

**A DETAILED METALLOGENIC STUDY OF THE MCFAULDS LAKE CHROMITE
DEPOSITS, NORTHERN ONTARIO**

(Thesis Format: Monograph)

by

Jordan Elliot Laarman

**Department of Earth Sciences
Graduate Program in Geology**

**Submitted in partial fulfillment
of the requirements for the degree of
Doctor of Philosophy**

**The School of Graduate and Postdoctoral Studies
The University of Western Ontario
London, Ontario
© Jordan Elliot Laarman, 2013**

ABSTRACT

The Black Label, Black Thor and Big Daddy chromite deposits are a series of chromitite layers that are hosted by the 2734.5 +/-1.0 Ma 'Ring of Fire' Intrusion in the McFaulds Lake greenstone belt of Northern Ontario. Over 4200 electron microprobe analyses and 142 laser ablation ICP-MS analyses were performed on chromite and record individual fractionation sequences of chromitite below the metre scale.

In comparing results, the dunite-hosted Black Thor chromites are higher grade with 53 to 49 wt. % Cr₂O₃, more primitive than Black Label chromites at 50 to 46 wt. % Cr₂O₃. Heterogeneous growth of orthopyroxene oikocrysts in Black Label chromitite accounts for increased silicate content. Massive chromitite at Big Daddy shows remarkable homogeneity at 50 to 51 wt. % Cr₂O₃. The homogeneity of the massive ore is attributed to development of chromitite layers by double diffusive convection. A strong linear regression of increasing Cr₂O₃ with MgO from disseminated to massive chromite at all deposits indicates the primary chromite compositions are magmatic. Elemental variation in the chromites include decreasing Cr, increasing Fe, slightly decreasing Al and decreasing Mg due to differentiation. Near constant low-Al compositions are characteristic of komatiitic chromite.

Laser ablation results show trends of depletion in Ti, V, Zn, Mn and Co, but enrichment in Ni and Sc, consistent with fractionation of chromitite. The chromitites contain mineral inclusions of pyroxene, igneous amphibole, and phlogopite that have very magnesian contents suggesting a source in the ultramafic magma. The host dunite and pyroxenite have negative Nb-Ta and Zr-Hf anomalies that signify an inherent contamination of ultramafic magma by TTG crust. The Ring of Fire Intrusion has been autohydrated, causing pervasive serpentinization and tremolitization of host dunite and pyroxenite. Secondary ferrichromite with higher wt. % FeO_T and Cr₂O₃ forms as rims on primary chromites, thereby enriching the Cr content of the ore. The rims of primary chromites are leached of Mg and Al leaving high Cr and Fe. The released Mg and Al forms magnesian clinocllore that contains up to 9 wt. % Cr₂O₃.

Key words: Black Thor, Big Daddy, Ring of Fire, chromite, deposits, double diffusive convection, massive chromitite, magma mixing, ferrichromite, silicate inclusions

ACKNOWLEDGEMENTS

There has been lots of support for me in the undertaking of this thesis. I would first like to thank Cliffs Natural Resources Inc. for the funding of probe analyses and logistical support for flying to and feeding me while I was at the bush camp the number of years I've worked for them on their drill programs. I'd also like to thank KWG Resources Inc. for logistical support at their camp on their drill programs. I'd like to thank both companies of course for the funding of the probe work. The project has been quite an adventure from the start with getting the interest of a few junior companies, input from Jon Scoates and sampling instruction from Tony Naldrett, then company take overs, new personnel, getting new interest for the funding and the applying for SEG grants. I would like to thank the SEG Canada Foundation and the internal grants at Western which also helped in the funding of the work. I'd like to acknowledge my NSERC IPS-2 grant which I received for two years on my term at Western. There has been very good instruction and advice for everyone involved with the laser ablation work under the TGI-4 program from the GSC. I'd like to acknowledge the funding from the GSC and help from Michel Houlé, who pulled me into doing the laser work; Simon Jackson in how to use the machine, advice from Marcus Burnham and Philippe Pagé on the choosing of the isotopes and much help in getting the laser work done from Zhaoping Yang of the GSC.

The microprobe work on the chromites and silicates is the meat of this thesis and I would like to give much appreciation to Bob Barnett for his performing of the analyses, teaching how the microprobe works, showing me how to identify phlogopites and pyroxenes under the microscope, giving me his input on the interpretation of the mineral chemistries, and of course his steady ambition to probe all those grains. Without him this thesis wouldn't have been possible to say the least. I would like to thank Jim Renaud for also probing some chromites too.

I would like to thank my advisor Norm Duke for his way of making me know the answer at the start and then filling in all the blanks with the evidence. Norm has always inspired me with his positive outlook on solving a problem. He came to the Cliffs camp one summer in helping me describe what I'm seeing in drill core and then made a report, which helped lift off some of the petrographic work. His input in the discussion of immiscible oxide melts and origin of the silicate inclusions were much appreciated.

Finally, I want to thank all of my family; my parents, brothers and sisters for continual moral support through my working of this thesis, for giving me food and a place to stay during my term at Western. Thank you for helping me persevere through this time, your love always being there when I need it – thank you. I want to thank Bonnie and rest of the Grootenboer family for my residence there in Thunder Bay while working in between rotations at the Cliffs camp. Bonnie, you're such a great friend to me and you always keep my spirit alive, thank you always.

TABLE OF CONTENTS

Abstract	i
Acknowledgements	ii
Table of Contents	iii
List of Figures	vi
List of Tables	xviii
CHAPTER 1: INTRODUCTION	
1.1 McFaulds Lake Chromite Deposits	1
1.2 Thesis Objective	1
1.3 Location and Climate	2
1.4 Previous Work	4
1.5 Methods	5
1.5.1 XRF (X-Ray Fluorescence spectrometry) and ICP-MS (Inductively Coupled Plasma-Mass Spectrometry)	6
1.5.2 Full Spectrum PGE analysis	6
1.5.3 Electron Microprobe Analysis	7
1.5.4 Laser Ablation ICP-MS	7
CHAPTER 2: GEOLOGICAL SETTING	
2.1 Oxford-Stull Domain	9
2.1.1 McFaulds Lake Greenstone Belt	12
2.2 Deformation	20
CHAPTER 3: PETROGRAPHY	
3.1 Introduction	25
3.2 Footwall granodiorite	30
3.3 Dunite-harzburgite	33
3.4 Oikocrystic harzburgite	35
3.5 Disseminated chromite	38
3.6 Chromitite	43
3.6.1 Heavily disseminated chromite	43
3.6.2 Intermittent chromitite beds	43
3.6.3 Semi-massive chromite	45
3.6.4 Massive chromite	53
3.7 Magmatic Breccia	58
3.8 Heterogeneous pyroxenite	63
3.9 Pyroxenite-olivine pyroxenite	63
3.10 Gabbro-leucogabbro	70
3.11 Hangingwall mafic metavolcanic	74
CHAPTER 4: GEOCHEMISTRY	
4.1 Introduction	75
4.2 Whole rock geochemistry	75
4.2.1.1 Major oxides	75

4.2.1.2 Up section major oxide variation	78
4.2.1.2.1 Black Label: DDH BT-09-31	78
4.2.1.2.2 Black Thor: DDH BT-08-10 & BT-09-17	81
4.2.1.2.3 Big Daddy: DDH FW-08-19	86
4.2.1.3 Binary major oxide variations	88
4.2.1.3.1 Black Label (Fig. 4.12)	88
4.2.1.3.2 Black Thor (Fig. 4.13)	88
4.2.1.3.3 Big Daddy (Fig. 4.14)	92
4.2.2 Trace element earth geochemistry	94
4.2.2.1 Primitive mantle-normalized multielement plots	94
4.2.2.1.1 Black Label	94
4.2.2.1.2 Black Thor	96
4.2.2.1.3 Big Daddy	99
4.2.2.2 $(La/Sm)_{cn}$ vs. $(Gd/Yb)_{cn}$	99
4.3 Full spectrum PGE analysis	101
4.3.1 Primitive mantle normalized PGE plots of host rocks	101
4.3.2 Primitive mantle normalized PGE plot of chromitite	103
4.4 Mineral chemistry of host silicates	105
4.4.1 Olivine	105
4.4.2 Pyroxene	105
4.4.3 Amphibole	109
4.4.4 Phlogopite	116
4.4.5 Chlorite	120

CHAPTER 5: MINERALIZATION

5.1 Introduction	130
5.2 Metal assay variation	130
5.2.1 Up section wt. % Cr_2O_3 , Pt, Pd, Ni and Cu ppm variation	130
5.2.1.1 Black Label (Figs. 5.1 and 5.2)	131
5.2.1.2 Black Thor (Figs. 5.3, 5.4, 5.5 and 5.6)	133
5.2.1.3 Big Daddy (Fig. 5.7)	137
5.2.2 Binary metal assay variation	139
5.3 Chromite mineral chemical variation	143
5.3.1 Up section mineral chemistry of chromite	145
5.3.1.1 Black Label	151
5.3.1.2 Black Thor BT-08-10	160
5.3.1.3 Black Thor BT-09-17	161
5.3.1.4 Big Daddy	176
5.3.2.1 Black Label binary chromite chemistry	199
5.3.2.2 Black Thor BT-08-10 binary chromite chemistry	204
5.3.2.3 Black Thor BT-09-17 binary chromite chemistry	209
5.3.2.4 Big Daddy binary chromite chemistry	213
5.4 Laser ablation ICP-MS analysis of chromite	222
5.4.1 Chromite/Chromite in MORB trace element plots	222
5.4.2 Binary trace element variation	224

CHAPTER 6: DISCUSSION	
6.1 Introduction	230
6.2 Tectonic discrimination of chromite	230
6.2.1 The Cr# vs. Mg# plot	230
6.2.2 The Ternary Cr-Fe ³⁺ -Al plot	233
6.3 Origin of chromite: An Evaluation of Irvine's 1975 model	233
6.4 Silicate Inclusions in Chromite	239
6.5 Origin of chromite: Irvine's 1977 magma mixing model	249
6.6 Evidence for magmatic differentiation by double diffusive convection: The electron microprobe results	255
6.6.1 Magmatic differentiation	255
6.6.2 Double diffusive convection mineralization	257
6.6.3 Formation of massive chromite by post-cumulus growth	261
6.7 Evaluation of the conduit model	264
6.8 Retrogression of chromite with hydration of the intrusion	267
CHAPTER 7: CONCLUSIONS	274
7.1 Conclusions	274
7.2 Summary	277
REFERENCES	281
APPENDIX 1: Core logs for DDH BT-09-31, BT-08-10, BT-09-17 and FW-08-19	296
APPENDIX 2: Sample List – BT-08-10	315
BT-09-31 & BT-09-17	320
FW-08-19	326
APPENDIX 3: Whole rock geochemistry & Full Spectrum PGE	330
APPENDIX 4: Silicate mineral chemistry data -	337
Olivine	338
Orthopyroxene	342
Clinopyroxene	344
Amphibole	350
Phlogopite	377
Chlorite	385
APPENDIX 5: Chromite mineral chemistry data -	401
BT-09-31	402
BT-08-10	423
BT-09-17	439
FW-08-19	442
APPENDIX 6: Chromite laser ablation data	459

List of Figures

Figure 1.1	Location map of the McFaulds Lake chromite deposits	3
Figure 2.1	Geological map of the Superior Geological Province	10
Figure 2.2	Aeromagnetic map of the Oxford-Stull Domain	11
Figure 2.3	Simplified geological map of the McFaulds Lake area	13
Figure 2.4	Geological map of the Ring of Fire Intrusion	15
Figure 2.5	Generalized stratigraphic column of the Ring of Fire Intrusion	15
Figure 2.6	Geology of the Blackbird chromite deposit	17
Figure 2.7	Geology of the Big Daddy chromite deposit	18
Figure 2.8	Geology of the Black Label and Black Thor chromite deposits	19
Figure 2.9	Quartz monzonite diapirism at the Koitelainen Intrusion	21
Figure 2.10	Drill section through Big Daddy DDH FW-08-19	23
Figure 2.11	Drill section through Black Thor DDH BT-08-10	23
Figure 2.12	Dextral strike-slip faults in the Black Thor chromitites	24
Figure 3.1	Drill section of Black Label DDH BT-09-31	26
Figure 3.2	Drill section of Black Thor DDH BT-08-10	27
Figure 3.3	Drill section of Black Thor DDH BT-09-17	28
Figure 3.4	Drill section of Big Daddy DDH FW-08-19	29
Figure 3.5	Photograph of granodiorite drill core	32
Figure 3.6	Photograph of dunite drill core	32
Figure 3.7	Photomicrograph of dunite with disseminated chromite-a	34
Figure 3.8	Photomicrograph of dunite with disseminated chromite-b	34
Figure 3.9	Pyroxene replacement of dunite in drill core-a	36

Figure 3.10	Pyroxene replacement of dunite in drill core-b	36
Figure 3.11	Pyroxene replacement of dunite in drill core-c	37
Figure 3.12	Photograph of oikocrystic harzburgite drill core	37
Figure 3.13	Photomicrograph of tremolitization of pyroxene	39
Figure 3.14	Photomicrograph of primary olivines and pyroxenes in talc	39
Figure 3.15	Photograph of disseminated chromite in dunite	40
Figure 3.16	Photomicrograph of interstitial chromite	40
Figure 3.17	Photomicrograph of net-textured chromite in dunite	41
Figure 3.18	Photomicrograph of interstitial chromite in oikocrystic harzburgite	41
Figure 3.19	Photograph of kaemmererite vein alteration	42
Figure 3.20	Photomicrograph of talc-rimmed olivines in net-textured chromite	42
Figure 3.21	Photograph of an intermittent chromite bed	44
Figure 3.22	Photograph of alternating intermittent chromite beds	44
Figure 3.23	Photograph of cumulus pyroxene interbanded with chromite	46
Figure 3.24	Photograph of net-textured semi-massive chromite	46
Figure 3.25	Photomicrograph of chain-like net-textured chromite	47
Figure 3.26	Photomicrograph of silicate inclusions in chromites	47
Figure 3.27	Photomicrograph of the incomplete annealing of a chromite grain	49
Figure 3.28	Photomicrograph of the concentric annealing of chromite grains	49
Figure 3.29	Backscatter image of multiple silicate inclusions in chromite	50
Figure 3.30	Backscatter image of minerals within a silicate inclusion	50
Figure 3.31	Photomicrograph of silicate inclusions in igneous amphibole	51
Figure 3.32	Backscatter image of silicate inclusions in igneous amphibole	51

Figure 3.33	Photomicrograph of the incomplete annealing of chromite around a phlogopite grain	52
Figure 3.34	Photomicrograph of chromite with interstitial phlogopite	52
Figure 3.35	Photograph of Black Thor massive chromite	54
Figure 3.36	Photograph of Big Daddy massive chromite	54
Figure 3.37	Photograph of oikocrystic pyroxene patches in massive chromite	55
Figure 3.38	Photograph of chicken-track texture of pyroxene in chromite	55
Figure 3.39	Photomicrograph of tremolitized oikocrystic pyroxene in massive chromite	56
Figure 3.40	Photomicrograph of interstitial chlorite in massive chromite	56
Figure 3.41	Photomicrograph of chlorite in brittle failure of massive chromite	56
Figure 3.42	Photograph of Black Label massive chromite	57
Figure 3.43	Photomicrograph of interstitial carbonate in massive chromite	59
Figure 3.44	Photograph of occluded silicate in chromite	59
Figure 3.45	Photograph of silicate layering in massive chromite	60
Figure 3.46	Photograph of deformation fabrics in chromite	60
Figure 3.47	Photomicrograph of adcumulus fracturing in massive chromite	61
Figure 3.48	Photograph of magmatic breccias	61
Figure 3.49	Photograph of sulphides in magmatic breccias	62
Figure 3.50	Photograph of heterogeneous olivine pyroxenite	64
Figure 3.51	Photograph of filter pressed layers in heterogeneous pyroxenite	64
Figure 3.52	Photograph of pyroxenite	65
Figure 3.53	Photograph of original bronzite in pyroxenite	65
Figure 3.54	Photomicrograph of pyroxenite	67

Figure 3.55 Photograph of disseminated chromite in pyroxenite	67
Figure 3.56 Photomicrograph of disseminated chromite in pyroxenite	68
Figure 3.57 Green aphyric ultramafic units in pyroxenite	68
Figure 3.58 Photograph of gabbro	71
Figure 3.59 Photomicrograph of green tremolite with surrounding biotite in gabbro	71
Figure 3.60 Photomicrograph of titanite alteration in gabbro	72
Figure 3.61 Photomicrograph of igneous amphibole in gabbro	72
Figure 3.62 Photograph of leucogabbro	73
Figure 4.1 Plot of Mg % vs. depth from assays of Black Label DDH BT-09-31	79
Figure 4.2 Plot of Fe % vs. depth from assays of Black Label DDH BT-09-31	79
Figure 4.3 Plot of Ca % and Al % vs. depth from assays of Black Label DDH BT-09-31	80
Figure 4.4 Plot of Mg % vs. depth from assays of Black Thor DDH BT-08-10	82
Figure 4.5 Plot of Fe % vs. depth from assays of Black Thor DDH BT-08-10	82
Figure 4.6 Plot of Ca % and Al % vs. depth from assays of Black Thor DDH BT-08-10	83
Figure 4.7 Plot of Mg % vs. depth from assays of Black Thor DDH BT-09-17	84
Figure 4.8 Plot of Fe % vs. depth from assays of Black Thor DDH BT-09-17	84
Figure 4.9 Plot of Ca % and Al % vs. depth from assays of Black Thor DDH BT-09-17	85
Figure 4.10 Plot of Ni, Fe %, Mg and Al % vs. depth from assays of Big Daddy DDH FW-08-19	87
Figure 4.11 Plot of Ca % vs. depth from assays of Big Daddy DDH FW-08-19	87
Figure 4.12 Binary plots of Cr vs. Mg, Cr vs. Al, Cr vs. Fe, Al vs. Mg, Fe vs. Mg and Ca vs. Mg from assays of Black Label DDH BT-09-31.	89

Figure 4.13	Binary plots of Cr vs. Mg, Cr vs. Al, Cr vs. Fe, Al vs. Mg, Fe vs. Mg and Ca vs Mg from assays of Black Thor DDH BT-08-10. Binary plots of Al vs. Mg and Ca vs. Mg from assays of Black Thor DDH BT-09-17	90
Figure 4.14	Binary plots of Cr vs. Mg, Cr vs. Al, Cr vs. Fe, Al vs. Mg, Fe vs. Mg and Ca vs. Mg from assays of Big Daddy DDH FW-08-19	93
Figure 4.15	Primitive mantle multielement plot of dunite-harzburgite in DDH BT-09-31	95
Figure 4.16	Primitive mantle multielement plot of pyroxenite in all three deposits	95
Figure 4.17	Primitive mantle multielement plot of dunite-harzburgite in DDH BT-08-10 and FW-08-19	97
Figure 4.18	Primitive mantle multielement plot of gabbro in DDH BT-09-17	97
Figure 4.19	Plot of $(La/Sm)_{cn}$ vs. $(Gd/Yb)_{cn}$ for Black Label, Black Thor and Big Daddy host rocks	100
Figure 4.20	Primitive mantle PGE plot of dunite-harzburgite in DDH BT-08-10 and FW-08-19	102
Figure 4.21	Primitive mantle PGE plot of dunite-harzburgite in DDH BT-09-31	102
Figure 4.22	Primitive mantle PGE plot of pyroxenite from all three deposits	104
Figure 4.23	Primitive mantle PGE plot of chromitite from all three deposits	104
Figure 4.24	Plot of $Mg/(Mg+Fe_{2+})$ vs. depth for chromite and olivine in Black Label DDH BT-09-31	106
Figure 4.25	Ternary plot of pyroxene compositions	107
Figure 4.26	Ternary plot of clinopyroxene compositions in sample 486211	108
Figure 4.27	Ternary plot of orthopyroxene compositions in sample 486211	108
Figure 4.28	Plot of Ti vs. Al total for pyroxene in five samples	110
Figure 4.29	Plot of Mg # vs. Si for amphiboles with $(Na+K)_A \geq 0.50$; $(Ca+NaB) \geq 1.00$; $0.50 < NaB < 1.50$ with nomenclature of Leake et al. (1997). A winchite is plotted for amphiboles with $(Na+K)_A < 0.50$; $(Ca+NaB) \geq 1.00$; $0.50 < NaB < 1.50$	111
Figure 4.30	Plot of tetrahedral Al vs. A site Na and K for all the amphiboles	113

Figure 4.31	Plot of tetrahedral Al – A site Na and K vs. octahedral Al+2Ti+Cr for all the amphiboles	113
Figure 4.32	Plot of Mg # vs. Si for amphiboles with $CaB \geq 1.50$; $(Na+K)A > 0.50$; $Ti < 0.50$; $AlVI \geq Fe^{3+}$ with nomenclature of Leake et al. (1997)	114
Figure 4.33	Plot of $Mg/(Mg+Fe^{2+})$ vs. depth (m) for pargasite-edenite in Black Label DDH BT-09-31	115
Figure 4.34	Plot of Mg # vs. Si for amphiboles with $CaB \geq 1.50$; $(Na+K)A < 0.5$ with nomenclature of Leake et al. (1997).	117
Figure 4.35	Plot of wt. % Al_2O_3 vs. wt. % TiO_2 for phlogopite compositions	118
Figure 4.36	Ternary Ba-K-Na plot for phlogopites	119
Figure 4.37	Plot of wt. % MgO vs. depth for phlogopite in Black Label DDH BT-09-31	121
Figure 4.38	Plot of wt. % Cr_2O_3 vs. depth for phlogopite in Black Label DDH BT-09-31	122
Figure 4.39	Plot of wt. % Cr_2O_3 vs. wt. % MgO for phlogopite	123
Figure 4.40	Plot of wt. % Cr_2O_3 vs. wt. % TiO_2 for phlogopite	123
Figure 4.41	Classification of McFaulds Lake chlorites after Hey (1954)	124
Figure 4.42	Classification of chlorites in DDH BT-09-31 after Hey (1954)	125
Figure 4.43	Classification of chlorites in DDH BT-08-10 and BT-09-17 after Hey (1954)	126
Figure 4.44	Plot of wt. % Cr_2O_3 vs. wt. % Al_2O_3 for chlorite	128
Figure 4.45	Plot of wt. % Cr_2O_3 vs. wt. % MgO for chlorite	128
Figure 5.1	Plot of Cr_2O_3 , Fe and Pt + Pd vs. depth from assays of Black Label DDH BT-09-31	132
Figure 5.2	Plot of Ni and Cu vs. depth from assays of DDH BT-09-31	132
Figure 5.3	Plot of Cr_2O_3 , Fe and Pt + Pd vs. depth from assays of Black Thor DDH BT-08-10	134

Figure 5.4	Plot of Ni and Cu vs. depth from assays of DDH BT-08-10	134
Figure 5.5	Plot of Cr ₂ O ₃ , Fe and Pt + Pd vs. depth from assays of Black Thor DDH BT-09-17	135
Figure 5.6	Plot of Ni and Cu vs. depth from assays of DDH BT-09-17	135
Figure 5.7	Plot of Cr ₂ O ₃ , Fe and Pt + Pd vs. depth from assays of Big Daddy DDH FW-08-19	138
Figure 5.8	Binary plots of Ti, V, Zn, Mn and Ni vs. Cr from assays of Black Label DDH BT-09-31	140
Figure 5.9	Binary plots of Ti, V, Zn, Mn and Ni vs. Cr from assays of Black Thor DDH BT-08-10	141
Figure 5.10	Binary plots of Ti, V, Zn, Mn and Ni vs. Cr from assays of Big Daddy DDH FW-08-19	142
Figure 5.11	Backscatter image of massive chromite with sample points shown	144
Figure 5.12	Backscatter image of sample 486044, chromite #1 with sample points shown	146
Figure 5.13	Plot of chromite evolution in Black Thor sample 486044, chromite #1	146
Figure 5.14	Backscatter image of sample 486044, chromite #2 with sample points shown	147
Figure 5.15	Plot of chromite evolution in Black Thor sample 486044, chromite #2	147
Figure 5.16	Backscatter image of sample 486129 with sample points shown	148
Figure 5.17	Plot of chromite evolution in Black Thor sample 486129	148
Figure 5.18	Plot of major oxide variation from disseminated to massive chromite in the chromite cores of the first fifty samples analysed in Black Thor DDH BT-08-10	150
Figure 5.19	Variation of wt. % major oxide with height up section (down hole) in Black Thor DDH BT-08-10 for chromite cores of first fifty samples analysed	150

Figure 5.20	Plot of Cr ₂ O ₃ wt. % vs. depth for Black Label DDH BT-09-31	152
Figure 5.21	Plot of MgO wt. % vs. depth for Black Label DDH BT-09-31 with various zones and pulses shown	153
Figure 5.22	Plot of Cr/(Cr+Al+Fe ₃₊) vs. depth for Black Label DDH BT-09-31	154
Figure 5.23	Plot of Mg/(Mg+Fe ₂₊) vs. depth for Black Label DDH BT-09-31	155
Figure 5.24	Plot of FeO wt. % vs. depth for Black Label DDH BT-09-31	156
Figure 5.25	Plot of Cr/Fe vs. depth for Black Label DDH BT-09-31	157
Figure 5.26	Plot of Al ₂ O ₃ wt. % vs. depth for Black Label DDH BT-09-31	158
Figure 5.27	Plot of Fe ₂ O ₃ wt. % vs. depth for Black Label DDH BT-09-31	159
Figure 5.28	Plot of Cr/Fe vs. depth for Black Thor DDH BT-08-10	162
Figure 5.29	Plot of MgO wt. % vs. depth for Black Thor DDH BT-08-10 with various zones and pulses shown	163
Figure 5.30	Plot of Mg/(Mg+Fe ₂₊) vs. depth for Black Thor DDH BT-08-10	164
Figure 5.31	Plot of Cr ₂ O ₃ wt. % vs. depth for Black Thor DDH BT-08-10	165
Figure 5.32	Plot of Cr/(Cr+Al+Fe ₃₊) vs. depth for Black Thor DDH BT-08-10	166
Figure 5.33	Plot of FeO wt. % vs. depth for Black Thor DDH BT-08-10	167
Figure 5.34	Plot of Al ₂ O ₃ wt. % vs. depth for Black Thor DDH BT-08-10	168
Figure 5.35	Plot of Fe ₂ O ₃ wt. % vs. depth for Black Thor DDH BT-08-10	169
Figure 5.36	Plot of Cr ₂ O ₃ wt. % vs. depth for Black Thor DDH BT-09-17	170
Figure 5.37	Plot of MgO wt. % vs. depth for Black Thor DDH BT-09-17	171
Figure 5.38	Plot of Cr/(Cr+Al+Fe ₃₊) vs. depth for Black Thor DDH BT-09-17	172
Figure 5.39	Plot of Mg/(Mg+Fe ₂₊) vs. depth for Black Thor DDH BT-09-17	173
Figure 5.40	Plot of Cr/Fe vs. depth for Black Thor DDH BT-09-17	175
Figure 5.41	Plot of Al ₂ O ₃ wt. % vs. depth for Black Thor DDH BT-09-17	177
Figure 5.42	Plot of FeO wt. % vs. depth for Black Thor DDH BT-09-17	178

Figure 5.43	Plot of Fe_2O_3 wt. % vs. depth for Black Thor DDH BT-09-17	179
Figure 5.44	Plot of Cr_2O_3 wt. % vs. depth for the first part of Big Daddy DDH FW-08-19	180
Figure 5.45	Plot of MgO wt. % vs. depth for the first part of Big Daddy DDH FW-08-19	181
Figure 5.46	Plot of $\text{Cr}/(\text{Cr}+\text{Al}+\text{Fe}_{3+})$ vs. depth for the first part of Big Daddy DDH FW-08-19	182
Figure 5.47	Plot of $\text{Mg}/(\text{Mg}+\text{Fe}_{2+})$ vs. depth for the first part of Big Daddy DDH FW-08-19	183
Figure 5.48	Plot of Cr/Fe vs. depth for the first part of Big Daddy DDH FW-08-19	184
Figure 5.49	Plot of Al_2O_3 wt. % vs. depth for the first part of Big Daddy DDH FW-08-19	186
Figure 5.50	Plot of FeO wt. % vs. depth for the first part of Big Daddy DDH FW-08-19	187
Figure 5.51	Plot of TiO_2 wt. % vs. depth for the first part of Big Daddy DDH FW-08-19	188
Figure 5.52	Plot of Fe_2O_3 wt. % vs. depth for the first part of Big Daddy DDH FW-08-19	189
Figure 5.53	Plot of Cr_2O_3 wt. % vs. depth for Big Daddy DDH FW-08-19	190
Figure 5.54	Plot of MgO wt. % vs. depth for Big Daddy DDH FW-08-19 with various zones and pulses shown	191
Figure 5.55	Plot of $\text{Cr}/(\text{Cr}+\text{Al}+\text{Fe}_{3+})$ vs. depth for Big Daddy DDH FW-08-19	192
Figure 5.56	Plot of $\text{Mg}/(\text{Mg}+\text{Fe}_{2+})$ vs. depth for Big Daddy DDH FW-08-19	193
Figure 5.57	Plot of Cr/Fe vs. depth for Big Daddy DDH FW-08-19	195
Figure 5.58	Plot of FeO wt. % vs. depth for Big Daddy DDH FW-08-19	196
Figure 5.59	Plot of Al_2O_3 wt. % vs. depth for Big Daddy DDH FW-08-19	197
Figure 5.60	Plot of Fe_2O_3 wt. % vs. depth for Big Daddy DDH FW-08-19	198

Figure 5.61	Binary plot of Cr ₂ O ₃ vs. MgO wt. % for Black Label DDH BT-09-31 with paths of chromite evolution shown	200
Figure 5.62	Black Label Layers 1 and 2 of DDH BT-09-31	200
Figure 5.63	Binary plot of Al ₂ O ₃ vs. MgO wt. % for Black Label DDH BT-09-31	202
Figure 5.64	Binary plot of FeO vs. MgO wt. % for Black Label DDH BT-09-31	202
Figure 5.65	Binary plot of TiO ₂ vs. Fe ₂ O ₃ wt. % for Black Label DDH BT-09-31	203
Figure 5.66	Binary plot of TiO ₂ vs. Cr ₂ O ₃ wt. % for Black Label DDH BT-09-31	203
Figure 5.67	Binary plot of TiO ₂ vs. FeO wt. % for Black Label DDH BT-09-31	205
Figure 5.68	Binary plot of ZnO vs. Cr ₂ O ₃ wt. % for Black Label DDH BT-09-31	205
Figure 5.69	Binary plot of NiO vs. Cr ₂ O ₃ wt. % for Black Label DDH BT-09-31	206
Figure 5.70	Binary plot of Cr ₂ O ₃ vs. MgO wt. % for Black Thor DDH BT-08-10 with paths of chromite evolution shown	207
Figure 5.71	Binary plot of Al ₂ O ₃ vs. MgO wt. % for Black Thor DDH BT-08-10	207
Figure 5.72	Binary plot of FeO vs. MgO wt. % for Black Thor DDH BT-08-10	208
Figure 5.73	Binary plot of TiO ₂ vs. Cr ₂ O ₃ wt. % for Black Thor DDH BT-08-10	208
Figure 5.74	Binary plot of ZnO vs. Cr ₂ O ₃ wt. % for Black Thor DDH BT-08-10	210
Figure 5.75	Binary plot of NiO vs. Cr ₂ O ₃ wt. % for Black Thor DDH BT-08-10	210

Figure 5.76	Binary plot of MnO vs. Cr ₂ O ₃ wt. % for Black Thor DDH BT-08-10	211
Figure 5.77	Binary plot of Cr ₂ O ₃ vs. MgO wt. % for Black Thor DDH BT-09-17 with paths of chromite evolution shown	212
Figure 5.78	Binary plot of Al ₂ O ₃ vs. MgO wt. % for Black Thor DDH BT-09-17	212
Figure 5.79	Binary plot of FeO vs. MgO wt. % for Black Thor DDH BT-09-17	214
Figure 5.80	Binary plot of TiO ₂ vs. Cr ₂ O ₃ wt. % for Black Thor DDH BT-09-17	214
Figure 5.81	Binary plot of ZnO vs. Cr ₂ O ₃ wt. % for Black Thor DDH BT-09-17	215
Figure 5.82	Binary plot of NiO vs. Cr ₂ O ₃ wt. % for Black Thor DDH BT-09-17	215
Figure 5.83	Binary plot of MnO vs. Cr ₂ O ₃ wt. % for Black Thor DDH BT-09-17	215
Figure 5.84	Binary plot of Cr ₂ O ₃ vs. MgO wt. % for Big Daddy DDH FW-08-19 with paths of chromite evolution shown	217
Figure 5.85	Binary plot of Al ₂ O ₃ vs. MgO wt. % for Big Daddy DDH FW-08-19	217
Figure 5.86	Binary plot of FeO vs. MgO wt. % for Big Daddy DDH FW-08-19	219
Figure 5.87	Binary plot of TiO ₂ vs. Cr ₂ O ₃ wt. % for Big Daddy DDH FW-08-19	219
Figure 5.88	Binary plot of ZnO vs. Cr ₂ O ₃ wt. % for Big Daddy DDH FW-08-19	220
Figure 5.89	Binary plot of NiO vs. Cr ₂ O ₃ wt. % for Big Daddy DDH FW-08-19	220
Figure 5.90	Binary plot of MnO vs. Cr ₂ O ₃ wt. % for Big Daddy DDH FW-08-19	221

Figure 5.94 Chromite in MORB trace element plot of Black Label DDH BT-09-31	223
Figure 5.95 Chromite in MORB trace element plot of Black Thor DDH BT-08-10	223
Figure 5.96 Chromite in MORB trace element plot of Big Daddy DDH FW-08-19	225
Figure 5.97 Binary plots of Cr vs. Ti, V, Zn, Mn, Ni, Co, Sc and Ga ppm for Black Label DDH BT-09-31	226
Figure 5.98 Binary plots of Cr vs. Ti, V, Zn, Mn, Ni, Co, Sc and Ga ppm for Black Thor DDH BT-08-10	227
Figure 5.99 Binary plots of Cr vs. Ti, V, Zn, Mn, Ni, Co, Sc and Ga ppm for Big Daddy DDH FW-08-19	229
Figure 6.1 Cr # vs. Mg # plot of McFaulds Lake chromites with other layered intrusion and komatiite chromites of the world	231
Figure 6.2 Cr # vs. Mg # plot of McFaulds Lake chromites with other chromite deposits of the world	231
Figure 6.3 Ternary Cr-Fe ³⁺ -Al plot of the McFaulds Lake chromites with other layered intrusion and komatiite chromites of the world	234
Figure 6.4 The annealing process from Hulbert and Von Gruenewaldt (1985)	241
Figure 6.5 Phase Relations in the System Olivine-Silica-Chromite as determined by Irvine (1977)	251
Figure 6.6 Differing primitive mantle trace element patterns of dunite and pyroxenite	253
Figure 6.7 Differing primitive mantle PGE patterns of dunite and pyroxenite	253
Figure 6.8 Double diffusive convection model	258
Figure 6.9 Double diffusive convection cells in a magma chamber	258
Figure 6.10 Step-wise double diffusive chromite-PGE mineralization	260
Figure 6.11 Figure showing thickness, grade and wt. % Cr in the 36 m-thick ore zone at Big Daddy	265
Figure 6.12 Residual gravity map with chromitite zones plotted	268

List of Tables

Table 3.1	Summary of drill holes	31
Table 4.1	Major oxide wt. % in DDH samples	76

CHAPTER 1

INTRODUCTION

1.1 McFaulds Lake Chromite Deposits

Three new chromite deposits have been discovered in the McFaulds Lake area of the “Ring of Fire” District in the James Bay Lowlands region of northern Ontario. The largest Black Thor deposit is up to 46 m thick with 40 % Cr₂O₃ in massive chromitite that extends along strike for 2.6 km. These new discoveries of high grade chromite have associated PGE enrichment and are only exceeded by deposits such as the Bushveld Complex in South Africa, the Great Dyke of Zimbabwe and Kazakhstan for global chromium resources. Historically, the main source of chromite has been in South Africa, however this new resource will allow North America to sustain itself. Mining is planned with a 30 year mine life predicted. This operation will have a major impact on the economic development of Northern Ontario. These new chromite deposits are classified with the group of stratiform magmatic Cr/PGE ores in layered complexes (Duke, 1988). Better understanding of their formation will facilitate stratigraphic correlation, thus instrumental in defining an exploration vector. The occurrence of multiple zones of basal massive vs. disseminated styles of mineralization indicates primary magmatic cumulate concentration of the chromite.

1.2 Thesis Objective

The objective of this project is to investigate the origin of the McFaulds Lake chromite deposits. The chromite deposits have undergone an igneous crystallization history that has in turn been modified by a pervasive hydration overprint. Therefore the origin of the chromite deposits involves both a study of the magmatic crystallization of the chromite and the retrogressive hydration that has since modified the grade of the ores. The study provides a detailed geochemical profile of chromite in three deposits: the Black Label, Black Thor and Big Daddy chromitites. It involves petrographic analysis of primary igneous chromite and associated hydrous silicate mineralogy; whole rock

geochemical and full spectrum PGE analysis of chromite and chromite host rock; mineral chemical analysis of host rock silicates and silicates in association with chromite; detailed electron microprobe analyses of chromite in the three deposits and laser ablation trace geochemical analysis of chromite minerals. Results will be discussed in the final chapter.

The project is both field and laboratory-based, focusing on drill core since there is only sparse outcrop in the muskeg-covered lowlands. The logging of drill core allows sampling of chromitite layers in igneous stratigraphy. Basal lithologies of the intrusion consist of dunite-peridotite and oikocrystic harzburgite hosting disseminated to heavily disseminated chromite with intermittent beds of semi-massive to massive chromite and local magmatic chromite breccia. Overlying units include heterogeneous olivine pyroxenite and pyroxenite capped by leucogabbro-gabbro-norite. These lithologies are pervasively hydrated with essentially complete serpentinization of olivine; the serpentine coexists with talc, tremolite, chlorite, kaemmererite, and magnetite.

The mineral chemistry of the various chromitites at Big Daddy, Black Label and Black Thor needs to be documented for metallurgical purposes. The higher and more consistent Cr# in the more massive chromitite makes such zones most profitable to mine. Cr# measured in 3 strategic drill holes can be correlated to trends of chromitites in other drill holes along strike. In addition to bulk rock wt. % Cr₂O₃, microprobe data is crucial in documenting the complex chromite mineral chemistry of the ore.

1.3 Location and Climate (from Aubut, 2010)

The McFaulds Lake chromite deposits are located in an area of complete muskeg cover in the James Bay Lowlands (Fig. 1.1). The site location for core storage is at Esker Camp serving as a hub for helicopter supported drill programs. It is located in northwestern Ontario, Canada, approximately 250 km north of the town of Nakina and 80 km east of the native village of Webequie. The camp is situated in the Porcupine Mining Division in area BMA 527861 (G-4306) with UTM NAD 83 coordinates of 547544E, 5843918N. The Black Label and Black Thor deposits are held by Cliffs Natural Resources Inc. while the Big Daddy deposit is 75 % owned by Cliffs and 25 % owned by KWG Resources Inc.

The James Bay Lowlands area has a typical continental climate with extreme temperature fluctuations from the winter to summer seasons. During the summer months

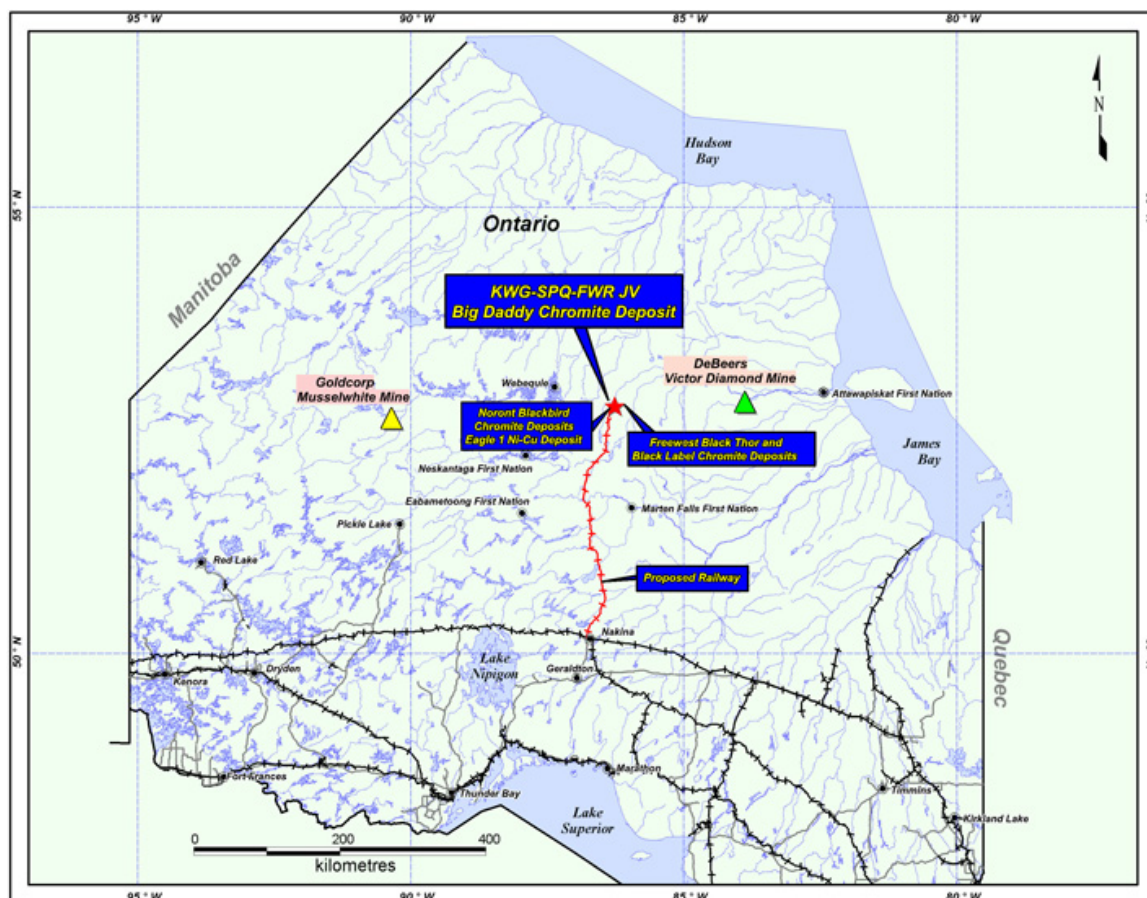


Figure 1.1. Location map of the McFaulds Lake chromite deposits. Source from www.kwgresources.com.

this can be moderated by the maritime effects of James and Hudson Bays. Summer temperatures range between 10°C and 35°C, with a mean temperature of 13°C in July. Winter temperatures usually range between -10°C and -55°C with an average January temperature of -23°C. Lakes typically freeze-up in mid-October and break-up is usually in mid-April. The region usually receives approximately 610 mm of precipitation per year, with about 1/3 originating as snow during the winter months. On a yearly basis the area averages about 160 days of precipitation per year.

1.4 Previous Work

Previous work relevant to this thesis include several investigations that provide petrographic and microprobe data in private company reports, NI-43-101 reports are available on both the Black Label-Black Thor and Big Daddy deposits (Aubut, 2010, 2012; Barrie, 2010; Gowens, 2009; Karagas, 2009; Metsaranta, 2010, 2011, 2012; Scoates, 2008a, 2008b, 2009a, 2009b; Tuchscherer, 2010). The junior companies involved in this early phase of work before being bought out by Cliffs Natural Resources Inc. include: Freewest Resources Inc. which held Black Label-Black Thor, Spider Resources Inc. who owned 25 % of Big Daddy and KWG Resources Inc. still owns 25 % of Big Daddy. The drilling of Black Label-Black Thor was carried out by Freewest Resources Inc. while Big Daddy was first drilled by Spider-KWG. The drilling history relevant to the drill holes of this study is as follows: In November 2008, DDH BT-08-10 was drilled as one of the first holes that cored Black Label-Black Thor. Subsequent drilling programs containing DDH BT-08-17 and BT-09-31 were drilled in the winter of 2008-2009. DDH FW-08-19 was drilled as one of the first nineteen drill holes at Big Daddy in the winter of 2008. Drilling continued in 2008 for DDH FW-08-05 to FW-08-23 and up to FW-09-60 into 2009. The drill program for Black Label-Black Thor continued in 2009 to DDH BT-09-113. The 2010 Black Thor holes drilled under Cliffs' operation include DDH BT-10-114 to BT-10-174. The 2011 Black Label-Black Thor drill holes include DDH BT-11-175 to BT-11-203. Big Daddy drilling under Cliffs' operation occurred in fall-winter 2011-2012 for DDH FW-11-61 to FW-11-112.

During the early 2008-2009 drill programs by Freewest and Spider-KWG, several technical reports were written on the petrography and preliminary whole rock assays of the host rocks and chromitites to Black Label-Black Thor and Big Daddy (Scoates,

2008b, 2009a, b). This preliminary work involved the first classification of the host rocks and chromitites for drilling purposes and included considerable detailed petrographic descriptions supplemented with hand sample and thin section photographs, as well as core logging notes that proved useful for the petrography chapter of this thesis. Scoates (2008a) cites several whole rock analyses similar to the whole rock geochemistry reported in this thesis.

As a component of the 2008 Freewest drill program, XRF, XRD and SEM-EDS analyses were performed on 27 samples from three drill holes. Sixty-nine single element determinations were performed by Karagas (2009). These analyses provided the initial framework for the undertaking of electron microprobe work reported in this thesis. Other technical reports that proved useful included the technical draft drill report to Freewest by Tuchscherer et al. (2010), an NI-43-101 on Black Label-Black Thor by Aubut (2010) of the Sibley Basin Group, and NI-43-101 reports on Big Daddy by Gowens (2009) of Micon International Ltd. and by Aubut (2012). Whole rock geochemical and metal assay data was provided by Spider-KWG and Freewest for the 3 strategic drill holes chosen for this study. Barrie (2010) reported on PGE mineralogy of the Black Thor deposit. Tuchscherer (2010) compiled a map of the Black Label-Black Thor zones on the basis of drill core information and a similar map was also provided by Spider-KWG. Metsaranta (2010, 2011 and 2012) has several reports for Summary of Field Work of the Ontario Geological Survey and these were considered in the writing of the geology chapter.

1.5 Methods

The four holes drilled by Freewest Resources and Spider-KWG Resources, including BT-08-10, BT-09-17, BT-09-31 and FW-08-19 were logged by the author. Representative lithologies were sampled for petrographic, whole rock XRF (X-ray Fluorescence Spectrometry) and ICP-MS (Inductively Coupled Plasma – Mass Spectrometry), electron microprobe mineral, laser ablation ICP-MS and full spectrum PGE analyses. Details of the logging and number of samples analysed are found in the following chapters. Polished thin sections of 30 µm thickness were made for petrographic and mineral chemical analysis, 100 µm thick slides were made for the laser ablation work.

1.5.1 XRF (X-Ray Fluorescence Spectrometry) and ICP-MS (Inductively Coupled Plasma-Mass Spectrometry)

The samples chosen for XRF and ICP-MS were first slabbed and polished thin sections were made for preliminary examination of texture and mineralogy utilizing both transmitted and reflected light microscopy. The rock samples were later crushed into powders and analysed by XRF and ICP at Activation Laboratories in Ancaster, Ontario. Sample preparation included the crushing to a nominal minus 10 mesh (1.7 mm), mechanically split (riffled) and then pulverized to 95 % minus 150 mesh (105 microns). In preparation for XRF whole rock geochemical analysis, the samples were homogenized by lithium metaborate/tetraborate fusion. The resulting molten beads were rapidly digested in a weak nitric acid solution and then were analysed by XRF and ICP. A base metal suite and sulphide sulphur were determined on an aquia regia extraction with an ICP/OES (Inductively Coupled Plasma-Optical Emission Spectroscopy) finish. For the aquia regia extraction, a combination of concentrated hydrochloric and nitric acids were used to leach total sulphide, oxide and silicate. A partial extraction was also analysed by ICP-MS for lower detection limits. ICP-MS analysis was also employed on samples for trace elements and REE. In preparation, these samples were again reduced by lithium metaborate/tetraborate fusion into beads that were digested in weak nitric acid to be analysed by ICP-MS.

1.5.2 Full spectrum PGE analysis

The same samples analysed by XRF and ICP were analysed for full spectrum PGE along with six other samples. Nickel sulphide fire assay was carried out on 50 g samples. The samples were fired at 1100 degrees C whereby nickel sulphide droplets scavenged the PGE and formed buttons at the bottom of the crucible. The nickel sulphide buttons were dissolved in concentrated HCl and the resulting residues which contained all the PGE and Au were collected on a filter paper. This residue undergoes 2 irradiations and 3 separate counts to measure all the PGE and Au. An INAA (Instrumental Neutron Activation Analysis) finish was later performed on the samples. Elements of Os, Ir, Ru, Rh, Pt, Pd, Au and Re were analysed with the respective detection limits of 2, 0.1, 5, 0.2, 5, 2 and 0.5 ppb.

1.5.3 Electron Microprobe Analysis

Electron microprobe analysis was performed on over 300 samples mostly by R.L. Barnett Geoanalytical Consulting Ltd using a JEOL Model 733 electron microprobe equipped with five wavelength spectrometers and using the Tracor Northern Automation System. A subset of the 300 samples was further analysed by Jim Renaud of Renaud Geological Consulting Ltd using a similar JEOL Model 733 microprobe. Thin sections were carbon coated to prevent charging during analysis. Samples were analysed with an accelerating voltage of 45 kV, a beam current of 10 nA and an electron beam width of 2 μm . Standards from the Smithsonian Institute were used to calibrate for Si, Ti, Al, Cr, Fe, Mn, Mg, Zn and Ni. Ferrous/ferric recalculations were later made for Fe.

1.5.4 Laser Ablation ICP-MS

Laser ablation ICP-MS was performed on 37 samples at the Geological Survey of Canada facility in Ottawa, Ontario under the supervision of Simon Jackson. Analyses were made on 100 μm thick polished thin sections. The thick sections were necessary to reduce spalling and allow longer ablation times to improve detection limits. Before analysis in Ottawa, an internal standard of FeO_T was needed for calibration to correct for variable ablation yield. Accordingly, polished chromites were analysed by microprobe for FeO_T before the LA ICP-MS analysis. After the microprobe work, the carbon coating was removed from the sections so as to not interfere with the LA analyses. Scans were made and circles drawn on the thin sections for select chromite grains prior to and in order to speed up the choice of grains for ablating. The laser ablation was conducted on a Photon-Machines Analyte 193 excimer laser ablation system ($\lambda=193$ nm) with a Helex ablation cell and an Agilent 7700x quadrupole ICP-MS. The software package used for data reduction was GLITTERTM. The analyses were conducted using a 69 μm or an 86 μm spot size, a 14 Hz frequency, 40 % of 5 mJ energy during a total acquisition of 100 seconds (~40 seconds for the gas blank and ~60 seconds for the chromite). In addition to the trace elements analysed (Sc^{45} , Ti^{47} , Ti^{49} , V^{51} , Mn^{55} , Co^{59} , Ni^{60} , Zn^{66} , Ga^{69} , Ga^{71}), other elements (Mg^{25} , Al^{27} , Si^{29} , Ca^{42} , Cr^{53} , Fe^{57} , Cu^{63} , Cu^{65} , Ge^{73} , As^{75} , Sr^{88} , Y^{89} , Zr^{90} , Zr^{91} , Nb^{93} , Mo^{95} , Mo^{98} , Ru^{99} , Ru^{101} , Ru^{102} , Rh^{103} , Ru^{104} , Pd^{105} , In^{115} , Sn^{118} , Sb^{121} , La^{139} , Ce^{140} , Yb^{174} , Hf^{178} , Ta^{181} , W^{182} , Os^{189} , Ir^{191} , Os^{192} , Ir^{193} , Pt^{195} , Pb^{206} , Pb^{207} , Pb^{208} , Th^{232} , U^{238}) were monitored during chromite ablation to control the nature of the ablated

material by identifying contaminants like the presence of included phases. Care was taken in selecting isotopes where there was no interference with argides and where there was acceptable range in uncertainty. For those elements where there were two isotopes, the isotopes that were chosen that had a lower range of uncertainty were Ti^{49} , Ga^{71} , Zr^{91} , Mo^{95} and Pb^{206} . For other elements with two isotopes, isotopes chosen on a basis of no interference with argides were Ru^{102} , Ir^{193} , Os^{192} , and Cu^{63} . Standards used for calibration include GSE-1G and Po726 for sulphide. The standards GOR 128 and BCR-2G were used for quality control standard and blanks.

CHAPTER 2

GEOLOGICAL SETTING

2.1 Oxford-Stull Domain

The McFaulds Lake chromite deposits are hosted in the Ring of Fire Intrusion, located in the McFaulds Lake Greenstone Belt in Northern Ontario. Regionally, this greenstone belt is located in the Oxford-Stull Domain of the former Sachigo Subprovince in the greater Archean Superior Province (Fig. 2.1). The Neoproterozoic 2870-2707 Ma. Oxford-Stull Domain is interpreted to form an intracratonic rift setting separating the Mesoproterozoic North Caribou Terrane from the more northerly Hudson Bay Terrane (Stott et al. 2010).

The Oxford-Stull Domain is a WNW-ESE striking granite-greenstone terrane that is bounded to the north by the North Kenyon Fault and to the south by the Stull-Wunnummin and Gods Lake Narrows shear zones. The latter are known to host several lode gold occurrences (Tuchscherer et al., 2009; Fig. 2.2). A larger SSW-NNE oriented unknown fault also cross-cuts the terrane in the region of the Ring of Fire Intrusion (Vaillancourt, 2003). These same faults control the emplacement of other mafic intrusions in the region, including the Highbank Lake-Fishtrap Lake intrusive complex and the Winiskisis Channel gabbros (Metsaranta and Houlé, 2012). The eastern extension of the terrane is the La Grande Domain in Quebec which hosts chromite occurrences in the Menarik Complex (Stott et al., 2010; Houlé, 2000; fig. 2.1).

The Big Trout Lake Complex, which is 50 km to the ESE, is a layered intrusion in the Sachigo Greenstone Belt that may have formed in a similar setting to the Ring of Fire Intrusion. It consists of a basal peridotite zone overlain by an anorthosite to quartz gabbro and finally monzodiorite. The peridotite intruded as two distinct magmas in 5 pulses: 1 pulse forming lower peridotite followed by 4 pulses forming upper peridotite higher in stratigraphy. The peridotite is generally olive green due to its high olivine

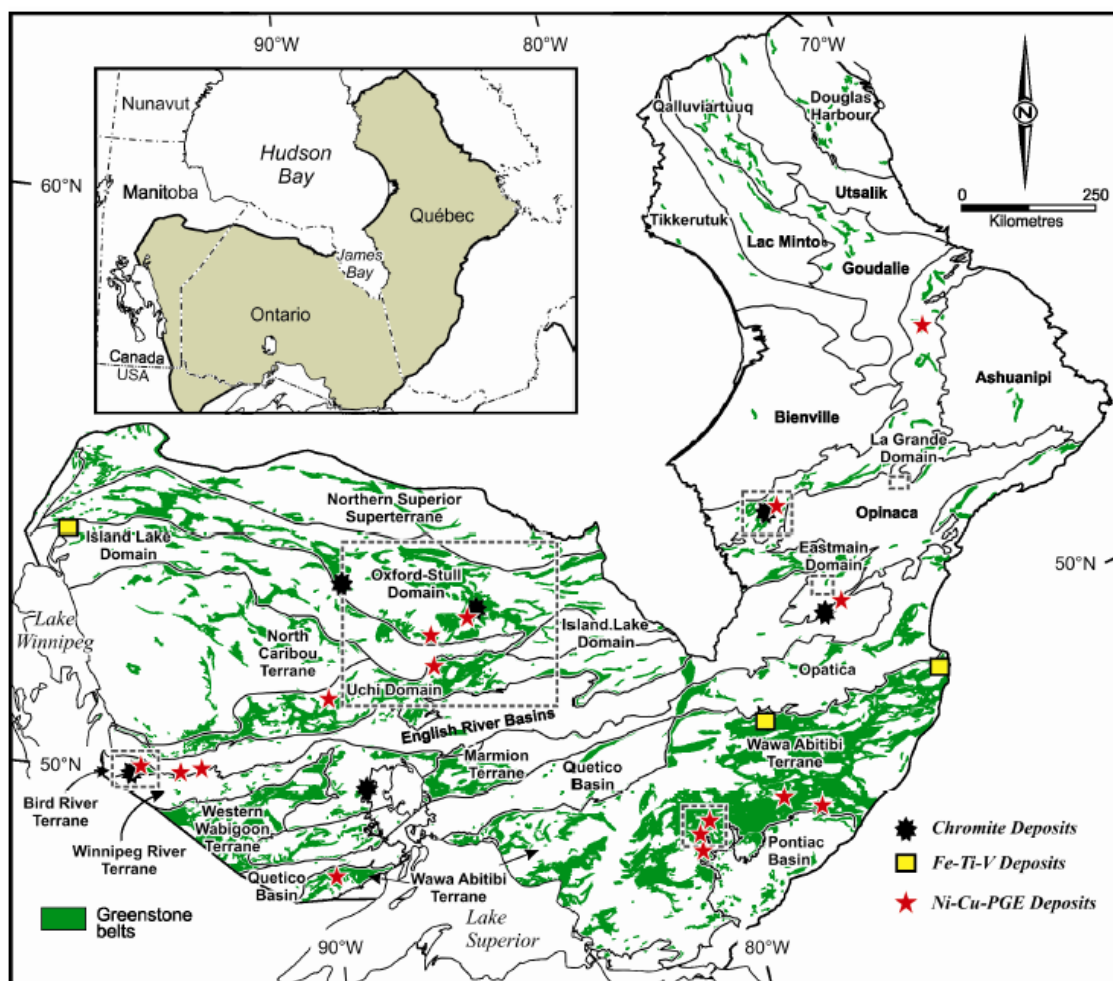


Figure 2.1. Geological map of the Superior Geological Province. The Oxford-Stull Domain is found within the large dashed box. Another near-contemporaneous chromite deposit is the Menarik Complex in the La Grande Domain (outlined in small box). From Houle, Leshar and Metsaranta (2012).

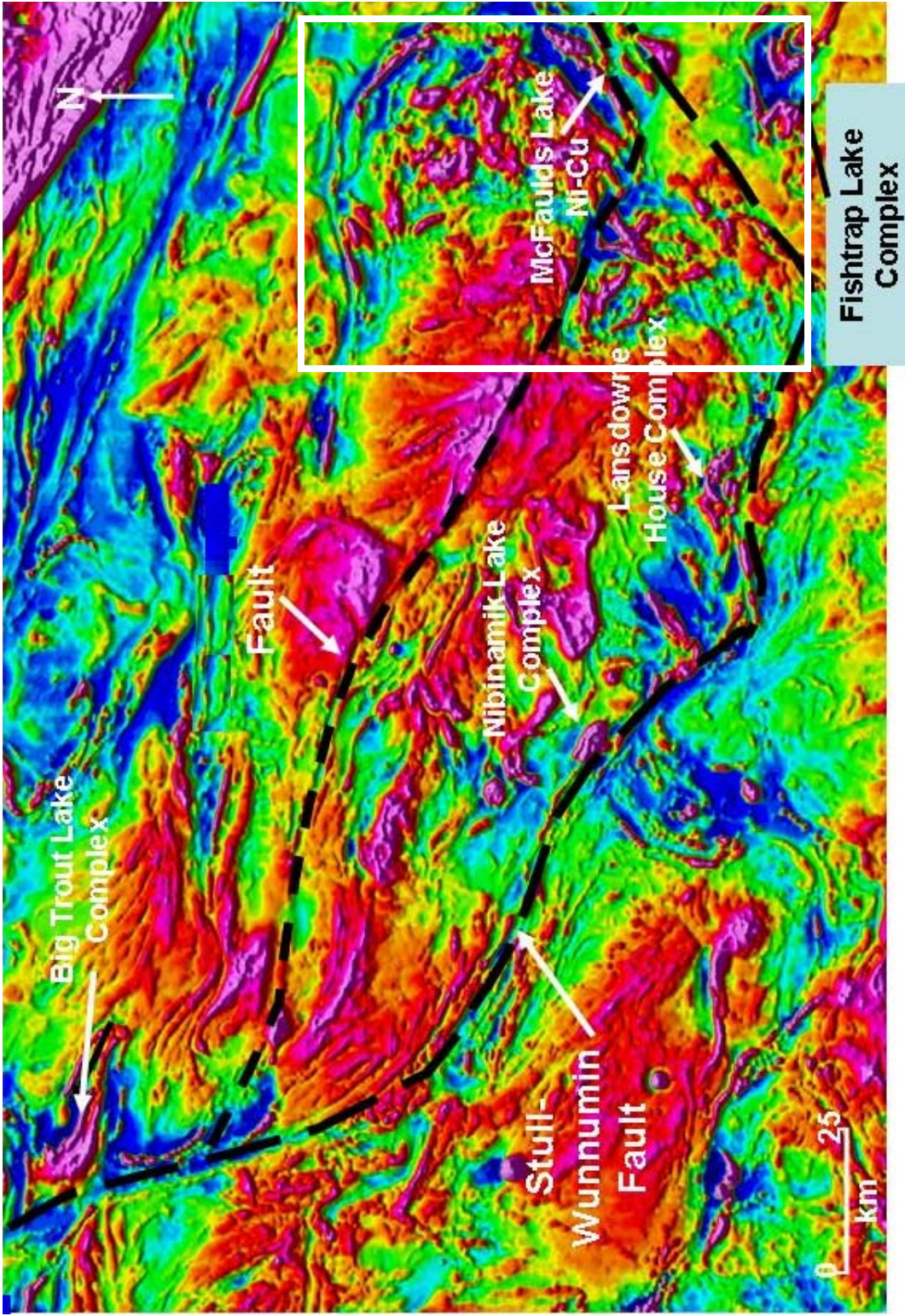


Figure 2.2. Aeromagnetic map of the Oxford-Stull Domain showing emplacement of intrusios along large WNW-ESE striking crustal faults. The Ring of Fire Intrusion is outlined in the box. From James Bay Resources Ltd. Website.

content, contains poikilitic orthopyroxene with interlayers of chromitite and magmatic sulphides occurring at the base of the pulses. The one pulse of lower peridotite has a trend of increasing olivine content with stratigraphic height due to the presence of poikilitic orthopyroxene in its lower portion. Chromitite layers increase towards the base. It is distinguished from the other pulses by greater increasing $(\text{MgO}+\text{FeO})/\text{Al}_2\text{O}_3$ with $\text{SiO}_2/\text{Al}_2\text{O}_3$ that parallels lesser increasing $(\text{MgO}+\text{FeO})/\text{Al}_2\text{O}_3$ with $\text{SiO}_2/\text{Al}_2\text{O}_3$ for the successive pulses (Borthwick, 1984).

The Oxford-Stull Domain is made up of granitoids and greenstones that form dome and keel structures where the supracrustal greenstone belts (keels) wrap around central granitoid batholiths (domes). The batholith in the Winisk Lake-Muketei River area is an unnamed quartz monzonite to trondhjemite with sinuous bodies of quartz diorite in the Muketei River Area (Thurston et al., 1979). Such quartz monzonite diapirs have been described in other parts of the world such as in the 2.8 Ga Kiviaapa Dome to the Koitelainen Intrusion and associated chromite deposits in Finland (Mutanen and Huhma, 2001 and Mutanen, 1997). Metsaranta and Houlé (2010) describe the pluton in the Muketei River Area as a foliated biotite tonalite to granodiorite with cross-cutting tonalite to quartz diorite bodies indicating multiple intrusive ages. Since there is the presence of both biotite and amphibole varieties of tonalite, TTG (tonalite-trondhjemite-granodiorite) suites in the North Caribou Terrane form from varying degrees of combined melting of garnet-amphibolite subducting slabs and hornblende-dominated fractional crystallization (Wyman et al., 2011). This batholith is the basement to the Ring of Fire Intrusion. The granodiorite has a determined age of $2773.4\pm 0.9\text{Ma}$ (Mungall et al., 2010). Observation of drill core has shown it to be younger than the intrusion (see petrography chapter). However, there are biotite xenoliths in the granodiorite that are possibly from an older basement crust. The basement Kiviaapa batholith to the Koitelainen Intrusion has been described by Mutanen (1997) to be a biotite-plagioclase mica gneiss. There may be a similar foliated basement TTG to the Ring of Fire Intrusion.

2.1.1 McFaulds Lake Greenstone Belt

Volcanism began in the McFaulds Lake Greenstone Belt with the eruption of various successions of mafic to felsic dominated volcanics defining five different packages (Fig. 2.3).

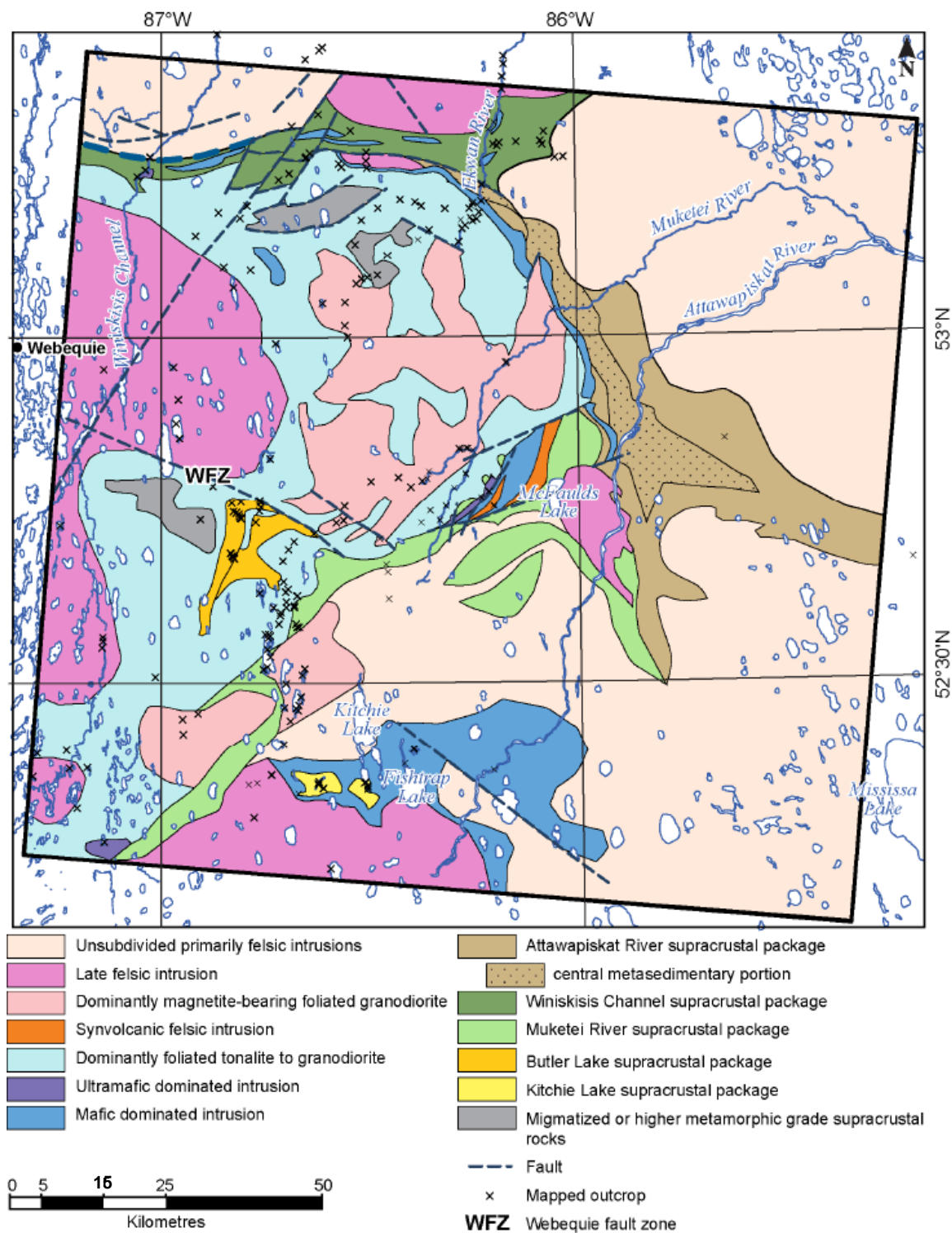


Figure 2.3. Simplified geological map of the McFaulds Lake area showing distribution of the supracrustal packages. From Metsaranta and Houlé (2012).

The Muketei River supracrustal package is both footwall and hangingwall to the synvolcanic Ring of Fire Intrusion. Locally, lower mafic volcanic and gabbros have been found in the footwall to the Blackbird and Black Horse chromitites to the east of the granodiorite contact. Volcanism began ca. 2770.7 ± 0.8 Ma with the eruption of footwall mafic volcanics (Mungall, Azar and Hamilton, 2011). Although geochemistry has not been determined, the mafic volcanics are probably ocean floor MORB volcanics similar to such MORB basalts of the Hayes River Group in the western part of the Oxford-Stull Domain. The mafic volcanics locally show pillowed facies with intercalated cherty iron formation (Metsaranta and Houlé, 2011).

The Ring of Fire Intrusion is a layered komatiitic sill that hosts the Eagle's Nest sulphide deposits and McFaulds Lake chromite deposits. The layered complex gives rise to the arcuate shaped magnetic anomaly on the airborne aeromagnetic map (Fig. 2.2). The southwest conduit to the intrusion hosts the Eagle's Nest deposits (Fig. 2.4). The Eagle's Nest magmatic sulphides accumulated in a shallowly plunging or subhorizontal keel structure at the base of a dike-like chonolith. It has been subsequently deformed into a vertically plunging shoot of sulphide mineralization occurring on the west margin of a north-south striking dike (Mungall et al., 2010). The Eagle's Nest deposits are comprised of disseminated, net textured and massive sulphides of pyrrhotite, pentlandite and chalcopyrite with subsidiary accessory amounts of magnetite. Total measured and indicated reserves are 11 Mt at 1.78 % Ni and 0.98 % Cu together with significant Pt and Pd (Baldwin, 2012). This mineralization is attributed to sulphide saturation following extensive contamination of the komatiitic magma by granodiorite country rock. The presence of abundant magnetite-rich xenoliths in the intrusion records assimilation of iron formation, which may have added sulphide to the magma to induce sulphide liquid saturation (Mungall et al., 2010). Host rocks to the deposit include harzburgite, lherzolite and marginal gabbro (Mungall et al., 2010).

The Ring of Fire Intrusion is a layered sill of dunite, peridotite, chromitite, pyroxenite, gabbro, leucogabbro, and gabbronorite (Tuchscherer et. al, 2009; Fig. 2.5). This ultramafic complex is up to 500 metres thick and has been traced for over 15 kilometres along strike (Aubut, 2012; Fig. 2.4). The Blackbird chromite deposit occurs within the main dunite sequence near the Eagle's Nest deposit. This deposit comprises a

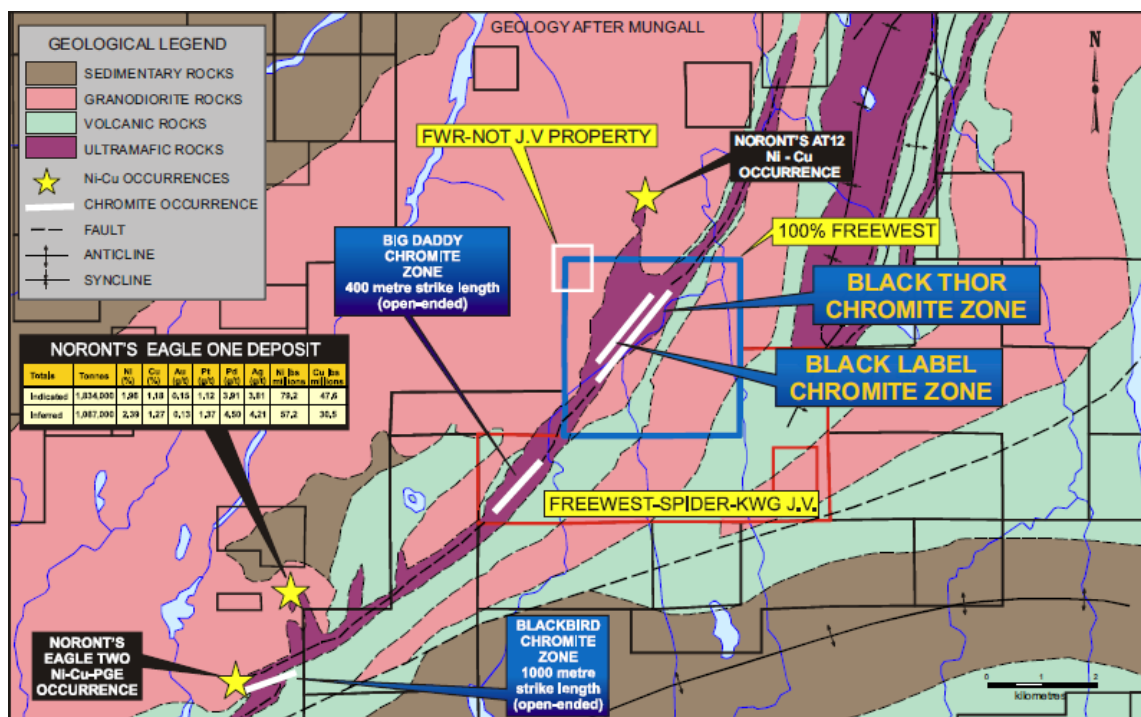


Figure 2.4. Geology map of the Ring of Fire Intrusion showing location of the Eagle’s Nest sulphide and McFaulds Lake chromite deposits. Geology after Mungall.

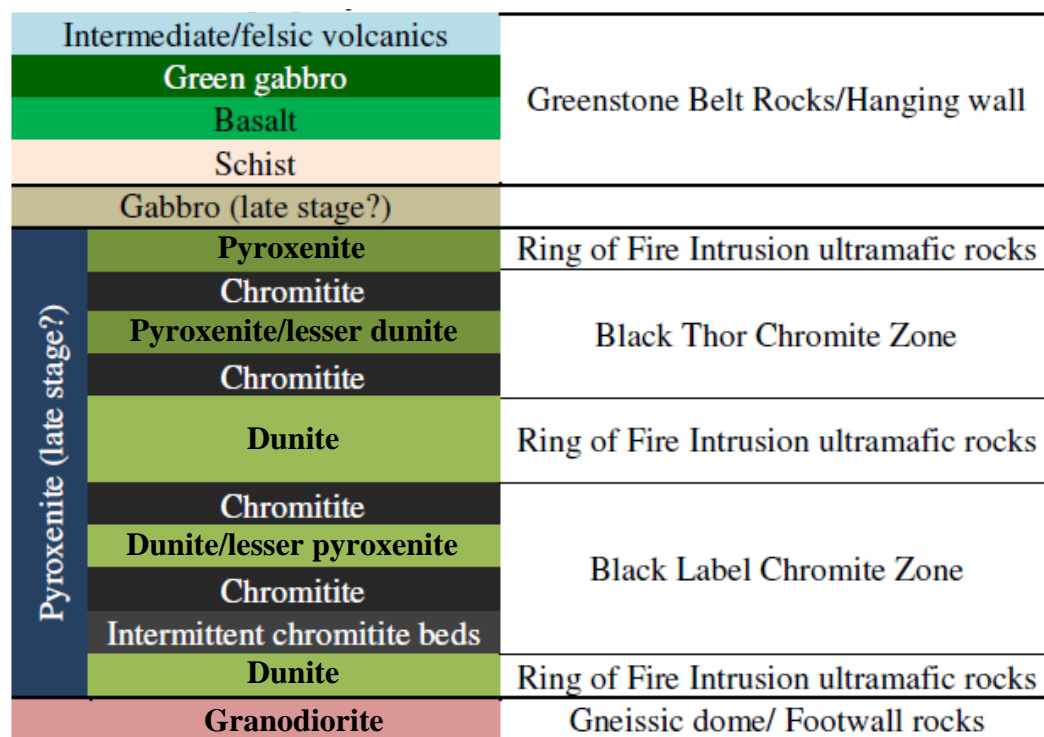


Figure 2.5. Generalized stratigraphic column of the Ring of Fire Intrusion at Black Label-Black Thor. Modified from Tuschcherer (2010).

series of steeply dipping chromitite lenses that have been overturned and young to the east (Fig. 2.6). Cr/(Cr+Al) ratios of chromite cores show little variability with an average value of 0.68 for all five zones in the Blackbird deposit (Azar and Mungall, 2010). Detailed electron microprobe analysis of chromite cores reveals Cr/(Cr +Al) atomic ratios from 0.63-0.77 and Mg/(Mg + Fe²⁺) atomic ratios from 0.12-0.62 (Azar, 2010). Generally Cr/(Cr +Al) is positively correlated with the Mg-number. The chromitites have been hypothesized to have formed as a result of assimilation of banded iron formation by a picritic ultramafic magma (Mungall, 2008).

The Black Horse and Big Daddy chromite deposits occur 5 km north of Blackbird and 3 km south of Black Thor. The Big Daddy deposit was the first chromite deposit discovered in the area and has a measured and indicated resource of 37.4 Mt at 28.5 % Cr₂O₃ (Aubut, 2012). This deposit is stratiform between lower dunite and overlying pyroxenite (Fig. 2.7). Various types of chromite mineralization have been observed including disseminated chromite (1 to 20% chromite), semi-massive chromite and massive >80% chromite. The main chromitite layer is up to 60 m thick and has been traced over 1.4 km along strike (Aubut, 2012). The chromite is present as fine euhedral grains typically 100 to 200 µm within peridotite and in the higher grade portions within dunite. Chromite may be intensely fractured, with internal veinlets and spherical inclusions of silicate gangue (SGS Minerals Services, 2009 *in* Aubut, 2012).

The Black Creek and Black Label-Black Thor mineralization occurs 3 km northeast of Big Daddy. The Black Label deposits occur below the main dunite layer that hosts the Big Daddy deposit and so was an earlier mineralizing event (Fig. 2.8). The Black Label Chromite Zone has been drilled for over 2.2 km along strike. It is cross-cut by a pyroxenitic body to the north. Chromite is generally fine grained and disseminated in peridotite, locally forming chromite-bearing magmatic breccias and semi-massive bands to massive chromitite bands. Silicate fragments, in the form of rip up clasts and as ovoid blebs indicate chromite concentration in a highly dynamic magmatic environment. Fine-grained disseminated sulphides are locally associated with the chromitite bands (Aubut, 2010).

The Black Thor deposit has been traced along strike 2.6 km. It is the most extensive chromite bearing body in the region. It has a measured and indicated resource

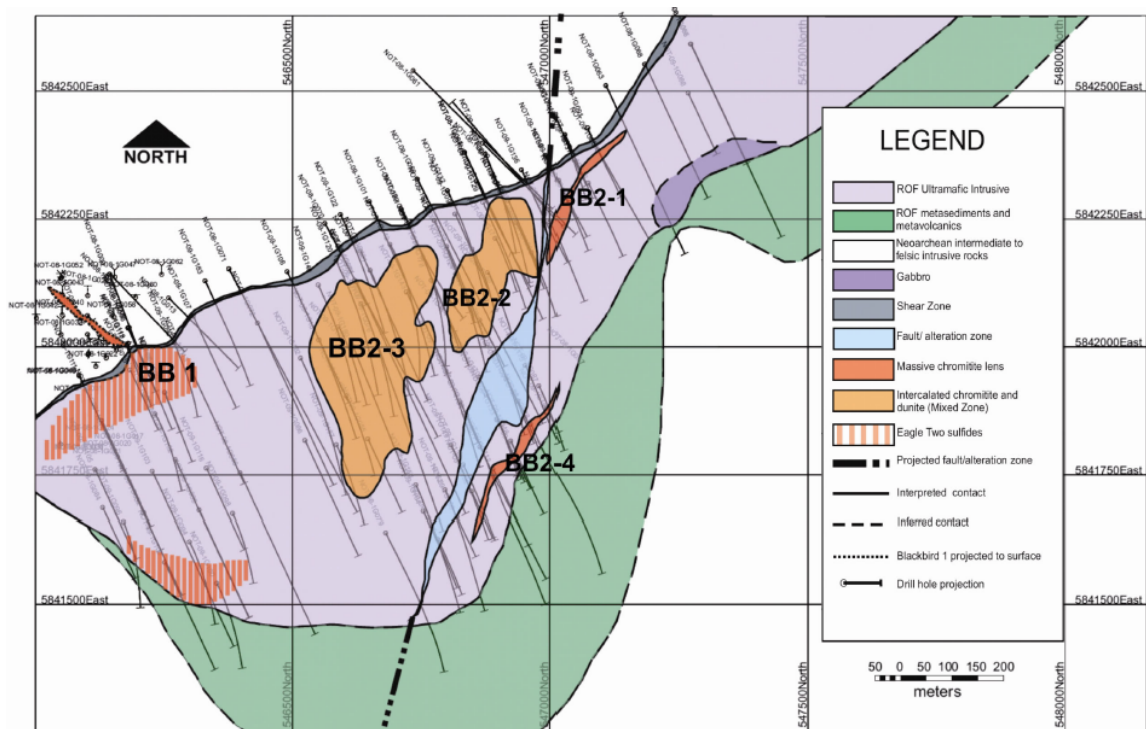


Figure 2.6. Geology of the Blackbird chromite deposit showing distribution of chromitite lenses. From Azar and Mungall (2010).

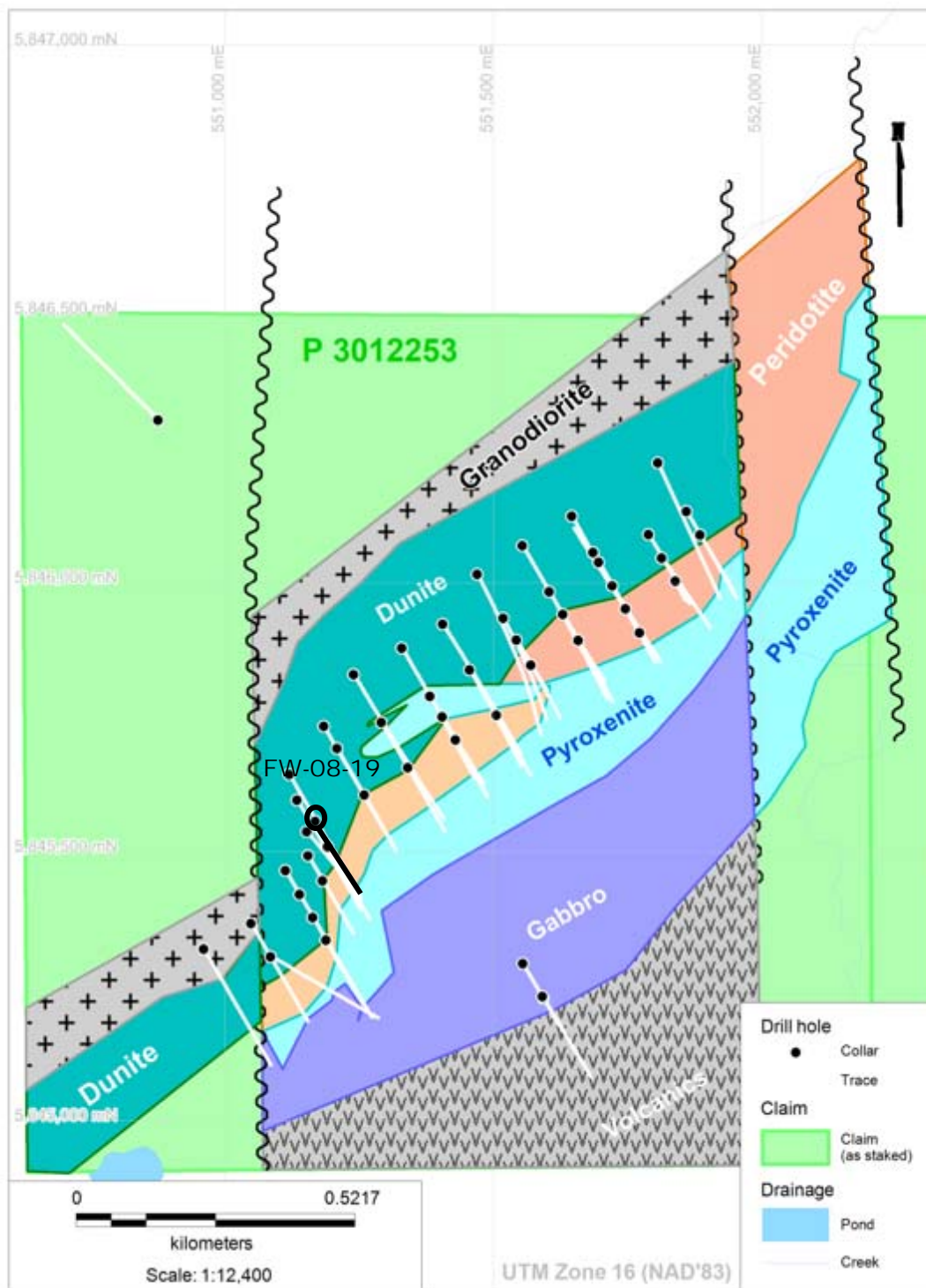


Figure 2.7. Geology of the Big Daddy chromite deposit. The chromite is between dunite and pyroxenite in orange. Diamond drill hole of study is shown. Map courtesy of KWG Resources Inc.

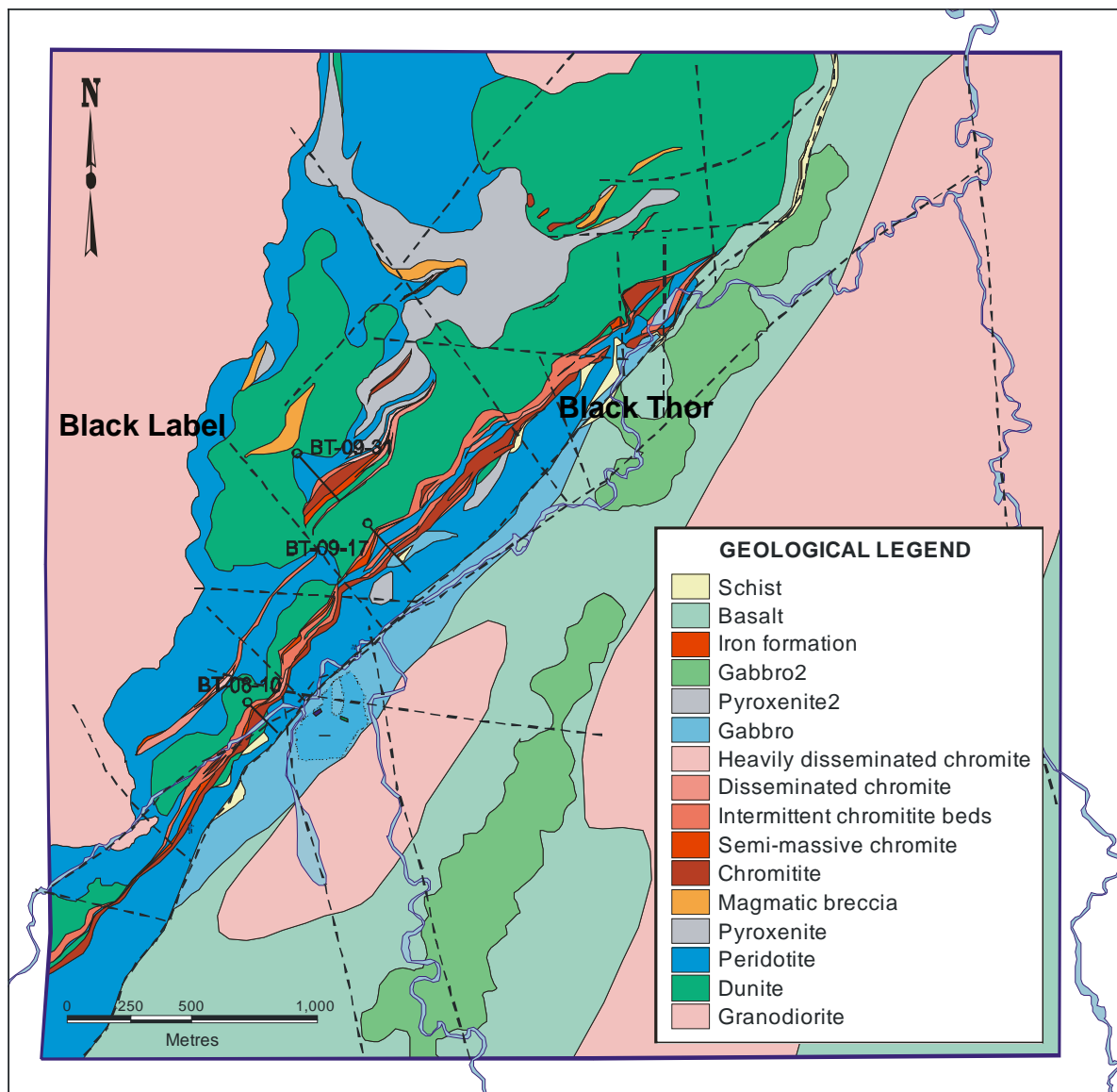


Figure 2.8. Geology of the Black Label and Black Thor chromite deposits. Diamond drill holes of study are shown. After Tuchscherer, courtesy of Freewest/Cliffs Natural Resource Inc.

of 111.9 Mt at 30.9 % Cr₂O₃ (Cliffs Natural Resources Inc., 2012 Annual Report, p. 54). It strikes SW/NE and has an overturned sub-vertical dip ranging between 70 and 85 degrees NW. The zone typically contains two chromitite layers (lower and upper) that can range in thickness from 10's of meters to over 100 m (i.e. DDH BT-09-37; Aubut, 2010). These layers are separated by a band of disseminated chromite in peridotite/dunite. Host lithologies consist of serpentinized peridotite, serpentinized dunite, dunite, and pyroxenite. The chromite is present as fine to heavily disseminated chromite in dunite/peridotite, intermittent chromite beds and semi-massive to massive chromitite. Because of its lateral continuity and uniformity the Black Thor chromite mineralization was likely deposited in a quiescent magmatic environment (Aubut, 2010). The leucogabbro at the top of the Big Daddy-Black Thor stratigraphy grades into the mafic volcanics of the Muketei River package. Hydration of the Ring of Fire Intrusion caused retrogression of the olivine and pyroxene to greenschist facies serpentine, talc, tremolite, chlorite, kaemmererite with trace to minor associated magnetite, sausserite, zoisite and titanite.

Overlying intermediate volcanics have been age dated at 2737±7 Ma (Rayner and Stott, 2005). The volcanics are composed of fine-grained tuff, rare coarse-tuff breccias and more flow-like lithologies (Metsaranta and Houlé, 2011). These volcanics are host to the McFaulds Lake VMS deposits. Intrusion of the mafic-dominated Thunderbird intrusion to the east of the Ring of Fire Intrusion was coeval with intermediate to felsic volcanism. This intrusion is one of a series of mafic intrusions in the area that are composed of gabbro-anorthosite-ferrogabbro±pyroxenite (Metsaranta and Houlé, 2011). An age of 2734.5±1.0 Ma has been determined for the ferrogabbro (Mungall et al., 2010). Significant V-Ti-Fe mineralization has been discovered In the Thunderbird intrusion.

2.2 Deformation

The Muketei River supracrustal package overlying the Ring of Fire Intrusion is overturned by the doming of the basement granodiorite batholith. An age of 2696±3 Ma has been determined from granodiorite within the core of the batholith (Rayner and Stott, 2005). The central granodiorite represents the age of “Kenoran” diapiric plutonism. Quartz monzonite diapirism is inferred to occur proximal to other intrusions such as the Koitelainen Intrusion and associated chromite deposits in Finland (Fig. 2.9). The Ring of

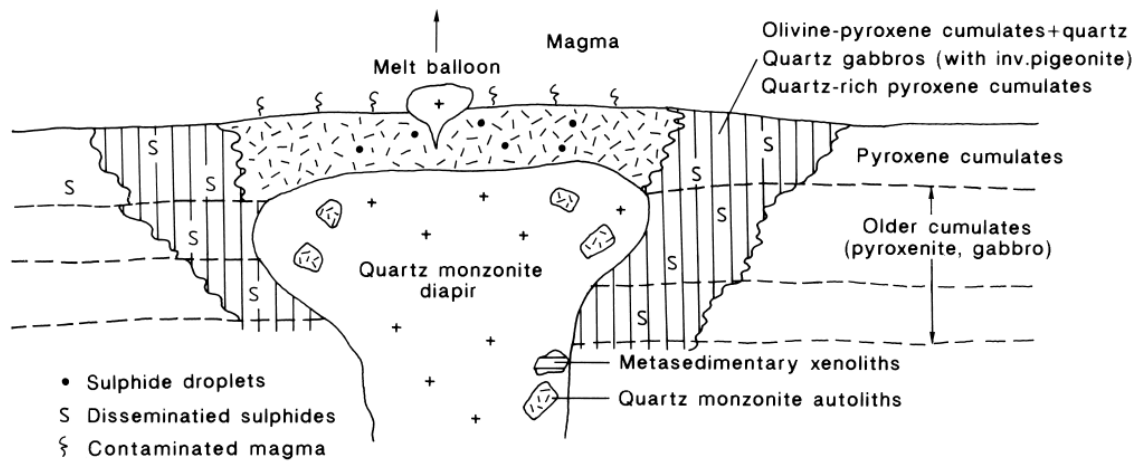


Figure 2.9. Quartz monzonite diapirism occurred in the vicinity of the Koitelainen Intrusion and associated chromite deposits in Finland. This is a similar scenario to the granodiorite diapirism in the vicinity of the Ring of Fire Intrusion. From Mutanen (1997).

Fire Intrusion hosting the chromitite dips steeply to the east as at Big Daddy or is overturned steeply to the west as at Black Label and Black Thor (Figs. 2.10 and 2.11). There is dextral strike-slip displacement of stratigraphic units in the intrusion (Fig. 2.12). The highest chromite layer in the eastern part of the Black Thor stratigraphy intersected in DDH BT-09-37 is a major zone of questionable provenance. This chromitite unit does not have a western extension and is bounded by mylonite. Late faults transecting the deposits give rise to incoherent fault gouges, fault breccias, coherent cataclastic breccias and ductile phyllonitic and mylonitic shear zones (Poulsen, 2010). Foliation fabrics are developed in serpentized units. Late aphanitic green and grey to brown micaceous to amphibole and feldspar-bearing lamprophyric dikes commonly intrude along these areas of structural weakness.

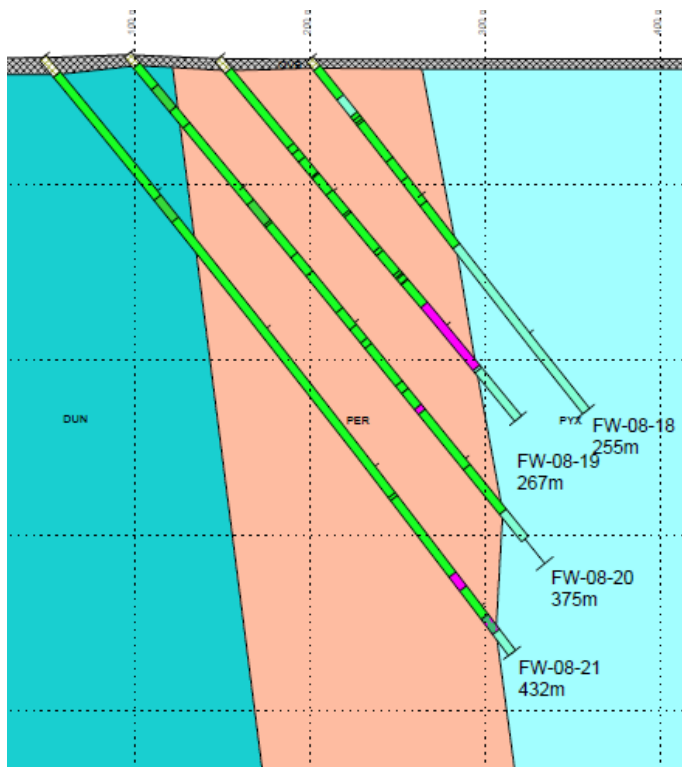


Figure 2.10. Drill section through Big Daddy DDH FW-08-19 showing the intrusion is plunging to the east, looking northeast.

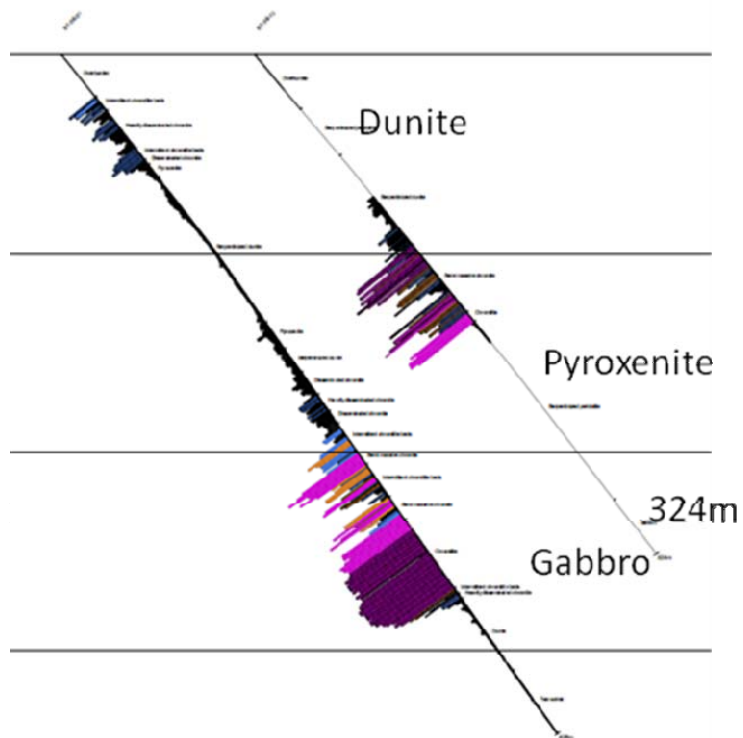


Figure 2.11. Drill section through Black Thor DDH BT-08-10 showing the intrusion is plunging to the west, looking northeast.

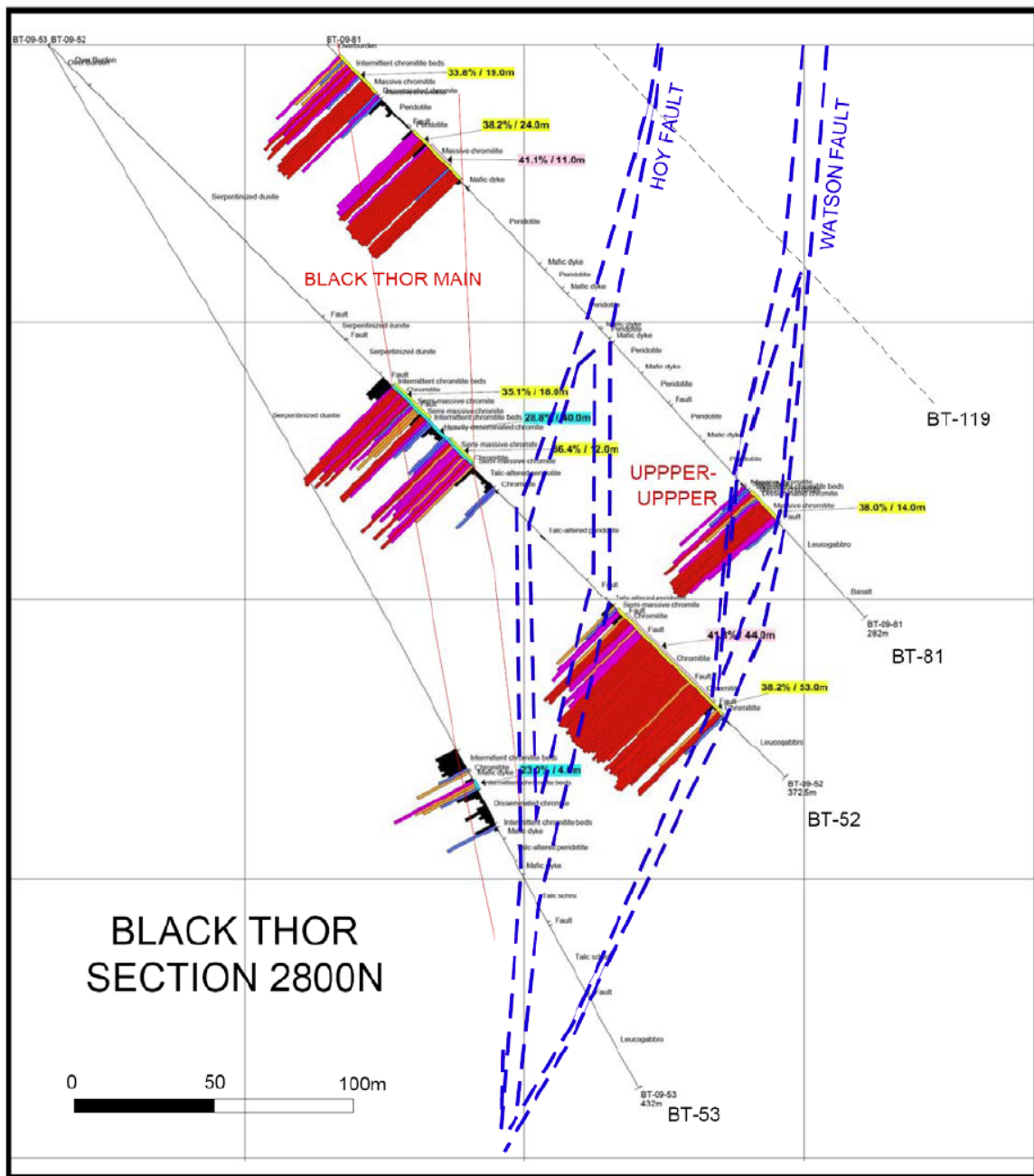


Figure 2.12. Dextral strike-slip faults offset some of the Black Thor chromitites such as the Upper-Upper zone chromitite in the northeast part of the Black Thor sequence. From Poulsen (2010).

CHAPTER 3

PETROGRAPHY

3.1 Introduction

This petrographic study of the McFaulds Lake chromite deposits entails both host lithologies to the chromite as well as the different styles of chromite mineralization. In order to define the host rock igneous stratigraphy, 13 drill holes were logged and photographs taken of key textures. Logging commenced in September 2009 and at this time 3 strategic holes were selected, one from each of the 3 deposits Black Label, Black Thor and Big Daddy. Detailed sampling resulted in selecting 600 samples of representative drill core. These are Black Label DDH BT-09-31, Black Thor BT-08-10 and BT-09-17 and Big Daddy FW-08-19 (Figs. 3.1 to 3.4; see figures 2.7 and 2.8 for drill plan, Appendix 1 for core logs and Appendix 2 for sample #s). Thirteen additional drill holes were logged over the summer of 2010 at McFaulds Lake, these were sited on the same section line as the initial strategic holes chosen for study. All three strategic holes were re-examined at this time to better detail the textures of the lithologies hosting the chromitite intervals. DDH BT-09-17 was re-examined in the summer of 2011 to characterize the uppermost chromitite hosted in leucogabbro. From June 2011 to March 2012, 53 drill holes were logged in conjunction with infill drill programs performed by Cliffs Natural Resources Inc. on the Black Label, Black Thor and Big Daddy chromite deposits. Further textures of lithologies and mineralization were documented and photographed to supplement the petrographic analysis. The petrographic investigation of the lithologies was carried out in April/May 2011 and in the summer-fall of 2012. Finally, textures of granodiorite and lamprophyres were investigated on a drill program for the Black Horse chromitite for KWG/Bold Ventures Inc. in the spring of 2013. Lithologies and chromitites in order of stratigraphy are as follows:

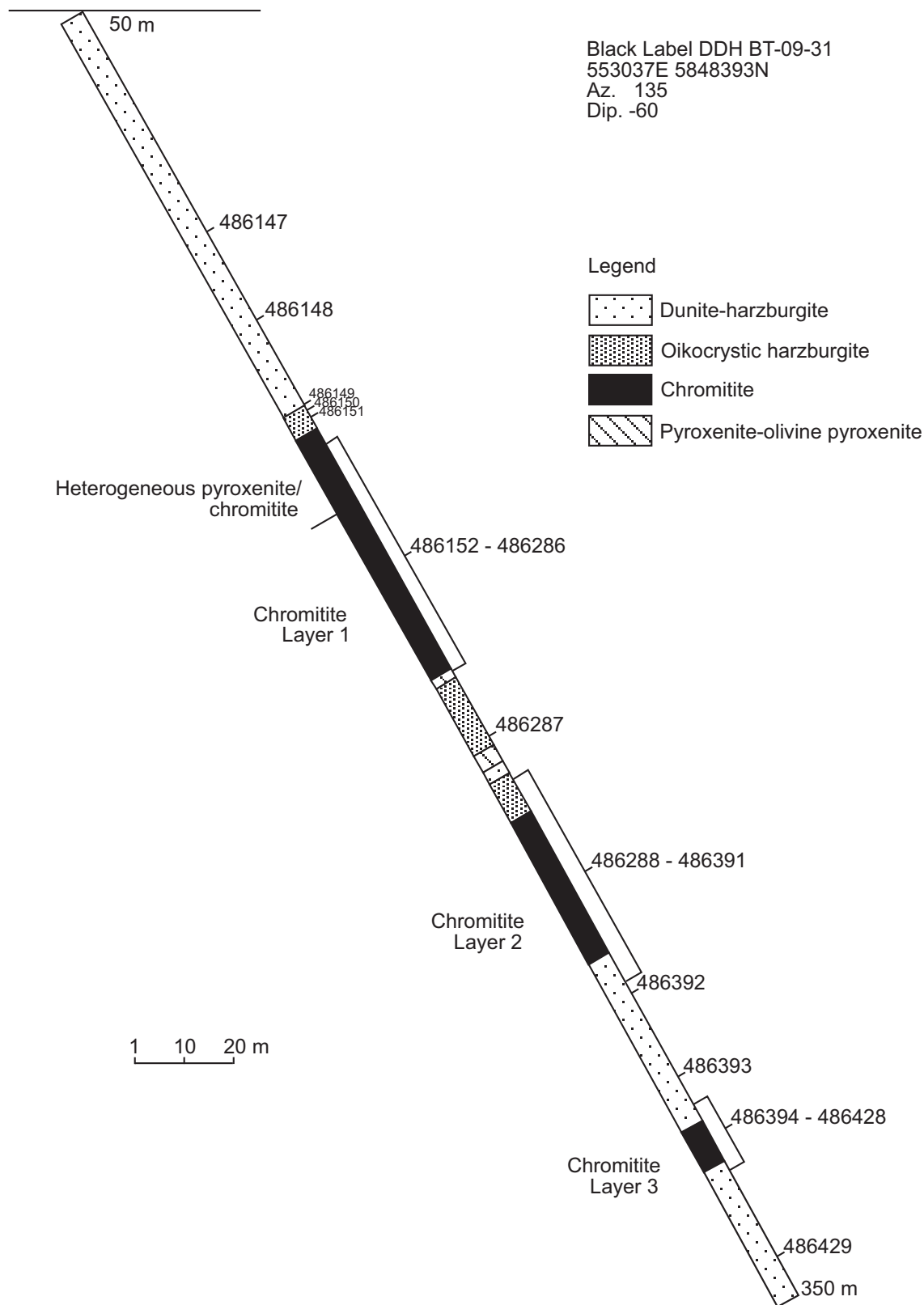


Figure 3.1: Drill section of Black Label DDH BT-09-31 from 50 to 350 m. Sample locations are numbered down the hole and mineralized zones are identified.

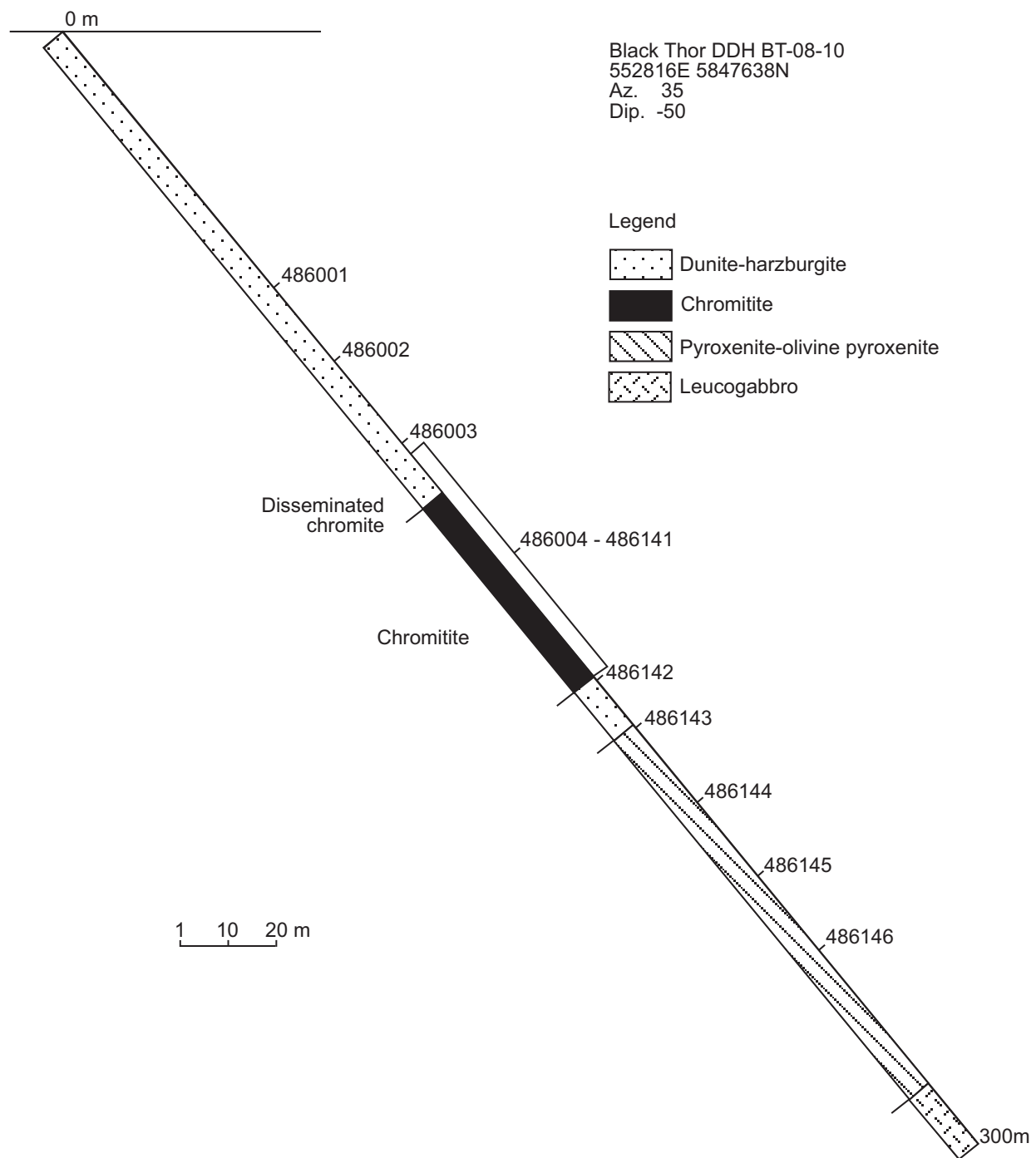


Figure 3.2: Drill section of Black Thor DDH BT-08-10 from 0 to 300 m. Sample locations are numbered down the hole and mineralized zones are identified.

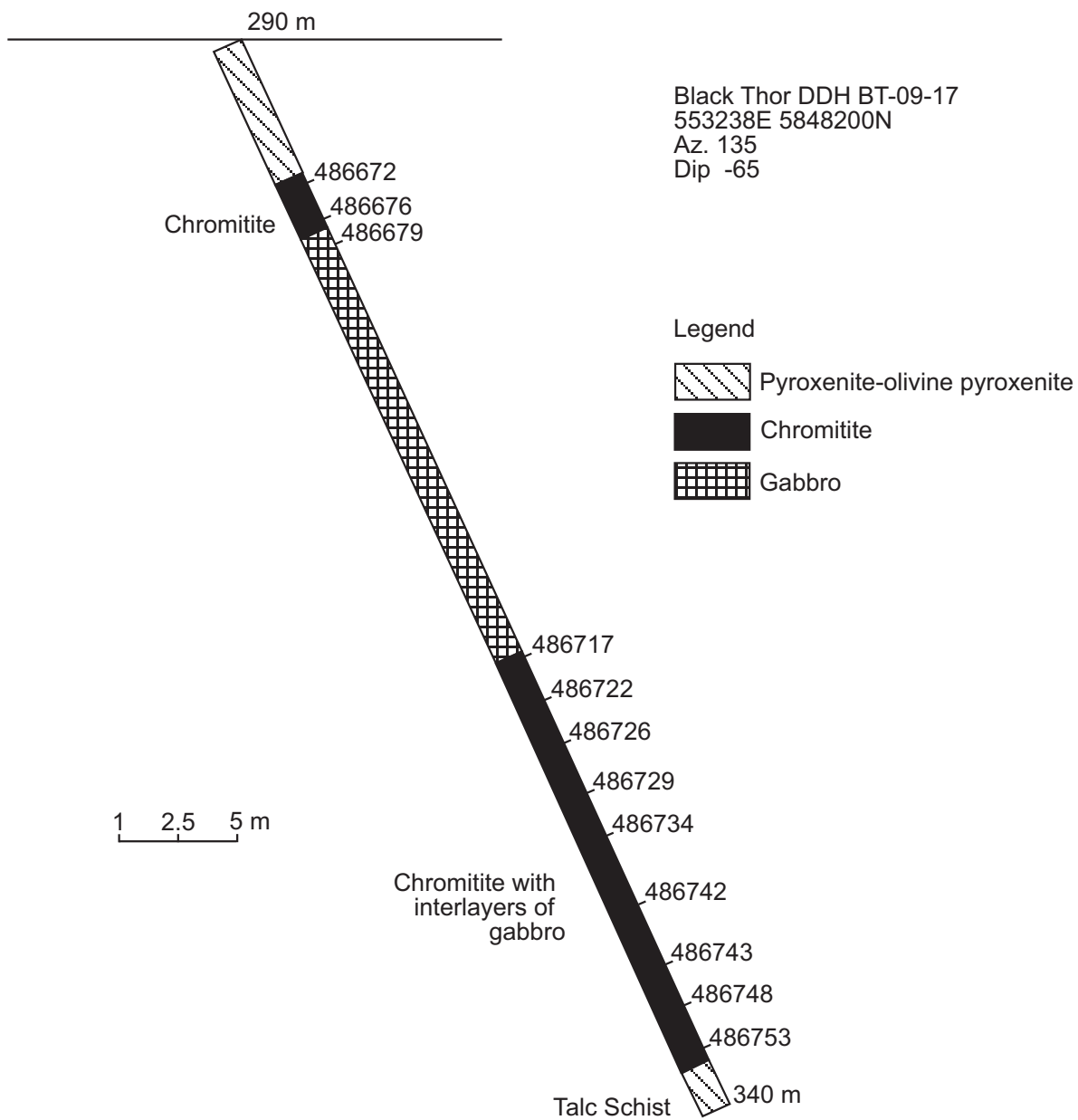


Figure 3.3: Drill section of Black Thor DDH BT-09-17 from 290 to 340 m. Sample locations are numbered down the hole and mineralized zones are identified.

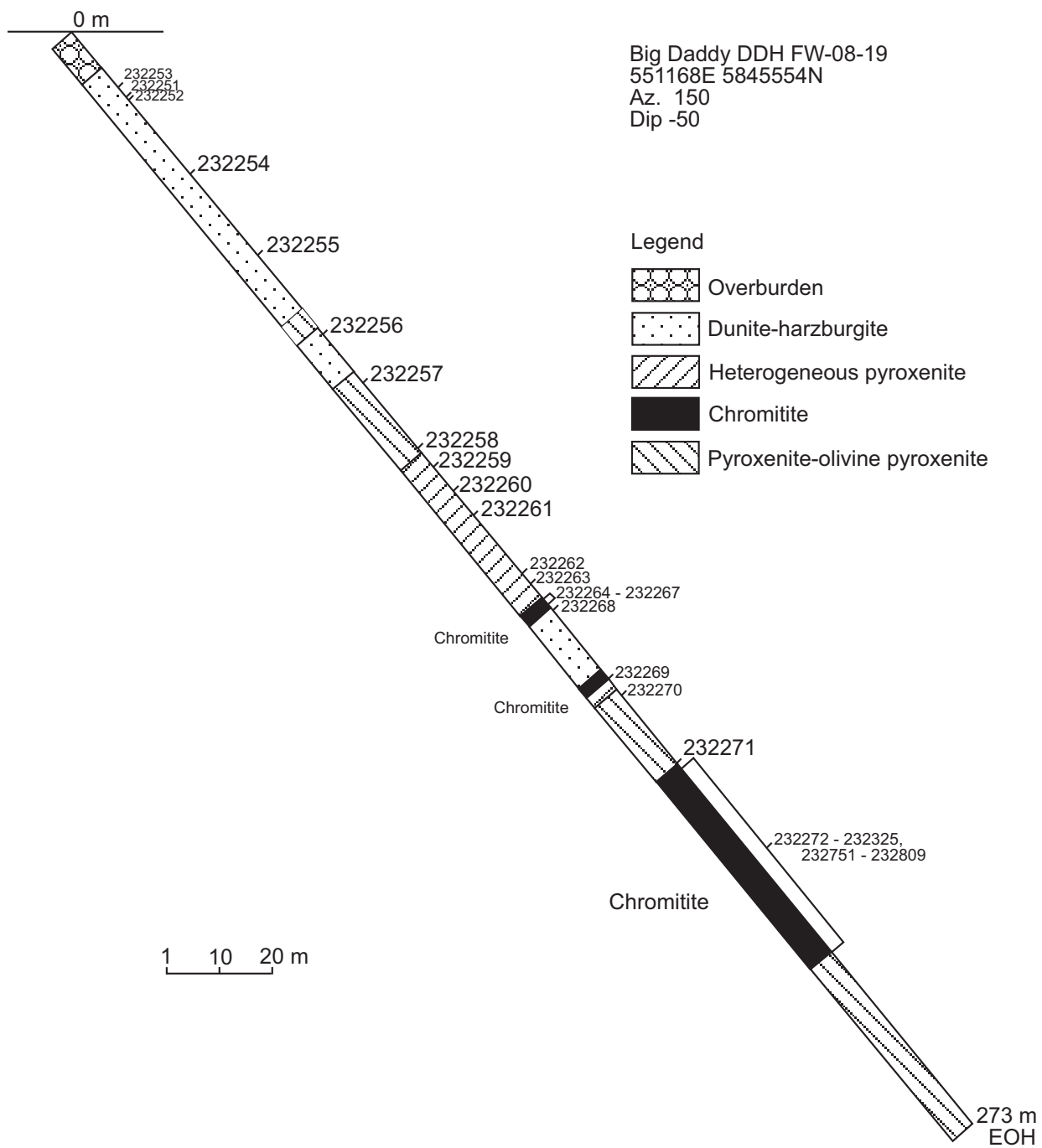


Figure 3.4: Drill section of Big Daddy DDH FW-08-19. Sample locations are numbered down the hole and mineralized zones are identified.

Hangingwall mafic metavolcanic
Gabbro-leucogabbro
Pyroxenite-olivine pyroxenite
Heterogeneous pyroxenite
Magmatic breccias
Massive chromite
Semi-massive chromite
Intermittent chromitite beds
Heavily disseminated chromite
Chromitite
Disseminated chromite
Oikocrystic harzburgite
Dunite-harzburgite
Footwall granodiorite

The characteristics of the lithologies from various drill holes that represent the three deposits are described below. The thin section descriptions from the 4 drill holes are supported by microprobe analyses. A list of all the drill holes with collar information are in Table 3.1.

3.2 Footwall granodiorite

Granodiorite forms the footwall rock to the west of the Ring of Fire Intrusion. The lithology is a massively textured, coarse-grained, quartz-rich hornblende granodiorite. There is up to 30 modal % coarse 1 cm hornblende or finer biotite, about 20 modal % quartz and 40-50 modal % feldspar with equal proportions of plagioclase and orthoclase (Fig. 3.5). The feldspars form tabular crystals up to 1 cm in size. Pink granodiorite commonly grades into more salt and pepper quartz diorite. This phase comprises 20 % quartz, 40 % feldspar and 30 % biotite or hornblende. Rounded quartz to tabular feldspar phenocrysts are up to 0.7 cm, sheafy interstitial hornblende is up to 1 cm sized crystals.

As observed in DDH BT-09-62, the dunite at the contact with granodiorite is highly silicified suggesting assimilation of silica at the contact with the intrusion. Close examination of the granodiorite contact with the ultramafic intrusion demonstrates the granodiorite is likely younger than the intrusion and not older basement gneiss. At the Black Horse chromitite (DDH FNCB-13-031 at 412.50 m), 0.4 cm acicular actinolite

Table 3.1: Summary of drill holes

Drill Hole	Easting	Northing	Depth (m)	Azimuth	Dip
Black Label					
BT-08-08	553721	5849242	423	135	-50
BT-09-26	553249	5848749	444	135	-50.47
BT-09-29	553272	5849136	384	135	-45.92
BT-09-31	553037	5848393	387	135	-60.78
BT-09-62	553164	5849663	193	270	-45
BT-11-176	554050	5849065	291	315	-45
BT-11-179	554262	5849138	365	315	-45
Black Thor					
BT-08-10	552816	5847638	324	135	-50
BT-09-17	553238	5848200	381	135	-65
BT-09-23	553491	5848508	399	140	-60.56
BT-09-37	553969	5849010	555	135	-59.11
BT-10-128	553200	5848093	159	135	-45
BT-10-133	553555	5848238	216	315	-45
BT-11-185	552356	5846691	252	315	-45
BT-11-194	552556	5846634	381	315	-45
BT-11-197	553426	5848566	645	130	-60
BT-11-200	553929	5849044	684	130	-65
Big Daddy					
FW-08-19	551168	5845554	273	150	-50
FW-09-34	551237	5845833	?	150	-50
FW-11-61	551698	5845733	309	16	-51
FW-11-83	551169	5845054	390	330	-68
FW-11-87	551236	5845146	458.7	330	-68
FW-12-93	551954	5845891	390	6.7	-46
FW-12-94	551954	5845891	426	6.7	-60
FW-12-97	551954	5845891	231	330.06	-45
FW-12-106	551731	5845676	486	360	-68
FW-12-108	551903	5845979	117	329.5	-45
FW-12-112	551731	5845676	510	296.17	-64
Blackbird					
NOT-08-1628					
Black Horse					
FNCB-13-030	547756	5843277	774	180	-70
FNCB-13-031	547451	5843171	978	180	-70
FNCB-13-032	547756	5843277	861	152	-73
FNCB-13-033	547451	5843171	861	160	-64



Figure 3.5. Granodiorite is basement to the Ring of Fire Intrusion. Sample is from 148.33 m in DDH BT-09-62.



Figure 3.6. Dunite is composed of light green fine grained round cumulus serpentinized olivine with interstitial chromite. Sample is from 33.48 m in DDH BT-08-08.

occurs as randomly oriented crystals in pyroxenite in contact with granodiorite. Actinolite growth in the bordering pyroxenite suggest thermal metamorphism due to heat from intruding granodiorite. Coarse rounded blue quartz crystals occur near the granodiorite contact. These quartz crystals are similar to silicified ultramafic occurring at the contact in DDH BT-09-62 at Black Label. The blue quartz may be a silica overprint from the granodiorite intrusion, rather than an assimilation texture.

Notably, the western granodiorite typically exhibits a fresh, undeformed equigranular texture in contrast to gneissic basement. Also, several small granodiorite dikes have been observed cross-cutting the dunite in DDH FNCB-13-033. As seen in DDH FNCB-13-031, FNCB-13-030 and FNCB-13-032, there is a blue quartz zone in a shear zone bordered by biotite and then chlorite alteration into pyroxenite. This is analogous to the occurrence of younger granodiorite along a major fault zone such as the late post-tectonic stocks to the Destor Porcupine Fault Zone in the Abitibi Greenstone Belt (Kishida, 1984). Biotite alteration of pyroxenite suggests potassic metasomatic fluids from the granodiorite. Also, biotite xenoliths observed in the granodiorite (eg. at 514.33m in DDH FNCB-13-031) are possible assimilated basement TTG inclusions by the granodiorite. Such xenoliths are probably similar to those observed in the quartz monzonite diapir to the Koitelainen Intrusion in Finland (Fig. 2.9). For geochemistry, on the $\text{CaO}/(\text{Na}_2\text{O}+\text{K}_2\text{O})$ vs. SiO_2 plot from Feng and Kerrich (1992), a single granodiorite sample from Azar (2010) plots in the field of the syntectonic tonalite-granodiorite-granite-quartz monzodiorite series (TGGM) of the Round Lake Batholith to the Larder Lake Group in the Abitibi Greenstone Belt. These are in contrast to the older synvolcanic TTG which have higher $\text{CaO}/(\text{Na}_2\text{O}+\text{K}_2\text{O})$ and SiO_2 contents.

3.3 Dunite-harzburgite

At Black Thor and Black Label, dunite is composed of totally serpentinized olivine. Serpentinization of the dunite results in: 1) a light green colour of a highly weathered unit; 2) a variation of aqua green to dark green colour with foliated dark blue/black iowaite vein alteration; 3) a uniform dark/black; 4) or a uniform apple green colour (Leshner and Houle, 2011) – see figs. 3.6, 3.7). Ultra fine magnetite is ubiquitous in the serpentine (Fig. 3.8). Notably, the primary meso to adcumulate textures are well preserved. Fine to medium grained round cumulus olivines form massive cumulates

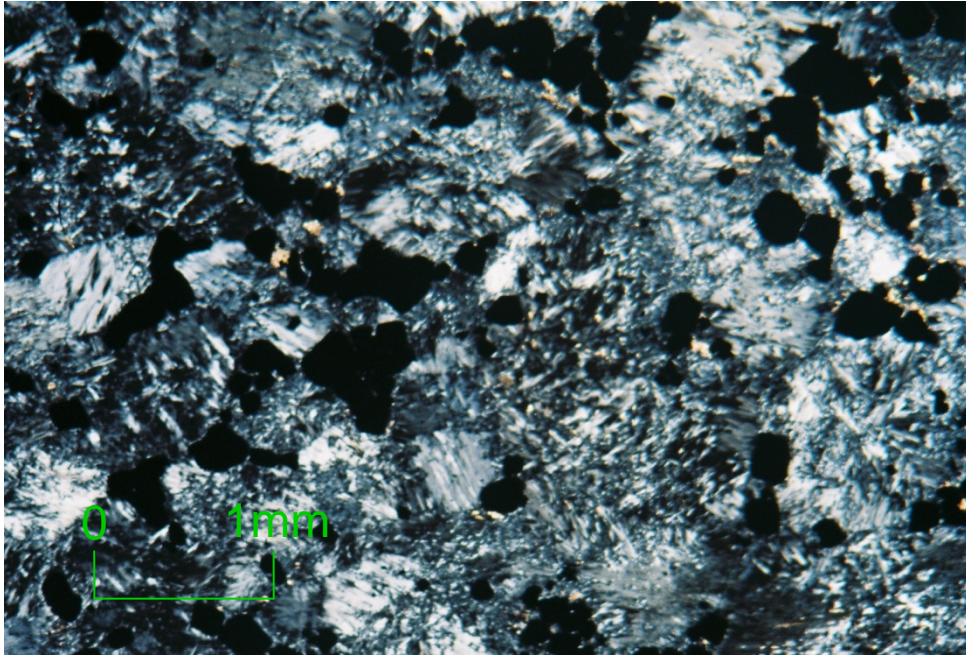


Figure 3.7. Thin section showing serpentinized olivine in dunite with very fine grained disseminated chromite. Sample 486008 is from 117 m in DDH BT-08-10.

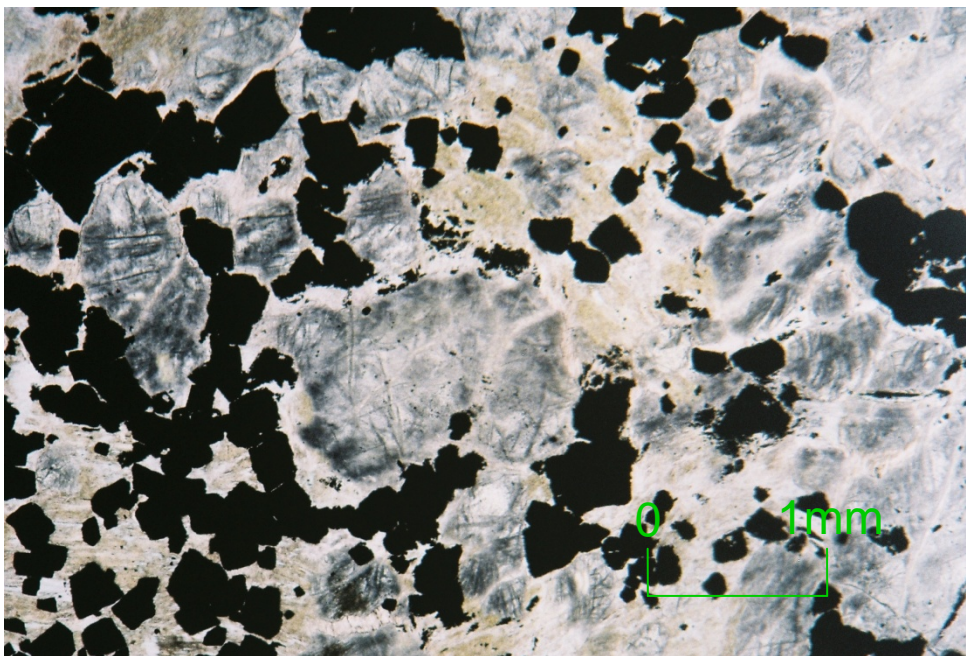


Figure 3.8. The serpentine is frosted with ultrafine magnetite. Note the chain-like network of chromite interstitial to cumulus olivine. Sample 486165 is from 155.8 m in DDH BT-09-31.

cross-cut by serpentine-carbonate veins and scattered magnetite veinlets. Often there is very fine cumulus chromite interstitial to olivine forming “olivine-chromite heteradcumulate.” Interstitial magnetite occurs as a result of replacement of primary cumulus chromite in heteradcumulate and may signify chromite replacement to magnetite during serpentinization.

With increasing orthopyroxene, the dunite becomes harzburgite. The harzburgite is similarly serpentinized, characteristically dark grey to green in colour. Intercumulus anhedral pyroxene envelopes the olivine, most commonly occurring as an olivine-rich meso to orthocumulate. Compositionally the harzburgite zones from near total olivine to an 85:15 olivine to pyroxene ratio. Often there is increasing metasomatic pyroxene after the primary pyroxene which gives patchy replacement of olivine. This is evident by textures of medium to coarse patchy encroachment of pyroxene on protolith textures of fine, often white talc-altered, round cumulus olivines in holes BT-11-197 and FW-11-87 (Figs. 3.9, 3.10 and 3.11). This leads to the talc/tremolite replacement on the rinds of olivine observed in sample 486234 at 183.4 m in DDH BT-09-31. Notably, metasomatic pyroxene was probed and results are presented by the mineral chemistry of pyroxene in the geochemistry chapter.

3.4 Oikocrystic harzburgite

Oikocrystic harzburgite occurs above the main dunite sequence and below the chromitites of the Black Label deposit and occasionally within the Black Thor sequence. Serpentinized, fine cumulus olivine is surrounded by coarse, up to 1.5 cm diameter, pyroxene oikocrysts that account for 35 modal % of the rock (Fig. 3.12). Oikocrystic harzburgite often occurs in dunite-peridotite sequences above previous pyroxenite, such as in DDH FW-09-34. The occurrence of common intercumulus minerals suggests the presence of larger amounts of pore liquid material surrounding the cumulus olivine. Jackson (1961), in his observation of the Stillwater Intrusion in Wager and Brown (1967), noted that in areas where the amount of pore material was greatest, there was a higher rate of crystal accumulation in the basin. Therefore, the intercumulus textures must have formed in a more dynamic system which suggests the Black Label harzburgites and chromitites formed under faster rates of crystallization. Like dunite, the oikocrystic harzburgite occasionally contains interstitial very fine cumulus chromite.



Figure 3.9. Coarse grained massive grey pyroxene at right replaces medium grained olivine. Sample is from 306.38 m in DDH BT-11-197. Diameter of core is 46.7 mm.

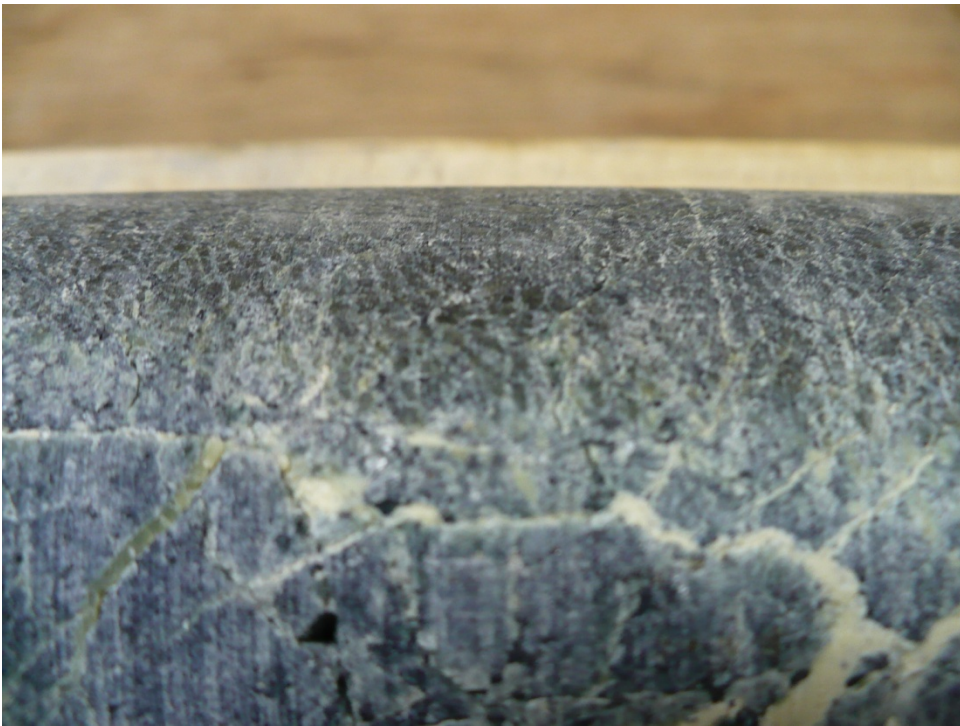


Figure 3.10. Closeup of coarse grey pyroxene (out of focus) replacing cumulus dark green olivine (in focus) as in Figure 3.1. Sample is from 306.38 m in DDH BT-11-197. Diameter of core is 46.7 mm.



Figure 3.11. Patchy grey coarse grained pyroxene at right replaces pale grey-white talc-altered cumulus olivine. There is very fine interstitial chromite. Sample is from 381.57 m in DDH FW-11-87. Diameter of core is 46.7 mm.



Figure 3.12. Harzburgite containing 35 modal % 1 cm oval to rounded tremolitized oikocrysts of pyroxene in serpentinized fine grained dark cumulus olivine groundmass. Sample is from 143.6 m in DDH BT-09-31.

In thin section, the serpentinized olivine is enveloped by talcose and tremolitized, replaced pyroxene. Incipient to pervasive replacement by highly birefringent tremolite occurs along the cleavage planes of the pyroxenes (Fig. 3.13). Electron microprobe analysis of the tremolite shows Cr-bearing tremolite and non Cr-bearing tremolite. The rarer Cr-bearing tremolites indicate chromite replacement to magnetite during hydration supplied Cr content to the enveloping orthopyroxene. The few primary olivines, pleochroic brown orthopyroxenes and igneous amphiboles microprobed have grains yielding Fo #s of 83-90 for cumulus olivine and Mg #s of 0.87-0.99 for cumulus orthopyroxene (Fig. 3.14).

3.5 Disseminated chromite

In the chromite mineralized dunite, fine grained cumulus olivine is bordered by very fine, interstitial, cumulus chromite (Fig. 3.15). There is typically 5 to 10 modal % disseminated chromite that occurs as interstitial chromite and thin bands. Up to 15 modal % light grey intercumulus pyroxene accompanies the olivine. The interstitial chromite often concentrates to form mm-scale layers. In thin section, minute equant intercumulus chromites rim larger serpentinized cumulus olivine, thereby showing that it is second to crystallize after olivine (Fig. 3.16). Intercumulus chromite is often associated with and altered to brown platy chlorite grains after orthopyroxene (Fig. 3.17). Only rarely is chromite included in olivine. The interstitial chromite is included within intercumulus pyroxene indicating chromite crystallization before pyroxene (Fig. 3.18). The concentric growth of fine cumulus chromite around olivine clearly demonstrates crystallization next after olivine prior the pyroxene. Pyroxene crystallized as oikocrysts around the chromite that rims the olivine. The order of crystallization for both dunite and oikocrystic harzburgite is: cumulus olivine → cumulus chromite → intercumulus orthopyroxene.

Some of the intercumulus orthopyroxene has been hydrated to chlorite. This chlorite has been confirmed by electron microprobe to be either chromian chlorite or kaemmererite (for Cr₂O₃ of over 7 wt. %; Fig. 3.19). Orthopyroxene has also been hydrated to talc as many of the olivines are surrounded by talc rims and then chromite (Fig. 3.20). The talc was originally primary intercumulus pyroxene.

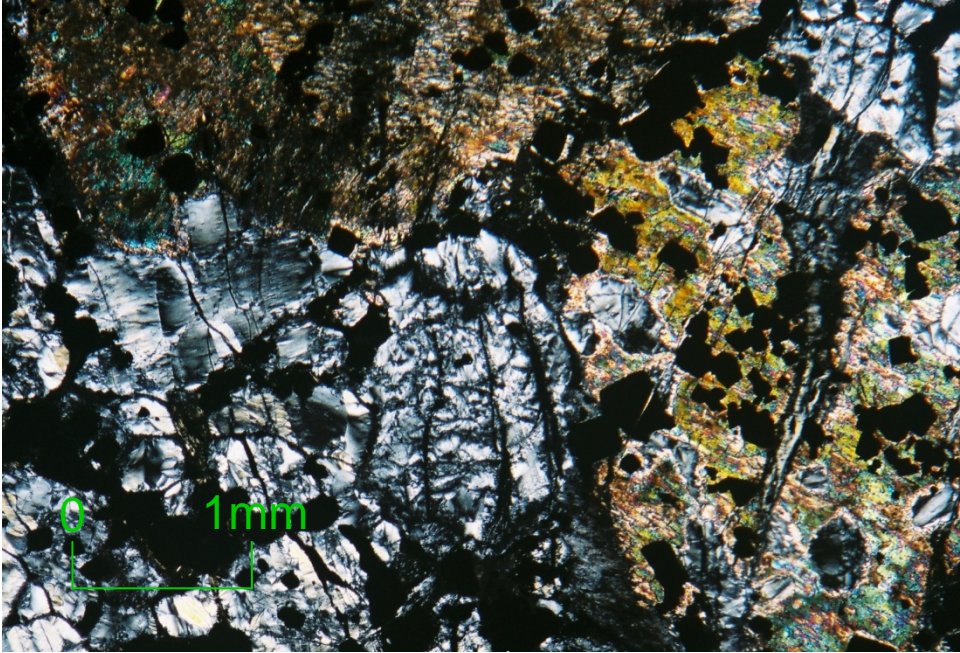


Figure 3.13. Incipient to pervasive replacement by highly birefringent tremolite along the cleavage planes of the pyroxene. Note low order serpentinized olivine in contrast to higher order tremolitic pyroxene. Sample 486153 is from 151.8 m in DDH BT-09-31.

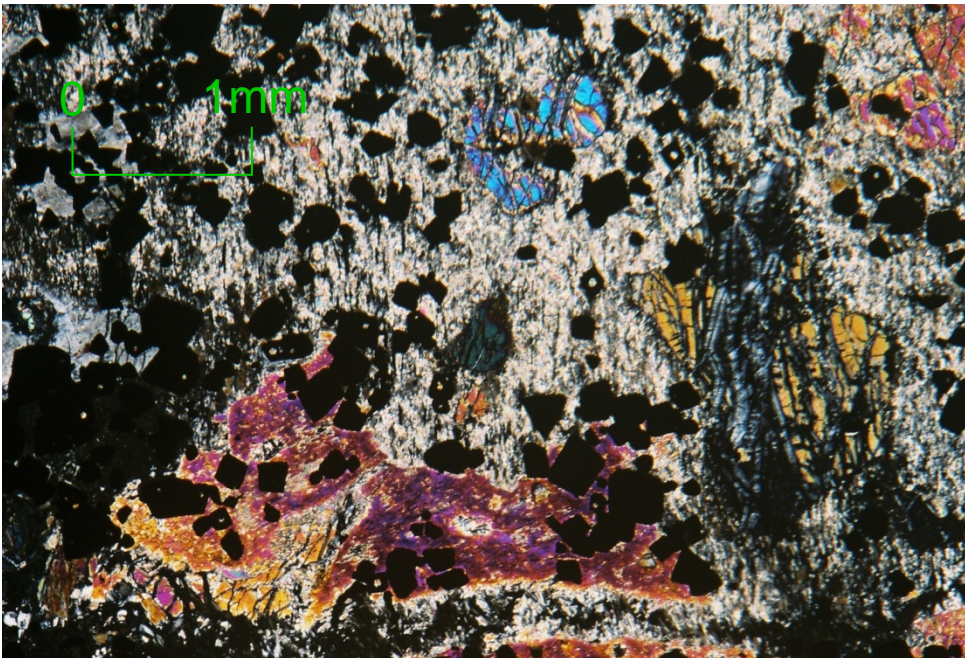


Figure 3.14. Relict micro-fractured olivine occurring with larger tabular, highly birefringent igneous amphibole in a talcose groundmass. Also shown are very finely disseminated euhedral chromite. Sample 486163 is from 155 m in DDH BT-09-31.



Figure 3.15. Up to 20 modal % very fine interstitial chromite hosted in light green fine grained serpentinized olivine, forming olivine-chromite heteradcumulate. Sample is from 59 m in DDH BT-08-10.

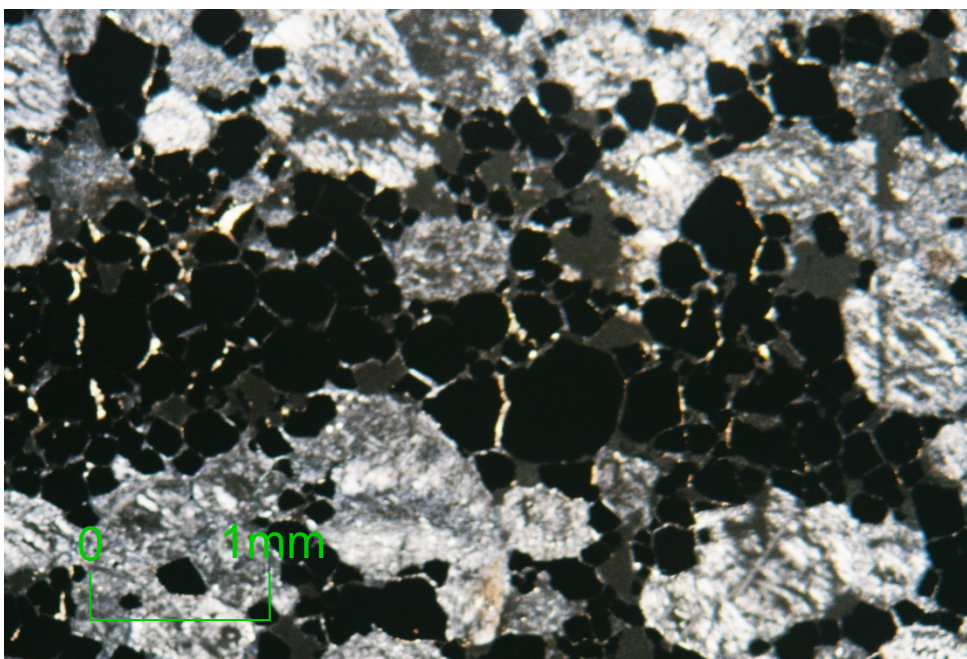


Figure 3.16. Minute intercumulus chromite surrounding coarser grained serpentinized cumulus olivine clearly demonstrating intercumulus chromite crystallization. Sample 486009 is from 117.7 m in DDH BT-08-10.

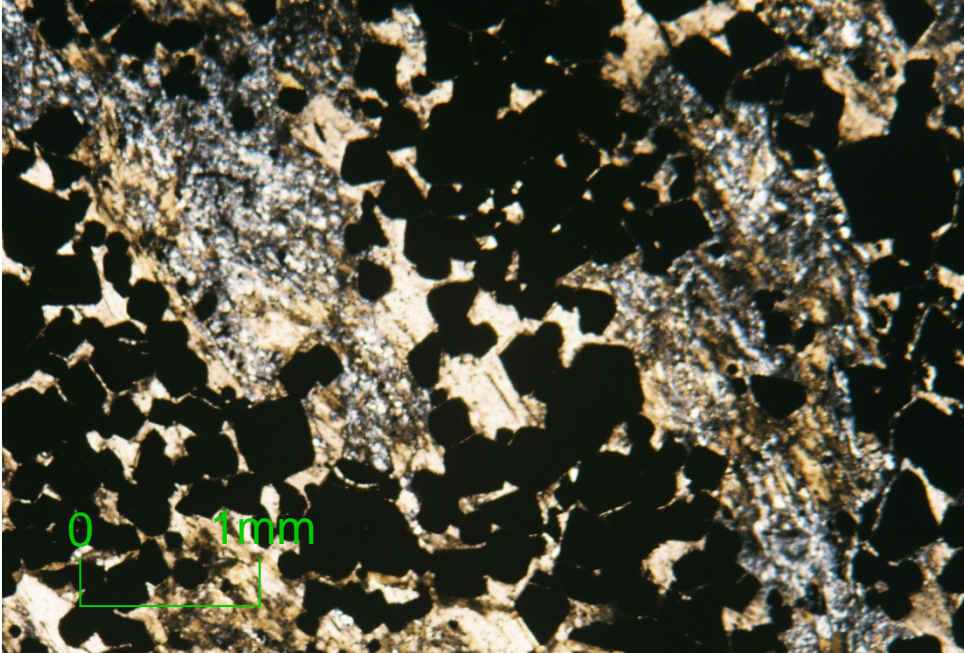


Figure 3.17. Chromite grains surrounding the olivines are in association with brown platy chlorite grains after orthopyroxene. Sample is from 259 m (sample 486350) in Black Label DDH BT-09-31. Also note the chain-like texture of the chromites.

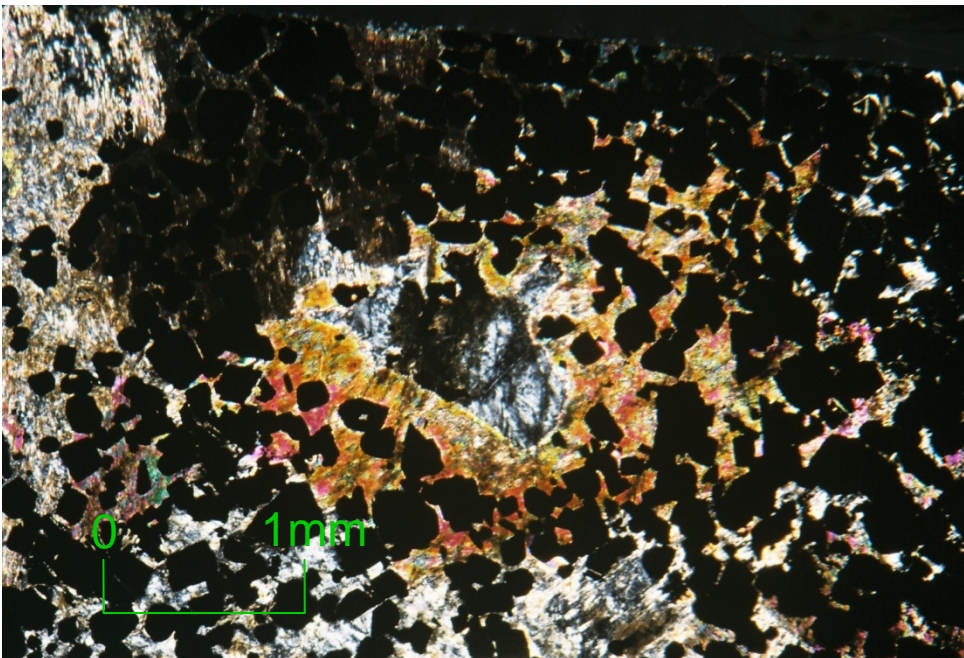


Figure 3.18. Interstitial chromite in oikocrystic harzburgite surrounds the serpentinized olivine and, in turn, occurs in intercumulus tremolitized pyroxene. This shows an order of crystallization of cumulus olivine \rightarrow cumulus chromite \rightarrow intercumulus orthopyroxene. Sample 486155 is from 151.8 m in DDH BT-09-31.



Figure 3.19. Often there is kaemmererite alteration in the chromitites. Kaemmererite is a purple, high Cr-bearing chlorite that forms due to the retrogression of pyroxene that occurs in close association with chromite. Sample is of a vein of kaemmererite that envelops coexisting dolomite and cross-cuts the chromitite. From 339.17 m in DDH FW-11-87. Diameter of core is 46.7 mm.

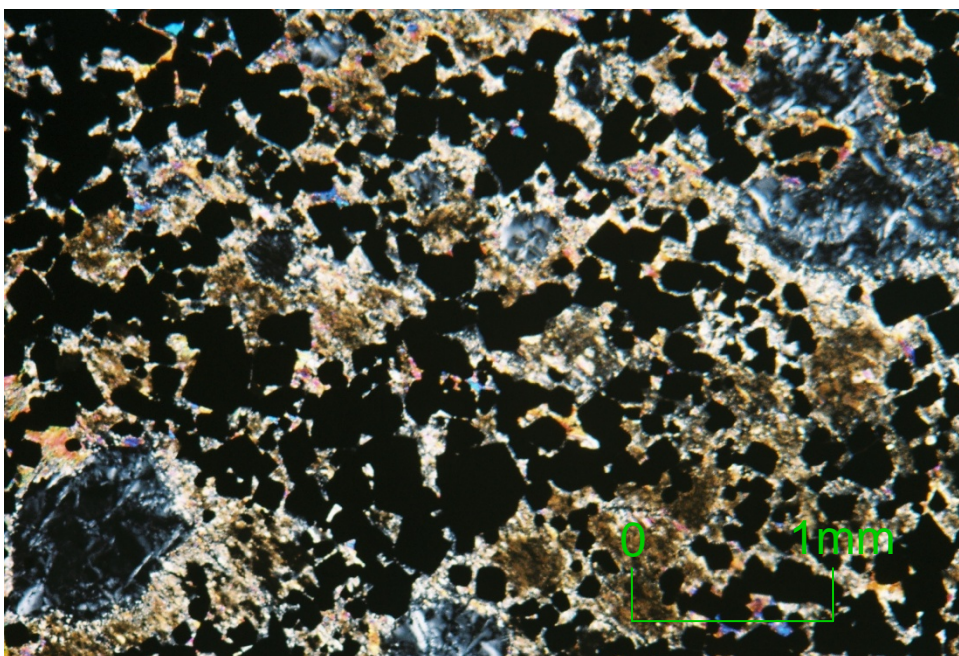


Figure 3.20. Often serpentinized olivines have talc rims due to retrogression of surrounding intercumulus pyroxene that encroaches on the olivines. Sample 486234 is from 183.4 m in DDH BT-09-31.

3.6 Chromitite

3.6.1 Heavily disseminated chromite

As with weak disseminated chromite described above, heavily disseminated chromite also occurs interstitial to cumulus olivine. Heavily disseminated chromite accounts for 25 to 40 modal %. At basal contacts with the massive chromitite there is usually an increase in chromite to 50 modal %. The interstitial chromite is either disseminated or weakly layered/foliated. The host generally is harzburgite with cumulus olivines within intercumulus pyroxene. Intercumulus pyroxene minerals is darker grey and commonly metasomatically replaces the cumulus olivine in patches throughout the unit (Figs. 3.9 to 3.11). The olivine and pyroxene is pervasively serpentinized, tremolitized and replaced by talc. Talc after the intercumulus pyroxene continues to replace olivine until olivine is completely ghostly-grey talc-altered. The presence of talc suggests there were CO₂ fluids involved in the hydration of the pyroxene.

3.6.2 Intermittent chromitite beds

Intermittent chromitite beds generally, but not always, occur between disseminated and semi-massive to massive chromite sequences. These beds range from 10 to up to 30 cm in thickness. Intermittent silicate layers form up to 50 cm to 1 m intervals of dunite, or pyroxenite, often with disseminated chromite. Disseminated chromite in intervening silicate layers generally contain 25 to 30 modal % chromite. Hole DDH BT-10-128 intersected large-scale, 3 m thick, massively textured intermittent chromitite beds separated by metre-scale sections of pyroxenite. These beds have contacts and internal bands that well display primary igneous layering. The igneous layers are later deformed, however, the primary layering often does not reflect the foliation and plunge of the chromite ore shoots. The chromite textures are well preserved, in contrast to the silicate lithologies. Chromite is not easily replaced, is denser and more resistant to alteration than the surrounding olivines and pyroxenes.

As well displayed in DDH BT-08-10, the intermittent beds often have sharp basal and grade upward into dunite. Excellent top directions are defined by sharp basal massive chromitite contacts against cumulate dunite hosting minor intercumulus chromite (Fig. 3.21). Upward increasing nodular olivine concentrates until cumulus olivine forms dunite with diminishing intercumulus chromite, followed by another knife sharp contact



Figure 3.21. An intermittent bed of chromite shows knife sharp lower contacts and cumulus to chain chromite upper contacts with overlying olivine cumulate. Sample is from 135.8 m in DDH BT-08-10.



Figure 3.22. Intermittent chromitite beds alternate with olivine cumulate dunite in DDH BT-08-10.

at the base of overlying massive chromitite (Fig. 3.22). The beds of sharp lower massive chromite grading upward into interstitial chromite with increasing cumulus olivine are a result of the settling of chromite layers (Kaçira, 1971). Higher up in the section, there are cumulus contacts below the lower and above the upper contacts of the chromite layers indicating a change in the order of crystallization from olivine back into chromite. Then higher up, the beds are reversely graded with coarser cumulus olivine grading up to fine interstitial chromite with sharp lower contacts of the chromite with the next cycle. This demonstrates dominant crystallization in the olivine field followed by chromite. Intermittent chromitite beds also show crystallization of cumulus chromite plus pyroxene where pyroxene is the dominant host silicate before the overlying chromitite interval. An example would be the layered beds with cumulus pyroxene in DDH BT-09-17 (Fig. 3.23).

3.6.3 Semi-massive chromite

Semi-massive chromite is olivine or pyroxene cumulate with 45 to 70 modal % chromite (Fig. 3.24). Interstitial very fine cumulus chromite is disseminated within cumulus olivine and/or pyroxene or as groundmass to dispersed cumulus olivine and/or pyroxene. Layering is common, with up to 5 cm wide chromite bands. Disseminated chromite grades to heavily disseminated to semi-massive, and finally to massive chromite. There is no general pattern as to the location of the various types of chromitite.

An excellent example of semi-massive chromite in thin section is the Black Label chromitite of BT-09-31. This chromitite has high silicate content, the chromite occurs in chain-like textures interstitial to serpentinized olivine (Fig. 3.25). These chromites contain more silicate inclusions, atoll textures, which are swiss cheese-like holes in the chromite containing silicate (Fig. 3.26). The silicate inclusions at 155 m depth have the same cleavage plane orientations as the surrounding tremolite, suggesting the chromites underwent subsequent growth or annealing around the host silicate. Annealing/sintering is a reequilibration of chromite around silicate melt has been postulated for the origin of the swiss cheese-like textures in the Bushveld chromites (Hulbert and Von Gruenewaldt, 1985). These silicate inclusions have been investigated by detailed microprobe analyses. They are of serpentine or tremolite composition, sometimes with the occurrence of both mineral inclusions in one chromite grain. In some cases, either single chromites, or a few



Figure 3.23. Intermittent beds of cumulus pyroxene alternating with very fine, massive cumulus chromite. Sample is from 81.80 m in DDH BT-09-17. Diameter of core is 46.7 mm.



Figure 3.24. Semi massive chromite: Chromite occurs as 45 to 70 modal % interstitial very fine cumulus chromite disseminated within cumulus olivine or as dominant groundmass chromite bearing cumulus olivine. Sample is from DDH BT-11-185. Diameter of core is 46.7 mm.

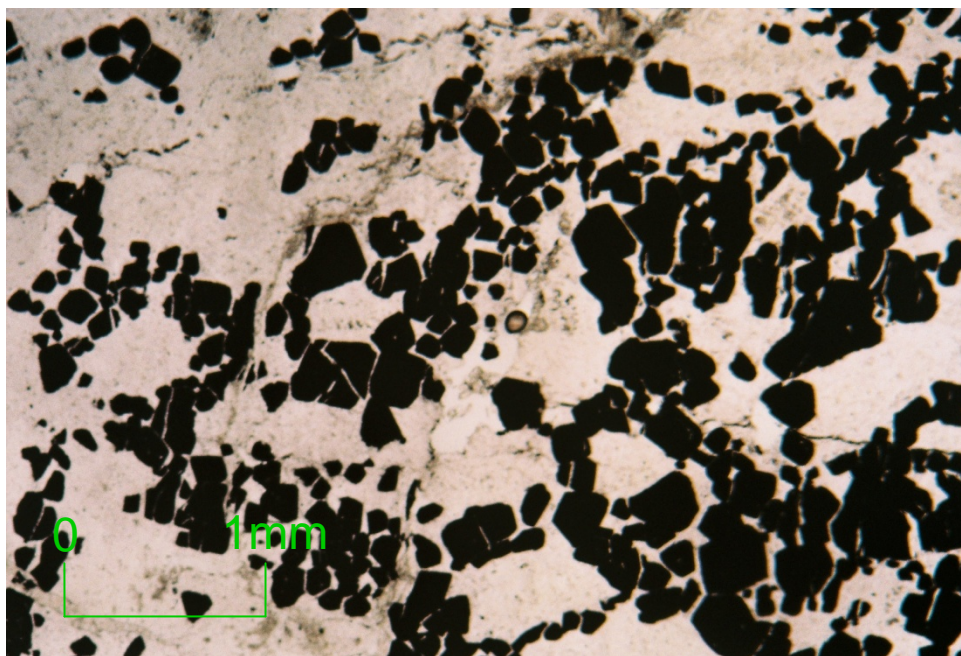


Figure 3.25. In semi-massive chromite, the chromites occur in chain like networks interstitial to serpentinized olivine. Sample 486033 is from 130.8 m in DDH BT-08-10.

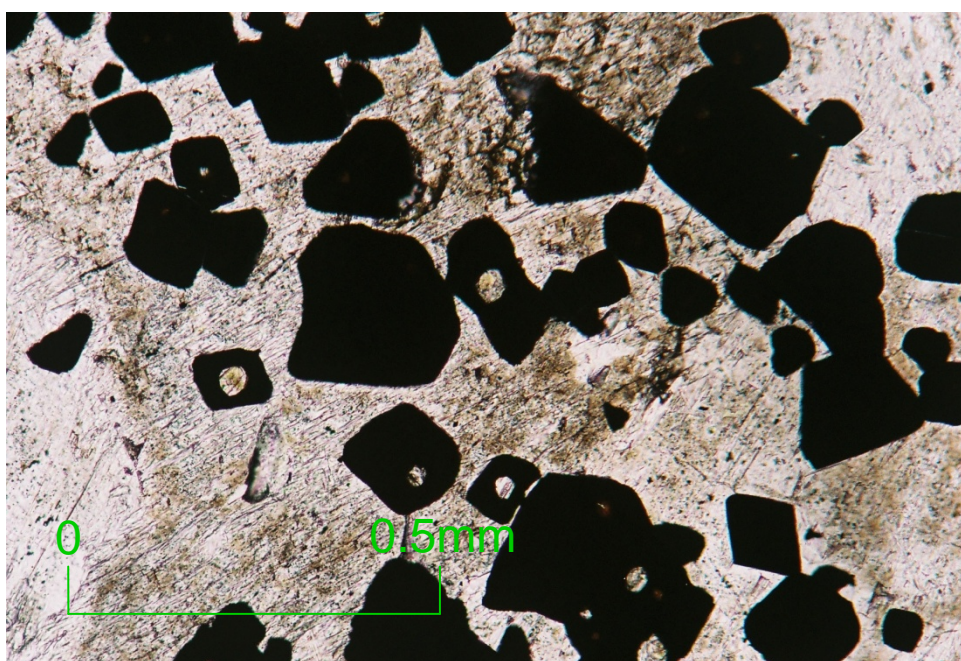


Figure 3.26. Chromites often contain silicate inclusions, which are rounded swiss cheese-like holes in the chromite containing silicate. In this sample, the silicate inclusions have the same cleavage plane orientations within them as the surrounding tremolite which suggests the chromites underwent subsequent annealing processes around the host tremolite. Sample 486163 is from 155 m in DDH BT-09-31.

fine chromites grown concentrically together, appear to partially envelop silicate from the host rock (Figs. 3.27 and 3.28). The incomplete growth of chromite around the silicate shows that the chromite primarily crystallized in equilibrium with the surrounding silicate i.e. the olivine dunite. In some cases, the sintering would occur after cumulus olivine-pyroxene-chromite segregation as some of the chromites envelop both serpentine (after olivine) and tremolite (after pyroxene).

The investigation of silicate inclusions demonstrates a larger range in mineral species than has been reported in other chromites in the world. In addition to serpentine and tremolite there are inclusions of Na-Ca amphibole, Ca amphibole, K and Na-phlogopite, chromian diopside, Ni sulphide and even albite. The silicate inclusions often have unique compositions, as in the case of Na-phlogopite and albite, and are often different than the cumulus minerals (Fig. 3.29). A single inclusion can contain igneous amphibole (edenite) that displays retrogressive zoning to tremolite, along with the occurrence of albite and phlogopite (Fig. 3.30). The suite of minerals constitute melt inclusions that show a unique crystallization environment within the inclusion. In some cases, however, amphibole such as pargasite can occur both within host cumulates and within silicate inclusions in the chromite. Sample 486163 at 155 m in DDH BT-09-31 shows relic igneous amphibole in cumulate hosting chromite with silicate inclusions of the same igneous amphibole composition (Figs. 3.31 and 3.32). Chromite probably encapsulated residual melt that crystallized at lower temperatures. Phlogopite analysed in the host cumulates is less Na-bearing than phlogopite in the silicate inclusions. Some textures suggest phlogopite was also incorporated by the growing chromite rather than being crystallized from fluids post entrapment. Sample 486353 at 260.6 m in DDH BT-09-31 shows chromite growing around a phlogopite grain (Fig. 3.33). Chromite in association with igneous amphibole and phlogopite is found in other stratiform intrusions such as the Stillwater Complex (Page and Zientek, 1987). In sample 486352 at 260.2 m in DDH BT-09-31, there is the common association of chromite with surrounding phlogopite (Fig. 3.34).

The silicate inclusions generally form large spheres within most chromite grains. Silicate inclusions of different composition can inhabit growth planes in larger chromites. The size of these central “swiss cheese” inclusions and also nature of growth within the

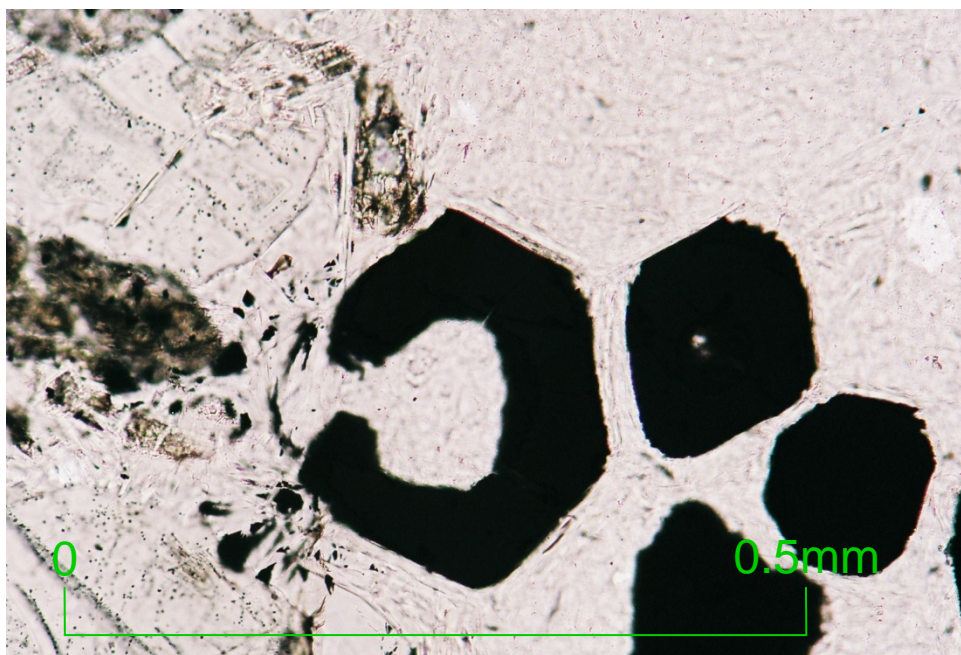


Figure 3.27. Incomplete annealing of a single chromite grain. Sample 486268 is from 197 m in DDH BT-09-31.

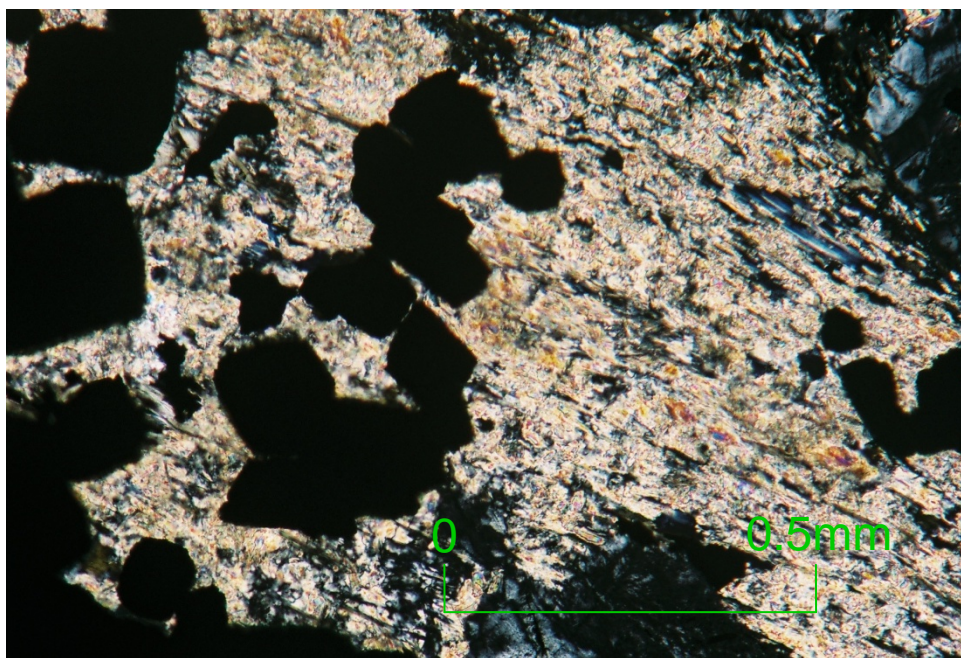


Figure 3.28. In some of the chromitite, either single chromite, or a few fine chromites grown concentrically together, appear to partially envelop silicate from the host rock, suggestive of initial stages of annealing. Note the surrounding talc-altered pyroxene. Sample 486185 is from 164 m in DDH BT-09-31.

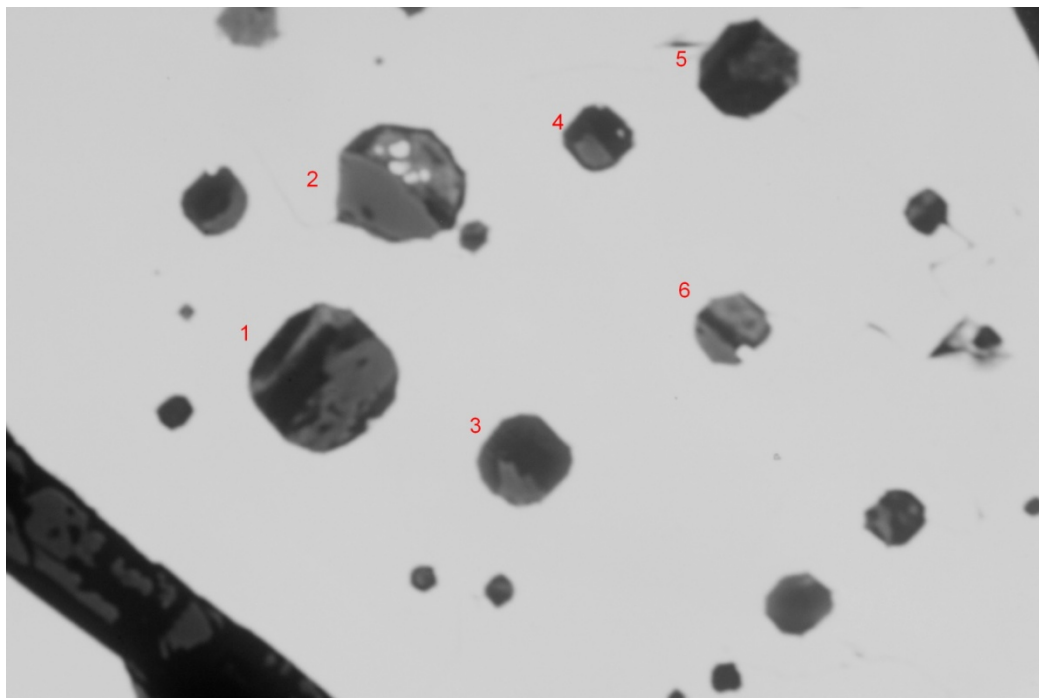


Figure 3.29. Various silicate inclusions are sometimes found along growth planes within chromite. In this case, the various inclusions all have unique compositions. Sample 486211, image_0022 at 174.4 m in DDH BT-09-31.

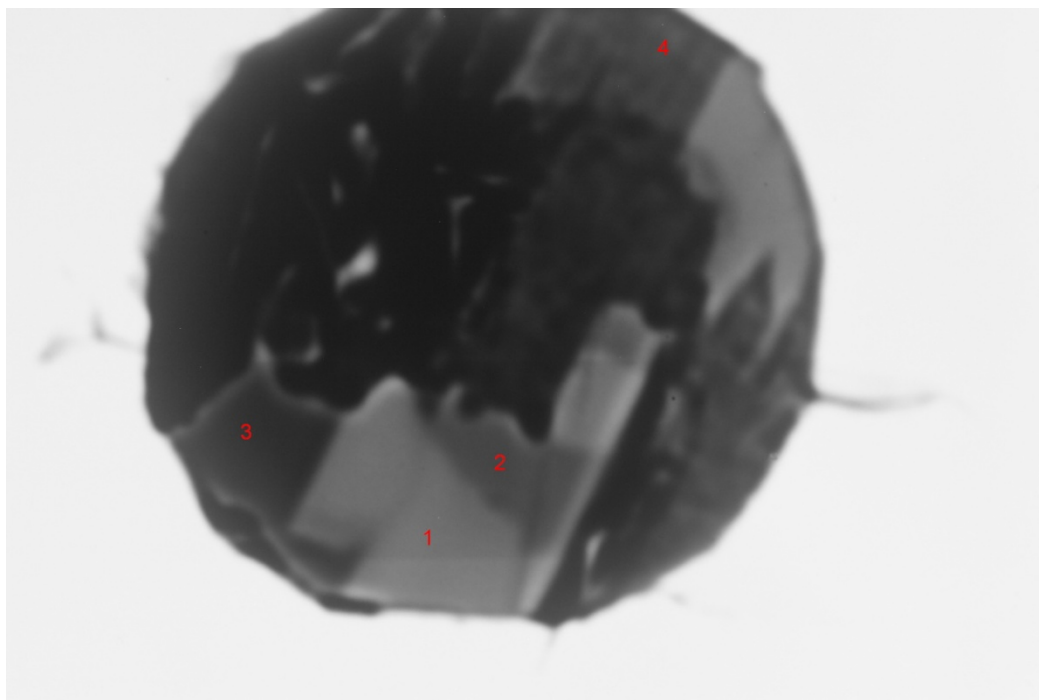


Figure 3.30. A single silicate inclusion contains igneous edenite in point 1 that displays zoning to tremolite at point 2. Also shown is an albite at point 3 and a phlogopite at point 4. From sample 486211, image_0010 at 174.4 m in DDH BT-09-31.

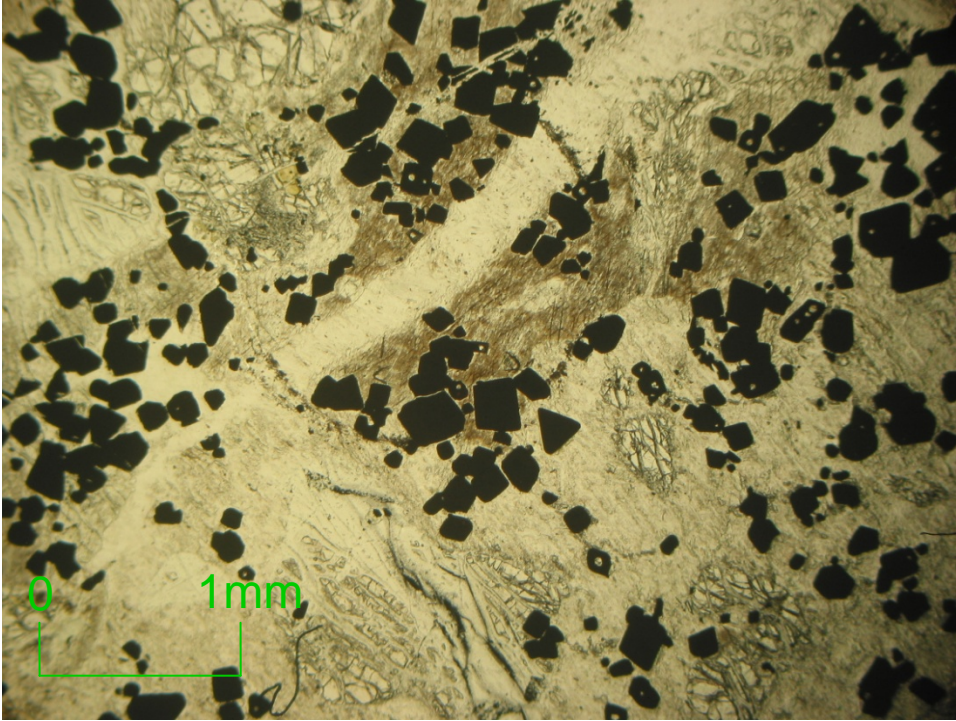


Figure 3.31. Silicate inclusions with the same composition as the surrounding igneous amphibole. Note the amphibole is the brown mineral in PPL. Sample 486163 is from 155 m in DDH BT-09-31.

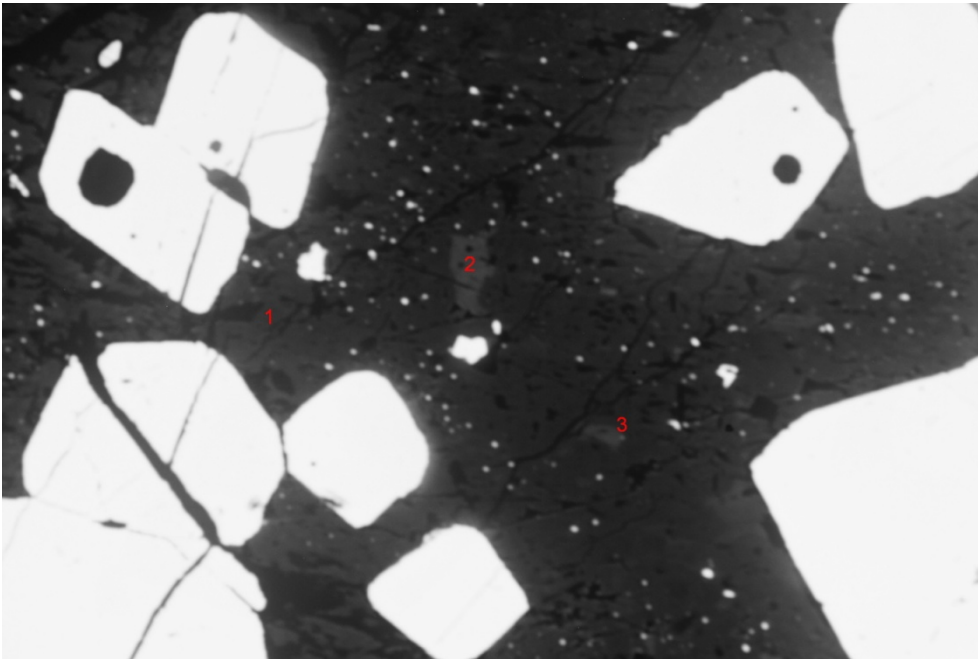


Figure 3.32. Sample 486163 shows relic igneous amphibole at points 2 and 3 that hosts chromite with silicate inclusions of the same igneous amphibole composition. Point 1 is secondary tremolite. Image_0031 at 155 m in DDH BT-09-31.

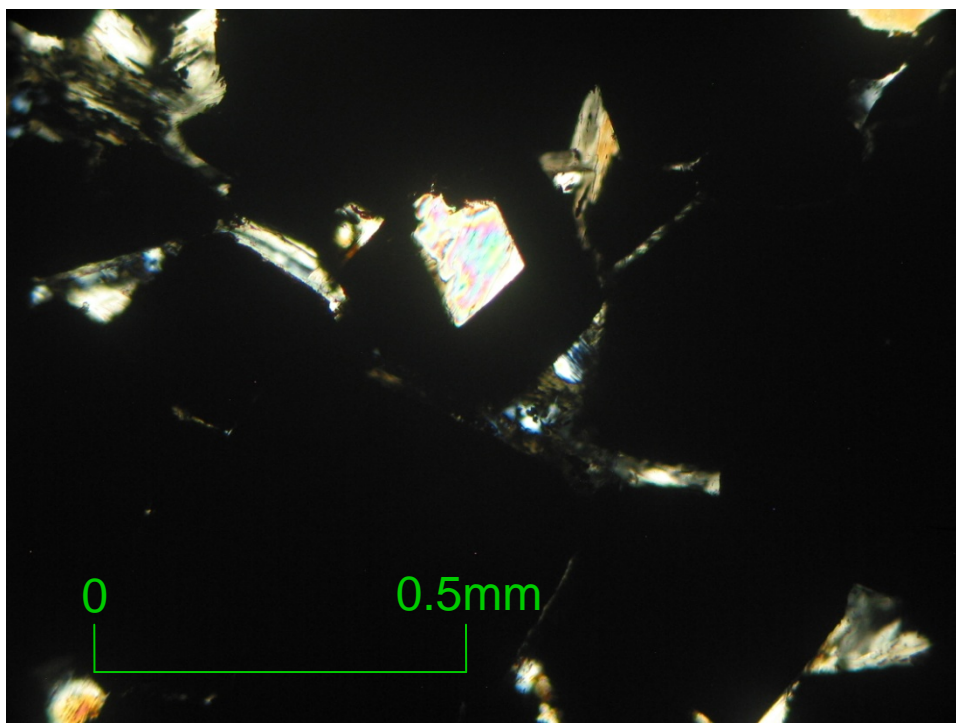


Figure 3.33. In this sample, chromite is observed to grow around and include the highly birefringent phlogopite grain. Sample 486353 is from 260.6 m in DDH BT-09-31.

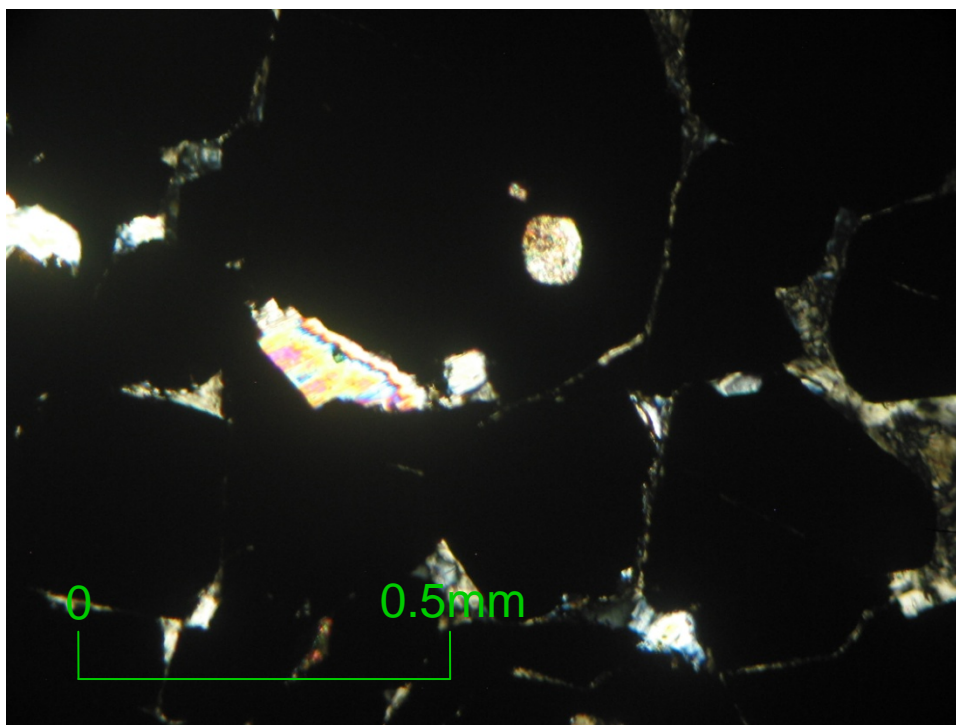


Figure 3.34. Phlogopite is found as both silicate inclusion in the chromite and in the silicate interstitial the chromites. Sample 486352 is from 260.2 m in DDH BT-09-31.

chromite suggests they were intimately encapsulated as melt while chromite was growing. Chromite encapsulates amphibole, serpentinized olivine and tremolitized pyroxenes by sintering. The melt responsible for the inclusions was residual within the crystal mushes. There are often fractures around the inclusions and entry points where melt was encapsulated in chromite. Negative crystal outlines of the inclusions reflect the cubic symmetry of the host chromite. There was probably also the later H₂O autohydration inclusions. More details in the discussion of the silicate inclusions are provided in chapter 6.

3.6.4 Massive chromite

Massive chromitite is composed of mesocumulus to adcumulus fine grained granular chromite with minor intercumulus tremolite after pyroxene. At Black Thor, the lower chromitites, between dunite and olivine pyroxenite, are the highest grade with over 90 modal % chromite and contain fewer oikocrystic pyroxene (Fig. 3.35). The Big Daddy chromitite is similarly high grade as Black Thor (Fig. 3.36). Chromitites with more intercumulus pyroxene show textures of lighter coloured/less dense chromite-bearing intercumulus pyroxene patches in a darker/more dense chromitite adcumulate (Fig. 3.37). The oikocrysts usually occur as large 1.5 to 5 cm wide patches of white to grey depending on the concentration of included chromite. In some chromitites, there are occasional chicken track textures of intercumulus pyroxene networks lacing the chromite (Fig. 3.38). In thin section, the lighter coloured areas of the intercumulus pyroxene in the massive chromite is characterized by birefringent tremolite after pyroxene. The darker areas contain lesser altered tremolitized pyroxene (Fig. 3.39). Clinocllore, is locally observed as a minor hydration product of original orthopyroxene (Fig. 3.40). Chromian clinocllore preferentially occurs where there has been brittle failure of original chromite (Fig. 3.41).

The Black Label chromitites are more heterogeneous than the Black Thor chromitites and contain wavy, lensoidal and magmatic breccia textures indicating a dynamic depositional environment (Fig. 3.42). Within the chromitites, the lighter areas often appear as single cleaved oikocrysts overgrowing cumulus aggregates of olivine and pyroxene. The lower Black Label (Layer 1) chromitite contains up to 15-20 modal % oikocrystic pyroxene and cumulus olivine content, identifying host pyroxene-oikocrystic



Figure 3.35. The lower Black Thor massive chromitite is the highest grade with over 90 modal % chromite. The chromitite is composed of massive granular very fine chromite with lesser intercumulus pyroxene (grey areas) content which gives the chromite a higher Cr/Fe ratio. Sample is from 160 m in DDH BT-08-10.

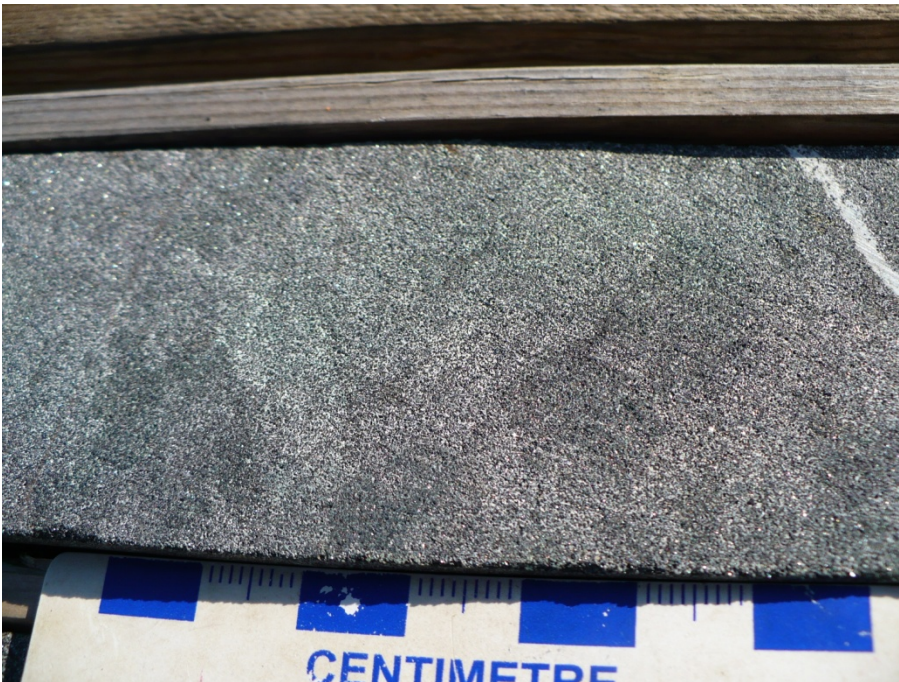


Figure 3.36. The Big Daddy massive chromitite is similarly high grade as the Black Thor chromitite. The chromitite has about 90 modal % chromite or more and high Cr/Fe ratio. Sample is from 212.20 m in DDH FW-08-19.



Figure 3.37. Chromitite intercumulus pyroxene show textures of lighter coloured/less dense chromite-bearing intercumulus pyroxene patches in a darker/more dense chromitite accumulate. Intercumulus pyroxene degrades the chromitite to 75 to 85 modal % chromite and lowers the Cr/Fe ratio. Sample is from 228.35 m in DDH FW-11-61. Diameter of core is 46.7 mm.



Figure 3.38. More infrequent are chicken track networks of intercumulus pyroxene in chromitite. Sample is from 94.30 m in DDH BT-10-133. Diameter of core is 46.7mm.

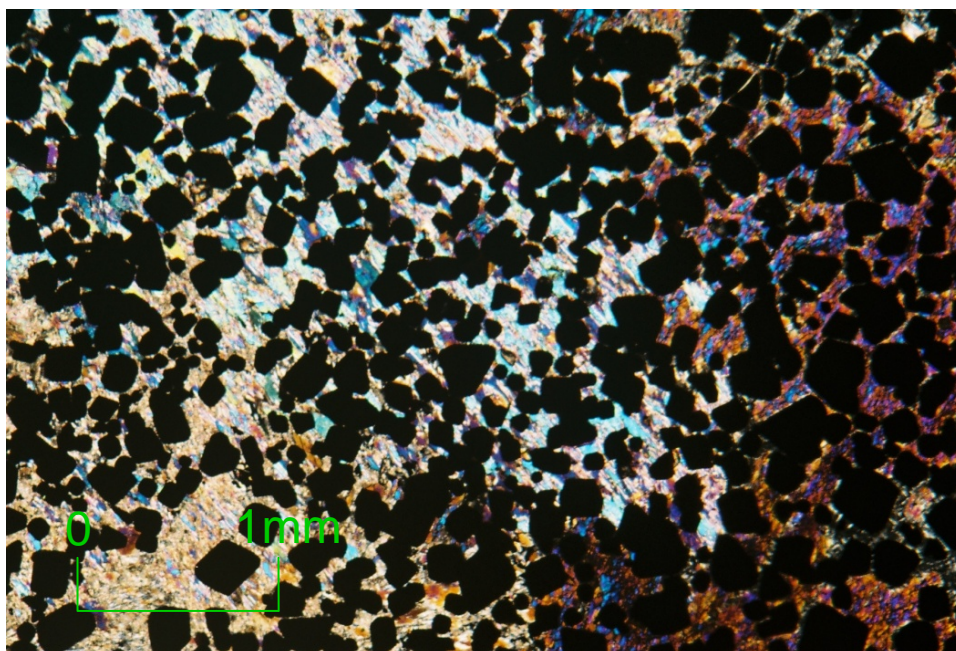


Figure 3.39. Lighter coloured areas with intercumulus pyroxene are now composed of birefringent tremolite. Note the cleavage planes of single oikocrysts of tremolite that envelop the chromite. The chromite is very fine grained with mesocumulate textures. Sample 486272 is from 198.6 m in DDH BT-09-31.

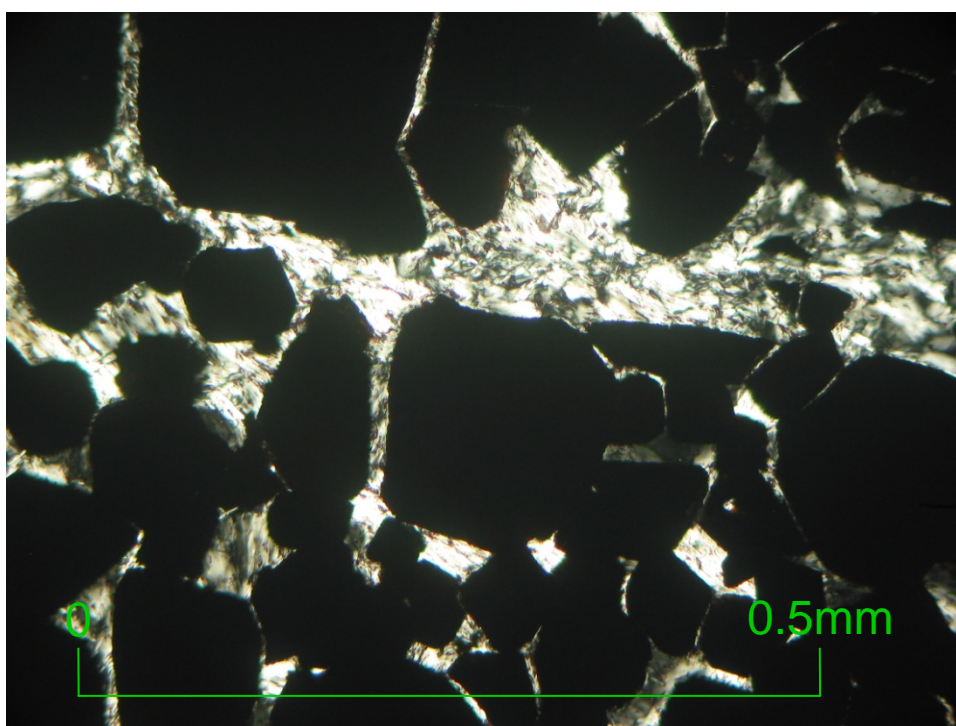


Figure 3.40. Chlinochlore is locally observed interstitial the chromites in massive chromitite. It is the alteration product of original intercumulus orthopyroxene. Sample 486022 is from 126.4 m in DDH BT-08-10.

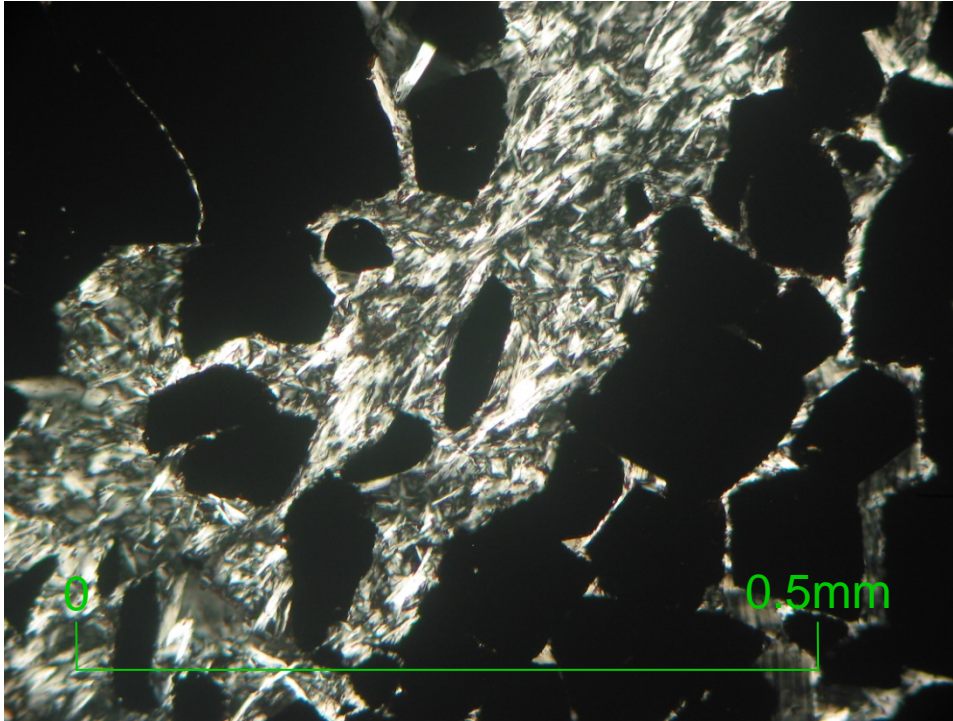


Figure 3.41. Chromian clinocllore occurs where there has been brittle failure of original chromite as opposed to non-Cr-bearing clinocllore that occurs in the interstitial groundmass. Sample 486020 is from 125.6 m in DDH BT-08-10.



Figure 3.42. The Black Label chromitites are lower grade than Black Thor and Big Daddy chromitites. Layer 1 of Black Label is more heterogeneous and contains wavy, lensoidal and magmatic breccia textures. Sample is from 174 m in DDH BT-09-26.

cumulus olivine harzburgite. Not all pyroxene is oikocryst, some occurs as large amoeboid patches in both Black Label and Black Thor chromitite. Some of the massive chromitites also contain interstitial carbonate after pyroxene which is probably magnesite (Fig. 3.43).

Often massive chromitites contain round aggregates of either olivine or pyroxene (Fig. 3.44). Pyroxene aggregates in the chromitites appear medium grey whereas cumulus aggregates of olivine appear white. The pyroxene hosts disseminated cumulus chromite whereas the olivine does not. The silicate aggregates commonly form singular “beaded” to composite layers, signifying primary magmatic layering.(Fig. 3.45).

Other features of massive chromitite include common deformation fabrics, rare hematite alteration and a variety of veins. Foliations commonly overprint the primary magmatic fabrics near faulted contacts (Fig. 3.46). In thin section, deformation is often represented in the incipient fracturing of adcumulus chromite that may be a result of compaction (Fig. 3.47). Chromitites are often wholesale hematite-altered as seen by the red-brown colouration of the ores (Fig. 3.44). Thin talc-carbonate-serpentine veinlets are often scattered within chromitites due to volume expansion related to serpentinization. Some of the veins have kaemmererite on the fracture coatings, which is a chromian chlorite alteration of the chromite (Fig. 3.19).

3.7 Magmatic Breccia

A few drill holes at Black Label intersect magmatic breccia developed after crystallization of chromitite. In DDH BT-11-176, the magmatic breccia occurs after the Layer 2 massive chromitite in the transition from oikocrystic harzburgite to dunite. Magmatic breccia consists of rounded up to 6 cm fragments of dunite in a lighter coloured pyroxenite and olivine matrix. Proportion of clasts to matrix is 70:30 or higher with variable clast size. This unit is chromite mineralized with occasional up to 5 cm massive chromitite clasts (Figure 3.48). This unit is also occasionally sulphide mineralized with interstitial pyrrhotite-pentlandite-chalcopyrite, disseminations and veinlets ranging from 0.5 to up to 8 modal % (Fig. 3.49).

In DDH BT-11-179, magmatic breccia occurs after the Layer 1 massive chromitite in the transition from oikocrystic harzburgite to heterogeneous pyroxenite. The fragments are dominantly fine grained cumulus olivine with intercumulus pyroxene.

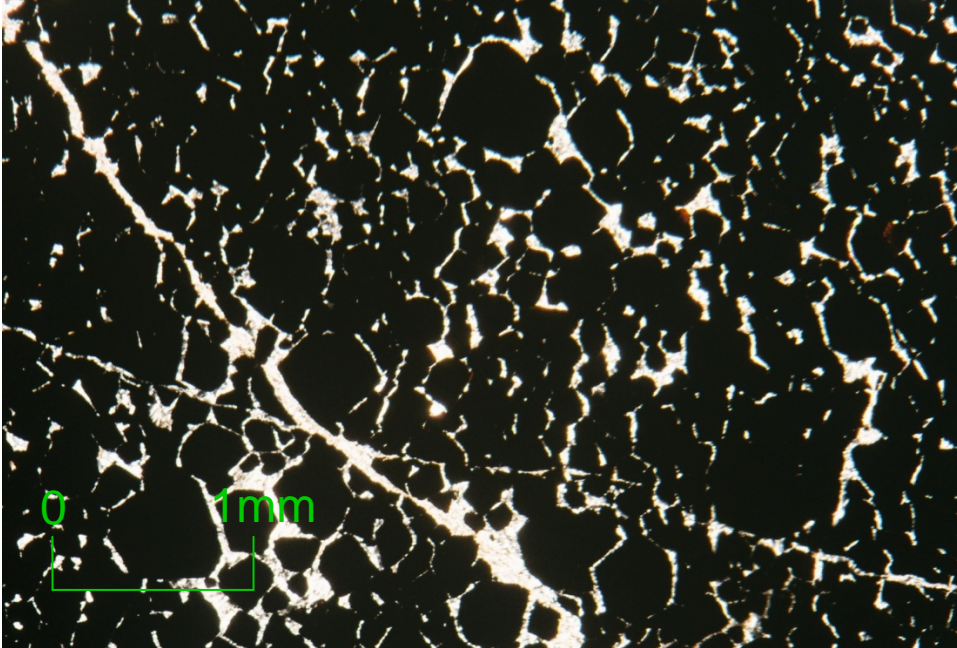


Figure 3.43. Some of the massive chromitites contain interstitial high birefringent magnesite after pyroxene. Note the chromite in this sample shows fracturing and is cross-cut by magnesite veins. Sample 486094 is from 155.6 m in DDH BT-08-10.



Figure 3.44. Talc altered olivines to aggregates of olivine often occur as beds in the massive chromitites. Note the red hematite alteration of the chromite on the fracture coating. Sample is from 69.75 m in DDH BT-10-133. Diameter of core is 46.7 mm.



Figure 3.45. Silicate aggregate (mostly olivine) form “beaded” layers signifying magmatic layering. Sample is from 382.3 m in the Blackbird DDH NOT-08-1628.



Figure 3.46. Chromitite often contains deformation fabrics proximal to pyroxenite. The brown fracturing of the chromitite lowers the Cr content. There is abundant calcite veinleting associated with the deformation. Also note the occluded silicate layering. Sample is from 474 m in DDH BT-11-200. Diameter of core is 46.7 mm.

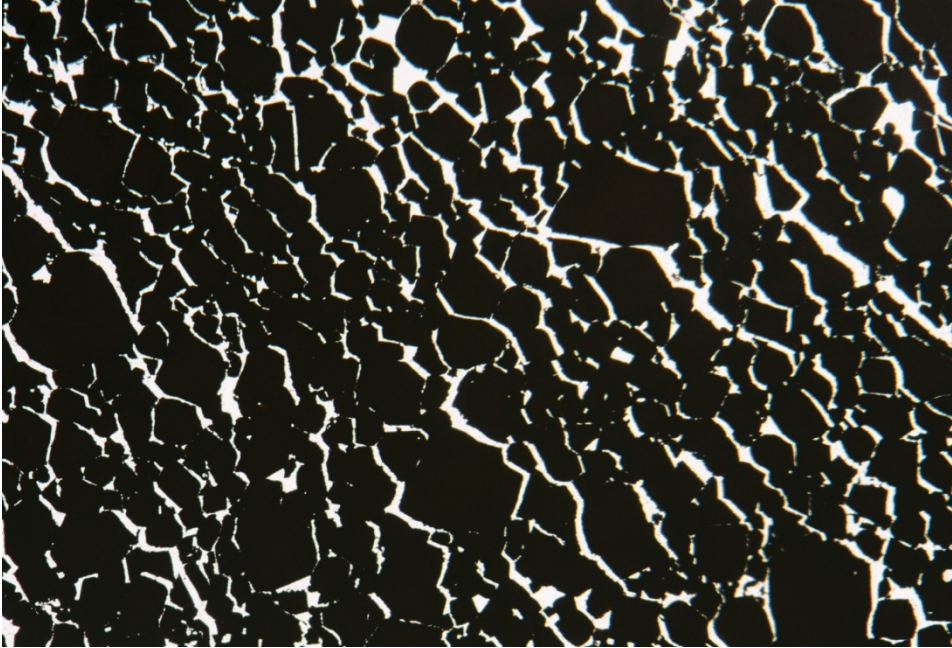


Figure 3.47. Fractured adcumulus massive chromite. The same orientation of the fractures is indicative of compaction of the chromites along those planes. Sample 486025 is from 127.6 m in DDH BT-08-10.

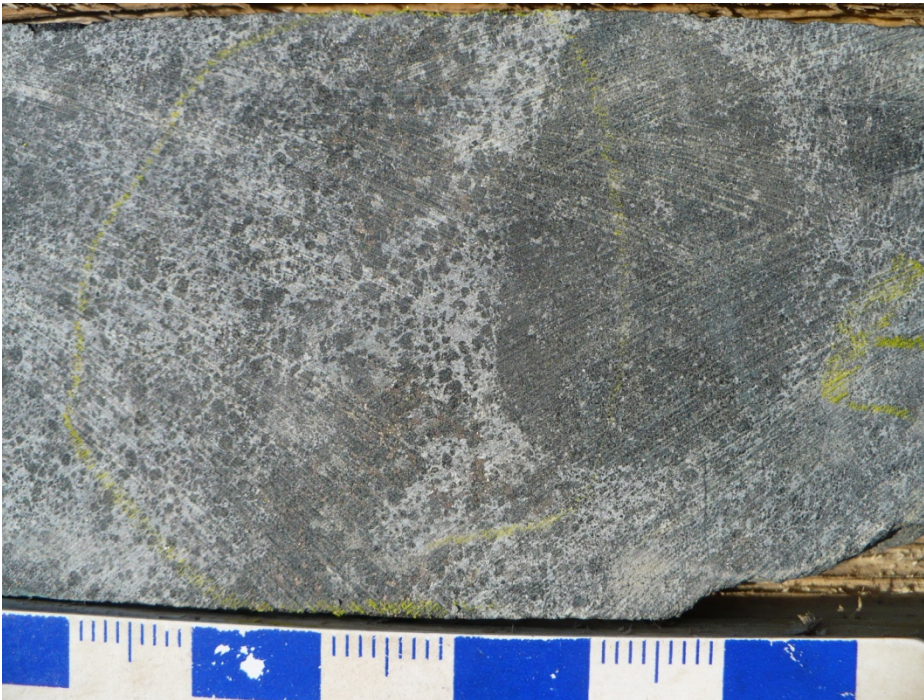


Figure 3.48. Magmatic breccias contain up to 3.5cm rounded fragments of chromite, and smaller dunite clasts in a light grey intercumulus pyroxene matrix. Sample is from 230.84 m in DDH BT-09-29.



Figure 3.49. Fine interstitial po-pn-cpy sulphides in magmatic breccia. Sample is from 244.68 m in DDH BT-09-29.

The host is serpentinized pyroxene-oikocrystic harzburgite and individual oikocrysts range up to 2 cm in size. From 290.40 to 290.70 m, there is coarse wispy pentlandite in serpentinized dunite. Light grey pyroxenite occurs from 297.10 to 298.62 m. Then there is oikocrystic magmatic breccia with more intercumulus pyroxene content and finer olivine clasts to 306 m. Patchy chromite is disseminated in this section ranging up to 8 Cr % in a few 1.5 m intervals.

3.8 Heterogeneous pyroxenite

Heterogeneous pyroxenite is dark green and light grey-coloured and ranges from olivine orthopyroxenite to harzburgite that consists of 50:50 dark olivine to light grey orthopyroxene (Fig. 3.50). Olivine forms fine to medium grained cumulus aggregates in diffuse patches up to 1 cm in size. Orthopyroxene occurs as light grey, up to 3 mm, sheafy cumulus minerals that have been tremolitized. The patchy association of pyroxene with olivine has been interpreted by Leshar (pers. communication, 2011), to be the result of replacement of primary olivine by a pyroxenitic magma. Like the textures of dunite-harzburgite, there is coarse patchy encroachment of pyroxene on fine cumulus olivine.

Occasionally cumulus olivine occurs as filter pressed layers within a pyroxene groundmass that may show a fabric orientation (Fig. 3.51). This filter pressed layering is probably formed as pyroxene melt was pressed out leaving behind thin compact olivine layers. Evidence of this being a form of compaction is the common occurrence of this layered olivine pyroxenite at the upper contacts of chromitites below major pyroxenite sequences, before the units grade into pyroxenite. The new pulse of pyroxenite would press the underlying olivine into layers within the unit.

3.9 Pyroxenite-olivine pyroxenite

Pyroxenites above the main chromitite zones are light grey medium to coarse grained massive units composed of sheafy to tabular, cumulus pyroxene (Fig. 3.52). The units locally have a cumulus olivine content ranging from 10 to up to 35 modal %. In areas where olivine pyroxenite is present, the crystallization sequence is dunite → chromitite → olivine pyroxenite → pyroxenite. Otherwise crystallization is dunite → chromitite → pyroxenite.



Figure 3.50. Mottled heterogeneous olivine pyroxenite contains a patchy association of 50:50 dark, fine to medium grained cumulus olivine to light grey, up to 3 mm, tremolitized, sheafy cumulus orthopyroxene. Sample is from 147.3 m in DDH FW-08-19.



Fig. 3.51. Filter pressed olivine layers occur in another heterogeneous pyroxenite. Sample is from 173.37 m in DDH BT-09-23.



Figure 3.52. Pyroxenites are light grey medium to coarse grained massive units composed of sheafy to tabular, cumulus pyroxene. Sample is from 35 m in DDH BT-10-133. Diameter of core is 46.7 mm.



Figure 3.53. Primary bronzite in pyroxenite distinguished by their bronze colours and cleavage. Sample is from 34 m in DDH FW-12-108. Diameter of core is 46.7 mm.

The pyroxenites have a variety of textures. Medium grained pyroxenite is commonly comprised of orthopyroxene. Occasionally, bronzite primocrysts make up segments of FW-12-108 (Fig. 3.53). Medium grey pyroxenite is mostly composed of light grey tremolitized pyroxene. Wholesale replacement by green radial fibrous tremolite can eradicate original pyroxene. In the bronzitite of FW-12-108, the tremolitization of pyroxenes is displayed by minor veinlets (Fig. 3.53). Coarse grained pyroxenite is commonly foliated and altered to talc. Large sections of the coarse grained talcose pyroxenite has pink hematite alteration. Rather commonly large 1.5 cm, rounded poikilitic pyroxene megacrysts enclose medium grained pyroxene. Poikilitic pyroxene accounts for 8 to 15 modal % of the composition and are identified by a darker, somewhat ghostly appearance.

Near the contacts with overlying leucogabbro, the pyroxenite is mylonitized and distinguished from the leucogabbro in that it is more greenish in colour contains no feldspar content. Leucogabbro, in contrast, is grey in colour with feldspar. It is unclear if the pyroxenes in pyroxenite occur in a cumulus fabric as similar textures have been reported in Pykes Hill komatiitic pyroxenites which could have a metasomatic origin (Leshner, pers. communication 2011). Under thin section, pyroxenite comprises tabular, anhedral, haphazardly oriented pyroxene that has been pervasively talcose-altered and incipiently tremolitized (Fig. 3.54). Tremolite usually occurs along the cleavage planes of pyroxene minerals that has been pseudomorphed by fine masses of talc. The pyroxenites are usually devoid of interstitial chromite and cap the chromitite sequences.

Although they cap the sequences, it is still argued that the pyroxenite is related to chromite mineralization. In DDH BT-10-17, pyroxenite above the first chromite sequence (above the initial dunite) and the pyroxenite in pyroxenite-chromitite-dunite cycles higher up in stratigraphy contain wispy interstitial and bands of chromite grading up to cumulus pyroxene in some of the cycles (Fig. 3.55). In thin section, the chromite in pyroxenite occurs in a vermicular habit and is retrogressed at the margins in contrast to regular euhedral chromite (Fig. 3.56). This is similar to the vermicular habit of pyroxenite-bearing chromites in ophiolites (Matsumoto and Arai, 2001). The gradation of chromite to pyroxene probably indicates the pyroxenes are cumulus within these chromitite zones. The occurrence of chromite mineralization with pyroxenite above the

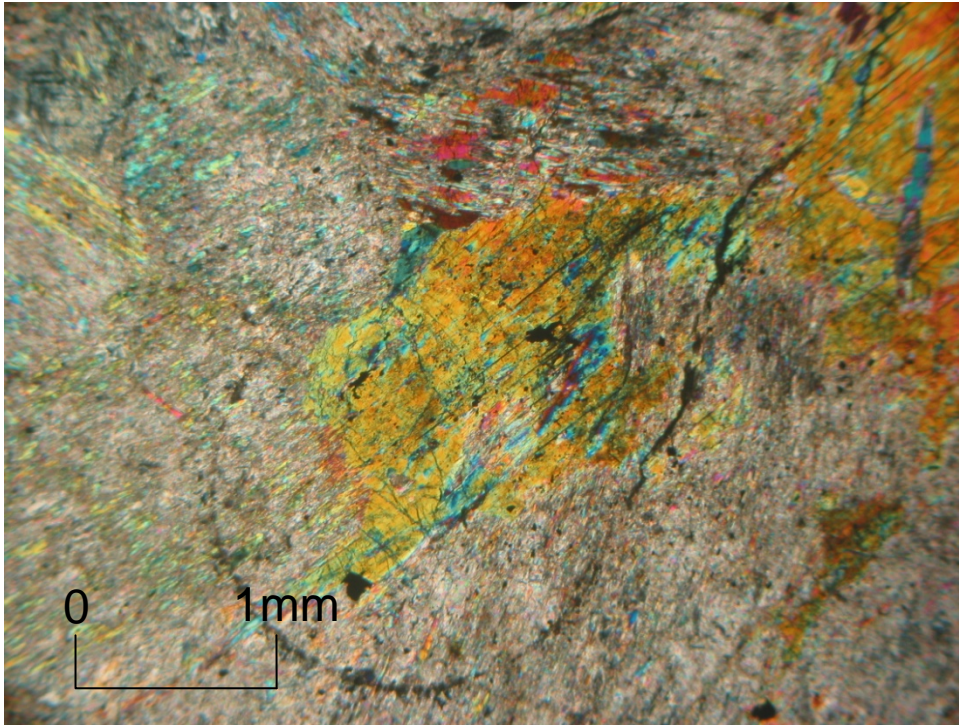


Figure 3.54. Pyroxenite contains tabular, anhedral, randomly oriented pyroxene that has been pervasively talcose-altered and incipiently tremolitized. Sample 232257 is from 87.49 m in DDH FW-08-19.



Figure 3.55. Pyroxenite occasionally contains disseminated chromite in the form of wispy interstitial chromite and bands that are finer grained than chromite in dunite. Sample is from 102.7 m in DDH BT-09-17. Diameter of core is 46.7 mm.

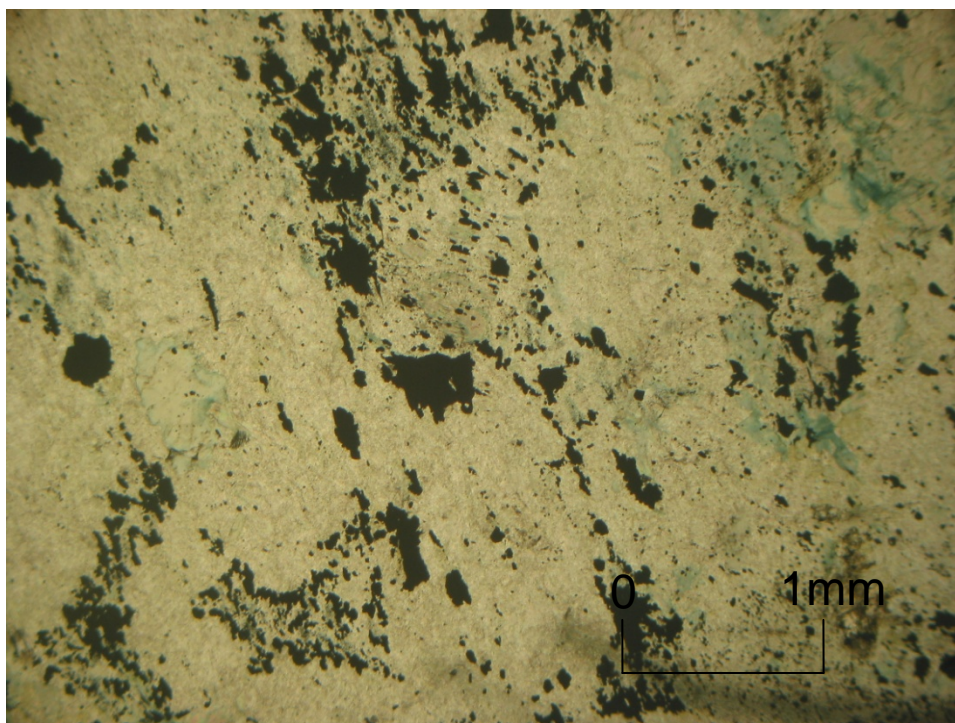


Figure 3.56. Disseminated interstitial chromite in pyroxenite occurs in a vermicular habit in a groundmass of talc and is retrogressed at the margins in contrast to regular euhedral chromite in dunite. Sample 232270 is from 165.38 m in DDH FW-08-19.



Figure 3.57. Green aphyric unit (middle core tube) is pale green and aphanitic with often the occurrence of clumps of euhedral plagioclase crystals (not shown in this sample). Sample is from 309.4 m in DDH BT-11-197. Diameter of core is 46.7 mm.

dunite is probably indicative of chromite mineralizing with a pulse of pyroxenite. The occurrence of chromitite above the pyroxenite can be explained by additions of new pulses of dunite overlying the pyroxenite. All this is more akin to a mixture of magmas involved with mineralization as proposed by Irvine (1977) and Irvine et al. (1983). In thin section, the chromites in the pyroxenites, although inferred to be cumulus, do not display igneous textures since the minerals have been obliterated at the edges and within the grains by replacement pyroxene.

There are sometimes green, aphanitic chloritized to talc-altered aphyric layers within the pyroxenite. Often these layers are found near the tops of the pyroxenites proximal to the leucogabbro, but have also been found within the pyroxenite sequences. The interlayers mostly have a green aphanitic chloritized groundmass that may contain a few plagioclase phenocrysts in clumps (Fig. 3.57). These layers have been interpreted to be komatiite by Leshner, C.M. (pers. communication, 2011). Sometimes there are plagioclase phenocrysts in the layers as shown by white, up to 0.5cm wide augen to oval shaped aggregates foliated in the pyroxenites at the tops of massive pyroxenite sequences. Weathering of the feldspars leaves behind vesicles in an orange weathered and talcose altered interlayer. Examples of these drill holes include DDH FW-12-93, -94, -97, -106, and -112.

Another examination of these green aphyric units shows that they are products of the hornfelsing of lamprophyre dikes against pyroxenite. In DDH FNCB-13-032, there is an abundance of these units in a pyroxenite interval from 667 to 672 m depth in the hole. Ultramafic-mafic dikes are described as consisting of light aqua-green, aphyric, aphanitic chlorite with sharp margins with pyroxenite. In larger dike sets, there is first green chlorite at the contact with pyroxenite and dark brown very fine grained biotite alteration in the interiors of the dikes. Then inner from the biotite zone is a fresh textured amphibole-feldspar fine grained lamprophyre dike. So zoning is from pyroxenite → talc phyllonite pyroxenite → sharp contact → green chlorite → brown biotite → amphibole-feldspar mafic dike to → brown biotite → green chlorite → sharp contact → talc phyllonite pyroxenite → pyroxenite. The green chlorite-biotite seen in these units is therefore the thermal aureole of a lamprophyre dike on the pyroxenite.

3.10 *Gabbro-Leucogabbro*

In DDH BT-09-17, there is biotite gabbro cross-cutting the chromitite in the upper parts of the Black Thor deposit. The unit is a salt and pepper textured, medium- to coarse-grained, massive gabbro that contains dominant white cumulus plagioclase and lesser green rounded up to 5 mm cumulus tremolite after early crystallizing orthopyroxene (Fig. 3.58). The green tremolites are in turn rimmed by and occur in association with finer tabular to needly brown biotite after late igneous amphibole. In thin section, the tremolites have high birefringence, two oblique cleavages and sometimes have a radial fibrous habit. The tremolites are surrounded by tabular, brown pleochroic biotite (Fig. 3.59). The plagioclase crystals occur as colourless twinned tabular crystals with cloudy sausserite alteration and overprinted by blue epidote, zoisite and albite alteration after primary plagioclase. Titanite and hexagonal to columnar apatite are accessory (Fig. 3.60). There appears to be a zonation from brown primary biotite to sericite on the margins to the central green tremolite. The tremolites contain centres of dark green lamellae that are remnants to be from titanium of primary pargasitic hornblende (Fig. 3.61). There is accessory magnetite.

The rock may be called leuconorite since there are a few occurrences of coarse cumulus bronzite. The tremolite:biotite:plagioclase ratio is dominantly 40:30:30 and ranges to 00:20:80 leucogabbro. The unit contains the coarsest bronzite orthopyroxene with finer tremolite at the base of the sequence at 299 m depth. Upward, there is more fine grained brown biotite in association with coarse green tremolite. Plagioclase increases up to 80 modal % by 309.80 m and then the rock is finer grained tremolite-dominant with plagioclase at 30 modal %. Unlike the ultramafic layered series the gabbro roof appears relatively fresh and unaltered. There is approximately 1-2 modal % pyrrhotite + pyrite + chalcopyrite. The chromitites that are cross-cut by the gabbro are massive and contain sharp contacts with the gabbro.

Leucogabbro is a massive light grey feldspar and quartz-phyric plagioclase-orthopyroxene cumulate overlying the pyroxenite that dominates the upper differentiated lithologies of the intrusion (Fig. 3.62). The contact of leucogabbro with pyroxenite is often faulted with either a mylonite as in DDH FW-11-83 or a hematized fault breccia as in DDH BT-11-185. In other drillholes such as DDH FW-11-87, the contact between

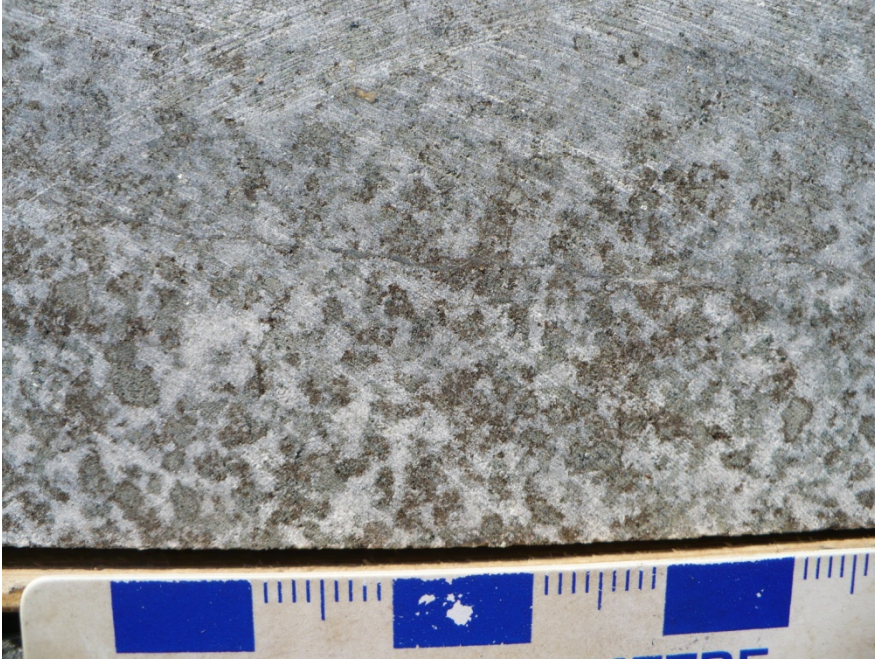


Figure 3.58. Gabbro is a salt and pepper textured, medium- to coarse-grained unit with white cumulus plagioclase and lesser green rounded up to 5 mm cumulus tremolite after early crystallizing orthopyroxene. The green tremolites are in turn rimmed by and occur in association with finer tabular to needle brown biotite after late igneous amphibole. Sample is from 314.87 m in DDH BT-09-17.

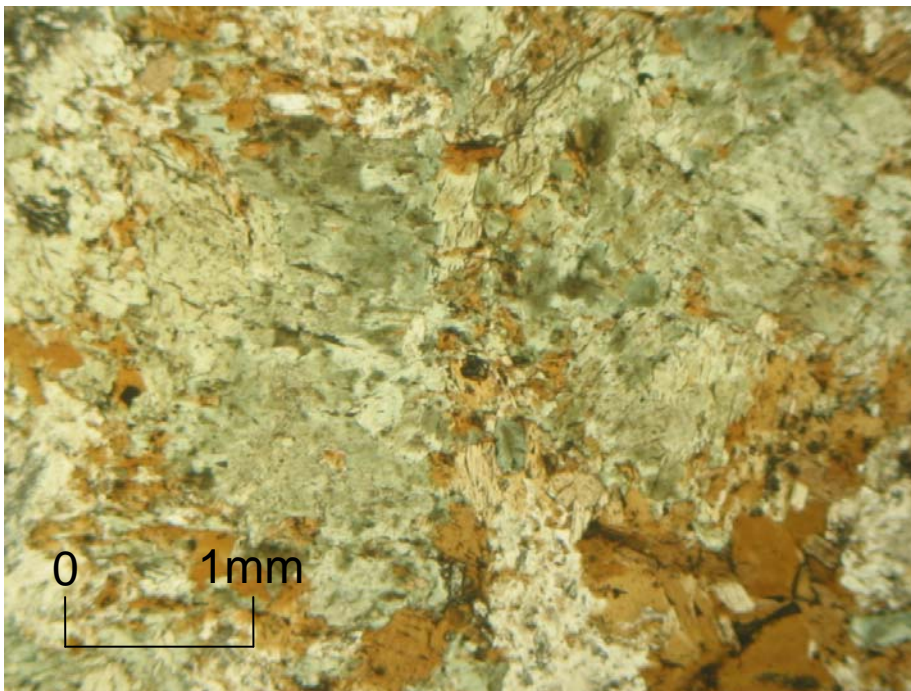


Figure 3.59. In thin section, green tremolites are surrounded by tabular, brown in PPL, one cleavage biotite laths. The tremolite-biotites are in turn surrounded by colourless plagioclase. Sample 486679 is from 299.6 m in DDH BT-09-17.

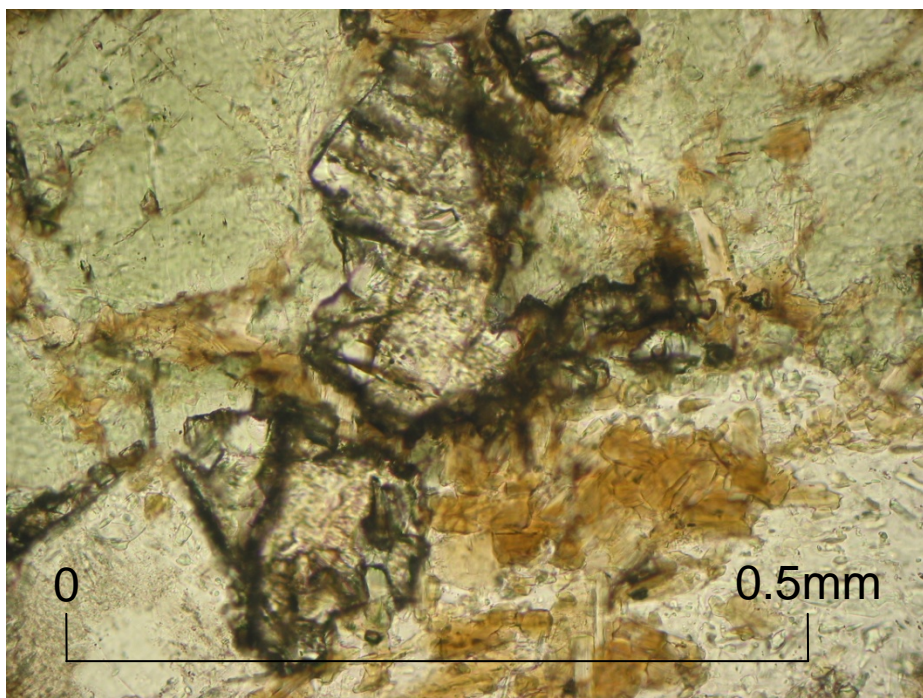


Figure 3.60. There is also titanite alteration (brown, high relief) with hexagonal to columnar apatite (small white crystals in the titanite) present in the gabbro that relates to higher temperature upper greenschist facies alteration. Sample 486679 is from 299.6 m in DDH BT-09-17.

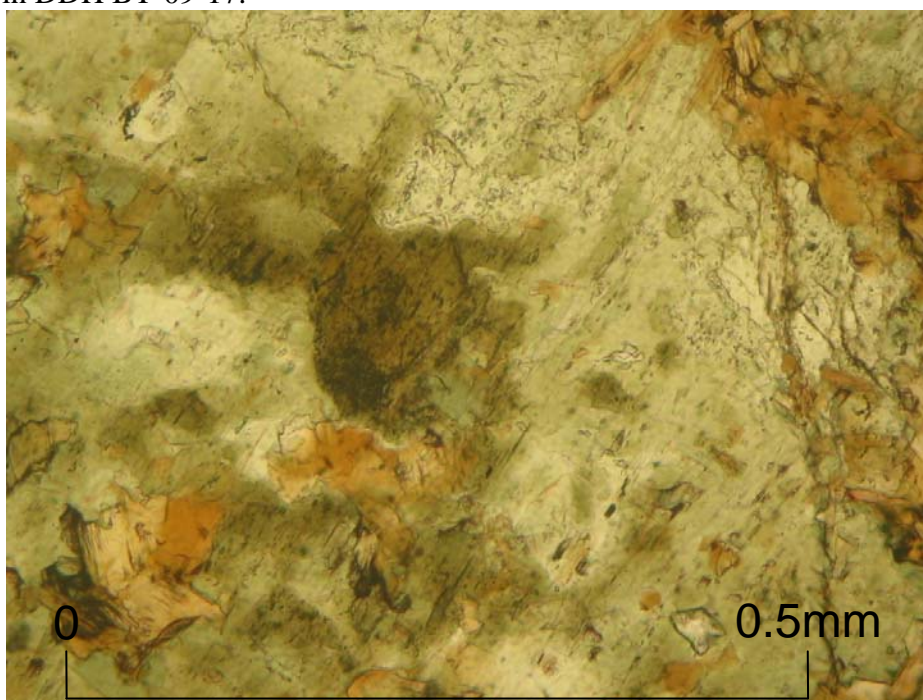


Figure 3.61. The tremolites contain deep green central patches with lamellae that are interpreted to be from titanium ions in late paragonitic hornblende. Sample 486679 is from 299.6 m in DDH BT-09-17.



Figure 3.62. Leucogabbro is a massive light grey feldspar and quartz-phyric plagioclase-orthopyroxene cumulate. Sample is from 483.65 m in DDH BT-09-37.

leucogabbro and pyroxenite is marked by the disappearance of feldspar in the pyroxenite, but having a gradation from the pyroxenite to leucogabbro in terms of the same tremolitized cumulus pyroxene.

The leucogabbro above the pyroxenite in DDH BT-11-185 begins with a fine to medium grained dark vs. light pyroxene gabbro or gabbro which lacks the medium to coarse feldspar. After the basal gabbro, there is leucogabbro with a feldspar content of 30 modal % in proportion to surrounding darker green tremolitized pyroxene. This is followed by a coarse silicified section of feldspar and quartz veins in pyroxene from 47 to 40 m in that hole. From 43.26 to 37 m, the leucogabbro contains veiny to patchy coarser grained feldspar-quartz silicification. From 37 to 31.53 m, there is leucogabbro with a 75:35 pyroxene to feldspar composition. Porphyritic feldspars are up to 0.5 cm wide grains. This section continues to 29 m depth in that hole. Sometimes pink feldspar is observed making the unit locally granophyric.

3.11 Hangingwall mafic metavolcanic

Mafic volcanic occurs when the leucogabbro loses its feldspar, becomes very fine grained grading into mafic volcanic lithology. The appearance of a gradational contact supports the idea that the gabbro is melted roof rock rather than being a differentiate of the ultramafic intrusion. The gradation of gabbro into mafic volcanic could be due to assimilation of wallrock mafic volcanic by gabbro. In DDH BT-11-200, the mafic volcanic is first medium grey like the groundmass of the gabbro, but progressively becomes darker green-grey chloritized down the hole. From 656.82 to 660.15 m, the unit is a true dark green basalt with 12 modal % clotty pyrrhotite mineralization. From 660.15 to the end of the hole at 684 m, the basalt is light green-grey chloritized with quartz banding, coarse quartz veins and interlayers of pegmatitic leucogabbro. In DDH BT-11-194, the metabasalt is green chloritized and aphanitic with Cross-cutting pink feldspar veins. From 678 to 684 m in DDH BT-11-200, the volcanic is recrystallized with medium grained feldspar at a composition of 60:40 chlorite to feldspar.

CHAPTER 4

GEOCHEMISTRY

4.1 Introduction

The geochemistry of the McFaulds Lake Intrusion is presented as whole rock geochemistry of major oxides, analyses of major element variation in previous assays, trace element geochemistry, full spectrum PGE analysis of host rock and chromite and electron microprobe mineral chemical analysis of silicates. Trace element and rare earth element analyses were performed on the same representative whole rocks reported for the three chromite deposits. Results are listed in Appendix 3.

4.2 Whole rock geochemistry

Whole rock geochemical analysis was carried out on 26 drill core samples from four drill holes that represent the three deposits: DDH FW-08-19 for Big Daddy; BT-08-10 for Black Thor; and BT-09-31 for Black Label. Two of the samples were collected from DDH BT-09-17 to represent the upper gabbro at Black Thor. Previous bulk rock geochemistry reported by Spider-KWG-Freewest and Freewest databases have been examined and interpreted along with this data. Full results are listed in Appendix 3. Discussion of bulk rock geochemical trends is for major element oxide and trace element/REE.

4.2.1.1 Major oxides

The lithologies analysed for major oxides include dunite, oikocrystic harzburgite, heterogeneous olivine pyroxenite, pyroxenite and gabbro. Results are displayed in Table 4.1.

The Black Label dunite is the most primitive of the intrusion with an MgO content of 41 to 45 wt. % MgO. The Black Thor dunitites is also primitive with 40 to 41 wt. % MgO. The Big Daddy dunite is more evolved with 36 to 41 wt. % MgO. The evolution in the Big Daddy dunitites is likely due to differentiation as there was a greater

Table 4.1: Major oxide wt. % in DDH samples.

Big Daddy	SiO₂ wt. %	TiO₂ wt. %	Al₂O₃ wt. %	FeO wt. %	CaO wt. %	MgO wt. %
Dunite	35 to 41	0.07 to 0.11	0.9 to 3.5	12 to 18	0.03 to 0.54	36 to 41
Heterogeneous pyroxenite	44	0.08	2.0	14	0.68	38
Pyroxenite	48 to 55	0.12 to 0.20	2.0 to 3.6	9 to 16	0.3 to 6.5	26 to 31
Black Thor						
Dunite	40 to 41	0.08 to 0.09	2.0 to 2.1	12 to 13	0.2	40 to 41
Pyroxenite	46 to 55	0.06 to 0.13	1.4 to 2.5	10 to 12	0.04 to 2.4	30 to 40
Gabbro	51 to 53	0.6 to 1.02	16 to 18	7 to 8	4.7 to 8.1	7 to 11
Black Label						
Dunite	34 to 42	0.05 to 0.10	0.7 to 3.0	13 to 15	0.01 to 0.2	41 to 45
Oikocrystic harzburgite	36 to 44	0.07 to 0.22	1.3 to 3.8	14 to 18	1.0 to 1.6	33 to 39
Pyroxenite	42	0.22	4.9	12	9.0	27

subset sampled in that drill hole. The dunites show degrees of crustal contamination, as evidenced by a source magma chemistry with high Cs, Ba and Rb contents. Notably, the dunites from the Big Daddy suite are located more proximal to the basement tonalite. All the dunites of the three deposits have low wt. % CaO and Al₂O₃ due to lack of pyroxene crystallization. Notably, the wt. % FeO contents is more elevated in the dunite than pyroxenite due to higher Fe in olivine.

The pyroxenites are distinctly more evolved than the dunites with 26 to 40 wt. % MgO. The Black Thor pyroxenites are the most primitive with 30 to 40 wt. % MgO. The more primitive pyroxenite combined with the primitive dunite at Black Thor makes this the most primitive of the three deposits. In contrast, the Black Label pyroxenite sample is much more evolved at 27 wt. % MgO. The Big Daddy pyroxenite is generally more evolved like Black Label. Although, there are more evolved pyroxenites in Big Daddy, the trace element geochemistry of the Big Daddy pyroxenites suggests they have a primitive source like that at Black Thor. Therefore, although there is more contamination in the Big Daddy suite, overall, the setting of the Big Daddy is more primitive and more like Black Thor than Black Label in terms of geochemistry of the pyroxenite.

Transitional lithologies like heterogeneous olivine pyroxenite and oikocrystic harzburgite are local to the Big Daddy and Black Label suites respectively. Heterogeneous pyroxenite does not just occur at Big Daddy, but in the other deposits as well. The sample selected from Big Daddy is representative of the transitional chemistry between dunite and pyroxenite. As will be observed in the major element trends of Big Daddy, the heterogeneous pyroxenite probably formed as a result of uptake of olivine in pyroxenite from the lower dunite followed by the replacement of olivine by pyroxene in these samples. The MgO content of the heterogeneous pyroxenite is at 38 wt. % and contains more pyroxene with higher Al₂O₃ content at 2.0 wt. % and SiO₂ content at 44 wt. %.

Oikocrystic harzburgite, an olivine cumulate with poikilitic pyroxene that is transitional from the dunite to pyroxenite in Black Label, has 33 to 39 wt. % MgO. Pyroxene is evident by the elevated Al₂O₃ and CaO contents of 4.9 and 9.0 wt. % respectively. Although there is higher CaO content, this probably reflects the tremolitization of primary orthopyroxene. Relic pyroxenes have parallel extinction

diagnostic of orthopyroxene. The Ca content of tremolite is derived from CO₂ fluid metasomatism

The two samples of gabbro proximal to the upper chromitite at Black Thor are much more evolved than the other samples due to modal plagioclase. SiO₂ contents vary between 51 and 53 wt. % and Al₂O₃ contents vary between 16 to 18 wt. %.

4.2.1.2 Up section major oxide variation

4.2.1.2.1 Black Label: DDH BT-09-31

Geochemical trends in major oxide variation are best represented by the major element plots based on reported assays for the three drill holes. A stratigraphic column of lithologies is presented for each drill hole for all the following variation plots. The legend for the lithologies is the same as that presented on the drill sections of the holes (Figs. 3.1 to 3.4). Major element variation is demonstrated for the lithologies bordering the chromitites of the three deposits. The Black Label interval begins at a depth of about 150 m (Figs. 4.1 to 4.3). From 150 to 164.70 m, there is elevated Mg % in heterogeneous olivine pyroxenite. Then from 164.70 to 203.50 m, there is the main chromitite interval composed of clasts of oikocrystic pyroxenite as wavy bands in a semi-massive chromitite. There are various replenishments of chromitite in this interval as indicated by peaks in Mg % content. Fe % varies inversely in the chromitite as it substitutes with Mg %. After 203.50 m, there is pyroxenite that contains decreased Mg % while increased Ca % and Al % content. The next interval begins at 228 m. From 228 to 237 m, there is oikocrystic harzburgite with generally high Mg % content due to dominance of cumulus olivine. Within this unit, Mg % decreases with height probably due to differentiation. Ca and Al % contents are intermediate since there is both olivine and pyroxene in the unit. From 237 to 270 m, there are intermittent chromitite beds with replenishments as evidenced by peaks in Mg % and Fe % content. Al % is elevated as it varies with Cr content. After 270 m, there is dunite that is characterized by decreased Al % and increased Mg % content. The last interval from 306 to 320m intersects the last beds of chromite within a dominant dunite sequence. Fe and Al % contents are elevated in association with Cr content.

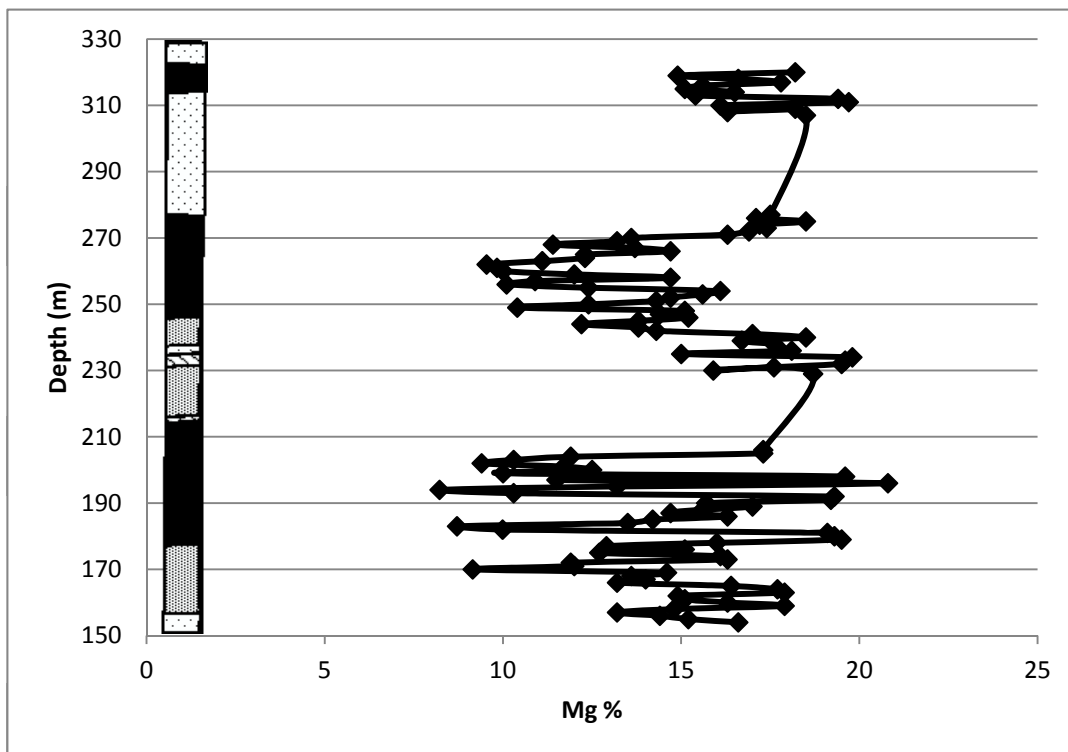


Figure 4.1. Plot of Mg % vs. depth (m) from assays of Black Label DDH BT-09-31 with stratigraphic column. See Figure 3.1 for legend.

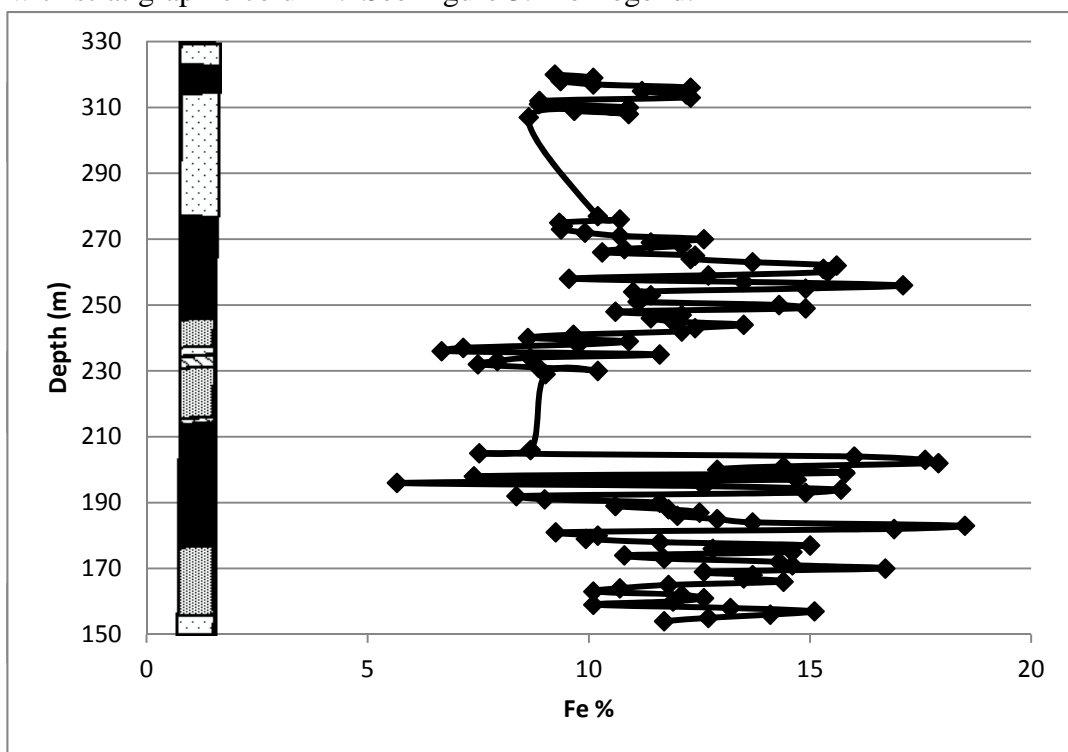


Figure 4.2. Plot of Fe % vs. depth (m) from assays of Black Label DDH BT-09-31 with stratigraphic column. See Figure 3.1 for legend.

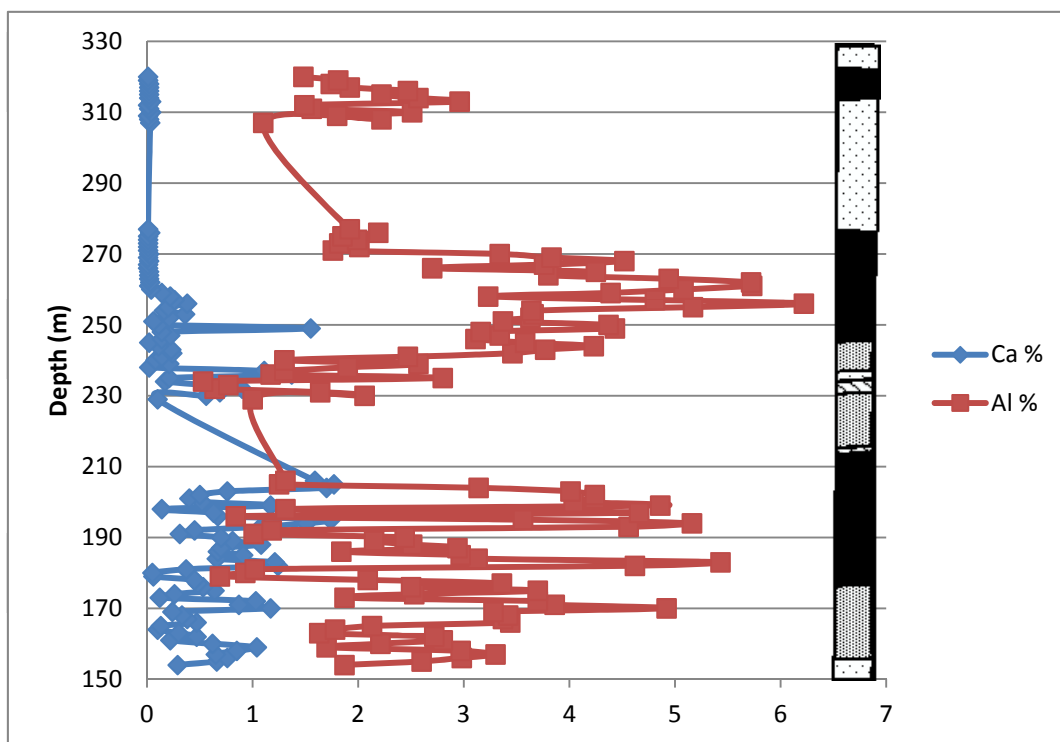


Figure 4.3. Plot of Ca % and Al % vs. depth (m) from assays of Black Label DDH BT-09-31 with stratigraphic column. See Figure 3.1 for legend.

4.2.1.2.2 Black Thor: DDH BT-08-10 & BT-09-17

The major oxide variation across Black Thor is shown for DDH BT-08-10, beginning with dunite at 94 m depth (Figs. 4.4 to 4.6). From 94 to 124.70 m, there is general decreasing Mg % and Fe % with depth indicative of a differentiating dunite pulse. From 124.70 to 168.20 m, there are various intermittent to semi-massive beds of chromite alternating with cumulus olivine dunite. Mg % increases in the areas of cumulus olivine and is lower in content within the chromite beds. Fe % peaks in these chromite beds is due to more silicate exchange in disseminated chromite as opposed to massive chromitite. From 155 to about 160 m, there is a trend of decreasing Mg % indicative of magma evolution in a chromitite interval. Fe % is antipathetic to Mg % and increases with substitution as the chromites become more evolved. Another Mg % and Fe % trend occurs from 168.20 to 174.20 m, where there is a section of massive chromitite with lower Mg % content. This shows a trend of decreasing Mg % and increasing Fe % with depth in the chromite interval indicative of magma evolution in the chromitite. Above the chromitite from 174.20 to 187.10 m, there is dunite showing a large replenished increase in Mg % content. Al % generally increases directly with Cr content within the drill hole sequence,.

Samples from DDH BT-09-17 are different than samples from the other drillholes as chromitite is related to pyroxenite intruded by upper gabbro. The interval of interest that contains the upper chromitite is from 290 to 345 m (Figs. 4.7 to 4.9). The interval begins with a pyroxenite above the previous chromitite layer at 290 m. The pyroxenite contains high Mg % but lower Al % and Ca % contents in comparison to the overlying gabbro. From 296.30 to 298.80 m, there is the first chromitite horizon sandwiched between pyroxenite and gabbro. The chromitite is distinguished by a peak in Fe % in comparison to low Fe % in background pyroxenite and gabbro. Above the chromitite there is gabbro with elevated Ca % and Al %. From 298.80 to 318.70 m, there is a trend of decreasing Al % from 8.4 to 7.8 %. This represents evolution in anorthite content of plagioclase to lower anorthite with height. A trough in Al % at 304 m coincided with high Ca % which represents abundance of tremolitized pyroxene over plagioclase. Higher up in the gabbro from 311 to 318.70 m, there is increased Ca % with the fractionation of pyroxene in association with plagioclase. Notably, the wt. % SiO₂ and

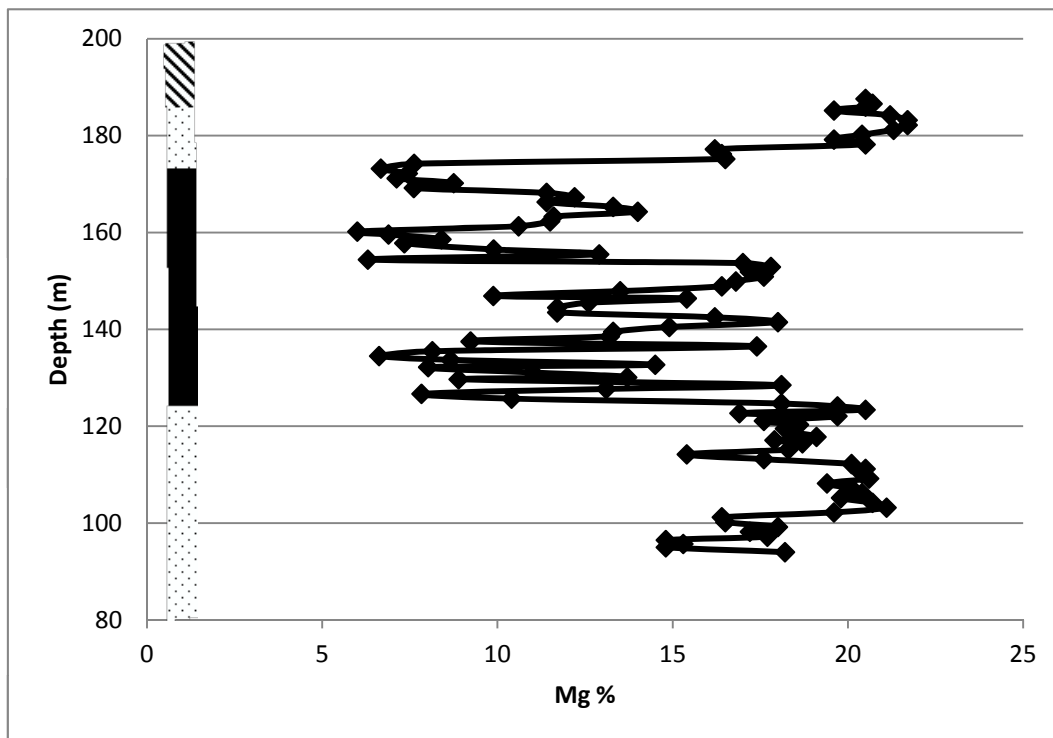


Figure 4.4. Plot of Mg % vs. depth (m) from assays of Black Thor DDH BT-08-10 with stratigraphic column. See Figure 3.1 for legend.

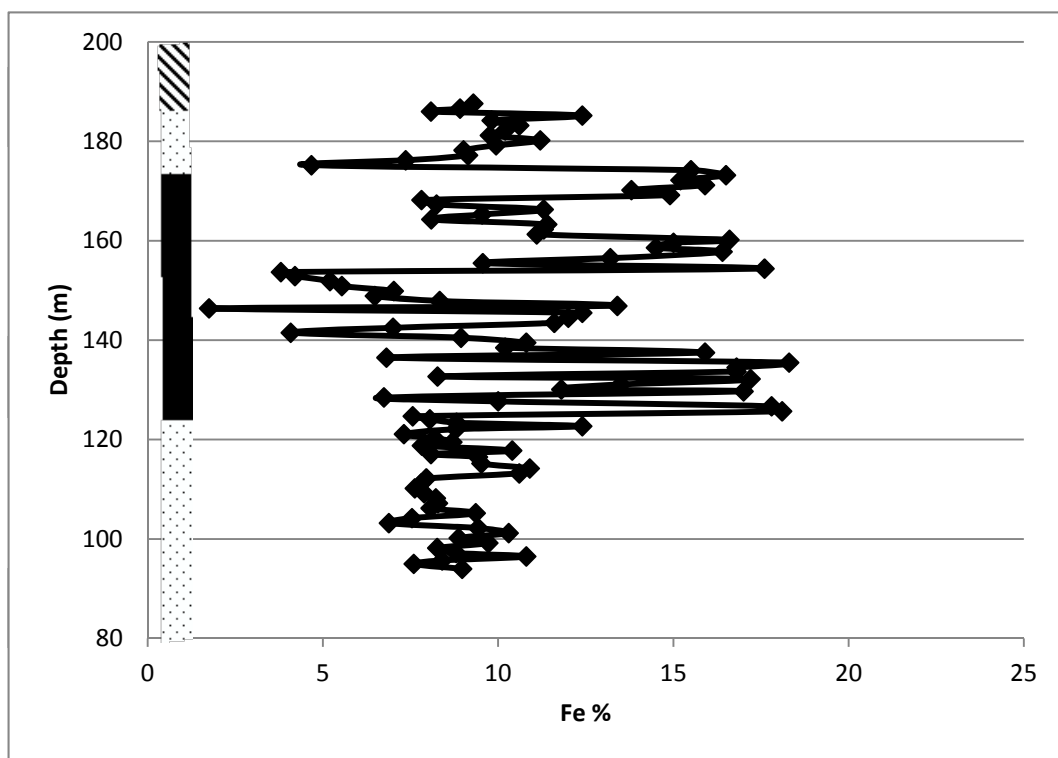


Figure 4.5. Plot of Fe % vs. depth (m) from assays of Black Thor DDH BT-08-10 with stratigraphic column. See Figure 3.1 for legend.

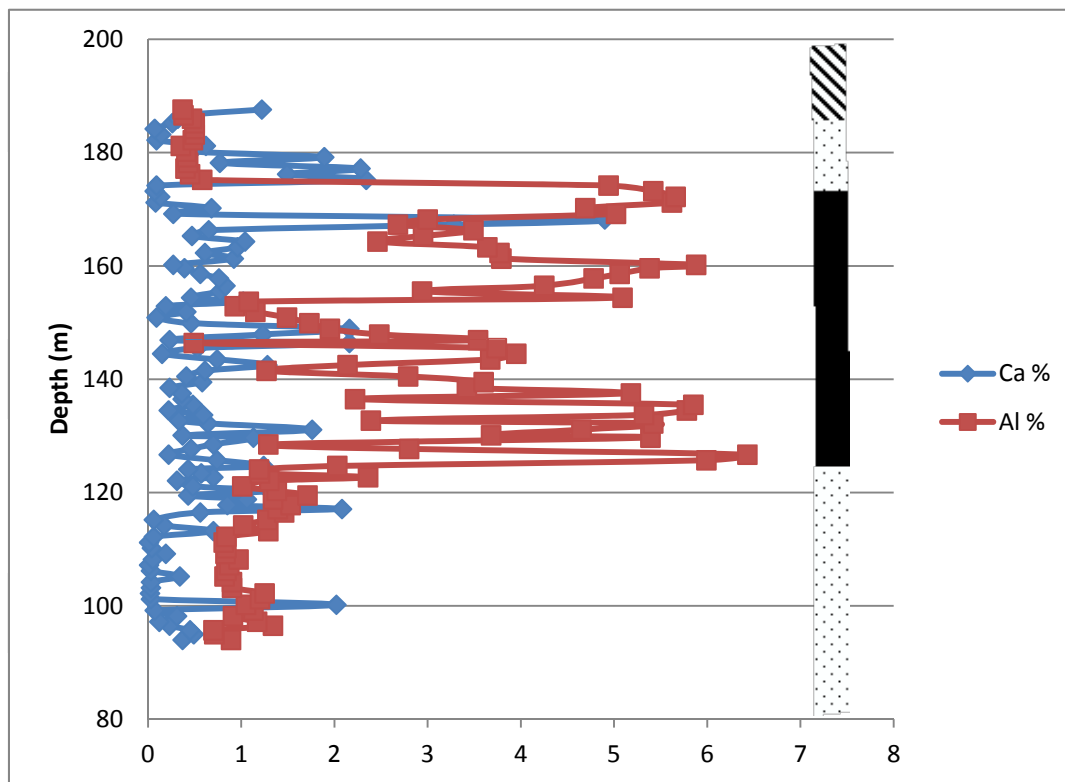


Figure 4.6. Plot of Ca % and Al % vs. depth (m) from assays of Black Thor DDH BT-08-10 with stratigraphic column. See Figure 3.1 for legend.

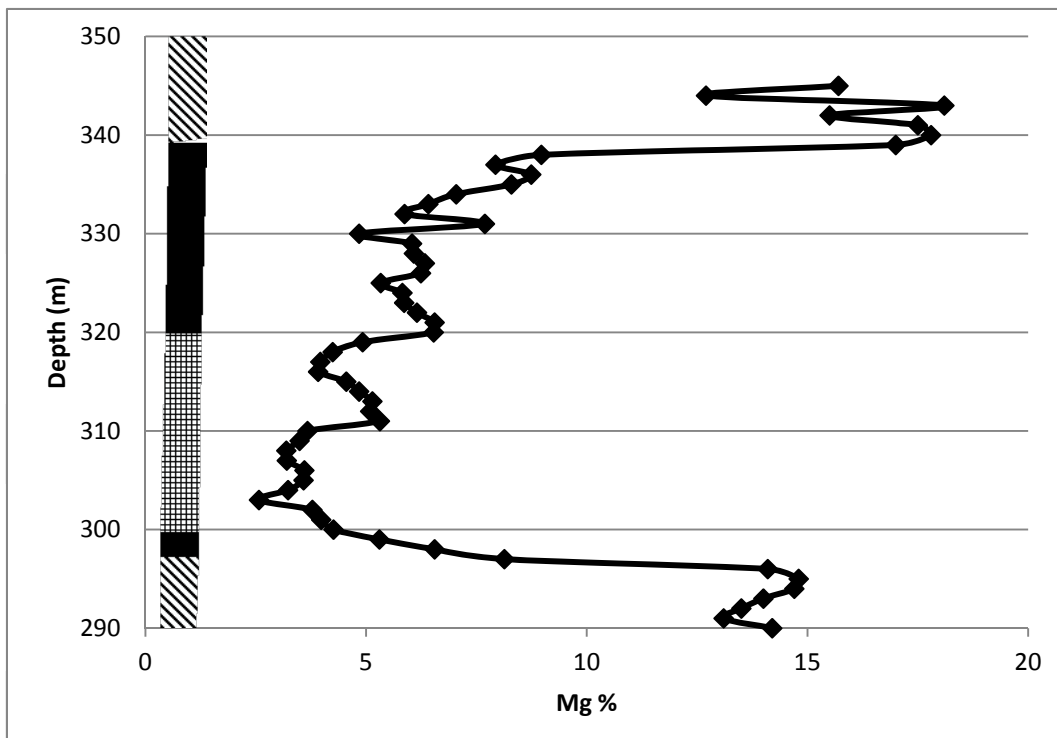


Figure 4.7. Plot of Mg % vs. depth (m) from assays of Black Thor DDH BT-09-17 with stratigraphic column. See Figure 3.1 for legend.

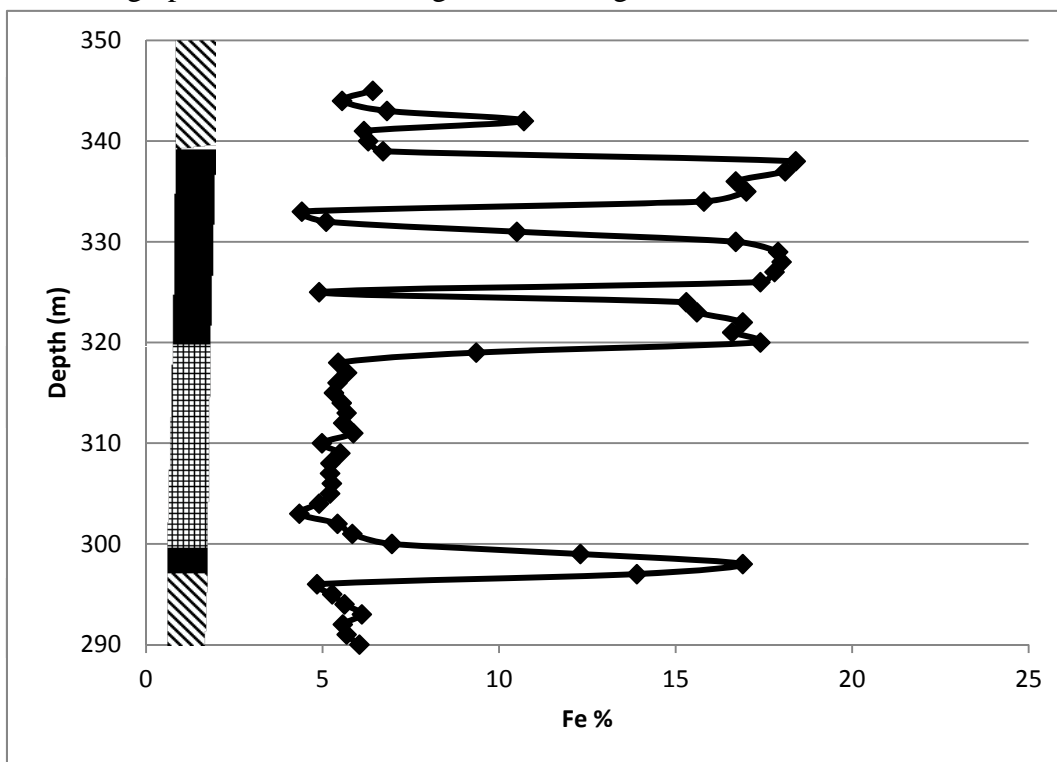


Figure 4.8. Plot of Fe % vs. depth (m) from assays of Black Thor DDH BT-09-17 with stratigraphic column. See Figure 3.1 for legend.

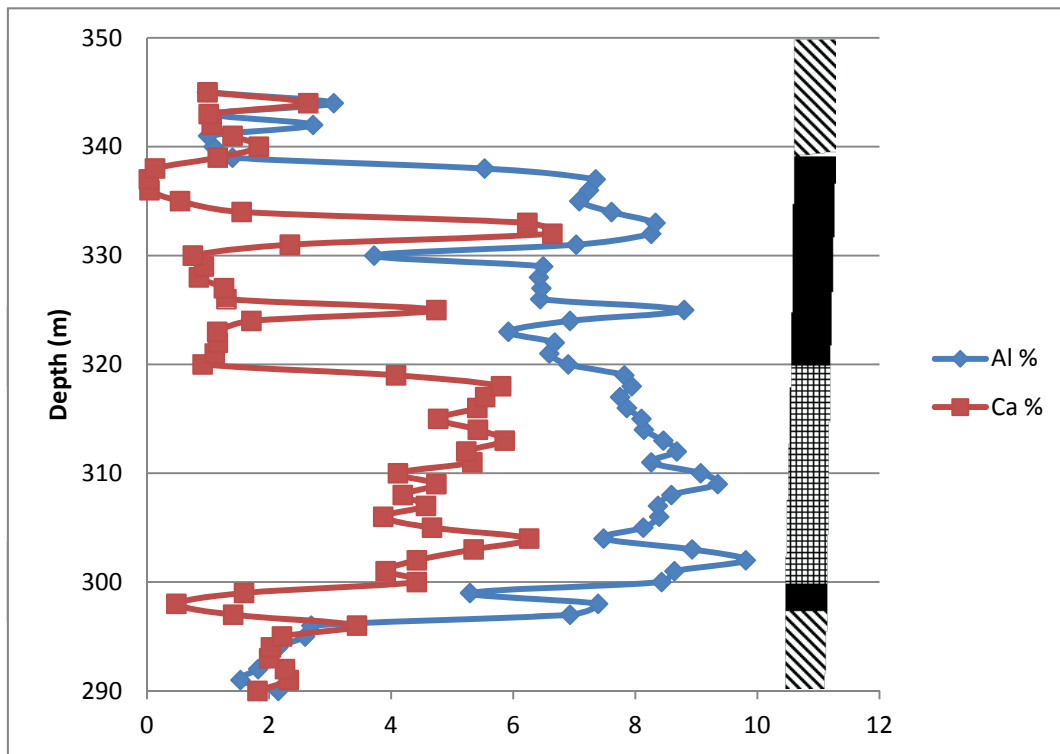


Figure 4.9. Plot of Ca % and Al % vs. depth (m) from assays of Black Thor DDH BT-09-17 with stratigraphic column. See Figure 3.1 for legend.

Na₂O contents increase upward in this section with evolution of the gabbro, well demonstrated by the increase in wt. % SiO₂ and Na₂O in the two gabbros analysed. The increase in modal % pyroxene is also evident by increase in Mg % upward in the gabbro. The main chromitite interval, from 318.70 to 337.90 m, is characterized by peaks in Fe %. There appears to be a decreasing trend in Mg % in the first chromite pulse from 318.70 to 325 m which may be due to differentiation. However, in the above pulses there is increased Mg %. The higher Mg % contents may be due to retrogression of the chromites to higher Mg % along with higher Al % as there is reduction in Fe with heat of the gabbro. Above the chromitite from 337.90 to 345 m, there is again pyroxenite with high Mg % and low Ca and Al %.

4.2.1.2.3 Big Daddy: DDH FW-08-19

Big Daddy is represented by DDH FW-08-19. From 9 to 64.50 m, there are three increases in Mg % that probably represent three replenishments of olivine cumulus magma to form dunite that alternates with pyroxenite (Fig. 4.10 to 4.11). From 64.50 to 100 m, there appears to be a megapulse of dunite, as evident by an overall decreasing trend in Mg %. Within this sequence are two pulses of decreasing Mg % with height from dunite to pyroxenite. They are from 64.50 to 73.97m and 73.97 to 105.39 m. Two replenishment trends of increased Mg wt. % occur in the interval of heterogeneous olivine pyroxenite from 105.39 to 129 m and from 129 to 141.50 m. With increased Mg %, there is generally elevated Fe % due to olivine content. From 141.50 to 144.14 m, there is semi-massive chromite with cumulus pyroxene. From 144.14 to 159.37 m, there is replenishment in Mg % with a dunite pulse. From 159.37 to 162.00 m, there is massive chromitite characterized by no Si % along with Fe % and Al % peaks. There is heterogeneous pyroxenite with elevated Mg %. from 162.00 to 164.20 m. From 164.20 to 183.00 m, there is a drop in Mg % in a new pyroxenite sequence. Notably, there is increased Ca % in the pyroxenite due to presence of tremolite and also increased Al % as Al substitutes into the pyroxene structure. From 183.00 to 229.64 m, there is the main section of massive chromitite. Within this sequence, there is an overall decreasing trend of Mg % while an increasing trend Fe % as Fe substitutes with Mg in the chromite structure. The overall decreasing Mg % trend is due to evolution from bottom to top of

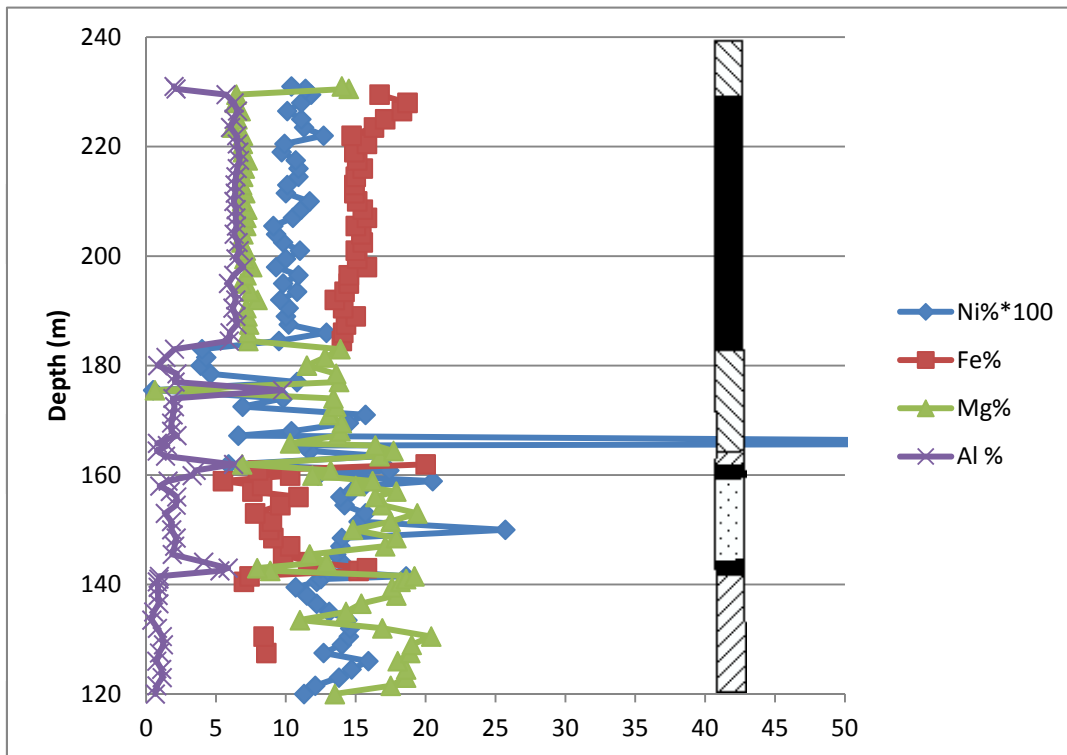


Figure 4.10. Plot of Ni %*100, Fe %, Mg % and Al % vs. depth (m) from assays of Big Daddy DDH FW-08-19 with stratigraphic column. See Figure 3.1 for legend.

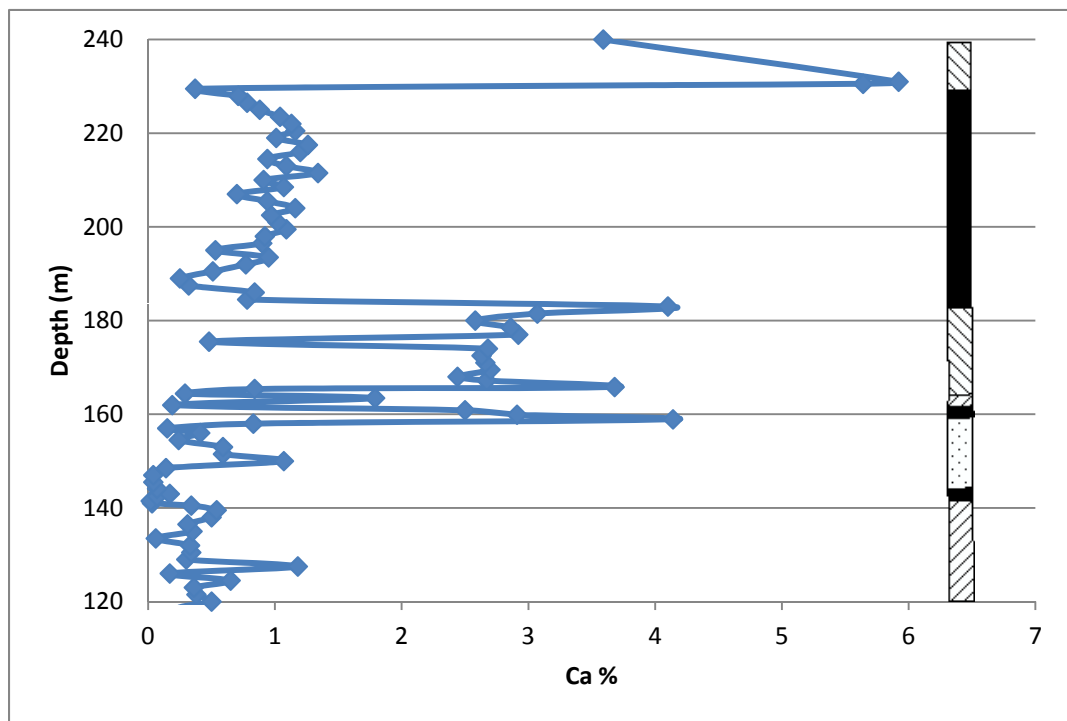


Figure 4.11. Plot of Ca % vs. depth (m) from assays of Big Daddy DDH FW-08-19 with stratigraphic column. See Figure 3.1 for legend.

the chromite sequence. Although there are trends of Mg and Fe %, Al % stays relatively constant at 6.5 wt. % Al. Above the chromitite is pyroxenite with elevated Ca %.

4.2.1.3 Binary major oxide variations

4.2.1.3.1 Black Label (Fig. 4.12)

The Black Label deposit displays variation to more evolved compositions, both in more evolved chromite and more pyroxene in the system. On a Cr ppm vs. Mg % plot, there is a general trend of decreasing Cr with increasing Mg %, reflective of more cumulus chromite and less cumulus olivine. On a Cr ppm vs. Al % plot, there is a convex upward trend of increasing Cr ppm with increasing Al % content. Again, with increased Cr, there is increased Al with substitution. The leveling off at the high Cr end of the plot is due to the effect of interstitial poikilitic pyroxene providing chromitite more exchange with higher aluminous compositions.

For Cr ppm vs. Fe %, there is a large spread of values over a general increasing Cr with increasing Fe % trend. There is increased Fe % with increased chromite content as before. However, the large spread in compositions is due to the increase in the amount of ferrichromite in the Black Label deposits as opposed to the other deposits. Since ferrichromite is non-igneous, there is no general enrichment trend in its origin. Where there is semi-massive chromite with interstitial silicate, there is greater amount of enriched Fe-bearing ferrichromite due to silicate-oxide exchange during hydration.

Igneous evolution in the Black Label chromitite is displayed well by linear negative correlative trends of decreasing Al and Fe % with Mg %. The decreases are due to substitution with Cr and Mg respectively and the predominance of those elements in more massive chromite-bearing vs. disseminated chromite-bearing cumulates.

There is no correlation on the Ca % vs. Mg % plot. There are however a large amount of Ca-enriched lithologies on a broad range of Mg % due to tremolite in more pyroxene-bearing lithologies. There is, in contrast, less pyroxene in the Big Daddy and Black Thor intercepts. Notably, the pyroxenes were probably more affected by Ca metasomatism during hydration to cause irregularity in the Ca signatures.

4.2.1.3.2 Black Thor (Fig. 4.13)

The Black Thor deposit shows more complete evolution in major element variation between the less chromite-bearing disseminated and the more massive

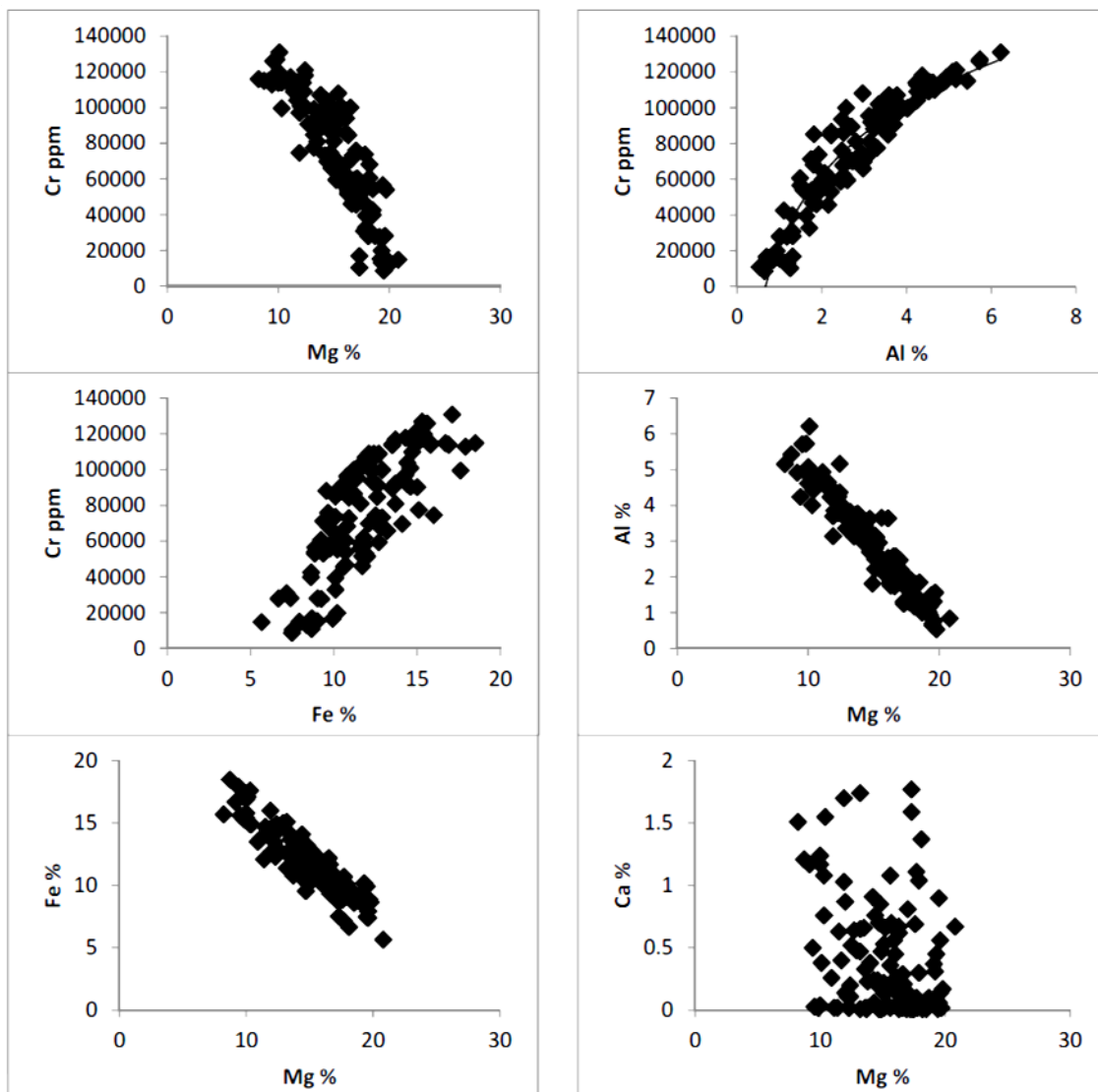


Figure 4.12. Binary plots of Cr vs. Mg, Cr vs. Al, Cr vs. Fe, Al vs. Mg, Fe vs. Mg and Ca vs. Mg from assays of Black Label DDH BT-09-31.

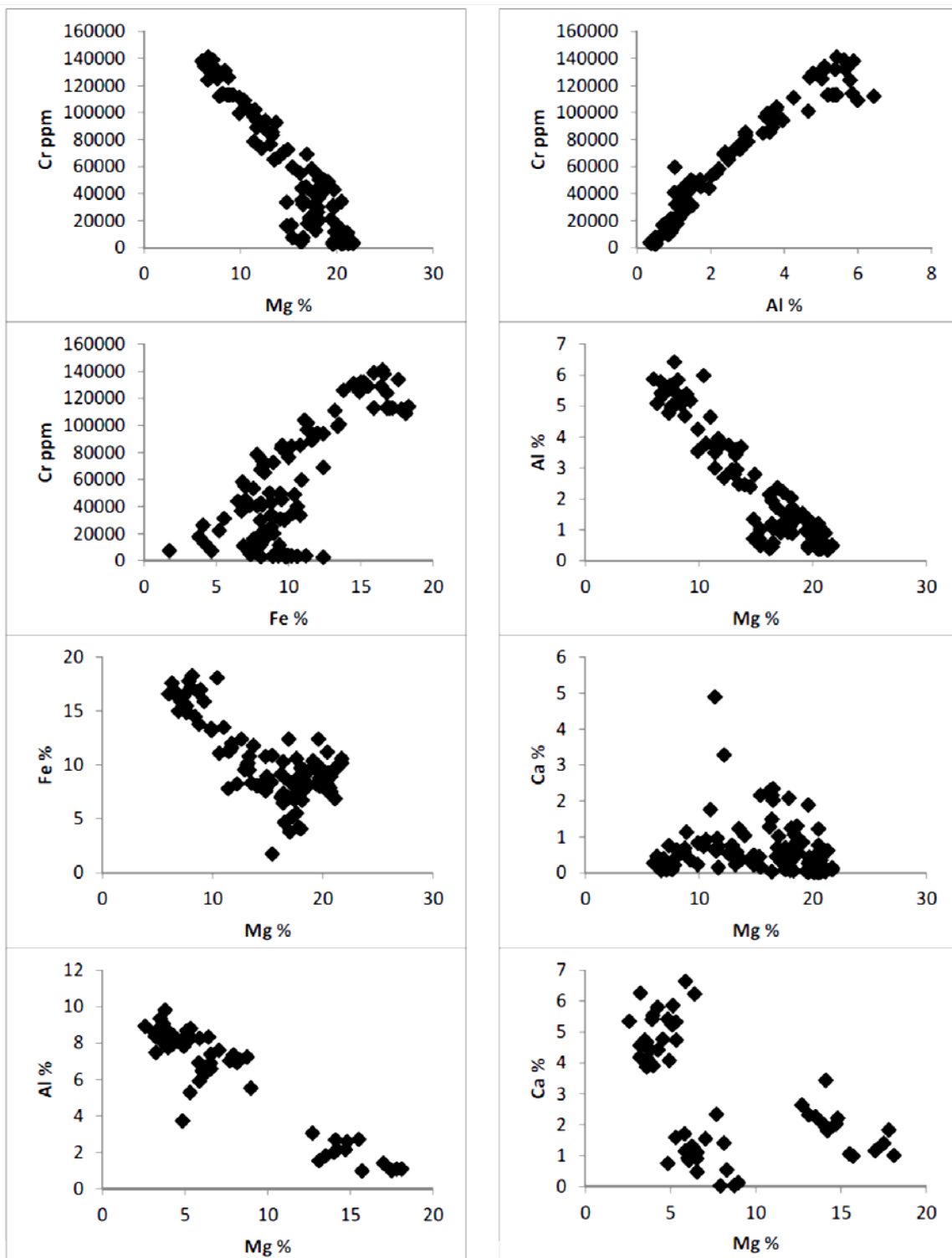


Figure 4.13. Binary plots of Cr vs. Mg, Cr vs. Al, Cr vs. Fe, Al vs. Mg, Fe vs. Mg and Ca vs. Mg from assays of Black Thor DDH BT-08-10. The bottom two plots are of Al vs. Mg and Ca vs. Mg from assays of Black Thor DDH BT-09-17.

chromite-bearing lithologies. On the Cr ppm vs. Mg % plot, there is a distinct negative correlation of increasing Mg % with decreasing Cr ppm. This trend reflects the greater Cr ppm in the more massive chromites vs. the more evolved disseminated chromites that have undergone silicate exchange. The trend of decreasing Cr ppm with differentiation is characteristic of chromite deposits of layered intrusions such as Bushveld (Stowe, 1994). With increased evolution of the chromitite, there is increasing Al content as well due to Cr-Al substitution in the individual chromites.

For Cr ppm vs. Fe %, there is also a trend of increasing Fe % with Cr ppm with magma evolution in the chromitites – the more massive chromitites containing less Fe % due to more primitive compositions. There is an increasing trend of Fe % in many of the less Cr-bearing lithologies due to increased Fe % in the olivine of dunite. At the high Cr-bearing end, there are also some high Fe-bearing chromitites or chromite-olivine cumulates that plot off the trend. These are representative rims on primary chromites that have been retrogressed leaving behind Cr-enriched and Fe-enriched ferrichromites on the rims of the primary chromites.

The Al % vs. Mg % plot shows a distinct negative correlation of decreasing Al % with increasing Mg %. This trend is also evident of the magma evolution in the chromitites where the more massive chromitites have greater Al % than the more primitive Mg-rich chromite-olivine cumulates. This is again due to Cr-Al substitution, the more chromite in the rock, the higher the Al content. Fe varies similarly with Mg as it does with Cr, only in an inverse way. There is another evolutionary trend of the more chromite-bearing lithologies containing more Fe % content. Again, some Mg-enriched dunitites contain elevated Fe within the olivine. Also, there is enrichment in Fe % at the low Mg % end that goes above the trend due to enriched Fe in ferrichromite-bearing chromitites.

The Ca % vs. Mg % plot, enrichment in Ca % shows no correlation. Enrichment in Ca % is probably due to secondary tremolite replacement of pyroxene. Notably, there are two outliers of high Ca-bearing lithologies which are intercumulus pyroxene-bearing semi-massive chromitites.

A few binary trends are useful for analyzing the composition of the gabbro vs. chromitite vs. pyroxenite in DDH BT-09-17. On a Al % vs. Mg % plot, igneous

evolution occurs with increasing Al % from pyroxenite to gabbro. The massive chromitite plots with intermediate Al % and Mg % compositions between the gabbro and pyroxenite. On a Ca % vs. Mg % plot, the gabbros plot at higher Ca % than the pyroxenite due to plagioclase controlled fractionation. The relatively low Ca % of the pyroxenite is indicative of predominant orthopyroxene fractionation.

4.2.1.3.3 Big Daddy (Fig. 4.14)

On binary variation plots, the Big Daddy deposit shows trends of magma evolution from the most primitive dunite through to the heterogeneous olivine pyroxenite to the chromitite and associated pyroxenite lithologies. Below the 2 % Cr mark on a Cr ppm vs. Mg % plot, chromite increases slightly with increasing Mg % up to 21 % Mg. Most of the data from the dunite plot in an area of chromite accumulation below a line of increasing Cr with Mg %. However, with evolution of the units, there is also a large negative correlation of Cr with Mg %. At the high Cr end of the trend, there is a cluster representative of the samples in the massive chromitite interval. Between the massive chromitite and the dominant cumulus olivine dunite lithologies are fewer intermediate lithologies that contain intermediate (semi-massive) chromite with intermediate Mg content between massive and disseminated chromite. This shows a direct negative correlation of Cr with decreasing modal % chromite. The observation of there being high Cr and low Cr-bearing clusters with few intermediate compositions shows the “it’s massive or it’s not there at all” nature of the Big Daddy chromitite as seen in this drill hole.

The Cr ppm vs. Al % plot shows a positive correlation of Cr ppm and Al % content. Therefore, there will be more partitioning of Al into the spinel structure as opposed to dunite that contains little Al %. Notably, the massive enriched chromitite contains the highest Al % content. This is probably due to silicate exchange with the surrounding dominant pyroxenite host lithology. The same correlation exists between Cr ppm and Fe % as Fe % increases with evolution of the chromitites.

The Al % vs. Mg % plot shows Al % generally increases with decreasing Mg % as there is more Al % in the chromitites than in the other lithologies. Pyroxenites with lower Mg % content also have elevated Al % content due to Al substitution into pyroxene. Fe % increase with decreasing Mg % content is not as obvious since many

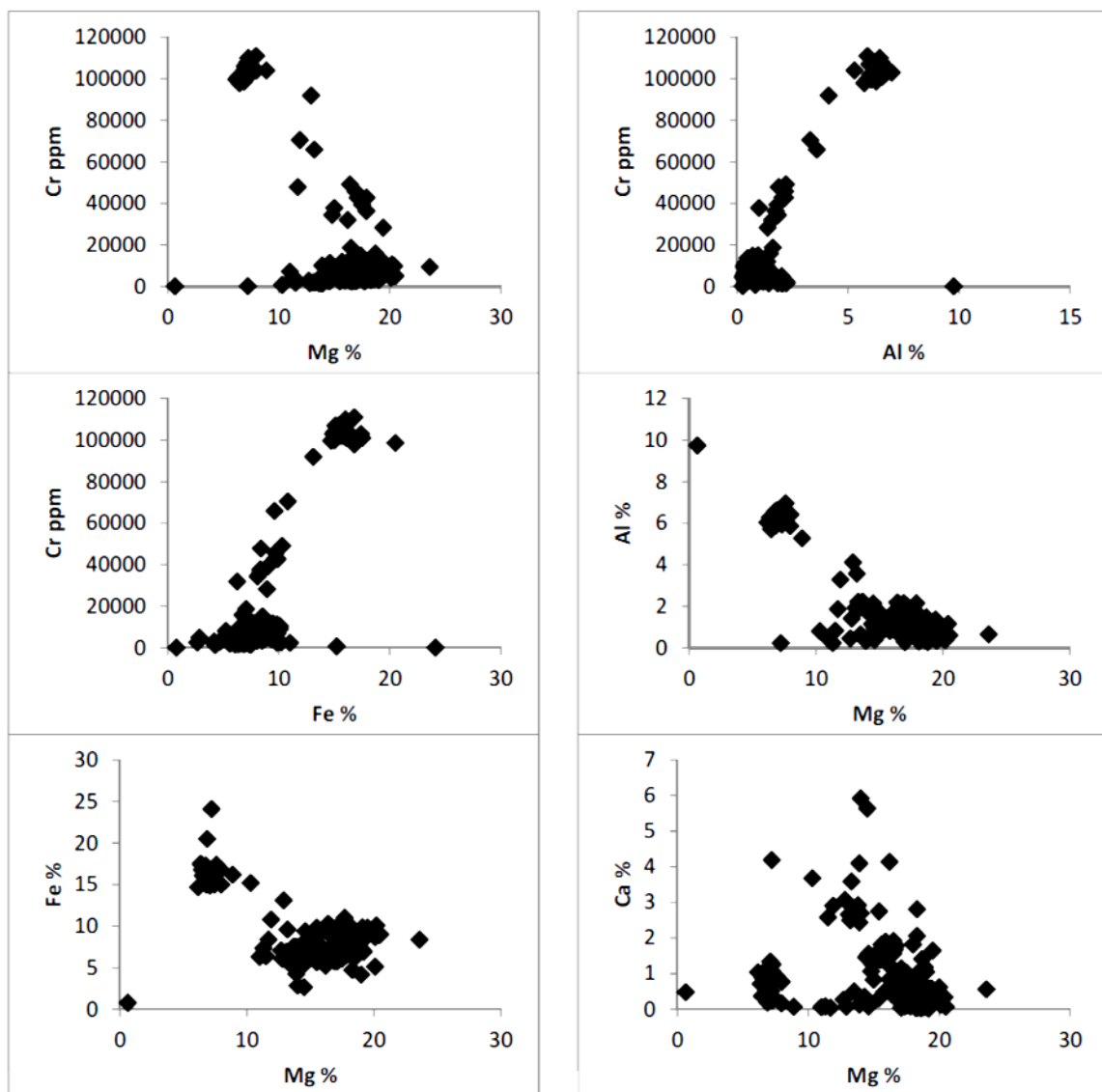


Figure 4.14. Binary plots of Cr vs. Mg, Cr vs. Al, Cr vs. Fe, Al vs. Mg, Fe vs. Mg and Ca vs. Mg from assays of Big Daddy DDH FW-08-19.

samples contain more pyroxene which have lower Fe % contents. Generally, the more chromite, the more Fe content due to its partitioning in the spinel structure.

The Ca % vs. Mg % plot identifies a broad increase of Ca % content in the more evolved pyroxene-bearing lithologies as opposed to the dunites. The Ca is not admitted into the spinel structure, so the olivine-chromite cumulus and massive chromite-bearing lithologies have limited Ca % content.

4.2.2 Trace element geochemistry

4.2.2.1 Primitive mantle-normalized multielement plots

4.2.2.1.1 Black Label

The Black Label chromite deposit is hosted in the main dunite and pyroxenite sequences stratigraphically lower than Black Thor. On a PM-normalized diagram, the Black Label dunite is the most primitive with the lowest overall REE (Fig. 4.15). They were probably the first units to crystallize among the host rocks to the three chromite deposits. The dunites are enriched in light rare earth elements (LREE) relative to heavy rare earth elements (HREE) and contain negative Nb-Ta, negative Zr-Hf, and positive Ti anomalies. These collectively indicate crustal contamination of komatiite. For trends in REE, the dunites and oikocrystic harzburgites show LREE enrichment over middle rare earth elements (MREE) with $(La/Sm)_{cn}$ ratios between 1.94 and 4.70, MREE depletion over HREE with $(Gd/Yb)_{cn}$ ratios of 0.68 to 1.05, and $(Eu/Eu^*)_{cn}$ ratios of 0.41 to 1.50. $(La/Sm)_{cn}$ ratios have an average ratio of 3.02 which is slightly larger than Big Daddy and larger than Black Thor. The ratios are similar to Big Daddy, only the overall REE are lower in the Black Label dunites.

LREE enrichment in Black Label identifies crustal contamination of an original komatiite as such LREE and LILE enrichment is commonly linked to crustal contamination (Leshner, 2005). LREE enrichment coinciding with negative Nb-Ta and Zr-Hf anomalies is due to crustal contamination in komatiites by tonalite-trondhjemite-granodiorite suites (Leshner, 2005 and Hollings & Kerrich, 1999). Low Al tonalities in the North Caribou Terrane have been characterized by LREE enrichment and negative Nb-Ta and Zr-Hf anomalies (Wyman et al., 2011). For the case of Black Label, the LREE enrichment along with enrichment in Cs-Rb-Ba suggests greater degree of crustal contamination in these dunites in contrast to Black Thor. Although the $(La/Sm)_{cn}$ ratios

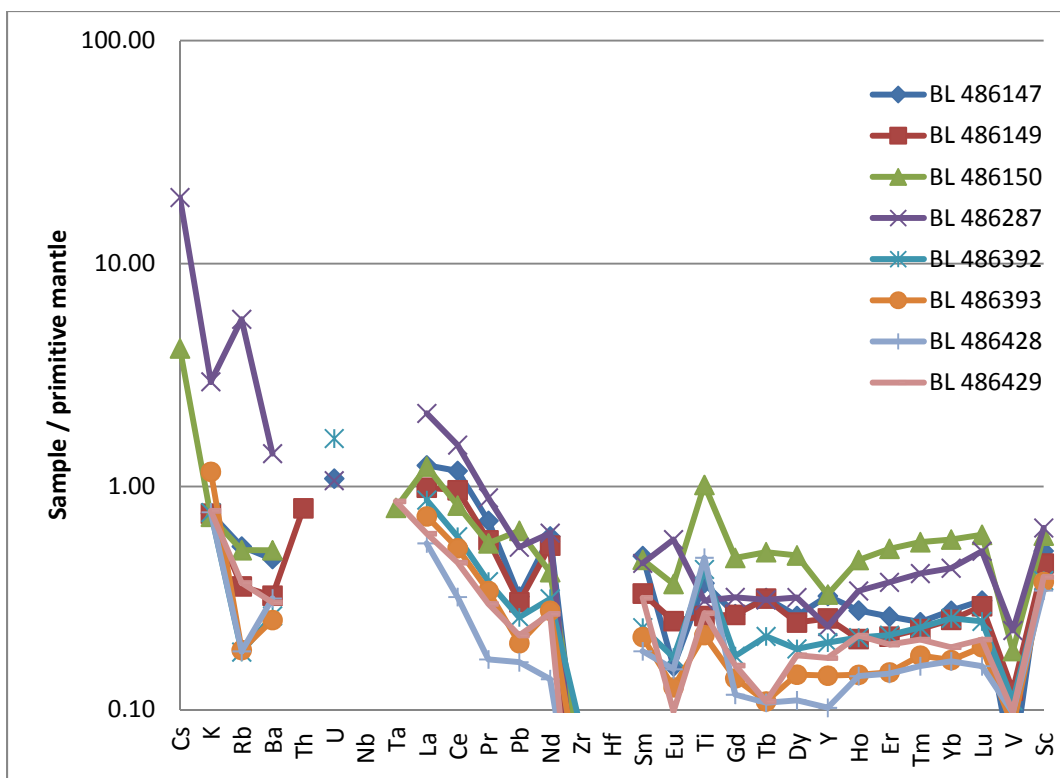


Figure 4.15. Primitive mantle normalized multi-element plot of dunite-harzburgite from Black Label DDH BT-09-31. Normalizing values of McDonough and Sun (1995).

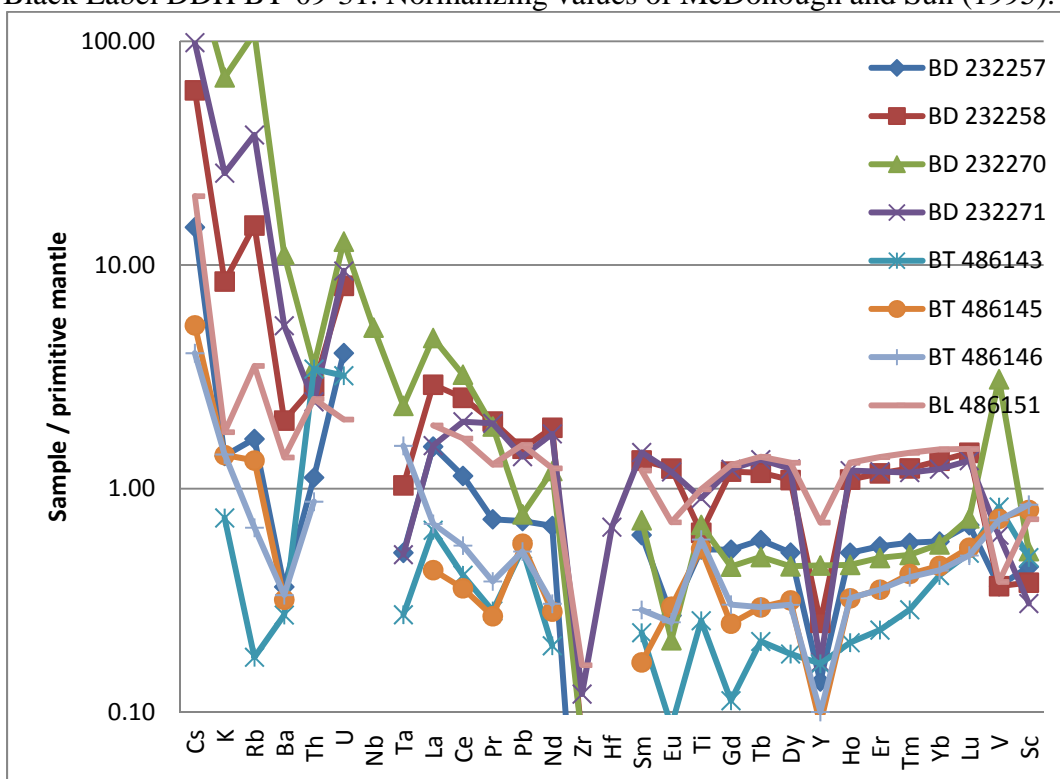


Figure 4.16. Primitive mantle normalized multi-element plot of pyroxenite from all 3 deposits. Normalizing values of McDonough and Sun (1995).

are larger than Black Thor, the Black Label dunites are more primitive with lower abundance in overall REE along with their signature MREE depletion characteristic of primitive aluminum-undepleted komatiite (AUK).

Notably, the REE compositions of the oikocrystic harzburgite samples are intermediate between Black Label dunite and Black Label pyroxenite (Fig. 4.15). The origin of the oikocrystic pyroxene at the top of a dunite sequence is related to the initiation of pyroxene crystallization, following the fractionation of pyroxene-laden magma (pyroxenite) in this sequence. Intermittent beds of chromite have been found associated with these wavy banded oikocrystic units and in DDH BT-11-176, oikocrystic harzburgite units are found in association with the magmatic breccias. The dynamic textures in these units indicate the chromite probably originated with a mixture of pyroxene-laden magma to drive the magma into the chromite field for crystallization. This mixing of pyroxene is suggested by the REE contents being intermediate that of dunite and pyroxenite.

One sample of Black Label pyroxenite was analysed and shows a highly evolved composition similar to the Big Daddy pyroxenite (Fig. 4.16). The sample displays LREE and LILE content that is lower than that of Big Daddy, but higher than Black Thor. The pyroxenite displays slight LREE enrichment relative to HREE and contains negative Nb-Ta, negative Zr-Hf and negative Y anomalies suggestive of crustal contamination. There is LREE enrichment over MREE with $(La/Sm)_{cn}$ of 1.59; MREE depletion over HREE with $(Gd/Yb)_{cn}$ of 0.85, and the $(Eu/Eu^*)_{cn}$ ratio is 0.57.

4.2.2.1.2 Black Thor

The Black Thor chromite deposit is hosted in main dunite with pyroxenite higher in stratigraphy. On a PM-normalized diagram, the Black Thor dunites are enriched in LREE relative to HREE and contain negative Nb-Ta, negative Zr-Hf, and positive Ti anomalies (Fig. 4.17). The dunites display LREE enrichment over MREE with $(La/Sm)_{cn}$ ratios between 1.68 and 2.11, MREE depletion over HREE with $(Gd/Yb)_{cn}$ ratios of 0.64 to 0.83, and $(Eu/Eu^*)_{cn}$ ratios of 0.44 to 0.63. The $(La/Sm)_{cn}$ ratios are lesser than the Big Daddy dunites and are depleted in MREE. The relative LREE non-enrichment is probably reflective of primitive AUK komatiite (Leshner et al., 1999). HREE enrichment over MREE is a characteristic signature of AUK komatiite or boninite (Leshner et al.,

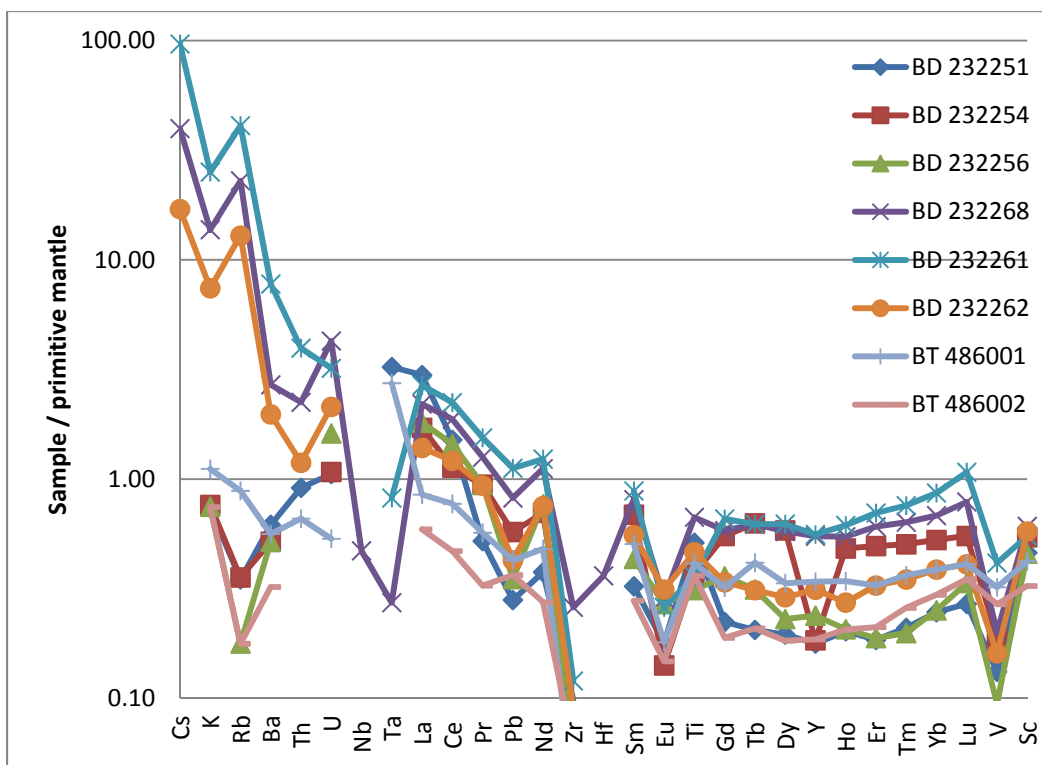


Figure 4.17. Primitive mantle normalized multi-element plot of dunite-harzburgite from Black Thor DDH BT-08-10 and Big Daddy DDH FW-08-19. Normalizing values of McDonough and Sun (1995).

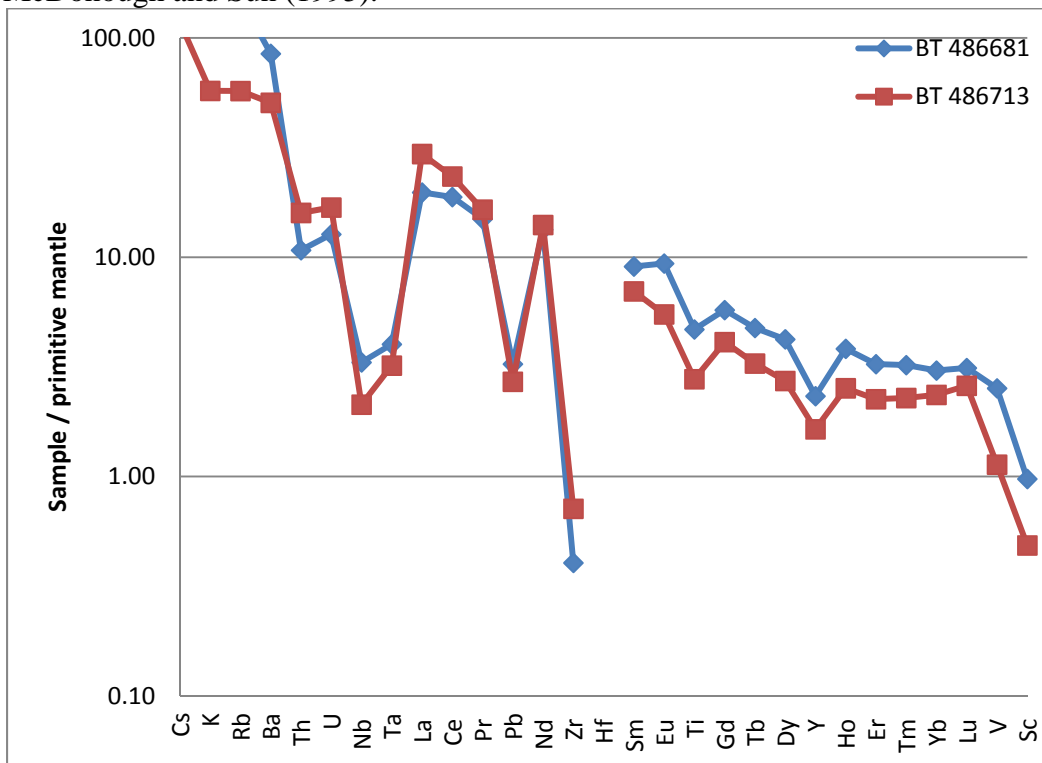


Figure 4.18. Primitive mantle normalized multi-element plot of gabbro from Black Thor DDH BT-09-17. Normalizing values of McDonough and Sun (1995).

1999, Kerrich, 1997 and Barnes, 1989). Like Big Daddy, the rocks show evidence of crustal contamination by TTG with the negative Nb-Ta, Zr-Hf anomalies. However, there is no local contamination as evidenced by depletion LILE of Cs-Rb-Ba, but generally reflective of an AUK signature.

The Black Thor pyroxenites are depleted in overall REE compared to Big Daddy and Black Label and are the most primitive pyroxenites (Fig. 4.16). These pyroxenites are also enriched in LREE relative to HREE and contain negative Nb-Ta, negative Zr-Hf, negative Y and positive Ti anomalies suggestive of crustally contaminated komatiite. The pyroxenites display LREE enrichment over MREE with $(La/Sm)_{cn}$ ratios between 2.42 and 2.87, MREE depletion over HREE with $(Gd/Yb)_{cn}$ ratios of 0.28 to 0.70, and $(Eu/Eu^*)_{cn}$ ratios of 0.51 to 1.42. The MREE are strongly depleted relative to HREE compared to Big Daddy which reflect that of HREE-enriched primitive AUK (Leshner et al., 1999).

In Black Thor DDH BT-09-17, there is gabbro cross-cutting the chromitite and it is located higher in stratigraphy than the pyroxenite. The gabbros are enriched in overall trace elements and REE relative to the other lithologies due their more evolved composition (Fig. 4.18). Although more enriched, the gabbros display similar REE trends of LREE enrichment, negative Nb-Ta, Zr-Hf and Y anomalies as the other lithologies which probably indicate they form an upper differentiate of the same layered intrusion. The negative Nb-Ta along with negative Ti anomalies is related to TTG contaminant. TTGs are considered to be formed by partial melting of hydrous basalt at the base of a thickened oceanic island arc, leaving a rutile-bearing eclogitic residue (Huang et al., 2012). The differences between the gabbros and the other lithologies are that the gabbros do not have HREE enrichment and have negative Ti anomalies: $(La/Yb)_{cn}$ ratios are 6.48 to 12.53 in contrast to an average $(La/Yb)_{cn}$ ratio of 3.60 in the other lithologies. This shows that the gabbros are not komatiitic, but are rather melted roof rocks after mafic volcanics. For REE ratios, the gabbros display LREE enrichment over MREE with $(La/Sm)_{cn}$ ratios between 2.18 and 4.23, MREE enrichment over HREE with $(Gd/Yb)_{cn}$ ratios of 1.74 to 1.89, and $(Eu/Eu^*)_{cn}$ ratios of 0.99 to 1.26.

4.2.2.1.3 Big Daddy

The Big Daddy chromite deposit is hosted in main dunite and pyroxenite lithologies along with transitional heterogeneous olivine pyroxenite. On a PM-normalized diagram, the Big Daddy dunites and heterogeneous pyroxenite are enriched in LREE relative to HREE and contain negative Nb-Ta, negative Zr-Hf, negative Y and positive Ti anomalies (Fig. 4.17). The dunites display LREE enrichment over MREE with $(La/Sm)_{cn}$ ratios between 2.49 and 9.19, MREE slight depletion or enrichment over HREE with $(Gd/Yb)_{cn}$ ratios of 0.76 to 1.43, and $(Eu/Eu^*)_{cn}$ ratios of 0.23 to 0.70. Five of the samples have $(La/Sm)_{cn}$ between 2.49 and 4.18 while sample 232251 with $(La/Sm)_{cn}$ at 9.19 is an exception. The enrichment of LREE to MREE and HREE reflects crustal contamination like that in Black Label. Although HREE are depleted relative to LREE, they are slightly enriched relative to MREE which could reflect an AUK signature (Leshner et al., 1999 and Kerrich, 1997). There are also positive Ti anomalies which would reflect the komatiite. For large ion lithophile elements (LILE) of Cs-Rb-Ba, there is strong enrichment in the Big Daddy dunites reflecting crustal contamination by continental crust. LILE are enriched in continental crust in contrast to depletion in komatiites by themselves (Leshner, 1999). The heterogeneous pyroxenite displays the higher REE content and LILE content than all the dunites and is notably transitional to the higher REE and LILE contents of the Big Daddy pyroxenites.

The Big Daddy pyroxenites are also enriched in LREE relative to HREE, but have more enrichment in overall REE than the dunites (Fig. 4.16). On a PM-normalized diagram, the pyroxenites also contain negative Nb-Ta, negative Zr-Hf, negative Y and positive Ti anomalies and are even more enriched in Cs-Rb-Ba. The samples display LREE enrichment over MREE with $(La/Sm)_{cn}$ ratios between 1.94 and 6.52, MREE slight depletion over HREE with $(Gd/Yb)_{cn}$ ratios of 0.80 to 0.92, and $(Eu/Eu^*)_{cn}$ ratios of 0.36 to 0.97. The negative Nb-Ta, Zr-Hf and positive Ti anomalies reflect crustal contamination in komatiite. Local contamination of the pyroxenites, like the dunites, is reflected by enriched Cs-Rb-Ba.

4.2.2.2 $(La/Sm)_{cn}$ vs. $(Gd/Yb)_{cn}$

A $(La/Sm)_{cn}$ vs. $(Gd/Yb)_{cn}$ plot can be used to distinguish the different host rocks to the three chromite deposits. Most of the samples plot in a $(Gd/Yb)_{cn}$ range from 0.75

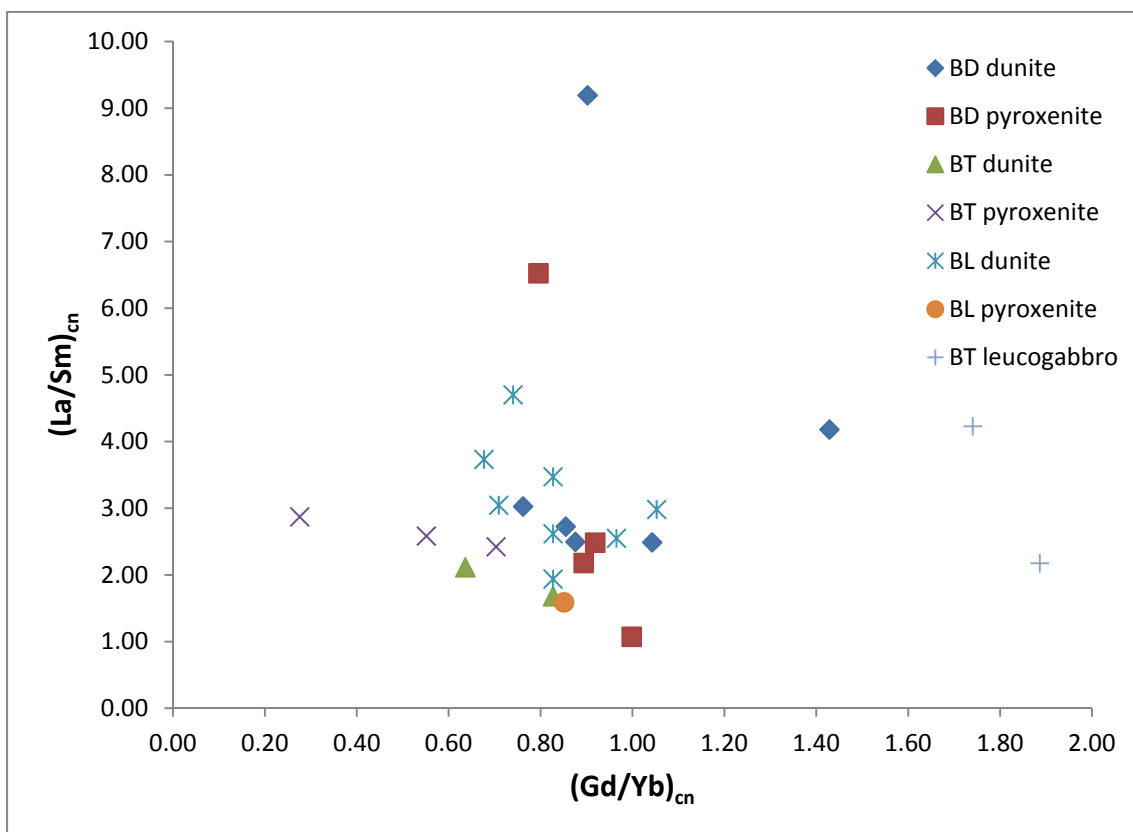


Figure 4.19. Plot of $(La/Sm)_{cn}$ vs. $(Gd/Yb)_{cn}$ for Black Label, Black Thor and Big Daddy host rocks. Normalizing values of McDonough and Sun (1995).

to 1.0 (Fig. 4.19). This range for both dunite and pyroxenite suggests the host magmas to the deposits are aluminum-undepleted komatiites or AUK. AUK at Pykes Hill, Quebec, for example, plot between 0.8 and 1.2 mark whereas aluminum-depleted komatiites (ADK) of the Tisdale suite plot between 1.2 and 1.6 (Kerrick, 1997). Although $(\text{Gd}/\text{Yb})_{\text{cn}}$ falls within the range, the $(\text{La}/\text{Sm})_{\text{cn}}$ ratio will be more enriched in the samples due to crustal contamination by TTG. The $(\text{La}/\text{Sm})_{\text{cn}}$ ratios are from 1.5 to 4.0 rather than near 0.5 for Pykes Hill. For the individual deposits, the Black Label dunites are the most enriched in $(\text{La}/\text{Sm})_{\text{cn}}$ while the Black Thor dunites are the most depleted. There was probably more crustal contamination in Black Label. The Big Daddy dunites are crustally contaminated in the range approaching that of Black Label. For $(\text{Gd}/\text{Yb})_{\text{cn}}$, the Black Thor dunites contain less $(\text{Gd}/\text{Yb})_{\text{cn}}$ than the others and are more primitive in composition. For pyroxenite, Big Daddy and Black Label pyroxenites plot as similar evolved with greater $(\text{Gd}/\text{Yb})_{\text{cn}}$ compositions than the Black Thor pyroxenites.

4.3 Full spectrum PGE analysis

Full spectrum PGE analysis was performed on dunites, pyroxenites and chromitites of the Black Thor, Black Label and Big Daddy deposits. The 26 samples analysed for whole rock geochemistry were also analysed for full spectrum PGE. Six more samples of chromitite were analysed for full spectrum PGE, two from each deposit. Results are listed in Appendix 3.

4.3.1 Primitive mantle normalized PGE plots of host rocks

In comparing the dunites and pyroxenites hosting the three chromite deposits, the dunites are more enriched in IPGE (Os, Ir, Ru) than the pyroxenites, but have similar PPGE (Rh, Pt, Pd). Dunites have $\text{Pd}/\text{Ir}_{\text{mn}}$ contents of 1.60 to 21.98 compared to pyroxenites with $\text{Pd}/\text{Ir}_{\text{mn}}$ contents of 0.65 to 26.2. This is similar to komatiites reported by Barnes et al. (1985) where peridotitic komatiites have Pd/Ir of ~ 10 while pyroxenitic komatiites have Pd/Ir of ~ 30 . The more primitive PGE chemistry of the dunites compared to the pyroxenites is probably due to the higher degree of partial melting in magmas that fractionated the dunites. For individual deposits, the Big Daddy dunites are more enriched in PPGE than the Black Thor dunites indicating there was more sulphur saturation in the Big Daddy lithologies (Fig. 4.20). The Big Daddy dunites have $\text{Pd}/\text{Ir}_{\text{mn}}$ contents of 6.49 to 21.98 compared to Black Thor dunites with $\text{Pd}/\text{Ir}_{\text{mn}}$ contents of 1.60 to

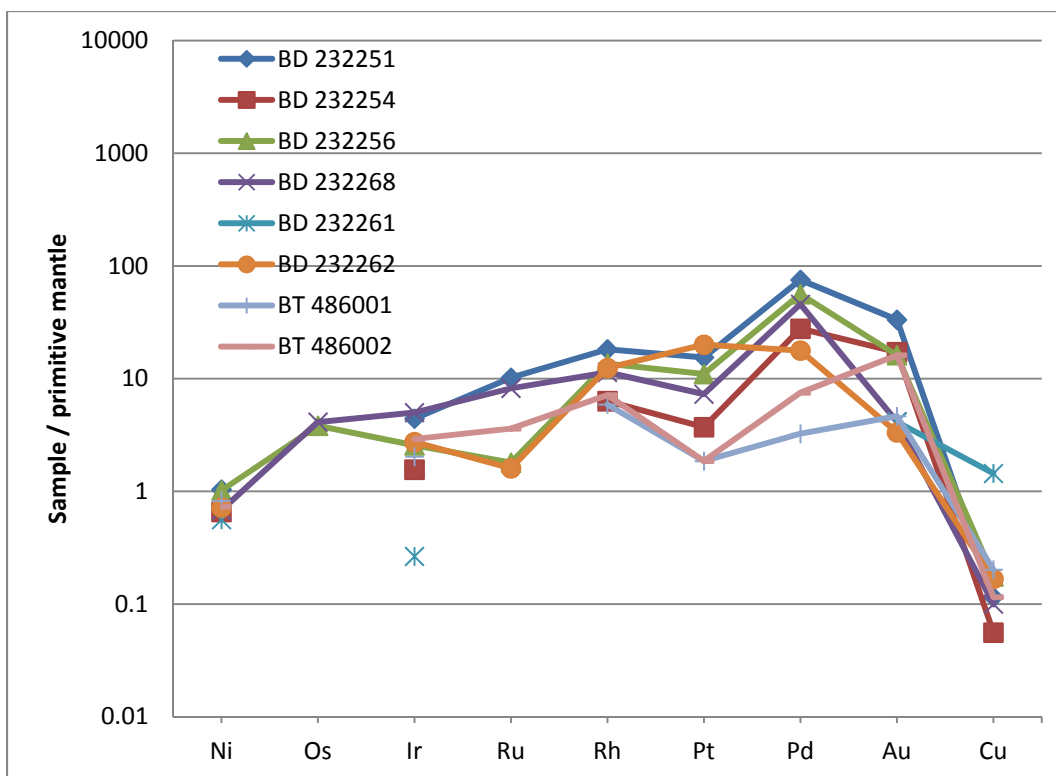


Figure 4.20. Primitive mantle normalized PGE plot of dunite-harzburgite from Black Thor DDH BT-08-10 and Big Daddy DDH FW-08-19. Normalizing values of Barnes et al. (1987).

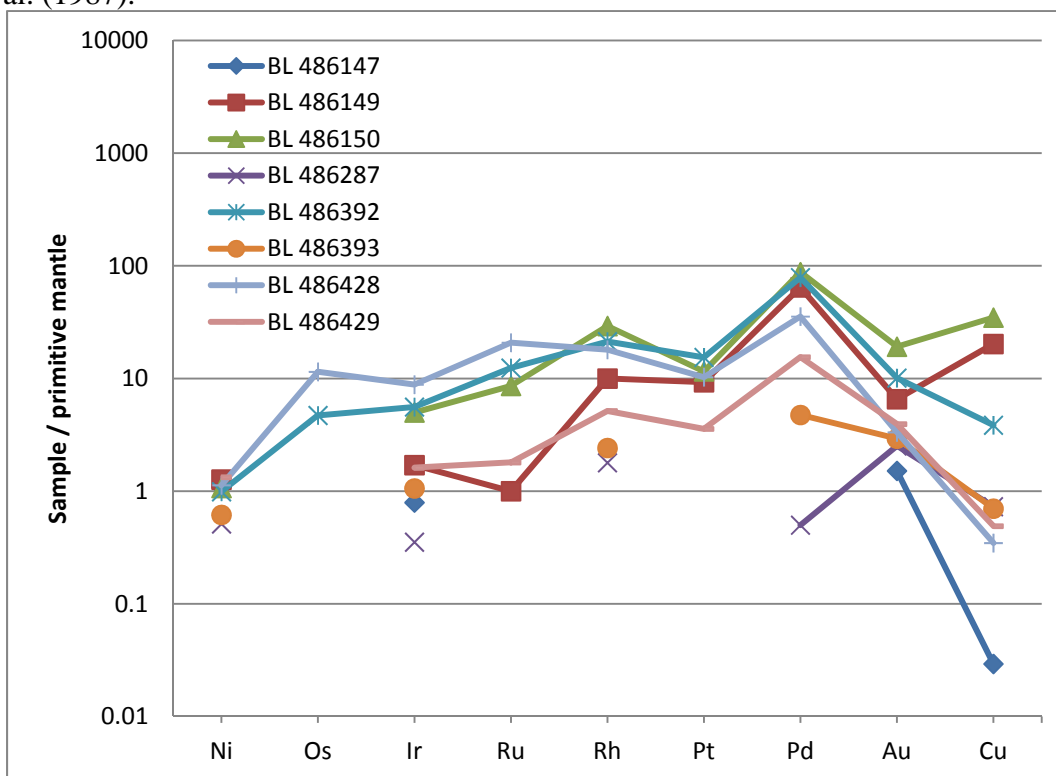


Figure 4.21. Primitive mantle normalized PGE plot of dunite-harzburgite from Black

2.58. This is probably related to the Big Daddy lithologies being more evolved than the Black Thor lithologies. The Black Label dunites are most enriched in IPGE with up to 30 ppm Ir and are enriched in PPGE like the Big Daddy dunites with up to 423 ppm Pt and Pd (Fig. 4.21). The Black Label dunites have up to Pd/Ir_{mn} contents of 4.02 to 17.6. Enrichment in IPGE reflects the more primitive PGE signatures of the Black Label dunites. Along with enrichment in dunites, the Black Label pyroxenite is the most enriched in PGE compared to the other pyroxenites (Fig. 4.22). The Black Label pyroxenite is also the most fractionated pyroxenite with Pd/Ir_{mn} of 26.2. The Big Daddy pyroxenites have Pd/Ir_{mn} contents of 2.32 to 21.97. The Black Thor pyroxenites are the most primitive with Pd/Ir_{mn} contents of 0.65 to 14.17. The overall PGE are noticeably different between the dunites and pyroxenites. The two lithologies probably reflect two magmas – an olivine and a fractionated pyroxene magma - that were mixed to precipitate the chromitites. The IPGE-rich dunites would reflect new S-saturated magmas that mixed with less IPGE-bearing S-undersaturated pyroxenites, thus chromitites being produced by magma mixing according to Irvine's model.

4.3.2 Primitive mantle normalized PGE plot of chromitite

For the PGE signature of the chromitites, all the deposits are enriched in both IPGE and PPGE with slightly more enrichment in PPGE (Fig. 4.23). These chromitites appear to have similar PGE patterns in comparison to the Blackbird chromitite, reported by Azar (2010). The relatively low PGE of the chromitites suggests the intrusion is largely sulphur undersaturated. Pd/Ir_{mn} contents range from 0.64 to 9.57. The enrichment in IPGE is due to the presence of IPGE inclusions in chromite. Inclusions of Rh, Ir, Os, Ru were detected in the chromite of Black Thor during the laser ablation work. These are probably multiple PGE minerals including laurite and others. The Black Label chromitite are the least enriched in Os, Ir, Ru and Rh compared to the Black Thor and Big Daddy chromitites since they are the most evolved. Enrichment in Cu in Black Label indicates the presence of sulphide in this deposit. For Pt contents, the Black Thor and Big Daddy chromitites contain more Pt with contents of 279 ppm for Black Thor and 266 ppm for Big Daddy, compared to 133 ppm for Black Label. Although the Black Label chromitites have proportional higher Pd with Pd/Pt ratio in one of the samples at 3.22, and usually have higher Pd contents e.g. assays of DDH BT-09-31.

Label DDH BT-09-31. Normalizing values of Barnes et al. (1987).

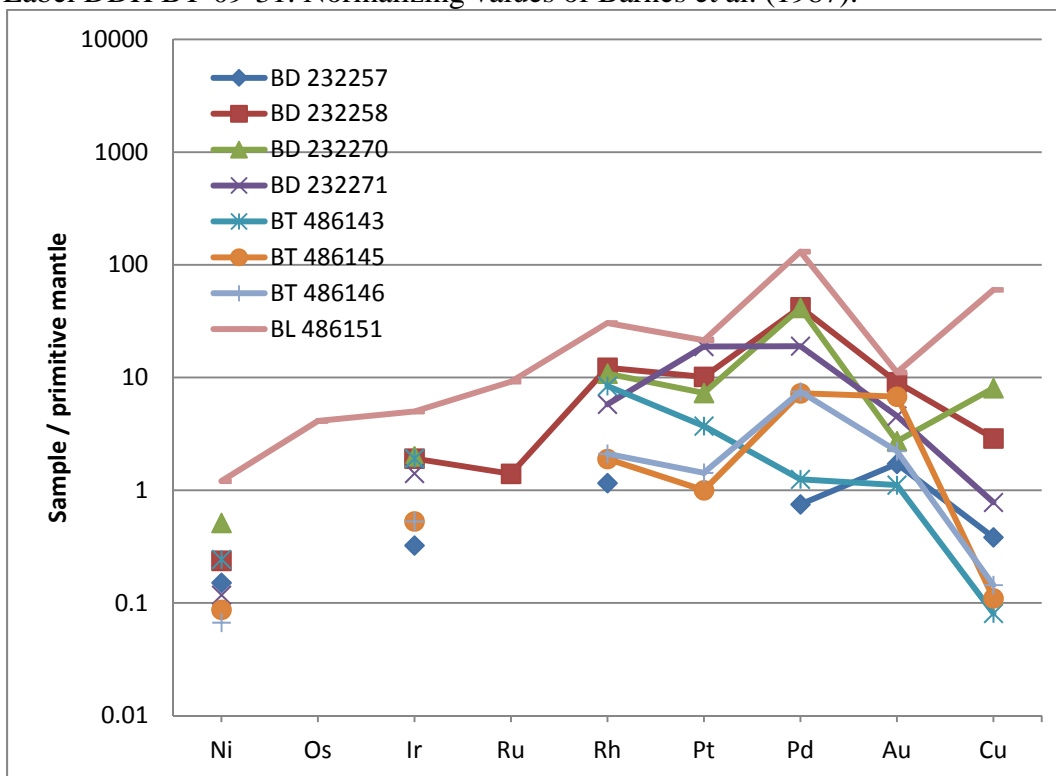


Figure 4.22. Primitive mantle normalized PGE plot of pyroxenite from all 3 deposits. Normalizing values of Barnes et al. (1987).

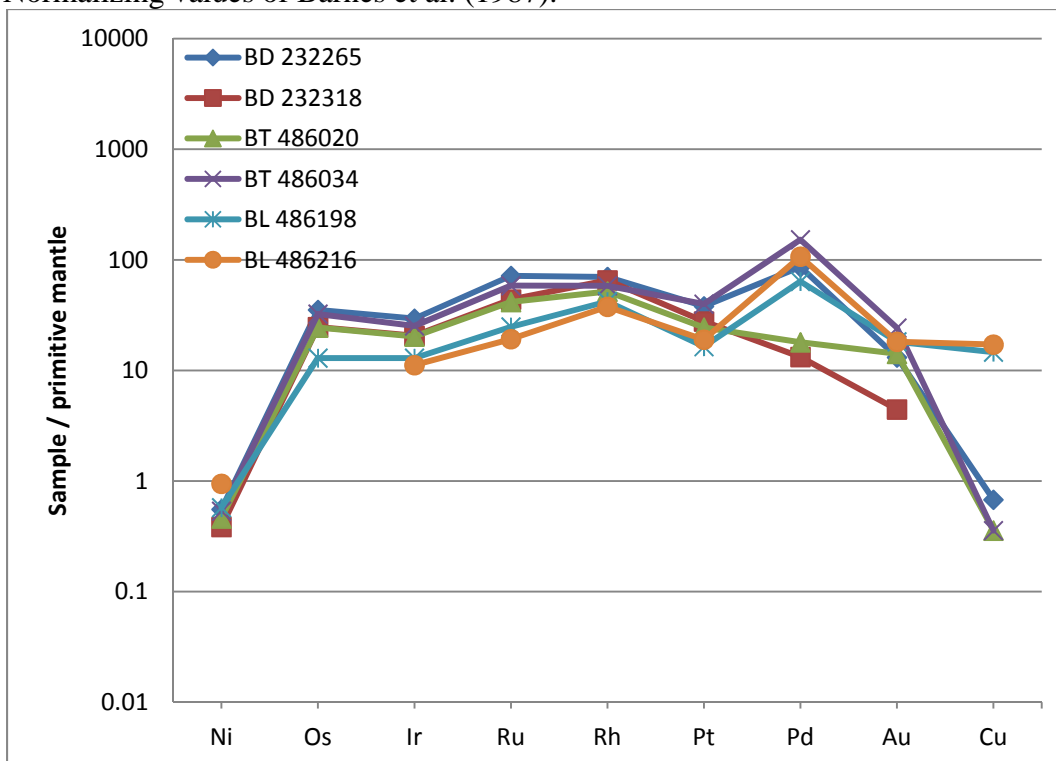


Figure 4.23. Primitive mantle normalized PGE plot of chromitite from all 3 deposits. Normalizing values of Barnes et al. (1987).

4.4 Mineral chemistry of host silicates

Electron microprobe analysis was performed on primary host silicates, minerals in silicate inclusions in chromites and on retrogressive silicate to the chromite. A total of 465 point analyses were determined for the silicates, not including serpentine, talc and albite. These last three minerals were not included in the database. Of the 465 analyses, 32 point analyses were performed for olivine, 45 for pyroxene, 202 for amphibole, 61 for phlogopite and 125 for chlorite. Analyses are listed in Appendix 4.

4.4.1 Olivine

Olivines were probed in only a few samples where there was remnant fresh olivine and pyroxene in DDH BT-09-31. Since there is very little primary olivine remaining due to pervasive hydration to serpentine, reporting of complete chemistries of Mg # up section in the intrusion is not possible. However, the few remnant olivine grains in the chromitites plot in compositions reflective of that layer, which gives evidence of difference in Mg # between the chromitites (Fig. 4.24). The Layer 1 olivines have lower Mg # between 85.7 to 90.77 compared to the Layer 2 olivines with Mg # between 90.68 and 94.41 reflective of the more primitive chromites in Layer 2 than in Layer 1.

4.4.2 Pyroxene

Primary intercumulus pyroxene has been pervasively retrogressed to hydrothermal tremolite and talc. Fresh pyroxene was analysed where preserved in five samples in Black Label DDH BT-09-31. Notably, no primary pyroxene is preserved in the Black Thor and Big Daddy drill holes. On a pyroxene ternary plot, the pyroxenes are classified as diopsides and augites for clinopyroxene and pigeonites and enstatites for orthopyroxenes (Fig. 4.25). In sample 486211 at 174.4 m, there is a trend of ferrosilite depletion in three pyroxenes from the main cluster of pyroxenes in the diopside-augite field (Fig. 4.26). The three offset pyroxenes are due to magmatic metasomatism of the primary pyroxene cluster. These pyroxenes have ferrosilite component at 2.83 to 3.39 % whereas the primary pyroxenes have ferrosilite at 4.73 to 5.60 %. This trend in Mg enrichment is due to replacement of the primary pyroxenes by metasomatic pyroxene.

Another trend evident in the diopside-augite cluster is the increase in wollastonite component in the primary pyroxenes from 45.70 to 47.79 %. This trend is due to core to rim diffusion in the relic pyroxenes due to melt metasomatism. Evidence of the core to

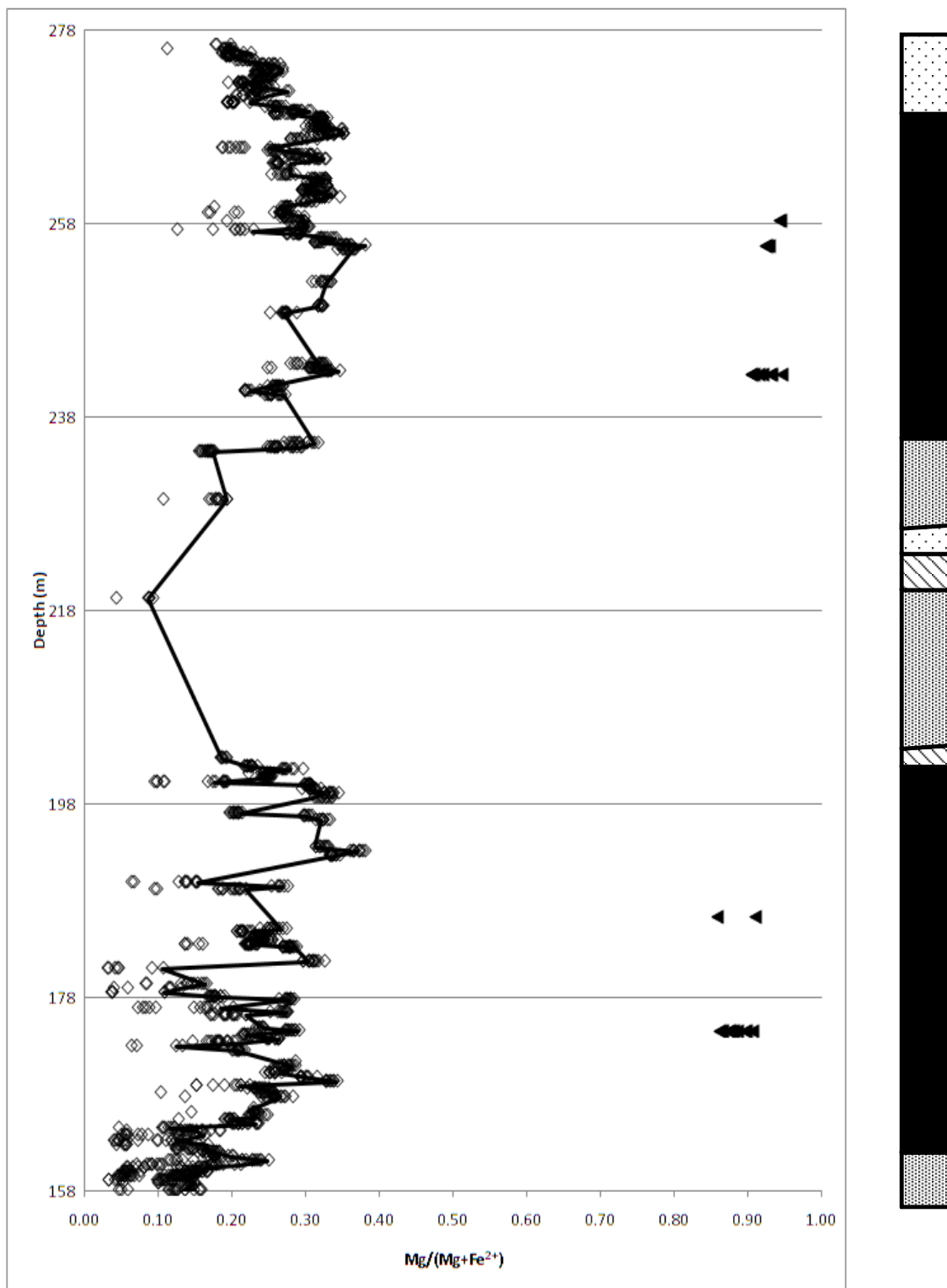


Figure 4.24. Plot of $\text{Mg}/(\text{Mg}+\text{Fe}^{2+})$ vs. depth (m) for Black Label DDH BT-09-31. The trend line plots through chromite cores. Diamonds are chromites while triangles are olivines.

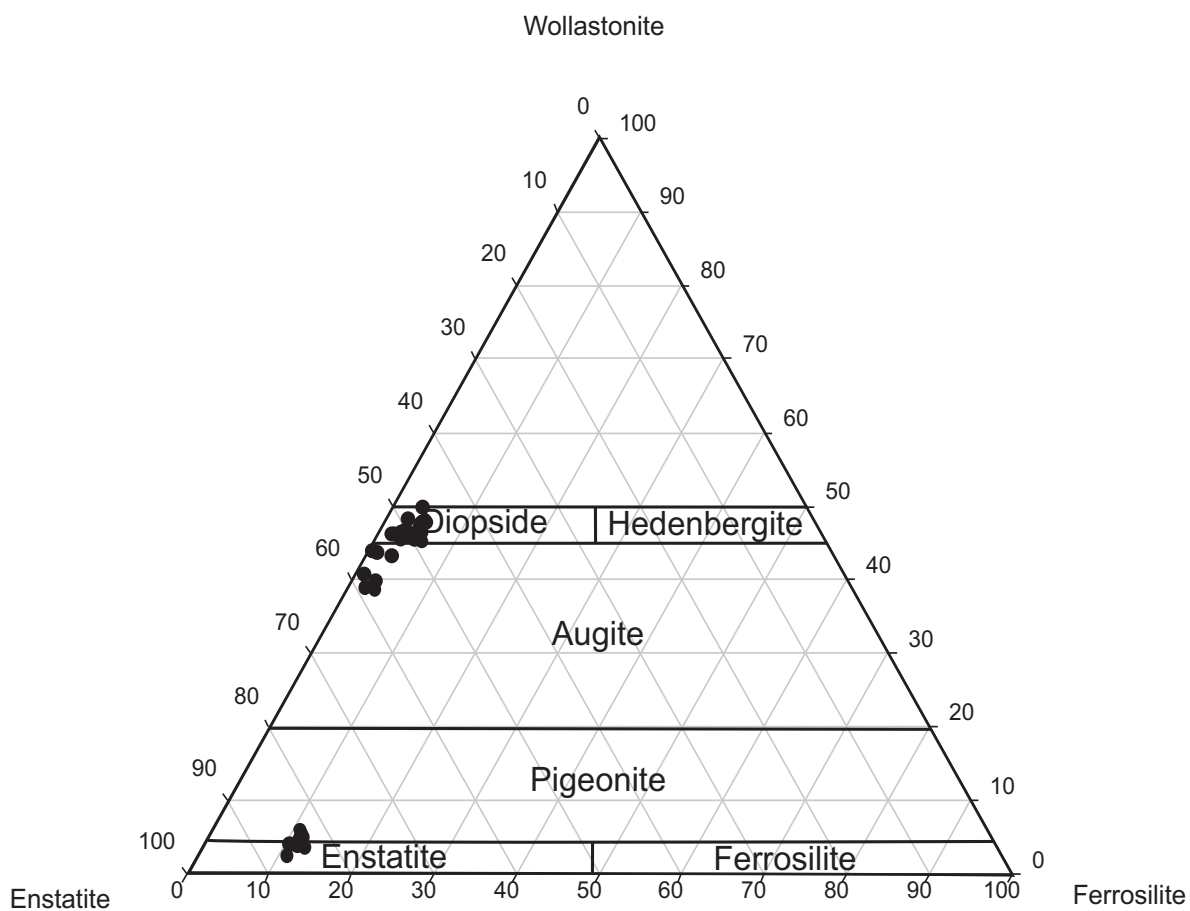


Figure 4.25. Ternary plot of pyroxene compositions.

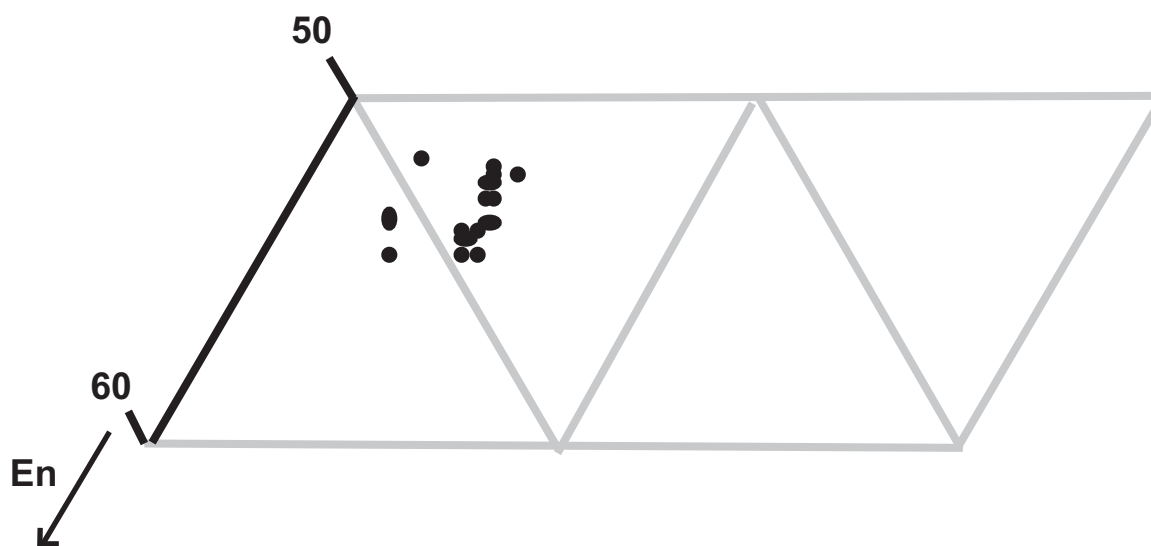


Figure 4.26. Ternary plot of clinopyroxene compositions in sample 486211.

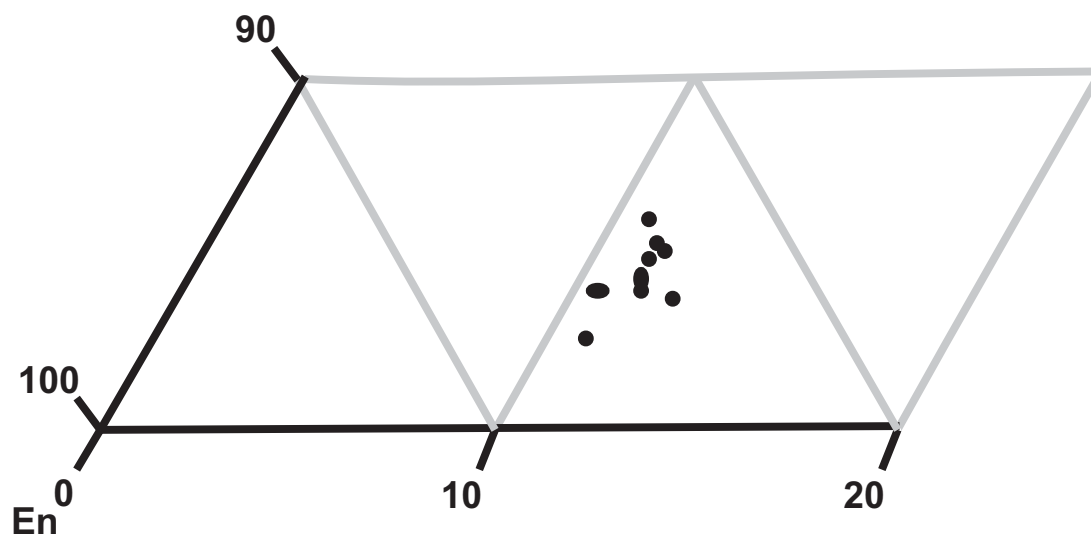


Figure 4.27. Ternary plot of orthopyroxene compositions in sample 486211.

rim diffusion is the variation from a core pyroxene at point 4 in sample 486211image_0001 at 45.40 % Wo to a rim pyroxene at point 3 at 46.90 % Wo. Diffusion to greater wollastonite component is also evident in the orthopyroxenes of sample 486211 (Fig. 4.27). Wollastonite increases from core orthopyroxene at 2.46 % Wo to rim orthopyroxene at 5.99 % Wo.

Primary pyroxenes occur as both poikilitic phases in the host olivine cumulate and the chromitite and as minerals in the chromite-hosted silicate inclusions. The primary pyroxenes are characterized by elevated non-pyroxene quadrilateral components such as wt. % TiO₂ and wt. % Cr₂O₃. The chromian diopsides have up to 0.33 wt. % TiO₂ and 1.74 wt. % Cr₂O₃ while the orthopyroxenes have up to 0.22 wt. % TiO₂ and 0.80 wt. % Cr₂O₃. The trend of decreasing Ti from primary to metasomatic to hydrothermal pyroxene is displayed on a plot Ti vs. total Al where the primary pyroxenes have higher Ti and Al contents (Fig. 4.28).

Hydrothermal diopsides were also detected in sample 486155 at 151.8 m in Black Label DDH BT-09-31. These represent higher T metamorphism of pyroxene into diopside stability after tremolite at 450 °C temperature (Winter, 2001). These pyroxenes have almost no non-quadrilateral components and high MgO at up to 21.71 wt. %.

4.4.3 Amphibole

The McFaulds Lake chromites have associated of both primary igneous and secondary retrogressive amphiboles. The amphiboles probed in this study are from Black Label DDH BT-09-31 and Black Thor DDH BT-09-17. All the amphiboles analysed are divided into three groups according to the nomenclature of Leake et al. (1997). Notably, Cr is not accounted for in this classification scheme. There are three types of igneous amphibole: the magnesiotaramites-magnesiokatophorites-winchites, the pargasites-edenites and the tschermakites-magnesiornblendes. On a plot of Mg # vs. Si for $(\text{Na}+\text{K})_{\text{A}} > \text{or} < 0.50$; $(\text{Ca}+\text{Na}_{\text{B}}) \geq 1.00$; $0.50 < \text{Na}_{\text{B}} < 1.50$, the first group of amphiboles range from the bulk cluster of lower Si-bearing magnesiotaramites and magnesiokatophorites with Si between 6.47 and 6.81 that trend in Si enrichment to four winchite compositions with Si ranging from 7.49 to 7.819 (Fig. 4.29). The bulk cluster of magnesiotaramites-magnesiokatophorites consists of silicate inclusion amphiboles found in both the Layer 1 and Layer 2 Black Label chromitites. On a Al^{IV} vs. Na_A+K diagram,

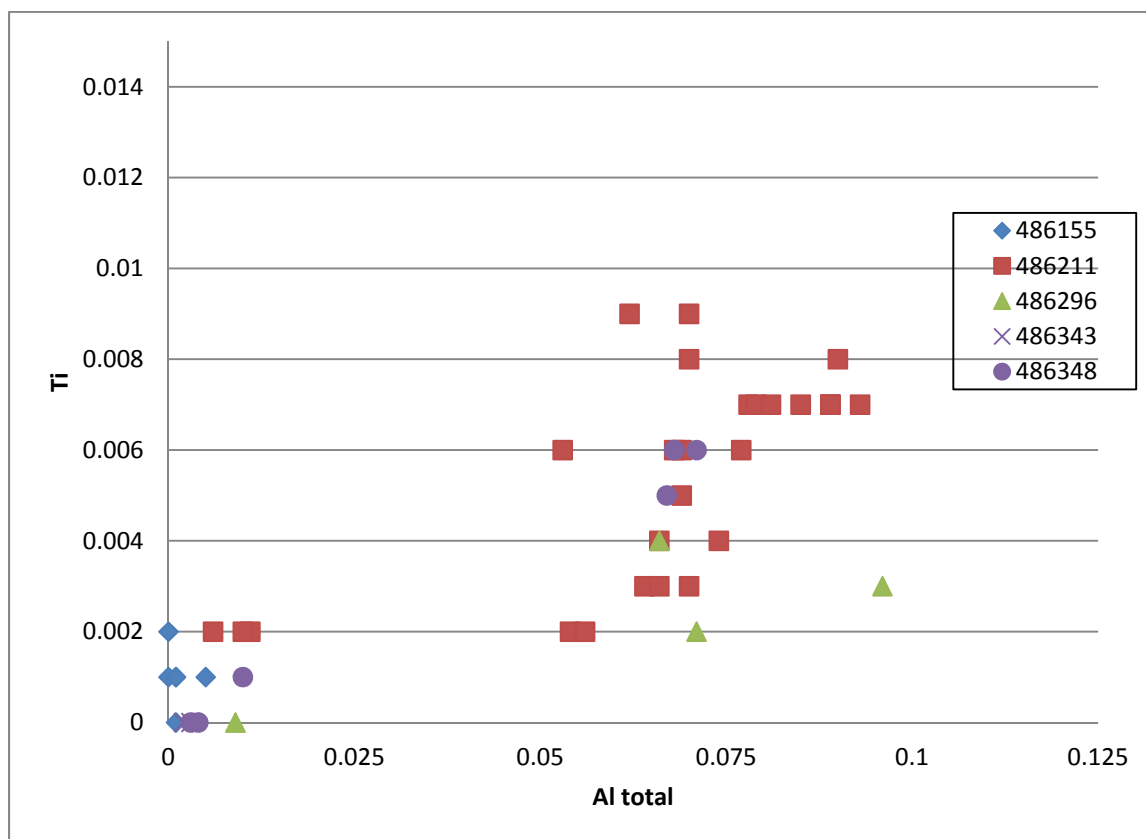


Figure 4.28. Plot of Ti vs. Al total for pyroxene in five samples.

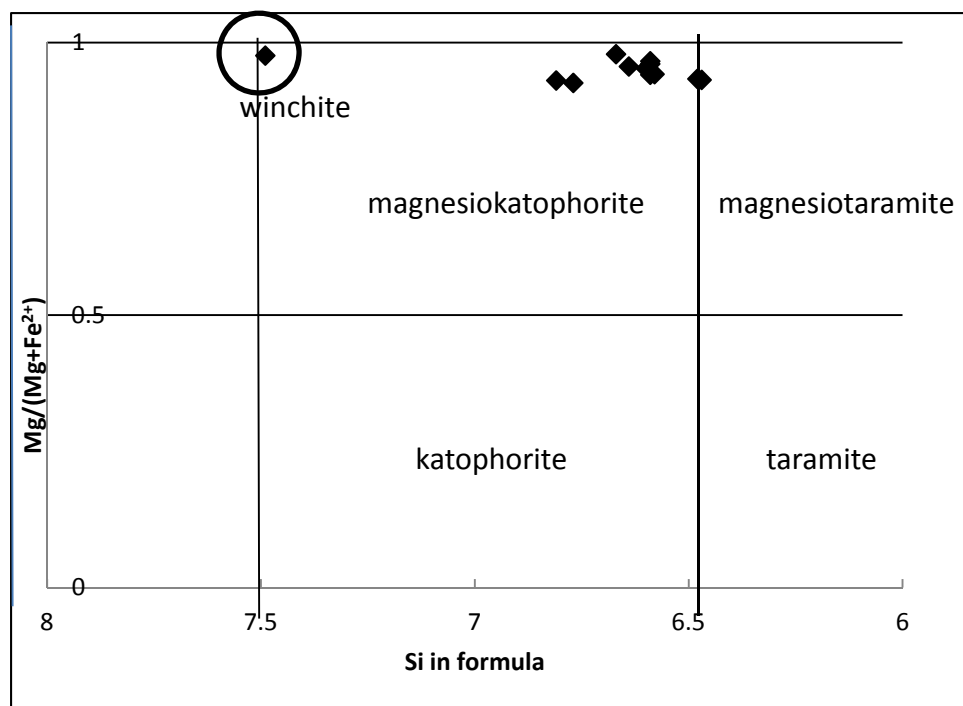


Figure 4.29. Plot of Mg # vs. Si for amphiboles with $(Na+K)_A \geq 0.50$; $(Ca+Na_B) \geq 1.00$; $0.50 < Na_B < 1.50$ with nomenclature of Leake et al. (1997). A winchite is plotted for amphiboles with $(Na+K)_A < 0.50$; $(Ca+Na_B) \geq 1.00$; $0.50 < Na_B < 1.50$.

these amphiboles plot in the range of igneous amphiboles with $\text{Na}_A + \text{K}$ greater than 0.5 which have relatively similar Al^{IV} compositions of about 1.1 to 1.45 (Fig. 4.30). The winchite is the only exception and occurs along the 1:1 magnesiohornblende to tremolite trend and has a $\text{Na}_A + \text{K}$ value of 0.49. On a $\text{Al}^{\text{IV}} - (\text{Na}, \text{K})_A$ vs. $\text{Al}^{\text{VI}} + 2\text{Ti} + \text{Cr}$ diagram, the amphibole with the highest Ti number is a magnesiotaramite while the amphibole with the highest Cr number is a magnesiokatophorite (Fig. 4.31). The winchite plotted on the Mg # vs. Si diagram with Si of 7.49 is from a relatively bright silicate inclusion mineral that occurs with albite in silicate inclusions at 273.6 m depth in the Black Label Layer 2 chromitite. The other three winchite compositions that did not run through the Papike calculation with Si from 7.81 to 7.819 are three point analyses from a single silicate inclusion amphibole from sample 486211 at 174.4 m.

The pargasites-edenites plot on a diagram of Mg # vs. Si for $\text{Ca}_B \geq 1.50$; $(\text{Na} + \text{K})_A > 0.50$; $\text{Ti} < 0.50$ (Fig. 4.32). There is one large cluster that plots in the range of Si between 6.37 and 6.99 while one point analysis plots at Si of 7.24. Within the range of these amphiboles, there is a trend of increasing Si and Mg # that probably reflects igneous evolution of decreasing Mg # in the amphiboles. On a plot of Mg # vs. depth for Black Label DDH BT-09-31, the amphiboles in Black Label Layer 2 from 232 to 321 m in DDH BT-09-31 have a higher amount of high Mg # amphiboles than Layer 1 amphiboles from 155 to 186 m which probably reflects the more primitive chromite compositions of Layer 2 (Fig. 4.33). A trend of decreasing Mg # with height from 255.6 m to 273.6 m in Layer 2 from 0.98 to 0.90 is suggestive of a differentiation trend. Notably, two pargasite compositions were detected (analyses 33 and 34 at 155 m) for igneous amphibole that surrounds silicate inclusion-bearing chromites with amphiboles of the same composition in the silicate inclusions. On a Al^{IV} vs. $\text{Na}_A + \text{K}$ diagram, the pargasites-edenites have the highest range of Al^{IV} compositions in the range of amphiboles with $\text{Na}_A + \text{K}$ greater than 0.5 (Fig. 4.30). The Al^{IV} compositions range from 1.01 to 1.66. On a $\text{Al}^{\text{IV}} - (\text{Na}, \text{K})_A$ vs. $\text{Al}^{\text{VI}} + 2\text{Ti} + \text{Cr}$ diagram, the pargasites-edenites plot in the large cluster of igneous amphiboles with high Ti and Cr contents (Fig. 4.31).

The tschermakites-magnesiohornblendes plot with and are replaced by retrogressive tremolite as the third type of amphibole. On a Mg # vs. Si diagram for $\text{Ca}_B \geq 1.50$; $(\text{Na} + \text{K})_A < 0.5$, there is a Si enrichment trend with associated Mg enrichment that

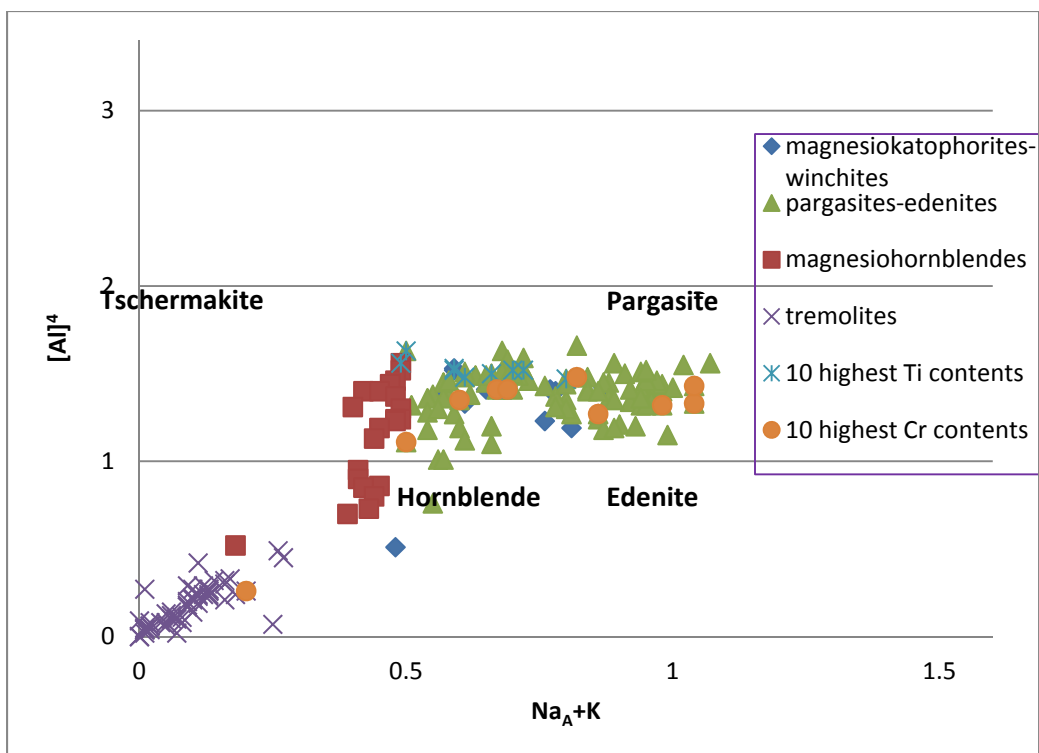


Figure 4.30. Plot of tetrahedral Al vs. A site Na and K for all the amphiboles after Deer et al. (1997).

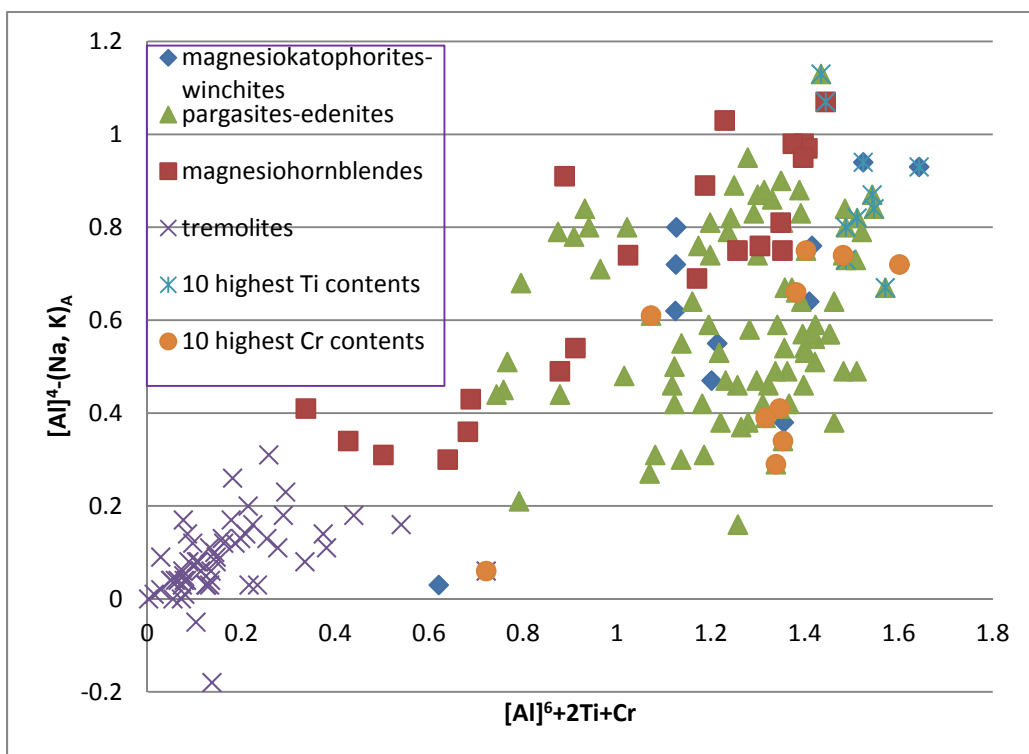


Figure 4.31. Plot of tetrahedral Al – A site Na and K vs. octahedral Al+2Ti+Cr for all the amphiboles.

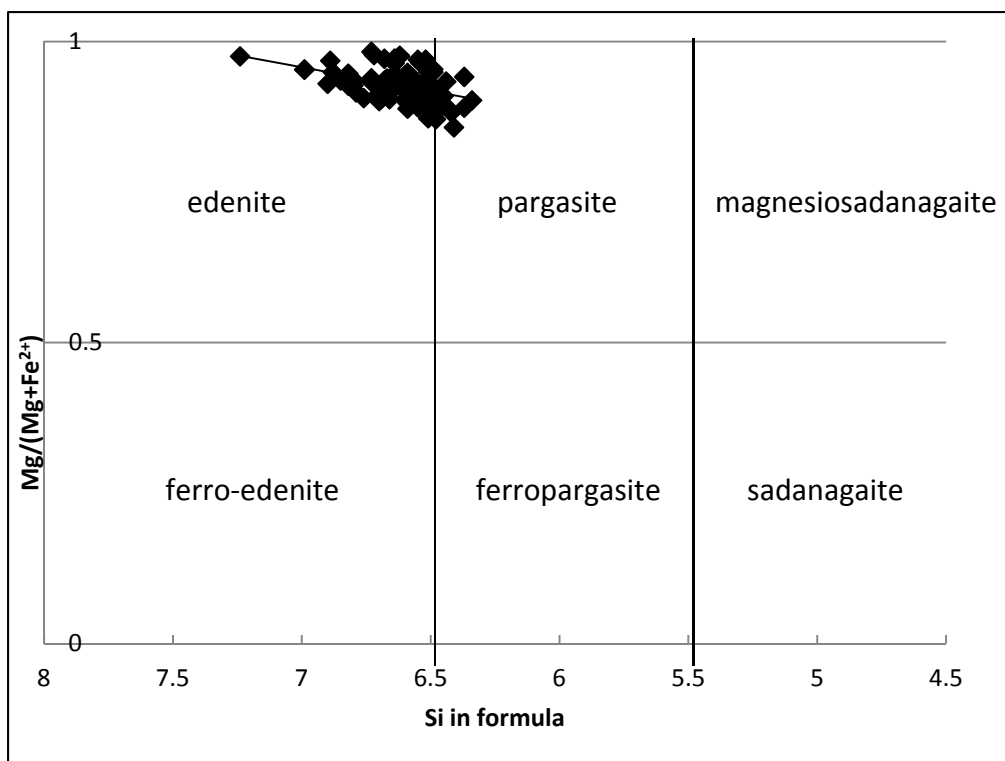


Figure 4.32. Plot of Mg # vs. Si for amphiboles with $Ca_B \geq 1.50$; $(Na+K)_A > 0.50$; $Ti < 0.50$; $Al^{VI} \geq Fe^{3+}$ with nomenclature of Leake et al. (1997).

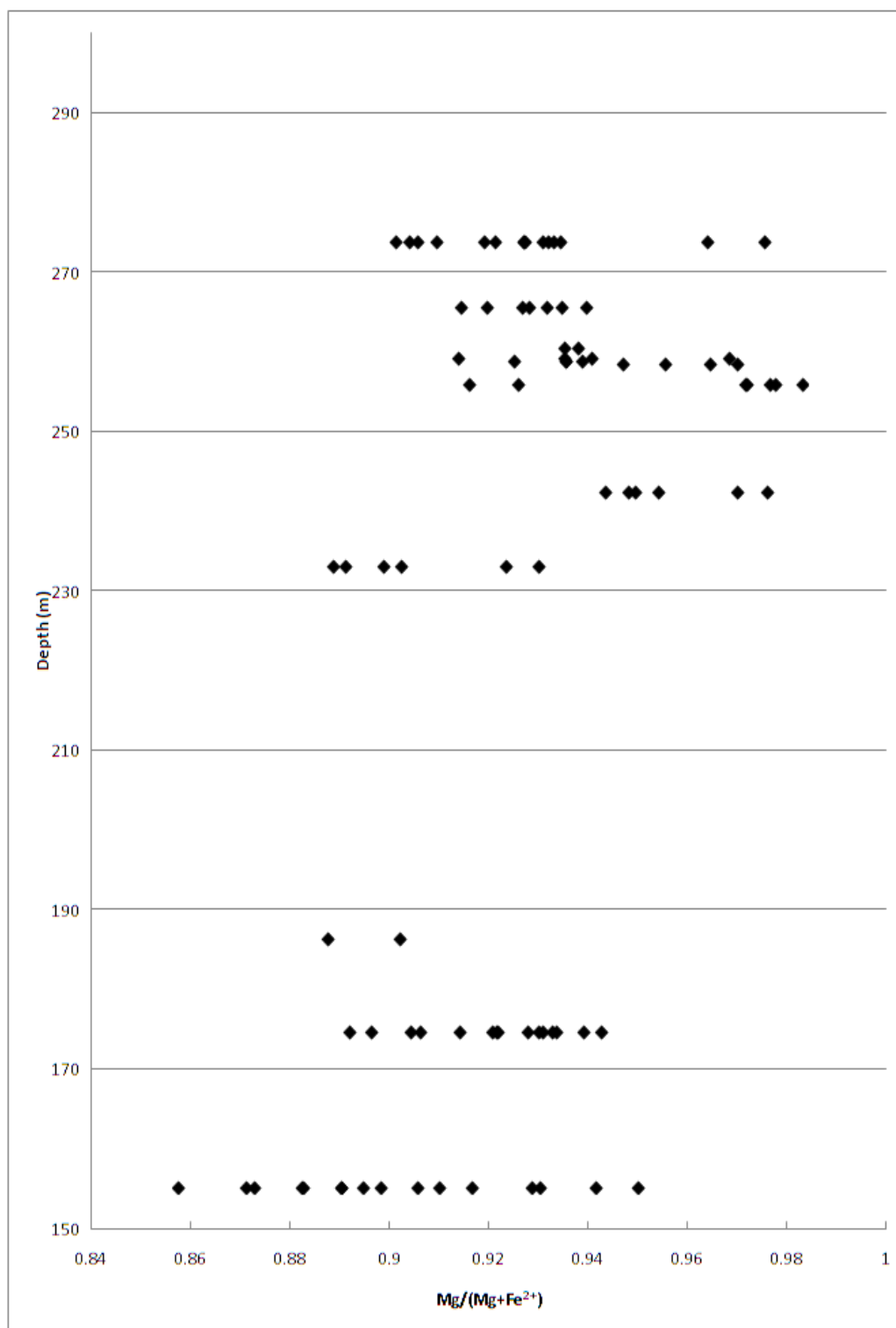


Figure 4.33. Plot of $\text{Mg}/(\text{Mg}+\text{Fe}^{2+})$ vs. depth (m) for pargasite-edenite in Black Label DDH BT-09-31.

represents the retrogression of pargasite to magnesiohornblende and further to tremolite (Fig. 4.34). This trend is better observed on a Al^{IV} vs. Na_A+K diagram where there is decreasing Na_A+K with decreasing Al^{IV} from pargasite to tremolite (Fig. 4.30). Evidence of this retrogression is the presence of chromian tremolite in analysis 71 of sample 486211 at 174.4 m that occurs as tabular grains adjacent to a crack in a silicate inclusion with pargasite. Notably, relics of pargasite at 155 m are observed in poikiloblastic chromian tremolite which represents replacement tremolite. Also, secondary zonation is observed from edenite to tremolite from points 1 to 2 in zoned amphibole sample 486211 image_0010, 174.4m depth (see petrography chapter, silicate inclusions). The retrogressive trend is also observed as decreasing $Al^{IV}-(Na+K)_A$ with decreasing $Al^{VI}+2Ti+Cr$ where the replacement tremolites have lower Ti and Cr contents than the pargasites and other igneous amphiboles (Fig. 4.31). A large amount of the tremolites are also replacement of primary chromian diopsides. One tremolite with elevated Cr (analysis 40 in sample 486211) is a poikiloblastic tremolite that replaces poikilitic chromian diopside that occurs as a patchy poikilitic pyroxene interstitial to massive chromite. The Mg enrichment evident in the pyroxenes as a whole represents initial retrogression toward more Mg-enriched tremolites. Finally, there are also high Mg hydrothermal vein tremolites present at 321 m in Black Thor DDH BT-09-17 with Mg #s of 0.96 to 0.99. These tremolites are zoned and their presence indicates higher T prograde alteration of the upper chromitites in that layer.

4.4.4 Phlogopite

The phlogopite probed in Black Label DDH BT-09-31 is unusual due to Ti and Cr enrichment similar to phlogopites found in other chromite-bearing rocks. On a plot of wt. % Al_2O_3 vs. wt. % TiO_2 , the phlogopite plots with high Al_2O_3 at 6.89 to 15.49 wt. % and enriched TiO_2 in the primitive mantle box; and they plot with compositions below the box on a kimberlite trend (Fig. 4.35). This would lead one to interpret that these minerals to be sourced directly from the mantle. The phlogopites are hosted within round silicate inclusions in the chromites and also in the surrounding matrix. The phlogopites in the common groundmass are more regular K phlogopites while those in the silicate inclusions are K and more Na-enriched phlogopites. Variation between the K and Na-enriched compositions is seen on a ternary Ba-K-Na plot (Fig. 4.36). Since Na

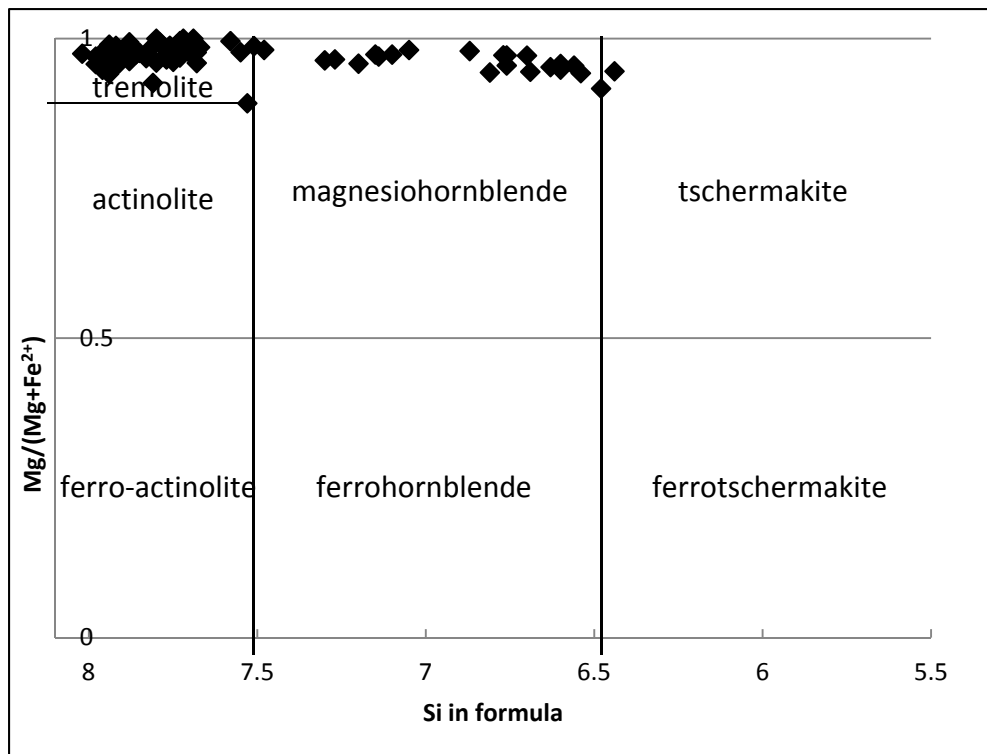


Figure 4.34. Plot of Mg # vs. Si for amphiboles with $Ca_B \geq 1.50$; $(Na+K)_A < 0.5$ with nomenclature of Leake et al. (1997).

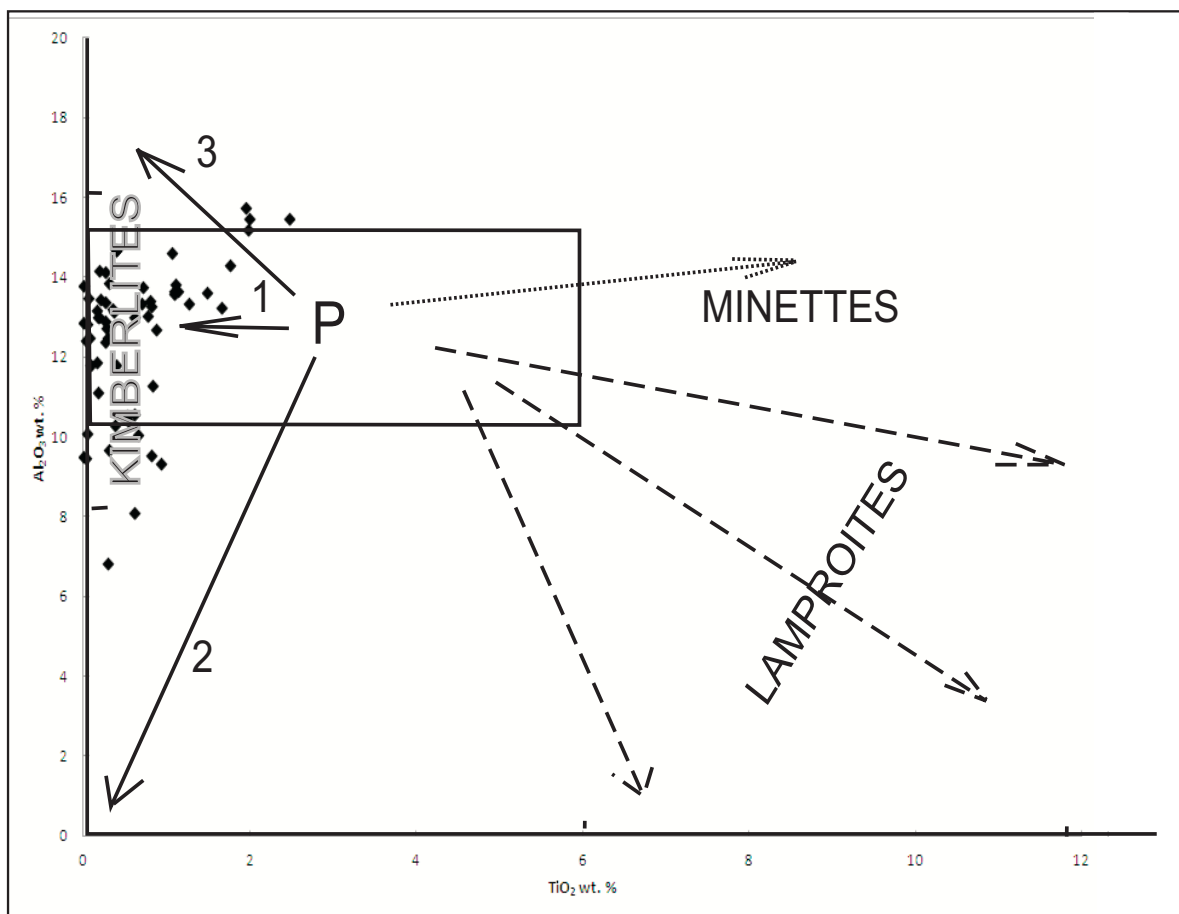


Figure 4.35. Plot of wt. % Al_2O_3 vs. wt. % TiO_2 for phlogopite compositions. Fields are after Mitchell (1986).

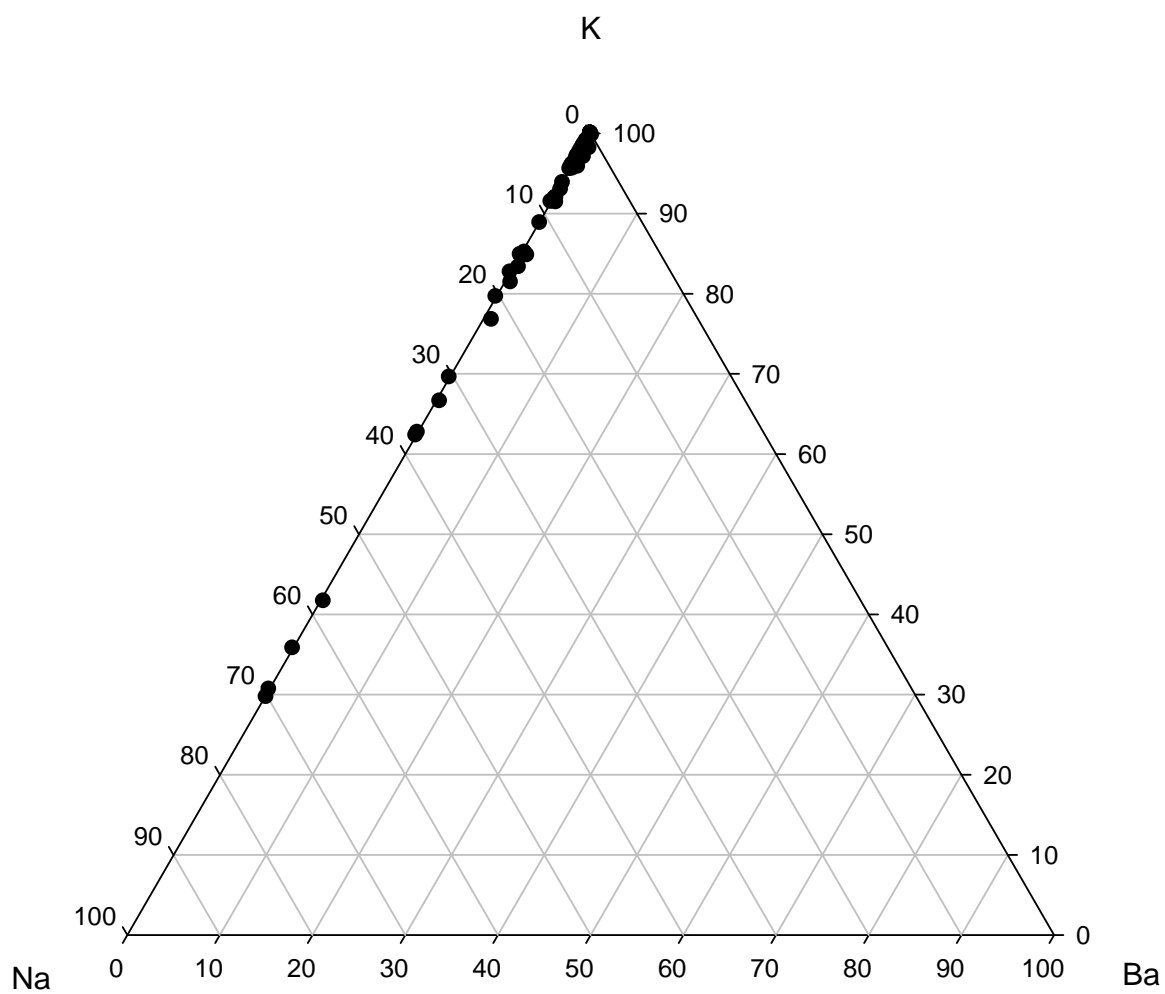


Figure 4.36. Ternary Ba-K-Na plot for phlogopite.

phlogopites are in the silicate inclusions and not in the groundmass, this could lead one to interpret that the silicate inclusion phlogopites are different than the groundmass phlogopites, possibly encapsulated as metasomatized mantle nodules within the chromites.

However, with variation of wt. % MgO and Cr₂O₃ with up section height, it is shown that the phlogopites (with mostly silicate inclusion phlogopites being represented here) have lower MgO/higher Cr₂O₃ contents in Black Label Layer 1 and higher MgO/lower Cr₂O₃ in Layer 2 (Figs. 4.37 and 4.38). The Layer 2 inclusions are therefore more primitive and reflect the trends of more MgO-rich chromites in Layer 2 than in Layer 1. This trend is also seen in the plot of Mg # variation of pargasite-edenite with up section height. A correlation of decreasing wt. % MgO with increasing wt. % Cr₂O₃ is evident due to Mg-Cr substitution with igneous evolution in the phlogopites (Fig. 4.39). On a plot of wt. % Cr₂O₃ vs. wt. % TiO₂, there is a correlation of increasing Cr with Ti that is similar to that observed in metasomatic phlogopites of the upper mantle (Fig. 4.40; Erlank et al., 1987). In the case of these phlogopites, they were probably enriched in Cr and Ti in the presence of residual melt. It appears therefore that the phlogopite compositions define trends of igneous evolution in Ti and Cr phlogopites and are more akin to ultramafic intrusive-hosting phlogopites in a layered intrusion. The Ti and Cr enrichment in more Na-bearing phlogopites in some of the silicate inclusions has probably been derived from the surrounding chromites themselves similar to phlogopites in the Stillwater Complex (Page and Zientek, 1987). This is discussed in more depth in chapter 6.

4.4.5 Chlorite

Chlorites were analysed from three drill holes: Black Label DDH BT-09-31, Black Thor DDH BT-08-10 and Black Thor DDH BT-09-17. On a Fe # vs. Si plot, the chlorites plot as a range of Si vs. Al with very magnesian compositions from sheridanite to clinocllore to penninite (Figs. 4.41 to 4.43). The Mg content of the chlorites reflect the Mg content of the chromites in the various zones. The Black Label chlorites are divided between those found in the Layer 1 and Layer 2 chromite intervals. The Layer 1 chlorites are the four analyses that plot in a separate cluster of higher Fe # than the other chlorites and reflect the higher Fe # of the host chromitites (Fig. 4.42). The Layer 2

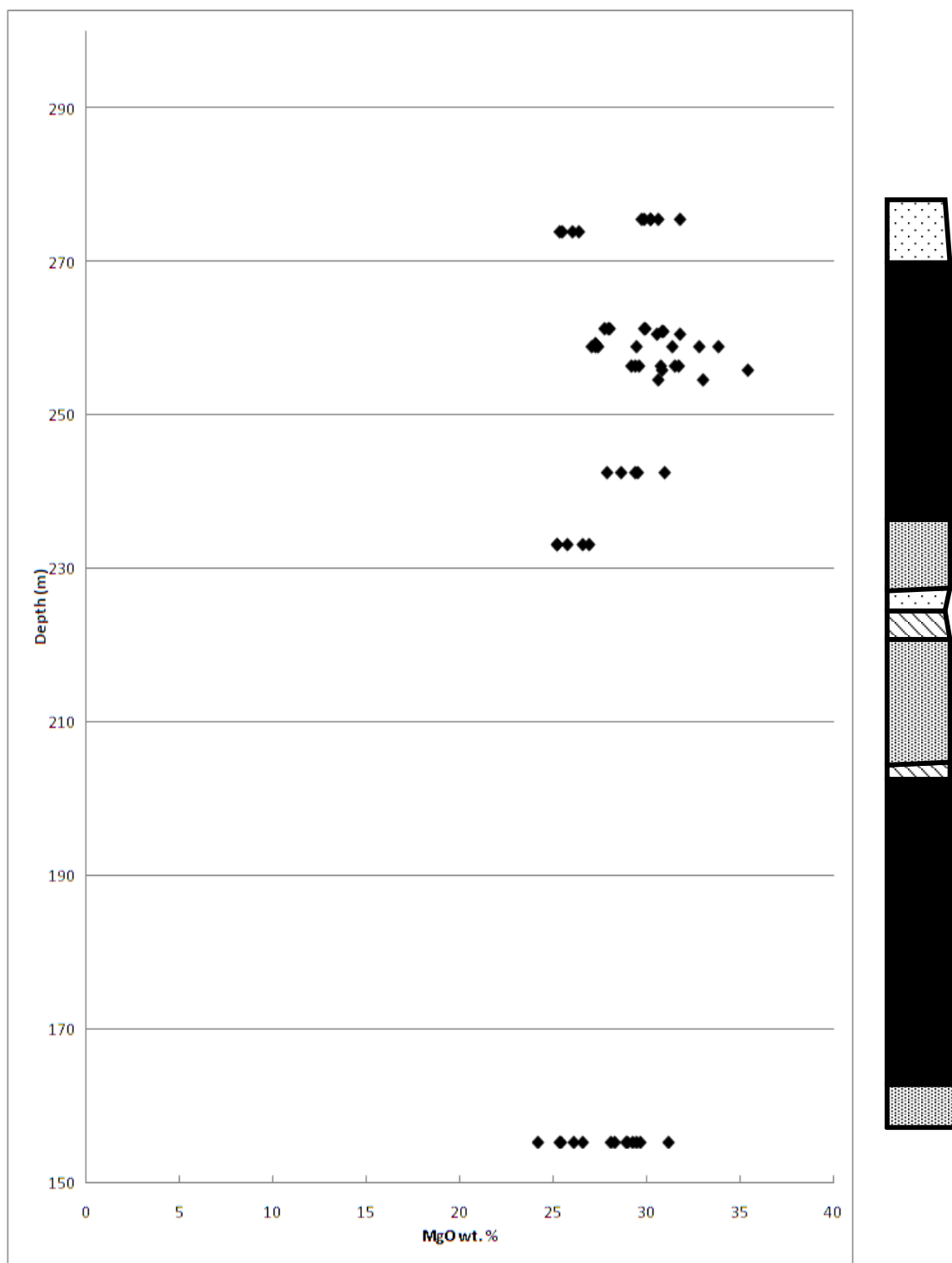


Figure 4.37. Plot of wt. % MgO vs. depth (m) for phlogopite in Black Label DDH BT-09-31.

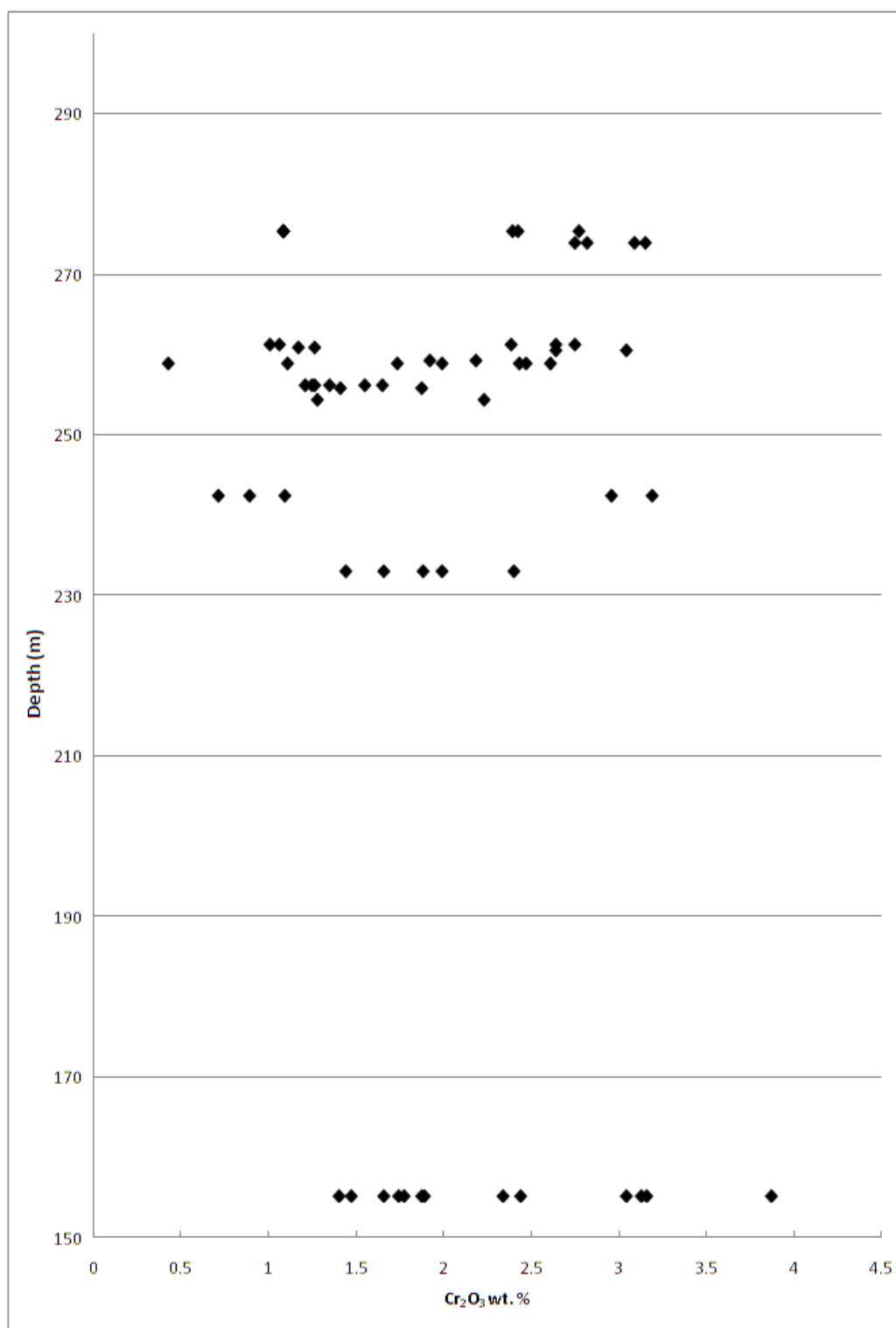


Figure 4.38. Plot of wt. % Cr_2O_3 vs. depth (m) for phlogopite in Black Label DDH BT-09-31.

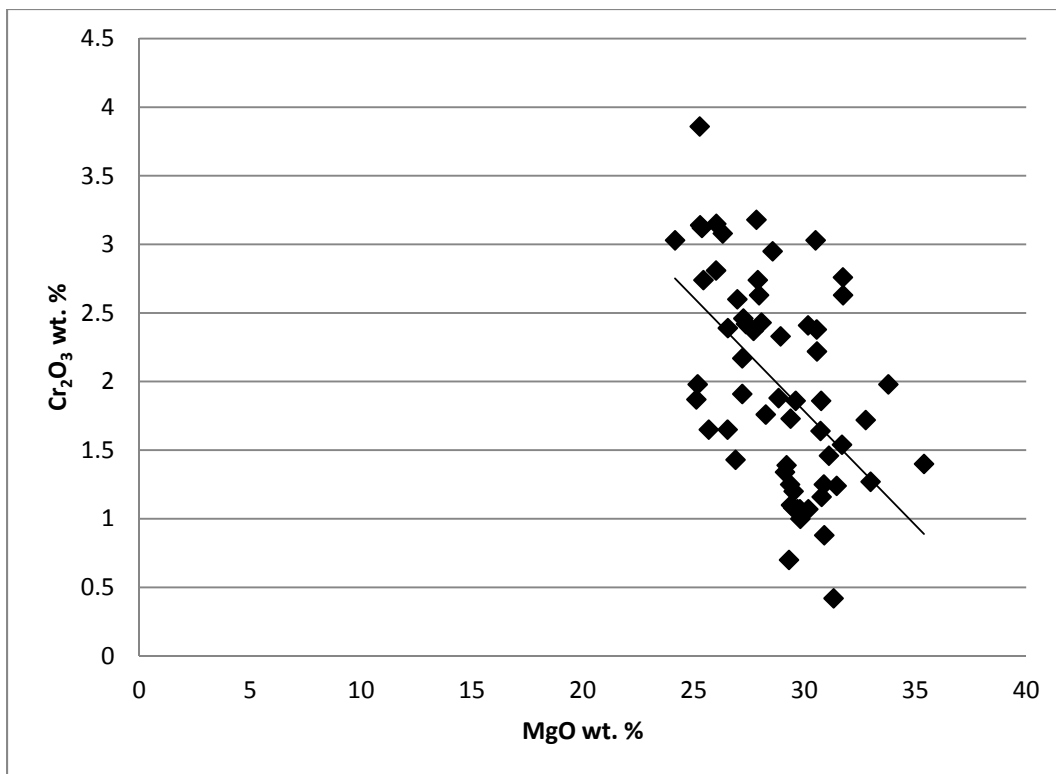


Figure 4.39. Plot of wt. % Cr_2O_3 vs. wt. % MgO for phlogopite.

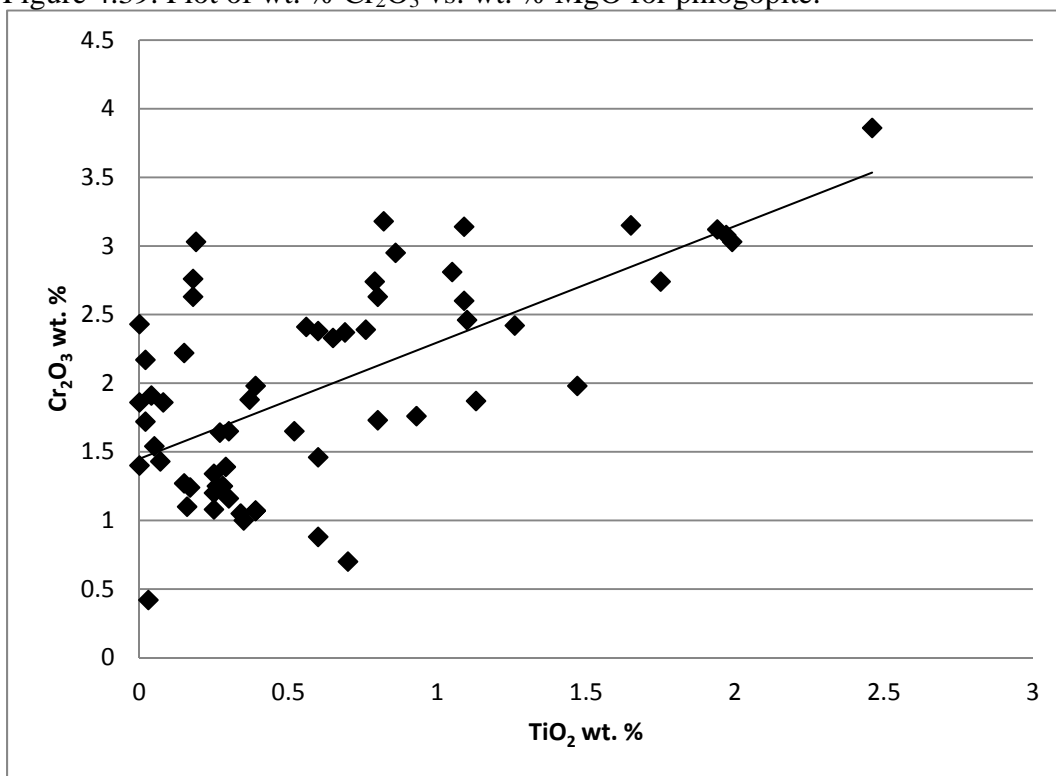


Figure 4.40. Plot of wt. % Cr_2O_3 vs. wt. % TiO_2 for phlogopite.

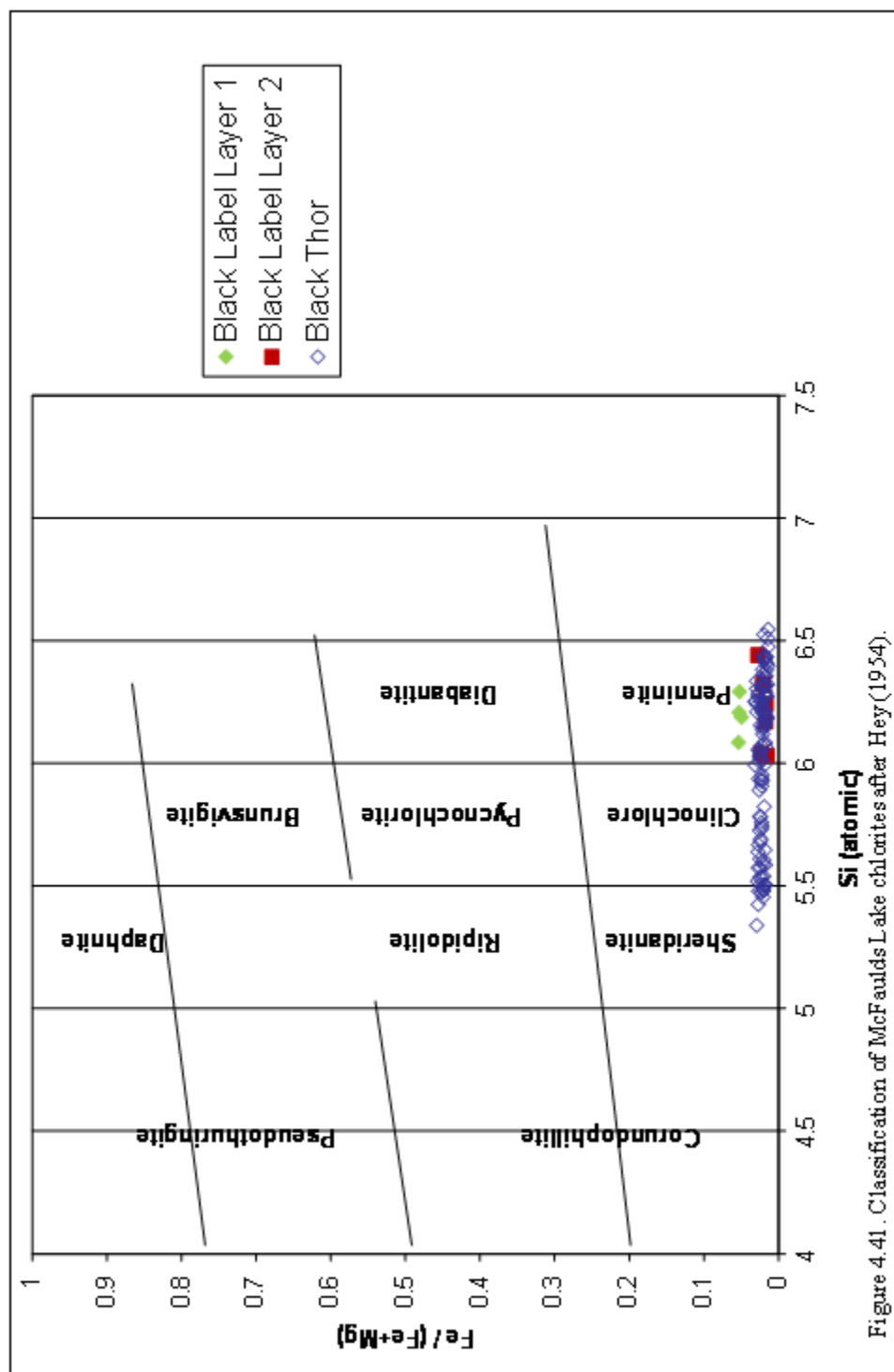


Figure 4.41 . Classification of McFaulds Lake chlorites after Hey (1954).

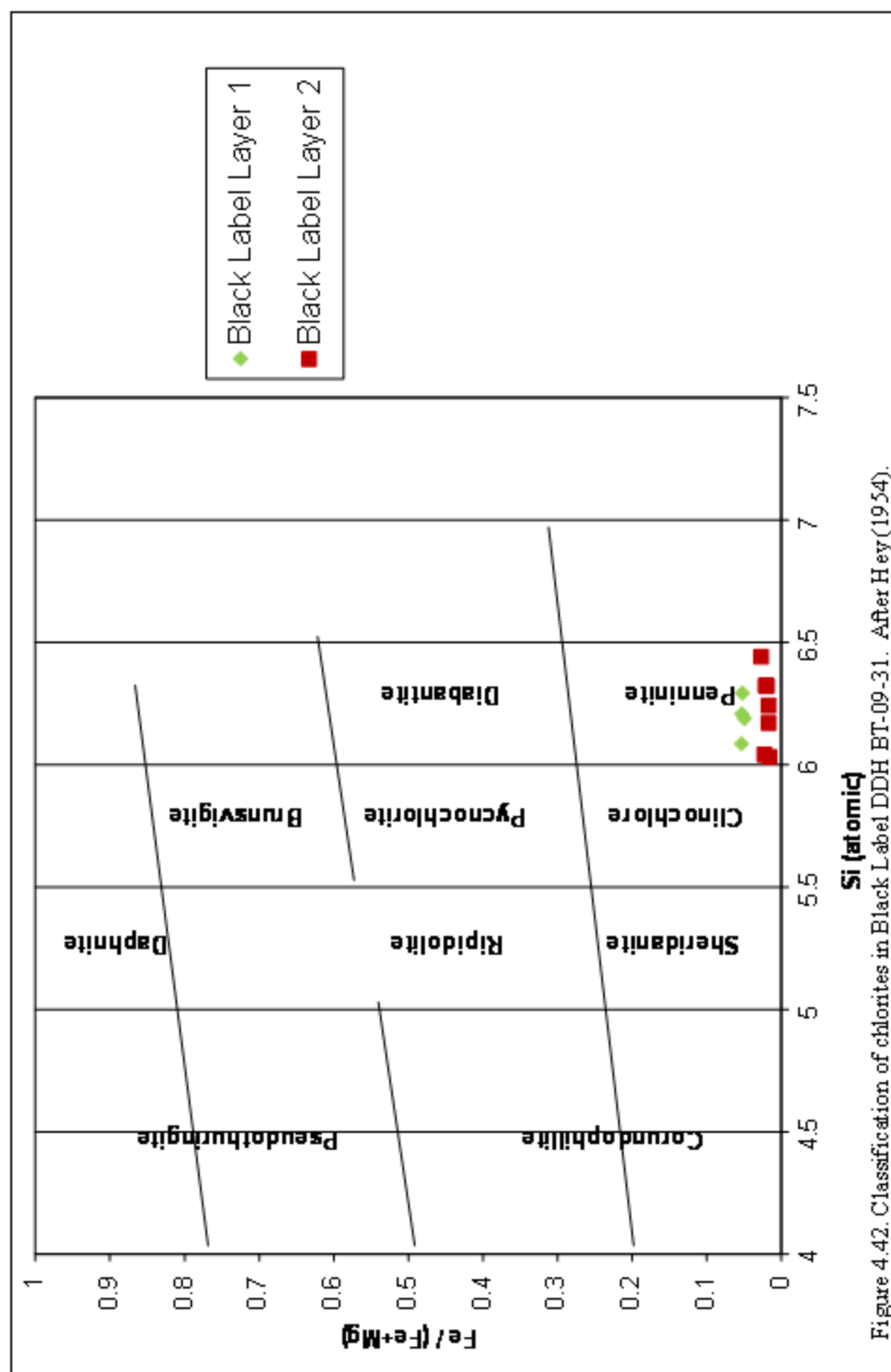


Figure 4.42. Classification of chlorites in Black Label DDH BT-09-31. After Hey (1954).

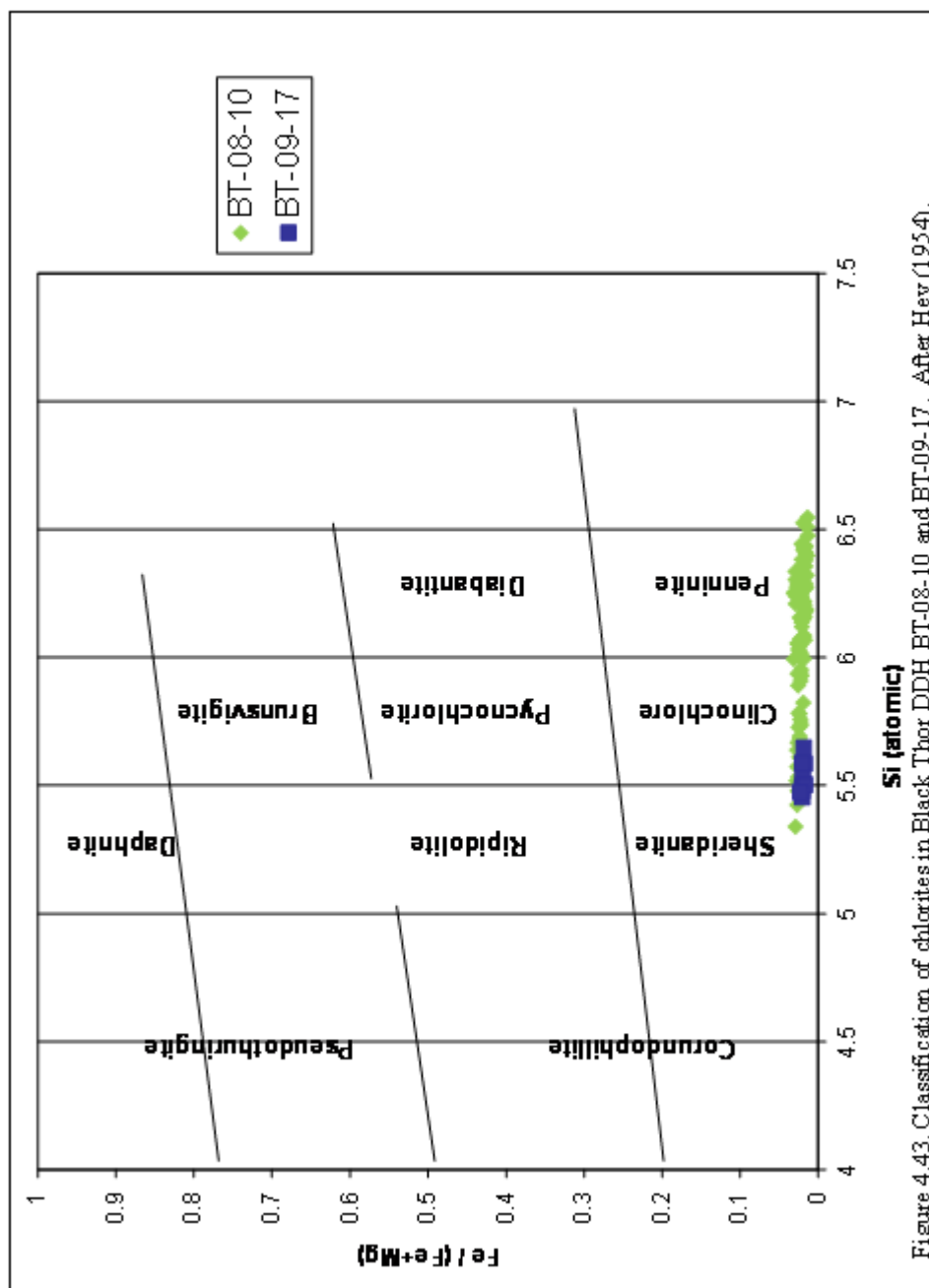


Figure 4.43. Classification of chlorites in Black Thor DDH BT-08-10 and BT-09-17. After Hey (1954).

chlorites, on the other hand, are more primitive with lower Fe # more similar to the Black Thor chlorites (Figs. 4.41 and 4.42).

There is a large range of chlorite compositions in the Black Thor chromites analysed. Three types of chlorite have been probed in the samples: 1) chlorites found in the round silicate inclusions in chromite; 2) chlorites found in the matrix of host dunites and chromitites; 3) and chlorites found as inclusions in the reaction margins of chromites. The chlorites are distinguished on a plot of wt. % Cr_2O_3 vs. wt. % Al_2O_3 (Fig. 4.44). The chlorites found in the round silicate inclusions plot as the four analyses 43 to 46 which are from sample 486034 at 131.2m in DDH BT-08-10. Three of these chlorites have high Al_2O_3 at 20 wt. % and elevated Cr_2O_3 at up to 2.63 wt. %. The fourth chlorite has lower Al_2O_3 at 15.53 wt. % and higher Cr_2O_3 at 3.66 wt. % as Cr substitutes with Al. The high Al_2O_3 and elevated Cr_2O_3 contents of these minerals are derived from the high Al and Cr contents of the host chromites. They probably formed from retrogression of chromite and host amphiboles and other minerals found within the round inclusions. The chlorites found in the host silicate and surrounding chromites have lower Al_2O_3 contents of 13 to 15 wt. % and either do or do not contain elevated Cr_2O_3 . Those with elevated Cr_2O_3 either replace interstitial chromian tremolite occurring interstitial in massive chromitites or are found as chromian chlorites in fractures where there has been mobility of Cr. It has been noted in the petrography chapter that the fracture chlorites all have elevated Cr while other interstitial chlorites either do or do not have elevated Cr. The chlorites found as inclusions in the reaction margins of chlorites are similar to the chlorites found in the round silicate inclusions with elevated Al_2O_3 from 16 to 20 wt. % and elevated Cr_2O_3 up to 2.55 wt. %. Some of these chlorites plot with lower Al_2O_3 and are similar to the matrix chlorites but with higher Cr_2O_3 , up to 5.75 wt. %. The high Cr, low Al is due to substitution of Cr for Al, as in the round silicate inclusion-bearing chlorites.

On a wt. % Cr_2O_3 vs. wt. % MgO plot, there is an overall trend of decreasing Cr_2O_3 with increasing MgO in the chlorites as a whole; however, there are two trends within the Black Thor DDH BT-08-10 and Black Label chromites for increasing Cr_2O_3 with MgO (Fig. 4.45). Overall, the chlorites are found as very Cr-rich (up to 9.61 wt. % Cr_2O_3) minerals coexisting with the upper chromites of DDH BT-09-17, lesser Cr-rich (1.6 to 7.17 wt. % Cr_2O_3) chlorites co-existing with chromite in DDH BT-08-10 and

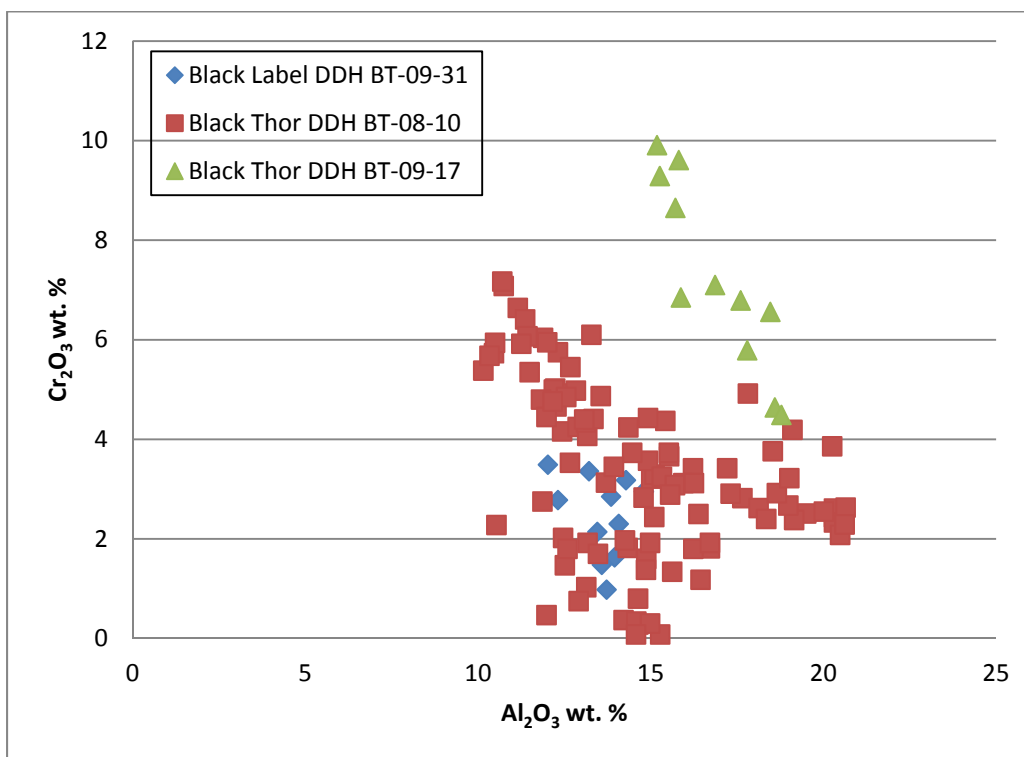


Figure 4.44. Plot of wt. % Cr_2O_3 vs. wt. % Al_2O_3 for chlorite.

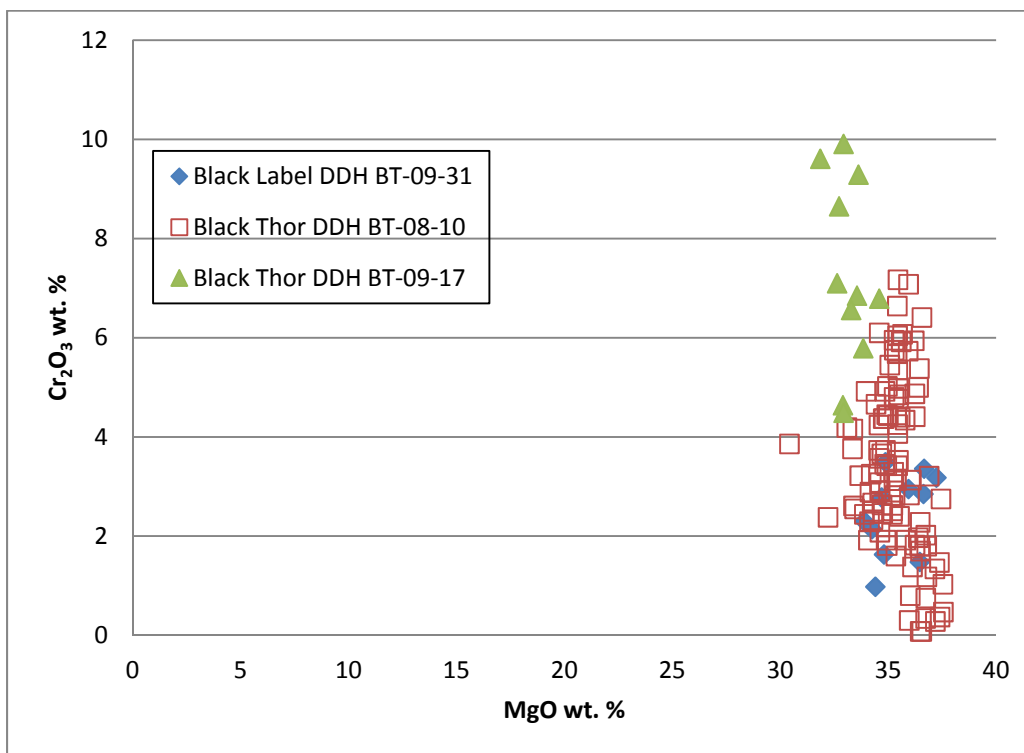


Figure 4.45. Plot of wt. % Cr_2O_3 vs. wt. % MgO for chlorite.

DDH BT-09-31, and low Cr-bearing regular chlorites coexisting with serpentine in the host dunites to the chromitites.

The high chromian chlorites of DDH BT-09-17 have lower Mg contents since there is Mg enrichment with higher T retrogression of these chromites from core to rim. This would not result in as high Mg content in the resulting chlorite due to mass balance. However, the high Cr enrichment of ferrichromite on the rims of these chromites serves to also enrich the Cr contents in the resulting chlorites. On the wt. % Cr_2O_3 vs. wt. % Al_2O_3 diagram, the DDH BT-09-17 chromites follow a separate trend of decreasing Cr_2O_3 with increasing Al_2O_3 than the other chlorites (Fig. 4.44). The chlorites as a whole generally decrease in Cr content with substitution with Al. However, the DDH BT-09-17 chlorites retrogressed at higher temperatures resulting in increased Cr and Al contents and substitution of the two elements under these conditions.

The two lower trends of increasing Cr_2O_3 with MgO are a result of Mg and Cr enrichment with the diffusion of Mg and Cr ions of the primary chromite as retrogression in the resulting chromites (Fig. 4.45). It was also noted in the petrography chapter that Cr is enriched in chlorites along fractures where there has been more retrogression of chromites as opposed to some of the interstitial groundmass to the chromites where there has not been this diffusion.

Finally the low Cr, high Mg chlorites are pristine clinochlores that occur with serpentine in the dunite host to the chromites and as chlorites surrounding chromite where there has not been mobility of Cr. Clinochlore is a result of low T greenschist hydration of the silicates.

CHAPTER 5

MINERALIZATION

5.1 Introduction

The nature of the chromite mineralization at McFaulds Lake is defined by an initial investigation of drillhole assay data, by electron microprobe analysis of major element chemistry of chromite, and by a laser ablation study of trace element chemistry of chromite.

5.2 Metal assay variation

Chromium oxide (wt. % Cr_2O_3), base and precious metals analyses are reported for three DDH holes representative of the three chromite deposits: DDH FW-08-19 for Big Daddy; BT-08-10 for Black Thor; and BT-09-31 for Black Label. These assays are reported on the exploration drill programs by Freewest-Spider-KWG for Big Daddy, and by Freewest for Black Thor and Black Label. Discussion of assay trends presented below are divided into up section Cr_2O_3 wt. %, Pt, Pd, Ni and Cu variation. This is followed by wt. % Cr_2O_3 vs. Ni, Ti, Zn and Mn variation for the Black Label, Black Thor and Big Daddy deposits respectively.

5.2.1 Up section wt. % Cr_2O_3 , Pt, Pd, Ni and Cu ppm variation

Assay values for whole rock wt. % Cr_2O_3 , ppb Pt+Pd and ppm Ni were investigated as a preliminary framework to performing electron microprobe work on chromite. This data shows basic trends of replenishment and differentiation in terms of Cr_2O_3 and Ni. Also, associated peaks in Pt+Pd mineralization provide evidence for double diffusive convection processes being involved in PGE concentration in the chromitites and host lithologies. Although helpful to understanding of gross trends through each of the chromitite intervals, care must be taken as the whole rock wt. % Cr_2O_3 , ppm Ni and ppb Pt+Pd represent the content of chromite + silicate rather than chromite alone; the variation in chromite chemistry is determined through electron

microprobe analyses. The up section variation in these metals is presented for the Black Label, Black Thor and Big Daddy drill holes in sections 5.2.1.1 to 5.2.1.3.

5.2.1.1 Black Label (Figs. 5.1 and 5.2)

In Black Label DDH BT-09-31, there are trends of increasing wt. % Cr_2O_3 upward, identifying repeated pulsing of chromite layers within alternating lithologies in three separate chromitite intervals. The first chromite interval at Black Label is from 154 to 206 m. From 154 to 165 m, there are two initial chromite replenishments with peaks at 14 wt. % Cr_2O_3 . Between 165 to 210 m, there is an overall trend of differentiation with decreasing wt. % Cr_2O_3 . However, in the overall trend, there are individual chromite replenishment peaks in wt. % Cr_2O_3 that increase in Cr_2O_3 with each successive replenishment. Pt+Pd show peaks that are offset from the replenishments in Cr_2O_3 , usually beneath each Cr_2O_3 layer. These PGE peaks probably represent sulphur saturation near the bottom and top boundaries of a convection layer.

PGE peaks at the tops and bottoms of convection layers have been known to occur in other layered complexes such as the Bushveld Complex. They have been attributed to represent initial sulphur saturation of a magma that initially convected near the top and bottom boundary layers of double diffusive convection cells (Rice and von Gruenewaldt, 1994). In the overall interval, Pt+Pd values have signatures of primary Pt+Pd in the top silicate at 206 m and the bottom of the interval at 156 m. With increased stratigraphic height between, there is a decreasing cascading upward trend of Pt+Pd values due to saturations with each chromite replenishment upward in the sequence.

For Cr_2O_3 , the individual replenishments of Cr_2O_3 in the overall differentiation trend reflect massive to lensy and discontinuous beds of chromitite hosted in pyroxenite between sections of dunite. Along with replenishments in Cr_2O_3 , there are peaks in Ni contents within the dunites that occur after each successive chromite layer. The Ni contents of the dunites increase upward in the section due to replenishing supply of magma. Cu contents show an overall increasing upward trend reflecting higher Cu contents with increased fractionation.

The second chromite interval is from 229 to 277 m. At first there is silicate with little chromite mineralization. Then from 248 to 270 m, there is a series of chromite replenishments that increase in wt. % Cr_2O_3 upward from 248 to 257, followed by a

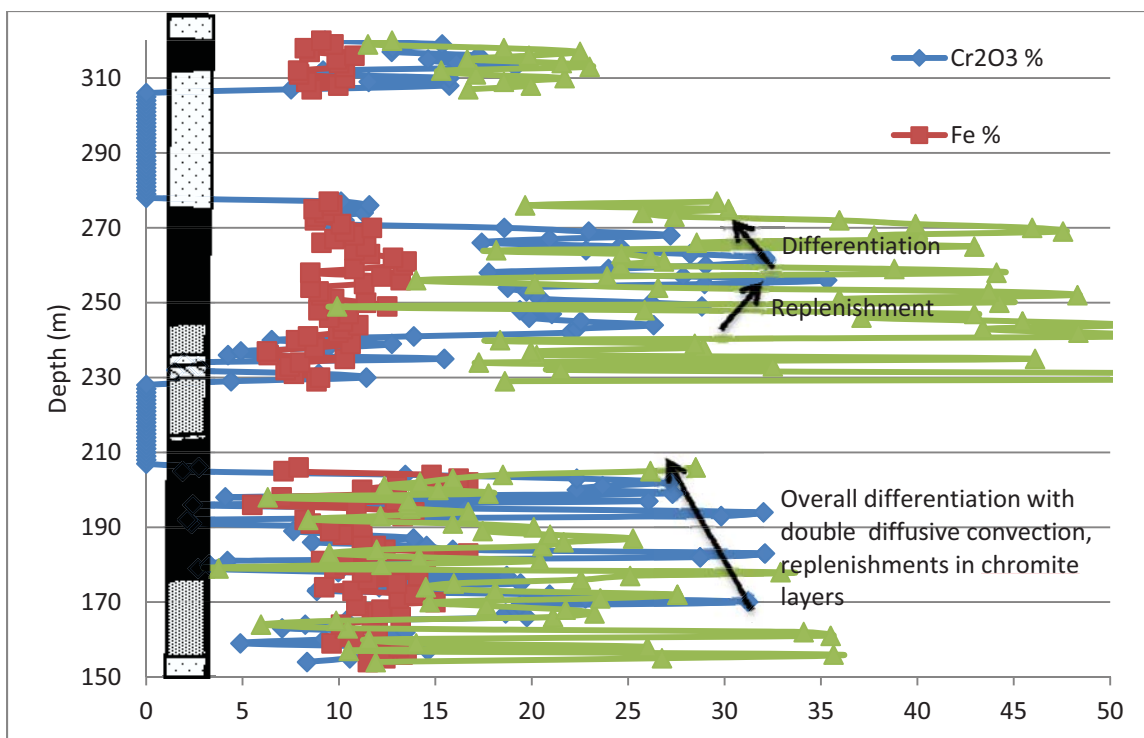


Figure 5.1. Plot of Cr₂O₃, Fe and Pt + Pd vs. depth from assays of Black Label DDH BT-09-31 with trends in replenishment and differentiation shown.

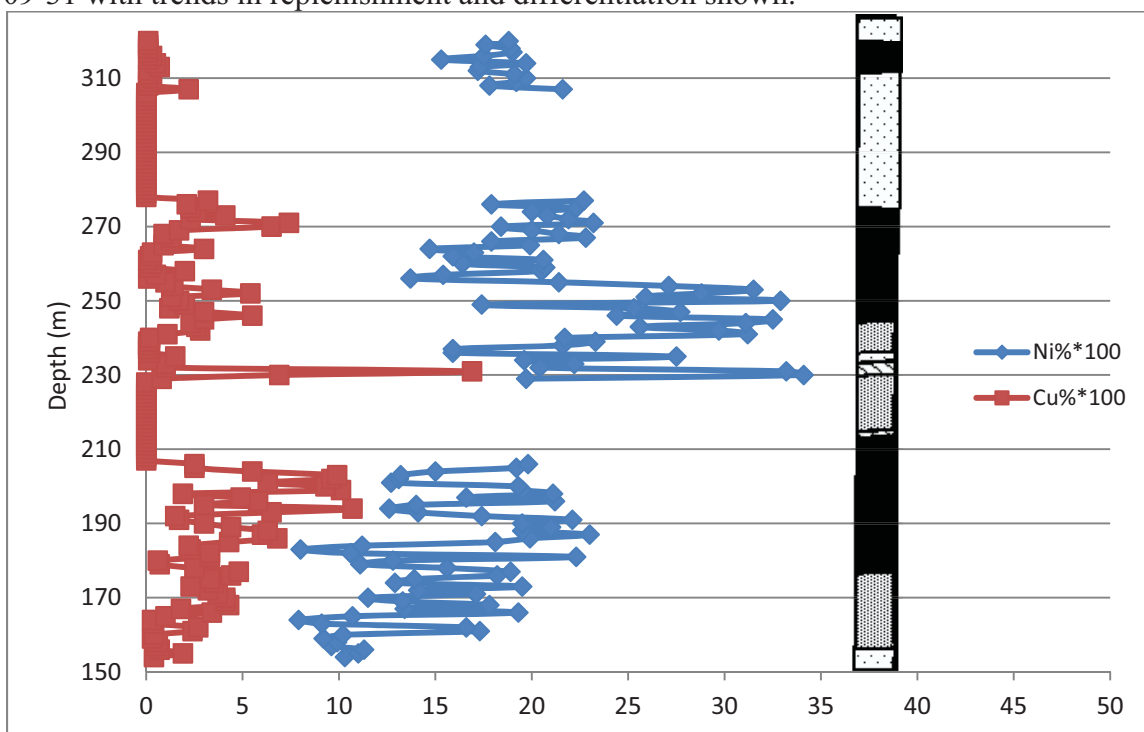


Figure 5.2. Plot of Ni and Cu vs. depth from assays of DDH BT-09-31.

decrease in wt. % Cr_2O_3 in the replenishments upward from 257 to 270 m. Cr_2O_3 contents reach a maximum of 35.32 wt. % at 256 m. The interval from 248 to 257 m is a section of the chromitite dominated by replenishing intermittent chromitite layers alternating with dunite while the section from 257 to 270 m contains minor chromite beds in dominant dunite that represents a differentiation sequence.

For PGE, the sequence begins at 229 m with high ppb Pt+Pd in the basal silicate with little chromite at 424 ppb Pt and 1330 ppb Pd. There are also high Ni and Cu peaks at 3410 ppm Ni and 1690 ppm Cu which suggests basal sulphide mineralization. Then from 244 to 272 m, there is a sequence starting with high ppb Pt+Pd at the base with 311 ppb Pt and 745 ppb Pd and decreasing in a cascading trend upward with each convection cycle of chromite mineralization. The roof of the sequence contains high ppb Pt+Pd at 254 ppb Pt and 697 ppb Pd at 269 m depth due to saturation at the top of the convecting magma. For Ni, from 236 to 253 m, the Ni contents have been increasing upward with each replenishment of dunite in the sequence. After 253 m, there is a sharp decrease in Ni ppm followed by another replenishing trend of increasing Ni with each dunite replenishment. Notably the Ni contents are higher from 236 to 253 m consistent with more primitive magma replenishments. Cu is elevated where there is high Ni.

The third chromite interval is from 307 to 318 m and contains chromite layers in a dominant dunite sequence. There are a few minor replenishments increasing in wt. % Cr_2O_3 upward followed by decrease. The interval shows a differentiation trend in dunite with a few chromite beds. Evidence for more dominant fractionation is in the decreasing upward trend of Ni ppm contents. PGE contents are low compared to the other chromite intervals.

5.2.1.2 Black Thor (Figs. 5.3, 5.4, 5.5 and 5.6)

Black Thor DDH BT-08-10 is characterized by intermittent chromite pulses alternating with dunites. Evident grading in chromitite layers is interpreted to be due to switches in and out of the stability fields of olivine and chromite. PGE contents are lower than Black Label as there are fewer episodes of sulphur saturation probably due to the lower silica content of the magma.

The first minor beds of chromite appear between 112 to 124 m, and these show an upward differentiation pattern of decreasing wt. % Cr_2O_3 . The host lithology is light

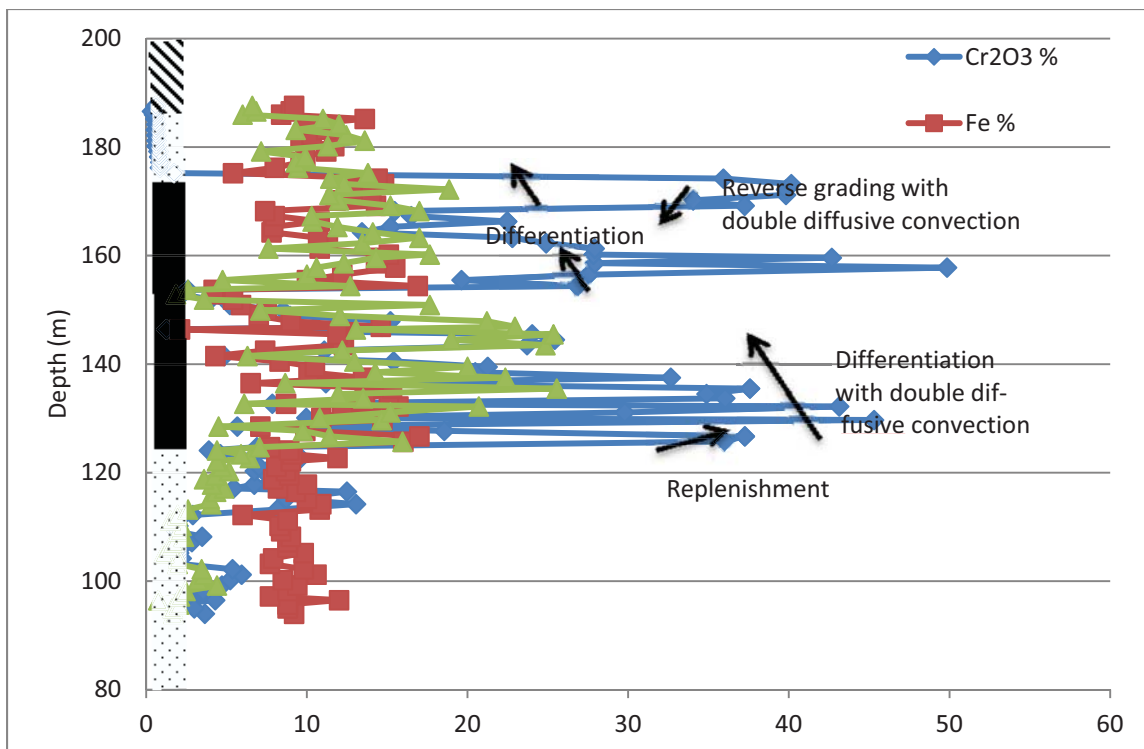


Figure 5.3. Plot of Cr₂O₃, Fe and Pt + Pd vs. depth from assays of Black Thor DDH BT-08-10 with trends in replenishment and differentiation shown.

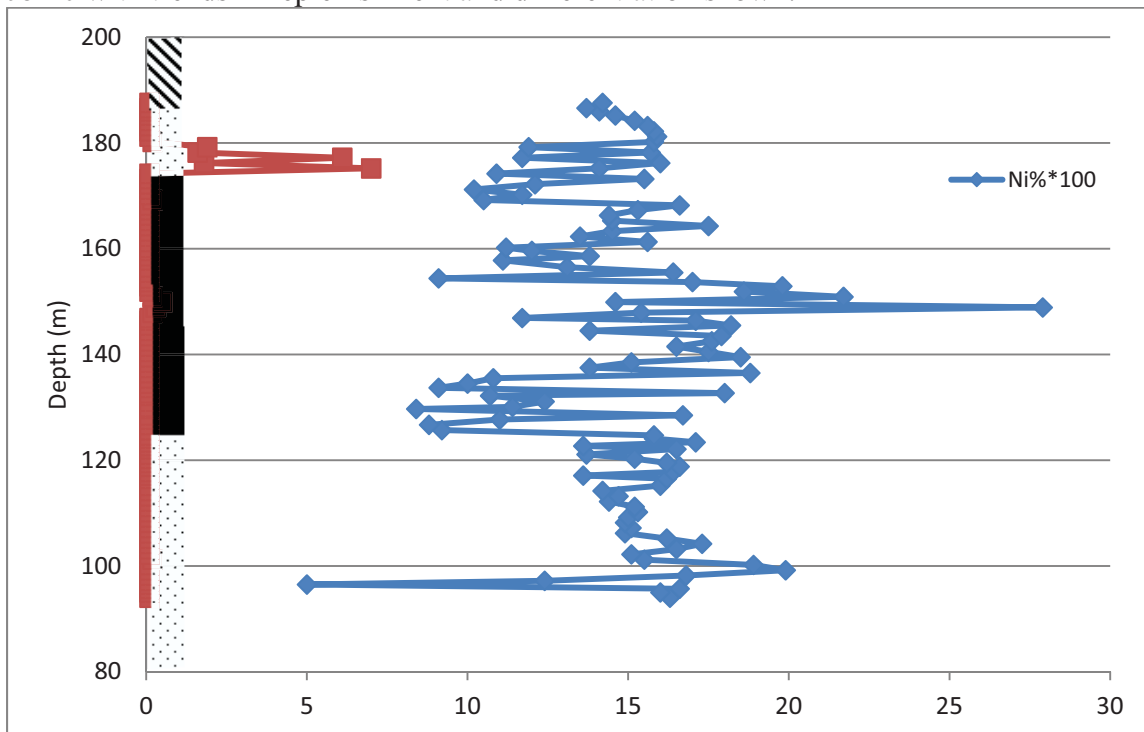


Figure 5.4. Plot of Ni and Cu vs. depth from assays of DDH BT-08-10.

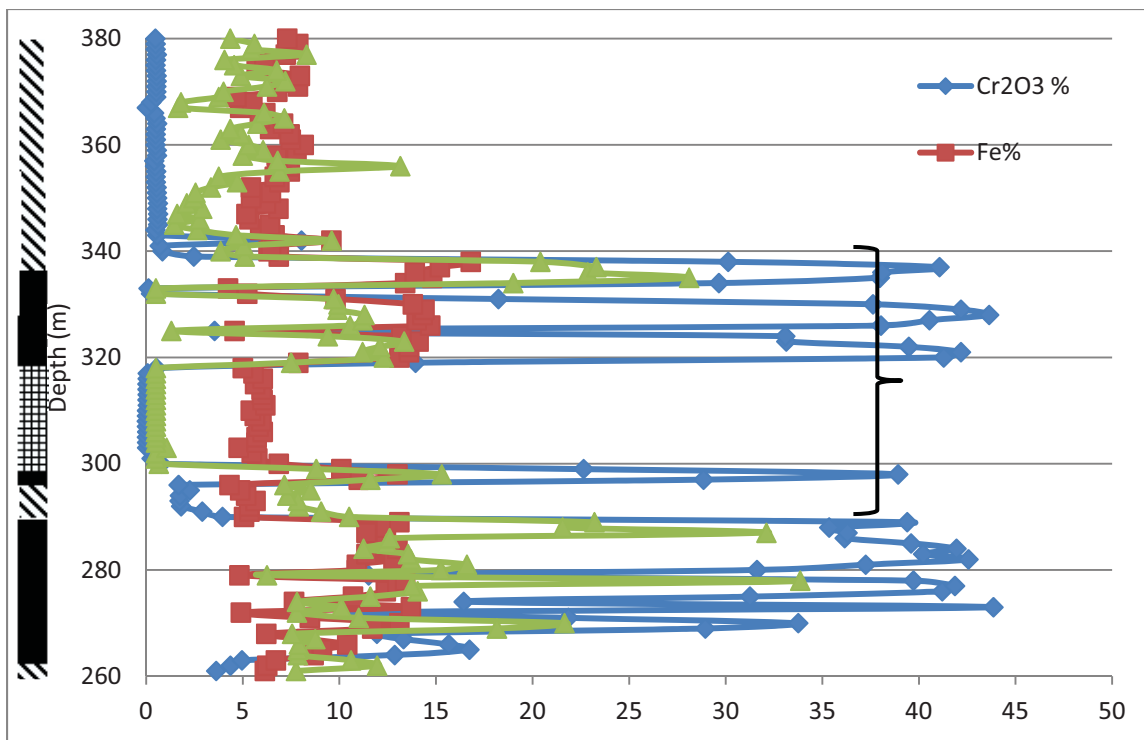


Figure 5.5. Plot of Cr₂O₃, Fe and Pt + Pd vs. depth from assays of Black Thor DDH BT-09-17 with chromitite interval analysed in bracket.

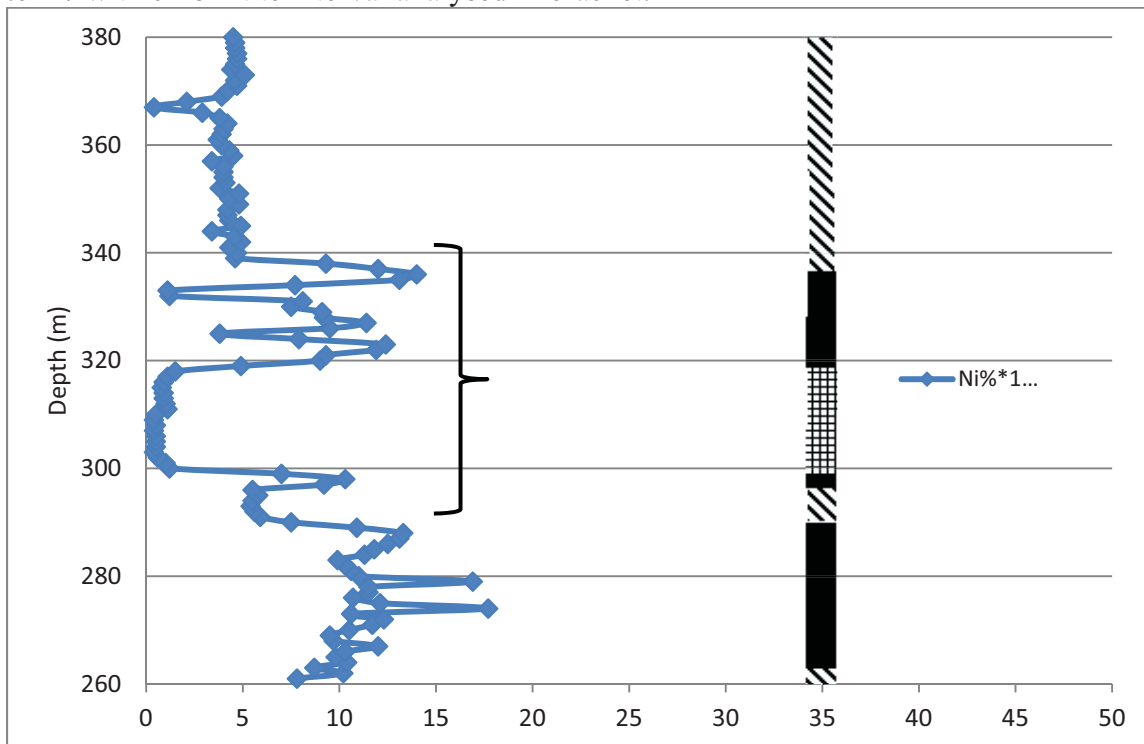


Figure 5.6. Plot of Ni and Cu vs. depth from assays of DDH BT-09-17.

green serpentinized dunite. From 124 to 152 m, there is an interval of intermittent chromitite beds that are variably 1 to 50 cm thick that alternate with dunite. The beds contain layers of chromite that fine upward to chain textures of cumulus chromite and olivine as chromite is filter pressed through the overlying dunite pulses. The individual chromite beds are identified by replenishments in wt. % Cr_2O_3 that successively increase upward from 124 to 130 m. From 130 to 152 m, replenishments in wt. % Cr_2O_3 of individual pulses follow an overall decreasing trend in wt. % Cr_2O_3 due to more dominant differentiation in the sequence. Pt+Pd peaks correspond with Cr_2O_3 replenishments. Ni ppm increases upward with each dunite pulse between the chromite beds. At 149 m, there is a peak at 2790 ppm Ni along with elevated Cu that is possibly due to sulphide.

From 152 to 165 m, there is another chromitite interval where there is a dominant replenishment of wt. % Cr_2O_3 followed by decreasing wt. % Cr_2O_3 in replenishments from 157.8 to 165 m. Ni ppm increases with each dunite pulse between the chromite layers. From 162 to 168.20 m, there are cumulus contacts below the lower and above the upper contacts of the chromite layers indicating a change in the order of crystallization of chromite and olivine. Above 168.20 m, beds then contain cumulus olivine grading up to chromite that indicate dominant cumulus olivine over cumulus chromite mineralization. There are then upward replenishments of increasing wt. % Cr_2O_3 as the magma switches back to the chromite stability field from 168.20 to 174.20 m. At 174.20 m, there is a sharp upper contact of the chromitite bed followed by the main dunite again. Notably, there are peaks in Cu ppm at 175 m depth above the chromite layer which are probably due to sulphur saturation at the upper contact.

The Black Thor deposit in DDH BT-09-17 intersects chromitite located within host pyroxenite and gabbro lithologies which shows trends in greater enrichment in wt. % Cr_2O_3 compared to the other chromitites in that particular drill hole. The sequence is found from 290 to 345 m depth. At 290 m, there is first pyroxenite with elevated Ni ppm. From 296.30 to 298.80 m, there is a pulse of chromite represented by up to 38.92 wt. % Cr_2O_3 . Along with a peak in wt. % Cr_2O_3 , there is a peak of 306 ppb Pt+Pd. From 298.80 to 318.70 m, there is gabbro. In contrast to the pyroxenite, there is little Ni in the gabbro and the unit is devoid of Pt, Pd and chromite. From 318.70 to 339 m, there are

three chromite sequences that alternate with gabbro, giving rise to troughs in wt. % Cr_2O_3 . Cr_2O_3 contents reach a maximum of 43.63 wt. % and possibly show trend in increasing Cr_2O_3 upward. These could be indicative of enrichment in wt. % Cr_2O_3 with retrogression of the chromites. Pt+Pd ppb show the highest peak in the third sequence where there is more silica for greater sulphur saturation. Above the sequence from 339 to 345 m, there is again pyroxenite similar to the first pyroxenite at 290 m.

5.2.1.3 Big Daddy (Fig. 5.7)

Big Daddy DDH FW-08-19 begins with a sequence of dunite with intervening pyroxenites and heterogeneous olivine pyroxenite as the system changes from cumulus olivine to pyroxene followed by chromite mineralization. There are a few intervals of chromite mineralization before the main sequence from 141.50 to 144.14 m and from 159.37 to 162.00 m that show replenishments in wt. % Cr_2O_3 and associated peaks in ppb Pt+Pd. In the interval of pyroxenite before the lower contact with the main massive chromitite sequence, there is high ppb Pt+Pd within 20 m of the contact. This possibly represents remobilized PGE since it is not in one horizon with visible sulphide, however it is not fully understood. Some sulphide is present since there is a large peak of 8480 ppm Ni at 165 m (Fig. 4.10). In the company logs, sulphide has been noted with predominately po with minor py and trace cpy. The mineralization style follows the foliation where it is semi massive but it appears to be fine grained disseminated on fracture surfaces. Notably, similar fracture pyrite has been noted immediately above the chromitite/pyroxenite contact which shows a similar peak in Pt+Pd.

The massive chromitite begins after the pyroxenite at 183 m and continues to 229 m. Within the sequence, wt. % Cr_2O_3 is consistently high at between 33 to 39 wt. % Cr_2O_3 . The chromitite sequence is divided into three intervals. The first two there is increasing wt. % Cr_2O_3 followed by decreasing wt. % Cr_2O_3 from 183 to 192 m and from 192 to 208.5 m. From 208.5 to 229m, there is an overall decreasing trend in wt. % Cr_2O_3 . The increases in wt. % Cr_2O_3 are due to replenishments while the decreasing trends are differentiation trends. Pt+Pd values are offset by these increases and decreases probably due to individual sulphur saturations in the top and bottoms of double diffusive convection cells as at Black Label.

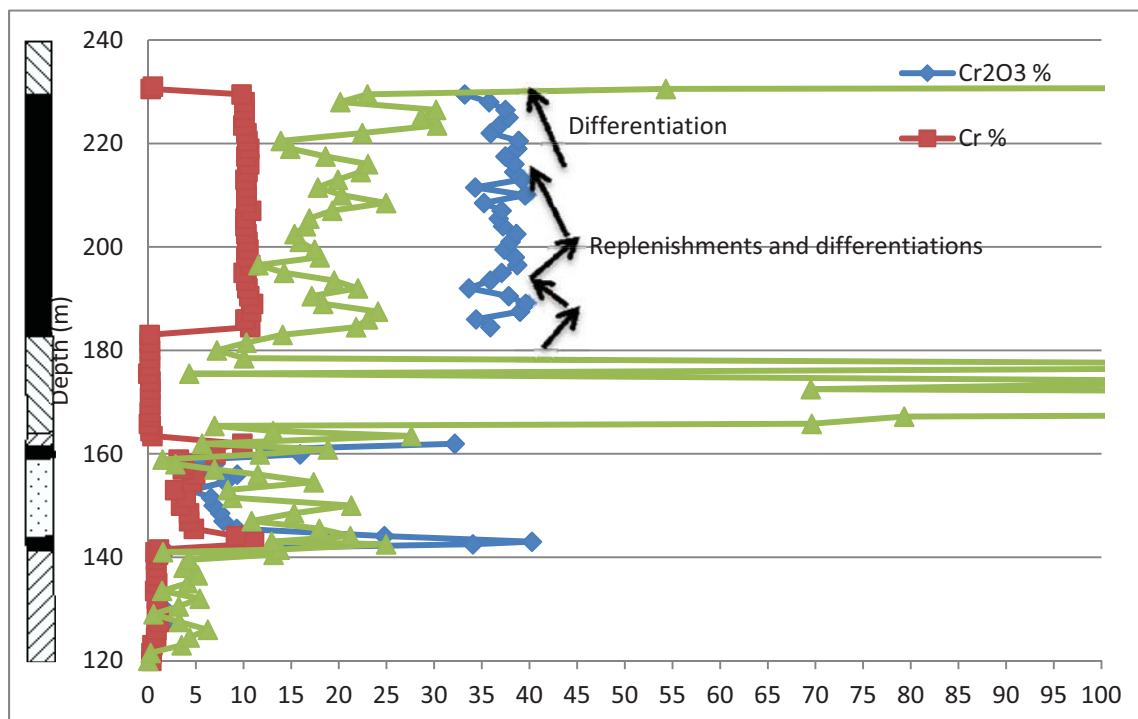


Figure 5.7. Plot of Cr₂O₃, Fe and Pt + Pd vs. depth from assays of Big Daddy DDH FW-08-19 with trends in replenishment and differentiation shown.

Above the upper contact of the chromitite, there is pyroxenite again. There is high ppm remobilized Pt+Pd again in the background pyroxenite. Notably, there are medium grained fracture pyrite sulphides just above the upper contact. The unit is bleached due to talc, indicative of intense hydrothermal alteration.

5.2.2 Binary metal assay variation

Binary metal plots that represent association of Ti, Zn and Mn with modal % chromite are displayed for Black Label (Fig. 5.8). Ni contents, on the other hand, do not show a correlation. For Ti ppm vs. Cr ppm, Ti increases with Cr, demonstrating Ti is partitioned into chromite grains than into silicate. Zn shows an even stronger correlation as Zn partitions into chromite, however, there are also Zn contents that are above the main trend due to sulphide mineralization. Mn generally correlates with Cr like Ti and Zn, however, there is variable Mn content in host dunite vs. pyroxenite. Pyroxenite contains more elevated Mn compared to the dunite. V contents are interesting in that they show two trends of increasing V ppm vs. Cr ppm. These represent the two chromitite intervals of Black Label. The first chromitite interval follows the lower trend plus the higher sloped trend of increasing V ppm vs. Cr ppm. The second chromitite interval only follows the lower sloped trend. The higher V in the first chromitite interval is due to higher V with differentiation of the chromitite in the first chromitite interval while the second chromitite interval is more primitive. These same trends can be shown for the Ti % vs. Cr ppm for these two intervals. The third interval follows the same trend as the second interval only with lower V and Cr contents.

Black Thor BT-08-10 shows well defined positive correlations of Ti, V and Zn with Cr (Fig. 5.9). There is a strong association of these metals with modal % chromite. Mn also shows a positive correlation but more diffuse. The consistent trend in Mn reflects only one host lithology to the chromite which is dunite. Ni contents show a diffuse negative correlation with Cr while an antipathetic positive correlation with Mg %. Therefore, Ni in Black Thor is more strongly associated with Ni in olivine of the dunite pulses.

Big Daddy also shows well defined correlations, although many of the samples plot as either low in the various metal contents or at high metal contents in the massive chromitite (Fig. 5.10). The fewer intermediary metal contents reflect increasing Ti, V, Zn

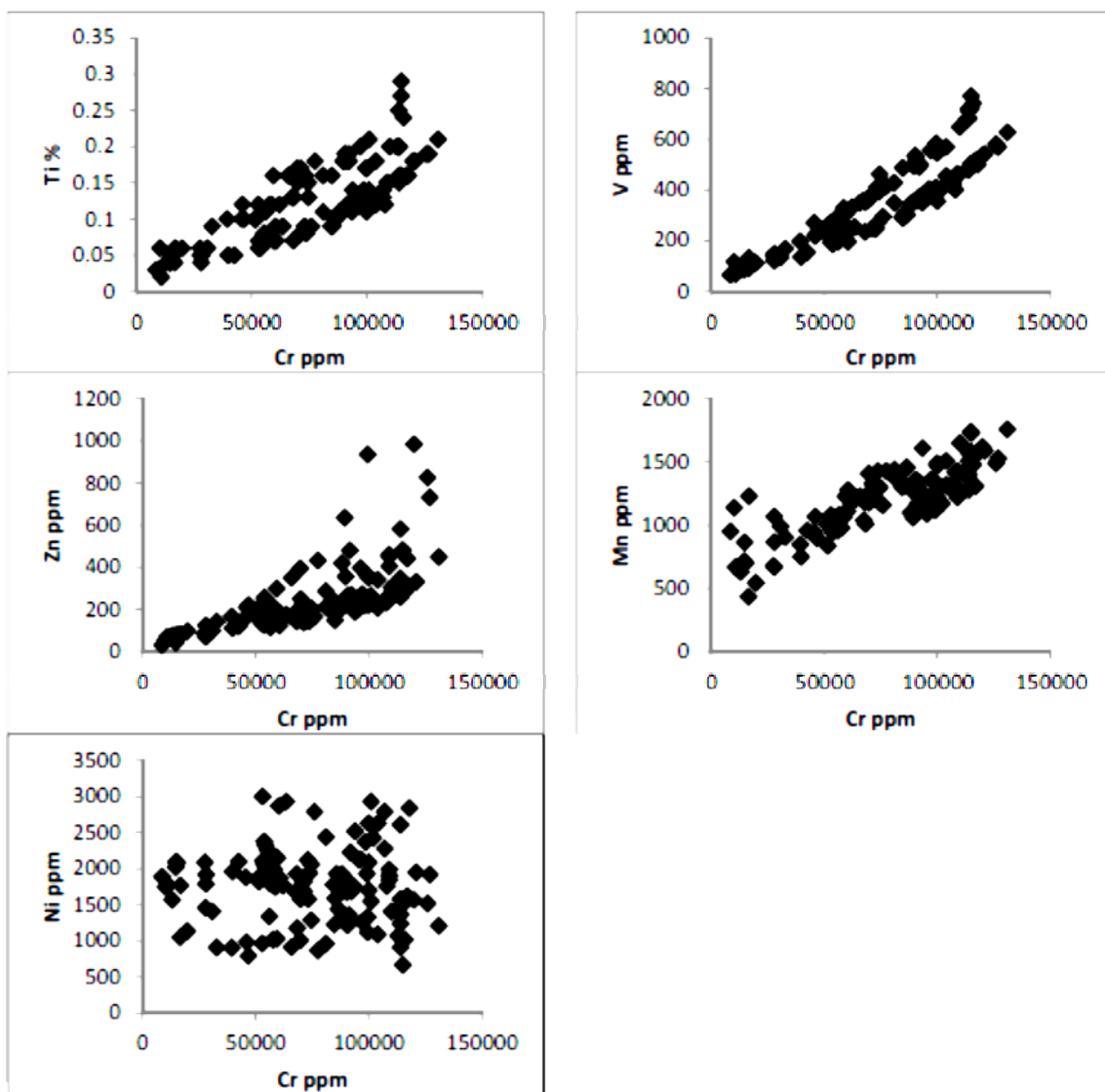


Figure 5.8. Binary plots of Ti, V, Zn, Mn and Ni vs. Cr from assays of Black Label DDH BT-09-31.

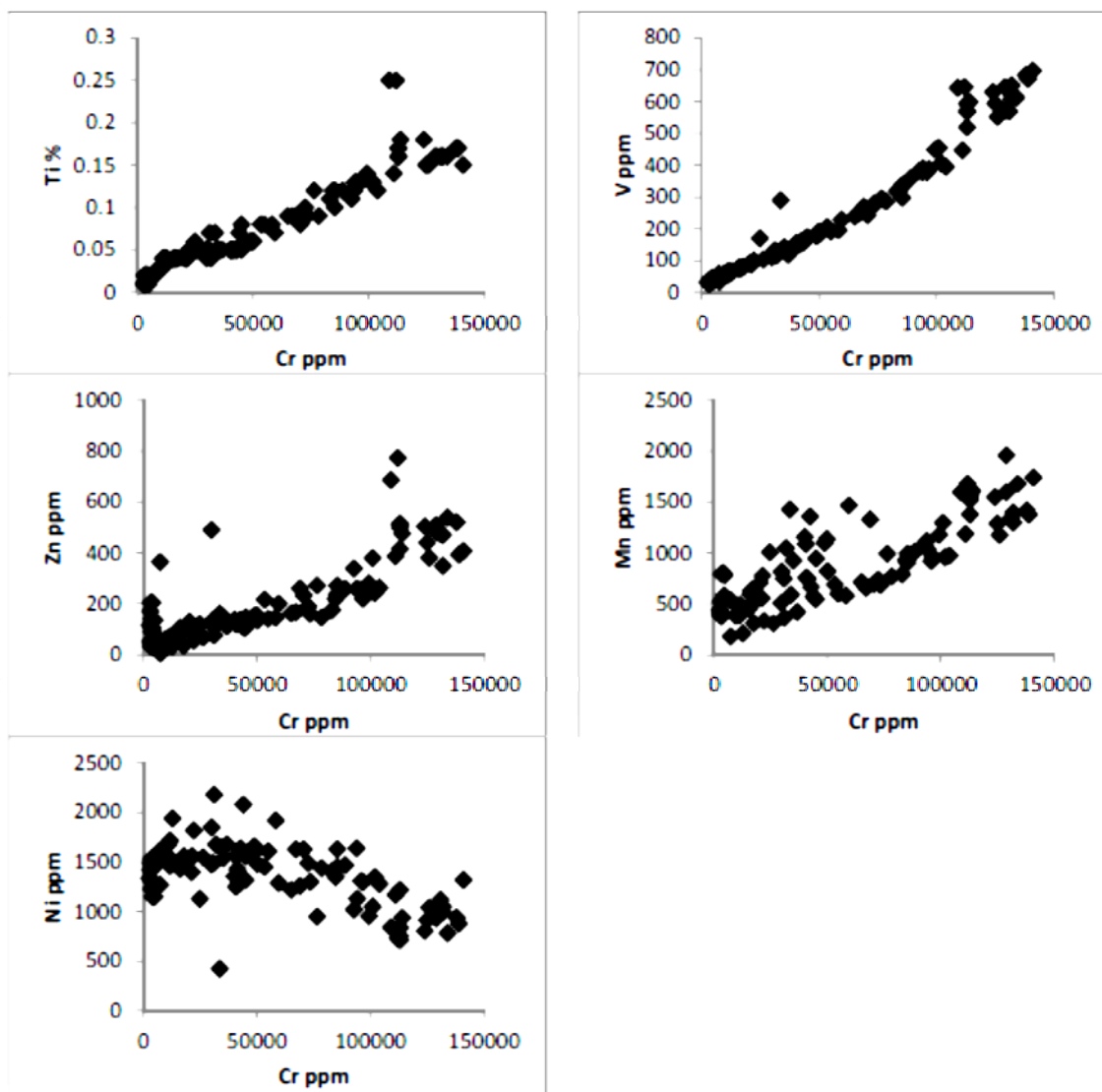


Figure 5.9. Binary plots of Ti, V, Zn, Mn and Ni vs. Cr from assays of Black Thor DDH BT-08-10.

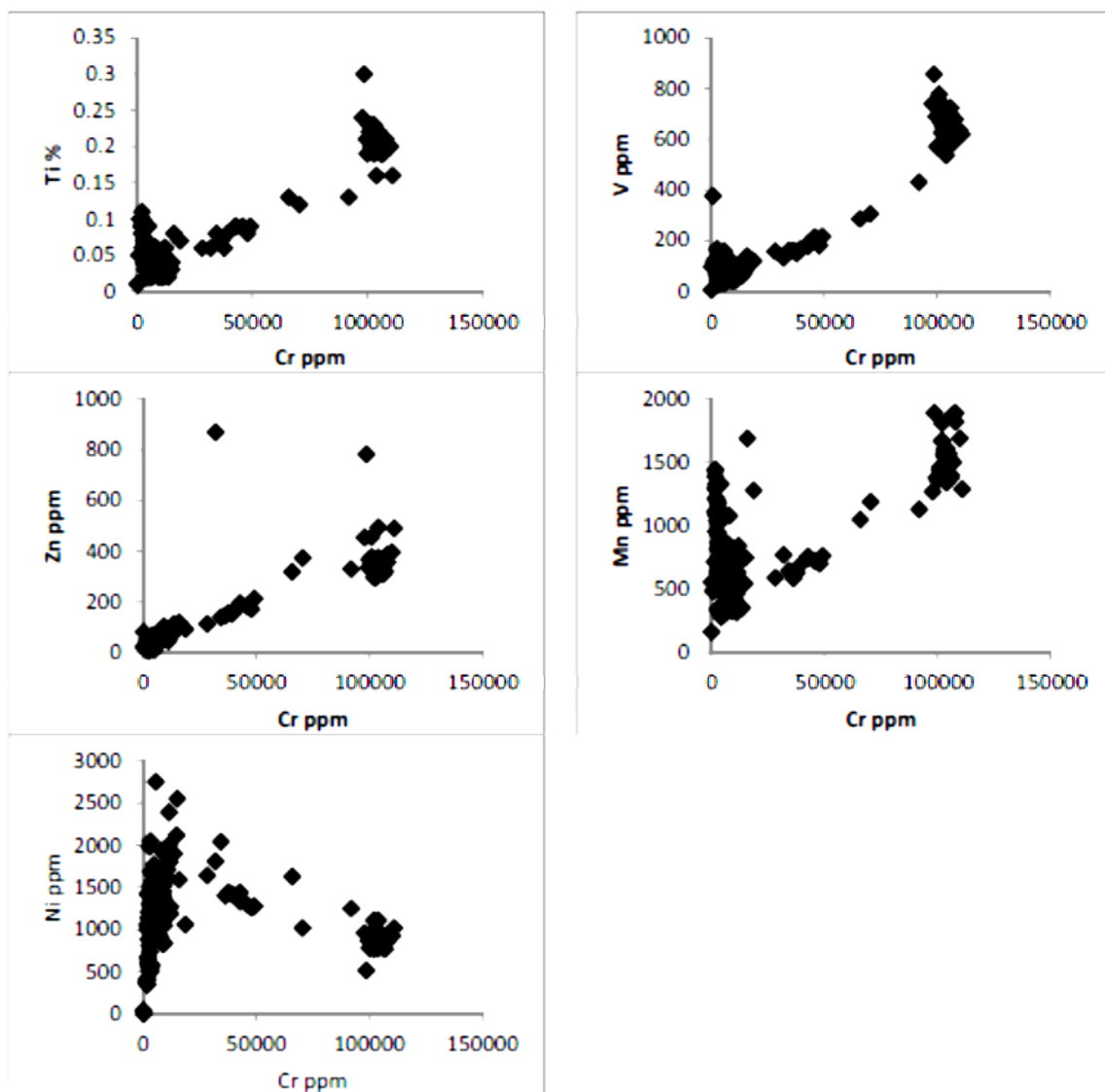


Figure 5.10. Binary plots of Ti, V, Zn, Mn and Ni vs. Cr from assays of Big Daddy DDH FW-08-19.

with increased modal % chromite. Mn show a broad correlation although many samples contain Mn that do not follow the trend as there is considerable cumulus pyroxene-bearing lithologies with elevated Mn and the chromitite is more varied in Mn with evolution to bordering pyroxenite. The same variability in metals is reflected in Ti and V as well for the massive chromitite interval. Ni shows negative correlation with Cr and shows a subtle positive correlation with Mg % due to Ni in cumulus olivine-bearing dunite.

5.3 Chromite mineral chemical variation

A major effort was made to define the mineral chemical variation in the McFaulds Lake chromite deposits. Electron microprobe analysis has been carried out on 300 samples with over 4200 point analyses on samples spaced 20 cm to 1 m apart across individual gravitational cycles. Generally, up to 8 point analyses are made of each chromite sample. More point analyses are needed where there is evident textural variation in modal chromite (i.e. mineral zoning), there is variation in grain size, and higher ferrichromite content (Fig. 5.11). The microprobe work outlines the primary differentiation sequences as well as the effects of secondary hydration on chromite mineral chemistry. Results are listed in Appendix 5.

The microprobe analyses document original igneous compositions best preserved in the cores of large chromite grains in massive chromitite. The smaller, more isolated disseminated chromites have undergone greater silicate exchange. Primary compositions retained in larger grains best define igneous fractionation. Ferrichromite developed on the rims of original grains relates to secondary hydration. Specific chromite mineral chemistry therefore relates to both primary adcumulate sintering and secondary hydrous retrogression.

Current microprobe data shows Cr_2O_3 loss from 55 to 51 wt. % for centres of grains up section. Grain margins and disseminated smaller grains show up section chemistries of 49 to 47 wt. % Cr_2O_3 . Disseminated chromites have generally undergone more silicate exchange, reporting 48 wt. % Cr_2O_3 . Other elemental variation in the chromites includes increasing Fe, slightly decreasing Al and decreasing Mg due to magmatic differentiation. Near constant low-Al compositions are characteristic of komatiitic chromites. High grade chromite with higher wt. % FeO_T forms as retrograde

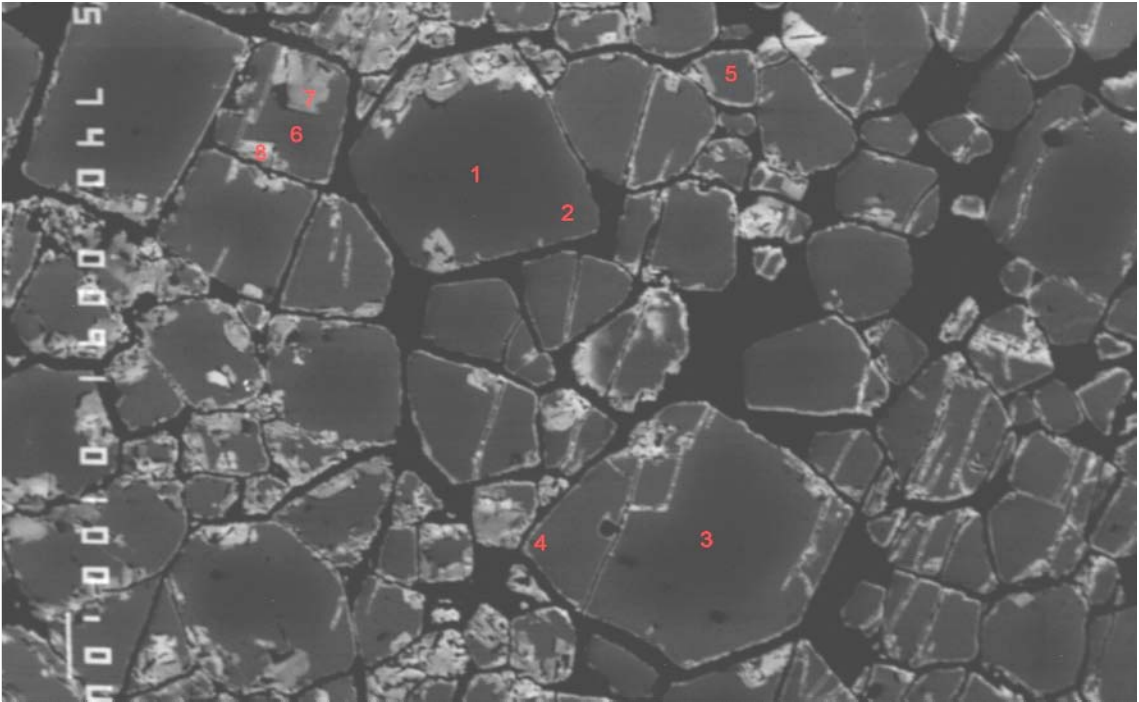


Figure 5.11. Backscatter image of massive chromite with sample points shown. The light grey to white areas on the rims of the chromites is ferrichromite alteration. Note the zoning in the grains due to diffusion. Sample points were taken of chromite cores and diffused margins of large and small grains as well as the ferrichromite rims.

ferrichromite rims. Original magmatic chromites are leached of Mg and Al leaving high Cr and Fe behind as ferrichromite.

The ferrichromite content has the effect of increasing or decreasing the Cr content of the ores. Cr-enriched ferrichromites are found as retrogression on the more primitive chromitites while Cr-depleted ferrichromites are found as further retrogression on disseminated chromite. The evolution of the chromites from core to rim to ferrichromite is illustrated in ferrichromite-bearing chromitites in three samples of massive chromite in DDH BT-08-10 (Figs. 5.12 to 5.17). In sample 486044 at 135.2 m, there is primary chromite with 52.18 wt. % Cr_2O_3 , 9.17 wt. % MgO, 19.78 wt. % FeO and 14.09 wt. % Al_2O_3 (Figs. 5.12 to 5.13). Due to increased diffusion towards the margin of the grain, there is then depletion of Cr_2O_3 and MgO to 50.04 and 8.87 wt. % respectively with enrichment in Al_2O_3 and FeO to 14.69 and 20.19 wt. % respectively. In one intermediate ferrichromite, there is enrichment in Cr_2O_3 and FeO to 57.84 and 22.27 wt. % respectively while depletion in Al_2O_3 and MgO with substitution to 9.87 and 7.28 wt. % respectively. In a more enriched ferrichromite, Cr_2O_3 and FeO increase to 59.94 and 21.53 wt. % respectively while Al_2O_3 and MgO decrease to 7.97 and 7.06 wt. % respectively. The ferrichromite occurs in association with chromian chlorite. There is later growth of Cr-depleted ferrichromite with relic grains of chlorite that decrease in Cr_2O_3 , Al_2O_3 and MgO to 48.90, 6.92 and 5.76 wt. % while FeO enriches to 23.50 wt. %. Notably, Fe_2O_3 has a composition of 13 wt. % compared to the earlier Cr-enriched ferrichromite at 2.47 wt. % Fe_2O_3 . The same trend is seen in another chromite from sample 486044 at 135.2 m, but there is an increase from core to rim in Cr_2O_3 in the primary chromite grain (Figs. 5.14 to 5.15). In sample 486129 at 169.6 m, Cr_2O_3 enriches to up to 65.11 wt. % with FeO at 23.25 wt. % while Al_2O_3 and MgO decrease to 2.62 and 5.16 wt. % respectively (Figs. 5.16 to 5.17).

5.3.1 Up section mineral chemistry of chromite

Detailed electron microprobe analysis was performed on chromitite intervals through the three deposits. Up section plots showing variation of wt. % Cr_2O_3 and wt. % MgO vs. depth are provided for the three chromite deposits in section 5.2.1. Comparable Cr #s ($\text{Cr}/(\text{Cr}+\text{Al}+\text{Fe}^{3+})$) and Mg #s ($\text{Mg}/(\text{Mg}+\text{Fe}^{2+})$) are plotted to supplement the wt. % Cr_2O_3 and wt. % MgO. Cr/Fe ($\text{Cr}_2\text{O}_3/\text{FeO}_T$) diagrams are also indicators of magma

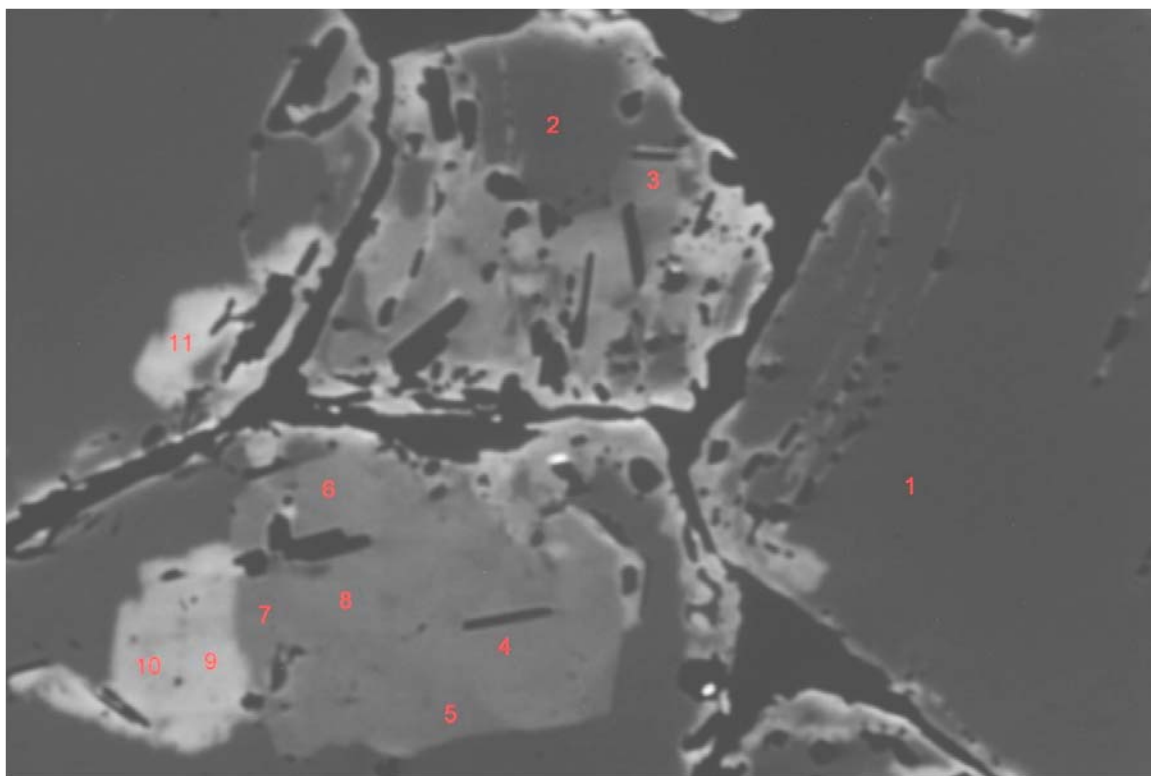


Figure 5.12. Backscatter image of sample 486044, chromite #1 with sample points shown.

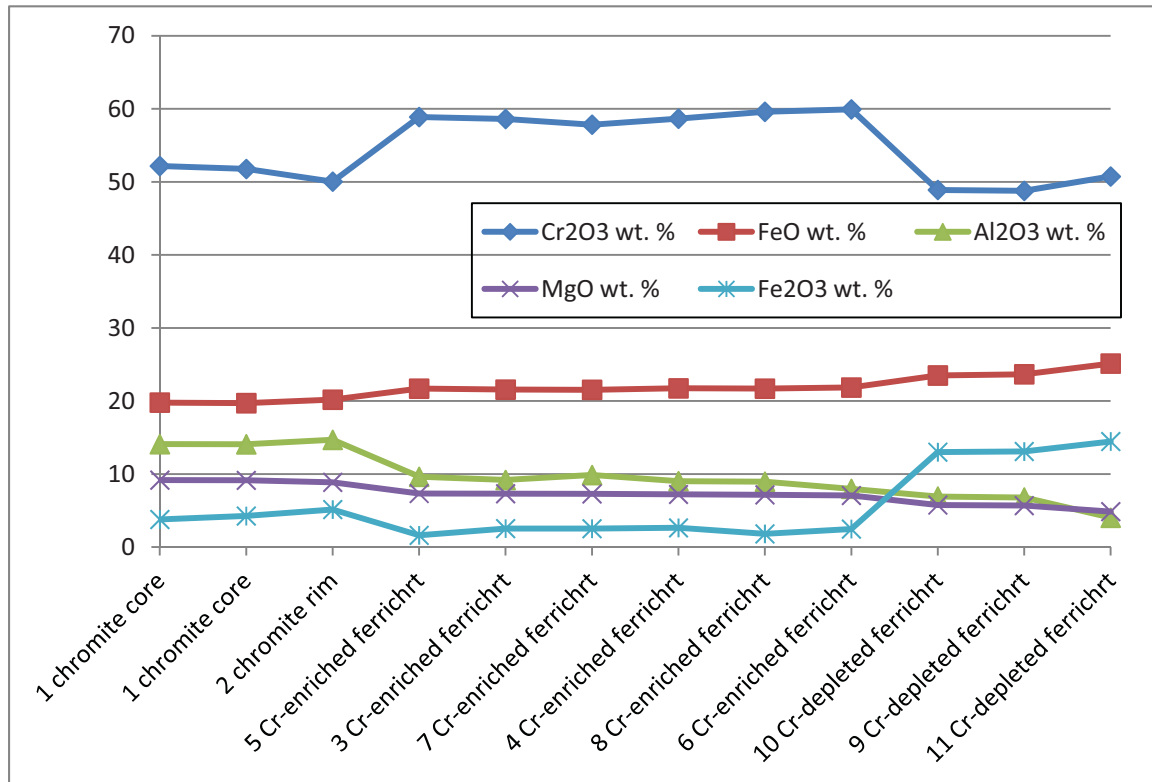


Figure 5.13. Plot of chromite evolution in Black Thor sample 486044, chromite #1.

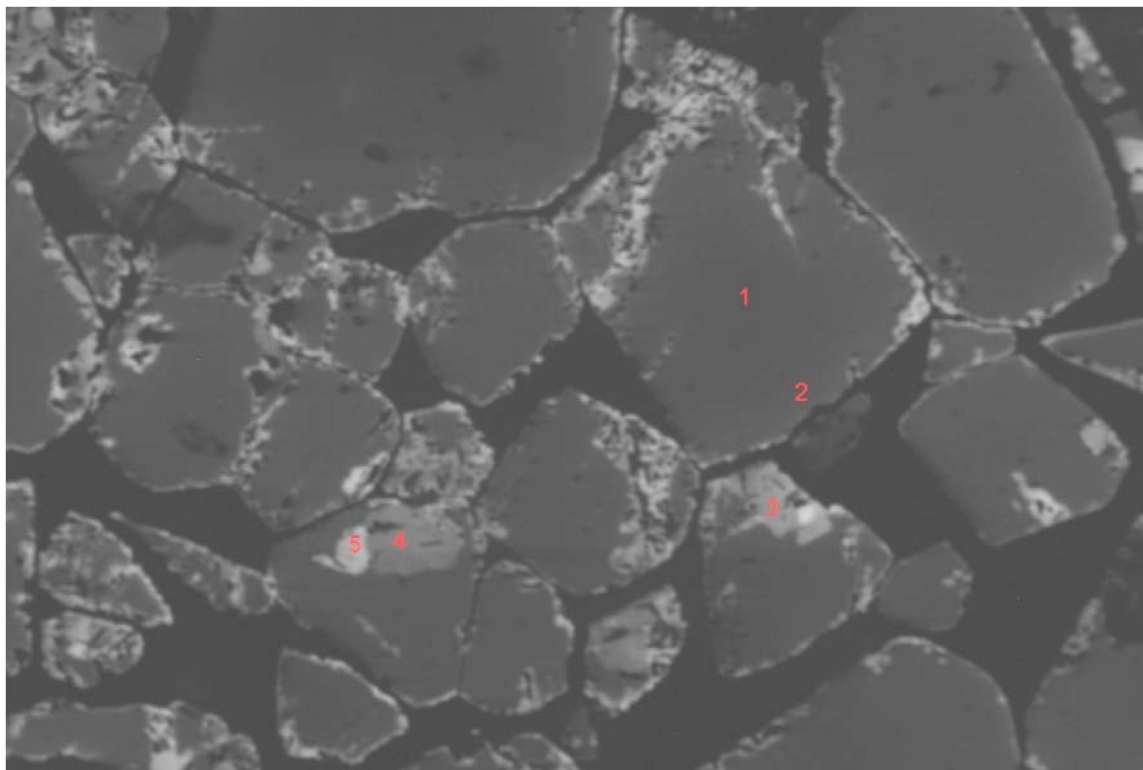


Figure 5.14. Backscatter image of sample 486044, chromite #2 with sample points shown.

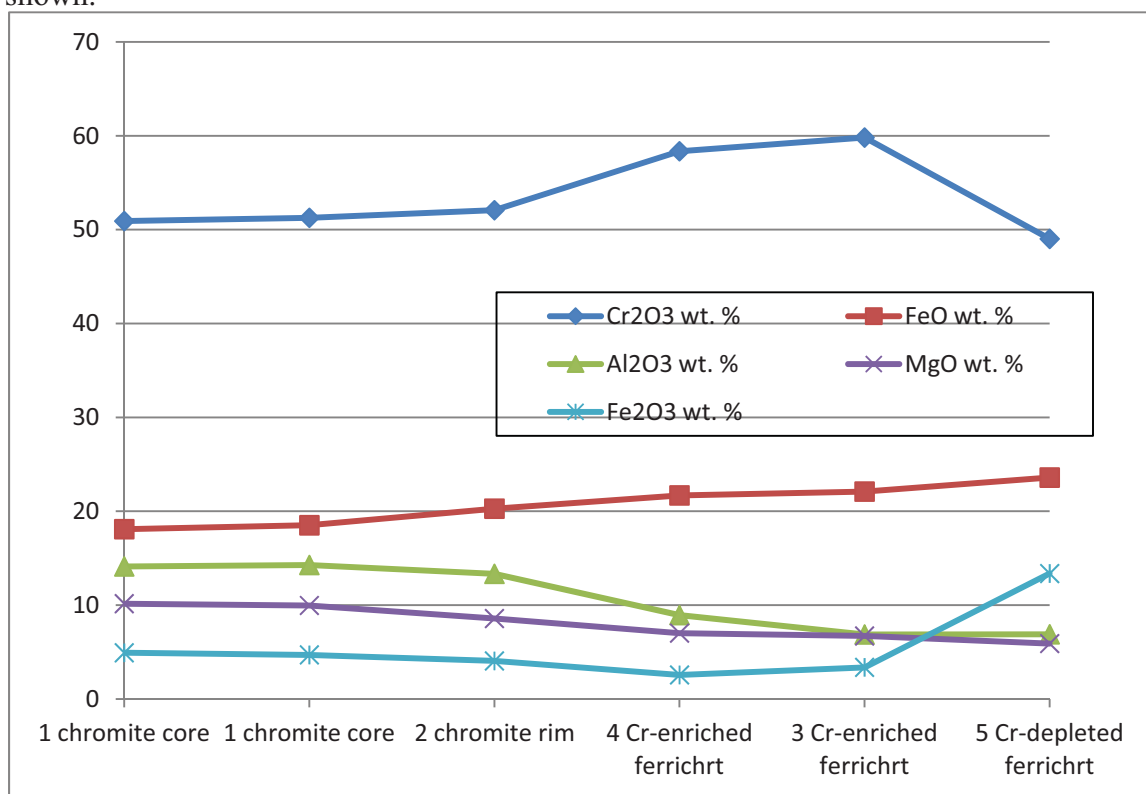


Figure 5.15. Plot of chromite evolution in Black Thor sample 486044, chromite #2.

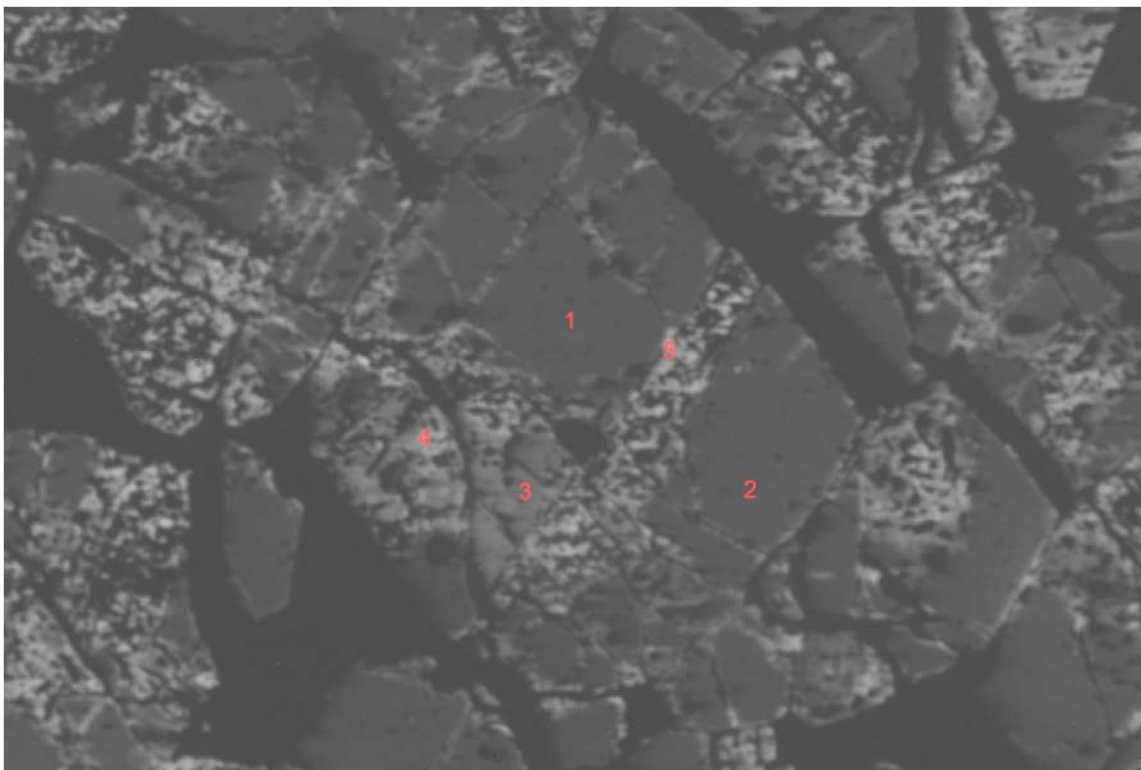


Figure 5.16. Backscatter image of sample 486129 with sample points shown.

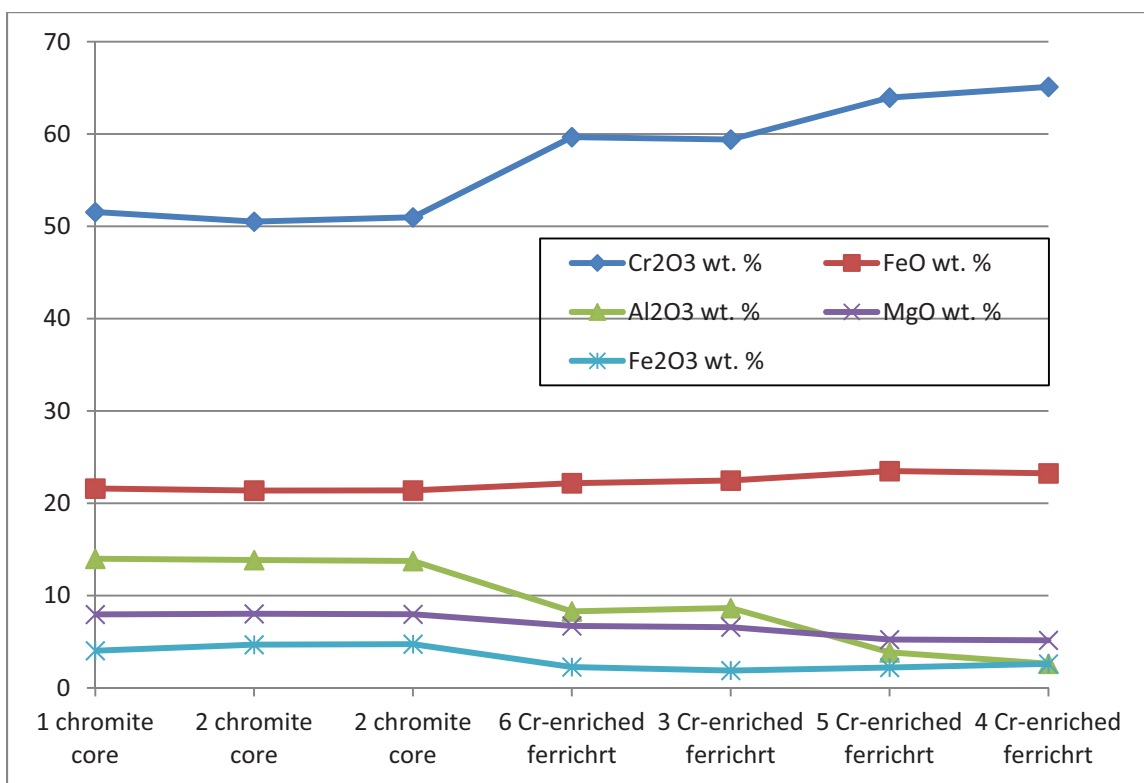


Figure 5.17. Plot of chromite evolution in Black Thor sample 486129.

evolution, but more importantly provide economic grades of the three deposits. There is a major difference from higher grade chromitites with Cr/Fe of 2 to 2.5 to lower grade with Cr/Fe of 1 to 1.7. The lower Cr/Fe is an indicator of more modal silicate degrading the ore. Also plotted are wt. % Al_2O_3 and wt. % FeO. Plots of wt. % Fe_2O_3 and wt. % TiO_2 for total chromite illustrate the range of spinel compositions between ferrochromite and magnetite, due to primary igneous fractionation and secondary retrogression of the chromites. Black Label analyses are from DDH BT-09-31; Black Thor from DDH BT-08-10 and Big Daddy from DDH FW-08-19. Another section of chromitite was probed in DDH BT-09-17 for chromitite hosted in gabbro. Note that since the host sill is overturned, increasing drill hole depths register increasing height in sill stratigraphy.

The microprobe analyses also show details of the deposits in terms of binary variation of major oxides and metals as an aid in tectonic discrimination. Section 5.3.2 documents the binary variation of Black Label, Black Thor and Big Daddy in terms of wt. % Cr_2O_3 , Al_2O_3 and FeO vs. wt. % MgO along with the metals of wt. % TiO_2 , ZnO, MnO and NiO vs. wt. % MgO.

In comparing trends of the three chromite deposits, the Black Thor chromites are highest grade with more primitive magmatic compositions in terms of Cr and Mg than the Black Label chromites. Heterogeneous pyroxene oikocrystic harzburgites host the Black Label chromitite, and more heterogeneous textures are displayed by the chromite ores themselves. With higher modal % silicate in the chromitite there is more silicate exchange accounting for the lower 50 to 46 wt. % Cr_2O_3 in Black Label chromite compared to 53 to 49 wt. % Cr_2O_3 in Black Thor. In addition to the more primitive composition of Black Thor chromite, magmatic variation grossly accounts for the lower wt. % Cr_2O_3 in disseminated chromite grains. Although lower Cr_2O_3 contents occur with more silicate exchange in disseminated grains, a strong linear regression from massive to disseminated grains reflects magmatic differentiation in forming massive through to disseminated chromite (Fig. 5.18). In terms of trends of other oxides, wt. % Al_2O_3 varies antipathetically with wt. % Cr_2O_3 and wt. % FeO varies antipathetically with wt. % MgO (Fig. 5.19). TiO_2 also increases with decreasing wt. % MgO, though there is less variation in wt. % TiO_2 in the deposits.

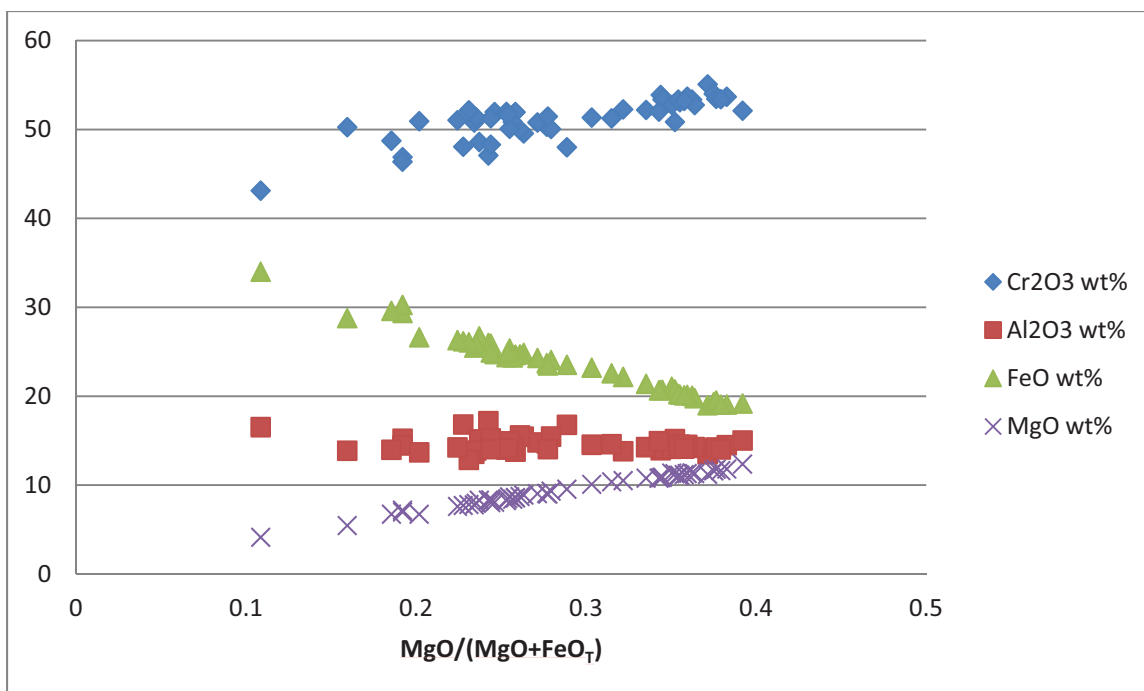


Figure 5.18. Plot of major oxide variation from disseminated to massive chromite in the chromite cores of the first fifty samples analysed in Black Thor DDH BT-08-10.

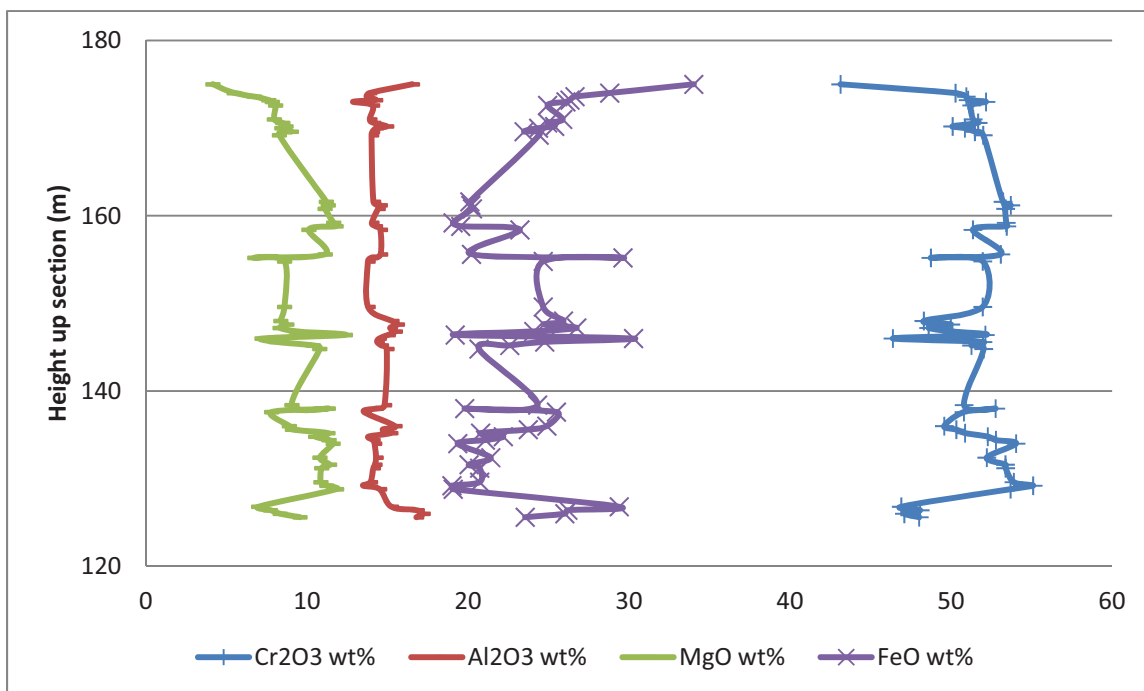


Figure 5.19. Variation of wt. % major oxide with height up section (down hole) in Black Thor DDH BT-08-10 for chromite cores of first fifty samples analysed.

The massive chromitite at Big Daddy shows remarkable homogeneity at 50 to 51 wt. % Cr₂O₃. This is higher than reported assay data for wt. % Cr₂O₃, which is accounted for by the minor silicate. The homogeneity of the massive ores is attributed to development of chromite layers by double diffusive convection (Rice and von Gruenewaldt, 1994). With little silicate in the massive zones there is less silicate exchange, much less than observed in the exchanged chromitites of the Black Thor and Black Label intersections. Variations from core to rim in all chromite is essentially due to diffusion during secondary hydration.

5.3.1.1 Black Label

The two chromitite intervals probed in BT-09-31 have markedly different mineral chemistries. First, from 158 to 161 m, the Cr₂O₃ and MgO values in disseminated chromite are low with maximum contents of 42 to 44 wt. % Cr₂O₃ and up to 4.67 wt. % MgO (Figs. 5.20 to 5.23). Notably, FeO contents are high ranging from 26 to 30 wt. % (Fig. 5.24). The first chromitite interval from 161 to 203 m comprises 4 zones defined by 4 pulses of decreasing wt. % MgO with height (Fig. 5.21). Cr/Fe ratios are lower with between 0.98 and 2.26 for magmatic compositions and as low as 0.41 for alteration rim Cr-enriched to Cr-depleted ferrichromites (Fig. 5.25). Within this first interval, wt. % Al₂O₃ contents are more elevated in these chromites than in the chromites from the second interval, except for the low wt. % Al₂O₃ contents in the Cr-enriched to Cr-depleted ferrichromites (Fig. 5.26). The trend in wt. % Al₂O₃ is also evident in wt. % TiO₂ where the first interval contains higher wt. % TiO₂ than the second interval.

The first pulse from the first interval is from 161 to 164 m and contains the lowest wt. % MgO and wt. % Cr₂O₃. The next two pulses are larger up to 20 m in thickness, and contain well defined differentiation sequences of decreasing wt. % MgO. Within these two pulses are individual replenishments with MgO peaks followed by decreasing wt. % MgO. The second pulse contains two subzones with wt. % MgO decreasing in the second subzone from 176 to 179 m. Notably, there is a large amount of Cr-depleted ferrichromite detected at the top of this subzone as displayed by enriched Fe₂O₃ compositions (Fig. 5.27). There appears to be an association of Cr-depleted ferrichromite with evolved chromite. This is due to more diffusion and leaching of ions to form the Cr-depleted ferrichromite where there is a greater proportion of adjacent silicate.

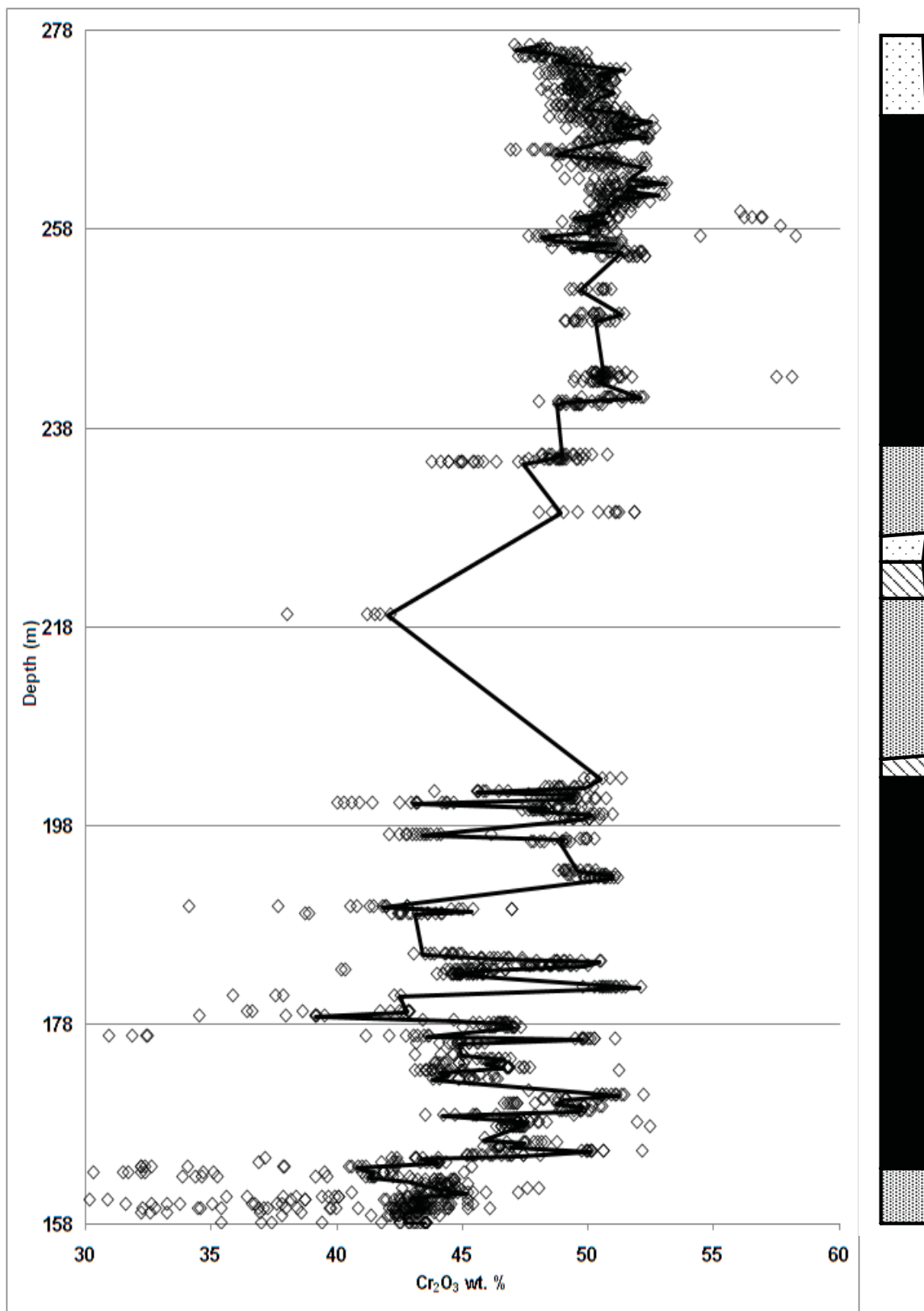


Figure 5.20. Plot of Cr₂O₃ wt. % vs. depth (m) for Black Label DDH BT-09-31. The trend line plots through chromite cores.

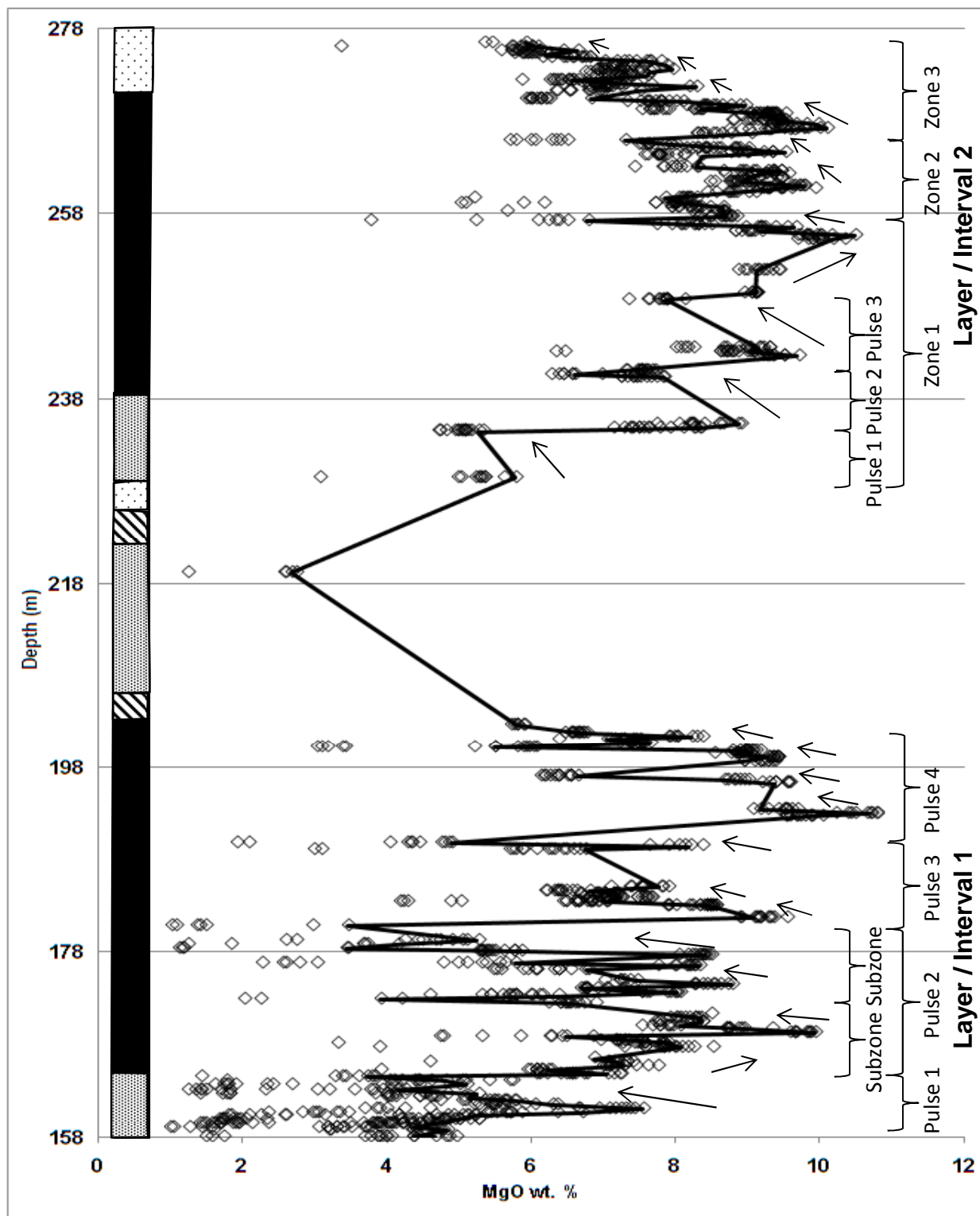


Figure 5.21. Plot of MgO wt. % vs. depth (m) for Black Label DDH BT-09-31 with various zones and pulses shown. The trend line plots through core compositions. Arrows pointing to the right represent replenishment while arrows pointing left represent differentiation.

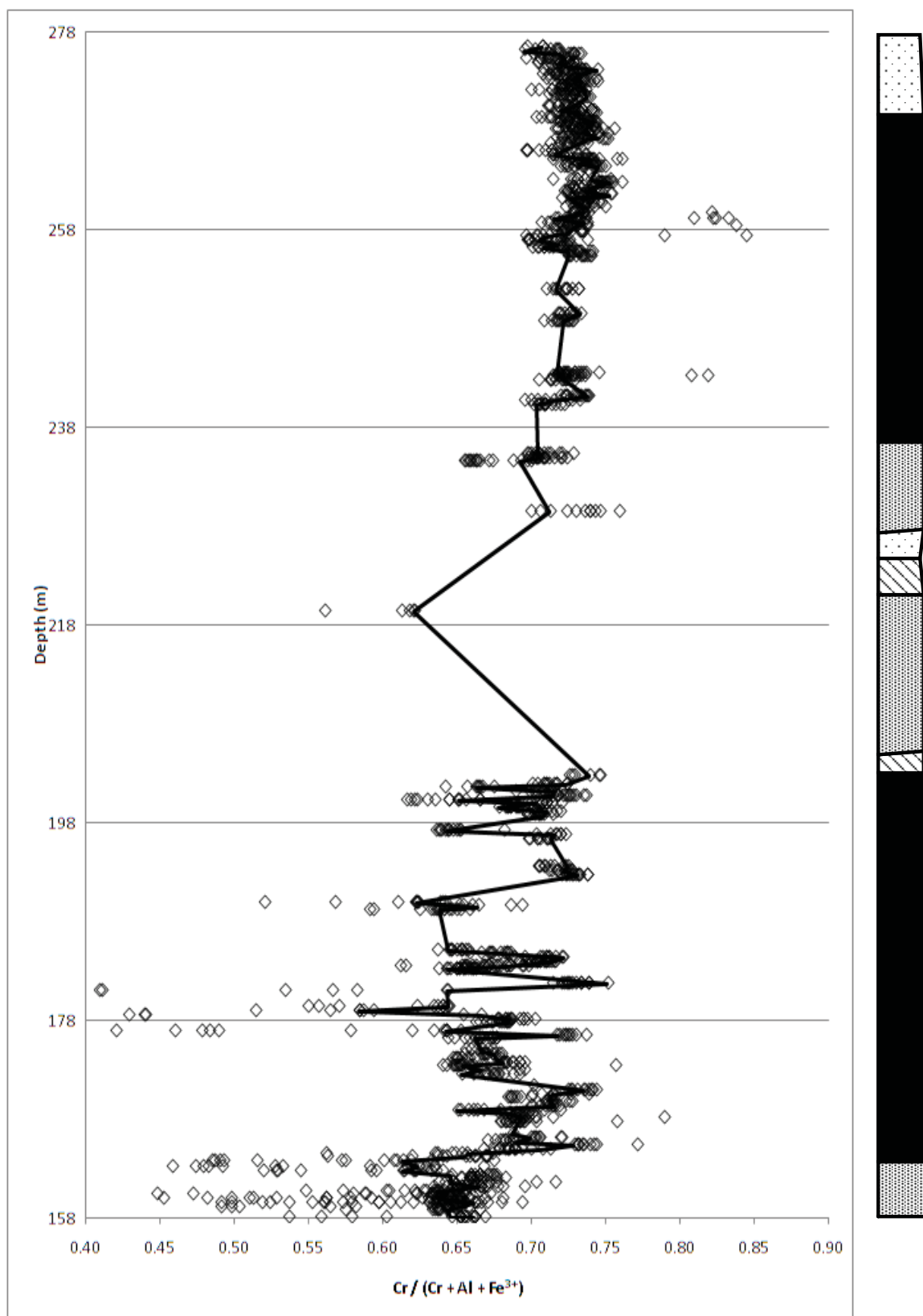


Figure 5.22. Plot of $\text{Cr}/(\text{Cr}+\text{Al}+\text{Fe}^{3+})$ vs. depth (m) for Black Label DDH BT-09-31. The trend line plots through chromite cores.

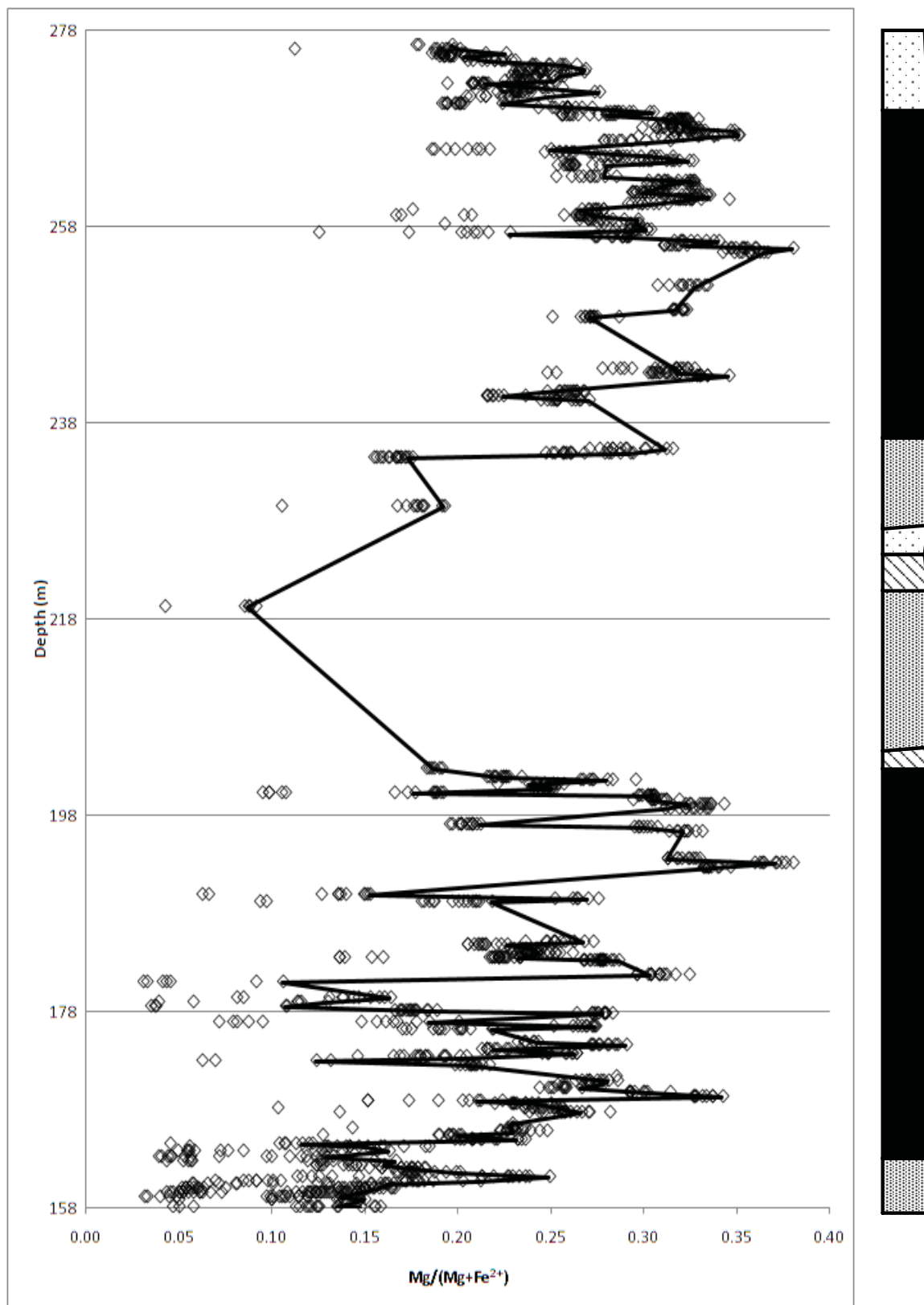


Figure 5.23. Plot of $\text{Mg}/(\text{Mg}+\text{Fe}^{2+})$ vs. depth (m) for Black Label DDH BT-09-31. The trend line plots through chromite cores.

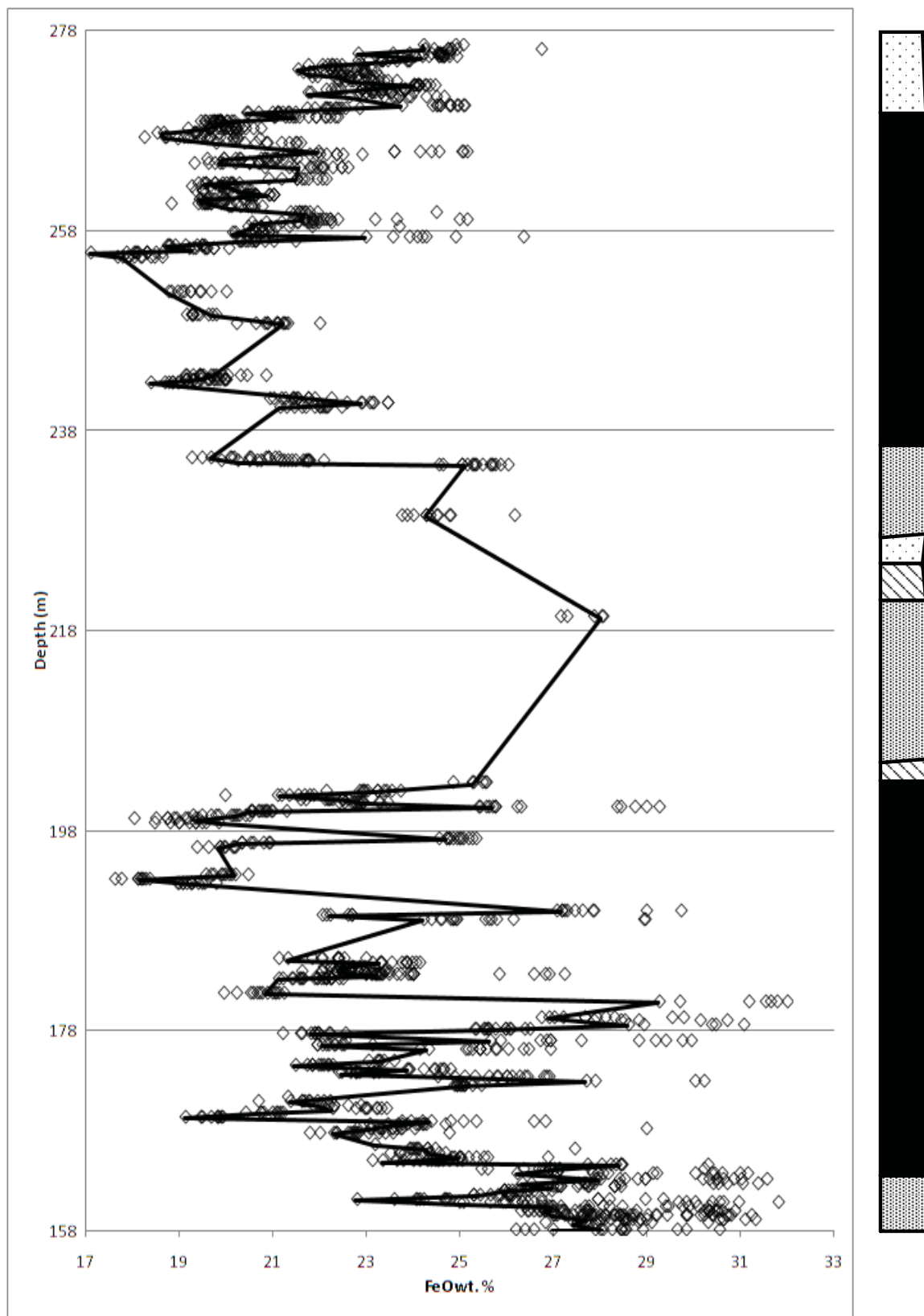


Figure 5.24. Plot of FeO wt. % vs. depth (m) for Black Label DDH BT-09-31. The trend line plots through chromite cores.

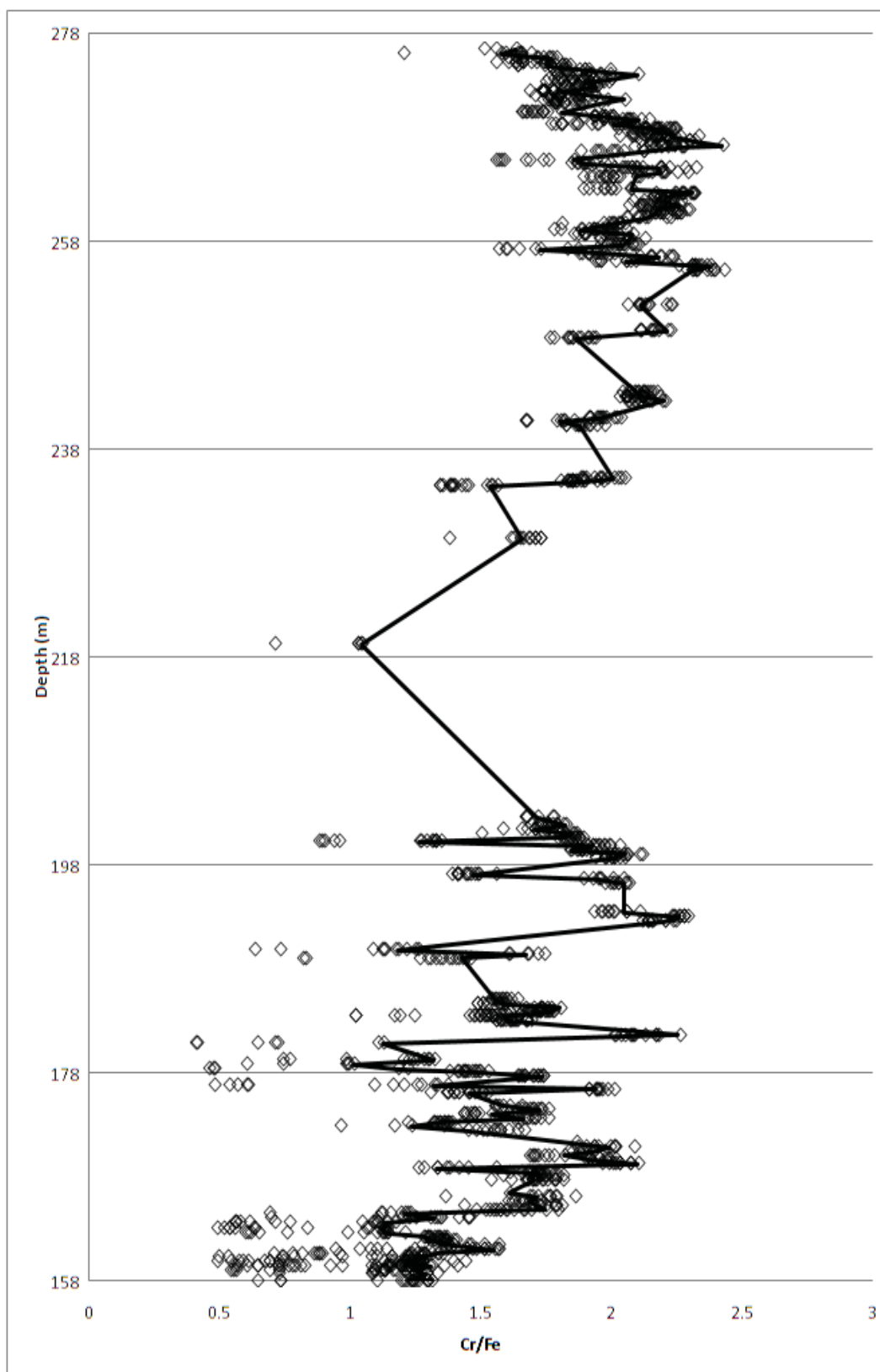


Figure 5.25. Plot of Cr/Fe vs. depth (m) for Black Label DDH BT-09-31. The trend line plots through chromite cores.

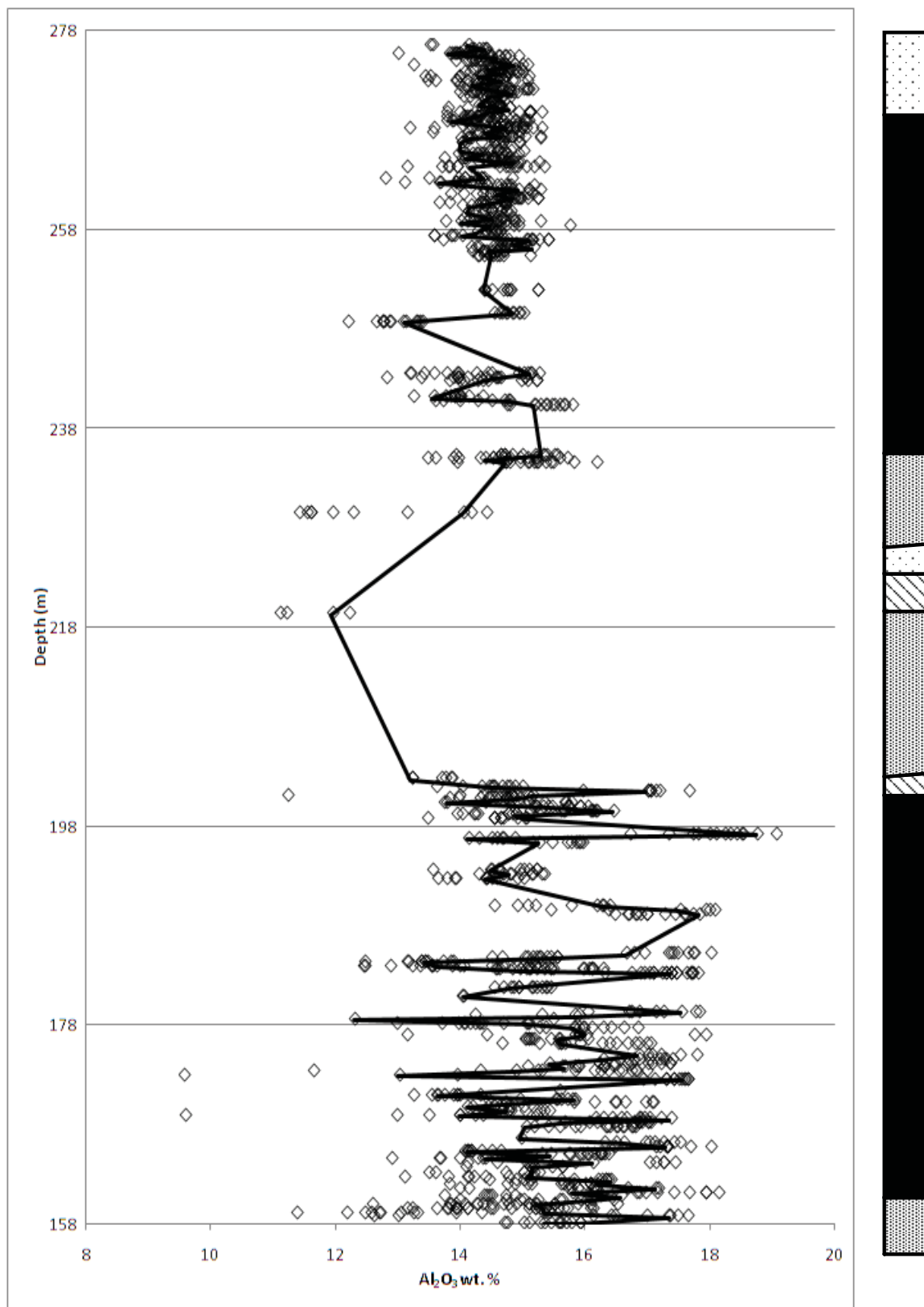


Figure 5.26. Plot of Al_2O_3 wt. % vs. depth (m) for Black Label DDH BT-09-31. The trend line plots through chromite cores. Ferrichromites are not displayed.

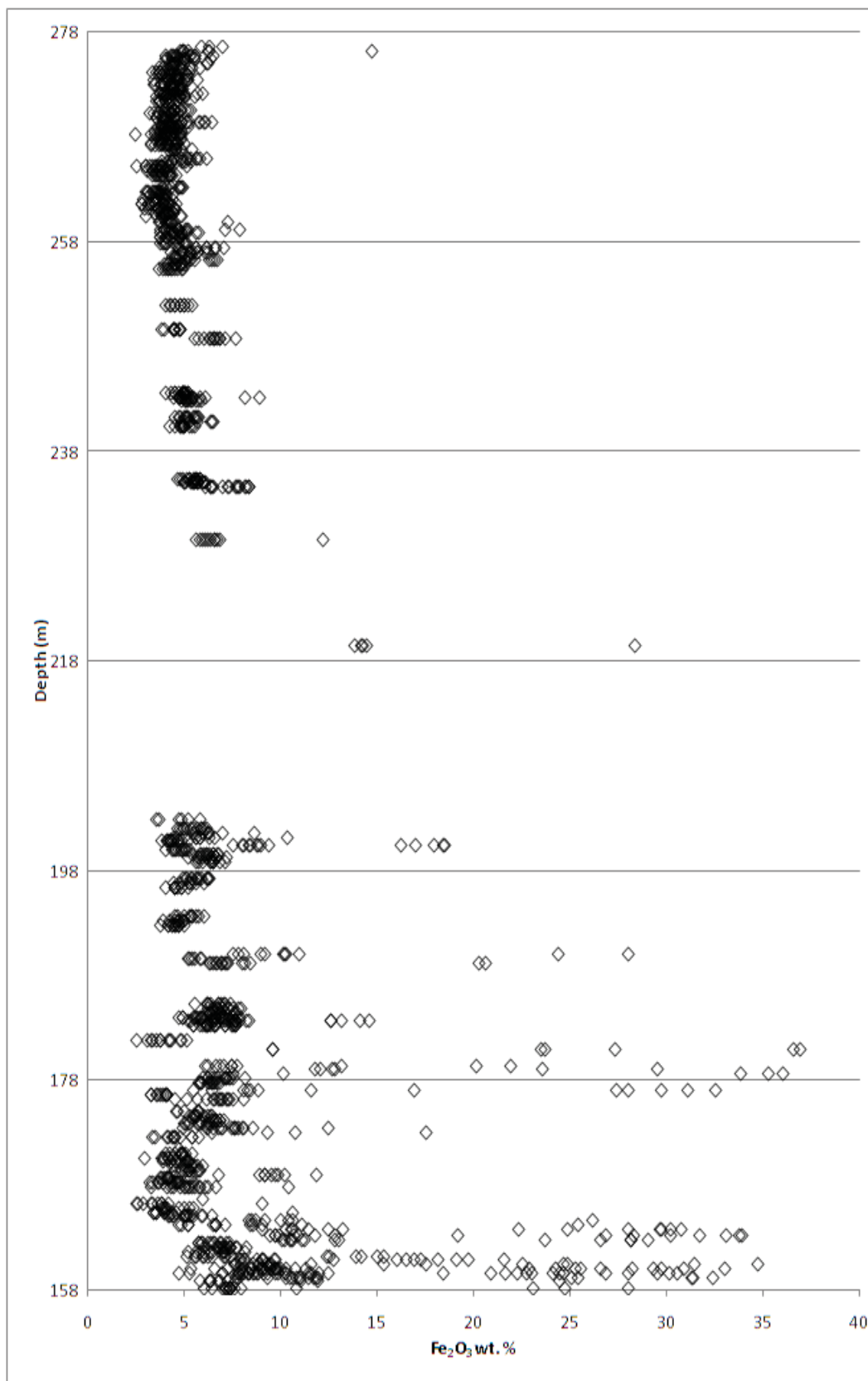


Figure 5.27. Plot of Fe₂O₃ wt. % vs. depth (m) for Black Label DDH BT-09-31.

The third pulse contains three subzones of decreasing wt. % Cr_2O_3 with height, following the pattern of differentiation shown by the MgO contents. In the fourth pulse of the chromitite interval, with each new replenishment the Cr_2O_3 contents remained high at about 50 wt. % Cr_2O_3 . However, individual differentiation sequences of decreasing Cr_2O_3 wt. % with height can be picked out within up to 6m thick mini-pulses. These mini cycles possibly formed by convection cells within the larger pulse of magma (Rice and von Gruenewaldt, 1994; Naldrett et al., 2010).

The second chromitite interval is from 229 to 276 m and contains 3 zones from 229 to 257 m, 257 to 265 m and from 265 to 276 m characterized by separate subsets of elevated wt. % Cr_2O_3 separated by troughs of low wt. % Cr_2O_3 . Notably, the Cr_2O_3 values are consistently high at above 50 wt. % suggesting a primitive chromitite interval. In the first zone, 3 pulses of replenished MgO are followed by decreasing MgO trends. Cr/Fe ratios are higher and more primitive in this second interval with between 1.82 and 2.42 for magmatic chromite compositions and as low as 1.38 for alteration rim Cr-enriched to Cr-depleted ferrichromites. With each successive replenishment, there is an overall increase in the MgO values. This suggests the influx of more primitive magma. The high peaks above 53 wt. % Cr_2O_3 with low wt. % MgO are Cr-enriched ferrichromites due to secondary hydration. In the second zone, there are 2 pulses with the second being larger, and having higher wt. % MgO and Cr_2O_3 than the second. Notably, more secondary Cr-enriched ferrichromite has been detected in this first pulse. The second pulse shows marked decreasing wt. % MgO with height while the Cr_2O_3 values decrease to a lesser extent. The third zone contains 3 to 4 pulses on an overall trend of decreasing Cr_2O_3 wt. % with height. The first pulse from 259 to 270 m contains higher wt. % MgO than the others and is well differentiated. The second pulse is poorly developed. The 3rd to 4th pulses from 272 to 276 m begin with more elevated MgO that decreases past 274 m. The overall decreasing trend in Cr_2O_3 wt. % in this zone also reflects igneous differentiation.

5.3.1.2 Black Thor BT-08-10

Black Thor DDH BT-08-10 contains chromite of more primitive but also more variable composition due to diffusion processes accompanying greater ferrichromite replacement during retrogression. Therefore, plots of core + margin of igneous chromite

have been separated from replacement ferrichromite. Cr/Fe ratios in the drill hole are less for disseminated but more for primitive and higher grade overall than Black Label with between 1.53 and 2.90 for magmatic compositions and as low as 0.74 for alteration rim Cr-enriched to Cr-depleted ferrichromites (Fig. 5.28). Some Cr-enriched ferrichromites in the upper part of the hole above 154 m have enriched Cr/Fe to the range of 2.50 to 2.95, thereby increasing the grade of the ore. From 114 to 124 m there are two zones of low MgO chromite disseminated in dunite (Figs. 5.29 to 5.30). The first zone from 114 to 118.5 m, comprises two pulses with trends of decreasing wt. % MgO with height. The second zone from 118.5 to 124 m also contains 2 pulses with decreasing wt. % MgO with height.

Above 124 m, chromite shows elevated wt. % Cr₂O₃ in intermittent beds of massive chromitite (Figs. 5.31 to 5.32). Between 124 and 127 m there is a well differentiated sequence showing decreasing wt. % MgO and Cr₂O₃ with height. A large zone of chromitite between 127 and 150 m can be subdivided into two zones from 127 to 136 m and 136 to 150 m based on Cr₂O₃ contents. These chromitites begin with high Cr₂O₃ wt. % contents and show a marked trend of decreasing MgO and Cr₂O₃ with height. In the first subzone, Cr₂O₃ contents reach 54 wt. % suggesting very primitive magma.

The upper zone from 150 to 174 m, also show trends of decreasing MgO and Cr₂O₃ wt. % with height. Notably, there is only a slight decrease in wt. % Cr₂O₃. This may be explained by development of chromite convection cells. A number of replenishments of high MgO may be also attributed to successive convection cells (Rice and von Gruenewaldt, 1994). Also shown are variation of FeO, Al₂O₃ and Fe₂O₃ with height (Figs. 5.33 to 5.35).

5.3.1.3 Black Thor BT-09-17

The Black Thor upper chromitite in DDH BT-09-17 displays trends in the mineral chemistry of chromite that are different than DDH BT-08-10 and the other chromite deposits. Instead of decrease in wt. % Cr₂O₃ and wt. % MgO from core to rim that is most common with silicate exchange of chromite in the other deposits, there is enrichment in wt. % Cr₂O₃ and wt. % MgO that effectively increases the grade of the ores (Figs. 5.36 to 5.39). With enrichment in Cr₂O₃ and MgO, there is enrichment in Cr/Fe

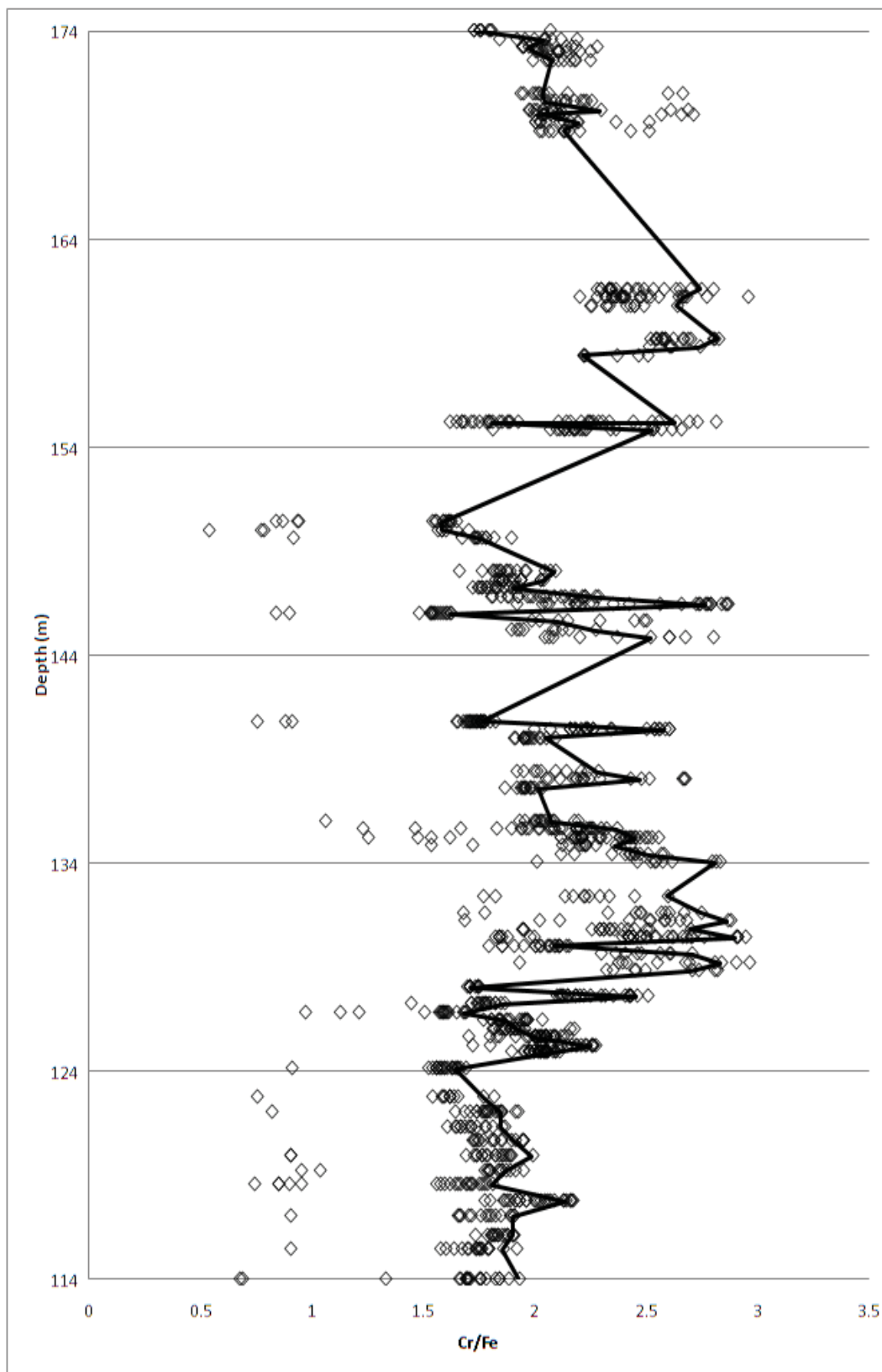


Figure 5.28. Plot of Cr/Fe vs. depth (m) for Black Thor DDH BT-08-10. The trend line plots through chromite cores.

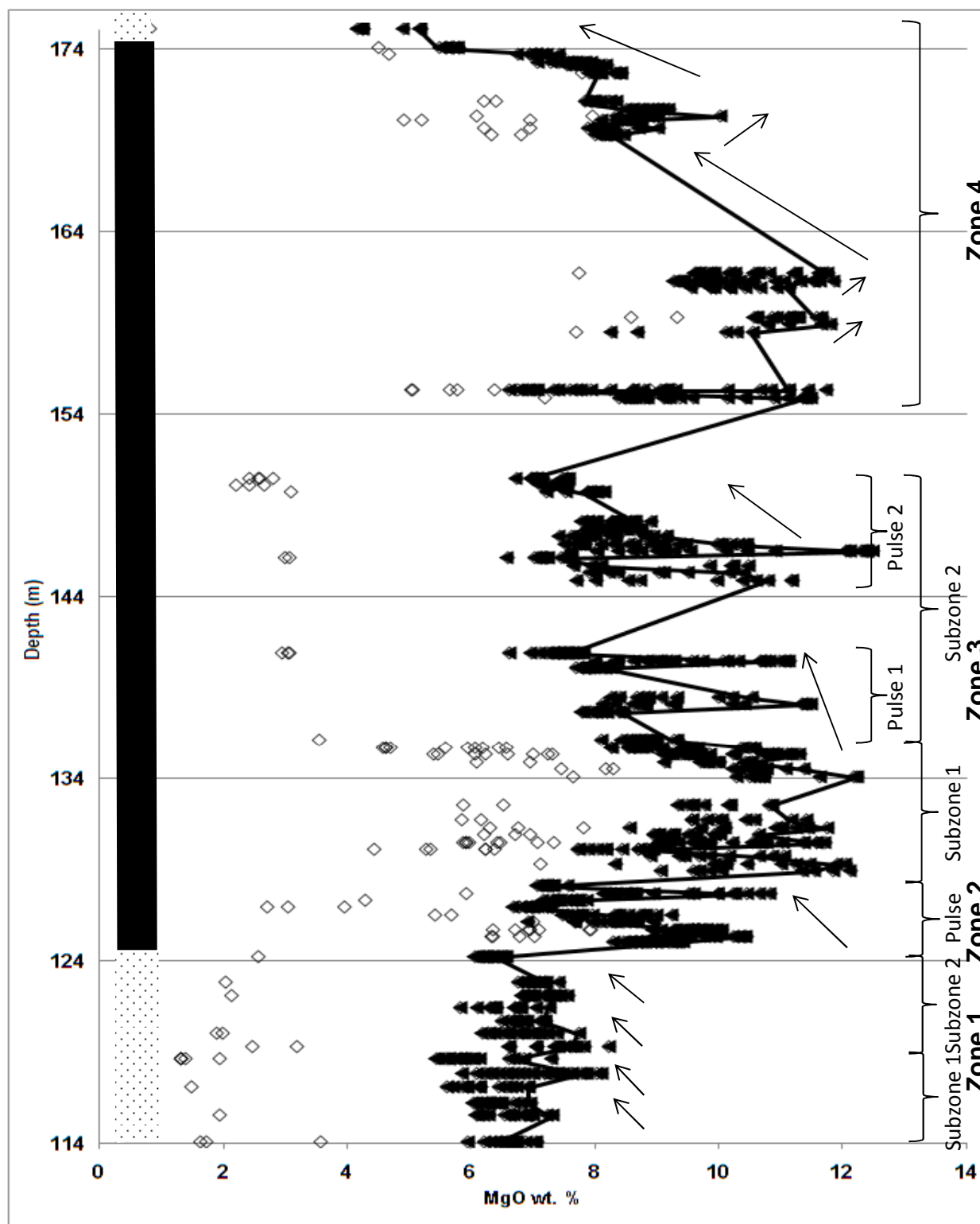


Figure 5.29. Plot of MgO wt. % vs. depth (m) for Black Thor DDH BT-08-10 with various zones and pulses shown. Dark triangles are chromite core + margins; while diamonds are ferrichromites. The trend line plots through core compositions. Arrows pointing to the right represent replenishment while arrows pointing left represent differentiation.

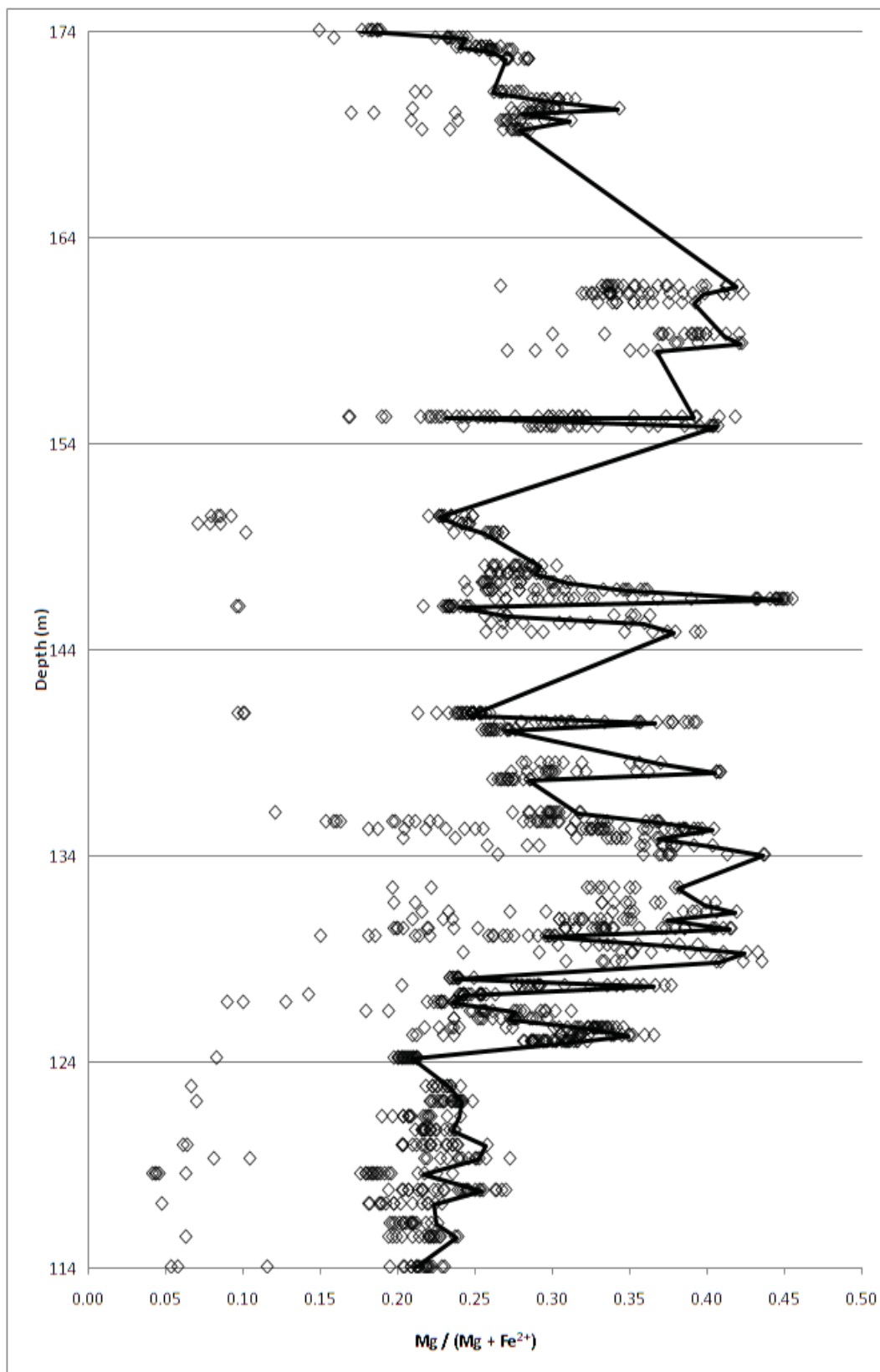


Figure 5.30. Plot of $\text{Mg}/(\text{Mg}+\text{Fe}^{2+})$ vs. depth (m) for Black Thor DDH BT-08-10. The trend line plots through chromite cores.

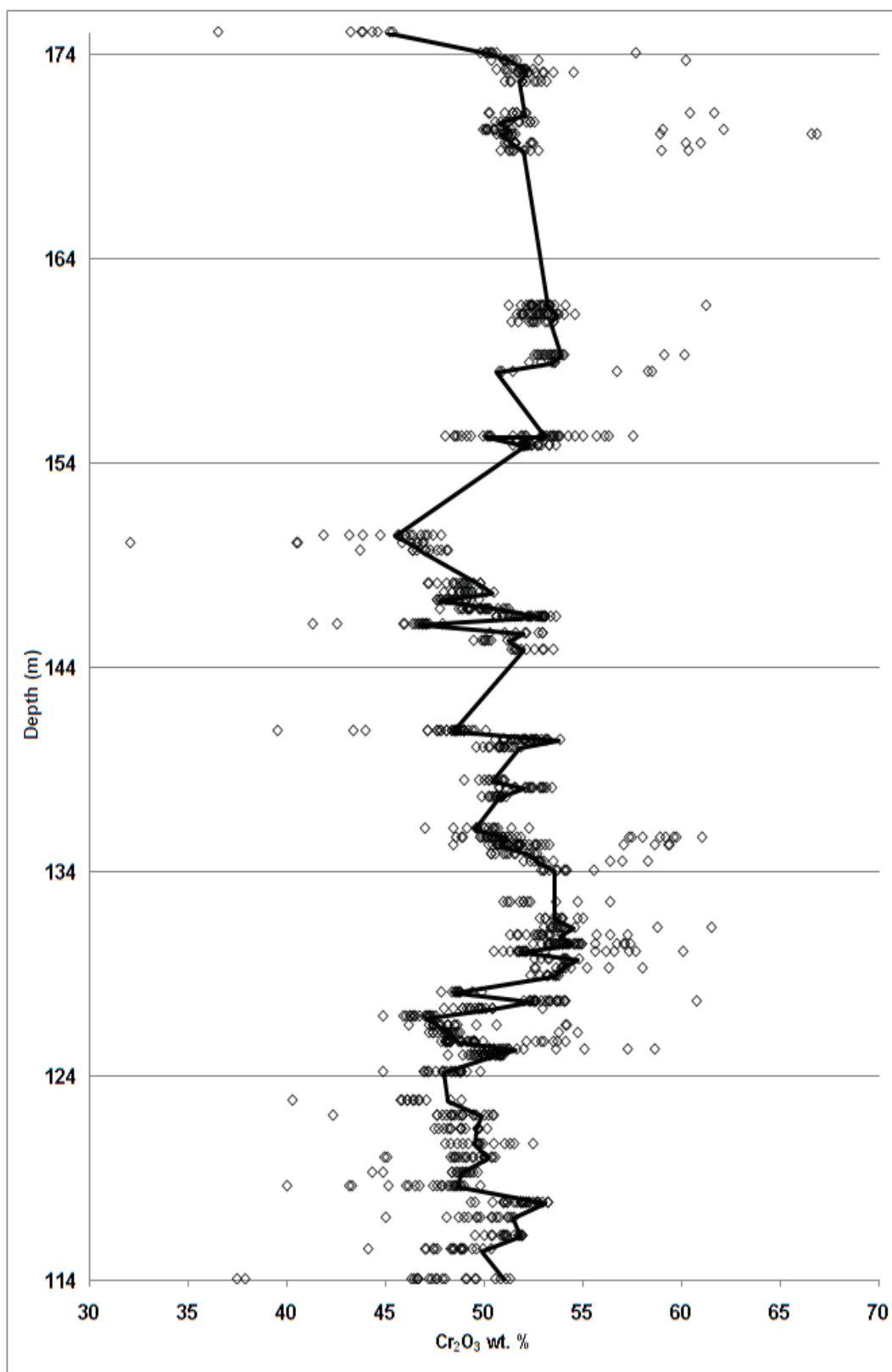


Figure 5.31. Plot of Cr₂O₃ wt. % vs. depth (m) for Black Thor DDH BT-08-10. The trend line plots through chromite cores.

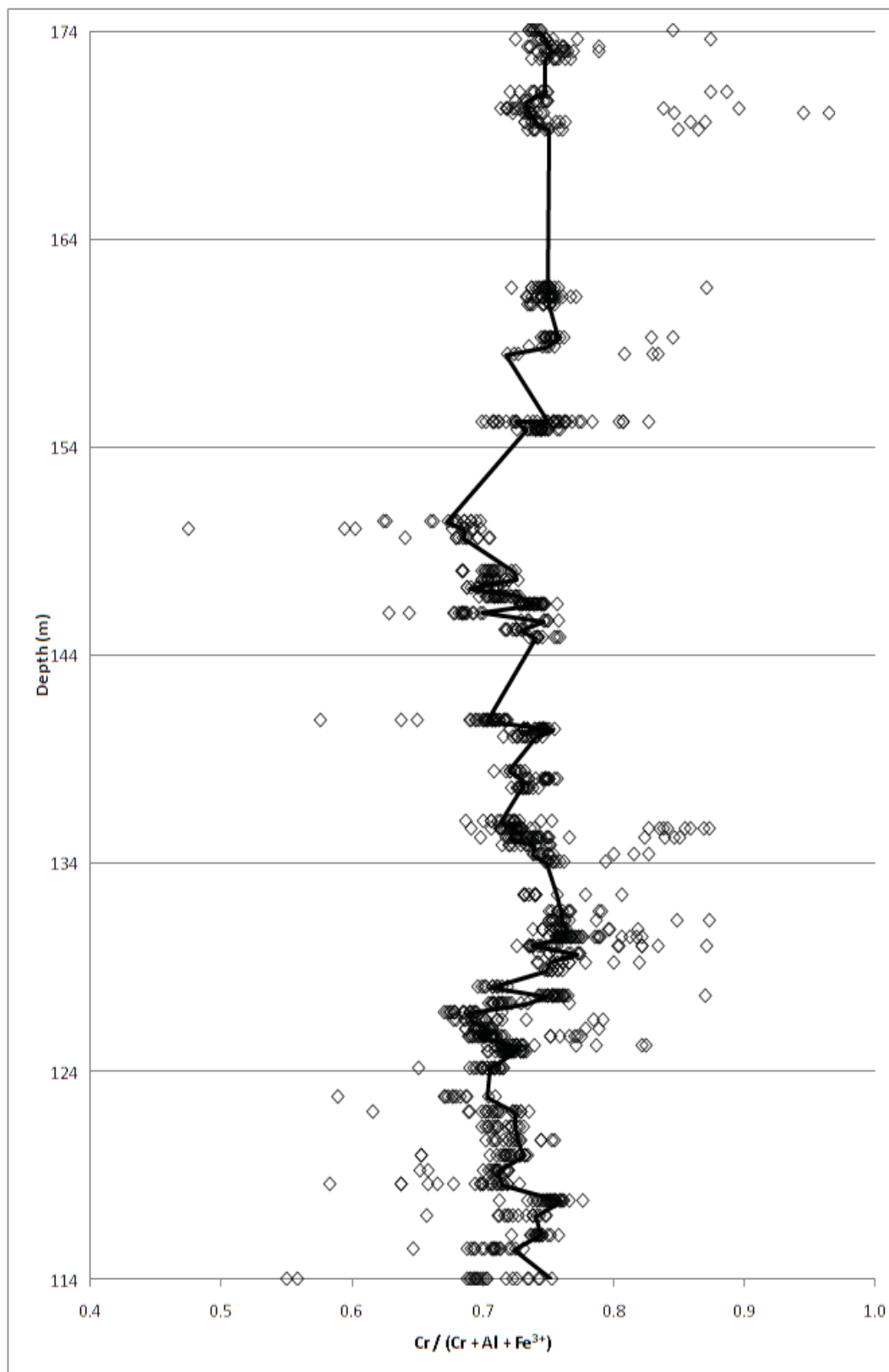


Figure 5.32. Plot of $\text{Cr}/(\text{Cr}+\text{Al}+\text{Fe}^{3+})$ vs. depth (m) for Black Thor DDH BT-08-10. The trend line plots through chromite cores.

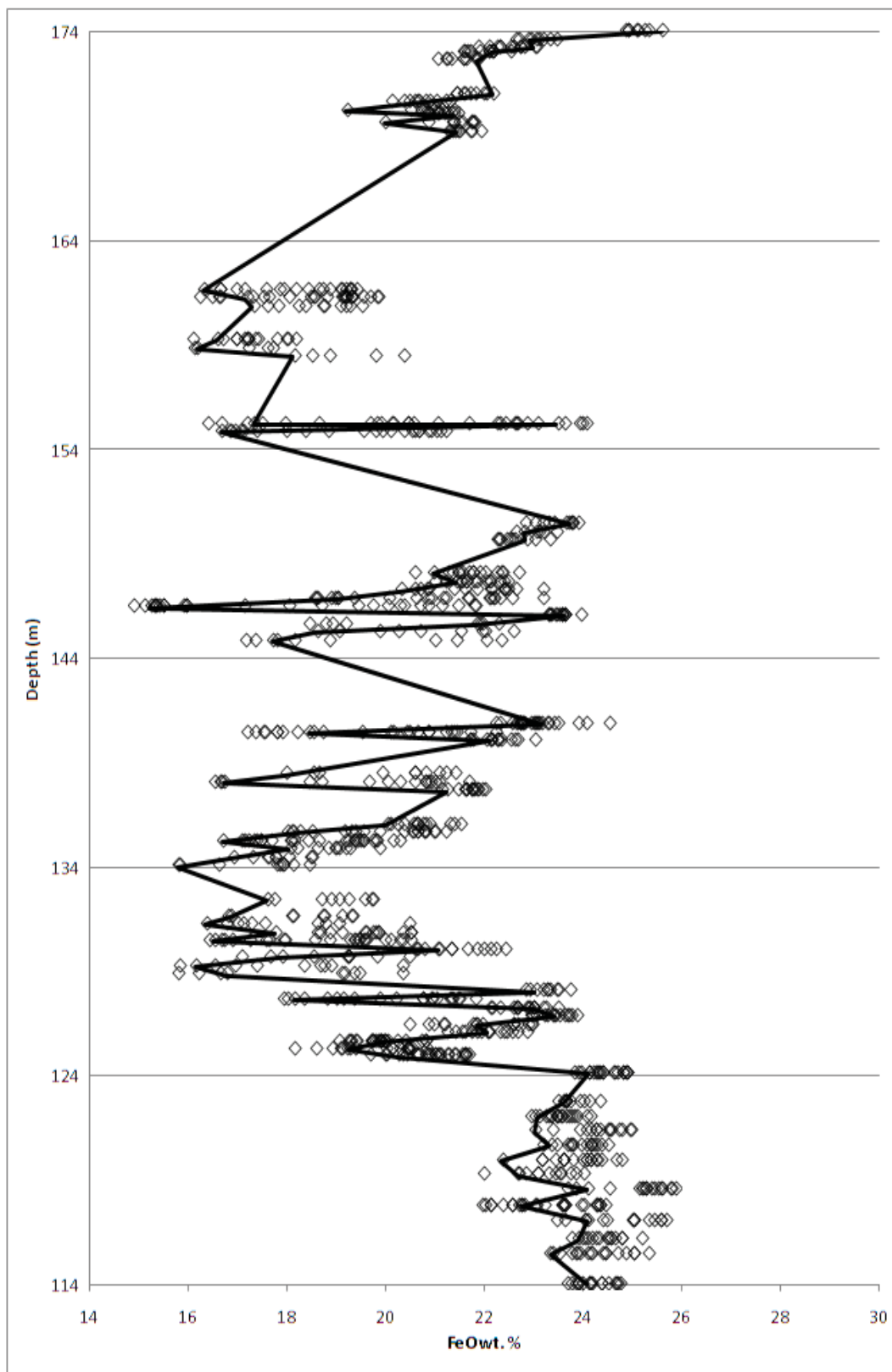


Figure 5.33. Plot of FeO wt. % vs. depth (m) for Black Thor DDH BT-08-10. The trend line plots through chromite cores.

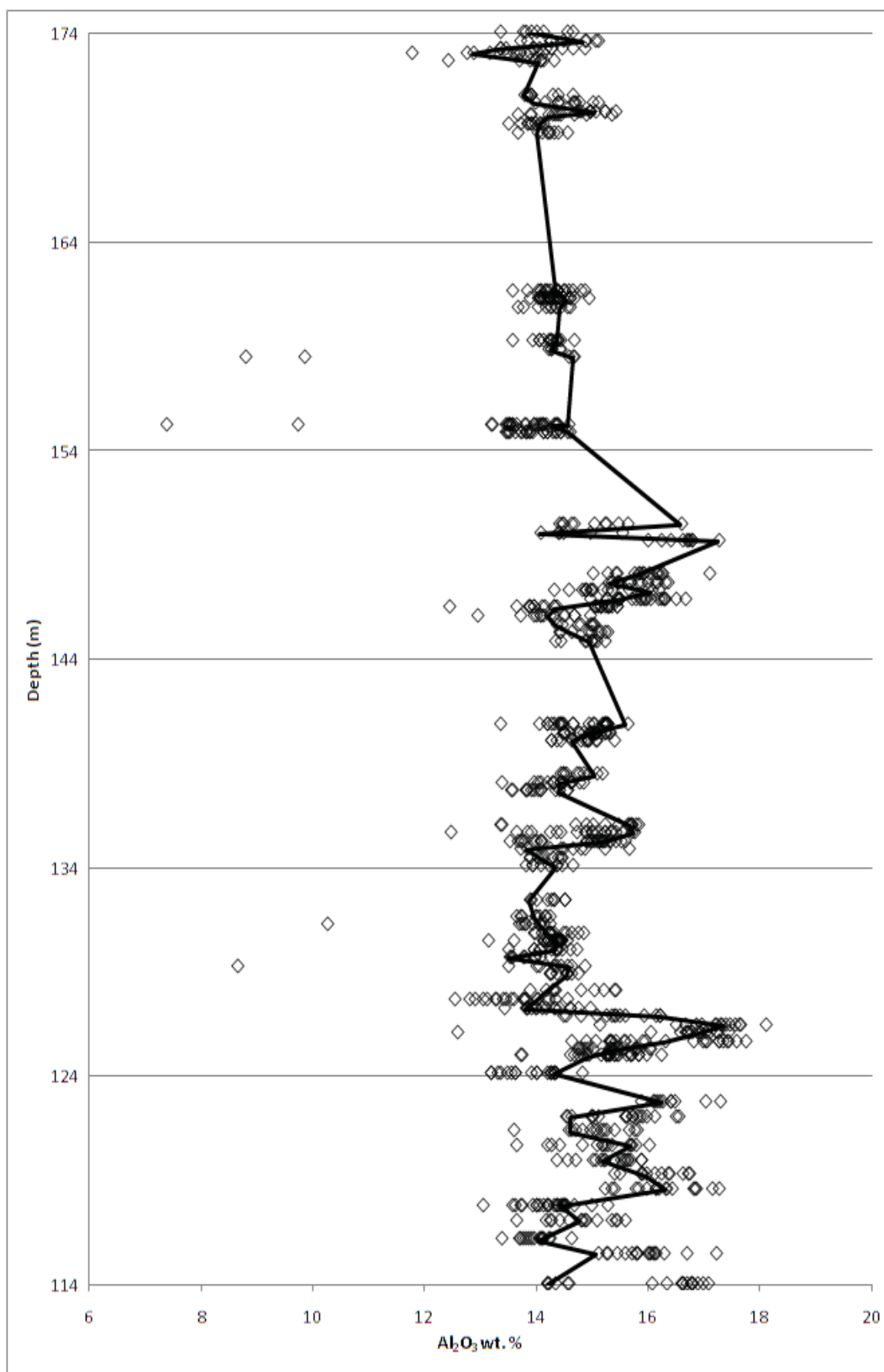


Figure 5.34. Plot of Al₂O₃ wt. % vs. depth (m) for Black Thor DDH BT-08-10. The trend line plots through chromite cores. Ferrichromites are not displayed.

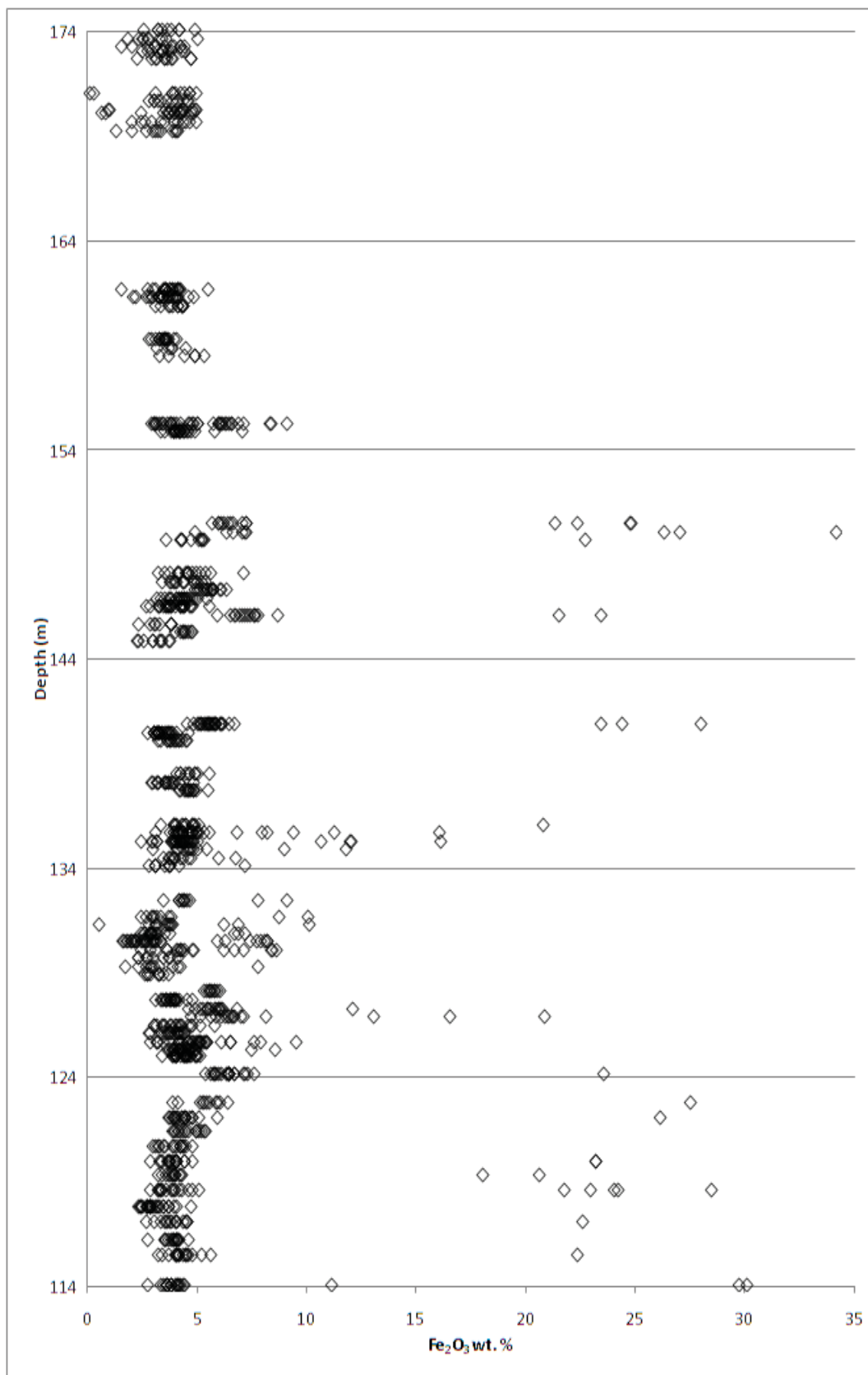


Figure 5.35. Plot of Fe₂O₃ wt. % vs. depth (m) for Black Thor DDH BT-08-10.

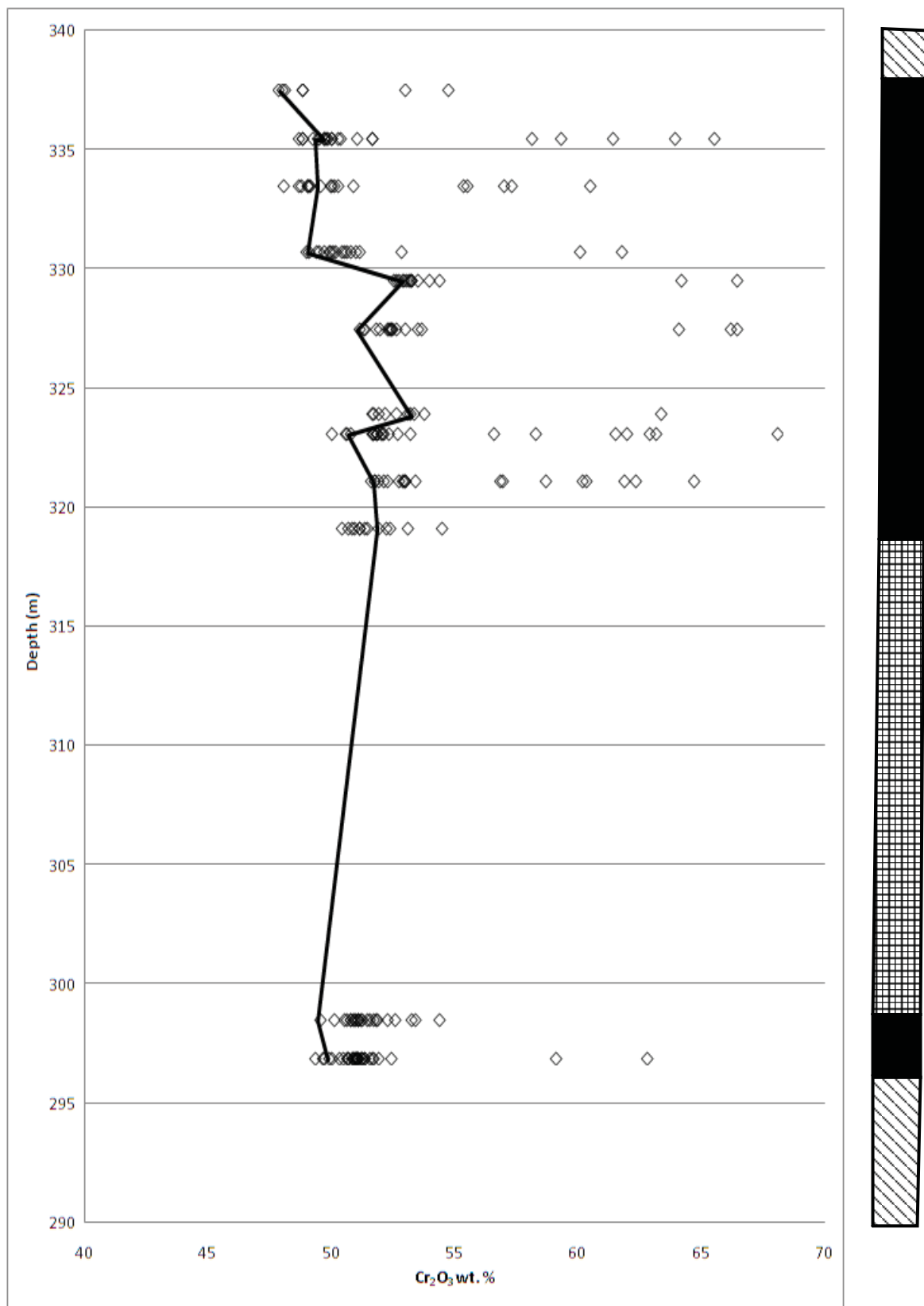


Figure 5.36. Plot of Cr₂O₃ wt. % vs. depth (m) for Black Thor DDH BT-09-17. The trend line plots through chromite cores.

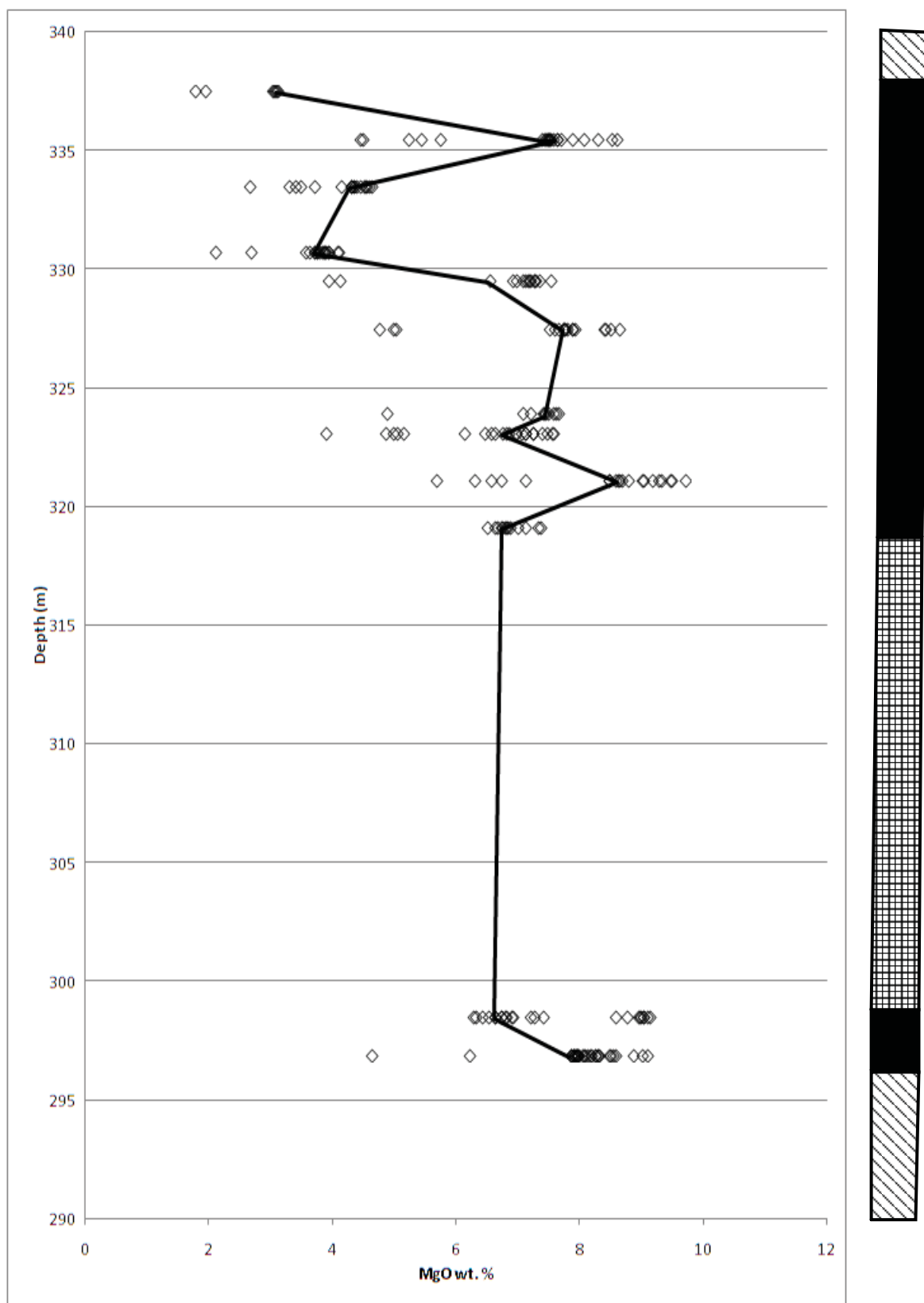


Figure 5.37. Plot of MgO wt. % vs. depth (m) for Black Thor DDH BT-09-17. The trend line plots through chromite cores.

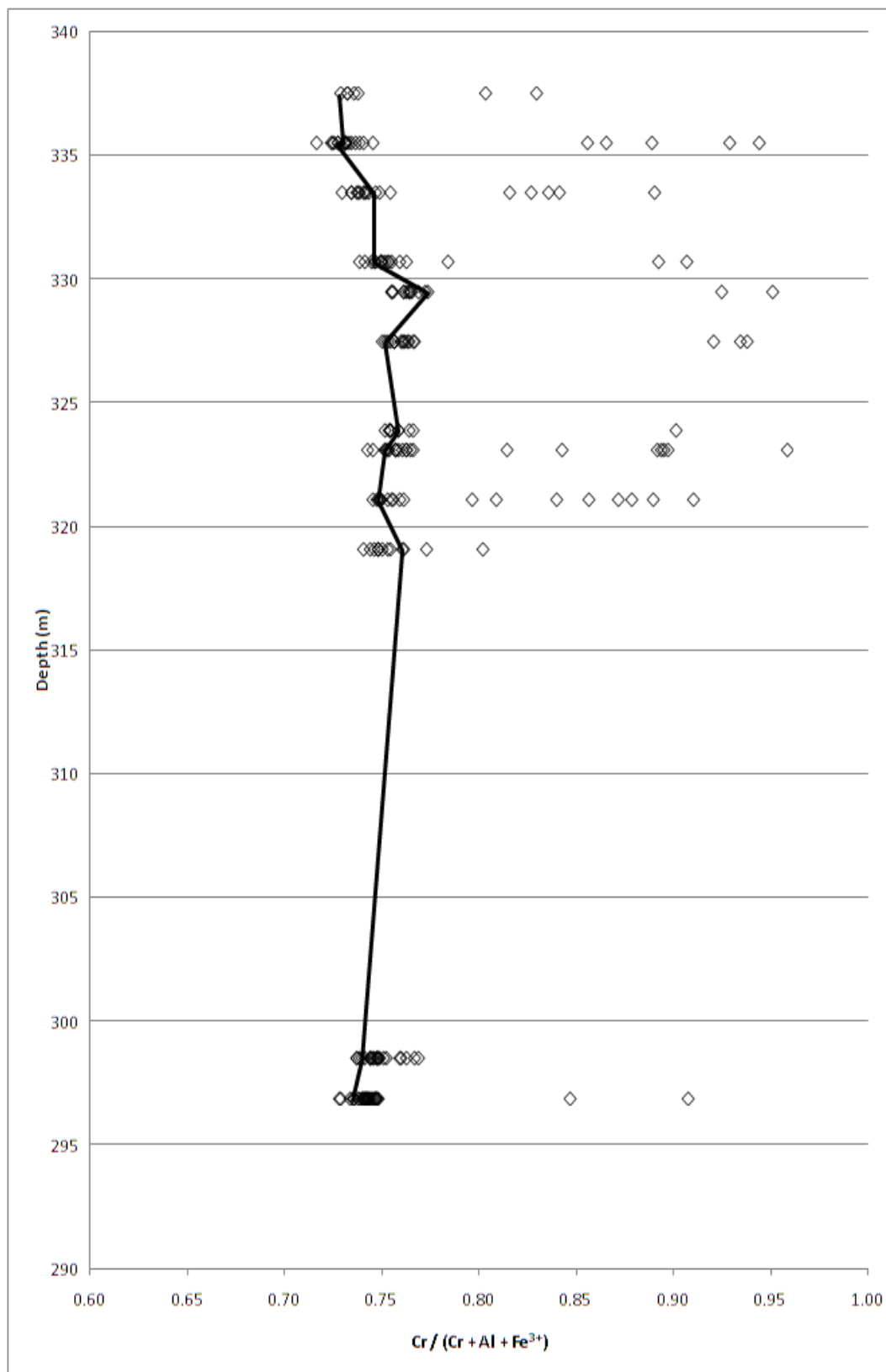


Figure 5.38. Plot of $\text{Cr}/(\text{Cr}+\text{Al}+\text{Fe}^{3+})$ vs. depth (m) for Black Thor DDH BT-09-17. The trend line plots through chromite cores.

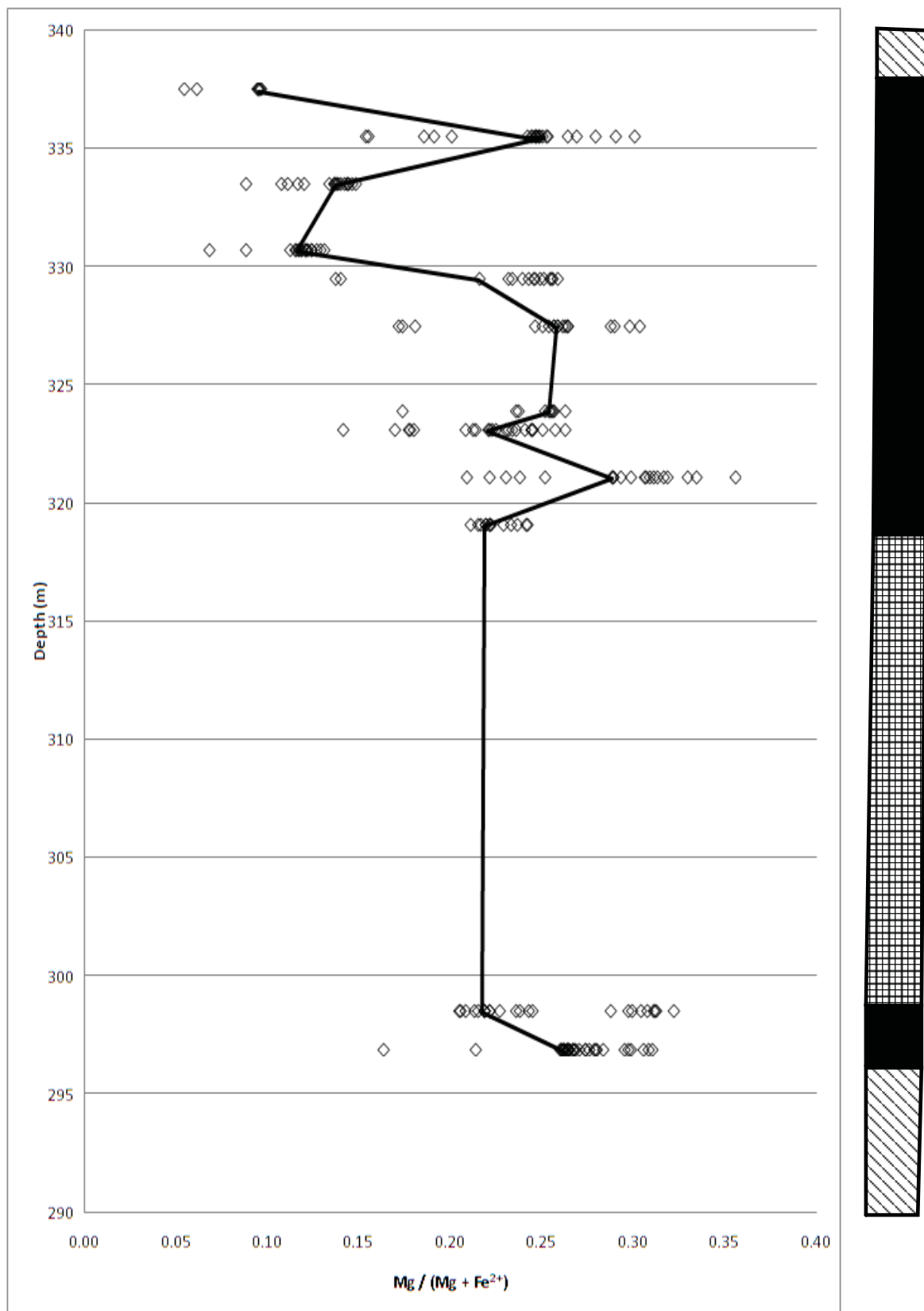


Figure 5.39. Plot of $\text{Mg}/(\text{Mg}+\text{Fe}^{2+})$ vs. depth (m) for Black Thor DDH BT-09-17. The trend line plots through chromite cores.

from core to margin with ratios of between 1.88 and 2.44 for magmatic chromite (Fig. 5.40). In contrast to other drill holes, the Cr-enriched ferrichromites serve to enrich the upper chromitites in Cr/Fe with compositions reaching up to 3.03 with retrogression. The high Cr/Fe in the ferrichromites is due to the decrease in FeO_T in these chromites.

In the drill hole sequence, there are two chromitite intervals, the first situated between pyroxenite and gabbro and the second situated between gabbro and pyroxenite. In the lower interval, from core to margin of the grains, there is an increase in Cr_2O_3 , Al_2O_3 and MgO while a decrease in FeO_T that occurs due to silicate exchange with retrogressive fluids. Evidence for retrogression is “zoning” toward the margins that also occur along interior cracks and rims with associated alteration rim replacement chromite. Along with these trends, retrogression has been observed with the occurrence of bright alteration margins (similar to ferrichromite) with enriched 61.75 wt. % Cr_2O_3 , low 6.45 wt. % Al_2O_3 , low 4.62 wt. % MgO and elevated 23.84 wt. % FeO_T . These are probably Cr-enriched ferrichromites, although the ferric iron content is not as high.

Retrogression has also been observed with the occurrence of chrome chlorites and tremolites with very little wt. % FeO_T which could be interpreted as hydrothermal tremolite in contrast with tremolite that results from the replacement pyroxene. Also, higher up in the second chromitite interval, the chromites are more diffused with increased Cr_2O_3 , Al_2O_3 , but with decreased MgO to 4 to 6 wt. %. It appears that the upper chromitites underwent higher temperature hydrothermal metamorphism to the tremolite field in the lower parts but have been more retrogressed in the upper parts of the upper chromitite. The lower T retrogression in the upper part is probably a later hydration overprint. The chromites in the upper parts of the zone are more non-uniform, broken up and enriched in silicate due to late influx of retrogressive fluids. In the two intervals, since only 12 samples were analysed in the chromitite and the differentiation and replenishment trends are masked by these retrogressive Cr_2O_3 and MgO enrichments, primary igneous signatures are too overprinted to interpret any fine scale cryptic layering.

For variation of major oxides with depth, the lower chromitite interval from 296.30 to 298.80 m contains more primary chromite than the second interval. The chromites show uniformity in the back scatter images with evidence for primary cores in well zoned chromites. From 296.80 to 298.40 m, the samples begin with wt. % Cr_2O_3 at

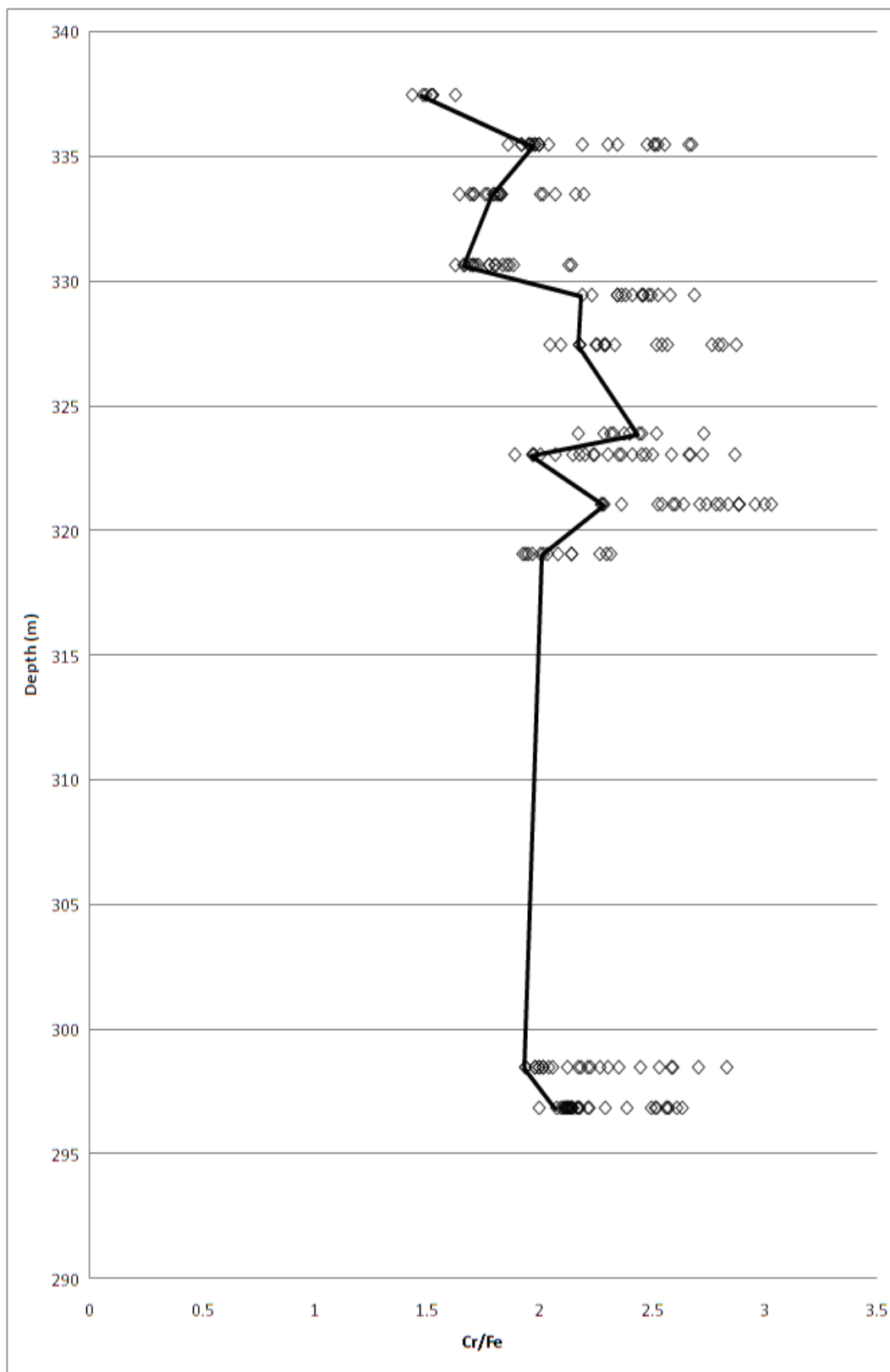


Figure 5.40. Plot of Cr/Fe vs. depth (m) for Black Thor DDH BT-09-17. The trend line plots through chromite cores.

49.59 wt. % Cr_2O_3 and increase upward to 52 to 54 wt. % Cr_2O_3 with retrogression. MgO decreases from 7.95 to 6.62 wt. % MgO in the igneous cores but shows enriched zonation on the margins to 9.01 wt. % MgO. Other trends include a decrease in wt. % Al_2O_3 while increase in wt. % FeO in the igneous core from the first to the second sample (Figs. 4.41 and 4.42). However there is an increase in wt. % Al_2O_3 , while decrease in wt. % FeO in the silicate exchanged zoned margins. The alteration rim chromites at 59.06 and 62.75 wt. % Cr_2O_3 have no wt. % Fe_2O_3 and low FeO at 23.41 and 24.61 wt. %.

The second chromitite interval is from 318.70 to 339 m. There are three sequences as seen from the variation in wt. % Cr_2O_3 from the assays. In the microprobed chromites, the first chromite sequence is from 319 to 324 m. There is a decrease in wt. % Cr_2O_3 in the igneous cores going up the sequence, however, Cr_2O_3 contents are enriched to up to 53.36 wt. % Cr_2O_3 on the diffused margins. MgO increases up to 9.69 wt. % MgO with retrogressive silicate exchange. Within the overall second interval, alteration rims report up to 68.03 wt. % Cr_2O_3 in chromite. Fe_2O_3 contents in the overall DDH BT-09-17 are more depleted than the Fe_2O_3 contents of the other drill holes (Fig. 4.43). The second chromite sequence from 326 to 331 m shows an enrichment in wt. % Cr_2O_3 in the cores followed by a decrease in wt. % Cr_2O_3 . With retrogression, the margins are enriched to 53.9 wt. % Cr_2O_3 . MgO decreases from 7.72 to a low 3.69 wt. % MgO in the cores along with margins. These chromites are not as uniform as the chromites in the lower sequences, due to considerable fracturing and silicate exchange. It is interpreted that primary compositions are not preserved. In the third chromite sequence from 334 to 338 m, MgO increases to 7.37 wt. % MgO probably due to a new pulse along with retrogressive enrichment in wt. % MgO. Cr_2O_3 concentrations at 49.47 wt. % are not as high, however, due to lack of primary chromite signatures. Notably, Fe_2O_3 becomes more elevated from 3.14 to 4.47 wt. % Fe_2O_3 in these more evolved chromites.

5.3.1.4 Big Daddy

Before the main chromitite in Big Daddy DDH FW-08-19, there is a sequence of dunite, heterogeneous pyroxenite and pyroxenite with intervening chromites. The chromites microprobed in this section are usually disseminated chromites found in dunite and sometimes pyroxenite. At 13.50 m depth, there is first a band of primitive chromite in dunite that contains high wt. % Cr_2O_3 and MgO (Figs. 5.44 to 5.48). In contrast there

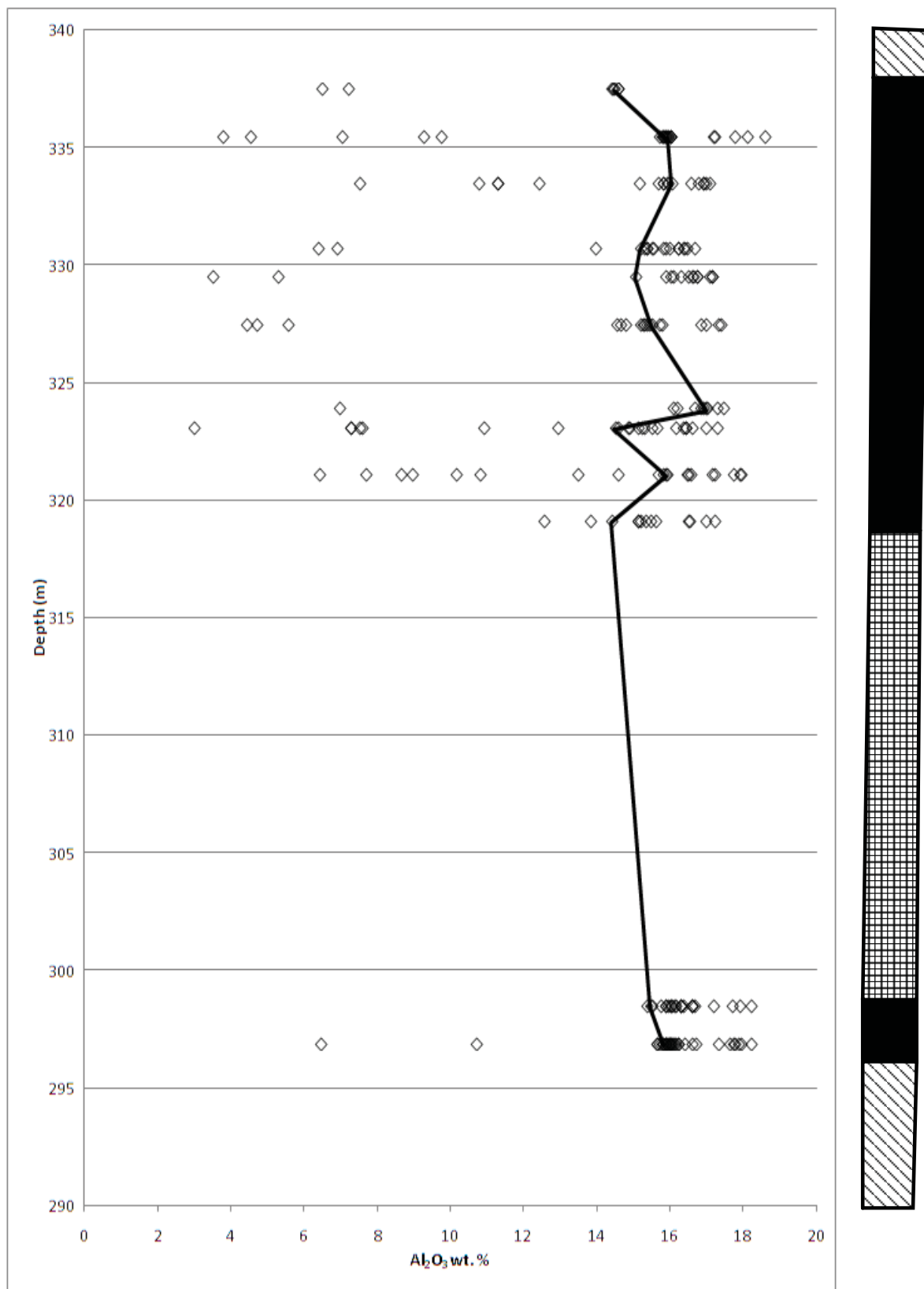


Figure 5.41. Plot of Al_2O_3 wt. % vs. depth (m) for Black Thor DDH BT-09-17 with ferrichromite displayed. The trend line plots through chromite cores.

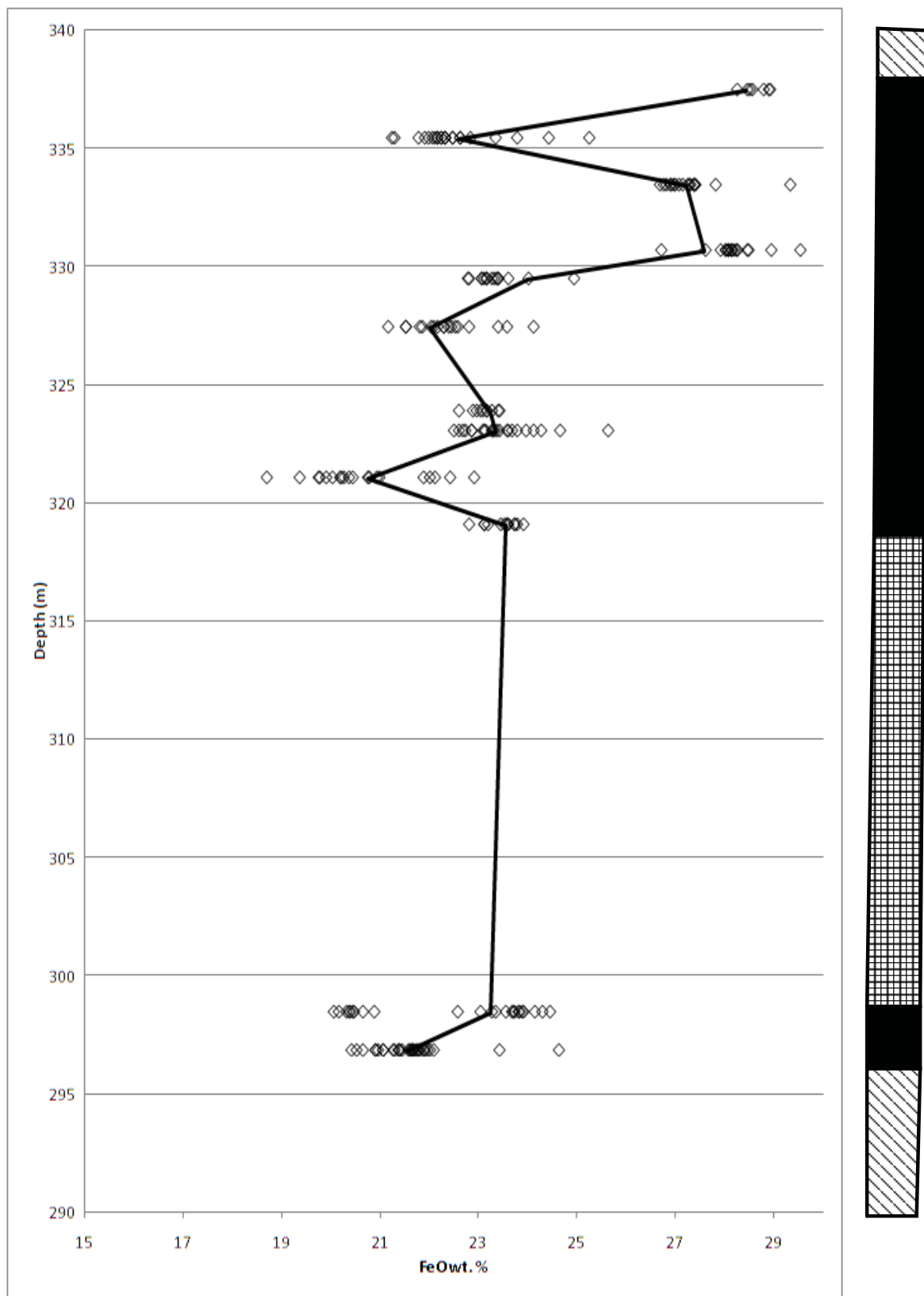


Figure 5.42. Plot of FeO wt. % vs. depth (m) for Black Thor DDH BT-09-17. The trend line plots through chromite cores.

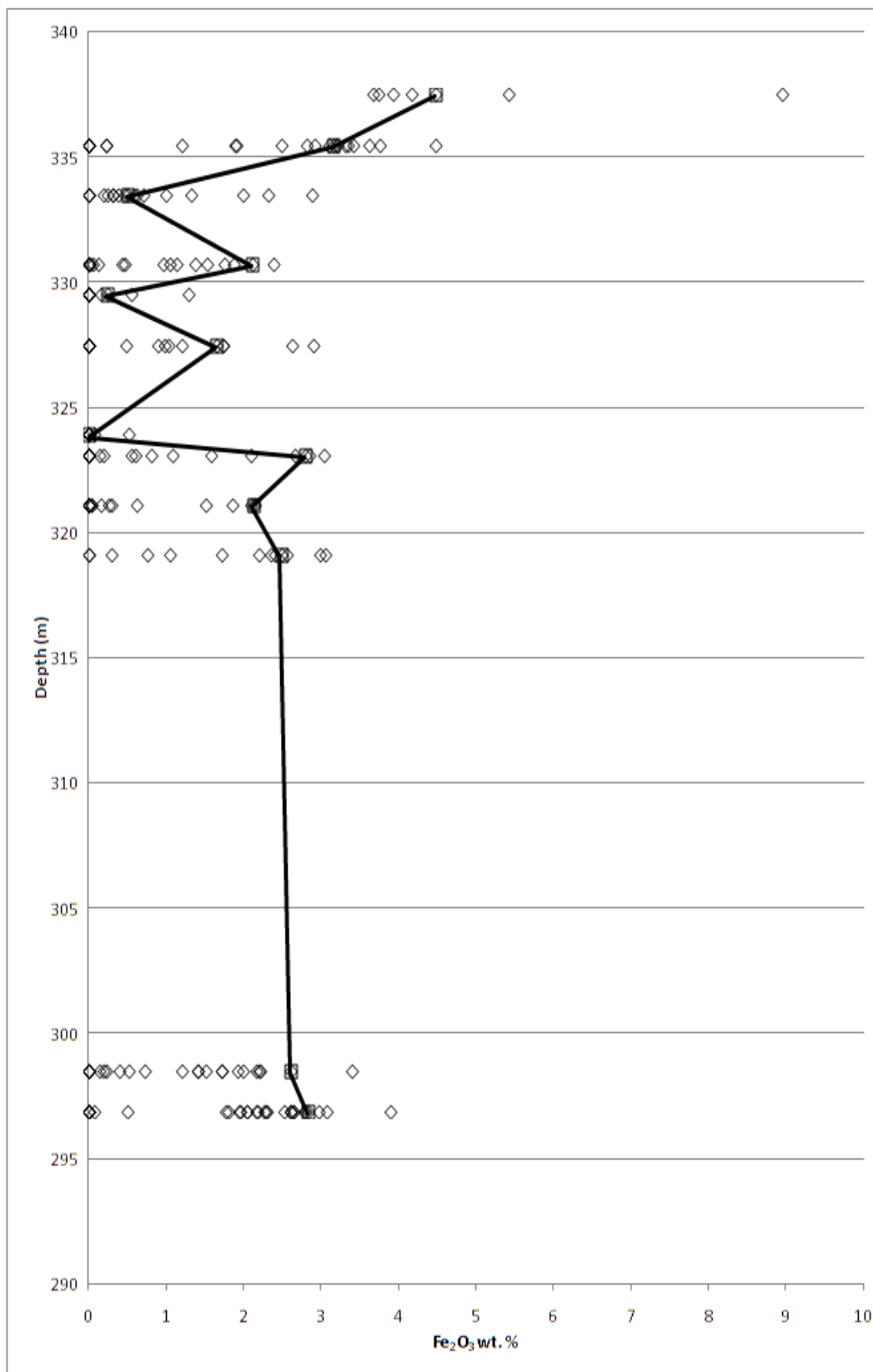


Figure 5.43. Plot of Fe₂O₃ wt. % vs. depth (m) for Black Thor DDH BT-09-17. The trend line plots through chromite cores.

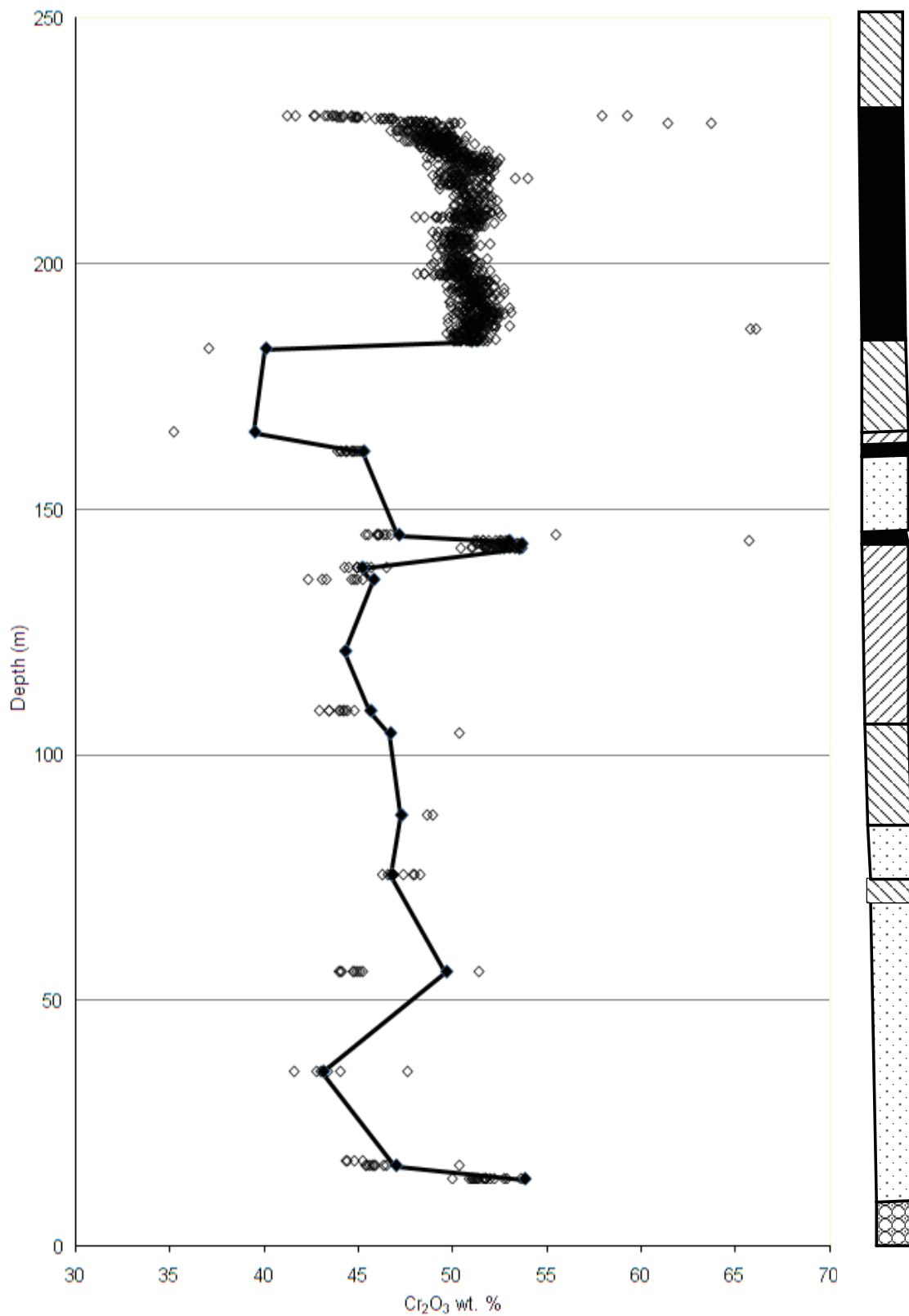


Figure 5.44. Plot of Cr₂O₃ wt. % vs. depth (m) for the first part of Big Daddy DDH FW-08-19. The trend line plots through chromite cores.

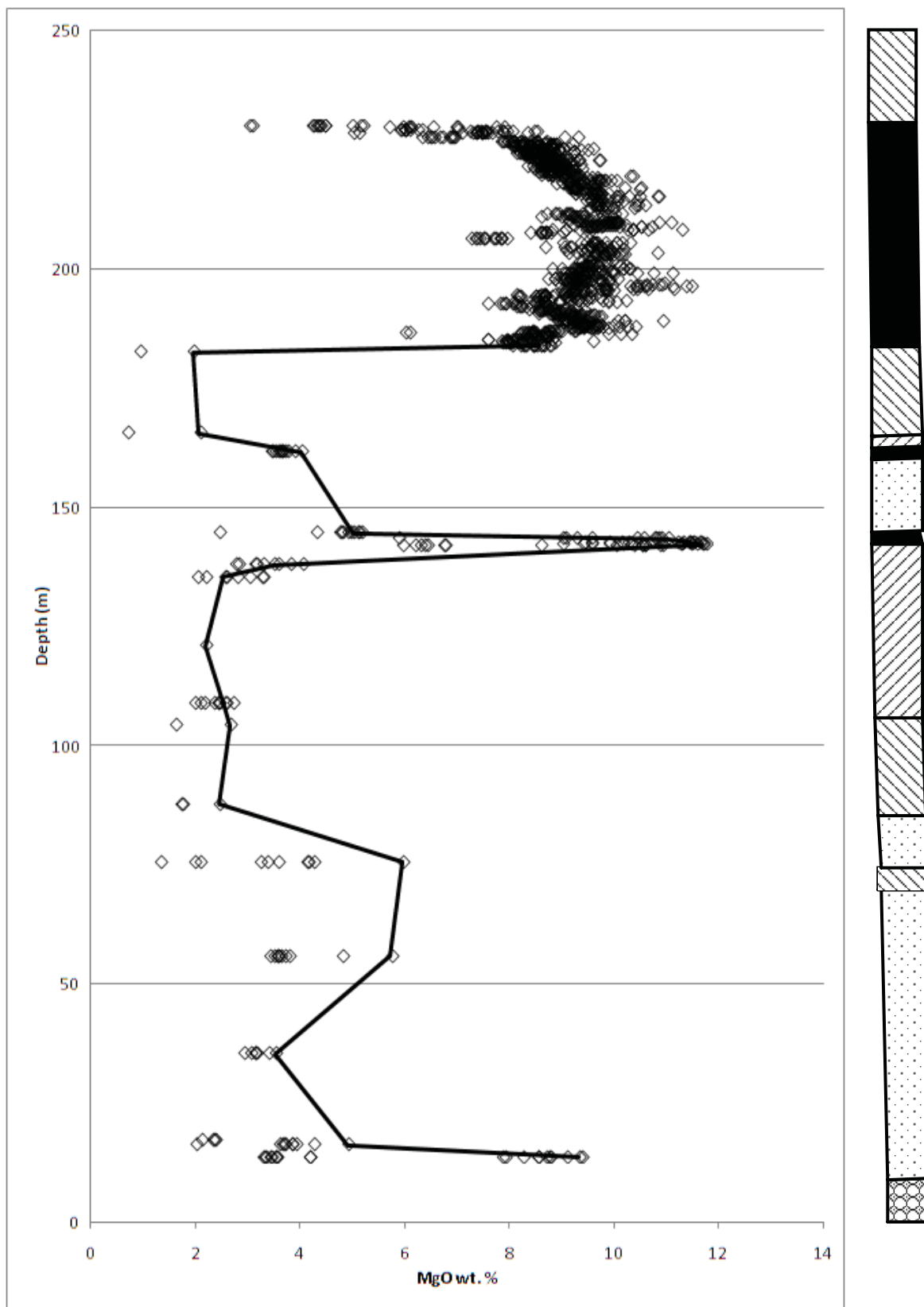


Figure 5.45. Plot of MgO wt. % vs. depth (m) for the first part of Big Daddy DDH FW-08-19. The trend line plots through chromite cores.

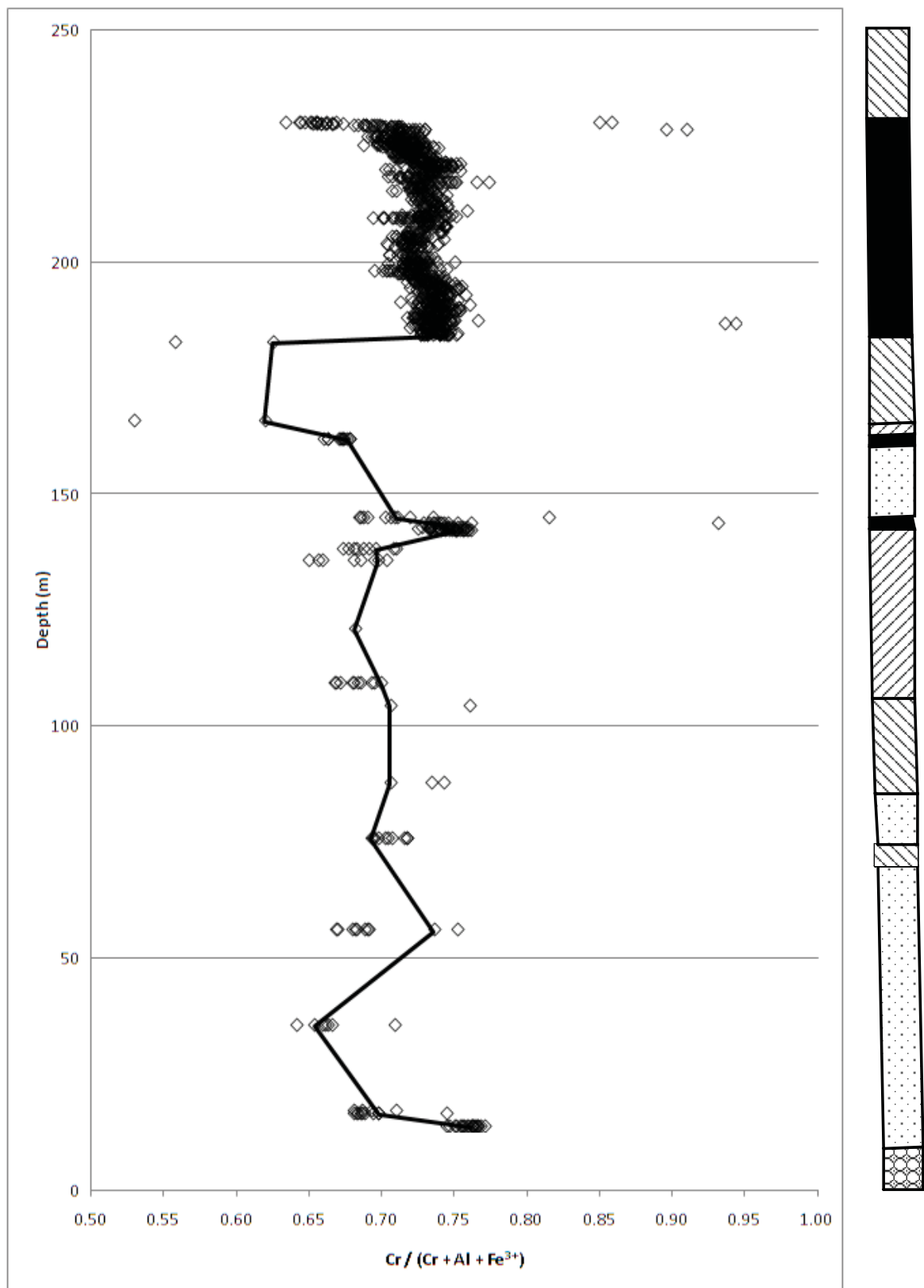


Figure 5.46. Plot of $\text{Cr}/(\text{Cr}+\text{Al}+\text{Fe}^{3+})$ vs. depth (m) for the first part of Big Daddy DDH FW-08-19. The trend line plots through chromite cores.

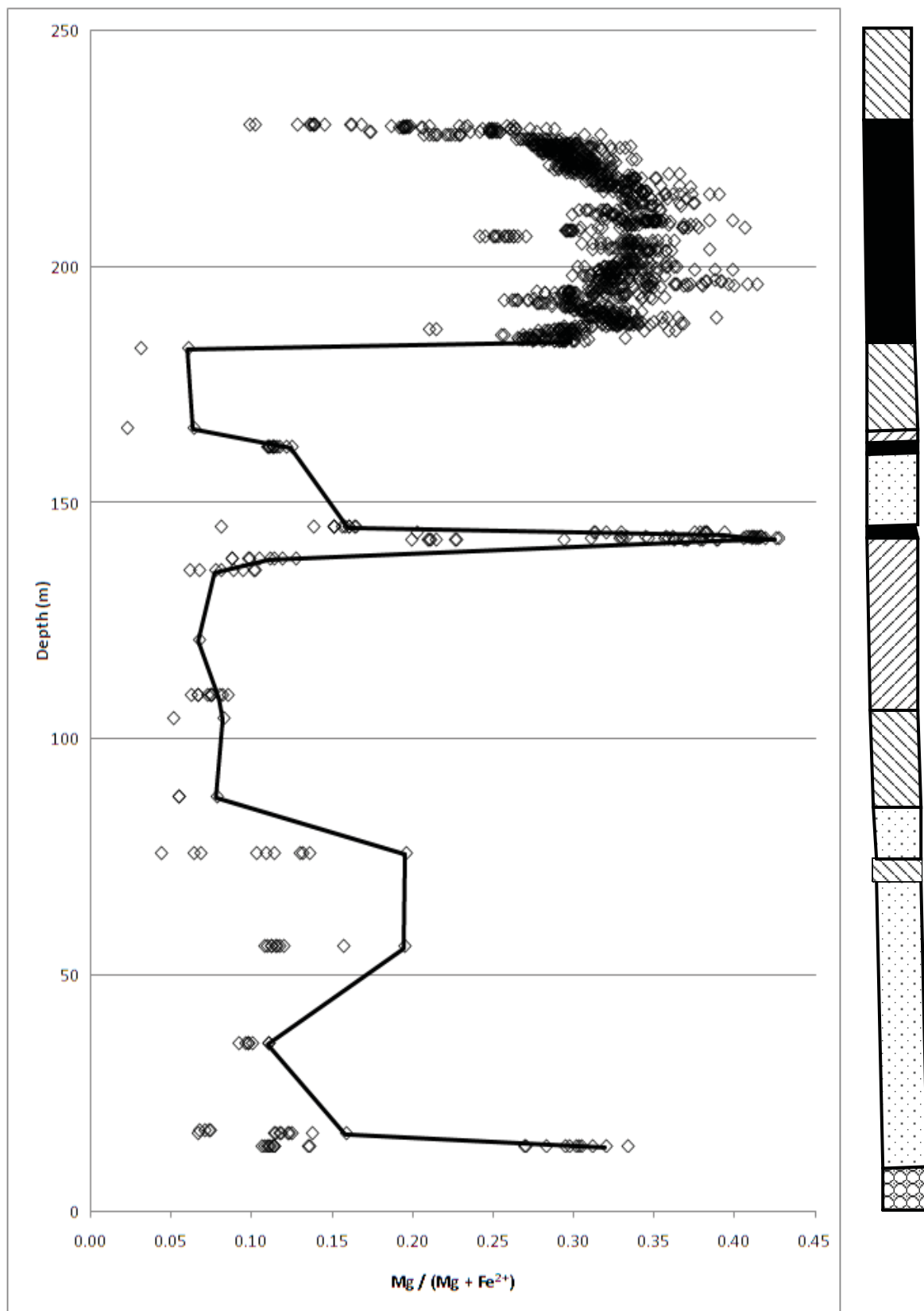


Figure 5.47. Plot of $\text{Mg}/(\text{Mg}+\text{Fe}^{2+})$ vs. depth (m) for the first part of Big Daddy DDH FW-08-19. The trend line plots through chromite cores.

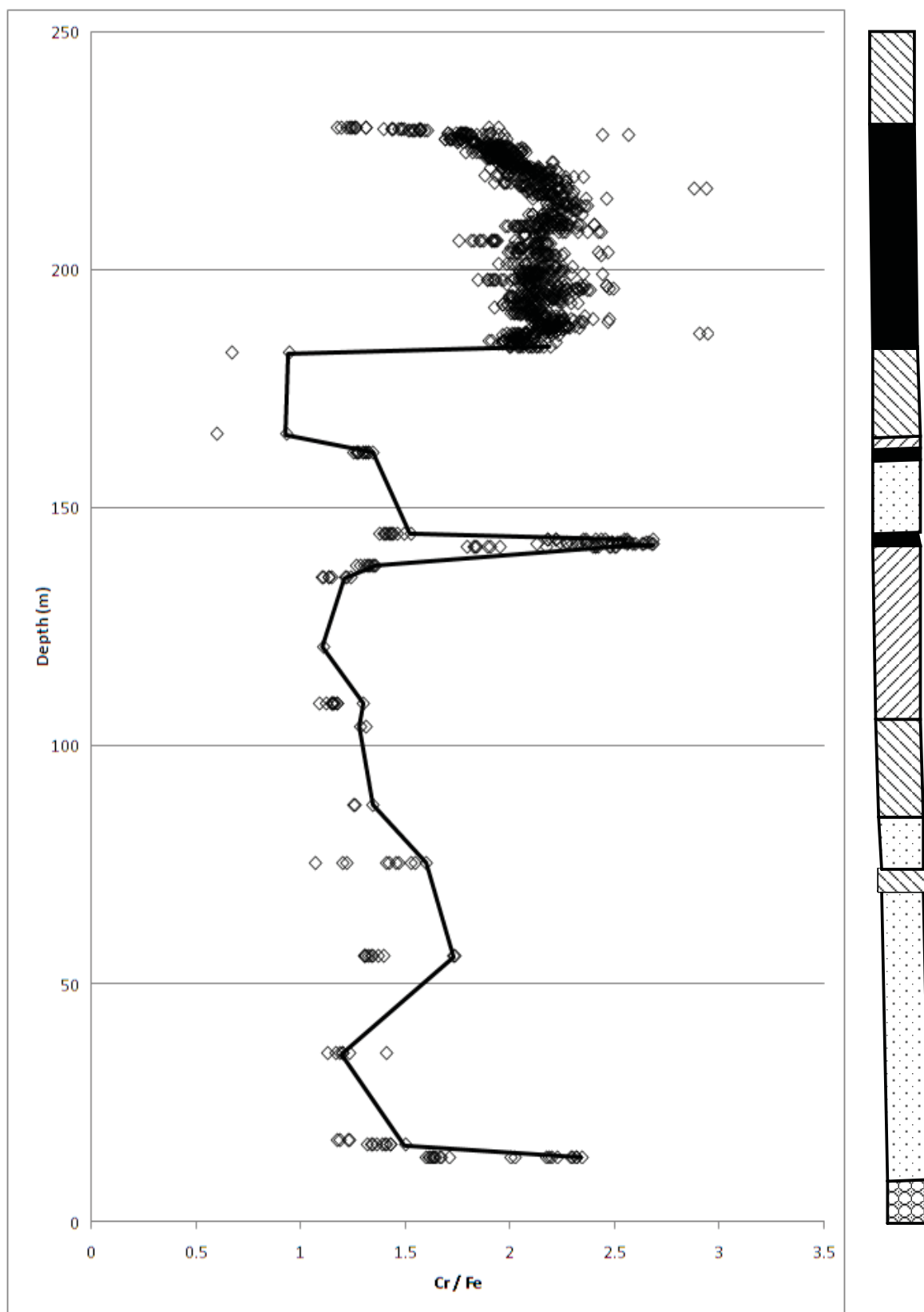


Figure 5.48. Plot of Cr/Fe vs. depth (m) for the first part of Big Daddy DDH FW-08-19. The trend line plots through chromite cores.

is low wt. % Al_2O_3 and FeO (Figs. 5.49 to 5.50). This chromite band is located in dunite just above a small layer of pyroxenite and is interpreted to form due to the mixing of a new dunite pulse with pyroxenite. Another such layer occurs at 20.10 m. At 16.07 m, disseminated interstitial chromite in dunite is more evolved in composition with lower wt. % Cr_2O_3 and MgO and higher wt. % Al_2O_3 and FeO . The dunite continues to 69.40 m. At first there is differentiation from 16.07 to 35.20 m toward lower wt. % Cr_2O_3 and MgO with intervening pyroxenite. Then there is a new pulse of dunite after beginning somewhere after 33.36 m with higher wt. % Cr_2O_3 and MgO at 55.62 m depth. Pyroxenite begins after 64.00 m above a faulted contact with the dunite. Another pulse of dunite occurs from 73.97 to 84.94 m and contains more primitive chromite at 75.36 m. From 74.36 to 135.2 m, the interstitial chromite in the host units become steadily more evolved as there is differentiated pyroxenite that grades into heterogeneous olivine pyroxene to harzburgite. This represents a mixed unit interpreted to be caused by magma mixing of a pulse of pyroxenite with dunite to form chromitite in an overlying pulse. Compositions show increasing wt. % FeO , wt. % TiO_2 while decreasing wt. % Al_2O_3 in the pyroxenite (Fig. 5.51). Lower wt. % Al_2O_3 is due to retrogression in the pyroxenite. From 141.50 to 144.14 m, there is a chromitite layer containing semi-massive chromitite in cumulus pyroxene and olivine. The chromitite contains the highest wt. % Cr_2O_3 and MgO with 53.45 wt. % Cr_2O_3 and 11.68 wt. % MgO making it the most primitive chromitite in the sequence. Then compositions are lower again in an overlying disseminated chromite-bearing dunite. The chromites then become progressively more evolved from 144.50 to 182.40 m as the dunite grades into heterogeneous olivine pyroxenite and in turn pyroxenite. Chromite in pyroxenite is vermicular in texture with low wt. % Cr_2O_3 and MgO . Within this first sequence, there are ferrichromites that contain higher wt. % Cr_2O_3 and wt. % Fe_2O_3 (Fig. 5.52).

The main Big Daddy interval begins at 183.80 m depth. It is all massive chromitite and therefore demonstrates a markedly different compositional trend than Black Thor and Label. MgO and Cr_2O_3 compositions are more uniform in the chromites (Figs. 5.53 to 5.56). This is especially reflected in constant Cr_2O_3 from one zone to another. The main chromitite interval in the hole is from 183 to 230 m and is divided into 4 main zones as defined by troughs in wt. % MgO . With constant Cr_2O_3

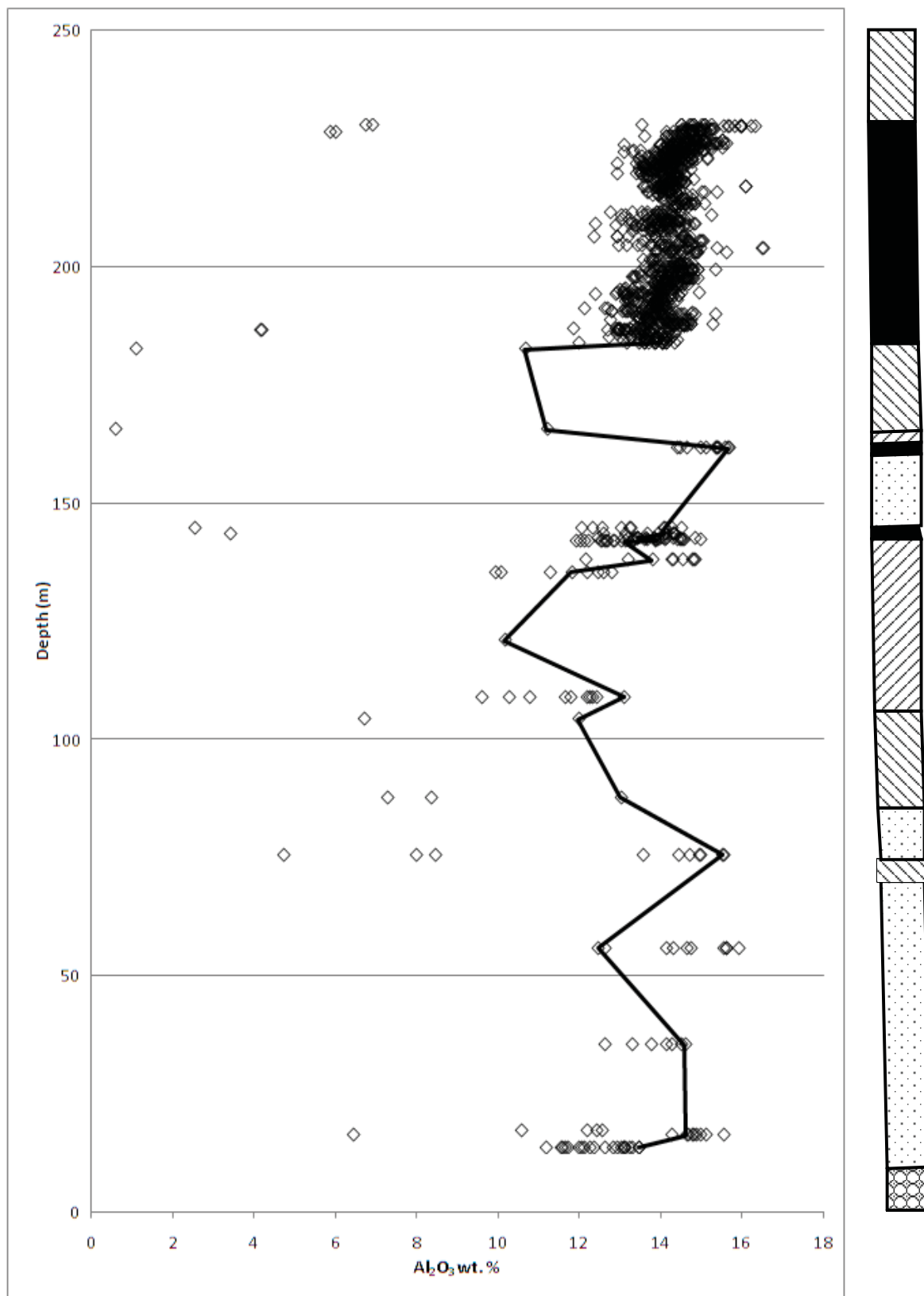


Figure 5.49. Plot of Al₂O₃ wt. % vs. depth (m) for the first part of Big Daddy DDH FW-08-19. The trend line plots through chromite cores.

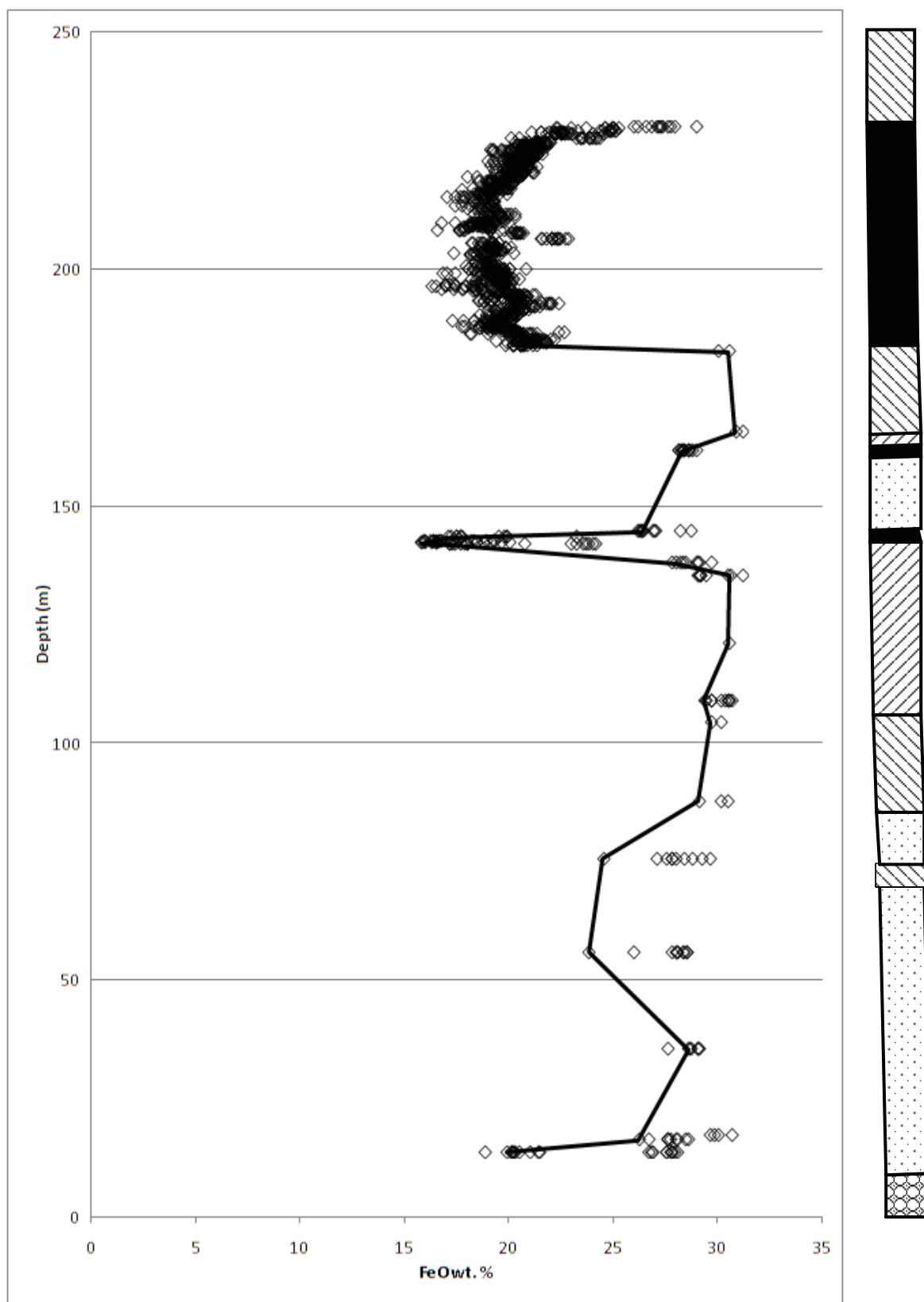


Figure 5.50. Plot of FeO wt. % vs. depth (m) for the first part of Big Daddy DDH FW-08-19. The trend line plots through chromite cores.

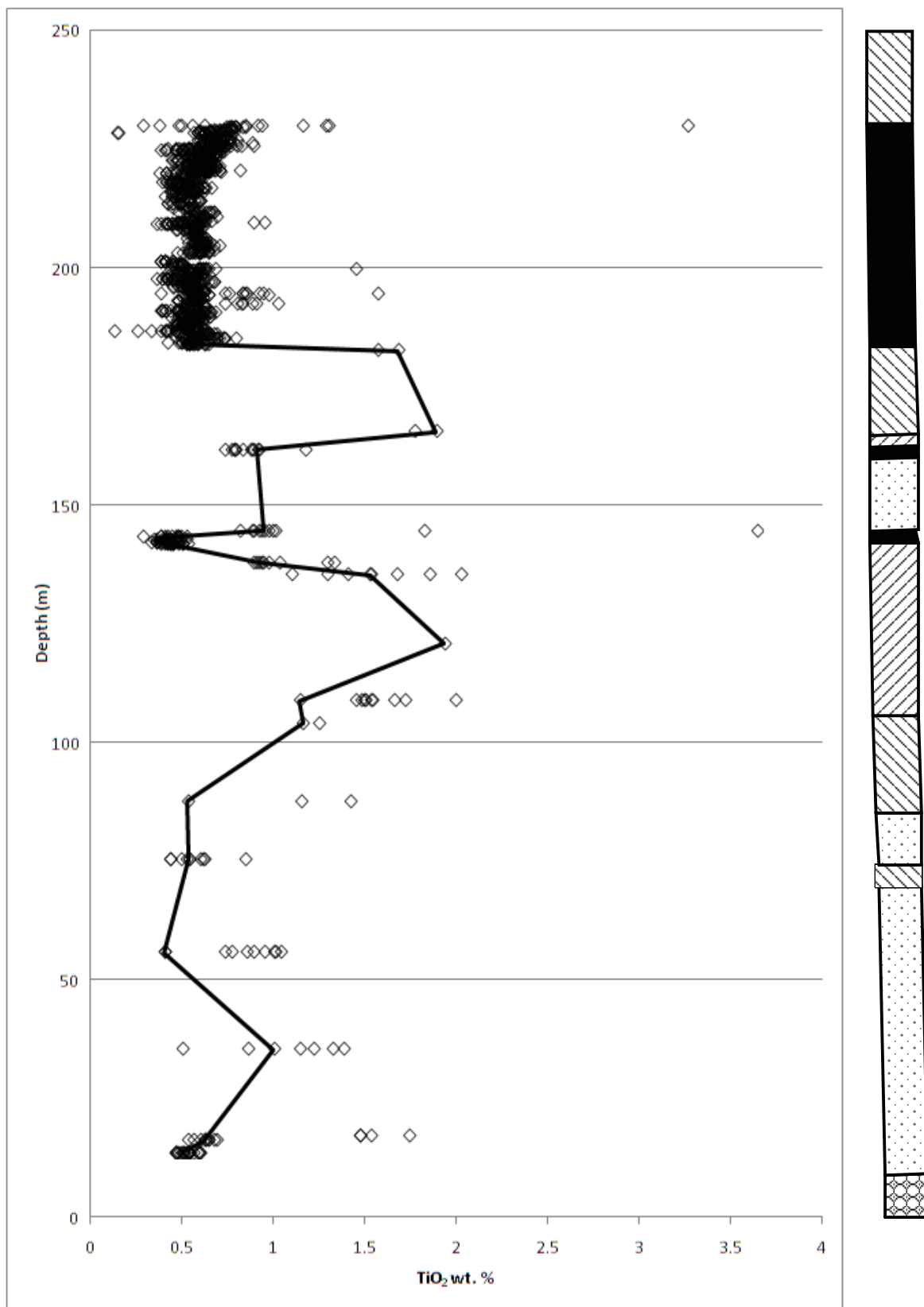


Figure 5.51. Plot of TiO₂ wt. % vs. depth (m) for the first part of Big Daddy DDH FW-08-19. The trend line plots through chromite cores.

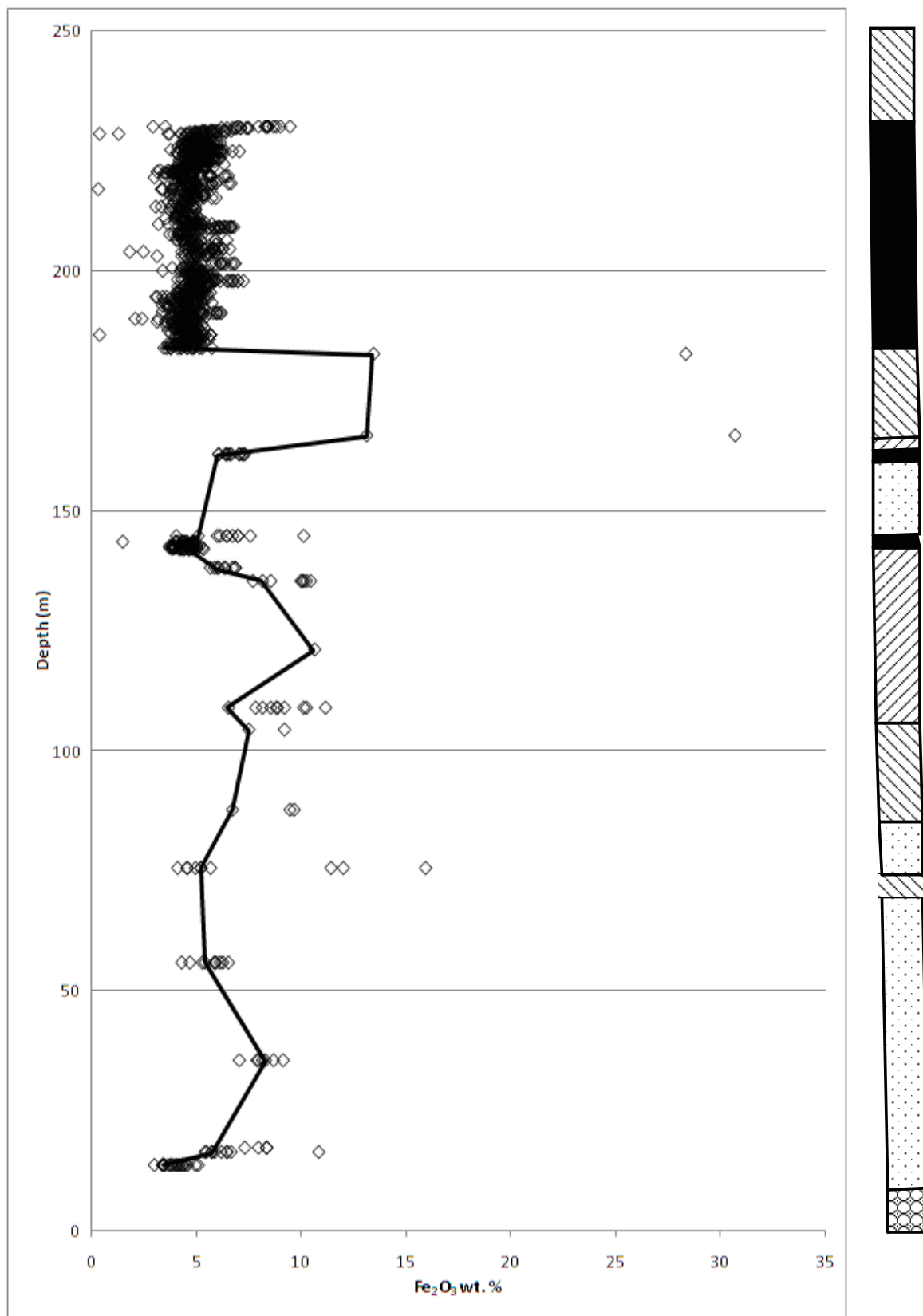


Figure 5.52. Plot of Fe₂O₃ wt. % vs. depth (m) for the first part of Big Daddy DDH FW-08-19. The trend line plots through chromite cores.

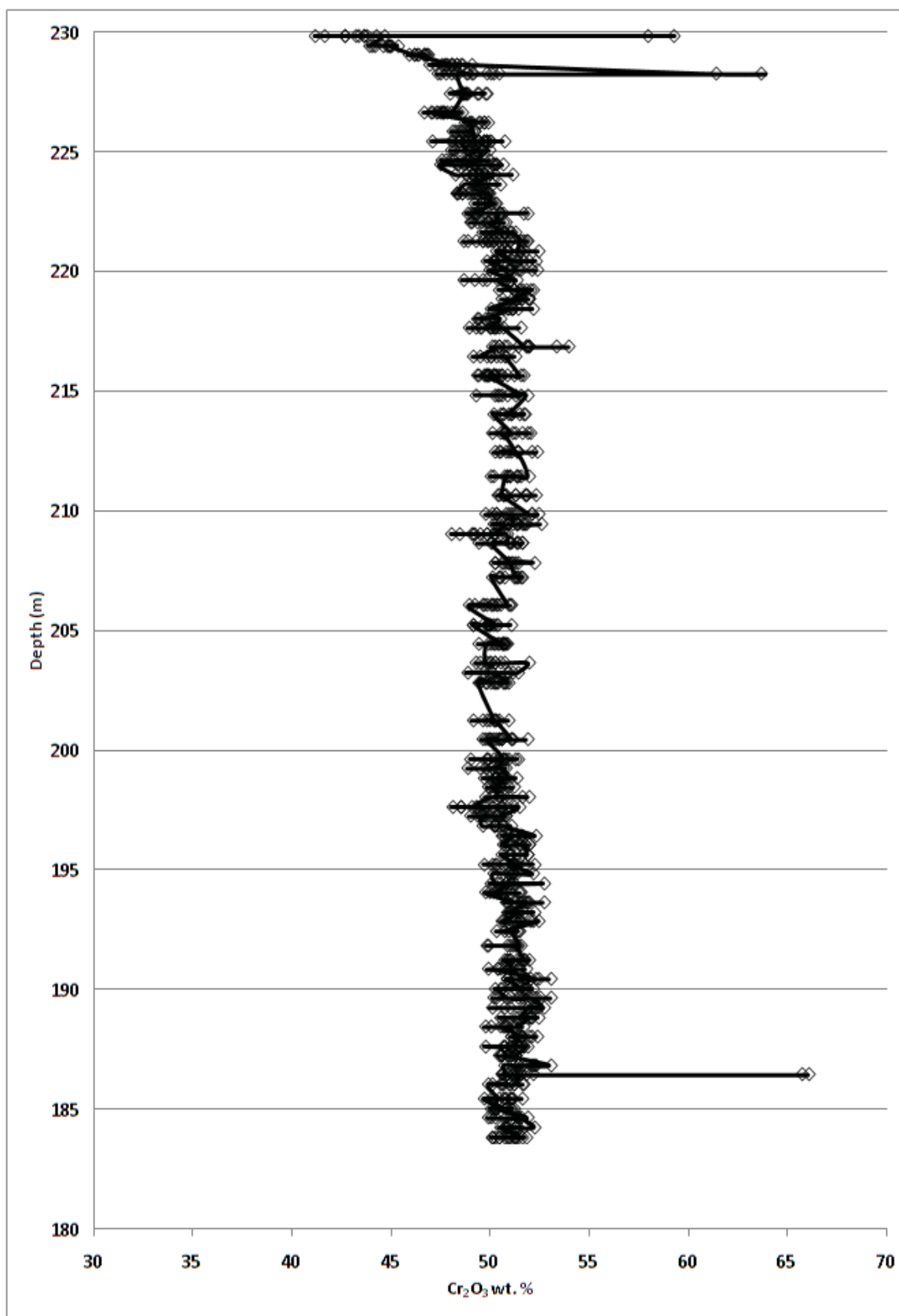


Figure 5.53. Plot of Cr₂O₃ wt. % vs. depth (m) for Big Daddy DDH FW-08-19.

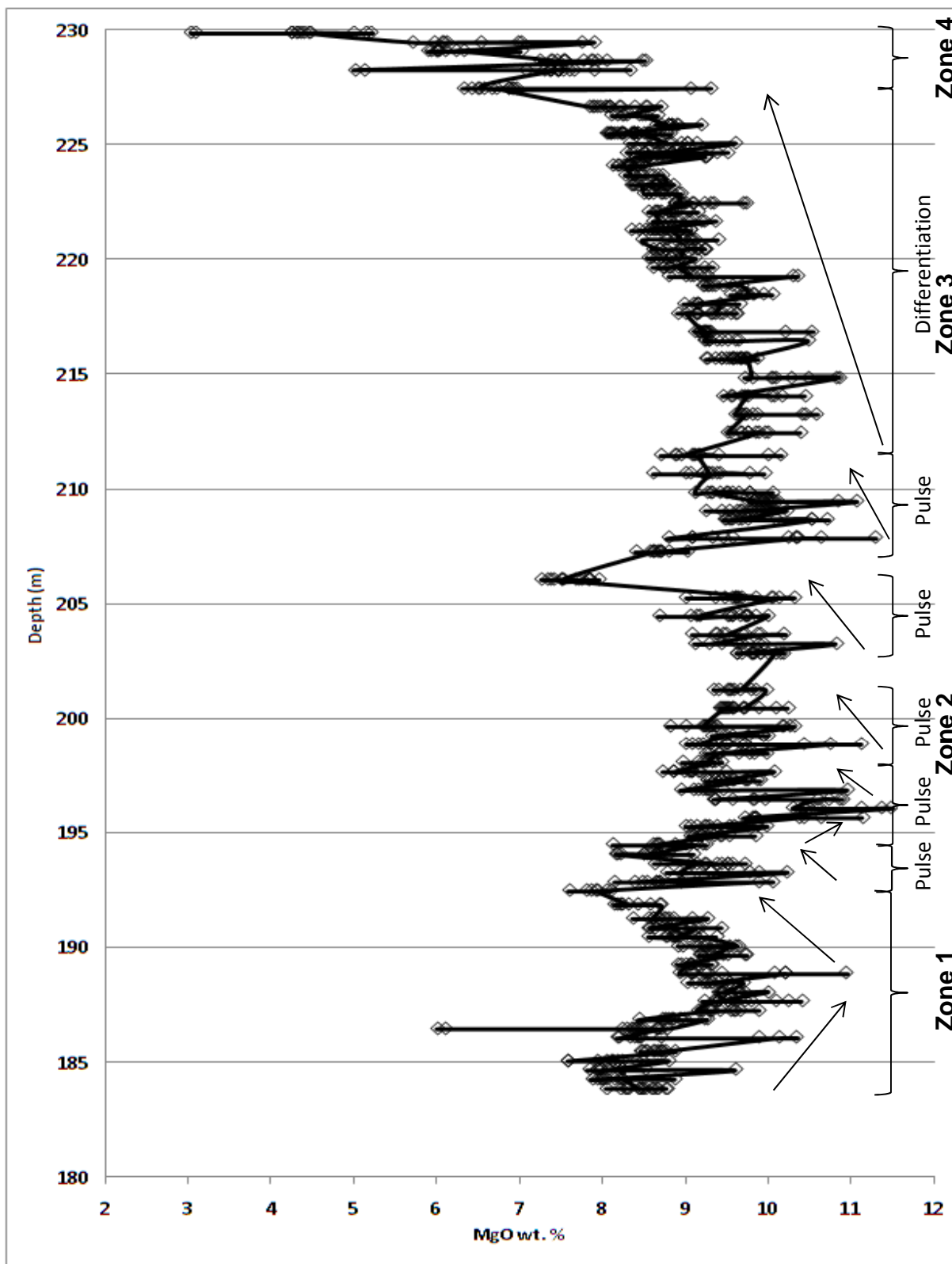


Figure 5.54. Plot of MgO wt. % vs. depth (m) for Big Daddy DDH FW-08-19 with various zones and pulses shown. Arrows pointing to the right represent replenishment while arrows pointing left represent differentiation.

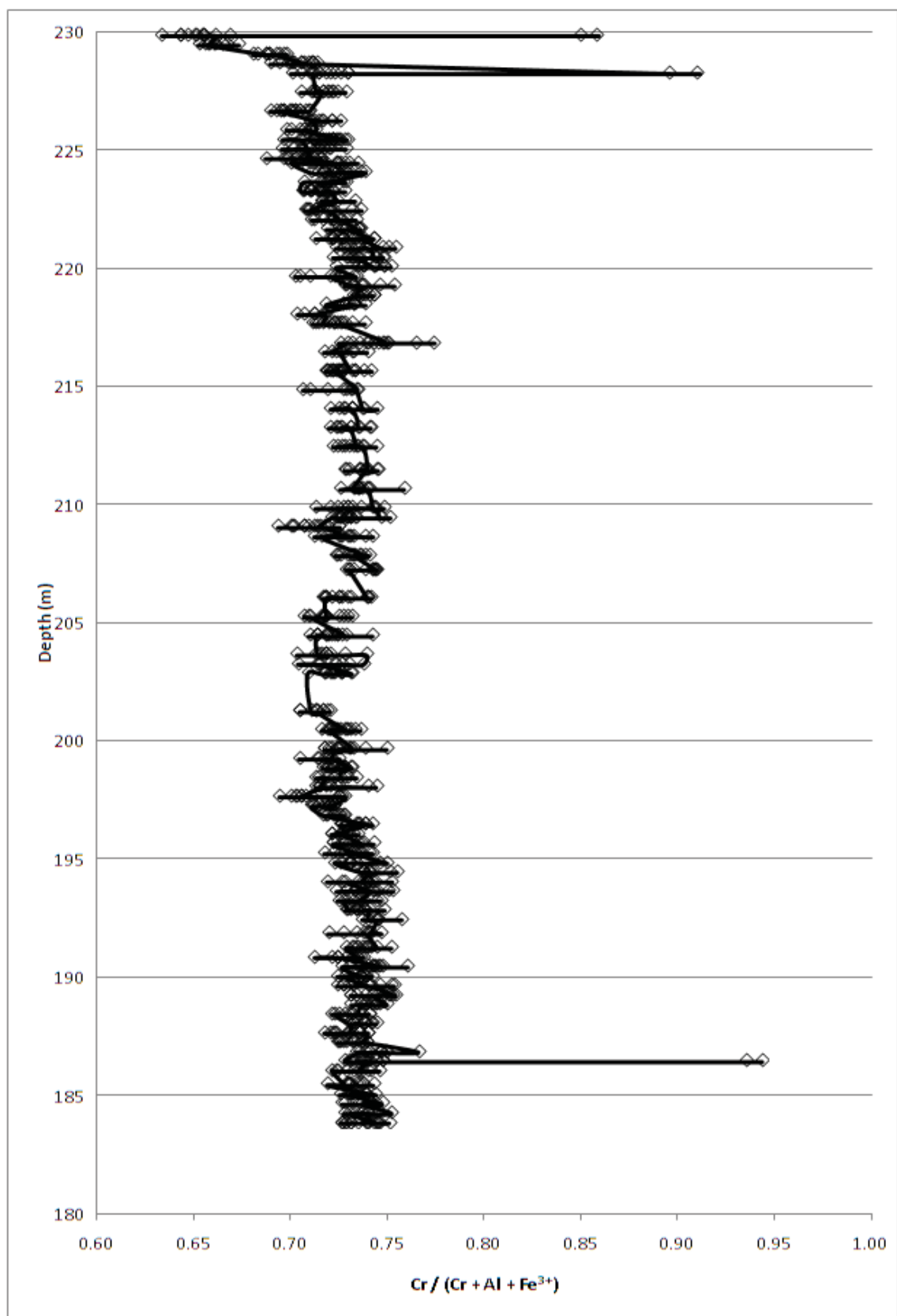


Figure 5.55. Plot of $\text{Cr}/(\text{Cr}+\text{Al}+\text{Fe}^{3+})$ vs. depth (m) for Big Daddy DDH FW-08-19.

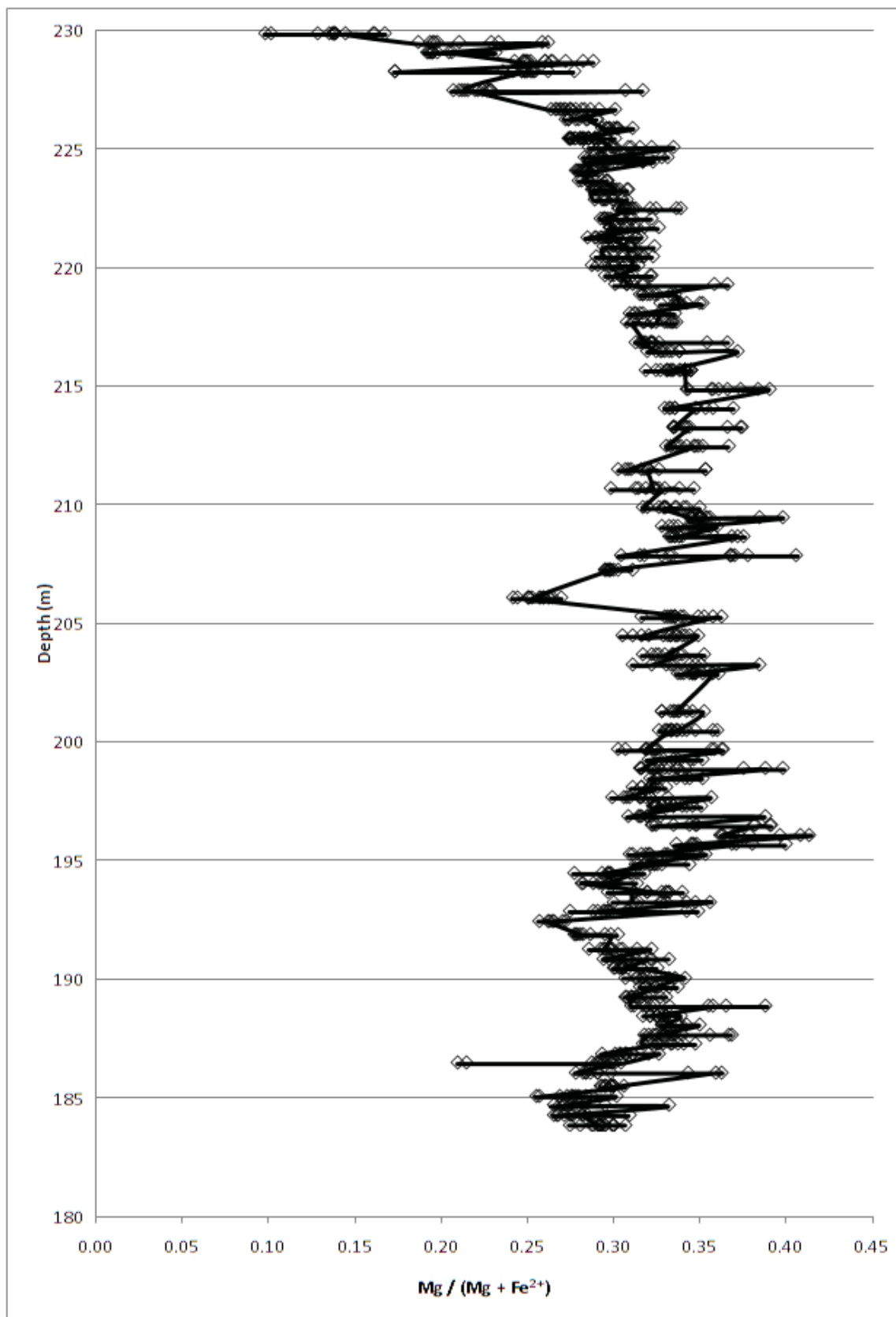


Figure 5.56. Plot of $\text{Mg}/(\text{Mg}+\text{Fe}^{2+})$ vs. depth (m) for Big Daddy DDH FW-08-19.

compositions, Cr/Fe is consistent at 2.25 for magmatic chromite, but tapers off near the upper contact with pyroxenite to lower Cr/Fe of down to 1.17 (Fig. 5.57). Minor variability in Cr/Fe is due to more variable wt. % MgO or FeO (Fig. 5.58). Cr-enriched ferrichromite where present enriches the Cr/Fe ratio. The first zone from 183 to 192 m, begins with two minor replenishments in wt. % MgO followed by decreasing wt. % MgO with height from 187 to 192 m. Chromite compositions are at 51 wt. % Cr₂O₃. The second zone from 192 to 206 m, begins with a pulse from 192 to 194 m at lower wt. % MgO followed by three successive pulses beginning at 11.46 wt. % MgO that decreases successively upward. Chromite compositions are constant at 50 wt. % Cr₂O₃. The third zone from 206 to 227 m, starts with a pulse at 11.27 wt. % MgO that decreases with height from 206 to 211 m. From 211 to 227 m there is a large well defined differentiation sequence. Chromite compositions decrease subtly from 51 to 47 wt. % Cr₂O₃ as the interval approaches the upper contact with pyroxenite. From 227 to 230 m is a contact zone with a pronounced decrease to 3 wt. % MgO and 41 wt. % Cr₂O₃ toward the contact. This zone is probably depleted due to silicate exchange with pale grey to white globular shaped aggregates of pyroxene. Also, there is more ferrichromite in this zone indicating higher degrees of hydration.

Al₂O₃ contents show a different pattern of variation in the Big Daddy interval. For wt. % Al₂O₃, the interval can be divided into three zones from 183 to 203 m, from 203 to 216 m and from 216 to 230 m (Fig. 5.59). The first zone shows a general trend of slightly increasing wt. % Al₂O₃ from 13.14 to 14.85 wt. % Al₂O₃. These contents are antipathetic the decreasing differentiation trend of the Cr₂O₃ contents. From 203 to 216 m, the Al₂O₃ contents first decrease and then increase in a concave pattern, due to replenishment followed by differentiation. Then from 216 to 230 m, there is another general increase in wt. % Al₂O₃ toward the contact with differentiation and silicate exchange with pyroxenite. The difference between the Al₂O₃ and MgO trends is due to less variation of Al₂O₃ and Cr₂O₃ within the complete convection cycles in massive chromitite compared to the more variable pattern of the Black Label and Thor intervals. Ferrichromites that are plotted have very low wt. % Al₂O₃. For wt. % Fe₂O₃ variation, contents are below 10 wt. % Fe₂O₃ and therefore do not show the retrogression to Cr-depleted ferrichromite as in Black Thor and Label (Fig. 5.60).

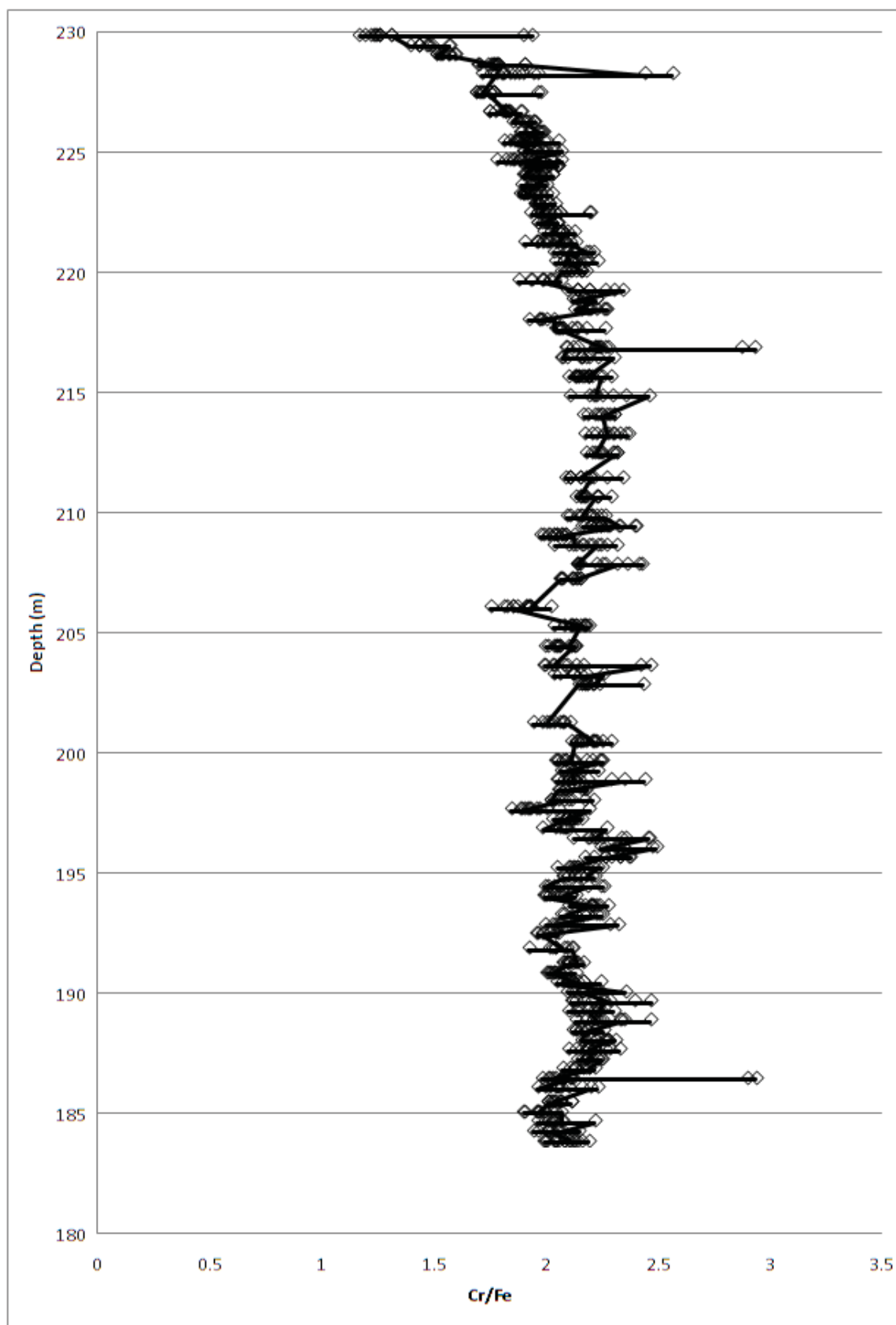


Figure 5.57. Plot of Cr/Fe vs. depth (m) for Big Daddy DDH FW-08-19.

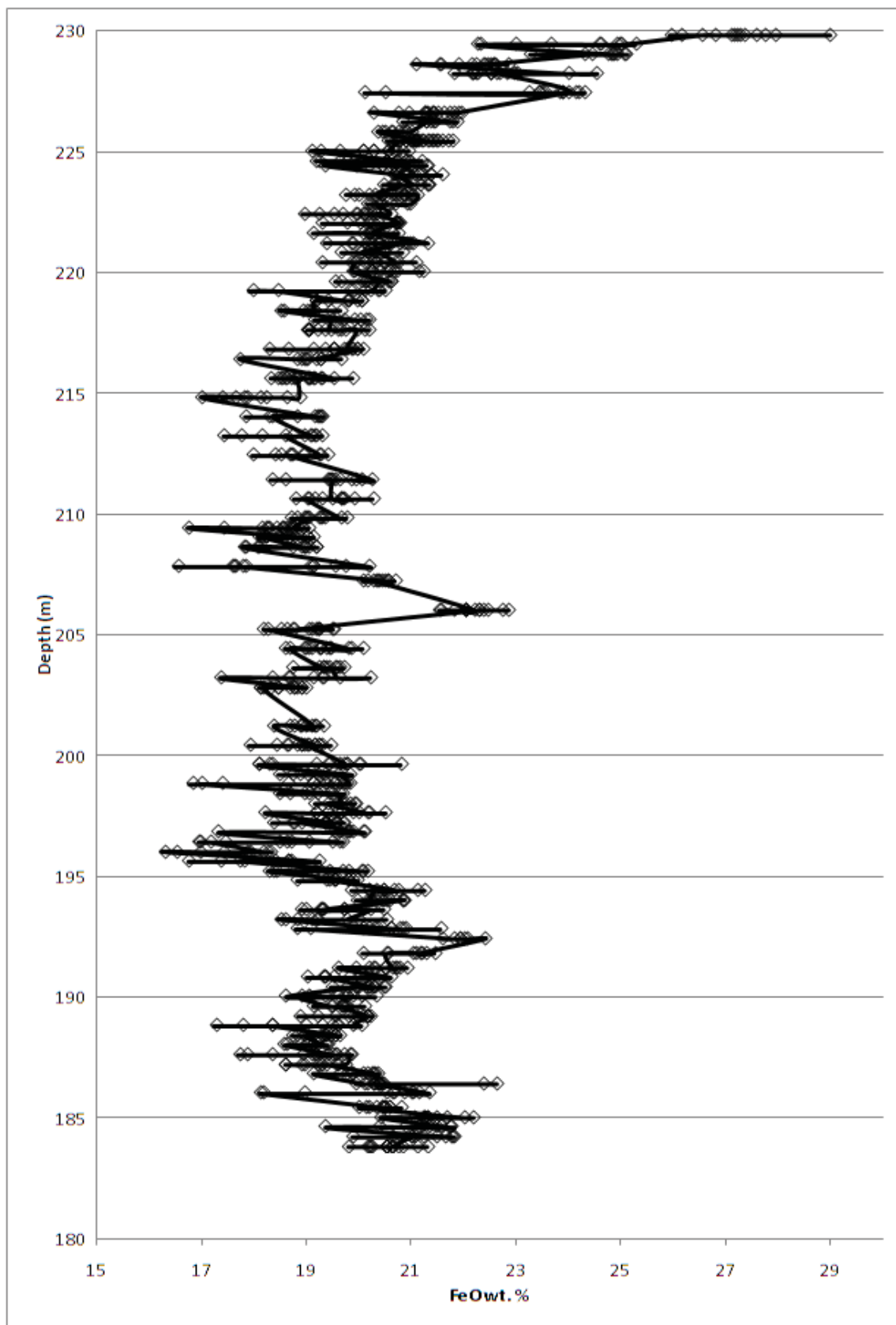


Figure 5.58. Plot of FeO wt. % vs. depth (m) for Big Daddy DDH FW-08-19.

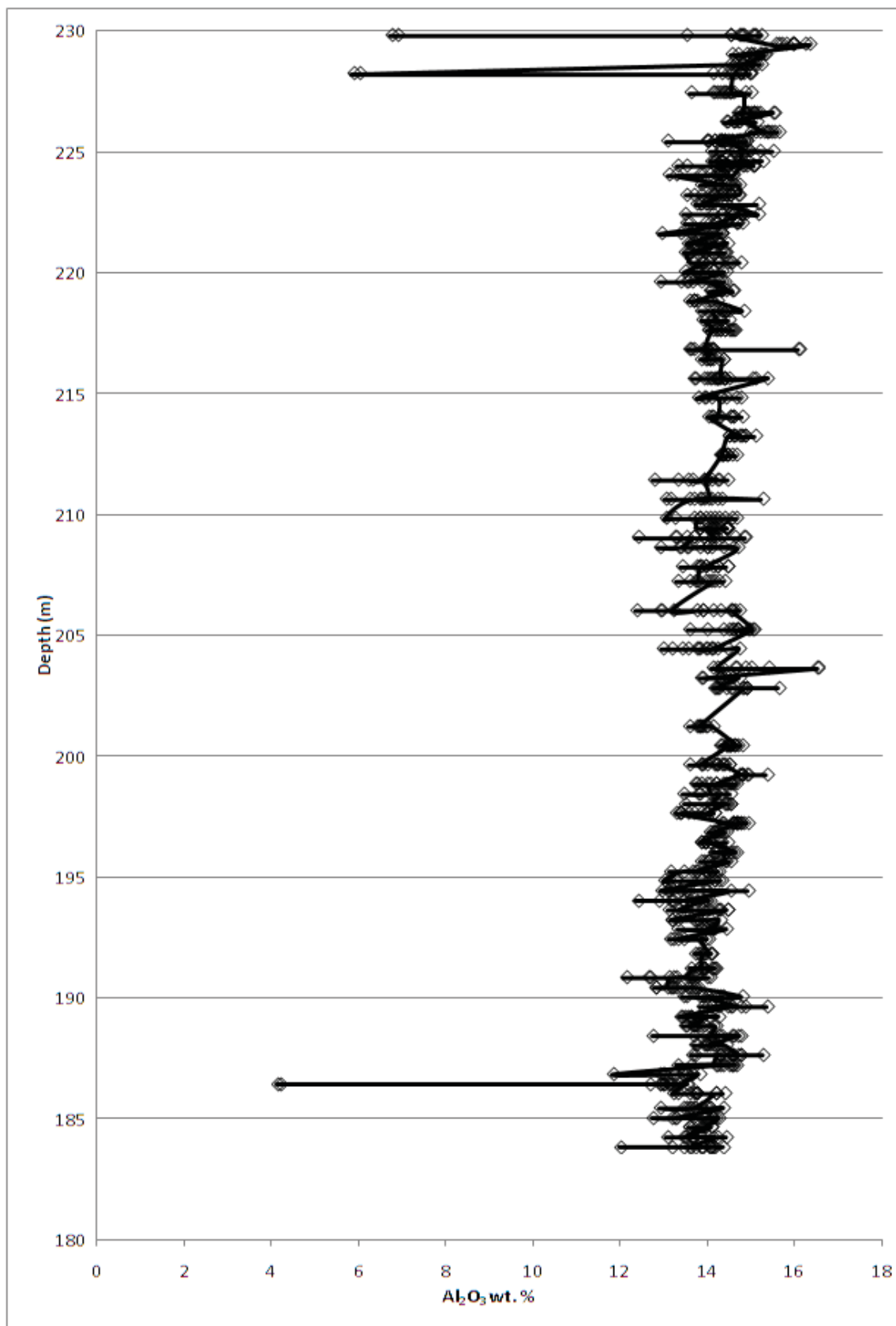


Figure 5.59. Plot of Al₂O₃ wt. % vs. depth (m) for Big Daddy DDH FW-08-19.

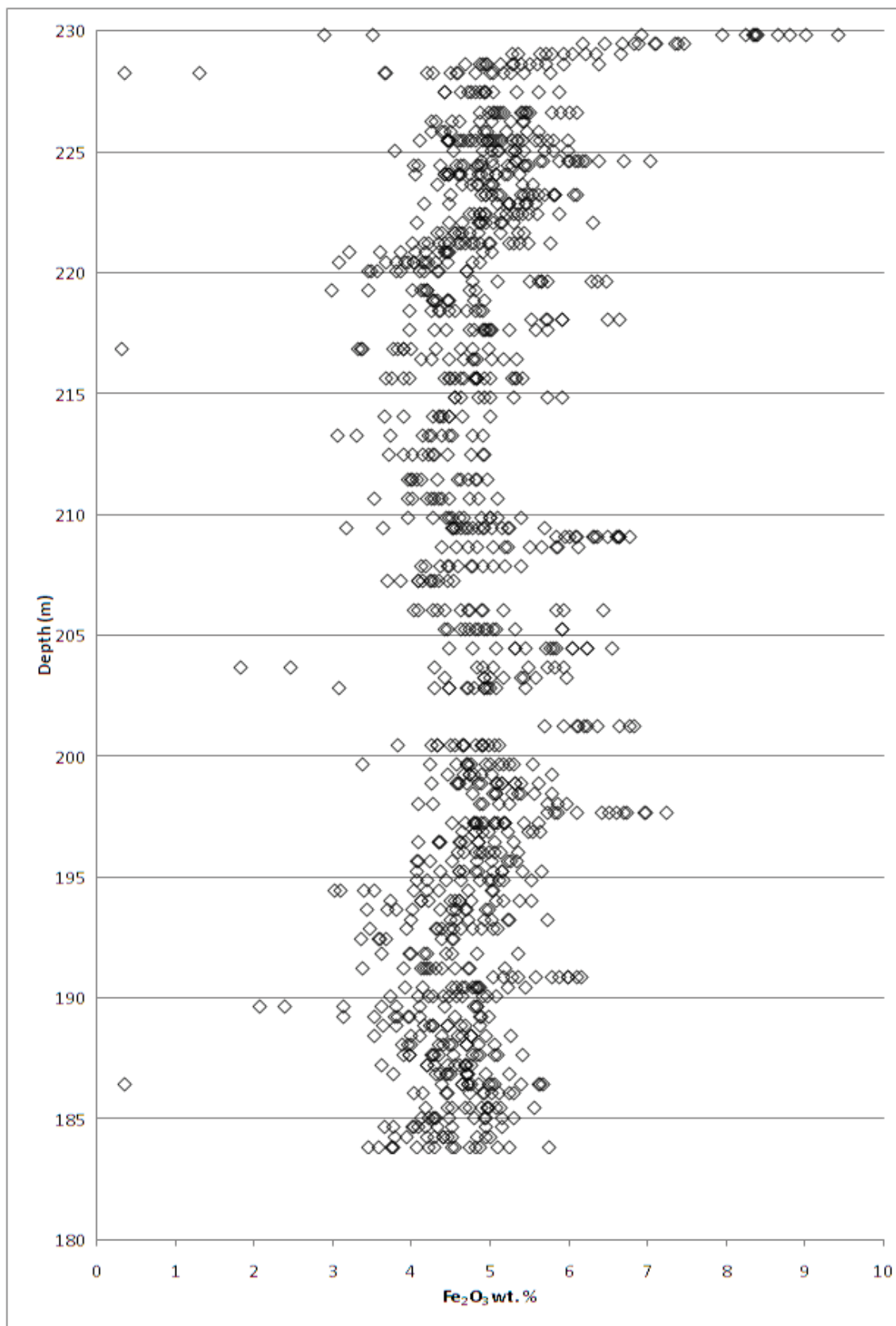


Figure 5.60. Plot of Fe₂O₃ wt. % vs. depth (m) for Big Daddy DDH FW-08-19.

5.3.2.1 Black Label binary chromite chemistry

The Black Label chromites show interesting trends in terms of wt. % Cr₂O₃ vs. wt. % MgO. Within DDH BT-09-31, two separate chromitite intervals are delineated as Layer 1 and Layer 2 (Figs. 5.61 to 5.62). Overall, there is a well defined positive correlation of increasing wt. % Cr₂O₃ with increasing wt. % MgO. Layer 1 is the bottom chromitite horizon from 161 to 203 m and is characterized by both lower and higher trends of increasing wt. % Cr₂O₃ with wt. % MgO. Layer 1 overlaps Layer 2 on the higher trend since here it represents the primary cores of the more massive chromitites that show igneous evolution from high wt. % Cr₂O₃ and MgO to lower wt. % Cr₂O₃ and MgO. Although, Layer 1 also plots on the lower trend because there is more differentiation to lower wt. % Cr₂O₃ and wt. % MgO in the disseminated chromites of this sequence vs. the more primitive larger grains of the massive chromites.

A general observation of the Black Label chromites is that chromitites are not as high grade as that of Black Thor and Big Daddy. This is due to the amount of intercumulus pyroxene content in the ore that causes the chromites to be more silica-enriched than the more primitive Black Thor and Big Daddy chromites. In the lower left of the plot, a number of Cr-depleted ferrichromites have been detected that have low MgO and a drop in Cr₂O₃ compared to the other chromites. In contrast, Cr-enriched ferrichromites are plotted off the trend and contain abnormally high wt. % Cr₂O₃ but low wt. % MgO.

There are several paths for chromite evolution as the primary grains undergo diffusion at their margins and in turn contain alteration replacement rims with retrogression. One path is from Layer 1 (chromite evolution 1). First the chromite crystallized out of the melt to form the primary core composition. With diffusion towards the margin, Mg and Cr contents are leached and exchanged with surrounding silicate. In turn, the chromite is retrogressed to a very MgO and Cr₂O₃-depleted ferrichromite at the rim. Another common example is that of chromite evolution 2 where an original chromite grain undergoes silicate exchange/diffusion at the margin thereby leaching both Cr and Mg components, but gaining Al and Fe components. Another path that could happen involves a chromite in Layer 2. A more primitive chromite is crystallized out of the melt. As it undergoes diffusion, Cr is again leached, but this time,

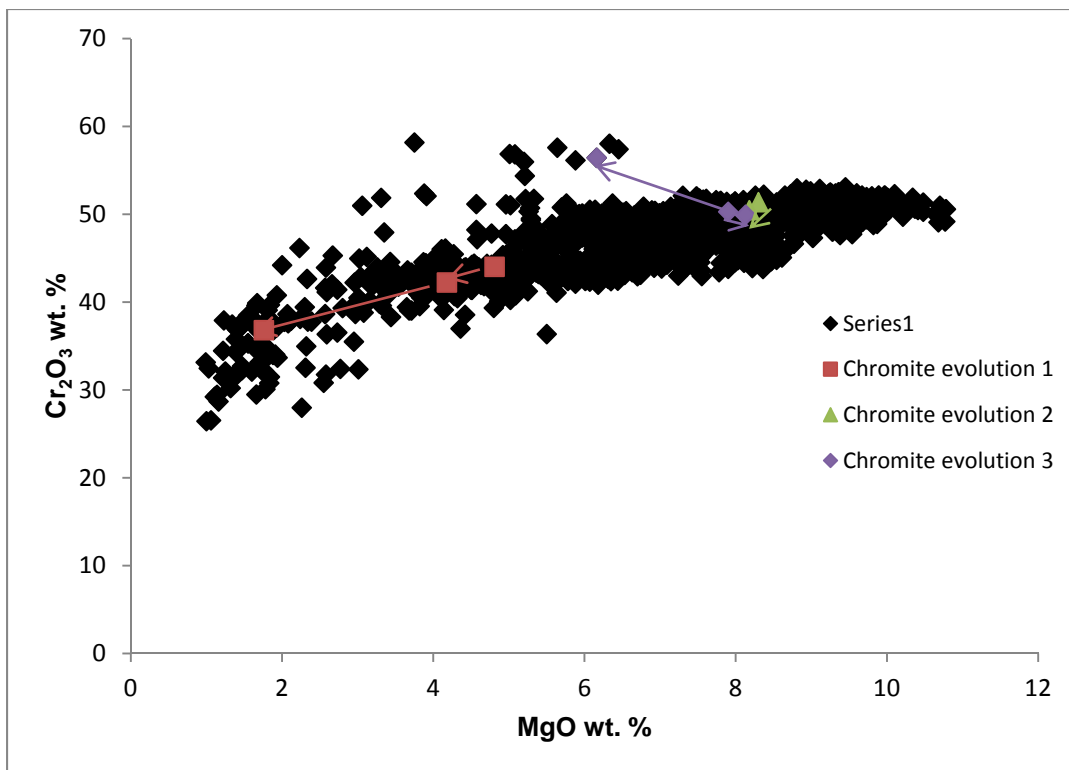


Figure 5.61. Binary plot of Cr_2O_3 vs. MgO wt. % for Black Label DDH BT-09-31 with paths of chromite evolution shown.

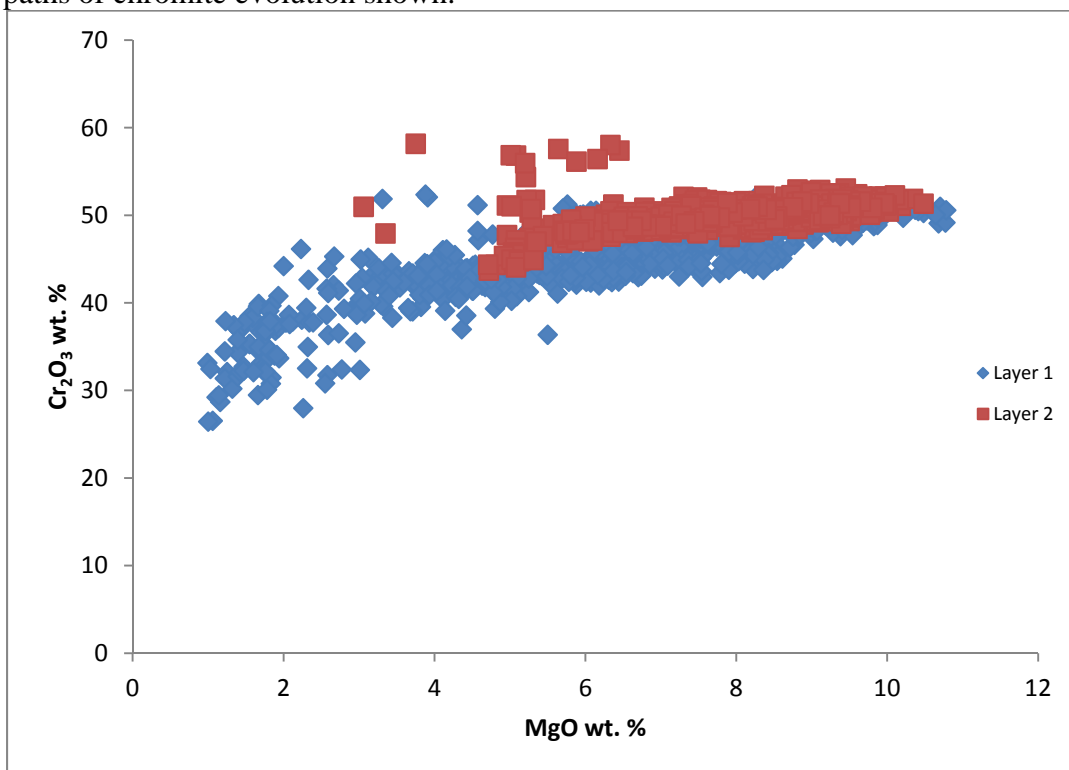


Figure 5.62. Black Label layers 1 and 2 of DDH BT-09-31. The primary, higher Cr_2O_3 and MgO cores of massive chromite from layer 1 are overlapped by the chromites of layer 2.

Mg is gained. Although there are sometimes increases in Mg and Al or sometimes even increases in Cr, the path mostly taken is that of diffusion to leach Cr and Mg and gain Al and Fe to eventually be replaced by ferrichromite. So this grain is eventually replaced by a Cr-enriched and high ferric iron-bearing ferrichromite as the last composition on the replacement rim.

For wt. % Al_2O_3 vs. wt. % MgO variation, wt. % Al_2O_3 is not well correlated with wt. MgO, but more or less shows a constant composition for the primitive chromite compositions as seen by the overlap of Layers 1 and 2 at lower wt. % Al_2O_3 and higher wt. % MgO (Fig. 5.63). In Layer 1, many of the more disseminated chromites contain higher wt. % Al_2O_3 reflective of silicate exchange with interstitial pyroxene. There is a well defined positive correlation in the transition of the chromites to Cr-enriched to Cr-depleted ferrichromites. With increasing Fe_2O_3 , there is a great decrease in wt. % Al_2O_3 with substitution. Therefore, the Cr-enriched to Cr-depleted ferrichromites show a substantial decrease in wt. % Al_2O_3 .

FeO shows a well defined correlation antipathetic to MgO (Fig. 5.64). With both diffusion and differentiation of the primary chromites, there is an increase in wt. % FeO from core to margin to Cr-enriched or Cr-depleted ferrichromite and from massive to disseminated chromites that have undergone more silicate exchange.

A Binary plot of wt. % TiO_2 vs. wt. % Fe_2O_3 demonstrates the behaviour of Fe vs. Ti in the Fe-Ti trend (Fig. 5.65). Most of the samples plot as a cluster with low wt. % TiO_2 at low wt. % Fe_2O_3 . With fractionation of olivine or pyroxene from the magma, the Fe/Mg ratio and Ti contents of the melt increase so there is enrichment of these elements in the more differentiated chromites (Barnes and Roeder, 2001). The trend is then accentuated by the reaction of the chromites with the intercumulus magma to produce the high TiO_2 -bearing Cr-depleted ferrichromites (Barnes and Roeder, 2001). With continuation toward magnetite, the wt. % TiO_2 contents decrease again at the highest wt. % Fe_2O_3 . This trend is common to chromites of MORB basalts and also stratiform layered intrusion chromitites.

For binary plots of metals, wt. % TiO_2 shows a subtle negative correlation with increasing wt. % Cr_2O_3 since there is more wt. % TiO_2 in the differentiated chromites (Fig. 5.66). There is a large increase in wt. % TiO_2 toward the Cr-depleted

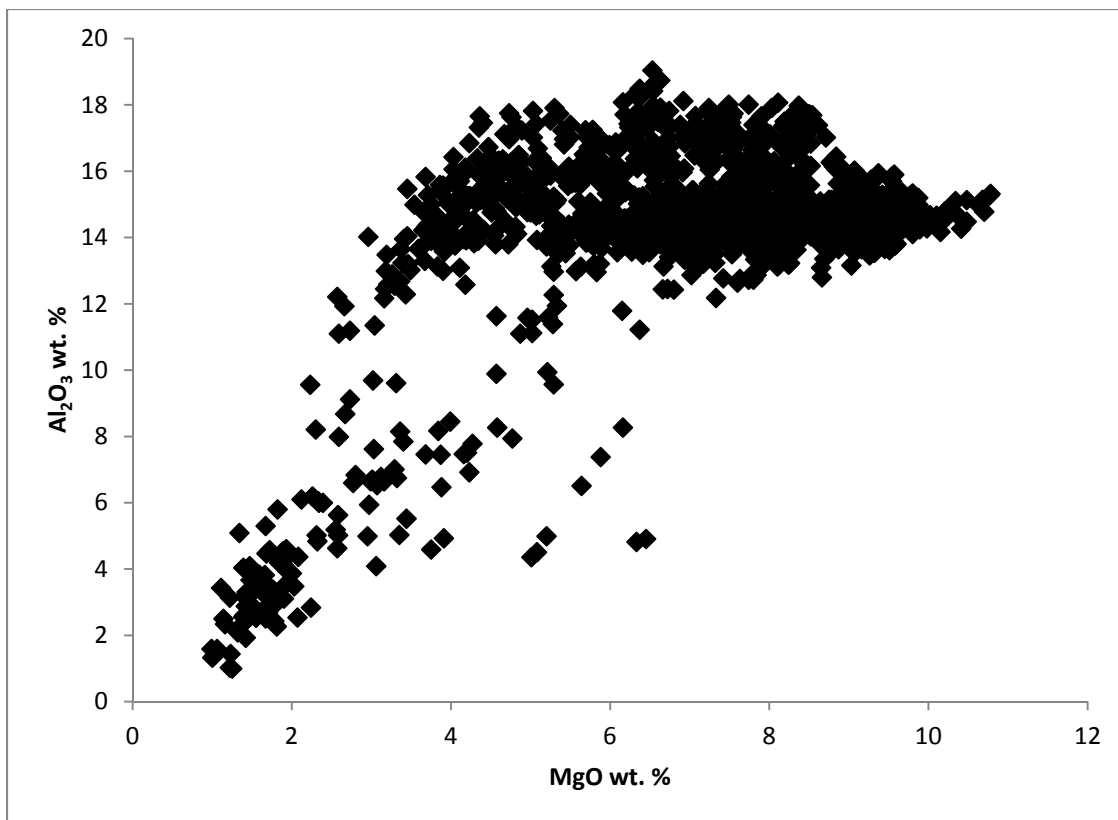


Figure 5.63. Binary plot of Al₂O₃ vs. MgO wt. % for Black Label DDH BT-09-31.

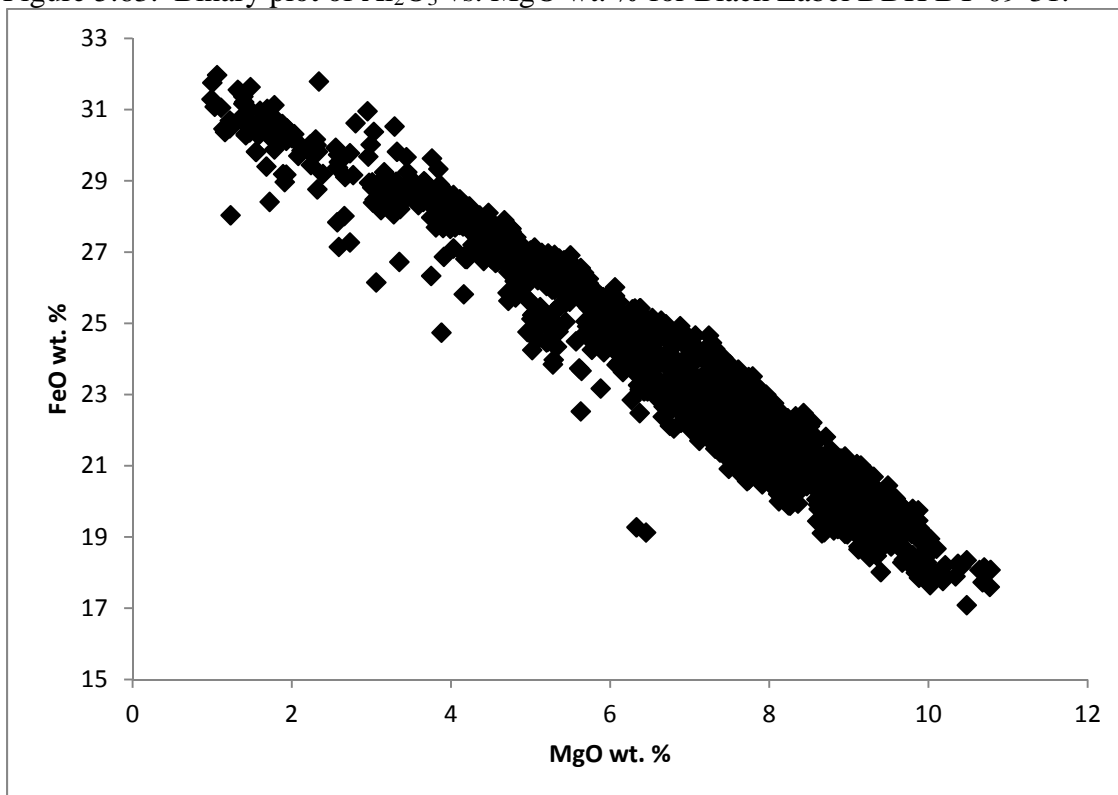


Figure 5.64. Binary plot of FeO vs. MgO wt. % for Black Label DDH BT-09-31.

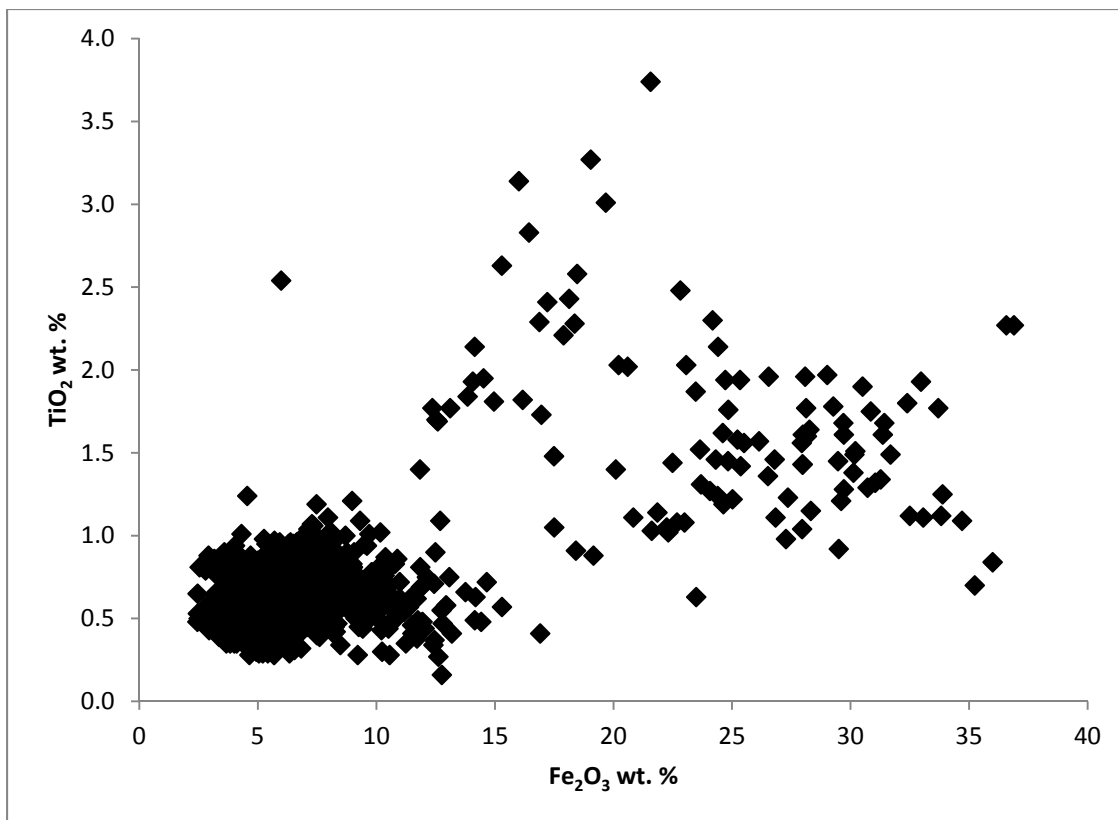


Figure 5.65. Binary plot of TiO_2 vs. Fe_2O_3 wt. % for Black Label DDH BT-09-31.

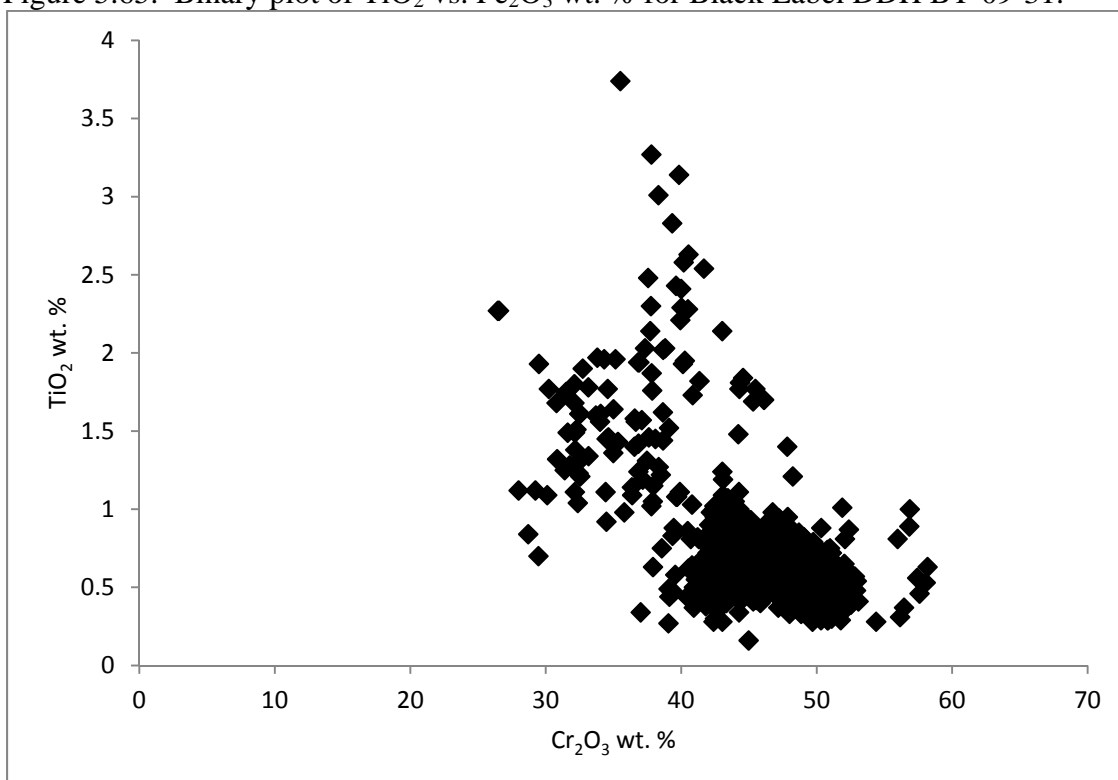


Figure 5.66. Binary plot of TiO_2 vs. Cr_2O_3 wt. % for Black Label DDH BT-09-31.

ferrichromites. For wt. % TiO_2 vs. wt. % FeO , there is a well defined igneous fractionation trend of increasing wt. % TiO_2 with wt. % FeO (Fig. 5.67). Above this trend are TiO_2 -enriched Cr-depleted ferrichromites that have high wt. % FeO . For wt. % ZnO vs. wt. % Cr_2O_3 , the chromites are separated into clusters for Layers 1 and 2 (Fig. 5.68). Layer 1 overlaps the higher and lower wt. % ZnO clusters at low and high wt. % Cr_2O_3 respectively, while Layer 2 overlaps the lower wt. % ZnO at higher wt. % Cr_2O_3 . The decrease in wt. % ZnO with increasing wt. % Cr_2O_3 is due increase in ZnO with differentiation. For wt. % NiO vs. wt. % Cr_2O_3 , NiO correlates with Cr_2O_3 in two layers (Fig. 5.69). Layer 1 has lower wt. % NiO at lower wt. % Cr_2O_3 than Layer 2.

5.3.2.2 *Black Thor BT-08-10 binary chromite chemistry*

Black Thor DDH BT-08-10 displays similar variation to Black Label, with more Cr-enriched ferrichromites analysed along with Cr-depleted ferrichromites. On a wt. % Cr_2O_3 vs. wt. % MgO diagram, there is a well defined correlation of wt. % Cr_2O_3 with MgO from the primitive to the differentiated chromites (Fig. 5.70). Typical paths of chromite evolution are displayed similar to Black Label. The Cr-depleted ferrichromites plot off the trend at lower wt. % Cr_2O_3 and wt. % MgO and the ferrichromites plot off the trend with high wt. % Cr_2O_3 at lower wt. % MgO . The Black Thor chromites are the most primitive with compositions reaching 54 wt. % Cr_2O_3 and 12 wt. % MgO which are even higher than Layer 2 of Black Label. Although primitive, there is still variation from massive to disseminate chromites that characterize the igneous evolution of other stratiform layered intrusions such as the Great Dyke (Wilson, 1982).

For wt. % Al_2O_3 vs. wt. % MgO , Black Thor shows the same trends as Black Label with a constant Al_2O_3 composition for the primitive chromites and diffusing to higher wt. % Al_2O_3 at the margins (Fig. 5.71). The Cr-enriched to Cr-depleted ferrichromites plot on a well defined trend of decreasing Al with substitution of Fe^{3+} . For wt. % FeO vs. wt. % MgO , there is a well defined negative correlation with substitution from the massive to disseminated chromites. Notably, the wt. % FeO contents are lower in Black Thor than Black Label (Fig. 5.72).

For binary plots of metals, wt. % TiO_2 shows a subtle negative correlation with wt. % Cr_2O_3 (Fig. 5.73). The TiO_2 compositions of Black Thor are lower than Black Label. Also displayed are the high TiO_2 Cr-depleted ferrichromites at low wt. % Cr_2O_3

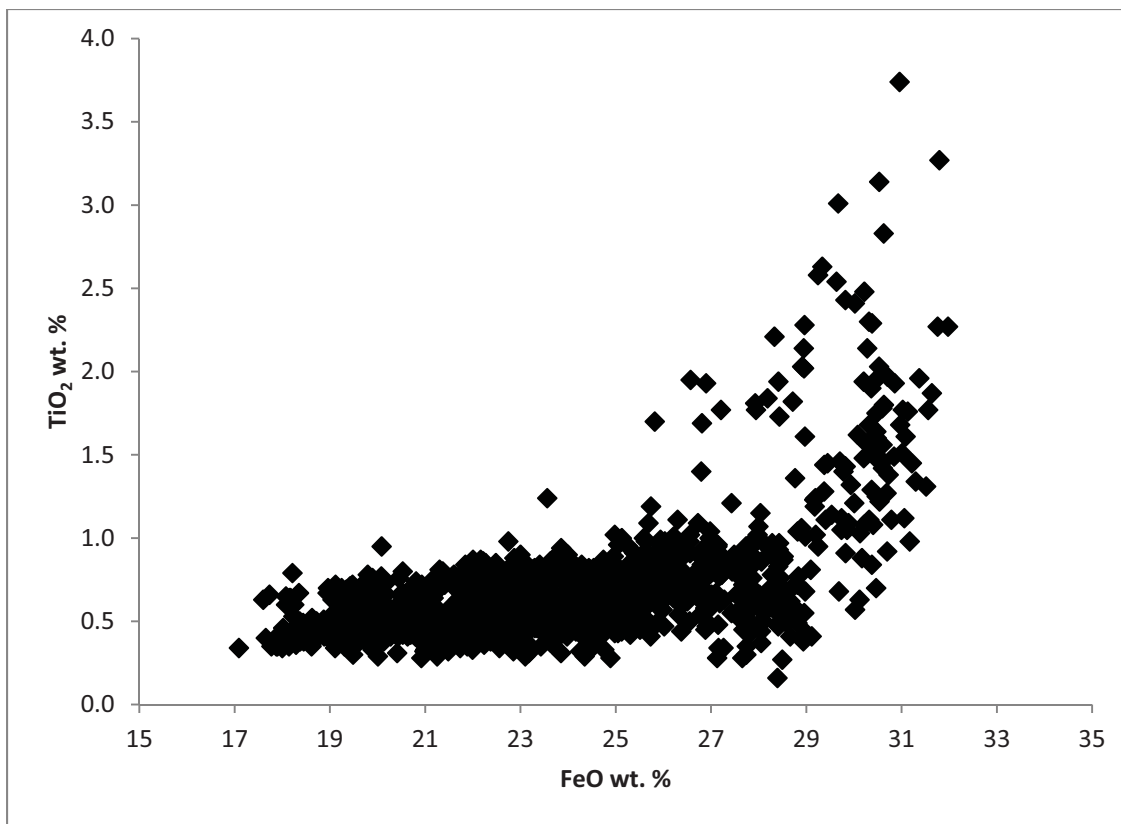


Figure 5.67. Binary plot of TiO₂ vs. FeO wt. % for Black Label DDH BT-09-31.

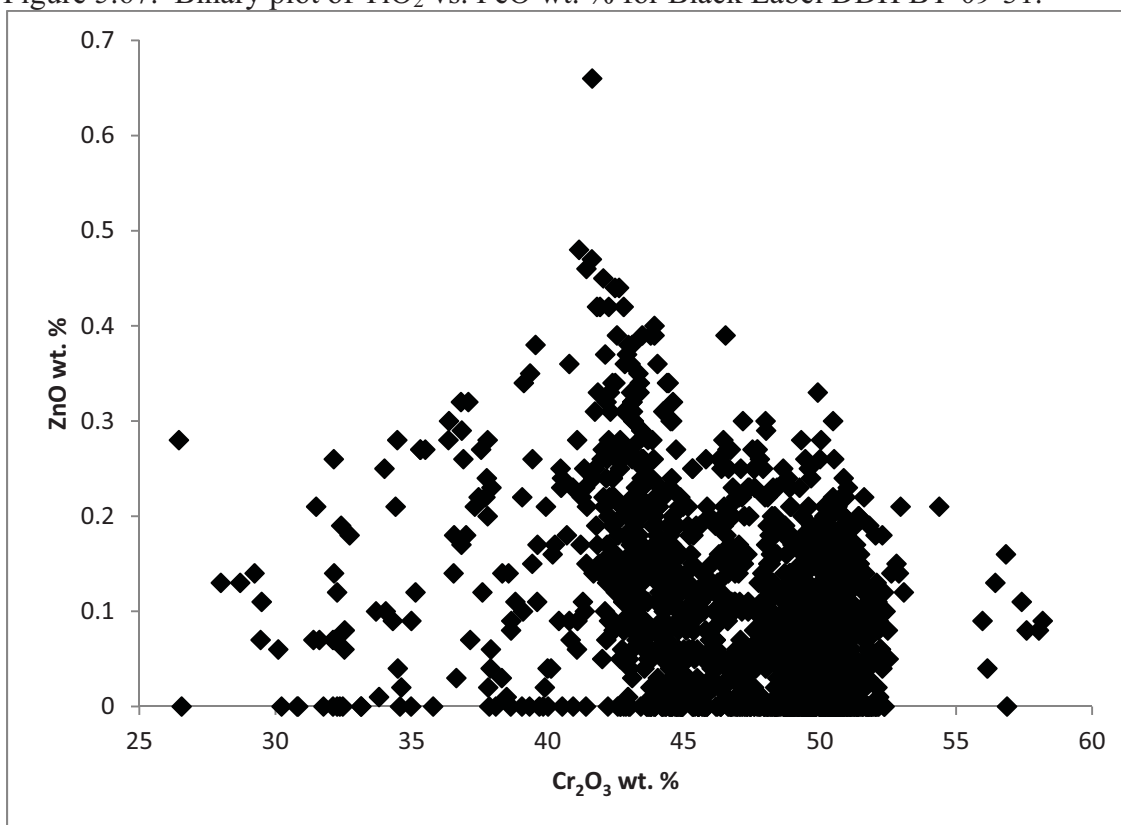


Figure 5.68. Binary plot of ZnO vs. Cr₂O₃ wt. % for Black Label DDH BT-09-31.

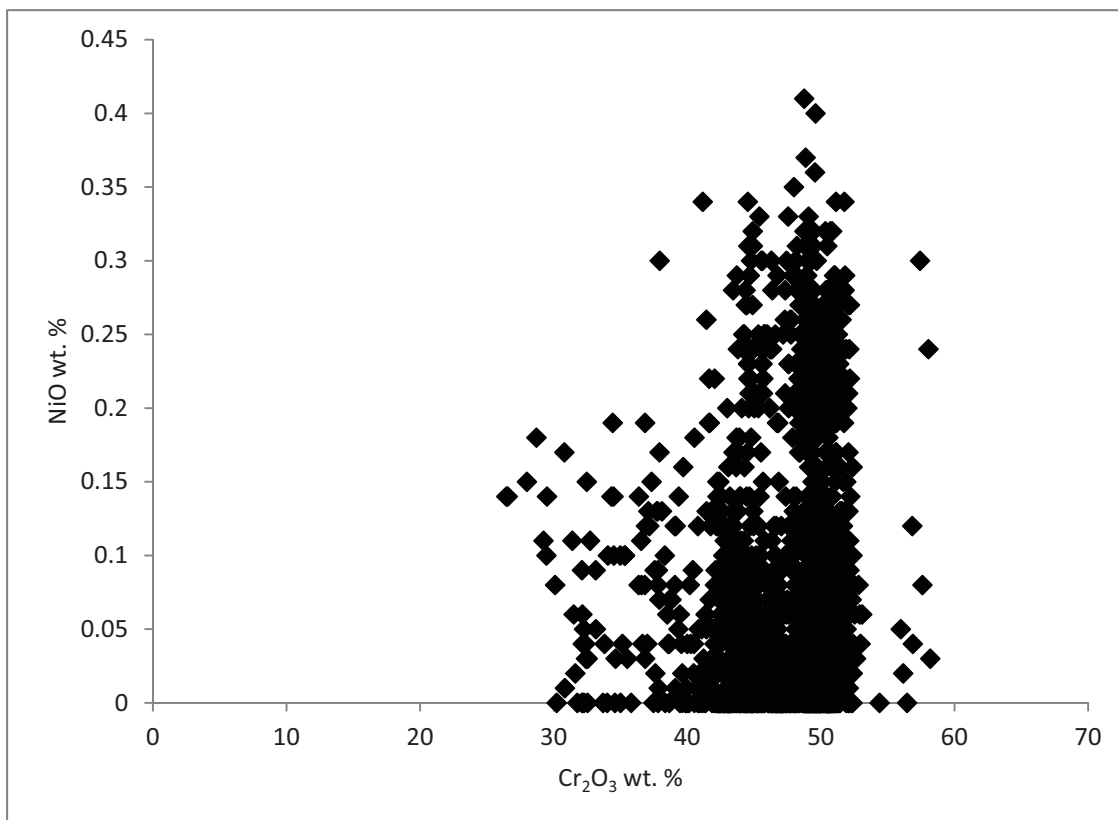


Figure 5.69. Binary plot of NiO vs. Cr₂O₃ wt. % for Black Label DDH BT-09-31.

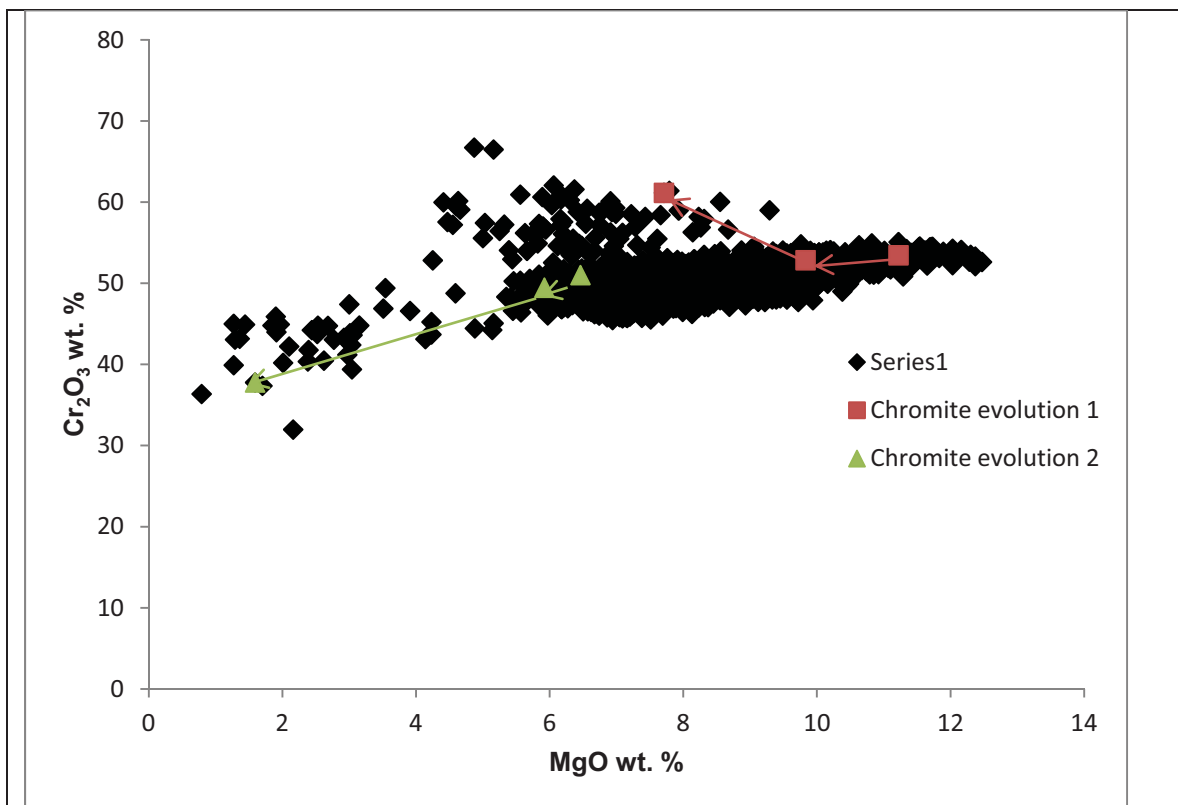


Figure 5.70. Binary plot of Cr_2O_3 vs. MgO wt. % for Black Thor DDH BT-08-10 with paths of chromite evolution shown.

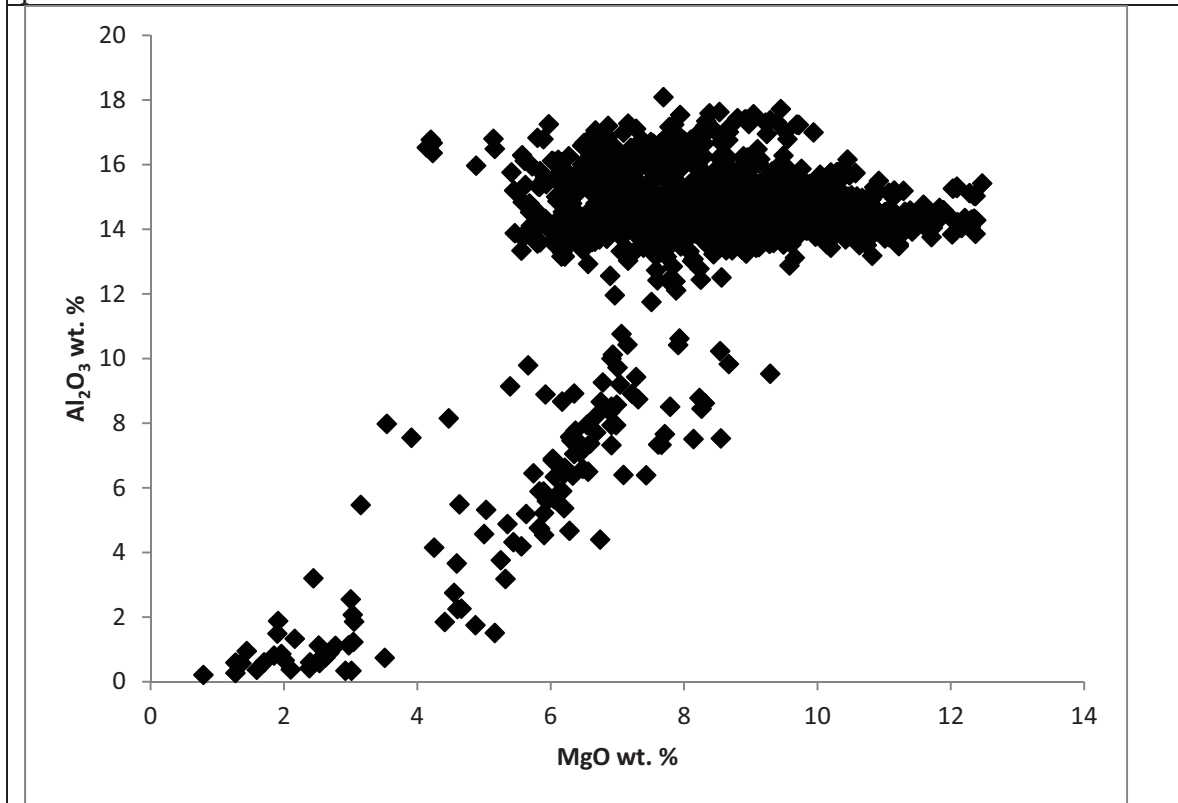


Figure 5.71. Binary plot of Al_2O_3 vs. MgO wt. % for Black Thor DDH BT-08-10.

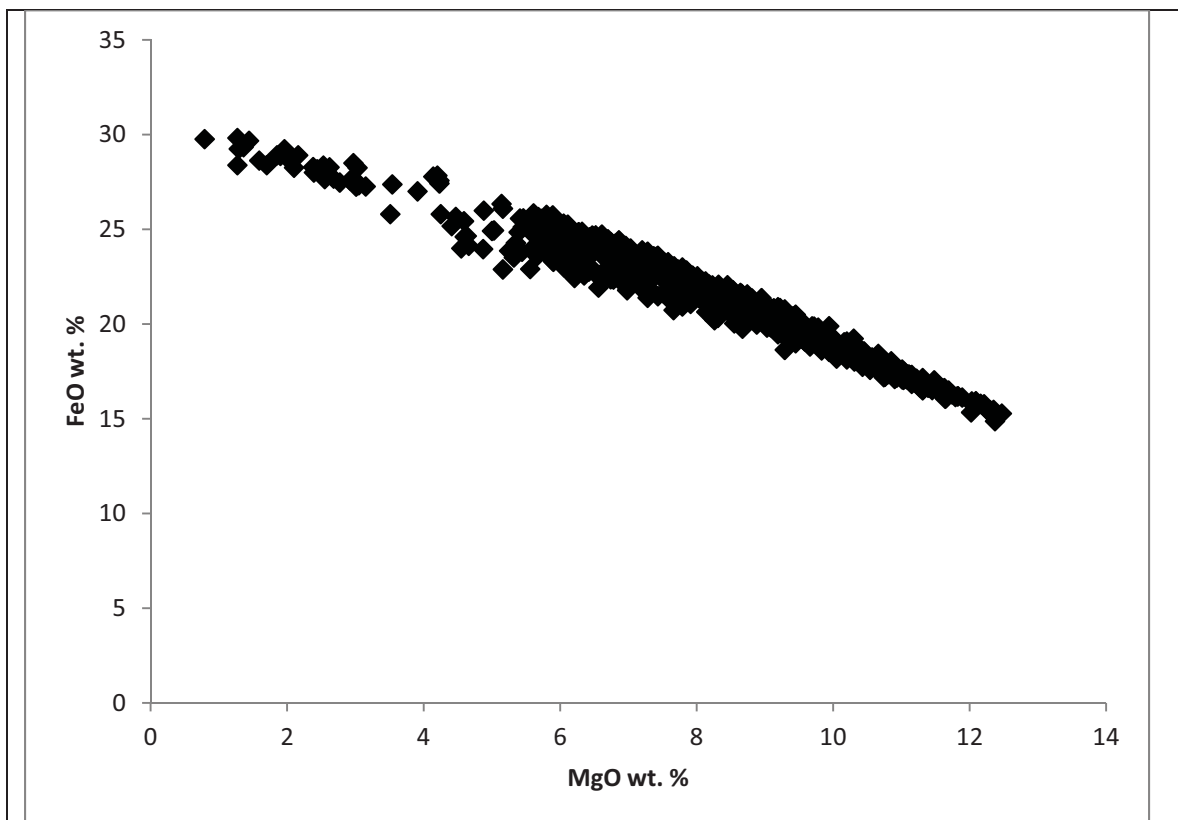


Figure 5.72. Binary plot of FeO vs. MgO wt. % for Black Thor DDH BT-08-10.

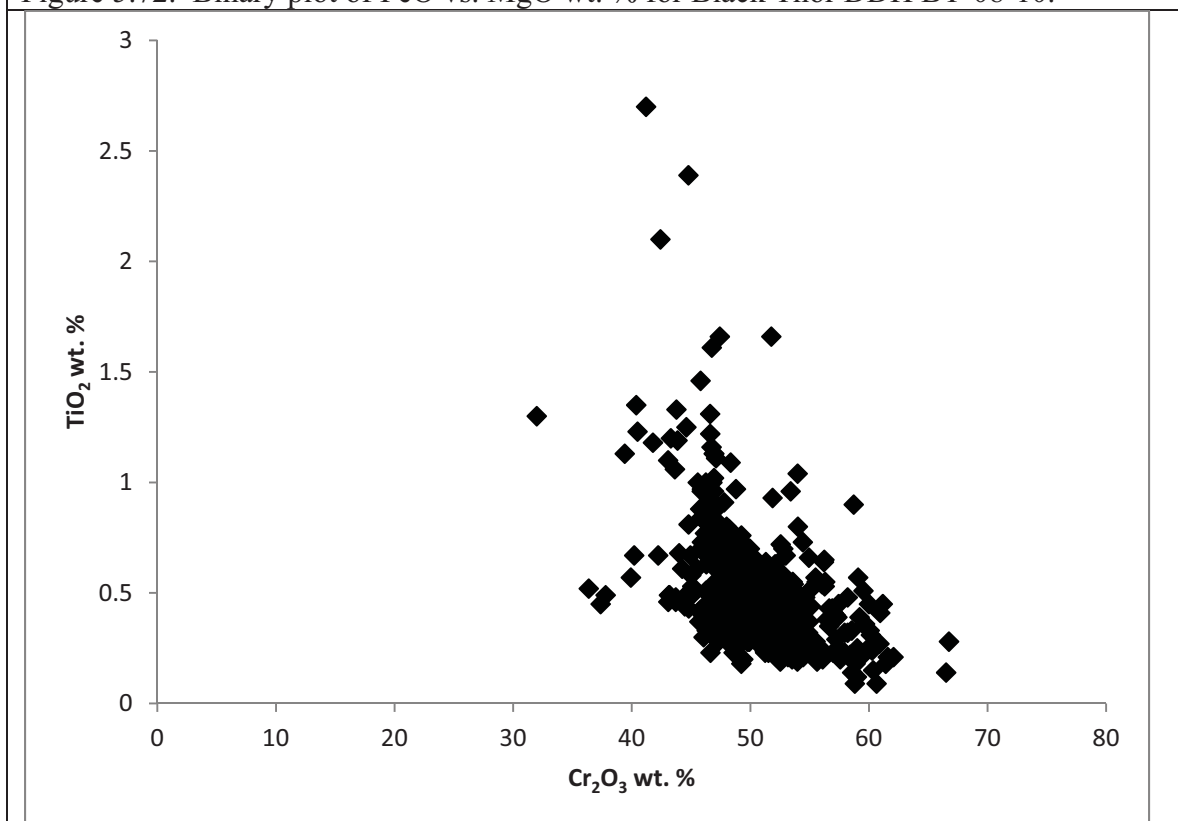


Figure 5.73. Binary plot of TiO₂ vs. Cr₂O₃ wt. % for Black Thor DDH BT-08-10.

and the low TiO_2 ferrichromites at high wt. % Cr_2O_3 . Wt. % ZnO increases with decreased wt. % Cr_2O_3 due to differentiation (Fig. 5.74). The ZnO contents are lower than ZnO of Layer 1 in Black Label. The NiO contents of Black Thor are noticeably lower than Black Label for both layers of Black Label (Fig. 5.75). Wt. % MnO shows a slight negative correlation with wt. % Cr_2O_3 . This is due to MnO increasing with differentiation (Fig. 5.76).

5.3.2.3 Black Thor BT-09-17 binary chromite chemistry

The upper chromitite of DDH BT-09-17 show similar binary variation of major oxides as the other chromite deposits but contains trends of chromite enrichment rather than depletion due to retrogression. On a wt. % Cr_2O_3 vs. wt. % MgO diagram, there is increased wt. % Cr_2O_3 with wt. % MgO similar to the other deposits, only the chromites evolve in the direction from lower to higher wt. % Cr_2O_3 and wt. % MgO with retrogression (Fig. 5.77). This can be seen in the chromite evolution 1 trend on the diagram where core to margin compositions increase from 51.70 to 52.21 wt. % Cr_2O_3 in one of the grains. The later alteration rims of the chromites have even higher wt. % Cr_2O_3 compared to the Cr-enriched ferrichromites in the other deposits. Chromites enrich to as high as 68.03 wt. % Cr_2O_3 . Notably, there are two separated chromite composition clusters on the diagram. Most of the chromites contain more primitive and higher wt. % Cr_2O_3 and wt. % MgO while the lower compositions are from more evolved chromites higher up in the second chromitite interval in the drill hole.

For wt. % Al_2O_3 vs. wt. % MgO variation, there are trends of increasing wt. % Al_2O_3 with wt. % MgO from the cores to rims due to retrogression (Fig. 5.78). Al_2O_3 compositions are higher compared to the other chromites of Black Thor DDH BT-08-10 to as high as 18.57 wt. % Al_2O_3 . This higher Al_2O_3 content is probably due to enrichment of Al_2O_3 with higher retrogression that overprints the primary chemistry. From primary chromite core to alteration rim, there is a well defined positive correlation of decreasing wt. % Al_2O_3 with decreasing wt. % MgO . This trend shows these rim chromites are behaving the same as Cr-enriched to Cr-depleted ferrichromites in the other deposits ie. Al is substituting with Cr. For wt. % FeO vs. wt. % MgO variation, there is a well defined negative correlation of wt. % FeO and MgO that is characteristic of all the

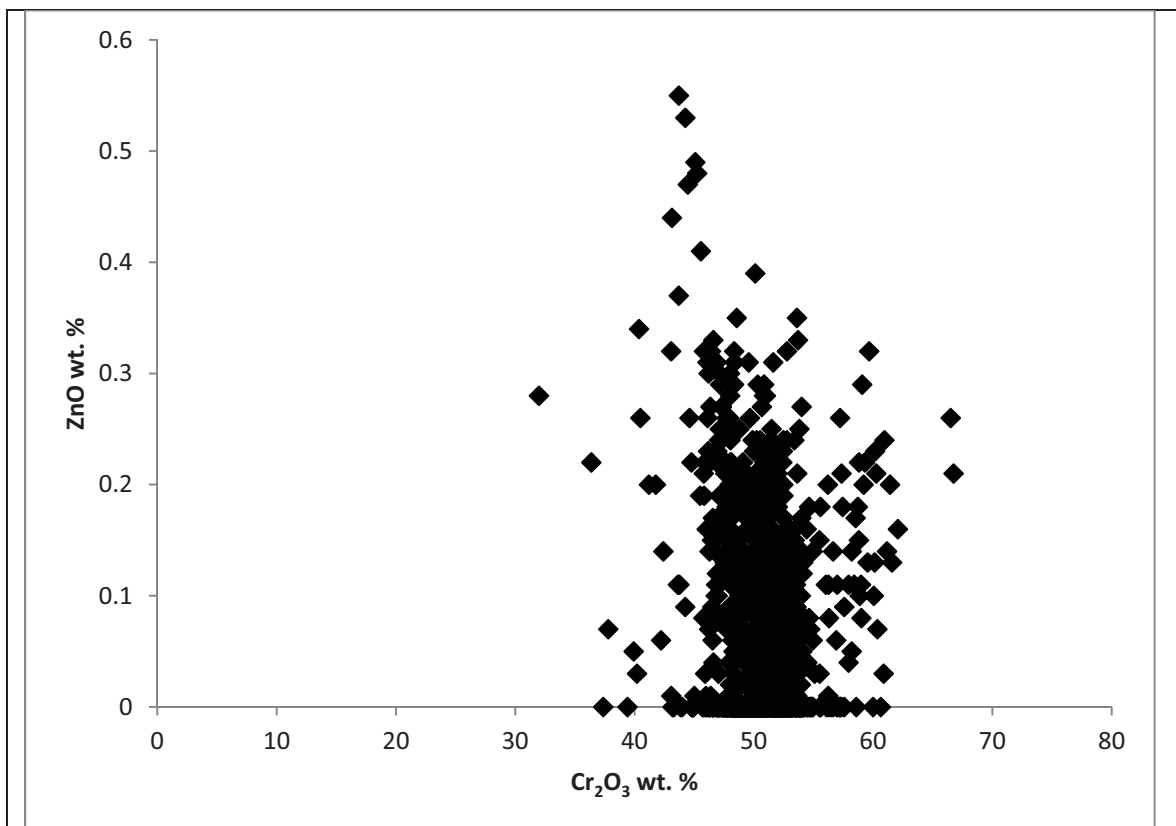


Figure 5.74. Binary plot of ZnO vs. Cr₂O₃ wt. % for Black Thor DDH BT-08-10.

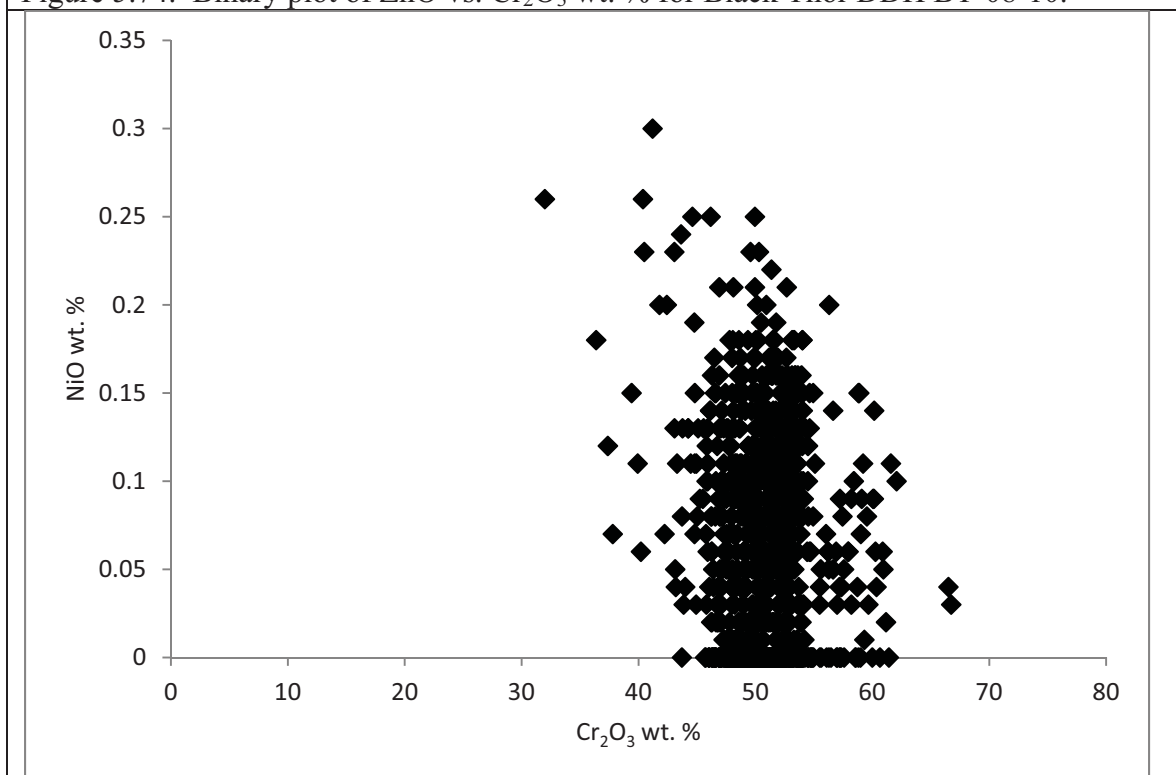


Figure 5.75. Binary plot of NiO vs. Cr₂O₃ wt. % for Black Thor DDH BT-08-10.

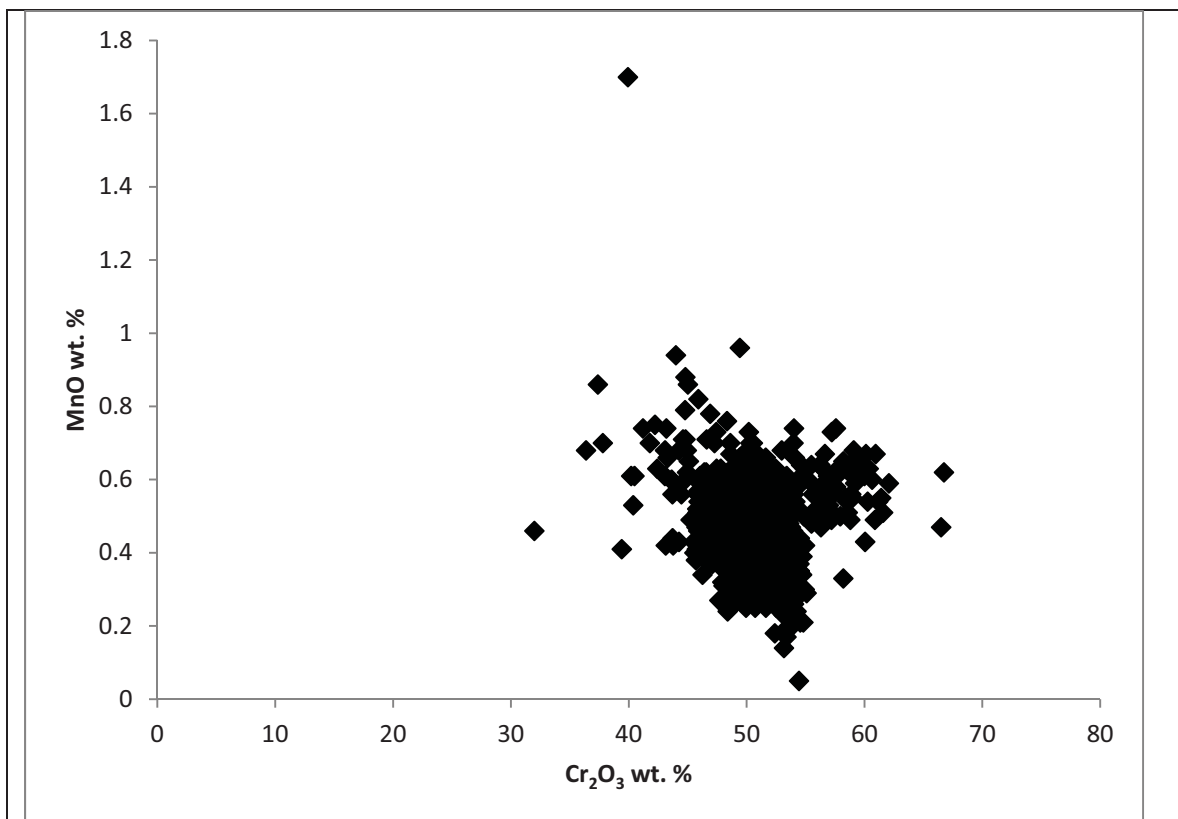


Figure 5.76. Binary plot of MnO vs. Cr₂O₃ wt. % for Black Thor DDH BT-08-10.

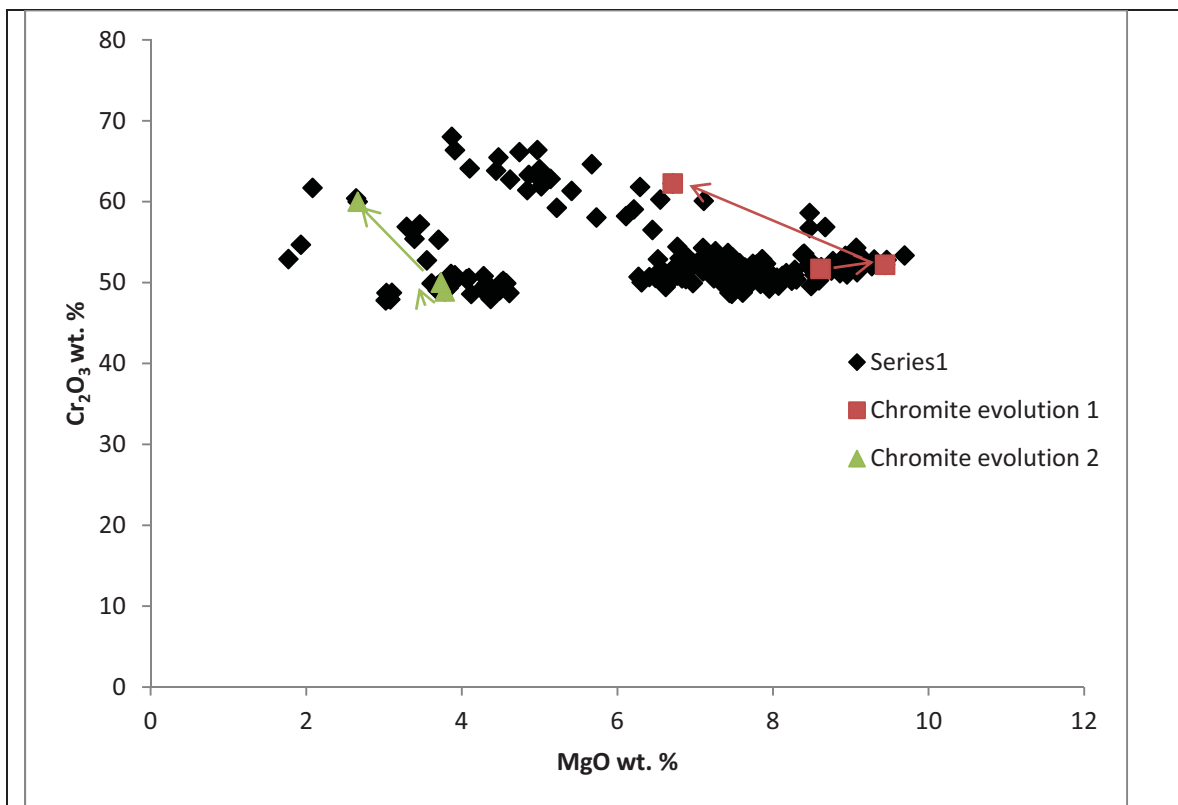


Figure 5.77. Binary plot of Cr_2O_3 vs. MgO wt. % for Black Thor DDH BT-09-17 with paths of chromite evolution shown.

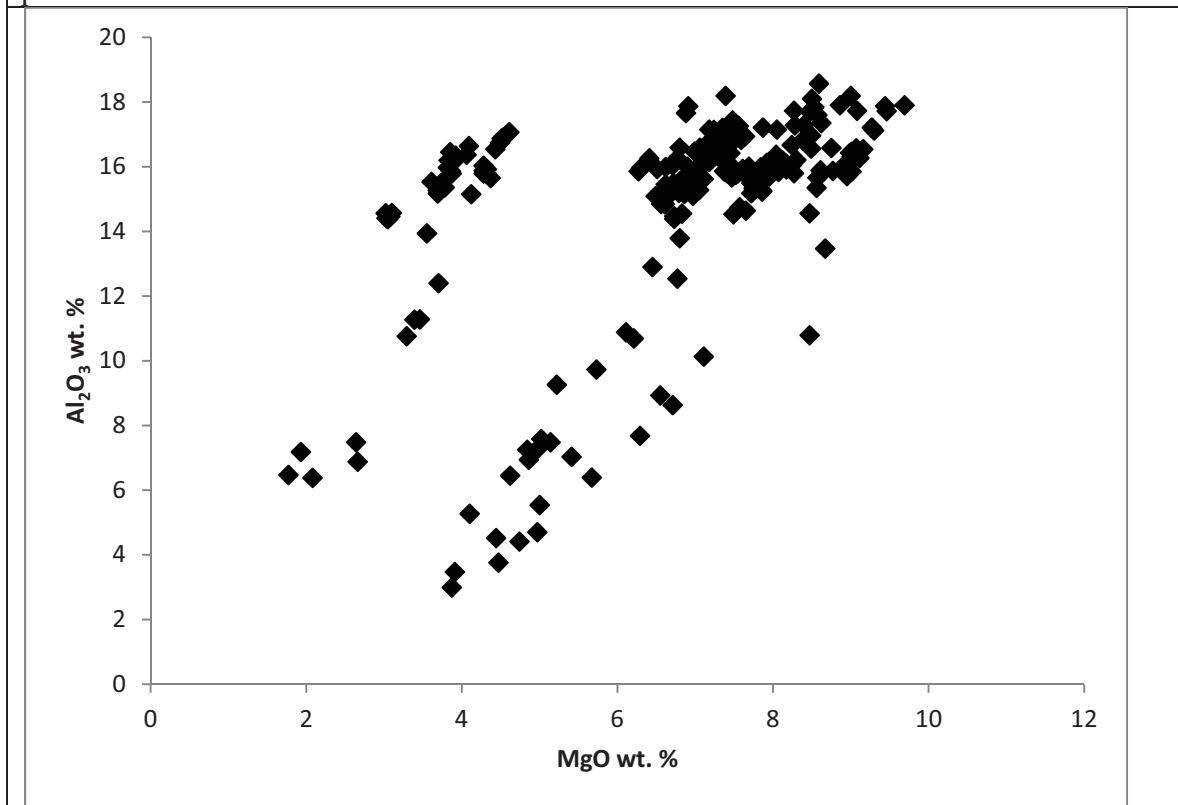


Figure 5.78. Binary plot of Al_2O_3 vs. MgO wt. % for Black Thor DDH BT-09-17.

deposits (Fig. 5.79). Notably, the alteration rim chromites are even more depleted in wt. % FeO and fall off the trend with decreasing wt. % MgO.

For other oxides, wt. % TiO₂ increases with decreasing wt. % Cr₂O₃ (Fig. 5.80). Therefore, wt. % TiO₂ does not increase with retrogression from core to margin in the chromites. ZnO is variable but also increases with decreasing wt. % Cr₂O₃ (Fig. 5.81). NiO is low in these chromites since the pyroxenites are not elevated in Ni ppm (Fig. 5.82). MnO increases with decreasing wt. % Cr₂O₃ like the other oxides (Fig. 5.83).

5.3.2.4 Big Daddy binary chromite chemistry

The Big Daddy chromites show relatively uniform compositions for major element and metals in contrast to the other deposits. For wt. % Cr₂O₃ vs. wt. % MgO variation, there is a positive linear correlation of increasing wt. % Cr₂O₃ with increasing wt. % MgO in the igneous chromites (Fig. 5.84). The lower wt. % MgO-bearing chromites have more scattered wt. % Cr₂O₃ contents than most of the chromites in the high MgO region. These chromites are from disseminated chromites hosted as minor cumulus phases in the dunites, heterogeneous pyroxenites and pyroxenites located below the main massive chromitite. The different contents of these chromites is due to differentiation in those pulses. Then from 7.33 to 11.68 wt. % MgO, there are chromites in the massive chromitite that plot on a well defined trend of increasing Cr₂O₃ with MgO. The slope of the trend is small compared to the other chromite deposits since there is not as much variation in the more complete convection cycles of these massive chromites. A few chromites plotting from 35 to 40 wt. % Cr₂O₃ are from the more retrogressed chromites in the pyroxenites. Also plotted are a few Cr-enriched ferrichromite with high wt. % Cr₂O₃ contents.

For wt. Al₂O₃ vs. wt. % MgO variation, most of the Al₂O₃ contents are constant with respect to wt. % MgO since there is little pyroxene to promote pyroxene-chromite substitution of Al₂O₃ (Fig. 5.85). The Al₂O₃ contents plot from 12 to 14 wt. % Al₂O₃ with lesser variation for the massive chromitite interval. The Al₂O₃ contents are lower than Black Label and Black Thor since there is less differentiation. Notably, wt. % Al₂O₃ does not plot above 16 wt. % Al₂O₃ as it does in the other deposits, even in the disseminated chromite. The disseminated and massive chromites have compositions from 11 to 15 wt. % Al₂O₃. However, Al₂O₃ is higher in the intermediate chromitite at

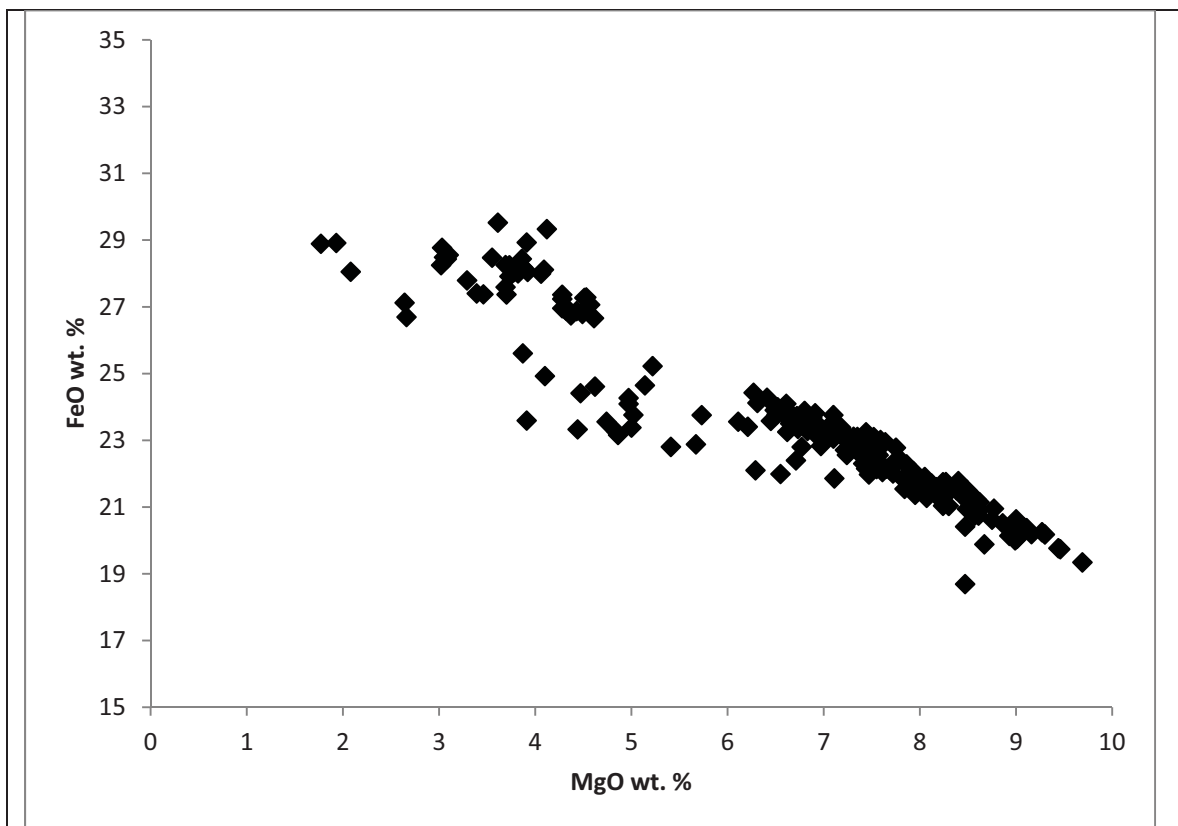


Figure 5.79. Binary plot of FeO vs. MgO wt. % for Black Thor DDH BT-09-17.

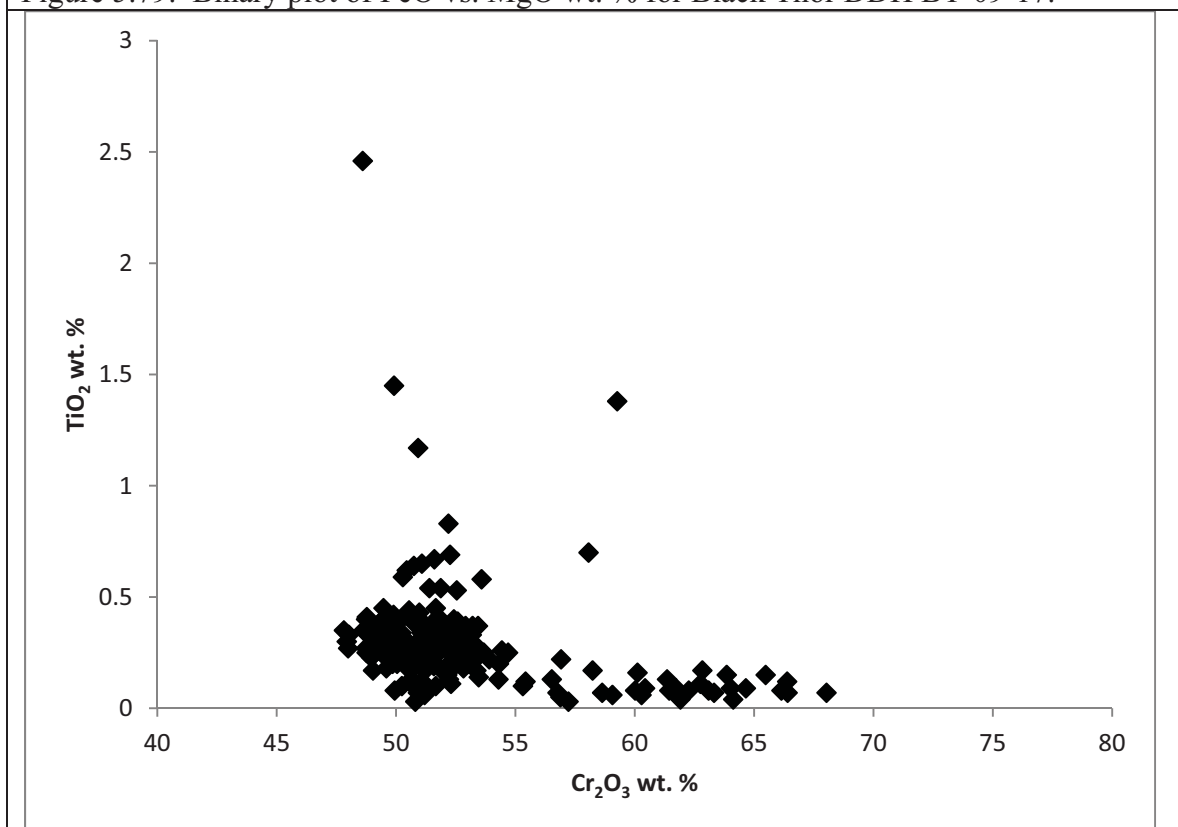


Figure 5.80. Binary plot of TiO₂ vs. Cr₂O₃ wt. % for Black Thor DDH BT-09-17.

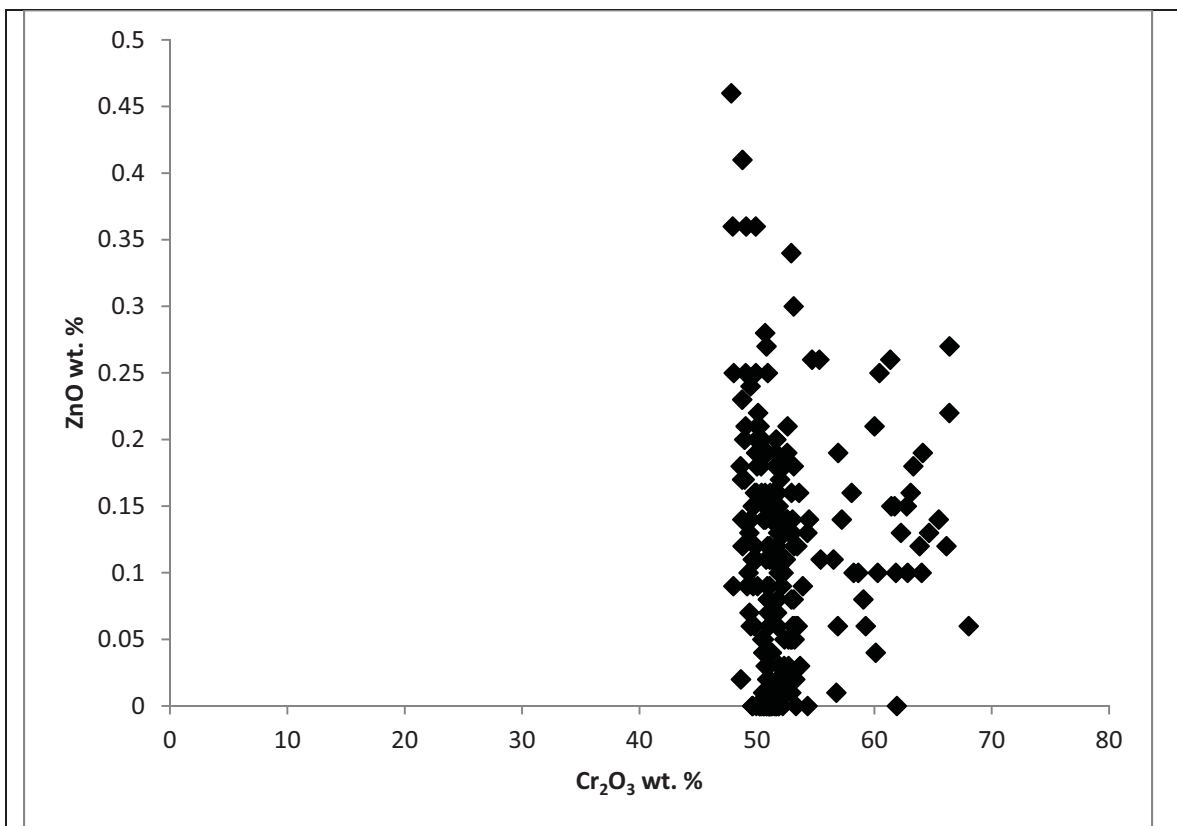


Figure 5.81. Binary plot of ZnO vs. Cr₂O₃ wt. % for Black Thor DDH BT-09-17.

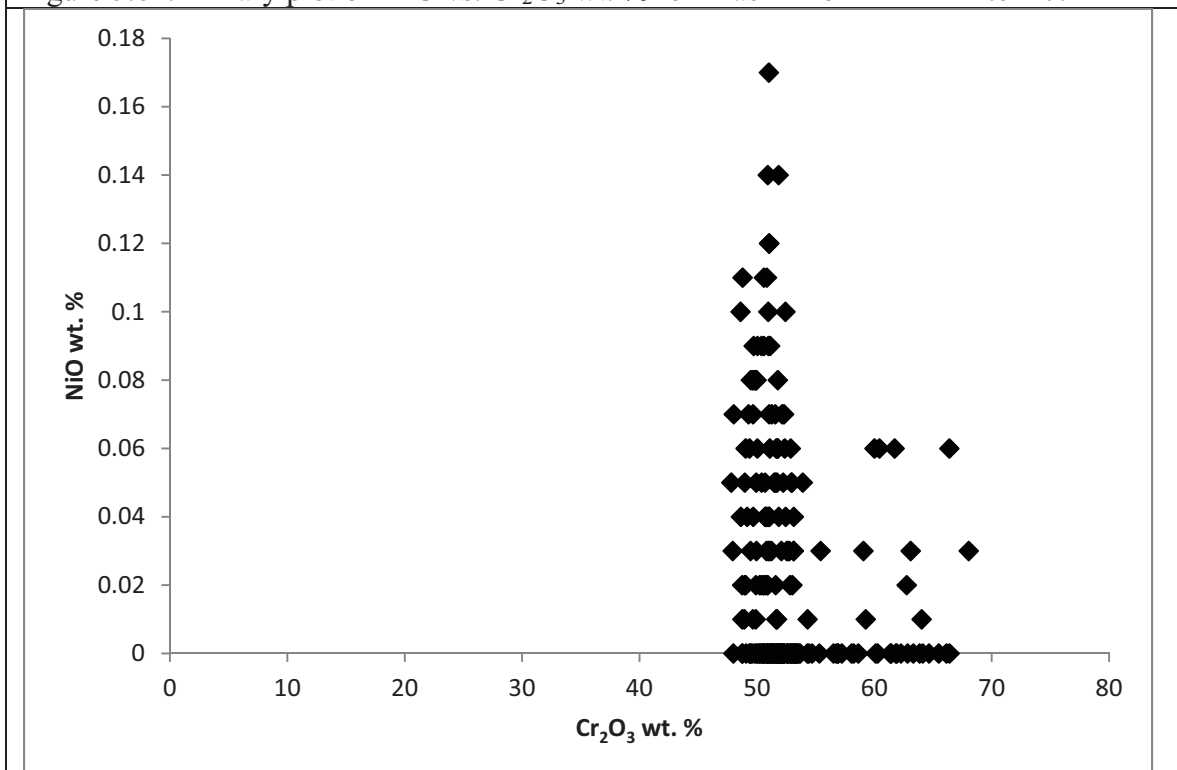
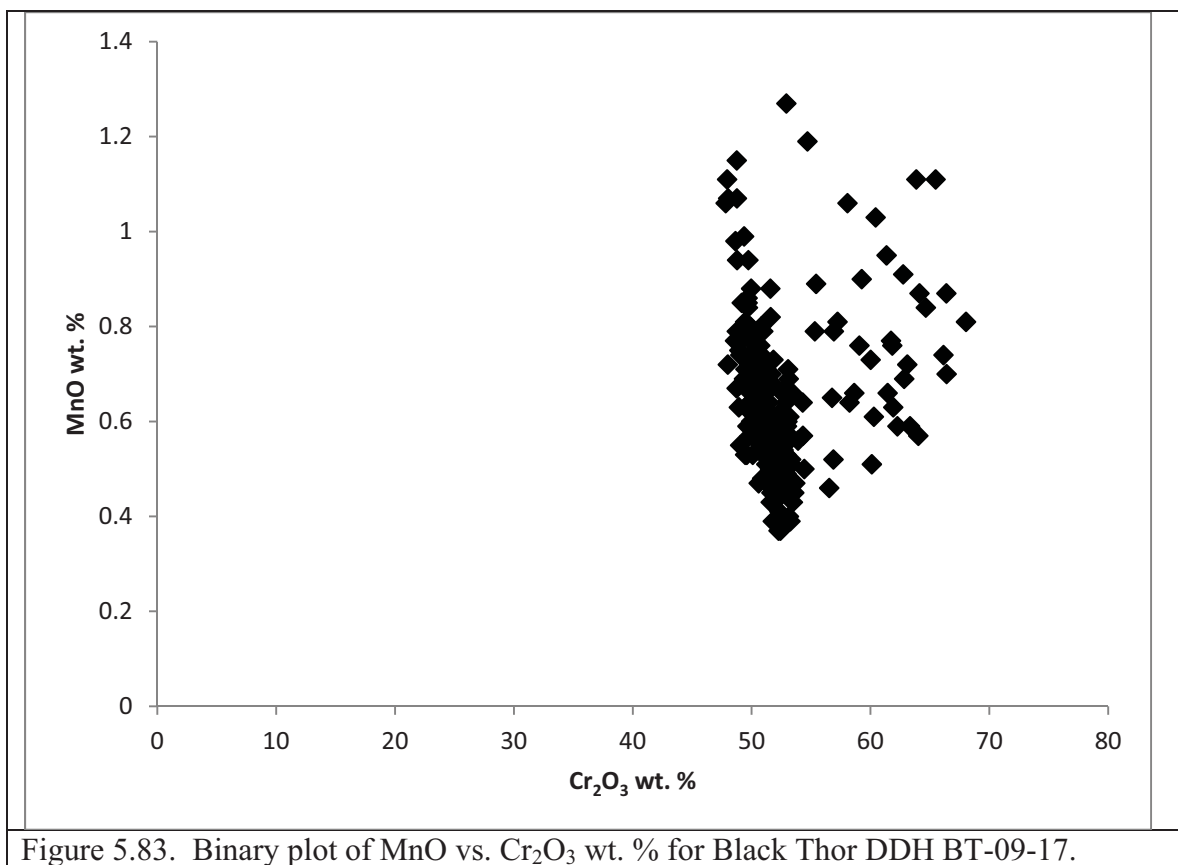


Figure 5.82. Binary plot of NiO vs. Cr₂O₃ wt. % for Black Thor DDH BT-09-17.



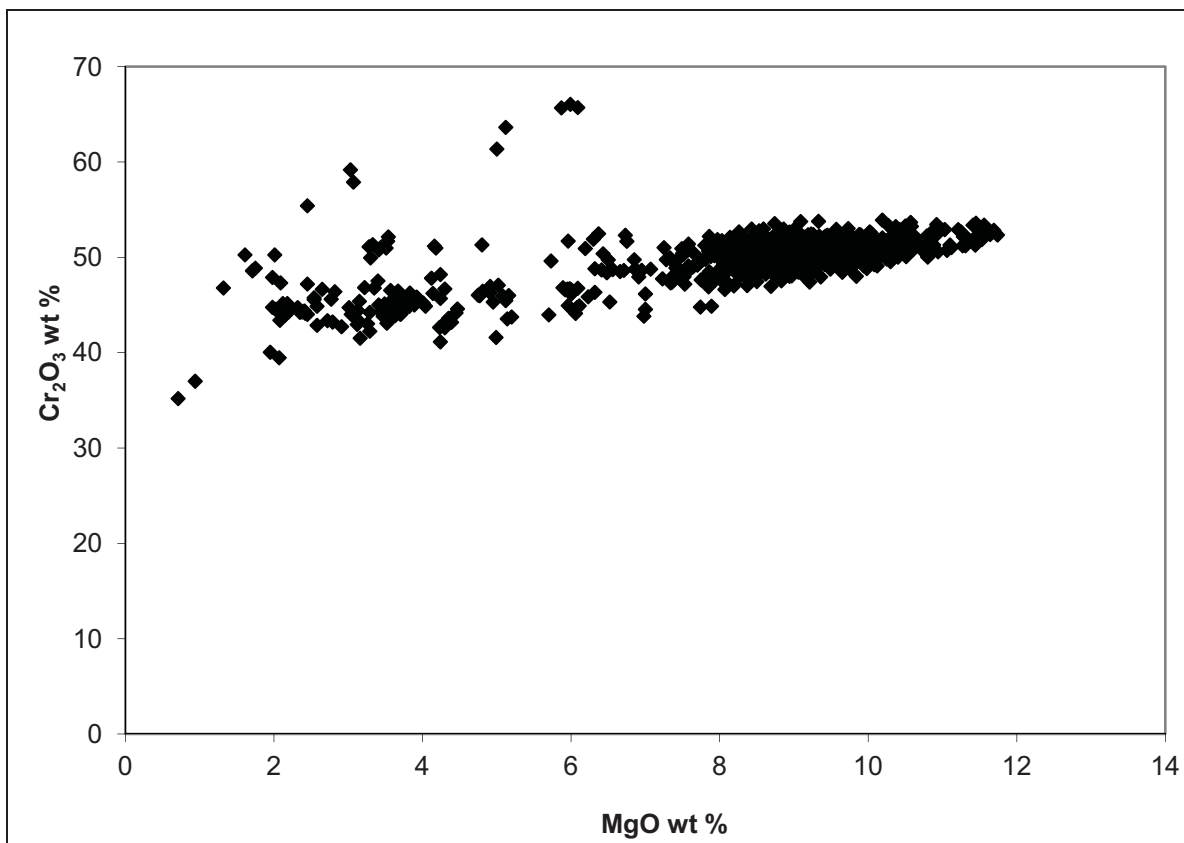


Figure 5.84. Binary plot of Cr₂O₃ vs. MgO wt. % for Big Daddy DDH FW-08-19.

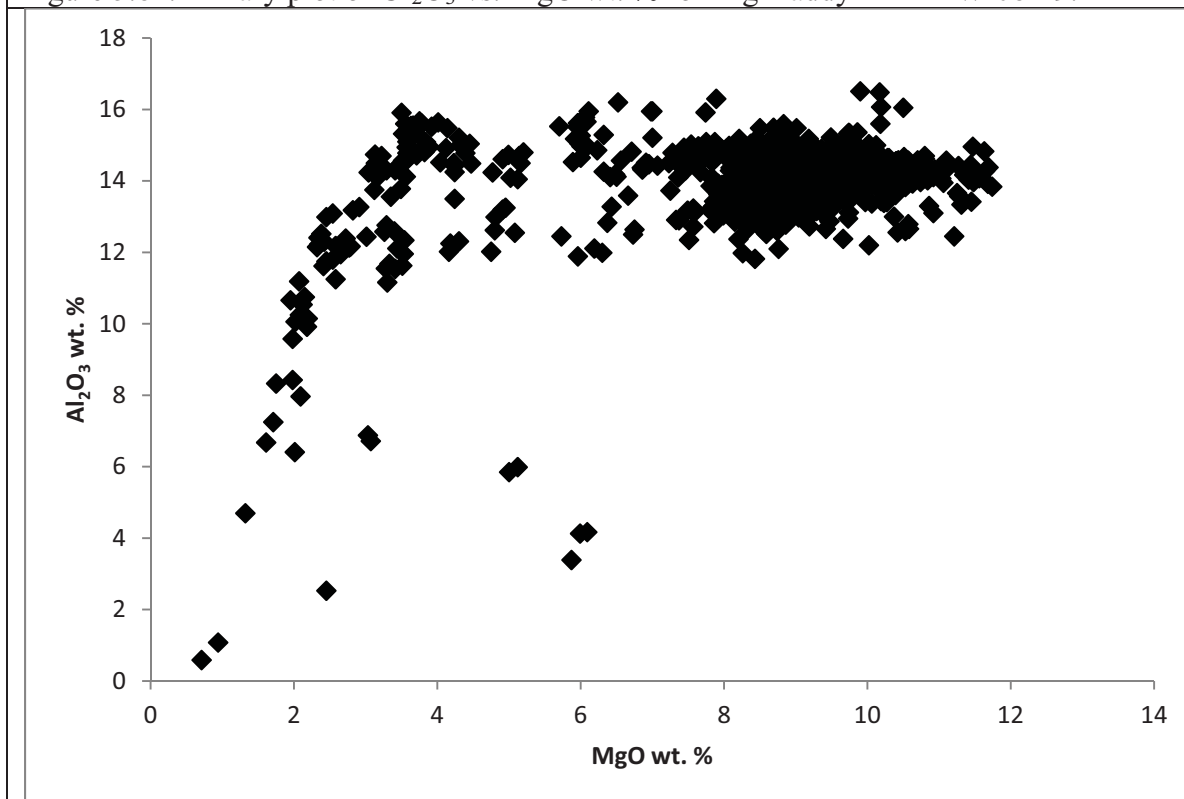


Figure 5.85. Binary plot of Al₂O₃ vs. MgO wt. % for Big Daddy DDH FW-08-19.

161.50 m depth. In the samples with more intermediate modal % chromite i.e. chromite ranging in between massive and disseminated chromite, the chromitites are hosted by heterogeneous pyroxenite and dunite. The chromitites probably mineralized in a magma driven toward more pyroxene stability rather than being constantly primitive due to repetitive replenishment of chromite pulses that are closer to olivine stability as in the massive chromitite interval. And the disseminated chromites primarily mineralized in cumulus olivine dunite sequences where there is less Al_2O_3 content. Notably, there is lower wt. % Al_2O_3 in the disseminated chromites while higher wt. % Al_2O_3 in the intermediate chromites of e.g. Black Thor which supports this observation.

For wt. % FeO vs. wt. % MgO, there is similar separation of disseminated vs. massive chromite regions that are visible in the wt. % Cr_2O_3 vs. wt. % MgO variation diagrams (Fig. 5.86). There is a general well defined trend of decreasing wt. % FeO with increasing wt. % MgO with substitution of the elements from more primitive to differentiated chromites. From 7.33 to 11.68 wt. % MgO, there is a large bunch of analyses with lower wt. % FeO that represent the massive chromites.

For binary plots of metals, there is a slight negative correlation of decreasing wt. % TiO_2 with increasing wt. % Cr_2O_3 with evolution of the chromites (Fig. 5.87). Higher wt. % TiO_2 samples represent evolved chromites of the disseminated chromite-bearing host lithologies located beneath the main zone. The negative correlation is also reflected in the wt. % ZnO vs. wt. % Cr_2O_3 (Fig. 5.88). The ZnO contents are elevated to 0.2 wt. % ZnO as in other deposits except for Layer 1 of Black Label. There are many samples of elevated ZnO above 0.2 wt. that reflect the more differentiated chromites in the host rocks below the main chromitite. The wt. % NiO vs. wt. % Cr_2O_3 shows a well defined correlation of increasing wt. % NiO with increasing wt. % Cr_2O_3 reflecting the igneous variation of the chromites (Fig. 5.89). NiO contents are high to 0.4 wt. % NiO which is similar to the higher wt. % NiO of Layer 2 in Black Label. The high NiO contents reflect the predominance of primary chromite that is present at these stratigraphic levels of Big Daddy and Black Label. MnO clusters at between 0.4 and 0.8 wt. % MnO at 50 wt. % Cr_2O_3 (Fig. 5.90). There is also a negative correlation of decreasing wt. % MnO with decreasing wt. % Cr_2O_3 reflecting higher MnO in the more differentiated disseminated chromites.

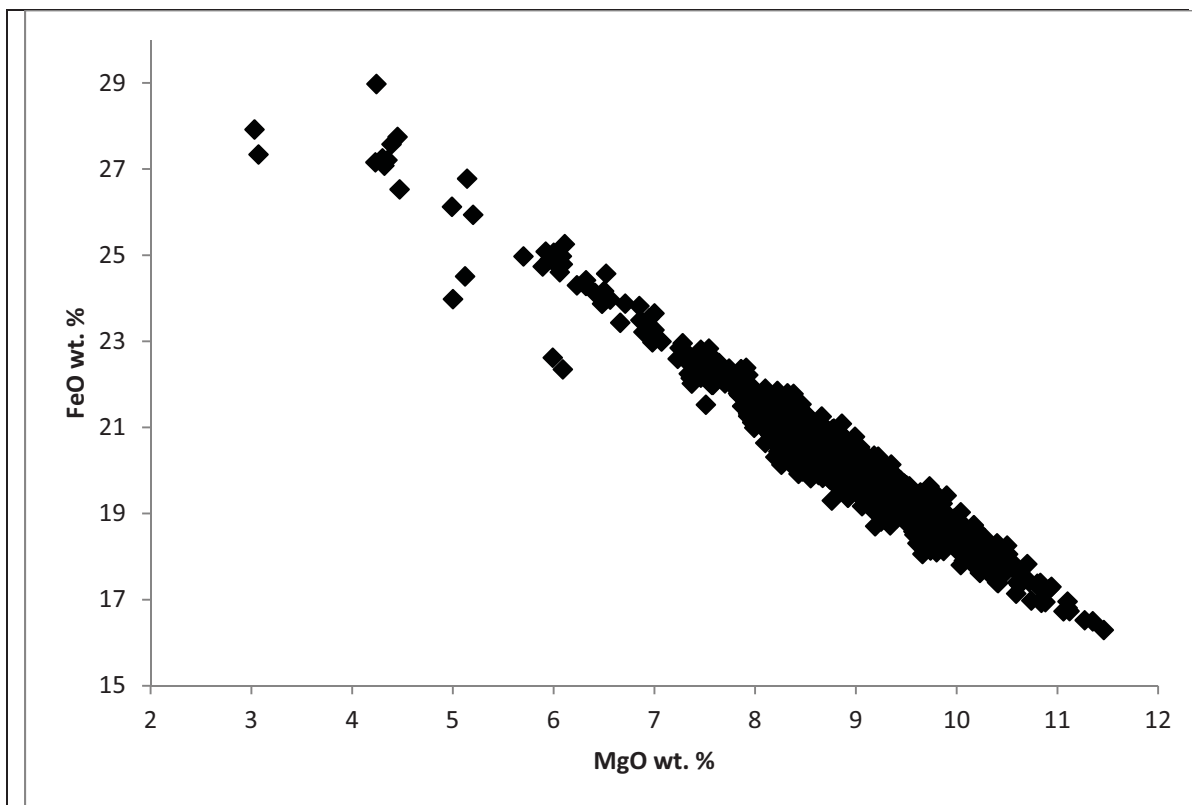


Figure 5.86. Binary plot of FeO vs. MgO wt. % for Big Daddy DDH FW-08-19.

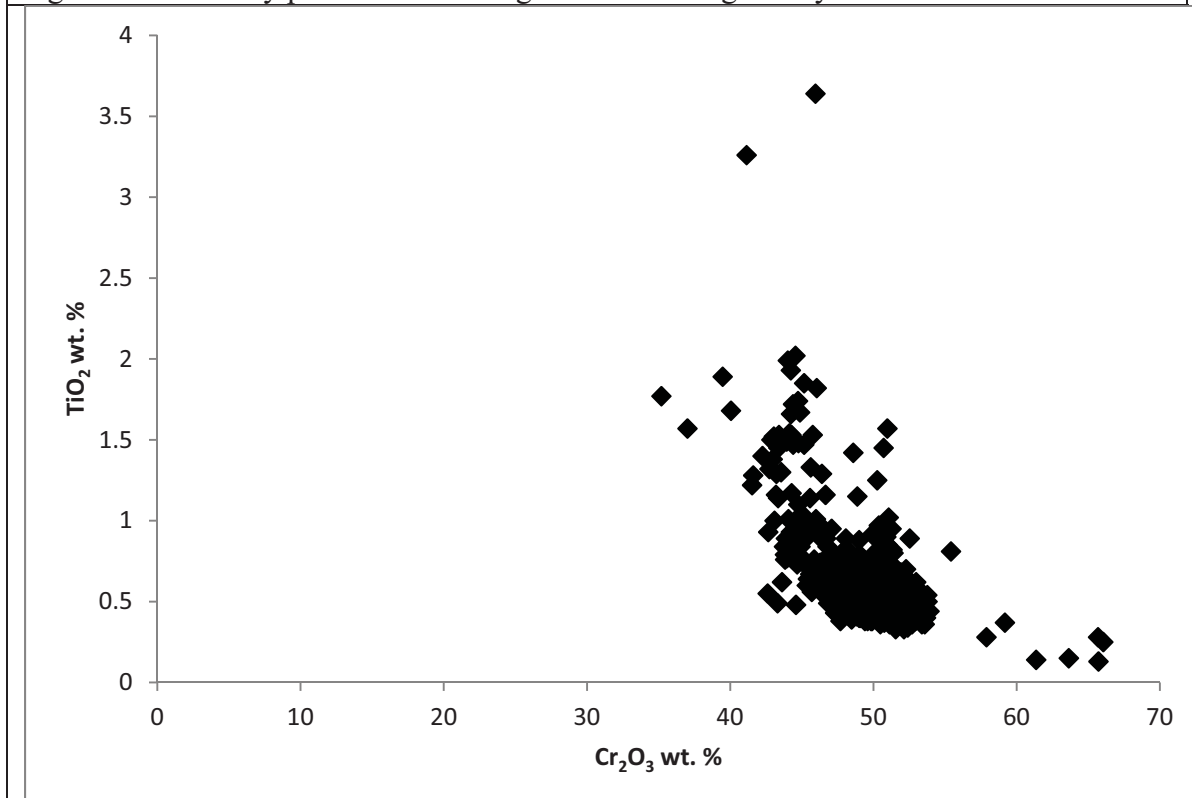


Figure 5.87. Binary plot of TiO₂ vs. Cr₂O₃ wt. % for the Big Daddy DDH FW-08-19 massive chromitite interval.

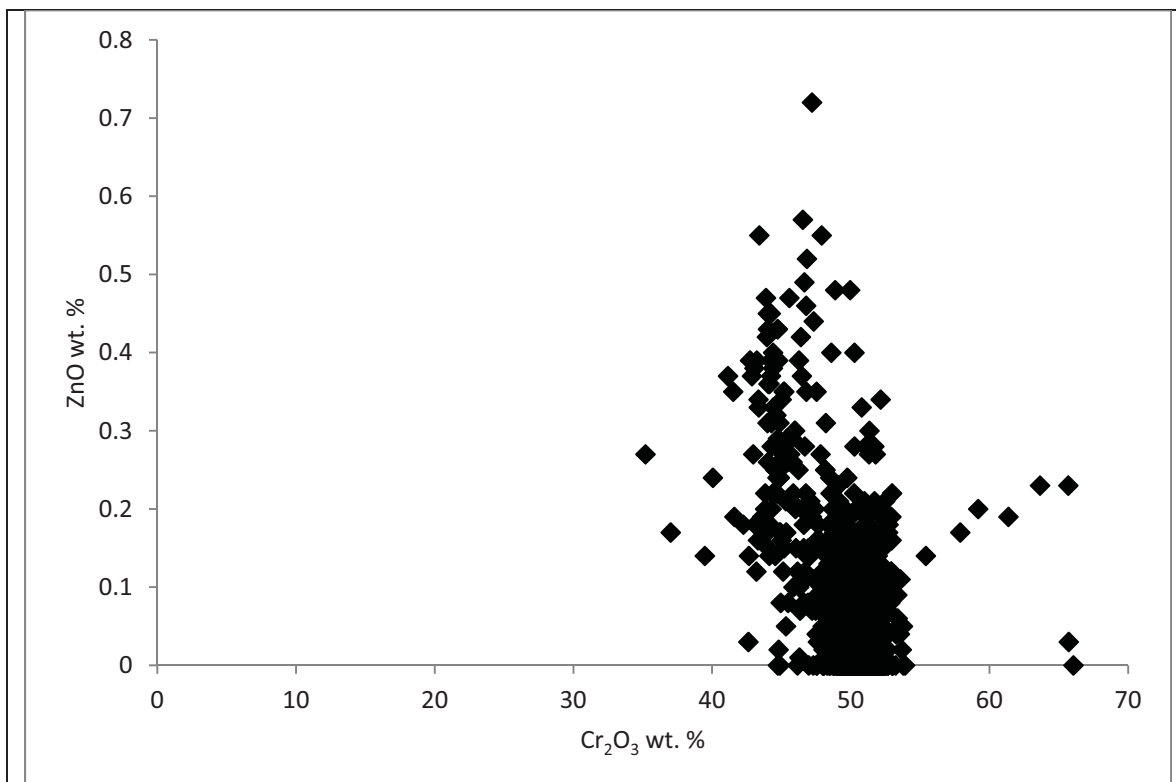


Figure 5.88. Binary plot of ZnO vs. Cr₂O₃ wt. % for the Big Daddy DDH FW-08-19 massive chromitite interval.

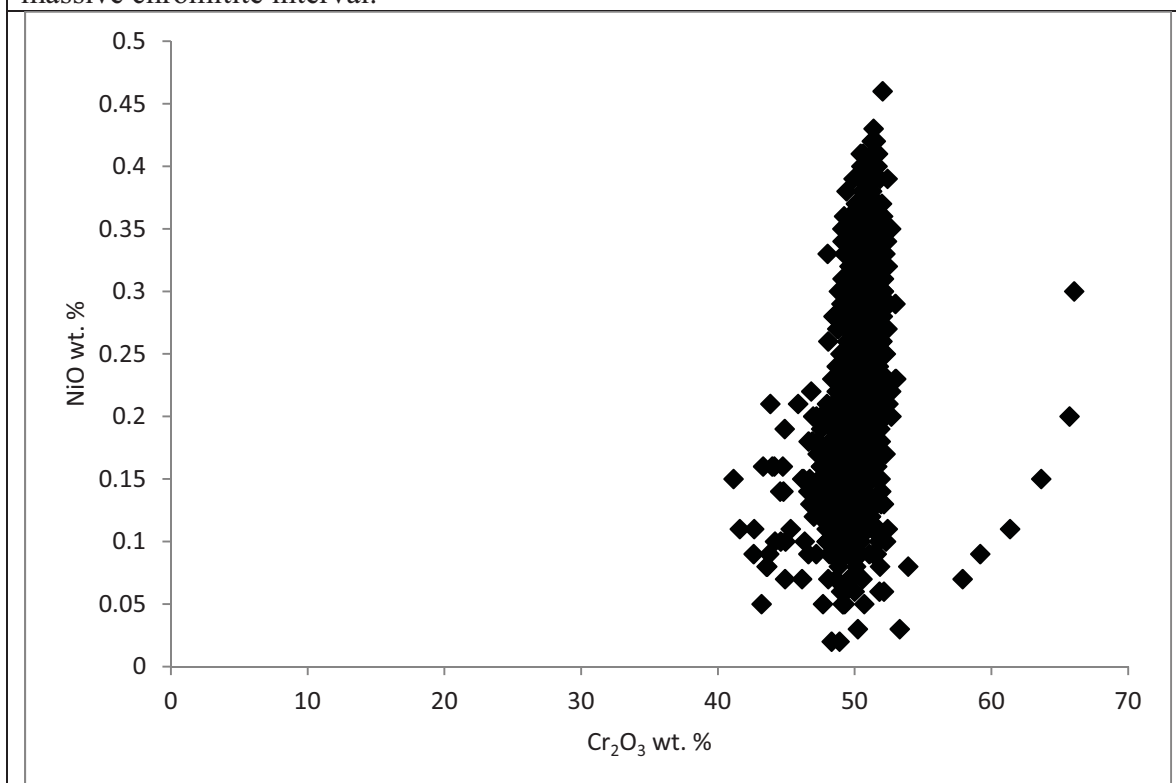


Figure 5.89. Binary plot of NiO vs. Cr₂O₃ wt. % for the Big Daddy DDH FW-08-19 massive chromitite interval.

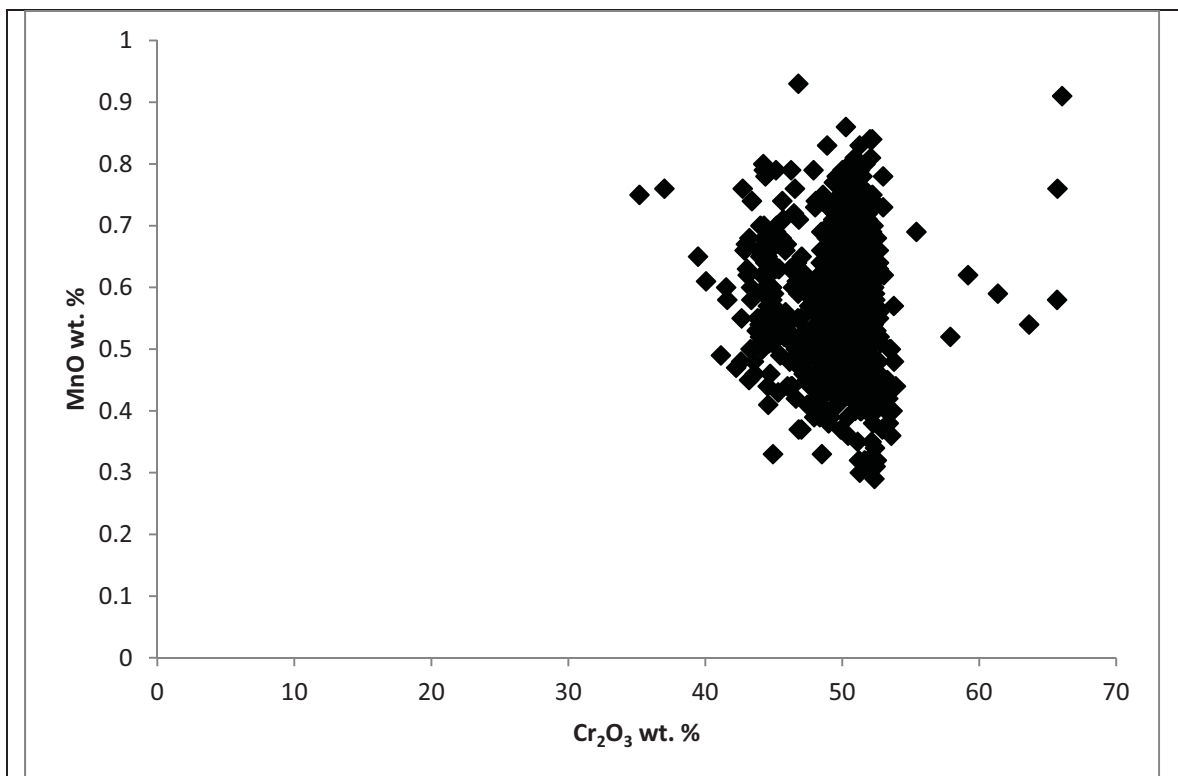


Figure 5.90. Binary plot of MnO vs. Cr₂O₃ wt. % for the Big Daddy DDH FW-08-19 massive chromitite interval.

5.4 Laser ablation ICP-MS analysis of chromite

Laser ablation ICP-MS analysis was carried out on chromites from three drill holes from the three deposits: Black Label DDH BT-09-31, Black Thor DDH BT-08-10 and Big Daddy DDH FW-08-19. There were 142 laser point analyses taken from 35 samples with up to 5 to 6 analyses taken per sample. The goal of the laser ablation work was to characterize the trace element signatures and variability of the three deposits with possible insights into using these signatures for an exploration vector. Trace elements of Sc, Ti, V, Mn, Co, Ni, Zn, Ga are reported and plotted on chromite normalized to chromite in MORB trace element plots. Binary variation of these elements with Cr is reported below. Another output of the analysis is an analysis of Ru, Rh, Pd, Os, Ir and Pt PGE in the deposits. However, the PGE in most of the samples are below detection limits, so they are not reported below. See Appendix 6 for the total suite of elements analysed by laser ablation.

5.4.1 Chromite/Chromite in MORB trace element plots

The laser geochemical results of the three deposits were analysed at the GSC facility in Ottawa May 16 to 18 and December 18 to 21, 2012. Results were first organized on an excel spreadsheet with care to subtract bad analyses. Chromite/chromite in MORB-normalized diagrams were then plotted for a useable suite of elements based on Pagé's work on the Thetford chromitites (Pagé, 2009).

The MORB chromite normalized patterns of the chromites reflect that of layered intrusion chromitites with large positive Ti anomalies and increased Fe contents and large negative Sc anomalies. There is also evolution in the patterns from more primitive komatiite to more evolved intrusion patterns where komatiites typically contain lower but positive Ti, negative Ni and negative Sc anomalies (Pagé and Barnes, 2012). The Black Label chromitites have high positive Ti anomalies indicating fractionated magma chemistry (Fig. 5.91). Zn and Co are elevated, again indicating these chromitites being more evolved. The Black Label chromitites are highest in Fe content and lowest in Mg content. There is more elevated Zn content in the disseminated chromite of Black Label. There are distinct negative Ni anomalies at Black Label in contrast to the other chromitites which indicates these chromitites are more evolved.

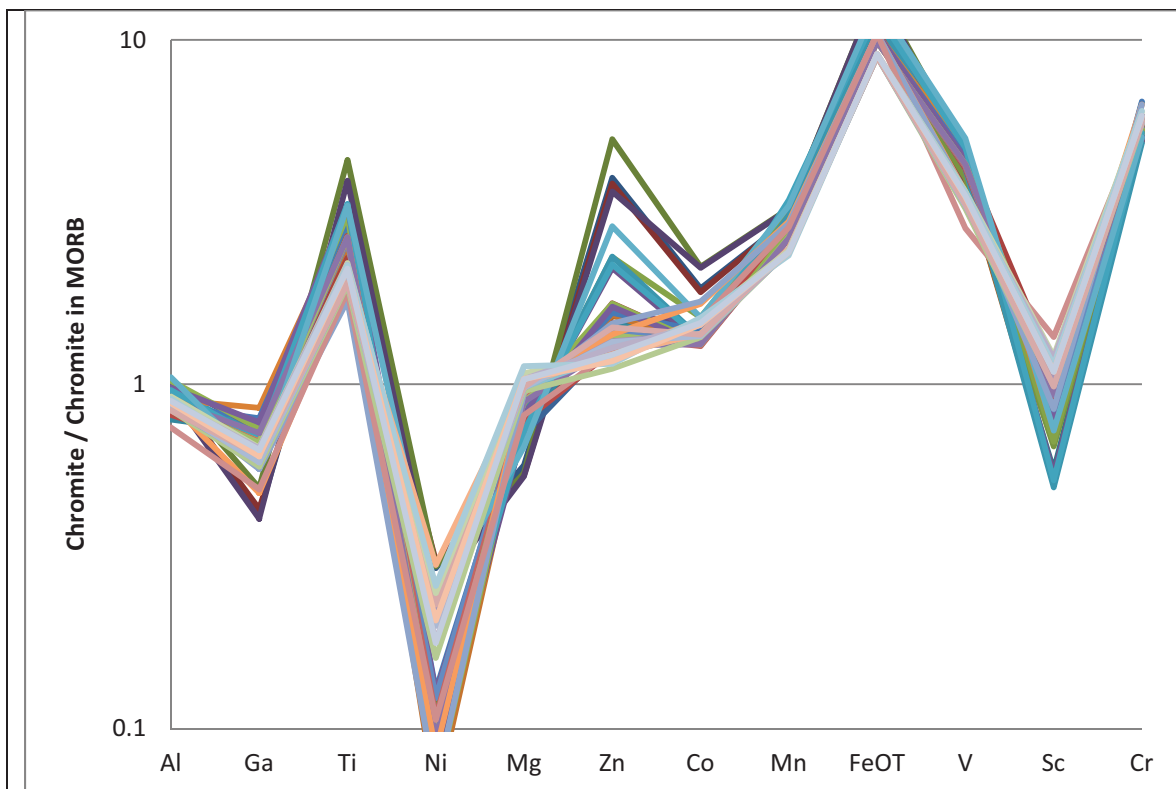


Figure 5.91. Chromite in MORB normalized trace element plot of Black Label DDH BT-09-31. Normalizing values of Pagé and Barnes (2009).

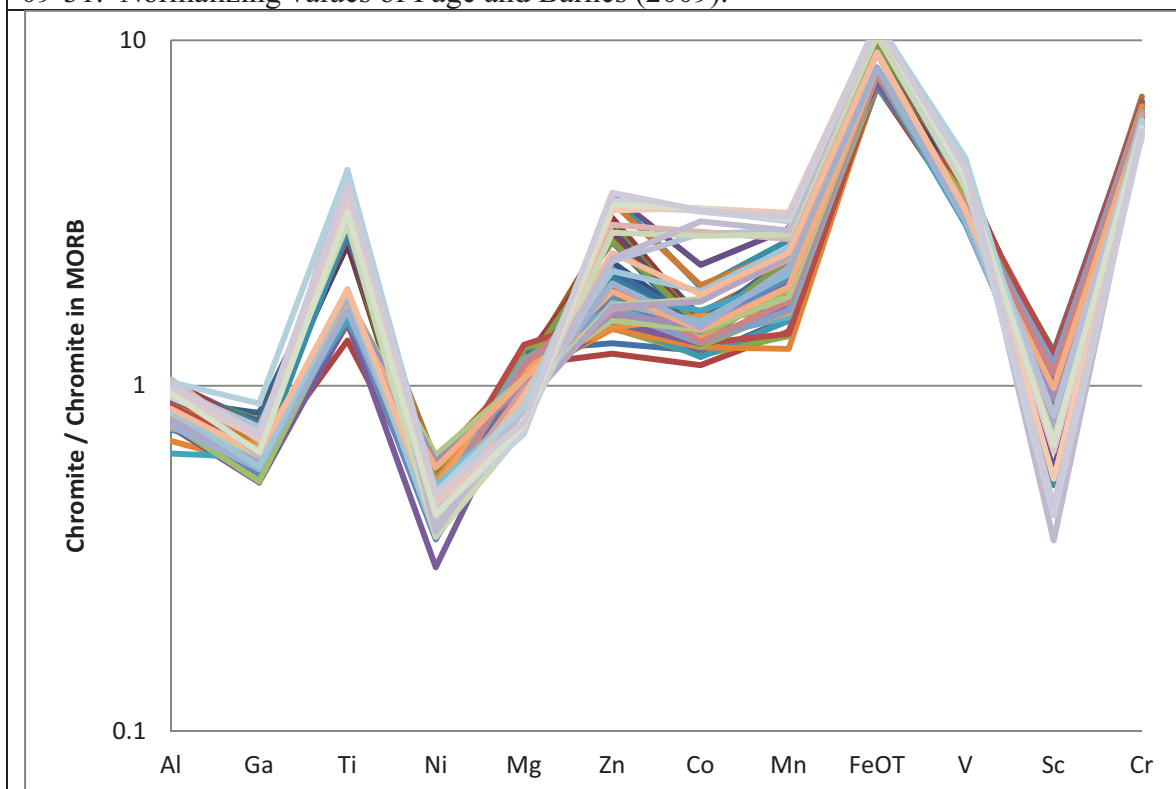


Figure 5.92. Chromite in MORB normalized trace element plot of Black Thor DDH BT-08-10. Normalizing values of Pagé and Barnes (2009).

At Black Thor, there are 2 subsets, a more differentiated and primitive sample (Fig. 5.92). The primitive komatiitic sample has a lesser positive Ti anomaly and lesser Zn and Co similar to the Great Dyke pattern, though being enriched in Fe (Jiménez et al., 2012). The more differentiated suite has a greater positive Ti anomaly with greater Zn and Co, more like Bushveld. V contents of the chromitites are high, in common with layered intrusion chromites in contrast to more primitive komatiite chromites.

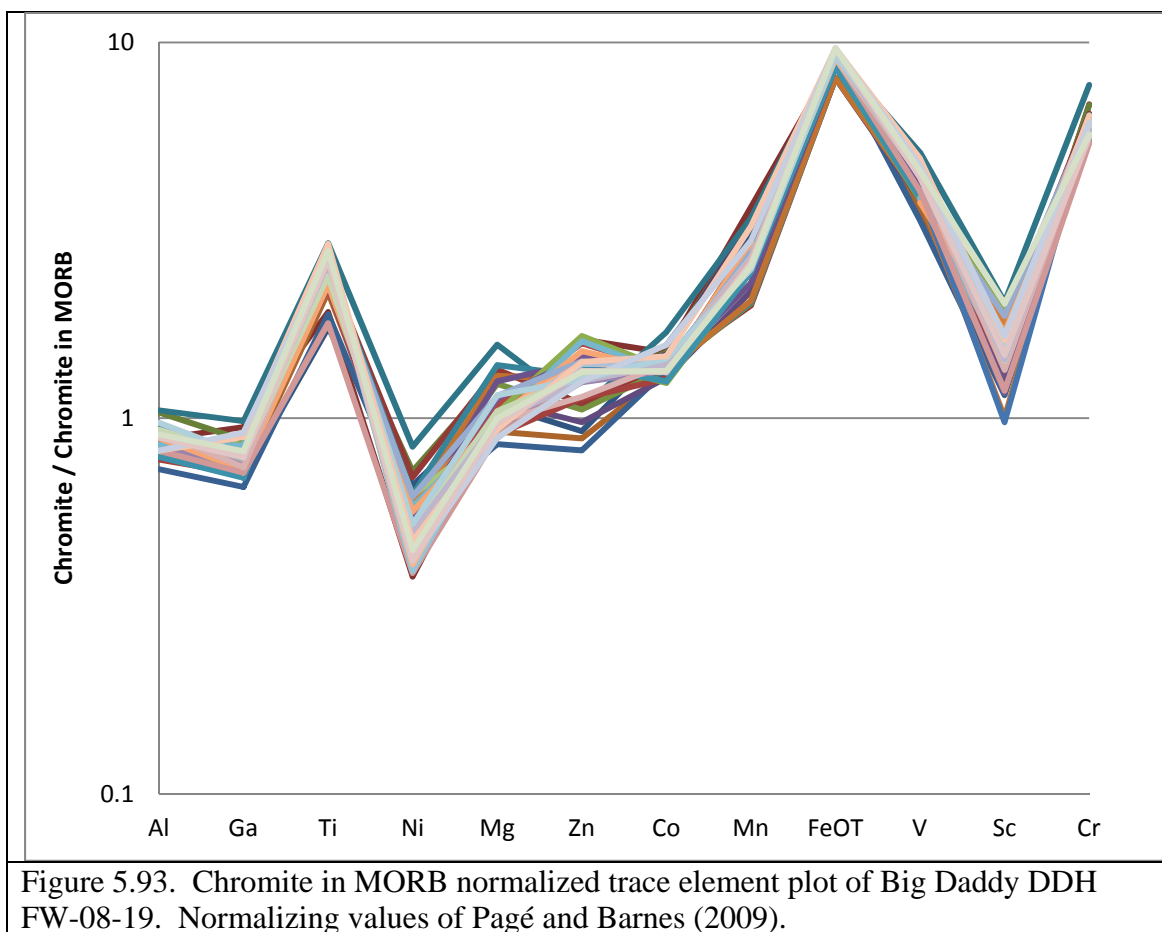
The Big Daddy chromitites consistently show positive Ti anomalies, but contain the most depleted Zn and Co, probably reflecting their primitive nature (Fig. 5.93). They are not, however, as primitive as the first subset of Black Thor. Notably, the Sc contents are more elevated. Mn contents are higher in Big Daddy and Black Label than Black Thor since they are more differentiated.

5.4.2 Binary trace element variation

The chromitites show trends of the elements vs. Cr that are indicative of fractionation from the more massive to disseminated chromites. Fractionation trends are displayed by increases of Ti, V, Co, Ga, Zn, Mn vs. Cr while decreases in Ni and Sc vs. Cr. Specific results from the three deposits are presented below.

The Black Label chromitites show the most fractionated magma chemistry of the three deposits (Fig. 5.94). Trace element concentrations include 2350 to 6012 ppm Ti, 794 to 1448 ppm V, 516 to 2392 ppm Zn, 2086 to 3016 ppm Mn, and 110 to 542 ppm Ni. For binary variation, fractionation trends are displayed by negative correlations of Zn, V and Mn with Cr and a positive correlation of Sc with Cr. Sc behaves incompatibly similar to Ni in these deposits. Ni appears to show a positive correlation and generally increases with Cr. Although showing fractionation with depleting trends of Cr in komatiitic chromites such as Alexo, Ga shows an enriching trend suggestive of it behaving incompatibly like Ni and Sc (Méric et al., 2012). Ga shows this positive correlation in all the deposits. Ti and Co vs. Cr plots no significant trend.

The Black Thor chromitites are the most primitive of the deposits with trace element concentrations that include 1125 to 2792 ppm Ti, 819 to 1277 ppm V, 575 to 1577 ppm Zn, 1125 to 2792 ppm Mn, and 526 to 1112 ppm Ni (Fig. 5.95). For binary variation, fractionation trends are displayed by negative correlations of Ti, Zn, Mn and Co with Cr and positive correlations of Ni and Sc with Cr. Ti shows two negative



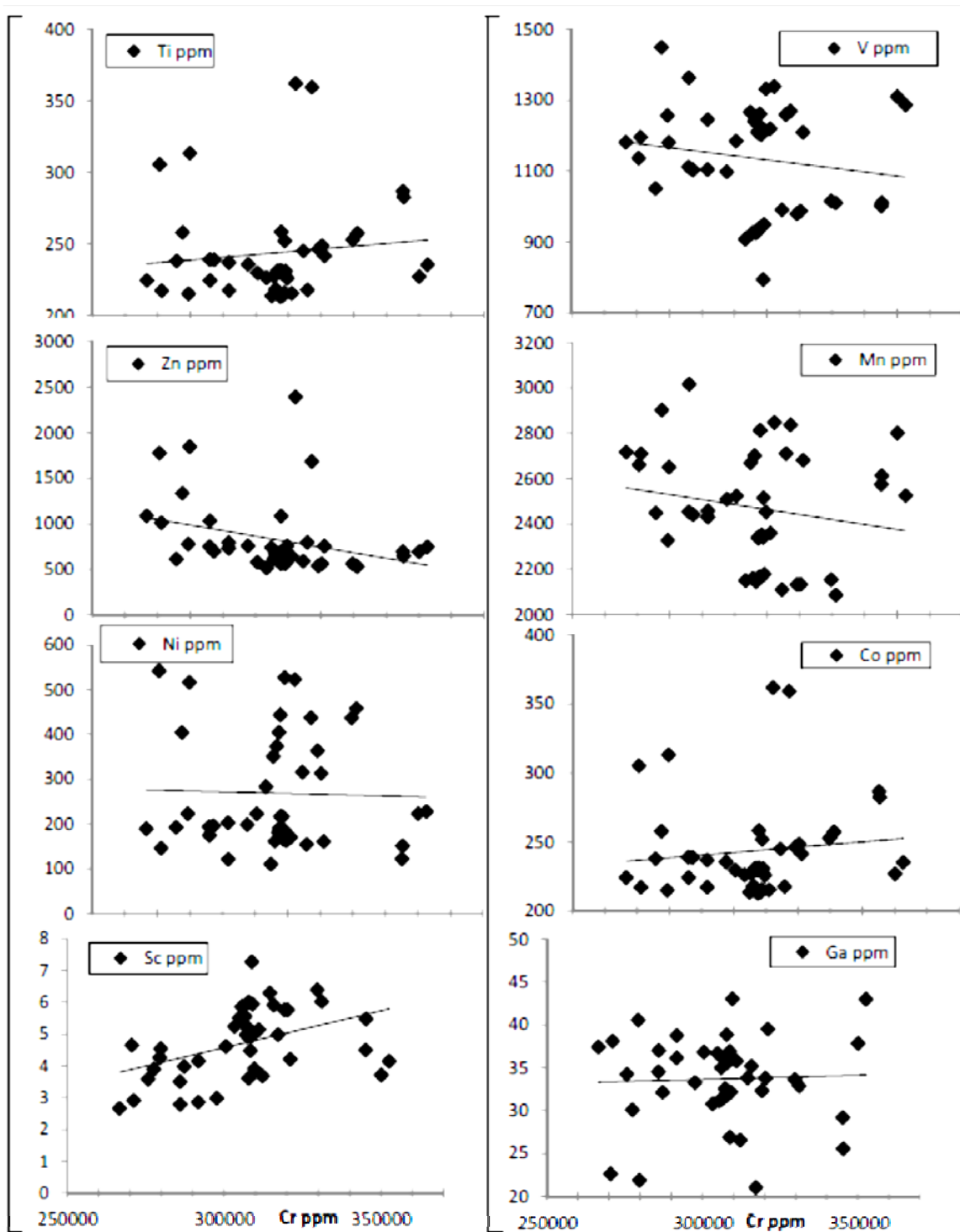


Figure 5.94. Binary plots of Cr vs. Ti, V, Zn, Mn, Ni, Co, Sc and Ga ppm for Black Label DDH BT-09-31.

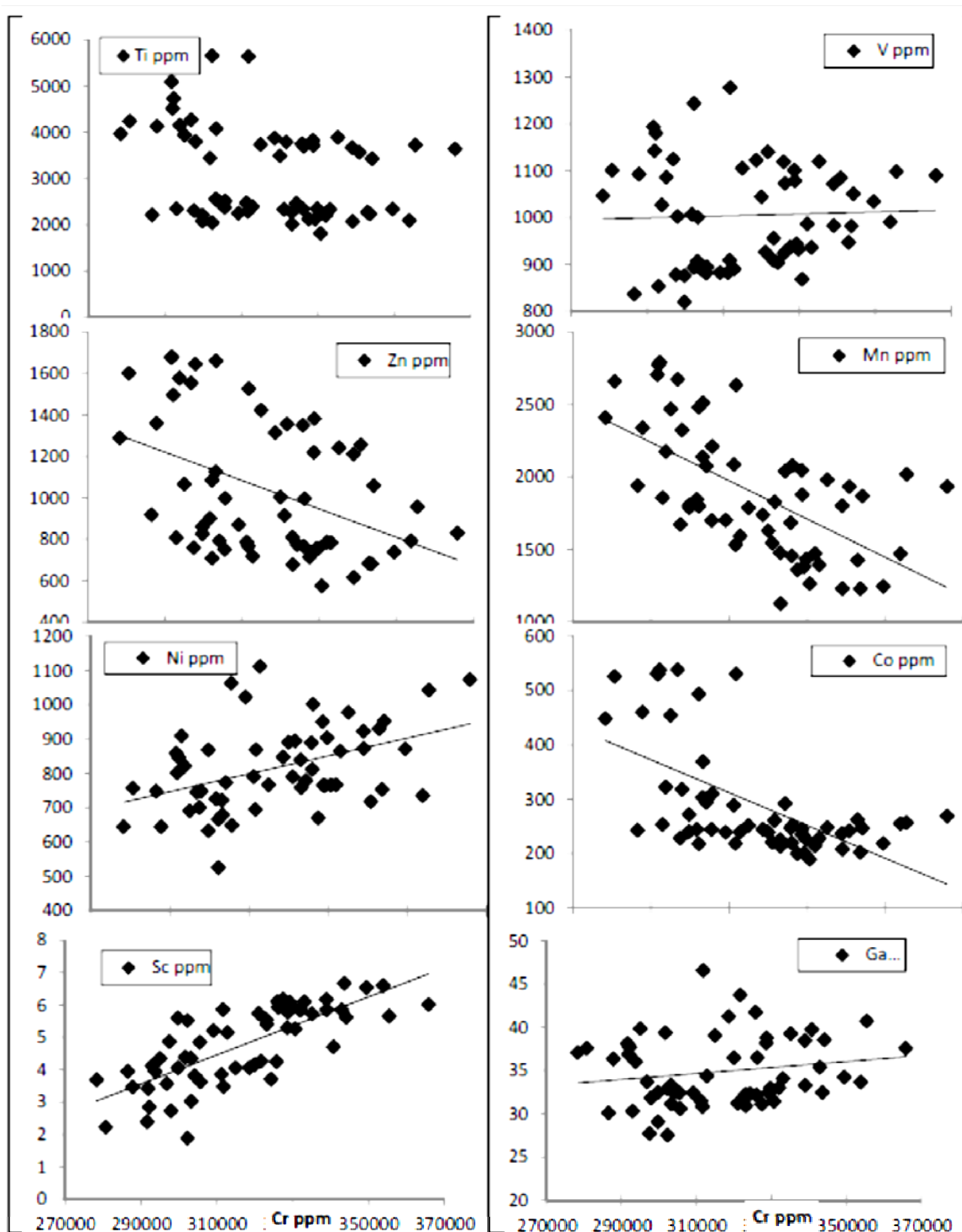


Figure 5.95. Binary plots of Cr vs. Ti, V, Zn, Mn, Ni, Co, Sc and Ga ppm for Black Thor DDH BT-08-10.

correlation trends for higher and lower Ti concentrations representative of two different sample subsets of the deposit, one being more primitive than the other. Zn and Mn show well defined correlations. V appears to show a weak negative correlation. Ga again shows a negative correlation. Ni and Sc also show well defined positive correlations indicative of fractionation.

The Big Daddy chromitites show less but similar variability as the other deposits (Fig. 5.96). Trace element concentrations include 2336 to 3923 ppm Ti, 940 to 1425 ppm V, 381 to 769 ppm Zn, 1758 to 3209 ppm Mn, and 668 to 1482 ppm Ni. Ni is higher and reflects the primitive character of the deposit like Black Thor. Mn contents are higher than the other deposits. Many of the Ni contents are high since the samples are all from massive chromite. For binary variation, correlations are less well defined but show negative correlations for Ti, Zn and possibly Mn with Cr. Correlations are positive for Ni and Sc with Cr. Ga shows a variable but negative correlation.

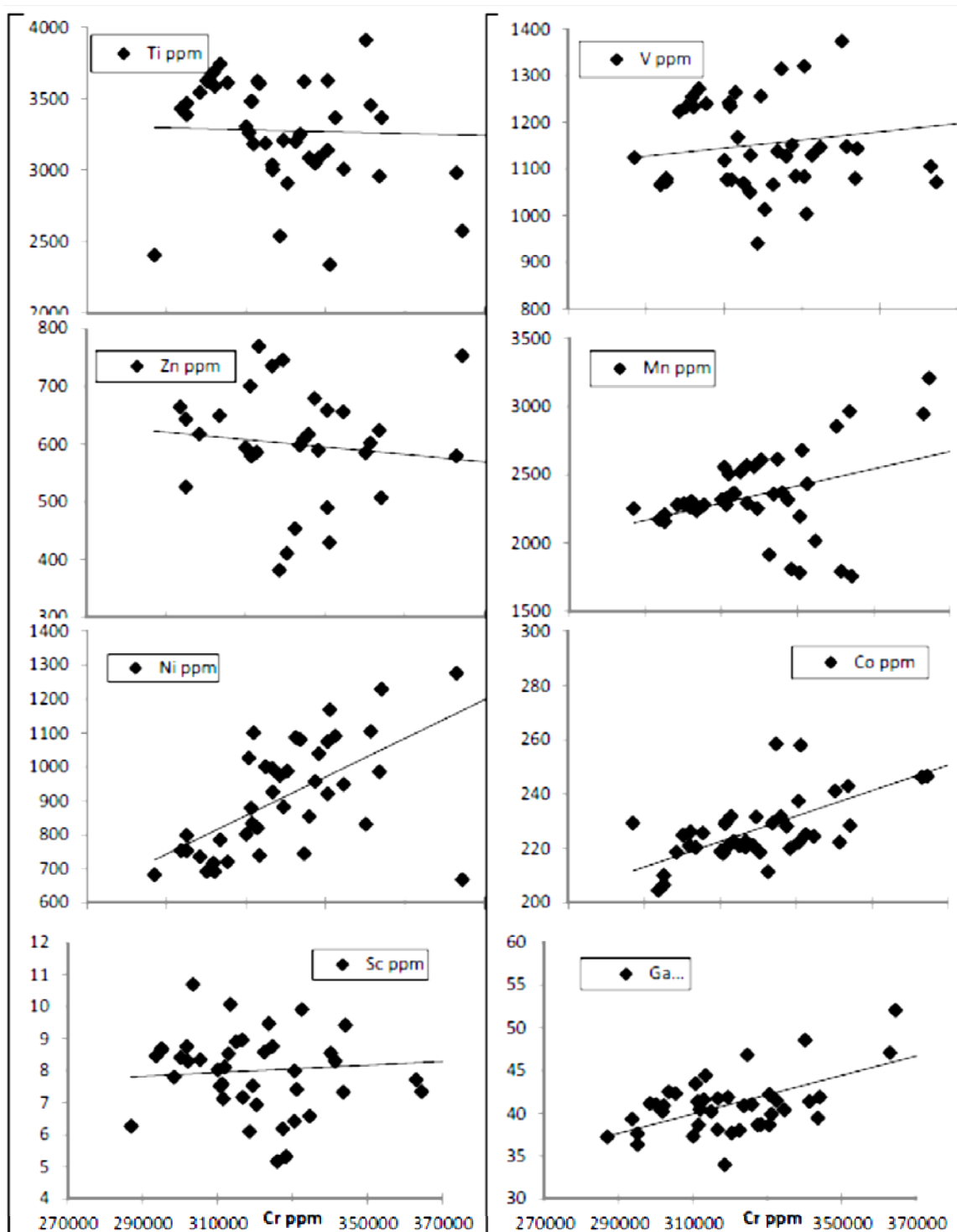


Figure 5.96. Binary plots of Cr vs. Ti, V, Zn, Mn, Ni, Co, Sc and Ga ppm for Big Daddy DDH FW-08-19.

CHAPTER 6

DISCUSSION

6.1 Introduction

For discussion of the McFaulds Lake deposits, the chromites are first plotted on tectonic discrimination diagrams to compare the chromites with other deposits of the world and indicate the type setting. Origin of chromite as it pertains to these deposits is then discussed in terms of an evaluation of Irvine's (1975) model, followed by a discussion of silicate inclusions leading up an evaluation of Irvine's (1977) proposal for chromite genesis. Magma mixing is proposed for origin and is further refined by advocating the double diffusive convection model. Postcumulus chromite growth is then discussed and an evaluation is made of the conduit theory for chromite origin. Finally, the late hydration overprint is discussed in terms of chromite ore modification.

6.2 Tectonic discrimination of chromite

6.2.1 The Cr# vs. Mg# plot

Chromites can be distinguished between komatiitic, layered intrusion and other environments such as ophiolitic by means of the Cr# vs. Mg# catio ratio plot (Figs. 6.1 and 6.2). In comparison to other chromites of the world, the McFaulds Lake chromites plot well in the fields of stratiform mafic intrusions and komatiite with the exception of the ferrichromites. In comparison to komatiite chromites, the McFaulds Lake chromites are similarly high in Cr/Al for the most primitive chromites. The primitive chromites of McFaulds Lake are most similar to the Great Dyke chromites. Other komatiitic chromites such as those from the Selukwe dataset, the Hartley Complex and the Wedza Complex and the Shurugwi dataset are however, slightly more Cr/Al-rich due to high Cr and low Al and more Mg-rich. There is not much pyroxene in the komatiitic magmas to exchange Al into the chromite structures. Also, lack of differentiation tends to make these deposits plot at a higher Mg composition. There is still substantial variation in Mg#

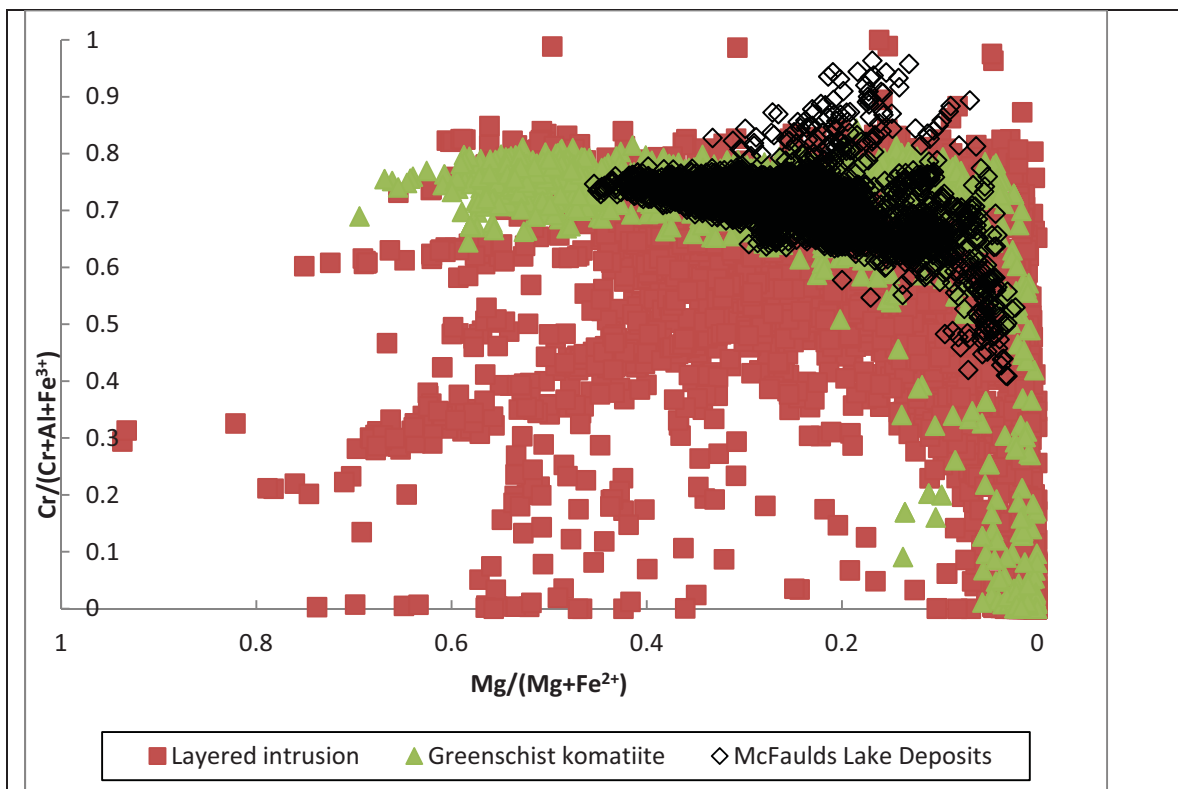


Figure 6.1. Cr # vs. Mg # plot of McFaulds Lake chromites with other layered intrusion and komatiite chromites of the world. World chromite data is from Barnes and Roeder (2001).

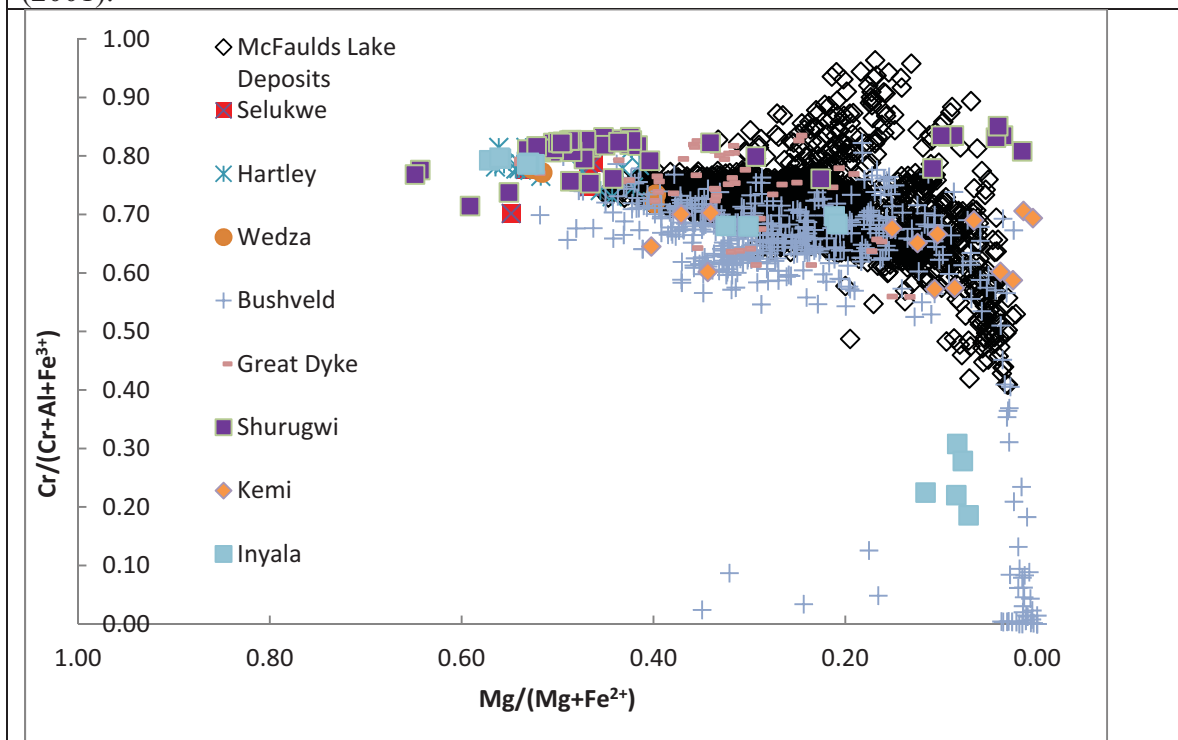


Figure 6.2. Cr # vs. Mg # plot of McFaulds Lake chromites with other chromite deposits of the world. World chromite data is from Barnes and Roeder (2001).

in the Great Dyke deposits, but only up to a Mg# composition of 0.218. The McFaulds Lake deposits then follow a trend toward decreasing Cr# with decreasing Mg# as is evident in other stratiform layered intrusions. However, other stratiform complexes that follow this trend do not plot at high Cr# and high Mg# compositions. A similar stratiform complex that follows a trend of decreasing Cr# with decreasing Mg# is the Bushveld Complex. Although having the same trend, the Bushveld chromites have overall lower Cr# than McFaulds Lake. The lower Cr# of Bushveld is due to the predominance of pyroxene to exchange Al with the chromite to lower the Cr#.

With increasing differentiation i.e. as the chromites go to lower Mg# composition along the increasing Fe-Ti trend, there are lower Cr#s in the McFaulds Lake chromites. Since there is a strong correlation of decreasing Cr# with decreasing Mg# in the McFaulds Lake chromites, this would indicate magmatic evolution typical of a differentiated intrusion. The McFaulds Lake deposits plot on an overall trend of primitive komatiite to more differentiated with increasing Fe-Ti and finally to more pyroxene-dominated differentiated compositions. The primitive McFaulds Lake chromites are similar to the Great Dyke komatiitic chromites; they become more differentiated along an increasing Fe-Ti trend similar to Great Dyke followed by Bushveld; and then decrease Cr# with differentiation and pyroxene fractionation similar to Bushveld chromite.

Another thick chromitite deposit, the Kemi Intrusion chromitite deposit is plotted for comparison. Although similar in thickness, the Kemi deposit is lower in grade at lower Cr# than the McFaulds Lake deposits and rather plots similar to the Bushveld complex. For comparison to the main chromites, the Cr-enriched to Cr-depleted ferrichromites of McFaulds Lake are also plotted. There is a much larger dataset for these secondary chromites in McFaulds Lake than for other chromites of the world. Unusual trends in Cr# enrichment with decreasing Mg# is evident in the Cr-enriched ferrichromites which is significant for higher grade chromite ores. The trend toward Cr-enrichment occurs with retrogression of the chromite rims. In contrast to Cr-enrichment, retrogression also produces a secondary chromite trend to low Cr# compositions with low Mg# in the Cr-depleted ferrichromites.

6.2.2 The Ternary Cr-Fe³⁺-Al plot

The ternary Cr-Fe³⁺-Al plot is also used for tectonic discrimination of chromites. On a Cr-Fe³⁺-Al plot, the McFaulds Lake deposits plot well in the field for komatiites and in the komatiitic part of the layered intrusions (Fig. 6.3). They plot near the corner of high Cr but lower Fe³⁺ and low Al. The lower Fe³⁺ and Al is typical of low Al-bearing undifferentiated komatiites. Although lower in Fe³⁺, there is still more Fe³⁺ in the McFaulds Lake chromites than in the komatiite chromites. This is similar to the Mg#-Cr# diagram in that the McFaulds Lake deposits follow an Fe-Ti trend with more differentiation than komatiite chromites. However, the broad overlap of the McFaulds Lake deposits with the komatiite field clearly shows the deposits have komatiite affinity i.e. primary chromite of komatiite composition. Like the Cr#-Mg# plots, there are also fields for the Cr-enriched to Cr-depleted ferrichromites. All the secondary chromites plot with low Al since Al is either substituted for Cr or Fe³⁺ in the chromite structure. The Cr-enriched ferrichromites plot at compositions intermediate between Cr and Fe³⁺ while the Cr-depleted ferrichromites plot toward the Fe³⁺ end. There is a subset of high Cr, low Fe³⁺ and low Al ferrichromites near the Cr apex of the plot. These represent the Cr-enriched ferrichromites of the upper chromitite of DDH BT-09-17 that follow a different trend than the other secondary chromites of the other deposits.

6.3 Origin of chromite: An Evaluation of Irvine's 1975 model

The origin of the McFaulds Lake chromite deposits is linked to the petrography and geochemistry of the host rocks and ores themselves. The deposits as a whole may be classified with stratiform magmatic Cr/PGE ores in layered complexes (Duke, 1988). Stratiform chromite deposits are formed by magmatic segregation during fractional crystallization (fractionation) of mafic-ultramafic magma. The precise reasons why massive chromite cumulate layers form have not been entirely understood. In the first of Irvine's models (Irvine, 1975) he suggested a mechanism whereby a chromite saturated picritic tholeiite liquid becomes more siliceous by contamination (assimilation) with granitic material or alternatively by blending with a more siliceous differentiate of the parent magma, thereby causing chromite to precipitate. In this model, the original magma is contaminated while coprecipitating olivine and minor chromite. A period

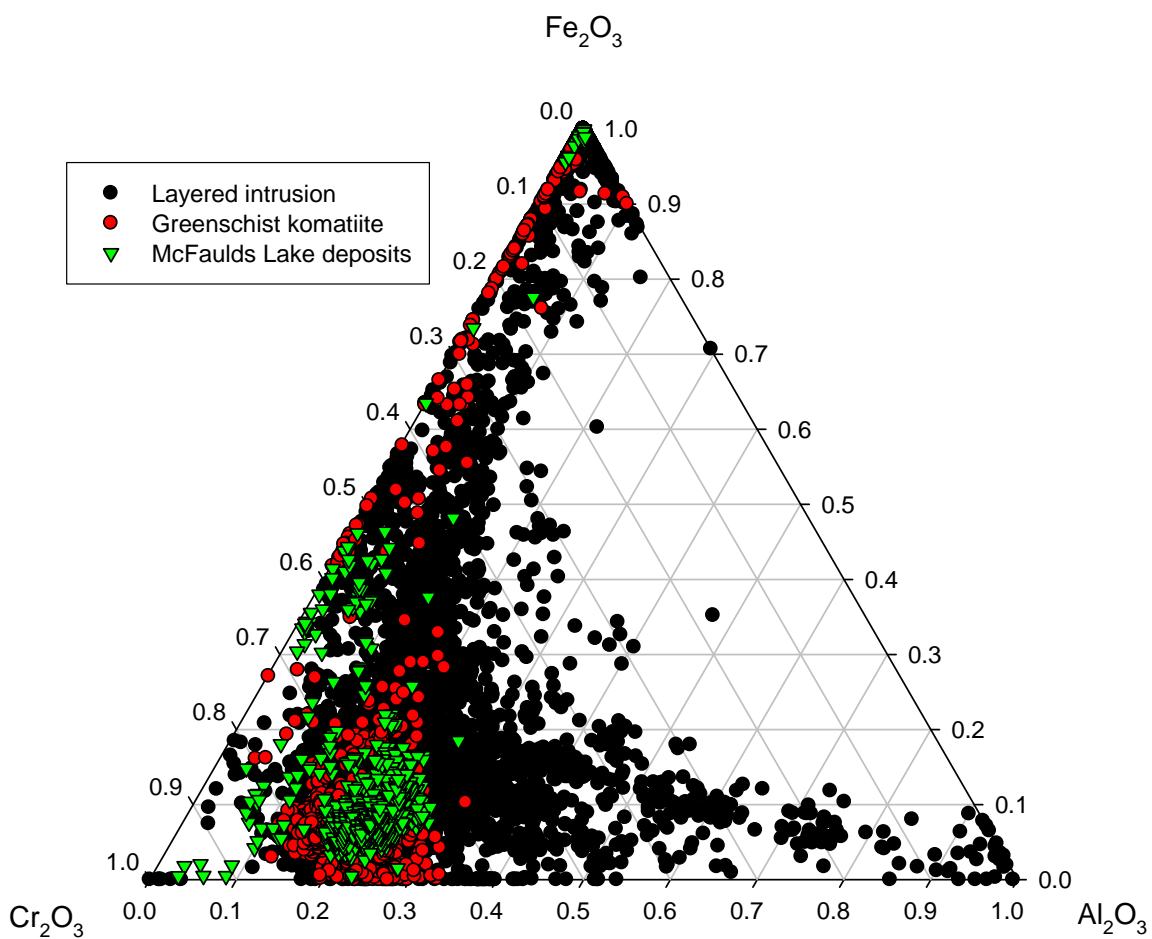


Figure 6.3. Ternary Cr-Fe³⁺-Al plot of the McFaulds Lake chromites with other layered intrusion and komatiite chromites of the world. World chromite data is from Barnes and Roeder (2001).

follows when chromite precipitates alone, and then, because the liquid is enriched in silica, orthopyroxene crystallizes instead of olivine (Irvine, 1975).

In the case of the McFaulds Lake deposits, initial crystallization of an olivine-chromite cumulate is indicated by dunite with disseminated chromite followed by the transition into massive chromite alone. However, what is not explained by this model is how the magma migrates into chromite-alone stability. It is assumed that this occurs with decreasing temperature as this is the dominant control of fractional crystallization. However, this does not explain the sudden onset of massive chromite from the disseminated chromite-bearing dunite. The magma needs to be directly shifted into the chromite-only field. A mechanism for driving melt chemistry from the chromite-only field to pyroxene is by crustal contamination. A contaminant would raise the silica content of the olivine magma so that it shifts directly into chromite stability. This would ideally work in the case of a chromite-laden pulse of magma after crystallization of chromite and olivine, that injects some silica-rich country rock to directly raise the silica of the melt to pyroxene stability. Although this model explains the transition of olivine to massive chromite, there is no explanation for the sudden break from chromite back into the pyroxene stability field. In other words, there are two modes of magma emplacement occurring one after the other which is an unlikely scenario. The appearance of intermittent chromitite beds after disseminated chromite suggests that there were intermittent pulses of magma to separate out chromite layers rather than a single magma batch being fractionated into chromite stability. There must have been episodic pooling and dithering of the magma to the right composition to cause the rainout of chromite layers eventually forming the massive chromitite zone.

There are several problems with Irvine's 1975 model. As suggested by Irvine (1977) and Mondal (2010), it takes an enormous amount of silica to migrate the melt to pyroxene stability. Rollinson (1997) in his discussion of the komatiitic chromites in Inyala, Zimbabwe, counters this argument by saying that for komatiitic melts, the melts have a high melting temperature sufficient to assimilate silica in the formation of chromite from olivine along with the later surrounding pyroxenites. There the pyroxenites are in the transition zone of dunite with country rock. In McFaulds Lake, the chromite compositions plot similarly to komatiitic chromites of the Great Dyke yet

contain pyroxenites similar to the intrusion in Inyala. Also, from the primitive mantle multielement plots, it can be observed that the dunites are of komatiitic affinity, with crustal contamination signatures evident of incorporation of TTG. However, the pyroxenites at McFaulds Lake appear to contain pyroxenite in an ordered layered series from dunite to pyroxenite with leucogabbro melted roof rock. From the primitive mantle multielement plots, it can be seen that the pyroxenites appear to be originated from komatiitic melts that have been contaminated by TTG, similar to dunite but with more contamination. However, both are part of the same series of intrusives that have incorporated TTG. Since there was inheritance of a crustal contamination signature in the dunite below the chromite intervals, this would suggest that TTG assimilation was already inherent in the magmas before chromite crystallization.

The leucogabbro has been argued as to not be a part of the layered series but as melted roof rock to the intrusion. True, the leucogabbro has distinct evolved signatures from the dunite and pyroxenite; however, there also appears to be a crustal contaminant signature of TTG in the leucogabbro as well. In drill core, the leucogabbro contains textures of large scale silicification of an original gabbro that are probably from the injection of TTG or other country rock since these are non-igneous. However, this implies that the gabbro existed and was overprinted by silicification, not that the gabbro itself originated as a result of silicification. Roof rock assimilation is evidenced by typical granophyric textures of coarse pink K-spar patches that occur in some of the feldspathic zones. Therefore the upper gabbro likely developed as a “typical granophyres” in the roof of the intrusion. It represents the crustally contaminated border of the intrusion and not the pyroxenite. Other clues to it being the roof of the intrusion are its large extent in the Ring of Fire intrusion and its abrupt change from pyroxenite, as opposed to it being a gradational replacement zone. Therefore, since the pyroxenite is not located at the contact of the wallrock, it is probably not a transition replacement zone of chromite with wall rock as implied for the origin of komatiitic chromite in Inyala by Rollinson (1997).

Another problem with the Irvine (1975) model is that it is only applied to cases of silica addition. Often in chromitites, there is the sequence of dunite to chromitite to pyroxenite which implies a migration of the melt with lowering of temperature and silica

contamination from olivine to chromite to pyroxene on the liquidus. However, not all chromitites occur in this sequence order. In the second layer of Black Label, there is pyroxenite before the chromitite which is followed in turn by oikocrystic harzburgite and dunite. In the first layer of Black Label DDH BT-09-31, the oikocrystic harzburgite is a transitional unit with crystallization of more intercumulus pyroxene from dunite to pyroxenite. In the second interval of that drill hole however, the oikocrystic unit is transitional from pyroxenite to oikocrystic unit/chromitite to dunite with a small pulse of dunite in between the pyroxenite and oikocrystic unit. This explains the onset of cumulus olivine rainout.

In Big Daddy DDH FW-08-19, there is a sequence of pyroxenite followed by the transitional heterogeneous pyroxenite unit, then chromitite followed by dunite resulting in the sequence order of pyroxenite to chromitite to dunite. In the second chromitite layer of DDH BT-09-17 there is first pyroxenite followed by cumulus pyroxene with chromite, then chromitite with minor dunite and then pyroxenite. In these scenarios, the chromitite is related to the migration of the melt from pyroxene to chromite to olivine. Notably, most chromitite layers occur in the sequence from dunite to chromitite to pyroxenite. Since this reversal in crystallization order involves an increase in temperature, the migration of the melt to eventual olivine could only work with magma mixing rather than a fractionation mechanism. There is no way of depleting the melt of silica except for some sort of mixture with a primitive melt which is inferred to be the mechanism for chromite origin.

Another problem with the model is that the chromite is related to the magma chemistry of the host rocks and not the assimilated. If a new dunite pulse was contaminated by TTG to mineralize chromite, the presence of variable plagioclase content with variable contamination would cause variable Cr contents of the ores. However, in the Big Daddy massive chromitite interval, the chromites that were probably derived from various replenishments have a consistent Cr_2O_3 composition up section. The chromites all have primitive Cr_2O_3 compositions related to the chromite that are primitive and closer to olivine stability rather than being lowered by plagioclase content of an assimilated. In their discussion of the Bushveld chromitites, Naldrett et al. (2009) show that Al_2O_3 content of chromite mineralized in equilibrium with plagioclase will be

buffered by the high Al_2O_3 content of plagioclase. The effect is to raise the $\text{Cr}/(\text{Cr}+\text{Al})$ or lower the Al_2O_3 content of the chromite since the chemical potential of Al_2O_3 is over its maximized value and is buffered by plagioclase (Naldrett et al., 2009). In the Big Daddy massive chromitite, there is no enrichment or depletion in Al_2O_3 in the chromite that would result due to the presence of plagioclase, as would be present in a crustally contaminated dunite pulse.

In the sequences of dunite to chromitite to pyroxenite, it may be argued that there was replacement of pyroxene by olivine to drive the melt into chromite stability. This is the mechanism thought to be the origin of some podiform chromitites. In the harzburgitic mantle the migration of an intercumulus melt causes replacement of pyroxene, incorporation of silica and the precipitation of pods of chromitite (Matsumoto and Arai, 2001). Or in a layered intrusion sequence, the influx of a primitive melt could dissolve and assimilate the roof pyroxenite of an intrusion and precipitate chromitite (Pagé, 2010). However, there appears to be several stacked sequences of dunite to chromitite to pyroxenite where there are large thicknesses of the later pyroxenite. It is unlikely that the large sequences of pyroxenite are all a result of roof contamination when there are later higher and more primitive sequences of chromitite in Black Label Layer 2 for example. Also the occurrence of some reversed crystallization orders of pyroxenite to chromitite to dunite and the presence of cumulus chromite in pyroxenite makes it unlikely that the pyroxenite was a result of roof assimilation.

The evidence that is missing is the lack of xenoliths in drill core that would be injected by the magma for incorporation into the melt. Mungall (2008) outlines the presence of iron formation xenoliths for the Eagle's Nest deposit and proposed the same incorporation of contaminant in the formation of the Blackbird deposit chromites. The assimilation of TTG is inherent to the trace element geochemistry of the McFaulds Lake dunites and pyroxenites. Iron formation has been observed as xenolith in the Black Creek chromite deposit (Lavigne, pers. communication, 2013). However, there have been no xenoliths detected in the McFaulds Lake chromite layers that would explain the formation of the large chromite layers.

Another means proposed for chromite formation is straight fractionation. This would explain the presence of cumulus chromite and olivine in disseminated chromite-

bearing dunite. Though, often in deposits such as Big Daddy, there is chromite disseminated in dunite followed by thick massive chromitite before overlying pyroxenite. What would cause a chromite-only crystallization change from chromite + olivine? There appears to be no mechanism of dithering and keeping the intercumulus melt in the chromite only field in order to produce up to 40 m thickness of chromitite. And of course the sequence of pyroxenite to chromite to dunite is not explained.

6.4 Silicate Inclusions in Chromite

There has been evidence used to support chromite origin by silica addition by means of the presence of silicate inclusions with minerals such as albite and amphibole. This interpretation was made in Irvine (1975). The presence of serpentine, chlorite or tremolite would be explained as the result of replacement of olivine. However, silicate inclusions of albite and amphibole are foreign to the surrounding retrograded serpentines and tremolites of the intrusive dunites and pyroxenites. The Kemi deposit in Finland is a chromite deposit similar in thickness to the McFaulds Lake deposits. Alapieti et al. (1989) described the Kemi deposit in detail and concluded that it is a stratiform chromite deposit in an ultramafic layered intrusion. He proposed that chromite crystallization was initiated by silica addition/silica contamination. Evidences for silica addition were round silicate inclusions of serpentine, amphibole or albite in chromite grains. The presence of albite inclusions in chromite hosted by dunite suggested entrapment of wallrock contaminant. Spandler et al. (2005) discuss the presence of mineral inclusions of enstatite, aspidolite (Na-phlogopite), magnesiokatophorite (Na-Ca amphibole), albite and diopside. Spandler et al. (2005) referenced Page and Zientek (1987), proposing that Na amphiboles and micas significantly more Na-rich than the primary amphibole and phlogopite of the surrounding cumulates, are exotic, related to contamination of the primary magma by a Na-rich trondhjemitic melt.

In the McFaulds Lake chromites, silicate inclusions of serpentine and tremolite have been observed in the chromites. The inclusions of serpentine and tremolite in the chromites of this study have been documented to undergo sintering as evidenced by the concentric growth of chromites around olivines and also adcumulus growth with the presence of incomplete chromites growing around silicate. In these cases, the resultant inclusions have compositions and sometimes cleavage planes that are the same as the

surrounding tremolite silicate. Therefore, these inclusions are shown to be a result of sintering similar to silicate inclusions of chromites in the Bushveld Complex (Hulbert and Von Gruenewaldt, 1985; Fig. 6.4). However, exotic inclusions of chromian diopside, chromian magnesiokatophorite, chromian Na-phlogopite and albite have also been found in the chromites. This would appear to suggest they are exotic inclusions involved in the origin of the chromite that were a result of contamination. The McFaulds Lake dunites and pyroxenites have trace element compositions that show crustal contamination of komatiite by Na-rich TTG. However, the magnesiokatophorites analysed have high TiO_2 contents similar to that of late igneous amphiboles in ultramafic intrusions. Primary pargasites, for example, often have high TiO_2 concentrations (Embey-Isztin, 1976). Borisova (2012) in his discussion of silicate inclusions in the Oman ophiolite chromitites, discusses that the high Ti and Cr contents of the amphiboles indicate either a magmatic or high T hydrothermal environment of formation, since these elements are less mobile in the presence of low T aqueous fluids. So these amphiboles would be magmatic.

Another observation is that primary pargasite occurs as a relic grain interior to tremolite in the host silicate to the chromite in sample 486163 that has silicate inclusions of the same pargasite composition. This is evidence that the mineral inclusions are residual amphiboles similar to that of the surrounding host rock and are therefore not exotic. A similar scenario could be suggested for the Na-phlogopite although the Na-phlogopite was not found in the host silicate. Though Cr-bearing Na-, titanian phlogopites occur as late stage igneous phases in other olivine-chromite cumulates such as the host rocks to the B chromitites in the Stillwater Complex (Page and Zientek, 1987). High Cr and Ti contents in phlogopites have been shown to be enriched by metasomatism in zoning trends of phlogopites of South Africa (Field et al., 1989). If the McFaulds Lake inclusions were a result of high T metasomatism, this would affect the chemistries of the chromites themselves with enrichment in silica and titanium. However, titanium distribution has shown to be less at the cores of the chromites rather than being enriched. The lower Ti as well as primitive high Cr and high Mg contents suggest that the chemistries of the chromites are primary residual melt rather than enriched by metasomatism. Another evidence of the phlogopite being postcumulus is the presence of similar K phlogopites in the surrounding host rocks and evidence of chromite in the

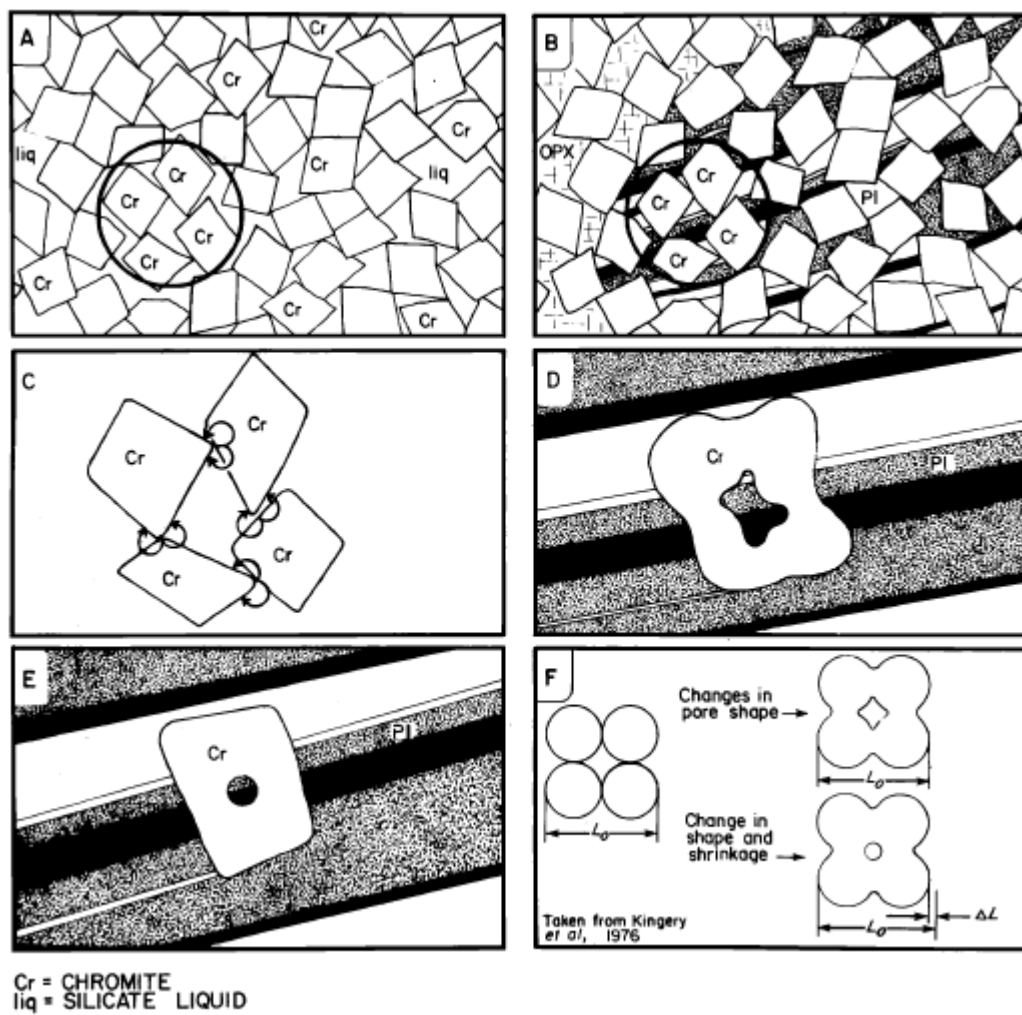


Fig. 6.4. Annealing process for the formation of silicate inclusions/atoll structures in chromite. From Hulbert and Von Gruenewaldt (1985).

intermediate stages of enveloping phlogopite minerals (See petrography chapter, silicate inclusions). Such evidence of the annealing of chromite around phlogopite has also been documented in chromites of the Western Laouni mafic intrusion in Algeria (Lorand and Cottin, 1987).

Sometimes the magesiokatophorite has been subsequently altered or the magnesiokatophorite replaces original clinopyroxene which is different alteration than the low T hydration of silicate surrounding the chromite. This shows that the silicate inclusions are often isolated from the silicate surrounding the chromite and reflects a different alteration. Often Na-katophorites have been found in silicate inclusions where there is no igneous amphibole surrounding the chromite. This could be explained by possible slumping of pulses that could have mobilized the chromite from the surroundings. In such a circumstance, the chromite composition would still be relatively similar to the surrounding host rock olivine or pyroxene magma. Another explanation that seems more plausible is that the minerals formed from residual melt encapsulated in the growing chromite. This explanation is discussed below in the discussion of Sharpe's (1983) thesis.

The high Ti and Cr compositions of the silicate inclusion-bearing amphiboles and phlogopites appear to be mantle compositions. On a Cr_2O_3 vs. Al_2O_3 plot of the phlogopites analysed, the minerals plot in the primitive mantle box and follow a trend of high Mg compositions similar to kimberlites. Also the Ti and Cr-enriched magnesiokatophorites and pargasites are similar to such amphiboles found in mantle nodules of kimberlites of the Jagersfontein and Kimberley kimberlites (Field et al., 1989). Page and Zietek (1987) discuss similar mantle-like compositions for the hornblendes and phlogopites of the Stillwater Intrusion. They reference Arima and Edgar (1981) for the solubility of titanium of phlogopites in mantle compositions. However, Page and Zietek (1987) state that the phlogopites certainly did not crystallize at high pressure and temperature mantle regimes. In their analysis of postcumulus hornblende and phlogopite compositions with height of the Stillwater Intrusion, they have shown that these compositions reflect the chromite content of the surrounding rocks. McElduff and Stumpfl (1991) have proposed that these minerals found in silicate inclusions form in the same process of postcumulus amphibole and phlogopite in the layered chromitites of the

Troodos Complex. Lorand and Cottin (1987), in their study of the silicate inclusions in chromites of the Western Laouni mafic intrusion, also concluded that the inclusions are postcumulus like the surrounding postcumulus amphiboles and phlogopites and are a result of residual liquids and late magmatic fluids.

Therefore, the silicate inclusion amphiboles and phlogopites should mimic the chromite contents of the host rocks like those of the Stillwater Intrusion. On a plot of wt. % MgO and wt. % Cr₂O₃ with height in DDH BT-09-31, it is shown that the Layer 2 chromites are more primitive than the Layer 1 chromites with higher wt. % MgO and wt. % Cr₂O₃. With the same variation in the phlogopites, it is also shown that the Layer 2 silicate inclusion phlogopites have higher wt. % MgO than the Layer 1 phlogopites. The wt. % Cr₂O₃ would show a reverse trend due to the substitution of Mg with Cr in phlogopite. For variation of Mg # with height in the same drill hole for pargasite-edenites compositions, it is also shown that Layer 2 silicate inclusion amphiboles have higher Mg # than the Layer 1 amphiboles.

It might be argued that phlogopite and amphibole mantle nodules were incorporated by the chromites from the varying primitive nature of the pulses that formed these layers. However, it is shown that the chemistry of the chromite in the Layer 1 chromitite reflects the mineralogy of the host oikocrystic harzburgite that lowers the Cr/Fe content of the chromites in that layer. Therefore, the lower Cr and Mg chromites of that layer are not reflective of a less primitive pulse. Also, it would remain to be explained why there would be mantle nodules incorporated in the chromites if the chromite itself crystallized in the magma chamber. The fractionation trends in the chromites give strong evidence that the chromites formed in a magma chamber rather than in mantle-like podiform chromitites. The newly formed chromites would have to peculiarly extract a large amount of mantle nodules from the surrounding host rock that has no evidence of the presence of mantle nodules itself. In fact, the igneous amphiboles that have been found with similar compositions to the silicate inclusion amphiboles are relic postcumulus amphiboles like those in the Stillwater Intrusion. This shows that the phlogopites and amphiboles in the silicate inclusions are derived as residual melts encapsulated by the chromite and reflect the differentiated layers rather than as mantle

nodules in the chromites. The chromite and titanium contents are derived from the chromite rather than forming under high pressure and temperature regimes of the mantle.

The presence of evolved albite in the inclusions would also preclude mantle origin. Albite would not crystallize as late igneous phases in the ultramafic McFaulds Lake complex like the amphiboles and phlogopites. Therefore, the origin of albite needs to be explained. It is suggested that the same Na-rich melt that produced the Na-magnesiokatophorites was involved in the crystallization of albite as Na-rich residual. One suggestion in the past from Irvine (1981) is that the albitic and other “granitic” inclusions formed as a result of an enhanced silica immiscibility effect with oxidation of chromite in the presence of FeO and Fe₂O₃. In such a circumstance, it might happen that the mixing lines of chromite between olivine and pyroxene will intersect the solvus and precipitate the silica-rich immiscible liquid as inclusion. Another theory for precipitation of albite is the reequilibration of previous inclusions due to metasomatism of the chromites. Often there are other salt species present in these inclusions that could allude to ingress of later fluids. The inclusions appear to be wholly enclosed by the chromite, and some fractures appear to be late with no retrogression which argues against a pathway for these migrating fluids. However, other silicates such as tremolites, chlorites and talcs that crystallized within the chromites formed the same way as later hydration metasomatism of the silicates and chromites. Clues to there being metasomatism of ionized salts are the presence of chlorites that require silicon from an outside source that can not be provided from the chromite spinels themselves.

Although there is evidence of metasomatism with retrogression, it is unlikely that the albite formed in a similar way. First of all, the retrogressive fluids are unrelated to the high alkali compositions of the albites. Also, in sample 486349, albite inclusions appear to have igneous textures in association with chromium titanian magnesiokatophorites and phlogopites. Since the magnesiokatophorites and phlogopites are interpreted as being magmatic, this is suggested for the albite as well. Albite, like phlogopite, has not been found outside of the inclusions. Also, it is not a late stage igneous mineral of an intrusion like igneous amphibole and phlogopite.

One thesis from Sharpe (1983) on chromitites in the Thetford Ophiolite Complex describes trends in chemistries of chromites and olivines toward secondary fluid

inclusion trains occurring in both chromite and olivine. The effect of the fluids on chromite was to slightly enrich the grains in ferrous and ferric iron, while decrease in Cr, Mg and Al. The effect of the fluids on olivine was to decrease the SiO₂ and MgO of olivine while increase in K₂O, CaO and NaO (Sharpe, 1983). From those observations, Sharpe (1983) concluded that the fluid that flowed through the rocks after formation contained significant amounts of Na, Ca and possible some iron. Further analysis of primary inclusions in chromite has shown that the fluids caused enrichment in Na₂O, MgO, SiO₂ and CaO, decrease in Al, Cr and Fe while no significant change in K or Ti. In comparing to inclusions in other deposits, Sharpe (1983) suggests the inclusions are not primary silicates that were included in the chromites, but were a result of later fluid to precipitate the serpentine, talc, chlorite, sulfides, pargasitic amphiboles, albite and sodic layer silicates described in these other complexes (Watkinson and Mainwaring, 1980 *in* Sharpe, 1983).

In the McFaulds Lake chromites, these types of silicates are found in the chromites, which suggests they were later incorporated into the chromites due to encapsulation of residual melt and later hydration. The enrichment in Na₂O, MgO and CaO would not be involved in forming the Na-katophorites after silicate is included since similar pargasite was found as late stage amphibole in the silicate host before being included in the chromite. However, Na-katophorites are not like the typical pargasites with lower Na₂O and CaO found as later stage igneous amphibole in complexes such as the Stillwater Complex. Sharpe (1983) suggested that the fluid inclusion trains observed in the Thetford chromites and olivines were from magmatic fluids. Clues to these fluids as being magmatic are the alkali and CaO along with MgO enrichment toward the inclusion trains. Clues to these being fluids rather than igneous melt are the textures of bubbles of fluid trains hosting the fluids and the enrichment or depletion in elements of the chromite and olivine toward these trains.

In the McFaulds Lake chromites, some of the inclusions are found as trains along growth planes in the chromites, in a similar habit to the fluid inclusion trains to the Thetford chromites. Their distribution along a growth plane in the chromite suggests incorporation of fluid during growth of the chromites since it is unlikely the chromite grew around aggregates of silicate all along the edge of the chromite (Fig. 3.29,

petrography chapter). Therefore the association of the inclusions with the growth planes suggests these were real magmatic fluids/residual melts. Sharpe (1983) mentions how there was no change in TiO_2 toward the inclusions. This suggests Ti was not mobile but represents a magmatic component to the inclusions rather than being a metasomatic feature. The Na-magnesiokatophorites of the McFaulds Lake chromites have high MgO, Na_2O and CaO similar to enrichments in these elements provided by the magmatic fluids of Sharpe (1983). Since the amphiboles are igneous with high TiO_2 and have peculiarly high MgO, Na_2O and CaO than regular pargasites, it is interpreted these inclusions as well as katophorite found in the silicate host are derived from residual melt. Naphlogopite may have been derived from similar fluids. K_2O was enriched by these fluids in the olivines of Sharpe (1983) and was probably also enriched in the formation of phlogopite.

Albite may have crystallized from these residual melts. Notably, in the fluids of Sharpe (1983), there is also enrichment in Al_2O_3 and a high enrichment in SiO_2 . These elements along with Na_2O would result in the formation of the albite in the inclusions. It may be that the albite grew in the inclusion or could have been the result of magmatic fluids being incorporated along fractures. Fractures have been found to occur along possible points of entry into silicate inclusions. Notably, retrogressive zoning has not been seen along these fractures like the retrogression that is involved in the formation of later chlorite within the chromites. However, these fluids are a different composition than the retrogressive fluids and would not cause the same extent of depletion in Cr, Mg while enrichment in Fe as the retrogressive fluids. Sharpe (1983) notes these trends in the chromites are subtle in the case of these magmatic fluids. Albite has not been found like amphibole and phlogopite as late stage igneous phases in the silicate host to the chromite. This is probably due to albite forming from residual melts specific to the chromite it is encapsulated in. Usually, albite is found in cases of granophyres and incorporation of wall rock in the intrusion. Since there is no indication of wallrock contamination in the immediate surrounding dunites and pyroxenites, and cracks have been found in association with the silicate inclusions, the albite probably grew within the silicate inclusions from residual melt.

This may or may not be the case for the igneous amphiboles and phlogopites since the growth and incorporation in some cases incorporated pargasite whereas in other cases magnesiokatophorite is found in the inclusion but not in surrounding silicate. Either the chromites were later mobilized in a different location than surroundings with slumping or filter pressing or the magnesiokatophorite grew in these cases in the inclusion. It appears more probable that the amphibole grew within the inclusion since chromite surrounds other exotic minerals such as the Na phlogopites. Either way, all these minerals are late stage phases to the intrusion, and since there is not a magmatic chemical association of the chromite with these minerals, they all crystallized as melt encapsulated by the chromite. It could have been argued that in some circumstances, the negative crystal faces of the silicate inclusions within the chromite make them in equilibrium with growing chromites. However, closer examination shows that these negative crystal faces of the inclusions surround an inclusion of multiple minerals and are not related to single crystal growths in the chromite. Therefore, these structures are interpreted to be wholly related to the crystal face structure of the chromite itself. The nature of how the chromite grew around the silicate is either by annealing or adcumulus growth of individual chromites.

There are other references to katophorite, Na-phlogopite and albite silicate inclusions in chromite being formed from precipitation of magmatic fluids. McElduff and Stumpfl (1991) argue the inclusions in the Troodos chromitites are intimately linked to a reducing chloride-rich fluid within the magmatic system where chromite is either transported within this fluid or extracted from the melt. An Na-rich and Ca-rich hydrous phase probably separated from the melt due to decreasing pressure related to the opening of the system (McElduff and Stumpfl, 1991). Within the Troodos chromitites, the layered complex chromites have different compositions of silicate inclusions than the lower mantle podiform chromites. The podiform chromites bear orthopyroxene, clinopyroxene, hornblende, olivine, serpentine and chlorite while the chromites in the layers bear pargasitic amphibole, serpentine, chlorite and albite (McElduff and Stumpfl, 1991). The latter set of inclusions is more similar to the pargasite, serpentine, chlorite and albite found in McFaulds Lake chromites. Inclusions in Troodos have been noted to become more Na and Fe-rich toward these layered cumulate chromites. The

compositional difference of the inclusions is probably reflective of the different environments of formation – the layered chromites being more evolved and alkalic than the podiform mantle chromites.

The association of these inclusions with layered chromite suggests the inclusions are related to the magma chemistry of the chromite evolution, rather than being exotic assimilants. Li et al. (2005) discuss the inclusions of the Merensky Reef and explain the Ti and Na-rich compositions as being due to volatiles that formed with dissolution of rutile and pyroxene as the fluids were expelled from the underlying cumulus pile. In the Merensky Reef chromites, silicate inclusions have been found to contain Na phlogopite that is more Na-rich than the matrix, similar to the case of there being Na phlogopites only in the inclusions of the McFaulds Lake chromites. Li et al. (2005) report oxygen isotopic data of the inclusions as having a bulk $d^{18}\text{O}$ value of 7 ‰. Plagioclase-orthopyroxene, orthopyroxene-chromite and orthopyroxene-phlogopite δ values suggested equilibration temperatures near 1200 °C using the fractionation factors of Zheng (1991, 1993) in Li et al. (2005). This shows that higher T magmatic fluids were involved rather than low T fluids in the precipitation of these alkali minerals. The addition of Na-K rich fluid occurred during chromite crystallization on the floor of the magma chamber (Li et al., 2005).

It appears that the exotic minerals in the silicate inclusions crystallized from residual melt encapsulated by the growing chromite. In sample 486211, there appears to be an association of silicate inclusion with the finer more disseminated grains rather than the larger chromites. The observation of more silicate inclusions in chain-like disseminated chromite was also made in the semi-massive chromitites of this study. Also, inclusions are found along growth planes within original chromites. Since the inclusions are preferentially found in smaller, later chromites, this would suggest that there are multiple generations of chromite in the samples: the first being primary magmatic chromite crystallization of larger, primitive chromites in the melt followed by further growth of chromite that encaptured the melt that later precipitated the silicate inclusions. The later growth of chromite that encaptured magmatic fluids is suggested by the presence of enriched Cr_2O_3 in the inclusions of diopside, magnesiokatophorite and phlogopite. The fact that there is Cr_2O_3 in these minerals suggests these minerals

incorporated Cr₂O₃ from pre-existing chromite. Since magmatic fluids have been shown by Sharp (1983) to cause subtle exchange with chromite, it is possible that the chromites in the presence of inclusions have slightly more diffused compositions. Although, there has not been evidence observed for this in these chromites, perhaps since diffusion is subtle.

The primary silicate inclusion minerals have unique compositions. The phlogopites and igneous amphiboles appear similar to metasomatic phlogopites and amphiboles in the upper mantle. Although these inclusions are not from the upper mantle, they probably formed from essentially similar magma chemistries. Page and Zientek (1987) concluded that the postcumulus phlogopites and amphiboles derived their chromium from the chromites themselves. Lorand and Cottin (1987) concluded that the minerals are a result of dissolution of chromite. In their discussion of metasomatic minerals in peridotite nodules of kimberlites, Erlank et al. (1987) suggest these minerals inherit Cr from the Cr-spinel with the Mg being of peridotite heritage. An overall reaction for the formation of metasomatic minerals in the upper mantle is Olivine + enstatite + garnet + diopside₁ + Cr-spinel + fluid (K₂O etc., H₂O, CO₂) → phlogopite + K-richterite ± diopside₂ + Cr-spinel₂ ± calcite ± LIMA, ilmenite, rutile, armalcolite, sulphides. The same magnesian olivines and pyroxenes + chromite + fluids are probably involved in the formation of the silicate inclusion minerals. Notably, the pyroxenes, amphiboles, phlogopites, and chlorites probed in this study all have very magnesian compositions. These minerals would be linked to the magnesian heritage of the host magma to the chromite. Albite, which has a more crustal-like composition, is suggested to be derived from the transformation of plagioclase toward its Na-end member due to hydrothermal fluids (Lorand and Cottin, 1987). This is also suggested by the presence of Na-phlogopite and Na-magnesiokatophorite in the inclusions alone as opposed to the surrounding silicate host rock.

6.5 Origin of chromite: Irvine's 1977 magma mixing model

Since there are problems with the theory of silica addition alone, it is proposed that the chromitites crystallized by means of magma mixing of two different magmas. In the case of the McFaulds deposits, one difference between the magmas is the lesser vs. more crustally contamination in the pyroxenite vs. dunite. Irvine (1977) explains that in a

magma chamber, there was first differentiation causing accumulation of dunite to pyroxenite, and then a new replenishing olivine-laden magma pulse mixes with the residual melt, left after pyroxene accumulation, to drive the melt into the chromite stability field to rainout chromite (Fig. 6.5). Eventually with fractionation the melt will migrate into the pyroxene only field. This order of crystallization is seen in the petrography of the oikocrystic harzburgite/semi-massive chromitites where olivine crystallized first followed by chromite which is in turn overgrown by intercumulus pyroxene. Specifically, Irvine (1977) demonstrated that if a new input of magma was injected into one that had reached a higher degree of fractionation, the resultant mixing action could inhibit the fractional crystallization of silicate minerals such as olivine and orthopyroxene and permit the crystallization of chromite alone. As illustrated in Figure 6.5, the mixing of liquid A which is on the olivine – chromite cotectic, with liquid D on the orthopyroxene field may, provided that points on the mixing line lie above the liquidus surface, culminate in a hybrid magma such as AD which will intersect the liquidus in the chromite field on cooling. Hence it will crystallize chromite alone while it moves to point X on the olivine – chromite cotectic, and thereafter it will continue to crystallize chromite and olivine.

It has been shown that the decrease in the solubility of chromite in basaltic magma in equilibrium with chromite per degree centigrade fall in temperature is greater at high (1,300°C – 1,400°C) than at low (1,100°C – 1,200°C) temperature. Due to this concave – upward curvature of the solubility curve, the mixing of two magmas at different temperatures saturated (or nearly saturated) in chromite places the resultant mixture above the saturation curve, which suggests that point AD in Figure 6.5 is likely to lie above the liquidus. The suggestions by Irvine (1977) are consistent with observations on chromitites in layered intrusions. Most significant amongst these observations is the fact that most of these chromitite layers occur at the base of well defined cyclic units (e.g. Bushveld Complex and Great Dyke in Southern Africa) or at/near the base of similar cyclic units. Further evidence comes from the textures of the underlying rock units which indicate a common cotectic crystallization of chromite with olivine or orthopyroxene showing that the magmas previously in the chambers were

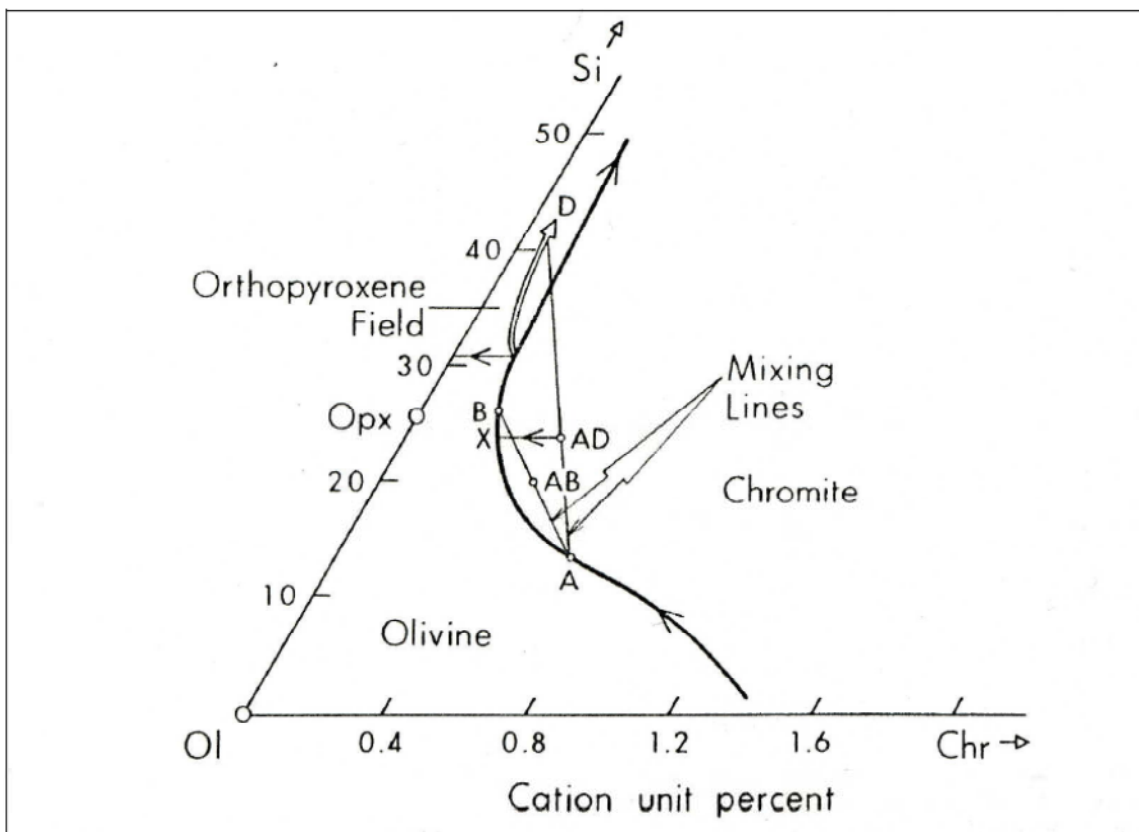


Figure 6.5. Phase Relations in the System Olivine-Silica-Chromite as determined by Irvine (1977) illustrating the consequence of mixing primitive magma (A) with well fractionated (D) and slightly fractionated (B) variants of the same primitive magma. From Naldrett et al. (1990) *in*: Gowans (2009).

saturated with respect to chromite. In the case of the McFaulds Lake chromitites, the Cr-saturated magma would be the melts that accumulated either the dunite or the pyroxenite.

There is evidence for magma mixing for the McFaulds Lake chromitites in the different multielement and PGE chemistries between the host dunites and pyroxenites of the three chromite deposits. The differences in trace element patterns are due to evolved and more crustally contaminated vs. primitive and less crustally contaminated magmas before the onset of chromite crystallization. Barnes and Maier (1999) have shown that in the Bushveld Complex, the magma mixing of a high-MgO basalt or U-magma that is SiO₂ and LILE-enriched and the A- or tholeiitic magma would result in the mineralization of the Merensky Reef PGE sulphide zone. Other evidence of there being two magmas are in the higher PGE, lower Pd/Ir of the U-magma in contrast to the lower PGE and higher Pd/Ir of the A-magma (Barnes and Maier, 1999). The terms of the two magmas involved are derived by studies on the J-M Reef by Todd et al. (1982) where U-type refers to an ultramafic magma that is PGE-rich and A-type refers to an anorthositic magma that is sulphur-rich. There is evident contrast in the behavior of the elements between the dunite and pyroxenite of the three deposits. For the trace element compositions, the dunites are more trace element and REE-depleted and provide primitive fresh magmas to the more evolved pyroxenites (Fig. 6.6). Contrasting REE contents are evident in other deposits such as the more crustally contaminated upper peridotites vs. the websterites of the Kemi Intrusion in Finland (Linkermann, 2010).

Mungall (2012) further explains the model as the mixing of S-undersaturated, high IPGE-bearing magma with S-saturated low IPGE, higher Pt/Pd restite, in this case, the mixing of a parental picrite with mantle residue. In the case of the McFaulds Lake chromite deposits, there was mixing of a S-undersaturated, higher IPGE:PPGE U-type olivine-bearing magma with S-saturated, lower IPGE:PPGE A-type pyroxene-laden magma. In the case of Black Label, there would be the magma mixing of a highly S-undersaturated dunite with the highest S-saturated pyroxenite of the three deposits (Fig. 6.7). Contrasting PGE contents of dunite vs. pyroxenite are also evident in the higher IPGE:PPGE peridotites vs. the lower IPGE:PPGE websterites of the Kemi Intrusion (Linkermann, 2010). For Black Thor, the dunite is not as highly undersaturated which probably makes it more capable of precipitating PGE sulphide. Pyroxenite is less highly

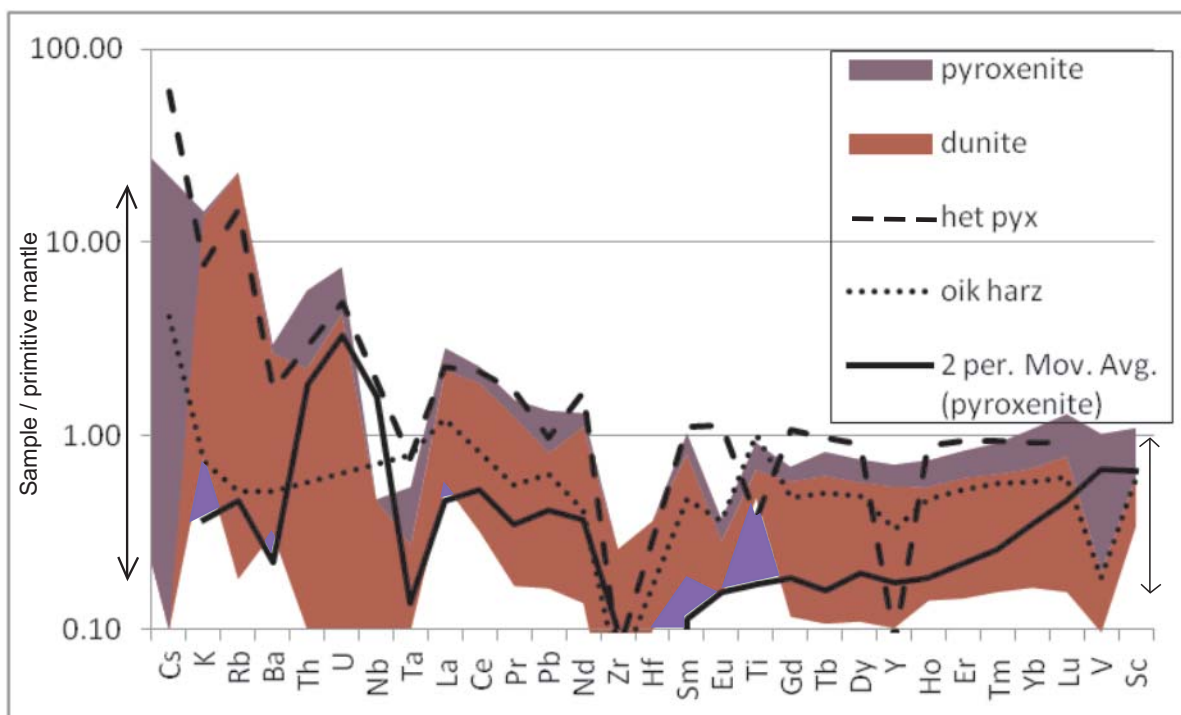


Figure 6.6. Different primitive mantle normalized multi-element patterns of dunite and pyroxenite give evidence of magma mixing of the different compositions. Intermediate heterogeneous pyroxenite and oikocrysticharzburgite are also plotted.

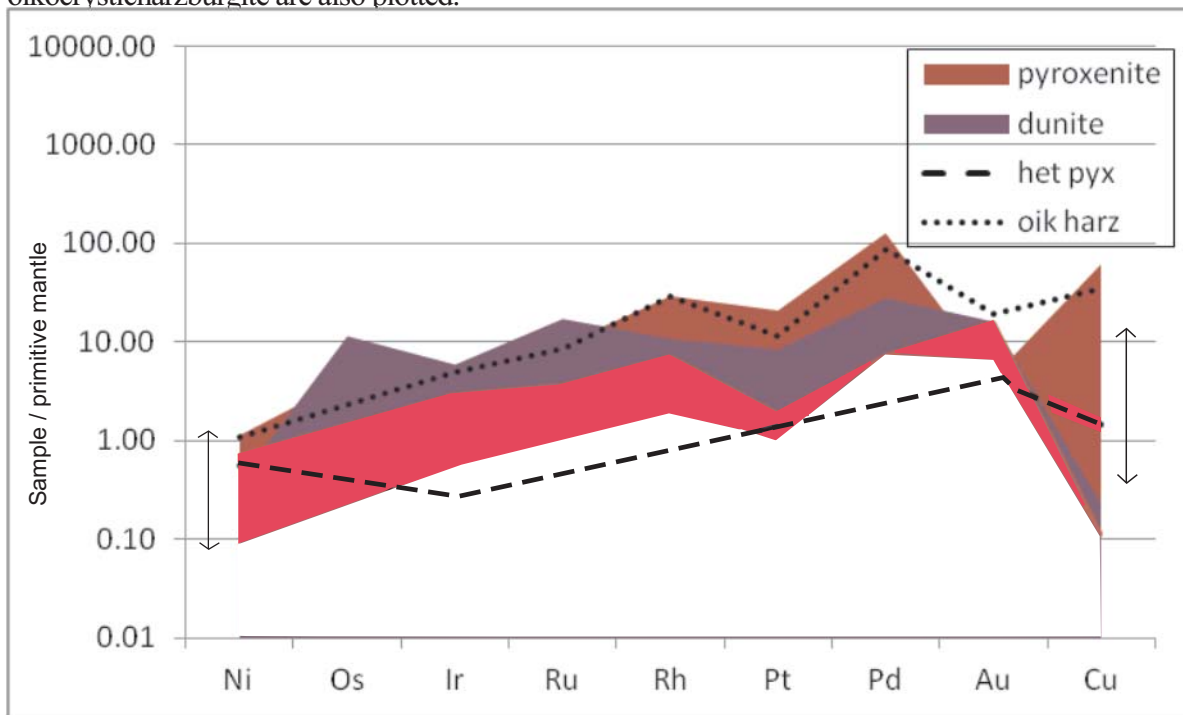


Figure 6.7. Different primitive mantle normalized PGE patterns of both dunite and pyroxenite give evidence of magma mixing of the different compositions. Intermediate heterogeneous pyroxenite and oikocrysticharzburgite are also plotted.

S-saturated. In this case, a S-saturated, crustally contaminated pyroxene magma probably mixed with S-undersaturated, less crustally contaminated dunite magma to cause chromite crystallization. The case is similar with Big Daddy, only there is more evidence of LILE enrichment within the dunites and pyroxenites which is probably a local phenoma since this signature is not found in all the samples. In terms of petrography, intermediate compositions of heterogeneous pyroxenite in Big Daddy and oikocrystic harzburgite in Black Label show intermediate trace element and PGE chemistries between the dunites and pyroxenites of the deposits.

At McFaulds Lake, a U-type olivine-laden magma, represented by dunite, is the main carrier of Cr_2O_3 with the amount of Cr_2O_3 increasing rapidly with the amount of olivine (Sharpe and Irvine, 1983). In the deposits, disseminated chromite-bearing dunites commonly contain finer intercumulus to cumulus chromite that surrounds the primary olivine grains. The A-type pyroxenite, in contrast, is close to saturation with chromite even when Cr-free. Therefore there is not more than trace Cr_2O_3 in the pyroxene-laden magma before there is crystallization of chromite (Sharpe and Irvine, 1983). This trace chromite is characterized by the disseminated chromite in pyroxenite. The mixing of Cr-undersaturated olivine magma with Cr-saturated residual pyroxene magma will then cause the precipitation of chromite that segregate into layers.

Textures of interstitial and net-textured chromite may suggest evidence for separation of an immiscible oxide melt. The separation of an immiscible oxide melt, as described by Pavlov (1977) is the process of liquation of an ore-silicate melt and the crystallization of the two separated liquids, essentially silicate and essentially oxide in nature. In this definition, it is noted that the two liquids are just separated without any particular order of crystallization. In the Black Label and Black Thor sequences, it was noted that the chromite crystallizes post olivine from the melt left behind in the interstices of the olivine cumulate. This makes sense if the melt is driven toward chromite stability after separation of cumulus olivine. Therefore, any olivine cumulate can leave behind an immiscible chromite melt.

In their discussion of podiform mantle chromites, the same interstitial chromite textures are evident due to this unmixing (Ballhaus, 1998). However, although this is evident in disseminated chromites, there needs to be a condition where massive chromite

is formed without there being wholesale mantle melting (Ballhaus, 1998). That is, if immiscible oxide melts were separated out of an olivine magma everywhere, there would be a common occurrence of chromite with dunite. However, the massive chromitite horizons are typically found between dunite and pyroxenite sequences with distinct chemistries as far as Cr-saturation. It would be more probable for separation of an immiscible oxide melt under certain conditions where the magma reaches Cr stability near certain evolved olivine magmas and certain primitive pyroxene magmas. However, the limited occurrence of massive chromite within these lithologies suggests the chromites are a product of the specific mixing of two different magmas and is more site specific than would be suggested by separation of an oxide melt.

The magma mixing of differing trace element and PGE-bearing magmas is more difficult to explain for chromitites since chromites host PGE as alloys in their structure in contrast to the silicates and have very little trace element and REE (Barnes and Maier, 1999). Therefore, the chromites can not be represented as magma compositions with olivine and pyroxene. The very thick chromitite intervals also make them harder to explain for a simple mixing model since some condition needs to keep the magma dithering in chromite stability. Therefore another mechanism is needed to explain the presence of the thick chromitite layers: namely, double diffusive convection after repetitive injections of magma.

6.6 Evidence for magmatic differentiation by double diffusive convection: The electron microprobe results.

6.6.1 Magmatic differentiation

Past microprobe studies demonstrate that chromite compositions vary substantially with respect to changes in Mg#, Cr/(Cr+Al), $\text{Cr}^{3+}/(\text{Fe}^{3+}+\text{Fe}^{2+})$ and elemental Cr^{3+} , Fe^{3+} and Al contents. Research has shown that Cr, Cr/Al, Cr/Fe and Mg# typically decreases while Al and Fe increases from basal chromitites upward in stratigraphy (Cameron, 1982, 1977; Irvine, 1975; Eales and Reynolds, 1986; Jackson, 1969). Commonly there is increase in Cr and Cr/Al while Fe decreases, making Cr/Fe increase while the Mg# decreases (Eales and Reynolds, 1986; Teigler and Eales, 1993; Teigler, 1999; Engelbrecht, 1985). The explanation for the general decrease in Cr, Cr/Al, Cr/Fe and Mg # and general increase in Al and Fe relates to disseminated chromitites hosted in

more evolved magma i.e. from dunite at the bottom, to pyroxenite, to leucogabbro at the top. Increasing Cr, Cr/Al, and lower Cr/Fe towards the top of intervals relates to differentiation from primary dunite to pyroxenite, and then a new pulse of magma mixes with the residual melt to drive this mixed magma batch into the chromite stability field and causes rainout of new chromite towards the tops of some intervals. Eales and Reynolds (1986) and Naldrett (2009) also document trends in enrichment in Cr/Al in the UG 2 chromitite and explain the increase as due to Al declining in the spinel phase after plagioclase is nucleated in the liquid.

In the McFaulds Lake chromites, there is evidence of magmatic differentiation in the form of cascading upward decreasing trends in MgO and Cr₂O₃, while increasing FeO and Al₂O₃ with height in layers, one on top of the other with pulses evident at the decimeter scale. These trends are particularly evident in the Black Label and Black Thor drill intercepts analysed. From one pulse to the next, there are enrichment trends in MgO and Cr₂O₃, while decreasing FeO and Al₂O₃. Since there is an association of increasing MgO with Cr₂O₃ and there is no plagioclase observed in the zones, the interpretation of increasing Cr/Al in the deposits as due to the buffering by plagioclase can be discarded. Rather, since MgO decreases with Cr₂O₃ and chromite is known to be a petrogenetic indicator of the melt, it is interpreted that these trends are due to replenishing pulses of magma followed by differentiation trends of the magma afterward (Irvine, 1965).

Evidence that the chromite is chemically related to the host rock are the high vs. low Al₂O₃ content of the Black Label Layer 1 vs. Layer 2, from which greater Al₂O₃ reflects greater pyroxene. In Layer 1, the greater silicate content also lowers the Cr/Fe ratio with more disseminated chromite. A few primary olivines have also been probed in the two layers where olivines of Layer 1 are more evolved with Fo #s of 80 to 85 whereas olivines of Layer 2 are more primitive with Fo #s of up to 94. Another evidence of these major oxide trends being due to magmatic differentiation is that they are common in layered intrusions and have relatively good antipathetic correlations to each other: MgO being antipathetic with FeO and Cr₂O₃ being antipathetic with Al₂O₃ due to direction substitution of the elements in the tetrahedral and octahedral sites of the chromite structure. These direct correlations have also been documented from other intrusions such as the Bushveld Complex (Stowe, 1994).

From disseminated to massive chromite, there are trends toward homogeneity in Cr_2O_3 as can be seen in the Big Daddy massive chromitite intercept. Although there is less of a decrease of Cr_2O_3 upward in each pulse, there is still a more direct decrease in MgO. This phenomenon has not been studied to any extent in other massive chromitite intervals of the world. Since there is no plagioclase in the surrounding lithologies to buffer the Al and cause an increase in Cr, it is proposed that the lesser decrease upward of Cr in these cycles is due to double diffusive convection. The theory is explained below.

6.6.2 Double diffusive convection mineralization

Double diffusive convection is a type of magma mixing where a flux of one property of a system is imposed on the gradient of another property with a different molecular diffusivity to produce a series of convecting layers (Campbell, 1996). A magma with a compositional density gradient when cooled from above will break up into two horizontal convective layers separated by an interface or boundary layer across which heat and composition are transported by molecular diffusion. Heat is transferred across the interfaces and causes instability and convection in the layers above and below, while the composition of the layer changes little to preserve “stable” density steps between the layers (Fig. 6.8). Total density is greatest in the bottom layer and density contrasts in a system will increase in time between individual double diffusive convection systems (Fig. 6.8).

There is a trend of increasing density in the bottom layer while decreasing density in the top since there is a loss of heat in the bottom layer while a gain of heat in the top (Fig. 6.8). In a layered intrusion chromite-PGE interval, the gain in density in the bottom layer is shown by replenishment with increasing Cr, and Cr/Al in the chromitite upward while the decreasing density in the top layer is shown by less decreasing Cr and reverse grading in the chromitite downward. An example of this system in progress is the top vs. bottom chromitite intervals in DDH BT-08-10. For PGE, top and bottom peaks in PGE first mineralize with initial sulphur saturation in the respective top and bottom convective layers in a double diffusively convecting chromite-PGE mineralizing system (Fig. 6.9).

At the early stages, the PGE contents increase more so in the bottom convective layer while decrease in the top convective layer due to the respective increasing density of mineralization in the bottom convective layer while decreasing the density in the top

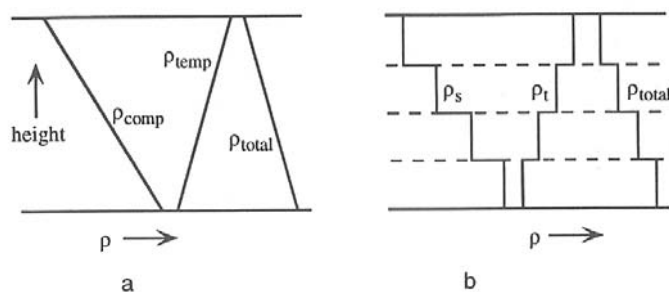


Figure 6.8. Double diffusive convection. a) In the magma chamber, density of crystallization is greatest toward the bottom convective layer, while temperature is initially the lowest in bottom convective layer. The density contrasts in the chamber cause development of the separate convection cells. b) With time, a series of double diffusion convection systems develop in a step-wise manner with density increasing toward the bottom layer due to settling mineralization and contrast in temperature. With time, the bottom convective layer increases in temperature with burial of cumulate and/or mineralization (Campbell, 1996).

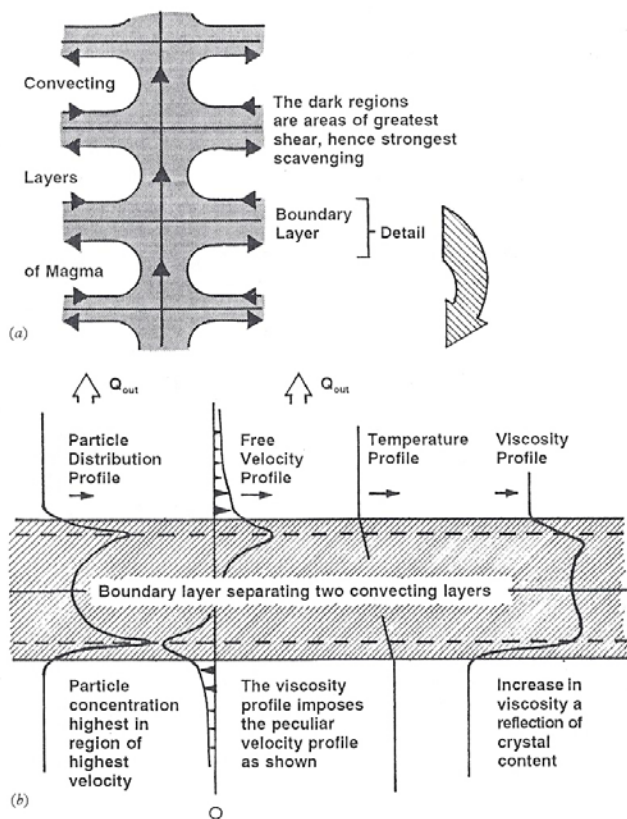


Figure 6.9: Double diffusion convection cells in the magma chamber with associated mineralization: a) The boundary layer is contained between top and bottom convective layers of a double diffusive convection system. Upwellings of magma heat the bottom of the overlying top layer which in turn cycles down into the bottom convective layer. b) Details of boundary layer: Heat first transports up with fluid, then cools down and crystallizes refractory chromite and PGE in top and bottom peaks of the respective top and bottom convective layers. With time there is an increasing velocity in top convective layer thereby increasing the mineralization, while decreasing velocity in the bottom convective layer. This is due to the temperature differences between the top and bottom layers (Rice and von Gruenewaldt, 1994).

convective layer (Fig. 6.9). Eventually, however, the PGE will increase from the top boundary layer downward since temperature drives higher velocity flow of magma in the top layer, while the bottom layer obtains slower velocity magma with more crystal accumulation (Fig. 6.9: Rice and von Gruenewaldt, 1994). Even though there is less velocity for mineralization with time in the bottom convective layer, there will still be a trend of less decreasing Cr upward since more mineralization in the top convective layer will be coupled by gravitational settling of this mineralization downward which accumulates the PGE in the bottom layer (Fig. 6.10: Rice and von Gruenewaldt, 1994). Therefore, with time there will be a pattern of increasing chromite-PGE inward ie. from the top convective layer downward and from the bottom convective layer upward in the most evolved chromite-PGE intervals.

In the McFaulds Lake chromites of the Big Daddy interval, it can be seen that there are less decreasing Cr_2O_3 contents while MgO decreases to a further extent. Although this phenomenon is has not been studied in any detail, one thesis by Johnson (2012) on the study of the podiform chromitites in Kazakhstan also considers prominent changes in Mg # vs. Cr # with depth of the chromitite. Johnson (2012) gave two proposals for this pattern: the first that there could be reequilibration of chromite with olivine in order to decrease the Mg # or that this was a result of increased chromite to olivine with densification of the magma upward in the profile. Johnson (2012) notes that the fine-scale layering and structural continuity of the massive chromitite would need to be preserved under these conditions.

For the Big Daddy massive chromitite, it is suggested that the pattern is not due to chromite reequilibrating with olivine because there is no cumulus olivine present in the massive chromitite. However, there are definitely higher chromite to olivine contents. Therefore, there is probably densification of the magma with the actual preservation of fine-scale layering in these compositions which makes them truly magmatic. Further explanation of the double diffusive convection with the densification of the magma is proposed. One factor critical for this convection to occur is the contrasting diffusivities between a Cr-saturated olivine magma and a Cr-undersaturated pyroxene magma. The olivine magma would have a higher diffusivity than the pyroxene magma. With a new pulse of olivine magma mixed into the pyroxene magma, the diffusion of Cr from the

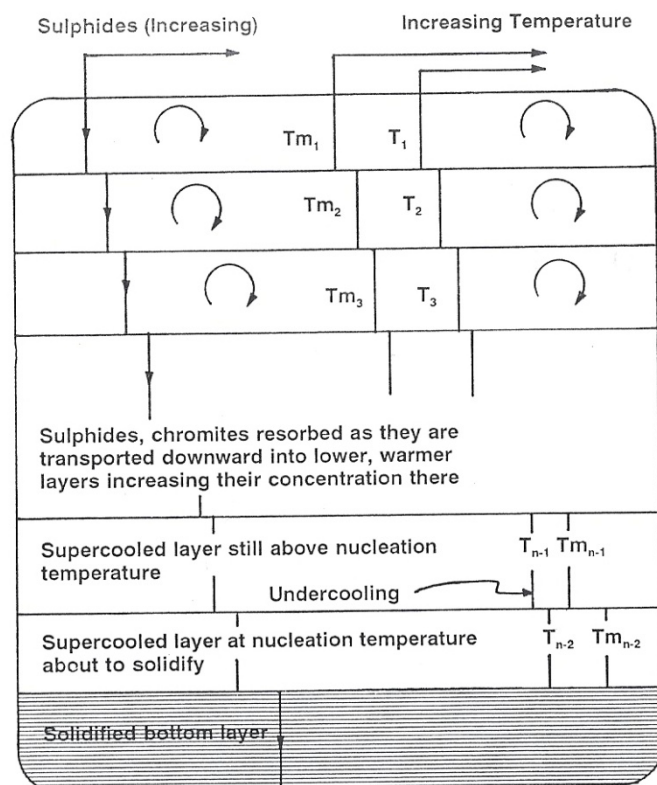


Figure 6.10: Double diffusive chromite-PGE mineralization. Separate systems develop with step-wise chromite-PGE mineralization where refractory chromite and PGE mineralize with increasing velocity of magma in the top convective layer, thereby increasing mineralization with gravitational settling in the bottom convective layer. Over time, the bottom convective layer mineralization will continue to be replenished from rainout from the top convective layer. Therefore patterns of increasing chromite-PGE from the top layer downward and bottom layer upward will develop with development of each step-wise double diffusive convection system grading upward in the magma chamber (Rice and von Gruenewaldt, 1994).

olivine magma to the pyroxene magma will cause Cr saturation and crystallization. After Cr is saturated in the underlying pyroxene magma, there will in turn be convective overturn of the resulting melt upward that will be less Cr-saturated and less dense. The next olivine magma layer higher up in sequence will mix with this less dense melt and the process will continue higher up in stratigraphy. There will be periodic interruptions in this sequence by new replenishments of olivine magma as evident by peaks in MgO contents within the overall differentiation trend. Noticeably in the 3rd pulse of the Layer 1 in Black Label, there is also more of a transition of the regular fractionating pulses to this double diffusive convecting condition. This would then progress to the more complete mineralization of the Big Daddy massive chromitite intervals. The double diffuse convection is also documented by the primary top and bottom peak PGE mineralization of many of the chromitite intercepts in all the drill holes analysed. These peaks of PGE that are commonly offset by the chromite mineralizations are due to primary individual sulphur saturating conditions of the PGE with the surrounding silicates at the beginning of the bottom layer going upward and the top layer mineralizing downward.

6.6.3 Formation of massive chromite by post-cumulus growth

In the petrography of intermittent chromitite beds, semi-massive chromite and massive chromite, there are observations in the chromite grains that alludes to post-cumulus growth of chromite following the pulsing events. In the intermittent chromitite beds, there are textures of layers with first chromite only, followed by cumulus olivine that contains intercumulus finer grained chromite. Textures of chromite interstitial to cumulus olivine suggest the chromite formed after cumulus olivine segregation. In semi-massive chromite, net to chain-like textures of intercumulus chromite within olivine also suggests this in situ crystallization. In the semi-massive chromites, the abundance of silicate inclusions within the chromites of these chains suggests the growth of adcumulus chromite. It was suggested earlier in this chapter that the occurrence of silicate inclusions in smaller chromites vs. no inclusions in larger chromites points to two generations of chromite: one being the early magmatic chromite and the second being a second-stage chromite that encaptured residual melts from the expulsion of these fluids from the cumulus pile. The fact that these silicate inclusions formed from expulsion of fluids after

cumulus segregation makes sense if their occurrence is after the larger primary chromite grains.

The presence of chromite growing in equilibrium with later igneous phases also suggests that chromite may have crystallized in the presence of H₂O. Azar (2010) cites Bannister et al. (1998) in her thesis on the Blackbird chromitites that H₂O lowers the liquidus temperature of chromite and associated olivine or pyroxene phase crystallization. This may suggest that the crystallization temperatures for growth of chromite are in fact lower than that as proposed from magmatic models of Irvine. Bannister et al. (1998) notes in her study of chromite in the Paricutin lava flows that when orthopyroxene crystallizes in equilibrium with chromite, the orthopyroxene dissolves Cr of the chromite to raise the Cr content of the orthopyroxene.

In the silicate inclusion samples, Cr-bearing pyroxene was observed in a silicate inclusion. Earlier it was suggested that the fact that there is Cr in the pyroxene, amphiboles and phlogopites suggests these silicates incorporated the Cr from the pre-existing chromite. Although there was pre-existing chromite, the chromite probably grew in equilibrium with the silicates as suggested by Bannister et al. (1998), by the Cr content in the silicates and by the fact that the magmatic fluids were encaptured in a growing chromite grain. Since Cr is also found in the amphiboles and phlogopites, it is suggested that the chromite also grew in equilibrium with these late igneous phases and that chromite probably also grew at lower crystallization temperatures. The lower crystallization temperatures and the presence of the silicate inclusions in chromite together suggest that H₂O was involved in the crystallization of chromite and associated igneous phases at least in the area of the silicate inclusions.

A hydrous component to chromite crystallization has been suggested by authors such as Johan (1986) and Boudreau (1999) in their discussion of hydrous silicate inclusions. A hydromagmatic model may be suggested for the chromitite deposits as a whole. The presence of a large amount of chromite with little magma volume may be explained by H₂O that raises the Cr content of the melt to promote chromite crystallization. This may suggest why there is plagioclase-bearing leucogabbro that occurs early after a relatively small intrusive sequence of dunite-chromitite-pyroxenite in

the Ring of Fire Intrusion. H₂O may have lowered the liquidus of orthopyroxene and in turn plagioclase crystallization according to the model of Bannister et al. (1998).

More evidence for in situ crystallization is observed in the massive chromite. In massive chromite, the chromites that were probed have more primitive larger grains and also more differentiated smaller grains. It was noted that there was more diffusion to lower Mg and Cr in the smaller grains. However, the fact that there is a general association of lower Mg and Cr with the smaller grains could be evidence that they were later grown in the intercumulus of the larger grains. In Big Daddy DDH FW-08-19, the Cr contents of the chromitite horizon appear homogeneous up the interval while there appears to be more variation in Mg content. The fact that the Mg contents are decoupled from the Cr contents shows that there was probably double diffusive convection involved in mineralizing complete chromite layers that were a result of pulses.

However, even though there is considerable primitive pulsing as seen in the Mg variation with height, there is also evidence of homogenization of these pulses, especially in the large differentiated section of the hole. There are numerous Mg pulses, but Mg contents seem to rise from below and move up through these mini-pulses. In other words, there are not perfect differentiations represented by these pulses. This is probably evidence of adcumulus growth of chromite after initial segregation of primary chromite. Another clue for adcumulus chromite is the chromite layer at the top of the section of DDH BT-08-10. The last of the chromite has a sharp boundary with the overlying dunite. Double diffusive convection could explain the formation at the top convecting layer, however, there would still be some sort of differentiation after that top layer. It is probably that chromite was formed in the intercumulus and migrated upward until trapped by an impermeable barrier at the overlying dunite sequence. Also, the adcumulus textures that fill the voids in the massive chromitites can be explained by further growth of the magmatic chromites.

In terms of silicate content, in Black Label DDH BT-09-31, there are a number of sections of oikocrystic harzburgite bearing chromite that is intercumulus to olivine but is overgrown by orthopyroxene. It was determined that the crystallization sequence was then olivine → chromite → intercumulus orthopyroxene. In the massive chromitites, there is often tremolitized intercumulus pyroxene in the matrix of the chromites. The

formation of amoeboid intercumulus pyroxene after chromite might be showing that the chromite continued to form from the reaction of the olivine and chromite with the surrounding melt. In this case, it would be a Cr and pyroxene-bearing liquid. After chromite is mineralized from the mixing of the Cr and pyroxene-bearing melt, the melt goes into pyroxene stability and pyroxene crystallizes. It is noteworthy, that the chromitite in Black Label Layer 1 reflects the textures of oikocrystic pyroxene in the host oikocrystic harzburgite. Therefore, primary chromite probably formed with the mixing of this pyroxene-bearing oikocrystic unit with dunite. Many of the samples reflect primary chromite after this mixing event. However, possibly where samples show chromite more into the intercumulus pyroxene farther away from the primary cumulus olivine, and where chromite has encapsulated inclusions, the chromite probably formed from this reaction.

In Black Thor DDH BT-08-10, some of the intercumulus pyroxene in the massive chromitite has been probed to be chromian diopside whereas other times it is orthopyroxene. Diopside has been observed as an interstitial phase to chromitites in the Uralian-Alaskan complexes of Asia (Krause et al., 2007). In these chromitites, the diopsides contain enriched La/Lu contents relative to cumulus diopside in neighbouring clinopyroxenites. Enriched diopsides have also been observed on the rims of cumulus diopside in the clinopyroxenites. Krause et al. (2007) concluded that the enriched rim and interstitial diopsides are fractionated residual melt in the pore space of the solidifying cumulate and are accessory minerals. The diopside would represent a hydrous fluid enriched in LREE which developed during the final crystallization of the pore liquid (Krause et al., 2007). In the McFaulds Lake chromites, hydrous melts that formed along with chromite crystallization have been documented in the silicate inclusions. Within these inclusions, there is also the presence of chromian diopside which gives evidence for it being a late stage igneous phase. Notably, the diopsides are chromian diopsides which implies the incorporation of Cr post-magmatic the primary chromite.

6.7 Evaluation of the conduit model

The McFaulds Lake chromites are high in grade with 50 wt% Cr₂O₃ in many of the layers with very thick intercepts. Also there has been evidence documented of magmatic breccias and deformations with sulphide mineralization, as at Black Label,

which alludes to some dynamic emplacement of the layers. There also needs to be a significant amount of magma to cause the precipitation of so much chromite. Conditions for the amount of Cr required in the magma to mineralize the amount of Cr have been discussed by Naldrett (2009) and are shown in Fig. 6.11.

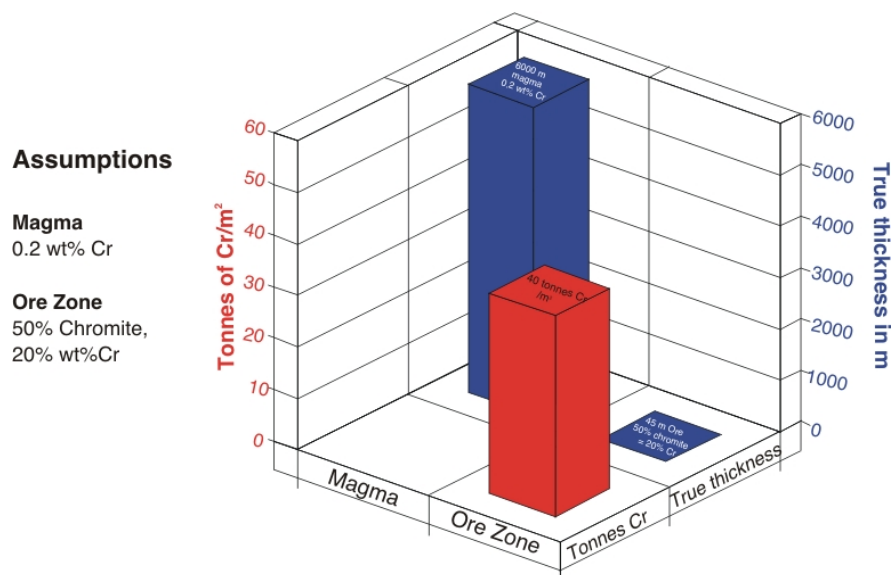


Fig. 6.11 Figure showing thickness, grade and wt% Cr in the 36 m-thick ore zone at Big Daddy, the tonnes of chromium this would amount to over each square m of the sill, and the value of magma required to produce this chromium, assuming that the magma contained 0.2 wt% Cr (a reasonable estimate for the magma likely to have produced the sill). – Naldrett (2009a)

The argument is that if there is so much chromite – a 36 m zone in Big Daddy – then there needs to have been a lot of magma to have produced so much chromite by gravitational processes. However, there does not have to be so much magma if there was a central pooling of the magmas in a conduit before being injected into layers. And the layers would still be settled out as differentiation cycles similar to that observed in the deposits. A key to debating such a case for the McFaulds deposits is to document the olivine and pyroxene silicate mineral chemistries upward in the layers along with the chromite. If olivine and pyroxene differentiate along with the chromite, then they probably mineralized by gravitational processes. If chromite was mineralized in the conduit, it would not settle out in association with the magma chemistry of the surrounding silicates which would have been gravitationally settled. In the McFaulds

intrusion, most of the olivine and pyroxene has been replaced by serpentine-tremolite-chlorite, so an in-depth study on silicate is not possible. A few olivines in samples from Layers 1 and 2 have been probed to have compositions relative to the primary chromite chemistries in those layers: Layer 1 having Fo #s of 80 to 85 in contrast to the more primitive chromite-bearing Layer 2 which has Fo #s of up to 94. Hence, this is evidence for the association of more primitive olivine with more primitive chromite layers. Also there is evidence of magmatic variation of pargasitic amphibole and phlogopite in the two layers of DDH BT-09-31.

In spite of no detailed study on primary silicates of McFaulds Lake, the olivine and pyroxene chemistries have been studied in another massive chromitite deposit, namely the 8 m-thick Ipueiro-Medrado chromitites in Brazil. These chromites have chemistries that relate to the silicate chemistries and have been proposed to mineralize by gravitational processes (Marques, 2003). Therefore, for other massive chromitites, it appears there is direct correlation of silicate-oxide that suggests gravitational segregation.

However, another important point about McFaulds Lake is that the chromite is komatiitic. Massive chromite from a different komatiitic chromite occurrence in Nunavut has been microprobed to compare with the McFaulds Lake deposits. It has compositions of 52 to 55 wt. % Cr_2O_3 , 26 to 27 wt. % FeO_T , 11 to 12 wt. % Al_2O_3 and 6 wt. % MgO . Diffusion of the chromitite is even similar with depletion of Cr_2O_3 and FeO_T to 48 and 25.75 wt. % respectively and enrichment in Al_2O_3 and MgO to 16 and 7 wt. % respectively. These compositions are very similar to the higher temperature hydrothermally retrogressed upper chromitite of DDH BT-09-17. Low-Mg komatiites can have up to 0.4 % or 3500 to 4000 ppm Cr in the magma, more than the basalts in the above diagram at 0.2 % (Baird et al., 1996).

The dunite and pyroxenite lithologies hosting the Cr deposits have been demonstrated to be aluminum-undepleted komatiite. More work needs to be done to investigate the primary magma chemistry of the intrusion. However, the chemistries of the cumulates show that the system is not basaltic as Naldrett (2009) proposed but contains more primitive magmas with higher partial melting conditions and therefore contain higher Cr to generate more chromium reserves. Other similar komatiitic-hosted thick chromitite deposits of the world include Ipueiro-Medrado, Kemi, Selukwe and

Nkomati SA (Mungall, 2010). Notably, these deposits are mineralized by many injections, one on top of the next, so there could have been many scenarios of mixing of new pulses with old ones to dither the magma in chromite stability.

Therefore, it is assumed that major amounts of chromite can be generated by a komatiite magma if there is this constant dithering. Although, to generate so much magma interaction, there should be conduit sites for feeders to the zones. As a general picture, the intrusion becomes more evolved from NW to SE from Black Label to Black Thor, while laterally the chromite mineralization branches off in doublets in the pyroxenites as it tends to do in more evolved lithologies moving NW from Big Daddy to Black Label and from Black Thor BT-09-10 to Black Thor BT-09-17. In the Black Thor zone specifically, there are 3 separate zones that differ laterally along strike: the SW zone, the Central Zone, and the NE zone with Upper-Upper Zone (Fig. 6.12). Areas where these zones intersect are domains of discontinuity. In the discontinuity between the SW and Central Zone, there appears to be NW-SE oriented displacements. These are probably faults. However, along with the fault displacement, the chromitite zones vary differently along both sides of the fault. Toward the SW, the chromitites become more massive while toward the NE, the zones branch off in doublets. Since the zones occur along the same orientation along strike on both sides of the faults, it is possible that these are feeder conduit sites for the magmas that injected into the chambers to mineralize the chromite. Notably, the intrusion has been overturned so care needs to be taken in this interpretation. However, given the preservation of the primary intermittent bedding and layering of the zones, it is possible that this is accurate. Discontinuities have been shown to be possible feeder sites in other complexes such as that of the discordant IRUP (iron-rich ultramafic pegmatite) localities in the Bushveld Complex (Reid et al., 2012).

6.8 Retrogression of chromite with hydration of the intrusion

The McFaulds Lake chromites have textures resulting from pervasive hydration, causing complete serpentinization and uralitization of host dunite and pyroxenite respectively. Along with hydration of silicates, there was reconstitution of the primary chromite ores to form either Cr-enriched or Cr-depleted ferrichromite and associated chromian chlorite. The host silicate to the chromite deposits have very few primary silicates preserved. There are a few primary olivines and orthopyroxenes preserved with

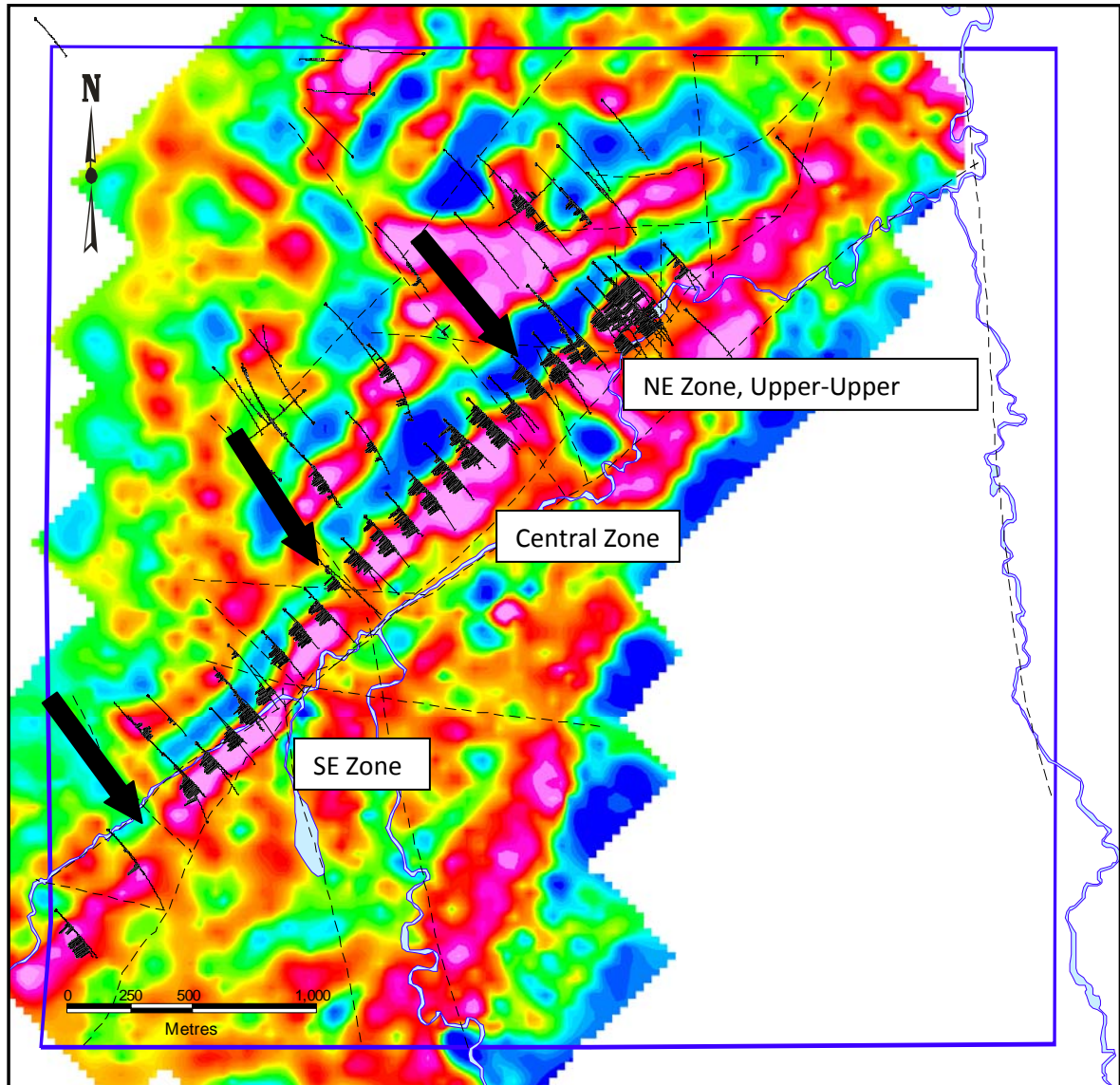


Figure 6.12. Residual gravity map with chromitite zones plotted and labeled. Possible feeder conduit sites are indicated by arrows in areas of discontinuity. From Tuchscherer (2010).

compositions suggestive of cumulus segregation of a magnesian magma. Olivines have been replaced with serpentine as evidenced by the pseudomorphing of serpentine on original cumulus olivine grains. Pyroxenes have been replaced by tremolite and talc as evidenced by tremolitization along the cleavage planes of orthopyroxene. Chemical compositions of serpentine are lizardite to antigorite and amphiboles after pyroxene are pristine magnesian tremolites. Another retrogressive mineral includes chlorite that occurs in association with chromite. The textures of serpentine after olivine suggest temperatures of formation of around 300-350 °C of H₂O hydration of the silicates (Winter, 2001).

Unlike the almost total replacement of the host silicates, the chromites are preserved with original cumulus associations of chromite in disseminated to massive chromite layers throughout the drill holes. Although, the ores have been modified and reconstituted first by diffusion with retrogressive fluids with further replacement to either Cr-enriched ferrichromite with chromian chlorite or Cr-depleted ferrichromite. Diffusion has the effect of depleting the primary chromites of Cr₂O₃ and MgO while enriching the grains in Al₂O₃ and FeO. Backscatter images of lighter areas on the margins of the grains and along cracks in the grains give evidence of variation in the chromite compositions with retrogression. The retrogression would be a result of fluids as the diffusion occurs from core to rim and along cracks where there is fluid access.

Three types of ferrichromite serve to either enrich or deplete the original chromites in Cr₂O₃. In the bulk of the samples analysed, there is either enrichment or depletion in ores with hydration. Evidence of the association of ferrichromite with the hydration that produced serpentine is not seen in massive chromitite due to absence of silicate. However, the massive chromitites occur in the same section as the serpentized disseminated chromite-bearing dunites so are inferred to undergo the same overprint. Cr-enriched ferrichromites serve to enrich the ores to compositions of up to 65 wt. % Cr₂O₃. Chlorite laths accompany ferrichromite developed interior to the primary chromite grains. The occurrence of chlorites within the primary chromite suggests breakdown and replacement of the chromite. Specifically, there must have been Si mobility in order to produce the chlorite.

Similar ferrichromite and chlorite relations in chromitites has been documented in other studies. Beeson and Jackson (1969) and Onyeagocha (1964) suggest the reaction: chromite + olivine + pyroxene + H₂O = ferrichromite + chlorite + magnetite + serpentine. In the McFaulds Lake chromites, this reaction is indicated by the simultaneous serpentinization and tremolitization with ferrichromitization and chloritization of the chromites. Cr-enriched ferrichromite and chlorite are not found in association with serpentine but rather in association with interstitial chlorite or tremolite. So there was no reaction to produce both the chlorite and ferrichromite with serpentine. Bliss and MacLean (1975) suggest there was first serpentinization. A later reaction of chromite with serpentine produces the ferrichromite and chlorite at higher grades of alteration. There is no evidence in the immediate vicinity of these ferrichromites to suggest higher degrees of alteration except for the tremolitization in DDH BT-09-17. Since there are pervasively serpentinized dunites within the same section as the massive chromites, higher degrees of hydration probably play no role.

However, in the chromites analysed, there are no associations of the ferrichromite and chlorite with serpentine and also no relations of the minerals with olivine and pyroxene. This is since the altered chromites occur within massive chromitites with no surrounding silicate rock (except for the chlorite interstitial the chromite). The chlorites are pristine Mg clinochlores with high MgO to 35 wt. %, but with low FeO_T at 1 to 2 wt. %. For mass balancing, it is inferred that the Mg and Al diffuse from the chromite into chlorite, while the Fe and Cr diffuse into the ferrichromite. There is lowering of the Cr and Mg from core to margin of the chromite grains with diffusion of these atoms into chlorite. Al and Fe however go up with substitution with Cr and Mg respectively. There must also be some SiO₂ in the metasomatizing fluids to cause the enrichment of SiO₂ in the chlorites. The SiO₂ is probably transported with the ingress of hot water.

After retrogression of the chromites to Cr-enriched ferrichromite, there was oxidation of the grains to Cr-depleted ferrichromite. Cr is degraded along with Mg and Al, while Fe increases with an especially large enrichment in ferric iron to 13 wt. % Fe₂O₃. This trend is seen in the last chromite evolution of samples 486044 and 486126 in Black Thor. It cannot be said that the Cr-depleted ferrichromite in these samples formed the same way as the bulk of Cr-depleted ferrichromites found in the drill hole intervals.

However, the association of Cr-depleted ferrichromites with more retrogressed disseminated chromites, the tendency to form chromian magnetite with further retrogression, and the fact that these grains have relics of previous chlorite suggests that these grains are similar to most of the other Cr-depleted ferrichromites. The only difference is that most of the other Cr-depleted ferrichromites have been depleted to within the 30 percentile range of Cr_2O_3 . Chromian magnetites are known to form as further retrogression from ferrichromite in other deposits of the world (Ashley, 1975 and Kapsiotis et al., 2007). The Cr-depleted ferrichromites are not exactly chromian magnetites but show the same tendency toward enrichment in ferric iron and depletion in Cr. Some magnetites have been found in the chromites of this study as well as magnetite veins cross-cutting chromite are a result of retrogression along with the magnetite with serpentine.

The chromitites of DDH BT-09-17 are the third type of ferrichromite observed in the McFaulds Lake chromites analysed. These upper chromitites have ferrichromites of high Cr-enrichment while depletion in FeO to 68 wt. % Cr_2O_3 and 20 wt. % FeO. The high Cr-enrichment along with lowering of FeO served to enrich not only the Cr content of the ores, but the Cr/Fe ratio as well. In most ferrichromites, there is a trend toward Fe-enrichment along with Cr-enrichment with hydration. The McFaulds Lake chromites have in general undergone this retrogression to enrich the Fe in these secondary chromites. However, there is a lowering of Fe in the case of DDH BT-09-17.

The lowering of FeO with ferrichromite is not well documented in the literature. One suggestion by Hamlyn and Keays (1979) regarding the Panton Sill in Australia is that the lowering of FeO in those chromites occurred with postcumulus reequilibration of the chromite. Although, it is not understood why there would be reequilibration of chromite to reduce the FeO here while enrich the FeO in chromites in the other drill hole intercepts, since they have the same mineral assemblages. An earlier paper by Hamlyn (1975) mentions that the Panton Sill chromites with this trend are the case of higher temperature chromite. Metamorphosed more aluminous spinels have undergone higher grades of amphibolite metamorphism to cause precipitation of Fe-depleted ferrichromite with hornblende. The higher T metamorphism would occur as a result of metasomatism under conditions of lower oxygen activity which would result in a reduction of FeO in the

ferrichromite. In DDH BT-09-17, there is evidence that the chromitites underwent higher T metamorphism in the thermal aureole of a neighbouring cross-cutting gabbro that itself underwent autohydration. The heat from the gabbro would reequilibrate the chromite to higher metamorphic conditions toward that seen in the Panton Sill, though not crystallizing hornblende. Hydrothermal tremolite and epidote-zoisite and sphene mineralogy of the gabbro constrain metamorphism in the upper greenschist field to above 500 °C (Apted and Liou, 1983).

In association with the Cr-enriched ferrichromite, there is pristine MgO-rich tremolite that is interpreted to be prograde. The tremolite shows textures of zoning in the grains from a core Cr₂O₃-enriched core to a Cr₂O₃-depleted margin. This shows that the tremolite is not just a replacement of clinopyroxene, but that there was an earlier Cr-enriching event. Chromian-enriched tremolites are seen elsewhere in the McFaulds Lake chromites as chromian tremolites after chromian pyroxene. However, the crystal zoning present and MgO-rich chemistries suggests these tremolites are hydrothermal. It may be that there are other hydrothermal tremolites elsewhere in drill core. However, the presence of this phase along with the ferrichromite and higher T epidotes and sphenes in the gabbro suggests the condition of higher T hydrothermalism of both gabbro and altered chromite.

In general, it is shown that the Ring of Fire Intrusion underwent complete hydration to eradicate primary chemistries of olivine and pyroxene. This autohydration occurred as a result of subsolidus cooling of this synvolcanic komatiitic sill. Autohydration had the effect of convecting water from the seawater interface down and from the bottom of the intrusion upward through stratigraphy. The intrusion cooled from the base of the intrusion upwards from magmatic temperatures of 1300°C at olivine and chromite crystallization to temperatures of 950°C in the roof gabbro. Encapsulation of residual melt crystallized with the sintering of chromites at lower temperatures of 700°C. Finally, the intrusion hydrated with the circulation of water rich in SiO₂ and CO₂, as low as 350°C with modification to serpentine. The fluids cooled the intrusion from the bottom dunites upward to the latest leucogabbros. The leucogabbros were the last to cool and retained their heat to 500°C while the lower cumulates were cooled to 350°C. Therefore, conditions of prograde modification of the upper chromitites in DDH BT-09-

17 were retained and preserved the higher T assemblages of tremolite, epidote, titanite, high Cr/Fe ferrichromite that are present in both gabbro and chromitite.

This autohydration supports that the Ring of Fire Intrusion is a subvolcanic sill. The intrusion is overlain by mafic volcanics and later intermediate volcanic that have been age dated to be coeval with the upper ferrogabbro. Other clues to synvolcanic volcanism are the komatiitic chemistry of the intrusion, the lack of thick stratigraphy that would be more suggestive of large layered intrusions, and the occurrence of thin chert horizons in the pyroxenites of some holes drilled in the Black Horse stratigraphy. These cherty silicalites represent the silicification barriers to the convecting fluids that one might see in a hydrothermal VMS system. They are found in pyroxenites which are in turn overlain by silicified volcanics of this subvolcanic to volcanic system.

CHAPTER 7

CONCLUSIONS

7.1 Conclusions

A number of conclusions can be drawn from the study of the McFaulds Lake chromite deposits. One is that the electron microprobe analyses on the chromite minerals give evidence of magmatic variation. Magmatic chemistries of the chromite minerals are displayed by linear enrichment of wt. % Cr_2O_3 vs. MgO from disseminated to massive chromite. Linear variations are also evident in the negative linear correlation of FeO vs. MgO. The variability of Cr_2O_3 and MgO with down hole depth give evidence that chromite mineralized by means of repeating successive primitive pulses or replenishments followed by differentiations with height of the intrusion. Evidence of replenishments are the occurrence of periodic Cr_2O_3 and MgO peaks or increases that are followed by decreases of Cr_2O_3 and MgO with differentiation before there is another replenishment. These pulses occur at the cm to metre scale in the chromitites.

The Black Thor and Big Daddy chromites are higher grade and distinguished from the Black Label chromites. The compositions of the Black Thor and Big Daddy chromites range from 49 to 53 wt. % Cr_2O_3 while the Black Label chromites range from 46 to 50 wt. % Cr_2O_3 . The Black Thor and Big Daddy chromites also have higher Cr/Fe at 1.53 to 2.90 in contrast to the lower Cr/Fe of Black Label at 0.98 to 2.42. In the Black Label chromites, there are textures of pyroxene oikocrysts and olivine aggregates with wavy layering suggestive of dynamic deposition with magma mixing with oikocrystic pyroxene-bearing ultramafics. With greater modal % silicate, there are lower Cr_2O_3 and MgO contents which makes the ore lower grade than the Black Thor and Big Daddy chromites. The Black Label chromites are also distinguished from the Black Thor and Big Daddy chromites in the laser ablation analyses. There are higher negative Ni

anomalies and higher positive Ti and Fe anomalies suggestive of more fractionated chromites.

The massive chromitite of Big Daddy DDH FW-08-19 shows more subtle change in Cr_2O_3 vs. depth in contrast to the more varying Cr_2O_3 compositions from the massive to the disseminated chromites in Black Label DDH BT-09-31 and Black Thor BT-08-10. Even though, there is subtle change in wt. % Cr_2O_3 in the massive chromite, pulses are still evident in the variation of wt. % MgO with depth. The high Cr_2O_3 and MgO compositions of the chromites and less variation from core to rim rule out the possibility that these chromites have been reequilibrated to mask primary compositions. Also there is the same variation in core chromite compositions in the massive Big Daddy chromites as the massive chromites of the Black Label and Black Thor intercepts. Therefore, the similar Cr_2O_3 compositions of the Big Daddy chromites are probably a result of real igneous processes. A theory for subtle decrease of wt. % Cr_2O_3 upward is that these chromites are a result of a cascading effect of double diffusive convection cells upward. Repeating convection cells cause chromite deposition in upward succession whereby the more progressively filled cells have more primitive Cr_2O_3 compositions. Upward in stratigraphy, the double diffusive convection effect wanes and differentiation is evident by the slightly decreasing Cr_2O_3 compositions before the next pulse takes place.

The chromites mineralized as both primitive settled chromites and later in situ chromites. In some of the replenishments of the Big Daddy chromites, there are distinctly higher MgO compositions than the MgO compositions in the chromites higher in a pulse. The distinction of high, early MgO compositions from lower, later MgO compositions support evidence of there being two generations of chromite: an early primitive settled chromite and a later in situ crystallized chromite. The occurrence of distinct high MgO compositions vs. lower MgO compositions at the same depth in some instances indicates that the variability of core compositions is due to some chromites being early settled chromites while others follow with later in situ crystallization of the interstitial melt. There is variation from lower to higher core wt. % Cr_2O_3 and MgO compositions in all the chromite intercepts which indicates that this succession in chromite mineralization is characteristic of all types of chromite. For textural evidence, massive chromites often contain very primitive cores of large grains that are the early

settled chromites along with later smaller chromite cores that are later in situ chromites with lower Cr_2O_3 and MgO chemistries. Textures of chain and net-textured chromites in semi-massive chromites support the crystallization of chromites interstitial to cumulus olivines.

Round silicate inclusions in some chromites vs. no inclusions in others supports the interpretation that there was an early deposition of primary settled chromite followed by in situ chromite that encaptured late igneous melt exsolved from a compressed cumulus igneous pile. The silicate inclusions have igneous amphibole and phlogopite with high Ti compositions that identify original igneous minerals. The prevalence of these inclusions in chain and net-textured semi-massive chromites suggests these chromites are later in-situ chromites that encaptured residual liquid. The idea that the primary core chromites do not have these inclusions and that the inclusions are late igneous phases of the intrusion rules out the possibility that they are remnants of exotic contaminants that were involved in chromite crystallization.

The chromites reached stability by magma mixing between the olivine and pyroxene fields, rather than by means of silic contamination. This is suggested by the fact that silicate inclusions are related to magmatic fluids introduced with compression of the igneous pile, the fact that the chromites occur between dunite and pyroxenite lithologies in any order, the fact that disseminated cumulus chromite sometimes occurs in pyroxenite before a massive chromite interval (e.g. DDH BT-09-17), the lack of evidence of assimilated xenoliths, the occurrence of both pyroxene and olivine inclusions in juxtaposed chromites and the distinction of trace element and full spectrum PGE signatures of dunite vs. pyroxenite.

There is variation of decreasing wt. % Cr_2O_3 and MgO in the chromites from core to margin of chromite grains that is evidence of zoning in the chromites. Since the location of this zoning is prevalent on outer margins, along cracks of grains, in smaller grains and surrounding silicate inclusions, the zoning is attributed to retrogression rather than silicate exchange with primary intercumulus silicate. The decrease in wt. % Cr_2O_3 and MgO is due to silicate exchange with interstitial and rim retrogressive chlorites. This diffusion is part of the modification of the chromite with hydration.

The primary chromites were later retrogressed to rim ferrichromite and chlorite. Mg and Cr ions are leached from the chromite while Al is enriched due to reaction forming ferrichromite and chlorite. The formation of ferrichromite and chlorite occurs along with the serpentinization of the dunites and tremolitization and chloritization of the pyroxenites. These reactions occur as the intrusion underwent greenschist subsolidus hydration at 300-350°C.

In the chromites of DDH BT-08-17, there is different variation with diffusion from chromite core to rim to lower wt. % Cr₂O₃, but higher wt. % MgO. The variation of Cr₂O₃ and MgO with depth do not show much evidence of magmatic fractionation. There is evidence of zoned tremolite interstitial the chromite grains in massive chromite in this interval. Since there is increase in wt. % MgO rather than decrease and there is zoned tremolite, it is proposed that this upper chromitite underwent higher temperature retrogression than the chromites in the other intercepts. The chromitite in this intercept is intercalated with gabbro. Petrography of the gabbro shows tremolite replacement of pyroxene, epidote-saussurite replacement of plagioclase and sphene mineralogy that support higher temperature retrogression in the gabbro. The bulk rock chemistry of the gabbro shows that it contains nil Ni and Cr and is therefore not saturated to warrant chromite mineralization. The higher T retrogression of the gabbro, the nil Ni and Cr and the intercalation of massive with no disseminated chromite in gabbro support the interpretation that the gabbro intrudes the upper chromitite, and that the heat of the gabbro caused prograde alteration to higher degrees C in both the gabbro and surrounding chromitite. Therefore, the diffusion to higher wt. % MgO from core to rim in the chromites is due to higher T retrogression. Along with diffusion to higher wt. % MgO, there was retrogression to higher wt. % Cr₂O₃ in the altered ferrichromite rims. It is proposed that higher T retrogressive fluids caused Cr₂O₃ enrichment in the ferrichromite rims to these chromite. These ferrichromites have the highest Cr₂O₃ compositions and serve to enrich the chromite ores in the interval.

7.2 Summary

From the study of the McFaulds Lake chromite a sequence of events can be deduced:

1. Regional WNW-ESE trending faults and NNE-SSW oriented faults related to rifting are the locus of the magma to the Ring of Fire magma chamber.

2. As the komatiitic Ring of Fire magma intruded the Oxford-Stull Terrane basement TTG, there was crustal contamination of the magma to produce large negative Nb-Ta and Zr-Hf anomalies in the geochemical signatures of the komatiitic magma.
3. The feeders of the Ring of Fire intrusion intruded in NW-SE oriented faults that are seen as displacement of the linear chromite zones.
4. In the McFaulds Lake sequence of the Ring of Fire magma chamber, there was first the pulsing and settling of primitive dunite. On the roof of the initial magma chamber, there was pyroxenite. In the Black Label sequence, primitive pulses of magma represented by the dunite mixed with pyroxene under dynamic conditions to crystallize oikocrystic harzburgite. In this dynamic environment, there was magma mixing of pyroxene in the primitive olivine pulse to dither the magma into the Cr field and crystallize the Black Label Layer 1 chromitite within the oikocrystic harzburgite. The dynamic features of the oikocrystic harzburgite are also suggested by magmatic breccias and wavy, pyroxene-rich textures in the Black Label chromite. The oikocrystic pyroxene has the effect of decreasing the Cr/Fe ratio of the chromite ore.
5. With differentiation of pyroxenite and additional mixing to produce oikocrystic harzburgite, there was the introduction of a primitive Mg pulse of magma to migrate the magma into Cr stability again in the Black Label Layer 2 chromitite. This chromitite is more primitive and reflects the chemistry of this dunite pulse. Dunite is being differentiated in this chamber at this time. It is Cr-saturated, and when there is slight dithering of the magma to a composition closer to pyroxene, another chromitite horizon will form such as the Black Label Layer 3 chromitite.
6. There is a large sequence of primitive dunite between the Black Label and Black Thor sequences. This dunite is probably very primitive and well below Cr saturation.
7. As the dunite sequence evolves in composition, the magma approaches Cr stability and mineralizes disseminated interstitial chromite followed by intermittent pulses of interstitial chromite in dunite in the DDH BT-08-10. New

chromite layers separate out of the magma as the melt migrates into Cr stability from the more evolved olivine.

8. Further in BT-08-10 sequence, the melt migrates in the Cr field closer to pyroxene and the chromite itself grades into pyroxenite. There is a massive layer at the top of the sequence where there is olivine-only crystallization. Not far above this sequence, there is only pyroxenite. The evidence of there being a large sequence of pyroxenite after this chromite interval and that the pyroxenite has higher degrees of crustal contamination of TTG that affects it differently than the underlying dunite suggests to some extent that the pyroxenite was a later differentiate that a primitive olivine magma mixed in to cause chromite saturation. At first chromite is disseminated with evolved dunite; however, the presence of cumulus pyroxene evident in the drill core along with the associated development of a massive layer of chromite suggests dithering occurred from a pyroxene to chromite magma with the mixing in of olivine.
9. In other nearby areas of the same intrusion at Big Daddy DDH FW-08-19, there is massive chromitite hosted in pyroxenite. The intermittent pulses in the Black Thor-Big Daddy deposits as a whole build up into layers upwards and outwards within double diffusive convective cycles of magma. These convection cycles cause separation of chromite into semi-massive net-textured chromitites followed by massive chromitites. Along with crystallization of semi-massive and massive chromite, there is the exsolution of magmatic fluids from the cumulus pile that are captured by the growing chromite grains. Further modification of the chromite includes adcumulus growth of the in situ chromites unto massive chromite.
10. In the layers higher up in the Black Thor sequence, there is primarily pyroxenite. Some mini-pulses of dunite cause the magma to migrate into chromite stability again from pyroxene to mineralize the upper chromitites such as in DDH BT-09-17.
11. Later in the upper chromite sequence of BT-09-17, there was the intrusion of gabbro into the upper chromitite that underwent higher T prograde modification of the upper chromitite. Within this chromite, ferrichromite is enriched to up to 68 wt. % Cr_2O_3 and hydrothermal tremolite becomes stable in nearby silicate.

12. As the subvolcanic Ring of Fire Intrusion underwent subsolidus cooling, there was autohydration by fluids that circulated from the seawater interface down through the stratigraphy of the intrusion. The primary olivines and pyroxenes of the dunite and pyroxenite retrogress into serpentine, tremolite, talc and chlorite. In the chromitites themselves, the original magmatic signatures of the chromites are well preserved with some areas of retrogression where there is zoning in the grains and replacement rims. In the zoned chromites, Mg and Cr are diffused out of the chromites causing enrichment in Fe and Al. Further retrogression results in diffusion of Fe and Cr that causes the crystallization of enriched Cr ferrichromite rims to the chromite. In this reaction, Mg and Al diffuses and dissolves from the chromite into the chlorite associated with the ferrichromite.
13. Further retrogression of the chromites causes the formation of Cr-depleted chromite which is more oxidized and has less Cr. Often, the Cr-depleted ferrichromite is found in association with more Cr-depleted disseminated chromites in the Black Label and Black Thor olivine-chromite cumulates. As hydrous fluids advanced upward in stratigraphy, the gabbros and upper chromitite were the last to cool and undergo retrogression to produce the MgO-depleted chromites in the upper part of the upper chromitite.
14. The Ring of Fire Intrusion was finally overturned as a result of late Kenoran granodiorite diapirism in the Oxford-Stull Terrane. This caused the steep plunges and overturning of the stratigraphy in the Black Label-Black Thor and Big Daddy sequences. Deformation fabrics often overprint the chromitites in massive chromites, together with Cr-enrichment in chromian chlorite and kaemmererite vein alteration.

REFERENCES

- Alapeiti, T. T., Huhtelin, T.A., 2005, The Kemi Intrusion and Associated Chromitite Deposit. Geological Survey of Finland, Guide 51a. p. 13-32.
- Alapieti, T.T., Kujanpää, J., Lahtinen, J.J. and Papunen, H. 1989. The Kemi Stratiform Chromitite Deposit, Northern Finland. *Economic Geology*, 84, p. 1057-1077.
- Apted, M.J. and Liou, J.G. 1983. Phase relations among Greenschist, Epidote-Amphibolite, and Amphibolite in a Basaltic System. *In: Studies in Metamorphism and Metasomatism: A special volume of the American Journal of Science*, 283-A, p. 328-354.
- Arndt, N.T. 1977. Thick, Layered Peridotite-Gabbro Lava Flows in Munro Township, Ontario. *Canadian Journal of Earth Sciences*, 14, p. 2620-2637.
- Arndt, N.T. 1975. Ultramafic Rocks of Munro Township and Their Volcanic Setting. *Unpublished Ph.D. thesis*, University of Toronto, p. 1-300.
- Arndt, N.T and Fowler, N.D. 2004. Textures in Komatiites and Variolitic Basalts. Grenoble France: LGCA. Ottawa, ON: Department of Earth Sciences & Ottawa Carleton Geoscience Centre, p. 1-28.
- Arndt, N.T. and Leshner, C.M. Komatiite. Grenoble, France: LGCA. Sudbury, ON, Canada: Mineral Exploration Research Centre, Department of Earth Sciences, Laurentian University, Sudbury, Ontario, Canada.
- Arndt, N.T. and Nisbet, E.G. (eds.) 1982. Komatiites. George Allen & Unwin., London, U.K. 526 pages.
- Ashley, P.M. 1975. Opaque mineral assemblage formed during serpentinization in the Coolac ultramafic belt, New South Wales. *Journal of the Geological Society of Australia*, 22, part 1, p. 91-102.
- Aubut, A. June 27, 2012. National Instrument 43-101 Technical Report Big Daddy chromite deposit McFaulds Lake Area, Ontario, Canada Porcupine Mining Division, NTS 43D16 Mineral Resource Estimation Technical Report Prepared For KWG Resources Inc. Sibley Basin Group, p. 1-64.
- Aubut, A. January 10, 2010. National Instrument 43-101 Technical Report McFauld's Lake Area, Ontario, Canada Black Thor Chromite Deposit Mineral Resource Estimation Technical Report Prepared For Freewest Resources Canada Inc. Sibley Basin Group, p. 1-65.
- Azar, B.A. 2010. The Blackbird Chromite Deposit, James Bay Lowlands of Ontario, Canada: Implications for Chromitite Genesis in Ultramafic Conduits and Open Magmatic Systems. *Unpublished M.Sc. thesis*, University of Toronto, p. 1-154.

- Azar, B.A. and Mungall, J.E. June 21-24, 2010. Geochemistry of the Blackbird Chromite Deposit, McFauld's Lake, Ontario. 11th International Platinum Symposium, Sudbury, Ontario. Ontario Geological Survey Miscellaneous Release – Data 269.
- Baird, A.M., Leshner, C.M., Larson, M.S., Gilles, S.L. 1996. Chromium variations in cumulate komatiites. Abstracts with Programs - Abstracts with Programs - Geological Society of America, 28, issue 7, p. 92.
- Ballhaus, C. 1998. Origin of Podiform Chromite Deposits by Magma Mingling. *Earth and Planetary Science Letters*, 156, p. 185-193.
- Bannister, V., Roeder, P. and Poustovetov, A. 1998. Chromite in the Paricutin lava flows (1943–1952). *Journal of Volcanology and Geothermal Research*, 87, p. 151–171.
- Barnes, S-J. and Maier, W.D. 1999. The fractionation of Ni, Cu and the noble metals in silicate and sulphide liquids, *in*: Keays, R.R., Leshner, C.M., Lightfoot, P.C. and Farrow, C.E.G. (eds.), *Dynamic processes in magmatic ore deposits and their application in mineral exploration*, Geological Association of Canada, Short Course Volume 13, p. 69-106.
- Barnes, S-J., Naldrett, A.J, Gorton, M.P. 1985. The Origin of the Fractionation of Platinum-group Elements in Terrestrial Magmas. *Chemical Geology*, 53, p. 303-323.
- Barnes, S.J. 1998. Chromite in Komatiites, 1. Magmatic Controls on Crystallization and Composition. *Journal of Petrology*, 39, p. 1689-1720.
- Beeson, M.H. and Jackson, E.D. 1969. Chemical Composition of Altered Chromites from the Stillwater Complex, Montana. *The American Mineralogist*, 54, p. 1084-1100.
- Bliss, N.W.; MacLean, W.H. 1975. The paragenesis of zoned chromite from central Manitoba. *Geochimica et Cosmochimica acta*, 39, p. 973-990.
- Borisova, A.Y., Ceuleneer, G., Kamenetsky, V.S., Arai, S., Bějina, F., Abily, B., Bindeman, I.N., Polvé, N., De Parseval, P., Aigouy, T. and Pokrovsky, G.S. 2012. A New View on the Petrogenesis of the Oman Ophiolite Chromitites from Microanalyses of Chromite-hosted Inclusions. *Journal of Petrology*, 53, no. 12, p. 2411-2440.
- Boudreau, A. 1999. Fluid Fluxing of Cumulates: The J-M Reef and Associated Rocks of the Stillwater Complex, Montana. *Journal of Petrology*, 10, no. 5, p. 755-772.
- Cameron, E.N. 1982. The Upper Critical Zone of the Eastern Bushveld Complex – Precursor of the Merensky Reef. *Economic Geology*, 77, p. 1307-1327.
- Cameron, E.N. 1980. Evolution of the Lower Critical Zone, Central Sector, Eastern Bushveld Complex, and Its Chromite Deposits. *Economic Geology*, 75, p. 845-871.

- Cameron, E.N. 1978. The Lower Zone of the Eastern Bushveld Complex in the Olifants River Trough. *Journal of Petrology*, 19, part 3, p. 437-462.
- Cameron, E.N. 1977. Chromite in the Central Sector of the Eastern Bushveld Complex, South Africa. *American Mineralogist*, 62, p. 1082-1096.
- Campbell, I.H. 1996. Fluid Dynamic Processes in Basaltic Magma Chambers. *In: Cawthorn ed., R.G. Layered Intrusions. Elsevier Science B.V.*, p. 45-76.
- Campbell, I.H. and Murck, B.W. 1993. Petrology of the G and H Chromitite Zones in the Mountain View Area of the Stillwater Complex, Montana. *Journal of Petrology*, 34, part 2, p. 291-316.
- Candia, M.A.F., Gaspar, J.C., Gergely, E., Szabo, A.J. 1997. Ferrichromita: Revisão e Implicações Petrogenéticas. *Revista Brasileira de Geociências*, 27, Issue 4, p. 349-354.
- Cooper, R.W. October 4-10, 2009. Field, Petrographic and Mineralization Characteristics of Mafic Layered Intrusions, University of Minnesota-Duluth – Still water Complex.
- Cooper, R.W. July 2002. Stratigraphy and chromite mineralization of the Peridotite zone, Stillwater Complex, Montana, with descriptions of field sites in the Mountain View area, *In: 9th International Platinum Symposium Geology and Guide, Stillwater Complex, Montana, USA.*, p. D-1 – D-68.
- Cotterill, P. 1969. The Chromite Deposits of Selukwe, Rhodesia. *Economic Geology Monograph* 4, p. 23-40.
- Dare, S.A.S., Pearce, J.A., McDonald, I. and Styles, M.T. 2009. Tectonic discrimination of peridotites using fO_2 -Cr# and Ga-Ti-FeIII systematic in chrome-spinel. *Chemical Geology*, 261, p. 199-216.
- Deer, W.A., Howie, R.A. and Zussman, J. 1997. *Rock-Forming Minerals: Double-chain silicates*, Volume 2B Second Edition. The Geological Society, London, 764 pages.
- Devaraju, D.C., Alapieti, T.T., Kaukonen, R.J. and Sudhakara, T.L. 2007. Chemistry of Cr-spinels from Ultramafic Complexes of Western Dharwar Craton and its Petrogenetic Implications. *Journal Geological Society of India*, 69, p. 1161-1175.
- Duke, J.M. 1988. Magmatic Segregation Deposits of Chromite. *In: Roberts, R.G. and Sheahan, P.A., eds. Ore Deposit Models. Geological Association of Canada*, p. 133-144.
- Eales, H.V. 1987. Upper Critical Zone Chromitite Layers at R.P.M. Union Section Mine Western Bushveld Complex. *In: Stowe, C.W., ed. Evolution of Chromium Ore Fields. Van Nostrand Reinhold Company. New York*, p. 144-168.

- Eales, H.V. and Costin, G. 2012. Crustally Contaminated Komatiite: Primary Source of the Chromitites and Marginal, Lower, and Critical Zone Magmas in a Staging Chamber Beneath the Bushveld Complex. *Economic Geology*, 107, p. 645-665.
- Eales, H.V. and Reynolds, I.M. 1986. Cryptic Variations within Chromitites of the Upper Critical Zone, Northwestern Bushveld Complex. *Economic Geology*, 81, p. 1056-1066.
- Eales, H.V., de Klerk, W.J. and Teigler, B. 1990. Evidence for magma mixing processes within the Critical and Lower Zones of the northwestern Bushveld Complex, South Africa. *Chemical Geology*, 88, p. 261-278.
- Embey-Isztin, A. 1976. Amphibole/Lherzolite Composite Xenolith from Szigliget, North of the Lake Balaton, Hungary. *Earth and Planetary Science Letters*, 31, p. 297-304.
- Engelbrecht, J.P. 1985. The Chromites of the Bushveld Complex in the Nietverdiend Area. *Economic Geology*, 80, p. 896-910.
- Erlank, A.J., Waters, F.G., Hawkesworth, C.J., Haggerty, S.E., Allsopp, H.L., Rickard, R.S. and Menzies, M. 1987. Evidence for Mantle Metasomatism in Peridotite Nodules from the Kimberley Pipes, South Africa. *In: Menzies, M.A. and Hawkesworth, C.J. eds. 1987. Mantle Metasomatism. Academic Press, Inc. (London) Ltd., p. 221-311.*
- Feng, R. and Kerrich, R. 1992. Geochemical evolution of granitoids from the Archean Abitibi Southern Volcanic Zone and the Pontiac subprovince, Superior Province, Canada: Implications for tectonic history and source regions. *Chemical Geology*, 98, p. 23-70.
- Field, S.W., Haggerty, S.E. and Erlank, A.J. 1989. Subcontinental metasomatism in the region of Jagersfontein, South Africa. *Special Publication – Geological Society of Australia*, 14.2, p. 771-783.
- Finnigan, C.S., Brenan, J.M., Mungall, J.E. and McDonough, W.F. 2008. Experiments and Models Bearing on the Role of Chromite as a Collector of Platinum Group Minerals by Local Reduction. *Journal of Petrology*, 49, p. 1647-1665.
- Gain, S.B. 1985. The Geologic Setting of the Platiniferous UG-2 Chromitite Layer on the Farm Maandagshoek, Eastern Bushveld Complex. *Economic Geology*, 80, p. 925-943.
- González Jiménez, J.M., Griffin, W.L., Locmelis, M., O'Reilly, S.Y. and Pearson, N.J. 2012. Contrasted minor- and trace-element compositions of spinel in chromitites of different tectonic settings. Australian Research Council Centre of Excellence for Core to Crust Fluid Systems.

- Gowans, R. and Murahwi, C. March 31, 2009. Spider Resources Inc. KWG Resources Inc. Freewest Resources Inc. McFaulds Lake Joint Venture Property NI 43-101 Technical Report on the Big Daddy Chromite Deposit and Associated Ni-Cu-PGE James Bay Lowlands, Northern Ontario. Micon International Limited Mineral Industry Consultants, p. 1-72.
- Hamlyn, P. 1975. Chromite alteration in the Panton Sill, East Kimberley Region, Western Australia. *Mineralogical Magazine*, 40, p. 181-192.
- Hamlyn, P.R. and Keays, R.R. 1979. Origin of chromite compositional variation in the Panton Sill, Western Australia. *Contributions to Mineralogy and Petrology*, 69, p. 75-82.
- Hatton, C.J. and Von Gruenewaldt, G. 1987. The Geological Setting and Petrogenesis of the Bushveld Chromitite Layers. *In: Stowe, C.W., ed. Evolution of Chromium Ore Fields*. Van Nostrand Reinhold Company. New York, p. 109-143.
- Hey, M.H. 1954. A New Review of the Chlorites. *Mineralogical Magazine*, 30, p. 277-292.
- Hiemstra, S.A. 1986. The Distribution of Chalcophile and Platinum-Group Elements in the UG-2 Chromitite Layer of the Bushveld Complex. *Economic Geology*, 81, p. 1080-1086.
- Hiemstra, S.A. 1985. The Distribution of Some Platinum-Group Elements in the UG-2 Chromitite Layer of the Bushveld Complex. *Economic Geology*, 80, p. 944-957.
- Hollings, P. and Kerrich, R. 1999. Trace element systematics of ultramafic and mafic volcanic rocks from the 3 Ga North Caribou greenstone belt, northwestern Superior Province. *Precambrian Research*, 93, p. 257-279.
- Houlé, M. 2000. *Pétrologie et Métallogénie du Complexe de Menarik, Baie James, Québec, Canada*. *Unpublished M.Sc. thesis*, Laval University, 450 pages.
- Huang, J., Xiao, Y., Gao, Y., Hou, Z. and Wu, W. 2012. Nb-Ta fractionation induced by fluid-rock interaction in subduction-zones; constraints from UHP eclogite- and vein-hosted rutile from the Dabie orogen, central-eastern China. *Journal of Metamorphic Geology*, 30, issue 8, p. 821-842.
- Hulbert, L.J. and Von Gruenewaldt, G. 1985. Textural and Compositional Features of Chromite in the Lower and Critical Zones of the Bushveld Complex South of Potgietersrus. *Economic Geology*, 80, p. 872-895.
- Irvine, T.N. 1981. A Liquid-density Controlled Model for Chromitite Formation in the Muskox Intrusion. *In: Carnegie Institution of Washington Year Book 80 1980-1981*, p. 317-324.

- Irvine, T.N. 1980. Magmatic Infiltration Metasomatism, Double-diffusive Fractional Crystallization, and Adcumulus Growth in the Muskox Intrusion and Other Layered Intrusions. *In: Hargraves, R.B., ed. Physics of Magmatic Processes.* Princeton University Press, Princeton, New Jersey, p. 325-384.
- Irvine, T.N. 1977. Origin of chromitite layers in the Muskox intrusion and other stratiform intrusions: A new interpretation. *Geology*, 5, p. 273-277.
- Irvine, T.N. 1975. Crystallization sequences of the Muskox intrusion and other layered intrusions - II. Origin of chromitite layers and similar deposits of other magmatic ores: *Geochimica et Cosmochimica Acta*, 39, p.991-1020.
- Irvine, T.N. 1967. Chromian Spinel as a Petrogenetic Indicator, Part 2. Petrologic Applications. *Canadian Journal of Earth Sciences*, 4, p. 71-103.
- Irvine, T.N., Keith, D.W., and Todd, S.G. 1983. The J-M Platinum-Palladium Reef of the Stillwater Complex, Montana: II. Origin by Double-Diffusive Convective Magma Mixing and Implications for the Bushveld Complex. *Economic Geology*, 78, p. 1287-1334.
- Jackson, E.D. July 7-14, 1969. The Cyclic Unit in Layered Intrusions – A Comparison of Repetitive Stratigraphy in the Ultramafic Parts of the Stillwater, Muskox, Great Dyke, and Bushveld Complexes. *In: Visser, D.J.L. and Von Gruenewaldt, G, eds. Symposium on the Bushveld Igneous Complex and Other Layered Intrusions.* The Geological Society of South Africa Special Publication, No. 1, p. 391-424.
- Jan, M.Q. and Windley, B.F. 1990. Chromite Spinel-Silicate Chemistry in Ultramafic Rocks of the Jijal Complex, Northwest Pakistan. *Journal of Petrology*, 31, part 3, p. 667-715.
- Jiménez, J.M.G, Griffin, W.L., Locmelis, M., O'Reilly, S.Y, Pearson, N.J. 2012. Contrasted minor- and trace-element compositions of spinel in chromitites of different tectonic settings. Australian Research Council Centre of Excellence for Core to Crust Fluid Systems.
- Johan, Z. 1986. Chromite Deposits in the Massif Du Sud Ophiolite, New Caledonia: Genetic Considerations. *In: Petrascheck, W., Karamata, S., Kravchenko, G.G., Johan, Z., Economou, M. and Engrin, T., eds. Chromites UNESCO's IGCP-197 Project Metallogeny of Ophiolites*, p. 311-339.
- Johnson, C. 2012. Podiform Chromite at Voskhod, Kazakhstan. *Unpublished PhD thesis*, Cardiff University, 449 pages.
- Kaçira, N. 1971. Geology of Chromitite Occurrences and Ultramafic Rocks of the Thetford Mines – Disraeli Area, Quebec. *Unpublished PhD thesis*, The University of Western Ontario, 247 pages.

- Kapsiotis, A., Tsikouras, B., Grammatikopoulos, T., Karipi, S. and Hatzipanagiotou, K. 2007. On the Metamorphic Modification of Cr-spinel Compositions from the Ultrabasic Rocks of the Pindos Ophiolite Complex (NW Greece). *Bulletin of the Geological Society of Greece*, 40, p. 781-793.
- Kerrick, R. and Fan, J. 1997. Geochemical characteristics of aluminum-depleted and undepleted komatiites and HREE-enriched low-Ti tholeiites, western Abitibi greenstone belt: A heterogeneous mantle plume-convergent margin environment. *Geochimica et Cosmochimica Acta*, 61, no. 22, p. 4723-4744.
- Khalil, K.I. and El-Makky, A.M. 2009. Alteration Mechanisms of Chromian-Spinel during Serpentinization at Wadi Sifein Area, Eastern Desert, Egypt. *Resource Geology*, 59, No. 2, p. 194–211.
- Kishida, A. 1984. Hydrothermal Alteration Zoning and Gold Concentration at the Kerr-Addison Mine, Ontario, Canada. *Unpublished* PhD thesis, The University of Western Ontario, 231 pages.
- Krause, J., Brüggemann, G.E., Pushkarev, E.V. 2007. Accessory and Rock Forming Minerals Monitoring the Evolution of Zoned Mafic–ultramafic Complexes in the Central Ural Mountains. *Lithos*, 95, p. 19-42.
- Layton-Matthews, D., Leshner, C.M., Burnham, O.M., Hulbert, L., Peck, D.C., Golightly, J.P. and Keays, R.R. 2010. Exploration for Komatiite-Associated Ni-Cu-(PGE) Mineralization in the Thompson Nickel Belt, Manitoba. *In: The Challenge of Finding New Mineral Resources: Global Metallogeny, Innovative Exploration, and New Discoveries Volume II: Zinc-Lead, Nickel-Copper-PGE, and Uranium. Society of Economic Geologists Special Publication Number 15*, p. 513-538.
- Leake, B.E., Woolley, A.R., Arps, C.E.S., Birch, W.D., Gilbert, M.C., Grice, J.D., Hawthorne, F.C., Kato, A., Kisch, H.J., Krivovichev, V.G., Linthout, K., Laird, J., Mandarino, J.A., Maresch, W.V., Nickel, E.H., Rock, N.M.S., Schumacher, J.C., Smith, D.C., Stephenson, N.C.N., Ungaretti, L., Whittaker, E.J.W., and Youshi, G., 1997, Nomenclature of amphiboles: Report of the subcommittee on amphiboles of the International Mineralogical Association, Commission on new minerals and mineral names: *American Mineralogist*, 82, p. 1019–1037.
- Leake, B.E. 1978. Nomenclature of Amphiboles. *Canadian Mineralogist*, 16, p. 501-520.
- Lee, C.A. and Parry, S.J. 1988. Platinum-Group Element Geochemistry of the Lower and Middle Group Chromitites of the Eastern Bushveld Complex. *Economic Geology*, 83, p. 1127-1139.
- Lee, C.A. and Tredoux, M. 1986. Platinum-Group Element Abundances in the Lower and the Lower Critical Zones of the Eastern Bushveld Complex. *Economic Geology*, 81, p. 1087-1095.

- Leshner, C.M. 2005. February 10-11, 2005. Mineral Deposit Short Courses: Magmatic Ni-Cu-PGE Sulfide Deposits, University of Ottawa Department of Earth Sciences.
- Leshner, C.M., Burnham, O.M., Keays, R.R., Barnes, S.J. and Hulbert, L. 1999. Geochemical discrimination of barren and mineralized komatiites in dynamic ore-forming magmatic systems, *in*: Keays, R.R., Leshner, C.M., Lightfoot, P.C. and Farrow, C.E.G. (eds.), Dynamic processes in magmatic ore deposits and their application in mineral exploration, Geological Association of Canada, Short Course Volume 13, p. 451-477.
- Li, C., Maier, W.D. and De Waal, S.A. 2001. The Role of Magma Mixing in the Genesis of PGE Mineralization in the Bushveld Complex: Thermodynamic Calculations and New Interpretations. *Economic Geology*, 96, p. 653-652.
- Li, C., Ripley, E.M., Sarkar, A., Shin, D. and Maier, W.D. 2005. Origin of Phlogopite-orthopyroxene Inclusions in Chromites from the Merensky Reef of the Bushveld Complex, South Africa. *Contributions to Mineralogy and Petrology*, 150, p. 119-130.
- Linkermann, S.A. 2010. Emplacement of the 2.44 Ga ultramafic layered Kemi intrusion, Finland: PGE, geochemical and Sm-Nd isotopic implications. *Unpublished M.Sc. thesis*, Rhodes University, 155 pages.
- Linkermann, S.A., Prevec, S.A. and Alapieti, T.T. 2010. Chrome and PGE Behaviour from the Kemi Intrusion, Finland: Geochemical and Sm-Nd Isotopic Implications. 11th International Platinum Symposium, Sudbury, Ontario. Ontario Geological Survey Miscellaneous Release – Data 269.
- Lorand, J.P. and Cottin, J.Y. 1987. Na-Ti-Zr-H₂O mineral inclusions indicating postcumulus chrome-spinel dissolution and recrystallization in the Western Laouni mafic intrusion, Algeria. *Contributions to Mineralogy and Petrology*, 97, p. 251-263.
- Maier, W.D., Barnes, S-J. and Groves, D.I. 2010. Formation of PGE Reefs Due to Magma Chamber Subsidence and Mobility of Cumulate Slurries. 11th International Platinum Symposium June 21st-24th, 2010. Geological Survey, Miscellaneous Release–Data 269.
- Maier, W.D. and Barnes, S-J. 2009. Formation of PGE Deposits in Layered Intrusions. *In*: Li, C. and Ripley, E.M., *editors*. *New Developments in Magmatic Ni-Cu and PGE Deposits*. Geological Publishing House. Beijing, p. 250-276.
- Maier, W. and Barnes, S-J. 2008. Platinum-group elements in the UG1 and UG2 chromitites, and the Bastard reef, at Impala platinum mine, western Bushveld Complex, South Africa: Evidence for late magmatic cumulate instability and reef constitution. *South African Journal of Geology*, 111, p. 159-176.

- Marques, J.C. and Filho, F.F. 2003. The Chromite Deposit of the Ipueira-Medrado Sill, São Francisco Craton, Bahia State, Brazil. *Economic Geology*, 98, p. 87–108.
- Mathez, E. 2010. Did Bushveld chromitites originate as crystal mushes? *In: The Association Between Chromite and PGEs. 11th International Platinum Symposium*, Sudbury, Ontario, Canada, June 21-24, 2010 Workshop Notes.
- Matsumoto, I. and Arai, S. 2001. Petrology of Dunite/harzburgite with Decimeter-scale Stratification in a Drill Core from the Tari-Misaka Ultramafic Complex, Southwestern Japan. *Journal of Mineralogical and Petrological Sciences*, 96, p. 19-28.
- McDonough, W.F. and Sun, S-S. 1995. The Composition of the Earth. *Chemical Geology*, 120, p. 223-253.
- McElduff, B. and Stumpfl, E.F. 1991. The Chromite Deposits of the Troodos Complex, Cyprus – Evidence for the Role of a Fluid Phase Accompanying Chromite Formation. *Mineralia Deposita*, 26, p. 307-318.
- McLaren, C.H. and DeVilliers, J.P.R. 1982. The Platinum-Group Chemistry and Mineralogy of the UG-2 Chromitite Layer of the Bushveld Complex. *Economic Geology*, 77, p. 1348-1366.
- Méric, J., Pagé, P., Barnes, S-J. and Houlé, M.G. 2012. Geochemistry of Chromite from the Alexo Komatiite, Dundonald Township: Preliminary Results from Electron Microprobe and Laser Ablation Inductively Coupled Plasma Mass Spectrometric Analyses. *In: Summary of Field Work and Other Activities 2012*. Ontario Geological Survey, Open File Report 6280, p. 46-1 to 46-12.
- Metsaranta, R.T. 2010. Project Unit 10-004. McFaulds Lake Area Regional Compilation and Bedrock Geology Mapping Project. *In: Summary of Field Work and Other Activities 2010*. Ontario Geological Survey, Open File Report 6260, p. 17-1 to 17-5.
- Metsaranta, R.T. and Houlé, M.G. 2012. Project Unit 10-004. Progress on the McFaulds Lake (“Ring of Fire”) Region Data Compilation and Bedrock Geology Mapping Project. *In: Summary of Field Work and Other Activities 2012*. Ontario Geological Survey, Open File Report 6280, p. 43-1 to 43-12.
- Metsaranta, R.T. and Houlé, M.G. 2011. Project Unit 10-004. McFaulds Lake Area Regional Compilation and Bedrock Mapping Project Update. *In: Summary of Field Work and Other Activities 2011*. Ontario Geological Survey, Open File Report 6270, p. 12-1 to 12-12.
- Mitchell, R.H. 1986. *Kimberlites – Mineralogy, Geochemistry and Petrology*. Plenum Press, New York and London, 442 pages.
- Mondal, S.K. and Mathez, E.A. 2007. Origin of the UG2 Chromitite Layer, Bushveld Complex. *Journal of Petrology*, 48, p. 495-510.

- Mungall, J.E. 2010a. The Association Between Chromite and PGEs. 11th International Platinum Symposium, Sudbury, Ontario, Canada, June 21-24, 2010 Workshop Notes.
- Mungall, J.E. 2010b. Coprecipitation of Chromite and PGM in Mafic Magmas. *In: The Association Between Chromite and PGEs. 11th International Platinum Symposium, Sudbury, Ontario, Canada, June 21-24, 2010 Workshop Notes.*
- Mungall, J.E. 2008. Formation of massive chromitite by assimilation of iron formation in the Blackbird Deposit, Ontario, Canada; *Eos, Transactions, American Geophysical Union, 89, Supplement, Abstract V11A-201.*
- Mungall, J.E., Azar, B., Atkinson, J. and Harvey, J.D. June 21-24, 2010. The Eagle's Nest Komatiite-Hosted Ni-Cu-PGE Sulphide Deposit in the James Bay Lowlands, Ontario. 11th International Platinum Symposium, Sudbury, Ontario. Ontario Geological Survey Miscellaneous Release – Data 269.
- Mungall, J.E., Harvey, J.D., Balch, S.J., Azar, B., Atkinson, J. and Hamilton, M.A. 2010. Eagle's Nest: A Magmatic Ni-Sulfide Deposit in the James Bay Lowlands, Ontario, Canada. *In: The Challenge of Finding New Mineral Resources: Global Metallogeny, Innovative Exploration, and New Discoveries Volume II: Zinc-Lead, Nickel-Copper-PGE, and Uranium. Society of Economic Geologists Special Publication Number 15, p. 539-557.*
- Mungall, J.E., Jenner, F., Arculus, R. and Mavrogenes, J. June 24-29, 2012. PGE systematics of refractory mantle: role of Pt alloy. Montréal, Canada. The 22nd V.M. Goldschmidt Conference: Earth in Evolution, Abstract.
- Murck, B.W. and Campbell, I.H. 1986. The Effects of Temperature, Oxygen Fugacity and Melt Composition on the Behaviour of Chromium in Basic and Ultrabasic Melts. *Geochimica et Cosmochimica Acta, 50, p. 1871-1887.*
- Mutanen, T. 1997. Geology and ore petrology of the Akanvaara and Koitelainen mafic layered intrusions and the Keivitsa-Satovaara layered complex, northern Finland. Geological Survey of Finland Bulletin 395, 233 pages.
- Mutanen, T. and Huhma, H. 2001. U-Pb Geochronology of the Koitelainen, Akanvaara and Keivitsa Layered Intrusions and Related Rocks. Geological Survey of Finland Special Paper 33, p. 229-246.
- Naldrett, A.J. 2010. PGE content of Chromitites and the distribution of PGE throughout the Bushveld. *In: The Association Between Chromite and PGEs. 11th International Platinum Symposium, Sudbury, Ontario, Canada, June 21-24, 2010 Workshop Notes.*
- Naldrett, A.J. September 22, 2009a. Report on visit to Spider-KWG and Freewest properties, September 16th-19th, 2009. A.J. Naldrett TOGA Technical and Exploration Services Inc.

- Naldrett, A.J. 2009b. Fundamentals of Magmatic Sulfide Deposits. *In: Li, C. and Ripley, E.M., eds. New Developments in Magmatic Ni-Cu and PGE Deposits.* Geological Publishing House. Beijing, p. 1-26.
- Naldrett, A.J., Kinnaird, A.W., Yudovskaya, M., McQuade, S., Chunnett, G. and Stanley, C. 2009. Chromite composition and PGE content of Bushveld chromitites: Part 1 – the Lower and Middle Groups. *Applied Earth Science (Transitions to the Institute of Mineralogy and Metallogeny B)*, 118, no. 3/4, p. 131-161.
- Naldrett, A. J., Wilson, A., Kinnaird, J., Yudovskaya, M. and Chunnett, G. 2012. The origin of chromitites and related PGE mineralization in the Bushveld Complex: new mineralogical and petrological constraints. *Mineralia Deposita*, 47, p. 209–232.
- Naslund, H.R and McBirney, A.R. 1996. Mechanisms of Formation of Igneous Layering. *In: Cawthorn ed., R.G. Layered Intrusions.* Elsevier Science B.V., p. 1-44.
- Nicholson, D.M. & Mathez, E.A. 1991. Petrogenesis of the Merensky Reef in the Rustenburg section of the Bushveld Complex. *Contributions to Mineralogy and Petrology*, 107, p. 293-309.
- Ohnenstetter, D., Watkinson, D.H., Jones, P.C. and Talkington, R. 1986. Cryptic Compositional Variation in Laurite and Enclosing Chromite from the Bird River Sill, Manitoba. *Economic Geology*, 81, p. 1159-1168.
- Onyeagocha, A.C. 1974. Alteration of Chromite from the Twin Sisters Dunite, Washington. *American Mineralogist*, 59, p. 608-612.
- Page, N.J. and Zientek, M.L. 1987. Composition of Primary Postcumulus Amphibole and Phlogopite within an Olivine Cumulate in the Stillwater Complex, Montana. *U.S. Geological Survey Bulletin* 1674-A, p. A1-A35.
- Pagé, P. 2010. Chromitites from ophiolitic complexes and their PGE mineralization: The Thetford Mines Ophiolite, Québec, Canada. *In: The Association Between Chromite and PGEs. 11th International Platinum Symposium, Sudbury, Ontario, Canada, June 21-24, 2010 Workshop Notes.*
- Pagé, P. and Barnes, S-J. June 30, 2012. Trace elements in chromite from various settings: Their use in provenance studies and as an exploration tool. *In: Beaudoin, G., Dare, S., Pagé, P. and King, J. Fe-oxide Workshop: Processes that control the composition of Fe-oxides in ore deposits.* Montreal, Canada, p. 1-33.
- Pagé, P. and Barnes, S-J. 2009. Using Trace Elements in Chromites to Constrain the Origin of Podiform Chromitites in the Thetford Mines Ophiolite, Québec, Canada. *Economic Geology*, 104, p. 997-1018.
- Pagé, P., Barnes, S-J., Bédard, J.H., Zientek, M.L. 2012. In situ determination of Os, Ir, and Ru in chromites formed from komatiite, tholeiite and boninite magmas: Implications for chromite control of Os, Ir and Ru during partial melting and crystal fractionation. *Chemical Geology* 302–303, p. 3–15.

- Pavlov, N.V., Grigoryeva, I. & Tsepina, A.I. 1977. Chromite nodules as an indicator of liquation of a magmatic melt. *International Geology Review*, 19, p. 43-56.
- Peltonen, P. 1995. Crystallization and Re-equilibration of Zoned Chromite in Ultramafic Cumulates, Vammala Ni-Belt, Southwestern Finland. *The Canadian Mineralogist*, 33, p. 521-535.
- Penberthy, C.J. and Merkle, R.K.W. 1999. Lateral Variations in the Platinum-Group Element Content and Mineralogy of the UG2 Chromitite Layer, Bushveld Complex. *South African Journal of Geology*, 102, part 3, p. 240-250.
- Percival, J.A. 2007. Geology and Metallogeny of the Superior Province, Canada. *In: Goodfellow, W.D., ed. Mineral Deposits of Canada: A Synthesis of Major Deposit-Types, District Metallogeny, the Evolution of Geological Provinces, and Exploration Methods: Geological Association of Canada, Mineral Deposits Division, Special Publication No. 5*, p. 903-928.
- Percival, J.A. 2006. Mineral Deposits of Canada: Geology and Metallogeny of the Superior Province, Canada. Geological Survey of Canada and the Mineral Deposits Division of the Geological Association of Canada.
- Prendergast, M.D. 2008. Archean Komatiitic Sill-hosted Chromite Deposits in the Zimbabwe Craton. *Economic Geology*, 103, p. 981-1004.
- Prendergast, M.D. 1987. The Chromite Ore Field of The Great Dyke, Zimbabwe. *In: Stowe, C.W., ed. Evolution of Chromium Ore Fields. Van Nostrand Reinhold Company. New York*, p. 89-108.
- Rayner, N. and Stott, G.M. 2005. Discrimination of Archean domains in the Sachigo Subprovince: a progress report on the geochronology. *In: Summary of Field Work and Other Activities 2005, Ontario Geological Survey, Open File Report 6172*, p. 10-1 to 10-21.
- Reid, D.L., Laidler, N., Cross, C., Veksler, I. and Keiding, J. May 27-29, 2012. Ultraferrous Silicate Magmatism and Immiscibility: Evidence from the Bushveld Complex, South Africa. GAC-MAC Joint Annual Meeting: St. John's Geoscience at the Edge, Abstracts, Volume 35, p. 115-116.
- Rice, A. and Von Gruenewaldt, G. 1994. Convective scavenging and cascade enrichment in Bushveld Complex melts: possible mechanism for concentration of platinum-group element and chromite in mineralized layers. *Transitions to the Institute of Mineralogy and Metallogeny, Sect B: Applied earth science*, p. B31-B38.
- Roeder, P.L. Chromite: 1994. From the fiery rain of chondrules to the Kilauea Iki Lava Lake. *The Canadian Mineralogist*, 32, p. 729-746.

- Roeder, P.L. and Campbell, I.H. 1985. The effect of postcumulus reactions on Composition of Chrome-Spinels from the Jimberlana Intrusion. *Journal of Petrology*, 26, part 3, p. 763-786.
- Roeder, P.L. and Poustovetov, A. 2001. Growth Forms and Composition of Chromian Spinel in MORB Magma: Diffusion-controlled Crystallization of Chromian Spinel. *The Canadian Mineralogist*, 39, p. 397-416.
- Roeder, P.L. and Reynolds, I. 1991. Crystallization of Chromite and Chromium Solubility in Basaltic Melts. *Journal of Petrology*, 32 (5), p. 909-934.
- Rollinson, H.R. 1997. The Archean Komatiite-Related Inyala Chromitite, Southern Zimbabwe. *Economic Geology*, 92, p. 98-107.
- Rollinson, H.R. 1995. The relationship between chromite chemistry and the tectonic setting of Archaean ultramafic rocks. *In: Blenkinsop, T.G. and Tromps, P., eds. Sub-Saharan Economic Geology. Amsterdam, Balkema, p. 7-23.*
- Scoates, R.F.J. August 24-29, 2009. Report on Visit to Freewest's McFauld's Lake Exploration Camp.
- Scoates, R.F.J. April 20, 2009. Report on Drill Core Examination of Some Black Label and Big Thor Chromitite Intersections For Freewest Resources Limited.
- Scoates, R.F.J. March 25, 2009. Report on Drill Core Examination of Some Big Daddy Drill Holes for Spider Resources Ltd. - KWG Resources Ltd. - Freewest Resources Ltd. McFauld's Lake Joint-Venture.
- Scoates, R.F.J. December 30, 2008. Report on Drill Core Examination of Some Black Thor Drill Holes for Freewest Resources Ltd.
- Scoates, R.F.J. February 22, 2008. Report on Thin Sections and New Whole Rock and Trace Element Analyses from Freewest's McFauld's Lake Drill Hole.
- Scoon, R.N. and Teigler, B. 1994. Platinum-Group Element Mineralization in the Critical Zone of the Western Bushveld Complex: I. Sulfide Poor-Chromitites below the UG-2. *Economic Geology*, 89, p. 1094-1121.
- Sharpe, J.L. 1983. Chromitite and Associated Ultramafic Rocks, Black Lake, Quebec. *Unpublished H.BSc. thesis, The University of Western Ontario, 73 pages.*
- Sharpe, M.R. and Irvine, T.N. 1983. Melting Relations of Two Bushveld chilled Margin Rocks and Implications for the Origin of Chromitite. *In: Carnegie Institution of Washington Year Book 82 1982-1983, p. 295-300.*
- Spandler, C., Mavrogenes, J. and Arculus, R. 2005. Origin of chromitites in layered intrusions: Evidence from chromite-hosted melt inclusions from the Stillwater Complex. *Geology*, 33, no. 11, p. 893-896.

- Sproule, R.A., Leshner, C.M., Ayer, J.A., Thurston, P.C., Herzberg, C.T. Spatial and temporal variations in the geochemistry of komatiites and komatiitic basalts in the Abitibi greenstone belt. *Precambrian Research*, 115, p. 153–186.
- Sun, S-S. and McDonough, W.F. 1989. Chemical and isotopic systematic of oceanic basalts: implications for mantle compositions and processes. Geological Society, London, Special Publications, 42, p. 313-345.
- Stowe, C.W. 1987. Chromite Deposits of the Shurugwi Greenstone Belt, Zimbabwe. *In*: Stowe, C.W., *ed.* Evolution of Chromium Ore Fields. Van Nostrand Reinhold Company. New York, p. 71-88.
- Stowe, C.W. 1994. Compositions and Tectonic Settings of Chromite Deposits through Time. *Economic Geology*, 89, p. 528-546.
- Teigler, B. and Eales, H.V. 1993. Correlation between chromite composition and PGE mineralization in the Critical Zone of the Western Bushveld Complex. *Mineralium Deposita*, 28, p. 291-302.
- Teigler, B. 1999. Chromite chemistry and platinum-group element distribution of the LG6 Chromitite, northwestern Bushveld Complex. *South African Journal of Geology*, 102, part 3, p. 282-285.
- Tuchscherer, M.G., Hoy, D., Johnson, M., Shinkle, D., Kruze, R., Holmes, M. July 2009. Fall 2008 to Winter 2009 Technical Drill Report on The Black Thor Chromite Deposit Black Label Chromite Deposit and Associated Ni-Cu-PGEs McFaulds Property (100 %) James Bay Lowlands, Northern Ontario Latitude 52°78' N, Longitude -86°20', Freewest Resources Canada Inc., p. 1-48.
- Vaillancourt, C., Sproule, R.A., MacDonald, C.A. and Leshner, C.M. 2003. Investigation of mafic-ultramafic intrusions in Ontario and implications for platinum group element mineralization: Operation Treasure Hunt; Ontario Geological Survey, Open File Report 6102, 335 pages.
- Von Gruenewaldt, G., Hatton, C.J., Merkle, R.K.W. 1986. Platinum-Group Element-Chromitite Associations in the Bushveld Complex. *Economic Geology*, 81, p. 1067-1079.
- Von Gruenewaldt, G., Hulbert, L.J. and Naldrett, A.J. 1989. Contrasting platinum-group element concentration patterns in cumulates of the Bushveld Complex. *Mineralium Deposita*, 24, p. 219-229.
- Wager, L.R. and Brown, G.M. 1967. Layered Igneous Rocks. Edinburgh and London, U.K.: Oliver & Boyd Ltd. 588 pages.
- Wilson, A.H. 1982. The Geology of the Great 'Dyke', Zimbabwe: The Ultramafic Rocks. *Journal of Petrology*, 23, Part 2, p. 240-292.

- Winter, J.D. 2001. *An Introduction to Igneous and Metamorphic Petrology*. Prentice Hall Inc., Upper Saddle River, New Jersey, 700 pages.
- Wyman, D.A., Hollings, P., Biczok, J. 2011. Crustal evolution in a cratonic nucleus: Granitoids and felsic volcanic rocks of the North Caribou Terrane, Superior Province Canada. *Lithos*, 123, p. 37-49.
- Zhu, D. 2012. Origin of sulfide in the massive chromitites in the Bushveld Complex. State Key Laboratory of Ore Deposit Geochemistry, Institute of Geochemistry, Chinese Academy of Sciences, Guizhou, P. R. China 550002, p. 1-11.

APPENDIX 1

Core logs for DDH BT-09-31, BT-08-10, BT-08-17 and FW-08-19

Drill Hole Log

BT-09-31

Hole ID: BT-09-31 Project: Freewest Year 2009 Claim: TWP:
 Grid X: Easting: Grid Azimuth: Dip Casing:
 Grid Y: Northing: Datum: True Azimuth: Elev (m): Core Size: Casing (m): Tar
 Drill Start: Log Start: Drill Company: Drilled for: Freewest Resources Inc.
 Drill Finish: Log Finish: Foreman: Storage:
 Surveyed Logged by: Checked by: Comments:

From	To	Lithology	Code
0.00	18.00	Overburden	
18.00	126.00	Dunite	
126.00	142.50	Serpentinized dunite	
142.50	142.86	Pyroxenite	
142.86	144.62	Poikilitic serpentinized dunite	
144.62	145.14	Pyroxenite	
145.14	147.75	Poikilitic dark serpentinized dunite	
147.75	164.70	Heterogeneous pyroxenite/chromitite	
164.70	203.50	Chromitite	
203.50	205.90	Pyroxenite	
205.90	207.30	Poikilitic serpentinized dunite	
207.30	207.70	Pyroxenite	
207.70	221.80	Heterolithic serpentinized dunite	
221.80	222.60	Pyroxenite	
222.60	224.33	Dark serpentinized dunite	
224.33	225.00	Pyroxenite	
225.00	228.00	Dark serpentinized dunite	

Drill Hole Log

BT-09-31

From	To	Lithology	Code
228.00	237.00	Poikilitic serpentized dunite	
237.00	270.00	Semi-massive chromitite	
270.00	309.30	Serpentinized dunite	
309.30	318.65	Intermittent chromitite beds	
318.65	387.00	Serpentinized dunite	

Drill Hole Log

BT-09-31

From	To	Lithology	Code	Sample	From
0.00	18.00	Overburden			
18.00	126.00	Dunite Homogeneous light grey-green to apple green fine grained olivine altered dunite. This interval contains dominant green dunite with alternating 1.5m sections of dark serpentinized dunite until get to underlying dark serpentinized dunite. Dark serpentinized sections are more highly talc veined. The unit contains a few 20cm wide plagioclase-pyroxene gabbro intrusions associated with dark altered sections.			
126.00	142.50	Serpentinized dunite Dark serpentinized homogeneous dunite. The unit contains X-cutting gabbros to anorthosites.			
	131.34	132.27	Gabbro		
		Unit X-cuts dunite is leucocratic with plagioclase-pyroxene composition and contains associated disseminated chalcopyrite-pyrrhotite sulphides.			
142.50	142.86	Pyroxenite Apophyse of leucocratic dark pyroxene-rich unit X-cutting darker dunite and contains medium grained pyrrhotite sulphides. Unit is oriented 60° to CA.			
142.86	144.62	Poikilitic serpentinized dunite Olive green 1cm round orthopyroxene poikilitic dark serpentinized dunite is a hybrid unit before underlying contact zone with pyroxenite. This unit is fine disseminated pyrrhotite?-mineralized to 3% in between dark fine olivines as it is probably a basal pulse after the overlying pyroxenite. Photos 27 and 28 are of oriented orthopyroxene oikocrysts at 40° to CA in dunite groundmass at 143.60m.			
144.62	145.14	Pyroxenite Leucocratic orthopyroxenite same as unit above.			

Drill Hole Log

BT-09-31

From	To	Lithology	Code	Sample	From
145.14	147.75	Poikilitic dark serpentinized dunite The unit is same as above pyroxenite only with more intermixing pyroxenite and intercumulus to disseminated chromitite mineralization.			
147.75	164.70	Heterogeneous pyroxenite/chromitite Interval of heterogeneous leucocratic orthopyroxenite with intercumulus grey chromitite surrounding up to 1.5cm patches of orthopyroxene - oikocrysts in spots. Dark serpentinized dunite is minor and consists of fine 1-2mm ovoidal dark olivine dunite in the intercumulus of the dominant orthopyroxenite-chromitite. Photo 29 is of poikilitic orthopyroxenes and intercumulus chromitite in unit at 149.5m.			
164.70	203.50	Chromitite Semi-massive to massive chromitite with mixture of pyroxenite and olivine dunite groundmass rock. Beds of chromitite are not layered with the cumulates but occurs as fragments and massive beds that are lensy and discontinuous with sharp contacts with surrounding rock. Photo 30 at 170.20m is of a bed of chromitite with sharp contact with cumulus dunite that contains interstitial chromitite. The massive chromitite in the beds contain large oikocrysts of orthopyroxene. Photo 32 shows lensoidal layering of chromitite in pyroxenite at 176m. It appears massive chromitite, layers and fragments are contained in pyroxenitic portions and interstitial chromitite occurs in darker dunitic portions. Photos 33 and 34 are of massive chromitite with oikocrysts of orthopyroxene and density contrast light vs. heavy chromitite spots at 182m. Intervals between beds are variable at 10 to 30 to 50cm intervals occupied by darker dunite and. A large interstitial section is from 167.2 to 168m. Larger continuous massive chromitite sections are toward the bottom contact from 181.1 to 181.3m, 192.3 to 194m and from 200.20 to 203.30m that contains dunite fragments and orthopyroxenite spots (photo 35 at 201.30m). These sections are associated with pyroxenite toward the bottom contact of this zone from 201 to 205.90m.			
203.50	205.90	Pyroxenite Leucocratic orthopyroxenite with some pulsing dunite portions.			
205.90	207.30	Poikilitic serpentinized dunite			

Drill Hole Log

BT-09-31

From	To	Lithology	Code	Sample	From
207.30	207.70	Pyroxenite Leucocratic unit with sharp contacts with dunite.			
207.70	221.80	Heterolithic serpentized dunite This unit is continuous with poikilitic orthopyroxenes to large orthopyroxene fragments up to 4cm in size throughout to areas of dominant cumulus pyroxenite with surrounding dunite. Photos 36 and 37 at 220.70m are of fragmented orthopyroxene texture in dark dunite groundmass. Foliations of orthopyroxenes is 45° to CA.			
221.80	222.60	Pyroxenite Leucocratic pyroxenite.			
222.60	224.33	Dark serpentized dunite			
224.33	225.00	Pyroxenite			
225.00	228.00	Dark serpentized dunite Dominant unit with some intervening pyroxenite.			
228.00	237.00	Poikilitic serpentized dunite Up to 234.90, the unit contains areas of pyroxene-poikilitic dark dunite. At 229.82m, is where some beds of chromitite begin. At 230.35m is photo 38 of diffuse layering and clasts of pyroxenite in chromitite - this is not a dominant texture in this hole as opposed to hole 30. Pyroxenite sections are from 234 to 234.40m, 235.35 to 2335.84m and 236.3 to 236.75m.			

Drill Hole Log		BT-09-31	
From	To	Lithology	Code
237.00	270.00	Semi-massive chromitite From 237 to 255m are intermittent beds of chromitite and interstitial chromite in dunite intervals. Groundmass is dark olivine dunite. At 241.70m is photo 38 of diffuse talc-rimmed olivine cumulate overprinted fragments of pyroxenite that also appear as oikocrysts - this section is from 241 to 243m. From 255 to 264m is more dominant interstitial chromitite with cumulus dunite textures - photo 39 is of lesser cumulus dunite at 255m whereas photo 40 is of more dominant cumulus dunite at 258.30m. The chromitite becomes less in abundance down hole with more just interbanding and predominant olivine cumulus. Photo 41 at 269.70m is a fragment of dunite surrounded by interstitial chromitite and cumulus dunite.	
270.00	309.30	Serpentinized dunite The unit contains disseminated chromite from 270 to 277m. This unit is a homogeneous prolific green talc-serpentine-magnetite veined throughout giving ghosted dunite textures among veins. Unit varies from more dark serpenitized to green olivine-rich. It continues to the end of the hole and surrounding the last chromitite interval. Photo 42 is at 303.4m of prolific veined unit.	
309.30	318.65	Intermittent chromitite beds Generally 20 to 30cm spaced up to 30cm chromitite beds with intervals of serpenitized dunite.	
318.65	387.00	Serpentinized dunite Same unit as above.	

Drill Hole Log

BT-08-10

Hole ID:	BT-08-10	Project:	Freewest	Year:	2008	Claim:	TWP:
Grid X:		Easting:		Grid Azimuth:		Dip	Casing:
Grid Y:		Northing:		True Azimuth:		Elev (m):	Casing (m):
Drill Start:		Log Start:		Drill Company:		Drilled for:	Freewest Resources Inc.
Drill Finish:		Log Finish:		Foreman:		Storage:	
Surveyed	<input type="checkbox"/>	Logged by:		Checked by:		Comments:	

From	To	Lithology	Code
0.00	35.60	Overburden	
35.60	66.37	Serpentinized peridotite	
66.37	124.70	Serpentinized dunite	
124.70	168.20	Semi-massive intermittent chromitite beds	
168.20	174.20	Chromitite	
174.20	187.10	Serpentinized dunite	
187.10	289.12	Pyroxenite	

BT-08-10

Drill Hole Log

From	To	Lithology	Code	Sample	From
0.00	35.60	Overburden			
35.60	66.37	Serpentinized peridotite			
		Not relogged.			
66.37	124.70	Serpentinized dunite			
		This unit is green-grey bleached highly wholesale talc-serpentine altered. Olivines are green 1-2mm round ovoidal minerals throughout. The unit is bleached light green-grey up to 86.7 where the unit is darker serpentine but still talc-altered and contains more picrolitic serpentine and talc irregular veins. Olivines are dark serpentine-altered in this section. Unit is more green dunite spotted and patchy toward this darker more serpentine-altered dunite. Photo 20 is of bleached light green dunite at 82.8m. The darker dunite could be the top of the pulse. The unit is bleached light green dunite again starting at 98.36m down. This dunite hosts the chromite. It is very crumbly and altered up to 124.7m. The unit contains 0.5 to 1% disseminate chromite and bed fractures of chromitite. Photo 21 is of crumbly dunite at 101.5m.			
124.70	168.20	Semi-massive intermittent chromitite beds			
		Intermittent chromitite beds contain intercumulus contacts with cumulus olivines in dunite. The beds are variably 1 to 50cm thick. In chromitite-bearing dunite, the unit is darker less bleach and grey-green in colour with the olivines as grey minerals up to 3mm in size. The chromitite beds sometimes contain gradational upper cumulus contacts with dunite and sharp lower contacts with dunite indicating grading in beds and topping of the chromitites to down the hole. Photo 22 is at 130.67m with sharp upper contact and cumulus lower contact in chromitite bed. Photo 23 is grading to more disseminated chromitite to lower down the hole at 135.8m. Sometimes there are cumulus contacts on the dunites on both the upper and lower contacts indicating a mixture of magma, however dominant grading indicates topping to down the hole - this occurs between 162 to the lower contact of lower massive chromitite interval at 174.20m. Photo 24 is of the general intermittent beds in this interval. In the chromitite beds, there are spotted lighter grey to darker chromitite density contrast textures - photo 25 is of the lighter less dense chromite up to 1.5cm irregular patches in more dense darker chromitite groundmass at 160m. There is irregular up to 2mm talc-serpentine white fracture veining in the chromitite beds.			

Drill Hole Log				BT-08-10	
From	To	Lithology	Code	Sample	From
168.20	174.20	Chromitite Section of dominant massive chromitite with some reverse bedding of sharp upper contacts and cumulus lower contacts in dunite intervals indicating intermittent pulsing of dunite in dominant chromitite at this level. And upper contact is more intermittent bedded to cumulus graded whereas upper contact of this massive chromitite interval is sharp with no more beds with underlying dunite. Photo 26 is a general photo of bedded upper contact and non-bedded/sharp lower contact.			
174.20	187.10	Serpentinized dunite Light green wholes talc and serpentine altered dunite. Chromitite occurs as irregular fractures up to 1.5cm wide in this interval. Toward lower contact with pyroxenite, the dunite has 10cm wide dark serpentine-altered cumulus olivine beds grading up into intercumulus pyroxenite in cycles until dunite quits and it's just pyroxenite.			
187.10	289.12	Pyroxenite The unit is a grey, homogeneous fine grained dirty looking composition due to dark and light preferential talc-serpentine-altered orthopyroxenes. The pyroxenes are sheafy rhombus-shaped grains. The unit is first darker and coarser grained pyroxenitic (up to 3mm grains) from 187.10 to 193.45m, then generally fine grained down the hole.			

Drill Hole Log

BT-09-17

Hole ID: BT-09-17 Project: Freewest Year 2009 Claim: TWP:
 Grid X: Easting: UTM Zone: Grid Azimuth: Dip Casing:
 Grid Y: Northing: Datum: 8/31/2009 True Azimuth: Elev (m): Core Size: Casing (m): Tar
 Drill Start: Log Start: Log Finish: Drill Company: Drilled for: Freewest Resources Inc.
 Drill Finish: Log Finish: Foreman: Storage:
 Surveyed Logged by: Checked by: Comments:

From	To	Lithology	Code
0.00	14.00	Overburden	
14.00	39.00	Serpentinized dunite	
39.00	85.50	Disseminated chromite zone	
85.50	145.20	Orthopyroxenite	
145.20	173.00	Dunite	
173.00	180.95	Semi-massive chromitite	
180.95	242.00	Talc-altered pyroxenite	
242.00	252.00	Intermittent chromite beds/semi-massive chromitite	
252.00	263.80	Talc-altered pyroxenite	
263.80	267.50	Intermittent chromite beds	
267.50	289.10	Chromitite	
289.10	296.30	Serpentinized pyroxenite	
296.30	298.80	Chromitite	
298.80	318.70	Leucogabbro	
318.70	337.90	Chromitite	
337.90	381.00	Talc schist	

Drill Hole Log

BT-09-17

From	To	Lithology	Code	Sample	From
0.00	14.00	Overburden			
14.00	39.00	Serpentinized dunite			
		From 26.7 to 26.88m is a geochem sample of dark serpentinized dunite. The unit is sheared with foliated olivine and talc alteration at 60° to CA.			
39.00	85.50	Disseminated chromite zone			
		Disseminated intercumulus chromite to bands in altered dunite. TS samples from 40.71 to 40.85m, 61.83 to 61.93m and 80.90 to 81m (photo 40 chromite and silicate banding). Chromite increases in the intercumulus toward the lower contact with the pyroxenite. There is more developed intermittent bedding of chromitite in pyroxenite. Some more semi-massive chromitite parts are from 61.5 to 75.40m.			
85.50	145.20	Orthopyroxenite			
		Geochem samples from 90.20 to 90.35m and 136.15m. The unit homogeneous grey with 2-3mm sheafy pyroxenes throughout. From 129 to contact with dunite/chromitite at 147m, the unit is more sheared looking with dark serpentinized parts present in between dominant pyroxene groundmass in shear. Foliation is 60° to CA at 139m.			
145.20	173.00	Dunite			
		Chromite horizon is at contact of orthopyroxenite with dunite in intercumulus interstitial and bands in dunite. Sharp contact of orthopyroxenite with dunite. TS samples are from 152.60 to 152.70m and of reef interval after 169m from 171.25 to 171.35m of intercumulus banded chromitite with dunite. More chromite beds occur from 169 to 173m. Massive chromitite sections in this interval are from 149 to 149.50m, 150.14 to 150.50m, 173 to 175.7m. In the interval from 173 to 175.7m, the chromitite begins with gradational cumulus dunite leading to more massive interstitial chromite. Grading to more massive chromitite is down the hole in these areas. Photo 43 at 174.7m shows the grading to more massive chromitite and sharp lower contact of dunite indicating a pulse of dunite and then going into chromite field. In this interval, the chromitite contains irregular lighter matches of less dense chromitite in massive denser chromitite groundmass.			

Drill Hole Log		BT-09-17	
From	To	Lithology	Code
173.00	180.95	Semi-massive chromitite	
TS sample from 179.87 to 180m.			
180.95	242.00	Talc-altered pyroxenite	
Sharp contact with overlying chromitite and no fragments of chromitite in pyroxenite due to it being an upper pulse. The unit contains a few small chromite intervals down the hole. In the chromite intervals, it appears there is sharp upper contact of pyroxenite parts and then they grade up to more interstitial chromitite. Geochem samples are from 183.94 to 184.09m and from 210.63 to 210.78m.			
242.00	252.00	Intermittent chromitite beds/semi-massive chromitite	
From 249.25 to 249.35m is TS sample of semi-massive chromitite.			
252.00	263.80	Talc-altered pyroxenite	
Geochem sample from 262.54 to 262.84m.			
263.80	267.50	Intermittent chromitite beds	
267.50	289.10	Chromitite	
Semi-massive up to 274.50m. Massive chromitite is lower down from basal pulse of pyroxenite. From 267.30 to 267.38 and from 284.07 to 284.17m are TS samples of chromitite. The unit contains what appears as a lot of density contrast textures throughout. From 286.5m to the end, there are grading textures of cumulus pyroxenite up to more interstitial chromitite indicating successive pulses of pyroxenite topping down the hole and grading into the chromite fields. There's a lower contact of chromitite with pyroxenite with successive pulse of pyroxenite.			

Drill Hole Log				BT-09-17	
From	To	Lithology	Code	Sample	From
289.10	296.30	Serpentinized pyroxenite			
296.30	298.80	Chromitite			
		Massive chromitite interval. TS sample from 297.10 to 297.21m.			
298.80	318.70	Leucogabbro			
		Grey to salt and pepper, medium- to coarse-grained, massive gabbro that shows early crystallizing green rounded up to 5mm cumulus clinopyroxene rimmed by and in association with finer sheaty to needly brown bronzite and interstitial plagioclase with trace magnetite. The bronzite rims shows it crystallized after the clinopyroxene. Rarely the bronzites are coarser rounded cumulus minerals. The opx:opx:pl ratios is dominantly 40:30:30 and ranges to 00:20:80 leucogabbro. The unit contains the coarsest orthopyroxene with finer clinopyroxene at the base. Upward, orthopyroxenes become fine grained and clinopyroxenes are coarse. Plagioclase increases up to 80% to 309.80m and then the rock is finer crained clinopyroxene cumulus-dominant with plagioclase at 30%. Unlike the ultramafic layered series the gabbro roof is fresh and unaltered. Contains approximately 1-2% pyrrhotite + pyrite + chalcopyrite. Upper contact with massive chromite is highly fractured and obscured, lower contact with chromitite is approximately 35 degrees ca. From 300.56 to 300.66m and from 314.77 to 314.87m are samples of gabbro - photo 41 at 300.56m. The gabbro is first coarse grained and then gets gradationally fine down the hole to the chromitite interval.			
318.70	337.90	Chromitite			
		The massive chromitite begins with a sharp contact with gabbro. Leucogabbro occurs from 330.20 to 333.90m. Dalmatianite chromitite occurs throughout the massive chromitite interval to 330.50m. TS samples of massive to dalmatianite chromitite are from 320.90 to 321m and from 335.90 to 336m.			
337.90	381.00	Talc schist			

Drill Hole Log

FW-08-19

Hole ID: FW-08-19	Project: Freewest	Year: 2008	Claim:	TWP:
Grid X:	Easting:	Grid Azimuth:	Dip	Casing:
Grid Y:	Northing:	True Azimuth:	Elev (m):	Casing (m):
Drill Start:	Log Start:	Drill Company:	Drilled for:	Freewest Resources Inc.
Drill Finish:	Log Finish:	Foreman:	Storage:	
Surveyed <input type="checkbox"/>	Logged by:	Checked by:	Comments:	

From	To	Lithology	Code
0.00	9.00	Overburden	
9.00	11.89	Dark serpentinized peridotite	
11.89	13.36	Pyroxenite	
13.36	64.50	Dark serpentinized peridotite	
64.50	69.40	Fault	
69.40	73.97	Pyroxenite	
73.97	84.94	Dark serpentinized peridotite	
84.94	105.39	Pyroxenite	
105.39	141.50	Heterolithic ultramafic	
141.50	144.14	Chromitite	
144.14	159.37	Peridotite	
159.37	162.00	Chromitite	
162.00	164.20	Heterogeneous peridotite	
164.20	183.00	Pyroxenite	
183.00	229.64	Chromitite	
229.64	273.00	Pyroxenite	

Drill Hole Log

FW-08-19

From	To	Lithology	Code	Sample	From
0.00	9.00	Overburden Hornblende granite boulders with minor fossiliferous limestone.			
9.00	11.89	Dark serpentinized peridotite Dark serpentinized cumulate ovoidal 1-2mm dark olivine-bearing unit that contains veins of talc-altered leucocratic pyroxenite running through and cumulus up to 4mm equant rhombus pyroxenes.			
11.89	13.36	Pyroxenite Leucocratic wholesale talc-altered and scalet red hematite irregular fracture veined pyroxenite.			
13.36	64.50	Dark serpentinized peridotite Dark serpentinized ovoidal olivine peridotite with irregular fractures and veins of hematite-serpentine with intruding leucocratic pyroxenites. Unit is often wholesale purple oxidation-altered on olivines in unit. Unit contains fragments of chromitite, interstitial disseminated chromite in between the olivines and chromitite fractures. Photo 1 is of chromitite fragments up to 4cm long in peridotite at 13.36m. Photo 2 is of a 1.5cm wide pyroxenite vein containing purple/mauve kaemmerite on the sides at 13.80m. The unit contains thin fracture veinlets of asbestos throughout down hole. Another patch of chromitite occurs at 20.10m. Photo 3 is of dark serpentinized cumulat olivine peridotite at 34.24m. Photo 4 is of vein altered kammerite/stichtite and scalet red hematite associated with pyroxenite veining at 34.53m. Foliation in purple oxidation veins is 40° to CA at 34.24m to 45° to CA at 51.40m. Unit is progressively oxidation veined toward fault lower contact with pyroxenite at 45° to CA at 58.13m - photo5 of purple veins.			
16.18	17.10	Pyroxenite Leucocratic talc-altered pyroxenite has sharp upper contact and more cumulus contact of cumulus pyroxenes toward lower serpentinized peridotite.			
26.60	28.00	Pyroxenite Leucocratic unit contains lots of platy serpentine.			

Drill Hole Log			FW-08-19		
From	To	Lithology	Code	Sample	From
32.13	32.70	Pyroxenite			
33.32	33.36	Pyroxenite Altered leucocratic unit.			
64.50	69.40	Fault Photo 6 is of scalet red iddingsite alteration in the core. The core is all broken up as a contact zone with underlying pyroxenite. Red alteration is associated with the pyroxenite.			
69.40	73.97	Pyroxenite Leucocratic altered orthopyroxenite with irregular talc veins at contact with underlying peridotite.			
73.97	84.94	Dark serpentinized peridotite Dark serpentinized dunite unit with cumulate olivine.			
84.94	105.39	Pyroxenite Unit is talc vein altered and coarse sheafy pyroxenitic at upper contact with peridotite. Unit contains areas of wholesale iddingsite alteration. Unit contains cumulus olivine gradational contact with underlying peridotite.			
105.39	141.50	Heterolithic ultramafic Heterogeneous dominant cumulus up to 0.5cm ovoidal olivine-bearing with intercumulus pyroxene unit. Unit contains an interstitial chromite with fragments of pyroxenite in interval from 114.15 to 115.50m - photo 7 at 114.86m. The unit is first peridotitic up to the chromite interval. Then above the chromite, the unit is heterogeneous pyroxenite in peridotite (evidence of magma mixing) gradationally up to 129m where the unit becomes dominant dark serpentinized peridotite. Photo 8 at 119m of heterogeneous pyroxene in peridotite unit. Within the heterogeneous ultramafic, there are large green orthopyroxene oikocrysts enveloping the intercumulus groundmass in the unit that look like sheared large fragments of orthopyroxenite? - photo 9 at 120.66m. Foliation is 45° to CA. The unit is peridotite up to 136.60m where the unit gradationally becomes heterogeneous pyroxenitic. Foliation is prevalent in this heterogeneous interval at 40° to CA at 147.3m - photo 11. At 141m,			

Drill Hole Log

FW-08-19

From	To	Lithology	Code	Sample	From
		the unit becomes dark peridotite again and a chromitite interval begins at lower contact. Photo 10 is of large poikilitic green orthopyroxene sheared on foliation at 135.95m.			
141.50	144.14	Chromitite			
		Semi-massive interstitial chromitite interval with beads of pyroxene layering in areas and darker cumulate olivine parts.			
144.14	159.37	Peridotite			
		At 158.70m, the unit becomes more talc-altered and veined toward underlying interval of chromitite indicating change of units to pyroxenite. The unit contains massive chromitite fragments that pinch out, indicating they're probably large space-occupying fragments in the dunite? - photo 12 at 146.70m.			
159.37	162.00	Chromitite			
		Massive chromitite with lighter areas of less dense chromitite in darker more dense chromitite groundmass.			
162.00	164.20	Heterogeneous peridotite			
		Dominant dark cumulate olivine-bearing peridotite with larger up to 1cm round cumulus leucocratic orthopyroxene coming through. Unit is talc-altered at upper contact with chromitite.			
164.20	183.00	Pyroxenite			
		Leucocratic pyroxenite talc-serpentinized. Unit has sharp lower contact with large chromitite interval. Unit contains up to 1.5cm large round brown bronzite orthopyroxene oikocrysts enveloping and surrounded by finer up to 2mm orthopyroxenes.			
183.00	229.64	Chromitite			
		Massive chromitite interval. Unit contains large up to 2cm sheafy oikocrysts of orthopyroxene that are lighter grey but chromite-bearing than the darker groundmass chromitite. Photo 13 at 212.20m and photo 14 at 216.55m of oikocrysts. From 227.70m to the lower contact, there are large globular leucocratic patches of orthopyroxenite probably fragment from intermixing of lower pyroxenite or density contrast chromitiites that are			

Drill Hole Log		FW-08-19	
From	To	Lithology	Code
		overprinted by the oikocystic orthopyroxenes. Photo 15 at 228m of globules of chromitite. Photo 16 of the large 46m chromitite interval.	
229.64	273.00	Pyroxenite Leucocratic orthopyroxenite. Photos 17, 18 and 19 of orthopyroxenite - large oikocrysts of orthopyroxene surrounded and enveloping smaller 2mm sheafy orthopyroxenes in groundmass. Medium grained pyrite sulphides occur in talc-altered unit at upper contact. The unit is whiter more differentiated in PGE-bearing interval from 229 to 238m before it is darker homogeneous afterward. Unit contains patches to veins of dark cumulate olivine/serpentine in areas.	

APPENDIX 2

- Sample Lists:**
- 1. BT-08-10**
 - 2. BT-09-31 & BT-09-17**
 - 3. FW-08-19**

BT-08-10**Sample # Depth (m)**

486001	69	Whole rock	dunite, light grey green
486002	89	Whole rock	dark dunite
486003	111.32	Whole rock	light green altered crumbly dunite
486004	114		
486005	114.7		
486006	115.4		
486007	116.1		
486008	117		
486009	117.7		
486010	118.5		
486011	119.2		
486012	119.9		
486013	120.6		
486014	121.3		
486015	122		
486016	122.7		
486017	124.1		
486018	124.9		
486019	125.2		
486020	125.6		
486021	126		
486022	126.4		
486023	126.8		
486024	127.2		
486025	127.6		
486026	128		
486027	128.4		
486028	128.8		
486029	129.2		
486030	129.6		
486031	130		
486032	130.4		
486033	130.8		
486034	131.2		
486035	131.6		
486036	132		
486037	132.4		
486038	132.8		
486039	133.2		
486040	133.6		
486041	134		
486042	134.4		

486043	134.8
486044	135.2
486045	135.6
486046	136
486047	136.4
486048	136.8
486049	137.2
486050	137.6
486051	138
486052	138.4
486053	138.8
486054	139.2
486055	139.6
486056	140
486057	140.4
486058	140.8
486059	141.2
486060	141.6
486061	142
486062	142.4
486063	142.8
486064	143.2
486065	143.6
486066	144
486067	144.4
486068	144.8
486069	145.2
486070	145.6
486071	146
486072	146.4
486073	146.8
486074	147.2
486075	147.6
486076	148
486077	148.4
486078	148.8
486079	149.2
486080	149.6
486081	150
486082	150.4
486083	150.8
486084	151.2
486085	151.6
486086	152.2

486087	152.6
486088	153
486089	153.6
486090	154
486091	154.4
486092	154.8
486093	155.2
486094	155.6
486095	156
486096	156.4
486097	156.8
486098	157.2
486099	157.6
486100	158.2
486101	158.4
486102	158.8
486103	159.2
486104	159.6
486105	160
486106	160.4
486107	160.8
486108	161.2
486109	161.6
486110	162
486111	162.4
486112	162.8
486113	163.2
486114	163.6
486115	164
486116	164.4
486117	164.8
486118	165.2
486119	165.6
486120	166
486121	166.4
486122	166.8
486123	167.2
486124	167.6
486125	168
486126	168.4
486127	168.8
486128	169.2
486129	169.6
486130	170

486131	170.2		
486132	170.6		
486133	171		
486134	171.4		
486135	171.8		
486136	172.2		
486137	172.6		
486138	173		
486139	173.2		
486140	173.6		
486141	174		
486142	175	Whole rock	dunite
486143	188	Whole rock	pyroxenite
486144	208	Whole rock	pyroxenite
486145	228	Whole rock	pyroxenite
486146	248	Whole rock	pyroxenite

BT-09-31				BT-09-17			
Sample #	Depth (m)			Sample #	Depth (m)		
486147	101.9	Whole rock	green dunite	486672	296.8		
486148	122	Whole rock	dark dunite	486676	298.4		
486149	142	Whole rock	dark dunite	486681	299		gabbro
486150	143.18	Thin section	oikocrysts	486713	315.4		gabbro
486151	145	Whole rock	pyroxenite	486717	319		
486152	151.4			486722	321		
486153	151.8			486726	323		
486154	151.2			486729	325.4		
486155	151.8			486734	327.4		
486156	152.2			486742	330.6		
486157	152.6			486743	333.4		
486158	153			486748	335.4		
486159	153.4			486753	337.4		
486160	153.8						
486161	154.2						
486162	154.6						
486163	155						
486164	155.4						
486165	155.8						
486166	156.2						
486167	156.6						
486168	157						
486169	157.6						
486170	158						
486171	158.4						
486172	158.6						
486173	159						
486174	159.4						
486175	159.8						
486176	160.2						
486177	160.6						
486178	161						
486179	161.4						
486180	161.8						
486181	162.2						
486182	162.6						
486183	163						
486184	163.6						
486185	164						
486186	164.4						
486187	164.8						
486188	165.2						

486189	165.6
486190	166
486191	166.4
486192	166.8
486193	167.2
486194	167.6
486195	168
486196	168.4
486197	168.8
486198	169.2
486199	169.6
486200	170
486201	170.4
486202	170.8
486203	171.2
486204	171.6
486205	172
486206	172.4
486207	172.8
486208	173.2
486209	173.6
486210	174
486211	174.4
486212	174.8
486213	175.2
486214	175.6
486215	176
486216	176.4
486217	176.8
486218	177.2
486219	177.6
486220	178
486221	178.4
486222	178.8
486223	179.2
486224	179.6
486225	180
486226	180.4
486227	180.8
486228	181.2
486229	181.6
486230	182
486231	182.2
486232	182.6

486233	183
486234	183.4
486235	183.8
486236	184.2
486237	184.6
486238	185
486239	185.4
486240	185.8
486241	186.2
486242	186.6
486243	187
486244	187.4
486245	187.8
486246	188.2
486247	188.6
486248	189
486249	189.4
486250	189.8
486251	190.2
486252	190.6
486253	191
486254	191.4
486255	191.8
486256	192.2
486257	192.6
486258	193
486259	193.4
486260	193.8
486261	194.2
486262	194.6
486263	195
486264	195.4
486265	195.8
486266	196.2
486267	196.6
486268	197
486269	197.4
486270	197.8
486271	198.2
486272	198.6
486273	199
486274	199.4
486275	199.8
486276	200.2

486277	200.6	
486278	201	
486279	201.4	
486280	201.8	
486281	202.2	
486282	202.6	
486283	203	
486284	203.4	
486285	203.8	
486286	204.2	
486287	219.2	Whole rock oikocrysts
486288	229.4	
486289	229.8	
486290	230.2	
486291	230.8	
486292	231	
486293	231.4	
486294	231.8	
486295	232.2	
486296	232.8	
486297	233.2	
486298	233.6	
486299	234.4	
486300	234.8	
486301	235.2	
486302	235.6	
486303	236	
486304	236.4	
486305	236.8	
486306	237.2	
486307	237.6	
486308	238	
486309	238.4	
486310	238.8	
486311	240.2	
486312	240.6	
486313	241	
486314	241.4	
486315	241.8	
486316	242.2	
486317	242.6	
486318	243	
486319	243.4	
486320	243.8	

486321	244.2
486322	244.6
486323	245
486324	245.4
486325	245.8
486326	246.2
486327	246.6
486328	247
486329	247.4
486330	247.8
486331	248.2
486332	248.6
486333	249.4
486334	251.8
486335	252.2
486336	252.6
486337	253
486338	253.4
486339	253.8
486340	254.2
486341	255.2
486342	255.6
486343	256
486344	256.4
486345	256.8
486346	257.2
486347	257.6
486348	258.2
486349	258.6
486350	259
486351	259.6
486352	260.2
486353	260.6
486354	261
486355	261.4
486356	261.8
486357	262.2
486358	262.6
486359	263
486360	264.2
486361	264.6
486362	265
486363	265.4
486364	265.8

486365	266.6
486366	267
486367	267.2
486368	267.6
486369	268
486370	268.4
486371	268.8
486372	269.2
486373	269.6
486374	270
486375	270.4
486376	270.8
486377	271.2
486378	271.6
486379	272
486380	272.4
486381	272.8
486382	273.2
486383	273.6
486384	274
486385	274.4
486386	274.8
486387	275.2
486388	275.6
486389	276
486390	276.4
486391	276.8

FW-08-19

Sample #	Depth (m)		
232251	16.07	Whole rock	peridotite
232252	16.86	Whole rock	pyroxenite
232253	13.5	Thin section	chromitite fragment
232254	35.2	Whole rock	peridotite
232255	55.62	Whole rock	peridotite
232256	75.36	Whole rock	peridotite
232257	87.49	Whole rock	pyroxenite
232258	104	Whole rock	pyroxenite
232259	108.76	Whole rock	peridotite
232260	114.58	Thin section	frags of pyroxenite in chromitite
232261	120.7	Whole rock	heterogeneous peridotite
232262	135.2	Whole rock	peridotite
232263	137.83	Whole rock	foliation in heterogeneous peridotite
232264	141.7		
232265	142.1		
232266	142.5		
232267	143.17		
232268	144.49	Whole rock	peridotite
232269	161.5		
232270	165.38	Whole rock	pyroxenite
232271	182.4	Whole rock	pyroxenite
232272	183.8		
232273	184.2		
232274	184.6		
232275	185		
232276	185.4		
232277	186		
232278	186.4		
232279	186.8		
232280	187.2		
232281	187.6		
232282	188		
232283	188.4		
232284	188.8		
232285	189.2		
232286	189.6		
232287	190		
232288	190.4		
232289	190.8		
232290	191.2		
232291	191.8		
232292	192.4		

232293	192.8
232294	193.2
232295	193.6
232296	194
232297	194.4
232298	194.8
232299	195.2
232300	195.6
232301	196
232302	196.4
232303	196.8
232304	197.2
232305	197.6
232306	198
232307	198.4
232308	198.8
232309	199.2
232310	199.6
232311	200
232312	200.4
232313	200.8
232314	201.2
232315	201.6
232316	202
232317	202.4
232318	202.8
232319	203.2
232320	203.6
232321	204
232322	204.4
232323	204.8
232324	205.2
232325	206
232751	206.6
232752	207.2
232753	207.4
232754	207.8
232755	208.2
232756	208.6
232757	209
232758	209.4
232759	209.8
232760	210.2
232761	210.6

232762	211
232763	211.4
232764	211.8
232765	212.4
232766	212.8
232767	213.2
232768	213.6
232769	214
232770	214.4
232771	214.8
232772	215.2
232773	215.6
232774	216
232775	216.4
232776	216.8
232777	217.2
232778	217.6
232779	218
232780	218.4
232781	218.8
232782	219.2
232783	219.6
232784	220
232785	220.4
232786	220.8
232787	221.2
232788	221.6
232789	222
232790	222.4
232791	222.8
232792	223.2
232793	223.6
232794	224
232795	224.4
232796	224.6
232797	225
232798	225.4
232799	225.8
232800	226.2
232801	226.6
232802	227
232803	227.4
232804	227.8
232805	228.2

232806	228.6
232807	229
232808	229.4
232809	229.8

APPENDIX 3**Whole Rock Geochemistry and Full Spectrum PGE**

Method	Analyte	Unit	232251	232254	232256	232257	232258	232261	
			BD dunite	BD dunite	BD dunite	BD pyroxenite	BD pyroxenite	BD peridotite	
FUS-XRF	SiO ₂	%	31.7	35.5	35.4		52	50.4	39.1
FUS-XRF	Al ₂ O ₃	%	2.44	1.18	0.82		1.9	3.35	1.76
FUS-XRF	Fe ₂ O ₃ (T)	%	16.5	12.7	12.7		8.61	8.51	12.5
FUS-XRF	MnO	%	0.124	0.056	0.051		0.145	0.182	0.125
FUS-XRF	MgO	%	32.1	35.79	36.37		29.28	27.07	34.26
FUS-XRF	CaO	%	0.08	0.03	0.48		2.13	3.95	0.61
FUS-XRF	Na ₂ O	%	< 0.01	< 0.01	< 0.01		< 0.01	0.08	< 0.01
FUS-XRF	K ₂ O	%	0.02	0.02	0.02		0.04	0.24	0.68
FUS-XRF	TiO ₂	%	0.1	0.07	0.06		0.11	0.13	0.07
FUS-XRF	P ₂ O ₅	%	< 0.01	0.01	0.01		0.01	0.01	0.01
FUS-XRF	Cr ₂ O ₃	%	6.74	1.69	2.19		0.52	0.45	0.6
FUS-XRF	V ₂ O ₅	%	0.041	0.015	0.014		0.013	0.018	0.013
FUS-XRF	LOI	%	9.76	11.5	11.6		5.7	5.7	10.9
FUS-XRF	Total	%	99.58	98.57	100.1		100.4	100.1	100.6
AR-MS	Li	ppm	23.2	15.5	16.3		2.9	4.5	8.4
AR-MS	Be	ppm	< 0.1	0.1	< 0.1		< 0.1	< 0.1	< 0.1
AR-MS	B	ppm	33	39	50		27	19	130
AR-MS	Na	%	0.017	0.011	0.012		0.013	0.017	0.017
AR-MS	Mg	%	> 10.0	> 10.0	> 10.0		5.64	5.41	> 10.0
AR-MS	Al	%	0.35	0.41	0.2		0.75	1.26	0.85
AR-ICP	P	%	0.002	0.002	0.002		0.002	0.002	0.002
AR-ICP	S	%	0.082	0.008	0.085		0.026	0.044	0.068
AR-MS	K	%	< 0.01	< 0.01	< 0.01		0.02	0.18	0.58
AR-MS	Ca	%	0.05	0.02	0.36		0.34	0.6	0.28
AR-MS	V	ppm	10	14	7		29	29	31
AR-MS	Cr	ppm	779	959	665		987	993	631
AR-ICP	Ti	%	< 0.01	< 0.01	< 0.01		0.02	0.03	0.02
AR-MS	Mn	ppm	335	266	219		277	496	797
AR-MS	Fe	%	6.84	7.5	7.55		2.59	2.31	7.53
AR-MS	Co	ppm	227	92.7	159		38.6	29.6	92.9
AR-MS	Ni	ppm	1870	1160	1800		285	447	1000
AR-MS	Cu	ppm	2.9	1.38	4.36		10.1	76.2	36
AR-MS	Zn	ppm	20.2	9.3	5.2		5.7	5.2	16.7
AR-MS	Ga	ppm	1.16	1.14	0.65		1.81	2.57	2.16
AR-MS	Ge	ppm	0.2	0.2	0.2		0.1	0.1	0.2
AR-MS	As	ppm	6.1	4	1.9		0.8	0.8	0.9
AR-MS	Se	ppm	0.5	0.2	0.1		< 0.1	< 0.1	< 0.1
AR-MS	Rb	ppm	0.2	0.2	0.1		1	9	23.2
AR-MS	Sr	ppm	2.4	1.7	3		3.3	2.8	5.5
AR-MS	Y	ppm	0.73	0.74	0.96		0.59	1.08	2.27
AR-MS	Zr	ppm	1	0.9	0.5		0.1	0.8	1.2
AR-MS	Sc	ppm	7.2	8.3	7		7.3	6.2	8.5
AR-MS	Mo	ppm	1.01	0.31	0.19		0.09	0.08	0.11
AR-MS	Ag	ppm	0.119	0.026	0.048		0.005	< 0.002	< 0.002
AR-MS	Cd	ppm	< 0.01	< 0.01	< 0.01		0.01	< 0.01	< 0.01
AR-MS	In	ppm	< 0.02	< 0.02	< 0.02		< 0.02	< 0.02	0.04
AR-MS	Sn	ppm	0.05	0.05	0.06		0.06	0.13	0.27
AR-MS	Sb	ppm	0.03	< 0.02	< 0.02		< 0.02	< 0.02	< 0.02
AR-MS	Te	ppm	0.15	0.06	0.11		< 0.02	0.06	< 0.02
AR-MS	Cs	ppm	< 0.02	< 0.02	< 0.02		0.11	0.45	0.68
AR-MS	Ba	ppm	3.9	3.2	3.2		2.4	13.3	48.4
AR-MS	W	ppm	< 0.1	< 0.1	< 0.1		< 0.1	< 0.1	< 0.1
AR-MS	Re	ppm	0.001	0.001	0.001		0.001	< 0.001	< 0.001
AR-MS	Tl	ppm	< 0.02	< 0.02	< 0.02		0.02	0.05	0.11
AR-MS	Pb	ppm	0.43	0.17	0.9		0.52	0.89	1.79
AR-MS	Bi	ppm	0.08	0.02	0.05		< 0.02	0.04	< 0.02
FUS-MS	Nb	ppm	< 0.2	< 0.2	< 0.2		< 0.2	< 0.2	< 0.2
FUS-MS	La	ppm	1.85	1.04	1.1		1	1.89	1.64
FUS-MS	Ce	ppm	2.42	1.77	2.27		1.91	4.27	3.54
FUS-MS	Pr	ppm	0.13	0.23	0.23		0.19	0.52	0.38
FUS-MS	Nd	ppm	0.46	0.84	0.92		0.87	2.39	1.49
FUS-MS	Sm	ppm	0.13	0.27	0.17		0.26	0.56	0.35
FUS-MS	Eu	ppm	0.027	0.021	0.04		0.043	0.195	0.039
FUS-MS	Gd	ppm	0.12	0.29	0.19		0.3	0.67	0.35
FUS-MS	Tb	ppm	0.02	0.06	0.03		0.06	0.12	0.06
FUS-MS	Dy	ppm	0.13	0.38	0.15		0.36	0.76	0.41
FUS-MS	Ho	ppm	0.03	0.07	0.03		0.08	0.17	0.09
FUS-MS	Er	ppm	0.08	0.21	0.08		0.25	0.53	0.3
FUS-MS	Tm	ppm	0.014	0.033	0.013		0.04	0.086	0.05
FUS-MS	Yb	ppm	0.11	0.23	0.11		0.27	0.62	0.38
FUS-MS	Lu	ppm	0.018	0.036	0.022		0.048	0.101	0.071
FUS-MS	Hf	ppm	< 0.1	< 0.1	< 0.1		< 0.1	< 0.1	< 0.1
FUS-MS	Ta	ppm	0.12	< 0.01	< 0.01		0.02	0.04	0.03
FUS-MS	Th	ppm	0.07	< 0.05	< 0.05		0.09	0.23	0.3
FUS-MS	U	ppm	0.02	0.02	0.03		0.08	0.16	0.06
NI-FINA	Os	ppb	< 2	< 2	13		< 2	< 2	< 2
NI-FINA	Ir	ppb	15	5.3	8.7		1.1	6.5	0.9
NI-FINA	Ru	ppb	51	< 5	9		< 5	7	< 5
NI-FINA	Rh	ppb	17.3	6	12.9		1.1	11.6	< 0.2
NI-FINA	Pt	ppb	108	26	77		< 5	71	< 5
NI-FINA	Pd	ppb	301	111	225		3	168	< 2
NI-FINA	Au	ppb	33	17	16		1.7	9	4.1
NI-FINA	Re	ppb	< 5	< 5	< 5		< 5	< 5	< 5
NI-FINA	Mass	q	15	15	15		25	25	25

Method	Analyte	Unit S		232265	232268	232270	232271
		232262	BD dunite	BD chromitite	BD dunite	BD pyroxenite	BD pyroxenite
FUS-XRF	SiO ₂	%	35.8			35	44.8
FUS-XRF	Al ₂ O ₃	%	1.85			3.13	3.1
FUS-XRF	Fe ₂ O ₃ (T)	%	14.4			10.6	14.8
FUS-XRF	MnO	%	0.082			0.083	0.07
FUS-XRF	MgO	%	35.11			35.32	28.02
FUS-XRF	CaO	%	0.07			0.04	0.29
FUS-XRF	Na ₂ O	%	< 0.01			< 0.01	< 0.01
FUS-XRF	K ₂ O	%	0.2			0.37	1.95
FUS-XRF	TiO ₂	%	0.09			0.13	0.14
FUS-XRF	P ₂ O ₅	%	0.01			0.01	0.01
FUS-XRF	Cr ₂ O ₃	%	1.76			4.75	0.48
FUS-XRF	V ₂ O ₅	%	0.019			0.029	0.053
FUS-XRF	LOI	%	10.9			10.8	6.5
FUS-XRF	Total	%	100.3			100.3	100.2
AR-MS	Li	ppm	2.2			4.1	8
AR-MS	Be	ppm	< 0.1			< 0.1	< 0.1
AR-MS	B	ppm	111			67	60
AR-MS	Na	%	0.013			0.028	0.018
AR-MS	Mg	%	> 10.0			> 10.0	> 10.0
AR-MS	Al	%	0.68			0.99	1.63
AR-ICP	P	%	0.003			0.004	0.001
AR-ICP	S	%	0.071			0.08	0.42
AR-MS	K	%	0.18			0.31	1.66
AR-MS	Ca	%	0.04			0.02	0.12
AR-MS	V	ppm	12			15	242
AR-MS	Cr	ppm	415			1070	1440
AR-ICP	Ti	%	< 0.01			0.01	0.03
AR-MS	Mn	ppm	433			300	408
AR-MS	Fe	%	8.2			4.22	8.88
AR-MS	Co	ppm	126			66	83
AR-MS	Ni	ppm	1280			1210	959
AR-MS	Cu	ppm	4.17			2.5	211
AR-MS	Zn	ppm	9.5			24.6	6.4
AR-MS	Ga	ppm	1.65			2.21	8.95
AR-MS	Ge	ppm	0.2			0.2	0.3
AR-MS	As	ppm	0.8			1	0.9
AR-MS	Se	ppm	< 0.1			0.2	1.5
AR-MS	Rb	ppm	7.3			13	64.5
AR-MS	Sr	ppm	3.2			1.3	2.1
AR-MS	Y	ppm	1.27			2.23	1.93
AR-MS	Zr	ppm	0.9			2.6	0.8
AR-MS	Sc	ppm	8.9			9.4	8.5
AR-MS	Mo	ppm	0.08			0.22	0.08
AR-MS	Ag	ppm	< 0.002			< 0.002	< 0.002
AR-MS	Cd	ppm	< 0.01			0.01	< 0.01
AR-MS	In	ppm	< 0.02			< 0.02	< 0.02
AR-MS	Sn	ppm	0.13			0.21	0.19
AR-MS	Sb	ppm	< 0.02			0.22	< 0.02
AR-MS	Te	ppm	0.07			0.03	0.16
AR-MS	Cs	ppm	0.12			0.28	1.54
AR-MS	Ba	ppm	12.3			16.8	72.8
AR-MS	W	ppm	< 0.1			< 0.1	< 0.1
AR-MS	Re	ppm	< 0.001			0.001	0.004
AR-MS	Tl	ppm	0.03			0.04	0.18
AR-MS	Pb	ppm	0.7			0.91	0.57
AR-MS	Bi	ppm	0.02			0.05	0.06
FUS-MS	Nb	ppm	< 0.2			0.3	3.5
FUS-MS	La	ppm	0.85			1.35	3.03
FUS-MS	Ce	ppm	1.92			2.97	5.37
FUS-MS	Pr	ppm	0.23			0.31	0.49
FUS-MS	Nd	ppm	0.91			1.35	1.52
FUS-MS	Sm	ppm	0.22			0.32	0.3
FUS-MS	Eu	ppm	0.047			0.043	0.033
FUS-MS	Gd	ppm	0.18			0.31	0.25
FUS-MS	Tb	ppm	0.03			0.06	0.05
FUS-MS	Dy	ppm	0.19			0.38	0.31
FUS-MS	Ho	ppm	0.04			0.08	0.07
FUS-MS	Er	ppm	0.14			0.26	0.22
FUS-MS	Tm	ppm	0.023			0.042	0.035
FUS-MS	Yb	ppm	0.17			0.3	0.26
FUS-MS	Lu	ppm	0.027			0.052	0.051
FUS-MS	Hf	ppm	< 0.1			0.1	< 0.1
FUS-MS	Ta	ppm	< 0.01			0.01	0.09
FUS-MS	Th	ppm	0.09			0.17	0.28
FUS-MS	U	ppm	0.04			0.08	0.25
NI-FINA	Os	ppb	< 2		120	14	< 2
NI-FINA	Ir	ppb	9.3		100	17	6.8
NI-FINA	Ru	ppb	8		358	41	< 5
NI-FINA	Rh	ppb	11.8		66.6	10.8	10.3
NI-FINA	Pt	ppb	140		266	51	51
NI-FINA	Pd	ppb	71		345	183	166
NI-FINA	Au	ppb	3.3		13	4.1	2.7
NI-FINA	Re	ppb	< 5		< 5	< 5	< 5
NI-FINA	Mass	q	15		5	15	25

Method	Analyte	Unit S 232318	486001	486002	486020	486034
		BD chromitite	BT dunite	BT dunite	BT chromitite	BT chromitite
FUS-XRF	SiO ₂	%		36.5	35.9	
FUS-XRF	Al ₂ O ₃	%		1.85	1.75	
FUS-XRF	Fe ₂ O ₃ (T)	%		11.7	10.9	
FUS-XRF	MnO	%		0.069	0.093	
FUS-XRF	MgO	%		36.13	36.67	
FUS-XRF	CaO	%		0.21	0.2	
FUS-XRF	Na ₂ O	%		< 0.01	< 0.01	
FUS-XRF	K ₂ O	%		0.03	0.02	
FUS-XRF	TiO ₂	%		0.08	0.07	
FUS-XRF	P ₂ O ₅	%		0.01	0.01	
FUS-XRF	Cr ₂ O ₃	%		2.82	3.41	
FUS-XRF	V ₂ O ₅	%		0.015	0.019	
FUS-XRF	LOI	%		11	11.3	
FUS-XRF	Total	%		100.4	100.3	
AR-MS	Li	ppm		0.2	< 0.1	
AR-MS	Be	ppm		< 0.1	< 0.1	
AR-MS	B	ppm		38	37	
AR-MS	Na	%		0.01	0.008	
AR-MS	Mg	%		> 10.0	> 10.0	
AR-MS	Al	%		0.54	0.35	
AR-ICP	P	%		0.003	0.002	
AR-ICP	S	%		0.1	0.077	
AR-MS	K	%		< 0.01	< 0.01	
AR-MS	Ca	%		0.16	0.14	
AR-MS	V	ppm		24	20	
AR-MS	Cr	ppm		1010	1220	
AR-ICP	Ti	%		< 0.01	< 0.01	
AR-MS	Mn	ppm		215	281	
AR-MS	Fe	%		5.66	4.83	
AR-MS	Co	ppm		102	86.1	
AR-MS	Ni	ppm		1470	1300	
AR-MS	Cu	ppm		5.03	2.86	
AR-MS	Zn	ppm		5.2	3.9	
AR-MS	Ga	ppm		1.73	1.57	
AR-MS	Ge	ppm		0.3	0.3	
AR-MS	As	ppm		2.7	1.3	
AR-MS	Se	ppm		0.2	< 0.1	
AR-MS	Rb	ppm		0.5	0.1	
AR-MS	Sr	ppm		1.8	6.5	
AR-MS	Y	ppm		1.38	0.75	
AR-MS	Zr	ppm		0.4	0.6	
AR-MS	Sc	ppm		6.5	5	
AR-MS	Mo	ppm		0.12	0.07	
AR-MS	Ag	ppm		< 0.002	< 0.002	
AR-MS	Cd	ppm		< 0.01	0.01	
AR-MS	In	ppm		< 0.02	< 0.02	
AR-MS	Sn	ppm		0.08	< 0.05	
AR-MS	Sb	ppm		0.03	0.03	
AR-MS	Te	ppm		< 0.02	< 0.02	
AR-MS	Cs	ppm		< 0.02	< 0.02	
AR-MS	Ba	ppm		3.5	2	
AR-MS	W	ppm		0.5	0.2	
AR-MS	Re	ppm		< 0.001	0.001	
AR-MS	Tl	ppm		0.22	0.14	
AR-MS	Pb	ppm		6.85	5.73	
AR-MS	Bi	ppm		0.1	0.06	
FUS-MS	Nb	ppm		< 0.2	< 0.2	
FUS-MS	La	ppm		0.52	0.36	
FUS-MS	Ce	ppm		1.22	0.74	
FUS-MS	Pr	ppm		0.14	0.08	
FUS-MS	Nd	ppm		0.58	0.33	
FUS-MS	Sm	ppm		0.2	0.11	
FUS-MS	Eu	ppm		0.027	0.022	
FUS-MS	Gd	ppm		0.17	0.1	
FUS-MS	Tb	ppm		0.04	0.02	
FUS-MS	Dy	ppm		0.22	0.12	
FUS-MS	Ho	ppm		0.05	0.03	
FUS-MS	Er	ppm		0.14	0.09	
FUS-MS	Tm	ppm		0.024	0.017	
FUS-MS	Yb	ppm		0.17	0.13	
FUS-MS	Lu	ppm		0.027	0.023	
FUS-MS	Hf	ppm		< 0.1	< 0.1	
FUS-MS	Ta	ppm		0.1	< 0.01	
FUS-MS	Th	ppm		0.05	< 0.05	
FUS-MS	U	ppm		0.01	< 0.01	
NI-FINA	Os	ppb	84	< 2		83
NI-FINA	Ir	ppb	70	6.9	9.9	69
NI-FINA	Ru	ppb	219	< 5	18	208
NI-FINA	Rh	ppb	62	5.6	6.8	49.2
NI-FINA	Pt	ppb	194	13	13	171
NI-FINA	Pd	ppb	53	13	30	72
NI-FINA	Au	ppb	4.4	4.6	16	14
NI-FINA	Re	ppb	< 5	< 5	< 5	< 5
NI-FINA	Mass	q	5	15	15	5

Method	Analyte	Unit S		486143	486145	486146	486147	486149
		BT pyroxenite	BT pyroxenite	BT pyroxenite	BT pyroxenite	BL dunite	BL dunite	
FUS-XRF	SiO ₂	%	41.3	51	51.2	36.7	35.6	
FUS-XRF	Al ₂ O ₃	%	1.23	2.35	2.11	0.65	1.46	
FUS-XRF	Fe ₂ O ₃ (T)	%	10.7	9.56	9.23	11.5	13.1	
FUS-XRF	MnO	%	0.138	0.189	0.159	0.035	0.089	
FUS-XRF	MgO	%	35.71	28	28.14	37.72	36.61	
FUS-XRF	CaO	%	0.04	2.22	1.9	0.2	0.07	
FUS-XRF	Na ₂ O	%	< 0.01	< 0.01	< 0.01	< 0.01	< 0.01	
FUS-XRF	K ₂ O	%	0.02	0.04	0.04	0.02	0.02	
FUS-XRF	TiO ₂	%	0.05	0.11	0.12	0.07	0.05	
FUS-XRF	P ₂ O ₅	%	0.01	0.01	0.01	0.01	0.01	
FUS-XRF	Cr ₂ O ₃	%	0.5	0.47	0.46	0.64	0.7	
FUS-XRF	V ₂ O ₅	%	0.014	0.017	0.017	< 0.003	0.008	
FUS-XRF	LOI	%	10.8	5.75	5.84	12.3	11.6	
FUS-XRF	Total	%	100.5	99.74	99.19	99.75	99.21	
AR-MS	Li	ppm	0.1	0.3	0.2	< 0.1	0.4	
AR-MS	Be	ppm	< 0.1	< 0.1	< 0.1	< 0.1	< 0.1	
AR-MS	B	ppm	24	10	9	51	65	
AR-MS	Na	%	0.009	0.012	0.011	0.009	0.008	
AR-MS	Mg	%	> 10.0	6.14	4.77	> 10.0	> 10.0	
AR-MS	Al	%	0.6	0.99	0.74	0.21	0.55	
AR-ICP	P	%	< 0.001	< 0.001	0.001	0.002	0.002	
AR-ICP	S	%	0.002	0.006	0.009	0.101	0.699	
AR-MS	K	%	< 0.01	0.01	< 0.01	< 0.01	< 0.01	
AR-MS	Ca	%	< 0.01	0.12	0.16	0.13	0.05	
AR-MS	V	ppm	62	58	57	4	9	
AR-MS	Cr	ppm	1300	1750	1650	497	628	
AR-ICP	Ti	%	< 0.01	0.02	0.02	< 0.01	< 0.01	
AR-MS	Mn	ppm	825	468	435	206	557	
AR-MS	Fe	%	6	2.9	2.79	6.56	7.73	
AR-MS	Co	ppm	92.2	33.1	27.1	123	205	
AR-MS	Ni	ppm	435	164	126	1910	2240	
AR-MS	Cu	ppm	2.02	2.9	3.8	0.72	501	
AR-MS	Zn	ppm	27.9	16.7	14.4	5.1	7.4	
AR-MS	Ga	ppm	2.33	2.31	1.92	0.82	1.02	
AR-MS	Ge	ppm	0.3	0.2	0.2	0.2	0.3	
AR-MS	As	ppm	0.9	0.5	0.3	0.7	1	
AR-MS	Se	ppm	< 0.1	< 0.1	< 0.1	< 0.1	1.2	
AR-MS	Rb	ppm	0.1	0.8	0.4	0.3	0.2	
AR-MS	Sr	ppm	< 0.5	1.1	1.8	0.9	1	
AR-MS	Y	ppm	0.67	0.38	0.43	1.29	1.03	
AR-MS	Zr	ppm	< 0.1	< 0.1	< 0.1	0.4	0.1	
AR-MS	Sc	ppm	7.6	13.1	13.8	7.8	6.9	
AR-MS	Mo	ppm	0.03	0.03	< 0.01	0.04	0.06	
AR-MS	Ag	ppm	< 0.002	< 0.002	< 0.002	0.003	0.122	
AR-MS	Cd	ppm	< 0.01	< 0.01	< 0.01	< 0.01	< 0.01	
AR-MS	In	ppm	< 0.02	< 0.02	< 0.02	0.03	0.02	
AR-MS	Sn	ppm	< 0.05	< 0.05	< 0.05	< 0.05	0.09	
AR-MS	Sb	ppm	< 0.02	< 0.02	< 0.02	< 0.02	< 0.02	
AR-MS	Te	ppm	< 0.02	< 0.02	< 0.02	< 0.02	0.27	
AR-MS	Cs	ppm	< 0.02	0.04	0.03	< 0.02	< 0.02	
AR-MS	Ba	ppm	1.7	2.1	2.2	2.9	2	
AR-MS	W	ppm	< 0.1	< 0.1	< 0.1	< 0.1	< 0.1	
AR-MS	Re	ppm	< 0.001	< 0.001	< 0.001	< 0.001	0.002	
AR-MS	Tl	ppm	< 0.02	< 0.02	< 0.02	0.03	0.16	
AR-MS	Pb	ppm	0.26	0.24	0.25	3.94	19.3	
AR-MS	Bi	ppm	< 0.02	< 0.02	< 0.02	< 0.02	0.02	
FUS-MS	Nb	ppm	< 0.2	< 0.2	< 0.2	< 0.2	< 0.2	
FUS-MS	La	ppm	0.4	0.28	0.45	0.75	0.6	
FUS-MS	Ce	ppm	0.65	0.6	0.93	1.83	1.51	
FUS-MS	Pr	ppm	0.07	0.07	0.1	0.17	0.14	
FUS-MS	Nd	ppm	0.24	0.36	0.39	0.71	0.65	
FUS-MS	Sm	ppm	0.09	0.07	0.12	0.19	0.13	
FUS-MS	Eu	ppm	0.013	0.047	0.04	0.023	0.037	
FUS-MS	Gd	ppm	0.06	0.14	0.17	0.14	0.14	
FUS-MS	Tb	ppm	0.02	0.03	0.03	0.03	0.03	
FUS-MS	Dy	ppm	0.12	0.22	0.21	0.17	0.16	
FUS-MS	Ho	ppm	0.03	0.05	0.05	0.04	0.03	
FUS-MS	Er	ppm	0.1	0.16	0.16	0.11	0.09	
FUS-MS	Tm	ppm	0.019	0.029	0.028	0.016	0.015	
FUS-MS	Yb	ppm	0.18	0.21	0.2	0.12	0.11	
FUS-MS	Lu	ppm	0.034	0.038	0.035	0.02	0.019	
FUS-MS	Hf	ppm	< 0.1	< 0.1	< 0.1	< 0.1	< 0.1	
FUS-MS	Ta	ppm	0.01	< 0.01	0.06	< 0.01	< 0.01	
FUS-MS	Th	ppm	0.26	< 0.05	0.07	< 0.05	0.06	
FUS-MS	U	ppm	0.06	< 0.01	< 0.01	0.02	< 0.01	
NI-FINA	Os	ppb	< 2	< 2	< 2	< 2	< 2	
NI-FINA	Ir	ppb	6.5	1.8	1.8	2.7	5.8	
NI-FINA	Ru	ppb	< 5	< 5	< 5	< 5	5	
NI-FINA	Rh	ppb	8	1.8	2	< 0.2	9.5	
NI-FINA	Pt	ppb	26	7	10	< 5	65	
NI-FINA	Pd	ppb	5	29	30	< 2	258	
NI-FINA	Au	ppb	1.1	6.7	2.2	1.5	6.5	
NI-FINA	Re	ppb	< 5	< 5	< 5	< 5	< 5	
NI-FINA	Mass	g	25	25	25	25	25	

Method	Analyte	Unit	486150	486151	486198	486216	486287	486392
			BL oik perid	BL pyroxenite	BL chromitite	BL chromitite	BL oik perid	BL dunite
FUS-XRF	SiO ₂	%	32.2	38.8			39.5	32
FUS-XRF	Al ₂ O ₃	%	3.49	4.52			1.18	2.16
FUS-XRF	Fe ₂ O ₃ (T)	%	16.3	11.2			12.5	11
FUS-XRF	MnO	%	0.191	0.472			0.136	0.109
FUS-XRF	MgO	%	30.22	25			34.97	36.26
FUS-XRF	CaO	%	1.45	8.39			0.9	0.03
FUS-XRF	Na ₂ O	%	< 0.01	< 0.01			< 0.01	< 0.01
FUS-XRF	K ₂ O	%	0.02	0.05			0.08	0.02
FUS-XRF	TiO ₂	%	0.2	0.2			0.06	0.08
FUS-XRF	P ₂ O ₅	%	0.01	0.02			0.01	0.01
FUS-XRF	Cr ₂ O ₃	%	6.54	4.09			0.61	5.07
FUS-XRF	V ₂ O ₅	%	0.047	0.033			0.011	0.025
FUS-XRF	LOI	%	8.82	6.57			10.5	13
FUS-XRF	Total	%	99.43	99.21			100.6	99.65
AR-MS	Li	ppm	1.9	6.4			7.3	0.1
AR-MS	Be	ppm	< 0.1	< 0.1			< 0.1	< 0.1
AR-MS	B	ppm	70	55			58	87
AR-MS	Na	%	0.01	0.012			0.012	0.012
AR-MS	Mg	%	> 10.0	> 10.0			> 10.0	> 10.0
AR-MS	Al	%	0.69	1.54			0.51	0.28
AR-ICP	P	%	0.002	0.006			0.001	0.002
AR-ICP	S	%	1.119	1.108			0.08	0.138
AR-MS	K	%	< 0.01	0.03			0.05	< 0.01
AR-MS	Ca	%	0.25	1.27			0.27	0.01
AR-MS	V	ppm	14	30			17	8
AR-MS	Cr	ppm	1440	2150			675	1010
AR-ICP	Ti	%	< 0.01	0.03			< 0.01	< 0.01
AR-MS	Mn	ppm	645	1610			784	476
AR-MS	Fe	%	5.72	3.83			7.23	4.45
AR-MS	Co	ppm	145	124			93.4	87.2
AR-MS	Ni	ppm	1950	2250			918	1720
AR-MS	Cu	ppm	886	1570			18.3	93.9
AR-MS	Zn	ppm	6.9	29			11.4	11.9
AR-MS	Ga	ppm	2.35	3.12			1.18	0.92
AR-MS	Ge	ppm	0.3	0.3			0.3	0.3
AR-MS	As	ppm	1	1.3			0.5	0.9
AR-MS	Se	ppm	1.5	2.2			< 0.1	0.4
AR-MS	Rb	ppm	0.3	2.1			3.2	0.1
AR-MS	Sr	ppm	3.2	6.7			3.4	< 0.5
AR-MS	Y	ppm	1.36	3			0.96	0.79
AR-MS	Zr	ppm	0.6	1.7			0.2	0.8
AR-MS	Sc	ppm	9.5	11.8			10.1	5.7
AR-MS	Mo	ppm	0.08	0.07			< 0.01	0.06
AR-MS	Ag	ppm	0.062	0.041			0.024	0.01
AR-MS	Cd	ppm	< 0.01	0.07			< 0.01	< 0.01
AR-MS	In	ppm	0.02	0.03			< 0.02	< 0.02
AR-MS	Sn	ppm	0.08	0.06			0.06	< 0.05
AR-MS	Sb	ppm	< 0.02	< 0.02			< 0.02	< 0.02
AR-MS	Te	ppm	0.18	0.18			0.03	0.14
AR-MS	Cs	ppm	0.03	0.15			0.14	< 0.02
AR-MS	Ba	ppm	3.3	9			8.8	1.6
AR-MS	W	ppm	< 0.1	< 0.1			< 0.1	< 0.1
AR-MS	Re	ppm	0.003	0.003			0.001	0.001
AR-MS	Tl	ppm	0.07	0.05			0.03	0.02
AR-MS	Pb	ppm	16.7	7.4			1.78	1.39
AR-MS	Bi	ppm	0.06	0.05			< 0.02	0.11
FUS-MS	Nb	ppm	< 0.2	< 0.2			< 0.2	< 0.2
FUS-MS	La	ppm	0.77	1.23			1.31	0.52
FUS-MS	Ce	ppm	1.33	2.78			2.44	0.92
FUS-MS	Pr	ppm	0.14	0.33			0.22	0.09
FUS-MS	Nd	ppm	0.51	1.56			0.75	0.37
FUS-MS	Sm	ppm	0.19	0.5			0.18	0.09
FUS-MS	Eu	ppm	0.056	0.111			0.087	0.025
FUS-MS	Gd	ppm	0.26	0.71			0.17	0.09
FUS-MS	Tb	ppm	0.05	0.14			0.03	0.02
FUS-MS	Dy	ppm	0.33	0.9			0.21	0.12
FUS-MS	Ho	ppm	0.07	0.2			0.05	0.03
FUS-MS	Er	ppm	0.23	0.62			0.16	0.09
FUS-MS	Tm	ppm	0.038	0.1			0.027	0.015
FUS-MS	Yb	ppm	0.26	0.69			0.19	0.11
FUS-MS	Lu	ppm	0.041	0.104			0.034	0.016
FUS-MS	Hf	ppm	< 0.1	0.2			< 0.1	< 0.1
FUS-MS	Ta	ppm	0.03	< 0.01			< 0.01	< 0.01
FUS-MS	Th	ppm	< 0.05	0.2			< 0.05	< 0.05
FUS-MS	U	ppm	< 0.01	0.04			0.02	0.03
NI-FINA	Os	ppb	< 2	14		44	< 2	16
NI-FINA	Ir	ppb	17	17		44	38	19
NI-FINA	Ru	ppb	43	46		124	96	62
NI-FINA	Rh	ppb	27.8	29		40	35.8	20.2
NI-FINA	Pt	ppb	81	150		115	133	108
NI-FINA	Pd	ppb	352	524		255	428	315
NI-FINA	Au	ppb	19	11		18	18	10
NI-FINA	Re	ppb	< 5	< 5		< 5	< 5	< 5
NI-FINA	Mass	g	15	15		5	5	25

Method	Analyte	Unit	486393	486428	486429	486681	486713
			BL dunite	BL dunite	BL dunite	BT gabbro	BT gabbro
FUS-XRF	SiO ₂	%	34	29.4	33.5	49.3	53
FUS-XRF	Al ₂ O ₃	%	0.61	2.63	0.88	17.4	16.3
FUS-XRF	Fe ₂ O ₃ (T)	%	10.9	12	10.8	6.67	8.2
FUS-XRF	MnO	%	0.097	0.156	0.154	0.036	0.106
FUS-XRF	MgO	%	38.83	35.18	38.48	10.26	6.84
FUS-XRF	CaO	%	0.01	0.01	0.01	4.62	8.04
FUS-XRF	Na ₂ O	%	< 0.01	< 0.01	< 0.01	4.23	4.34
FUS-XRF	K ₂ O	%	0.03	0.02	0.02	3.48	1.72
FUS-XRF	TiO ₂	%	0.04	0.09	0.05	0.99	0.6
FUS-XRF	P ₂ O ₅	%	0.01	< 0.01	0.01	0.32	0.25
FUS-XRF	Cr ₂ O ₃	%	0.95	7.02	1.33	0.05	0.06
FUS-XRF	V ₂ O ₅	%	0.006	0.033	0.012	0.048	0.032
FUS-XRF	LOI	%	14.9	13.7	14.8	2.72	1.1
FUS-XRF	Total	%	100.2	100.2	99.96	100.1	100.5
AR-MS	Li	ppm	< 0.1	< 0.1	< 0.1	35	12.7
AR-MS	Be	ppm	< 0.1	< 0.1	< 0.1	0.2	0.2
AR-MS	B	ppm	100	48	49	26	10
AR-MS	Na	%	0.009	0.01	0.01	0.178	0.24
AR-MS	Mg	%	> 10.0	> 10.0	> 10.0	4.98	1.76
AR-MS	Al	%	0.18	0.23	0.24	4.12	2.35
AR-ICP	P	%	0.002	0.002	0.002	0.128	0.105
AR-ICP	S	%	0.071	0.072	0.075	0.01	0.027
AR-MS	K	%	< 0.01	< 0.01	< 0.01	2.32	0.9
AR-MS	Ca	%	0.01	< 0.01	< 0.01	1.32	2.04
AR-MS	V	ppm	6	7	7	206	94
AR-MS	Cr	ppm	419	958	439	154	120
AR-ICP	Ti	%	< 0.01	< 0.01	< 0.01	0.37	0.26
AR-MS	Mn	ppm	640	707	1010	170	320
AR-MS	Fe	%	6.36	4.27	6.09	3.29	2.91
AR-MS	Co	ppm	124	72.2	172	31.3	19.5
AR-MS	Ni	ppm	1050	1950	2270	124	59.7
AR-MS	Cu	ppm	16.7	8.39	11.7	56.8	50.8
AR-MS	Zn	ppm	6.8	7.9	12.8	14	22.7
AR-MS	Ga	ppm	0.58	0.79	0.77	12.1	7.02
AR-MS	Ge	ppm	0.2	0.2	0.3	0.2	0.2
AR-MS	As	ppm	0.5	0.6	0.6	0.7	0.4
AR-MS	Se	ppm	< 0.1	< 0.1	0.4	< 0.1	< 0.1
AR-MS	Rb	ppm	0.1	0.1	0.2	93.7	36
AR-MS	Sr	ppm	< 0.5	< 0.5	< 0.5	97	162
AR-MS	Y	ppm	0.55	0.4	0.66	10.3	7.39
AR-MS	Zr	ppm	0.4	0.2	0.1	4.4	7.9
AR-MS	Sc	ppm	5.5	5.1	5.8	16.4	8.3
AR-MS	Mo	ppm	0.04	0.07	0.05	0.31	0.6
AR-MS	Ag	ppm	0.013	< 0.002	< 0.002	< 0.002	< 0.002
AR-MS	Cd	ppm	< 0.01	< 0.01	< 0.01	0.02	0.01
AR-MS	In	ppm	< 0.02	< 0.02	< 0.02	0.02	< 0.02
AR-MS	Sn	ppm	< 0.05	< 0.05	< 0.05	0.44	0.29
AR-MS	Sb	ppm	< 0.02	< 0.02	< 0.02	< 0.02	< 0.02
AR-MS	Te	ppm	0.11	0.03	0.05	< 0.02	< 0.02
AR-MS	Cs	ppm	< 0.02	< 0.02	< 0.02	5.3	0.92
AR-MS	Ba	ppm	1.5	1.9	1.8	576	350
AR-MS	W	ppm	< 0.1	< 0.1	< 0.1	0.2	< 0.1
AR-MS	Re	ppm	< 0.001	0.001	0.001	< 0.001	< 0.001
AR-MS	Tl	ppm	< 0.02	< 0.02	0.03	0.55	0.2
AR-MS	Pb	ppm	0.86	0.51	0.49	1.6	0.85
AR-MS	Bi	ppm	< 0.02	0.02	< 0.02	0.04	0.09
FUS-MS	Nb	ppm	< 0.2	< 0.2	< 0.2	2.3	1.5
FUS-MS	La	ppm	0.43	0.33	0.36	13.2	20.1
FUS-MS	Ce	ppm	0.8	0.49	0.69	32.5	41
FUS-MS	Pr	ppm	0.08	0.04	0.07	4.01	4.5
FUS-MS	Nd	ppm	0.32	0.16	0.31	17.6	18.8
FUS-MS	Sm	ppm	0.08	0.07	0.12	3.92	3.07
FUS-MS	Eu	ppm	0.018	0.022	0.014	1.53	0.912
FUS-MS	Gd	ppm	0.07	0.06	0.08	3.33	2.42
FUS-MS	Tb	ppm	0.01	0.01	0.01	0.5	0.35
FUS-MS	Dy	ppm	0.09	0.07	0.11	3.03	1.99
FUS-MS	Ho	ppm	0.02	0.02	0.03	0.61	0.41
FUS-MS	Er	ppm	0.06	0.06	0.08	1.52	1.07
FUS-MS	Tm	ppm	0.011	0.01	0.013	0.232	0.167
FUS-MS	Yb	ppm	0.07	0.07	0.08	1.46	1.15
FUS-MS	Lu	ppm	0.012	0.01	0.013	0.225	0.19
FUS-MS	Hf	ppm	< 0.1	< 0.1	< 0.1	1.1	1.3
FUS-MS	Ta	ppm	< 0.01	< 0.01	0.03	0.16	0.13
FUS-MS	Th	ppm	< 0.05	< 0.05	< 0.05	0.89	1.34
FUS-MS	U	ppm	< 0.01	< 0.01	< 0.01	0.26	0.35
NI-FINA	Os	ppb	< 2	39	< 2	< 2	< 2
NI-FINA	Ir	ppb	3.6	30	5.5	0.3	< 0.1
NI-FINA	Ru	ppb	< 5	104	9	< 5	< 5
NI-FINA	Rh	ppb	2.3	17.1	4.9	< 0.2	< 0.2
NI-FINA	Pt	ppb	< 5	72	25	< 5	< 5
NI-FINA	Pd	ppb	19	142	62	< 2	< 2
NI-FINA	Au	ppb	2.9	3.3	3.9	5.5	4.1
NI-FINA	Re	ppb	< 5	< 5	< 5	< 5	< 5
NI-FINA	Mass	g	15	15	25	25	25

APPENDIX 4

Silicate Mineral Chemistry data:

- 1. Olivine**
- 2. Orthopyroxene**
- 3. Clinopyroxene**
- 4. Amphibole**
- 5. Phlogopite**
- 6. Chlorite**

TABLE 4: OLIVINE, BLACK LABEL, J. LAARMAN, JULY 2012, R.L.B.

	1	2	3	4	5	6	7	8
STO2	40.31	40.51	40.12	40.84	40.09	40.16	40.00	40.07
TIO2	.00	.00	.00	.03	.03	.06	.00	.05
A2O3	.00	.00	.00	.00	.00	.00	.01	.03
C2O3	.02	.05	.03	.00	.10	.07	.05	.00
FEO	12.64	12.62	12.52	9.30	10.25	10.44	12.36	11.96
MGO	47.33	47.12	47.42	49.52	49.26	49.08	47.04	47.51
MNO	.21	.18	.22	.03	.06	.08	.32	.33
CAO	.00	.00	.00	.05	.04	.00	.04	.04
K2O	.03	.01	.09	.01	.03	.09	.05	.04
NA2O	.00	.00	.25	.00	.07	.01	.02	.01
NIO	.01	.00	.01	.20	.20	.20	.00	.00
SUM	100.55	100.49	100.66	99.98	100.13	100.19	99.89	100.04
SI	.996	1.000	.991	.999	.986	.987	.994	.993
AL	.000	.996	.000	.991	.000	.986	.000	.995
AL	.000	.000	.000	.000	.000	.000	.000	.000
TI	.000	.000	.000	.001	.001	.001	.000	.001
CR	.000	.001	.001	.000	.002	.001	.001	.000
FE	.261	.261	.259	.190	.211	.215	.257	.248
MN	.004	.004	.005	.001	.001	.002	.007	.007
MG	1.742	1.734	1.746	1.805	1.805	1.799	1.743	1.755
CA	.000	.000	.000	.001	.001	.000	.001	.001
K	.001	.000	.003	.000	.001	.003	.002	.001
NA	.000	.000	.012	.000	.003	.000	.001	.000
NI	.000	2.009	.000	2.025	.004	2.029	.000	2.013
O	4.000	.000	4.000	.004	4.000	.004	4.000	4.000
FO	86.97	86.94	87.10	90.47	89.55	89.34	87.15	87.62
FA	13.03	13.06	12.90	9.53	10.45	10.66	12.85	12.38
F/M	.152	.152	.151	.106	.117	.120	.151	.145
F/FM	.132	.132	.131	.096	.105	.107	.131	.127

- 1 *** BL-09-31 486163 DARK GREY IN IM00312
- 2 SINGLE DEEP RED IM0781
- 3 MINUTE RELIC LOBL-09-31 ER LEFT IM 0178
- 4 *** BL-09-31 486211 OLIV INT BL-09-31 REPL BY CR-TREM
- 5 INT BL-09-31 CHROMITE BL-09-31 HOLES, S-1, IM0005
- 6 ADJ OLIVINE SPOT 13
- 7 OLV * IST TIME
- 8 OLV AGAIN IM 581 C-1

TABLE 4: OLIVINE, BLACK LABEL, J. LAARMAN, JULY 2012, R.L.B.

	9	10	11	12	13	14	15	16
STO2	39.81	39.90	39.86	39.45	39.43	40.16	40.14	39.79
TIO2	.02	.00	.00	.02	.02	.00	.00	.00
A2O3	.02	.00	.00	.00	.00	.00	.00	.00
C2O3	.09	.09	.09	.05	.00	.00	.00	.05
FEO	11.34	13.28	13.29	13.63	13.63	12.26	12.26	11.91
MGO	48.39	46.87	46.82	46.85	46.85	47.78	47.79	48.03
MNO	.30	.19	.19	.14	.14	.22	.22	.23
CAO	.04	.00	.00	.00	.00	.00	.00	.00
K2O	.00	.00	.00	.02	.02	.00	.00	.01
NA2O	.00	.04	.01	.00	.02	.00	.00	.01
NIO	.18	.31	.11	.00	.09	.09	.06	.06
SUM	100.19	100.68	100.37	100.14	100.20	100.51	100.47	100.09
SI	.984	.989	.990	.984	.984	.991	.991	.986
AL	.001	.984	.000	.984	.000	.000	.000	.000
AL	.000	.000	.000	.000	.000	.000	.000	.000
TI	.000	.000	.000	.000	.000	.000	.000	.000
CR	.002	.002	.002	.001	.000	.000	.000	.001
FE	.234	.275	.276	.284	.284	.253	.253	.247
MN	.006	.004	.004	.003	.003	.005	.005	.005
MG	1.783	1.732	1.734	1.742	1.742	1.758	1.759	1.774
CA	.001	.000	.000	.000	.000	.000	.000	.000
K	.000	.000	.000	.001	.001	.000	.000	.000
NA	.000	.002	.000	.000	.001	.000	.000	.000
NI	.004	2.030	.002	2.031	.002	2.017	.001	2.028
O	4.000	4.000	4.000	4.000	4.000	4.000	4.000	4.000
FO	88.38	86.28	86.26	85.97	85.97	87.42	87.42	87.79
FA	11.62	13.72	13.74	14.03	14.03	12.58	12.58	12.21
F/M	.135	.161	.162	.165	.165	.147	.147	.142
F/FM	.119	.139	.139	.142	.142	.128	.128	.124

9 OLIV BL-09-31 OPX, C-3, IM 0590

10 REPL BY CHL GRAINS ACROSS SAMPLE

11 REPL BY CHL

12 AGAIN

13 REPLY BY CHL

14 CHL GRAINS ACROSS SAMPLE

15 CHL GRAINS ACROSS SAMPLE

16 CHL GRAINS ACROSS SAMPLE

TABLE 5: ORTHOPYROXENE, BLACK LABEL, J. LAARMAN, JULY 2012, R.I.B.

	1	2	3	4	5	6	7	8
STO2	55.94	55.00	55.80	55.79	55.72	55.12	55.22	55.09
TIO2	.09	.22	.21	.14	.06	.10	.12	.14
A2O3	1.32	1.28	1.65	1.62	1.35	1.53	1.71	1.77
C2O3	.55	.80	.54	.59	.35	.70	.62	.50
FEO	7.62	7.79	7.34	7.15	7.50	7.82	8.64	7.74
MGO	31.32	32.07	31.51	32.36	32.85	31.73	32.09	31.72
MNO	.01	.15	.21	.34	.32	.29	.26	.33
CAO	2.81	2.25	3.16	2.10	1.30	2.01	1.91	2.58
K2O	.06	.32	.05	.01	.01	.05	.00	.09
NA2O	.23	.26	.02	.01	.04	.00	.00	.00
NIO	.20	.20	.11	.11	.18	.18	.11	.11
SUM	100.15	100.34	100.60	100.22	99.68	99.53	100.69	100.07
SI	1.957	1.930	1.943	1.944	1.950	1.942	1.929	1.932
AL	.043	2.000	.057	.056	2.000	.058	.070	.068
AL	.012	*	.011	.010	*	.005	.000	.006
TI	.002	*	.005	.004	*	.003	.003	.004
CR	.015	*	.015	.016	*	.019	.017	.014
FE	.223	*	.214	.208	*	.230	.252	.227
MN	.000	*	.006	.010	*	.009	.008	.010
MG	1.633	*	1.636	1.680	*	1.666	1.670	1.658
CA	.105	*	.118	.078	*	.076	.071	.097
K	.003	*	.002	.000	*	.002	.000	.004
NA	.016	*	.001	.001	*	.000	.001	.000
NI	.006	2.015	.003	.003	2.012	.005	.003	.003
O	6.000	*	6.000	6.000	*	6.000	6.000	6.000
ENST	83.26	84.27	83.14	85.42	86.46	84.47	83.76	83.66
WO	5.37	4.25	5.99	3.98	2.46	3.85	3.58	4.89
FERR	11.37	11.48	10.87	10.59	11.08	11.68	12.65	11.45
F/M	.137	.139	.134	.130	.134	.143	.156	.143
F/FM	.120	.122	.119	.115	.118	.125	.135	.125

1 **** BL-09-31 486211 OPX INT W OLIV C-2

2 OPX INT W OLIV C-2

3 OPX INT W C OLIV W CHROMITE INCL

4 OPX AT MARGIN

5 OPX INT W OLIV, C-3, IM 0590

6 OPX INT W OLIV, C-3, IM 0590

7 BIRFR ORANGE OPX, C-4, IM 592

8 BRIFR ORANGE OPX, C-4, IM 592

TABLE 5: ORTHOPYROXENE, BLACK LABEL, J. LAARMAN, JULY 2012, R.I.B.

	9
STO2	55.93
TIO2	.12
A2O3	1.62
C2O3	.62
FEO	7.93
MGO	31.49
MNO	.27
CAO	2.63
K2O	.04
NA2O	.00
NIO	.11
SUM	100.76
SI	1.947 *
AL	.053 2.000
AL	.013 *
TI	.003 *
CR	.017 *
FE	.231 *
MN	.008 *
MG	1.634 *
CA	.098 *
K	.002 *
NA	.000 *
NI	.003 2.009
O	6.000 *
ENST	83.24
WO	5.00
FERR	11.76
F/M	.146
F/FM	.128

9 WITH CLEAVAGE

TABLE 2: CLINOPYROXENE, BLACK LABEL, J LAARMAN, JULY 2013 R.L.B.

	1	2	3	4	5	6	7	8
STO2	55.42	55.48	54.65	55.11	56.69	55.27	53.16	53.73
TIO2	.02	.00	.06	.04	.02	.04	.24	.21
A2O3	.02	.03	.00	.00	.12	.03	2.19	1.60
C2O3	.00	.05	.04	.08	.12	.18	1.35	1.07
FEO	2.40	2.30	1.46	1.34	1.53	2.03	2.96	3.32
MGO	21.71	19.90	19.35	19.38	21.45	21.25	16.68	16.48
MNO	.31	.23	.23	.27	.14	.24	.09	.06
CJO	20.21	22.33	24.07	23.91	19.64	20.56	23.19	23.26
K2O	.03	.00	.00	.00	.08	.04	.04	.10
NA2O	.02	.02	.02	.03	.09	.01	.54	.67
SUM	100.14	100.34	99.88	100.16	99.88	99.65	100.44	100.50
SI	1.988	1.996	1.981	1.989	2.021	1.992	1.934	1.955
AL	.001	.001	.000	.000	.000	.001	.066	.045
AL	.000	.000	.000	.000	.005	.000	.027	.024
TI	.001	.000	.002	.001	.001	.001	.007	.006
CR	.000	.001	.001	.002	.003	.005	.039	.031
FE	.072	.069	.044	.040	.046	.061	.090	.101
MG	1.161	1.067	1.046	1.042	1.140	1.141	.904	.894
MN	.009	.007	.007	.008	.004	.007	.003	.002
CA	.777	.861	.935	.925	.750	.794	.904	.907
K	.001	.000	.000	.000	.004	.002	.002	.005
NA	.001	2.023	.001	2.036	.006	.001	.038	.047
O	6.000	6.000	6.000	6.000	6.000	6.000	6.000	6.000
ENST	57.76	53.43	51.64	51.93	58.89	57.17	47.64	47.00
WO	38.65	43.10	46.17	46.05	38.76	39.76	47.61	47.69
FERR	3.58	3.47	2.19	2.01	2.36	3.06	4.74	5.31
F/M	.070	.071	.049	.047	.044	.060	.103	.115
F/FM	.066	.067	.047	.045	.042	.057	.093	.103

- 1 **** BL-09-31 486155
- 2 ANOTHER METAS DIOFSIDE W TALC
- 3 ANOTHER IN TALC HOST
- 4 ANOTHER GRAIN
- 5 IN CHL-TALC
- 6 AGAIN
- 7 **** BL-09-31 486211 C-1 INST TO CHROMITE, BRIGHT
- 8 RELICT IGNEOUS CPX IN CR-TREMOLITE

TABLE 2: CLINOPYROXENE, BLACK LABEL, J LAARMAN, JULY 2013 R.L.B.

	9	10	11	12	13	14	15	16
STO2	53.69	52.68	53.01	53.07	52.50	52.40	53.27	52.88
TIO2	.21	.26	.27	.28	.25	.27	.31	.25
A2O3	1.80	1.80	1.84	1.62	2.07	2.05	2.09	1.98
C2O3	1.07	1.15	1.21	1.12	1.48	1.32	1.12	1.25
FEO	2.98	3.32	3.23	3.11	3.23	3.14	3.04	3.55
MGO	16.77	17.32	17.01	17.00	17.75	17.50	16.76	17.45
MNO	.00	.00	.04	.04	.01	.10	.01	.09
CAO	23.48	22.81	23.13	23.00	22.63	22.55	23.05	22.43
K2O	.06	.36	.05	.78	.03	.30	.04	.10
NA2O	.46	.36	.41	.36	.41	.44	.46	.39
SUM	100.52	100.06	100.20	100.38	100.36	100.07	100.15	100.37
SI	1.949	1.928	1.935	1.939	1.913	1.917	1.940	1.927
AL	.051	2.000	.065	2.000	.087	2.000	.060	2.000
AL	.026	*	.014	*	.002	*	.030	*
TI	.006	*	.007	*	.007	*	.008	*
CR	.031	*	.033	*	.043	*	.032	*
FE	.090	*	.102	*	.098	*	.093	*
MG	.907	*	.945	*	.964	*	.910	*
MN	.000	*	.000	*	.000	*	.000	*
CA	.913	*	.895	*	.884	*	.900	*
K	.003	*	.017	*	.036	*	.002	*
NA	.032	2.009	.029	2.017	.029	2.033	.032	2.022
O	6.000	*	6.000	*	6.000	*	6.000	*
ENST	47.48	48.68	47.98	48.19	49.54	49.34	47.84	49.06
WO	47.79	46.08	46.90	46.86	45.40	45.70	47.29	45.33
FERR	4.73	5.24	5.11	4.95	5.06	4.97	4.87	5.60
F/M	.100	.108	.108	.104	.102	.104	.102	.117
F/FM	.091	.097	.097	.094	.093	.094	.093	.105

9 ANOTHER
 10 CPX INT W CHROMITE IM 0001
 11 ADJ RELICT CPX SPOT 3 IM 2013 02 07 0001
 12 ADJ RELICT CPX SPOT 3 IM 2013 02 07 0001
 13 INCL SPOT 4
 14 INCL SPOT 4
 15 RELICT GRAIN IN AMPH C-1 IM 0003
 16 ANOTHER SPOT 3

TABLE 2: CLINOPYROXENE, BLACK LABEL, J LAARMAN, JULY 2013 R.L.B.

	25	26	27	28	29	30	31	32
STO2	1.935	1.959	1.954	2.029	2.010	1.997	1.990	1.997
TIO2	.065	2.000	.046	2.000	.000	2.010	.004	.003
A2O3	.031	*	.020	*	.003	*	.000	.000
C2O3	.003	*	.004	*	.000	*	.000	.000
FEO	.037	*	.026	*	.000	*	.000	.000
MGO	.116	*	.094	*	.068	*	.027	.013
MNO	.932	*	.921	*	1.002	*	1.166	1.107
CJO	.003	*	.002	*	.005	*	.001	.003
K2O	.860	*	.927	*	.898	*	.818	.873
NA2O	.000	*	.000	*	.000	*	.001	.002
SUM	.027	2.009	.023	1.934	.001	1.979	.003	.008
SI	6.000	*	6.000	*	6.000	*	6.000	6.000
AL	.041	2.000	.046	2.000	.000	2.010	.004	.003
TI	.030	*	.020	*	.003	*	.000	.000
CR	.002	*	.004	*	.000	*	.000	.000
FE	.026	*	.020	*	.000	*	.000	.000
MG	.094	*	.093	*	.074	*	.100	.013
MN	.932	*	.921	*	.887	*	1.166	1.107
CA	.003	*	.002	*	.005	*	.001	.003
K	.860	*	.927	*	.898	*	.818	.873
NA	.000	*	.000	*	.000	*	.001	.002
O	.027	2.005	.023	1.934	.001	1.979	.003	.008
ENST	48.85	48.73	47.43	46.41	50.91	47.02	57.99	55.53
WO	45.08	46.38	47.78	49.69	45.62	47.97	40.65	43.80
FERR	6.07	4.90	4.79	3.90	3.47	5.01	1.36	.67
F/M	.128	.109	.104	.089	.074	.118	.024	.015
F/FM	.113	.098	.094	.082	.069	.105	.023	.015

25 *** BL-09-31 486296 SMALL RELICT DOMAIN CPX C-3
 26 WITH CPX RELIC C-1 IM801,02 16 0002
 27 CPX RELIC AGAIN SPOT 3 02 16 0002
 28 SPOT 4
 29 ***** BL-09-31 486343 INT W CHROMITE C-1 IM 0786,00
 30 HYD DIOPSIDE
 31 *** BL-09-31 486348 CPX C-1 IM0854
 32 REPL OLIV C-1

TABLE 2: CLINOPYROXENE, BLACK LABEL, J LAARMAN, JULY 2013 R.L.B.

	33	34	35	36	37	38	39	40
STO2	53.50	53.66	53.85	54.66	55.94	55.00	55.80	55.79
TIO2	.18	.21	.21	.04	.09	.22	.21	.14
A2O3	1.55	1.59	1.65	.23	1.32	1.28	1.65	1.62
C2O3	1.63	1.74	1.74	.44	.55	.80	.54	.59
FEO	2.15	2.09	2.20	.94	7.62	7.79	7.34	7.15
MGO	17.66	17.47	17.48	20.61	31.32	32.07	31.51	32.36
MNO	.03	.00	.00	.25	.01	.15	.21	.34
CAO	22.85	22.54	22.34	22.69	2.81	2.25	3.16	2.10
K2O	.01	.00	.00	.04	.06	.32	.05	.01
NA2O	.96	.88	.88	.10	.23	.26	.02	.01
SUM	100.52	100.18	100.35	100.00	99.95	100.14	100.49	100.11
SI	1.939	1.948	1.950	1.970	1.959	1.931	1.944	1.945
AL	.061	2.000	.050	2.000	.041	2.000	.056	2.000
AL	.006	*	.021	*	.013	*	.012	*
TI	.005	*	.006	*	.002	*	.006	*
CR	.047	*	.050	*	.015	*	.015	*
FE	.065	*	.067	*	.223	*	.214	*
MG	.954	*	.944	*	1.635	*	1.637	*
MN	.001	*	.000	*	.008	*	.006	*
CA	.888	*	.867	*	.105	*	.118	*
K	.000	*	.000	*	.003	*	.014	*
NA	.067	2.033	.062	2.019	.016	2.013	.001	2.011
O	6.000	*	6.000	*	6.000	*	6.000	*
ENST	50.04	50.14	50.27	55.04	83.26	84.27	83.14	85.42
WO	46.54	46.50	46.18	43.55	5.37	4.25	5.99	3.98
FERR	3.42	3.37	3.55	1.41	11.37	11.48	10.87	10.59
F/M	.069	.067	.071	.032	.137	.139	.134	.130
F/FM	.065	.063	.066	.031	.120	.122	.119	.115

33 SMALL BRIGHT DOMAIN

34 SMALL REL IGN CPX IN AMPH, IM02 20 0015

35 SMALL REL IGN CPX IN AMPH, IM02 20 0015

36 REL-ALT CPX IN INCL IM0016

37 *** BL-09-31 486211 OPX INT W OLIV C-2

38 OPX INT W OLIV C-2

39 OPX INT W C OLIV W CHROMITE INCL

40 OPX AT MARGIN

TABLE 2: CLINOPYROXENE, BLACK LABEL, J LAARMAN, JULY 2013 R.L.B.

	41	42	43	44	45
STO2	55.72	55.12	55.22	55.09	55.93
TIO2	.06	.10	.12	.14	.12
A2O3	1.35	1.53	1.71	1.77	1.62
C2O3	.35	.70	.62	.50	.62
FEO	7.50	7.82	8.64	7.74	7.93
MGO	32.85	31.73	32.09	31.72	31.49
MNO	.32	.29	.26	.33	.27
CAO	1.30	2.01	1.91	2.58	2.63
K2O	.01	.05	.00	.09	.04
NA2O	.04	.00	.01	.00	.00
SUM	99.50	99.35	100.58	99.96	100.65
SI	1.952	1.943	1.930	1.933	1.948
AL	.048	2.000	.070	2.000	.052
AL	.008	*	.000	*	.014
TI	.002	*	.003	*	.003
CR	.010	*	.017	*	.017
FE	.220	*	.231	*	.231
MG	1.715	*	1.671	*	1.635
MN	.009	*	.008	*	.008
CA	.049	*	.072	*	.098
K	.000	*	.000	*	.002
NA	.003	2.015	.001	2.024	.000
O	6.000	*	6.000	*	6.000
ENST	86.46	84.47	83.76	83.66	83.24
WO	2.46	3.85	3.58	4.89	5.00
FERR	11.08	11.68	12.65	11.45	11.76
F/M	.134	.143	.156	.143	.146
F/FM	.118	.125	.135	.125	.128
41 OPX INT W OLIV, C-3, IM 0590					
42 OPX INT W OLIV, C-3, IM 0590					
43 BIRFR ORANGE OPX, C-4, IM 592					
44 BRIFR ORANGE OPX, C-4, IM 592					
45 WITH CLEAVAGE					

TABLE 1: AMPHIBOLE, BLACK LABEL-BLACK THOR, J LAARMAN, JULY 2013

	1	2	3	4	5	6	7	8
STO2	55.64	57.65	46.51	46.01	46.03	45.38	45.47	44.39
TIO2	.09	.03	2.57	2.79	3.18	2.66	3.71	4.58
A2O3	1.73	.36	8.91	9.33	9.17	9.81	10.40	10.59
C2O3	1.38	.13	3.02	2.73	2.63	3.32	2.65	2.63
FEO	2.46	2.67	3.58	3.87	3.50	3.51	3.95	4.09
MGO	23.15	23.50	18.49	18.76	19.70	18.83	18.32	18.79
MNO	.05	.04	.00	.01	.03	.00	.00	.01
C2O	12.75	12.57	9.31	9.79	9.42	9.48	10.12	10.28
K2O	.04	.04	.15	.17	.15	.43	.25	.12
NA2O	.00	.17	4.42	4.31	4.24	4.50	2.76	2.68
SUM	97.29	97.16	96.96	97.77	98.05	97.92	97.63	98.16
SI	7.691	* 7.936	* 6.639	* 6.535	* 6.503	* 6.449	* 6.442	* 6.278
AL	.282	7.972	1.361	8.000	1.497	8.000	1.551	8.000
AL	.000	* .000	.138	* .097	* .030	* .092	* .178	* .042
TI	.009	* .003	* .276	* .298	* .338	* .284	* .395	* .487
CR	.151	* .014	* .341	* .307	* .294	* .373	* .297	* .294
FE	.284	* .307	* .427	* .460	* .414	* .417	* .468	* .484
MG	4.769	* 4.822	* 3.934	* 3.972	* 4.149	* 3.989	* 3.869	* 3.961
MN	.006	5.220	.000	5.133	.004	5.227	.000	5.207
CA	1.888	* 1.854	* 1.424	* 1.490	* 1.426	* 1.443	* 1.536	* 1.558
K	.007	* .007	* .027	* .031	* .027	* .078	* .045	* .022
NA	.000	1.895	.045	1.906	1.223	2.674	1.187	2.707
O	23.000	* 23.000	* 23.000	* 23.000	* 23.000	* 23.000	* 23.000	* 23.000
ANTH	68.70	69.05	68.00	67.08	69.28	68.19	65.87	65.99
WO	27.20	26.55	24.61	25.16	23.81	24.68	26.16	25.95
GEDR	4.10	4.40	7.39	7.76	6.91	7.13	7.97	8.06
F/M	.061	.065	.109	.116	.101	.105	.121	.122
F/FM	.057	.061	.098	.104	.091	.095	.108	.109

1 **** BL-09-31 485153
2 **** BL-09-31 486155 IN CHL-TALC

3 **** BL-09-31 486163 INCL

4 ANOTHER INCL

5 ANOTHER INCL

6 ANOTHER INCL

7 INCL 1 IM 2013 02 09 0029

8 INCL 1 IM 2013 02 09 0029

TABLE 1: AMPHIBOLE, BLACK LABEL-BLACK THOR, , J LAARMAN, JULY 2013

	9	10	11	12	13	14	15	16
STO2	44.61	44.20	57.99	45.03	46.30	46.35	45.05	57.99
TIO2	3.90	3.95	.11	4.50	3.17	3.87	3.52	.02
A2O3	10.87	10.61	.46	10.83	9.48	9.90	10.81	.45
C2O3	2.80	3.21	.22	3.07	2.48	2.65	1.41	.85
FEO	3.88	4.11	1.99	3.66	3.58	3.65	4.09	2.59
MGO	18.56	17.50	24.11	17.65	19.73	19.05	17.96	24.08
MNO	.00	.04	.07	.09	.11	.04	.05	.09
CAO	9.95	9.49	11.79	9.15	10.03	9.88	11.51	11.44
K2O	.07	.07	.00	.04	.08	.06	.33	.00
NA2O	2.76	3.62	.25	4.03	2.56	2.69	2.20	.18
SUM	97.40	96.80	96.99	98.05	97.52	98.14	96.93	97.69
SI	6.337	6.346	7.951	6.362	6.539	6.505	6.432	7.921
AL	1.663	1.654	8.000	1.638	1.461	1.495	1.568	8.000
AL	.156	.142	.025	.165	.117	.142	.251	.000
TI	.417	.427	.011	.478	.337	.408	.378	.002
CR	.314	.364	.024	.343	.277	.294	.159	.092
FE	.461	.494	.228	.432	.423	.428	.488	.296
MG	3.930	3.745	4.927	3.717	4.154	3.985	3.822	4.903
MN	.000	5.278	.008	.011	5.320	.005	.006	.010
CA	1.514	1.460	1.732	1.385	1.518	1.486	1.761	1.674
K	.013	.013	.000	.007	.014	.011	.060	.000
NA	.760	2.287	1.008	1.104	2.496	.732	.609	.048
O	23.000	23.000	23.000	23.000	23.000	23.000	23.000	23.000
ANTH	66.55	65.72	71.54	67.16	68.16	67.55	62.95	71.33
WO	25.65	25.62	25.15	25.03	24.91	25.18	29.00	24.36
GEDR	7.81	8.66	3.31	7.81	6.94	7.26	8.04	4.30
F/M	.117	.133	.048	.119	.105	.109	.129	.062
F/FM	.105	.117	.046	.107	.095	.098	.115	.059

9 INT W TALC PHLOG

10 INCL 2 BRIGHT

11 BRIGHT IN HOST SPOT 4

12 OUTER BRIGHT

13 BRIGHT INCL SPOT 5

14 BRIGHT INCL 7

15 IN ADJ HOT, REL ,BRIGHT

16 ADJ C GRAIN

TABLE 1: AMPHIBOLE, BLACK LABEL-BLACK THOR, J LAARMAN, JULY 2013

	17	18	19	20	21	22	23	24
STO2	44.83	59.15	47.65	50.86	45.78	46.73	44.46	46.02
TIO2	1.67	.06	1.28	.33	1.90	1.61	3.82	4.09
A2O3	11.72	.50	9.71	5.69	10.73	10.39	11.01	10.23
C2O3	3.19	.22	2.63	1.79	1.70	1.47	2.45	2.58
FEO	4.34	1.93	4.06	3.88	4.46	4.22	4.61	3.71
MGO	17.86	24.64	18.84	21.69	18.47	18.93	16.81	17.76
MNO	.08	.06	.12	.09	.11	.05	.02	.05
CAO	11.22	11.47	10.86	12.23	12.14	11.93	10.04	9.82
K2O	.95	.42	.39	1.09	.31	.43	.09	.09
NA2O	2.65	.20	2.21	1.07	2.48	2.30	3.97	4.15
SUM	98.51	98.65	97.75	98.72	98.08	98.06	97.28	98.50
SI	6.357	7.971	6.719	7.094	6.485	6.591	6.366	6.471
AL	1.643	8.000	1.281	8.000	1.515	8.000	1.634	8.000
AL	.316	.050	.332	.030	.276	.318	.224	.167
TI	.178	.006	.136	.035	.202	.171	.411	.433
CR	.358	.023	.293	.197	.190	.164	.277	.287
FE	.515	.218	.479	.453	.528	.498	.552	.436
MG	3.775	4.949	3.960	4.510	3.900	3.980	3.588	3.722
MN	.010	5.151	.014	5.235	.013	5.136	.002	5.055
CA	1.705	1.656	1.641	1.828	1.842	1.803	1.540	1.480
K	.172	.072	.070	.194	.056	.077	.016	.016
NA	.729	2.605	.604	2.315	.681	2.509	1.102	2.627
O	23.000	23.000	23.000	23.000	23.000	23.000	23.000	23.000
ANTH	62.98	72.54	65.14	66.42	62.19	63.37	63.16	66.02
WO	28.44	24.27	26.99	26.92	29.38	28.71	27.12	26.24
GEDR	8.59	3.19	7.88	6.67	8.43	7.93	9.72	7.74
F/M	.139	.045	.125	.103	.139	.127	.155	.119
F/FM	.122	.043	.111	.093	.122	.112	.134	.106

17 REL BRIGHT CENTRAL

18 REPL CR-TI AMPH

19 REL BRIGHT TOP RIGHT C-3 IM 0784

20 RELICT IN CR-TREM TOP RIGHT

21 REL BRIGHT SMALL SPOT 2

22 ANOTHER SMALL RELIC SPOT 3

23 INCL LOWER LEFT

24 ANOTHER INCL

TABLE 1: AMPHIBOLE, BLACK LABEL-BLACK THOR, , J LAARMAN, JULY 2013

	25	26	27	28	29	30	31	32
STO2	47.91	43.71	44.53	44.38	43.50	43.43	45.15	45.15
TIO2	2.51	2.16	2.18	3.95	2.20	2.12	3.87	3.89
A2O3	9.62	12.13	11.56	10.95	12.19	11.63	10.37	10.40
C2O3	.89	2.99	3.10	2.48	2.62	2.78	3.20	3.20
FEO	4.21	4.95	4.63	4.18	4.91	4.66	3.67	3.85
MGO	20.51	17.17	16.97	16.92	16.45	16.99	17.78	17.68
MNO	.04	.09	.07	.08	.09	.08	.04	.03
CAO	10.55	11.76	11.78	9.95	11.91	11.76	9.87	9.83
K2O	.11	.47	.21	.04	.66	.17	.01	.54
NA2O	1.90	2.54	2.62	3.96	2.52	2.71	4.23	4.37
SUM	98.25	97.97	97.65	96.89	97.05	96.33	98.19	98.71
SI	6.678	6.251	6.362	6.367	6.281	6.301	6.389	6.380
AL	1.322	8.000	1.638	8.000	1.719	8.000	1.611	8.000
AL	.258	* .295	* .309	* .218	* .355	* .289	* .118	* .111
TI	.263	* .232	* .234	* .426	* .239	* .231	* .412	* .413
CR	.098	* .338	* .350	* .281	* .299	* .319	* .358	* .332
FE	.491	* .592	* .553	* .502	* .593	* .565	* .434	* .455
MG	4.261	* 3.660	* 3.614	* 3.618	* 3.540	* 3.674	* 3.750	* 3.724
MN	.005	5.376	.011	5.128	.011	5.037	.005	5.077
CA	1.576	* 1.802	* 1.803	* 1.529	* 1.842	* 1.828	* 1.496	* 1.488
K	.020	* .086	* .038	* .007	* .122	* .031	* .002	* .097
NA	.513	2.109	.726	2.567	.705	2.669	1.161	2.659
O	23.000	* 23.000	* 23.000	* 23.000	* 23.000	* 23.000	* 23.000	* 23.000
ANTH	67.34	60.46	60.53	64.05	59.24	60.55	66.01	65.71
WO	24.90	29.76	30.20	27.07	30.83	30.13	26.34	26.26
GEDR	7.76	9.78	9.27	8.88	9.92	9.32	7.65	8.03
F/M	.116	.165	.155	.141	.171	.157	.117	.123
F/FM	.104	.141	.135	.124	.146	.135	.105	.110

25 INCL IN ADJ CHROMITE
 26 SMALL REL IN CR-TREM KOST
 27 ADJ BRIGHT
 28 INCL IN CHROM C-1 IM09-003
 29 RELIC IN CRTREM SPOT 2
 30 RELIC SPOT 3
 31 INCL IN IM0001-1
 32 BRIGHT INCL SPOT 1 IM 003-1

TABLE 1: AMPHIBOLE, BLACK LABEL-BLACK THOR, , J LAARMAN, JULY 2013

	33	34	35	36	37	38	39	40
STO2	46.59	46.53	45.33	50.79	56.98	53.66	56.56	56.64
TIO2	1.47	2.13	4.08	.19	.10	.41	.06	.13
A2O3	12.02	9.98	10.65	1.48	1.30	3.16	.87	1.50
C2O3	1.07	3.12	3.15	6.08	.89	1.68	.58	1.05
FEO	3.59	3.41	3.64	4.83	1.63	1.67	1.28	1.88
MGO	19.19	20.56	17.44	22.07	23.91	22.86	23.92	23.78
MNO	.08	.11	.08	.02	.00	.00	.00	.00
CAO	11.26	9.62	9.80	12.10	12.59	12.96	12.91	12.86
K2O	.03	.27	.14	.58	.05	.13	.05	.07
NA2O	3.47	2.50	4.49	.33	.43	.96	.35	.50
SUM	98.77	98.23	98.80	98.47	97.88	97.49	96.58	98.41
SI	6.493	6.521	6.380	7.198	7.782	7.440	7.820	7.722
AL	1.507	1.479	1.620	1.247	1.445	.516	.142	.241
AL	.467	.170	.147	.000	.000	.000	.000	.000
TI	.154	.224	.432	.020	.010	.043	.006	.013
CR	.118	.346	.351	.681	.096	.184	.063	.113
FE	.418	.400	.428	.572	.186	.194	.148	.214
MG	3.986	4.295	3.659	4.662	4.867	4.724	4.929	4.832
MN	.009	.013	.010	.002	.000	.000	.000	.000
CA	1.681	1.445	1.478	1.837	1.842	1.925	1.912	1.879
K	.005	.048	.025	.105	.009	.023	.009	.012
NA	.938	2.624	1.225	2.728	.114	.258	.094	.132
O	23.000	23.000	23.000	23.000	23.000	23.000	23.000	23.000
ANTH	65.50	69.96	65.74	65.92	70.58	69.04	70.52	69.78
WO	27.63	23.53	26.56	25.98	26.72	28.13	27.36	27.13
GEDR	6.88	6.51	7.70	8.09	2.70	2.83	2.12	3.10
F/M	.107	.096	.120	.123	.038	.041	.030	.044
F/FM	.097	.088	.107	.110	.037	.039	.029	.042

33 INCL ADJ CHROMITE SPOT 2

34 INCL SMALL L CENTRAL IM 781

35 INCL TO RIGHT DARK OLIV IM 781

36 *** BL-09-31 486211 C-1 INST TO CHROMITE

37 C-1 INST TO CHROMITE

38 REPL CPX C-1

39 INCL CHROMITE

40 ENCL CPX RELIC IM02 07 0001

TABLE 1: AMPHIBOLE, BLACK LABEL-BLACK THOR, , J LAARMAN, JULY 2013

	41	42	43	44	45	46	47	48
STO2	55.62	55.53	46.09	45.37	57.89	45.00	44.90	44.63
TIO2	.11	.17	3.76	3.75	.02	3.95	3.91	3.63
A2O3	1.73	2.11	10.14	10.07	.52	10.75	10.75	9.56
C2O3	1.17	1.09	2.78	2.82	.50	2.97	3.10	3.10
FEO	1.55	1.62	2.64	2.58	1.64	2.84	3.02	2.78
MGO	23.27	23.00	18.73	18.54	24.35	18.04	18.00	18.05
MNO	.01	.00	.01	.03	.00	.00	.00	.00
CAO	12.58	13.28	9.37	9.98	12.55	10.17	10.34	10.50
K2O	.08	.09	.16	.18	.05	.10	.10	.39
NA2O	.53	.57	4.61	4.65	.30	3.54	3.65	4.31
SUM	96.65	97.46	98.29	97.97	97.82	97.36	97.77	96.95
SI	7.712	* 7.656	* 6.472	* 6.415	* 7.890	* 6.384	* 6.359	* 6.407
AL	.283	7.994	1.528	8.000	.084	7.973	1.641	8.000
AL	.000	* .000	* .149	* .093	* .000	* .181	* .153	* .025
TI	.011	* .018	* .397	* .399	* .002	* .421	* .416	* .392
CR	.128	* .119	* .309	* .315	* .054	* .333	* .347	* .352
FE	.180	* .187	* .310	* .305	* .187	* .337	* .358	* .334
MG	4.809	* 4.727	* 3.920	* 3.907	* 4.947	* 3.815	* 3.800	* 3.862
NN	.001	5.130	.001	5.086	.000	5.189	.000	5.074
CA	1.869	* 1.962	* 1.410	* 1.512	* 1.833	* 1.546	* 1.569	* 1.615
K	.014	* .016	* .029	* .032	* .009	* .018	* .018	* .071
NA	.142	2.025	1.255	2.693	.079	1.921	1.002	2.589
O	23.000	* 23.000	* 23.000	* 23.000	* 23.000	* 23.000	* 23.000	* 23.000
ANTH	70.13	68.75	69.51	68.26	71.01	66.95	66.35	66.46
WO	27.25	28.53	25.00	26.41	26.31	27.13	27.40	27.79
GEDR	2.62	2.72	5.50	5.33	2.68	5.91	6.25	5.74
F/M	.038	.040	.079	.079	.038	.088	.094	.086
F/FM	.036	.038	.074	.073	.036	.081	.086	.080

41 REPL CPX SPOT 4
42 REPL CPX
43 INCL IN CHROMITE
44 TI CR NA AMPH
45 TREMOLITE ENCL CHROMITE
46 SPOT 3 IM0007
47 ADJ DOMAIN SPOT 4
48 ANOTHER

TABLE 1: AMPHIBOLE, BLACK LABEL-BLACK THOR, , J LAARMAN, JULY 2013

	49	50	51	52	53	54	55	56
STO2	44.43	45.24	45.56	45.61	57.23	43.84	44.10	56.00
TIO2	3.55	3.70	3.44	3.17	.06	3.30	3.36	.14
A2O3	10.31	10.51	9.77	10.06	.52	10.51	10.42	1.54
C2O3	3.28	3.47	3.16	3.28	1.16	3.15	3.27	1.12
FEO	2.83	2.36	2.46	2.45	1.74	3.74	3.60	1.52
MGO	18.88	18.34	18.79	18.45	24.21	17.35	17.31	23.53
MNO	.00	.00	.00	.00	.00	.00	.00	.00
CAO	10.43	8.42	10.30	9.96	10.26	10.97	10.69	12.82
K2O	.20	.10	.15	.21	.05	.93	.16	.12
NA2O	4.32	4.57	4.80	4.96	1.89	4.13	4.18	.49
SUM	98.23	96.71	98.43	98.15	97.12	97.92	97.09	97.28
SI	6.296	6.440	6.422	6.443	7.871	6.290	6.340	7.718
AL	1.704	1.560	1.578	1.557	.084	1.710	1.660	.250
AL	.017	.203	.045	.117	.000	.067	.106	.000
TI	.378	.396	.365	.337	.006	.356	.363	.015
CR	.367	.391	.352	.366	.126	.357	.372	.122
FE	.335	.281	.290	.289	.200	.449	.433	.175
MG	3.988	3.891	3.948	3.884	4.963	3.710	3.709	4.833
MN	.000	.000	.000	.000	.000	.000	.000	.000
CA	1.583	1.284	1.556	1.507	1.512	1.686	1.647	1.893
K	.036	.018	.027	.038	.009	.170	.029	.021
NA	1.187	1.261	1.312	1.358	.504	1.149	1.165	.131
O	23.000	23.000	23.000	23.000	23.000	23.000	23.000	23.000
ANTH	67.51	71.32	68.14	68.37	74.35	63.47	64.08	70.03
WO	26.81	23.54	26.85	26.53	22.65	28.85	28.45	27.43
GEDR	5.68	5.15	5.01	5.09	3.00	7.68	7.48	2.54
F/M	.084	.072	.073	.075	.040	.121	.117	.036
F/FM	.078	.067	.068	.069	.039	.108	.104	.035

49 ADJ DARK DOM

50 RANDOM INCL

51 BRIGHT PHASE S-1 IM0010

52 SPOT 1 AGAIN

53 DARKER SPOT 2

54 3 PHASES IN CIRC DOMAIN 3

55 NA CA AMPH AGAIN SPOT 1

56 ENCL CHROMITE W CIRC INCL, SPOT 8

TABLE 1: AMPHIBOLE, BLACK LABEL-BLACK THOR, , J LAARMAN, JULY 2013

	57	58	59	60	61	62	63	64
STO2	55.80	56.69	56.25	45.47	45.61	45.99	45.82	46.34
TIO2	.08	.07	.20	3.74	3.64	2.89	2.59	3.54
A2O3	1.26	1.13	1.47	10.11	9.77	8.75	9.17	9.52
C2O3	.52	.97	.88	2.72	2.99	3.33	2.86	3.17
FEO	1.82	1.63	1.86	3.09	2.97	2.24	3.43	2.49
MGO	24.19	24.57	24.32	18.75	18.98	19.09	18.30	19.25
MNO	.00	.00	.00	.00	.00	.00	.00	.02
CAO	12.02	10.80	12.22	10.42	10.34	10.29	11.58	10.09
K2O	.07	.18	.29	.23	.10	.16	.13	.10
NA2O	.54	.36	.50	2.60	2.57	4.13	3.87	4.32
SUM	96.30	96.40	97.99	97.13	96.97	96.87	97.75	98.84
SI	7.751	7.824	7.700	6.454	6.479	6.562	6.524	6.481
AL	.206	.176	.237	1.546	1.521	1.438	1.476	1.519
AL	.000	.008	.000	.146	.114	.033	.063	.050
TI	.008	.007	.021	.399	.389	.310	.277	.372
CR	.057	.106	.095	.305	.336	.376	.322	.351
FE	.211	.188	.213	.367	.353	.267	.408	.291
MG	5.008	5.054	4.962	3.967	4.018	4.060	3.884	4.013
MN	.000	.000	.000	.000	.000	.000	.000	.002
CA	1.789	1.597	1.792	1.585	1.574	1.573	1.767	1.512
K	.012	.032	.051	.042	.018	.029	.024	.018
NA	.145	.096	.133	.716	.708	1.142	1.068	1.171
O	23.000	23.000	23.000	23.000	23.000	23.000	23.000	23.000
ANTH	71.46	73.90	71.22	67.03	67.59	68.81	64.10	69.00
WO	25.52	23.35	25.72	26.78	26.47	26.66	29.16	26.00
GEDR	3.02	2.75	3.06	6.20	5.93	4.53	6.74	5.01
F/M	.042	.037	.043	.092	.088	.066	.105	.073
F/FM	.041	.036	.041	.085	.081	.062	.095	.068

57 INST TREM SPOT 9
58 INT W REPL METAS DIOPSIDE C-11
59 ADJ TO CRACK POSS RETRO NA-CA AMPH
60 COMP INCL 5 REL BRIGHT
61 REPL BY CR-TALC INCL 5
62 INCL 1 SPOT 1
63 INCL 2 W SULPH
64 INCL 3 BRIGHT

TABLE 1: AMPHIBOLE, BLACK LABEL-BLACK THOR, , J LAARMAN, JULY 2013

	73	74	75	76	77	78	79	80
STO2	55.83	56.67	56.05	56.53	44.75	46.38	59.04	57.14
TIO2	.09	.13	.10	.08	1.67	1.50	.02	.07
A2O3	.49	1.15	1.74	2.05	11.40	11.10	.66	.62
C2O3	1.79	.78	1.10	1.53	1.86	1.74	.18	.41
FEO	3.42	2.15	1.31	1.37	4.83	4.64	1.62	1.75
MGO	23.43	23.48	23.60	23.70	17.52	18.28	24.55	23.79
MNO	.09	.07	.00	.10	.13	.03	.10	.05
CAO	12.72	13.23	13.12	12.79	11.86	11.69	12.41	13.12
K2O	.02	.01	.01	.02	.74	.82	.02	.00
NA2O	.18	.41	.53	.65	2.44	2.66	.26	.27
SUM	98.06	98.08	97.56	98.82	97.20	98.84	98.86	97.22
SI	7.714	7.762	7.697	7.670	6.425	6.525	7.937	7.858
AL	.080	.186	.282	.328	1.575	1.475	.063	.100
AL	.000	.000	.000	.000	.354	.365	.042	.000
TI	.009	.013	.010	.008	.180	.159	.002	.007
CR	.196	.084	.119	.164	.211	.194	.019	.045
FE	.395	.246	.150	.155	.580	.546	.182	.201
MG	4.825	4.793	4.831	4.793	3.750	3.833	4.919	4.876
MN	.011	.008	.000	.011	.016	.004	.011	.006
CA	1.883	1.941	1.930	1.859	1.825	1.762	1.788	1.933
K	.004	.002	.002	.003	.136	.147	.003	.000
NA	.048	.109	.141	.171	.679	.726	.068	.072
O	23.000	23.000	23.000	23.000	23.000	23.000	23.000	23.000
ANTH	67.93	68.66	69.89	70.40	60.93	62.42	71.41	69.56
WO	26.51	27.81	27.93	27.31	29.65	28.69	25.95	27.57
GEDR	5.56	3.53	2.18	2.28	9.42	8.89	2.64	2.87
F/M	.084	.053	.031	.035	.159	.143	.039	.042
F/FM	.078	.050	.030	.034	.137	.125	.038	.041

73 WITHIN CHL GRAINS ACROSS SAMPLE

74 WITHIN CHL GRAINS ACROSS SAMPLE

75 **** BL-09-31 486229

76 AGAIN

77 **** BL-09-31 486241 NEAR C-1 RELIC

78 BRIGHT RELIC IM0004-1

79 ENCL HOST

80 SMALL INCL IM0806 NEAR OLIV RELIC 241

TABLE 1: AMPHIBOLE, BLACK LABEL-BLACK THOR, , J LAARMAN, JULY 2013

	81	82	83	84	85	86	87	88
STO2	57.38	57.87	44.68	45.36	44.41	58.44	46.08	45.94
TIO2	.08	.00	3.09	3.22	2.95	.00	2.17	2.96
A2O3	.65	.81	9.69	10.50	13.19	.51	9.55	10.92
C2O3	.42	.58	2.36	2.15	2.57	.97	2.36	2.91
FEO	1.29	2.40	3.82	3.78	3.43	2.26	3.29	3.74
MGO	24.07	23.00	17.03	17.46	17.38	23.90	19.09	17.91
MNO	.07	.16	.15	.10	.11	.10	.13	.13
CAO	13.63	13.07	11.22	10.98	10.62	12.54	10.72	10.52
K2O	.02	.00	.00	.02	.01	.00	.01	.00
NA2O	.24	.24	4.09	4.19	4.32	.13	4.33	4.13
SUM	97.85	98.13	96.13	97.76	98.99	98.85	97.73	99.16
SI	7.837	* 7.898	* 6.478	* 6.448	* 6.226	* 7.902	* 6.538	* 6.431
AL	.105	7.942	1.522	8.000	1.774	8.000	1.462	8.000
AL	.000	* .028	* .134	* .207	* .405	* .000	* .134	* .232
TI	.008	* .000	* .337	* .344	* .311	* .000	* .232	* .312
CR	.045	* .063	* .271	* .242	* .285	* .104	* .265	* .322
FE	.147	* .274	* .463	* .449	* .402	* .256	* .390	* .438
MG	4.900	* 4.679	* 3.680	* 3.700	* 3.632	* 4.817	* 4.037	* 3.737
MN	.008	5.109	.018	4.903	.013	5.047	.016	5.073
CA	1.995	* 1.911	* 1.743	* 1.672	* 1.595	* 1.817	* 1.630	* 1.578
K	.003	* .000	* .000	* .004	* .002	* .000	* .002	* .000
NA	.064	2.062	1.150	2.893	1.174	2.771	1.191	2.822
O	23.000	* 23.000	* 23.000	* 23.000	* 23.000	* 23.000	* 23.000	* 23.000
ANTH	69.58	68.17	62.52	63.55	64.52	69.92	66.65	64.96
WO	28.32	27.84	29.61	28.73	28.34	26.37	26.90	27.43
GEDR	2.09	3.99	7.87	7.72	7.14	3.71	6.44	7.61
F/M	.032	.063	.131	.125	.114	.055	.101	.121
F/FM	.031	.059	.116	.111	.103	.053	.091	.108

81 NEAR OLIV REL 241

82 *** BL-09-31 486296 HOST TO CHROMITE BY C-3 FEB13

83 ADJ HOLE

84 ADJ HOLE

85 TI CR CA-NA AMPH W TALC, IM0004

86 COMP INCL 1 IM0009

87 BRIGHT INCL 2

88 BRIGHT INCL 3

TABLE 1: AMPHIBOLE, BLACK LABEL-BLACK THOR, , J LAARMAN, JULY 2013

STO2	105	106	107	108	109	110	111	112
TIO2	45.96	58.12	46.73	46.82	47.06	46.48	47.18	58.58
A2O3	2.70	.00	2.27	2.55	2.64	2.69	2.75	.00
C2O3	10.13	.20	9.52	9.39	9.60	10.25	9.76	.28
FEO	1.92	.64	2.60	2.91	3.00	3.17	3.08	.26
MGO	19.25	1.31	1.60	1.96	1.95	1.95	2.19	1.44
MNO	.09	23.68	20.45	19.52	19.41	19.18	18.91	24.09
CJO	.00	.00	.02	.08	.02	.05	.08	.00
K2O	10.87	13.52	10.84	10.39	10.56	10.47	10.82	13.34
NA2O	.00	.03	.01	.02	.04	.06	.04	.07
SUM	2.87	.00	2.57	2.77	2.82	2.96	2.86	.08
	96.39	97.50	97.32	96.41	97.10	97.26	97.67	98.14
SI	6.534	7.945	6.570	6.641	6.629	6.547	6.621	7.949
AL	1.466	8.000	1.430	1.359	1.371	1.453	1.379	.045
AL	.231	.000	.148	.210	.223	.249	.236	.000
TI	.289	.000	.240	.272	.280	.285	.290	.000
CR	.292	.069	.368	.326	.334	.353	.342	.028
FE	.228	.150	.188	.232	.230	.230	.257	.163
MG	4.079	4.825	4.286	4.127	4.075	4.027	3.956	4.873
MN	.011	5.130	.002	.010	.002	.006	.010	.000
CA	1.656	.000	1.633	1.579	1.594	1.580	1.627	1.940
K	.000	.005	.002	.004	.007	.011	.007	.012
NA	.791	2.447	.701	.762	.770	.808	.778	.021
O	23.000	23.000	23.000	23.000	23.000	23.000	23.000	23.000
ANTH	68.41	69.37	70.18	69.50	69.09	68.99	67.74	69.85
WO	27.77	28.47	26.74	26.59	27.02	27.07	27.86	27.80
GEDR	3.83	2.15	3.08	3.92	3.89	3.94	4.40	2.34
F/M	.059	.031	.044	.059	.057	.059	.067	.034
F/FM	.055	.030	.043	.055	.054	.055	.063	.032

105 BRIGHT CENTRAL IM 0010

106 DARK AT END

107 SMALLER AMPH GRAIN

108 GREY PHASE INCL 3

109 GREY PHASE INCL 3

110 GREY PHASE AGAIN

111 AGAIN

112 NEEDLES IN TALC

TABLE 1: AMPHIBOLE, BLACK LABEL-BLACK THOR, J LAARMAN, JULY 2013

	129	130	131	132	133	134	135	136
STO2	45.89	58.89	46.22	57.98	57.50	45.50	46.13	47.79
TIO2	3.17	.03	3.19	.03	.18	2.52	1.96	2.06
A2O3	10.59	.70	10.80	.87	1.06	10.60	11.21	9.29
C2O3	3.32	3.19	2.57	.73	.99	3.39	1.18	3.08
FEO	2.93	1.08	2.49	1.39	1.50	2.17	3.28	2.73
MGO	17.92	24.55	19.36	24.00	24.04	19.71	19.45	19.29
MNO	.00	.00	.00	.00	.00	.02	.00	.00
CAO	10.14	12.98	10.81	13.49	13.31	11.31	11.84	11.16
K2O	.05	.03	.04	.01	.01	.04	.05	.07
NA2O	3.48	.32	3.14	.26	.33	3.18	2.86	2.87
SUM	97.49	98.77	98.62	98.76	98.92	98.44	97.96	98.34
SI	6.490	7.920	6.444	7.842	7.780	6.382	6.483	6.679
AL	1.510	8.000	1.556	8.000	.169	1.618	1.517	1.321
AL	.254	.031	.218	.000	.000	.133	.340	.209
TI	.337	.003	.334	.003	.018	.266	.207	.216
CR	.371	.020	.283	.078	.106	.376	.131	.340
FE	.347	.121	.290	.157	.170	.255	.386	.319
MG	3.777	4.921	4.023	4.838	4.848	4.120	4.074	4.018
MN	.000	5.086	.000	5.077	.000	.002	.000	.000
CA	1.536	1.870	1.615	1.955	1.929	1.700	1.783	1.671
K	.009	.005	.007	.002	.002	.007	.009	.012
NA	.954	2.500	.849	2.471	.087	.865	.779	.778
O	23.000	23.000	23.000	23.000	23.000	23.000	23.000	23.000
ANTH	66.73	71.19	67.86	69.61	69.78	67.83	65.27	66.88
WO	27.14	27.06	27.24	28.13	27.77	27.98	28.56	27.81
GEDR	6.12	1.76	4.90	2.26	2.44	4.19	6.18	5.31
F/M	.092	.025	.072	.032	.035	.062	.095	.079
F/FM	.084	.024	.067	.031	.034	.059	.086	.074

129 MAIN GRAIN PRIOR TO INCORP
130 *** BL-09-31 486348 ANOTHER METAS DIOPSIDE REPL OL
131 SMALL INCL IN SMALL CHROMITE C-1
132 C AMPH INCL, IM0856, 02 20 0011
133 BRIGHT IN SMALL INCL IM02 20 0011
134 INCL BRIGHT, IM0955, 02 20 0014
135 ENCL AMPH DARK ZONE
136 OUTER BRIGHTER ZONE

TABLE 1: AMPHIBOLE, BLACK LABEL-BLACK THOR, , J LAARMAN, JULY 2013

	169	170	171	172	173	174	175	176
STO2	46.16	47.81	51.82	58.12	57.11	51.08	56.78	55.72
TIO2	2.65	.58	.42	.01	.11	.39	.02	.06
A2O3	9.50	8.67	5.69	.72	1.26	7.30	1.79	1.89
C2O3	3.16	2.65	1.56	.70	1.04	2.37	1.84	2.69
FEO	1.46	2.48	1.50	.64	.62	1.62	.52	.72
MGO	20.00	20.01	21.53	24.46	24.27	21.21	23.74	23.20
MNO	.00	.16	.09	.11	.07	.14	.08	.14
CAO	10.23	12.65	12.99	13.71	13.51	12.75	13.49	13.47
K2O	.05	.49	.22	.02	.03	.31	.05	.07
NA2O	4.84	1.99	1.42	.24	.31	1.58	.37	.45
SUM	98.05	97.49	97.24	98.73	98.33	98.75	98.68	98.41
SI	6.491	* 6.755	* 7.222	* 7.846	* 7.754	* 7.037	* 7.697	* 7.616
AL	1.509	8.000	.778	.115	.202	.963	.286	.304
AL	.065	* 1.198	* .156	* .000	* .000	* .223	* .000	* .000
TI	.280	* .062	* .044	* .001	* .011	* .040	* .002	* .006
CR	.351	* .296	* .172	* .075	* .112	* .258	* .197	* .291
FE	.172	* .293	* .175	* .072	* .070	* .187	* .059	* .082
MG	4.192	* 4.214	* 4.472	* 4.922	* 4.912	* 4.355	* 4.797	* 4.726
MN	.000	5.060	.019	.013	.008	.016	.009	.016
CA	1.541	* 1.915	* 1.940	* 1.983	* 1.965	* 1.882	* 1.959	* 1.973
K	.009	* .088	* .039	* .003	* .005	* .054	* .009	* .012
NA	1.320	2.870	.384	.063	.082	.422	.097	.119
O	23.000	* 23.000	* 23.000	* 23.000	* 23.000	* 23.000	* 23.000	* 23.000
ANTH	70.99	65.62	67.90	70.54	70.70	67.80	70.39	69.70
WO	26.10	29.82	29.45	28.42	28.29	29.30	28.75	29.09
GEDR	2.91	4.56	2.65	1.04	1.01	2.91	.87	1.21
F/M	.041	.074	.041	.017	.016	.047	.014	.021
F/FM	.039	.069	.040	.017	.016	.045	.014	.020

169 SMALL RELIC IN TALC

170 *** BT-08-10 486722 INST

171 INST

172 ANOTHER INST

173 ANOTHER INST

174 ANOTHER INST

175 INT W CHL

176 INT W INST CR-CHLORITE

TABLE 1: AMPHIBOLE, BLACK LABEL-BLACK THOR, , J LAARMAN, JULY 2013

	177	178	179	180	181
STO2	49.23	50.89	56.16	51.79	49.02
TIO2	.52	.45	.06	.35	.44
A2O3	8.46	7.05	1.64	6.13	7.95
C2O3	2.15	1.83	1.47	2.46	2.83
FEO	2.02	1.76	.61	1.82	2.51
MGO	20.29	20.67	24.23	21.32	20.40
MNO	.19	.13	.13	.14	.13
CAO	12.50	12.35	13.75	12.45	12.44
K2O	.46	.37	.03	.26	.41
NA2O	2.08	1.80	.33	1.80	2.09
SUM	97.90	97.30	98.41	98.52	98.22
SI	6.881	* 7.107	* 7.649	* 7.153	* 6.860
AL	1.119	8.000	.263	7.913	1.140
AL	.275	* .267	* .000	* .150	* .171
TI	.055	* .047	* .006	* .036	* .046
CR	.238	* .202	* .158	* .269	* .313
FE	.236	* .206	* .069	* .210	* .294
MG	4.227	* 4.302	* 4.919	* 4.389	* 4.255
NN	.022	5.053	.015	5.015	.015
CA	1.872	* 1.848	* 2.007	* 1.842	* 1.865
K	.082	* .066	* .005	* .046	* .073
NA	.564	2.518	.087	2.099	.567
O	23.000	* 23.000	* 23.000	* 23.000	* 23.000
ANTH	66.72	67.69	70.32	68.14	66.34
WO	29.55	29.07	28.69	28.60	29.08
GEDR	3.73	3.23	.99	3.26	4.58
F/M	.061	.051	.017	.052	.073
F/FM	.058	.049	.017	.049	.068
177 CENTRAL BRIGHT ZONE IM0005					
178 BRIGHT CENTRAL AGAIN, IM0005					
179 DARK MARGINAL ZONE					
180 BRIGHTER SPOT 3					
181 BRIGHTER SPOT 3					

Paplike Recalculation for Amphibole

	Si	Al4	Tet	Al6	F2	F3	Mg	Mn	Ti	Cr	Oct	Xoct	Ca	NaiM4	M4	NaA	K	A	Ca	Mg	F2	
1	7.73	0.27	8	0.01	0.05	0.24	4.79	0.01	0.01	0.151	5.1	0.1	1.9	0	0	2	0	0.01	0.01	28.16	71.11	0.73
2	7.94	0.06	8	0	0.3	0	4.82	0	0	0.014	5.14	0.14	1.86	0	0	2	0.04	0.01	0.05	26.57	69.09	4.34
3	6.77	1.23	8	0.3	0.32	0.12	4.01	0	0.28	0.341	5.03	0.03	1.45	0.51	2	0.73	0.03	0.76	0.25	25.11	69.35	5.54
4	6.65	1.35	8	0.23	0.31	0.16	4.04	0	0.3	0.307	5.04	0.04	1.52	0.44	2	0.77	0.03	0.8	25.84	68.86	5.3	
5	6.6	1.4	8	0.15	0.21	0.21	4.21	0	0.34	0.294	5.13	0.13	1.45	0.43	2	0.75	0.03	0.78	24.67	71.75	3.58	
6	6.58	1.42	8	0.26	0.25	0.18	4.07	0	0.29	0.373	5.05	0.05	1.47	0.48	2	0.79	0.08	0.87	25.44	70.29	4.27	
7	6.54	1.46	8	0.3	0.24	0.24	3.92	0	0.4	0.297	5.1	0.1	1.56	0.34	2	0.43	0.05	0.47	27.25	68.6	4.15	
8	6.37	1.63	8	0.16	0.25	0.25	4.02	0	0.49	0.294	5.16	0.16	1.58	0.26	2	0.48	0.02	0.51	27.04	68.75	4.2	
9	6.44	1.56	8	0.29	0.23	0.23	3.99	0	0.42	0.314	5.17	0.17	1.54	0.29	2	0.48	0.01	0.49	26.69	69.25	4.06	
10	6.47	1.53	8	0.3	0.28	0.22	3.82	0	0.43	0.364	5.06	0.06	1.49	0.45	2	0.58	0.01	0.59	26.62	68.28	5.1	
11	7.96	0.04	8	0.03	0.2	0.03	4.93	0.01	0.49	0.343	5.05	0.05	1.41	0.54	2	0.58	0.01	0.59	25.8	69.23	4.96	
13	6.48	1.52	8	0.32	0.27	0.17	3.79	0.01	0.41	0.294	5.21	0.21	1.73	0.06	2	0.01	0	0.01	25.27	71.88	2.85	
14	6.63	1.37	8	0.23	0.21	0.21	4.21	0.01	0.34	0.277	5.22	0.22	1.54	0.24	2	0.47	0.01	0.49	25.8	70.6	3.6	
15	6.6	1.4	8	0.26	0.22	0.22	4.04	0	0.41	0.294	5.16	0.16	1.51	0.33	2	0.41	0.01	0.42	26.14	70.09	3.77	
16	6.48	1.52	8	0.31	0.35	0.14	3.85	0.01	0.38	0.159	5.04	0.04	1.77	0.19	2	0.43	0.06	0.49	29.7	64.47	5.83	
17	7.96	0.04	8	0.04	0.27	0.03	4.93	0.01	0	0.092	5.28	0.28	1.68	0.04	2	0.01	0	0.01	24.45	71.59	3.96	
18	6.48	1.52	8	0.48	0.35	0.17	3.85	0.01	0.18	0.358	5.05	0.05	1.74	0.21	2	0.53	0.18	0.07	24.28	72.54	3.19	
19	7.98	0.02	8	0.06	0.22	0	4.96	0.01	0.01	0.023	5.25	0.25	1.66	0.05	1.96	0	0.07	0.05	28.1	67.8	4.1	
20	6.81	1.19	8	0.45	0.24	0.24	4.01	0.01	0.14	0.293	5.1	0.1	1.66	0.23	2	0.38	0.07	0.47	24.28	72.54	3.19	
21	7.14	0.86	8	0.08	0.14	0.32	4.54	0.01	0.03	0.197	5.12	0.12	1.84	0.04	2	0.25	0.2	0.44	28.24	69.65	2.12	
23	6.55	1.45	8	0.35	0.39	0.15	3.94	0.01	0.2	0.19	5.04	0.04	1.86	0.1	2	0.59	0.06	0.65	30.08	63.65	6.28	
24	6.63	1.37	8	0.37	0.3	0.2	4	0.01	0.17	0.164	5.06	0.06	1.81	0.13	2	0.5	0.08	0.58	29.64	65.41	4.95	
27	6.48	1.52	8	0.37	0.54	0.02	3.65	0	0.42	0.277	5.01	0.01	1.57	0.43	2	0.7	0.02	0.71	27.23	63.41	9.36	
28	6.59	1.41	8	0.32	0.43	0.01	3.79	0.01	0.46	0.288	5	0	1.51	0.49	2	0.66	0.02	0.68	26.31	66.17	7.52	
29	6.69	1.31	8	0.27	0.25	0.25	4.27	0	0.26	0.096	5.29	0.29	1.58	0.13	2	0.38	0.02	0.4	25.91	70.06	4.04	
30	6.37	1.63	8	0.46	0.46	0.14	3.73	0.01	0.24	0.338	5.04	0.04	1.84	0.12	2	0.59	0.09	0.68	30.45	61.84	7.71	
31	6.51	1.49	8	0.5	0.54	0.03	3.7	0.01	0.24	0.335	5.01	0.01	1.84	0.15	2	0.59	0.04	0.63	30.35	60.81	8.84	
32	6.48	1.52	8	0.37	0.49	0.02	3.68	0.01	0.43	0.281	5.01	0.01	1.56	0.44	2	0.69	0.01	0.69	27.19	64.31	8.51	
33	6.41	1.59	8	0.52	0.6	0	3.61	0.01	0.24	0.299	4.99	0	1.88	0.12	2	0.6	0.12	0.72	30.84	59.24	9.92	
34	6.42	1.58	8	0.45	0.5	0.07	3.75	0.01	0.24	0.319	5.02	0.02	1.86	0.12	2	0.66	0.03	0.69	30.49	61.27	8.24	
35	6.54	1.46	8	0.31	0.4	0.04	3.84	0	0.42	0.358	5.01	0.01	1.53	0.46	2	0.73	0	0.73	26.54	66.48	6.98	
36	6.52	1.48	8	0.29	0.47	0	3.81	0	0.42	0.332	4.99	0	1.52	0.48	2	0.74	0.1	0.84	26.27	65.71	8.03	
37	6.51	1.49	8	0.49	0.21	0.21	4	0.01	0.15	0.118	5.08	0.08	1.69	0.24	2	0.7	0.01	0.71	28.61	67.83	3.56	
38	6.64	1.36	8	0.32	0.2	0.2	4.37	0.01	0.23	0.346	5.35	0.35	1.47	0.18	2	0.51	0.05	0.56	24.33	72.31	3.37	
39	6.53	1.47	8	0.34	0.44	0	3.74	0.01	0.44	0.351	4.97	0	1.51	0.49	2	0.77	0.03	0.79	26.56	65.74	7.7	
40	7.53	0.26	7.79	0	0.59	0.01	4.88	0	0.02	0.681	5.5	0.08	1.92	0	2	0.09	0.11	0.2	26.03	66.02	7.95	
41	7.82	0.18	8	0.03	0.09	0.09	4.89	0	0.01	0.096	5.11	0.11	1.85	0.04	2	0.08	0.01	0.08	27.09	71.55	1.37	
42	7.51	0.49	8	0.03	0.06	0.13	4.77	0	0.04	0.184	5.04	0.04	1.94	0.02	2	0.24	0.02	0.26	28.69	70.38	0.93	
43	7.85	0.14	7.99	0	0.12	0.03	4.95	0	0.01	0.063	5.1	0.08	1.92	0	2	0.09	0.01	0.1	27.47	70.79	1.74	
44	7.77	0.23	8	0.01	0.13	0.08	4.86	0	0.01	0.113	5.1	0.1	1.89	0.01	2	0.12	0.01	0.13	27.46	70.63	1.91	
46	7.76	0.24	8	0.05	0.09	0.09	4.84	0	0.01	0.128	5.08	0.08	1.88	0.04	2	0.1	0.01	0.12	27.62	71.05	1.33	
47	7.7	0.3	8	0.05	0.12	0.07	4.76	0	0.02	0.119	5.01	0.01	1.97	0.01	2	0.14	0.02	0.16	28.82	69.42	1.76	
50	6.59	1.41	8	0.3	0.25	0.07	3.99	0	0.4	0.309	5.02	0.02	1.44	0.54	2	0.74	0.03	0.76	25.31	70.37	4.32	
51	6.55	1.45	8	0.26	0.31	0	3.99	0	0.41	0.315	4.97	0	1.54	0.46	2	0.85	0.03	0.88	26.42	68.25	5.33	
53	7.92	0.08	8	0	0.18	0	4.96	0	0	0.054	5.15	0.15	1.84	0.01	2	0.07	0.01	0.08	26.33	71.05	2.61	
54	6.52	1.48	8	0.35	0.28	0.07	3.89	0	0.43	0.333	5.02	0.02	1.58	0.4	2	0.59	0.02	0.61	27.45	67.72	4.83	
55	6.5	1.5	8	0.34	0.33	0.04	3.88	0	0.43	0.347	5.01	0.01	1.6	0.38	2	0.64	0.02	0.66	27.59	66.79	5.62	
56	6.56	1.44	8	0.21	0.34	0	3.95	0	0.4	0.352	4.91	0	1.65	0.35	2	0.88	0.07	0.95	27.8	66.46	5.74	
57	6.44	1.56	8	0.21	0.29	0.05	4.08	0	0.39	0.367	5.02	0.02	1.62	0.36	2	0.85	0.04	0.89	27.06	68.12	4.82	
58	6.59	1.41	8	0.39	0.14	0.14	3.98	0	0.41	0.391	5.06	0.06	1.31	0.62	2	0.67	0.02	0.69	24.16	73.2	2.64	
59	6.57	1.43	8	0.23	0.3	0	4.04	0	0.37	0.352	4.95	0	1.59	0.41	2	0.94	0.03	0.96	26.85	68.14	5.01	
61	6.6	1.4	8	0.32	0.3	0	3.98	0	0.34	0.366	4.94	0	1.54	0.46	2	0.94	0.04	0.97	26.54	68.37	5.09	
64	7.93	0.07	8	0.01	0.14	0.06	5	0	0.01	0.107	5.21	0.21	1.52	0.26	2	0.24	0.01	0.25	22.86	75.02	2.12	

Paplike Recalculation for Amphibole

	Si	Al4	Tet	Al6	F2	F3	Mg	Mn	Ti	Cr	Oct	Xoct	Ca	NaM4	M4	NaA	K	A	Ca	Mg	F2
65 3 PHASES IN CIRC DOMAIN 3	6.44	1.56	8	0.26	0.46	0	3.8	0	0.36	0.357	4.88	0	1.73	0.27	0	0.9	0.17	1.08	28.85	63.47	7.68
66 NA CA AMPH AGAIN SPOT 1	6.5	1.5	8	0.31	0.44	0	3.8	0	0.37	0.372	4.92	0	1.69	0.31	0	0.88	0.03	0.91	28.45	64.07	7.48
67 ENCL CHROMITE W CIRC INCL, SPOT 8	7.76	0.24	8	0.02	0.08	0.09	4.86	0	0.01	0.122	5.07	0.07	1.9	0.03	0	0.1	0.02	0.13	27.8	70.98	1.22
68 INST TREM SPOT 9	7.77	0.21	7.98	0	0.18	0.03	5.02	0	0.01	0.057	5.24	0.21	1.79	0	0	0.15	0.01	0.16	25.64	71.78	2.58
69 INT W REPL METAS DIOPSIDE C-11	7.86	0.14	8	0.05	0.11	0.08	5.08	0	0.01	0.038	5.32	0.32	1.61	0.07	0	0.03	0.03	0.06	23.64	74.8	1.56
71 ADI TO CRACH POSS RETRO NA-CA AMPH	7.75	0.24	7.99	0	0.2	0.01	4.99	0	0.02	0.095	5.23	0.2	1.8	0	0	0.13	0.05	0.18	25.77	71.35	2.88
72 COMP INCL 5 REL BRIGHT	6.56	1.44	8	0.28	0.19	0.19	4.03	0	0.41	0.305	5.09	0.09	1.61	0.3	0	0.43	0.04	0.47	27.64	69.17	3.2
73 REPL BY CR-TALC INCL 5	6.6	1.4	8	0.26	0.18	0.18	4.09	0	0.4	0.336	5.11	0.11	1.6	0.29	0	0.43	0.02	0.45	27.28	69.66	3.06
74 INCL 1 SPOT 1	6.73	1.27	8	0.24	0.27	0	4.16	0	0.32	0.376	4.99	0	1.61	0.39	0	0.78	0.03	0.81	26.66	68.8	4.53
75 INCL 2 W SJUPH	6.66	1.34	8	0.24	0.42	0	3.97	0	0.28	0.322	4.9	0	1.8	0.2	0	0.9	0.02	0.92	29.16	64.1	6.74
76 INCL 3 BRIGHT	6.63	1.37	8	0.23	0.25	0.05	4.1	0	0.38	0.351	5.01	0.01	1.55	0.44	0	0.76	0.02	0.78	26.21	69.55	4.24
77 INCL 4 BRIGHT	6.66	1.44	8	0.21	0.34	0.01	4.01	0	0.42	0.342	5	0	1.58	0.42	0	0.78	0.02	0.8	26.64	67.62	5.74
78 LOWER LEFT	6.59	1.41	8	0.11	0.38	0	4.05	0	0.41	0.367	4.95	0	1.64	0.36	0	0.92	0.02	0.94	27.01	66.7	6.29
79 INCL 1 0025	7.67	0.33	8	0.01	0.07	0.14	4.81	0	0.01	0.194	5.04	0.04	1.94	0.01	0	0.16	0.01	0.17	28.48	70.45	1.07
80 INCL 1	6.76	1.24	8	0.23	0.41	0	3.96	0	0.34	0.369	4.94	0	1.59	0.41	0	0.85	0.01	0.86	26.59	66.47	6.94
81 REPL OLIV C-1	7.83	0.17	8	0.15	0.16	0	4.76	0.02	0.01	0.165	5.1	0.1	1.84	0.01	1.96	0	0.09	0.09	27.28	70.38	2.34
82 C POIK INST TO CHROM, IM0586	7.71	0.29	8	0.05	0.06	0.11	4.76	0.01	0.02	0.124	5.02	0.02	1.88	0	2	0	0.11	0.12	28.08	71.63	0.29
83 C POIK INST TO CHROM, IM0586	7.58	0.42	8	0.05	0.02	0.21	4.79	0.02	0.02	0.168	5.12	0.12	1.88	0	2	0	0	0	25.45	71.5	3.05
84 WITHIN CHL GRAINS ACROSS SAMPLE	7.91	0.09	8	0	0.21	0.08	4.95	0	0	0.028	5.24	0.24	1.76	0	2	0	0	0	25.45	71.5	3.05
85 WITHIN CHL GRAINS ACROSS SAMPLE	7.81	0.08	7.89	0	0.39	0.01	4.89	0.01	0.01	0.196	5.31	0.09	1.91	0	2	0.05	0	0.05	26.55	68.01	5.44
86 WITHIN CHL GRAINS ACROSS SAMPLE	7.8	0.19	7.98	0	0.2	0.05	4.81	0.01	0.01	0.084	5.08	0.05	1.95	0	2	0.11	0	0.11	28.01	69.14	2.86
87 **** BL-09-31 486229	7.74	0.26	8	0.02	0.05	0.1	4.86	0	0.01	0.119	5.04	0.04	1.94	0.02	2	0.13	0	0.13	28.35	70.94	0.71
88 AGAIN	7.74	0.26	8	0.07	0.08	0.08	4.84	0.01	0.01	0.164	5.08	0.08	1.88	0.04	2	0.13	0	0.14	27.63	71.21	1.16
89 **** BL-09-31 486241 NEAR C-1 REL	6.5	1.5	8	0.45	0.48	0.11	3.79	0.02	0.18	0.211	5.03	0.03	1.85	0.12	2	0.56	0.14	0.7	30.17	61.98	7.85
90 BRIGHT REUC IM0004-1	6.59	1.41	8	0.45	0.42	0.13	3.87	0	0.16	0.194	5.04	0.04	1.78	0.18	2	0.55	0.15	0.7	29.3	63.72	6.99
91 ENCL HOST	7.94	0.06	8	0.04	0.14	0.05	4.92	0.01	0	0.019	5.16	0.16	1.79	0.05	2	0.02	0	0.02	26.13	71.89	1.98
92 SMALL INCL IM0806 NEAR OLIV REUC	7.88	0.1	7.98	0	0.19	0.01	4.89	0.01	0.01	0.245	5.1	0.06	1.94	0	2	0.07	0	0.07	27.63	69.69	2.68
94 NEAR OLIV REL 241	7.86	0.1	7.96	0	0.13	0.02	4.91	0.01	0.01	0.045	5.08	0	2	0	2	0.06	0	0.07	28.41	69.79	1.8
95 **** BL-09-31 486296 HOST TO CE BY CHROM	7.92	0.08	8	0.05	0.22	0.05	4.69	0.02	0	0.063	5.04	0.04	1.92	0.05	2	0.02	0	0.02	28.07	68.71	3.22
100 ADJ HOLE	6.59	1.41	8	0.28	0.47	0	3.75	0.02	0.34	0.271	4.86	0	1.77	0.23	2	0.94	0	0.94	29.61	62.52	7.87
101 ADJ HOLE	6.55	1.45	8	0.34	0.46	0	3.76	0.01	0.35	0.242	4.92	0	1.7	0.3	2	0.87	0	0.88	28.73	63.55	7.72
102 TI CR CA-NA AMPH W TALC, IM0000 4	6.34	1.66	8	0.56	0.4	0.01	3.7	0.01	0.32	0.285	5	0	1.63	0.37	2	0.82	0	0.83	28.38	64.6	7.02
103 COMP INCL 1 IM00009	7.95	0.05	8	0.03	0.23	0.03	4.85	0.01	0	0.104	5.15	0.15	1.83	0.02	2	0.01	0	0.01	26.49	70.22	3.28
104 BRIGHT INCL 2	6.64	1.36	8	0.27	0.34	0.06	4.1	0.02	0.24	0.265	5.02	0.02	1.66	0.33	2	0.88	0	0.89	27.17	67.3	5.53
105 BRIGHT INCL 3	6.57	1.43	8	0.41	0.43	0.01	3.82	0.02	0.32	0.322	5	0	1.61	0.38	2	0.76	0	0.76	27.5	65.11	7.39
106 INCL CENTRAL IM0919	7.89	0.11	8	0.01	0.13	0.07	4.84	0.01	0	0.116	5.06	0.06	1.88	0.07	2	0.08	0	0.08	27.47	70.7	1.83
107 WIDE LATH IM0010	6.9	1.1	8	0.35	0.31	0.1	4.12	0	0.14	0.248	5.03	0.03	1.69	0.28	2	0.66	0	0.66	27.56	67.29	5.15
108 **** BL-09-31 486316 PRIMARTY PHEN PHLC	6.49	1.51	8	0.4	0.21	0.15	3.94	0.01	0.33	0.331	5.04	0.04	1.58	0.38	2	0.63	0.05	0.68	27.58	68.82	3.61
109 INCL 3 IM 09 0005	6.49	1.51	8	0.44	0.19	0.19	3.94	0.01	0.32	0.269	5.08	0.08	1.54	0.38	2	0.59	0.02	0.61	27.17	69.52	3.31
110 SMALL REL BRIGHT REL IM09 0005	7.48	0.52	8	0.33	0.09	0.09	4.7	0	0.02	0.057	5.24	0.24	1.63	0.13	2	0.18	0	0.18	25.43	73.1	1.47
111 REUCT DOMAIN EXOTIC AMPH C-2	8.02	0	8.02	0.05	0.13	0	5.06	0.01	0	0.022	5.25	0.25	1.67	0.04	1.96	0	0	0	24.38	73.69	1.92
112 INCL 3 AGAIN IM0005	6.59	1.41	8	0.46	0.16	0.16	3.95	0	0.32	0.315	5.05	0.05	1.46	0.49	2	0.55	0.1	0.65	26.21	70.88	2.91
113 LARGE COMP INCL IN RANDOM CHROM	6.55	1.45	8	0.39	0.13	0.13	4.19	0.01	0.33	0.338	5.19	0.19	1.51	0.3	2	0.57	0	0.57	25.9	71.83	2.27
114 INT W ALBTITE	6.59	1.41	8	0.4	0.22	0	4.02	0.01	0.34	0.373	4.99	0	1.51	0.49	2	0.84	0	0.84	26.23	70.01	3.75
115 INT W ALBTITE IM02 10 0007	6.6	1.4	8	0.41	0.24	0	4	0.01	0.33	0.351	4.98	0	1.51	0.49	2	0.84	0	0.84	26.33	69.47	4.19
116 INCL IN PRIMARY OLIV	7.89	0	7.89	0	0.11	0	5.16	0	0	0.002	5.27	0.06	1.94	0	2	0	0	0	26.95	71.47	1.58
117 BRIGHT PHASE INCL 0008	6.7	1.3	8	0.44	0.12	0.12	4.12	0.01	0.26	0.388	5.08	0.08	1.64	0.28	2	0.48	0.01	0.49	27.89	70.03	2.09
118 BRIGHT PHASE INCL 0008	6.62	1.38	8	0.26	0.11	0.11	4.47	0.02	0.27	0.373	5.24	0.24	1.61	0.14	2	0.6	0.02	0.62	26.06	72.11	1.83
119 SMALL ORANGE IM818	7.69	0.29	7.98	0	0	0.11	4.96	0	0.02	0.036	5.08	0.03	1.97	0	2	0.12	0	0.12	28.44	71.56	0
120 SMALL BRFR ORANGE IM818	7.73	0.27	8	0.03	0.02	0.09	4.87	0	0.01	0.035	5.02	0.02	1.98	0.01	2	0.13	0	0.13	28.82	70.93	0.26
121 **** BL-09-31 486342 BRGT CEIM 001NTRA	6.62	1.38	8	0.39	0.1	0.1	4.17	0.01	0.29	0.321	5.06	0.06	1.69	0.25	2	0.55	0	0.55	28.33	69.98	1.69
122 BRIGHT CENTRAL IM 0010	6.64	1.36	8	0.37	0.12	0.12	4.15	0.01	0.29	0.292	5.05	0.05	1.68	0.26	2	0.54	0	0.54	28.31	69.74	1.95
123 DARK AT END	7.98	0.02	8	0.01	0.15	0	4.85	0	0	0.069	5.01	0.01	1.99	0	2	0	0	0.01	28.48	69.37	2.15

	Si	Al4	Tet	Al6	F2	F3	Mg	Mn	Ti	Cr	Oct	Xoct	Ca	NaM4	M4	NaA	K	A	Ca	Mg	F2	
Paplike Recalculation for Amphibole																						
181 INCL1 BRIGHT IM0016	6.49	1.51	8	0.34	0.34	0	3.86	0.01	0.38	0.317	4.94	0	1.59	0.41	2	0.94	0	0.94	27.46	66.72	5.82	
182 ADJ INCL BRIGHT	6.68	1.32	8	0.38	0.28	0	3.84	0	0.35	0.382	4.85	0	1.59	0.41	2	0.94	0	0.94	27.85	67.32	4.83	
183 ADJ INCL BRIGHT	6.48	1.52	8	0.35	0.33	0	3.86	0	0.37	0.362	4.92	0	1.64	0.36	2	0.95	0	0.95	28.1	66.22	5.68	
184 ADJ INCL BRIGHT	6.45	1.55	8	0.36	0.38	0	3.82	0.01	0.35	0.34	4.92	0	1.62	0.38	2	1.02	0	1.02	27.82	65.72	6.46	
185 ADJ INCL BRIGHT	6.59	1.41	8	0.41	0.3	0	3.83	0	0.36	0.352	4.89	0	1.59	0.41	2	0.92	0	0.92	27.76	67.02	5.21	
186 INCL IM 0935	6.8	1.2	8	0.28	0.32	0	4.07	0	0.23	0.329	4.9	0	1.75	0.25	2	0.92	0	0.93	28.44	66.35	5.21	
187 CR,TI CA-NA AMPH IM0001-1	6.82	1.18	8	0.3	0.32	0	4.06	0	0.23	0.321	4.91	0	1.74	0.26	2	0.87	0	0.87	28.39	66.34	5.28	
188 AMPH CENTRAL AGAIN	6.81	1.19	8	0.32	0.3	0	4.04	0	0.24	0.336	4.9	0	1.72	0.28	2	0.88	0.01	0.89	28.35	66.73	4.92	
189 BRIGHT OUTER ZONE	6.68	1.32	8	0.32	0.28	0	3.99	0	0.28	0.384	4.86	0	1.77	0.23	2	0.94	0.01	0.95	29.32	66.11	4.57	
190 SMALL RELIC IN TALC	6.64	1.36	8	0.25	0.16	0.01	4.29	0	0.29	0.351	5	0	1.58	0.42	2	0.93	0.01	0.94	26.16	71.13	2.71	
191 **** BT-08-10 486722 INST	6.88	1.12	8	0.35	0.23	0.07	4.29	0.02	0.06	0.296	5.02	0.02	1.95	0.03	2	0.52	0.09	0.61	30.13	66.29	3.59	
192 INST	7.3	0.7	8	0.25	0.17	0.01	4.52	0.01	0.04	0.172	5	0	1.96	0.04	2	0.35	0.04	0.39	29.48	67.96	2.56	
193 ANOTHER INST	7.88	0.12	7.99	0	0.03	0.05	4.94	0.01	0	0.075	5.03	0.01	1.99	0	2	0.06	0	0.07	28.62	71.01	0.37	
194 ANOTHER INST	7.8	0.2	8	0	0	0.07	4.94	0.01	0.01	0.112	5.03	0.02	1.98	0	2	0.08	0.01	0.09	28.58	71.42	0	
195 ANOTHER INST	7.15	0.85	8	0.35	0.12	0.07	4.42	0.02	0.04	0.258	5.02	0.02	1.91	0.07	2	0.36	0.06	0.42	29.63	68.56	1.81	
196 INT W CHL	7.79	0.21	8	0.08	0.03	0.03	4.86	0.01	0	0.197	5.01	0.01	1.98	0.01	2	0.09	0.01	0.1	28.89	70.72	0.39	
197 INT W INST CR-CHLORITE	7.76	0.24	8	0.07	0.06	0.03	4.81	0.02	0.01	0.291	4.99	0	2.01	0	2.01	0.12	0.01	0.13	29.2	69.95	0.85	
198 CENTRAL BRIGHT ZONE IM0005	6.99	1.01	8	0.4	0.21	0.03	4.29	0.02	0.06	0.238	5.01	0.01	1.9	0.09	2	0.48	0.08	0.56	29.69	67.04	3.27	
199 BRIGHT CENTRAL AGAIN, IM0005	7.2	0.8	8	0.38	0.19	0.02	4.36	0.02	0.05	0.202	5	0	1.87	0.12	2	0.37	0.07	0.44	29.15	67.86	2.99	
200 DARK MARGINAL ZONE	7.72	0.27	7.98	0	0	0.07	4.96	0.02	0.01	0.158	5.05	0.05	2.02	0	2.02	0.09	0.01	0.09	28.98	71.02	0	
201 BRIGHTER SPOT 3	7.27	0.73	8	0.29	0.16	0.05	4.46	0.02	0.04	0.269	5.02	0.02	1.87	0.11	2	0.38	0.05	0.43	28.84	68.7	2.46	
202 BRIGHTER SPOT 3	6.99	1.01	8	0.33	0.21	0.09	4.34	0.02	0.05	0.313	5.02	0.02	1.9	0.07	2	0.5	0.07	0.58	29.47	67.22	3.31	

TABLE 6: PHLOGOPIITE, BLACK LABEL, J LAARMAN, JULY 2013 R.L.B.

	1	2	3	4	5	6	7	8
STO2	38.27	38.87	38.90	39.93	43.19	41.07	44.46	47.10
TIO2	.00	.00	1.99	1.94	1.65	2.46	.60	.93
A2O3	12.90	13.84	15.50	15.76	13.28	15.49	8.13	9.38
C2O3	1.86	2.43	3.03	3.12	3.15	3.86	1.46	1.76
FEO	2.82	3.04	3.08	3.53	3.02	2.78	3.56	1.68
MGO	29.60	28.06	24.16	25.37	26.02	25.27	31.10	28.25
MNO	.00	.00	.00	.00	.05	.00	.04	.00
BAO	.00	.00	.00	.00	.00	.00	.00	.03
CAO	.00	.00	.41	.00	.80	.00	.00	.13
K2O	5.70	8.10	4.52	4.44	2.45	2.57	2.94	2.01
NA2O	.08	.13	1.80	1.28	2.90	3.83	.18	3.13
SUM	91.23	94.47	93.39	95.37	96.51	97.33	92.47	94.40
SI	5.548	5.526	5.505	5.518	5.841	5.538	6.216	6.386
AL	2.204	2.318	2.495	2.482	2.116	2.461	1.339	1.499
AL	.000	.000	.090	.085	.000	.000	.000	.000
TI	.000	.000	.212	.202	.168	.249	.063	.095
CR	.213	.273	.339	.341	.337	.412	.161	.189
FE	.342	.361	.365	.408	.342	.313	.416	.191
MG	6.396	5.946	5.096	5.226	5.245	5.079	6.481	5.709
MN	.000	.000	.000	.000	.006	.000	.005	.000
CA	.000	.000	.062	.000	.116	.000	.000	.019
EA	.000	.000	.000	.000	.000	.000	.000	.002
K	1.054	1.469	.816	.783	.423	.442	.524	.348
NA	.022	1.077	.494	1.372	.760	1.001	.049	.823
O	22.000	22.000	22.000	22.000	22.000	22.000	22.000	22.000
F/M	.053	.061	.072	.078	.066	.062	.065	.033
F/FM	.051	.057	.067	.072	.062	.058	.061	.032

1 **** BL-09-31 486163 INCL 1 IM 2012 02 09 0029 DARKER PHASE

2 DARKER

3 INT W CR-TI-AMPH, INCL 2

4 PHLOG INT W AMPH

5 C PLATE IN INCL 3

6 C PLATE IN INCL 3

7 ADJ PHASE IN INCL

8 DARKER SPOT 4

TABLE 6: PHLOGOPIITE, BLACK LABEL, J LAARMAN, JULY 2013 R.L.B.

	9	10	11	12	13	14	15	16
STO2	47.84	46.13	45.93	46.23	42.90	39.22	39.75	43.40
TIO2	.80	.29	.37	.65	.30	1.13	1.47	.07
A2O3	9.58	6.85	10.34	10.08	9.71	13.69	13.65	12.51
C2O3	1.73	1.39	1.88	2.33	1.65	1.87	1.98	1.43
FEO	1.62	3.06	1.92	1.46	5.52	3.31	3.37	3.27
MGO	29.37	29.19	28.83	28.92	26.53	25.12	25.18	26.89
MNO	.00	.00	.00	.00	.14	.19	.10	.04
BAO	.05	.05	.08	.15	.18	.00	.00	.00
CAO	.16	.10	.19	.10	.25	.14	.16	.05
K2O	1.89	2.52	7.27	6.29	6.89	6.30	6.08	3.19
NA2O	1.73	.82	.40	.80	.05	.74	.84	1.25
SUM	94.77	90.40	97.21	97.01	94.12	91.71	92.58	92.10
SI	6.414	6.545	6.208	6.228	6.111	5.683	5.697	6.087
AL	1.514	1.145	1.647	1.600	1.630	2.317	2.303	1.913
AL	.000	.000	.000	.000	.000	.021	.003	.154
TI	.081	.031	.038	.066	.032	.123	.158	.007
CR	.183	.156	.201	.248	.186	.214	.224	.159
FE	.182	.363	.217	.164	.658	.401	.404	.384
MG	5.870	6.173	5.808	5.807	5.633	5.426	5.379	5.621
MN	.000	.000	.000	.000	.017	.023	.012	.005
CA	.023	.015	.028	.014	.038	.022	.025	.008
EA	.003	.003	.004	.008	.010	.000	.000	.000
K	.323	.456	1.253	1.081	1.252	1.164	1.111	.571
NA	.450	.799	.105	.209	.014	.208	.233	.340
O	22.000	22.000	22.000	22.000	22.000	22.000	22.000	22.000
F/M	.031	.059	.037	.028	.120	.078	.077	.069
F/FM	.030	.056	.036	.028	.107	.073	.072	.065

9 DARKER SPOT 4
10 REL DARK S-1 IM0008
11 ADJ DARKER GRAIN
12 AGAIN
13 ADJ SPOT 5
14 **** BL-09-31 486296 INCL
15 INCL PHLOG IM0914
16 2ND INCL

TABLE 6: PHLOGOPITE, BLACK LABEL, J LAARMAN, JULY 2013 R.L.B.

	25	26	27	28	29	30	31	32
SI	5.557	5.910	5.679	5.585	5.762	5.585	5.810	5.817
AL	2.207	7.765	1.999	7.678	2.159	7.772	2.076	7.887
AL	.000	* .000	* .000	* .000	* .000	* .000	* .000	* .000
TI	.016	* .000	* .009	* .029	* .027	* .018	* .027	* .030
CR	.249	* .154	* .211	* .186	* .134	* .139	* .150	* .139
FE	.226	* .133	* .211	* .129	* .121	* .130	* .144	* .135
MG	6.469	* 7.342	* 6.562	* 6.582	* 6.231	* 6.667	* 6.161	* 6.138
MN	.000	6.960	.002	7.632	.004	6.995	.004	6.930
CA	.000	* .012	* .005	* .000	* .002	* .003	* .005	* .005
EA	.001	* .000	* .000	* .000	* .000	* .000	* .000	* .000
K	.926	* .217	* 1.055	* 1.062	* 1.236	* .992	* 1.329	* 1.412
NA	.017	.943	.000	.229	.000	1.060	.000	1.356
O	22.000	* 22.000	* 22.000	* 22.000	* 22.000	* 22.000	* 22.000	* 22.000
F/M	.035	.018	.033	.020	.020	.020	.020	.022
F/FM	.034	.018	.032	.020	.020	.020	.023	.022
25 BRIGHT PHLG INCL IM 0022								
26 ***** BL-09-31 486342 DARKER PHASE IM0010								
27 INT GREY LEVEL IM776,777								
28 ***** BL-09-31 486343 INT W CHROMITE C-1 IM 0786,0014								
29 INT W CHROMITE C-1 IM 0786,0014								
30 INT W CHROMITE C-1 IM 0786,0014								
31 INT W CHROMITE C-1 IM 0786,0014								
32 ADJ REGION								
SUM	92.34	91.26	91.81	91.14	92.51	91.81	92.71	94.00

TABLE 6: PHLOGOPIITE, BLACK LABEL, J LAARMAN, JULY 2013 R.L.B.

	33	34	35	36	37	38	39	40
STO2	38.72	40.43	42.49	42.62	40.10	36.74	41.70	39.55
TIO2	.05	.03	1.09	1.10	.16	.02	1.26	.39
A2O3	13.52	10.11	13.63	13.86	11.15	9.49	13.38	11.85
C2O3	1.54	.42	2.60	2.46	1.10	1.72	2.42	1.98
FEO	1.06	7.11	1.51	1.39	3.12	3.22	1.26	2.14
MGO	31.69	31.31	26.97	27.24	29.39	32.76	27.36	33.78
MNO	.00	.09	.00	.00	.01	.00	.00	.00
BAO	.00	.02	.06	.14	.08	.02	.22	.09
CAO	.03	.05	.05	.01	.04	.01	.00	.00
K2O	4.42	1.66	9.15	9.01	7.15	2.09	9.15	3.74
NA2O	.00	.08	.17	.08	.07	.00	.14	.09
SUM	91.03	91.31	97.72	97.91	92.37	86.07	96.89	93.61
SI	5.523	5.807	5.794	5.789	5.782	5.566	5.744	5.520
AL	2.273	1.711	2.190	2.211	1.894	1.694	2.172	1.949
TI	.000	.000	.000	.007	.000	.000	.000	.000
TI	.005	.003	.112	.112	.017	.002	.131	.041
CR	.174	.048	.280	.264	.125	.206	.264	.218
FE	.126	.854	.172	.158	.376	.408	.145	.250
MG	6.738	6.703	5.481	5.515	6.316	7.398	5.617	7.027
MN	.000	.011	7.619	.000	.001	.000	.000	.000
CA	.005	.008	.007	.001	.006	.002	.000	.000
EA	.000	.001	.003	.007	.005	.001	.012	.005
K	.804	.304	1.591	1.561	1.315	.404	1.608	.666
NA	.000	.809	.022	.021	.020	.000	.037	.024
O	22.000	22.000	22.000	22.000	22.000	22.000	22.000	22.000
F/M	.019	.129	.031	.029	.060	.055	.026	.036
F/FM	.018	.114	.030	.028	.056	.052	.025	.034

33 WITHIN CHROMITE W SYMPLECTITE TEXTURE SPOT 3

34 *** BL-09-31 486349 SPOT 2 IM0018,0964

35 INCL 5 IN SMALL CHROMITE

36 INCL 5 SPOT 1 MICA IM0020

37 INT GREY SPOT 3 IM0020

38 SPOT 1 IM0021

39 SPOT 1 IM0021

40 SPOT 1 IM0021

TABLE 6: PHLOGOPIITE, BLACK LABEL, J LAARMAN, JULY 2013 R.L.B.

	41	42	43	44	45	46	47	48
STO2	45.87	43.95	37.75	41.41	38.62	39.33	40.80	40.25
TIO2	.02	.04	.19	.18	.26	.30	.34	.35
A2O3	12.46	12.86	13.49	14.19	14.17	13.88	13.23	13.18
C2O3	2.17	1.91	3.03	2.63	1.25	1.16	1.05	1.00
FEO	1.47	1.40	1.31	1.24	.92	.98	.91	1.01
MGO	27.19	27.19	30.50	31.74	30.87	30.77	29.85	29.81
MNO	.00	.00	.00	.00	.00	.00	.00	.00
BAO	.08	.06	.05	.05	.02	.01	.00	.08
CAO	.00	.00	.03	.00	.04	.00	.00	.00
K2O	6.04	7.79	5.15	5.95	5.86	6.06	8.15	7.92
NA2O	.68	.44	.08	.17	.25	.09	.16	.15
SUM	95.98	95.64	91.58	97.56	92.26	92.58	94.54	93.75
SI	6.203	6.040	5.421	5.568	5.482	5.558	5.703	5.675
AL	1.797	1.960	2.283	2.248	2.370	2.311	2.179	2.190
AL	.189	.123	.000	.000	.000	.000	.000	.000
TI	.002	.004	.021	.018	.028	.032	.036	.037
CR	.232	.208	.344	.280	.140	.130	.116	.111
FE	.166	.161	.157	.139	.109	.116	.106	.119
MG	5.481	5.570	6.528	6.361	6.531	6.482	6.220	6.265
MN	.000	.000	.000	.000	.000	.000	.000	.000
CA	.000	.000	.005	.000	.006	.000	.000	.000
EA	.004	.003	.003	.003	.001	.001	.003	.004
K	1.042	1.365	.943	1.020	1.061	1.092	1.453	1.424
NA	.178	1.224	.022	.044	1.067	.025	1.499	.041
O	22.000	22.000	22.000	22.000	22.000	22.000	22.000	22.000
F/M	.030	.029	.024	.022	.017	.018	.017	.019
F/FM	.029	.028	.024	.021	.016	.018	.017	.019
41 ***	BL-09-31	486350	C-1	OUTER ZONE	SPOT 5	IM0004		
42	SPOT 5							
43 ***	BL-09-31	486352	BRIGHT	AT	TOP	IM0024		
44	BRIGHT	AT	TOP	IM0024				
45 ***	BL-09-31	486353	INCL	IN	CHROMITE	C-1	IM0847	
46	ADJ	BRIGHTER						
47 ***	BL-09-31	486354	C	PHLOG	PLATE	C-1	IM833-836	
48	C	PHLOG	PLATE	C-1	IM833-836			

TABLE 6: PHLOGOPITE, BLACK LABEL, J LAARMAN, JULY 2013 R.L.B.

	57	58	59	60	61
STO2	37.53	37.67	37.56	37.18	36.99
TIO2	.39	.39	.18	.56	.60
A2O3	14.71	14.73	13.04	10.35	10.59
C2O3	1.07	1.07	2.76	2.41	2.38
FEO	1.03	1.03	2.68	5.12	5.64
MGO	29.68	30.17	31.73	30.16	30.55
MNO	.00	.00	.03	.00	.00
BAO	.04	.04	.00	.08	.02
CAO	.00	.00	.00	.00	.03
K2O	6.59	6.59	4.97	4.15	3.67
NA2O	.13	.13	.10	.24	.30
SUM	91.17	91.82	93.05	90.25	90.77
SI	5.419	5.402	5.347	5.508	5.449
AL	2.503	2.489	2.187	1.807	1.838
AL	.000	.000	.000	.000	.000
TI	.042	.042	.019	.062	.066
CR	.122	.121	.311	.282	.277
FE	.124	.124	.319	.634	.695
MG	6.387	6.448	6.732	6.659	6.707
MN	.000	.000	.004	.000	.000
CA	.000	.000	.000	.000	.000
EA	.002	.002	.000	.005	.001
K	1.214	1.205	.902	.784	.690
NA	.036	.036	.028	.069	.086
O	22.000	22.000	22.000	22.000	22.000
F/M	.019	.019	.048	.095	.104
F/FM	.019	.019	.046	.087	.094

57 PHLOG INST TO CHROMITE C-1 IM0826

58 ADJ COARSE PLATE, C-1 IM0826

59 SMALL INCL TOP IM 0826

60 ADJ BRIGHT INCL C-1 IM930

61 ADJ BRIGHT INCL C-1 IM930

TABLE 3: CHLORITE, BLACK LABEL-BLACK THOR, J LAARMAN, JULY 2013 R.L.B.

	1	2	3	4	5	6	7	8
STO2	31.14	32.15	32.58	31.97	31.37	32.09	33.70	34.91
TIO2	.00	.00	.00	.02	.01	.03	.00	.00
A2O3	14.07	13.95	13.72	13.45	13.21	14.80	14.28	13.58
C2O3	2.30	1.63	.98	2.14	3.36	2.95	3.18	1.48
FEO	3.42	3.24	3.38	3.42	1.05	1.49	1.16	1.82
MGO	33.89	34.80	34.40	34.25	36.66	35.94	37.23	36.46
MNO	.00	.00	.00	.00	.00	.00	.00	.00
CAO	.00	.00	.00	.00	.00	.00	.00	.01
K2O	.01	.00	.00	.01	.00	.06	.00	.41
NA2O	.03	.00	.30	.02	.02	.00	.04	.04
SUM	84.86	85.77	85.36	85.28	85.68	87.36	89.59	88.71
SI	6.085	* 6.188	* 6.292	* 6.207	* 6.031	* 6.041	* 6.170	* 6.441
AL	.000	6.188	.000	6.292	.000	6.031	.000	6.170
AL	3.240	* 3.164	* 3.123	* 3.077	* 2.993	* 3.283	* 3.081	* 2.952
TI	.000	* .000	* .000	* .003	* .001	* .004	* .000	* .000
CR	.355	* .248	* .150	* .328	* .511	* .439	* .460	* .216
FE	.559	* .522	* .546	* .555	* .169	* .235	* .178	* .281
MG	9.870	* 9.983	* 9.903	* 9.911	* 10.505	* 10.084	* 10.161	* 10.026
MN	.000	14.024	.000	13.917	.000	14.179	.000	13.880
CA	.000	* .000	* .000	* .000	* .000	* .000	* .000	* .002
K	.002	* .000	* .000	* .002	* .000	* .014	* .000	* .096
NA	.011	.014	.112	.112	.007	.007	.014	.014
O	28.000	* 28.000	* 28.000	* 28.000	* 28.000	* 28.000	* 28.000	* 28.000
F/M	.057	.052	.055	.056	.016	.023	.017	.028
F/FM	.054	.050	.052	.053	.016	.023	.017	.027

1 **** BL-09-31 486155 INT W TALC ENCL DIOP

2 **** BL-09-31 486211 CHL INITIAL

3 CHL GRAINS ACROSS SAMPLE

4 CHL GRAINS ACROSS SAMPLE

5 **** BL-09-31 486383 INCL 3 LATH

6 **** BL-09-31 486348 INT W HASTINGSITE IM02 20 001

7 ASSOC W CR-TREM INCL IM0856

8 INCL 4

TABLE 3: CHLORITE, BLACK LABEL-BLACK THOR, J LAARMAN, JULY 2013 R.L.B.

	9	10	11	12	13	14	15	16
STO2	32.32	33.57	32.07	29.69	31.54	33.21	30.54	27.89
TIO2	.00	.00	.00	.00	.00	.00	.00	.00
A2O3	12.02	13.85	12.31	20.30	14.79	15.01	19.50	19.15
C2O3	3.49	2.85	2.78	2.44	2.83	3.21	2.51	2.38
FEO	1.31	1.13	1.26	1.57	1.19	1.19	1.59	1.42
MGO	34.87	36.63	34.69	33.89	35.98	36.89	35.20	32.21
MNO	.00	.00	.00	.10	.07	.05	.06	.09
CAO	.00	.00	.00	.06	.02	.02	.04	.03
K2O	.00	.09	.16	.08	.03	.03	.02	.05
NA2O	.00	.00	.00	.03	.00	.02	.00	.00
SUM	84.01	88.12	83.27	88.16	86.45	89.63	89.46	83.22
SI	6.324	6.241	6.321	5.534	5.995	6.084	5.610	5.507
AL	.000	.000	.000	.466	.005	.000	.390	.493
AL	2.771	3.034	2.859	3.992	3.308	3.240	3.830	3.963
TI	.000	.000	.000	.000	.000	.000	.000	.000
CR	.540	.419	.433	.360	.425	.465	.365	.372
FE	.214	.176	.208	.245	.189	.182	.244	.234
MG	10.169	10.150	10.191	9.415	10.193	10.072	9.637	9.480
MN	.000	.000	.000	.016	.011	.008	.009	.015
CA	.000	.000	.000	.012	.004	.004	.008	.006
K	.000	.021	.040	.019	.007	.007	.005	.013
NA	.000	.000	.000	.011	.000	.007	.000	.000
O	28.000	28.000	28.000	28.000	28.000	28.000	28.000	28.000
F/M	.021	.017	.020	.028	.020	.019	.026	.026
F/M	.021	.017	.020	.027	.019	.019	.026	.026

9 **** BL-09-31 486340 IM0857

10 **** BL-09-31 486350 DARKER

11 **** BL-09-31 486387 INST TO CHROMITE C-1 IM0B19

12 **** BT-08-10 486020 INST TO CHROMITE C-1

13 ADJ INST

14 OPPOSITE SIDE

15 ANOTHER INST

16 WITHIN FRACTURE ZONE W FABRIC 0579

TABLE 3: CHLORITE, BLACK LABEL-BLACK THOR, J LAARMAN, JULY 2013 R.L.B.

	17	18	19	20	21	22	23	24
STO2	29.63	32.82	31.09	33.04	33.25	31.81	32.19	32.01
TIO2	.00	.05	.02	.00	.02	.02	.00	.00
A2O3	15.10	16.44	16.71	14.33	14.63	15.62	13.70	15.11
C2O3	2.44	1.18	1.81	1.82	.80	1.34	3.13	3.29
FEO	1.23	1.62	1.44	1.43	1.54	1.49	1.38	1.61
MGO	35.19	36.79	34.95	36.24	36.02	37.16	36.07	35.25
MNO	.06	.06	.06	.09	.08	.08	.06	.09
CAO	.03	.01	.07	.00	.02	.01	.02	.02
K2O	.06	.03	.02	.00	.00	.00	.00	.00
NA2O	.03	.14	.00	.14	.22	.05	.00	.00
SUM	83.77	89.14	86.17	87.09	86.58	87.58	86.55	87.38
SI	5.823	6.022	5.908	6.209	6.264	5.953	6.119	6.031
AL	.177	.000	.092	.000	.000	.047	.000	.000
AL	3.319	3.555	3.650	3.173	3.248	3.398	3.069	3.354
TI	.000	.007	.003	.000	.003	.003	.000	.000
CR	.379	.171	.272	.270	.119	.198	.470	.490
FE	.202	.249	.229	.225	.243	.233	.219	.254
MG	10.307	10.062	9.900	10.151	10.114	10.365	10.219	9.898
MN	.010	.009	.010	.014	.013	.013	.010	.014
CA	.006	.002	.014	.000	.004	.002	.004	.004
K	.015	.007	.005	.000	.000	.000	.000	.000
NA	.011	.033	.000	.051	.080	.018	.000	.000
O	28.000	28.000	28.000	28.000	28.000	28.000	28.000	28.000
F/M	.021	.026	.024	.024	.025	.024	.022	.027
F/FM	.020	.025	.024	.023	.025	.023	.022	.026

17 WITHIN FRACTURE ZONE W FABRIC 0579
 18 *** BT-08-10 486021 INST TO CHROMITE, C-1
 19 ADJ REGION
 20 ANOTHER INST
 21 ANOTHER INST CHLORITE
 22 ANOTHER INST CHLORITE
 23 WITHIN LINEAR ZONE OF FAILURE 0574
 24 ADJ LINEAR

TABLE 3: CHLORITE, BLACK LABEL-BLACK THOR, J LAARMAN, JULY 2013 R.L.B.

	25	26	27	28	29	30	31	32
STO2	32.65	31.11	30.50	31.03	32.53	30.65	29.55	30.52
TIO2	.00	.00	.02	.00	.05	.01	.00	.02
A2O3	14.25	17.65	18.12	18.34	16.23	17.31	18.98	20.41
C2O3	1.97	2.82	2.62	2.40	1.80	2.91	2.67	2.46
FEO	1.60	1.54	1.53	1.44	1.64	1.60	1.69	1.55
MGO	36.39	35.31	35.21	35.52	36.46	34.61	34.28	34.74
MNO	.06	.02	.04	.04	.04	.10	.11	.10
CAO	.03	.00	.02	.01	.02	.01	.03	.03
K2O	.01	.00	.01	.00	.00	.01	.00	.03
NA2O	.02	.00	.03	.00	.00	.00	.00	.01
SUM	86.98	88.45	88.10	88.78	88.77	87.21	87.31	89.87
SI	6.155	5.780	5.692	5.734	6.003	5.783	5.573	5.574
AL	.000	.220	.308	.266	.000	.217	.427	.426
AL	3.166	3.644	3.677	3.727	3.529	3.632	3.791	3.967
TI	.000	.000	.003	.000	.007	.001	.000	.003
CR	.294	.414	.387	.351	.263	.434	.398	.355
FE	.252	.239	.239	.223	.253	.252	.267	.237
MG	10.226	9.778	9.795	9.783	10.028	9.733	9.637	9.458
MN	.010	.003	.006	.006	.006	.016	.018	.015
CA	.006	.000	.004	.002	.004	.002	.006	.006
K	.002	.000	.002	.000	.000	.002	.000	.007
NA	.007	.016	.011	.000	.000	.000	.000	.004
O	28.000	28.000	28.000	28.000	28.000	28.000	28.000	28.000
F/M	.026	.025	.025	.023	.026	.028	.029	.027
F/FM	.025	.024	.024	.023	.025	.027	.029	.026

25 INST AWAY FROM BRITTLE ZONE

26 *** BT-08-10 486022 INST TO CHROMITITE, UNZONED

27 INST TO CHROMITITE, UNZONED

28 INST TO CHROMITE, NO APPARENT ALT

29 INT ASSOC W BRIGHT RIMS ON CHROMITE

30 ADJ GRAIN ALONG

31 ADJ INST RECRYST CHL

32 ADJ TO AN INST REG IN CROM ALT

TABLE 3: CHLORITE, BLACK LABEL-BLACK THOR, J LAARMAN, JULY 2013 R.L.B.

	41	42	43	44	45	46	47	48
STO2	34.17	29.38	28.86	29.88	31.20	31.15	31.42	29.95
TIO2	.00	.01	.00	.01	.00	.00	.00	.03
A2O3	12.51	20.30	20.30	20.64	15.53	15.42	14.92	20.48
C2O3	1.47	2.61	2.33	2.63	3.66	4.37	3.57	2.08
FEO	1.31	1.71	1.69	1.69	1.44	1.64	2.00	1.39
MGO	37.37	33.39	34.29	34.71	34.70	34.77	34.58	34.61
MNO	.00	.06	.02	.12	.12	.05	.09	.07
K2O	.00	.04	.03	.04	.05	.04	.03	.01
CAO	.00	.02	.03	.01	.04	.05	.02	.07
NA2O	.02	.01	.00	.00	.00	.02	.01	.01
SUM	86.85	87.53	87.55	89.73	86.74	87.51	86.64	88.70
SI	6.420	5.518	5.424	5.479	5.930	5.890	5.993	5.535
AL	.000	.482	.576	.521	.070	.110	.007	.465
AL	2.770	4.011	3.921	3.939	3.409	3.326	3.346	3.996
TI	.000	.001	.000	.001	.000	.000	.000	.004
CR	.218	.388	.346	.381	.550	.653	.538	.304
FE	.206	.269	.266	.259	.229	.259	.319	.215
MG	10.466	9.347	9.607	9.487	9.831	9.799	9.831	9.534
NN	.000	.010	.003	.019	.019	.008	.015	.011
CA	.000	.008	.006	.008	.010	.008	.006	.002
K	.000	.005	.007	.002	.010	.012	.005	.017
NA	.007	.004	.000	.000	.000	.007	.004	.004
O	28.000	28.000	28.000	28.000	28.000	28.000	28.000	28.000
F/M	.020	.030	.028	.029	.025	.027	.034	.024
F/FM	.019	.029	.027	.028	.025	.027	.033	.023

41 ANOTHER

42 *** 486034 C-1 INCL IN OUTER ZONE

43 C-1 INCL IN OUTER ZONE

44 ANOTHER INCL

45 ANOTHER INCL

46 ADJ HIGHLY ALT INST

47 ADJ HIGHLY ALT INST

48 INT W CC

TABLE 3: CHLORITE, BLACK LABEL-BLACK THOR, J LAARMAN, JULY 2013 R.L.B.

	49	50	51	52	53	54	55	56
STO2	29.35	29.83	31.38	30.55	32.96	34.40	33.44	30.70
TIO2	.00	.00	.07	.00	.00	.00	.03	.00
A2O3	20.61	20.01	14.87	18.65	12.46	11.98	12.91	15.32
C2O3	2.29	2.55	1.60	2.92	2.02	.47	.75	3.25
FEO	1.27	1.19	1.09	1.52	1.36	1.33	1.42	1.66
MGO	34.13	33.44	35.35	34.62	36.74	37.55	36.74	34.21
MNO	.06	.10	.08	.10	.00	.00	.00	.03
CAO	.04	.01	.04	.04	.00	.00	.01	.06
K2O	.01	.00	.06	.01	.00	.00	.04	.00
NA2O	.02	.00	.02	.01	.00	.00	.09	.00
SUM	87.78	87.13	84.53	88.42	85.54	85.73	85.43	85.23
SI	5.482	5.606	6.068	5.682	6.310	6.525	6.382	5.936
AL	.518	.394	.000	.318	.000	.000	.000	.064
AL	4.018	4.037	3.388	3.769	2.811	2.678	2.903	3.427
TI	.000	.000	.010	.000	.000	.000	.004	.000
CR	.338	.379	.245	.429	.306	.070	.113	.497
FE	.198	.187	.176	.236	.218	.211	.227	.268
MG	9.502	9.366	10.189	9.597	10.485	10.616	10.451	9.859
MN	.009	.016	.013	.016	.000	.000	.000	.005
CA	.008	.002	.002	.008	.000	.000	.002	.012
K	.002	.000	.015	.002	.000	.000	.010	.000
NA	.007	.018	.007	.004	.000	.000	.033	.000
O	28.000	28.000	28.000	28.000	28.000	28.000	28.000	28.000
F/M	.022	.022	.019	.026	.021	.020	.022	.028
F/FM	.021	.021	.018	.026	.020	.019	.021	.027

49 INT W CC
50 C INST TO CHROMITITE
51 MATRIX OPP, MARGIN
52 INCL IN CHROMITE
53 *** BT-08-10 486040
54 CHL W SERP
55 CHL W SERP
56 *** BT-08-10 486044 INST TO CHROMITITE

TABLE 3: CHLORITE, BLACK LABEL-BLACK THOR, J LAARMAN, JULY 2013 R.L.B.

	57	58	59	60	61	62	63	64
STO2	29.79	33.37	34.59	32.27	33.49	32.53	32.09	34.17
TIO2	.00	.00	.00	.00	.00	.01	.02	.01
A2O3	12.43	13.17	13.47	15.70	12.88	12.27	16.38	13.16
C2O3	4.16	1.92	1.70	3.08	4.25	4.66	2.50	4.07
FEO	1.65	1.33	1.24	1.46	1.73	1.74	1.42	1.91
MGO	33.36	35.82	36.49	34.60	35.43	34.43	34.30	35.44
MNO	.07	.07	.07	.06	.08	.06	.06	.10
CAO	.10	.02	.04	.02	.03	.00	.02	.05
K2O	.00	.00	.00	.00	.00	.00	.00	.00
NA2O	.00	.00	.04	.00	.02	.01	.00	.01
SUM	81.56	85.70	87.64	87.19	87.91	85.71	86.79	88.92
SI	6.055	6.361	6.432	6.072	6.286	6.276	6.050	6.335
AL	.000	.000	.000	.000	.000	.000	.000	.000
AL	2.977	2.958	2.951	3.481	2.849	2.789	3.639	2.875
TI	.000	.000	.000	.000	.000	.001	.003	.001
CR	.668	.289	.250	.458	.631	.711	.373	.597
FE	.280	.212	.193	.230	.272	.281	.224	.296
MG	10.106	10.177	10.113	9.703	9.913	9.901	9.638	9.794
MN	.012	.011	.011	.010	.013	.010	.010	.016
CA	.022	.004	.008	.004	.006	.000	.004	.010
K	.000	.000	.000	.000	.000	.000	.000	.000
NA	.000	.000	.014	.000	.007	.004	.000	.004
O	28.000	28.000	28.000	28.000	28.000	28.000	28.000	28.000
F/M	.029	.022	.020	.025	.029	.029	.024	.032
F/FM	.028	.021	.020	.024	.028	.029	.024	.031

57 INST TO CHROMITITE

58 REL DARK DOMAIN

59 REL DARK DOMAIN

60 BRIGHT DOMAIN

61 ANOTHER INST

62 ANOTHER INST

63 DARK

64 BRIGHTER

TABLE 3: CHLORITE, BLACK LABEL-BLACK THOR, J LAARMAN, JULY 2013 R.L.B.

	73	74	75	76	77	78	79	80
STO2	33.29	30.82	30.05	33.23	33.87	34.26	33.17	34.11
TIO2	.04	.04	.04	.00	.00	.01	.00	.00
A2O3	14.92	19.01	18.53	13.93	13.55	11.49	12.23	13.12
C2O3	4.43	3.22	3.76	3.45	4.87	5.35	5.02	4.34
FEO	1.34	1.56	1.62	2.00	1.17	1.05	1.16	1.23
MGO	35.00	33.68	33.34	34.83	36.23	35.44	34.96	35.78
MNO	.06	.10	.04	.09	.11	.13	.08	.11
CAO	.01	.00	.01	.03	.02	.05	.02	.03
K2O	.00	.00	.00	.00	.00	.00	.00	.03
NA2O	.00	.00	.00	.00	.01	.00	.03	.01
SUM	89.09	88.43	87.39	87.56	89.83	87.78	86.67	88.76
SI	6.148	5.726	5.667	6.250	6.216	6.435	6.313	6.322
AL	.000	.274	.333	.000	.000	.000	.000	.000
AL	3.247	3.887	3.785	3.087	2.930	2.543	2.743	2.865
TI	.006	.006	.006	.000	.000	.001	.000	.000
CR	.647	.473	.561	.513	.707	.795	.755	.636
FE	.207	.242	.255	.315	.180	.165	.185	.191
MG	9.634	9.326	9.371	9.764	9.910	9.922	9.918	9.884
MN	.009	.016	.006	.014	.017	.021	.013	.017
CA	.002	.000	.002	.006	.004	.010	.004	.006
K	.000	.000	.000	.000	.000	.000	.000	.007
NA	.000	.000	.000	.000	.004	.000	.011	.004
O	28.000	28.000	28.000	28.000	28.000	28.000	28.000	28.000
F/M	.022	.028	.028	.034	.020	.019	.020	.021
F/M	.022	.027	.027	.033	.019	.018	.020	.021

73 INCL ANOTHER CHROMITE
74 IN DOMAIN FERRICHRONITE
75 ANOTHER INCL
76 ADJ GDMASS
77 *** BT-08-10 486129 INST
78 INST
79 ANOTHER INST
80 INST TO POROUS

TABLE 3: CHLORITE, BLACK LABEL-BLACK THOR, J LAARMAN, JULY 2013 R.L.B.

	81	82	83	84	85	86	87	88
STO2	32.59	30.19	34.04	34.38	34.19	34.12	32.84	33.62
TIO2	.00	.02	.03	.00	.00	.05	.00	.00
A2O3	13.28	19.10	13.34	11.15	11.36	11.88	12.53	12.83
C2O3	6.10	4.19	4.41	6.64	6.41	6.04	4.92	4.98
FEO	1.34	1.65	1.05	1.10	.97	1.12	.98	1.08
MGO	34.58	33.08	36.25	35.42	36.56	35.43	34.85	35.46
MNO	.10	.06	.13	.07	.05	.06	.05	.06
CAO	.03	.02	.01	.03	.02	.05	.03	.02
K2O	.00	.01	.00	.05	.00	.00	.00	.00
NA2O	.01	.01	.03	.02	.01	.04	.00	.01
SUM	88.03	88.33	89.29	88.86	89.57	88.79	86.20	88.06
SI	6.137	5.638	6.270	6.409	6.321	6.353	6.276	6.290
AL	.000	.362	.000	.000	.000	.000	.000	.000
AL	2.947	3.842	2.896	2.449	2.475	2.607	2.822	2.828
TI	.000	.003	.004	.000	.000	.007	.000	.000
CR	.908	.619	.642	.979	.937	.889	.743	.737
FE	.211	.258	.162	.171	.150	.174	.157	.169
MG	9.706	9.208	9.953	9.841	10.075	9.833	9.927	9.888
MN	.016	13.788	.020	13.452	.008	13.520	.008	13.631
CA	.006	.004	.002	.006	.004	.010	.006	.004
K	.000	.002	.000	.012	.000	.000	.000	.000
NA	.004	.010	.011	.013	.004	.014	.000	.004
O	28.000	28.000	28.000	28.000	28.000	28.000	28.000	28.000
F/M	.023	.029	.018	.019	.016	.019	.017	.018
F/FM	.023	.028	.018	.018	.015	.018	.016	.018

81 SMALL INCL IN CHROMITE

82 SMALL INCL IN CHROMITE

83 C INST

84 WIDE VEINLET

85 WIDE VEINLET

86 ALONG VEINLET

87 IN ADJ INT

88 IN ADJ INT

TABLE 3: CHLORITE, BLACK LABEL-BLACK THOR, J LAARMAN, JULY 2013 R.L.B.

STO2	105	106	107	108	109	110	111	112
TIO2	32.34	31.72	32.38	32.23	31.97	31.48	32.19	33.08
A2O3	.00	.01	.00	.00	.02	.00	.00	.00
C2O3	14.58	12.66	15.27	11.43	10.70	10.33	14.98	14.57
FEO	.34	3.53	.08	6.07	7.17	5.68	.30	.08
MGO	1.04	1.13	1.16	1.00	1.18	1.19	1.12	1.22
MNO	36.73	35.47	36.48	35.66	35.45	35.41	35.97	36.55
CAO	.00	.00	.00	.00	.00	.00	.00	.00
K2O	.00	.00	.00	.00	.00	.00	.00	.00
NA2O	.00	.00	.05	.00	.00	.00	.00	.00
SUM	85.03	84.52	85.42	86.39	86.49	84.09	84.56	85.50
SI	6.182	* 6.175	* 6.157	* 6.187	* 6.164	* 6.219	* 6.183	* 6.279
AL	.000	6.182	.000	6.157	.000	6.164	.000	6.183
AL	3.284	* 2.904	* 3.422	* 2.586	* 2.431	* 2.405	* 3.391	* 3.259
TI	.000	* .001	* .000	* .000	* .003	* .000	* .000	* .000
CR	.051	* .543	* .012	* .921	* 1.093	* .887	* .046	* .012
FE	.166	* .184	* .184	* .161	* .190	* .197	* .180	* .194
MG	10.465	* 10.291	* 10.340	* 10.203	* 10.188	* 10.427	* 10.298	* 10.341
NN	.000	13.967	.000	13.958	.000	13.871	.000	13.914
CA	.000	* .000	* .000	* .000	* .000	* .000	* .000	* .000
K	.000	* .000	* .000	* .000	* .000	* .000	* .000	* .000
NA	.000	.000	.018	.018	.000	.000	.000	.000
O	28.000	* 28.000	* 28.000	* 28.000	* 28.000	* 28.000	* 28.000	* 28.000
F/M	.016	.018	.018	.016	.019	.019	.017	.019
F/FM	.016	.018	.018	.015	.018	.019	.017	.018

105 *** BT-08-10 486133 CHLORITE

106 CHL GRAINS ACROSS SAMPLE

107 CHL GRAINS ACROSS SAMPLE

108 CHL GRAINS ACROSS SAMPLE

109 CHL GRAINS ACROSS SAMPLE

110 CHL GRAINS ACROSS SAMPLE

111 CHL GRAINS ACROSS SAMPLE

112 CHL GRAINS ACROSS SAMPLE

TABLE 3: CHLORITE, BLACK LABEL-BLACK THOR, J LAARMAN, JULY 2013 R.L.B.

	121	122	123	124	125
STO2	29.58	28.47	29.52	29.06	29.32
TIO2	.01	.00	.01	.02	.00
A2O3	15.26	16.86	15.18	17.79	18.46
C2O3	9.29	7.10	9.91	5.79	6.56
FEO	1.07	1.06	1.24	1.05	1.39
MGO	33.62	32.63	32.93	33.84	33.28
MNO	.12	.10	.16	.08	.10
CAO	.01	.03	.02	.03	.05
K2O	.02	.00	.00	.01	.00
NA2O	.00	.00	.00	.00	.00
SUM	88.98	86.25	88.97	87.67	89.16
SI	5.585 *	5.505 *	5.588 *	5.502 *	5.474 *
AL	.415 6.000	.495 6.000	.412 6.000	.498 6.000	.526 6.000
AL	2.980 *	3.346 *	2.974 *	3.470 *	3.536 *
TI	.001 *	.000 *	.001 *	.003 *	.000 *
CR	1.387 *	1.085 *	1.483 *	.867 *	.968 *
FE	.169 *	.171 *	.196 *	.166 *	.217 *
MG	9.461 *	9.404 *	9.291 *	9.549 *	9.262 *
NN	.019 14.017	.016 14.023	.026 13.970	.013 14.068	.016 13.999
CA	.002 *	.006 *	.004 *	.006 *	.010 *
K	.005 *	.000 *	.000 *	.002 *	.000 *
NA	.000 .007	.000 .006	.000 .004	.000 .009	.000 .010
O	28.000 *	28.000 *	28.000 *	28.000 *	28.000 *
F/M	.020	.020	.024	.019	.025
F/FM	.019	.020	.023	.018	.025
121 BRIGHT INST					
122 ADJ DARKER					
123 ADJ BRIGHT AGAIN					
124 INTST W AMPH					
125 INT W ZONED AMPH, IM0005					

APPENDIX 5

Chromite Mineral Chemistry data -
BT-09-31
BT-08-10
BT-09-17
FW-08-19

Black Label BT-09-31

	SiO2	TiO2	Al2O3	Cr2O3	Fe2O3	FeO	MnO	MgO	ZnO	NiO	TOTAL
1 CHR **** SAMPLE 170	0.01	1	15.33	43.5	6.96	26.97	0.59	4.67	0.26	0.13	99.43
2 CHR BRIGHT OUTER RIND SPOT 3	0.04	1.43	2.54	35.32	27.97	29.82	0.53	1.55	0.27	0.1	99.57
3 CHR SPOT 7	0.03	0.83	15.27	39.35	10.78	26.18	0.37	4.8	0.35	0.14	98.10
4 CHR SPOT 1, 01-09-3833	0	0.91	15.56	42.41	7.07	26.56	0.4	4.84	0.27	0	98.02
5 CHR SPOT 1 AGAIN	0	0.88	15.67	42.48	7.15	26.38	0.55	4.94	0.16	0.04	98.25
6 CHR **** SAMPLE 171 REL L CENTRAL, SPOT 1, 0	0.01	0.99	15.91	42.78	7.53	28.03	0.41	4.36	0.27	0.1	100.39
7 CHR NEAR MARGIN SPOT 2	0.03	0.88	15.42	43.37	7.29	28.44	0.56	3.85	0.22	0.02	100.08
8 CHR L CENTRAL SPOT 3	0	0.96	15.9	43.45	6.37	27.89	0.45	4.35	0.24	0.03	99.64
9 CHR AT MARGIN SPOT 4	0.07	1.07	14.99	43.44	7.28	27.99	0.6	3.98	0.29	0.01	99.72
10 CHR W CIRC SERP SPOT 5	0	2.54	14.69	41.67	5.98	29.63	0.57	3.76	0.24	0.19	99.27
11 CHR SMALLER SPOT 5	0	0.87	14.74	42.85	7.92	28.52	0.52	3.67	0.21	0	99.29
12 CHR BRIGHT MARGIN SPOT 6	0.45	1.94	4.57	36.9	24.71	28.41	1.28	1.72	0.26	0.12	100.36
13 CHR AGAIN	0.1	2.03	4.09	37.32	23.06	30.53	0.59	1.47	0.21	0.15	99.55
14 CHR SURR CIRC SERP SPOT 7	0	1.06	15.59	42.98	7.34	28.90	0.62	3.86	0.12	0	100.46
15 CHR SURR CIRC SERP SPOT 7	0	0.97	15.57	43.1	7.17	28.43	0.5	3.9	0.38	0.1	100.12
16 CHR W CIRC INCL SERP, SPOT 7	0	0.89	15.76	43.24	7.35	28.52	0.48	4.04	0.23	0.04	100.56
17 CHR W CIRC INCL SERP, SPOT 7	0	0.93	15.09	43.51	7.33	28.24	0.59	3.97	0.25	0.04	99.95
18 CHR **** SAMPLE 172 L CENTRAL, SPOT 1, 01-10	0	0.84	17.35	42.66	6.33	27.42	0.44	4.82	0.28	0.05	100.18
19 CHR AT MARGIN SPOT 2	0.03	0.81	17.46	41.29	6.32	27.56	0.45	4.4	0.11	0.02	98.45
20 CHR AT MARGIN SPOT 2	0.04	0.81	17.32	42.28	6.27	27.72	0.51	4.35	0.33	0	99.63
21 CHR ANOTHER GRAIN SPOT 3	0	0.9	16.97	42.25	7.17	27.48	0.5	4.73	0.27	0.12	100.40
22 CHR W CIRC INCL SERP AFTER OLIV? SPOT 4	0.01	0.9	17.63	42.06	6.79	27.66	0.57	4.76	0.15	0.08	100.61
23 CHR W CIRC INCL SERP AFTER OLIV? SPOT 4	0.03	0.8	16.11	42.34	6.74	26.81	0.53	4.51	0.22	0.12	98.20
24 CHR SMALLER SPOT 5	0	0.87	16.39	42.39	7.62	27.96	0.54	4.33	0.24	0.15	100.49
25 CHR ANOTHER SPOT 6	0	0.86	16.45	44.01	5.74	27.87	0.41	4.5	0.18	0.06	100.09
26 CHR ANOTHER CENTRAL, SPOT 7	0.03	0.81	12.59	42.91	11.84	29.09	0.64	3.21	0.37	0.01	101.51
27 CHR ANOTHER CENTRAL, SPOT 7	0.02	0.72	12.99	41.94	10.98	28.81	0.46	3.18	0.14	0.05	99.29
28 CHR BRIGHT MARGINAL ZONE, SPOT 8	0.21	2.14	3.52	37.71	24.41	30.28	0.71	1.58	0.22	0.13	100.90
29 CHR **** SAMPLE 173 W CIRC SERP, SPOT 1, 01-	0.04	0.58	13.24	43.16	10.80	28.48	0.54	3.39	0.3	0.11	100.64
30 CHR W CIRC SERP, SPOT 1, 01-10-3839	0.04	0.62	12.45	42.27	11.69	28.54	0.46	3.17	0.22	0.09	99.55
31 CHR ANOTHER DEARK CENTRAL, SPOT 2	0	0.68	12.17	43.05	11.83	28.97	0.63	3.16	0.17	0.08	100.74
32 CHR ANOTHER DEARK CENTRAL, SPOT 2	0.04	0.69	11.35	42.87	11.87	28.48	0.67	3.04	0	0.08	99.09
33 CHR ANOTHER CENTRAL, SPOT 4	0.03	0.69	12.68	43.78	10.22	28.21	0.65	3.36	0.39	0.13	100.14
34 CHR ANOTHER SPOT 5	0.01	0.57	12.55	43.13	11.37	28.54	0.62	3.29	0.2	0.12	100.40
35 CHR ANOTHER SPOT 6	0	0.62	13.02	43.46	11.00	28.66	0.64	3.49	0.16	0.11	101.16
36 CHR ANOTHER SPOT 6	0.01	0.6	12.7	42.54	10.93	28.06	0.61	3.28	0.39	0.14	99.26
37 SAMPLE 173 DARK CENTRAL SPOT 1 PIC 577	0.00	0.85	15.33	42.71	7.63	27.70	0.14	4.38	0.21	0.12	99.07
38 BRIGHT MARGIN SPOT 2 PIC 577	0.01	1.22	2.78	38.49	25.02	30.54	0.19	1.55	0.01	0.06	99.87
39 DARK CENTRAL SPOT 3 PIC 577	0.00	0.56	14.32	43.11	9.26	28.83	0.14	3.69	0.06	0.04	100.02
40 BRIGHT MARGIN SPOT 4 PIC 577	0.00	1.34	1.59	33.15	31.27	31.29	0.16	0.99	0.00	0.05	99.84
41 DARK CENTRAL SPOT 1 PIC 578	0.00	0.48	13.90	42.24	10.58	27.98	0.21	3.75	0.42	0.15	99.71
42 BRIGHT MARGIN SPOT 2 PIC 578	0.11	1.80	1.00	32.11	32.39	30.63	0.16	1.25	0.07	0.09	99.60
43 DARK CENTRAL SPOT 1 PIC 579	0.00	0.77	15.41	43.18	7.75	28.83	0.25	3.88	0.16	0.00	100.24
44 BRIGHT SPOT 2 PIC 579	0.00	1.42	3.16	36.84	25.36	30.61	0.20	1.41	0.29	0.03	99.32
45 RANDOM GRAIN DARK CENTRAL	0.00	0.64	13.30	42.79	10.41	28.58	0.20	3.67	0.00	0.11	99.70
46 RANDOM GRAIN BRIGHT MARGIN	0.00	1.61	1.41	32.47	31.36	31.08	0.28	1.03	0.00	0.15	99.39
47 CHR **** SAMPLE 174 L GRAIN CENTRAL, SPOT 1	0	0.98	15.25	42.18	8.30	27.86	0.54	4.21	0.26	0.04	99.62
48 CHR SPOT 1 CENTRAL AGAIN	0.01	1	15.33	43.5	6.96	26.97	0.59	4.67	0.26	0.13	99.43
49 CHR NEAR MARGIN SPOT 2	0.04	0.82	15.35	42.29	8.51	27.41	0.6	4.34	0.16	0.02	99.54
50 CHR NARROW BRIGHT MARGIN SPOT 3	0.04	1.43	2.54	35.32	27.97	29.82	0.53	1.55	0.27	0.1	99.57
51 CHR ANOTHER CENTRAL SPOT 3	0	0.8	14.8	43.28	8.04	27.06	0.43	4.57	0.21	0.12	99.32
52 CHR BRIGHT MARGIN SPOT 5	0.06	0.34	17.66	37	12.40	27.26	0.6	4.36	0.18	0.04	99.90
53 CHR BRIGHT MARGIN INCL MG-CHL, SPOT 6	0.04	1.11	4.47	34.41	26.83	29.40	0.52	1.68	0.21	0.19	98.87
54 CHR V BRIGHT INST	0.07	1.24	4.54	36.83	24.39	29.19	0.58	1.89	0.17	0.19	99.09
55 CHR V BRIGHT INST	0.12	1.19	4.6	37.15	24.63	29.18	0.65	1.93	0.07	0.12	99.64
56 CHR ANOTHER CENTRAL, SPOT 7	0	0.85	15.19	42.25	8.58	27.00	0.47	4.7	0.09	0.14	99.27
57 CHR ANOTHER CENTRAL SPOT 8	0.01	0.78	15.44	41.98	9.06	27.22	0.42	4.63	0.26	0.03	99.83
58 CHR **** SAMPLE 174 L CENTRAL, SPOT 1, 01-10	0.02	0.87	15.18	43.54	7.76	27.57	0.5	4.44	0.16	0.11	100.15
59 CHR AT MARGIN SPOT 2	0.08	0.57	13.59	43.13	11.36	27.81	0.59	3.91	0.31	0.07	101.42
60 CHR AT MARGIN SPOT 2	0.07	0.48	13.9	42.16	11.94	27.77	0.63	3.87	0.32	0.04	101.18
61 CHR ANOTHER SPOT 3	0.02	0.78	13.9	42.84	9.80	28.28	0.44	3.8	0.18	0.11	100.14
62 CHR ANOTHER CENTRAL, SPOT 4	0	0.85	13.76	43.96	8.29	27.70	0.66	4.05	0.14	0.03	99.44
63 CHR ANOTHER SPOT 5	0.05	0.9	14.46	43.68	8.76	28.26	0.59	3.86	0.28	0.18	101.02
64 CHR ANOTHER SPOT 5	0	0.86	14.1	44.35	7.76	28.06	0.51	4.01	0.17	0.07	99.89
65 CHR ANOTHER CENTRAL, SPOT 6	0.04	0.88	15.34	43.39	7.80	27.63	0.62	4.32	0.22	0.07	100.31
66 CHR AT MARGIN SPOT 7	0.02	1.02	13.13	42.61	10.16	27.98	0.54	3.83	0.26	0.13	99.68
67 CHR BRIGHT MARGIN SPOT 8	0.13	1.9	2.58	32.72	30.50	30.36	0.55	1.47	0.18	0.11	100.50
68 SAMPLE 174 DARK CENTRAL SPOT 1 PIC 581	0.00	0.49	13.92	43.82	9.25	28.42	0.10	3.84	0.15	0.07	100.06
69 INT DOMAIN SPOT 2 PIC 581	0.00	0.71	14.09	42.59	9.69	28.73	0.07	3.77	0.18	0.02	99.85
70 ANOTHER DARK DOMAIN SPOT 3 PIC 581	0.00	0.43	13.78	43.63	10.21	28.99	0.18	3.66	0.00	0.00	100.88
71 BRIGHT MARGIN SPOT 4 PIC 581	0.00	1.38	3.30	32.17	30.12	30.73	0.19	1.43	0.07	0.04	99.43
72 DARK DOMAIN SPOT 1 PIC 582	0.00	0.41	13.20	42.15	11.51	28.66	0.20	3.46	0.07	0.05	99.71
73 BRIGHT MARGIN SPOT 2 PIC 582	0.00	1.45	2.60	34.49	29.47	31.21	0.16	1.40	0.04	0.10	100.92
74 DARK CENTRAL SPOT 1 PIC 583	0.00	0.72	15.56	44.24	6.91	27.79	0.13	4.51	0.31	0.05	100.22
75 BRIGHT MARGIN SPOT 2 PIC 583	0.00	0.91	6.05	42.65	18.41	29.82	0.09	2.33	0.25	0.06	100.57
76 DARK CENTRAL SPOT 3 PIC 583	0.00	0.62	15.70	46.03	4.66	28.48	0.09	4.11	0.15	0.00	99.85
77 BRIGHT MARGIN SPOT 4 PIC 583	0.03	1.05	6.10	37.90	22.24	29.85	0.23	2.12	0.04	0.07	99.64
78 DARK CENTRAL SPOT 1 PIC 584	0.00	0.66	16.11	42.62	8.24	28.31	0.24	4.18	0.44	0.00	100.81

Black Label BT-09-31

	SiO2	TiO2	Al2O3	Cr2O3	Fe2O3	FeO	MnO	MgO	ZnO	NiO	TOTAL
79 BRIGHT MARGIN SPOT 2 PIC 584	0.01	1.27	3.83	38.33	24.07	30.68	0.24	1.59	0.14	0.00	100.16
80 DARK CENTRAL SPOT 3 PIC 584	0.01	0.66	15.64	43.38	7.98	28.39	0.24	4.06	0.34	0.09	100.79
81 BRIGHT MARGIN SPOT 4 PIC 584	0.00	1.11	5.30	39.89	20.83	30.78	0.18	1.67	0.02	0.00	99.79
82 DARK CORE SPOT 5 PIC 584	0.00	0.73	14.50	43.24	8.71	28.40	0.14	3.98	0.22	0.06	99.98
83 BRIGHT MARGIN SPOT 6 PIC 584	0.01	1.08	3.82	39.62	22.99	30.40	0.13	1.66	0.17	0.02	99.90
84 DARK CENTRAL SPOT 7 PIC 584	0.00	0.57	16.06	45.16	5.23	28.60	0.06	4.03	0.12	0.09	99.92
85 BRIGHT MARGIN SPOT 8 PIC 584	0.00	1.03	4.38	40.79	21.61	30.13	0.18	1.93	0.09	0.12	100.25
86 DARK CENTRAL SPOT 9 PIC 584	0.00	0.56	15.09	44.38	7.61	28.11	0.13	4.21	0.34	0.00	100.42
87 BRIGHT MARGIN SPOT 10 PIC 584	0.00	1.08	4.19	39.69	22.68	30.21	0.21	1.84	0.00	0.16	100.06
88 CHR **** SAMPLE 175 CENTRAL, SPOT 1, 01-10-3	0	0.68	15.21	43.18	9.43	26.80	0.59	5	0.17	0.14	101.20
89 CHR SPOT 1, 01-10-3843	0.04	0.74	14.33	42.95	9.16	26.44	0.57	4.81	0.01	0.06	99.12
90 CHR AT MARGIN SPOT 2	0.04	0.67	14.48	42.99	9.76	26.67	0.71	4.69	0.13	0.07	100.21
91 CHR ANOTHER SPOT 3	0.03	0.65	13.8	43.44	9.69	26.70	0.55	4.56	0.2	0.09	99.71
92 CHR BRIGHT MARGIN SPOT 4	0.06	2.3	3.48	37.76	24.18	30.31	0.75	2.03	0.24	0.13	101.24
93 CHR BRIGHT MARGIN SPOT 4	0.03	2.48	3.11	37.55	22.82	30.22	0.59	1.9	0.27	0.09	99.05
94 CHR ANOTHER SPOT 5	0.09	0.81	15.18	43.45	8.99	26.29	0.59	5.14	0.11	0.17	100.82
95 CHR ANOTHER SPOT 5	0	0.8	14.76	43.29	8.38	26.41	0.55	5	0.12	0.09	99.40
96 CHR ANOTHER SPOT 6	0.03	0.65	14.26	43.39	9.63	27.12	0.53	4.58	0.11	0	100.29
97 CHR ANOTHER SPOT 6	0.01	0.61	14.06	44.38	9.03	27.18	0.51	4.54	0.15	0.08	100.55
98 CHR ANOTHER SPOT 6	0.04	0.66	13.9	43.03	9.78	26.96	0.56	4.34	0.2	0.1	99.57
99 CHR SMALLER SPOT 7	0.03	0.53	13.83	44.49	9.38	27.55	0.43	4.29	0.18	0.02	100.73
100 CHR SMALLER SPOT 7	0.07	0.55	12.58	43.57	10.71	26.81	0.54	4.18	0.09	0.05	99.15
101 SAMPLE 175 UNZONED SPOT 1 PIC 585	0.02	0.50	15.87	45.15	6.55	26.55	0.17	5.25	0.19	0.03	100.28
102 UNZONED SPOT 2 PIC 585	0.00	0.68	16.07	45.34	5.28	26.79	0.21	5.25	0.00	0.00	99.62
103 DARK CENTER SPOT 3 PIC 585	0.00	0.34	15.09	44.26	8.47	27.16	0.17	4.77	0.07	0.09	100.42
104 BRIGHT MARGIN SPOT 4 PIC 585	0.22	1.36	4.84	34.98	26.51	28.76	0.27	2.32	0.00	0.10	99.36
105 DARK CENTRAL SPOT 1 PIC 586	0.00	0.35	14.23	42.66	11.24	27.75	0.20	4.41	0.00	0.07	100.91
106 BRIGHT MARGIN SPOT 2 PIC 586	0.00	1.93	2.77	29.49	32.97	30.85	0.15	1.66	0.11	0.14	100.07
107 DARK CENTRAL SPOT 3 PIC 586	0.00	0.62	16.49	42.81	7.18	27.20	0.06	4.85	0.31	0.02	99.55
108 BRIGHT MARGIN SPOT 4 PIC 586	0.00	1.78	2.68	33.14	29.27	30.59	0.21	1.70	0.00	0.09	99.46
109 DARK CENTRAL SPOT 5 PIC 586	0.00	0.55	15.50	42.97	8.88	27.43	0.18	4.79	0.00	0.07	100.37
110 BRIGHT MARGIN SPOT 6 PIC 586	0.01	1.60	3.95	33.69	28.15	30.48	0.18	1.94	0.10	0.00	100.10
111 DARK CENTER SPOT 7 PIC 586	0.00	0.49	15.09	43.11	9.65	26.94	0.21	4.92	0.32	0.03	100.76
112 BRIGHT MARGIN SPOT 8 PIC 586	0.00	1.75	3.14	31.49	30.85	30.47	0.13	1.84	0.21	0.06	99.94
113 DARK CORE SPOT 10 PIC 586	0.00	0.55	14.88	42.50	9.92	27.68	0.13	4.55	0.12	0.00	100.32
114 BRIGHT EDGE SPOT 11 PIC 586	0.03	1.56	3.13	36.64	25.50	30.29	0.27	1.70	0.03	0.04	99.19
115 DARK CENTER SPOT 12 PIC 586	0.00	0.72	15.49	43.45	7.94	27.67	0.08	4.75	0.07	0.04	100.22
116 BRIGHT EDGE SPOT 13 PIC 586	0.00	1.58	3.38	36.56	25.23	30.32	0.16	1.76	0.18	0.08	99.25
117 DARK CENTRAL SPOT 14 PIC 586	0.00	0.30	14.66	42.48	10.24	27.74	0.20	4.16	0.16	0.06	99.99
118 BRIGHT MARGIN SPOT 15 PIC 586	0.04	1.61	3.16	32.53	29.71	30.42	0.15	1.71	0.06	0.00	99.40
119 SAMPLE 176 DARK SPOT SPOT 1 PIC 589	0.00	0.44	14.99	42.21	9.42	28.05	0.08	4.15	0.00	0.02	99.35
120 DARK CENTER SPOT 2 PIC 589	0.00	0.59	16.01	41.82	9.46	27.66	0.18	4.67	0.17	0.05	100.61
121 INT SPOT SPOT 3 PIC 589	0.00	0.56	16.43	42.48	7.58	28.44	0.08	4.03	0.34	0.07	100.01
122 IN BRIGHT AREA SPOT 4 PIC 589	0.00	1.05	5.63	43.94	17.49	29.74	0.16	2.58	0.00	0.00	100.59
123 BRIGHT AREA SPOT 5 PIC 589	0.00	1.68	3.08	30.79	31.42	30.32	0.14	1.83	0.00	0.17	99.43
124 DARK DOMAIN SPOT 1 PIC 588	0.00	0.78	16.09	43.23	7.88	26.96	0.16	5.22	0.21	0.11	100.65
125 DARK DOMAIN SPOT 2 PIC 588	0.00	0.28	15.90	43.03	9.21	27.13	0.23	4.90	0.11	0.00	100.78
126 DARK DOMAIN SPOT 3 PIC 588	0.00	0.58	14.94	43.10	8.75	26.94	0.22	4.83	0.03	0.09	99.48
127 DARK DOMAIN SPOT 4 PIC 588	0.00	0.46	13.96	41.92	11.50	27.72	0.11	4.15	0.42	0.05	100.29
128 DARK DOMAIN SPOT 5 PIC 588	0.00	0.57	6.78	45.16	15.29	28.18	0.26	3.12	0.03	0.00	99.39
129 DARK DOMAIN SPOT 6 PIC 588	0.00	1.45	2.84	38.09	24.83	29.45	0.22	2.24	0.00	0.13	99.25
130 BRIGHT MARGIN SPOT 7 PIC 588	0.00	1.62	2.54	38.64	24.61	30.08	0.23	2.07	0.00	0.04	99.82
131 RANDOM GRAIN UNZONED	0.00	0.60	15.22	42.40	9.35	26.38	0.20	5.20	0.15	0.07	99.57
132 DARK CENTRAL SPOT 1 PIC 590	0.00	0.58	15.58	42.60	8.86	26.88	0.12	5.03	0.15	0.05	99.85
133 BRIGHT MARGIN SPOT 2 PIC 590	0.03	1.09	2.43	30.10	34.70	29.88	0.18	1.78	0.06	0.08	100.33
134 DARK CORE SPOT 3 PIC 590	0.01	0.76	14.70	43.67	8.49	26.70	0.16	5.11	0.11	0.07	99.78
135 BRIGHT RIND SPOT 4 PIC 590	0.00	1.44	4.63	38.65	22.49	29.38	0.21	2.57	0.08	0.00	99.44
136 RANDOM DARK CORE	0.00	0.82	15.61	43.33	7.65	26.77	0.20	5.10	0.35	0.03	99.86
137 SAMPLE 177 UNZONED RANDOM DARK	0.00	1.02	16.56	42.96	8.02	24.98	0.15	6.70	0.38	0.01	100.77
138 RANDOM DARK CORE	0.00	0.96	16.09	42.71	7.85	25.05	0.24	6.34	0.13	0.08	99.45
139 DARK DOMAIN SPOT 1 PIC 591	0.00	1.02	16.23	42.44	8.10	26.56	0.12	5.63	0.22	0.07	100.38
140 BRIGHT MARGIN SPOT 2 PIC 591	0.01	3.27	6.00	37.79	19.03	31.79	0.20	2.34	0.28	0.08	100.80
141 DARK CORE SPOT 3 PIC 591	0.00	0.83	14.86	43.37	8.99	25.89	0.15	5.72	0.28	0.02	100.11
142 BRIGHT MARGIN SPOT 4 PIC 591	0.00	2.41	6.65	39.99	17.20	30.02	0.24	2.99	0.04	0.04	99.58
143 DARK CENTRAL SPOT 5 PIC 591	0.03	0.81	14.37	43.21	9.00	25.96	0.18	5.39	0.19	0.00	99.14
144 BRIGHT MARGIN SPOT 6 PIC 591	0.00	2.83	6.84	39.33	16.43	30.62	0.23	2.80	0.00	0.05	99.14
145 DARK CENTRAL SPOT 7 PIC 591	0.00	0.88	16.05	43.31	7.55	26.32	0.23	5.68	0.09	0.00	100.12
146 BRIGHT MARGIN SPOT 8 PIC 591	0.00	2.43	6.75	39.61	18.13	29.82	0.17	3.32	0.11	0.00	100.34
147 DARK CENTRAL SPOT 9 PIC 591	0.00	0.98	14.45	44.22	7.89	25.63	0.17	5.86	0.05	0.11	99.36
148 BRIGHT MARGIN SPOT 10 PIC 591	0.00	2.29	7.62	40.01	16.87	30.38	0.21	3.03	0.00	0.00	100.41
149 DARK CENTRAL SPOT 11 PIC 591	0.00	0.90	14.48	43.79	9.05	26.14	0.23	5.69	0.00	0.08	100.37
150 BRIGHT MARGIN SPOT 12 PIC 591	0.01	3.01	5.52	38.31	19.67	29.67	0.29	3.44	0.03	0.10	100.05
151 DARK CENTRAL SPOT 13 PIC 591	0.00	0.74	14.41	43.94	8.74	26.43	0.15	5.39	0.00	0.00	99.79
152 BRIGHT MARGIN SPOT 14 PIC 591	0.00	3.14	7.01	39.83	16.00	30.53	0.22	3.29	0.00	0.00	100.02
153 DARK ZONE INT W PENT SPOT 1 PIC 592	0.00	0.94	14.72	42.76	9.60	26.30	0.07	5.65	0.09	0.07	100.20
154 DARK ZONE SPOT 2 PIC 592	0.00	1.01	13.73	43.10	9.70	26.21	0.12	5.42	0.26	0.00	99.55
155 BRIGHT MARGIN SPOT 3 PIC 592	0.00	3.74	4.99	35.50	21.56	30.96	0.24	2.95	0.27	0.03	100.24
156 DARK DOMAIN SPOT 4 PIC 592	0.00	1.09	17.40	36.37	12.69	26.72	0.19	5.50	0.30	0.14	100.40
157 SAMPLE 178 DARK DOMAIN SPOT 1 PIC 593	0.00	0.59	16.81	44.33	7.08	23.56	0.25	7.36	0.13	0.00	100.11

Black Label BT-09-31

	SiO2	TiO2	Al2O3	Cr2O3	Fe2O3	FeO	MnO	MgO	ZnO	NiO	TOTAL
158 BRIGHT MARGIN SPOT 2 PIC 593	0.03	1.84	7.45	44.56	13.84	28.18	0.26	3.87	0.17	0.22	100.43
159 DARK CENTER SPOT 3 PIC 593	0.00	0.56	15.78	45.15	7.02	22.76	0.14	7.54	0.21	0.10	99.26
160 BRIGHT MARGIN SPOT 4 PIC 593	0.00	2.14	7.46	43.02	14.14	28.95	0.26	3.68	0.04	0.00	99.69
161 DARK CENTRAL SPOT 5 PIC 593	0.00	0.73	16.85	44.22	7.35	24.04	0.13	7.42	0.00	0.00	100.74
162 BRIGHT MARGIN SPOT 6 PIC 593	0.06	1.77	8.45	44.29	12.36	27.94	0.21	3.99	0.09	0.00	99.16
163 DARKEST DOMAIN SPOT 1 PIC 594	0.12	0.40	17.92	45.84	5.08	24.65	0.20	6.63	0.02	0.04	100.90
164 INT DOMAIN SPOT 2 PIC 594	0.00	0.53	17.13	45.00	5.89	24.20	0.09	7.06	0.06	0.02	99.98
165 BRIGHT MARGIN SPOT 3 PIC 594	0.01	1.81	6.92	44.33	14.95	27.92	0.24	4.23	0.00	0.06	100.48
166 DARK DOMAIN SPOT 1	0.00	0.82	17.91	44.72	5.47	24.66	0.12	7.24	0.01	0.00	100.95
167 BRIGHT MARGIN SPOT 2	0.00	0.90	8.27	47.17	12.48	26.73	0.20	4.58	0.30	0.00	100.63
168 RANDOM UNZONED GRAIN	0.00	0.66	16.95	45.33	5.53	24.05	0.10	7.14	0.06	0.12	99.94
169 ANOTHER RANDOM UNZONED GRAIN	0.00	0.51	17.41	44.27	6.20	24.68	0.17	6.65	0.13	0.08	100.10
170 ANOTHER RANDOM UNZONED GRAIN	0.01	0.79	17.65	44.51	6.00	24.11	0.16	7.30	0.30	0.00	100.83
171 RANDOM DARK CORE	0.00	0.56	18.12	43.92	6.35	24.76	0.12	6.92	0.20	0.00	100.96
172 RANDOM BRIGHT MARGIN	0.00	2.63	8.17	40.53	15.29	29.33	0.17	3.84	0.00	0.18	100.14
173 CHR **** SAMPLE 179 L CENTRAL, SPOT 1, 01-10	0.03	0.87	17.12	44.01	6.95	25.40	0.61	6.28	0.19	0.04	101.50
174 CHR CENTRAL, SPOT 1, 01-10-3844	0.07	0.84	16.67	43.26	7.02	25.26	0.45	6.03	0.07	0	99.67
175 CHR CIRC SERP INCL, SPOT 1, 01-10-3844	0.02	0.95	17.16	43.31	7.08	25.26	0.49	6.34	0.26	0.08	100.95
176 CHR AT MARGIN SPOT 2	0.03	0.98	16.11	42.5	8.10	26.03	0.5	5.6	0.15	0.06	100.06
177 CHR ANOTHER SPOT 3	0	0.82	15.75	43.57	6.97	25.85	0.53	5.48	0.15	0.02	99.14
178 CHR AT MARGIN SPOT 4	0	0.94	15.87	43.99	6.26	26.00	0.67	5.42	0.06	0.1	99.31
179 CHR ANOTHER SPOT 5	0	0.92	16.33	44.65	5.55	25.62	0.47	5.89	0.04	0.14	99.61
180 CHR AT MARGIN SPOT 6	0	0.92	16.14	43.77	6.36	26.05	0.53	5.48	0.14	0.11	99.50
181 CHR ENCL CIRC SERP, SPOT 7	0	0.76	15.72	44.8	5.77	25.79	0.59	5.44	0.06	0.08	99.01
182 CHR ANOTHER SPOT 8	0	0.69	14.12	47.52	5.99	26.09	0.63	5.25	0.27	0.02	100.58
183 CHR ANOTHER SPOT 8	0	0.64	13.96	47.98	5.12	26.05	0.56	5.2	0	0.09	99.60
184 CHR **** SAMPLE 180 L CENTRAL, SPOT 1, 01-10	0	0.89	16.18	43.3	7.63	25.93	0.47	5.78	0.13	0.08	100.39
185 CHR L CENTRAL, SPOT 1, 01-10-3845	0	0.85	15.98	43.44	7.15	26.01	0.51	5.48	0.26	0.02	99.70
186 CHR AT MARGIN SPOT 2	0	0.96	15.72	43.81	7.69	26.44	0.64	5.47	0.05	0.1	100.88
187 CHR AT MARGIN SPOT 2	0	0.98	15.81	44.43	6.82	26.55	0.49	5.4	0.19	0.14	100.81
188 CHR AT MARGIN SPOT 2	0.03	1	15.13	44.28	7.10	26.24	0.53	5.33	0.16	0.02	99.82
189 CHR SURR CIRC SERP, SPOT 3	0.01	0.98	15.64	44.07	7.30	26.16	0.58	5.52	0.21	0.08	100.55
190 CHR ANOTHER CENTRAL, SPOT 4	0	0.96	16.06	44.47	6.64	25.93	0.66	5.75	0.12	0.1	100.68
191 CHR ANOTHER CENTRAL, SPOT 4	0	0.99	15.59	43.97	6.99	25.94	0.49	5.62	0.21	0.06	99.86
192 CHR AT MARGIN SPOT 5	0	0.96	16.07	44.3	6.96	26.39	0.58	5.61	0.11	0.05	101.03
193 CHR AT MARGIN SPOT 5	0	0.96	16.06	43.92	6.69	26.09	0.57	5.65	0.08	0.01	100.03
194 CHR SMALL SPOT 6	0.01	0.9	14.85	44.63	8.16	26.93	0.62	5.07	0.19	0.04	101.40
195 CHR SMALL SPOT 6	0	0.98	13.8	44.04	7.34	26.44	0.62	4.72	0.03	0.1	98.08
196 CHR SMALL SPOT 6	0	0.93	15.06	45.13	5.98	26.81	0.44	5.04	0.05	0.02	99.46
197 CHR SMALL SPOT 7	0	0.91	14.73	44.24	7.34	26.26	0.52	5.19	0.22	0	99.40
198 CHR **** SAMPLE 181 SPOT 1, 01-11-3846	0	1.04	16.4	42.93	7.12	26.98	0.62	5.14	0.11	0.06	100.40
199 CHR SPOT 1, 01-11-3846	0	0.95	16.31	44.08	6.50	27.13	0.56	5.05	0.21	0.08	100.87
200 CHR SPOT 1 01-11-3846	0	0.97	15.6	44.06	5.70	27.08	0.65	4.58	0.14	0.1	98.88
201 CHR AT MARGIN SPOT 2	0.02	0.96	14.87	44.55	6.78	28.29	0.49	4.05	0.24	0	100.25
202 CHR ANOTHER CENTRAL, SPOT 3	0.02	0.95	16.2	43.46	6.30	27.73	0.52	4.44	0.13	0.12	99.87
203 CHR AT MARGIN SPOT 4	0	0.97	14.44	44.49	7.28	28.28	0.62	3.99	0.23	0	100.30
204 CHR SMALLER SPOT 5	0	0.93	15.11	44.57	6.88	28.28	0.6	4.1	0.3	0.03	100.80
205 CHR SMALLER SPOT 5	0	0.93	15	44.63	6.42	28.42	0.5	4	0.11	0.08	100.09
206 CHR ENCL CIRC SERP, SPOT 6	0	0.89	16.36	43.81	5.71	27.49	0.53	4.65	0.01	0.09	99.54
207 CHR ANOTHER CENTRAL, SPOT 7	0	0.92	16.32	43.98	6.17	27.72	0.64	4.6	0.16	0.01	100.53
208 CHR ANOTHER CENTRAL, SPOT 7	0.01	0.96	15.81	43.14	5.92	27.14	0.56	4.43	0.3	0.01	98.27
209 CHR ANOTHER CENTRAL, SPOT 7	0.05	0.91	16.26	43.82	5.82	27.06	0.53	4.69	0.24	0.02	99.39
210 SAMPLE 182 DARK DOMAIN SPOT 1	0.00	0.54	15.07	41.25	11.01	26.32	0.17	5.25	0.22	0.00	99.83
211 DARK DOMAIN, SPOT 1, PIC 596	0.01	0.54	14.20	41.36	11.16	27.64	0.19	4.22	0.10	0.06	99.48
212 BRIGHT MARGIN, SPOT 2 PIC 596	0.01	1.96	2.92	35.14	26.54	30.49	0.31	1.76	0.12	0.04	99.30
213 DARK CENTRAL, SPOT 3 PIC 596	0.00	0.58	14.38	39.55	12.94	28.40	0.11	3.82	0.38	0.04	100.20
214 BRIGHT MARGIN, SPOT 4 PIC 596	0.00	1.96	2.56	34.31	28.08	31.37	0.12	1.39	0.09	0.14	100.02
215 DARK CENTRAL, SPOT 1 PIC 597	0.00	0.55	13.09	41.07	12.74	27.76	0.17	4.11	0.06	0.05	99.61
216 BRIGHT MARGIN, SPOT 2 PIC 597	0.00	1.77	2.88	34.57	28.12	31.02	0.17	1.69	0.00	0.00	100.23
217 DARK CORE, SPOT 3 PIC 597	0.03	0.28	14.10	42.38	10.55	27.65	0.14	3.99	0.19	0.00	99.32
218 BRIGHT MARGIN, SPOT 4 PIC 597	0.01	1.52	2.99	39.09	23.64	30.39	0.19	1.81	0.10	0.01	99.76
219 RANDOM DARK CENTRAL	0.04	0.62	14.11	42.83	10.04	26.50	0.15	4.83	0.36	0.05	99.52
220 RANDOM BRIGHT MARGIN	0.02	1.97	2.27	33.80	29.01	30.70	0.10	1.81	0.01	0.04	99.74
221 ANOTHER RANDOM DARK CENTRAL	0.01	0.59	13.78	42.15	10.45	27.84	0.14	3.99	0.24	0.05	99.24
222 ANOTHER RANDOM DARK CENTRAL	0.00	0.67	15.17	41.42	10.12	27.68	0.14	4.50	0.15	0.05	99.90
223 ANOTHER RANDOM DARK CENTRAL	0.00	0.66	14.76	41.40	10.47	27.53	0.24	4.51	0.00	0.06	99.63
224 SAMPLE 183 RANDOM DARK CENTRAL	0.00	0.55	15.00	42.18	9.42	28.77	0.16	3.75	0.13	0.00	99.96
225 RANDOM BRIGHT MARGIN	0.06	1.64	2.51	34.99	28.26	30.47	0.16	1.67	0.09	0.00	99.85
226 DARK CENTRAL SPOT 1 PIC 598	0.00	0.59	15.16	41.44	9.88	27.97	0.13	4.13	0.21	0.13	99.64
227 BRIGHT MARGIN SPOT 2 PIC 598	0.02	1.25	1.03	31.39	33.88	30.48	0.14	1.22	0.07	0.11	99.58
228 DARK CENTER SPOT 3 PIC 598	0.05	0.61	13.58	42.07	10.65	27.88	0.03	3.92	0.21	0.02	99.03
229 BRIGHT MARGIN SPOT 4 PIC 598	0.00	1.77	2.09	30.22	33.70	31.56	0.19	1.32	0.00	0.00	100.84
230 DARK CENTER SPOT 5 PIC 598	0.00	0.55	14.99	41.78	9.71	28.95	0.11	3.54	0.19	0.13	99.95
231 BRIGHT MARGIN SPOT 6 PIC 598	0.00	1.49	2.36	31.61	31.68	30.84	0.14	1.39	0.07	0.02	99.60
232 DARK CENTRAL SPOT 7 PIC 598	0.00	0.38	13.48	41.81	11.71	28.94	0.19	3.19	0.42	0.03	100.14
233 BRIGHT MARGIN SPOT 8 PIC 598	0.02	1.11	1.93	32.14	33.06	30.32	0.19	1.42	0.26	0.06	100.51
234 DARK CORE SPOT 9 PIC 598	0.00	0.50	14.70	40.93	10.83	28.50	0.18	3.80	0.00	0.02	99.46
235 BRIGHT MARGIN SPOT 10 PIC 598	0.00	0.88	8.21	39.44	19.15	30.17	0.13	2.30	0.26	0.00	100.54
236 DARK CENTER SPOT 11 PIC 598	0.00	0.16	9.69	44.97	12.76	28.39	0.15	3.02	0.21	0.00	99.35

Black Label BT-09-31

	SiO2	TiO2	Al2O3	Cr2O3	Fe2O3	FeO	MnO	MgO	ZnO	NiO	TOTAL
237 BRIGHT MARGIN SPOT 12 PIC 598	0.01	1.46	4.32	34.62	26.79	30.61	0.16	1.81	0.02	0.03	99.83
238 DARK CENTER SPOT 13 PIC 598	0.03	0.69	15.25	41.74	9.69	27.89	0.15	4.24	0.25	0.12	100.05
239 BRIGHT MARGIN SPOT 14 PIC 598	0.01	1.51	3.21	32.26	30.20	31.00	0.14	1.47	0.00	0.00	99.80
240 SAMPLE 184 DARK CENTRAL SPOT 1 PIC 599	0.00	0.64	15.16	40.79	10.59	26.21	0.27	5.09	0.36	0.00	99.11
241 BRIGHT MARGIN SPOT 2 PIC 599	0.00	1.29	3.42	32.26	30.72	30.37	0.19	1.73	0.12	0.05	100.15
242 DARK CENTRAL SPOT 3 PIC 599	0.02	0.58	15.11	41.09	10.25	28.15	0.16	4.05	0.09	0.02	99.52
243 BRIGHT MARGIN SPOT 4 PIC 599	0.01	1.21	5.02	32.54	29.60	30.01	0.14	2.31	0.08	0.03	100.94
244 DARK CORE SPOT 5 PIC 599	0.00	0.44	15.46	40.41	10.50	27.81	0.21	4.11	0.09	0.09	99.12
245 BRIGHT MARGIN SPOT 6 PIC 599	0.00	1.49	3.31	32.15	30.16	30.43	0.09	1.76	0.14	0.00	99.53
246 DARK CENTRAL SPOT 7 PIC 599	0.00	0.66	15.61	42.24	8.98	27.93	0.14	4.43	0.20	0.05	100.24
247 BRIGHT MARGIN SPOT 8 PIC 599	0.00	1.68	3.38	32.11	29.69	30.97	0.12	1.60	0.00	0.00	99.55
248 DARK CENTER SPOT 9 PIC 599	0.00	0.62	15.62	40.52	11.40	27.05	0.23	5.00	0.24	0.00	100.68
249 BRIGHT MARGIN SPOT 10 PIC 599	0.00	1.02	6.00	37.79	22.31	29.20	0.24	2.39	0.20	0.09	99.23
250 DARK CENTER SPOT 1 PIC 600	0.01	0.37	14.08	40.92	12.45	28.05	0.22	3.93	0.23	0.00	100.26
251 BRIGHT MARGIN SPOT 2 PIC 600	0.00	1.56	4.18	34.00	27.94	30.60	0.22	1.88	0.25	0.00	100.63
252 DARK CENTER SPOT 3 PIC 600	0.00	0.41	8.68	45.31	13.18	29.11	0.11	2.67	0.25	0.00	99.72
253 BRIGHT W CHL SPOT 4 PIC 600	0.00	1.76	3.25	37.85	24.84	31.13	0.21	1.78	0.00	0.01	100.83
254 CHR **** SAMPLE 185 L CENTRAL, SPOT 1, 01-11	0.02	0.82	15.09	43.97	6.61	26.93	0.61	4.43	0.22	0.14	98.83
255 CHR CENTRAL, SPOT 1, 01-11-3847	0	0.68	15.14	43.92	6.57	26.75	0.51	4.41	0.39	0.14	98.52
256 CHR CENTRAL, SPOT 1, 01-11-3847	0	0.66	16.11	44.03	7.08	27.01	0.56	4.81	0.36	0.07	100.69
257 CHR CENTRAL, SPOT 1, 01-11-3847	0.03	0.78	15.82	43.72	6.62	26.88	0.71	4.59	0.21	0.09	99.44
258 CHR AT MARGIN SPOT 2	0	0.62	14.09	43.22	8.36	27.10	0.63	4.03	0.22	0.12	98.40
259 CHR AT MARGIN SPOT 2	0.05	0.56	15.03	42.24	8.49	26.91	0.53	4.18	0.28	0	98.27
260 CHR AT MARGIN SPOT 2	0.05	0.67	15.13	42.18	9.01	27.10	0.46	4.37	0.17	0.12	99.26
261 CHR ANOTHER CENTRAL, SPOT 3	0	0.83	17.12	43.47	5.15	25.43	0.5	5.73	0.23	0.07	98.53
262 CHR ANOTHER CENTRAL, SPOT 3	0	0.76	17.24	43.89	5.16	25.58	0.54	5.69	0.26	0.09	99.21
263 CHR AT MARGIN SPOT 4	0	0.84	17.02	43.96	4.83	26.80	0.44	5.03	0.22	0.05	99.19
264 CHR SMALLER SPOT 6	0	0.75	17.43	42.38	6.45	26.66	0.53	5.07	0.34	0.03	99.64
265 CHR SMALLER SPOT 6	0.04	0.88	17.23	44.28	4.69	26.34	0.41	5.4	0.17	0.04	99.48
266 CHR V SMALL CENTRAL, SPOT 7	0.04	0.57	14.57	41.68	11.04	27.76	0.54	4.08	0.14	0.07	100.50
267 CHR BRIGHT M W CHL INCL, SPOT 8	0.04	1.94	3.38	36.81	25.33	30.20	0.77	1.76	0.32	0.08	100.64
268 CHR **** SAMPLE 186 L CENTRAL, SPOT 1, 01-11	0	0.83	14.39	43.36	8.30	28.41	0.56	3.71	0.18	0.12	99.86
269 CHR AT MARGIN SPOT 2	0.05	0.76	13.96	42.11	10.34	28.45	0.57	3.41	0.37	0.09	100.12
270 CHR BRIGHT MARGIN SPOT 3'	0.08	1.57	2.88	37.08	26.13	30.28	0.53	1.42	0.32	0.13	100.43
271 CHR ANOTHER SPOT 4	0.02	0.77	14.33	43.06	8.63	27.70	0.68	3.81	0.33	0.16	99.48
272 CHR SMALLER SPOT 6	0	0.67	12.89	43.97	8.43	28.21	0.6	3.26	0.17	0.09	98.28
273 CHR SMALLER SPOT 6	0.01	0.63	14.25	43.1	9.13	28.01	0.52	3.78	0.32	0.05	99.80
274 CHR ANOTHER SPOT 7 CENTRAL	0	0.7	13.66	42.3	10.53	28.32	0.59	3.59	0.31	0.03	100.03
275 CHR SMALLER SPOT 8	0.02	0.54	13.65	43.04	9.98	28.43	0.57	3.37	0.36	0	99.96
276 CHR **** SAMPLE 187 L CENTRAL, SPOT 1, 01-11	0	0.73	15.43	47.36	4.19	23.34	0.44	7.04	0.1	0.04	98.67
277 CHR L CENTRAL, SPOT 1, 01-11-3850	0.04	0.74	15.28	48.02	4.10	23.10	0.55	7.12	0.11	0	99.06
278 CHR AT MARGIN SPOT 2	0	0.71	16.13	46.5	4.96	24.74	0.53	6.47	0.05	0	100.10
279 CHR SMALLER SPOT 3	0	0.73	16.22	46.88	5.45	23.98	0.45	7.23	0	0.03	100.98
280 CHR SMALLER SPOT 3	0	0.78	15.95	46.02	4.42	23.77	0.55	6.72	0.08	0.01	98.29
281 CHR SMALLER SPOT 3	0	0.69	16.23	46.85	5.01	23.63	0.48	7.21	0.03	0.08	100.21
282 CHR ANOTHER CENTRAL, SPOT 4	0	0.71	16.03	47.33	4.31	24.12	0.56	6.76	0.05	0.1	99.97
283 CHR AT MARGIN SPOT 5	0	0.85	16.26	45.45	6.40	24.92	0.59	6.51	0.19	0.06	101.23
284 CHR AT MARGIN SPOT 5	0.06	0.69	15.71	45.33	5.88	24.60	0.57	6.07	0.11	0	99.03
285 CHR ANOTHER CENTRAL, SPOT 6	0.01	0.77	15.73	46.1	5.09	24.28	0.5	6.55	0.05	0	99.08
286 CHR AT MARGIN SPOT 7	0	0.69	16.35	46.73	5.30	25.01	0.47	6.55	0	0.07	101.17
287 CHR AT MARGIN SPOT 7	0	0.66	15.9	45.29	4.94	24.36	0.57	6.11	0.12	0.09	98.04
288 CHR AT MARGIN SPOT 7	0	0.7	16	45.09	5.05	24.44	0.47	6.21	0.14	0.01	98.12
289 CHR AT MARGIN SPOT 7	0	0.68	16.23	45.68	5.87	24.54	0.46	6.6	0.14	0	100.20
290 CHR SMALLER SPOT 8	0	0.73	16.3	45.13	5.20	24.50	0.5	6.38	0.05	0.05	98.84
291 SAMPLE 188 UNZONED SPOT 2 PIC 602	0.00	0.44	14.10	50.09	4.56	24.98	0.19	6.23	0.06	0.13	100.79
292 UNZONED SPOT 3 PIC 602	0.00	0.51	14.15	49.87	3.93	24.99	0.19	6.06	0.15	0.12	99.97
293 UNZONED SPOT 4 PIC 602	0.00	0.59	14.31	49.94	4.13	25.33	0.21	6.12	0.18	0.00	100.81
294 UNZONED SPOT 5 PIC 602	0.00	0.46	14.48	50.04	3.93	25.49	0.13	5.93	0.28	0.01	100.75
295 UNZONED SPOT 6 PIC 602	0.00	0.58	14.63	49.67	3.34	24.79	0.15	6.26	0.24	0.02	99.68
296 DARK DOMAIN SPOT 7 PIC 602	0.00	0.49	14.15	49.89	3.49	24.86	0.17	6.07	0.17	0.00	99.29
297 BRIGHT DOMAIN SPOT 8 PIC 602	0.03	0.81	4.93	52.08	10.56	26.87	0.20	3.91	0.13	0.00	99.52
298 UNZONED DARK SPOT 9 PIC 602	0.00	0.53	14.05	50.10	4.35	25.58	0.21	5.97	0.00	0.06	100.85
299 UNZONED DARK SPOT 10 PIC 602	0.00	0.51	14.09	50.52	3.50	25.17	0.08	6.07	0.26	0.00	100.20
300 UNZONED DARK SPOT 11 PIC 602	0.00	0.43	14.12	50.52	3.34	24.98	0.18	6.14	0.00	0.00	99.70
301 SAMPLE 189 UNZONED DARK SPOT 1 PIC 604	0.00	0.77	17.28	46.90	3.85	24.35	0.09	7.27	0.03	0.04	100.58
302 UNZONED DARK SPOT 2 PIC 604	0.00	0.75	17.12	45.77	5.44	23.70	0.14	7.61	0.00	0.09	100.62
303 UNZONED DARK SPOT 3 PIC 604	0.00	0.61	16.45	46.36	5.19	23.78	0.20	7.27	0.00	0.00	99.86
304 UNZONED DARK SPOT 5,6 PIC 604	0.00	0.74	17.30	46.33	4.03	24.31	0.19	7.09	0.10	0.00	100.09
305 UNZONED DARK SPOT 7 PIC 604	0.00	0.65	18.01	46.44	3.81	23.49	0.14	7.74	0.05	0.05	100.38
306 UNZONED DARK SPOT 8 PIC 604	0.00	0.59	17.30	46.38	4.65	23.69	0.11	7.43	0.25	0.00	100.40
307 UNZONED DARK SPOT 9 PIC 604	0.00	0.69	17.67	46.45	3.99	24.66	0.16	7.07	0.02	0.00	100.71
308 UNZONED DARK SPOT 10 PIC 604	0.00	0.44	17.30	46.24	4.96	24.16	0.21	7.02	0.13	0.07	100.53
309 UNZONED DARK SPOT 11 PIC 604	0.00	0.82	17.18	46.44	3.95	24.53	0.08	6.99	0.20	0.06	100.26
310 SAMPLE 190 UNZONED DARK SPOT 1 PIC 605	0.00	0.50	16.48	48.67	2.49	23.92	0.08	7.06	0.00	0.06	99.26
311 UNZONED DARK SPOT 2 PIC 605	0.00	0.84	16.60	47.45	3.79	24.28	0.22	7.20	0.00	0.00	100.38
312 UNZONED DARK SPOT 3 PIC 605	0.00	0.64	16.96	47.36	3.24	24.10	0.13	7.04	0.04	0.14	99.64
313 UNZONED DARK SPOT 4 PIC 605	0.00	0.77	16.30	48.06	3.76	23.90	0.15	7.31	0.00	0.21	100.46
314 UNZONED DARK SPOT 5 PIC 605	0.00	0.76	17.09	47.93	3.28	24.28	0.11	7.32	0.00	0.10	100.87
315 DARK ZONE SPOT 6 PIC 605	0.00	0.65	17.02	46.66	4.11	24.04	0.16	7.15	0.00	0.12	99.91

Black Label BT-09-31

	SiO2	TiO2	Al2O3	Cr2O3	Fe2O3	FeO	MnO	MgO	ZnO	NiO	TOTAL
316 BRIGHT MARGIN SPOT 7 PIC 605	0.02	1.21	9.89	48.23	8.97	27.43	0.20	4.57	0.10	0.02	100.64
317 UNZONED SPOT 8 PIC 605	0.00	0.90	17.41	46.18	3.58	23.99	0.16	7.39	0.00	0.00	99.61
318 UNZONED SPOT 9 PIC 605	0.00	0.79	17.24	47.41	2.79	24.06	0.20	7.13	0.23	0.06	99.91
319 UNZONED SPOT 10 PIC 605	0.00	0.81	17.51	47.74	2.54	24.46	0.06	7.28	0.01	0.00	100.40
320 CHR **** SAMPLE 191 ANOTHER SPOT 2	0	0.7	14.95	45.81	5.90	23.15	0.45	6.87	0.26	0.02	98.11
321 SAMPLE 194 DARKEST SPOT SPOT 1 PIC 606	0.01	0.66	16.58	46.93	3.25	23.37	0.12	7.28	0.00	0.00	98.21
322 INT DOMAIN SPOT 2 PIC 606	0.00	0.66	16.79	46.63	4.02	23.25	0.00	7.57	0.14	0.00	99.06
323 BRIGHT DOMAIN SPOT 3 PIC 606	0.00	0.56	15.91	47.40	5.00	22.59	0.14	7.83	0.20	0.01	99.64
324 BRIGHT DOMAIN SPOT 3 PIC 606	0.01	0.64	15.58	47.33	6.19	21.76	0.15	8.51	0.16	0.02	100.35
325 DARK DOMAIN SPOT 4 PIC 606	0.00	0.71	15.16	47.07	5.74	22.35	0.18	8.00	0.00	0.00	99.20
326 BRIGHT DOMAIN SPOT 5 PIC 606	0.75	0.87	6.47	52.37	10.38	24.74	0.15	3.88	0.00	0.16	99.77
327 UNZONED SPOT 6 PIC 606	0.00	0.70	16.72	46.48	4.97	22.82	0.17	7.89	0.21	0.01	99.97
328 DARK SPOTS SPOT 7 PIC 606	0.00	0.62	15.83	46.72	5.71	22.76	0.06	7.78	0.27	0.00	99.75
329 MAIN GRAIN SPOT 8 PIC 606	0.00	0.70	16.31	46.92	5.51	22.75	0.24	7.98	0.22	0.00	100.63
330 MAIN GRAIN SPOT 9 PIC 606	0.00	0.73	15.38	46.29	6.59	22.80	0.11	7.82	0.16	0.00	99.88
331 MAIN GRAIN SPOT 10 PIC 606	0.00	0.62	16.49	46.49	5.24	22.70	0.15	7.83	0.16	0.12	99.79
332 MAIN GRAIN SPOT 11 PIC 606	0.00	0.54	16.48	47.22	4.28	22.65	0.15	7.77	0.20	0.00	99.29
333 MAIN GRAIN SPOT 12 PIC 606	0.00	0.56	16.33	47.30	5.17	23.54	0.15	7.57	0.02	0.00	100.64
334 MAIN GRAIN SPOT 13 PIC 606	0.00	0.69	15.03	47.20	6.07	22.28	0.16	8.07	0.02	0.03	99.55
335 MAIN GRAIN SPOT 14 PIC 606	0.00	0.60	16.60	46.49	5.37	23.03	0.14	7.80	0.11	0.00	100.14
336 RANDOM GRAIN	0.00	0.66	16.38	47.26	4.75	22.34	0.15	8.23	0.04	0.01	99.82
337 RANDOM GRAIN	0.01	0.58	16.74	47.03	4.39	21.97	0.24	8.15	0.16	0.12	99.39
338 SAMPLE 195 UNZONED GRAIN SPOT 1 PIC 607	0.00	0.83	17.04	47.05	3.63	24.00	0.08	7.41	0.00	0.09	100.13
339 UNZONED GRAIN SPOT 2 PIC 607	0.00	0.70	16.84	47.13	4.45	23.24	0.07	7.79	0.22	0.01	100.46
340 UNZONED GRAIN SPOT 3 PIC 607	0.00	0.80	16.76	47.10	4.23	23.26	0.17	7.83	0.03	0.00	100.18
341 UNZONED GRAIN SPOT 4 PIC 607	0.00	0.86	16.05	47.98	3.16	23.63	0.20	7.25	0.22	0.01	99.36
342 UNZONED GRAIN SPOT 5 PIC 607	0.00	0.77	15.65	47.59	5.46	23.09	0.17	7.90	0.00	0.02	100.65
343 DARK ZONE SPOT 6 PIC 607	0.00	0.60	16.18	47.91	4.59	23.33	0.20	7.54	0.25	0.00	100.60
344 BRIGHT MARGIN SPOT 7 PIC 607	0.00	1.01	9.61	51.88	4.30	28.98	0.17	3.31	0.00	0.00	99.26
345 UNZONED GRAIN SPOT 8 PIC 607	0.00	0.60	16.85	46.80	4.53	23.30	0.12	7.57	0.20	0.02	99.99
346 UNZONED GRAIN SPOT 9 PIC 607	0.00	0.86	16.76	47.34	3.32	23.74	0.12	7.50	0.00	0.00	99.64
347 UNZONED GRAIN SPOT 10 PIC 607	0.00	0.70	16.88	47.13	4.64	23.51	0.12	7.79	0.00	0.00	100.77
348 UNZONED GRAIN SPOT 11 PIC 607	0.00	0.61	16.99	47.09	4.57	23.55	0.22	7.56	0.15	0.00	100.75
349 UNZONED GRAIN SPOT 12 PIC 607	0.00	0.59	16.84	48.29	3.60	23.72	0.16	7.46	0.18	0.04	100.88
350 UNZONED GRAIN SPOT 13 PIC 607	0.00	0.66	17.00	47.36	3.87	23.06	0.09	7.82	0.23	0.00	100.09
351 RANDOM UNZONED GRAIN	0.00	0.69	16.45	46.56	4.74	22.78	0.09	7.82	0.18	0.00	99.31
352 SAMPLE 196 UNZONED GRAIN SPOT 1 PIC 608	0.05	0.87	17.20	46.64	3.75	23.67	0.18	7.30	0.25	0.10	100.01
353 UNZONED GRAIN SPOT 2 PIC 608	0.00	0.76	17.36	46.53	4.04	23.42	0.16	7.51	0.39	0.10	100.27
354 UNZONED GRAIN SPOT 3 PIC 608	0.00	0.81	16.56	46.80	4.16	24.05	0.11	7.15	0.23	0.01	99.88
355 UNZONED GRAIN SPOT 4 PIC 608	0.00	0.76	16.14	46.59	5.26	23.05	0.25	7.66	0.20	0.00	99.91
356 UNZONED GRAIN SPOT 5 PIC 608	0.00	0.75	16.28	47.71	4.13	23.72	0.16	7.33	0.27	0.04	100.39
357 UNZONED GRAIN SPOT 6 PIC 608	0.00	0.63	16.93	46.42	5.14	24.21	0.16	7.17	0.15	0.03	100.84
358 UNZONED GRAIN SPOT 7 PIC 608	0.00	0.75	16.65	46.98	4.60	24.26	0.19	7.22	0.00	0.03	100.68
359 UNZONED GRAIN SPOT 8 PIC 608	0.00	0.65	16.87	47.09	4.12	24.08	0.09	7.17	0.25	0.00	100.32
360 UNZONED GRAIN SPOT 9 PIC 608	0.00	0.83	17.01	47.02	3.72	24.17	0.10	7.27	0.17	0.00	100.29
361 UNZONED GRAIN SPOT 10 PIC 608	0.00	0.70	16.84	47.25	3.94	24.67	0.15	6.94	0.00	0.04	100.53
362 UNZONED RANDOM	0.00	0.94	16.42	47.23	4.03	23.85	0.12	7.50	0.00	0.06	100.15
363 CHR **** SAMPLE 203 AS TEST	0	0.81	15.58	47.55	4.68	21.30	0.55	8.48	0.05	0	99.00
364 CHR **** SAMPLE 197 LARGE GRAIN CENTRAL, SPO	0	0.76	13.97	44.18	9.79	24.35	0.46	6.48	0.08	0.06	100.13
365 CHR SMALL SPOT 2	0	0.53	15.21	46.29	6.72	23.75	0.45	6.84	0.19	0.01	99.98
366 CHR SMALL SPOT 3	0	0.64	13.48	45.35	9.09	23.93	0.56	6.41	0.18	0.1	99.74
367 CHR SMALL CENTRAL, SPOT 4	0	0.62	12.96	45.43	10.15	25.06	0.67	5.83	0.12	0.05	100.90
368 CHR OUTER ZONE INCL MG-CHLORITE SPOT 5	0	1.4	7.94	47.82	11.83	26.79	0.67	4.77	0	0.07	101.29
369 CHR ANOTHER SPOT 6	0	0.5	14.21	44.6	9.12	24.17	0.46	6.24	0.32	0.06	99.67
370 CHR REL LARGE LIKELY PRIMARYM, NOT IN PHOTO	0	0.7	14.34	43.44	8.85	26.56	0.54	4.73	0.29	0.09	99.54
371 CHR ANOTHER REL LARGE, CENTRAL GR 8	0	0.55	13.96	45.49	9.48	24.76	0.52	6.27	0.12	0.02	101.17
372 CHR AT MARGIN	0.04	0.73	9.57	49.35	9.70	25.32	0.62	5.29	0.13	0.06	100.81
373 CHR **** SAMPLE 198 L CENTRAL, SPOT 1, 12-28	0	0.72	14.75	49.68	5.02	19.12	0.5	9.93	0.12	0	99.83
374 CHR AT MARGIN SPOT 2	0	0.69	15.26	48.78	5.76	19.65	0.46	9.82	0.03	0	100.45
375 CHR ANOTHER L CENTRAL. SPOT 3	0	0.78	15.33	49.05	5.19	19.79	0.38	9.8	0	0.08	100.40
376 CHR AT MARGIN SPOT 4	0	0.76	15.4	49.59	4.50	19.89	0.53	9.65	0.06	0	100.38
377 CHR SMALLER SPOT 5	0	0.7	15.2	48.91	5.73	19.46	0.52	9.87	0.08	0.01	100.48
378 CHR SMALL SPOT 6	0	0.64	15.01	49.6	5.16	19.79	0.51	9.64	0	0	100.36
379 CHR INST SPOT 7	0	0.61	14.79	49.9	5.24	19.86	0.34	9.63	0.05	0.05	100.46
380 CHR INST SPOT 8	0	0.63	14.75	50	4.84	19.80	0.46	9.57	0	0.01	100.06
381 CHR SMALLEST SPOT 9	0	0.71	14.65	49.34	5.64	19.42	0.49	9.84	0	0	100.09
382 CHR **** SAMPLE 199 L CENTRAL SPOT 1, 12-28-	0	0.58	14.17	50.5	4.97	20.97	0.49	8.74	0.04	0.06	100.52
383 CHR AT MARGIN SPOT 2	0	0.6	14.6	49.38	5.11	20.71	0.44	8.85	0.08	0	99.77
384 CHR ANOTHER L CENTRAL, SPOT 3	0	0.66	14.1	49.79	5.90	20.71	0.57	8.93	0.07	0.05	100.78
385 CHR SMALLER SPOT 5	0	0.61	14.53	49.19	5.65	20.76	0.46	8.9	0	0.04	100.15
386 CHR INST SMALL SPOT 5	0	0.65	14.67	50.41	4.31	21.14	0.51	8.71	0.1	0	100.50
387 CHR INST SMALL SPOT 6	0	0.57	14.76	49.44	5.29	21.05	0.51	8.69	0.13	0	100.44
388 CHR INST SPOT 7	0	0.64	14.8	50.1	4.45	21.18	0.44	8.73	0.08	0.01	100.43
389 CHR INST SPOT 8	0	0.59	14.99	49.73	5.37	20.39	0.43	9.32	0.1	0.02	100.94
390 CHR INST SPOT 9	0	0.52	14.42	49.76	5.50	21.09	0.45	8.7	0	0.04	100.48
391 CHR **** SAMPLE 200 L GRAIN SPOT 1, 12-29-37	0	0.85	14.71	48.68	5.00	22.27	0.48	8.06	0.04	0	100.09
392 CHR AT MARGIN SPOT 2	0	0.98	15.81	46.74	5.25	22.74	0.48	7.9	0	0.05	99.96
393 CHR SPOT 4	0	0.9	17.07	47.11	3.88	23.00	0.45	7.96	0.02	0	100.39
394 CHR REL LARGE CENTRAL, SPOT 5	0	0.78	16.13	47.83	4.47	23.22	0.48	7.67	0.01	0	100.59

Black Label BT-09-31

	SiO2	TiO2	Al2O3	Cr2O3	Fe2O3	FeO	MnO	MgO	ZnO	NiO	TOTAL
395 CHR AT MARGIN SPOT 6	0	0.87	16.46	46.83	5.18	22.93	0.5	7.91	0.1	0.01	100.79
396 CHR SMALLER SPOT 7	0	0.76	16.47	47.11	5.16	22.97	0.43	7.88	0.06	0.06	100.90
397 CHR SMALLER SPOT 8	0	0.82	17.05	47.01	4.25	23.18	0.43	7.77	0.14	0.03	100.69
398 CHR SPOT 9	0	0.84	16.63	46.58	4.77	23.40	0.44	7.53	0.04	0.09	100.32
399 CHR SMALL SPOT 10	0	0.82	16.95	46.93	4.52	23.29	0.44	7.76	0.06	0.01	100.78
400 CHR **** SAMPLE 201 L CENTRAL, SPOT 1, 12-29	0	0.75	15.83	49	3.81	22.00	0.4	8.36	0	0.08	100.23
401 CHR AT MARGIN SPOT 2	0	0.84	15.7	48.11	4.92	21.84	0.6	8.36	0.19	0.01	100.57
402 CHR ANOTHER CENTRAL, SPOT 3	0	0.88	14.94	50.33	2.91	22.87	0.5	7.74	0	0.04	100.21
403 CHR AT MARGIN SPOT 4	0	0.77	15.54	48.57	3.88	21.94	0.49	8.14	0.08	0.02	99.44
404 CHR ANOTHER CENTRAL, SPOT 5	0	0.87	15.78	48.17	4.30	22.16	0.44	8.25	0.08	0	100.05
405 CHR SMALLER SPOT 7	0	0.82	14.42	49.03	4.11	22.28	0.6	7.7	0.01	0.04	99.01
406 CHR SMALLER SPOT 9	0	0.78	15.52	48.76	3.77	22.60	0.51	7.77	0.06	0.07	99.84
407 CHR V SMALL SPOT 10	0	0.82	15.59	49.06	4.11	22.27	0.5	8.19	0.14	0	100.68
408 CHR **** SAMPLE 202 L CENTRAL, SPOT 1, 12-29	0.26	0.62	13.23	52.13	4.81	20.66	0.49	8.26	0.05	0.08	100.58
409 CHR ANOTHER CENTRAL SPOT 1	0	0.5	13.63	51.24	4.82	21.35	0.51	8.34	0.13	0.05	100.57
410 CHR AT MARGIN SPOT 2	0	0.59	13.52	50.64	4.74	21.77	0.49	8.01	0.02	0.1	99.89
411 CHR ANOTHER CENTRAL, SPOT 3	0	0.53	13.6	51.38	4.44	21.61	0.41	8.3	0	0	100.26
412 CHR AT MARGIN SPOT 4	0	0.56	13.96	50.48	5.01	21.64	0.5	8.18	0.16	0.09	100.58
413 CHR SMALLER SPOT 5	0	0.56	13.92	51.03	4.22	21.60	0.39	8.26	0.08	0.05	100.11
414 CHR SMALLER SPOT 6	0	0.54	14.3	50.29	4.86	22.07	0.54	8	0.06	0.08	100.74
415 CHR SMALLER SPOT 7	0	0.59	13.87	50.84	4.88	21.92	0.45	8.11	0.19	0.06	100.91
416 CHR SMALLER SPOT 8	0	0.54	13.72	50.48	5.35	22.20	0.51	7.91	0.07	0.03	100.81
417 CHR SMALLEST SPOT 9	0	0.53	13.92	51	4.01	21.74	0.5	8.05	0.07	0.02	99.84
418 SAMPLE 206 UNZONED GRAIN SPOT 1 PIC 609	0.01	0.65	17.40	46.31	3.31	24.85	0.22	6.47	0.05	0.11	99.38
419 UNZONED GRAIN SPOT 2 PIC 609	0.00	0.75	17.09	45.20	4.44	25.25	0.22	6.23	0.18	0.02	99.39
420 UNZONED GRAIN SPOT 3 PIC 609	0.03	0.72	17.56	43.77	5.73	25.08	0.11	6.50	0.02	0.00	99.51
421 UNZONED GRAIN SPOT 4 PIC 609	0.00	0.75	17.29	44.00	5.37	24.96	0.07	6.46	0.11	0.11	99.12
422 UNZONED GRAIN SPOT 5 PIC 609	0.00	0.68	17.53	45.18	4.08	25.04	0.25	6.38	0.09	0.02	99.25
423 UNZONED GRAIN SPOT 6 PIC 609	0.00	0.80	17.29	45.33	4.74	24.92	0.14	6.71	0.09	0.08	100.10
424 UNZONED GRAIN SPOT 7 PIC 609	0.00	0.80	17.49	45.26	4.42	25.00	0.24	6.60	0.16	0.00	99.96
425 UNZONED GRAIN SPOT 8 PIC 609	0.00	0.65	17.58	45.41	4.31	25.02	0.18	6.52	0.00	0.14	99.81
426 UNZONED GRAIN SPOT 9 PIC 609	0.00	0.65	17.62	46.23	3.46	25.08	0.08	6.64	0.00	0.00	99.76
427 UNZONED GRAIN SPOT 10 PIC 609	0.00	0.78	16.90	44.76	5.33	24.92	0.20	6.54	0.09	0.01	99.53
428 UNZONED GRAIN SPOT 11 PIC 609	0.00	0.83	17.64	44.80	4.46	25.43	0.19	6.38	0.13	0.00	99.86
429 UNZONED RANDOM GRAIN	0.00	0.86	17.40	45.96	4.14	24.92	0.08	6.88	0.07	0.07	100.38
430 SAMPLE 207 DARK CENTRAL SPOT 1 PIC 610	0.00	0.45	13.00	44.44	9.25	27.68	0.15	3.90	0.34	0.06	99.27
431 DARK CENTRAL SPOT 2 PIC 610	0.00	0.57	9.56	46.17	10.70	30.02	0.15	2.23	0.07	0.20	99.67
432 DARK DOMAIN SPOT 1 PIC 612	0.00	0.76	13.92	45.60	6.41	27.87	0.18	4.19	0.11	0.00	99.03
433 BRIGHT DOMAIN SPOT 2 PIC 612	0.03	1.48	3.87	44.21	17.49	30.20	0.23	2.00	0.00	0.01	99.52
434 SAMPLE 208 RANDOM DARK	0.00	0.57	16.35	44.90	6.12	25.98	0.08	5.77	0.16	0.04	99.97
435 RANDOM BRIGHT	0.00	0.71	11.79	43.46	12.43	24.50	0.10	6.15	0.17	0.01	99.31
436 RANDOM DARK	0.00	0.76	14.88	44.06	8.54	24.86	0.06	6.36	0.21	0.08	99.80
437 UNZONED DARK SPOT 1 PIC 616	0.00	0.58	15.29	44.86	7.93	25.60	0.09	6.11	0.01	0.00	100.47
438 UNZONED DARK SPOT 2 PIC 616	0.00	0.66	16.97	43.68	6.46	26.77	0.04	5.42	0.21	0.04	100.25
439 UNZONED DARK SPOT 3 PIC 616	0.00	0.46	16.58	43.02	7.61	25.76	0.18	5.78	0.00	0.02	99.41
440 UNZONED DARK SPOT 4 PIC 616	0.00	0.62	16.79	43.47	6.94	25.29	0.29	5.99	0.39	0.01	99.78
441 UNZONED DARK SPOT 5 PIC 616	0.00	0.44	16.81	44.30	6.21	26.37	0.15	5.42	0.11	0.09	99.90
442 UNZONED DARK SPOT 6 PIC 616	0.00	0.63	16.72	43.73	6.74	26.25	0.14	5.73	0.00	0.01	99.96
443 UNZONED DARK SPOT 7 PIC 616	0.12	0.69	16.12	43.92	7.77	25.09	0.20	5.97	0.40	0.00	100.28
444 UNZONED DARK SPOT 8 PIC 616	0.00	0.76	16.51	43.68	6.86	26.42	0.16	5.67	0.05	0.00	100.12
445 UNZONED DARK SPOT 9 PIC 616	0.00	0.71	16.23	43.49	7.40	25.99	0.23	5.78	0.08	0.00	99.91
446 UNZONED DARK SPOT 10 PIC 616	0.00	0.45	11.63	51.17	4.86	26.88	0.33	4.57	0.02	0.00	99.91
447 UNZONED DARK SPOT 11 PIC 616	0.00	0.70	15.23	44.40	7.57	26.82	0.12	5.29	0.01	0.00	100.14
448 UNZONED DARK SPOT 12 PIC 616	0.00	0.89	15.82	43.23	7.54	26.10	0.24	5.69	0.10	0.00	99.62
449 UNZONED DARK SPOT 13 PIC 616	0.00	0.64	14.30	44.96	8.00	25.80	0.13	5.58	0.10	0.12	99.62
450 CHR **** SAMPLE 209 L CENTRAL, SPOT 1, 12-28	0	0.8	15.66	46.67	6.23	22.44	0.51	8.01	0.11	0	100.43
451 CHR MARGIN	0	0.68	15.88	47.4	5.25	23.12	0.47	7.59	0.06	0	100.45
452 CHR ANOTHER CENTRAL SPOT 3	0	0.73	15.07	46.78	6.26	22.83	0.44	7.53	0.1	0.08	99.82
453 CHR AT MARGIN SPOT 4	0	0.81	15.83	47.36	5.00	23.25	0.49	7.52	0.11	0	100.37
454 CHR ANOTHER CENTRAL SPOT 5	0	0.79	15.86	46.75	5.82	22.38	0.52	8	0.11	0.05	100.28
455 CHR AT MARGIN SPOT 6	0	0.77	15.61	46.71	6.08	23.14	0.41	7.63	0.03	0.02	100.40
456 CHR SMALLER SPOT 7	0	0.74	16.29	46.7	5.71	22.76	0.46	7.88	0.17	0.03	100.74
457 CHR SMALLER GRAIN 8	0	0.63	16.27	47.62	4.96	22.63	0.44	7.97	0.06	0	100.59
458 CHR SMALLEST SPOT 9	0	0.71	16.43	47.2	5.13	22.78	0.43	7.91	0.15	0.03	100.76
459 CHR SMALLEST SPOT 10	0	0.82	16.3	46.79	5.64	22.76	0.45	8.06	0.04	0	100.85
460 CHR **** SAMPLE 210 L CENTRAL, SPOT 1	0	0.61	15.41	45.94	6.60	23.87	0.62	6.71	0.12	0.08	99.96
461 CHR AT MARGIN SPOT 2	0	0.79	16.73	44.27	6.79	24.56	0.53	6.74	0.07	0.02	100.50
462 CHR ANOTHER CENTRAL SPOT 3	0	0.76	16.21	46.42	5.75	23.83	0.45	7.25	0.1	0.02	100.80
463 CHR AT MARGIN SPOT 4	0	0.8	17.19	43.84	6.60	23.91	0.54	7.02	0.28	0.03	100.20
464 CHR ANOTHER SPOT 5	0	0.78	16.67	45.01	6.37	24.79	0.55	6.67	0.05	0.01	100.90
465 CHR SMALLER SPOT 6	0	0.78	17.05	44.8	6.24	24.44	0.47	6.91	0.08	0.1	100.88
466 CHR ANOTHER SPOT 7	0	0.76	17.35	43.8	6.61	24.63	0.53	6.76	0	0.06	100.50
467 CHR ADJ GRAIN SPOT 8	0	0.7	17.35	44.18	6.46	24.20	0.47	7.04	0	0.05	100.45
468 CHR V SMALL SPOT 9	0	0.81	16.99	44	6.81	24.60	0.58	6.73	0.11	0.01	100.64
469 CHR ANOTHER SPOT 10	0.02	0.82	16.46	44.76	6.99	24.43	0.6	6.76	0.19	0.02	101.05
470 CHR **** SAMPLE 211 L CENTRAL, SPOT 1, 12-29	0	0.74	16.27	46.65	6.17	21.45	0.49	8.77	0.05	0	100.59
471 CHR AT MARGIN SPOT 2	0	0.69	17.39	45.08	6.41	21.72	0.49	8.61	0.1	0.04	100.53
472 CHR SMALLER SPOT 3	0	0.7	16.66	46.37	5.41	22.17	0.41	8.27	0.02	0.01	100.02
473 CHR SMALLER SPOT 4	0	0.71	16.55	46.13	6.30	22.26	0.45	8.26	0.12	0.03	100.81

Black Label BT-09-31

	SiO2	TiO2	Al2O3	Cr2O3	Fe2O3	FeO	MnO	MgO	ZnO	NiO	TOTAL
474 CHR REL LARGE CENTRAL, SPOT 5	0.01	0.82	16.84	46.83	5.24	21.94	0.48	8.52	0.03	0.15	100.86
475 CHR AT MARGIN SPOT 6	0	0.8	17.02	46.37	5.51	21.81	0.38	8.71	0.12	0	100.72
476 CHR SMALL SPOT 8	0	0.66	16.76	45.7	5.95	22.01	0.53	8.25	0	0.02	99.89
477 CHR SMALL SPOT 9	0	0.69	17.17	46	5.53	22.07	0.49	8.36	0.03	0.08	100.41
478 CHR V SMALL SPOT 10	0	0.78	17.29	45.49	5.59	21.82	0.55	8.51	0.06	0	100.09
479 CHR V SMALL SPOT 10	0	0.69	17.23	45.81	5.62	22.13	0.39	8.43	0	0.01	100.31
480 CHR **** SAMPLE 212 L CENTRAL, SPOT 1, 01-12	0	0.72	16.84	44.95	5.68	23.28	0.32	7.45	0	0.08	99.32
481 CHR AT MARGIN SPOT 2	0	0.7	17.51	44.04	5.70	23.22	0.49	7.35	0.13	0.05	99.19
482 CHR ANOTHER SPOT 3	0	0.61	17	44.56	4.96	23.23	0.58	7	0.03	0.05	98.03
483 CHR ANOTHER SPOT 3	0	0.59	17.2	44.91	4.60	23.02	0.47	7.28	0	0	98.07
484 CHR SPOT 3 AGAIN	0	0.66	17.06	44.52	5.61	23.35	0.38	7.21	0.15	0.06	99.00
485 CHR ANOTHER SPOT 4	0	1.24	17.78	43.03	4.55	23.56	0.53	7.24	0.16	0	98.09
486 SAMPLE 215 UNZONED DARK SPOT 1 PIC 617	0.00	0.63	14.64	45.53	7.47	24.13	0.19	6.74	0.00	0.00	99.33
487 UNZONED DARK SPOT 2 PIC 617	0.00	0.62	16.38	45.20	6.48	25.42	0.15	6.31	0.06	0.07	100.69
488 UNZONED DARK SPOT 3 PIC 617	0.00	0.54	16.78	43.99	7.14	25.23	0.10	6.36	0.15	0.00	100.30
489 UNZONED DARK SPOT 4 PIC 617	0.00	0.76	16.48	45.49	5.62	25.15	0.16	6.53	0.03	0.03	100.25
490 UNZONED DARK SPOT 5 PIC 617	0.00	0.80	15.91	44.87	6.71	25.77	0.11	6.06	0.22	0.00	100.45
491 UNZONED DARK SPOT 6 PIC 617	0.00	0.56	16.67	44.51	6.14	25.10	0.10	6.36	0.00	0.02	99.45
492 UNZONED DARK SPOT 7 PIC 617	0.00	0.70	16.26	44.38	7.21	26.01	0.06	6.06	0.07	0.00	100.75
493 UNZONED DARK SPOT 8 PIC 617	0.00	0.64	15.66	44.74	6.95	26.33	0.22	5.56	0.00	0.00	100.10
494 UNZONED DARK SPOT 9 PIC 617	0.00	0.84	16.97	44.82	4.49	25.75	0.20	5.88	0.21	0.06	99.22
495 UNZONED DARK SPOT 1 PIC 618	0.00	0.67	16.85	45.80	5.11	25.42	0.18	6.37	0.08	0.00	100.48
496 UNZONED DARK SPOT 2 PIC 618	0.00	0.65	15.25	44.71	8.00	25.42	0.22	6.04	0.27	0.00	100.56
497 UNZONED DARK SPOT 3 PIC 618	0.00	0.72	15.60	44.84	7.27	24.30	0.20	6.77	0.14	0.06	99.90
498 UNZONED DARK SPOT 4 PIC 618	0.00	0.76	15.60	44.71	6.77	25.53	0.16	5.94	0.16	0.12	99.75
499 UNZONED DARK SPOT 5 PIC 618	0.00	0.80	17.03	43.10	6.88	26.91	0.12	5.50	0.08	0.00	100.42
500 UNZONED DARK SPOT 6 PIC 618	0.00	0.66	15.56	45.17	6.49	26.45	0.13	5.47	0.10	0.00	100.03
501 SAMPLE 216 UNZONED DARK SPOT 1 PIC 619	0.00	0.74	15.08	50.00	3.69	22.18	0.10	8.27	0.26	0.00	100.32
502 UNZONED DARK SPOT 2 PIC 619	0.00	0.48	15.04	50.98	3.22	22.51	0.09	7.97	0.18	0.04	100.51
503 UNZONED DARK SPOT 3 PIC 619	0.00	0.62	15.12	50.16	3.51	22.13	0.20	8.14	0.20	0.04	100.12
504 UNZONED DARK SPOT 4 PIC 619	0.00	0.41	15.56	49.70	4.09	21.92	0.13	8.24	0.12	0.19	100.36
505 UNZONED DARK SPOT 5 PIC 619	0.00	0.60	15.01	49.92	4.03	21.94	0.16	8.20	0.33	0.06	100.24
506 UNZONED DARK SPOT 6 PIC 619	0.00	0.69	15.09	49.74	4.01	22.45	0.21	8.15	0.00	0.00	100.34
507 UNZONED DARK SPOT 7 PIC 619	0.00	0.49	15.57	49.76	3.95	22.04	0.12	8.32	0.18	0.00	100.44
508 UNZONED DARK SPOT 8 PIC 619	0.00	0.55	15.17	49.43	3.59	22.29	0.13	7.99	0.00	0.00	99.15
509 UNZONED DARK SPOT 9 PIC 619	0.00	0.48	15.43	50.18	3.87	22.32	0.17	8.17	0.12	0.04	100.78
510 UNZONED DARK SPOT 10 PIC 619	0.00	0.48	16.02	49.68	3.23	23.10	0.10	7.75	0.08	0.00	100.44
511 SAMPLE 217 DARK CENTRAL SPOT 1 PIC 621	0.00	0.67	15.91	42.97	8.01	26.68	0.21	5.10	0.27	0.11	99.93
512 BRIGHT MARGIN SPOT 2 PIC 621	0.00	1.04	6.68	32.36	27.95	28.81	0.23	3.01	0.00	0.04	100.13
513 DARK CENTRAL SPOT 3 PIC 621	0.00	0.60	14.40	42.02	11.51	25.84	0.25	5.55	0.27	0.04	100.48
514 BRIGHT MARGIN SPOT 4 PIC 621	0.00	1.23	6.60	32.41	27.35	29.16	0.19	2.77	0.19	0.03	99.94
515 DARK CENTRAL SPOT 5 PIC 621	0.00	0.54	17.73	43.37	6.40	26.82	0.12	5.36	0.33	0.06	100.73
516 BRIGHT MARGIN SPOT 6 PIC 621	0.01	1.28	5.02	31.76	29.71	29.37	0.20	2.58	0.00	0.00	99.94
517 DARK CENTRAL SPOT 7 PIC 621	0.00	0.60	17.91	43.58	5.41	26.93	0.22	5.30	0.11	0.04	100.09
518 BRIGHT MARGIN SPOT 8 PIC 621	0.00	1.12	6.19	27.99	32.50	29.74	0.20	2.26	0.13	0.15	100.27
519 DARK CENTRAL SPOT 9 PIC 621	0.86	0.41	13.12	41.08	16.90	22.53	0.08	5.63	0.28	0.00	100.89
520 BRIGHT MARGIN SPOT 10 PIC 621	0.00	1.32	5.19	30.83	31.04	29.93	0.08	2.55	0.00	0.01	100.95
521 RANDOM DARK	0.04	0.45	16.00	43.55	8.24	25.64	0.18	5.78	0.04	0.03	99.95
522 RANDOM DARK	0.00	0.55	15.88	42.68	8.82	27.58	0.16	4.76	0.00	0.10	100.52
523 RANDOM DARK	0.00	0.47	15.82	43.12	8.35	26.91	0.15	4.97	0.22	0.02	100.03
524 CHR **** SAMPLE 219 L CENTRAL, SPOT 1, 01-12	0	0.74	15.25	46.2	6.21	21.18	0.53	8.36	0.06	0.04	98.57
525 CHR SPOT 1 AGAIN	0	0.75	15.8	47	5.84	21.79	0.49	8.4	0.04	0.03	100.14
526 CHR SPOT 2 AT MARGIN	0	0.72	16.08	46.96	5.72	22.52	0.54	8.04	0	0	100.57
527 CHR ANOTHER CENTRAL, SPOT 2	0	0.77	16.39	44.93	6.52	21.57	0.48	8.37	0	0.13	99.16
528 CHR AT MARGIN SPOT 4	0	0.64	16.83	46.1	6.41	21.95	0.48	8.48	0.1	0.05	101.04
529 CHR AT MARGIN SPOT 4	0	0.64	16.61	47	5.79	22.20	0.49	8.38	0.04	0.01	101.16
530 CHR ANOTHER CENTRAL SPOT 5	0	0.71	15.34	46.88	6.39	21.59	0.49	8.33	0.14	0.06	99.93
531 CHR ANOTHER SPOT 6	0	0.71	15.82	46.62	6.21	21.92	0.5	8.32	0	0	100.10
532 CHR V SMALL SPOT 7	0	0.66	15.88	46.75	6.78	22.18	0.57	8.26	0.05	0	101.13
533 CHR V SMALL SPOT 7	0	0.63	15.94	46.02	6.44	21.87	0.45	8.21	0.04	0.02	99.63
534 CHR SMALLER SPOT 8	0	0.62	16.28	47.26	5.87	21.94	0.51	8.44	0.05	0.02	100.99
535 CHR SMALLER SPOT 8	0	0.66	15.96	45.75	6.67	21.88	0.6	8.16	0	0.03	99.71
536 CHR **** SAMPLE 220 CENTRAL, SPOT 1, 01-12-3	0	0.64	15.04	46.66	6.41	25.73	0.52	5.76	0.15	0.03	100.94
537 CHR SPOT 1, 01-12-3855	0	0.67	14.06	47.03	5.89	25.57	0.52	5.44	0.22	0	99.40
538 CHR ANOTHER SPOT 2	0	0.68	14.67	46.45	6.53	25.29	0.4	5.85	0.28	0.09	100.24
539 CHR ANOTHER SPOT 3	0	0.65	14.29	46.65	7.16	26.05	0.57	5.4	0.21	0.08	101.06
540 CHR ANOTHER SPOT 3	0	0.65	14.03	46.3	8.07	26.37	0.47	5.32	0.26	0.01	101.48
541 CHR ANOTHER SPOT 3	0	0.68	14.35	46.47	7.29	26.49	0.48	5.26	0.19	0.07	101.28
542 CHR ANOTHER SPOT 3	0	0.64	13.68	46.6	7.13	25.95	0.4	5.27	0.27	0.04	99.97
543 CHR ANOTHER SPOT 4	0	0.68	14.28	45.32	7.31	25.51	0.61	5.37	0.25	0.08	99.41
544 CHR W CIRC SERP INCL, SPOT 5	0	0.71	15.06	45.94	6.17	25.58	0.33	5.75	0.2	0.04	99.78
545 CHR V SMALL SPOT 6	0	0.68	15.09	46.16	6.97	26.06	0.54	5.6	0.19	0.06	101.35
546 CHR V SMALL SPOT 6	0	0.61	14.21	45.58	7.05	25.50	0.56	5.38	0.19	0	99.08
547 CHR V SMALL SPOT 7	0	0.63	13.95	46.76	6.64	25.94	0.48	5.3	0.2	0	99.90
548 CHR SPOT 8	0	0.59	12.97	46.37	7.49	25.32	0.58	5.29	0.09	0.08	98.78
549 CHR SPOT 8	0	0.75	14.13	46.65	6.20	25.61	0.57	5.49	0.2	0	99.60
550 SAMPLE 221 DARK DOMAIN SPOT 1 PIC 622	0.00	0.40	15.47	43.33	7.48	28.92	0.12	3.45	0.20	0.11	99.48
551 BRIGHT DOMAIN SPOT 2 PIC 622	0.00	1.12	3.43	29.23	33.82	31.06	0.20	1.11	0.14	0.11	100.22
552 DARK DOMAIN SPOT 1 PIC 623	0.00	0.49	12.29	44.58	10.12	28.59	0.23	3.43	0.20	0.06	99.98

Black Label BT-09-31

	SiO2	TiO2	Al2O3	Cr2O3	Fe2O3	FeO	MnO	MgO	ZnO	NiO	TOTAL
553 BRIGHT DOMAIN SPOT 2 PIC 623	0.01	0.84	2.34	28.70	35.99	30.37	0.14	1.16	0.13	0.18	99.86
554 UNZONED SPOT 2 PIC 624	0.00	0.70	2.50	29.45	35.23	30.46	0.14	1.14	0.07	0.10	99.80
555 SAMPLE 222 DARK DOMAIN SPOT 1 PIC 625	0.00	0.27	15.28	39.05	12.61	28.49	0.16	3.71	0.00	0.12	99.69
556 DARK DOMAIN SPOT 1 PIC 626	0.00	0.49	15.83	39.06	11.74	28.81	0.14	3.68	0.22	0.08	100.06
557 RANDOM DARK	0.00	0.63	5.80	37.91	23.49	30.12	0.13	1.82	0.06	0.17	100.12
558 DARK CENTRAL SPOT 1 PIC 627	0.00	0.44	15.88	39.12	12.03	27.86	0.23	4.14	0.34	0.12	100.15
559 RANDOM DARK	0.00	0.92	3.14	34.47	29.50	30.70	0.18	1.22	0.28	0.14	100.54
560 RANDOM DARK	0.00	0.47	14.22	39.43	12.79	28.41	0.15	3.65	0.15	0.06	99.33
561 SAMPLE 223 UNZONED SPOT 1 PIC 629	0.00	0.64	17.53	42.79	6.18	26.88	0.14	5.25	0.08	0.06	99.55
562 UNZONED SPOT 2 PIC 629	0.03	0.64	17.23	42.42	6.62	27.18	0.16	4.89	0.08	0.05	99.30
563 UNZONED SPOT 3 PIC 629	0.00	0.74	16.69	42.79	6.98	26.72	0.22	5.09	0.42	0.07	99.72
564 UNZONED SPOT 4 PIC 629	0.00	0.50	16.73	42.80	7.70	28.10	0.16	4.47	0.08	0.08	100.62
565 UNZONED SPOT 5 PIC 629	0.00	0.64	16.85	42.05	7.42	28.28	0.17	4.23	0.22	0.05	99.91
566 UNZONED SPOT 6 PIC 629	0.00	0.56	17.75	42.83	6.07	27.65	0.17	4.73	0.27	0.00	100.03
567 UNZONED SPOT 7 PIC 629	0.00	0.64	17.82	41.62	7.40	27.00	0.14	5.03	0.47	0.19	100.31
568 DARK ZONE SPOT 8 PIC 629	0.00	0.66	17.12	42.57	6.82	27.90	0.16	4.67	0.00	0.06	99.95
569 BRIGHT MARGIN SPOT 9 PIC 629	0.00	1.14	7.99	36.35	21.85	29.53	0.22	2.59	0.28	0.08	100.03
570 DARK CENTRAL SPOT 10 PIC 629	0.20	0.75	16.02	38.56	13.07	27.66	0.09	4.42	0.14	0.04	100.95
571 BRIGHT MARGIN SPOT 11 PIC 629	0.04	1.40	9.12	36.54	20.09	29.78	0.19	2.73	0.14	0.11	100.14
572 SAMPLE 227 UNZONED INT W PYRR SPOT 1 PIC 630	0.01	2.27	1.59	26.55	36.57	31.97	0.16	1.06	0.00	0.14	100.32
573 DARK ZONE SPOT 1 PIC 631	0.00	0.95	14.04	42.47	9.51	29.24	0.17	3.45	0.44	0.00	100.27
574 BRIGHT MARGIN SPOT 2 PIC 631	0.00	1.87	3.67	37.81	23.47	31.63	0.09	1.48	0.02	0.00	100.04
575 DARK CENTRAL SPOT 1 PIC 633	0.00	0.68	14.02	42.23	9.52	29.68	0.21	2.96	0.20	0.00	99.50
576 BRIGHT MARGIN SPOT 2 PIC 633	0.00	1.31	5.09	37.46	23.69	31.51	0.21	1.34	0.22	0.00	100.83
577 RANDOM UNZONED	0.00	0.98	4.04	35.79	27.27	31.17	0.15	1.39	0.00	0.00	100.79
578 RANDOM UNZONED	0.01	2.27	1.33	26.45	36.89	31.76	0.15	1.00	0.28	0.14	100.27
579 SAMPLE 229 UNZONED SPOT 1 PIC 635	0.00	0.58	15.29	51.42	3.00	21.01	0.14	9.15	0.00	0.01	100.60
580 UNZONED SPOT 2 PIC 635	0.00	0.65	14.80	52.04	2.45	20.84	0.11	9.08	0.18	0.00	100.16
581 UNZONED SPOT 3 PIC 635	0.00	0.46	14.91	51.07	3.74	20.20	0.15	9.35	0.15	0.00	100.03
582 UNZONED SPOT 4 PIC 635	0.00	0.49	15.34	50.72	3.47	21.20	0.06	8.90	0.11	0.00	100.30
583 UNZONED SPOT 5 PIC 635	0.00	0.42	15.42	50.16	4.71	20.69	0.15	9.31	0.00	0.01	100.87
584 UNZONED SPOT 6 PIC 635	0.00	0.42	15.13	50.55	4.14	20.65	0.07	9.16	0.14	0.00	100.25
585 UNZONED SPOT 7 PIC 635	0.00	0.53	14.66	50.48	4.81	19.92	0.09	9.54	0.30	0.03	100.35
586 UNZONED SPOT 8 PIC 635	0.00	0.51	14.53	50.36	5.09	20.50	0.07	9.28	0.04	0.11	100.49
587 UNZONED SPOT 9 PIC 635	0.00	0.54	14.84	50.86	4.26	20.76	0.12	9.26	0.00	0.00	100.64
588 UNZONED SPOT 10 PIC 635	0.00	0.47	14.91	51.24	3.27	20.56	0.05	9.17	0.10	0.00	99.77
589 UNZONED SPOT 11 PIC 635	0.00	0.72	15.20	49.70	3.69	21.11	0.09	8.87	0.16	0.00	99.54
590 UNZONED SPOT 12 PIC 635	0.00	0.50	15.15	50.65	4.19	20.96	0.10	9.12	0.00	0.08	100.75
591 UNZONED SPOT 13 PIC 635	0.01	0.61	15.36	50.99	3.23	21.05	0.10	9.10	0.00	0.06	100.51
592 CHR **** SAMPLE 233 SPOT 1, 05-08-4214	0.16	0.76	17.8	44.49	6.09	21.19	0.7	8.33	0	0.17	99.69
593 CHR SPOT 2	0.19	0.69	17.37	44.67	7.42	21.10	0.54	8.47	0	0.29	100.74
594 CHR AT MARGIN SPOT 3	0.17	0.8	16.29	44.52	7.60	21.37	0.66	7.9	0.14	0.34	99.79
595 CHR SPOT 4	0.13	0.57	16.72	44.18	7.60	21.54	0.61	7.86	0.09	0.25	99.55
596 CHR AT MARGIN SPOT 5	0.19	0.73	17.36	44.55	7.50	21.58	0.57	8.17	0.05	0.31	101.01
597 CHR SPOT 6	0.16	0.46	17.61	44.73	6.55	21.58	0.7	7.89	0	0.22	99.90
598 CHR SPOT 7	0.14	0.82	17.01	44.56	7.08	21.94	0.63	7.99	0	0.23	100.40
599 CHR SMALLER SPOT 8	0.17	0.72	17.45	43.89	7.53	21.41	0.67	8.22	0	0.18	100.23
600 CHR **** SAMPLE 233 1DPOT 1 04-07-4070	0.02	0.71	17.44	45.18	6.55	22.13	0.49	8.43	0.06	0.07	101.08
601 CHR SAMPLE 233 1DPOT 1 04-07-4070	0	0.85	17.7	45.37	5.41	22.24	0.45	8.46	0.08	0.04	100.60
602 CHR SPOT 2	0.01	0.73	17.69	44.82	5.40	21.63	0.49	8.54	0	0	99.31
603 CHR ANOTHER GRAIN SPOT 3	0.01	0.87	16.93	44.82	6.52	22.00	0.5	8.42	0	0.05	100.12
604 CHR AT MARGIN	0	0.76	17.08	44.87	6.57	21.88	0.57	8.47	0.02	0	100.22
605 CHR GRAIN 3 CENTRAL SPOT 5	0.05	0.8	17.28	45.09	7.07	22.11	0.51	8.51	0.08	0	101.51
606 CHR GRAIN 3 CENTRAL SPOT 5	0	0.77	17.72	45.78	5.80	22.12	0.62	8.5	0.13	0.11	101.55
607 CHR GRAIN 3 CENTRAL SPOT 5	0	0.79	17.28	44.72	6.33	22.39	0.34	8.33	0	0	100.18
608 CHR AT MARGIN SPOT 6	0	0.86	17.36	45.35	6.04	22.22	0.44	8.54	0	0.05	100.85
609 CHR AT MARGIN SPOT 6	0	0.81	17.08	44.77	6.16	22.07	0.37	8.39	0	0.03	99.68
610 CHR LA ANOTHER CENTRAL, SPOT 7	0.02	0.85	17.67	44.82	6.10	22.19	0.46	8.48	0.01	0.04	100.64
611 CHR AT MARGIN SPPT 8	0	0.85	17.22	45.72	6.15	22.48	0.5	8.43	0.02	0.01	101.39
612 CHR AT MARGIN SPPT 8	0.02	0.83	16.87	45.5	5.88	21.94	0.47	8.42	0.02	0	99.95
613 CHR **** SAMPLE 234 SPOY 1 04-08-4071	0.09	0.9	14.55	46.61	6.90	23.86	0.45	6.79	0.09	0.08	100.32
614 CHR SPOT 1 04-08-4071	0.03	0.81	14.94	45.85	6.32	23.23	0.55	7.02	0	0.06	98.81
615 CHR AT MARGIN SPOT 2	0.03	0.85	16.08	45.72	5.99	23.99	0.58	6.93	0.1	0	100.27
616 CHR AT MARGIN SPOT 2	0.05	0.78	16.09	46.17	5.32	23.98	0.52	6.81	0.07	0.01	99.80
617 CHR ANOTHER CENTRAL, SPOT 3	0.07	0.83	15.2	45.72	6.45	23.17	0.61	7.04	0.05	0	99.14
618 CHR AT MARGIN SPOT 4	0.03	0.76	15.44	46.64	5.14	23.71	0.53	6.82	0.03	0.03	99.13
619 CHR SMALLER SPOT 5	0	0.81	15.48	45.85	6.55	23.94	0.64	6.83	0.21	0.04	100.35
620 CHR SMALLER SPOT 6	0.05	0.8	15.97	45.17	6.33	23.62	0.59	6.91	0.13	0	99.57
621 CHR ANOTHER SPOT 7	0.03	0.81	15.42	45.07	6.71	23.18	0.64	7.03	0.1	0.05	99.04
622 CHR BRIGHT DOMAIN, SPOT 8	0.08	1.69	7.51	45.3	12.58	26.81	0.61	4.2	0.06	0.06	98.90
623 CHR BRIGHT DOMAIN, SPOT 8	0.06	1.77	7.78	45.47	13.11	27.21	0.74	4.27	0.12	0.1	100.62
624 CHR BRIGHT DOMAIN, SPOT 8	0.39	1.7	7.47	46.11	12.53	25.82	0.63	4.16	0.02	0	98.82
625 CHR ANOTHER BRIGHT SPOT 9	0.1	1.95	11.12	40.26	14.51	26.57	0.71	5.02	0.17	0.04	100.45
626 CHR ANOTHER BRIGHT SPOT 9	0.07	1.93	11.1	40.12	14.06	26.90	0.63	4.87	0.04	0	99.72
627 CHR SPOT 1, 05-08-4215	0.17	0.68	15.94	45.62	7.39	23.26	0.82	6.76	0.11	0.3	101.05
628 CHR AT MARGIN SPOT 2	0.15	0.65	14.56	44.88	7.84	23.09	0.63	6.43	0	0.27	98.51
629 CHR AT MARGIN SPOT 2	0.14	0.7	15.11	45.63	7.27	23.45	0.63	6.59	0.02	0.23	99.78
630 CHR SPOT 3	0.2	0.78	15.08	45.73	7.62	23.32	0.7	6.64	0.01	0.25	100.33
631 CHR AT MARGIN SPOT 4	0.2	0.66	14.6	46.24	7.53	23.23	0.58	6.48	0.19	0.24	99.94

Black Label BT-09-31

	SiO2	TiO2	Al2O3	Cr2O3	Fe2O3	FeO	MnO	MgO	ZnO	NiO	TOTAL
632 CHR SPOT 5	0.2	0.75	16.05	44.42	7.55	22.96	0.62	6.85	0.08	0.24	99.72
633 CHR AT MARGIN SPOT 6	0.17	0.71	15.33	44.65	8.27	23.28	0.71	6.64	0.06	0.21	100.04
634 CHR SMALLER SPOT 7	0.21	0.71	16.28	44.26	7.04	22.96	0.66	6.66	0.1	0.25	99.14
635 CHR ANOTHER SPOT 8	0.12	0.67	16.11	45.31	7.63	23.98	0.65	6.63	0.15	0.25	101.50
636 CHR ANOTHER SPOT 8	0.19	0.73	14.81	44.75	7.61	23.09	0.53	6.47	0.03	0.24	98.45
637 CHR ANOTHER SPOT 8	0.19	0.69	15.04	45	8.20	23.19	0.71	6.6	0.03	0.2	99.84
638 CHR **** SAMPLE 235 L CENTRAL, SPOT 1, 05-08	0.19	0.65	13.61	49.9	6.50	22.44	0.71	7.23	0.12	0.22	101.57
639 CHR CENTRAL, SPOT 1, 05-08-4217	0.19	0.63	12.43	48.43	6.88	22.05	0.63	6.8	0	0.17	98.21
640 CHR CENTRAL, SPOT 1, 05-08-4217	0.19	0.59	13.53	48.39	7.28	22.33	0.59	7.13	0.01	0.2	100.24
641 CHR AT MARGIN SPOT 2	0.21	0.57	13.84	48.5	6.92	22.48	0.69	6.98	0	0.2	100.39
642 CHR SPOT 3	0.17	0.62	13.21	49.48	7.03	22.47	0.73	7.17	0	0.18	101.06
643 CHR SPOT 3	0.19	0.63	12.87	48.79	6.56	22.01	0.58	7.02	0.01	0.2	98.86
644 CHR SPOT 4	0.16	0.53	13.52	49.24	6.79	22.64	0.64	7	0.04	0.25	100.81
645 CHR CENTRAL, SPOT 5	0.18	0.62	14.04	49.19	5.92	22.48	0.74	7.05	0	0.28	100.49
646 CHR AT MARGIN SPOT 6	0.21	0.62	13.51	47.58	7.80	22.60	0.71	6.78	0	0.23	100.04
647 CHR SPOT 7	0.13	0.54	12.45	48.75	7.50	22.61	0.76	6.72	0	0.19	99.65
648 CHR SPOT 8	0.2	0.68	13.33	48.37	6.56	22.30	0.62	6.94	0	0.18	99.19
649 CHR SAMPLE 235 SPOT 1 04-08-4072	0.17	0.78	13.97	47.08	7.04	21.60	0.53	7.64	0.07	0.04	98.93
650 CHR SAMPLE 235 SPOT 1 04-08-4072	0.1	0.78	14.9	47.75	5.84	22.43	0.5	7.66	0	0.03	99.99
651 CHR SAMPLE 235 SPOT 1 04-08-4072	0.07	0.7	14.69	47.47	5.79	22.33	0.53	7.51	0	0.07	99.16
652 CHR AT MARGIN SPOT 2	0.01	0.75	14.49	48.1	5.63	23.45	0.58	7.13	0	0.03	100.17
653 CHR ANOTHER CENTRAL, SPOT 3	0.07	0.79	14.99	48.41	5.44	22.94	0.49	7.6	0	0	100.72
654 CHR AT MARGIN SPOT 2	0	0.8	14.64	47.6	5.56	23.08	0.53	7.26	0.23	0	99.70
655 CHR ANOTHER CENTRAL, SPOT 5	0	0.73	15.27	47.6	4.87	22.81	0.55	7.46	0.1	0.01	99.40
656 CHR ANOTHER GRAIN SPOT 6	0.13	0.55	15.08	48.87	5.52	22.53	0.51	7.59	0	0	100.78
657 CHR SMALLER SPOT 7	0.03	0.69	15.39	48.07	4.91	22.93	0.44	7.56	0	0.02	100.04
658 CHR SMALLER SPOT 8	0	0.79	15.18	48	5.83	23.34	0.54	7.45	0.3	0	101.43
659 CHR SMALLER SPOT 8	0	0.76	15.19	47.64	4.68	23.37	0.41	7.22	0.05	0	99.32
660 CHR **** SAMPLE 236 CENTRAL, SPOT 1, 05-08-4	0.15	0.51	13.42	50.44	6.09	22.49	0.7	7.18	0.04	0.21	101.23
661 CHR CENTRAL, SPOT 1, 05-08-4218	0.18	0.56	13.35	50.39	6.25	22.93	0.7	6.93	0	0.2	101.50
662 CHR SPOT 2 AT AMRGIN	0.13	0.58	13.82	48.98	6.66	22.84	0.71	6.99	0	0.3	101.01
663 CHR WIRTHIN CIRC INCL, SPOT 3	0.14	0.47	13.13	48.97	6.34	22.67	0.7	6.67	0	0.17	99.25
664 CHR CENTRAL SPPT 4	0.14	0.56	13.35	49.66	6.82	22.68	0.59	7.2	0	0.18	101.18
665 CHR CENTRAL SPPT 4	0.16	0.56	13.14	49.2	6.86	22.22	0.69	7.12	0	0.24	100.20
666 CHR SPOT 5	0.2	0.54	12.44	48.71	7.52	22.38	0.67	6.66	0	0.27	99.39
667 CHR SPOT 6	0.14	0.58	13.42	48.7	6.49	22.31	0.65	7	0.1	0.24	99.63
668 CHR SPOT 7	0.16	0.62	13.46	47.88	7.57	22.42	0.73	6.91	0.13	0.29	100.18
669 CHR SPOT 8	0.16	0.56	13.87	48.56	6.28	22.08	0.79	7.13	0.01	0.21	99.65
670 CHR SPOT 9	0.19	0.56	13.71	47.29	7.71	22.21	0.81	6.89	0.02	0.26	99.65
671 CHR **** SAMPLE 237 SPOT 1 CENTRAL, 05-08-42	0.14	0.63	15.54	46.34	6.43	23.28	0.55	6.81	0	0.24	99.96
672 CHR AT MARGIN SPOT 2	0.2	0.62	15.54	45.06	7.89	23.31	0.73	6.56	0.02	0.21	100.14
673 CHR SPPT 3	0.11	0.59	14.64	45.66	7.49	23.10	0.69	6.62	0	0.21	99.11
674 CHR SPOT 4	0.15	0.62	15.25	45.31	6.95	23.51	0.55	6.41	0	0.2	98.95
675 CHR SPOT 4	0.14	0.65	15.44	46.58	6.16	24.11	0.73	6.21	0.01	0.25	100.29
676 CHR SPOT 4	0.15	0.57	15.15	46.71	6.73	23.73	0.78	6.39	0	0.19	100.40
677 CHR SPOT 5	0.12	0.65	15.02	45.69	7.27	23.84	0.65	6.35	0.02	0.22	99.83
678 CHR AT MARGIN SPOT 6	0.16	0.63	14.49	46.19	6.93	23.27	0.67	6.35	0.04	0.24	98.96
679 CHR SPOT 7	0.12	0.59	15.05	47.32	6.67	23.86	0.79	6.47	0	0.28	101.15
680 CHR SPOT 7	0.17	0.6	15.37	45.99	7.21	24.03	0.71	6.19	0.06	0.25	100.58
681 CHR SMALLER SPOT 8	0.18	0.65	15.27	46.8	6.41	23.95	0.7	6.3	0	0.19	100.45
682 CHR SPOT 8	0.17	0.57	15.21	45.66	7.72	23.83	0.65	6.36	0.02	0.15	100.34
683 CHR **** SAMPLE 238 SPOT 1, 05-08-4221	0.15	0.76	16.65	43.42	7.32	21.29	0.76	7.78	0	0.28	98.41
684 CHR SPOT 1, 05-08-4221	0.2	0.7	16.76	44.9	6.70	22.35	0.64	7.36	0	0.24	99.85
685 CHR AT MARGIN SPOT 2	0.17	0.63	17.74	42.98	6.86	21.81	0.71	7.55	0.05	0.2	98.70
686 CHR SPOT 3	0.19	0.56	17.33	43.79	6.74	21.12	0.67	7.9	0	0.17	98.46
687 CHR SPOT 3	0.18	0.63	18.01	44.77	5.51	22.38	0.66	7.49	0.04	0.18	99.85
688 CHR AT MARGIN SPOT 4	0.13	0.69	16.93	43.65	6.98	22.03	0.69	7.54	0	0.16	98.80
689 CHR AT MARGIN SPOT 4	0.16	0.64	17.47	44.58	6.29	22.36	0.63	7.52	0	0.2	99.85
690 CHR SPOT 5	0.2	0.72	17.72	44.2	6.19	22.51	0.6	7.37	0.02	0.24	99.77
691 CHR CENTRAL SPOT 7	0.21	0.72	17.4	44.46	7.10	22.00	0.59	7.8	0	0.27	100.55
692 CHR AT MARGIN SPOT 8	0.17	0.74	17.37	44.27	6.21	22.97	0.7	7.09	0	0.16	99.68
693 CHR AT MARGIN SPOT 8	0.16	0.69	17.64	44.54	6.14	22.39	0.68	7.53	0	0.23	100.01
694 CHR **** SAMPLE 248 CENTRAL, SPOT 1, 04-08-4	0	0.61	17.71	44.07	6.47	24.83	0.57	6.58	0.16	0.04	101.04
695 CHR SAMPLE 248 CENTRAL, SPOT 1, 04-08-4073	0	0.68	16.8	43.28	6.34	24.36	0.6	6.27	0.21	0.04	98.58
696 CHR SAMPLE 248 CENTRAL, SPOT 1, 04-08-4073	0.02	0.61	17.82	43.12	6.68	24.19	0.59	6.74	0.16	0	99.93
697 CHR AT MARGIN SPOT 2	0	0.67	16.98	43.54	7.13	26.12	0.46	5.73	0.07	0.1	100.80
698 CHR AT MARGIN SPOT 2	0	0.59	16.45	42.77	7.98	25.64	0.57	5.69	0.11	0	99.80
699 CHR ANOTHER CENTRAL, SPOT 3	0	0.65	16.78	43.85	6.89	24.84	0.56	6.3	0.19	0.02	100.08
700 CHR AT MARGIN SPOT 4	0	0.66	16.97	42.1	8.37	25.76	0.48	5.88	0.1	0	100.32
701 CHR AT MARGIN SPOT 4	0	0.61	16.66	42.53	8.11	25.51	0.4	5.86	0.26	0	99.94
702 CHR ANOTHER CENTRAL, SPOT 5	0	0.68	17.57	43.54	6.86	24.90	0.46	6.65	0.06	0	100.72
703 CHR ANOTHER CENTRAL, SPOT 5	0	0.66	16.68	44.1	6.26	24.55	0.36	6.48	0.12	0.03	99.25
704 CHR AT MARGIN SPOT 6	0.01	0.67	16.87	42.34	7.24	24.78	0.58	6.07	0.14	0	98.70
705 CHR AT MARGIN SPOT 6	0	0.61	17.43	42.88	6.62	24.92	0.46	6.23	0.15	0	99.30
706 CHR GRAIN 4 CENTRAL SPOT 7	0	0.63	17.59	42.45	6.93	24.57	0.54	6.44	0.13	0	99.28
707 CHR GRAIN 4 MARGIN SPOPT 8	0	0.65	17.25	42.42	7.09	25.60	0.54	5.78	0.13	0	99.46
708 CHR GRAIN 4 WHITE RIM SPOT 8	0.11	2.03	6.67	38.81	20.21	28.91	0.69	3.08	0.11	0.07	100.69
709 CHR GRAIN 1 WHITE RIM SPOT 10	0.05	2.02	5.94	38.66	20.59	28.95	0.72	2.97	0.09	0.07	100.06
710 CHR **** SAMPLE 249 CENTRAL, SPOT 1, 04-08-4	0	0.72	15.44	46.91	5.34	22.12	0.53	7.9	0.01	0	98.97

Black Label BT-09-31

	SiO2	TiO2	Al2O3	Cr2O3	Fe2O3	FeO	MnO	MgO	ZnO	NiO	TOTAL
711 CHR SPOT 2	0	0.59	16.36	46.88	5.16	22.68	0.7	7.62	0.11	0	100.10
712 CHR ANOTH GRAIN CENTRAL, SPIT 3	0	0.66	17.5	45.35	5.47	22.20	0.54	8.19	0.08	0	99.99
713 CHR GRAIN MARGIN SPOT 4	0	0.68	18.07	44.49	5.75	22.57	0.5	8.11	0.04	0	100.22
714 CHR GRAIN 3 SPOT 5	0	0.68	17.98	44.93	5.21	22.04	0.46	8.37	0.05	0	99.72
715 CHR GRAIN 4 SPOT 6	0	0.61	17.91	44.79	5.81	22.67	0.42	8.03	0.1	0	100.34
716 CHR **** SAMPLE 250 CENTRAL, SPOT 1, 04-08-4	0	0.77	16.27	41.84	9.11	27.17	0.54	4.89	0.33	0	100.92
717 CHR SAMPLE 250 CENTRAL, SPOT 1, 04-08-4077	0.01	0.82	16.16	41.21	8.93	27.16	0.45	4.78	0.17	0.03	99.71
718 CHR BRIGHT MARGIN SPOT 2	0.04	1.46	4.37	37.6	24.31	29.70	0.68	2.08	0.12	0.02	100.38
719 CHR BRIGHT MARGIN SPOT 2	0	0.82	15.19	41.73	10.20	27.81	0.64	4.34	0.31	0.02	101.06
720 CHR BRIGHT MARGIN SPOT 2	0	0.81	14.53	40.7	10.09	27.04	0.63	4.28	0.18	0.01	98.27
721 CHR BRIGHT MARGIN SPOT 2	0.01	0.86	15.05	40.47	10.88	27.60	0.58	4.32	0.25	0.02	100.04
722 CHR GRAIN 2 SPOT 4	0.15	1.61	3.51	34.05	27.98	28.97	0.77	1.91	0.1	0.1	99.15
723 CHR GRAIN 3 CENTYRAL, SPOT 5	0	0.88	16.37	42.73	7.51	27.27	0.61	4.84	0.2	0	100.41
724 CHR GRAIN 3 CENTYRAL, SPOT 5	0	0.78	16.26	42.72	7.78	27.22	0.63	4.75	0.26	0	100.40
725 CHR SMALLER CENTRAL	0	0.8	15.76	41.89	8.00	27.44	0.46	4.43	0.15	0.01	98.94
726 CHR ANOTHER CENTRAL SPOT 7	0	0.64	14.89	41.37	10.16	27.86	0.52	4.03	0.23	0	99.70
727 CHR ****SAMPLE 257 SPOT 1 03-08-4079	0	0.69	14.4	50.97	4.32	19.24	0.43	9.89	0.13	0	100.07
728 CHR AT MARGIN SPOT 2	0	0.71	14.39	49.82	4.65	19.13	0.33	9.86	0.02	0	98.91
729 CHR GRAIN 2 CENTRAL SPOT 3	0	0.66	14.48	50.52	4.53	19.51	0.49	9.67	0.07	0	99.93
730 CHR AT MARGIN SPOT 4	0	0.67	14.67	50.63	4.11	18.95	0.48	10.02	0.03	0	99.56
731 CHR GRAIN 3 CENTRAL SPOT 5	0	0.74	14.99	50.78	4.49	19.75	0.5	9.87	0.07	0	101.19
732 CHR GRAIN 3 CENTRAL SPOT 5	0	0.66	14.4	50.33	4.46	19.39	0.42	9.66	0.11	0	99.43
733 CHR AT AMRGIN SPOT 6	0	0.7	13.62	49.96	4.67	18.96	0.55	9.51	0.12	0	98.09
734 CHR AT AMRGIN SPOT 6	0	0.72	14.56	51.11	3.69	19.47	0.4	9.78	0.07	0	99.80
735 CHR SMALLER SPOT 7	0	0.63	13.89	49.76	4.96	19.05	0.52	9.53	0.11	0.01	98.47
736 CHR SMALLER SPOT 7	0	0.7	14.9	49.44	4.35	19.24	0.42	9.73	0.08	0	98.87
737 CHR SMALLER SPOT 8	0	0.69	13.76	50	4.67	19.05	0.46	9.58	0.09	0	98.30
738 CHR SMALLER SPOT 8	0	0.63	13.9	50.59	4.14	19.21	0.43	9.53	0.08	0	98.51
739 CHR **** SAMPLE 258 CENTRAL, SPOT 1, 04-08-4	0	0.64	14.78	50.98	4.90	18.15	0.51	10.7	0.15	0	100.81
740 CHR AT MARGIN SPOT 2	0	0.66	15.14	49.1	4.67	17.73	0.39	10.68	0	0	98.37
741 CHR AT MARGIN SPOT 2	0	0.63	15.28	49.18	4.67	17.60	0.33	10.77	0.13	0	98.59
742 CHR ANOTHER CENTRAL SPOT 3	0	0.67	15.13	50.29	4.17	18.35	0.46	10.48	0.02	0	99.57
743 CHR AT MARGIN SPOT 4	0	0.6	15.32	50.59	4.61	18.08	0.44	10.78	0.14	0	100.56
744 CHR ANOTHER CENTRAL SPOT 5	0	0.64	14.27	50.5	4.94	18.17	0.53	10.41	0.04	0	99.50
745 CHR AT AMRGIN SPOT 6	0	0.6	14.66	50.65	4.48	18.25	0.51	10.37	0.13	0	99.65
746 CHR ANOTHER CENTRAL SPOT 7	0	0.79	14.8	49.74	3.87	18.21	0.61	10.21	0.08	0	98.31
747 CHR ANOTHER CENTRAL SPOT 7	0	0.65	14.95	50.07	4.89	18.08	0.48	10.64	0.05	0	99.81
748 CHR *** SAMPLE 259 CENTRAL SPOT 1 03-08-3081	0	0.73	14.48	49.6	4.44	20.17	0.45	9.16	0	0	99.03
749 CHR AT MARGIN SPOT 2	0	0.65	15.2	49.16	5.36	19.70	0.44	9.68	0.14	0	100.34
750 CHR ANAOTHER SPOT 3	0	0.67	15.2	48.94	5.35	19.88	0.54	9.52	0.07	0	100.17
751 CHR AT MARGIN SPOT 4	0	0.61	14.94	49.04	5.30	19.66	0.53	9.53	0	0	99.61
752 CHR W CIRC INCL SPOT 5	0	0.62	14.58	50.23	4.92	20.02	0.5	9.41	0.05	0	100.33
753 CHR AT AMRGIN SPOT 6	0.02	0.67	14.6	49.89	4.60	19.54	0.45	9.51	0.11	0	99.39
754 CHR SPOT 7	0.01	0.76	15	49.99	5.22	20.45	0.4	9.49	0.11	0	101.42
755 CHR SPOT 7	0	0.77	15.08	49.39	5.67	20.08	0.64	9.59	0.1	0	101.32
756 CHR SPOT 7	0	0.65	14.47	48.74	5.58	19.89	0.45	9.27	0.05	0	99.10
757 CHR SPOT 8	0	0.71	13.54	49.01	6.00	19.96	0.5	9.07	0.05	0	98.84
758 CHR **** SAMPLE 266 LARGE CENTRAL, 1 03-08-4	0	0.66	15.25	48.89	4.48	19.83	0.5	9.38	0	0	98.99
759 CHR AT MARGIN SPOT 2	0	0.69	15.88	47.64	4.78	19.83	0.48	9.38	0.04	0.03	98.75
760 CHR AT MARGIN SPOT 2	0	0.69	15.15	48.19	5.14	19.34	0.46	9.56	0.15	0.03	98.72
761 CHR AT MARGIN SPOT 2	0	0.73	15.9	49.07	4.60	20.11	0.58	9.57	0.02	0	100.58
762 CHR GRAIN 2 SPOT 3	0	0.61	15.7	49.18	4.44	19.94	0.45	9.54	0	0	99.86
763 CHR GRAIN 2 SPOT 4	0	0.68	15.84	47.75	4.82	19.60	0.4	9.54	0.13	0	98.76
764 CHR GRAIN 3 SPOT 5	0	0.66	15.75	48.03	4.50	19.91	0.49	9.28	0.07	0	98.69
765 CHR GRAIN 3 SPOT 5	0	0.67	15.94	48.95	3.98	20.15	0.38	9.37	0.14	0	99.58
766 CHR GRAIN 4 SPOT 6	0	0.66	15.45	48.9	4.47	20.17	0.52	9.18	0.14	0.02	99.51
767 CHR *** SAMPLE 267 SPOT 1, 03-04-4086	0	0.45	14.11	49.03	5.36	20.30	0.51	8.68	0	0.05	98.49
768 CHR GRAIN 1 SPOT 2	0	0.54	14.57	48.58	5.95	20.32	0.44	9	0.08	0	99.48
769 CHR GRAIN 2 SPOT 3	0	0.56	14.49	49.79	5.19	20.76	0.49	8.79	0.16	0.02	100.25
770 CHR GRAIN 2 SPOT 4	0	0.51	14.66	49.87	5.54	20.91	0.56	8.81	0.15	0	101.00
771 CHR GRAIN 3 SPOT 5	0	0.65	14.64	49.62	4.74	20.51	0.57	8.94	0.06	0	99.72
772 CHR GRAIN 4 SPOT 6	0	0.51	14.27	49.85	5.23	20.87	0.45	8.71	0.04	0	99.93
773 CHR GRAIN 5 SPOT 7	0	0.49	14.85	50.16	4.43	20.56	0.48	8.87	0.21	0	100.05
774 CHR **** SAMPLE 268 SPOT 1 03-08-4089	0	0.57	18.74	43.41	5.34	24.70	0.56	6.63	0.08	0	100.02
775 CHR SPOT 2	0	0.68	17.71	42	6.21	24.76	0.52	6.18	0.05	0	98.11
776 CHR SPOT 2	0	0.7	17.8	42.39	6.18	24.53	0.55	6.35	0.24	0	98.74
777 CHR SPOT 2	0	0.63	18.31	42.66	5.87	25.06	0.48	6.31	0.05	0	99.37
778 CHR SPOT 3	0	0.6	19.04	43.1	5.08	24.98	0.44	6.53	0.1	0	99.87
779 CHR SMALLER GRAIN SPOT 3	0	0.65	18.51	43.91	5.03	24.92	0.57	6.5	0.17	0	100.26
780 CHR ANOTHER SPOT 4	0.04	0.59	18.49	42.92	6.14	24.83	0.58	6.37	0.2	0	100.17
781 CHR SMALL SPOT 7	0	0.69	17.32	42.73	6.26	24.75	0.53	6.24	0.06	0	98.58
782 CHR SMALL SPOT 7	0	0.73	18.08	43.23	5.27	25.15	0.6	6.16	0.14	0	99.36
783 CHR ANOTHER COARSE NO PHOTO	0	0.57	16.7	46.05	4.85	25.23	0.48	6.12	0.13	0	100.13
784 CHR AT MARGIN	0	0.62	17.98	44.04	5.53	24.70	0.57	6.54	0.17	0	100.15
785 CHR SMALLER IN MATRIX	0.01	0.78	18.23	43.66	5.62	25.31	0.56	6.37	0.15	0	100.69
786 CHR SMALLER IN MATRIX	0	0.74	18.42	43.5	5.68	24.98	0.6	6.54	0.15	0.05	100.67
787 CHR **** SAMPLE 272 CENTRAL SPOT 1, 05-09-42	0.19	0.5	15.03	49.76	5.53	19.81	0.64	8.94	0	0.2	100.60
788 CHR AT MARGIN SPOT 2	0.21	0.43	14.9	49	6.42	19.55	0.64	8.93	0.01	0.2	100.29
789 CHR CENTRAL SPOT 3	0.2	0.44	14.63	49.99	6.35	19.33	0.74	9.17	0	0.21	101.06

Black Label BT-09-31

	SiO2	TiO2	Al2O3	Cr2O3	Fe2O3	FeO	MnO	MgO	ZnO	NiO	TOTAL
790 CHR AT MARGIN SPOT 4	0.19	0.49	13.46	48.99	7.08	18.44	0.63	9.26	0	0.23	98.77
791 CHR SMALLER SPOT 5	0.19	0.47	14.52	50.38	5.70	19.47	0.67	9.09	0	0.2	100.69
792 CHR SMALLER SPOT 6	0.19	0.46	14.52	49.99	6.29	19.20	0.63	9.27	0	0.26	100.81
793 CHR SPOT 7	0.23	0.43	15.02	49.97	5.90	19.33	0.65	9.17	0	0.21	100.91
794 CHR SPOT 7	0.17	0.43	14.52	49.37	6.43	18.96	0.68	9.33	0	0.15	100.03
795 CHR SMALLER SPOT 8	0.19	0.49	14.67	48.81	6.43	18.96	0.68	9.21	0	0.22	99.65
796 CHR SMALL SPOT 9	0.23	0.42	14.62	49.33	6.83	18.78	0.63	9.37	0	0.23	100.44
797 CHR **** SAMPLE 273 L CENTRAL, SPOT 1, 05-08	0.2	0.49	14.88	50.16	5.62	19.37	0.53	9.28	0	0.21	100.73
798 CHR AT MARGIN SPOT 2	0.2	0.5	14.76	49.36	5.84	19.11	0.74	9.08	0.04	0.23	99.85
799 CHR CENTRAL SPOT 3	0.18	0.49	14.82	50.54	5.18	19.33	0.56	9.29	0	0.23	100.62
800 CHR AT MARGIN SPOT 4	0.22	0.46	14.01	48.35	7.12	18.02	0.7	9.4	0	0.23	98.50
801 CHR AT MARGIN SPOT 4	0.17	0.51	14.26	49.33	6.57	18.87	0.64	9.34	0	0.27	99.96
802 CHR CENTRAL SPOT 5	0.24	0.47	14.22	48.97	6.59	18.47	0.55	9.35	0	0.14	99.00
803 CHR AT MARGIN SPOT 6	0.25	0.52	14.87	50.01	6.38	19.15	0.58	9.41	0	0.23	101.40
804 CHR AT MARGIN SPOT 6	0.23	0.44	14.76	49.4	6.08	18.71	0.62	9.36	0	0.16	99.76
805 CHR ANOTHER SPOT 7	0.18	0.45	14.2	50.89	5.71	18.91	0.64	9.4	0.02	0.26	100.66
806 CHR SMALLER SPOT 8	0.2	0.5	13.93	50.39	6.36	18.72	0.71	9.42	0	0.22	100.45
807 CHR **** SAMPLE 274 CENTRAL, SPOT 1, 05-09-4	0.23	0.53	16.44	47.69	6.25	20.21	0.57	8.84	0	0.26	101.02
808 CHR CENTRAL, SPOT 1, 05-09-4225	0.22	0.67	16.08	48.1	6.00	20.13	0.68	8.86	0.09	0.23	101.06
809 CHR AT MARGIN SPOT 2	0.23	0.58	16.15	48.04	6.12	20.25	0.63	8.81	0	0.2	101.00
810 CHR AT MARGIN SPOT 2	0.24	0.58	15.11	47.58	6.43	19.46	0.65	8.75	0.02	0.2	99.01
811 CHR CENTRAL SPOT 3	0.18	0.53	16.1	48.72	5.80	20.40	0.57	8.91	0	0.22	101.43
812 CHR AT MARGIN SPOT 4	0.19	0.57	15.6	48.19	6.49	19.77	0.77	8.95	0	0.31	100.84
813 CHR CENTRAL SPOT 5	0.21	0.63	15.63	48.1	5.83	19.80	0.6	8.86	0.11	0.21	99.98
814 CHR AT MARGIN SPOT 6	0.3	0.95	16.06	47.86	5.35	20.08	0.59	8.84	0.01	0.18	100.23
815 CHR CENTRAL SPOT 7	0.22	0.6	15.27	47.32	6.71	19.27	0.61	9.02	0	0.21	99.23
816 CHR AT MARGIN SPOT 8	0.22	0.51	16.16	47.78	6.10	20.48	0.65	8.52	0	0.26	100.68
817 CHR SMALL SPOT 9	0.26	0.49	15.65	48.34	6.69	19.65	0.77	8.91	0	0.22	100.98
818 CHR *** SAMPLE 275 L CENTRAL SPOT 1, 04-09-4	0	0.67	15.39	48.27	5.05	20.51	0.58	9	0	0	99.47
819 CHR AT MARGIN SPOT 2	0	0.65	15.69	49.64	4.65	20.82	0.47	9.16	0.18	0	101.26
820 CHR AT MARGIN SPOT 2	0	0.8	15.71	48.01	4.32	20.53	0.55	8.99	0.04	0	98.94
821 CHR SMALLER SPOT 3	0	0.7	15.46	49.9	3.99	20.98	0.55	8.94	0.07	0	100.59
822 CHR AT MARGIN SPOT 4	0	0.7	15.3	48.76	4.95	20.70	0.59	8.95	0.07	0	100.02
823 CHR ANOTHER SPOY 5	0	0.66	15.14	48.7	4.78	20.74	0.52	8.78	0.12	0	99.44
824 CHR ANOTHER CENTRAL SPOT 6	0	0.72	15.91	49.26	4.52	20.93	0.57	9.11	0.09	0	101.10
825 CHR ANOTHER CENTRAL SPOT 6	0	0.64	15.91	48.25	4.83	20.67	0.5	9.05	0	0.03	99.88
826 CHR AT MARGIN SPOT 7	0	0.65	16.02	48.3	5.03	20.86	0.44	9.07	0.09	0	100.45
827 CHR SMALLER SPOT 8	0	0.76	15.72	49.4	4.50	21.26	0.54	8.95	0.06	0	101.19
828 CHR SMALLER SPOT 8	0	0.67	15.2	48.81	4.42	20.53	0.63	8.87	0	0	99.13
829 CHR SMALLER SPOT 9	0	0.74	15.19	48.68	5.24	20.81	0.5	8.97	0.11	0	100.23
830 CHR *** SAMPLE 276 CENTRAL 04-09-4095	0	1.09	13.77	43.07	9.31	25.68	0.59	5.49	0.16	0	99.16
831 CHR SAMPLE 276 CENTRAL 04-09-4095	0	1.11	14.39	44.25	7.95	26.30	0.48	5.48	0.09	0	100.05
832 CHR DARK CENTRAL SPOT 2	0	0.71	13.73	44.59	8.76	26.21	0.43	5.2	0.06	0	99.70
833 CHR BRIGHT MARGIN SPOT 3	0.05	1.82	8.15	41.34	16.16	28.71	0.65	3.36	0.25	0.01	100.51
834 CHR BRIGHT MARGIN SPOT 3	0.07	1.73	7.85	40.84	16.95	28.43	0.63	3.4	0.07	0.05	100.03
835 CHR ANOTHER V SMALL CENTRAL, NO PHOTO	0	1.19	15.68	43.08	7.47	25.74	0.52	5.91	0.13	0	99.72
836 CHR BRIGHT MARGIN	0.17	2.58	6.65	40.18	18.46	29.24	0.71	3.16	0.16	0.08	101.40
837 CHR BRIGHT MARGIN	0.21	2.28	6.7	40.49	18.36	28.96	0.64	3.01	0.23	0.04	100.92
838 CHR BRIGHT MARGIN	0.2	2.21	6.53	39.93	17.89	28.33	0.54	3.07	0.21	0.01	98.92
839 CHR V SMALL	0	1	15.75	42.42	8.69	25.59	0.47	6.01	0.09	0	100.02
840 CHR V SMALL	0	0.91	15.65	42.87	8.05	25.39	0.57	5.87	0.14	0	99.45
841 CHR ANOTHER SMALL CENTRAL	0	0.88	15.08	44.32	8.27	25.53	0.46	6.05	0.11	0	100.71
842 CHR ANOTHER SMALL CENTRAL	0	0.89	15.33	44.13	8.40	25.75	0.46	5.96	0.23	0	101.15
843 CHR ANOTHER SMALL CENTRAL	0	0.76	14.91	43.16	8.94	25.40	0.4	5.8	0.13	0.04	99.55
844 CHR **** SAMPLE 277 CENTRAL, SPOT 1, 04-09-4	0	0.69	14.94	49.2	4.80	22.89	0.56	7.64	0.1	0.02	100.84
845 CHR SAMPLE 277 CENTRAL, SPOT 1, 04-09-4096	0	0.7	14.77	49.29	4.29	22.72	0.6	7.55	0.13	0	100.05
846 CHR AT MARGIN SPOT 2	0	0.68	14.3	49.45	5.17	22.89	0.59	7.52	0.12	0	100.73
847 CHR AT MARGIN SPOT 2	0	0.73	13.8	49.33	4.06	22.68	0.48	7.22	0.17	0	98.47
848 CHR ANOTHER CENTRAL, SPOT 3	0	0.69	14.42	50.64	3.75	23.44	0.46	7.36	0	0	100.76
849 CHR ANOTHER CENTRAL, SPOT 3	0	0.59	13.95	48.99	4.67	22.40	0.55	7.33	0.14	0	98.62
850 CHR AT MARGIN SPOT 4	0	0.72	14.6	49.17	4.28	22.91	0.57	7.37	0.14	0	99.77
851 CHR ANOTHER CENTRAL, SPOT 5	0	0.65	15.11	48.12	4.42	22.50	0.51	7.56	0.07	0	98.94
852 CHR AT MARGIN SPOT 6	0	0.64	14.74	50.25	4.20	23.26	0.48	7.49	0.06	0.03	101.15
853 CHR AT MARGIN SPOT 6	0	0.64	14.72	48.76	4.58	22.72	0.55	7.45	0.08	0	99.50
854 CHR ANOTHER CENTRAL SPOT 7	0.01	0.66	14.84	48.94	4.42	22.76	0.51	7.45	0.18	0	99.77
855 CHR AT MARGIN SPOT 8	0	0.6	14.72	49.86	4.23	22.82	0.55	7.52	0.16	0	100.46
856 CHR AT MARGIN SPOT 8	0	0.65	14.54	50.19	4.12	23.26	0.53	7.36	0.09	0	100.73
857 CHR AT MARGIN SPOT 8	0	0.63	14.45	49.44	4.03	22.79	0.44	7.37	0.14	0	99.29
858 CHR **** SAMPLE 278 CENTRAL, SPOT 1, 06-09-4	0.26	0.66	15.15	49.43	4.55	22.60	0.57	7.04	0.01	0.31	100.58
859 CHR AT MARGIN SPOT 2	0.27	0.57	14.82	48.61	5.74	21.58	0.65	7.44	0.05	0.2	99.94
860 CHR CENTRAL SPOT 3	0.2	0.65	15.09	49.19	4.37	22.48	0.6	7.16	0	0.22	99.96
861 CHR SPOT 4	0.27	0.58	14.63	48.36	6.24	22.21	0.68	7.08	0.02	0.2	100.26
862 CHR CENTRAL SPOT 5	0.23	0.68	14.88	49.27	4.92	22.24	0.66	7.27	0.04	0.21	100.40
863 CHR AT MARGIN SPOT 6	0.19	0.6	14.33	48.92	5.59	22.15	0.64	7.24	0	0.21	99.87
864 CHR SMALLER SPOT 7	0.22	0.57	14.68	49.33	5.75	22.17	0.51	7.5	0.01	0.16	100.91
865 CHR SMALLER SPOT 7	0.22	0.63	13.98	47.95	6.50	21.69	0.73	7.27	0	0.14	99.11
866 CHR ANOTHER SPOT 8	0.25	0.64	14.8	49.18	5.53	22.10	0.62	7.4	0.01	0.2	100.73
867 CHR SPOT 9	0.26	0.57	11.22	47.58	10.29	22.48	0.67	6.37	0.08	0.23	99.75
868 CHR **** SAMPLE 279, CENTRAL, SPOT 1, 05-09-	0.19	0.58	17.18	46.74	5.41	21.75	0.61	7.92	0	0.29	100.67

Black Label BT-09-31

	SiO2	TiO2	Al2O3	Cr2O3	Fe2O3	FeO	MnO	MgO	ZnO	NiO	TOTAL
869 CHR AT MARGIN SPOT 2	0.22	0.47	16.99	45.54	6.90	21.32	0.63	7.97	0	0.24	100.28
870 CHR ANOTHER CENTRAL SPOT 3	0.19	0.68	16.99	45.56	6.22	21.15	0.59	8.22	0	0.23	99.82
871 CHR AT MARGIN SPOT 4	0.14	0.58	17.04	45.51	6.16	21.66	0.54	8.02	0	0.17	99.82
872 CHR ANOTHER CENTRAL SPOT 5	0.21	0.64	17.66	45.85	5.58	21.85	0.6	7.9	0	0.25	100.54
873 CHR AT MARGIN SPOT 6	0.25	0.67	17.03	46.36	6.16	21.07	0.57	8.29	0	0.28	100.68
874 CHR AT MARGIN SPOT 6	0.24	0.57	15.94	43.78	8.56	19.94	0.52	8.36	0.06	0.24	98.21
875 CHR SMALLER SPOT 8	0.14	0.52	17.11	45.76	5.93	21.50	0.59	8.01	0	0.25	99.81
876 CHR **** SAMPLE 280 CENTRAL, SPOT 1, 05-09-4	0.19	0.54	14.48	49.88	4.61	23.22	0.62	6.66	0	0.22	100.40
877 CHR AT MARGIN SPOT 2	0.25	0.64	14.73	48.77	5.10	22.93	0.73	6.62	0	0.22	99.99
878 CHR CENTRAL, SPOT 3	0.23	0.5	14.45	50.15	4.77	23.34	0.61	6.53	0	0.24	100.82
879 CHR CENTRAL, SPOT 3	0.22	0.53	13.6	48.56	5.64	22.12	0.6	6.75	0	0.22	98.24
880 CHR CENTRAL, SPOT 3	0.23	0.58	14.65	49.35	4.89	23.22	0.66	6.55	0.05	0.2	100.38
881 CHR AT MARGIN SPOPT 4	0.24	0.53	14.53	48.36	5.86	22.92	0.63	6.63	0	0.17	99.87
882 CHR SMALLER SPOT 5	0.29	0.57	14.98	49.43	5.30	23.50	0.66	6.45	0.07	0.22	101.47
883 CHR SMALLER SPOT 5	0.2	0.53	14.02	48.76	5.94	22.88	0.63	6.65	0	0.23	99.84
884 CHR SMALLER SPOT 6	0.21	0.62	14.85	49.57	4.98	23.71	0.62	6.55	0	0.24	101.35
885 CHR SMALLER SPOT 6	0.2	0.51	14.77	48.9	5.44	23.41	0.56	6.57	0	0.25	100.61
886 CHR SMALLER SPOT 7	0.23	0.54	14.32	48.81	5.85	22.84	0.58	6.71	0.03	0.26	100.17
887 CHR SMALL SPOT 9	0.2	0.54	14.5	48.21	6.14	22.98	0.58	6.7	0	0.28	100.13
888 CHR ****SAMPLE 282 CENTRAL, SPOT 1, 04-09-4097	0	0.51	13.2	50.51	4.64	25.28	0.43	5.8	0.15	0	100.51
889 CHR SAMPLE 282 CENTRAL, SPOT 1, 04-09-4097	0.09	0.48	13.21	50	5.74	24.83	0.56	5.87	0.1	0.01	100.88
890 CHR AT MARGIN SPOT 2	0.03	0.53	13.82	51.24	3.66	25.54	0.47	5.76	0.15	0	101.20
891 CHR AT MARGIN SPOT 2	0.02	0.46	13.68	50.01	5.14	25.24	0.48	5.89	0.11	0	101.02
892 CHR AT MARGIN SPOT 2	0	0.45	13.85	50.79	3.54	25.51	0.46	5.7	0.04	0	100.33
893 CHR AT MARGIN SPOT 2	0.02	0.57	13.74	49.75	4.80	25.46	0.5	5.79	0	0	100.63
894 CHR **** SAMPLE 287 DARK CENTRAL, SPOT 1, 05-09-4230	0.29	0.66	11.93	42.04	13.75	28.01	0.89	2.66	0.45	0.22	100.91
895 CHR DARK CENTRAL, SPOT 1, 05-09-4230	0.28	0.63	11.19	41.42	14.18	27.27	0.83	2.73	0.46	0.26	99.25
896 CHR OUTER ZONE SPOT 2	0.44	1.15	1.44	37.93	28.32	28.04	0.92	1.23	0.23	0.3	100.00
897 CHR ANOTHER ZONED, DARK CENTRAL, SPOT 3	0.31	0.49	12.21	41.63	14.15	27.84	0.82	2.57	0.66	0.22	100.90
898 CHR ANOTHER ZONED, DARK CENTRAL, SPOT 3	0.28	0.48	11.1	41.15	14.42	27.15	0.76	2.59	0.48	0.34	98.74
899 CHR **** SAMPLE 288 CENTRAL SPOT 1, 05-09-42	0.24	0.51	14.04	48.93	5.78	24.26	0.6	5.77	0	0.25	100.38
900 CHR AT MARGIN SPOT 2	0.28	0.51	14.41	48.48	5.89	24.77	0.68	5.35	0.07	0.25	100.69
901 CHR AT MARGIN SPOT 2	0.3	0.39	14.15	47.97	6.49	23.74	0.75	5.61	0	0.35	99.75
902 CHR BRIGHT AT MARGIN SPOT 3	0.21	0.75	4.09	50.98	12.12	26.15	0.85	3.06	0.04	0.29	98.54
903 CHR CENTRAL SPOT 4	0.28	0.37	13.13	50.33	5.56	24.47	0.8	5.26	0	0.22	100.43
904 CHR AT MARGIN SPOT 5	0.29	0.41	12.27	49.51	6.68	23.98	0.73	5.29	0	0.27	99.43
905 CHR CENTRAL SPOT 6	0.3	0.29	11.94	51.77	6.33	24.35	0.66	5.33	0.04	0.28	101.28
906 CHR CENTRAL SPOT 6	0.26	0.4	11.59	51.75	6.06	24.49	0.7	5.22	0	0.34	100.82
907 CHR CENTRAL SPOT 6	0.22	0.31	11.39	50.72	6.54	23.85	0.84	5.28	0.11	0.25	99.50
908 CHR AT MARGIN SPOT 7	0.25	0.33	11.58	51.14	6.20	24.76	0.73	4.96	0	0.19	100.14
909 CHR SMALLER SPOT 8	0.29	0.32	11.52	51.04	6.82	24.25	0.88	5.02	0.15	0.29	100.58
910 CHR **** SAMPLE 299 SPOT 1, CENTRAL, 05-10-4	0.19	0.44	14.71	47.42	6.34	25.12	0.72	5.26	0	0.3	100.51
911 CHR AT MARGIN SPOT 2	0.22	0.48	14.77	47.75	6.05	25.69	0.67	4.96	0.07	0.25	100.91
912 CHR AT MARGIN SPOT 2	0.23	0.37	13.93	47.16	6.34	24.52	0.7	5.08	0	0.25	98.59
913 CHR AT MARGIN SPOT 2	0.23	0.47	14.66	46.29	6.45	24.62	0.88	5.07	0.02	0.3	99.00
914 CHR SMALLER SPOT 3	0.23	0.46	15.21	45.76	7.25	25.28	0.83	5.04	0	0.24	100.30
915 CHR SPOT 4	0.22	0.47	15.09	45.39	8.11	25.65	0.65	4.97	0.05	0.33	100.93
916 CHR SPOT 4	0.21	0.42	14.72	45.53	8.28	25.30	0.75	5.06	0	0.3	100.57
917 CHR SMALLER SPOT 5	0.15	0.41	14.93	44.35	8.19	25.73	0.61	4.81	0	0.28	99.46
918 CHR SMALLER SPOT 7	0.16	0.45	15.34	43.7	7.74	25.63	0.66	4.72	0	0.29	98.70
919 CHR SMALLER SPOT 7	0.2	0.47	15.81	45.36	7.21	26.01	0.71	4.92	0.01	0.21	100.91
920 CHR SMALLER SPOT 7	0.16	0.49	15.17	44.37	7.84	25.86	0.73	4.71	0.06	0.27	99.65
921 CHR SPOT 6	0.22	0.49	16.18	44.89	6.90	25.32	0.74	5.15	0	0.32	100.21
922 CHR SPOT 6	0.19	0.54	15.42	44.95	6.41	25.23	0.64	5.02	0	0.24	98.64
923 CHR L RANDOM, CENTRAL, NO PHOTO	0.13	0.51	15.23	44.76	7.61	25.46	0.71	5.12	0.02	0.3	99.84
924 CHR AT MARGIN	0.23	0.54	15.48	44.07	7.71	25.02	0.73	5.08	0.08	0.2	99.14
925 CHR ADJ SMALLER	0.17	0.54	15.05	44.9	8.28	25.01	0.82	5.31	0.12	0.31	100.52
926 CHR **** SAMPLE 300 CENTRAL, SPOT 1, 05-10-4	0.17	0.49	13.46	49.53	5.88	19.88	0.78	8.26	0	0.22	98.67
927 CHR CENTRAL, SPOT 1, 05-10-4239	0.13	0.53	14.39	48.32	5.88	20.23	0.62	8.35	0	0.22	98.67
928 CHR AT MARGIN SPOT 2	0.14	0.43	13.87	48.82	5.61	21.38	0.69	7.38	0.06	0.2	98.57
929 CHR AT MARGIN SPOT 2	0.18	0.46	15.07	48.65	5.51	21.61	0.63	7.6	0	0.27	99.98
930 CHR ANOTHER CENTRAL, SPOT 3	0.17	0.52	15.7	48.97	5.00	20.72	0.65	8.33	0.09	0.29	100.44
931 CHR AT MARGIN SPOT 4	0.12	0.54	13.57	49.07	5.52	21.67	0.73	7.28	0.05	0.21	98.76
932 CHR ANOTHER CENTRAL SPOT 5	0.17	0.52	14.59	47.54	6.07	20.48	0.66	7.91	0.04	0.33	98.31
933 CHR ANOTHER CENTRAL SPOT 5	0.11	0.46	15.58	48.91	5.40	21.13	0.7	8.25	0	0.29	100.83
934 CHR ANOTHER CENTRAL SPOT 5	0.16	0.41	14.78	48.39	5.98	20.63	0.71	8.09	0	0.19	99.34
935 CHR AT MARGIN SPOT 6	0.19	0.45	14.51	49.72	5.68	21.77	0.75	7.47	0.16	0.2	100.90
936 CHR AT MARGIN SPOT 6	0.18	0.45	13.94	49.47	4.97	21.70	0.66	7.12	0.11	0.24	98.85
937 CHR CENTRAL SPOT 7	0.15	0.47	15.21	48.79	5.31	21.73	0.7	7.62	0.04	0.25	100.27
938 CHR AT MARGIN SPOT 8'R SC SM	0.16	0.49	15.19	48.75	4.94	21.73	0.65	7.55	0	0.25	99.72
939 CHR CENTRAL SPOT 9	0.14	0.51	14.5	48.8	5.65	21.29	0.65	7.76	0	0.31	99.61
940 CHR SPOT 10	0.14	0.47	14.29	48.43	5.60	21.47	0.72	7.4	0.03	0.25	98.80
941 CHR SPOT 10	0.19	0.44	14.93	48.15	5.36	21.20	0.75	7.48	0	0.29	98.79
942 CHR SPOT 10	0.11	0.5	14.69	48.67	5.45	22.06	0.73	7.36	0	0.27	99.85
943 CHR **** SAMPLE 301 SPOT 1 CENTRAL, 05-10-42	0.27	0.45	15.18	49.28	5.58	19.23	0.7	8.86	0	0.3	99.85
944 CHR AT MARGIN SPOT 2	0.19	0.45	13.9	50.06	4.88	20.87	0.69	7.72	0	0.23	98.99
945 CHR ANOTHER CENTRAL, SPOPT 3	0.15	0.47	14.63	50.67	5.11	20.15	0.87	8.65	0	0.25	100.95
946 CHR ANOTHER CENTRAL, SPOPT 3	0.19	0.46	14.68	48.83	5.21	19.45	0.7	8.6	0	0.21	98.33
947 CHR ANOTHER CENTRAL, SPOPT 3	0.14	0.46	15.3	48.97	5.25	19.66	0.7	8.89	0	0.24	99.62

Black Label BT-09-31

	SiO2	TiO2	Al2O3	Cr2O3	Fe2O3	FeO	MnO	MgO	ZnO	NiO	TOTAL
948 CHR AT MARGIN SPOT 4	0.17	0.45	14.68	49.62	5.77	20.51	0.76	8.39	0	0.16	100.51
949 CHR SMALLER SPOT 5	0.15	0.47	15.49	48.49	5.40	20.88	0.64	8.22	0.01	0.21	99.96
950 CHR SPOT 6	0.17	0.51	14.98	49.07	5.63	20.06	0.69	8.59	0	0.33	100.02
951 CHR SMALLER SPOT 7	0.15	0.5	15.37	48.14	5.58	20.47	0.74	8.24	0.1	0.3	99.59
952 CHR SPOT 7	0.18	0.5	14.63	48.08	5.79	20.09	0.68	8.2	0	0.3	98.45
953 CHR SPOT 7	0.11	0.47	15.33	49.36	4.64	21.02	0.68	8.18	0	0.26	100.04
954 CHR ANOTHER SPOT 8	0.13	0.47	14.82	49.81	4.74	21.09	0.66	8.04	0	0.26	100.02
955 CHR SPOT 9	0.17	0.48	15.53	48.4	5.48	20.83	0.6	8.21	0	0.27	99.97
956 CHR **** SAMPLE 311 SPOT 1, 05-09-4236	0.2	0.43	15.18	50.33	4.22	22.12	0.58	7.4	0	0.32	100.78
957 CHR AT MARGIN SPOT 2	0.22	0.4	15.34	48.78	5.47	21.86	0.71	7.39	0.01	0.24	100.43
958 CHR SPOT 3	0.14	0.42	14.78	49.34	4.86	22.03	0.69	7.32	0	0.24	99.82
959 CHR CENTRAL SPOT 4	0.2	0.42	15.26	50.5	4.45	21.61	0.62	7.81	0	0.28	101.15
960 CHR CENTRAL SPOT 4	0.14	0.41	15.17	48.74	5.36	21.13	0.72	7.83	0	0.41	99.91
961 CHR AT MARGIN SPOT 5	0.26	0.44	15.77	49.55	4.93	21.69	0.62	7.65	0	0.36	101.27
962 CHR AT MARGIN SPOT 5	0.27	0.43	14.73	49.56	5.23	21.26	0.68	7.58	0	0.19	99.93
963 CHR CENTRAL SPOT 6	0.2	0.37	15.46	49.59	4.90	21.45	0.62	7.72	0.03	0.4	100.73
964 CHR AT MARGIN SPOT 7	0.19	0.37	15.66	49.43	4.78	22.09	0.6	7.46	0	0.32	100.90
965 CHR AT MARGIN SPOT 7	0.2	0.39	15.58	49.45	4.76	21.97	0.7	7.43	0.05	0.28	100.81
966 CHR SMALLER SPOT 8	0.16	0.38	15.5	49.68	4.94	22.16	0.72	7.5	0	0.3	101.33
967 CHR SMALLER SPOT 8	0.15	0.46	15.63	49.07	4.94	22.44	0.79	7.24	0.11	0.31	101.15
968 CHR SMALLER SPOT 8	0.15	0.33	15.36	48.85	4.77	21.99	0.69	7.23	0	0.37	99.74
969 CHR **** SAMPLE 312 SPOT 1 05-09-4235	0.2	0.39	14.77	49.06	4.81	22.88	0.69	6.6	0	0.17	99.57
970 CHR SPOT 2	0.16	0.33	14.76	47.99	6.28	23.06	0.66	6.56	0.05	0.29	100.14
971 CHR LARGER CENTRAL NOT IN PHOTO	0.21	0.32	13.58	50.07	5.25	22.85	0.82	6.27	0.07	0.26	99.70
972 CHR AT MARGIN	0.26	0.37	13.7	51.24	5.03	23.14	0.83	6.37	0.01	0.22	101.17
973 CHR AT MARGIN	0.2	0.29	13.97	50.31	5.20	23.10	0.72	6.42	0	0.27	100.48
974 CHR V LARGE CENTRAL, NO PHOTO	0.19	0.34	14.69	49.41	5.65	22.56	0.73	6.96	0	0.26	100.79
975 CHR AT MARGIN	0.17	0.35	14.49	48.76	6.45	23.43	0.78	6.42	0.01	0.32	101.18
976 CHR AT MARGIN	0.17	0.44	14.26	48.91	6.39	23.44	0.63	6.55	0	0.28	101.07
977 CHR **** SAMPLE 313 L CENTRAL, SPOT 1, 05-09	0.21	0.36	13.55	52.12	4.93	22.23	0.56	7.3	0	0.24	101.50
978 CHR L CENTRAL, SPOT 1, 05-09-4234	0.2	0.32	13.24	51.26	5.10	21.48	0.73	7.32	0	0.21	99.86
979 CHR AT MARGIN SPOT 2	0.28	0.32	13.93	50.82	5.49	20.98	0.67	7.66	0	0.24	100.39
980 CHR SMALLER SPOT 3	0.22	0.32	14.34	51.29	4.73	21.16	0.77	7.71	0.05	0.28	100.87
981 CHR SMALLER SPOT 3	0.24	0.35	14.11	51.67	4.45	21.41	0.71	7.57	0	0.24	100.75
982 CHR SPOT 4	0.23	0.36	13.88	52.05	4.66	21.73	0.7	7.48	0	0.27	101.36
983 CHR SPOT 4	0.21	0.37	13.98	50.6	5.54	21.40	0.7	7.6	0	0.28	100.67
984 CHR SPOT 5	0.21	0.34	13.88	51.8	4.99	21.73	0.69	7.52	0	0.29	101.45
985 CHR SPOT 5	0.22	0.29	13.99	50.83	5.41	21.25	0.66	7.59	0.04	0.32	100.60
986 CHR SMALLER SPOT 6	0.22	0.35	13.96	51.68	5.06	21.88	0.7	7.45	0.04	0.22	101.56
987 CHR SMALLER SPOT 6	0.2	0.36	13.88	50.68	5.12	21.51	0.66	7.51	0	0.17	100.09
988 CHR SMALLER SPOT 7	0.22	0.36	13.83	50.73	5.64	21.43	0.8	7.52	0	0.22	100.76
989 CHR SMALLER SPOT 8	0.22	0.28	13.74	49.69	5.68	20.92	0.66	7.49	0	0.25	98.93
990 CHR **** SAMPLE 317 SPOT 1 CENTRAL, 05-10-42	0.15	0.43	14.04	50.52	4.78	18.74	0.6	9.21	0	0.22	98.70
991 CHR SPOT 1 CENTRAL, 05-10-4242	0.12	0.5	14.35	50.39	5.02	18.36	0.64	9.69	0.03	0.21	99.31
992 CHR AT MARGIN SPOT 2	0.13	0.51	14.25	50.89	5.28	19.34	0.57	9.34	0	0.21	100.52
993 CHR CENTRAL SPOT 3	0.18	0.47	14.95	50.12	5.33	19.15	0.58	9.36	0	0.19	100.33
994 CHR AT MARGIN SPOT 4	0.17	0.43	14.42	50.3	5.08	18.82	0.61	9.29	0	0.19	99.31
995 CHR ANOTHER CENTRAL, SPOT 5	0.19	0.4	13.81	50.15	5.73	18.65	0.63	9.12	0.05	0.24	98.97
996 CHR AT MARGIN	0.17	0.47	15.2	50.29	5.04	18.94	0.69	9.49	0	0.23	100.52
997 CHR SPOT 7	0.13	0.46	15.21	49.36	5.54	18.98	0.53	9.5	0	0.31	100.01
998 CHR SMALLER SPOT 9	0.17	0.46	15.05	50.02	5.14	19.33	0.51	9.27	0	0.21	100.16
999 CHR SPOT 9	0.15	0.49	13.97	49.72	5.83	18.82	0.66	9.25	0	0.16	99.05
1000 CHR **** SAMPLE 318 SPOT 1, CENTRAL, 05-10-4	0.16	0.35	14.58	50.61	5.03	19.30	0.65	9.03	0.05	0.23	99.99
1001 CHR AT MARGIN SPOT 2	0.15	0.4	15.01	51.17	4.90	19.74	0.6	9.22	0	0.2	101.39
1002 CHR AT MARGIN SPOT 2	0.19	0.43	15.02	50.4	4.75	19.56	0.59	8.98	0	0.25	100.18
1003 CHR CENTRAL SPOT 3	0.16	0.4	13.36	49.83	5.76	19.14	0.64	8.69	0	0.25	98.23
1004 CHR CENTRAL SPOT 3	0.17	0.41	14.56	51.14	4.67	19.96	0.51	8.86	0.03	0.17	100.48
1005 CHR CENTRAL SPOT 3	0.16	0.38	13.94	50.72	5.34	19.83	0.56	8.7	0	0.22	99.84
1006 CHR AT MARGIN SPOT 4	0.13	0.34	12.8	50.38	6.03	19.11	0.65	8.66	0.07	0.28	98.44
1007 CHR AT MARGIN SPOT 4	0.14	0.44	13.86	51.66	4.70	19.94	0.54	8.8	0.05	0.21	100.34
1008 CHR SMALLER CENTRAL SPOT 5	0.15	0.43	14.29	51.27	5.40	19.72	0.62	9.09	0.01	0.24	101.22
1009 CHR SMALLER CENTRAL SPOT 5	0.13	0.42	13.93	50.47	4.91	19.42	0.65	8.77	0	0.31	99.01
1010 CHR ANOTHER SPOT 6	0.12	0.4	14.4	50.51	5.11	19.98	0.64	8.72	0.09	0.22	100.19
1011 CHR SPOT 7	0.11	0.4	14.09	50.61	4.37	19.91	0.54	8.61	0	0.21	98.85
1012 CHR SMALLER SPOT 8	0.12	0.41	14.55	50.3	5.38	19.59	0.61	9.07	0	0.25	100.28
1013 CHR SMALLEST SPOT 9	0.11	0.37	13.94	50.63	4.71	19.79	0.63	8.62	0	0.23	99.03
1014 CHR SMALLEST SPOT 9	0.13	0.44	14.62	49.39	5.22	19.63	0.66	8.76	0	0.26	99.11
1015 CHR AT MARGIN SPOT 10	0.79	0.56	4.91	57.41	8.86	19.13	0.79	6.45	0.11	0.3	99.31
1016 CHR AT MARGIN SPOT 10	0.81	0.53	4.82	58.04	8.11	19.27	0.69	6.33	0.08	0.24	98.92
1017 CHR **** SAMPLE 319 SPOT 1, CENTRAL, 05-10-4	0.12	0.4	15.1	50.62	4.87	19.72	0.59	9.15	0.02	0.27	100.86
1018 CHR SPOT 1, CENTRAL, 05-10-4245	0.14	0.41	15.12	50.57	4.49	19.26	0.73	9.21	0	0.24	100.17
1019 CHR AT MARGIN SPOT 2	0.16	0.3	15.24	51.1	4.93	19.48	0.65	9.29	0	0.19	101.34
1020 CHR AT MARGIN SPOT 2	0.19	0.42	14.24	50.24	5.13	19.09	0.63	8.95	0	0.26	99.15
1021 CHR CENTRAL SPOT 3	0.12	0.48	14.42	50.71	5.04	19.40	0.56	9.16	0.1	0.32	100.30
1022 CHR AT MARGIN SPOT 4	0.17	0.34	14.92	50.29	4.85	19.42	0.6	8.99	0	0.22	99.80
1023 CHR CENTRAL SPOT 5	0.15	0.44	13.95	50.49	4.87	19.77	0.48	8.7	0	0.21	99.06
1024 CHR MARGIN SPOT 6	0.17	0.43	15.07	50.21	4.01	19.66	0.47	8.86	0	0.2	99.08
1025 CHR SPOT 7 CENTRAL	0.16	0.46	14.48	50.61	4.91	19.40	0.65	9.02	0	0.27	99.96
1026 CHR GRAIN CENTRAL SPOT 8	0.15	0.46	13.77	50.08	4.91	19.44	0.61	8.65	0	0.23	98.30

Black Label BT-09-31

	SiO2	TiO2	Al2O3	Cr2O3	Fe2O3	FeO	MnO	MgO	ZnO	NiO	TOTAL
1027 CHR GRAIN CENTRAL SPOT 8	0.15	0.42	15	50.19	4.70	19.13	0.57	9.28	0	0.2	99.64
1028 CHR CENTRAL, SPOT 1, 05-100-4246	0.19	0.29	13.17	50.79	5.04	20.01	0.48	8.12	0	0.21	98.29
1029 CHR CENTRAL, SPOT 1, 05-100-4246	0.19	0.33	13.18	50.84	5.18	19.89	0.61	8.24	0	0.14	98.60
1030 CHR AT MARGIN SPOT 2	0.15	0.42	13.92	50.1	4.48	20.29	0.56	8.16	0	0.15	98.23
1031 CHR SPOT 5	0.12	0.4	13.4	51.42	4.25	20.83	0.57	7.99	0	0.16	99.14
1032 CHR SPOT 6 GRAIN MARHIN	0.13	0.31	13.56	50.56	4.90	20.41	0.63	8.05	0.04	0.17	98.76
1033 CHR **** SAMPLE 332 SPI 1 CENTRAL, 05-11-425	0.12	0.48	13.1	50.29	6.34	21.23	0.62	7.88	0.01	0.24	100.30
1034 CHR AT MARGIN SPOT 2	0.17	0.39	12.64	49.06	7.59	21.05	0.59	7.6	0	0.22	99.31
1035 CHR CENTRAL SPOT 3	0.12	0.44	13.34	50.06	5.47	21.08	0.52	7.82	0	0.2	99.06
1036 CHR CENTRAL SPOT 3	0.13	0.41	13.3	50.78	5.68	21.08	0.64	7.88	0.01	0.27	100.18
1037 CHR AT MARGIN SPOT 4	0.13	0.37	13.27	50.66	6.01	21.20	0.63	7.87	0.02	0.17	100.32
1038 CHR CENTRAL SPOT 5	0.18	0.43	13.37	49.37	6.26	20.21	0.62	8.11	0	0.2	98.75
1039 CHR CENTRAL SPOT 5	0.12	0.43	13.06	49.34	6.83	20.86	0.62	7.88	0.02	0.25	99.41
1040 CHR AT MARGIN SPOT 6	0.18	0.41	12.75	49.52	6.65	20.80	0.7	7.63	0	0.16	98.80
1041 CHR AT MARGIN SPOT 6	0.14	0.48	12.73	49	6.55	20.61	0.6	7.74	0	0.27	98.12
1042 CHR AT MARGIN SPOT 6	0.16	0.38	12.83	51.02	6.51	21.28	0.68	7.76	0.02	0.19	100.83
1043 CHR SMALLER SPOT 7	0.12	0.45	12.18	50.32	7.07	21.97	0.53	7.33	0.01	0.21	100.19
1044 CHR SMALLER SPOT 8	0.19	0.56	12.73	49.39	6.79	20.85	0.54	7.8	0	0.17	99.02
1045 CHR SMALLER SPOT 8	0.14	0.67	12.87	49.64	6.46	21.20	0.58	7.84	0.01	0.21	99.62
1046 CHR **** SAMPLE 333 SPOT 1,K CENTRAL, 05-11-	0.1	0.43	14.84	51.35	3.90	19.69	0.62	9.11	0	0.23	100.27
1047 CHR AT MARGIN SPOT 2	0.09	0.37	14.93	50.12	4.70	19.59	0.64	9.04	0	0.22	99.70
1048 CHR OPPOSIRTE MARGIN SPOT 3	0.1	0.42	14.6	50.12	4.39	19.41	0.66	8.94	0.01	0.21	98.86
1049 CHR CENTRAL SPOT 4	0.11	0.42	14.71	51.13	4.44	19.76	0.56	9.1	0.05	0.17	100.45
1050 CHR CENTRAL SPOT 4	0.11	0.47	14.53	50.17	4.47	19.23	0.57	9.1	0	0.27	98.92
1051 CHR CENTRAL SPOT 4	0.11	0.42	14.74	50.41	4.37	19.35	0.59	9.12	0	0.21	99.33
1052 CHR AT MARGIN SPOT 7	0.2	0.42	14.99	50.26	4.38	19.13	0.54	9.1	0	0.2	99.22
1053 CHR SMALLER SPOT 8	0.12	0.39	14.82	49.71	4.77	19.28	0.54	9.08	0	0.21	98.92
1054 CHR SMALLER SPOT 8	0.13	0.49	14.92	50.39	3.79	19.27	0.59	9.1	0	0.21	98.89
1055 CHR SMALLER SPOT 9	0.09	0.45	14.64	49.63	4.75	19.25	0.68	9.04	0	0.25	98.78
1056 CHR **** SAMPLE 334 SPOT 1, CENTRAL, 05-11-4	0.2	0.44	14.37	49.67	5.33	18.73	0.59	9.12	0	0.26	98.71
1057 CHR AT MARGIN SPOT 2	0.13	0.44	14.36	50.54	5.17	19.39	0.61	9.15	0	0.19	99.98
1058 CHR SPOT 1 AGAIN	0.12	0.5	14.49	50.34	4.76	19.22	0.65	9.2	0	0.2	99.49
1059 CHR ANOTHER SPOT 3	0.09	0.48	14.74	49.38	4.91	18.80	0.55	9.42	0	0.23	98.60
1060 CHR CENTRAL SPOT 4	0.12	0.41	14.79	50.64	4.26	18.93	0.48	9.43	0	0.22	99.28
1061 CHR CENTRAL SPOT 4	0.17	0.53	15.22	49.68	4.73	19.01	0.65	9.32	0	0.2	99.51
1062 CHR CENTRAL SPOT 6	0.13	0.45	14.73	50.84	3.98	19.22	0.48	9.24	0	0.22	99.29
1063 CHR SMALLER SPOT 7	0.07	0.4	14.78	50.48	4.50	19.98	0.64	8.85	0.06	0.23	99.99
1064 CHR V SMALL SPOT 8	0.15	0.41	14.38	50.52	4.19	19.08	0.61	8.98	0	0.22	98.54
1065 CHR V SMALL SPOT 8	0.08	0.51	14.67	49.85	4.47	19.65	0.6	8.94	0	0.26	99.03
1066 CHR V SMALL SPOT 9	0.14	0.51	15.22	49.22	4.97	19.42	0.58	9.09	0	0.27	99.42
1067 CHR ****SAMPLE 341 SPOT 1 CENTRAL, 05-10-4248	0.1	0.35	14.5	51.11	4.86	17.77	0.54	10.18	0	0.26	99.67
1068 CHR SPOT 1	0.1	0.35	14.28	51.58	4.10	17.87	0.5	9.98	0	0.28	99.04
1069 CHR GRAIN MARGIN SPOT 2	0.09	0.4	14.45	50.55	4.30	17.86	0.65	9.88	0	0.18	98.36
1070 CHR GRAIN MARGIN SPOT 2	0.1	0.35	14.67	51.88	4.00	18.14	0.59	10.01	0	0.24	99.98
1071 CHR ANOTHER CENTRAL, SPOT 3	0.09	0.38	14.46	51.49	4.23	18.37	0.53	9.82	0	0.28	99.65
1072 CHR AT MARGIN SPOT 4	0.12	0.4	14.61	50.44	4.61	17.65	0.68	10.02	0	0.16	98.69
1073 CHR AT MARGIN SPOT 4	0.08	0.38	14.45	51.12	4.82	18.01	0.64	9.97	0.06	0.34	99.87
1074 CHR ANOTHER SPOT 5	0.15	0.44	14.25	52.16	4.16	18.18	0.61	9.89	0	0.22	100.06
1075 CHR AT MARGIN SPOT 6	0.1	0.35	15.1	51.89	3.83	17.90	0.56	10.34	0	0.15	100.21
1076 CHR SPOT 7	0.1	0.38	14.36	52.16	4.46	18.45	0.49	9.97	0.01	0.27	100.65
1077 CHR AT MARGIN SPOT 8	0.07	0.35	14.57	51.72	3.67	18.61	0.6	9.68	0	0.19	99.46
1078 CHR **** SAMPLE 342 SPOT 1, CENTRAL, 05-11-4	0.15	0.34	14.48	51.34	4.98	17.09	0.57	10.48	0	0.27	99.70
1079 CHR SPOT 2	0.14	0.43	14.34	52.06	3.94	18.47	0.48	9.8	0	0.17	99.82
1080 CHR CENTRAL SPOT 3	0.09	0.43	14.17	51.79	4.74	18.04	0.59	10.15	0	0.22	100.23
1081 CHR AT MARGIN SPOT 4	0.2	0.38	14.56	51.36	4.83	17.83	0.56	10	0	0.22	99.94
1082 CHR CENTRAL SPOT 5	0.14	0.36	14.36	52.03	4.75	18.29	0.54	9.98	0	0.21	100.66
1083 CHR CENTRAL SPOT 5	0.16	0.34	14.4	51.54	4.47	18.00	0.57	9.84	0	0.26	99.58
1084 CHR AT MARGIN SPOT 6	0.09	0.36	14.34	51.97	4.06	18.61	0.56	9.73	0	0.2	99.92
1085 CHR SMALLER SPOT 7	0.17	0.43	14.68	51.34	4.54	18.05	0.58	9.95	0.02	0.23	99.99
1086 CHR SMALLER SPOT 8	0.15	0.39	14.57	50.73	4.88	18.10	0.58	9.83	0	0.23	99.46
1087 CHR SMALLER SPOT 9	0.12	0.4	14.67	50.81	4.14	18.29	0.6	9.67	0	0.24	98.93
1088 CHR SMALLER SPOT 9	0.15	0.39	14.59	51.34	4.41	18.29	0.56	9.8	0	0.2	99.73
1089 CHR **** SAMPLE 343 SPOT 1 CENTRAL, 05-11-42	0.16	0.48	15.16	49.33	5.24	19.27	0.54	9.18	0	0.28	99.64
1090 CHR AT MARGIN SPOT 2	0.12	0.61	14.56	50.48	5.02	20.04	0.53	9.01	0.04	0.24	100.64
1091 CHR CENTRAL SPOT 3	0.2	0.5	14.24	48.47	6.21	19.19	0.59	8.81	0	0.2	98.41
1092 CHR CENTRAL SPOT 3	0.17	0.54	14.28	49.74	6.64	19.71	0.72	8.98	0.07	0.22	101.06
1093 CHR AT MARGIN SPOT 5	0.15	0.44	14.15	49.78	6.37	19.70	0.64	8.9	0	0.24	100.37
1094 CHR CENTRAL SPOT 6	0.1	0.39	14.6	50.21	5.02	19.52	0.6	9.08	0	0.2	99.71
1095 CHR AT MARGIN SPOT 5	0.19	0.42	14.68	49.85	5.29	19.31	0.54	9.03	0	0.19	99.50
1096 CHR SMALLER SPOT 7	0.18	0.39	14.63	49.43	6.55	19.53	0.53	9.05	0	0.27	100.56
1097 CHR SMALLER SPOT 8	0.15	0.46	14.51	49.28	5.47	19.57	0.61	8.81	0.01	0.2	99.07
1098 CHR **** SAMPLE 344 CENTRAL SPOT 1, 05-11-42	0.18	0.45	14.87	51.08	5.22	18.71	0.72	9.65	0.08	0.21	101.17
1099 CHR CENTRAL SPOT 1, 05-11-4255	0.15	0.42	14.93	50.89	4.56	18.74	0.66	9.53	0	0.28	100.16
1100 CHR AT MARGIN SPOT 2	0.17	0.39	14.86	50.64	4.49	19.11	0.6	9.18	0	0.24	99.68
1101 CHR CENTRAL SPOT 3	0.21	0.46	14.88	51.26	4.76	19.50	0.6	9.16	0	0.25	101.09
1102 CHR AT MARGIN SPOT 4	0.17	0.45	14.72	50.75	5.15	19.47	0.62	9.17	0	0.24	100.75
1103 CHR CENTRAL SPOT 5	0.19	0.42	14.74	50.99	4.49	18.77	0.62	9.37	0	0.26	99.85
1104 CHR AT MARGIN SPOT 6	0.16	0.4	14.9	50.48	4.62	19.35	0.53	9.12	0	0.26	99.82
1105 CHR ANOTHER SPOT 7	0.21	0.41	14.79	50.81	4.49	18.88	0.57	9.23	0.06	0.24	99.69

Black Label BT-09-31

	SiO2	TiO2	Al2O3	Cr2O3	Fe2O3	FeO	MnO	MgO	ZnO	NiO	TOTAL
1106 CHR SMALLER SPOT 8	0.17	0.44	15.02	50.17	4.33	19.45	0.57	8.97	0	0.21	99.33
1107 CHR **** SAMPLE 345 SPOT 1, CENTRAL, 05-11-4	0.19	0.45	15.12	48.76	5.30	20.26	0.63	8.31	0.09	0.2	99.31
1108 CHR AT MARGIN SPOT 2	0.21	0.48	15.25	48.53	5.41	20.61	0.63	8.12	0.03	0.24	99.51
1109 CHR CENTRAL SPOT 3	0.21	0.43	14.75	48.99	5.32	20.52	0.66	8.05	0	0.18	99.11
1110 CHR CENTRAL SPOT 3	0.18	0.43	14.62	51.24	4.80	21.46	0.53	8.08	0.05	0.16	101.55
1111 CHR CENTRAL SPOT 3	0.22	0.44	13.71	50.53	4.28	20.57	0.67	7.72	0.01	0.2	98.35
1112 CHR CENTRAL SPOT 3	0.19	0.33	14.69	50.17	4.94	21.00	0.61	7.93	0.03	0.2	100.08
1113 CHR AT MARGIN SPOT 4	0.25	0.42	15.05	48.67	6.18	20.38	0.68	8.24	0	0.2	100.07
1114 CHR CENTRAL SPOT 5	0.2	0.48	15.12	50.45	4.82	20.80	0.57	8.38	0	0.27	101.09
1115 CHR CENTRAL SPOT 5	0.25	0.48	15.03	49.24	5.24	20.45	0.51	8.27	0	0.19	99.67
1116 CHR SPOT 7	0.18	0.45	15.14	49.01	6.03	20.60	0.56	8.49	0	0.2	100.66
1117 CHR SPOT 8	0.2	0.5	15.38	48.39	5.62	20.31	0.78	8.31	0	0.28	99.76
1118 CHR SPOT 8	0.21	0.5	15.38	48.39	5.63	20.29	0.77	8.3	0	0.28	99.75
1119 CHR **** SAMPLE 346 POSS 346 SPOT 1, 05-11-4	0.07	0.57	14.02	48.16	5.53	22.96	0.57	6.77	0.12	0.11	98.88
1120 CHR SPOT 2	0.04	0.52	13.56	47.88	6.59	24.16	0.63	6.09	0.14	0.12	99.73
1121 CHR SPOT 3	0.03	0.54	13.89	48.28	6.11	23.89	0.61	6.37	0.23	0.12	100.07
1122 CHR SMALLER SPOT 4	0.04	0.28	9.94	54.38	4.64	24.89	0.74	5.21	0.21	0	100.32
1123 CHR SPOT 5	0.04	0.54	13.84	48.02	6.49	24.25	0.64	6.22	0.17	0.02	100.23
1124 CHR AT M W CHL INCL, SPOT 6	0.13	0.63	4.59	58.18	6.13	26.33	0.87	3.75	0.09	0.03	100.73
1125 CHR RANDOM	0	0.49	13.83	47.57	6.97	24.07	0.55	6.33	0.25	0.12	100.19
1126 CHR ANOTHER RANDOM	0.01	0.5	13.56	48.72	5.55	23.55	0.56	6.49	0.19	0.08	99.22
1127 CHR **** SAMPLE 347 CENTRAL, SPOT 1, 05-14-	0.04	0.38	14.25	50.05	4.86	20.13	0.7	8.69	0	0.05	99.15
1128 CHR AT MARGIN SPOT 2	0	0.49	14.41	50.16	3.97	20.97	0.54	8.32	0.14	0.06	99.07
1129 CHR CENTRAL SPOT 3	0.04	0.46	14.47	50.58	5.09	20.51	0.57	8.83	0.14	0.09	100.78
1130 CHR AT MARGIN SPOT 4	0	0.48	14.39	50.05	3.70	20.47	0.56	8.47	0.18	0.03	98.33
1131 CHR AT MARGIN SPOT 4	0	0.46	14.36	50.13	3.92	20.61	0.54	8.49	0.09	0.04	98.64
1132 CHR AT MARGIN SPOT 4	0	0.54	14.48	49.32	4.57	20.18	0.64	8.78	0.04	0.03	98.58
1133 CHR AT MARGIN SPOT 4	0	0.51	14.55	50.2	4.42	20.72	0.62	8.67	0	0.09	99.78
1134 CHR CENTRAL SPOT 5	0	0.5	14.61	49.57	4.97	20.89	0.54	8.63	0.02	0.03	99.76
1135 CHR AT MARGIN SPOT 6	0	0.51	14.56	50.56	3.82	20.87	0.54	8.6	0	0.05	99.51
1136 CHR CENTRAL SPOT 7	0	0.47	14.62	50.25	4.68	20.62	0.7	8.74	0.01	0.09	100.18
1137 CHR AT MARGIN SPOT 8	0.03	0.5	14.56	51.03	4.08	20.75	0.65	8.68	0.04	0.06	100.38
1138 CHR SMALLER SPOT 9	0	0.57	14.52	50.15	5.02	20.77	0.68	8.75	0.1	0.08	100.64
1139 CHR ****SAMPLE 348 CENTRAL, SPOT 1, 05-1404259	0	0.52	14.47	50.01	4.00	20.57	0.55	8.66	0	0	98.78
1140 CHR SAMPLE 348 CENTRAL, SPOT 1, 05-1404259	0	0.52	14.41	50.52	3.71	20.43	0.61	8.65	0.07	0.11	99.03
1141 CHR AT MARGIN SPOT 2	0	0.54	15.74	49.59	4.03	21.82	0.63	8.29	0.06	0.03	100.72
1142 CHR CENTRAL SPOT 3	0.03	0.53	14.44	50.85	3.70	21.33	0.59	8.22	0	0.11	99.80
1143 CHR AT MARGIN SPOT 4	0	0.48	14.91	49.39	4.67	21.05	0.6	8.39	0.14	0.08	99.71
1144 CHR LA NEAR MARGIN SPOT 7	0	0.48	14.7	50.15	4.75	20.92	0.56	8.63	0.13	0.08	100.40
1145 CHR AT M INCL CHL, SPOT 8	0.04	0.46	6.51	57.59	4.71	23.67	0.69	5.64	0.08	0.08	99.47
1146 CHR AT M INCL CHL, SPOT 8	0.04	0.57	14.84	50.4	4.46	20.71	0.73	8.68	0.2	0.02	100.65
1147 CHR SPOT 9	0.01	0.48	14.62	49.83	4.36	20.73	0.57	8.55	0	0.09	99.24
1148 CHR **** SAMPLE 349 SPOT 1, CENTRAL, 05-14-4	0	0.54	14	50.78	4.31	20.52	0.61	8.66	0.06	0.16	99.64
1149 CHR AT MARGIN SPOT 2	0	0.55	14.7	50.14	4.96	21.96	0.65	8.17	0.01	0.09	101.24
1150 CHR AT MARGIN SPOT 2	0	0.58	14.57	50.02	5.09	21.85	0.66	8.19	0.1	0.04	101.10
1151 CHR CENTRAL SPOT 3	0.04	0.51	14.2	50.27	4.70	20.84	0.59	8.46	0.05	0.05	99.71
1152 CHR AT MARGIN SPOT 4	0.1	0.58	14.83	48.91	5.56	21.15	0.5	8.34	0.03	0.09	100.09
1153 CHR CENTRAL SPOT 5	0.07	0.5	14.85	50.15	4.40	21.35	0.56	8.27	0.01	0.05	100.20
1154 CHR AT MARGIN SPOT 6	0	0.42	14.62	49.81	5.73	21.72	0.6	8.31	0	0.04	101.24
1155 CHR SPOT 7	0	0.47	13.74	50.81	4.35	21.51	0.61	7.94	0.16	0.08	99.68
1156 CHR SMALLER SPOT 8	0	0.54	15.26	49.6	4.82	21.75	0.6	8.29	0.12	0.1	101.08
1157 CHR SMALLER SPOT 8	0	0.53	14.91	49.98	3.71	21.80	0.52	8.04	0.08	0.02	99.59
1158 CHR SMALLEST SPOT, 9	0	0.55	14.42	50.33	4.78	22.24	0.5	8.01	0	0.07	100.90
1159 CHR SMALLEST SPOT, 9	0.01	0.46	14.09	50.2	4.45	21.50	0.65	7.93	0.17	0	99.46
1160 CHR **** SAMPLE 350 CENTRAL, SPOT 1, 05-14-4	0	0.51	14.51	49.43	5.16	21.63	0.59	8.09	0.13	0.07	100.12
1161 CHR AT MARGIN SPOT 2	0.01	0.47	14.65	50.34	3.92	21.68	0.61	7.99	0.1	0.05	99.82
1162 CHR AT M W CHL INCL, SPOT 3	0.04	0.89	4.51	56.83	7.84	24.96	0.7	5.08	0.16	0.12	101.12
1163 CHR AT M W CHL INCL, SPOT 3	0	1	4.36	56.87	7.09	25.13	0.84	5.01	0	0.04	100.34
1164 CHR CENTRAL SPOT 4	0	0.52	14.27	50.74	4.66	22.10	0.57	7.97	0.11	0.09	101.04
1165 CHR CENTRAL SPOT 4	0	0.53	14.04	50.29	4.65	21.85	0.65	7.9	0.06	0.07	100.04
1166 CHR AT MARGIN SPOT 5	0	0.6	14.62	49.96	4.61	21.97	0.53	8.13	0.07	0.01	100.50
1167 CHR AT MARGIN SPOT 6	0	0.31	7.38	56.15	4.66	23.17	0.68	5.88	0.04	0.02	98.29
1168 CHR AT MARGIN SPOT 6	0	0.37	8.27	56.44	5.06	23.63	0.71	6.16	0.13	0	100.78
1169 CHR CENTRAL, SPOT 7	0	0.53	14.45	51.18	3.90	22.20	0.47	7.95	0.16	0.1	100.94
1170 CHR CENTRAL, SPOT 7	0	0.52	14.14	49.59	4.02	21.64	0.53	7.71	0.25	0.01	98.41
1171 CHR CENTRAL, SPOT 7	0	0.53	14.47	51.1	3.95	22.20	0.49	8	0.07	0.06	100.88
1172 CHR CENTRAL, SPOT 7	0	0.47	14.57	49.63	5.03	21.81	0.65	7.97	0.16	0.02	100.30
1173 CHR AT MARGIN SPOT 8	0	0.56	14.4	50.33	4.20	22.36	0.55	7.71	0.11	0.08	100.30
1174 CHR SMALLER SPOT 9	0	0.52	14.83	50.4	4.33	22.06	0.67	8.01	0.13	0.02	100.97
1175 CHR SMALLER SPOT 10	0	0.54	14.66	50.24	3.73	21.94	0.53	7.93	0.08	0.05	99.69
1176 CHR ****SAMPLE 351 SPOT 1 CENTRAL, 05-14-4263	0	0.41	14.11	50.87	4.25	21.66	0.72	7.85	0.24	0.05	100.16
1177 CHR NEAR MARGIN SPOT 2	0	0.43	14.33	50.95	4.11	21.46	0.71	8.08	0.19	0.06	100.32
1178 CHR AT MARGIN SPOT 3	0	0.46	14.48	50.35	4.17	21.34	0.63	8.2	0.08	0.04	99.76
1179 CHR SMALLER SPOT 4	0	0.43	14.48	50.28	4.32	21.68	0.58	8.03	0.11	0.01	99.92
1180 CHR SMALLER SPOT 5	0	0.4	14.73	51.62	3.63	21.93	0.59	8.1	0.12	0.06	101.18
1181 CHR SMALLER SPOT 5	0	0.41	14.39	51.27	4.02	21.59	0.68	8.14	0.14	0.01	100.65
1182 CHR CENTRAL SPOT 7	0.01	0.48	14.72	50.83	4.27	21.53	0.6	8.29	0.12	0.12	100.97
1183 CHR CENTRAL SPOT 7	0	0.49	14.79	50.48	4.00	21.77	0.45	8.15	0.22	0.01	100.36
1184 CHR NEAR MARGIN SPOT 7	0	0.49	14.63	50.48	3.68	21.54	0.46	8.18	0.1	0.03	99.60

Black Label BT-09-31

	SiO2	TiO2	Al2O3	Cr2O3	Fe2O3	FeO	MnO	MgO	ZnO	NiO	TOTAL
1185 CHR INT W SILICATE SPOT 8	0.03	0.81	4.99	55.97	7.23	24.46	0.67	5.2	0.09	0.05	99.50
1186 CHR **** SAMPLE 352 SPPOT 1 CENTRTRAL, 05-14-	0	0.44	14.15	50.78	4.16	20.04	0.7	8.79	0.22	0.03	99.31
1187 CHR AT MARGIN SPOT 2	0.05	0.48	14.36	51.02	4.73	20.51	0.61	8.83	0.06	0.07	100.71
1188 CHR CENTRAL SPOT 3	0	0.54	14.53	51.66	3.52	20.08	0.62	9.11	0.14	0.15	100.34
1189 CHR AT MARGIN SPOT 4	0	0.41	14.61	50.51	4.82	20.27	0.65	9	0.01	0.1	100.38
1190 CHR SMALLER SPOT 5	0	0.57	14.39	50.81	3.99	20.52	0.68	8.74	0.12	0.08	99.90
1191 CHR SPOT 7	0	0.55	14.26	51.36	2.97	20.60	0.64	8.54	0.1	0.1	99.12
1192 CHR SMALLER SPOT 6	0	0.42	14.71	51.42	3.80	20.76	0.58	8.76	0.2	0	100.65
1193 CHR SMALLER SPOT 6	0	0.42	14.01	50.63	4.00	20.53	0.6	8.43	0.17	0.05	98.84
1194 CHR SMALLER SPOT 6	0	0.54	14.7	50.19	3.83	20.44	0.6	8.71	0.16	0.06	99.23
1195 CHR **** SAMPLE 353 SPOT 1, CENTRAL. 05-14-4	0	0.44	14.51	51.16	4.42	19.64	0.58	9.46	0.03	0.07	100.31
1196 CHR AT MARGIN SPPT 2	0.02	0.39	14.34	51.05	4.09	19.58	0.54	9.24	0.06	0.03	99.34
1197 CHR AT MARGIN SPOPT 3	0	0.45	13.65	51.38	3.81	19.51	0.5	9.16	0	0.09	98.55
1198 CHR AT MARGIN SPOPT 3	0	0.44	14.39	51.73	4.17	19.92	0.62	9.28	0.08	0.1	100.73
1199 CHR AT MARGIN SPOPT 3	0	0.47	14.34	50.89	3.41	19.37	0.57	9.29	0	0.03	98.37
1200 CHR CENTRAL SPOT 4	0	0.49	13.81	52.41	4.15	19.47	0.54	9.6	0.1	0.04	100.61
1201 CHR CENTRAL SPOT 4	0	0.48	14.47	51.22	4.38	18.81	0.57	9.93	0.08	0.08	100.02
1202 CHR AT MARGIN SPOT 5	0	0.51	14.71	51.91	3.99	20.21	0.52	9.44	0	0.05	101.34
1203 CHR AT MARGIN SPOT 5	0	0.46	14.64	51.21	3.94	19.65	0.53	9.47	0.04	0.02	99.96
1204 CHR CENTRAL SPOT 6	0	0.46	14.71	51.34	3.61	19.59	0.53	9.45	0	0.12	99.81
1205 CHR SMALLER SPOT 7	0	0.49	14.67	49.97	4.20	19.50	0.56	9.26	0.07	0.09	98.81
1206 CHR SMALLER SPOT 7	0	0.47	14.69	50.55	3.87	19.54	0.63	9.27	0.08	0.06	99.17
1207 CHR SMALLER SPOT 8	0	0.51	14.3	50.88	4.04	19.88	0.48	9.2	0.1	0.01	99.39
1208 CHR **** SAMPLE 354 SPOY 1 CENTRAL, 05-15-42	0	0.5	14.84	51.02	4.46	19.41	0.53	9.78	0	0.1	100.65
1209 CHR AT MARGIN SPOT 2	0	0.5	14.85	51.74	3.55	19.45	0.48	9.73	0.06	0.09	100.45
1210 CHR AT MARGIN SPOT 2	0	0.53	14.96	51.85	3.63	19.89	0.58	9.59	0.05	0.02	101.10
1211 CHR SPOT 3 CENTRAL	0	0.51	14.9	50.37	3.93	19.69	0.52	9.36	0.05	0.05	99.37
1212 CHR AT MARGIN SPOT 4	0	0.49	15.23	50.52	4.47	19.61	0.47	9.7	0.11	0.03	100.63
1213 CHR SMALLER SPOY 5	0	0.5	14.91	51.39	4.38	19.57	0.46	9.77	0.01	0.21	101.20
1214 CHR SMALLER SPOY 5	0	0.5	14.7	51.58	3.55	19.94	0.49	9.37	0.09	0.02	100.24
1215 CHR SMALLER SPOT 6	0	0.48	15.22	51.76	3.12	19.73	0.51	9.64	0	0.03	100.48
1216 CHR SMALLER SPOT 7	0	0.46	14.93	50.43	3.66	19.97	0.6	9.01	0.16	0.05	99.28
1217 CHR SMALLER SPOT 8	0	0.49	15.06	51.8	2.92	20.35	0.43	9.18	0.1	0.06	100.38
1218 CHR **** SAMPLE 355 SPOT 1, CENTRAL, 05-15-4	0	0.49	14.67	51.76	3.83	20.99	0.48	8.9	0.03	0.04	101.19
1219 CHR SPOT 1, CENTRAL, 05-15-4267	0	0.57	14.58	52.81	2.78	20.88	0.5	8.93	0.15	0.08	101.28
1220 CHR SPOT 1, CENTRAL, 05-15-4267	0	0.41	14.46	50.64	3.26	20.43	0.55	8.47	0.21	0.06	98.50
1221 CHR 355 SPOT 1, CENTRAL, 05-15-4267	0	0.54	14.23	52.96	3.11	21.00	0.5	8.81	0.21	0.04	101.40
1222 CHR 355 SPOT 1, CENTRAL, 05-15-4267	0	0.5	14.34	50.43	3.85	20.11	0.7	8.79	0.1	0	98.82
1223 CHR 355 SPOT 1, CENTRAL, 05-15-4267	0	0.45	14.47	51.23	3.47	20.38	0.53	8.83	0.13	0.01	99.50
1224 CHR AT MARGIN SPOT 2	0	0.47	15.05	50.53	4.17	20.13	0.74	9.08	0.14	0.02	100.34
1225 CHR CENTRAL SPOT 3	0	0.53	14.54	51.09	4.27	20.41	0.64	9.05	0.03	0.05	100.61
1226 CHR AT MARGIN SPOT 4	0	0.5	14.78	51.73	3.40	20.62	0.54	9	0.07	0.03	100.67
1227 CHR CENTRAL SPOT 5	0	0.61	14.78	51.7	3.07	20.92	0.68	8.77	0	0.09	100.62
1228 CHR AT MARGIN SPOT 4	0	0.54	14.73	51.02	4.51	20.62	0.62	9	0.23	0	101.27
1229 CHR AT MARGIN SPOT 4	0	0.52	13.82	50.3	4.10	19.91	0.54	8.86	0.05	0	98.10
1230 CHR SMALLER SPOT 7	0	0.52	14.85	51.49	2.76	20.59	0.47	8.83	0.14	0.05	99.70
1231 CHR SMALLER SPOT 8	0	0.52	15.14	51.18	3.44	21.01	0.6	8.75	0.06	0.08	100.77
1232 CHR SMALLER SPOT 8	0	0.45	14.04	51.05	3.22	20.47	0.54	8.52	0.07	0.01	98.37
1233 CHR SMALLER SPOT 8	0	0.46	14.58	50.63	3.95	20.49	0.59	8.74	0.16	0	99.60
1234 CHR **** SAMPLE 356 SPOT 1, 05-15-4268	0	0.44	14.92	51.46	3.44	20.26	0.64	9	0.15	0.1	100.40
1235 CHR AT MARGIN SPOT 2	0	0.6	15.09	49.98	3.92	20.02	0.64	9.15	0.08	0.05	99.53
1236 CHR AT MARGIN SPOT 3	0	0.41	14.62	51.44	3.61	19.48	0.69	9.4	0.02	0.03	99.70
1237 CHR AT MARGIN SPOT 4	0	0.52	15.27	50.07	4.01	19.45	0.67	9.46	0.09	0.1	99.64
1238 CHR CENTRAL SPOT 5	0	0.54	14.68	50.32	3.97	19.33	0.58	9.47	0.01	0.08	98.98
1239 CHR CENTRAL SPOT 5	0	0.49	14.75	50.51	4.00	19.50	0.52	9.46	0.07	0	99.30
1240 CHR AT MARGIN SPOT 6	0	0.55	14.39	50.76	3.51	19.92	0.56	9	0.12	0.07	98.88
1241 CHR SMALLER SPOT 7	0	0.5	15.08	50.67	4.34	20.45	0.63	9.14	0.01	0.04	100.85
1242 CHR SMALLER SPOT 8	0	0.5	14.82	51.54	2.82	20.51	0.5	8.9	0.03	0.07	99.68
1243 CHR **** SAMPLE 357 SPOT 1 CENTRAL, 05-15-42	0	0.53	14.4	51.66	3.66	20.12	0.48	9.23	0.02	0.09	100.19
1244 CHR AT MARGIN SPOT 2	0	0.49	14.71	50.95	3.14	19.93	0.53	9.04	0.13	0.05	98.96
1245 CHR CENYRAL SPOT 3	0	0.45	14.62	50.01	4.32	19.23	0.66	9.35	0.07	0.07	98.78
1246 CHR CENYRAL SPOT 3	0	0.46	14.75	51	3.99	19.88	0.62	9.24	0.05	0.1	100.09
1247 CHR AT MARGIN SPOT 4	0	0.55	14.79	50.4	4.06	19.63	0.52	9.35	0.18	0.08	99.57
1248 CHR CENTRAL SPOT 5	0	0.48	15.17	51.12	3.94	19.83	0.58	9.55	0	0.05	100.71
1249 CHR SMALLER SPOT 8	0	0.48	13.96	50.78	3.77	20.13	0.51	8.67	0.18	0.14	98.62
1250 CHR SMALLER SPOT 8	0	0.46	14.56	50.65	3.71	19.88	0.64	9.05	0.02	0.02	98.99
1251 CHR **** SAMPLE 358 SPOT 1, 05-15-358	0	0.41	13.66	53.08	3.77	19.54	0.59	9.45	0.12	0.06	100.69
1252 CHR SAMPLE 358 SPOT 1, 05-15-358	0	0.42	13.91	51.67	3.72	19.38	0.55	9.33	0.05	0.04	99.07
1253 CHR AT MARGIN SPOT 2	0	0.44	13.09	52.14	3.30	19.98	0.61	8.65	0.08	0.06	98.35
1254 CHR AT MARGIN SPOT 2	0	0.39	14.15	52.29	3.58	20.10	0.57	9.07	0.18	0	100.33
1255 CHR CENTRAL SPOT 3	0	0.39	14.03	52.52	3.36	19.72	0.41	9.36	0.05	0.06	99.90
1256 CHR AT MARGIN SPOT 4	0	0.48	14.21	52.9	3.03	20.25	0.57	9.11	0.14	0.06	100.74
1257 CHR AT MARGIN SPOT 4	0	0.54	13.65	51.29	4.00	20.07	0.57	8.87	0.19	0.01	99.19
1258 CHR CENTRAL SPOT 5	0	0.47	14.39	52.05	3.44	19.48	0.58	9.45	0.11	0.13	100.09
1259 CHR AT MARGIN SPPT 6	0	0.47	14.13	51.03	3.08	19.74	0.55	8.97	0.01	0.02	98.00
1260 CHR AT MARGIN SPPT 6	0	0.46	13.96	51.83	3.67	19.54	0.51	9.36	0.06	0.02	99.41
1261 CHR SMALLER SPOT 7	0	0.47	14.44	52.35	2.97	19.91	0.56	9.27	0.12	0	100.09
1262 CHR SMALLER SPOT 9	0	0.44	13.91	52.13	3.54	20.11	0.62	8.92	0.12	0.09	99.87
1263 CHR **** SAMPLE 359 SPOT 1, CENTRAL, 05-15-3	0	0.43	14.36	51.63	3.78	21.49	0.55	8.29	0.07	0.12	100.72

Black Label BT-09-31

	SiO2	TiO2	Al2O3	Cr2O3	Fe2O3	FeO	MnO	MgO	ZnO	NiO	TOTAL
1264 CHR AT MARGIN SPOT 2	0	0.52	14.06	49.54	4.65	21.73	0.53	7.83	0.05	0.09	99.00
1265 CHR CENTRAL SPOT 3	0	0.5	14.25	50.56	3.95	20.88	0.65	8.3	0.18	0.13	99.41
1266 CHR AT MARGIN SPOT 4	0	0.49	14.82	48.99	4.84	21.58	0.6	8	0.17	0.06	99.55
1267 CHR CENTRAL SPOT 5	0	0.45	13.94	51.54	3.85	22.13	0.54	7.8	0.08	0.08	100.41
1268 CHR AT MARGIN SPOT 6	0	0.51	12.77	51.32	4.07	22.03	0.54	7.42	0.17	0.06	98.89
1269 CHR CENTRAL SPOT 7	0	0.36	14.31	50.88	4.76	21.50	0.58	8.14	0.2	0.16	100.89
1270 CHR CENTRAL SPOT 7	0.07	0.44	13.48	50.94	4.88	21.15	0.63	7.93	0.22	0.12	99.86
1271 CHR SMALLER SPOT 8	0	0.52	14.05	50.76	4.66	21.92	0.61	7.99	0.16	0	100.68
1272 CHR SMALLER SPOT 8	0	0.55	14.31	50.2	4.26	21.66	0.53	8.05	0.05	0.13	99.74
1273 CHR **** SAMPLE 360, C SPOT 1, 05-15-4273	0	0.45	13.8	51.76	3.78	22.45	0.54	7.61	0.11	0.04	100.54
1274 CHR SAMPLE 360, C SPOT 1, 05-15-4273	0	0.47	13.69	51.62	4.17	22.02	0.63	7.74	0.22	0.12	100.69
1275 CHR AT MARGIN SPOT 2	0	0.52	13.78	49.94	4.20	21.79	0.63	7.57	0.12	0.11	98.66
1276 CHR AT MARGIN SPOT 2	0	0.47	14.6	50.06	4.10	21.32	0.65	8.11	0.17	0.06	99.54
1277 CHR CENTRAL SPOT 3	0	0.49	14.15	52.24	3.77	21.55	0.64	8.37	0.06	0.07	101.35
1278 CHR CENTRAL SPOT 3	0	0.46	13.13	50.45	4.55	20.80	0.57	8.1	0.03	0.14	98.23
1279 CHR CENTRAL SPOT 3	0	0.51	13.92	51.47	3.31	21.43	0.62	7.99	0.16	0.11	99.52
1280 CHR AT MARGIN SPOT 4	0	0.54	14.89	49.73	4.17	22.06	0.61	7.83	0.18	0.05	100.06
1281 CHR CENTRAL SPOT 5	0	0.48	13.92	50.86	3.82	21.77	0.64	7.76	0.12	0.08	99.44
1282 CHR AT MARGIN SPOT 6	0	0.57	14.86	51.07	3.64	22.60	0.55	7.78	0.12	0.15	101.33
1283 CHR AT MARGIN SPOT 6	0	0.55	14.75	50.52	3.60	22.25	0.64	7.76	0.17	0	100.24
1284 CHR SMALLER SPOT 7	0	0.5	15.03	49.79	3.53	22.01	0.66	7.73	0.08	0.09	99.41
1285 CHR SMALLER SPOT 8	0	0.48	15.16	50.32	4.28	22.44	0.59	7.86	0.19	0.04	101.37
1286 CHR SMALLER SPOT 8	0	0.53	14.71	48.7	4.35	21.84	0.57	7.74	0.08	0.01	98.54
1287 CHR SMALLER SPOT 8	0	0.5	15.32	49.24	3.44	21.94	0.58	7.75	0.17	0.03	98.96
1288 CHR **** SAMPLE 361 C SPOT 1, 05-15-4274	0	0.48	14.84	51.35	4.01	19.85	0.48	9.52	0.03	0.06	100.62
1289 CHR C SPOT 1, 05-15-4274	0	0.45	14.58	50.96	3.28	19.31	0.53	9.34	0	0.16	98.61
1290 CHR AT MARGIN SPOT 2	0	0.44	14.94	49.76	4.19	19.89	0.55	8.99	0.16	0.12	99.04
1291 CHR CENTRAL SPOT 3	0	0.52	14.9	50.55	3.68	19.72	0.62	9.21	0.16	0.08	99.44
1292 CHR AT MARGIN SPOT 4	0	0.55	15.24	50.91	3.54	20.66	0.5	9	0.09	0.1	100.58
1293 CHR CENTRAL SPOT 5	0	0.45	14.53	50.26	3.64	19.61	0.58	8.98	0.15	0.11	98.30
1294 CHR CENTRAL SPOT 5	0	0.52	14.78	52.19	3.34	20.17	0.54	9.32	0.06	0.14	101.06
1295 CHR SMALLER SPOT 6	0	0.43	14.7	51.05	3.62	20.48	0.49	8.85	0.15	0.01	99.77
1296 CHR SMALLER SPOT 7	0	0.47	14.7	51.11	3.03	20.47	0.51	8.75	0.05	0.1	99.19
1297 CHR SMALLER SPOT 8	0	0.48	14.76	50.68	3.91	20.70	0.59	8.75	0.1	0	99.97
1298 CHR ****SAMPLE 362 SPOT 1, CENTRAL, 05-15-4276	0	0.51	14.06	50.8	3.71	19.94	0.53	8.88	0.11	0.11	98.64
1299 CHR SPOT 1, CENTRAL, 05-15-4276	0	0.53	14.01	52.22	2.46	20.27	0.53	8.83	0.06	0.02	98.93
1300 CHR SPOT 1, CENTRAL, 05-15-4276	0	0.52	14.06	50.33	3.80	19.57	0.52	9	0.05	0.17	98.02
1301 CHR SPOT 1, CENTRAL, 05-15-4276	0	0.46	13.72	52.08	2.96	20.16	0.5	8.82	0.05	0.01	98.77
1302 CHR SPOT 1, CENTRAL, 05-15-4276	0	0.48	14.33	50.41	3.48	19.93	0.6	8.8	0.12	0.03	98.18
1303 CHR SPOT 1, CENTRAL, 05-15-4276	0	0.43	14.49	50.95	2.94	20.29	0.51	8.62	0.11	0.12	98.46
1304 CHR AT MARGIN SPOT 2	0	0.47	14.75	49.46	5.07	20.71	0.61	8.57	0.26	0.07	99.97
1305 CHR CENTRAL SPOT 3	0	0.53	14.43	49.4	4.20	20.79	0.45	8.42	0.04	0.07	98.33
1306 CHR CENTRAL SPOT 3	0	0.5	14.55	50.68	3.29	20.96	0.5	8.4	0.07	0.09	99.04
1307 CHR AT MARGIN SPOT 4	0	0.51	14.66	50.3	3.77	21.05	0.54	8.38	0.09	0.11	99.41
1308 CHR CENTRAL SPOT 5	0	0.5	14.52	50.63	3.77	20.80	0.6	8.5	0.17	0.05	99.55
1309 CHR AT MAREGIN SPOT 6	0	0.49	14.86	50.04	3.75	21.06	0.4	8.4	0.13	0.14	99.28
1310 CHR SMALLER SPOT 7	0	0.47	14.52	50.01	3.44	21.03	0.57	8.13	0.08	0.1	98.34
1311 CHR SMALLER SPOT 7	0	0.43	14.34	50.04	4.12	20.87	0.65	8.31	0.02	0.03	98.80
1312 CHR SMALLER SPOT 7	0	0.53	14.63	51.03	3.16	21.48	0.6	8.21	0.04	0.05	99.73
1313 CHR SMALL INSTN SPOT 8	0	0.53	14.51	50.63	3.58	21.18	0.67	8.29	0.1	0	99.49
1314 CHR **** SAMPLE 363 CENTRAL SPOT 1, 05-15-42	0	0.49	14.24	50.08	3.77	21.77	0.62	7.68	0.13	0.09	98.87
1315 CHR SAMPLE 363 CENTRAL SPOT 1, 05-15-4278	0	0.49	13.95	50.6	4.14	22.46	0.55	7.52	0	0.07	99.78
1316 CHR AT MARGIN SPOT 2	0	0.47	14.91	49.76	4.36	22.12	0.59	7.85	0.12	0.02	100.20
1317 CHR CXENTRAL SPOT 3	0.13	0.67	14.37	48.7	5.01	21.19	0.45	7.94	0.14	0.06	98.66
1318 CHR CXENTRAL SPOT 3	0	0.44	14.31	48.86	5.28	21.40	0.65	7.91	0.1	0.11	99.06
1319 CHR AT MARGIN SPOT 4	0	0.58	14.73	49.49	4.23	22.35	0.6	7.59	0.1	0.15	99.82
1320 CHR CENTRAL SPOT 5	0	0.52	14.07	49.95	4.32	21.42	0.58	8	0.08	0.07	99.01
1321 CHR AT MARGIN SPOT 6	0	0.51	14.64	48.65	4.90	21.98	0.53	7.62	0.25	0.12	99.20
1322 CHR SMALLER SPOT 7	0	0.56	14.17	48.94	4.79	21.91	0.6	7.61	0.21	0.01	98.80
1323 CHR SMALLER SPOT 7	0	0.56	14.7	49.45	4.08	22.34	0.51	7.62	0.11	0.04	99.41
1324 CHR SMALLER SPOT 8	0	0.49	14.26	50.75	4.50	22.88	0.65	7.47	0.1	0	101.10
1325 CHR **** SAMPLE 364 CENTRAL, SPOT 1, 05-15-4 1	0.15	0.49	14.01	49.22	5.07	21.95	0.52	7.3	0.08	0.03	98.82
1326 CHR AT MARGIN SPOT 2	0	0.5	14.68	48.33	4.81	24.37	0.59	6.27	0.05	0.07	99.67
1327 CHR CENTRAL SPOT 3	0.21	0.52	14.57	48.91	5.15	23.57	0.5	6.33	0.21	0.09	100.07
1328 CHR AT MARGIN SPOT 4	0	0.5	14.79	46.86	5.63	25.06	0.7	5.69	0.11	0	99.33
1329 CHR SMALLER SPOT 5	0	0.57	14.45	47.81	5.58	25.14	0.73	5.77	0.08	0.09	100.22
1330 CHR SMALLER SPOT 6	0	0.47	15	47.69	5.80	25.01	0.62	5.98	0.27	0.03	100.87
1331 CHR SMALLER SPOT 6	0	0.44	14.47	47.05	6.08	24.52	0.57	6.04	0.11	0	99.28
1332 CHR REL LARGE NO PHOTO	0	0.51	14.58	48.24	5.29	24.12	0.6	6.39	0.2	0.08	100.01
1333 CHR SMALLER NO PHOTO	0	0.53	14.51	48.42	4.39	23.58	0.59	6.5	0.23	0.08	98.83
1334 CHR **** SAMPLE 365, CENTRAL, SPOT 1, 05-16-	0	0.48	14.01	50.42	4.43	19.77	0.61	9.04	0	0.06	98.82
1335 CHR CENTRAL, SPOT 1, 05-16-4280	0	0.46	14.08	51.07	4.10	20.37	0.63	8.76	0.08	0.04	99.59
1336 CHR AT MARGIN SPOT 2	0	0.53	14.93	49.75	4.51	21.49	0.55	8.29	0.17	0.05	100.27
1337 CHR OPPOSITE MARGIN SPOT 3	0	0.5	14.6	49.49	5.38	21.46	0.61	8.37	0	0	100.42
1338 CHR CENTRAL SPOT 4	0	0.48	14.31	50.09	4.31	20.62	0.56	8.51	0.14	0.09	99.11
1339 CHR AT MARGIN SPOT 5	0	0.47	14.52	49.57	4.45	20.82	0.56	8.36	0.17	0.07	99.00
1340 CHR AT MARGIN SPOT 5	0	0.48	14.67	50.72	4.53	21.15	0.67	8.54	0.14	0.04	100.94
1341 CHR CENTRAL SPOT 6	0	0.54	14.01	50.7	4.71	20.85	0.66	8.64	0	0.01	100.12
1342 CHR SMALLER SPOT 7	0	0.55	14.67	49.59	4.79	21.31	0.51	8.4	0.1	0.03	99.95

Black Label BT-09-31

	SiO2	TiO2	Al2O3	Cr2O3	Fe2O3	FeO	MnO	MgO	ZnO	NiO	TOTAL
1343 CHR SMALLER SPOT 8	0	0.6	14.92	49.89	4.35	21.58	0.6	8.3	0.05	0.11	100.40
1344 CHR **** SAMPLE 366 CENTRAL, SPOTR 1, 05-16-	0	0.47	14.16	51.2	4.10	18.93	0.66	9.64	0	0.09	99.25
1345 CHR AT MARGIN SPOT 2	0	0.44	14.6	50.4	4.46	20.15	0.61	9.01	0	0.08	99.75
1346 CHR CENTRAL SPOT 3	0	0.52	14.61	51.13	4.19	19.57	0.46	9.58	0.11	0.07	100.24
1347 CHR AT MARGIN SPOT 4	0	0.51	15.26	50.99	3.76	20.19	0.58	9.3	0	0.11	100.70
1348 CHR SMALLER SPOT 5	0	0.48	14.69	51.36	3.99	20.12	0.43	9.29	0.1	0.08	100.54
1349 CHR SMALLER SPOT 6	0	0.45	14.09	52.36	3.42	19.99	0.48	9.23	0	0.1	100.12
1350 CHR SMALLER SPOT 7	0	0.47	14.49	50.56	4.08	20.22	0.52	8.9	0.1	0.1	99.44
1351 CHR SMALLER SPOT 8	0	0.48	14.12	52.3	3.24	20.70	0.61	8.73	0.05	0.07	100.29
1352 CHR SPOT 1 AGAIN	0	0.48	13.99	52.11	3.65	19.62	0.64	9.27	0.11	0.11	99.98
1353 CHR **** SAMPLE 367 CENTRAL, SPOT 1, 05-16-4	0	0.46	14.66	52.29	3.23	18.67	0.53	10.1	0.04	0.08	100.06
1354 CHR AT MARGIN SPOT 2	0	0.5	14.8	52.15	3.80	19.85	0.48	9.67	0.09	0.03	101.37
1355 CHR AT MARGIN SPOT 2	0	0.48	14.51	51.02	3.84	19.43	0.55	9.49	0	0.03	99.35
1356 CHR ANOTHER CENTRAL SPOT 3	0	0.41	14.49	51.15	4.63	18.70	0.58	9.99	0.03	0.09	100.06
1357 CHR AT MARGIN SPOT 4	0	0.49	15.02	50.65	4.03	19.51	0.56	9.6	0	0.03	99.89
1358 CHR SMALLER SPOT 5	0	0.48	14.92	50.36	4.30	19.08	0.47	9.79	0.03	0.08	99.51
1359 CHR SMALLER CENTRAL SPOT 6	0.24	0.53	14.81	50.76	4.96	18.23	0.59	9.83	0.01	0.11	100.07
1360 CHR SMALLER SPOT 7	0	0.45	15.27	50.08	4.58	19.20	0.6	9.77	0.09	0	100.04
1361 CHR SMALLER SPOT 8	0	0.45	14.7	49.77	4.56	19.16	0.55	9.49	0.1	0.02	98.80
1362 CHR SMALLER SPOT 8	0	0.55	14.75	50.29	3.72	19.62	0.51	9.31	0.08	0.02	98.85
1363 CHR **** SAMPLE 368 SPOT 1, CENTRAL, 05-16-4	0	0.52	14.4	51.37	3.92	18.62	0.59	9.96	0.04	0.12	99.54
1364 CHR AT MARGIN SPOT 2	0	0.53	14.28	50.14	4.73	19.51	0.63	9.31	0.1	0.01	99.24
1365 CHR ANOTHER CENTRAL SPOT 3	0	0.47	14.11	50.87	4.78	18.50	0.66	9.8	0.17	0.21	99.57
1366 CHR AT MARGIN SPOT 4	0	0.58	14.66	49.97	4.45	19.29	0.56	9.52	0.18	0.01	99.22
1367 CHR ANOTHER CENTRAL SPOT 5	0	0.53	14.42	51.76	3.94	19.82	0.53	9.48	0.08	0.03	100.58
1368 CHR AT MARGIN SPOT 6	0	0.48	14.55	51.57	4.15	19.36	0.55	9.65	0.13	0.13	100.58
1369 CHR SMALLER SPOT 7	0	0.49	14.22	51.43	3.43	19.30	0.43	9.45	0.15	0.04	98.94
1370 CHR SMALLER SPOT 8	0	0.57	14.93	51.42	3.79	20.13	0.62	9.41	0	0.02	100.89
1371 CHR SMALLER SPOT 8	0	0.56	14.26	52.38	3.77	20.19	0.59	9.32	0.1	0.02	101.20
1372 CHR SMALLER SPOT 8	0	0.51	13.54	51.9	3.68	19.31	0.62	9.32	0.08	0.02	98.98
1373 CHR **** SAMPLE 369 CENTRAL, SPOT 1, 05-16-4	0	0.49	14.57	51.08	3.99	20.16	0.62	9.06	0.13	0.03	100.13
1374 CHR CENTRAL, SPOT 1, 05-16-4284	0	0.48	14.17	52.17	3.44	19.98	0.62	9.2	0.01	0.04	100.10
1375 CHR AT MARGIN SPOT 2	0	0.49	14.41	50.86	4.69	20.30	0.51	9.12	0.09	0.03	100.50
1376 CHR AT MARGIN SPOT 2	0	0.49	13.16	50.87	4.74	19.66	0.57	9.03	0	0	98.53
1377 CHR AT MARGIN SPOT 2	0	0.52	13.56	50.77	3.98	19.87	0.69	8.77	0	0.08	98.24
1378 CHR AT MARGIN SPOT 2	0	0.52	14.64	51.52	3.23	20.71	0.59	8.8	0.04	0.03	100.08
1379 CHR CENTRAL SPOT 3	0	0.53	14.46	51.33	4.03	20.06	0.61	9.21	0.03	0.1	100.35
1380 CHR AT MARGIN SPOT 4	0	0.49	15.15	50.5	4.27	19.81	0.62	9.46	0	0.05	100.35
1381 CHR ANOTHER CENTRAL SPOT 5	0	0.51	14.74	51.08	3.57	19.58	0.43	9.44	0.16	0.07	99.59
1382 CHR AT MARGIN SPOT 6	0	0.5	14.97	51.97	3.72	20.20	0.57	9.42	0.09	0.04	101.48
1383 CHR AT MARGIN SPOT 6	0	0.48	14.59	52.62	2.44	20.38	0.55	8.99	0.14	0.03	100.22
1384 CHR AT MARGIN SPOT 6	0	0.49	14.87	52.11	3.75	20.16	0.68	9.43	0.02	0	101.51
1385 CHR AT MARGIN SPOT 6	0	0.45	14.54	51.25	3.91	19.63	0.7	9.35	0	0.03	99.86
1386 CHR ANOTHER CENTRASL SPOT 7	0	0.48	14.84	51.59	4.19	19.95	0.54	9.51	0.09	0.07	101.26
1387 CHR ANOTHER CENTRASL SPOT 7	0	0.5	14.87	51.11	3.94	19.60	0.65	9.49	0.07	0.07	100.30
1388 CHR ANOTHER CENTRASL SPOT 7	0	0.46	14.74	49.05	4.77	19.15	0.57	9.39	0.02	0.06	98.21
1389 CHR ANOTHER CENTRASL SPOT 7	0	0.51	14.98	51.35	3.84	20.06	0.68	9.37	0.02	0	100.81
1390 CHR ANOTHER CENTRASL SPOT 7	0	0.48	14.78	50.89	4.26	19.63	0.67	9.46	0	0.08	100.26
1391 CHR SMALLER SPOT 8	0	0.54	15.04	50.44	4.82	20.55	0.58	9.18	0.09	0	101.23
1392 CHR SMALLER SPOT 8	0	0.53	15.29	50.21	4.51	20.07	0.53	9.42	0.05	0.05	100.66
1393 CHR **** SAMPLE 370 CENTRAL SPOT 1, 05-17-42	0	0.49	14.87	50.24	4.40	20.26	0.46	9.09	0.1	0.07	99.98
1394 CHR AT MARGIN SPOT 2	0	0.54	14.97	50.85	4.05	20.18	0.62	9.24	0.1	0.01	100.57
1395 CHR CENTRAL SPOT 3	0	0.47	14.26	50.33	4.80	19.52	0.51	9.4	0.06	0	99.35
1396 CHR AT MARGIN SPOT 4	0.03	0.45	14.69	50.83	4.40	19.82	0.57	9.31	0.03	0	100.13
1397 CHR CENTRAL SPOT 5	0	0.5	14.02	51.74	3.95	19.96	0.43	9.22	0.12	0.08	100.02
1398 CHR AT MARGIN SPOT 6	0	0.45	14.52	51.29	3.42	20.37	0.49	8.9	0.03	0.07	99.53
1399 CHR SMALLER SPOT 7	0	0.53	14.62	49.85	4.52	19.91	0.58	9.14	0.07	0	99.22
1400 CHR SMALL INST SPOT 8	0.01	0.48	14.68	51.08	3.69	20.11	0.63	9.06	0	0.07	99.81
1401 CHR **** SAMPLE 371 L CENTRAL, SPOT 1, 05-17	0	0.45	14.21	51.54	3.97	19.78	0.55	9.25	0.02	0.13	99.91
1402 CHR AT MARGIN SPOT 2	0	0.49	14.37	51.33	3.92	20.08	0.58	9.17	0	0.02	99.96
1403 CHR CENTRAL SPOT 3	0	0.39	13.85	52.49	4.43	20.00	0.62	9.25	0.08	0.08	101.19
1404 CHR CENTRAL SPOT 3	0	0.38	13.77	51.87	4.13	19.50	0.57	9.31	0.08	0.02	99.63
1405 CHR CENTRAL SPOT 5	0	0.47	14.18	51.81	3.83	19.88	0.63	9.11	0.19	0.13	100.23
1406 CHR CENTRAL SPOT 5	0	0.4	13.86	51.1	4.66	19.88	0.63	9.01	0.16	0.02	99.72
1407 CHR AT MARGIN SPOT 6	0	0.43	14.05	51.05	4.11	19.87	0.51	9.05	0.12	0.03	99.22
1408 CHR SMALLER SPOT 7	0	0.42	14.08	51.35	4.39	19.72	0.6	9.26	0.03	0.07	99.92
1409 CHR SMALLER SPOT 8	0	0.45	15.04	50.07	4.68	19.83	0.55	9.34	0.08	0.08	100.12
1410 CHR SMALLER SPOT 8	0	0.44	14.86	51.01	3.99	19.84	0.46	9.35	0.11	0.1	100.16
1411 CHR SMALLER SPOT 8	0.03	0.45	14.57	51.82	3.77	19.73	0.53	9.4	0	0.1	100.40
1412 CHR SMALLER SPOT 8	0	0.4	14.77	51.37	4.17	19.99	0.53	9.37	0	0.06	100.66
1413 CHR AT MARGIN SPOT 2	0	0.46	14.99	50.04	4.53	19.84	0.61	9.26	0	0.12	99.85
1414 CHR CENTRAL SPOT 3	0	0.48	14.66	50.87	4.32	19.44	0.56	9.52	0.16	0.07	100.08
1415 CHR AT MARGIN SPOT 4	0.04	0.5	15.09	50.65	4.47	20.15	0.62	9.21	0.03	0.07	100.83
1416 CHR CENTRAL SPOT 5	0	0.46	14.49	51.4	3.59	19.69	0.5	9.34	0	0.11	99.58
1417 CHR AT MARGIN SPOT 6	0.02	0.48	15.01	50.31	4.27	19.77	0.66	9.29	0.05	0	99.87
1418 CHR CENTRAL SPOT 7	0	0.46	14.57	51.37	3.76	19.72	0.56	9.37	0	0.08	99.89
1419 CHR SMALLER SPOT 8	0	0.47	14.23	49.48	5.12	19.84	0.44	9.1	0.05	0.01	98.74
1420 CHR SMALLER SPOT 8	0	0.44	14.66	49.69	4.27	19.55	0.46	9.24	0	0.05	98.36
1421 CHR SMALLER SPOT 8	0.01	0.5	14.41	49.97	4.23	19.62	0.49	9.15	0.05	0.06	98.48

Black Label BT-09-31

	SiO2	TiO2	Al2O3	Cr2O3	Fe2O3	FeO	MnO	MgO	ZnO	NiO	TOTAL
1422 CHR SMALLER SPOT 8	0	0.53	14.88	49.98	4.16	19.85	0.55	9.24	0	0.06	99.25
1423 CHR **** SAMPLE 372 CENTRAL, SPPOT 1, 05-17	0	0.57	14.16	50.51	4.05	21.01	0.63	8.32	0.18	0.07	99.50
1424 CHR AT AMRGIN SPOT 2	0	0.5	14.25	49.51	5.21	21.89	0.59	7.84	0.17	0.08	100.03
1425 CHR CENTRAL SPOT 3	0	0.38	14.24	51.32	4.54	21.47	0.56	8.35	0.09	0.02	100.98
1426 CHR CENTRAL SPOT 3	0.03	0.46	14.44	50.79	4.33	21.25	0.49	8.36	0.07	0.11	100.32
1427 CHR AT MARGIN SPOT 4	0	0.38	14.3	49.99	5.09	22.37	0.51	7.69	0.03	0.06	100.42
1428 CHR AT MARGIN SPOT 4	0	0.46	14.04	48.95	5.94	22.32	0.52	7.65	0.03	0.02	99.93
1429 CHR CENTRAL SPOT 5	0	0.48	14.54	51.2	3.85	21.73	0.53	8.24	0.09	0.01	100.67
1430 CHR CENTRAL SPOT 5	0	0.53	14.56	49.99	4.84	21.42	0.63	8.29	0.17	0.04	100.46
1431 CHR CENTRAL SPOT 5	0.01	0.47	14.26	49.39	4.81	21.03	0.51	8.23	0.07	0.08	98.86
1432 CHR AT AMRGIN SPOT 6	0.03	0.45	14.1	49.93	5.11	22.10	0.5	7.73	0.07	0.06	100.08
1433 CHR SMALLER SPOT 7	0.04	0.43	14.4	49.2	6.04	22.20	0.53	7.8	0.07	0	100.72
1434 CHR SMALLER SPOT 7	0.03	0.48	13.76	48.36	5.77	21.55	0.61	7.62	0.06	0.07	98.31
1435 CHR SMALLER SPOT 7	0.01	0.49	14.06	49.26	4.17	21.90	0.55	7.53	0	0.02	98.00
1436 CHR SMALLER SPOT 7	0.18	0.47	14.28	48.77	6.38	21.31	0.51	7.9	0.01	0.05	99.86
1437 CHR SMALLER SPOT 8	0	0.47	14.13	49.2	5.67	22.12	0.61	7.68	0.13	0.07	100.08
1438 CHR **** SAMPLE 373 CENTRAL, SPOT 1, 05-18-4	0.04	0.48	14.46	51.37	4.38	20.42	0.61	8.96	0.01	0.1	100.83
1439 CHR CENTRAL, SPOT 1, 05-18-4289	0	0.51	13.96	51.57	4.01	20.45	0.61	8.87	0	0.06	100.03
1440 CHR AT MARGIN SPOT 2	0	0.48	15.11	49.35	4.46	21.08	0.64	8.42	0.03	0.08	99.66
1441 CHR SMALLER SPOT 3	0.03	0.53	13.76	50.63	3.77	20.95	0.56	8.13	0.03	0.1	98.50
1442 CHR SMALLER SPOT 3	0.02	0.49	14.56	50.56	3.86	21.10	0.54	8.36	0.06	0.08	99.64
1443 CHR SMALLER SPOT 4	0	0.56	15.09	50.65	3.92	21.31	0.52	8.64	0.07	0.05	100.80
1444 CHR SMALLER SPOT 4	0	0.5	15.1	50.92	3.94	21.07	0.61	8.75	0	0.1	100.98
1445 CHR SMALLER SPOT 5	0	0.49	15.11	49.87	4.48	21.31	0.51	8.54	0.04	0.03	100.39
1446 CHR SMALLER SPOT 6	0	0.48	14.91	50.24	3.52	21.19	0.5	8.38	0.04	0.03	99.29
1447 CHR SMALLER SPOT 7	0	0.48	14.46	49.54	4.60	20.66	0.6	8.51	0	0.1	98.95
1448 CHR SMALLEST SPOT 8	0	0.43	15.28	50.65	3.49	21.46	0.55	8.4	0.03	0.04	100.33
1449 CHR **** SAMPLE 374 CENTRAL SPOT 1, 05-18-41	0.02	0.44	14.39	51.42	4.30	22.33	0.61	7.78	0.2	0.09	101.58
1450 CHR CENTRAL SPOT 1, 05-18-4191	0	0.47	13.79	51.01	4.19	22.12	0.54	7.7	0.15	0.03	100.00
1451 CHR AT MARGIN SPOT 2	0	0.49	14.61	50.62	4.25	22.39	0.59	7.79	0.13	0.03	100.61
1452 CHR AT MARGIN SPOT 2	0	0.47	14.64	50.53	3.16	22.52	0.43	7.58	0	0	99.33
1453 CHR CENTRAL SPOT 3	0	0.52	14.57	50.23	4.25	22.19	0.46	7.9	0.09	0.04	100.26
1454 CHR AT MARGIN SPOT 4	0	0.49	14.48	50.66	3.91	22.31	0.57	7.77	0.06	0	100.25
1455 CHR CENTRAL SPOT 5	0.02	0.51	14.78	49.91	4.62	21.70	0.54	8.09	0.12	0.14	100.42
1456 CHR CENTRAL SPOT 5	0	0.55	14.78	50.69	3.58	22.08	0.54	8	0.09	0.01	100.32
1457 CHR CENTRAL SPOT 6	0	0.47	14.38	49.61	3.90	22.14	0.44	7.61	0.04	0	98.59
1458 CHR CENTRAL SPOT 6	0	0.46	14.1	50.31	3.64	21.87	0.63	7.63	0.02	0.06	98.71
1459 CHR AT MARGIN SPOT 7	0	0.5	14.63	49.56	4.18	22.46	0.6	7.5	0.06	0.03	99.52
1460 CHR SMALLER SPOT 8	0	0.47	14.43	51	3.39	22.84	0.61	7.32	0.13	0.03	100.22
1461 CHR **** SAMPLE 375 CENTRAL, SPOT 1, 05-18-4	0	0.48	14.28	49.99	4.37	23.74	0.47	6.82	0.02	0.14	100.31
1462 CHR AT MARGIN SPOT 2	0.01	0.47	14.62	48.62	5.16	24.78	0.64	6.12	0.05	0.02	100.50
1463 CHR AT MARGIN SPOT 2	0.08	0.49	14.57	48.91	5.26	24.75	0.43	6.21	0	0	100.70
1464 CHR AT MARGIN SPOT 2	0.03	0.49	14.38	48.85	4.84	24.55	0.52	6.19	0.03	0	99.88
1465 CHR ANOTHER CENTRAL SPOT 3	0.03	0.49	14.61	49.56	4.42	24.57	0.56	6.25	0.13	0.06	100.67
1466 CHR SMALLEWR SPOPT 4	0.01	0.48	14.59	48.45	5.00	24.50	0.58	6.11	0.09	0.2	100.01
1467 CHR SMALLER SPOT 5	0	0.49	14.38	48.88	4.19	24.39	0.57	6.12	0.13	0.02	99.17
1468 CHR SMALLER SPOT 6	0.02	0.51	14.59	49.22	3.92	24.94	0.51	5.99	0	0	99.69
1469 CHR SMALLER SPOT 7	0.02	0.5	14.45	49.3	4.44	24.92	0.5	5.99	0.13	0.07	100.31
1470 CHR SMALLER SPOT 7	0	0.48	14.54	48.71	3.99	24.77	0.51	5.95	0	0.04	98.99
1471 CHR SMALLEST SPOT 8	0	0.45	14.61	49.11	4.72	25.08	0.56	5.98	0.1	0.05	100.66
1472 CHR SMALLEST SPOT 8	0	0.48	14.5	49.25	4.50	25.04	0.56	5.91	0.23	0.04	100.51
1473 CHR SMALLEST SPOT 8	0.01	0.49	14.34	49.36	4.14	24.49	0.59	6.07	0.2	0.05	99.73
1474 CHR ****SAMPLE 377 SPOT 1, 05-18-4293	0	0.52	14.48	50.44	3.52	22.62	0.55	7.49	0	0.04	99.65
1475 CHR AT MARGIN SPOT 2	0.02	0.52	14.14	49.64	4.51	23.88	0.61	6.52	0.12	0.07	100.03
1476 CHR CENTRAL SPOT 3	0	0.46	14.64	49.94	3.67	23.35	0.43	6.99	0.09	0.08	99.65
1477 CHR SMALLER SPOT 4	0	0.44	14.66	49.41	4.66	23.55	0.54	6.93	0.07	0.07	100.33
1478 CHR SMALLER SPOT 4	0	0.53	14.8	49.61	3.98	23.69	0.48	6.94	0.02	0.06	100.11
1479 CHR CENTRAL SPOT 5	0	0.46	14.31	50.88	3.66	23.68	0.57	6.78	0.2	0.09	100.64
1480 CHR CENTRAL SPOT 5	0	0.51	14.56	49.91	3.70	23.61	0.52	6.81	0.06	0.11	99.79
1481 CHR SMALLER SPOT 6	0.01	0.53	14.4	49.39	4.18	23.93	0.57	6.53	0.02	0.12	99.68
1482 CHR SMALLER SPY 7	0	0.5	14.03	50.19	4.31	24.25	0.56	6.51	0	0.03	100.38
1483 CHR SMALLER SPOT 8	0	0.45	14.47	50.48	3.70	24.48	0.59	6.35	0.07	0.08	100.67
1484 CHR SMALLER SPOT 8	0	0.45	14.34	50.46	3.97	24.65	0.57	6.33	0	0.04	100.81
1485 CHR **** SAMPLE 378 CENTRAL, SPOT 1, 05-18-4	0	0.53	14.83	51	3.48	21.73	0.55	8.28	0.04	0	100.44
1486 CHR CENTRAL, SPOT 1, 05-18-4294	0	0.47	14.79	50.72	4.19	21.78	0.65	8.18	0.05	0.07	100.90
1487 CHR AT MARGIN SPOT 2	0	0.48	14.23	48.72	4.73	22.98	0.66	6.88	0.09	0.06	98.83
1488 CHR AT MARGIN SPOT 2	0	0.49	14.16	49.68	4.42	23.16	0.56	6.95	0.19	0.05	99.66
1489 CHR CENTRAL, SPOT 3	0	0.5	14.77	49.99	3.97	23.09	0.55	7.24	0.09	0.09	100.29
1490 CHR AT MARGIN SPOT 4	0.05	0.56	14.9	49.56	4.71	23.99	0.67	6.78	0	0.06	101.28
1491 CHR AT MARGIN SPOT 4	0.03	0.46	14.3	49.28	4.97	23.30	0.53	6.93	0.07	0.04	99.91
1492 CHR SMALLER SPPOT, 5	0.03	0.48	14.62	49.47	5.50	23.51	0.5	7.07	0.14	0.14	101.46
1493 CHR SMALLER SPPOT, 5	0	0.47	14.52	49.29	4.75	23.08	0.68	7.05	0.06	0.13	100.03
1494 CHR SMALLER SPOT 6	0	0.54	13.96	48.34	4.70	22.82	0.57	6.8	0.2	0.08	98.01
1495 CHR SMALLER SPOT 6	0.03	0.51	14.41	49.84	4.19	23.11	0.62	6.99	0.06	0.13	99.89
1496 CHR SMALLER SPOT 7	0	0.49	14.21	49.65	4.98	23.30	0.58	7.02	0.11	0.11	100.45
1497 CHR SMALLER SPOT 7	0	0.5	14.56	49.58	3.96	22.97	0.54	7.11	0.21	0	99.43
1498 CHR SMALLER SPOT 8	0.03	0.49	14.74	49.48	5.00	23.49	0.57	7.03	0.09	0.09	101.01
1499 CHR SMALLER SPOT 8	0.01	0.38	14.18	50.13	3.91	22.83	0.59	6.99	0.12	0.09	99.23
1500 CHR **** SAMPLE 379 SPOT 1 CENTRAL, 05-19-42	0	0.56	14.45	50.75	3.72	22.85	0.56	7.44	0.1	0.09	100.51

Black Label BT-09-31

	SiO2	TiO2	Al2O3	Cr2O3	Fe2O3	FeO	MnO	MgO	ZnO	NiO	TOTAL
1501 CHR SPOT 1 CENTRAL, 05-19-4296	0.01	0.48	14.62	50.01	4.09	22.23	0.53	7.65	0.13	0.08	99.83
1502 CHR AT MARGIN SPOT 2	0.07	0.58	14.77	48.07	5.87	22.88	0.7	7.14	0.06	0.12	100.26
1503 CHR CENTRAL SPOT 3	0.02	0.52	14.54	48.88	3.92	22.12	0.67	7.3	0.11	0.05	98.13
1504 CHR CENTRAL SPOT 3	0	0.52	14.67	49.97	3.86	23.09	0.52	7.23	0.08	0.06	100.00
1505 CHR AT MARGIN SPOT 4	0.03	0.54	14.33	49.12	4.06	23.32	0.49	6.72	0.02	0.16	98.80
1506 CHR AT MARGIN SPOT 4	0.04	0.51	14.33	49.56	4.92	23.14	0.7	6.95	0.15	0.1	100.40
1507 CHR CENTRAL SPOT 5	0.07	0.52	14.5	48.88	4.14	22.36	0.68	7.02	0.14	0.1	98.41
1508 CHR CENTRAL SPOT 5	0.09	0.48	14.05	49.08	4.32	22.43	0.51	6.97	0.12	0	98.05
1509 CHR CENTRAL SPOT 5	0.02	0.51	14.65	50.37	3.74	23.40	0.59	7.04	0.07	0.03	100.42
1510 CHR SMALLER SPOT 6	0.27	0.46	14.99	49.14	5.66	22.31	0.59	7.22	0	0.1	100.74
1511 CHR SMALLER SPOT 7	0.05	0.51	15.05	49.63	4.41	23.81	0.57	6.86	0	0.11	101.00
1512 CHR SMALLER SPOT 7	0.05	0.46	15.04	49.36	4.80	23.80	0.52	6.86	0.1	0.04	101.03
1513 CHR SMALLER SPOOT 8	0	0.5	15.09	49.42	4.14	23.71	0.6	6.9	0.07	0.08	100.50
1514 CHR SMALLER SPOOT 8	0.02	0.52	15.15	49.22	4.66	23.79	0.63	6.89	0.09	0.09	101.07
1515 CHR SMALLER SPOOT 8	0.01	0.48	14.75	48.58	4.17	23.29	0.6	6.78	0.04	0.03	98.74
1516 CHR **** SAMPLE 380 CENTRAL SPOT 1, 05-19-42	0.02	0.49	14.18	50.37	4.30	24.00	0.62	6.55	0.11	0.12	100.76
1517 CHR CENTRAL SPOT 1, 05-19-4297	0	0.52	14.46	49.4	4.79	24.10	0.53	6.63	0.15	0.05	100.63
1518 CHR AT MARGIN SPOT 2	0.03	0.45	14.24	49.16	4.86	24.05	0.74	6.31	0.03	0.05	99.92
1519 CHR CENTRAL SPOT 3	0	0.45	14.29	49.09	4.61	24.08	0.51	6.4	0.08	0.08	99.59
1520 CHR SMALLER SPOT 4	0.01	0.51	14.36	49.51	4.31	24.00	0.6	6.49	0.09	0.08	99.96
1521 CHR SMALLER SPOT 5	0	0.51	14.37	49.85	4.39	24.22	0.52	6.58	0.04	0.07	100.55
1522 CHR SMALLER SPOT 6	0	0.44	14.44	49.31	4.76	24.25	0.63	6.38	0.09	0.08	100.38
1523 CHR SMALLER SPOT 6	0	0.48	14.41	49.83	4.35	24.13	0.74	6.51	0.02	0.03	100.50
1524 CHR SMALLER SPOT 6	0	0.46	14.49	49.2	4.41	24.34	0.56	6.34	0.04	0.04	99.88
1525 CHR SMALLER SPOT 7	0.04	0.52	14.1	48.29	4.69	24.44	0.56	5.86	0.13	0.05	98.68
1526 CHR SMALLER SPOT 7	0.01	0.45	14.24	49.13	4.10	24.00	0.66	6.25	0.04	0.02	98.90
1527 CHR SMALLER SPOT 7	0.04	0.49	13.97	49.17	4.71	23.97	0.64	6.28	0.01	0.07	99.35
1528 CHR SMALLER SPOT 8	0	0.46	14.52	49.38	4.76	24.09	0.7	6.51	0.16	0	100.58
1529 CHR **** SAMPLE 381 CENTRAL, SPOT 1, 05-19-4	0	0.55	14.66	50.53	3.73	22.65	0.64	7.61	0	0.02	100.39
1530 CHR CENTRAL, SPOT 1, 05-19-4299	0	0.44	14.47	50.03	4.46	22.68	0.54	7.4	0.11	0.13	100.26
1531 CHR AT MARGIN SPOT 2	0.04	0.54	14.86	51.02	3.47	23.35	0.63	7.24	0.03	0.01	101.19
1532 CHR AT MARGIN SPOT 2	0.05	0.54	14.81	50.55	3.79	23.12	0.7	7.21	0.06	0.03	100.86
1533 CHR AT MARGIN SPOT 2	0	0.55	15.07	50.94	3.40	23.62	0.56	7.24	0.14	0	101.52
1534 CHR AT MARGIN SPOT 2	0.07	0.51	14.43	49.67	4.21	22.93	0.55	7.05	0	0.07	99.49
1535 CHR CENTRAL, SPOT 3	0.03	0.44	13.93	50.61	4.35	22.53	0.6	7.35	0.03	0.08	99.96
1536 CHR AT MARGIN SPOT 4	0.05	0.46	14.23	50.46	3.80	23.24	0.64	6.89	0	0	99.77
1537 CHR CENTRAL SPOT 5	0.01	0.43	13.46	50.98	4.29	22.39	0.65	7.3	0.15	0.05	99.71
1538 CHR AT MARGIN SPOT 6	0.03	0.46	13.9	50.38	3.95	23.43	0.5	6.79	0	0.03	99.47
1539 CHR SMALLER SPOT 7	0.01	0.49	13.57	50.86	3.90	22.80	0.64	7.14	0	0.02	99.43
1540 CHR SMALLER SPOT 8	0.07	0.51	14.1	49.8	4.80	23.07	0.53	7	0.09	0.05	100.02
1541 CHR **** SAMPLE 382 CENTRAL, SPOT 1	0.05	0.53	14.29	50.88	4.62	22.41	0.66	7.65	0.13	0.08	101.30
1542 CHR CENTRAL, SPOT 1	0.05	0.53	13.5	50.53	3.99	21.82	0.6	7.53	0.04	0.02	98.61
1543 CHR AT MARGIN SPOT 2	0.07	0.49	14.72	49.34	4.53	22.64	0.64	7.21	0.06	0.09	99.78
1544 CHR CENTRAL SPOT 3	0.06	0.47	14.46	49.06	4.20	21.93	0.55	7.37	0.13	0.09	98.32
1545 CHR CENTRAL SPOT 3	0.08	0.44	14.69	49.97	4.68	22.28	0.69	7.46	0.16	0.07	100.52
1546 CHR CENTRAL SPOT 3	0.03	0.49	14.7	50.12	3.39	22.43	0.73	7.31	0.07	0.05	99.33
1547 CHR AT MARGIN SPOT 4	0.1	0.43	14.31	50.02	5.09	22.62	0.75	7.21	0.09	0	100.62
1548 CHR CENTRAL SPOT 5	0.04	0.47	14.63	50.13	4.03	23.14	0.61	7.06	0.03	0.11	100.25
1549 CHR AT MARGIN SPOT 6	0.12	0.44	14.49	49.13	5.64	23.06	0.66	6.94	0.09	0.01	100.57
1550 CHR AT MARGIN SPOT 6	0.09	0.43	13.41	49.3	5.16	22.53	0.69	6.74	0.15	0.04	98.54
1551 CHR AT MARGIN SPOT 6	0.15	0.53	15.08	49.55	4.91	23.25	0.64	7	0.06	0.07	101.24
1552 CHR AT MARGIN SPOT 6	0.11	0.48	14.46	49.68	5.11	22.79	0.66	7.18	0.05	0.01	100.52
1553 CHR SMALLER SPOT 7	0.06	0.47	13.97	49.62	4.54	22.62	0.76	7	0.04	0	99.07
1554 CHR SMALLER SPOT 8	0.07	0.51	13.97	49.66	4.57	22.98	0.65	6.8	0.12	0.1	99.43
1555 CHR **** SAMPLE 383 CENTRAL, SPOT 1, 05-19-4	0.03	0.46	14.63	50.33	3.81	21.75	0.52	7.95	0	0.05	99.53
1556 CHR AT MARGIN SPOT 2	0.05	0.51	14.44	49.92	4.26	22.64	0.55	7.28	0.1	0.11	99.86
1557 CHR CENTRAL SPOT 3	0.04	0.54	14.14	49.46	4.53	21.85	0.55	7.67	0	0.08	98.86
1558 CHR AT MARGIN SPOT 4	0.09	0.55	14.39	48.96	5.12	22.94	0.63	6.98	0.05	0.08	99.79
1559 CHR CENTRAL SPOT 5	0.04	0.56	14.06	49.22	4.56	22.49	0.5	7.21	0.02	0.18	98.84
1560 CHR CENTRAL SPOT 5	0.09	0.52	14.65	48.71	4.67	22.24	0.61	7.22	0.11	0.13	98.95
1561 CHR CENTRAL SPOT 6	0.06	0.55	14.87	47.96	4.62	21.75	0.61	7.49	0.09	0.13	98.13
1562 CHR CENTRAL SPOT 6	0.06	0.49	14.34	49.54	4.20	22.39	0.54	7.26	0.05	0.09	98.96
1563 CHR SMALLER SPOT 7	0.03	0.49	14.58	48.51	4.58	22.97	0.54	6.94	0.04	0.08	98.77
1564 CHR SMALLER SPOT 7	0.07	0.47	14.75	49.03	4.48	23.19	0.54	6.91	0.05	0	99.49
1565 CHR SMALLER SPOT 8	0.07	0.52	14.98	48.23	4.21	22.89	0.52	6.9	0.05	0.09	98.46
1566 CHR SMALLER SPOT 8	0.12	0.61	14.91	48.36	5.11	22.90	0.65	7	0.09	0.07	99.82
1567 CHR V LARGE CENTRAL NO PHOTO	0.11	0.51	14.73	50.6	4.00	22.11	0.52	7.69	0.09	0.06	100.42
1568 CHR V LARGE CENTRAL NO PHOTO	0.13	0.48	14.68	49.31	4.32	21.63	0.6	7.45	0.28	0.07	98.95
1569 CHR **** SAMPLE 384 CENTRAL, SPOT 1, 05-19-4	0.08	0.45	14.44	51.42	3.28	21.52	0.61	7.88	0.09	0.13	99.90
1570 CHR AT MARGIN SPOT 2	0.12	0.4	14.18	49.82	4.19	22.24	0.72	7	0.06	0.08	98.81
1571 CHR AT MARGIN SPOT 2	0.04	0.46	14.46	50.48	3.74	22.95	0.57	7.18	0.01	0.04	99.92
1572 CHR CENTRAL SPOT 3	0.05	0.53	14.22	50.06	3.94	22.03	0.49	7.57	0.07	0.09	99.05
1573 CHR CENTRAL SPOT 3	0.1	0.43	14.65	50.8	3.51	22.31	0.56	7.39	0.11	0.06	99.92
1574 CHR AT MARGIN SPOT 4	0.13	0.43	14.77	48.53	5.25	22.41	0.61	7.11	0.12	0.06	99.42
1575 CHR CENTRAL, 5	0.06	0.47	14.43	48.68	4.32	22.21	0.57	7.17	0.08	0.04	98.03
1576 CHR CENTRAL, 5	0.07	0.51	14.85	51.05	3.66	22.89	0.66	7.4	0	0.08	101.17
1577 CHR CENTRAL, 5	0.07	0.53	14.49	49.19	3.95	22.31	0.54	7.24	0.04	0.06	98.42
1578 CHR CENTRAL, 5	0.1	0.55	14.66	49.61	4.99	22.55	0.58	7.4	0.11	0.12	100.67
1579 CHR CENTRAL SPOT 6	0.09	0.5	14.55	50.07	3.73	22.78	0.51	7.1	0.04	0.08	99.45

Black Label BT-09-31

	SiO2	TiO2	Al2O3	Cr2O3	Fe2O3	FeO	MnO	MgO	ZnO	NiO	TOTAL
1580 CHR SMALLER SPOT 8	0.08	0.49	14.96	48.92	4.68	23.07	0.62	6.99	0.03	0.09	99.93
1581 CHR **** SAMPLE 385 CENTRAL, SPOT 1, 05-19-4	0.08	0.54	14.71	49.26	5.38	22.34	0.65	7.62	0.01	0.07	100.66
1582 CHR CENTRAL, SPOT 1, 05-19-4303	0.12	0.52	14.64	49.73	4.71	22.03	0.66	7.58	0.08	0.02	100.09
1583 CHR AT MARGIN SPOT 2	0.09	0.51	14.69	49.28	4.77	22.81	0.56	7.17	0.1	0.03	100.02
1584 CHR CENTRAL SPOT 3	0.06	0.49	15.07	49.74	3.63	21.73	0.58	7.78	0	0.18	99.25
1585 CHR CENTRAL SPOT 3	0.05	0.47	14.98	49.95	3.83	22.88	0.55	7.27	0.09	0.02	100.09
1586 CHR CENTRAL SPOT 5	0.08	0.51	14.86	49.92	4.41	22.13	0.69	7.65	0.07	0.06	100.38
1587 CHR CENTRAL, SPOT 6	0.01	0.53	14.46	49.33	4.25	22.45	0.49	7.44	0.05	0.07	99.09
1588 CHR SMALLER SPOT 7	0.07	0.47	13.24	48.77	5.77	22.22	0.61	7.01	0.16	0.02	98.34
1589 CHR SMALLER SPOT 7	0.13	0.57	14.58	49.07	5.21	22.24	0.72	7.33	0.07	0.12	100.04
1590 CHR *** SAMPLE 386 CENTRAL, SPOT 1, 05-19-43	0.04	0.51	14.52	48.68	4.49	23.63	0.65	6.47	0.1	0.08	99.17
1591 CHR AT MARGIN SPOT 2	0.05	0.47	14.31	48.94	4.34	23.02	0.53	6.81	0	0.08	98.55
1592 CHR AT MARGIN SPOT 2	0.06	0.59	14.12	48.48	4.94	23.43	0.56	6.57	0.12	0.05	98.93
1593 CHR AT MARGIN SPOT 2	0.12	0.48	14.17	49.88	4.49	23.29	0.6	6.69	0.02	0.03	99.77
1594 CHR CENTRAL SPOT 3	0.03	0.53	14.29	48.67	4.76	23.33	0.64	6.68	0.06	0.09	99.08
1595 CHR CENTRAL SPOT 3	0.04	0.47	13.9	49.38	4.39	23.33	0.62	6.55	0.08	0.07	98.83
1596 CHR CENTRAL SPOT 4	0.08	0.47	14.21	49.47	4.31	23.88	0.68	6.26	0.04	0.04	99.43
1597 CHR CENTRAL SPOT 5	0.06	0.53	14.39	48.74	4.16	22.79	0.61	6.81	0.06	0.12	98.28
1598 CHR CENTRAL SPOT 5	0.08	0.49	14.27	49.38	4.53	23.26	0.56	6.74	0.09	0.01	99.41
1599 CHR CENTRAL SPOT 6	0.07	0.51	14.07	48.05	6.10	23.85	0.52	6.42	0.06	0.08	99.73
1600 CHR SMALLER SPOT 8	0.16	0.43	14.22	48.32	6.19	23.90	0.62	6.14	0.18	0.02	100.18
1601 CHR **** SAMPLE 387 CENTRAL, SPOT 1, 05-20-4	0.1	0.51	14.47	47.79	5.48	24.30	0.55	5.89	0.26	0.11	99.46
1602 CHR CENTRAL SPOT 2	0.04	0.48	14.37	48.02	4.73	23.83	0.62	6.08	0.29	0.07	98.53
1603 CHR CENTRAL SPOT 2	0	0.49	14.61	48.14	4.92	24.57	0.67	5.99	0.09	0.14	99.62
1604 CHR CENTRAL SPOT 3	0.08	0.49	14.58	49.13	4.32	24.18	0.63	6.18	0	0.11	99.70
1605 CHR SMALLER SPOT 4	0.06	0.51	14.77	49.54	4.06	24.92	0.67	5.93	0.05	0.07	100.58
1606 CHR SMALLER SPOT 4	0.1	0.53	14.68	48.94	3.98	24.54	0.63	5.93	0	0	99.33
1607 CHR SMALLER SPOT 5	0.1	0.56	14.34	47.44	5.49	24.65	0.59	5.76	0	0.01	98.94
1608 CHR SPOT 5	0.02	0.55	14.42	47.74	5.03	24.76	0.59	5.86	0.07	0.02	99.05
1609 CHR SMAZLLER SPOT 6	0.05	0.56	14.48	48.08	4.93	24.02	0.55	6.24	0.19	0.05	99.15
1610 CHR SMALLER SPOT 7	0.04	0.57	14.92	47.37	4.62	24.52	0.61	5.97	0.01	0.03	98.66
1611 CHR SMALLER SPOT 7	0.05	0.54	14.71	48.15	4.92	24.61	0.48	6.03	0.18	0.07	99.74
1612 CHR SMALLER SPOT 8	0.07	0.55	14.28	47.17	6.34	24.64	0.64	5.88	0.03	0.07	99.67
1613 CHR **** SAMPLE 388 SPOT 1, 05-21-4306	0.06	0.41	13.8	48.69	5.21	22.81	0.56	6.63	0.18	0.18	98.53
1614 CHR SPOT 1, 05-21-4306	0.05	0.52	13.88	49.39	4.51	23.55	0.57	6.43	0.18	0.11	99.19
1615 CHR AT MARGIN SPOT 2	0.02	0.34	12.99	48.89	5.50	24.50	0.6	5.57	0.23	0.02	98.66
1616 CHR AT MARGIN SPOT 2	0.06	0.44	13.85	47.59	6.46	23.91	0.58	6.11	0.25	0.06	99.31
1617 CHR CENTRAL SPOT 3	0.01	0.47	13.9	49.27	4.24	24.19	0.54	6.1	0.09	0.1	98.91
1618 CHR AT MARGIN SPOT 4	0.06	0.44	14.42	49.87	4.59	24.60	0.78	6	0.19	0.05	101.00
1619 CHR CENTRAL SPOT 5	0.06	0.39	14.3	48.24	5.52	24.37	0.57	5.92	0.18	0.12	99.67
1620 CHR CENTRAL SPOT 6	0	0.49	13.96	48.82	4.30	24.55	0.57	5.82	0.24	0.02	98.77
1621 CHR CENTRAL SPOT 6	0.01	0.5	13.97	47.91	4.92	24.53	0.58	5.77	0.11	0.06	98.36
1622 CHR CENTRAL SPOT 6	0.04	0.46	14.1	47.85	5.31	24.56	0.65	5.74	0.11	0.03	98.85
1623 CHR SMALLER SPOT 7	0.01	0.45	13.93	49.02	4.39	24.75	0.59	5.7	0.12	0.11	99.07
1624 CHR SMALLER SPOT 8	0.05	0.44	14.08	49.5	3.99	24.51	0.64	5.81	0.17	0	99.19
1625 CHR **** SAMPLE 389 SPOT 1 BAD POL, 05-21-43	0.01	0.55	14.06	48.25	4.86	24.92	0.55	5.71	0.13	0.08	99.12
1626 CHR NEAR RIND SPPOT 2	0	0.56	14.2	48.08	4.88	24.77	0.64	5.74	0.22	0.09	99.18
1627 CHR BRIGHT MARGIN	0.12	0.72	5.03	47.94	14.65	26.73	0.66	3.35	0.13	0.04	99.37
1628 CHR CENTRAL SPOT 4	0.06	0.59	14.28	48.08	5.16	24.72	0.55	5.9	0.07	0.03	99.44
1629 CHR CENTRAL SPOT 5	0.11	0.63	14.4	47.13	6.27	24.23	0.6	6.09	0.1	0.07	99.63
1630 CHR CENTRAL, SPOT 6	0.03	0.58	14.16	48.2	4.92	24.73	0.52	5.83	0.16	0.09	99.22
1631 CHR CENTRAL SPOT 7	0.12	0.56	14.39	48.36	6.18	24.81	0.58	5.99	0.02	0.12	101.13
1632 CHR SMALLER SPOT 8	0.03	0.56	14.35	48.42	4.74	24.42	0.64	5.99	0.16	0.11	99.42
1633 CHR **** SAMPLE 390 CENTRAL, SPOT 1, 05-21-4	0.12	0.51	14.11	48.1	5.82	24.19	0.64	5.92	0.15	0.12	99.68
1634 CHR AT MARGIN SPOT 2	0.02	0.43	13.53	47.62	6.22	25.04	0.68	5.44	0.08	0.02	99.08
1635 CHR AT MARGIN SPOT 2	0.12	0.47	13.5	47	6.96	24.88	0.66	5.35	0.05	0	99.00

Black Thor BT-08-10

	SiO2	TiO2	Al2O3	Cr2O3	Fe2O3	FeO	MnO	MgO	ZnO	NiO	TOTAL
1 CHR **** SAMPLE 486004 REL L CENTRAL	0	0.37	14.19	51.02	2.70	24.09	0.38	6.46	0	0	99.21
2 CHR AT MARGIN	0	0.35	14.32	49.47	3.59	24.61	0.55	5.92	0	0	98.81
3 CHR AT MARGIN	0	0.31	14.18	51.23	3.61	24.64	0.55	6.28	0	0	100.80
4 CHR BRIGHT AT M W INCL	0.01	0.49	0.37	37.79	29.67	28.64	0.7	1.59	0.07	0.07	99.40
5 CHR BRIGHT AT M W INCL	0	0.45	0.6	37.37	30.03	28.39	0.86	1.7	0	0.12	99.53
6 CHR ANOTHER REL C CENTRAL	0	0.42	14.17	50.74	3.55	23.83	0.56	6.69	0	0	99.96
7 CHR AT MARGIN	0	0.32	14.54	49.01	4.07	24.34	0.46	6.18	0	0	98.92
8 CHR AT MARGIN	0	0.31	14.56	50.45	3.75	24.36	0.63	6.37	0	0	100.44
9 CHR ANOTHER CENTRAL	0	0.44	16.31	47.95	4.15	23.74	0.56	7.01	0	0.01	100.18
10 CHR AT MARGIN	0	0.42	17.06	46.21	3.78	23.88	0.53	6.67	0	0.02	98.57
11 CHR AT MARGIN	0	0.5	16.96	46.32	4.18	24.14	0.54	6.7	0	0	99.34
12 CHR ANOTHER CENTRAL	0	0.42	16.03	48.93	3.29	23.65	0.47	7.03	0	0	99.82
13 CHR AT MARGIN	0	0.49	16.67	46.57	3.58	24.16	0.5	6.5	0	0	98.47
14 CHR AT MARGIN	0	0.44	16.6	47.24	3.39	23.88	0.5	6.71	0	0	98.76
15 CHR AT MARGIN	0	0.43	16.73	46.49	3.76	23.87	0.55	6.62	0	0	98.45
16 CHR AT MARGIN	0	0.42	16.85	47.1	4.29	24.11	0.48	6.86	0	0	100.11
17 CHR SMALLER CENTRAL	0	0.48	16.76	47.45	4.00	24.48	0.63	6.61	0	0	100.41
18 CHR BRIGHT MARGIN INCL SIL	0	0.39	7.98	49.42	11.06	27.38	0.96	3.54	0	0	100.73
19 CHR V SMALL	0	0.44	16.57	46.56	4.03	23.95	0.62	6.57	0	0	98.74
20 CHR V SMALL	0	0.49	16.77	47.51	4.36	24.73	0.55	6.61	0	0.05	101.07
21 CHR V SMALL	0	0.44	16.59	47.8	3.94	24.68	0.63	6.47	0	0	100.54
22 CHR **** SAMPLE 486006 L CENTRAL	0	0.46	15.07	49.86	3.94	23.36	0.43	7.29	0	0	100.40
23 CHR ANOTHER CENTRAL	0	0.34	15.26	50.27	3.33	23.31	0.46	7.21	0	0	100.17
24 CHR AT MARGIN	0	0.39	15.78	48.82	4.44	24.15	0.56	6.83	0	0	100.97
25 CHR AT MARGIN	0	0.36	15.41	48.31	4.10	23.91	0.49	6.6	0	0.01	99.19
26 CHR SMALLER CENTRAL	0	0.34	15.77	48.75	4.53	23.86	0.5	6.98	0	0	100.72
27 CHR SMALLER CENTRAL	0	0.37	15.76	48.65	3.98	23.73	0.57	6.87	0	0	99.93
28 CHR AT MARGIN	0	0.47	17.2	47.54	3.98	24.43	0.56	6.86	0	0	101.04
29 CHR AT MARGIN	0	0.46	16.67	48.28	3.99	24.39	0.57	6.86	0	0	101.22
30 CHR AT MARGIN	0	0.42	16.12	49.27	3.14	24.69	0.5	6.52	0	0	100.65
31 CHR ANOTHER REL LARGE	0	0.37	15.57	49.53	3.63	24.42	0.51	6.59	0	0	100.62
32 CHR SMALL RELICT CENTRAL	0	0.36	16.09	48.38	4.14	25.30	0.62	6.05	0	0	100.94
33 CHR SMALL RELICT CENTRAL	0	0.42	16.07	47.39	4.45	25.00	0.48	6.17	0	0	99.98
34 CHR ANOTHER CENTRAL	0	0.41	15.23	48.2	4.46	23.81	0.55	6.67	0	0	99.34
35 CHR ANOTHER	0	0.41	15.98	48.91	4.27	24.12	0.59	6.91	0	0	101.20
36 CHR ANOTHER	0	0.37	16.01	46.9	4.72	23.49	0.55	6.84	0	0	98.88
37 CHR ANOTHER	0	0.39	16	48.74	4.08	24.07	0.53	6.87	0	0	100.68
38 CHR SMALLER CENTRAL	0	0.38	16.26	46.94	5.12	24.85	0.6	6.27	0	0	100.42
39 CHR SMALL W INCL	0	0.38	15.67	47.27	5.58	25.01	0.7	6.09	0	0.01	100.71
40 CHR BRIGHT MARGIN	0	0.68	1.88	43.99	22.29	28.97	0.94	1.91	0	0.04	100.70
41 CHR **** SAMPLE 486007 REL LARGE	0	0.37	14.04	51.83	3.74	23.88	0.48	6.94	0	0	101.28
42 CHR REL LARGE	0	0.26	14.07	51.75	3.67	24.02	0.59	6.66	0	0.01	101.03
43 CHR REL LARGE	0	0.31	13.36	51.85	3.84	24.23	0.42	6.48	0	0	100.49
44 CHR AT MARGIN	0	0.37	14.2	50.76	4.02	24.55	0.46	6.43	0	0	100.79
45 CHR SMALLER CENTRAL	0	0.35	14.07	50.34	3.49	24.06	0.66	6.27	0	0	99.24
46 CHR AY MARGIN	0	0.32	14.6	49.42	4.53	24.49	0.66	6.23	0	0	100.25
47 CHR ANOTHER CENTRAL	0	0.36	13.92	51.59	2.67	24.76	0.56	6.01	0	0	99.88
48 CHR AT MARGIN NO RIND	0	0.45	14.23	50.25	3.53	24.61	0.55	6.15	0.05	0	99.82
49 CHR ANOTHER REL L CENTRAL	0	0.28	13.78	49.88	4.06	23.75	0.65	6.29	0	0	98.69
50 CHR ANOTHER REL L CENTRAL	0	0.29	13.73	50.9	3.88	24.29	0.58	6.24	0	0	99.91
51 CHR ANOTHER REL LARGE	0	0.34	13.84	51.67	3.47	24.44	0.44	6.43	0	0	100.64
52 CHR V SMALL	0	0.27	14.02	51.39	4.09	25.17	0.54	6.05	0	0	101.53
53 CHR V SMALL	0	0.34	13.7	51.1	4.05	24.75	0.66	6.07	0	0	100.68
54 CHR SMALL GRAIN	0	0.36	13.66	50.87	4.02	24.14	0.62	6.37	0	0	100.04
55 CHR SMALL	0	0.34	13.89	50.98	4.00	24.54	0.66	6.22	0	0	100.63
56 CHR REL L CENTRAL	0	0.4	14.1	50.97	3.85	23.97	0.4	6.79	0	0	100.49
57 CHR **** SAMPLE 486008 8 L CENTRAL	0	0.33	15.42	48	4.02	24.45	0.55	6.13	0.02	0	98.92
58 CHR L CENTRAL	0	0.39	15.05	49.73	3.73	24.99	0.58	6.12	0	0	100.59
59 CHR AT MARGIN	0	0.35	15.57	48.88	4.31	25.54	0.56	5.91	0	0	101.12
60 CHR SMALLER	0	0.41	15.4	49.49	4.00	25.55	0.65	5.93	0	0	101.43
61 CHR SMALLER	0	0.37	14.23	50.52	3.77	25.01	0.7	5.91	0	0.02	100.53
62 CHR SMALLER	0	0.37	15.31	50.31	2.63	25.32	0.7	5.83	0	0	100.46
63 CHR BRIGHT ALONG CRACK	0	0.51	0.95	44.92	22.54	29.68	0.68	1.44	0	0.03	100.75
64 CHR REL LARGE	0	0.31	14.14	50.64	3.91	24.01	0.53	6.55	0	0	100.09
65 CHR ANOTHER	0	0.31	14.39	51.12	2.99	24.37	0.39	6.42	0	0	99.99
66 CHR REL LARGE	0	0.31	14.24	51.25	3.51	24.03	0.4	6.71	0	0	100.45
67 CHR REL LARGE	0	0.37	14.77	51.44	3.28	24.07	0.45	6.92	0	0	101.31
68 CHR REL LARGE	0	0.31	13.61	51.07	3.60	23.60	0.5	6.62	0	0	99.31
69 CHR SMALLER	0	0.31	14.87	50.28	3.49	24.97	0.52	6.1	0	0	100.54
70 CHR REL LARGE	0	0.32	14.56	49.56	4.49	23.45	0.55	6.89	0	0	99.82
71 CHR V SMALL	0	0.33	14.84	48.62	4.44	25.41	0.67	5.58	0	0	99.88
72 CHR V SMALL	0	0.37	14.8	49.11	4.51	25.65	0.55	5.68	0	0	100.67
73 CHR **** SAMPLE 486009 REL L CENTRAL	0	0.29	14.47	52.14	2.88	22.67	0.42	7.61	0	0	100.48
74 CHR AT MARGIN	0	0.31	14.65	51.4	3.40	24.26	0.6	6.64	0	0	101.26
75 CHR AT MARGIN	0	0.28	14.49	51.77	2.93	24.26	0.58	6.54	0	0	100.85
76 CHR AT MARGIN	0	0.29	13.55	50.29	3.89	23.60	0.5	6.44	0	0	98.56
77 CHR REL L CENTRAL	0	0.37	14.43	53.11	2.36	22.73	0.43	7.76	0	0	101.19
78 CHR REL L CENTRAL	0	0.26	13.03	52.63	2.24	22.35	0.42	7.16	0	0	98.08
79 CHR REL L CENTRAL	0	0.26	14.17	51.9	3.07	22.55	0.5	7.47	0	0	99.92

Black Thor BT-08-10

	SiO2	TiO2	Al2O3	Cr2O3	Fe2O3	FeO	MnO	MgO	ZnO	NiO	TOTAL
80 CHR AT MARGIN	0	0.26	14.46	50.89	3.39	24.31	0.67	6.31	0	0	100.29
81 CHR V LARGE CENTRAL	0	0.31	14.37	52.84	2.47	23.19	0.4	7.39	0	0	100.97
82 CHR V LARGE CENTRAL	0	0.3	13.68	51.76	3.64	22.73	0.45	7.35	0	0	99.90
83 CHR AT MARGIN	0	0.27	13.71	52.61	2.82	23.61	0.47	6.84	0	0	100.33
84 CHR L CENTRAL	0	0.33	14.2	52.2	2.81	23.02	0.55	7.27	0	0	100.38
85 CHR AT MARGIN	0	0.2	13.98	49.4	4.01	23.93	0.61	6.06	0	0.02	98.21
86 CHR AT MARGIN	0	0.18	15.25	49.23	4.69	23.55	0.43	6.99	0	0	100.32
87 CHR ANOTHER L CENTRAL	0	0.23	14.03	51.52	3.66	23.01	0.45	7.17	0	0.06	100.43
88 CHR AT MARGIN	0	0.32	14.96	50.85	3.19	23.56	0.56	6.99	0	0	100.13
89 CHR REL L CENTRAL	0	0.29	14.42	52.06	2.70	22.10	0.43	7.84	0	0	99.84
90 CHR ANOTHER L CENTRAL	0	0.33	14.48	52.37	2.82	22.10	0.43	8.01	0	0.01	100.55
91 CHR AT MARGIN	0	0.35	13.99	51.82	2.80	23.98	0.52	6.58	0	0	100.04
92 CHR L CENTRAL	0	0.25	14.35	51.79	3.11	22.79	0.47	7.36	0	0.06	100.17
93 CHR SMALL INST	0	0.29	14.17	51.9	2.70	23.58	0.63	6.75	0	0	100.02
94 CHR SMALL	0	0.32	14.3	51.04	2.79	24.23	0.57	6.3	0	0	99.55
95 CHR L CENTRAL	0	0.3	13.9	53.13	2.40	22.53	0.44	7.6	0	0	100.30
96 CHR L CENTRAL	0	0.31	14.5	52.58	2.69	21.98	0.41	8.08	0	0.04	100.59
97 CHR L CENTRAL	0	0.32	14.34	52.04	2.32	21.94	0.4	7.81	0	0.06	99.22
98 CHR SMALL INST	0	0.32	13.6	51.08	2.63	24.44	0.63	5.84	0	0	98.54
99 CHR SMALL INST	0	0.27	14.11	50.91	3.23	24.31	0.59	6.19	0	0	99.61
100 CHR **** SAMPLE 486010 L CENTRAL	0	0.29	15.33	49.73	3.31	25.51	0.45	5.81	0	0	100.43
101 CHR BRIGHT ALT AT MARGIN	0	0.46	0.56	43.07	23.99	29.25	0.68	1.29	0.01	0.13	99.44
102 CHR BRIGHT ALT AT MARGIN	0	0.49	0.57	43.18	24.14	29.34	0.74	1.36	0	0.04	99.86
103 CHR L CENTRAL	0	0.29	16.3	48.65	3.17	24.07	0.48	6.66	0	0	99.63
104 CHR AT MARGIN	0	0.4	15.95	48.49	3.14	25.56	0.53	5.72	0	0	99.79
105 CHR BRIGHT MARGIN	0	0.58	0.59	45.01	22.92	29.83	0.86	1.27	0.01	0.08	101.14
106 CHR L CENTRAL	0	0.39	16.79	48.51	2.79	25.74	0.46	5.89	0	0.01	100.58
107 CHR L CENTRAL	0	0.27	15.76	48.22	3.21	25.58	0.6	5.41	0	0	99.05
108 CHR SMALL REMN	0	0.31	16.83	47.74	3.74	25.77	0.55	5.8	0	0	100.74
109 CHR SMALL REMN	0	0.3	17.25	46.05	4.72	25.37	0.57	5.97	0	0	100.22
110 CHR BRIGHT MARGINAL W LATHS	0.01	0.43	1.49	45.9	21.67	28.88	0.82	1.9	0	0.13	101.23
111 CHR REL L CENTRAL	0	0.36	16.81	48.34	3.27	24.52	0.54	6.59	0	0	100.43
112 CHR AT MARGIN	0	0.29	16.12	48.74	3.35	25.85	0.57	5.61	0	0	100.53
113 CHR AT MARGIN	0	0.23	15.2	46.63	5.05	25.13	0.59	5.45	0	0	98.28
114 CHR ANOTHER L CENTRAL	0	0.27	16.15	48.91	3.83	25.25	0.56	6.11	0	0	101.08
115 CHR ANOTHER L CENTRAL	0	0.35	15.37	47.49	3.96	25.25	0.42	5.62	0	0	98.46
116 CHR ANOTHER L CENTRAL	0	0.31	16.12	48.06	4.10	25.18	0.56	6.02	0	0	100.35
117 CHR ANOTHER L CENTRAL	0	0.28	15.8	47.3	4.56	25.20	0.43	5.84	0	0	99.42
118 CHR REL L CENTRAL	0	0.37	17.11	48.37	3.87	23.82	0.52	7.28	0	0	101.35
119 CHR REL L CENTRAL	0	0.36	16.41	47.77	3.53	23.67	0.53	6.83	0	0	99.10
120 CHR SMALLER RELICT CENTRAL	0	0.36	16.29	46.42	4.23	25.41	0.55	5.57	0.08	0	98.91
121 CHR BRIGHT ALTERATION	0.07	0.57	0.27	39.92	28.39	28.39	1.7	1.27	0.05	0.11	100.74
122 CHR **** SAMPLE 486011 L CENTRAL	0	0.38	15.95	48.82	3.85	22.68	0.46	7.62	0	0	99.77
123 CHR AT MARGIN	0	0.33	15.88	48.27	3.92	23.42	0.39	7.04	0	0	99.25
124 CHR ANOTHER REL L CENTRAL	0	0.35	16.33	49.55	3.18	22.64	0.44	7.8	0	0	100.29
125 CHR AT MARGIN NEAR NARFROW RIND	0	0.31	16.35	48.48	4.12	22.82	0.51	7.58	0	0	100.17
126 CHR SMALLER CENTRAL	0	0.36	16.72	48.55	4.19	23.52	0.56	7.39	0	0	101.29
127 CHR SMALLER CENTRAL	0	0.36	16.68	48.92	3.33	23.49	0.48	7.32	0	0	100.57
128 CHR BRIGHT MARGINAL RIND	0.02	0.61	3.2	44.24	20.55	28.17	0.68	2.44	0.09	0.13	100.14
129 CHR ANOTHER CENTRAL	0	0.28	15.86	49.24	4.27	21.98	0.28	8.2	0	0	100.11
130 CHR AT MARGIN NEAR RIND	0	0.27	16.09	49.13	3.91	23.27	0.43	7.35	0	0	100.45
131 CHR SMALLER	0	0.39	16.6	49.03	3.82	23.05	0.52	7.67	0	0.05	101.13
132 CHR SMALLER	0	0.41	15.85	49.38	3.53	23.07	0.43	7.48	0	0	100.14
133 CHR V SMALL	0	0.32	15.38	48.78	3.70	23.84	0.56	6.58	0	0	99.16
134 CHR ANOTHER V SMALL	0	0.38	15.47	48.29	3.66	23.72	0.48	6.6	0	0.09	98.70
135 CHR ANOTHER	0	0.35	16.2	48.7	3.94	23.99	0.31	7.03	0	0	100.52
136 CHR BRIGHT MARGINAL	0	0.43	5.47	44.8	17.95	27.27	0.88	3.15	0	0.11	100.06
137 CHR **** SAMPLE 486012 L CENTRAL	0	0.36	14.54	49.93	3.82	23.78	0.43	6.73	0	0	99.59
138 CHR L CENTRAL	0	0.37	15.56	48.48	3.73	24.65	0.41	6.26	0	0	99.45
139 CHR ANOTHER REL L CENTRAL	0	0.34	15.19	50.22	3.25	22.34	0.41	7.72	0	0	99.48
140 CHR NEAR MARGIN	0	0.31	15.6	48.59	4.01	23.14	0.32	7.2	0	0.02	99.19
141 CHR REL L CENTRAL	0	0.28	14.68	49.9	3.99	23.14	0.46	7.08	0	0	99.53
142 CHR ANOTHER L CENTRAL	0	0.44	15.49	49.39	3.97	23.58	0.38	7.22	0	0	100.48
143 CHR AT MARGIN	0	0.41	15.18	48.95	3.93	23.96	0.59	6.6	0	0.02	99.63
144 CHR ANOTHER L CENTRAL	0	0.44	15.37	50.47	3.61	23.58	0.38	7.37	0	0	101.22
145 CHR ANOTHER L CENTRAL	0	0.35	14.99	49.92	3.32	23.41	0.41	6.99	0	0	99.38
146 CHR AT MARGIN	0	0.34	15.62	48.41	3.66	24.23	0.36	6.48	0	0	99.11
147 CHR REL L CENTRAL	0	0.31	15.53	49.61	3.63	23.58	0.36	7.09	0	0	100.11
148 CHR AT MARGIN	0	0.43	15.84	48.2	4.36	24.05	0.52	6.79	0	0	100.20
149 CHR C ANGULAR CENTRAL	0	0.34	15.36	49.98	2.81	24.06	0.53	6.58	0	0	99.66
150 CHR AT MARGIN	0	0.3	15.84	49.31	4.38	24.13	0.44	6.96	0	0	101.36
151 CHR AT MARGIN	0	0.36	15.66	50.31	3.21	24.27	0.46	6.83	0	0	101.09
152 CHR AT MARGIN	0	0.34	15.03	48.81	3.68	24.14	0.47	6.35	0	0	98.82
153 CHR V SMALL	0	0.39	14.34	48.3	4.73	24.35	0.45	6.15	0	0	98.70
154 CHR V SMALL	0	0.39	15.14	49.01	3.93	24.75	0.34	6.29	0	0	99.85
155 CHR BRIGHT MARGIN	0	0.67	0.86	44.94	23.13	29.23	0.62	1.96	0	0.11	101.53
156 CHR BRIGHT MARGIN	0	0.5	0.81	44.81	23.16	28.91	0.71	1.85	0	0.15	100.90
157 CHR **** SAMPLE 486013 REL L CENTRAL	0	0.36	15.69	49.55	2.94	23.32	0.34	7.17	0	0	99.37
158 CHR AT MARGIN	0	0.37	15.64	47.93	4.73	23.71	0.54	6.85	0	0	99.77

Black Thor BT-08-10

	SiO2	TiO2	Al2O3	Cr2O3	Fe2O3	FeO	MnO	MgO	ZnO	NiO	TOTAL
159 CHR ANOTHER REL L CENTRAL	0	0.36	15.16	49.59	3.38	23.77	0.42	6.73	0	0.1	99.51
160 CHR AT MARGIN INSIDE RIND	0	0.37	15.76	48.79	4.29	24.48	0.34	6.7	0	0	100.73
161 CHR ANOTHER L CENTRAL	0	0.33	15.05	49.63	3.91	23.43	0.29	7.12	0	0	99.76
162 CHR AT MARGIN	0	0.33	15.2	49.5	4.19	24.26	0.4	6.67	0.04	0	100.59
163 CHR C ANG CENTRAL	0	0.31	14.18	51.2	3.47	23.18	0.33	7.18	0	0	99.85
164 CHR AT MARGIN	0	0.33	14.8	50.37	4.27	23.94	0.53	6.89	0	0	101.13
165 CHR AT MARGIN	0	0.35	14.38	50.94	3.20	24.06	0.47	6.59	0	0	99.99
166 CHR ADJ SMALLER	0	0.33	14.24	52.39	3.05	24.20	0.4	6.81	0	0.02	101.44
167 CHR ADJ SMALLER	0	0.33	13.62	51.41	3.17	23.66	0.33	6.66	0	0.05	99.23
168 CHR REL L CENTRAL	0	0.35	15.31	49.86	4.17	23.75	0.42	7.08	0	0.07	101.01
169 CHR AT MARGIN	0	0.34	16	48.18	3.98	24.35	0.55	6.47	0	0.01	99.88
170 CHR SMALLER	0	0.29	15.26	49.69	3.84	24.14	0.49	6.65	0	0	100.35
171 CHR SMALLER CENTRAL	0	0.36	15.65	48.51	4.17	24.14	0.48	6.65	0	0	99.96
172 CHR SMALL CENTRAL	0	0.36	15.15	49.11	4.41	24.15	0.44	6.69	0	0	100.31
173 CHR **** SAMPLE 486014 REL L CENTRAL	0	0.34	14.67	49.58	4.56	23.91	0.45	6.76	0	0.02	100.29
174 CHR AT MARGIN	0	0.45	15.06	48.08	4.91	24.54	0.46	6.37	0	0	99.87
175 CHR L TRIANG CENTRAL	0	0.4	14.8	49.6	3.83	24.04	0.38	6.67	0	0	99.72
176 CHR AT MARGIN NEAR RIND	0	0.29	15.38	48.75	4.43	24.47	0.51	6.39	0.02	0	100.24
177 CHR L ANG CENTRAL	0	0.34	14.6	49.56	4.24	23.00	0.31	7.24	0	0.01	99.30
178 CHR AT MARGIN	0	0.34	15.18	48.98	4.14	24.52	0.44	6.37	0	0	99.97
179 CHR ANOTHER L CENTRAL	0	0.45	14.93	48.68	5.05	24.12	0.44	6.76	0	0	100.43
180 CHR AT MARGIN INSIDE RIND	0	0.4	15.72	48.16	3.88	24.72	0.41	6.27	0	0	99.56
181 CHR SMALLER GRAIN	0	0.43	15.22	49.54	4.08	24.24	0.39	6.8	0	0	100.70
182 CHR AT MARGIN	0	0.42	15.78	47.83	4.92	24.32	0.48	6.67	0	0	100.42
183 CHR V SMALL	0	0.38	15.13	48.19	5.14	24.76	0.44	6.3	0	0	100.34
184 CHR SMALL CLUSTER	0	0.47	13.56	48.74	5.29	24.92	0.56	5.8	0	0	99.34
185 CHR SMALL CLUSTER	0	0.35	14.56	50.05	3.93	23.37	0.41	7.03	0	0	99.70
186 CHR V SMALL W WIDE RIND	0	0.44	15.63	47.34	4.35	24.24	0.58	6.34	0	0.01	98.93
187 CHR V SMALL W WIDE RIND	0	0.47	15.01	47.61	5.24	24.95	0.49	6.08	0	0	99.86
188 CHR **** SAMPLE 486015 REL L CENTRAL	0	0.37	14.6	49.9	4.36	23.07	0.36	7.33	0	0	100.00
189 CHR AT MARGIN	0	0.37	15.77	48.6	3.81	24.05	0.29	6.8	0	0	99.69
190 CHR ANOTHER L CENTRAL	0	0.36	14.99	48.81	3.85	23.22	0.45	6.91	0	0.02	98.62
191 CHR ANOTHER L CENTRAL	0	0.31	14.96	50.32	4.24	23.54	0.4	7.18	0	0.05	100.99
192 CHR ANOTHER L CENTRAL	0	0.35	14.54	49.38	3.90	23.32	0.34	6.9	0	0	98.73
193 CHR ANOTHER L CENTRAL	0	0.39	14.5	50.13	3.63	23.01	0.47	7.16	0	0	99.28
194 CHR AT MARGIN INSIDE RIND	0	0.33	15.56	47.52	5.85	23.73	0.49	6.97	0	0	100.46
195 CHR ANOTHER L CENTRAL	0	0.36	15.08	50.41	3.71	22.92	0.4	7.54	0	0	100.42
196 CHR AT MARGIN	0	0.33	16.09	49.53	4.07	23.56	0.4	7.41	0	0	101.39
197 CHR AT MARGIN	0	0.49	14.97	49.38	4.03	24.13	0.33	6.8	0	0	100.12
198 CHR INT SIZE CENTRAL	0	0.44	15.59	48.43	4.36	23.32	0.47	7.2	0	0	99.82
199 CHR AT MARGIN NEAR MARGINAL RIND	0	0.36	15.59	48.22	4.41	23.85	0.4	6.82	0	0	99.65
200 CHR BRIGHT MARGINAL ZONE	0.06	0.67	0.38	42.22	26.09	28.26	0.75	2.1	0.06	0.07	100.66
201 CHR SMALLER CENTRAL	0	0.38	16.47	48.24	4.42	23.46	0.39	7.42	0	0	100.77
202 CHR SMALLER CENTRAL	0	0.45	15.7	47.98	4.72	23.43	0.42	7.19	0	0	99.89
203 CHR AT MARGIN, NO RIND	0	0.3	16.52	47.48	5.05	23.68	0.38	7.2	0	0	100.61
204 CHR REL L CENTRAL	0	0.38	15.83	48.25	4.23	23.27	0.28	7.29	0	0	99.52
205 CHR REL L CENTRAL	0	0.35	15.68	47.8	4.70	23.80	0.27	6.91	0	0	99.51
206 CHR C ANGULAR CENTRAL	0	0.36	15.94	48.76	4.60	23.47	0.44	7.34	0	0	100.91
207 CHR C ANGULAR CENTRAL	0	0.36	15.88	48.79	3.95	23.63	0.56	7	0	0	100.18
208 CHR **** SAMPLE 486016 L CENTRAL, SPOT 1	0	0.45	16.24	48.16	4.04	23.63	0.35	7.21	0	0	100.07
209 CHR AT MARGIN NEAR OUTER RIND	0	0.37	16.99	45.69	5.25	23.57	0.38	7.09	0	0	99.35
210 CHR V BRIGHT NARROW MARGIN	0	0.67	0.66	40.2	27.44	28.73	0.61	2.01	0.03	0.06	100.41
211 CHR ADJ SMALLER SPOT 4	0	0.42	17.27	45.74	5.17	23.63	0.47	7.16	0	0	99.87
212 CHR CENTRAL SPOT 1 AGAIN	0	0.45	16.19	48.72	3.81	23.47	0.29	7.4	0	0	100.33
213 CHR ANOTHER GRAIN CENTRAL	0	0.37	16.14	46.96	5.36	23.62	0.39	7.09	0	0	99.93
214 CHR AT MARGIN	0	0.33	16.37	46.31	5.81	23.99	0.5	6.81	0	0	100.11
215 CHR ANOTHER REL LARGE CENTRAL	0	0.4	16.07	45.98	6.01	23.72	0.46	6.89	0.01	0	99.54
216 CHR AT MARGIN	0	0.42	16.44	46.03	6.32	24.33	0.59	6.74	0	0	100.87
217 CHR AT MARGIN	0	0.51	16.38	46.25	5.51	24.09	0.34	6.94	0	0	100.02
218 CHR ANOTHER REL LARGE CENTRAL	0	0.41	15.84	46.62	5.88	23.64	0.46	6.99	0	0.02	99.86
219 CHR AT MARGIN	0	0.46	16.09	46.58	5.11	23.90	0.44	6.81	0	0	99.38
220 CHR **** SAMPLE 486017 CENTRAL SPOT 1	0	0.42	14.31	47.98	5.69	24.11	0.53	6.39	0	0.04	99.47
221 CHR AT MARGIN	0	0.44	13.46	47.79	6.27	24.37	0.37	6.14	0	0	98.84
222 CHR AT MARGIN	0	0.4	14.3	48.17	6.43	24.33	0.45	6.55	0	0	100.62
223 CHR ADJ GRAIN CENTRAL	0	0.47	14.31	48.7	5.72	24.85	0.42	6.27	0.08	0	100.82
224 CHR ADJ GRAIN CENTRAL	0	0.42	13.59	47.1	6.36	24.24	0.46	6.03	0	0	98.20
225 CHR ADJ GRAIN CENTRAL	0	0.42	14.24	47.87	6.03	24.86	0.42	6.08	0.01	0	99.93
226 CHR ANOTHER GRAIN	0	0.42	14.23	48.63	5.77	24.66	0.44	6.31	0	0.01	100.48
227 CHR AT MARGIN	0	0.43	13.16	49.03	6.67	24.78	0.46	6.16	0	0	100.69
228 CHR NARROW BRIGHT MARGIN	0.01	0.81	0.58	44.78	23.50	28.37	0.6	2.53	0	0.07	101.25
229 CHR ADJ CENTRAL	0	0.3	13.28	46.9	7.10	23.79	0.46	6.17	0	0	98.00
230 CHR ADJ CENTRAL	0	0.33	13.52	48.69	5.95	24.20	0.45	6.24	0	0.04	99.42
231 CHR AT AMRGIN	0	0.35	13.16	47.05	7.08	23.87	0.38	6.21	0	0	98.10
232 CHR AT AMRGIN	0	0.4	13.98	48.24	7.22	24.58	0.49	6.43	0.09	0	101.43
233 CHR AT AMRGIN	0	0.28	13.59	49.73	6.41	24.63	0.29	6.48	0	0	101.41
234 CHR AT AMRGIN	0	0.32	13.33	46.83	7.53	24.10	0.37	6.18	0	0	98.66
235 CHR AT AMRGIN	0	0.46	13.88	48.72	6.41	24.36	0.5	6.53	0	0.01	100.87
236 CHR SMALLER CENTRAL	0	0.32	13.99	48.38	5.31	23.95	0.24	6.42	0	0.06	98.66
237 CHR SMALLER CENTRAL	0	0.32	14.17	48.77	5.57	24.29	0.33	6.45	0	0	99.90

Black Thor BT-08-10

	SiO2	TiO2	Al2O3	Cr2O3	Fe2O3	FeO	MnO	MgO	ZnO	NiO	TOTAL
238 CHR CLUSTER CENTRAL	0	0.43	14.8	47.43	6.63	24.87	0.39	6.32	0.08	0	100.95
239 CHR CLUSTER CENTRAL	0	0.46	14.24	47.77	6.40	24.80	0.43	6.21	0	0.02	100.33
240 CHR SMALLER GRAIN	0	0.39	14.28	48.49	5.76	24.25	0.43	6.5	0	0	100.11
241 CHR **** SAMPLE 486018 C CENTRAL	0	0.41	14.91	50.48	4.39	20.22	0.29	9.29	0	0	99.99
242 CHR AT MARGIN	0	0.46	15.13	50.68	3.36	21.36	0.35	8.55	0	0	99.90
243 CHR ANOTHER CENTRAL	0	0.41	14.8	50.65	3.87	20.59	0.41	8.89	0	0	99.62
244 CHR AT MARGIN	0	0.44	15.29	49.45	4.47	21.08	0.27	8.75	0	0	99.75
245 CHR ANOTHER	0	0.47	15.38	50.46	4.50	20.62	0.37	9.29	0	0	101.09
246 CHR ANOTHER	0	0.49	15.28	50.75	4.54	20.85	0.37	9.22	0	0.02	101.52
247 CHR ANOTHER	0	0.44	13.69	49.8	4.87	19.98	0.34	8.88	0	0.02	98.02
248 CHR ANOTHER	0	0.48	15.23	50.83	4.43	20.90	0.33	9.19	0	0	101.39
249 CHR ANOTHER	0	0.49	15.26	50.72	4.02	20.66	0.25	9.26	0	0	100.66
250 CHR ANOTHER	0	0.46	14.71	50.75	5.07	20.41	0.28	9.41	0	0	101.09
251 CHR ANOTHER	0	0.46	13.71	50.1	4.99	19.95	0.29	9.07	0	0	98.57
252 CHR ANOTHER	0	0.51	15.27	48.03	4.93	19.65	0.31	9.33	0	0	98.03
253 CHR CENTRAL AGAIN	0	0.46	15.45	48.79	4.36	20.31	0.26	9.07	0	0	98.70
254 CHR ANOTHER GRAIN	0	0.47	15.65	49.65	3.98	20.79	0.39	8.95	0	0	99.88
255 CHR AT MARGIN	0	0.43	15.8	49.07	4.40	20.96	0.44	8.79	0	0	99.89
256 CHR ANOTHER GRAIN CENTRAL	0	0.42	15.79	50.16	3.80	21.03	0.29	8.96	0	0	100.45
257 CHR AT MARGIN	0	0.37	15.65	49.54	3.94	20.98	0.34	8.73	0	0	99.54
258 CHR ANOTHER CENTRAL	0	0.48	15.38	50.55	4.21	21.60	0.42	8.66	0	0.03	101.32
259 CHR ANOTHER CENTRAL	0	0.46	14.57	49.82	3.99	21.21	0.48	8.27	0	0	98.80
260 CHR ANOTHER CENTRAL	0	0.35	14.87	50.84	3.95	21.57	0.32	8.43	0	0	100.33
261 CHR AT MARGIN	0	0.4	16.22	50.26	4.00	21.37	0.37	8.95	0	0	101.57
262 CHR AT MARGIN	0	0.44	15.68	50.15	4.29	21.57	0.32	8.74	0	0	101.19
263 CHR AT MARGIN	0	0.41	15.42	49.95	3.81	21.24	0.4	8.56	0	0.02	99.81
264 CHR SMALL INST	0	0.43	15.95	49.19	4.90	21.65	0.41	8.64	0	0	101.17
265 CHR SMALL INST	0	0.43	15.23	49.82	4.39	21.07	0.41	8.72	0	0	100.07
266 CHR ANOTHER SMALL INST	0	0.4	15.58	49.85	4.46	21.59	0.29	8.63	0	0	100.80
267 CHR INST	0	0.41	14.66	49.33	4.63	20.84	0.37	8.53	0	0.05	98.82
268 CHR INST	0	0.44	15.23	49.94	4.62	21.52	0.25	8.66	0	0	100.66
269 CHR **** SAMPLE 486019 L CENTRAL	0	0.45	15.45	51.55	4.08	19.24	0.3	10.3	0	0	101.37
270 CHR L CENTRAL	0	0.45	14.88	50.15	4.11	18.89	0.31	9.9	0	0	98.69
271 CHR L CENTRAL	0	0.43	14.99	50.12	4.53	18.13	0.32	10.42	0	0.04	98.98
272 CHR L CENTRAL	0	0.44	15.77	51.02	3.83	19.05	0.34	10.29	0	0	100.74
273 CHR AT MARGIN	0	0.39	14.8	50.6	3.91	20.45	0.42	8.93	0	0.01	99.51
274 CHR ANOTHER L CENTRAL	0	0.46	14.73	50.42	4.09	19.19	0.31	9.75	0	0	98.95
275 CHR ANOTHER L CENTRAL	0	0.43	15.3	51.11	3.68	19.36	0.27	9.93	0	0.04	100.12
276 CHR AT MARGIN	0	0.46	14.83	51.9	3.59	20.80	0.34	9.1	0	0.06	101.08
277 CHR AT MARGIN	0	0.42	15.31	50.18	4.84	20.44	0.44	9.26	0	0.05	100.93
278 CHR ANOTHER L CENTRAL	0	0.46	14.75	51.15	4.63	18.57	0.35	10.4	0	0.02	100.32
279 CHR AT MARGIN	0	0.4	15.72	49.61	4.68	20.25	0.34	9.4	0	0	100.40
280 CHR BRIGHT MARGIN W CHL INCL	0	0.51	7.58	54.95	7.41	23.93	0.42	6.29	0	0	101.09
281 CHR BRIGHT MARGIN W CHL INCL	0	0.55	7.46	53.57	8.50	23.58	0.56	6.31	0	0	100.53
282 CHR SMALLWER INST	0	0.42	15.35	50.72	4.15	20.44	0.27	9.37	0	0	100.72
283 CHR ANOTHER INST	0	0.45	16.02	49.43	4.90	20.50	0.32	9.45	0	0	101.07
284 CHR ANOTHER INST	0	0.42	15.4	49.61	4.42	20.09	0.27	9.35	0	0.01	99.57
285 CHR INT CENTRAL	0	0.41	15.51	49.93	4.23	20.40	0.36	9.19	0	0.02	100.05
286 CHR BRIGHT MARGINAL ZONE INCL CHL	0	0.14	8.57	58.58	3.92	22.77	0.51	6.99	0	0	101.47
287 CHR BRIGHT MARGINAL ZONE INCL CHL	0	0.24	8.66	57.19	3.82	22.76	0.49	6.75	0	0	99.90
288 CHR L CENTRAL	0	0.33	15.76	50.41	4.54	19.08	0.3	10.2	0	0	100.62
289 CHR AT MARGIN	0	0.45	16	50.16	4.17	20.44	0.4	9.44	0	0	101.06
290 CHR AT MARGIN	0	0.4	15.27	50.84	4.12	20.00	0.37	9.53	0	0	100.53
291 CHR **** SAMPLE 486020 GRAIN 1, 12-21-3629	0	0.51	16.28	48.71	4.90	19.95	0.49	9.49	0.12	0.15	100.60
292 CHR BRIGHT RIND AT MARGIN	0.13	0.96	6.38	53.39	9.46	22.92	0.61	6.33	0.24	0.06	100.49
293 CHR GRAIN 2 CENTRAL	0	0.67	16.79	48.01	4.24	19.72	0.58	9.55	0.18	0.15	99.89
294 CHR BRIGHT MARGIN	0.09	0.8	8.2	54	7.51	22.88	0.56	6.67	0.27	0.12	101.10
295 CHR GRAIN 3, CENTRAL	0	0.76	17	47.93	4.64	19.89	0.32	9.94	0.09	0.08	100.65
296 CHR AT MARGIN, NO RIND	0	0.6	17.31	48.03	4.11	20.37	0.45	9.39	0.16	0.13	100.55
297 CHR GRAIN 4 CENTRAL, 12-21-3632	0	0.68	17.23	47.71	4.14	19.87	0.4	9.72	0.07	0.12	99.94
298 CHR RIND AT MARGIN	0.01	0.49	10	53.61	6.04	22.66	0.52	6.91	0.35	0.13	100.73
299 CHR GRAIN 5, CENTRAL	0.06	0.69	17.02	49	3.38	20.02	0.36	9.52	0.2	0.1	100.35
300 CHR BRIGHT CENTRAL	0.04	0.36	12.11	52.48	5.32	21.47	0.5	7.88	0.19	0	100.34
301 CHR GRAIN 6 CENTRAL	0.03	0.67	17.24	48.02	4.48	19.89	0.46	9.69	0.22	0.11	100.81
302 CHR AT MARGIN, NO RIND	0.02	0.61	17.72	48.17	2.82	19.96	0.49	9.45	0.18	0.07	99.49
303 CHR ADJ BRIGHT DOMAIN, 12-21-3636	0.04	0.56	10.76	52.01	6.48	22.50	0.58	7.06	0.18	0.07	100.24
304 CHR GRAIN 7 CENTRAL, 12-21-3639	0	0.68	16.95	48.03	3.08	20.22	0.46	9.24	0.11	0	98.77
305 CHR AT MARGIN NO RIND	0	0.62	17.56	48.11	3.11	20.71	0.57	9.04	0.25	0	99.97
306 CHR GRAIN 8 CENTRAL	0.02	0.73	17.38	48.22	3.69	20.78	0.38	9.29	0.19	0.03	100.71
307 CHR AT MARGIN NO RIND	0	0.67	17.4	47.93	3.14	20.80	0.58	8.91	0.26	0.04	99.72
308 CHR * 2ND TIME, GRAIN 1 CENTRAL, 12-21-3632	0	0.59	15.57	48.62	5.26	19.35	0.4	9.76	0.12	0.13	99.80
309 CHR GRAIN 2 CENTRAL AS CHECK	0	0.57	15.65	49.07	4.77	19.73	0.46	9.55	0.2	0	100.00
310 CHR GRAIN 2 CENTRAL AGAIN	0	0.58	15.87	49.38	4.55	19.69	0.35	9.76	0.12	0.07	100.37
311 CHR AT MARGIN AWAY FROM RIND	0	0.59	15.91	48.21	5.41	19.78	0.46	9.54	0.18	0.09	100.16
312 CHR GRAIN 4 CENTRAL AS CHECK	0	0.61	15.4	49.38	5.04	19.39	0.32	9.88	0.16	0.09	100.27
313 CHR NEAR GRAIN 4 CENTRAL SPOT 1 12-21-3632	0	0.73	15.31	49.33	5.16	19.82	0.4	9.78	0.02	0.07	100.62
314 CHR AT MARGIN SANS RIND, SPOT 2	0	0.59	15.29	48.76	4.99	19.94	0.41	9.27	0.18	0.1	99.53
315 CHR ANOTHER GRAIN 5, CENTRAL, SPOT 1, 12-21-	0	0.59	15.04	49.84	5.10	19.02	0.35	10.02	0.12	0.17	100.25
316 CHR AT MARGIN NO RIND, SPOT 2	0	0.6	15.29	49.2	5.35	19.26	0.35	9.95	0.12	0.06	100.19

Black Thor BT-08-10

	SiO2	TiO2	Al2O3	Cr2O3	Fe2O3	FeO	MnO	MgO	ZnO	NiO	TOTAL
317 CHR BRIGHT AT MARGIN, SPOT 3	0	0.28	10.42	52.89	6.46	21.07	0.43	7.91	0.09	0.07	99.62
318 CHR GRAIN 6 CENTRAL SPOT 1 12-21-3639	0	0.6	14.6	49.41	4.98	19.23	0.36	9.65	0.1	0.08	99.01
319 CHR AT MARGIN NO RIND SPOT 2	0	0.63	14.87	48.72	5.10	19.24	0.42	9.55	0.19	0.08	98.80
320 CHR GRAIN 8 CENTRAL AGAIN SPOT 1 12-21-3639	0	0.63	15.28	49.41	4.53	19.68	0.32	9.55	0.21	0.08	99.69
321 CHR AT MARGIN	0	0.66	15.53	49.38	4.72	19.86	0.39	9.57	0.19	0.12	100.42
322 CHR BRIGHT AT MARGIN	0	0.7	8.35	52.77	7.85	22.36	0.55	6.89	0.32	0.14	99.94
323 CHR **** SAMPLE 486021 GRAIN 1 CENTRAL 12-21	0	0.69	16.9	48.25	3.36	22.05	0.47	8.23	0.19	0.11	100.25
324 CHR AT MARGIN NO RIND	0.05	0.71	16.54	48.39	3.60	22.66	0.5	7.66	0.31	0.1	100.52
325 CHR GRAIN 2 CENTRAL	0.02	0.72	17.4	47.3	4.25	21.23	0.41	8.93	0.12	0.06	100.45
326 CHR AT MARGIN NO RIND	0.04	0.6	17.01	48.03	4.01	21.39	0.37	8.67	0.17	0.01	100.30
327 CHR GRAIN 3 CENTRAL	0	0.72	17.2	47.09	4.36	22.08	0.43	8.32	0.22	0.1	100.52
328 CHR INNER SIDE OUTER RIND	0.03	0.67	17.21	47.81	3.62	21.90	0.48	8.32	0.12	0.1	100.26
329 CHR BRIGHT MARGINAL ZONE, ALT?	0.07	0.24	12.56	53.7	2.82	22.36	0.54	6.89	0.33	0.12	99.63
330 CHR GRAIN 4 CENTRAL	0.01	0.67	16.69	47.92	4.35	21.53	0.51	8.55	0.16	0.1	100.50
331 CHR AT MARGIN SANS RIND	0	0.65	16.64	48.51	3.49	22.29	0.45	8.07	0.19	0.1	100.39
332 CHR INSIDE MARGINAL RIND	0	0.61	16.7	48.29	3.87	21.82	0.49	8.28	0.29	0.1	100.46
333 CHR ANG BRIGHT MARGINAL ZONE	0.05	0.32	11.96	54.61	2.76	22.65	0.64	6.96	0.07	0.06	100.08
334 CHR GRAIN 5 TRIANG CENTRAL	0.02	0.64	16.01	48	4.17	22.43	0.52	7.66	0.3	0.03	99.78
335 CHR AT MARGIN	0.01	0.61	16.66	48.01	4.11	22.84	0.53	7.64	0.28	0.09	100.78
336 CHR GRAIN 6 CENTRAL	0	0.62	16.76	48.7	3.78	21.57	0.41	8.66	0.14	0.11	100.75
337 CHR AT MARGIN NO RIND	0	0.62	16.85	48.11	3.69	22.53	0.42	7.94	0.17	0.14	100.47
338 CHR GRAIN 7 CENTRAL	0.01	0.76	17.07	47.54	4.08	22.05	0.41	8.45	0.13	0.01	100.52
339 CHR AT MARGIN	0.02	0.62	16.9	47.27	4.05	21.72	0.48	8.18	0.24	0.1	99.58
340 CHR **** SAMPLE 486022 GRAIN 1 CENTRAL 12-21	0.06	0.68	17.35	47.65	4.00	21.83	0.48	8.33	0.22	0.13	100.73
341 CHR GRAIN 1 CENTRAL AGAIN	0	0.69	17.17	47.27	3.45	22.65	0.42	7.78	0.19	0.13	99.75
342 CHR DARK MARGIN	0.03	0.49	9.14	54.08	5.75	24.85	0.66	5.39	0.12	0.1	100.62
343 CHR GRAIN 2 CENTRAL	0	0.54	16.48	48.43	3.38	22.92	0.56	7.45	0.21	0.05	100.02
344 CHR AT MARGIN	0	0.7	16.65	48.56	3.12	22.95	0.49	7.54	0.35	0.16	100.51
345 CHR GRAIN 3 CENTRAL	0	0.63	16.83	48.07	3.68	22.88	0.55	7.72	0.12	0.07	100.55
346 CHR AT MARGIN NO RIND	0.01	0.68	16.94	47.39	4.19	21.94	0.57	8.29	0.12	0	100.13
347 CHR GRAIN 4 CENTRAL	0.04	0.64	17.19	47.11	5.08	21.16	0.57	8.69	0.3	0.14	100.92
348 CHR AT MARGIN	0.03	0.61	17.44	48.06	3.79	21.13	0.41	8.8	0.29	0.18	100.74
349 CHR GRAIN 5 CENTRAL	0.08	0.66	17.54	47.29	4.10	22.56	0.39	7.94	0.16	0.11	100.83
350 CHR AT MARGIN NO RIND	0.09	0.69	18.09	46.04	3.92	22.58	0.61	7.69	0.16	0.04	99.90
351 CHR SMALL BRIGHT DOMAIN AT MARGIN	0.11	0.44	9.79	54.01	4.53	23.60	0.74	5.66	0.14	0.18	99.19
352 CHR GRAIN 6 CENTRAL	0.05	0.63	17.3	47.71	4.64	20.44	0.55	9.22	0.26	0.06	100.86
353 CHR AT MARGIN NO RIND	0.04	0.66	17.59	47.6	3.01	21.73	0.38	8.38	0.21	0	99.60
354 CHR GRAIN 7 CENTRAL	0.06	0.69	17.26	48.43	3.36	20.85	0.41	8.97	0.18	0.11	100.32
355 CHR AT MARGIN	0.06	0.67	17.63	48.09	2.99	21.79	0.38	8.53	0.04	0	100.18
356 CHR * 2ND TIME GR 1 REG, SPOT 1 REL DARK, 12	0	0.58	15.11	49.47	4.70	20.95	0.49	8.75	0.06	0.1	100.21
357 CHR REL BRIGHT SPOT 2	0	0.57	14.3	50.54	4.22	22.45	0.45	7.7	0.17	0.11	100.51
358 CHR **** SAMPLE 496023 GRAIN 1 CENTRAL	0.1	0.83	16.18	47.07	5.11	23.42	0.44	7.21	0.24	0.03	100.63
359 CHR AT MARGIN	0.15	0.75	16.12	46.93	5.55	23.04	0.51	7.2	0.23	0.08	100.56
360 CHR BRIGHT MARGINAL	0.38	2.39	0.89	44.77	20.81	27.68	0.79	2.68	0.22	0.19	100.80
361 CHR GRAIN 2 CENTRAL	0.04	0.68	16.18	47.15	4.66	23.75	0.48	6.88	0.25	0.1	100.17
362 CHR BRIGHT MARGINAL RIND	0.09	1.31	7.55	46.6	13.02	27.01	0.71	3.91	0.33	0.15	100.68
363 CHR GRAIN 3 CENTRAL AGAIN	0.04	0.73	15.89	45.91	6.22	23.35	0.54	7.2	0.03	0.06	99.97
364 CHR AT MARGIN	0.03	0.73	14.78	47.17	6.54	23.61	0.5	6.94	0.29	0.08	100.67
365 CHR GRAIN 4 CENTRAL	0.03	0.79	15.23	46.9	6.36	23.65	0.51	6.98	0.31	0.16	100.93
366 CHR AT MARGIN NO RIND	0.06	0.7	15.05	46.35	7.08	22.96	0.53	7.26	0.27	0	100.26
367 CHR GRAIN 5, ADJ,M CENTRAL	0.05	0.75	14.46	47	6.43	23.85	0.48	6.65	0.16	0.08	99.90
368 CHR NEAR MARGINAL ALT	0.07	0.7	14.5	45.81	8.07	23.25	0.56	6.86	0.32	0.1	100.24
369 CHR REL BRIGHT MARGINAL ALT	0.17	1.66	2.55	47.42	16.49	27.40	0.73	3	0.19	0.15	99.76
370 CHR GRAIN 6 CENTRAL	0.05	0.71	15.33	46.28	6.03	23.69	0.47	6.76	0.22	0.02	99.55
371 CHR AT MARGIN	0.03	0.65	15.4	47.3	5.83	23.51	0.56	6.99	0.27	0.09	100.62
372 CHR GRAIN 7 CENTRAL	0.06	0.51	15.46	46.4	6.64	22.91	0.62	7.06	0.32	0.04	100.01
373 CHR AT MARGIN	0.06	0.71	15.57	46.12	6.96	23.20	0.47	7.21	0.26	0.14	100.70
374 CHR GRAIN 8 CENTRAL	0.06	0.7	15.37	46.11	6.59	23.40	0.5	6.87	0.31	0.14	100.05
375 CHR **** SAMPLE 486024 REL L CENTRAL	0	0.48	14.29	48.83	5.92	23.22	0.44	7.3	0	0	100.47
376 CHR AT MARGIN NO RIND	0	0.36	13.96	50.3	4.87	22.97	0.46	7.3	0	0	100.22
377 CHR ANOTHER L CENTRAL	0	0.41	13.41	48.35	6.01	22.29	0.42	7.13	0.32	0.04	98.38
378 CHR ANOTHER L CENTRAL	0	0.44	13.8	50.35	4.52	22.99	0.29	7.33	0	0	99.72
379 CHR AT MARGIN	0	0.46	14.07	49.05	5.95	22.57	0.36	7.67	0	0	100.13
380 CHR SMALLER CENTRAL	0	0.4	14.14	50	5.83	23.48	0.32	7.37	0	0	101.53
381 CHR SMALLER CENTRAL	0	0.4	13.97	49.62	6.09	23.17	0.37	7.41	0	0	101.03
382 CHR SMALLER CENTRAL	0	0.4	14.58	49.45	5.47	22.97	0.45	7.52	0	0	100.84
383 CHR REL L CENTRAL	0	0.39	13.82	49.77	5.46	22.90	0.49	7.29	0	0.03	100.15
384 CHR ANOTHER REL L CENTRAL	0	0.39	13.88	49.23	5.36	22.66	0.38	7.36	0	0	99.26
385 CHR ANOTHER CENTRAL	0	0.42	13.78	49.18	6.77	22.64	0.42	7.68	0	0	100.89
386 CHR BRIGHT MARGIN W CHL LATH AS INCL	0	0.34	4.15	52.84	12.04	25.81	0.53	4.25	0	0.01	99.97
387 CHR ANOTHER L CENTRAL	0	0.37	14.93	49.79	5.07	22.83	0.44	7.7	0	0	101.13
388 CHR ANOTHER L CENTRAL	0	0.37	14.57	47.83	5.56	22.10	0.41	7.59	0	0	98.43
389 CHR ANOTHER L CENTRAL	0	0.38	14.39	49.61	5.19	22.62	0.44	7.6	0	0	100.23
390 CHR AT MARGIN	0	0.38	14.73	49.62	5.76	22.88	0.45	7.73	0	0	101.55
391 CHR AT MARGIN	0	0.35	14.32	48.82	6.00	22.12	0.38	7.84	0	0.01	99.84
392 CHR **** SAMPLE 486025 L CENTRAL	0	0.37	14	52.39	3.59	18.14	0.18	10.43	0	0	99.10
393 CHR AT MARGIN	0	0.2	14.32	52.42	3.89	21.31	0.37	8.58	0	0	101.09
394 CHR AT MARGIN	0	0.31	14.2	51.88	3.86	21.01	0.39	8.64	0	0.02	100.31
395 CHR ANOTHER L CENTRAL	0	0.24	14.53	53.12	3.69	17.91	0.27	10.8	0	0	100.56

Black Thor BT-08-10

	SiO2	TiO2	Al2O3	Cr2O3	Fe2O3	FeO	MnO	MgO	ZnO	NiO	TOTAL
396 CHR AT MARGIN	0	0.25	13.75	53.61	3.49	21.47	0.48	8.47	0	0	101.52
397 CHR AT MARGIN	0	0.19	12.78	52.52	3.77	20.74	0.43	8.23	0	0.02	98.68
398 CHR AT MARGIN	0	0.21	13.23	52.18	4.02	20.72	0.4	8.44	0	0	99.20
399 CHR SMALLER GRAIN	0	0.29	13.43	52.98	3.96	18.30	0.32	10.2	0	0	99.49
400 CHR REL L CENTRAL	0	0.27	14.15	53.74	3.41	19.32	0.29	9.96	0	0.03	101.17
401 CHR REL L CENTRAL	0	0.24	13.78	53.94	3.95	18.77	0.37	10.25	0	0	101.31
402 CHR REL L CENTRAL	0	0.25	13.77	53.63	3.51	18.97	0.32	9.97	0.01	0	100.43
403 CHR AT MARGIN	0	0.19	12.51	53.96	4.10	20.89	0.35	8.56	0	0	100.56
404 CHR SMALL INST	0	0.29	13.25	53.21	3.35	20.18	0.41	8.93	0	0	99.63
405 CHR SMALL INST CENTRAL	0	0.29	13.53	54.05	3.55	19.86	0.42	9.49	0	0	101.19
406 CHR SMALL INST CENTRAL	0	0.26	12.88	52.48	4.74	19.10	0.3	9.58	0	0	99.33
407 CHR BRIGHT DOMAIN AT MARGIN	0	0.09	5.89	60.64	3.27	23.34	0.6	5.89	0	0	99.72
408 CHR L CENTRAL	0	0.22	13.57	53.27	4.48	18.00	0.19	10.64	0	0	100.37
409 CHR AT MARGIN	0	0.2	13.74	53.51	3.04	21.44	0.44	8.31	0	0	100.68
410 CHR AT MARGIN	0	0.28	13.02	52.27	3.71	21.28	0.29	8.12	0	0	98.97
411 CHR AT MARGIN	0	0.32	13.39	52.25	3.88	20.92	0.34	8.52	0	0	99.63
412 CHR V SMALL INST	0	0.33	13.98	52.76	3.76	21.81	0.42	8.3	0	0.05	101.41
413 CHR V SMALL INST	0	0.22	13.08	52.43	3.99	21.34	0.33	8.14	0	0	99.53
414 CHR SAMPLE 486026 REL LARGE	0	0.36	14.15	48.48	5.99	23.02	0.37	7.2	0	0	99.57
415 CHR ADJ GRAIN	0	0.34	14.27	48.53	5.48	23.17	0.37	7.03	0	0	99.19
416 CHR ANOTHER	0	0.4	15.17	47.68	5.75	22.82	0.27	7.54	0	0	99.63
417 CHR REL L CENTRAL	0	0.37	15.01	48.7	5.24	23.30	0.3	7.3	0	0	100.22
418 CHR AT MARGIN	0	0.23	14.3	48.58	5.59	22.91	0.33	7.14	0	0	99.08
419 CHR AT MARGIN	0	0.28	14.77	48.28	5.84	23.24	0.37	7.15	0	0	99.94
420 CHR SMALLER	0	0.37	15.37	48.65	5.39	23.72	0.25	7.26	0	0	101.01
421 CHR SMALLER	0	0.37	15.39	48.43	5.55	23.47	0.39	7.31	0	0	100.92
422 CHR V SMALL GRAIN	0	0.37	13.85	49.74	5.74	23.45	0.33	7.11	0	0.06	100.65
423 CHR SMALL	0	0.41	14.32	49.31	5.51	23.26	0.49	7.21	0	0.01	100.51
424 CHR **** SAMPLE 486028 L CENTRAL, SPOT 1, 12	0	0.43	14.54	53.54	3.40	16.76	0.32	11.53	0.08	0.15	100.75
425 CHR AT MARGIN SPOT 2	0	0.44	14.52	52.27	3.25	19.34	0.52	9.57	0.23	0.07	100.21
426 CHR ANOTHER CENTRAL SPOT 3	0	0.4	14.22	53.38	3.65	15.77	0.17	12.1	0	0.11	99.80
427 CHR ANOTHER SPOT 4	0	0.38	14.5	53.69	3.20	16.19	0.39	11.82	0.03	0.04	100.24
428 CHR ANOTHER SPOT 5	0	0.37	14.35	53.16	3.16	16.61	0.39	11.33	0.06	0.08	99.51
429 CHR SMALLER SPOT 6	0	0.4	14.6	53.13	2.57	19.43	0.5	9.68	0	0.09	100.40
430 CHR SMALL SPOT 7	0	0.47	14.24	52.71	2.71	20.32	0.43	9.04	0.13	0.03	100.28
431 CHR SMALL SPOT 8	0	0.4	14.72	53.06	2.81	19.13	0.38	10.02	0.01	0.05	100.58
432 CHR SMALLEST SPOT 9	0	0.42	14.23	53.52	2.67	19.09	0.49	9.83	0.11	0.08	100.44
433 CHR **** SAMPLE 486029 L GRAIN CENTRAL, SPOT	0	0.36	14.59	53.89	3.21	16.13	0.33	11.89	0.05	0.15	100.50
434 CHR AT MARGIN SPOT 2	0	0.4	14.85	53.81	1.67	18.65	0.54	10.03	0.25	0.08	100.28
435 CHR ANOTHER CENTRAL, SPOT 3	0	0.44	13.48	55.09	2.29	16.93	0.29	11.22	0.03	0.11	99.88
436 CHR AT MARGIN NO RIND, SPOT 4	0	0.42	14.34	52.44	4.04	18.32	0.41	10.44	0.08	0.05	100.54
437 CHR BRIGHT DOMAIN AT MARGIN SPOT 5	0.03	0.65	6.4	56.23	7.72	22.29	0.58	7.09	0.01	0.06	101.06
438 CHR DARKER SPOT 6	0	0.32	8.62	57.94	4.20	20.33	0.62	8.31	0.11	0.06	100.51
439 CHR SPOT 1 AGAIN	0	0.47	14.29	54.27	2.81	15.81	0.38	12.03	0.08	0.13	100.27
440 CHR SMALLER SPOT 7	0	0.43	14.03	53.81	2.97	16.52	0.31	11.45	0.14	0.07	99.73
441 CHR AT MARGIN SPOT 8	0	0.35	14.52	52.51	3.83	18.72	0.44	10.11	0.17	0.07	100.72
442 CHR SMALL INST, SPOT 9	0	0.35	13.97	54.02	2.65	18.86	0.45	9.9	0.07	0.18	100.44
443 CHR INST SPOT 10	0	0.42	14.41	53.55	2.87	17.36	0.44	10.99	0	0.12	100.16
444 CHR **** SAMPLE 486030 CENTRAL SPOT 1, 12-31	0	0.37	13.51	54.7	2.63	17.87	0.34	10.63	0	0.06	100.11
445 CHR AT MARGIN SPOT 2	0	0.37	13.52	54.06	2.29	20.47	0.42	8.87	0.05	0.03	100.08
446 CHR ANOTHER L CENTRAL SPOT 3	0	0.42	14.04	52.79	3.62	17.06	0.38	11.03	0	0.13	99.47
447 CHR AT MARGIN SPOT 4	0	0.38	13.96	53.1	3.72	19.20	0.52	9.84	0	0.03	100.74
448 CHR ANOTHER CENTRAL SPOT 5	0	0.37	13.93	53.89	3.43	17.62	0.43	10.85	0	0.1	100.62
449 CHR AT MARGIN SPOT 6	0	0.46	13.76	53.93	2.26	19.80	0.46	9.34	0.05	0.08	100.14
450 CHR SMALL INST SPOT 7	0	0.37	14.21	52.42	4.07	19.22	0.54	9.66	0.23	0.1	100.82
451 CHR SMALL INST SPOT 8	0	0.45	13.54	54.04	2.94	18.50	0.4	10.14	0.12	0.14	100.26
452 CHR SMALL INST SPOT 9	0	0.41	13.74	53.21	2.70	19.23	0.48	9.43	0.13	0.15	99.48
453 CHR **** SAMPLE 486031 CENTRAL	0	0.33	14.32	51.85	4.16	21.07	0.29	8.81	0	0	100.83
454 CHR CENTRAL	0	0.32	13.94	51.71	4.75	20.75	0.32	8.92	0	0	100.72
455 CHR ANOTHER CENTRAL	0	0.34	14.35	51.95	4.33	21.02	0.34	8.9	0	0	101.23
456 CHR ANOTHER CENTRAL	0	0.33	14.35	50.41	4.78	20.62	0.34	8.82	0	0	99.65
457 CHR BRIGHT AT MARGIN	0	0.2	5.37	56.09	8.36	22.87	0.49	6.2	0	0	99.58
458 CHR L CENTRAL	0	0.3	14.43	51.59	3.59	21.31	0.38	8.42	0	0	100.02
459 CHR AT MARGIN	0	0.33	14.7	51.9	2.41	21.97	0.3	8.02	0	0	99.63
460 CHR ANOTHER L CENTRAL	0	0.3	13.92	52.04	4.05	22.40	0.32	7.88	0	0	100.91
461 CHR ANOTHER L CENTRAL	0	0.31	14.04	52.05	2.79	22.21	0.33	7.72	0	0	99.45
462 CHR ANOTHER L CENTRAL	0	0.33	14.24	52.98	3.02	22.10	0.38	8.16	0	0	101.21
463 CHR ANOTHER L CENTRAL	0	0.31	13.47	51.52	3.60	21.83	0.44	7.7	0	0.02	98.89
464 CHR ANOTHER L CENTRAL	0	0.35	14.02	51.19	4.22	21.62	0.41	8.17	0	0	99.98
465 CHR INNER ZONE NEAR MARGIN	0	0.2	6.43	57.58	6.17	23.25	0.58	6.2	0	0	100.41
466 CHR BRIGHT MARGINAL ZONE	0	0.45	1.85	59.99	7.08	25.18	0.61	4.41	0	0	99.57
467 CHR ANOTHER SMALLER	0	0.35	14.57	51.67	4.17	21.32	0.4	8.68	0	0	101.16
468 CHR ANOTHER SMALLER	0	0.29	14.37	50.88	3.99	20.60	0.41	8.68	0	0	99.22
469 CHR BRIGHT AT MARGIN W INCL	0	0.38	3.76	56.46	8.55	23.87	0.63	5.25	0	0	98.91
470 CHR BRIGHT AT MARGIN W INCL	0	0.29	3.18	57.24	8.33	23.52	0.56	5.32	0	0	98.43
471 CHR ANOTHER OUT ZONE	0	0.2	7.05	55.51	6.64	22.57	0.59	6.35	0.03	0.04	98.99
472 CHR **** SAMPLE 486032 REL L CENTRAL	0	0.29	14.53	54.02	2.67	17.61	0.26	11.01	0	0	100.39
473 CHR AT MARGIN	0	0.26	13.58	52.8	3.01	19.41	0.29	9.34	0	0	98.69
474 CHR AT MARGIN	0	0.25	14.1	54.18	1.57	20.27	0.36	9.01	0	0.01	99.75

Black Thor BT-08-10

	SiO2	TiO2	Al2O3	Cr2O3	Fe2O3	FeO	MnO	MgO	ZnO	NiO	TOTAL
475 CHR ANOTHER CENTRAL	0	0.21	14.37	54.44	2.55	16.49	0.05	11.69	0	0	99.81
476 CHR AT MARGIN	0	0.23	14.29	53.7	2.78	19.57	0.52	9.55	0	0	100.64
477 CHR AT MARGIN	0	0.25	14.11	53.71	1.72	19.95	0.36	9.11	0	0	99.21
478 CHR ANOTHER CENTRAL	0	0.3	14.4	53.85	2.39	16.40	0.2	11.56	0	0	99.10
479 CHR SMALLER	0	0.28	14.39	54.1	1.88	18.53	0.34	10.2	0	0	99.72
480 CHR ANOTHER V LARGE CENTRAL	0	0.28	14.37	53.88	2.98	16.87	0.28	11.36	0	0.03	100.05
481 CHR AT MARGIN	0	0.27	14.16	53.55	2.05	19.26	0.25	9.64	0	0	99.19
482 CHR ANOTHER CENTRAL	0	0.21	14.42	54.23	2.18	16.70	0.24	11.34	0	0	99.32
483 CHR AT MARGIN	0	0.22	14.41	53.41	2.90	19.53	0.41	9.62	0	0	100.50
484 CHR ANOTHER INT CENTRAL	0	0.32	14.2	52.37	3.29	17.23	0.39	10.76	0	0.01	98.57
485 CHR ANOTHER INT CENTRAL	0	0.21	14.35	53.16	2.43	17.55	0.14	10.67	0	0	98.50
486 CHR ANOTHER INT CENTRAL	0	0.29	14.31	53.14	2.63	17.94	0.23	10.51	0	0	99.05
487 CHR BRIGHT AT M W INCL	0	0.39	4.74	57.33	8.17	23.84	0.56	5.84	0	0	100.87
488 CHR BRIGHT AT M W INCL	0	0.38	4.54	56.94	7.86	23.29	0.52	5.9	0	0	99.44
489 CHR ANOTHER C CENTRAL	0	0.29	14.42	54.55	2.14	16.65	0.21	11.54	0	0	99.79
490 CHR AT MARGIN	0	0.23	14.34	54.81	1.63	19.55	0.21	9.76	0	0	100.52
491 CHR AT MARGIN	0	0.31	14.2	53.49	3.09	19.33	0.34	9.85	0	0	100.61
492 CHR BRIGHT DOM W INCL CHL	0	0.32	7.08	54.86	7.68	22.96	0.5	6.44	0	0	99.84
493 CHR SMALLER GRAIN CENTRAL	0	0.25	14.25	54.51	1.80	20.47	0.44	9.06	0	0	100.78
494 CHR SMALLER GRAIN CENTRAL	0	0.28	14.12	53.85	1.97	20.31	0.38	9.03	0	0	99.95
495 CHR BRIGHT REACTION ZONE W INCL CHL	0	0.28	9.2	55.5	5.87	22.83	0.48	7.04	0	0	101.20
496 CHR BRIGHT REACTION ZONE W INCL CHL	0	0.25	8.74	54.73	6.24	21.86	0.39	7.31	0	0	99.53
497 CHR ANOTHER REL C GRAIN CENTRAL	0	0.2	13.12	53.88	3.28	18.82	0.5	9.66	0	0	99.47
498 CHR CENTRAL DOMAIN W CHL LATHS	0	0.37	7.28	54.71	7.34	22.97	0.51	6.4	0.07	0	99.66
499 CHR BRIGHTER W INCL AT MARGIN	0	0.43	5.59	56.64	8.14	23.83	0.67	5.94	0	0.05	101.30
500 CHR BRIGHTER W INCL AT MARGIN	0	0.41	5.22	57.01	8.02	23.85	0.6	5.9	0	0	101.00
501 CHR V SMALL INST	0	0.25	14.44	53.73	1.99	19.44	0.34	9.61	0	0	99.80
502 CHR ANOTHER V SMALL INST	0	0.24	14.17	53.24	2.94	19.37	0.33	9.65	0	0	99.94
503 CHR V LARGE CENTRAL	0	0.32	14.36	53.56	2.52	17.89	0.29	10.63	0	0.01	99.58
504 CHR V SMALL INST	0	0.26	14.39	53.19	2.11	20.07	0.26	9.18	0	0	99.46
505 CHR **** SAMPLE 486033 REL C CENTRAL	0	0.25	14.28	52.83	2.72	18.59	0.29	10	0	0	98.96
506 CHR AT MARGIN	0	0.21	14.46	52.42	2.56	19.72	0.36	9.21	0	0	98.94
507 CHR ANOTHER REL L CENTRAL	0	0.29	13.96	53.2	2.78	18.83	0.27	9.9	0	0	99.23
508 CHR AT MARGIN	0	0.22	14.24	52.64	2.85	19.84	0.37	9.19	0	0	99.35
509 CHR ANOTHER BRIGHT CENTRAL	0	0.32	14.19	53.25	2.78	19.55	0.29	9.62	0	0	100.00
510 CHR AT M W CHL INCL	0	0.4	5.9	57.18	6.82	23.36	0.57	6.17	0	0.04	100.44
511 CHR ANOTHER L CENTRAL	0	0.27	14.19	53.83	2.48	17.74	0.35	10.62	0	0.02	99.50
512 CHR AT MARGIN NO RIND	0	0.26	14.08	52.86	3.08	20.33	0.37	9.01	0	0	99.99
513 CHR V SMALL INST	0	0.28	13.94	53.16	2.86	20.48	0.36	8.92	0	0	100.00
514 CHR BRIGHT MARGIN W CHL LATH INCL	0	0.19	7.71	55.62	6.66	22.59	0.56	6.68	0	0	100.01
515 CHR ANOTHER L CENTRAL	0	0.2	14.22	52.55	3.18	18.65	0.31	9.92	0	0	99.04
516 CHR REL V LARGE CENTRAL	0	0.32	14.71	51.62	2.95	19.77	0.39	9.26	0	0	99.02
517 CHR NEAR MARGIN	0	0.25	14.21	51.55	3.45	19.82	0.46	9.03	0	0	98.77
518 CHR NEAR MARGIN	0	0.32	14.5	52.77	2.35	20.49	0.38	8.93	0	0	99.75
519 CHR ANOTHER MEDIUM CENTRAL	0	0.23	14.61	51.24	3.68	19.09	0.39	9.59	0	0	98.83
520 CHR ANOTHER MEDIUM CENTRAL	0	0.23	14.82	52.04	3.07	19.59	0.34	9.48	0	0	99.57
521 CHR AT MARGIN W CHL LATH INCL	0	0.23	7.32	56.28	7.13	22.53	0.53	6.91	0	0	100.93
522 CHR **** SAMPLE 486034 L CENTRAL, SPPT 1, 12	0	0.39	14.05	54.51	3.03	16.33	0.35	11.73	0.07	0.08	100.54
523 CHR AT MARGIN NO RIND, SPOT 2	0	0.36	13.78	53.82	2.73	19.02	0.53	9.7	0.06	0.13	100.13
524 CHR MARGINAL SPOT 3	0	0.4	10.23	53.6	6.80	20.44	0.58	8.54	0.01	0.06	100.66
525 CHR BRIGHT W INCL MG-CHLORITE, SPOT 5	0	1.04	4.67	53.98	10.08	23.02	0.7	6.28	0.17	0.14	100.08
526 CHR ANOTHER CENTRAL SPOT 6	0	0.4	13.9	53.3	3.85	17.24	0.49	10.99	0.06	0.06	100.29
527 CHR ANOTHER CENTRAL SPOT 6	0	0.33	13.72	53.31	3.76	17.09	0.3	11.01	0.02	0.12	99.66
528 CHR ANOTHER CENTRAL SPOT 6	0	0.43	14.11	53.38	3.55	17.51	0.42	10.9	0.05	0.14	100.50
529 CHR ANOTHER CENTRAL SPOT 6	0	0.4	14.02	52.92	3.49	18.75	0.43	10.05	0.05	0.04	100.15
530 CHR FOLIATED, SPOT 7	0	0.43	13.77	53.53	3.63	16.98	0.32	11.22	0	0.11	99.99
531 CHR SMALL INST SPOT 9	0	0.36	14.21	53.69	3.67	16.75	0.41	11.43	0.07	0.09	100.69
532 CHR W INCL AT MARGIN, SPOT 10	0	0.9	4.4	58.71	6.13	22.37	0.64	6.74	0.18	0.04	100.11
533 CHR CENTRAL SPOT 11	0	0.39	13.66	53.82	3.12	18.58	0.44	10.09	0.1	0.07	100.27
534 CHR BRIGHT AT MARGIN SPOT 12	0	0.18	8.51	61.41	0.46	20.94	0.55	7.79	0.2	0	100.04
535 CHR **** SAMPLE 486035 L CENTRAL, SPOT 1, 12	0	0.44	13.96	53.54	2.96	16.85	0.45	11.15	0.09	0.01	99.45
536 CHR SPOT 1 AGAIN	0	0.45	14.13	53.8	2.39	18.71	0.5	10.03	0.06	0.13	100.20
537 CHR AT MARGIN SPOT 2	0	0.33	13.63	52.75	3.79	19.29	0.42	9.54	0	0.12	99.87
538 CHR BRIGHT DOMAIN AT MARGIN SPOT 3	0	0.48	5.84	54.62	8.69	22.99	0.59	6.12	0.08	0.15	99.56
539 CHR L CENTRAL, SPOT 3	0	0.42	14.21	53.37	3.65	16.77	0.4	11.39	0.07	0.1	100.38
540 CHR AT MARGIN SPOT 4	0	0.43	14.15	53.02	2.86	19.09	0.43	9.78	0.07	0.08	99.91
541 CHR ANOTHER SPOT 5	0	0.4	13.99	53.89	3.31	18.06	0.44	10.56	0.14	0.09	100.88
542 CHR ANOTHER SPOT 5	0	0.43	13.69	53.83	2.93	18.11	0.4	10.42	0.02	0.08	99.90
543 CHR BRIGHT DOMAIN SPOT 6	0	0.66	4.76	54.93	10.01	23.80	0.63	5.82	0.14	0.08	100.82
544 CHR SMALLER SPOT 7	0	0.4	13.71	53.58	2.65	19.27	0.51	9.54	0	0.11	99.76
545 CHR SMALLER INST SPOT 8	0	0.43	14.02	52.98	3.08	18.72	0.52	9.93	0.03	0.11	99.82
546 CHR **** SAMPLE 486037 L GRAIN CENTRAL, 12-3	0	0.44	14.28	52.21	4.11	17.70	0.27	10.79	0.07	0.11	99.98
547 CHR AT MARGIN NO RIND, SPOT 2	0	0.42	13.89	51.7	4.34	19.22	0.57	9.55	0.07	0.05	99.81
548 CHR ANOTHER CENTRAL SPOT 3	0	0.4	14.28	52.13	4.14	18.68	0.33	10.17	0	0.15	100.27
549 CHR AT MARGIN SPOT 4	0	0.44	14.25	51.07	4.50	19.04	0.43	9.75	0.12	0.04	99.64
550 CHR ANOTHER L CENTRAL, SPOT 5	0	0.42	13.86	53.54	3.39	17.59	0.35	10.84	0	0.09	100.08
551 CHR AT MARGIN NO RIND SPOT 6	0	0.46	13.99	51.89	4.26	19.54	0.41	9.58	0	0.1	100.24
552 CHR SMALLER SPOT 7	0	0.46	14.48	51.24	4.36	19.71	0.51	9.46	0.06	0.07	100.35
553 CHR BRIGHT MARGIN INCL MG-CHL, SPOT 8	0	0.53	5.89	56.26	7.72	23.98	0.64	5.83	0.11	0.05	101.01

Black Thor BT-08-10

	SiO2	TiO2	Al2O3	Cr2O3	Fe2O3	FeO	MnO	MgO	ZnO	NiO	TOTAL
554 CHR LARGER CENTRAL, SPOT 9	0	0.49	14.48	51.9	4.29	18.87	0.47	10.13	0.07	0.09	100.79
555 CHR BRIGHT AT MARGIN W INCL MG-CHL, SPOT 10	0	0.45	6.59	54.63	9.02	22.88	0.61	6.48	0.18	0.13	100.97
556 CHR SMALL INST SPOT 12	0	0.46	14.17	50.85	4.61	19.69	0.49	9.32	0	0.13	99.72
557 CHR **** SAMPLE 486041 L CENTRAL, SPOT 1, 12	0	0.52	14.35	53.59	3.69	15.77	0.36	12.21	0.12	0.03	100.64
558 CHR AT MARGIN SPOT 2, 12-27-3747	0	0.42	14.62	52.79	3.07	17.81	0.49	10.63	0.03	0.11	99.97
559 CHR ANOTHER CENTRAL, SPOT 3	0	0.37	14.04	54.12	3.72	15.79	0.31	12.16	0	0.03	100.54
560 CHR AT MARGIN SPOT 4	0	0.37	13.91	53.53	3.66	17.77	0.39	10.71	0.05	0.12	100.52
561 CHR ANOTHER CENTRAL, SPOT 5	0	0.4	14.19	54.03	3.07	16.59	0.27	11.61	0	0.08	100.24
562 CHR AT MARGIN NO RIND SPOT 6	0	0.39	13.91	53.94	3.06	17.89	0.35	10.7	0.04	0.02	100.31
563 CHR BRIGHT AT MARGIN SPOT 7	0	0.57	7.34	55.49	7.13	21.26	0.64	7.61	0.15	0.03	100.22
564 CHR SMALL INST SPOT 8	0	0.37	13.79	52.89	4.12	17.87	0.48	10.48	0.14	0.08	100.21
565 CHR ANOTHER SPOT 9	0	0.37	14.34	53.23	3.45	18.09	0.45	10.55	0.07	0.07	100.61
566 CHR INST SPOT 10	0	0.42	14.43	52.9	2.74	18.43	0.42	10.26	0.02	0	99.62
567 CHR **** SAMPLE 486042 L CENTRAL, SPOT 1, 12	0	0.41	14.09	52.78	4.65	16.88	0.36	11.36	0.15	0.08	100.77
568 CHR AT MARGIN SPOT 2	0	0.47	13.87	51.91	4.32	17.75	0.56	10.43	0.1	0.1	99.51
569 CHR BRIGHT DOM AT MARGIN, SPOT 3	0	0.48	6.39	58.2	5.90	21.48	0.65	7.43	0.14	0.03	100.70
570 CHR REL L CENTRAL, SPOT 4	0	0.4	14.01	52.92	3.40	17.58	0.28	10.74	0.1	0.04	99.47
571 CHR NEW FIL SPOT 4 AGAIN	0	0.4	14.05	53.38	3.85	17.28	0.39	11.06	0.13	0.08	100.62
572 CHR AT MARGIN SPOT 5	0	0.45	14.36	52.63	3.92	18.02	0.55	10.6	0.08	0.03	100.64
573 CHR BRIGHT DOM AT MARGIN SPOT 6	0	0.43	8.45	56.9	4.53	20.21	0.61	8.26	0.06	0.06	99.51
574 CHR SMALLER SPOT 6	0	0.43	14.4	52.26	4.16	17.61	0.49	10.74	0.14	0.12	100.36
575 CHR SMALLER SPOT 7	0	0.45	14.27	52.43	3.91	17.73	0.52	10.66	0.08	0.08	100.13
576 CHR BRIGHT W INCL MG-CHL, SPOT 8	0	0.55	7.51	56.3	6.67	20.65	0.47	8.14	0.08	0.2	100.57
577 CHR SMALL INST SPOT 9	0	0.39	14.43	52.65	3.62	18.46	0.44	10.31	0.05	0.06	100.41
578 CHR SMALL INST SPOT 10	0	0.43	13.87	52.75	3.71	18.47	0.36	10.21	0.09	0.03	99.92
579 CHR **** SAMPLE 486043 L CENTRAL, SPOT 1, 12	0	0.47	13.82	52.27	4.61	18.03	0.41	10.52	0.01	0.16	100.30
580 CHR AT MARGIN NO RIND SPOTM 2	0	0.43	14.23	51.47	4.96	18.94	0.56	9.94	0.04	0.1	100.68
581 CHR BRIGHT NEAR LINEAR RETRO, SPOT 3	0	0.41	13.7	51.17	4.79	19.85	0.45	9.1	0.1	0.12	99.69
582 CHR ANOTHER L CENTRAL, SPOT 4	0	0.42	14.47	50.86	5.39	18.17	0.36	10.51	0	0.15	100.33
583 CHR AT MARGIN, SPOT 5	0	0.42	14.42	51.41	4.33	19.25	0.41	9.67	0.12	0.16	100.19
584 CHR ANOTHER SPOT 6	0	0.46	14.62	51.01	4.08	18.82	0.34	9.99	0.03	0.08	99.43
585 CHR BRIGHT SPOT 7	0	0.72	5.65	52.55	11.77	23.78	0.58	6.05	0.15	0.13	101.38
586 CHR INT BRIGHT SPOT 8	0	0.44	8.51	52.11	8.92	22.38	0.63	6.91	0.08	0.03	100.00
587 CHR SMALLER SPOT 9	0	0.42	15.64	50.43	4.56	18.60	0.35	10.39	0.06	0.14	100.59
588 CHR SMALLER SPOT 10	0	0.43	15.2	50.24	4.01	18.96	0.39	9.8	0.08	0.14	99.25
589 CHR INST SPOT 11	0	0.45	14.76	52.46	2.94	19.02	0.63	9.82	0.08	0.1	100.25
590 CHR V SMALL INST SPOT 12	0	0.46	14.84	50.22	4.65	19.17	0.4	9.74	0.1	0.09	99.68
591 CHR **** SAMPLE 486044 GRAIN 1 CENTRAL, 12-2	0.04	0.45	15.19	50.86	4.54	16.68	0.32	11.29	0.17	0.13	99.67
592 CHR AT MARGIN	0.08	0.46	15.55	50.67	4.27	18.40	0.36	10.25	0.21	0.05	100.30
593 CHR GRAIN 2 CENTRAL	0.05	0.47	15.5	51.14	4.10	17.44	0.38	10.92	0.15	0.13	100.28
594 CHR AT MARGIN NO RIND	0.07	0.4	15.27	51	4.17	19.42	0.47	9.51	0.28	0.03	100.62
595 CHR BRIGHT MARGIN	0.06	0.33	8.91	58.53	2.41	21.77	0.54	7.22	0.17	0	99.94
596 CHR GRAIN 2A CENTRAL	0.08	0.51	15.07	50.3	4.01	19.53	0.41	9.36	0.1	0.02	99.39
597 CHR REL BRIGHT MARGINAL DOMAIN	0.05	0.21	7.94	59.31	2.92	21.79	0.64	6.98	0.22	0.01	100.07
598 CHR ANOTHER BRIGHT DOMAIN AT MARGIN	0.05	0.23	9.43	56.98	2.84	21.39	0.53	7.28	0.11	0.03	98.87
599 CHR ANOTHER BRIGHT	0.12	0.39	6.5	59.2	4.02	21.93	0.59	6.56	0.2	0.11	99.62
600 CHR IMMED ADJ MAIN GRAIN	0.03	0.44	15.17	51.17	3.77	19.77	0.3	9.53	0.07	0.1	100.36
601 CHR ADJ GRAIN CENTRAL	0.02	0.41	15.16	50.64	4.16	20.25	0.5	9.15	0.04	0.03	100.37
602 CHR BRIGHT ANG DOMAIN	0.11	0.59	6.62	51.74	10.62	22.44	0.63	6.21	0.23	0.09	99.28
603 CHR GRAIN 4 CENTRAL	0.03	0.44	14.97	51.63	3.10	18.14	0.52	10.2	0.06	0.1	99.19
604 CHR AT MARGIN	0.03	0.46	15.11	50.56	4.12	19.16	0.51	9.66	0.08	0.12	99.81
605 CHR GRAIN 5 CENTRAL	0.01	0.5	14.97	51.63	3.82	18.07	0.25	10.67	0.13	0.07	100.11
606 CHR AT MARGIN	0.05	0.45	14.86	50.56	4.32	19.22	0.43	9.48	0.2	0.16	99.72
607 CHR SMALLER GRAIN	0.07	0.41	15.01	50.13	4.78	19.46	0.65	9.19	0.21	0.14	100.05
608 CHR GRAIN 6 CENTRAL, 12-21-3644	0.01	0.44	15.16	52.52	3.12	18.04	0.25	10.85	0.01	0.01	100.41
609 CHR AT MARGIN	0	0.41	14.89	51.36	3.89	19.33	0.51	9.62	0.19	0.1	100.30
610 CHR BRIGHT AT MARGIN	0.11	1.09	4.88	48.33	16.08	24.29	0.76	5.35	0.29	0.11	101.29
611 CHR GRAIN 7 CENTRAL	0.02	0.43	15.06	51.67	4.26	17.65	0.47	10.86	0.09	0.07	100.58
612 CHR GRAIN 8 CENTRAL, RANDOM, 12-21-3646,47	0.03	0.41	15.3	51.08	4.01	17.45	0.32	10.85	0.13	0.1	99.68
613 CHR AT MARGIN	0.02	0.46	15.4	50.78	3.91	19.53	0.35	9.7	0.13	0.06	100.33
614 CHR * 2ND TIME GR 2 REG, DARK, SPOT 1 12-21-	0	0.4	13.97	51.52	4.38	18.61	0.48	9.83	0.15	0.14	99.48
615 CHR ANOTHER DARK CENTRAL, SPOT 2	0	0.36	14.06	52.78	4.47	17.06	0.35	11.15	0.08	0.16	100.47
616 CHR INT, SPOT 3	0	0.42	14.04	53.19	3.95	17.30	0.35	11.1	0.06	0.08	100.49
617 CHR AT MARGIN SPOT 4	0	0.33	13.92	51.97	4.59	19.70	0.51	9.41	0	0.04	100.47
618 CHR BRIGHTEST SPOT 5	0.05	0.67	4.32	52.97	11.93	23.83	0.68	5.44	0.09	0.13	100.10
619 CHR BRIGHT AT MARGIN SPOT 6	0	0.64	6.9	50.54	11.98	23.59	0.64	6.03	0.19	0.15	100.66
620 CHR GR 6 REGION, L CENTRAL, SPOT 1, 12-21-364	0	0.42	13.51	51.52	4.99	17.20	0.27	10.74	0.2	0.08	98.93
621 CHR NEAR MARGIN NO RIND, SPOT 2	0.01	0.34	13.64	51.74	4.64	19.79	0.46	9.23	0	0.01	99.85
622 CHR ADJ GRAIN CENTRAL, SPOT 3	0	0.47	13.76	52.6	4.43	17.11	0.36	11.07	0.05	0.15	100.00
623 CHR AT MARGIN SPOT 4	0	0.36	13.69	52.46	4.38	20.13	0.44	9.08	0.24	0.09	100.87
624 CHR CENTRAL SPOT 1, 12-21-3647	0	0.39	14.07	51.76	4.73	17.35	0.39	10.8	0.05	0.17	99.71
625 CHR AT MARGIN SPOT 2	0	0.41	13.72	52.18	3.77	19.37	0.37	9.49	0.04	0.07	99.42
626 CHR **** SAMPLE 486045 CENTRAL, SPOT 1, 12-2	0.06	0.49	15.74	51.09	3.73	18.24	0.33	10.57	0	0.1	100.35
627 CHR AT MARGIN, SPOT 2	0.1	0.46	15.51	50.68	3.90	19.15	0.38	9.64	0.23	0.07	100.12
628 CHR GRAIN 2 CENTRAL, SPOT 3	0.1	0.55	15.33	50.26	4.12	19.36	0.44	9.53	0.1	0.04	99.83
629 CHR AT MARGIN, SPOT 4	0.07	0.55	15.21	50.04	4.23	20.53	0.45	8.94	0	0.01	100.02
630 CHR GRAIN 3 CENTRAL	0.03	0.56	14.69	50.32	4.32	19.84	0.62	9.08	0.17	0.14	99.77
631 CHR AT MARGIN	0.06	0.47	15.4	48.71	4.94	20.76	0.45	8.53	0.08	0.17	99.57
632 CHR GRAIN 4 CENTRAL	0.06	0.56	15.2	50.3	3.88	19.52	0.35	9.39	0.13	0.23	99.62

Black Thor BT-08-10

	SiO2	TiO2	Al2O3	Cr2O3	Fe2O3	FeO	MnO	MgO	ZnO	NiO	TOTAL
633 CHR AT MARGIN	0.09	0.49	14.86	50.52	4.29	21.21	0.54	8.24	0.24	0.08	100.56
634 CHR BRIGHT DOMAIN AT MARGIN	0.02	0.36	6.85	59.66	3.07	23.26	0.63	6.03	0.32	0.03	100.23
635 CHR ADJ GRAIN CENTRAL	0.06	0.54	15.06	49.67	4.70	20.97	0.38	8.54	0.26	0.09	100.27
636 CHR BRIGHT DOM NEAR MARGIN	0.06	0.5	8.89	49.81	11.20	24.12	0.52	5.92	0.17	0.12	101.31
637 CHR MARGINAL RIND	0.13	0.57	2.26	59.08	7.89	24.13	0.68	4.66	0.29	0.09	99.78
638 CHR GRAIN 5 CENTRAL, 12-21-3651	0.02	0.52	15.67	49.95	4.52	18.10	0.36	10.48	0.16	0.25	100.62
639 CHR AT MARGIN INSIDE RIND, 12-21-3652	0.06	0.46	15.29	50.12	3.97	20.62	0.59	8.59	0.13	0.15	99.99
640 CHR NARROW MARGIN	0.18	0.41	4.19	60.94	4.72	22.91	0.67	5.56	0.24	0.05	99.87
641 CHR GRAIN 6 CENTRAL	0.08	0.51	14.98	49.72	5.00	20.94	0.52	8.51	0.11	0.11	100.48
642 CHR AT MARGIN	0.04	0.49	14.85	50.86	4.01	20.79	0.48	8.72	0.13	0.06	100.43
643 CHR * 2ND TIME GR 1, SPOT 1, 12-21-3649	0	0.4	13.89	51.77	4.75	18.07	0.44	10.34	0.02	0.16	99.84
644 CHR AT MARGIN NO RIND SPOT 2	0.06	0.41	14.97	50.89	4.28	19.27	0.42	9.59	0.08	0.12	100.10
645 CHR ZONED GRAIN, DARK CENTRAL, SPOT 3	0	0.52	14.33	50.48	5.52	18.00	0.42	10.49	0.08	0.19	100.03
646 CHR AT MARGIN, SPOT 4	0.05	0.32	12.44	48.45	9.34	20.76	0.55	8.25	0.13	0.07	100.35
647 CHR GR 5 REG, LARGE GRAIN CENTRAL, SPOT 1, 1	0	0.47	14.4	51.56	4.91	18.47	0.37	10.37	0.08	0.18	100.41
648 CHR AT ALT MARGIN, SPOT 2	0	0.38	13.61	51.29	4.60	20.51	0.43	8.63	0.23	0.06	99.74
649 CHR MAIN GRAIN SPOT 1, 12-21-3652	0	0.4	13.81	51.05	5.28	20.62	0.46	8.76	0.11	0.16	100.65
650 CHR AT MARGIN SPOT 2 NO RIND	0.01	0.42	14.22	50.81	4.67	20.34	0.59	8.82	0.12	0.08	100.08
651 CHR BRIGHT DOMAIN INTERNAL, SPOT 3	0	0.2	7.41	58.81	4.04	22.78	0.63	6.42	0.22	0.15	100.65
652 CHR SPOT 4 EARLY-STAGE CONSUMPTION	0	0.25	7.95	57.35	4.13	22.57	0.56	6.54	0.21	0.04	99.60
653 CHR REL BRIGHT SPOT 5	0.02	0.97	3.66	48.78	15.99	25.44	0.63	4.59	0.1	0.14	100.31
654 CHR ADJ GRAIN SPOT 6	0	0.23	6.61	57.94	4.92	23.09	0.5	6.16	0.04	0.06	99.55
655 CHR BRIGHTEST AT MARGIN, SPOT 7	0.01	0.51	2.25	59.53	6.77	24.61	0.63	4.6	0.13	0.08	99.12
656 CHR BRIGHTEST MARGIN, SPOT 7	0.04	0.39	2.75	57.22	8.16	24.00	0.73	4.55	0.26	0.09	98.20
657 CHR **** SAMPLE 486046 GRAIN 1 CENTRAL	0.03	0.51	15.67	48.31	5.05	20.53	0.39	8.94	0.03	0.04	99.50
658 CHR BRIGHT MARGIN	0.17	1.13	0.74	46.9	20.75	25.80	0.78	3.51	0.22	0.21	100.22
659 CHR GRAIN 2 CENTRAL	0.04	0.55	15.67	49.52	4.24	20.01	0.38	9.26	0.2	0.08	99.95
660 CHR AT MARGIN	0.07	0.51	15.75	49	4.72	20.88	0.55	8.57	0.2	0.08	100.32
661 CHR GRAIN 3 CENTRAL	0	0.52	15.45	49.57	4.74	20.61	0.43	8.89	0.31	0.23	100.76
662 CHR AT MARGIN	0.03	0.51	15.64	49.92	3.92	21.36	0.51	8.5	0.09	0.05	100.52
663 CHR GRAIN 4 CENTRAL	0.03	0.44	14.99	50.3	4.32	21.26	0.44	8.41	0.16	0.09	100.44
664 CHR AT MARGIN	0.04	0.43	15.19	49.94	3.98	20.63	0.4	8.7	0.04	0.11	99.46
665 CHR GRAIN 5 CENTRAL	0.01	0.48	13.32	51.31	4.41	21.50	0.41	8.08	0.01	0.11	99.64
666 CHR INT	0.08	0.48	13.35	52.17	3.85	20.34	0.44	8.63	0.07	0.05	99.47
667 CHR AT MARGIN	0.04	0.47	15.66	50.09	3.86	20.59	0.59	8.83	0.15	0.04	100.33
668 CHR GRAIN 6 CENTRAL	0.06	0.52	15.61	50.37	3.31	20.20	0.52	8.98	0.12	0.11	99.80
669 CHR AT MARGIN	0.05	0.5	15.79	49.5	4.83	20.08	0.48	9.32	0.18	0.02	100.74
670 CHR GRAIN 7 CENTRAL, 12-21-3655	0.06	0.5	14.68	50.56	4.79	20.73	0.47	8.69	0.21	0.14	100.83
671 CHR AT MARGIN	0.05	0.52	14.87	50.43	4.39	20.78	0.37	8.81	0	0.14	100.36
672 CHR **** SAMPLE 486050 LARGE CENTRAL, SPOT 1	0	0.56	13.54	50.79	4.17	21.73	0.57	7.79	0.13	0.13	99.41
673 CHR AT MARGIN NO RIND SPOT 2	0	0.53	14.01	50.7	4.69	21.78	0.48	8.09	0.19	0.05	100.52
674 CHR ANOTHER CENTRAL, SPOT 3	0	0.55	14.06	50.51	4.45	21.60	0.51	8.18	0	0.08	99.94
675 CHR AT MARGIN SPOT 4	0	0.45	13.78	50.5	4.50	21.57	0.48	8	0.04	0.06	99.38
676 CHR SMALLER SPOT 5	0	0.58	14.06	50.11	4.78	21.61	0.45	8	0.39	0.12	100.10
677 CHR SMALLER SPOT 6	0	0.5	13.78	49.76	5.47	21.84	0.38	7.91	0.13	0.16	99.93
678 CHR V SMALL SPOT 7	0	0.48	13.93	50.2	4.89	21.86	0.48	7.95	0.04	0.06	99.84
679 CHR LARGE CENTRAL, SPOT 1, 12-25-3714	0	0.52	14.39	50.79	4.39	21.23	0.63	8.45	0.06	0.08	100.59
680 CHR AT MARGIN NO RIND, SPOT 2	0	0.52	13.52	50.75	4.53	21.98	0.54	7.75	0.06	0.1	99.75
681 CHR SMALLER SPOT 3	0	0.54	13.88	50.98	4.79	21.72	0.51	8.17	0.08	0.14	100.81
682 CHR SMALLER SPOT 4	0	0.61	13.82	50.66	4.54	21.94	0.46	8.02	0.02	0.11	100.19
683 CHR ANOTHER SPOT 5	0	0.42	14.54	50.31	4.14	21.10	0.5	8.38	0.07	0.04	99.50
684 CHR SMALLER SPOT 6	0	0.42	14.53	50.74	4.62	21.45	0.47	8.35	0.16	0.11	100.84
685 CHR SMALLER SPOT 7	0	0.54	14.31	50.44	4.78	21.73	0.4	8.17	0.23	0.15	100.75
686 CHR **** SAMPLE 486051 L CENTRAL, SPOT 1, 12	0	0.4	14.41	51.97	4.79	16.71	0.43	11.4	0	0.13	100.24
687 CHR SPOT 2 AT MARGIN	0	0.41	14.05	52.33	3.52	20.83	0.45	8.72	0.09	0.05	100.45
688 CHR ANOTHER C CENTRAL, SPOT 3	0	0.41	14.42	52.71	3.45	18.66	0.33	10.19	0.09	0.13	100.38
689 CHR AT MARGIN SPOT 4	0	0.42	14.18	50.67	4.12	21.05	0.41	8.31	0.27	0.04	99.47
690 CHR GRAIN 3 CENTRAL, SPOT 5	0	0.44	14.29	52.76	3.63	16.51	0.45	11.31	0.24	0.1	99.73
691 CHR AT MARGIN SPOT 6	0	0.41	14.59	51.01	3.89	19.64	0.42	9.28	0.18	0.12	99.54
692 CHR SMALLER SPOT 7	0	0.4	14.57	51.45	3.54	20.57	0.42	8.77	0.24	0.06	100.02
693 CHR SMALLER SPOT 8	0	0.43	14.45	50.68	4.11	20.96	0.42	8.59	0	0.06	99.70
694 CHR L CENTRAL, SPOT 1, 12-25-3716	0	0.37	14.27	53.05	3.63	16.63	0.32	11.46	0.02	0.03	99.78
695 CHR AT MARGIN SPOT 2	0	0.48	14.26	51.47	3.12	21.66	0.34	8.1	0.1	0.12	99.64
696 CHR L GRAIN CENTRAL, SPOT 3	0	0.41	14	53.32	3.81	16.63	0.48	11.33	0.04	0.18	100.19
697 CHR AT MARGIN SPOT 4	0	0.43	14.6	52.23	3.14	20.02	0.53	9.21	0.09	0.11	100.36
698 CHR AT MARGIN SPOT 4	0	0.42	13.93	52.88	3.14	20.79	0.48	8.77	0.03	0.05	100.48
699 CHR SMALLER SPOT 5	0	0.36	13.35	52.38	3.78	20.27	0.54	8.72	0.07	0.09	99.56
700 CHR SMALLER SPOT 6	0	0.4	14.74	52.9	2.95	18.43	0.44	10.4	0.01	0.02	100.29
701 CHR SMALLER SPOT 7	0	0.39	14.4	52.18	3.46	20.77	0.54	8.81	0	0.05	100.61
702 CHR V SMALL SPOT 8	0	0.45	14.81	52.01	2.86	20.89	0.43	8.81	0.02	0.07	100.35
703 CHR **** SAMPLE 486052 GRAIN 1 CENTRAL, SPO	0	0.46	15.05	50.39	4.60	17.97	0.45	10.51	0.02	0.15	99.59
704 CHR AT MARGIN SPOT 2	0	0.41	14.4	50.13	4.45	21.20	0.43	8.23	0.15	0.15	99.55
705 CHR SMALLER SPOT 3	0	0.51	15.15	50.16	4.00	19.91	0.51	9.3	0.01	0.09	99.64
706 CHR L CENTRAL SPOT 4	0	0.51	14.81	50.8	4.17	20.56	0.45	9.05	0	0.1	100.45
707 CHR AT MARGIN SPOT 5	0	0.5	14.69	49.64	4.97	21.05	0.39	8.66	0	0.07	99.97
708 CHR SPOT 6	0	0.43	14.47	50.6	4.85	18.62	0.42	9.98	0.11	0.14	99.63
709 CHR SMALLER SPOT 7	0	0.6	14.92	49.89	4.53	20.79	0.49	8.77	0.24	0.08	100.31
710 CHR SMALL SPOT 8	0	0.48	14.5	50.88	4.19	21.38	0.51	8.38	0.08	0.12	100.52
711 CHR CENTRAL SPOT 9	0	0.5	14.47	50.97	4.82	18.52	0.6	10.21	0	0.03	100.12

Black Thor BT-08-10

	SiO2	TiO2	Al2O3	Cr2O3	Fe2O3	FeO	MnO	MgO	ZnO	NiO	TOTAL
712 CHR AT MARGIN SPOT 10	0	0.52	14.75	48.9	5.49	20.57	0.46	8.86	0.06	0.03	99.64
713 CHR **** SAMPLE 486056 L TRIANG CENTRAL	0	0.3	14.25	50.84	3.99	22.12	0.33	7.83	0	0	99.66
714 CHR AT MARGIN	0	0.38	14.61	50.57	4.48	22.50	0.47	7.81	0	0	100.82
715 CHR ANOTHER L CENTRAL	0	0.36	14.63	51.76	3.57	22.11	0.37	8.16	0	0	100.96
716 CHR ANOTHER L CENTRAL	0	0.36	14.33	50.69	3.87	21.68	0.39	8.06	0	0	99.38
717 CHR AT MARGIN	0	0.4	14.77	50.93	3.17	22.32	0.26	7.88	0	0	99.73
718 CHR ANOTHER L CENTRAL	0	0.4	14.9	51.26	3.76	22.65	0.42	7.89	0	0	101.29
719 CHR ANOTHER L CENTRAL	0	0.41	14.24	50.68	3.56	22.26	0.38	7.67	0	0.01	99.21
720 CHR AT MARGIN	0	0.46	15.06	51.12	3.69	23.00	0.36	7.79	0	0.02	101.50
721 CHR ANOTHEWR L CENTRAL	0	0.42	14.4	51.45	3.27	21.70	0.32	8.23	0	0	99.79
722 CHR AT MARGIN	0	0.37	14.89	50.19	4.11	22.10	0.37	7.98	0	0.03	100.04
723 CHR SMALLER	0	0.42	15.36	49.51	4.44	22.01	0.45	8.14	0	0	100.33
724 CHR SMALLER INST	0	0.34	14.91	49.86	4.26	21.75	0.39	8.11	0	0	99.62
725 CHR V SMALL INST	0	0.41	14.9	50.72	3.72	22.60	0.41	7.78	0	0	100.54
726 CHR ANOTHER SMALL INST	0	0.26	14.84	50.96	4.12	22.24	0.47	7.94	0	0	100.83
727 CHR ANOTHER SMALL INST	0	0.3	15.04	50.11	3.93	22.23	0.47	7.79	0	0	99.87
728 CHR **** SAMPLE 486057 V L CENTRAL W INCL	0	0.31	14.91	53.78	2.70	18.43	0.26	10.66	0	0	101.05
729 CHR V L CENTRAL W INCL	0	0.32	14.93	52.35	3.20	17.78	0.37	10.73	0	0	99.68
730 CHR AT MARGIN	0	0.37	15.04	51.65	3.23	20.85	0.29	8.97	0	0	100.39
731 CHR ANOTH L NEARE CIRCC INCL	0	0.35	14.47	53.15	3.24	17.52	0.38	10.94	0	0	100.05
732 CHR AT MARGIN	0	0.36	15.21	52.29	2.97	21.36	0.35	8.81	0	0	101.35
733 CHR AT MARGIN	0	0.4	14.72	51.96	3.13	21.32	0.36	8.61	0	0.03	100.52
734 CHR ANOTHER L CENTRAL	0	0.35	15.06	51.95	3.83	17.34	0.37	11.11	0	0	100.01
735 CHR AT MARGIN	0	0.41	15.04	52.52	2.96	20.61	0.42	9.23	0	0	101.20
736 CHR AT MARGIN	0	0.34	15.03	52.57	3.09	20.84	0.32	9.13	0	0	101.32
737 CHR AT MARGIN	0	0.23	14.74	52.79	3.32	20.41	0.31	9.27	0	0	101.06
738 CHR AT MARGIN	0	0.34	14.45	51.49	3.36	20.07	0.44	9.05	0	0	99.20
739 CHR ANOTHER W CIRC INCL, CENTRAL	0	0.34	14.48	51.82	2.97	21.41	0.44	8.3	0	0	99.76
740 CHR AT MARGIN	0	0.31	15.3	52.01	3.67	20.13	0.41	9.54	0	0.02	101.39
741 CHR ANOTHER BRIGHT CENTRAL	0	0.34	14.57	52.26	3.19	17.78	0.28	10.63	0	0	99.05
742 CHR AT MARGIN	0	0.32	15.19	51.28	3.47	21.69	0.48	8.36	0	0	100.79
743 CHR GRAIN 1 CENTRAL AGAIN	0	0.32	14.93	52.97	3.19	17.88	0.41	10.81	0	0	100.51
744 CHR GRAIN 4 AT AMRGIN	0	0.41	15.06	50.84	3.65	18.51	0.37	10.13	0	0.08	99.06
745 CHR ANOTHER GRAIN BETWEEN TWO CIRC INCL	0	0.37	15.13	51.92	3.13	17.17	0.37	11.07	0	0	99.16
746 CHR AT MARGIN	0.08	0.52	14.81	50.44	3.78	18.18	0.43	10.05	0	0	98.29
747 CHR AT MARGIN	0	0.36	15.28	50.96	4.57	18.71	0.41	10.3	0	0.08	100.67
748 CHR L W ONE CIRC INCL	0	0.31	14.48	53.04	3.61	17.48	0.29	11.04	0	0	100.25
749 CHR AT MARGIN	0	0.34	14.99	50.9	3.70	22.22	0.45	7.98	0	0	100.58
750 CHR VERY SMALL INST GRAIN	0	0.33	15.01	51.41	4.01	19.49	0.4	9.72	0	0.06	100.43
751 CHR ANOTHER SMALL INST	0	0.38	14.97	52.54	2.95	21.18	0.43	8.84	0	0.02	101.32
752 CHR ANOTHER SMALL INST	0	0.35	15.23	50.91	3.54	20.46	0.51	9	0	0	100.00
753 CHR **** SAMPLE 486058 REL L GRAIN CENTRAL	0	0.6	15.18	48.48	4.49	24.50	0.41	6.59	0	0.05	100.30
754 CHR AT MARGIN	0	0.52	14.03	48.29	5.16	22.92	0.38	7.08	0.05	0	98.43
755 CHR AT MARGIN	0	0.51	14.17	49.29	5.45	22.97	0.49	7.4	0	0	100.28
756 CHR BRIGHT DOMAIN AT MARGIN	0.14	1.13	1.23	39.4	27.92	27.44	0.41	3.04	0	0.15	100.86
757 CHR ANOTHER REL L CENTRAL	0	0.55	15.23	47.04	5.61	22.77	0.41	7.46	0	0	99.06
758 CHR ANOTHER REL L CENTRAL	0	0.59	15.6	48.4	4.80	23.15	0.43	7.57	0	0.01	100.55
759 CHR AT MARGIN	0	0.56	14.63	48.37	5.47	22.71	0.31	7.64	0	0	99.69
760 CHR ANOTHER REL LARGE	0	0.61	15.22	47.66	5.80	23.25	0.46	7.4	0	0.05	100.45
761 CHR ANOTHER REL LARGE	0	0.55	15.25	47.54	5.14	22.73	0.43	7.49	0	0	99.13
762 CHR SMALLER GRAIN	0	0.5	14.43	48.67	5.32	23.02	0.44	7.29	0	0	99.67
763 CHR V SMALL GRAIN	0	0.5	14.38	48.88	5.74	22.71	0.37	7.65	0	0	100.22
764 CHR ANOTHER GRAIN CENTRAL	0	0.59	14.41	48.01	6.00	22.79	0.41	7.52	0	0	99.73
765 CHR BRIGHT MARGINAL ZONE	0.08	1.19	0.34	43.85	23.39	27.26	0.59	3.01	0	0.03	99.74
766 CHR BRIGHT MARGINAL ZONE	0.05	1.2	0.34	43.29	24.33	27.59	0.66	2.92	0	0.11	100.49
767 CHR ANOTHER V LARGE CENTRAL	0	0.57	15.19	47.99	5.75	24.05	0.53	6.94	0	0.04	101.07
768 CHR ANOTHER V LARGE CENTRAL	0.42	0.6	15.21	48.52	6.62	22.20	0.43	7.3	0.06	0	101.36
769 CHR ANOTHER V LARGE CENTRAL	0	0.59	15.24	48.72	5.01	23.89	0.35	7.2	0	0	101.00
770 CHR ANOTHER V LARGE CENTRAL	0	0.64	15.15	48.4	4.95	23.47	0.39	7.33	0	0	100.33
771 CHR ANOTHER V LARGE CENTRAL	0	0.61	15.19	47.04	6.08	23.06	0.5	7.41	0	0	99.89
772 CHR AT MARGIN	0	0.42	14.41	50.01	5.40	23.00	0.41	7.61	0	0	101.25
773 CHR AT MARGIN	0	0.42	14.62	48.87	6.04	22.71	0.4	7.72	0	0	100.79
774 CHR ANOTHER CENTRAL	0	0.47	14.17	48.88	5.78	22.53	0.45	7.6	0	0	99.89
775 CHR ANOTHER CENTRAL	0	0.58	14.36	47.69	5.53	22.66	0.45	7.31	0	0.05	98.63
776 CHR V SMALL	0	0.61	13.34	49.4	6.05	22.69	0.5	7.5	0	0	100.10
777 CHR L CENTRAL	0	0.69	14.92	48.23	5.49	23.39	0.49	7.37	0	0	100.58
778 CHR L CENTRAL	0	0.52	14.99	48.89	5.07	23.10	0.33	7.54	0	0.02	100.46
779 CHR L CENTRAL	0	0.65	15	47.52	5.48	23.29	0.43	7.26	0	0	99.63
780 CHR AT MARGIN	0	0.57	14.47	48.89	5.67	22.77	0.38	7.7	0	0	100.45
781 CHR AT MARGIN	0	0.56	14.3	48.53	6.43	22.63	0.38	7.79	0	0.02	100.63
782 CHR AT MARGIN	0	0.5	14.25	49.11	5.28	22.30	0.38	7.77	0	0	99.59
783 CHR **** SAMPLE 486068 L CENTRAL, SPOT 1, 12	0	0.46	14.95	52.02	3.32	17.68	0.48	10.78	0	0.06	99.75
784 CHR AT MARGIN SPOT 2	0	0.43	14.85	51.31	3.68	21.40	0.41	8.53	0.14	0	100.76
785 CHR ANOTHER CENTRAL SPOT 3	0	0.42	15.02	52.88	2.26	17.76	0.43	10.59	0.15	0.15	99.66
786 CHR AT MARGIN SPOT 4	0	0.44	14.32	51.53	3.62	22.02	0.53	8	0.03	0.02	100.51
787 CHR ANOTHER CENTRAL, SPOT 5	0	0.44	15.06	53.43	2.21	17.13	0.48	11.17	0	0.13	100.05
788 CHR SMALLER SPOT 6	0	0.48	14.97	51.49	3.27	18.84	0.52	9.95	0.08	0.05	99.65
789 CHR SMALLER SPOT 7	0	0.47	14.41	52.94	2.48	18.13	0.44	10.37	0	0.08	99.32
790 CHR SMALLER SPOT 8	0	0.43	15.2	52.46	3.20	17.32	0.35	11.15	0.06	0.12	100.29

Black Thor BT-08-10

	SiO2	TiO2	Al2O3	Cr2O3	Fe2O3	FeO	MnO	MgO	ZnO	NiO	TOTAL
791 CHR V SMALL SPOT 9	0.02	0.44	14.97	51.42	2.93	22.33	0.57	7.69	0.2	0.08	100.64
792 CHR ANOTHER SPOT 10	0	0.45	14.87	51.78	2.90	20.98	0.49	8.7	0.03	0.06	100.26
793 CHR **** SAMPLE 486069 L CENTRAL, SPOT 1, 12	0	0.63	14.61	51.26	4.44	18.58	0.49	10.38	0	0.08	100.48
794 CHR AT MARGIN SPOT 2	0	0.65	15.2	49.35	4.32	21.49	0.43	8.35	0.19	0.18	100.16
795 CHR ANOTHER DARK CENTRAL, SPOT 3	0	0.61	14.95	50.1	4.17	20.23	0.53	9.09	0.16	0.08	99.92
796 CHR AT MARGIN SPOT 4	0	0.62	14.92	49.93	4.30	22.56	0.5	7.89	0.03	0.01	100.76
797 CHR SMALLER CENTRAL, SPOT 5	0	0.65	15.08	50.25	3.94	20.68	0.48	9.02	0	0.08	100.17
798 CHR SMALLER SPOT 6	0	0.65	14.38	49.93	4.54	21.98	0.46	8	0.14	0.12	100.20
799 CHR LARGE CENTRAL, RANDOM, ANAL 7	0	0.49	14.4	51.08	4.72	19.86	0.45	9.49	0.03	0.04	100.55
800 CHR AT MARGIN ANAL 8	0	0.5	15.26	49.77	4.35	21.94	0.42	8.21	0.03	0.11	100.59
801 CHR ANOTHER L CENTRAL, ANAL 9	0	0.7	15.14	49.95	4.69	19.04	0.29	10.16	0	0.21	100.18
802 CHR **** SAMPLE 486070 V L CENTRAL, SPOT 1,	0	0.4	14.35	51.97	3.25	21.83	0.46	8.08	0.11	0.07	100.52
803 CHR AT MARGIN SPOT 2	0	0.42	14.71	52.84	3.07	18.88	0.37	10.18	0.04	0.04	100.55
804 CHR ANOTHER SPOT 3	0	0.4	14.93	51.47	3.73	19.16	0.37	9.83	0.16	0.05	100.10
805 CHR AT MARGIN SPOT 4	0	0.49	14.98	50.15	3.76	21.92	0.45	8.06	0	0.09	99.91
806 CHR SMALLER C SPOT 6	0	0.41	15.01	52.68	2.97	18.43	0.4	10.46	0	0.07	100.43
807 CHR AT MARGIN SPOT 7	0	0.36	14.76	50.93	3.75	21.89	0.59	7.93	0.12	0.08	100.42
808 CHR ANOTHER REL DARK SPOT 8	0	0.4	14.97	52.84	2.78	18.76	0.38	10.22	0.06	0.08	100.50
809 CHR NEAR ALT FRACTS SPOT 9	0	0.41	14.43	52.03	2.24	22.27	0.43	7.63	0.07	0.14	99.65
810 CHR **** SAMPLE 486071 GRAIN 1 CENTRAL, 12-2	0.07	1	14.46	46.24	7.00	23.32	0.57	7.08	0.07	0.08	99.89
811 CHR MARGINAL RIND	0.13	2.7	1.13	41.2	23.35	28.50	0.74	2.97	0.2	0.3	101.22
812 CHR GRAIN 2	0.02	1.61	14.21	46.74	5.87	23.61	0.54	7.43	0.14	0.02	100.19
813 CHR NEAR MARGINAL RIND	0.05	0.96	13.92	46.93	7.54	23.55	0.54	7.07	0.16	0.03	100.76
814 CHR GRAIN 3	0.06	1.22	14.93	46.61	6.47	23.27	0.45	7.58	0.04	0.1	100.74
815 CHR GRAIN 4 CENTRAL	0.03	0.77	14.48	46.38	7.60	23.43	0.48	7.19	0.01	0.05	100.42
816 CHR AT MARGIN	0.03	0.73	12.93	46.78	8.65	23.93	0.49	6.56	0.14	0.04	100.28
817 CHR GRAIN 5 CENTRAL	0.03	0.96	14.66	45.89	7.25	23.55	0.46	7.04	0.22	0.11	100.18
818 CHR AT MARGIN	0.07	1.13	13.99	46.95	6.87	23.44	0.59	7.11	0.12	0.02	100.29
819 CHR GRAIN 6	0	1	14.66	46.79	6.66	23.27	0.45	7.52	0.1	0.02	100.48
820 CHR GRAIN 7	0.03	0.93	14.29	46.53	7.52	23.56	0.54	7.11	0.06	0.15	100.72
821 CHR GRAIN 8 CENTRAL	0.05	0.91	14.05	47.78	6.72	23.61	0.57	7	0.08	0.18	100.94
822 CHR AT MARGIN	0.08	1.02	14.11	46.93	7.72	23.49	0.49	7.22	0.22	0	101.28
823 CHR GRAIN 9	0.06	1.46	14.05	45.8	7.10	23.60	0.52	7.15	0.21	0.03	99.98
824 CHR * 2ND TIME DARK CENTRAL, SPOT 1, 12-21-3	0	1.11	13.69	47.1	7.33	23.31	0.37	7.47	0.19	0.04	100.61
825 CHR SURROUNDING RIND SPOT 2	0.07	2.1	2.07	42.41	21.47	28.25	0.63	3.03	0.14	0.2	100.37
826 CHR **** SAMPLE 486072 GRAIN 1 CENTRAL, 12-2	0.03	0.47	14.33	52.84	4.35	15.21	0.32	12.35	0.11	0.09	100.10
827 CHR AT MARGIN NO RIND	0.08	0.47	15.27	50.77	3.66	20.34	0.48	8.98	0	0.04	100.09
828 CHR ADJ GRAIN 2 CENTRAL	0	0.55	15.32	52.9	2.83	15.94	0.46	12.09	0	0.11	100.19
829 CHR MARGIN	0.06	0.44	15.09	52.19	3.24	18.68	0.41	10.11	0.05	0.11	100.37
830 CHR ADJ SMALL INST GRAIN	0.02	0.5	13.92	50.84	4.69	20.83	0.63	8.36	0.28	0.14	100.21
831 CHR GRAIN 3 LARGE, CENTRAL	0.01	0.43	15.03	52.12	4.33	15.30	0.35	12.37	0.07	0.14	100.14
832 CHR INT	0.02	0.41	15.12	52.68	3.95	15.38	0.45	12.28	0.16	0.11	100.57
833 CHR AT MARGIN	0.05	0.43	15.41	50.51	3.55	20.03	0.33	9.12	0.14	0.13	99.70
834 CHR ADJ INST	0.02	0.45	15.24	50.55	3.20	21.79	0.45	8.01	0.15	0.13	99.99
835 CHR GRAIN 4 REL LARGE CENTRAL	0.03	0.5	15.42	52.64	3.56	15.28	0.38	12.47	0.05	0.17	100.50
836 CHR INT	0.03	0.4	14.28	52.78	4.73	15.09	0.45	12.38	0	0.1	100.24
837 CHR AT MARGIN	0.09	0.44	15.19	51.27	3.74	20.25	0.42	9.06	0.13	0.04	100.63
838 CHR GRAIN 5 CENTRAL	0.01	0.43	15.26	52.25	4.17	15.92	0.42	12.03	0.13	0.15	100.78
839 CHR AT MARGIN	0.07	0.47	15.13	51.6	2.63	20.68	0.41	8.73	0.05	0.05	99.81
840 CHR GRAIN 6 CENTRAL, 12-31-3658	0.02	0.45	15.04	53	3.62	15.47	0.43	12.35	0	0.07	100.45
841 CHR AT MARGIN	0.04	0.53	15.14	51.46	3.43	19.72	0.42	9.52	0.03	0.16	100.45
842 CHR GRAIN 7 CENTRAL	0.02	0.38	15.28	52.91	3.53	15.89	0.37	12.09	0.09	0.06	100.62
843 CHR AT MARGIN	0.07	0.51	15	51.13	4.22	18.02	0.47	10.44	0	0.12	99.98
844 CHR * 2ND TIME GR 1 REG, CENTRAL, SPOT 1 12-	0	0.39	13.86	53.3	4.20	14.88	0.39	12.37	0.12	0.13	99.64
845 CHR NARROW MARGIN LIKELY MAGMATIC, SPOT 2	0	0.37	13.61	51.45	4.58	19.41	0.53	9.27	0.08	0.1	99.40
846 CHR ANOTHER GRAIN CENTRAL SPOT 3	0	0.39	14.08	53.52	4.38	15.45	0.4	12.3	0.01	0.1	100.63
847 CHR BRIGHT MARGIN SPOT 4	0	0.4	13.85	52.77	3.16	21.10	0.37	8.6	0	0.04	100.29
848 CHR ADJ INST SPOT 5	0	0.47	13.93	51.74	3.72	21.77	0.51	8.01	0.1	0.14	100.39
849 CHR GR 6 REGION CENTRAL SPOT 1, 12-21-3658	0	0.4	14.3	53.02	4.17	15.29	0.41	12.31	0	0.09	99.99
850 CHR SPOT 2	0	0.4	13.84	52.49	4.28	15.34	0.35	12.02	0.02	0.07	98.81
851 CHR AT MARGIN SPOT 3	0	0.31	12.42	50.54	5.53	21.44	0.59	7.6	0.11	0	98.54
852 CHR SMALLER ZONED GRAIN, CENTRAL, SPOT 3	0	0.41	14.13	52.33	3.73	17.11	0.42	10.9	0	0.15	99.18
853 CHR **** SAMPLE 486073 GRAIN 1 CENTRAL, 12-2	0.04	0.45	14.93	50.88	4.51	18.87	0.38	9.95	0.22	0.03	100.26
854 CHR AT MARGIN	0.09	0.52	16.21	49.19	4.02	21.18	0.49	8.52	0.04	0.09	100.35
855 CHR GRAIN 2 CENTRAL	0.04	0.48	15.23	48.75	5.38	22.18	0.55	7.82	0.2	0.01	100.64
856 CHR AT MARGIN	0.07	0.49	16.64	49.12	3.64	21.65	0.42	8.3	0.14	0.14	100.60
857 CHR GRAIN 3 CENTRAL, 12-22-3662	0.04	0.5	15.47	50.07	4.48	20.04	0.5	9.33	0.1	0.03	100.56
858 CHR AT MARGIN	0.06	0.53	16.25	49.08	3.78	21.63	0.49	8.3	0.06	0.04	100.22
859 CHR GRAIN 4 12-22-3663	0.28	0.51	15.83	50.17	4.58	18.99	0.55	9.45	0.04	0.08	100.49
860 CHR AT MARGIN	0.07	0.5	16.28	49.62	3.44	21.13	0.42	8.63	0.02	0.08	100.19
861 CHR GRAIN 5 CENTRAL	0	0.51	15.44	50.98	3.72	19.01	0.36	10.17	0.05	0.02	100.26
862 CHR AT MARGIN	0.02	0.55	16.02	49.7	3.97	20.88	0.44	8.99	0.09	0.03	100.70
863 CHR GRAIN 6 CENTRAL	0.03	0.59	15.89	49	4.94	18.54	0.41	10.38	0	0.04	99.82
864 CHR AT MARGIN	0.05	0.47	16.48	49.15	4.25	20.58	0.47	9.1	0.07	0.02	100.65
865 CHR F GRAINED INST	0.01	0.5	15.92	47.63	4.83	22.15	0.5	7.81	0.14	0.06	99.55
866 CHR ADJ REL C CENTRAL	0.02	0.56	16.16	49.7	4.39	18.57	0.36	10.45	0.1	0.12	100.43
867 CHR ADJ INST	0	0.48	15.95	48.79	4.39	22.54	0.45	7.75	0.25	0.11	100.71
868 CHR GRAIN 7 CENTRAL	0.02	0.45	15.69	49.99	4.69	18.95	0.48	10.04	0.13	0.07	100.51
869 CHR AT MARGIN	0	0.45	16.26	50.14	3.27	20.83	0.55	8.89	0.18	0.05	100.62

Black Thor BT-08-10

	SiO2	TiO2	Al2O3	Cr2O3	Fe2O3	FeO	MnO	MgO	ZnO	NiO	TOTAL
870 CHR ANOTHER CENTRAL	0.06	0.5	15.76	48.61	4.25	22.08	0.7	7.66	0.09	0.09	99.80
871 CHR SMALL GRAIN	0.02	0.52	15.86	49.89	3.13	23.18	0.41	7.49	0.05	0.02	100.56
872 CHR * 2ND TIME CENTRAL, SPOT 1, 12-22-3660	0	0.47	15.24	51.12	4.13	19.33	0.31	9.98	0.14	0.05	100.77
873 CHR AT MARGIN SPOT 2	0	0.45	15.44	49.06	4.35	22.28	0.51	7.75	0.19	0.06	100.09
874 CHR GRAIN 4 DARK CENTRAL, SPOT 1, 12-22-3663	0	0.44	15.46	50.6	4.15	18.58	0.46	10.29	0	0.08	100.07
875 CHR AT MARGIN SPOT 2	0	0.44	15.41	49.74	4.23	22.11	0.47	8.09	0	0.06	100.55
876 CHR **** SAMPLE 486074 GRAIN 1 CENTRAL, 12-2	0	0.64	16.04	47.72	5.36	20.29	0.61	9.12	0.18	0.1	100.06
877 CHR AT MARGIN	0.06	0.71	14.85	47.64	5.97	22.38	0.44	7.63	0.25	0.01	99.94
878 CHR GRAIN 2 CENTRAL	0.08	0.74	15.64	47.53	6.02	21.58	0.43	8.33	0.17	0.13	100.65
879 CHR AT MARGIN	0.08	0.73	14.87	47.91	5.56	22.39	0.47	7.6	0.04	0.11	99.77
880 CHR GRAIN 3	0.06	0.79	15.32	48.19	5.29	20.80	0.54	8.78	0.06	0.04	99.87
881 CHR AT MARGIN	0.09	0.73	14.86	48.11	6.26	21.37	0.47	8.23	0.22	0.21	100.55
882 CHR GRAIN 4	0.04	0.8	15.98	47.5	5.66	20.83	0.45	8.93	0.25	0.09	100.53
883 CHR AT MARGIN	0.02	0.74	14.8	48.33	5.70	22.62	0.6	7.76	0.01	0.01	100.59
884 CHR SMALL	0.07	0.76	14.28	49.24	5.39	23.17	0.44	7.39	0	0	100.74
885 CHR GRAIN 5 CENTRAL	0.04	0.71	15.16	48.6	5.45	21.83	0.41	8.31	0.14	0.01	100.67
886 CHR AT MARGIN	0.07	0.67	14.95	48.46	5.69	22.13	0.53	7.89	0.05	0.1	100.54
887 CHR GRAIN 6	0.02	0.8	16.17	47.99	4.99	20.57	0.57	9.14	0.21	0.04	100.50
888 CHR AT MARGIN	0.07	0.73	14.98	49	5.26	22.47	0.52	7.83	0.07	0.05	100.98
889 CHR GRAIN 7 CENTRAL	0.05	0.58	14.56	49.65	5.64	20.67	0.53	8.8	0.09	0.1	100.66
890 CHR AT MARGIN	0.06	0.7	14.93	48.98	5.10	22.37	0.45	7.74	0.18	0.16	100.67
891 CHR SMALL GRAIN	0.03	0.59	15.26	48.98	4.81	22.09	0.54	7.98	0.08	0.06	100.42
892 CHR **** SAMPLE 486075 GRAIN 1, CENTRAL, 12-	0.03	0.52	15.28	48.97	5.33	21.62	0.54	8.31	0.08	0.06	100.73
893 CHR AT MARGIN	0	0.5	15.43	48.65	4.89	21.82	0.45	8.1	0.19	0.09	100.12
894 CHR AT MARGIN	0	0.58	15.85	49.08	4.29	21.52	0.43	8.49	0.22	0.06	100.52
895 CHR GRAIN 2 CENTRAL	0	0.59	15.66	49.2	4.38	21.51	0.47	8.5	0.14	0.07	100.52
896 CHR AT MARGIN	0	0.56	16.34	48.24	4.27	22.29	0.49	8.06	0	0.1	100.35
897 CHR GRAIN 3 CENTRAL	0	0.63	15.31	50.39	3.73	21.42	0.42	8.68	0	0.1	100.68
898 CHR ADJ INST	0	0.54	15.45	48.58	5.14	22.08	0.6	7.91	0.19	0.18	100.67
899 CHR GRAIN 4 CENTRAL	0	0.49	15.41	49.64	3.99	20.96	0.5	8.62	0.03	0.14	99.78
900 CHR AT MARGIN	0	0.53	16.12	48.23	4.76	22.01	0.44	8.14	0.18	0.13	100.55
901 CHR ADJ SMALLER	0	0.51	16.14	49.09	3.36	22.37	0.55	7.84	0.07	0.04	99.98
902 CHR GRAIN 5 CENTRAL	0	0.52	15.6	49.97	3.89	21.21	0.47	8.73	0.01	0.05	100.45
903 CHR AT MARGIN	0	0.6	15.97	47.88	4.76	21.78	0.56	8.21	0.01	0.12	99.89
904 CHR GRAIN 6 CENTRAL	0	0.45	15.79	48.88	4.95	21.60	0.51	8.45	0	0.09	100.72
905 CHR AT MARGIN	0	0.62	16.27	48.68	3.78	22.10	0.47	8.18	0.11	0.04	100.25
906 CHR ADJ SMALL GRAIN	0	0.52	15.65	49.27	3.95	22.44	0.55	7.84	0.02	0.04	100.29
907 CHR **** SAMPLE 486076 GRAIN 1 CENTRAL, 12-2	0	0.56	15.82	49.71	3.16	20.95	0.41	8.65	0.17	0.15	99.58
908 CHR AT MARGIN	0	0.5	17.07	47.07	4.71	21.75	0.45	8.37	0.08	0.1	100.10
909 CHR ADJ SMALL	0.03	0.52	14.99	47.53	7.07	22.31	0.5	7.86	0.12	0.07	101.01
910 CHR GRAIN 2 CENTRAL	0	0.56	16.14	48.89	4.43	21.53	0.55	8.56	0.07	0.08	100.81
911 CHR AT MARGIN	0	0.52	16.23	47.96	4.48	21.98	0.5	8.02	0.2	0.1	99.99
912 CHR GRAIN 3 CENTRAL	0	0.59	15.88	49.13	4.09	21.43	0.41	8.59	0.06	0.11	100.29
913 CHR AT MARGIN	0	0.53	15.4	48.69	4.92	22.22	0.55	7.85	0.15	0.13	100.44
914 CHR GRAIN 4 CENTRAL	0	0.55	16.12	49	4.09	21.47	0.46	8.62	0.02	0.03	100.36
915 CHR AT MARGIN	0	0.56	15.41	48.5	5.30	21.67	0.49	8.27	0.14	0.15	100.49
916 CHR INST	0	0.49	16	48.36	4.56	22.67	0.48	7.75	0	0.1	100.41
917 CHR GRAIN 5 CENTRAL	0	0.5	15.26	48.3	5.09	21.34	0.49	8.36	0.04	0	99.38
918 CHR AT MARGIN	0	0.55	15.8	48.84	4.52	21.87	0.44	8.27	0.21	0	100.50
919 CHR GRAIN 6 CENTRAL	0	0.53	15.73	49.7	3.46	21.25	0.52	8.46	0.1	0.15	99.90
920 CHR AT MARGIN	0	0.54	15.9	48.88	4.15	22.33	0.47	7.96	0.07	0.09	100.40
921 CHR GRAIN 7 CENTRAL	0	0.43	16.2	49.38	3.72	20.57	0.51	8.89	0.17	0.12	99.99
922 CHR AT MARGIN	0	0.54	16.16	47.03	5.53	21.73	0.52	8.23	0.03	0.13	99.90
923 CHR **** SAMPLE 486080 L CENTRAL, SPOT 1, 12	0	0.69	17.24	46.9	4.27	22.83	0.42	7.85	0.12	0.13	100.45
924 CHR AT MARGIN SPOT 2	0	0.82	16.67	46.24	5.05	22.25	0.47	8.13	0.08	0.06	99.78
925 CHR ANOTHER SPOT 3	0	0.63	16.7	46.28	5.25	23.00	0.51	7.5	0.22	0.06	100.15
926 CHR V SMALL SPOT 4	0	0.68	16.2	47.52	4.67	22.60	0.45	7.85	0.17	0	100.14
927 CHR SMALL SPOT 5	0	0.66	16.71	47.68	4.23	22.53	0.46	8.01	0.15	0	100.42
928 CHR REL LARGE CENTRAL, SPOT 6	0.04	0.67	15.97	48	4.17	23.31	0.47	7.19	0.07	0.17	100.06
929 CHR AT MARGIN SPOT 7	0	0.66	16.75	46.48	5.22	22.29	0.47	7.99	0.15	0.17	100.18
930 CHR SMALL CENTRAL, SPOT 9	0	0.69	16.77	48.04	3.52	22.22	0.42	8.1	0.24	0.05	100.05
931 CHR SMALL CENTRAL, SPOT 9	0	0.53	16.6	46.96	5.13	22.49	0.46	7.89	0.1	0.05	100.21
932 CHR CENTRAL, SPOT 10	0	0.69	16.38	47.14	5.14	22.43	0.52	7.97	0.19	0.05	100.52
933 CHR BRIGHT MARGIN SPOT 11	0.07	1.06	1.86	43.63	22.67	27.33	0.6	3.05	0.11	0.24	100.62
934 CHR **** SAMPLE 486081 CENTRAL SPOT 1, 12-25	0	0.88	14.05	46.2	7.15	22.79	0.51	7.23	0.3	0.08	99.20
935 CHR AGAIN	0	0.86	14.39	46.56	7.14	23.08	0.58	7.3	0.17	0.08	100.17
936 CHR BRIGHT MARGIN SPOT 2	0	1.3	1.33	31.98	34.08	28.91	0.46	2.16	0.28	0.26	100.76
937 CHR CENTRAL SPOT 3	0.06	0.9	14.45	46.51	6.28	22.63	0.54	7.33	0.09	0	98.79
938 CHR SPOT 3 AGAIN	0.03	0.88	14.93	45.76	7.00	23.03	0.41	7.38	0.08	0.07	99.57
939 CHR AT MARGIN SPOT 4	0	1.23	0.75	40.48	26.98	28.28	0.61	2.62	0.26	0.23	101.44
940 CHR SPOT 5	0	1.35	0.42	40.37	26.26	28.29	0.53	2.38	0.34	0.26	100.20
941 CHR L CENTRAL S 1, 12-26-3725	0	1.16	15.51	46.72	4.82	23.16	0.41	7.54	0.15	0.12	99.59
942 CHR AT MARGIN NEAR RIND	0	0.83	14.37	46.83	6.60	23.43	0.46	7.09	0.11	0.09	99.81
943 CHR **** SAMPLE 486082 LARGE CENTRAL, SPOT 1	0	0.61	16.58	45.49	5.59	23.74	0.43	6.94	0.19	0.09	99.66
944 CHR AT MARGIN SPOT 2	0	0.81	15.23	47.06	5.90	23.27	0.43	7.44	0.11	0.02	100.27
945 CHR ANOTHER SPOT 3	0	0.77	15	46.16	7.15	23.64	0.49	6.96	0.23	0.25	100.66
946 CHR ANOTHER SPOT 4	0	0.84	14.38	45.83	7.20	23.18	0.51	7.05	0.19	0.12	99.30
947 CHR ANOTHER SPOT 4	0	0.81	14.45	46.7	6.99	23.73	0.41	7	0.23	0.03	100.35
948 CHR AT MAREGIN SPOT 5	0.15	1.1	1.11	43.06	24.75	27.48	0.61	2.77	0.32	0.23	101.58

Black Thor BT-08-10

	SiO2	TiO2	Al2O3	Cr2O3	Fe2O3	FeO	MnO	MgO	ZnO	NiO	TOTAL
949 CHR ANOTHER CENTRAL, SPOT 6	0	0.78	14.66	46.92	6.46	23.77	0.49	6.94	0.17	0.03	100.22
950 CHR AT MARGIN SPOT 7	0.1	1.25	0.73	44.6	22.28	27.65	0.71	2.55	0.26	0.25	100.38
951 CHR AT MARGIN SPOT 7	0.06	1.33	1.12	43.76	21.28	28.02	0.42	2.52	0.11	0.13	98.75
952 CHR AT MARGIN SPOT 7	0	0.76	14.43	47.72	6.58	23.69	0.52	7.04	0.25	0.07	101.06
953 CHR AT MARGIN SPOT 7	0.01	1.18	0.6	41.78	24.66	28.01	0.7	2.39	0.2	0.2	99.73
954 CHR ANOTHER SPOT 8	0	1	15.44	45.56	6.37	22.80	0.4	7.51	0.41	0.13	99.62
955 CHR ANOTHER SPOT 8	0	0.97	15.61	45.91	6.13	23.00	0.57	7.55	0.08	0.1	99.92
956 CHR ANOTHER SPOY 9	0	0.9	15.21	46.28	6.05	23.38	0.56	7.13	0.14	0.16	99.81
957 CHR ANOTHER SPOT 10	0.04	0.89	14.6	47.31	5.90	23.87	0.59	6.7	0.27	0.07	100.24
958 CHR **** SAMPLE 486092 GRAIN 1, 12-20-3612	0	0.45	13.72	51.77	4.57	19.77	0.47	9.35	0	0.09	100.19
959 CHR AT MARGIN	0	0.39	14.09	51.88	3.95	19.91	0.45	9.19	0.06	0.13	100.06
960 CHR GRAIN 2 CENTRAL	0	0.38	14.58	52.05	4.38	16.65	0.43	11.39	0.09	0.07	100.02
961 CHR AT MARGIN	0.03	0.39	13.78	51.36	5.74	17.96	0.43	10.42	0.08	0.09	100.27
962 CHR ADJ SMALL	0	0.38	13.91	51.82	3.89	20.65	0.43	8.65	0.15	0.1	99.98
963 CHR GRAIN 3 CENTRAL	0	0.37	14.31	52.64	3.98	17.37	0.5	10.86	0.06	0.14	100.23
964 CHR AT MARGIN	0	0.49	13.59	52.81	3.29	21.09	0.53	8.45	0.09	0.14	100.48
965 CHR AT MARGIN	0	0.41	13.87	53.52	3.45	17.08	0.37	11.09	0.03	0.12	99.94
966 CHR GRAIN 4 CENTRAL	0	0.43	14.33	52.28	3.98	18.80	0.41	10.12	0.05	0.08	100.43
967 CHR AT MARGIN	0	0.45	13.48	51.77	4.33	21.19	0.54	8.37	0.06	0.02	100.20
968 CHR GRAIN 4 CENTRAL REGION AGAIN	0	0.39	14.4	52.09	4.16	18.36	0.34	10.39	0.06	0.07	100.26
969 CHR GRAIN 4 AT MARGIN AGAIN	0	0.41	13.5	51.83	4.35	20.84	0.42	8.55	0.11	0.11	100.12
970 CHR GRAIN 5 CENTRAL	0	0.37	13.78	51.96	4.17	20.90	0.38	8.59	0.12	0.11	100.39
971 CHR BRIGHT AT MARGIN	0	0.47	10.43	52	6.98	22.53	0.51	7.15	0.08	0.06	100.21
972 CHR GRAIN 6 CENTRAL	0	0.39	14.4	51.91	3.87	20.34	0.43	9.11	0.09	0.03	100.58
973 CHR AT MARGIN	0	0.41	14.11	51.95	4.20	19.53	0.38	9.55	0.03	0.16	100.32
974 CHR INST SMALLER	0	0.43	13.7	51.87	3.75	20.99	0.39	8.49	0.04	0.08	99.75
975 CHR GRAIN 8 CENTRAL, SPOT 1, 12-20-3612	0	0.37	14.52	52.67	4.47	16.83	0.38	11.38	0.11	0.21	100.94
976 CHR AT MARGIN, SPOT 2	0	0.42	13.81	51.93	4.14	20.64	0.52	8.77	0.04	0.06	100.33
977 CHR AT MARGIN AGAIN, SPOT 3	0	0.42	13.85	52.29	3.87	20.56	0.5	8.79	0.19	0.07	100.55
978 CHR SPOT 4 SMALLER GRAIN, 12-20-3612	0	0.39	13.44	52.6	4.10	20.51	0.45	8.84	0.12	0.05	100.50
979 CHR * AGAIN SAMPLE 92 FOR SURE SPOT 1 AS CHE	0	0.41	14.17	53.21	3.85	16.91	0.38	11.33	0.03	0.09	100.39
980 CHR AGAIN	0	0.4	14.27	52.16	4.66	16.81	0.31	11.33	0.12	0.1	100.17
981 CHR GRAIN BOTTOM RIGHT CENTRAL SPOT 5	0	0.45	14.17	53.22	4.13	17.03	0.25	11.48	0.01	0.05	100.79
982 CHR AT MARGIN	0	0.42	13.43	51.98	4.86	20.08	0.47	9.08	0.21	0.05	100.58
983 CHR **** SAMPLE 486093 L GRAIN CENTRAL, SPOT	0	0.53	14.29	50.06	4.75	23.46	0.53	7.06	0.11	0.15	100.95
984 CHR AT MARGIN SPOT 2	0	0.53	14.15	50.14	4.99	22.30	0.36	7.91	0.04	0.07	100.49
985 CHR GRAIN 2 CENTRAL	0	0.66	13.98	48.74	6.20	24.03	0.48	6.74	0.21	0.15	101.19
986 CHR GRAIN 2 CENTRAL	0	0.67	14.32	47.95	6.43	23.92	0.42	6.89	0.17	0.08	100.84
987 CHR GRAIN MARGIN	0	0.65	14.1	48.37	6.53	22.40	0.51	7.69	0.15	0.15	100.55
988 CHR SMALL GRAIN	0	0.52	13.42	49.81	6.25	22.22	0.46	7.75	0.18	0.09	100.71
989 CHR ADJACENT GRAIN	0	0.7	13.92	49.03	6.07	23.06	0.59	7.3	0.18	0.15	101.00
990 CHR ANOTHER GRAIN CENTRAL	0	0.67	14.11	48.42	6.00	23.60	0.49	6.94	0.21	0.09	100.53
991 CHR AT MARGIN	0	0.66	13.16	50.28	5.92	22.65	0.47	7.58	0.17	0.11	101.00
992 CHR ANOTHER GRAIN CENTRAL	0	0.65	14.37	48.52	5.70	23.97	0.38	6.79	0.21	0.16	100.75
993 CHR * AGAIN 93 GRAIN 1 CENTRAL, SPOT 1, 12-	0	0.5	14.07	49.24	5.93	22.84	0.45	7.39	0.21	0.11	100.73
994 CHR SPOT 2 AT MARGIN	0	0.48	14.33	50.15	4.95	21.66	0.47	8.22	0.07	0.04	100.38
995 CHR **** SAMPLE 486094 GRAIN 1 CENTRAL 12-20	0	0.43	14.56	53.08	3.21	17.31	0.32	11.12	0.06	0.06	100.15
996 CHR BRIGHT MARGIN SPOT 2	0	0.38	13.42	52.83	3.05	20.45	0.48	8.61	0.09	0.13	99.44
997 CHR GRAIN 2 DARK CENTRAL SPOT 3	0	0.49	14.33	51.74	4.54	17.18	0.33	11.1	0.06	0.13	99.89
998 CHR BRIGHTER MARGIN SPOT 4	0	0.32	13.37	53.43	3.68	20.37	0.48	8.87	0.16	0.1	100.78
999 CHR INST SPOT 5	0	0.45	13.45	52.82	3.87	20.10	0.49	9.12	0.02	0.13	100.45
1000 CHR INST SPOT 5	0	0.51	13.5	52.84	3.57	20.44	0.4	9.03	0.06	0.02	100.37
1001 CHR INST SPOT 5	0	0.42	13.51	51.97	4.20	19.80	0.49	9.15	0	0.13	99.67
1002 CHR INST SPOT 5	0	0.42	13.63	51.33	4.62	19.87	0.4	9.17	0.05	0.04	99.53
1003 CHR GRAIN 3 LARGE DARK CENTRAL SPOT 12 20 36	0	0.37	13.18	54.93	2.98	17.47	0.3	10.82	0.06	0.15	100.26
1004 CHR GRAIN 3 BRIGHT MAREGIN SPOT 2	0	0.41	13.51	51.85	4.00	20.44	0.55	8.6	0.13	0.13	99.62
1005 CHR CENTRAL AGAIN	0	0.42	13.76	54.48	3.38	16.38	0.37	11.71	0	0.1	100.60
1006 CHR GRAIN 4 INTERSTIAL SMALL	0	0.4	13.48	52.01	4.72	20.54	0.51	8.77	0.15	0.11	100.68
1007 CHR GRAIN 1 CENTRAL, 12-30-3618	0	0.4	13.93	53.76	3.75	16.65	0.47	11.42	0.04	0.12	100.54
1008 CHR GRAIN 1 CENTRAL, 12-30-3618	0	0.37	13.55	52.95	3.77	19.67	0.51	9.28	0.07	0.15	100.32
1009 CHR BRIGHT MARGIN SPOT 5	0	0.4	9.72	53.63	6.55	22.58	0.49	7	0.21	0.13	100.71
1010 CHR ANOTHER GRAIN CENTRAL, SPOT 6	0	0.37	14.02	53.28	3.09	20.13	0.58	9.14	0.12	0.01	100.74
1011 CHR BRIGHT DOM AT MARGIN INCL MG-CHL, SPOT 7	0	0.42	8.92	54.13	6.10	23.31	0.54	6.35	0.13	0.09	99.99
1012 CHR BRIGHT AT OPP MARGIN SPOT 8	0	0.45	5.32	57.44	6.82	24.95	0.62	5.03	0.18	0.08	100.88
1013 CHR GRAIN 3 CENTRAL AS CHECK SPOT 1	0	0.47	13.78	53.41	2.87	18.63	0.31	10.12	0.01	0.11	99.71
1014 CHR CENTRAL SPOT 4	0	0.42	14.06	53.5	3.36	17.94	0.38	10.65	0.08	0.09	100.48
1015 CHR AT MARGIN SPOT 5	0	0.43	13.54	53.28	2.99	21.04	0.39	8.58	0.01	0.11	100.37
1016 CHR ORIG GRAIN SPOT 2A	0	0.54	7.37	53.65	8.24	22.62	0.59	6.59	0.14	0.15	99.90
1017 CHR BRIGHT IN INST, SPOT 6	0.01	0.64	5.19	56.2	8.30	24.14	0.64	5.63	0.2	0.06	101.01
1018 CHR SPOT 7	0	0.54	6.45	56.03	7.03	24.21	0.55	5.74	0.11	0.07	100.73
1019 CHR INCL MG-PHLOG, SPT 8	0	0.55	4.57	55.58	9.06	24.92	0.51	5	0.18	0.05	100.42
1020 CHR **** SAMPLE 486101 LARGE GRAIN CENTRAL,	0	0.45	14.55	51.35	4.86	18.84	0.39	10.1	0.19	0.12	100.85
1021 CHR NEAR MARGIN SPOT 2	0	0.5	14.63	50.77	4.86	18.49	0.38	10.28	0.13	0.08	100.12
1022 CHR ANOTHER GRAIN CENTRAL, SPOT 3	0	0.51	14.65	50.64	5.28	18.12	0.38	10.53	0.17	0.13	100.41
1023 CHR INCL DOL, MG-CHL, SPOT 4	0	0.35	9.83	56.64	3.65	19.76	0.49	8.67	0.14	0.14	99.67
1024 CHR SPOT 5	0.05	0.32	8.78	58.2	3.23	20.35	0.33	8.23	0.05	0.09	99.63
1025 CHR BRIGHT MARGIN, SPOT 7	0	0.22	7.33	58.41	4.39	20.74	0.55	7.66	0.11	0.1	99.51
1026 CHR **** SAMPLE 486102 L GRAIN CENTRAL, SPOT	0.01	0.37	14.24	53.45	3.75	16.15	0.28	11.79	0.01	0.15	100.21
1027 CHR AT MARGIN SPOT 2	0	0.42	14.2	53.32	3.64	17.19	0.44	11.12	0.11	0.05	100.48

Black Thor BT-08-10

	SiO2	TiO2	Al2O3	Cr2O3	Fe2O3	FeO	MnO	MgO	ZnO	NiO	TOTAL
1028 CHR SMALLER SPOT 3	0	0.38	14.38	53.45	3.10	17.69	0.33	10.78	0.14	0.11	100.36
1029 CHR INT SIZE, DARK CENTRAL, SPOT 5	0	0.36	14.42	52.2	4.44	16.08	0.46	11.65	0.14	0.04	99.79
1030 CHR AT MARGIN SPOT 6	0.04	0.36	14.24	52.8	3.85	17.57	0.33	10.77	0.01	0.07	100.04
1031 CHR **** SAMPLE 486103 LARGE CENTRAL, SPOT 1	0	0.39	14.37	53.94	2.87	16.56	0.27	11.56	0.1	0.09	100.15
1032 CHR LARGE CENTRAL, SPOT 1, 12-24-3699	0	0.43	14.02	53.42	3.33	16.06	0.3	11.64	0.15	0.16	99.51
1033 CHR AT MARGIN NO RIND SPOT 2	0	0.33	13.91	52.76	4.03	17.18	0.37	10.93	0.04	0.08	99.62
1034 CHR ASSOC W RETRO, SPOT 3	0	0.42	14.02	53.3	3.54	17.18	0.31	11.1	0.07	0.08	100.02
1035 CHR ADJ LARGER, DARK CENTRAL, SPOT 4	0	0.46	13.54	53.88	3.42	16.93	0.31	11.22	0	0.13	99.89
1036 CHR AT MARGIN NO RIND SPOT 5	0	0.4	14.11	52.98	3.51	17.38	0.37	10.84	0.15	0.08	99.82
1037 CHR SMALL BRIGHT DOMAIN, SPOT 5	0.07	0.25	9.53	59.01	2.74	18.64	0.61	9.29	0.08	0.07	100.29
1038 CHR REL C CENTRAL, SPOT 7	0	0.38	14.33	52.66	3.46	16.66	0.32	11.27	0.02	0.14	99.25
1039 CHR AT MARGIN SPOT 8	0	0.39	14.24	53.56	3.25	18.14	0.34	10.58	0.09	0.09	100.69
1040 CHR BRIGHT SPOT 9	0	0.33	7.53	60.05	3.57	20.04	0.43	8.55	0.1	0.09	100.69
1041 CHR SMALLER GRAIN SPOT 9	0	0.38	14.32	53.24	3.45	16.94	0.41	11.22	0	0.14	100.10
1042 CHR SMALLER SPOT 10	0	0.39	14.24	53.75	3.23	17.11	0.39	11.17	0.07	0.12	100.47
1043 CHR V SMALL SPOT 11	0	0.45	14.65	52.93	3.64	17.34	0.46	11.09	0.1	0.13	100.79
1044 CHR REL L CENTRAL, SPOT 1, 12-24-3701	0	0.36	14.22	53.12	3.88	17.18	0.35	11.11	0.08	0.12	100.42
1045 CHR AT MARGIN NO RIND SPOT 2	0	0.39	14.19	53.45	3.23	17.97	0.4	10.58	0.12	0.08	100.41
1046 CHR SMALLER SPOT 4	0	0.39	14.41	52.46	3.44	17.76	0.42	10.61	0.07	0.04	99.59
1047 CHR SMALL SPOT 3	0	0.42	14.36	52.58	3.05	17.98	0.31	10.54	0.02	0	99.26
1048 CHR **** SAMPLE 486107 LARGE GRAIN, CENTRAL,	0	0.41	14.41	53.38	3.30	17.29	0.37	11.11	0.06	0.09	100.42
1049 CHR AT MARGIN SPOT 2	0	0.4	14.34	52.14	4.24	18.71	0.47	10.16	0	0.08	100.54
1050 CHR SMALLER, CENTRAL, SPOT 3	0	0.44	14.53	52.37	4.29	17.59	0.44	10.92	0.1	0.13	100.81
1051 CHR AT MARGIN SPOT 4	0	0.49	14.24	53.12	3.06	19.18	0.4	9.91	0	0.16	100.56
1052 CHR SMALLER SPOT 5	0	0.43	14.58	51.25	4.09	18.34	0.39	10.17	0.14	0.13	99.52
1053 CHR SMALLEST SPOT 6	0	0.42	14.32	51.62	4.29	19.06	0.46	9.85	0.11	0	100.13
1054 CHR LARGE GRAIN CENTRAL, SPOT 1, 12-23-3691	0	0.41	13.65	53.37	4.09	17.79	0.36	10.65	0.15	0.16	100.63
1055 CHR AT MARGIN	0	0.38	14	53.01	3.68	18.72	0.31	10.15	0	0.14	100.39
1056 CHR SMALLEST 3	0	0.36	13.74	52.29	4.24	19.48	0.44	9.53	0.03	0.01	100.12
1057 CHR REL C CENTRAL, SPOT 4	0	0.44	14.23	52.45	3.65	18.21	0.35	10.41	0.07	0.07	99.89
1058 CHR SMALL SPOT 5	0	0.46	14.15	52.57	3.82	19.25	0.47	9.84	0	0.1	100.66
1059 CHR **** SAMPLE 486108 GRAIN 1 DARK CENTRAL,	0	0.46	14.34	52.82	3.81	17.28	0.44	11.03	0.11	0.13	100.42
1060 CHR AT MARGIN NO RIND SPOT 2	0	0.34	14.21	52.59	3.22	19.12	0.48	9.65	0.03	0.1	99.74
1061 CHR OPP MARGIN SPOT 3	0	0.43	14.3	52.08	3.61	19.31	0.46	9.6	0.06	0.16	100.01
1062 CHR GRAIN 2 REL DARK CENTRAL	0	0.37	14.54	53.7	3.34	17.16	0.36	11.31	0.03	0.09	100.89
1063 CHR GRAIN 2 REL DARK CENTRAL	0	0.41	14.57	53.04	2.89	17.49	0.3	10.9	0.02	0.14	99.76
1064 CHR SPOT 5	0	0.47	13.86	53.62	2.16	19.52	0.46	9.39	0.06	0.16	99.70
1065 CHR REL BRIGHT AT MARGIN, SPOT 6	0	0.41	14.05	52.24	3.22	19.27	0.55	9.38	0.14	0.11	99.37
1066 CHR SMALL INST SPOT 7	0	0.37	14.38	52.66	3.17	19.66	0.38	9.43	0.12	0.16	100.34
1067 CHR SMALL SPOT 8	0	0.44	14.36	51.86	3.41	18.54	0.49	9.94	0.09	0.13	99.26
1068 CHR INST SPOT 9	0	0.41	14.01	51.52	4.79	19.13	0.51	9.74	0.13	0	100.21
1069 CHR GRAIN 8 CENTRAL, SPOT 1, 3680	0	0.39	14.2	53.94	3.40	16.44	0.42	11.61	0.02	0.16	100.58
1070 CHR REL BRIGHT MARGIN, SPOT 2	0	0.36	14.05	52.93	3.42	19.18	0.32	9.72	0.16	0.14	100.28
1071 CHR GRAIN 9 CENTRAL SPOT 3	0	0.41	14.57	54.49	2.05	16.62	0.35	11.53	0.04	0.12	100.19
1072 CHR AT MARGIN SPOT 2	0	0.35	14.02	51.91	4.54	18.03	0.46	10.31	0.06	0.17	99.84
1073 CHR INST GRAIN SPOT 3	0	0.39	14.19	53.12	3.38	19.27	0.4	9.77	0.11	0.15	100.78
1074 CHR SPOT 4	0	0.47	14.17	51.77	3.96	19.20	0.42	9.71	0.07	0.09	99.87
1075 CHR SMALL INST SPOT 5	0	0.38	14.13	53.16	2.62	19.83	0.45	9.24	0.12	0.09	100.02
1076 CHR SPOT 5	0	0.41	14.23	52.55	3.21	19.81	0.51	9.34	0.03	0.05	100.14
1077 CHR GRAIN 1 CENTRAL, SPOT 1, 12-23-3685	0.02	0.4	14.66	53.13	4.06	16.19	0.44	11.83	0.08	0.1	100.92
1078 CHR SPOT 2 AT MARGIN	0.01	0.44	14.92	51.93	3.94	18.50	0.32	10.46	0	0.11	100.62
1079 CHR ANOTHER REL C GRAIN, CENTRAL, SPOT 1	0	0.4	14.47	52.91	3.68	16.59	0.4	11.5	0.01	0.08	100.04
1080 CHR AT MARGIN SPOT 2	0	0.41	14.05	52.39	4.02	17.59	0.61	10.54	0.13	0.1	99.84
1081 CHR SMALLER INST SPOT 3	0	0.49	14.26	53.13	2.95	18.46	0.45	10.23	0.05	0.18	100.19
1082 CHR SMALL INST SPOT 4	0	0.45	14.09	52.73	3.61	18.79	0.5	10.02	0.04	0.09	100.32
1083 CHR SMALL INST SPOT 5	0.01	0.45	14.35	53.12	2.74	19.09	0.41	9.91	0	0.05	100.12
1084 CHR **** SAMPLE 486109 LARGE GRAIN CENTRAL,	0	0.45	14.35	53.25	3.48	16.30	0.29	11.74	0.03	0.11	100.00
1085 CHR AT MARGIN SPOT 2	0	0.45	14.48	51.77	4.03	17.83	0.28	10.6	0.12	0.19	99.75
1086 CHR GRAIN 2 SPOT 3	0	0.4	14.76	52.8	3.84	16.61	0.41	11.59	0	0.12	100.53
1087 CHR AT MARGIN SPOT 4	0	0.44	14.83	52.15	2.91	19.07	0.35	9.87	0.06	0.13	99.81
1088 CHR SMALLER GRAIN CENTRAL, SPOT 3	0	0.37	14.36	51.12	5.46	17.56	0.47	10.79	0	0.14	100.27
1089 CHR SPOT 1 AGAIN	0	0.44	14.35	54.03	3.02	16.62	0.3	11.63	0	0.15	100.54
1090 CHR SPOT 4	0	0.34	14.18	53.11	3.55	18.39	0.44	10.25	0.11	0.1	100.48
1091 CHR AT MARGIN SPOT 4	0	0.38	14.14	53.22	3.50	17.91	0.3	10.64	0.02	0.18	100.19
1092 CHR SMALLER GRAIN SPOT 5	0.02	0.43	14.45	52.03	4.13	18.61	0.36	10.14	0.12	0.16	100.45
1093 CHR SMALLER GRAIN 6	0	0.43	14.34	52.34	3.92	18.69	0.42	10.15	0.07	0.12	100.48
1094 CHR GRAIN 8	0	0.38	14.01	52.28	3.82	19.38	0.44	9.58	0.02	0.07	99.97
1095 CHR VERY SMALL SPOT 9	0	0.4	14.33	52.55	3.69	19.24	0.52	9.78	0	0.12	100.63
1096 CHR LARGE GRAIN CENTRAL, SPOT 1, 12-23-3687	0	0.42	14.12	53.22	3.52	16.93	0.4	11.19	0.09	0.08	99.97
1097 CHR AT MARGIN NO RIND	0	0.44	14.05	52.39	4.07	18.83	0.57	9.91	0.08	0.15	100.49
1098 CHR REL BRIGHT NEAR LINEAR, SPOT 3	0	0.44	13.54	52.23	4.16	19.05	0.45	9.61	0.2	0.08	99.77
1099 CHR SMALLER, DARK CENTRAL, SPOT 4	0	0.37	14.05	53.47	4.05	17.12	0.35	11.22	0.08	0.12	100.83
1100 CHR AT MARGIN SPOT 5	0	0.44	14.56	52.86	2.66	19.18	0.37	9.83	0.06	0.11	100.07
1101 CHR SMALLER GRAIN SPOT 6	0	0.43	14.63	52.72	3.40	18.15	0.42	10.54	0.02	0.15	100.46
1102 CHR SMALLER SPOT 7	0	0.42	14.21	52.31	3.47	19.28	0.51	9.64	0.04	0.04	99.92
1103 CHR SMALLEST SPOT 8	0	0.4	13.82	52.92	3.71	19.25	0.4	9.68	0.16	0.09	100.43
1104 CHR ADJ BRIGHT GRAIN	0	0.45	7.66	61.16	1.51	21.36	0.54	7.71	0.14	0.02	100.55
1105 CHR **** SAMPLE 486128 LARGE CENTRAL, SPOT 1	0	0.46	14	51.99	3.31	21.43	0.36	8.27	0.2	0.04	100.06
1106 CHR AT MARGIN SPOT 2	0	0.39	14.2	51.32	3.85	21.27	0.44	8.33	0.11	0.04	99.95

Black Thor BT-08-10

	SiO2	TiO2	Al2O3	Cr2O3	Fe2O3	FeO	MnO	MgO	ZnO	NiO	TOTAL
1107 CHR ANOTHER CENTRAL, SPOT 3	0	0.45	14.08	51.14	4.06	21.68	0.42	8.1	0.11	0.09	100.13
1108 CHR AT MARGIN NO RIND SPOT 4	0	0.39	14.17	52.21	2.63	21.39	0.5	8.12	0.12	0.07	99.60
1109 CHR SMALLER SPOT 5	0	0.46	14.52	50.71	3.96	21.46	0.49	8.23	0.05	0.15	100.03
1110 CHR AT MARGIN SPOT 6	0	0.46	14.28	51.4	3.17	21.33	0.5	8.14	0.22	0.08	99.58
1111 CHR SMALLER SPOT 7	0	0.49	14.37	51.87	3.03	21.71	0.41	8.15	0.18	0.08	100.29
1112 CHR SMALL BRIGHT SPOT 8	0	0.18	9.26	58.87	1.24	22.35	0.56	6.78	0.1	0.15	99.49
1113 CHR SMALLER SPOT 9	0	0.5	14.23	51.19	4.01	21.24	0.33	8.45	0.23	0.09	100.27
1114 CHR BRIGHT SPOT 10	0	0.24	7.54	60.26	1.96	23.09	0.54	6.3	0.21	0.06	100.20
1115 CHR SMALL SPOT 11	0	0.49	13.64	52.67	2.95	21.90	0.42	7.98	0.11	0.07	100.22
1116 CHR **** SAMPLE 486129 L CENTRAL, SPOT 1, 12	0	0.46	13.47	51.48	4.44	21.77	0.4	7.95	0.25	0.09	100.30
1117 CHR AT MARGIN SPOT 2	0	0.45	13.8	51.47	3.44	21.35	0.49	8.04	0.15	0.1	99.29
1118 CHR CENTRAL, SPOT 3	0	0.48	13.89	51.05	4.92	20.83	0.51	8.68	0.14	0.05	100.55
1119 CHR AT MARGIN SPOT 4	0	0.45	13.89	52.24	2.41	21.73	0.38	7.86	0.14	0.13	99.23
1120 CHR SMALL INST SPOT 5	0	0.43	13.96	51.12	4.29	21.53	0.47	8.16	0.08	0.09	100.13
1121 CHR SMALL SPOT 6	0	0.5	14.03	51.43	4.05	21.46	0.48	8.29	0.2	0.02	100.46
1122 CHR LARGE CENTRAL, SPOT 7	0.02	0.45	14.06	51.47	3.90	19.96	0.47	9.01	0.14	0.09	99.57
1123 CHR AT MARGIN SPOT 8	0	0.45	13.84	52.3	2.87	21.70	0.43	7.97	0.12	0.13	99.82
1124 CHR SMALL SPOT 9	0	0.36	14.09	50.93	4.61	21.34	0.42	8.22	0.13	0.2	100.30
1125 CHR BRIGHT AT MARGIN INCL MG-CHL, SPOT 10	0	0.26	7.94	60.12	1.99	22.18	0.67	6.91	0.13	0.09	100.29
1126 CHR SMALL SPOT 11	0	0.49	13.68	52.38	3.30	21.72	0.44	8.04	0.22	0.07	100.34
1127 CHR BRIGHT AT MARGIN SPOT 12	0	0.27	6.6	60.88	2.57	23.49	0.49	6.17	0.03	0.06	100.57
1128 CHR **** SAMPLE 486130 L CENTRAL, SPOT 1, 12	0	0.48	14.19	50.91	4.10	21.36	0.43	8.32	0.06	0.09	99.94
1129 CHR AT MARGIN NO RIND, SPOT 2	0	0.44	14.66	50.52	4.77	21.06	0.48	8.62	0.2	0.06	100.82
1130 CHR ANOTHER CENTRAL SPOT 3	0	0.47	14.4	51.33	3.61	21.22	0.4	8.48	0.02	0.13	100.06
1131 CHR AT MARGIN NO RIND, SPOT 4	0	0.38	13.88	51.47	3.88	21.44	0.45	8.09	0.05	0.18	99.82
1132 CHR BRIGHT AT MARGIN, SPOT 5	0.21	0.14	1.51	66.5	2.41	22.89	0.47	5.16	0.26	0.04	99.59
1133 CHR V SMALL	0	0.41	14.86	51.11	3.58	20.87	0.37	8.74	0.04	0.12	100.10
1134 CHR SMALL ONE END SPOT 6	0	0.4	14.26	51.06	4.25	21.31	0.37	8.44	0.05	0.04	100.19
1135 CHR V BRIGHT AT MARGIN, SPOT 7	0.03	0.28	1.75	66.74	0.76	23.96	0.62	4.87	0.21	0.03	99.26
1136 CHR LARGER CENTRAL, SPOT 8	0	0.42	14.32	50.85	3.93	20.83	0.49	8.42	0.29	0.06	99.61
1137 CHR AT MARGIN NO RIND, SPOT 9	0	0.5	13.85	51.31	3.68	21.03	0.42	8.33	0.23	0.06	99.42
1138 CHR SMALLER SPOT 10	0	0.47	13.65	50.88	4.67	20.80	0.55	8.51	0	0.09	99.62
1139 CHR SMALL INST, SPOT 11	0	0.43	14.36	50.88	4.20	21.18	0.41	8.48	0.02	0.11	100.07
1140 CHR SMALL ONE END PRIM, SPOT 12	0	0.47	15.31	50.75	3.43	21.03	0.43	8.71	0.13	0.06	100.32
1141 CHR BRIGHT HALF SPOT 13	0	0.09	10.12	58.8	0.61	22.38	0.49	6.93	0.15	0	99.57
1142 CHR **** SAMPLE 486131 L CENTRAL, SPOT 1, 12	0	0.64	15.03	51.3	3.54	19.19	0.39	10	0.01	0.17	100.26
1143 CHR AT MARGIN SPOT 2	0	0.49	14.77	50.42	3.78	21.37	0.47	8.32	0.09	0.07	99.78
1144 CHR BRIGHT SPOT 3	0	0.12	10.62	58.98	0.89	21.19	0.55	7.93	0.11	0	100.39
1145 CHR ANOTHER CENTRAL, SPOT 4	0	0.5	14.93	50.09	4.73	21.11	0.41	8.68	0.11	0.13	100.69
1146 CHR AT MARGIN SPOT 5	0	0.45	14.73	50.36	4.17	20.49	0.49	8.82	0.07	0.1	99.69
1147 CHR ANOTHER SPOT 6	0	0.56	14.94	50	4.86	20.71	0.43	8.99	0.03	0.17	100.69
1148 CHR BRIGHT MARGIN W INCL MG-CHLORITE, SPOT 7	0	0.21	6.34	62.07	0.96	22.98	0.59	6.06	0.16	0.1	99.48
1149 CHR ANOTHER SPOT 7	0	0.49	15.4	50.03	4.29	20.80	0.28	8.91	0.19	0.18	100.57
1150 CHR SMALLER SPOT 9	0	0.49	14.94	50.01	4.32	21.04	0.37	8.62	0.13	0.1	100.02
1151 CHR ANOTHER SPOT 10	0	0.47	15.21	49.87	4.89	20.94	0.46	8.84	0.07	0.11	100.86
1152 CHR ANOTHER SPOT 11	0	0.51	15.2	50.45	4.03	20.74	0.46	8.93	0.04	0.13	100.49
1153 CHR **** SAMPLE 486132 L CENTRAL, SPOT 1, 12	0	0.46	14.13	51.67	4.05	21.28	0.46	8.48	0	0.17	100.71
1154 CHR AT MARGIN SPOT 2	0	0.38	14.62	52.43	2.97	20.87	0.5	8.76	0.08	0.04	100.65
1155 CHR ANOTHER CENTRAL SPOT 3	0	0.47	13.96	50.73	4.49	20.77	0.48	8.56	0.1	0.08	99.64
1156 CHR AT MARGIN SPOT 4	0	0.45	14.99	52	2.74	20.63	0.29	8.98	0.15	0.13	100.35
1157 CHR SMALL SPOT 4	0	0.47	14.75	51.02	3.01	20.46	0.45	8.82	0.03	0.04	99.05
1158 CHR SMALL SPOT 5	0	0.5	14.66	50.43	4.55	20.09	0.45	9.17	0.17	0.08	100.10
1159 CHR ANOTHER SPOT 6	0	0.48	14.37	51.16	4.31	20.33	0.38	9.08	0.05	0.17	100.33
1160 CHR SMALLER SPOT 7	0	0.45	14.4	52.22	3.19	21.19	0.49	8.6	0	0.06	100.60
1161 CHR SMALL SPOT 8	0	0.47	14.37	52.21	3.28	20.65	0.31	9	0	0.12	100.42
1162 CHR SMALL SPOT 9	0	0.43	14.67	51.61	3.53	20.99	0.42	8.69	0.1	0.1	100.54
1163 CHR SMALLEST SPOT 10	0	0.37	15.08	51.16	3.85	20.57	0.47	8.91	0.22	0.09	100.72
1164 CHR **** SAMPLE 486133 L CENTRAL, SPOT 1, 12	0	0.43	13.76	52.06	3.80	22.16	0.55	7.82	0.04	0.1	100.72
1165 CHR AT MARGIN SPOT 2	0	0.4	13.81	51.56	3.84	21.57	0.44	8.06	0.07	0.11	99.85
1166 CHR ANOTHER CENTRAL, SPOT 3	0	0.46	13.89	51.36	4.35	21.95	0.51	7.96	0.04	0.16	100.69
1167 CHR AT MARGIN SPOT 4	0	0.5	14.37	51.98	3.04	21.56	0.55	8.2	0.13	0.12	100.44
1168 CHR ADJ SPOT 6	0	0.44	13.8	51.36	4.62	21.41	0.53	8.22	0.07	0.22	100.67
1169 CHR BRIGHT END, SPOT 7	0	0.15	8.67	60.35	0.07	23.20	0.63	6.17	0.07	0.04	99.36
1170 CHR ANOTHER SPOT 7	0	0.46	13.86	51.55	3.95	22.02	0.44	7.94	0.07	0.06	100.35
1171 CHR SMALL SPOT 8	0	0.42	14.63	50.14	4.91	21.41	0.35	8.32	0.21	0.2	100.59
1172 CHR INST SPOT 9	0	0.44	13.89	50.95	4.19	21.70	0.37	7.99	0.12	0.13	99.78
1173 CHR SMALL SPOT 10	0	0.43	14.26	50.21	4.61	21.80	0.47	7.91	0.09	0.18	99.96
1174 CHR SMALL BRIGHT SPOT 11	0	0.21	7.77	61.58	0.21	22.96	0.51	6.37	0.13	0.11	99.85
1175 CHR **** SAMPLE 486137 L CENTRAL, SPOT 1, 12	0	0.48	14.04	51.81	3.44	21.84	0.43	8.06	0.05	0.11	100.26
1176 CHR AT MARGIN SPOT 2	0	0.47	13.96	50.95	3.75	21.55	0.52	7.92	0.14	0.14	99.40
1177 CHR ANOTHER CENTRAL, SPOT 3	0.09	0.42	12.39	52.55	4.65	21.32	0.51	7.87	0	0.13	99.93
1178 CHR AT MARGIN SPOT 4	0	0.4	12.41	53.05	3.81	21.84	0.49	7.76	0	0.09	99.85
1179 CHR SMALLER SPOT 6	0	0.55	14.04	52.46	2.84	21.79	0.46	8.08	0.2	0.13	100.54
1180 CHR ANOTHER SPOT 6	0	0.53	13.67	51.24	4.63	21.61	0.42	8.28	0	0.1	100.48
1181 CHR ANOTHER CENTRAL, SPOT 7	0	0.52	14.06	51.27	3.44	21.84	0.38	8.04	0.06	0.02	99.62
1182 CHR AT MARGIN SPOT 8	0	0.43	13.94	51.8	3.56	21.19	0.4	8.37	0.07	0.11	99.87
1183 CHR SMALL SPOT 9	0	0.52	13.85	51.83	3.07	21.04	0.44	8.31	0.18	0.12	99.37
1184 CHR SMALL INST SPOT 10	0	0.46	14.09	52.01	3.02	21.22	0.35	8.39	0.08	0.1	99.72
1185 CHR SMALLEST SPOT 11	0	0.58	14.3	52.79	2.18	21.54	0.38	8.41	0.12	0.03	100.34

Black Thor BT-08-10

	SiO2	TiO2	Al2O3	Cr2O3	Fe2O3	FeO	MnO	MgO	ZnO	NiO	TOTAL
1186 CHR **** SAMPLE 486138 L CENTRAL, SPOT 1, 12	0	0.57	12.85	52.16	4.38	22.13	0.48	7.83	0.04	0.1	100.54
1187 CHR AT MARGIN SPOT 2	0	0.47	13.46	52.5	3.19	22.16	0.55	7.66	0.17	0.06	100.22
1188 CHR ANOTHER SPOT 3	0	0.51	12.73	53.41	3.36	22.51	0.46	7.58	0.06	0.11	100.73
1189 CHR ANOTHER CENTRAL, SPOT 4	0.2	0.73	11.75	54.42	2.89	21.64	0.43	7.51	0.16	0.06	99.79
1190 CHR AT MARGIN SPOT 5	0	0.49	13.87	52.93	2.67	21.69	0.46	8.17	0.07	0.1	100.45
1191 CHR ANOTHER CENTRAL, SPOT 6	0	0.49	13.68	51.09	4.27	21.58	0.56	7.97	0.09	0.16	99.89
1192 CHR AT MARGIN SPOT 7	0	0.46	14.09	51.57	3.36	21.54	0.62	8.03	0.16	0.02	99.86
1193 CHR OPP MARGIN SPOT 8	0	0.46	13.56	51.62	3.77	22.08	0.43	7.76	0.07	0.07	99.83
1194 CHR SMALL SPOT 9	0	0.55	13.61	51.61	3.64	21.88	0.62	7.8	0.03	0.18	99.92
1195 CHR SMALLER SPOT 10	0	0.46	13.15	52.86	3.40	22.07	0.58	7.74	0.1	0.07	100.43
1196 CHR SMALL SPOT 11	0	0.63	13.67	52.08	2.45	22.15	0.43	7.73	0	0.13	99.27
1197 CHR **** SAMPLE 486139 L GRAN CENTRAL, SPOT	0	0.52	13.32	52.04	3.87	23.00	0.46	7.26	0.2	0.08	100.75
1198 CHR AT MARGIN SPOT 2	0	0.55	13.43	51.98	3.48	22.80	0.49	7.39	0	0.13	100.25
1199 CHR SMALL SPOT 3	0	0.4	13.32	51.77	3.01	22.70	0.56	7.05	0.06	0.05	98.92
1200 CHR SPOT 4	0	0.93	14.84	51.87	1.48	22.69	0.59	7.82	0.04	0.05	100.32
1201 CHR SPOT 5	0	0.5	13.91	51.62	3.75	22.08	0.66	7.69	0.31	0.06	100.59
1202 CHR SMALL SPOT 6	0	0.43	14.44	51.93	2.69	21.86	0.49	7.91	0.21	0.06	100.02
1203 CHR SMALL SPOT 7	0	1.66	14.25	51.76	-0.27	23.03	0.5	7.65	0.15	0.07	98.80
1204 CHR IN CLEAR ZONE SPOT 8	0	0.53	14.62	52.38	1.96	22.29	0.57	7.77	0.12	0.08	100.32
1205 CHR SMALL SPOT 9	0	0.42	13.94	50.92	4.34	22.30	0.57	7.55	0.13	0.16	100.32
1206 CHR LARGER SPOT 10	0	0.41	14.25	51.05	4.17	22.57	0.47	7.61	0.11	0.08	100.72
1207 CHR SMALL SPOT 11	0	0.5	14.03	51.77	3.02	22.50	0.5	7.5	0.2	0.07	100.09
1208 CHR SMALL SPOT 12	0	0.43	14.14	50.53	4.20	22.23	0.63	7.54	0.06	0.15	99.91
1209 CHR **** SAMPLE 486140 REL LARG GRAIN SPOT 1	0.03	0.39	14.46	51.52	2.43	23.04	0.62	6.91	0.15	0.08	99.63
1210 CHR SPOT 2	0.01	0.49	14.83	51.37	2.51	22.92	0.45	7.4	0.15	0	100.13
1211 CHR OPP MARGIN SPOT 3	0	0.58	13.81	52.66	1.77	23.32	0.45	7.03	0.15	0.03	99.80
1212 CHR SMALLER SPOT 4	0.05	0.35	15.04	50.89	2.67	22.63	0.55	7.21	0.18	0.05	99.62
1213 CHR SMALL SPOT 5	0	0.37	14.87	51.02	2.71	23.16	0.59	7.02	0.12	0.11	99.97
1214 CHR REL LARGE SPOT 1, 12-24-3703	0	0.51	13.69	50.94	3.53	23.46	0.55	6.73	0.12	0.12	99.64
1215 CHR AT MARGIN SPOT 2	0.08	0.34	14.22	50.22	4.94	22.88	0.55	7.01	0.24	0.07	100.56
1216 CHR SMALLER SPOT 4	0.04	0.24	15.08	51.19	2.27	22.69	0.55	7.12	0.17	0	99.35
1217 CHR ANOTHER SPOT 5	0	0.31	14.24	50.94	3.34	23.09	0.58	6.93	0.1	0.06	99.58
1218 CHR BRIGHT MARGIN SPOT 6	0.09	0.31	5.49	60.15	3.23	24.65	0.63	4.63	0.23	0.14	99.55
1219 CHR **** SAMPLE 486141 LARGE GRAIN SPOT N1,	0	0.49	13.88	50.27	3.56	25.59	0.66	5.46	0	0.04	99.95
1220 CHR ANOTHER CENTRAL, SPOT 2	0	0.53	13.79	49.96	4.13	25.31	0.63	5.57	0.16	0.13	100.21
1221 CHR AT MARGIN SPOT 3	0	0.54	13.73	50.01	3.79	25.09	0.65	5.58	0.23	0.1	99.72
1222 CHR BRIGHT SPOT 4	0	0.24	8.15	57.57	2.48	25.66	0.74	4.47	0.09	0.05	99.45
1223 CHR REL LARGE SPOT 5	0.07	0.41	13.34	50.32	4.84	24.90	0.62	5.56	0.29	0.07	100.42
1224 CHR ANOTHER SPOT 6	0.05	0.48	13.99	50.06	4.14	24.89	0.63	5.77	0.07	0.14	100.21
1225 CHR AT MARGIN SPOT 7	0	0.51	14.62	50.18	3.17	25.21	0.73	5.76	0.11	0.05	100.35
1226 CHR SMALLER SPOT 8	0.03	0.52	14.11	50.55	3.32	25.05	0.65	5.7	0.14	0.13	100.20
1227 CHR SMALL SPOT 9	0.01	0.42	14.53	49.73	3.17	24.83	0.67	5.69	0.2	0.05	99.31
1228 CHR **** SAMPLE 486142 SMALL GRAIN DARK CENT	0.07	0.44	15.97	44.46	6.79	25.99	0.56	4.88	0.47	0.11	99.74
1229 CHR ANOTHER CENTRAL, SPOT 5	0.03	0.5	16.36	45.24	5.12	27.42	0.49	4.23	0.48	0.09	99.96
1230 CHR DARK CENTRAL, SPOT 1, 12-24-3708	0	0.53	16.49	45.09	5.84	26.10	0.65	5.16	0.49	0.13	100.47
1231 CHR DARK CENTRAL, SPOT 1, 12-24-3708	0	0.46	16.8	44.25	6.56	26.34	0.43	5.14	0.53	0.13	100.65
1232 CHR ANOTHER DARK CENTRAL, SPOT 6	0	0.48	16.77	43.71	6.65	27.84	0.44	4.2	0.55	0.08	100.73
1233 CHR ANOTHER DARK CENTRAL, SPOT 6	0	0.46	16.67	43.7	6.18	27.58	0.56	4.23	0.37	0	99.75
1234 CHR CENTRAL, SPOT 8	0	0.49	16.53	43.13	6.92	27.79	0.42	4.14	0.44	0.05	99.90
1235 CHR AT MARGIN SPOT 9	0.14	0.52	0.21	36.37	32.51	29.77	0.68	0.79	0.22	0.18	101.38

Black Thor BT-09-17

	SiO2	TiO2	Al2O3	Cr2O3	Fe2O3	FeO	MnO	MgO	ZnO	NiO	TOTAL
1 CHR **** SAMPLE 486672 CENTRAL IM 002 2	0.07	0.26	15.7	49.28	2.74	22.25	0.68	7.95	0.1	0.07	98.83
2 CHR CENTRAL IN 002 2	0	0.1	16.05	50.24	2.00	21.75	0.75	8.24	0	0	98.93
3 CHR CENTRAL IN 002 2	0	0.06	15.92	51.19	2.09	22.38	0.68	8.17	0	0	100.28
4 CHR CENTRAL IN 002 2	0	0.12	16.03	51.1	1.49	22.25	0.66	7.94	0	0	99.44
5 CHR AT MARGIN INNER ZONE	0	0.11	16.2	50.83	1.90	22.37	0.63	8.12	0	0	99.97
6 CHR OUTER ZONE	0	0.1	18.19	51.66	0.03	20.55	0.7	9	0	0	100.23
7 CHR CENTRAL	0	0.2	15.8	50.92	2.27	22.07	0.62	8.27	0.08	0.14	100.14
8 CHR CENTRAL	0	0.2	15.9	50.62	1.88	22.21	0.61	8.05	0	0	99.29
9 CHR DARKER MARGIN	0	0.64	16.67	50.74	0.82	21.44	0.59	8.24	0.03	0.04	99.13
10 CHR ANOTHER CENTRAL	0	0.22	16.11	50.87	1.39	21.74	0.62	8.16	0.02	0.02	99.01
11 CHR DARKER MARGIN	0	0.18	17.73	51.3	0.12	20.28	0.47	9.08	0	0	99.15
12 CHR SMALLER	0	0.18	16.56	49.59	1.95	21.56	0.53	8.49	0	0	98.66
13 CHR ANOTHER CENTRAL	0	0.26	15.84	49.64	2.12	21.87	0.59	8.07	0	0.08	98.25
14 CHR CENTRAL	0	0.21	16.21	50.4	1.48	21.44	0.6	8.3	0	0.05	98.54
15 CHR GRAIN 1 CENTRAL AGAIN	0	0.2	15.97	51.03	1.70	22.36	0.69	7.89	0	0.12	99.79
16 CHR GRAIN 1	0	0.2	15.97	51.04	1.71	22.36	0.69	7.9	0	0.12	99.82
17 CHR GRAIN 1 CENTRAL AGAIN	0	0.2	15.84	49.85	2.11	22.19	0.64	7.84	0.12	0.08	98.66
18 CHR GRAIN 1 CENTRAL AGAIN	0	0.2	15.61	50.93	1.55	22.09	0.59	7.88	0.01	0.04	98.74
19 CHR GRAIN 1 CENTRAL AGAIN	0	0.24	15.98	50.59	1.66	22.33	0.61	7.84	0	0.09	99.17
20 CHR GRAIN 1 CENTRAL AGAIN	0	0.22	15.74	50.96	1.96	22.51	0.65	7.88	0	0.1	99.82
21 CHR DARKER MARGIN	0	0.19	17.28	51.58	0.19	21.46	0.54	8.28	0	0.05	99.55
22 CHR DARKER AT MARGIN	0	0.18	17.7	52.35	0.00	20.08	0.5	8.47	0.11	0	99.39
23 CHR CENTRAL	0	0.19	15.61	50.97	1.72	22.31	0.53	7.84	0.07	0.09	99.16
24 CHR CENTRAL	0	0.21	15.78	50.84	1.95	22.22	0.74	7.96	0	0.11	99.62
25 CHR CENTRAL	0	0.24	15.86	51.47	1.68	22.53	0.64	7.93	0	0.05	100.23
26 CHR DARK MARGIN	0	0.18	17.6	51.83	0.00	20.24	0.73	8.57	0	0	99.15
27 CHR REL BRIGHT MARGIN	0	0.06	10.69	59.06	0.00	22.99	0.76	6.21	0.08	0.03	99.88
28 CHR BRIGHT CENTRAL SPOT 1 IM 0005-3	0	0.24	16.01	51.28	1.39	22.32	0.54	7.94	0.07	0	99.65
29 CHR SPOT 2 BRIGHT CENTRAL	0	0.17	16.12	50.58	1.46	22.08	0.62	7.92	0.04	0.02	98.86
30 CHR DARK REACTION MARGIN SPOT 3	0	0.21	17.84	50.97	0.00	20.45	0.64	8.53	0.08	0	98.72
31 CHR DARKEST MARGIN SPOT 5	0	0.21	17.9	51.18	0.00	19.95	0.58	8.86	0	0	98.68
32 CHR BRIGHT REPLACEMENT MARGIN SPOT 6	0.02	0.11	6.45	62.75	0.00	23.84	0.91	4.62	0.15	0.02	98.87
33 CHR BRIGHT CENTRAL	0.01	0.08	16.37	49.94	1.82	22.12	0.64	8.04	0	0	98.84
34 CHR **** SAMPLE 486676 BRIGHT CENTRAL,S1 000	0.01	0.24	15.45	49.47	1.97	23.82	0.63	6.62	0.06	0.08	98.15
35 CHR RELICT BRIGHT SPOT 1 0007-2	0	0.23	15.49	51.03	1.70	24.10	0.71	6.72	0.02	0.07	99.9
36 CHR ADJ DARK DOMAIN SPOT 2	0	0.12	16.65	50.54	0.58	22.69	0.68	7.24	0	0	98.49
37 CHR IM 0009-2	0	0.31	15.35	51.64	1.71	21.27	0.56	8.56	0	0.06	99.29
38 CHR AT MARGIN	0.01	0.28	16.32	52.23	0.30	19.95	0.54	9.01	0.02	0.05	98.68
39 CHR AT MARGIN	0.02	0.2	16.57	54.31	0.00	19.19	0.57	9.07	0	0.01	99.94
40 CHR AT MARGIN	0.03	0.22	16.08	53.32	0.00	19.74	0.52	8.93	0	0	98.84
41 CHR AT MARGIN	0.03	0.37	16.27	53.2	0.35	20.26	0.57	9.11	0.05	0	100.17
42 CHR AT MARGIN	0	0.36	16.12	52.53	0.52	20.30	0.56	8.98	0.01	0	99.33
43 CHR ANOTHER	0	0.3	15.85	51.8	1.53	20.69	0.53	9.01	0.13	0	99.68
44 CHR ANOTHER GRAIN BRIGHT CENTRAL	0.02	0.31	15.71	51.02	2.53	21.23	0.65	8.95	0.06	0.04	100.27
45 CHR DARK MARGIN	0	0.28	16.58	51.49	0.55	20.58	0.52	8.75	0.01	0	98.71
46 CHR 486676 IM 0010-2 SPOT 1 BRIGHT	0.01	0.03	16.04	50.8	1.49	24.15	0.8	6.71	0	0	99.88
47 CHR BRIGHT CENTRAL SPOT 2	0	0.21	16.26	50.88	1.13	23.96	0.64	6.77	0.09	0	99.82
48 CHR RELICT BRIGHT SPOT 3	0	0.21	16.59	51.19	0.98	24.07	0.66	6.8	0.14	0	100.54
49 CHR DARKER ALT SPOT 4	0	0.07	18.19	50.91	0.00	22.89	0.62	7.39	0.12	0	100.19
50 CHR REL BTIGHT CENTRAL SPOT 5	0	0.2	15.99	51.12	1.33	24.24	0.61	6.62	0.16	0.09	100.23
51 CHR DARK MARGIN ALT SPOT 6	0	0.26	17.87	51.76	0.00	22.51	0.58	6.91	0.11	0.06	100.06
52 CHR DARK MARGIN ALT SPOT 6	0	0.3	17.15	51.37	0.20	23.08	0.6	7.18	0.14	0	100
53 CHR REL BRIGHT CENTRAL IM 0011-2 SPOT 1	0.02	0.23	15.93	51.01	1.32	24.14	0.73	6.51	0.15	0.17	100.07
54 CHR REL BRIGHT SPOT 2	0	0.41	15.86	50.72	1.32	24.50	0.76	6.27	0.14	0.02	99.87
55 CHR V DARK AT M ALT SPOT 4	0	0.19	17.66	50.45	0.25	23.58	0.69	6.88	0.05	0	99.72
56 CHR REL BRIGHT CENTRAL	0	0.2	15.98	50.04	1.53	24.53	0.62	6.31	0.09	0.09	99.24
57 CHR DARKER AT MARGIN SPOT 6	0.01	0.24	16.26	50.69	1.20	24.54	0.59	6.41	0.15	0.04	100.01
58 CHR **** SAMPLE 486717 BRIGHT RELICT S-1 IM	0	0.27	14.39	51.85	1.93	24.04	0.56	6.73	0.1	0.04	99.72
59 CHR BRIGHT SPOT 2	0	0.27	13.79	53.01	1.83	23.90	0.6	6.8	0.13	0.02	100.17
60 CHR AT MARGIN	0	0.26	12.54	54.43	0.93	22.91	0.5	6.77	0.14	0	98.38
61 CHR 486717 IM 0012 1 BRIGHT CENTRAL SPOT 1	0	0.24	15.16	51.09	2.25	24.21	0.63	6.86	0.12	0.06	100.4
62 CHR IM 0012 1 BRIGHT CENTRAL SPOT 1	0	0.23	15.09	50.59	1.94	24.44	0.47	6.49	0.05	0.11	99.22
63 CHR STILL BRIGHJT SPOT 2	0	0.22	15.3	50.78	1.83	24.22	0.61	6.61	0.11	0.04	99.54
64 CHR DARK ALT AT MARGIN SPOT 3	0	0.54	16.52	51.39	0.65	23.43	0.47	7.1	0.16	0	100.2
65 CHR DARK ALT SPOT 4	0	0.11	16.47	52.3	0.00	22.65	0.52	6.99	0.03	0.07	99.14
66 CHR ADJ SPOT 1 AGAIN	0	0.21	15.09	50.38	2.29	24.19	0.6	6.65	0.16	0.09	99.43
67 CHR DARK ALT MARGIN SPOT 6	0	0.2	17.2	50.88	0.66	23.17	0.48	7.35	0.19	0	100.07
68 CHR REL BRIGHT SPOT 1 IMAGE 0013.1	0	0.21	15.57	51.06	1.67	24.04	0.63	6.81	0.09	0.03	99.94
69 CHR DARKER SPOT 2	0	0.15	16.94	52.14	0.05	22.96	0.5	7.31	0.1	0.07	100.22
70 CHR ANOTHER REL BRIGHT SPOT 3	0	0.26	15.45	51.26	1.38	24.01	0.54	6.72	0.11	0	99.6
71 CHR **** SAMPLE 486722 CENTRAL IM 0014-1	0.06	0.28	15.89	51.7	1.51	21.29	0.58	6.81	0.12	0.01	99.9
72 CHR CENTRAL IM 0014-1	0	0.27	15.79	51.7	1.63	21.33	0.58	8.62	0.07	0.05	99.88
73 CHR DARK MARGIN SPOT 2	0	0.13	17.87	52.21	0.00	19.28	0.54	9.44	0.13	0	99.6
74 CHR BRIGHT	0.04	0.08	8.63	62.26	0.00	21.62	0.59	6.71	0.13	0	100.06
75 CHR BRIGHT	0.13	0.05	7.68	61.83	0.00	22.24	0.76	6.29	0.1	0	99.08
76 CHR ANOTHER REGION IM 0018 1 DARK SPOT 1	0.01	0.29	16.43	51.84	0.59	20.02	0.52	8.99	0.15	0.14	98.92
77 CHR DARK SPOT 2	0.02	0.17	17.9	53.36	0.00	17.63	0.51	9.69	0.06	0	99.34
78 CHR INT W TREM	0.36	0.07	10.79	58.63	0.43	19.96	0.66	8.47	0.1	0	99.43
79 CHR SPOT 4	0.13	0.09	6.39	64.65	0.00	21.59	0.84	5.67	0.13	0	99.49

Black Thor BT-09-17

	SiO2	TiO2	Al2O3	Cr2O3	Fe2O3	FeO	MnO	MgO	ZnO	NiO	TOTAL
80 CHR REL DOMAIN SPOT 5	0.03	0.24	16.54	52.93	0.29	20.18	0.49	9.16	0.08	0	99.91
81 CHR REL BRIGHT CENT IM 00019 1 SPOT 1	0.04	0.31	15.66	51.55	1.60	21.23	0.5	8.57	0.15	0.07	99.52
82 CHR REL BRIGHT CENT IM 00019 1 SPOT 1	0.03	0.29	15.87	52.67	1.16	21.26	0.49	8.77	0.05	0	100.47
83 CHR INT SPOT 3	0.03	0.28	16.46	52.94	0.16	20.23	0.45	9.01	0.16	0	99.7
84 CHR DARKER SPOT 3	0	0.37	17.21	52.05	0.43	20.08	0.6	9.27	0.14	0	100.11
85 CHR DARKER SPOT 4	0.03	0.19	17.72	52.81	0.00	18.88	0.57	9.46	0.02	0.02	99.7
86 CHR V DARK ALT SPOT 5	0	0.26	17.12	52.87	0.09	19.97	0.59	9.3	0.05	0.06	100.31
87 CHR DARK INT SPOT 6	0.09	0.07	14.56	56.76	0.00	19.21	0.65	8.47	0.01	0	99.82
88 CHR VERY DARK	0.1	0.05	13.47	56.88	0.00	19.75	0.52	8.67	0.06	0	99.5
89 CHR SMALL BRIGHT SPOT 7	0.09	0.16	10.13	60.11	0.00	21.22	0.51	7.11	0.04	0	99.37
90 CHR SMALL BRIGHT SPOT 7	0.11	0.06	8.93	60.28	0.00	22.01	0.61	6.55	0.1	0	98.65
91 CHR **** SAMPLE 486726 IM 0023 SPOT 1 BRIGHT	0	0.44	14.55	50.54	2.19	23.69	0.62	6.83	0.04	0	98.68
92 CHR IM 0023 SPOT 1 BRIGHT	0	0.39	14.47	50.69	2.25	23.82	0.57	6.73	0.16	0.05	98.91
93 CHR BRIGHT SPOT 2	0	0.33	15.1	49.95	2.24	23.38	0.6	6.97	0.2	0.08	98.62
94 CHR DARKER ALT SPOT 3	0	0.33	17.25	52.07	0.00	21.28	0.6	7.56	0.02	0.03	99.14
95 CHR DARK ALT SPOT 4	0	0.3	16.14	51.74	0.79	22.86	0.68	7.37	0.06	0	99.86
96 CHR REL BRIGHT SPOT 5	0	0.36	15.47	51.96	0.42	22.86	0.56	6.95	0.17	0	98.71
97 CHR REL BRIGHT SPOT 5	0	0.4	15.62	51.77	0.70	23.16	0.39	7.11	0.08	0	99.16
98 CHR DARKER SPOT 6	0	0.29	16.96	51.63	0.00	21.87	0.48	7.53	0.2	0	98.96
99 CHR SMALL ALT BRIGHT, SPOT 7	0.39	0.08	7.25	61.44	0.00	23.79	0.66	4.84	0.15	0	98.6
100 CHR SMALL ALT BRIGHT, SPOT 7	0.23	0.04	7.58	61.91	0.00	23.30	0.63	5.02	0	0	98.71
101 CHR V BRIGHT SPOT 8	0.01	0.07	2.99	68.03	0.00	23.74	0.81	3.87	0.06	0.03	99.61
102 CHR SMALL PRIMARY SPOT 2 IM 0024	0	0.32	15.19	51.77	1.34	23.86	0.47	6.79	0.16	0.08	99.84
103 CHR SPOT 2	0	0.33	15.28	52.26	1.00	23.48	0.44	7.05	0.13	0	99.87
104 CHR REL BRIGHT SPOT 3	0	0.33	16.32	51.98	0.37	22.90	0.56	7.23	0.18	0	99.83
105 CHR DARKER ALT SPOT 4	0	0.24	16.42	52.6	0.00	22.39	0.57	7.45	0.21	0.03	99.91
106 CHR LINEAR BRIGHT SPOT 5	0.01	0.13	12.9	56.52	0.00	22.89	0.46	6.45	0.11	0	99.47
107 CHR NARROW FRACTURE SPOT 6	0.11	0.08	7.27	63.09	0.00	23.20	0.72	4.97	0.16	0.03	99.63
108 CHR ANOTHER REL BRIGHT PRIM S 1 IM 0025	0	0.35	14.85	51.64	1.73	24.26	0.61	6.56	0.2	0.01	100.04
109 CHR ADJ GRAIN BRIGHT SPOT 2	0	0.42	14.84	50.52	2.46	24.61	0.54	6.61	0.01	0.02	99.78
110 CHR AT MARGIN DARKER SPOT 3	0	0.23	16.58	51.59	0.00	22.43	0.57	7.22	0.18	0.02	98.82
111 CHR DARK INT	0	0.26	16.4	53.12	0.00	22.04	0.51	7.1	0.3	0.03	99.76
112 CHR SMALL BRIGHT SPOT 5	0.04	0.17	10.88	58.23	0.00	23.33	0.64	6.11	0.1	0	99.5
113 CHR BRIGHTER	0.03	0.17	7.48	62.83	0.00	23.58	0.69	5.14	0.1	0	100.02
114 CHR **** SAMPLE 486728 DARK CENTRAL S 1 IM 0	0.01	0.29	16.98	53.26	0.00	21.86	0.39	7.44	0.02	0	100.25
115 CHR ALT? SPOT 2	0	0.2	16.9	53.02	0.00	22.11	0.46	7.4	0.14	0	100.23
116 CHR SMALLER BRIGHTER SPOT 3	0.01	0.39	16.07	52.58	0.04	23.01	0.51	7.07	0.14	0	99.82
117 CHR SPOT 4	0	0.67	16.83	51.6	0.03	22.28	0.43	7.59	0.14	0	99.57
118 CHR SPOT 5	0	0.54	16.94	51.87	0.00	22.30	0.53	7.64	0	0	99.82
119 CHR SPOT 1 IM 0028	0.05	0.19	17.27	52.12	0.00	21.97	0.48	7.55	0.09	0	99.72
120 CHR SPOT 2	0.01	0.45	16.15	51.66	0.69	23.22	0.45	7.18	0.16	0	99.9
121 CHR ADJ GRAIN SPOT 3	0.01	0.25	16.63	53.67	0.00	21.93	0.47	7.42	0.03	0	100.41
122 CHR LINEAR SPOT 4	0.07	0.34	17.43	53.13	0.00	21.10	0.4	7.48	0.18	0.04	100.17
123 CHR BRIGHT SPOT 5	0.5	0.07	6.94	63.32	0.00	23.22	0.59	4.86	0.18	0	99.68
124 CHR **** SAMPLE 486734 REL BRIGHT S 1 IM0031	0	0.34	15.49	51.05	1.39	22.24	0.58	7.72	0	0.04	98.71
125 CHR REL BRIGHT S1 IM0031	0.02	0.3	15.26	52.3	0.99	22.01	0.44	7.86	0.18	0	99.26
126 CHR ADJ SPOT 2	0	0.34	17.35	51.91	0.00	20.43	0.47	8.62	0.03	0	99.15
127 CHR V BRIGHT SPOT 3	0.29	0.08	4.41	66.14	0.00	23.03	0.74	4.74	0.12	0	99.55
128 CHR POSS REL PRIM S 4	0	0.37	15.23	52.91	0.95	22.30	0.53	7.86	0.01	0	100.06
129 CHR ADJ ALT SPOT 5	0	0.28	15.75	52.36	0.82	22.13	0.4	7.91	0.13	0.06	99.75
130 CHR REL BRIGHT, PRIM SPOT 6	0	0.41	15.18	51.76	1.50	22.47	0.56	7.72	0.02	0.06	99.53
131 CHR AT MARGIN ALT SPOT 7	0.02	0.14	16.82	53.46	0.00	20.83	0.43	8.38	0.06	0	100.14
132 CHR REL BR PRIM S 1 IM 0032	0.01	0.4	14.75	52.42	1.48	22.78	0.37	7.57	0.11	0.1	99.84
133 CHR AGAIN	0	0.37	14.64	51.23	2.10	22.61	0.51	7.65	0.04	0.03	98.97
134 CHR DARK MARGIN SPOT 2	0	0.69	15.41	52.26	0.53	21.93	0.37	7.79	0.1	0	99.03
135 CHR SMALL BRIGHT PRIM S 3	0	0.37	14.53	51.26	2.29	23.03	0.47	7.49	0.04	0.07	99.32
136 CHR RE BR CENTRAL SPOT 4	0.01	0.24	15.68	52.34	0.86	22.52	0.41	7.74	0.05	0	99.76
137 CHR V BRIGHT SPOT 4A	0.22	0.09	5.54	64.02	0.00	22.78	0.57	5	0.1	0.01	98.33
138 CHR ALT PRIM SPOT 5	0	0.83	15.33	52.19	0.98	22.32	0.57	7.75	0	0	99.87
139 CHR DARK GRAIN PERV ALT SPOT 6	0	0.58	17.29	53.58	0.00	19.38	0.45	8.4	0.16	0	99.84
140 CHR DARK GRAIN PERV ALT SPOT 6	0.02	0.53	16.96	52.54	0.00	20.89	0.52	8.49	0.14	0.03	100.12
141 CHR BRIGHT SPOT 7	0.16	0.07	4.7	66.4	0.00	23.78	0.7	4.97	0.27	0	101.05
142 CHR **** SAMPLE 486739 SP 1 IM 0034	0	0.32	15.05	52.89	0.43	23.81	0.64	6.52	0.02	0	99.64
143 CHR DARKER SPOT 2	0	0.24	17.14	52.97	0.00	21.27	0.59	7.24	0.05	0.05	99.55
144 CHR DARKER SPOT 2	0.06	0.22	16.71	53.9	0.00	20.93	0.56	7.26	0.09	0.05	99.78
145 CHR ANOTHER GRAIN SPOT 3	0	0.23	16	53.12	0.00	22.69	0.69	6.9	0.08	0.03	99.74
146 CHR ALT SPOT 4	0	0.28	16.27	53.06	0.00	22.51	0.71	7.18	0.06	0	100.07
147 CHR V BRIGHT SPOT 5	0.61	0.12	3.47	66.38	0.00	24.75	0.87	3.91	0.22	0.06	100.39
148 CHR ADJ DARK SPOT 6	0	0.33	16.6	53.17	0.00	22.10	0.56	7.16	0.06	0	99.98
149 CHR SPOT 2 0038	0.03	0.38	15.86	52.44	0.36	23.20	0.62	6.97	0.11	0.04	99.97
150 CHR AT MARGIN SPOT 2	0	0.18	16.59	52.82	0.00	22.54	0.67	7.06	0.02	0	99.88
151 CHR ANOTH SPOT 3	0	0.32	17.12	52.69	0.00	22.17	0.54	7.52	0.03	0	100.39
152 CHR SPOT 4	0	0.26	17.06	52.57	0.00	21.45	0.66	7.33	0.19	0	99.52
153 CHR ANOTHER GRAIN SPOT 5	0	0.37	16.47	53.43	0.00	21.74	0.66	7.24	0.12	0	100.03
154 CHR ANOTHER GRAIN SPOT 5	0	0.35	16.7	53.17	0.00	21.64	0.61	7.15	0.12	0	99.74
155 CHR ANOTH GRAIN SPOT 6	0.03	0.13	16.05	54.29	0.00	21.87	0.64	7.1	0.13	0	100.24
156 CHR LINEAR BRIGHT SPOT 7	0.22	0.04	5.27	64.12	0.00	25.41	0.87	4.1	0.19	0	100.22
157 CHR **** SAMPLE 486742 SPOT 1 IM 0041	0.03	0.17	15.17	49.03	1.53	28.10	0.55	3.69	0.21	0.06	98.39
158 CHR SPOT 1 IM 0041	0	0.31	15.27	49.64	1.59	28.49	0.67	3.69	0.11	0.01	99.62

Black Thor BT-09-17

	SiO2	TiO2	Al2O3	Cr2O3	Fe2O3	FeO	MnO	MgO	ZnO	NiO	TOTAL
159 CHR ANOTHER GRAIN SPOT 2	0	1.45	15.53	49.91	1.11	27.98	0.66	3.61	0.25	0.02	100.41
160 CHR ANOTHER GRAIN SPOT 3	0	0.29	16.64	50.57	0.31	27.85	0.62	4.09	0.14	0	100.48
161 CHR ANOTHER GRAIN SPOT 3	0	0.26	16.34	50.69	0.30	27.82	0.67	3.92	0.28	0	100.25
162 CHR V BRIGHT SPOT 7	0	0.32	13.94	52.76	0.62	28.29	0.57	3.55	0.13	0.03	100.15
163 CHR V BRIGHT SPOT 7	0.32	0.09	6.38	61.72	0.00	28.91	0.77	2.08	0.15	0.06	100.48
164 CHR UNIFORM SPOT 4	0	0.29	15.79	49.83	1.33	28.35	0.57	3.87	0.16	0.08	100.14
165 CHR SPOT 5	0	0.2	15.97	50.35	0.52	27.95	0.62	3.82	0.18	0.02	99.58
166 CHR SPOT 6	0	1.17	16.2	50.92	0.00	27.13	0.54	3.91	0.25	0.02	100.14
167 CHR SPOT 6	0	0.62	16.37	50.44	0.00	27.09	0.62	4.06	0.2	0	99.4
168 CHR PRIMARY SPOT 1 IM 0042	0	0.33	15.36	48.92	1.97	28.42	0.63	3.78	0.2	0.01	99.42
169 CHR AT MARGIN SPOT 2	0	0.32	15.49	50	1.10	28.27	0.57	3.73	0.18	0	99.55
170 CHR ADJ GRAIN SPOT 3	0	0.31	16.2	49.35	1.03	28.14	0.69	3.83	0.13	0	99.58
171 CHR SPOT 4	0	0.29	15.33	49.45	1.23	28.04	0.53	3.73	0.24	0	98.71
172 CHR ADJ GRAIN SPOT 5	0	0.65	15.86	51.08	0.06	27.54	0.64	3.86	0.11	0	99.79
173 CHR SPOT 6	0	0.23	16.45	50.09	0.32	27.96	0.53	3.85	0.22	0	99.62
174 CHR BRIGHT SPOT 7	0.36	0.08	6.88	60.01	0.41	27.90	0.73	2.66	0.21	0.06	99.26
175 CHR **** SAMPLE 486743 S 1 IM 0043	0.03	0.27	15.65	47.99	2.16	27.37	0.72	4.37	0.09	0	98.44
176 CHR 1 IM 0043	0.03	0.23	15.78	48.95	1.73	27.41	0.79	4.32	0.17	0.02	99.26
177 CHR SPOT 2	0	0.45	16.03	49.47	0.79	26.97	0.71	4.28	0.14	0	98.76
178 CHR SPOT 3	0	0.29	16.9	50.22	0.45	27.09	0.7	4.53	0.21	0.02	100.37
179 CHR ANOTHER GRAIN SPOT 4	0	2.46	15.15	48.6	1.90	26.90	0.77	4.12	0.18	0.1	99.99
180 CHR DARKER SPOT 5	0	0.38	16.87	50.03	0.58	27.01	0.79	4.51	0.21	0.06	100.39
181 CHR DARKER ADJ GRAIN SPOT 6	0.01	0.42	15.92	49.89	0.87	26.82	0.8	4.32	0.36	0.01	99.33
182 CHR SMALL INTERNAL BRIGHT DOMAIN SPOT 7	0.01	0.12	11.27	55.42	0.36	27.42	0.89	3.39	0.11	0.03	98.98
183 CHR V BRIGHT SPOT 9	0.22	0.09	7.48	60.43	0.00	27.54	1.03	2.64	0.25	0.06	99.74
184 CHR POSS REL PRIM S 1 IM0045	0.02	0.32	16.54	49.04	0.94	26.92	0.74	4.43	0.25	0.02	99.13
185 CHR SPOT 2	0	0.23	15.79	48.96	1.58	27.32	0.75	4.28	0.2	0.05	99
186 CHR DARKER SPOT 3	0	0.27	16.97	49.93	0.47	26.91	0.74	4.57	0.19	0.05	100.05
187 CHR DARKER SPOT 4	0.02	0.27	17.07	48.73	0.61	26.63	0.67	4.61	0.17	0	98.72
188 CHR SPOT 5	0.04	0.28	16.74	49.07	1.07	27.01	0.77	4.49	0.36	0	99.72
189 CHR SUBPARALLEL LINEAR BRIGHT SPOT 6	0.03	0.22	10.76	56.91	0.01	27.57	0.79	3.29	0.19	0	99.77
190 CHR V BRIGHT SPOT 8	0.03	0.03	11.28	57.22	0.00	26.54	0.81	3.46	0.14	0	99.51
191 CHR SPOT 9	0.03	0.1	12.4	55.31	0.15	27.39	0.79	3.7	0.26	0	100.12
192 CHR SPOT 1 AGAIN	0	0.29	15.88	50.81	0.70	27.28	0.73	4.28	0.27	0.03	100.2
193 CHR ****SAMPLE 486748 CENTRAL PRIM SPOT 1	0	0.39	15.93	49.36	2.60	22.68	0.99	7.61	0.07	0.06	99.43
194 CHR CENTRAL PRIM SPOT 1 IM46	0	0.36	15.86	49.68	2.47	23.22	0.84	7.37	0.09	0.04	99.68
195 CHR PRIMARY SPOT 2	0	0.38	16	49.72	2.66	22.76	0.94	7.69	0.15	0.09	100.13
196 CHR SPOT 3	0	0.36	15.89	49.16	2.81	23.17	0.85	7.45	0.09	0.04	99.54
197 CHR ANOTHER GRAIN SPOT 14	0	0.41	15.84	48.77	3.47	23.13	0.94	7.61	0.12	0.11	100.05
198 CHR V BRIGHT SPOT 7	0.42	0.15	4.52	63.85	0.42	24.65	1.11	4.44	0.12	0	99.64
199 CHR SPOT 1 IM 0051	0	0.4	15.75	49.95	2.63	23.08	0.88	7.52	0.16	0.03	100.14
200 CHR SPOT 2	0	0.34	15.98	48.75	2.49	22.79	0.79	7.44	0.14	0.01	98.48
201 CHR SPOT 2	0	0.4	15.8	49.45	2.26	22.79	0.81	7.41	0.14	0.03	98.87
202 CHR DARKER SPOT 3	0	0.43	17.73	50.97	0.32	21.45	0.79	8.27	0.03	0.03	99.99
203 CHR REL BRIGHT SPOT 4	0	1.38	9.26	59.26	0.00	22.20	0.9	5.22	0.06	0.01	98.29
204 CHR REL BRIGHT SPOT 4	0	0.7	9.73	58.06	0.09	22.93	1.06	5.73	0.16	0	98.45
205 CHR SPOT 4	0	0.59	18.57	50.28	0.00	20.04	0.77	8.59	0	0	98.84
206 CHR SPOT 6 V BRIGHT	0.07	0.15	3.76	65.48	0.12	24.49	1.11	4.47	0.14	0	99.78
207 CHR REL PRIM S1 IM 0053	0	0.35	15.67	48.63	2.90	22.74	0.98	7.47	0.02	0.04	98.51
208 CHR REL PRIM S1 IM 0053	0	0.36	15.82	49.78	2.50	23.24	0.72	7.49	0.06	0	99.72
209 CHR SPOT 2	0	0.39	15.91	49.93	2.03	22.72	0.77	7.5	0.11	0.08	99.23
210 CHR SPOT 3	0	0.35	16.01	49.66	2.29	22.86	0.85	7.47	0.15	0.07	99.48
211 CHR SPOT 4	0	0.38	15.8	49.65	2.46	22.72	0.86	7.55	0.15	0.08	99.4
212 CHR SPOT 5	0	0.38	17.21	51.57	0.45	22.02	0.88	7.87	0.15	0	100.48
213 CHR SPOT 5	0	0.34	17.15	50.22	1.08	22.01	0.71	8.05	0	0	99.45
214 CHR SPOT 6	0	0.27	18.1	51.6	0.00	20.85	0.82	8.5	0.19	0	100.33
215 CHR SPOT 7	0.29	0.13	7.03	61.35	0.69	23.87	0.95	5.41	0.26	0	99.91
216 CHR **** SAMPLE 486753 S 1 IM 0055	0	0.3	14.46	47.93	3.43	29.37	1.11	3.08	0.36	0.03	99.73
217 CHR SPOT 2	0	0.25	14.57	48.76	2.98	29.40	1.07	3.1	0.41	0	100.24
218 CHR BRIGHT SPOT 3	0.11	0.34	6.47	52.92	6.51	31.09	1.27	1.77	0.34	0.05	100.21
219 CHR PRIN S 1 IM 0056	0	0.33	14.38	48.02	3.24	29.31	1.07	3.05	0.25	0.07	99.4
220 CHR MORE PRIM SPOT 2	0	0.4	14.41	48.74	2.96	29.40	1.15	3.03	0.23	0.02	100.05
221 CHR SPOT 3	0	0.35	14.56	47.81	2.95	28.95	1.06	3.02	0.46	0.05	98.91
222 CHR BRIGHT SPOT 4	0	0.25	7.18	54.69	4.07	30.12	1.19	1.93	0.26	0	99.28

Big Daddy FW-08-19

	SiO2	TiO2	Al2O3	Cr2O3	Fe2O3	FeO	MnO	MgO	ZnO	NiO	TOTAL
1 1 CHR * 232251 15.84m, CENTRAL S-1, 09-02-4541	0.07	0.56	14.25	45.69	6.44	26.70	0.71	4.24	0.21	0.05	98.28
2 2 CHR AT MARGIN SPOT 2	0.15	0.63	15.52	45.84	5.80	27.60	0.66	3.92	0.22	0.19	99.95
3 3 CHR CENTRAL SPOT 3	0.09	0.62	14.61	46.95	5.72	26.20	0.55	4.91	0.15	0.11	99.34
4 4 CHR AT MARGIN SPOT 4	0.09	0.69	14.94	46.26	5.46	27.57	0.79	3.83	0.39	0.13	99.6
5 5 CHR CENTRAL SPOT 5	0.09	0.67	14.77	45.58	6.18	28.01	0.54	3.71	0.21	0.16	99.3
6 6 CHR CENTRAL SPOT 6	0.06	0.64	14.86	45.79	6.61	28.40	0.67	3.65	0.26	0.14	100.42
7 7 CHR CENTRAL SPOT 6	0.1	0.64	14.65	45.42	6.44	28.04	0.56	3.59	0.26	0.13	99.19
8 8 CHR CENTRAL SPOT 7	0.08	0.6	15.09	45.34	5.69	27.56	0.63	3.84	0.17	0.14	98.57
10 10 CHR SMALLER SPOT 8	0.09	0.63	14.8	46.47	5.38	27.74	0.72	3.67	0.37	0.19	99.52
11 11 CHR BRIGHT AT MARGIN	0.14	0.53	6.41	50.26	10.81	28.58	0.86	2.01	0.28	0.15	98.95
13 13 CHR SINGLE GRAIN NO PHOTO	0.12	1.74	12.15	44.73	8.35	30.63	0.67	2.32	0.43	0.2	100.5
14 14 CHR SINGLE GRAIN NO PHOTO	0.06	1.47	10.54	45.16	7.95	29.62	0.79	2.12	0.27	0.28	97.47
15 15 CHR SINGLE GRAIN NO PHOTO	0.16	1.53	12.52	44.27	8.31	29.99	0.79	2.38	0.31	0.17	99.6
17 17 CHR DARKER	0.06	1.47	12.41	44.39	7.26	29.80	0.78	2.34	0.4	0.25	98.43
18 18 CHR * 232253 13.4m DARK CENTRAL, S-1 09-02-4	0.01	0.54	12.89	51.73	4.03	20.08	0.5	8.78	0	0.03	98.19
19 19 CHR DARK CENTRAL	0.01	0.6	13.22	51.25	3.74	20.23	0.62	8.54	0.01	0.17	98.02
20 20 CHR DARK CENTRAL	0	0.58	13.27	51.94	3.43	20.26	0.44	8.7	0.15	0.15	98.58
21 21 CHR AT MARGIN SPOT 2	0.07	0.51	12.25	50.98	4.28	26.88	0.57	4.18	0.2	0.16	99.65
22 22 CHR AT MARGIN SPOT 2	0.02	0.51	12.02	51.18	3.61	26.70	0.69	4.16	0.19	0.13	98.85
23 23 CHR CENTRAL SPOT 3	0.02	0.54	13.12	53.76	3.42	20.16	0.57	9.09	0.05	0.09	100.47
24 24 CHR CENTRAL SPOT 3	0.04	0.49	12.6	53.54	3.34	20.15	0.5	8.74	0.04	0.11	99.22
25 25 CHR AT MARGIN SPOT 4	0.07	0.47	11.68	51.34	3.97	27.75	0.68	3.33	0.3	0.16	99.36
26 26 CHR AT MARGIN SPOT 4	0.09	0.54	11.55	51.11	3.88	27.72	0.65	3.28	0.19	0.2	98.82
27 27 CHR CENTRAL SPOT 5	0.03	0.59	12.99	51.55	4.52	21.46	0.68	7.91	0.08	0.16	99.51
28 28 CHR AT MARGIN SPOT 6	0.14	0.52	11.96	51.69	4.44	27.77	0.72	3.53	0.28	0.09	100.69
29 29 CHR AT MARGIN SPOT 6	0.14	0.46	11.16	49.95	5.04	26.80	0.7	3.3	0.48	0.09	97.61
30 30 CHR AT MARGIN SPOT 6	0.07	0.48	11.63	50.98	4.30	27.49	0.7	3.51	0.21	0.12	99.06
31 31 CHR CENTRAL SPOT 7	0.07	0.46	12.82	51.65	4.94	21.35	0.58	7.86	0.08	0.15	99.47
32 32 CHR AT MARGIN SPOT 8	0.1	0.46	12.34	52.15	3.74	27.89	0.73	3.54	0.34	0.14	101.06
33 33 CHR AT MARGIN SPOT 8	0.11	0.59	11.54	50.78	4.34	27.49	0.66	3.41	0.33	0.1	98.92
34 34 CHR SPOT 1 AGAIN	0.05	0.53	13.43	52.79	2.94	20.46	0.51	8.53	0.16	0.14	99.24
35 35 CHR INST SPOT 9	0.07	0.56	12.11	51.05	4.16	28.04	0.68	3.44	0.28	0.11	100.08
36 36 CHR CENTRAL RANDOM	0.02	0.53	13.06	52.68	3.35	20.97	0.64	8.26	0.04	0.1	99.31
37 37 CHR ANOTHER CENTRAL RANDOM	0.03	0.5	13.46	53.78	3.44	19.90	0.48	9.33	0	0.2	100.77
38 38 CHR ANOTHER CENTRAL RANDOM	0	0.53	13.08	51.67	4.15	18.82	0.62	9.38	0.1	0.21	98.14
39 39 CHR * 232254 35.0m L CENTRAL	0.08	1	14.57	43.09	8.28	28.59	0.62	3.52	0.18	0.13	99.23
40 40 CHR AT MARGIN	0.11	0.86	14.24	44.02	7.86	28.69	0.7	3.04	0.43	0.21	99.37
41 41 CHR CENTRAL SPOT 3	0.12	1.22	14.1	41.52	9.12	28.63	0.6	3.16	0.35	0.11	98.02
42 42 CHR ANOTHER CENTRAL SPOT 4	0.1	1.38	13.75	42.96	8.14	29.00	0.67	3.12	0.27	0.19	98.76
43 43 CHR SMALLER SPOT 5	0.12	1.14	14.5	43.34	7.95	29.07	0.6	3.14	0.34	0.19	99.6
44 44 CHR CENTRAL SPOT 6	0.13	0.5	12.59	47.53	6.99	27.57	0.71	3.4	0.35	0.21	99.18
45 45 CHR CENTRAL SPOT 7	0.06	1.32	13.27	42.73	8.64	28.99	0.66	2.91	0.39	0.24	98.45
47 47 CHR * 232255 55.42m CENTRAL SPOT 1	0.09	0.4	12.45	49.62	5.39	23.82	0.61	5.73	0.13	0.18	97.88
50 50 CHR CENTRAL SPOT 1	0.03	0.77	15.61	44.85	5.23	28.07	0.6	3.78	0.31	0.11	98.83
51 51 CHR GRAIN 2	0.11	0.89	15.54	43.88	6.25	27.95	0.66	3.63	0.47	0.08	98.83
52 52 CHR ANOTHER SPOT 3	0.05	0.95	14.12	44.63	6.08	27.77	0.62	3.56	0.32	0.24	97.73
53 53 CHR ANOTHER SPOT 3	0	1.01	14.72	44.06	5.85	28.04	0.55	3.71	0.36	0.13	97.84
54 54 CHR ANOTHER SPOT 3	0.07	1.04	14.3	45.01	5.90	28.38	0.69	3.41	0.34	0.09	98.64
55 55 CHR ANOTHER	0.03	0.85	15.91	44.01	5.86	28.53	0.65	3.5	0.45	0.22	99.42
57 57 CHR CENTRAL SPOT 1 AGAIN	0.07	0.4	12.62	51.31	4.28	25.93	0.61	4.8	0.27	0.12	99.98
58 58 CHR ADJ SMALLER	0.01	0.73	15.6	45.2	4.63	28.30	0.7	3.55	0.35	0.06	98.67
59 59 CHR ADJ CENTRAL	0.02	1	14.61	44.72	6.48	28.49	0.66	3.57	0.43	0.16	99.49
60 60 CHR * 232256 75.14m CENTRAL SPOT 1 09-03-454	0.03	0.54	15.52	46.68	5.20	24.52	0.61	5.95	0.28	0.18	98.99
61 61 CHR AT MARGIN SPOT 2	0	0.61	15.48	46.22	4.54	27.52	0.63	4.14	0.25	0.14	99.08
62 62 CHR CENTRAL SPOT 3	0.02	0.6	13.56	46.78	4.92	27.76	0.59	3.35	0.46	0.13	97.68
63 63 CHR CENTRAL SPOT 3	0.05	0.54	14.94	46.54	5.64	28.00	0.76	3.57	0.57	0.17	100.21
64 64 CHR CENTRAL SPOT 4	0.05	0.52	14.43	48.2	4.54	27.08	0.58	4.24	0.31	0.2	99.7
65 65 CHR ZONED GRAIN SPOT 1 09-03-4547	0.07	0.49	14.7	46.83	5.19	28.36	0.71	3.22	0.52	0.11	99.68
66 66 CHR SPOT 2	0.08	0.43	8.43	47.9	11.41	29.20	0.79	1.98	0.55	0.1	99.72
67 67 CHR SPOT 2	0.09	0.43	7.97	47.32	11.96	28.79	0.62	2.09	0.44	0.18	98.69
68 68 CHR SPOT 3 INT W SIL	0.16	0.84	4.7	46.79	15.87	29.62	0.93	1.32	0.35	0.1	99.09
71 71 CHR REL LARGE CENTRAL	0	0.62	14.92	47.82	4.08	27.78	0.58	4.12	0.27	0.13	99.91
72 72 CHR * 232257 87.29m CENTRAL SPOT 1	0.13	0.53	12.99	47.2	6.70	29.09	0.6	2.45	0.72	0.12	99.86
74 74 CHR SPOT 2 CENTRAL	0.1	1.15	8.33	48.87	9.42	30.45	0.68	1.75	0.48	0.12	100.41
75 75 CHR SPOT 2 CENTRAL	0.1	1.42	7.25	48.59	9.61	30.16	0.75	1.71	0.4	0.16	99.19
78 78 CHR *232258 103.8m CENTRAL	0.15	1.25	6.68	50.26	9.19	30.17	0.59	1.61	0.4	0.15	99.53
79 79 CHR CENTRAL SPOT 2	0.08	1.16	11.95	46.65	7.48	29.68	0.51	2.65	0.49	0.2	100.1
80 80 CHR * 232259 108.5m L CENTRAL	0.06	1.99	11.75	44.02	7.82	30.63	0.53	2.45	0.26	0.14	98.87
81 81 CHR AT MARGIN SPOT 2	0.06	1.53	10.25	43.4	10.19	29.71	0.74	2.08	0.55	0.14	97.63
82 82 CHR CENTRAL SPOT 3	0.08	1.5	12.18	42.87	8.83	29.40	0.66	2.58	0.37	0.15	97.73
83 83 CHR CENTRAL SPOT 3	0.07	1.45	12.39	43.36	9.15	29.65	0.58	2.72	0.33	0.25	99.03
84 84 CHR CENTRAL SPOT 4	0.13	1.14	13.09	45.57	6.48	29.33	0.68	2.54	0.47	0.15	98.93
85 85 CHR CENTRAL W HOLE	0.11	1.66	12.23	44.24	8.52	30.54	0.59	2.35	0.37	0.18	99.93
87 87 CHR CENTRAL W HOLE	0.05	1.54	12.3	44.13	8.14	30.34	0.62	2.42	0.36	0.13	99.21
88 88 CHR ANOTHER CENTRAL	0.04	1.72	11.62	44.38	8.78	30.55	0.64	2.41	0.38	0.2	99.84
89 89 CHR SMALLER	0.12	1.49	10.75	43.94	11.11	30.49	0.53	2.15	0.42	0.23	100.12
90 90 CHR SMALLER	0.08	1.48	9.58	44.76	10.07	30.12	0.64	1.98	0.39	0.08	98.17
92 92 CHR * 232261 120.5m GRAIN 1	0.1	1.93	10.15	44.23	10.57	30.53	0.8	2.19	0.45	0.18	100.07
93 93 CHR * 232262 135.0m GRAIN 1	0.15	2.02	10.06	44.55	10.42	31.17	0.65	2.02	0.28	0.08	100.36

Big Daddy FW-08-19

	SiO2	TiO2	Al2O3	Cr2O3	Fe2O3	FeO	MnO	MgO	ZnO	NiO	TOTAL
94 94 CHR GRAIN 2	0.13	1.85	9.92	45.16	9.96	30.47	0.69	2.18	0.35	0.17	99.88
95 95 CHR L CENTRAL	0.05	1.53	11.8	45.76	8.10	30.58	0.52	2.54	0.29	0.22	100.58
96 96 CHR L CENTRAL	0.11	1.67	11.25	44.87	7.69	29.44	0.6	2.58	0.24	0.22	97.9
97 97 CHR ANOTHER	0.07	1.52	12.58	43.04	9.99	29.13	0.63	3.26	0.38	0.2	99.8
99 99 CHR ANOTHER	0.05	1.4	12.76	42.25	10.07	29.14	0.47	3.29	0.18	0.14	98.74
100 100 CHR AT MARGIN	0.15	1.29	12.17	43.22	10.20	29.08	0.68	2.79	0.39	0.11	99.06
102 102 CHR L CENTRAL	0.1	1.1	12.44	44.74	8.54	29.03	0.53	3.01	0.29	0.07	98.99
103 103 CHR * 232263 137.63m CENTRAL	0.08	0.89	14.74	44.42	6.80	29.02	0.64	3.13	0.33	0.13	99.5
104 104 CHR NEAR MARGIN	0.09	0.93	14.3	44.23	6.81	28.30	0.66	3.29	0.39	0.12	98.44
105 105 CHR SMALLER	0.04	0.97	14.52	44.88	6.35	27.81	0.58	4.04	0.17	0.11	98.83
106 106 CHR SURR HOLE	0.06	1.29	13.18	46.4	5.85	29.69	0.6	2.82	0.42	0.2	99.92
107 107 CHR SURR HOLE	0.05	1.33	12.14	45.62	6.67	29.12	0.74	2.77	0.27	0.24	98.28
108 108 CHR LARGER	0.06	0.92	13.78	45.12	5.94	27.96	0.63	3.49	0.12	0.16	97.59
109 109 CHR LARGER	0.06	0.94	14.78	44.84	5.62	28.17	0.67	3.58	0.25	0.09	98.44
110 110 CHR LARGER	0.05	0.9	14.24	45.39	6.03	28.93	0.63	3.15	0.29	0.15	99.16
111 111 CHR CENTRAL	0.01	1.03	14.81	44.86	6.27	28.41	0.63	3.82	0.26	0.19	99.66
112 112 CHR * 232264 141.5m CENTRAL S-1 09-03-454E	0.01	0.42	13.1	53.45	4.69	17.16	0.5	10.92	0.05	0.14	99.97
113 113 CHR CENTRAL SPOT 1	0	0.53	12.6	51.87	4.83	17.24	0.43	10.53	0.03	0.05	97.63
114 114 CHR AT MARGIN SPOT 2	0.09	0.45	12.5	52.32	4.32	22.94	0.55	6.73	0.19	0.21	99.86
115 115 CHR CENTRAL SPOT 3	0.01	0.45	12.66	53.25	4.57	17.41	0.44	10.58	0.04	0.16	99.11
116 116 CHR AT MARGIN SPOT 4	0.04	0.43	12.11	50.93	4.80	23.52	0.58	6.19	0.01	0.21	98.34
117 117 CHR CENTRAL SPOT 5	0	0.5	12.52	52.98	4.10	20.70	0.45	8.59	0.09	0.07	99.59
118 118 CHR AT MARGIN SPOT 6	0.08	0.43	12.83	52.48	4.18	23.97	0.45	6.37	0.21	0.16	100.74
119 119 CHR AT MARGIN SPOT 6	0.04	0.44	11.99	51.91	4.96	23.81	0.6	6.3	0.06	0.12	99.73
120 120 CHR CENTRAL SPOT 7	0	0.4	12.79	53.67	5.00	17.96	0.4	10.57	0.02	0.13	100.44
121 121 CHR CENTRAL SPOT 7	0	0.45	12.2	52.68	4.56	17.67	0.55	10.02	0.17	0.13	97.97
122 122 CHR CENTRAL SPOT 7	0	0.45	13	53.23	3.83	17.82	0.4	10.37	0	0.15	98.87
123 123 CHR SMALLER SPOT 8	0.05	0.38	11.89	51.71	5.30	24.12	0.58	5.96	0.21	0.14	99.81
124 124 CHR V SMALL SPOT 9	0.01	0.48	12.64	51.68	4.38	23.22	0.63	6.75	0.15	0.1	99.61
125 125 CHR CENTRAL SPOT 10	0	0.42	13.3	52.69	4.65	17.12	0.46	10.86	0.04	0.15	99.22
126 126 CHR AT MARGIN SPOT 11	0.02	0.43	13.28	50.38	4.40	23.69	0.46	6.43	0.08	0.15	98.88
127 127 CHR LARGE CENTRAL SPOT 12	0.02	0.5	13.83	52.43	4.27	17.98	0.31	10.53	0	0.2	99.64
128 128 CHR * 232265 141.9m CENTRAL S-1 09-03-454E	0	0.36	13.92	52.7	4.27	15.81	0.45	11.68	0.07	0.15	98.98
129 129 CHR INT SPOT 2	0	0.36	13.84	52.35	5.23	15.79	0.55	11.74	0.02	0.21	99.57
130 130 CHR AT MARGIN SPOT 3	0	0.46	14.44	51.79	3.87	18.78	0.4	9.9	0.27	0.16	99.68
131 131 CHR CENTRAL SPOT 4	0	0.39	14.38	52.84	4.56	16.26	0.44	11.69	0.08	0.26	100.44
132 132 CHR CENTRAL SPOT 4	0	0.36	14.08	53.38	4.24	16.47	0.38	11.56	0.06	0.2	100.3
133 133 CHR CENTRAL SPOT 4	0	0.4	13.57	52.17	3.96	15.97	0.43	11.28	0.05	0.17	97.6
135 135 CHR CENTRAL SPOT 4	0	0.48	13.66	52.67	3.94	16.51	0.48	11.25	0.02	0.09	98.71
136 136 CHR AT MARGIN SPOT 5	0	0.33	14.51	51.55	4.27	18.41	0.42	10.16	0.1	0.07	99.39
137 137 CHR CENTRAL SPOT 6	0	0.37	14.47	52.22	4.04	18.47	0.31	10.32	0.02	0.17	99.98
138 138 CHR SMALLER SPOT 7	0	0.41	14.96	51.63	3.89	16.49	0.32	11.47	0.02	0.16	98.96
139 139 CHR SMALL SPOT 8	0	0.47	14.54	50.94	4.81	19.65	0.4	9.57	0.13	0.11	100.13
140 140 CHR SMALL SPOT 8	0	0.42	13.86	51.71	3.79	19.12	0.47	9.4	0.16	0.19	98.74
142 142 CHR V SMALL SPOT 9	0	0.43	13.31	52.97	3.67	20.02	0.44	9.01	0.22	0.13	99.83
144 144 CHR * 232266 CENTRAL SPOT 1	0	0.43	14.04	53.38	3.88	16.65	0.38	11.41	0.11	0.18	100.07
145 145 CHR CENTRAL SPOT 1	0	0.36	13.42	53.58	4.96	16.62	0.36	11.45	0.11	0.18	100.54
146 146 CHR CENTRAL SPOT 1	0	0.41	12.45	52.91	4.43	15.90	0.41	11.21	0.12	0.11	97.51
147 147 CHR CENTRAL SPOT 1	0	0.43	14.12	51.87	4.52	16.19	0.32	11.53	0.05	0.17	98.75
148 148 CHR AT MARGIN SPOT 2	0	0.41	13.41	53.35	3.83	18.18	0.42	10.27	0.09	0.14	99.72
149 149 CHR CENTRAL SPOT 3	0	0.34	14.28	52.39	5.02	16.35	0.34	11.64	0.08	0.19	100.12
150 150 CHR CENTRAL SPOT 3	0	0.49	13.34	51.22	4.81	15.96	0.32	11.31	0.07	0.15	97.19
151 151 CHR AT MARGIN SPOT 4	0	0.46	13.82	51.47	4.88	18.30	0.47	10.13	0.11	0.17	99.32
152 152 CHR CENTRAL SPOT 5	0	0.46	14.83	52.52	4.17	16.72	0.32	11.63	0.04	0.17	100.44
153 153 CHR CENTRAL SPOT 5	0	0.41	14.45	51.28	4.77	16.36	0.3	11.44	0.18	0.09	98.8
154 154 CHR AT MARGIN SPOT 6	0	0.4	13.42	52.94	3.84	19.23	0.41	9.57	0.16	0.08	99.67
155 155 CHR CENTRAL SPOT 7	0	0.4	13.97	52.42	5.10	16.49	0.4	11.48	0.11	0.19	100.05
156 156 CHR SMALLER SPOT 8	0	0.52	13.61	52.35	3.65	18.86	0.29	9.9	0.1	0.02	98.94
157 157 CHR V SMALL SPOT 9	0	0.4	13.19	52.21	4.57	19.27	0.45	9.42	0.18	0.08	99.31
158 158 CHR * 232267 142.95m CENTRAL S-1 09-03-455I	0	0.38	14.07	52.92	4.04	17.07	0.37	11.03	0.12	0.23	99.82
159 159 CHR AT MARGIN SPOT 2	0	0.4	13.11	52.72	4.31	19.90	0.52	9.05	0.18	0.1	99.86
160 160 CHR CENTRAL SPOT 3	0	0.44	12.56	52.92	4.01	17.19	0.45	10.42	0.19	0.08	97.86
161 161 CHR CENTRAL SPOT 3	0	0.46	14.31	52.43	4.55	17.70	0.42	10.85	0.1	0.19	100.56
162 162 CHR CENTRAL SPOT 3	0	0.42	14.08	52.25	4.29	17.48	0.38	10.79	0.05	0.17	99.48
163 163 CHR AT MARGIN SPOT 4	0	0.52	14.27	51.23	4.46	19.51	0.41	9.56	0.06	0.2	99.77
164 164 CHR CENTRAL SPOT 5	0	0.49	14.3	52.49	4.37	17.65	0.53	10.89	0	0.14	100.42
165 165 CHR CENTRAL SPOT 5	0	0.38	13.91	51.87	4.83	17.62	0.49	10.56	0.12	0.13	99.43
166 166 CHR AT MARGIN SPOT 6	0	0.48	13.63	51.53	4.24	19.88	0.5	9.01	0.16	0.15	99.15
167 167 CHR CENTRAL SPOT 7	0	0.47	14.33	51.12	4.76	17.48	0.35	10.75	0.09	0.18	99.05
168 168 CHR V SMALL SPOT 8	0	0.48	14.13	51.55	3.96	19.72	0.48	9.27	0.15	0.11	99.45
171 171 CHR BRIGHT AT MARGIN	0.02	0.28	3.39	65.68	1.47	23.19	0.58	5.87	0.23	0.06	100.62
172 172 CHR * 232268 144.29m C CENTRAL SPOT 1	0	0.99	13.25	45.31	7.54	26.13	0.53	4.95	0.21	0.26	98.42
173 173 CHR AT MARGIN SPOT 2	0	3.64	12.55	45.95	4.00	28.73	0.67	5.08	0.3	0.19	100.71
176 176 CHR AT MARGIN SPOT 2	0	0.88	12.99	46.45	6.69	26.21	0.51	4.81	0.2	0.23	98.3
177 177 CHR CENTRAL SPOT 3	0.01	1.01	14.24	45.98	6.45	27.02	0.54	4.77	0.3	0.11	99.79
179 179 CHR SMALLER	0	0.89	12.31	46.69	6.93	26.97	0.64	4.3	0.12	0.08	98.23
181 181 CHR CENTRAL	0.01	0.97	13.2	46.29	6.08	26.26	0.51	4.91	0.01	0.08	97.71
182 182 CHR CENTRAL	0	0.95	14.09	47.08	5.08	26.38	0.49	5.02	0.21	0.17	98.96
184 184 CHR ANOTHER	0	1.82	12.02	46.04	5.97	26.86	0.53	4.75	0.15	0.2	97.75

Big Daddy FW-08-19

	SiO2	TiO2	Al2O3	Cr2O3	Fe2O3	FeO	MnO	MgO	ZnO	NiO	TOTAL
185 185 CHR ANOTHER	0	0.92	14.05	45.47	6.94	26.32	0.49	5.12	0.08	0.16	98.86
186 186 CHR INT AT MARGIN	0.1	0.81	2.53	55.41	10.08	28.14	0.69	2.45	0.14	0.16	99.5
188 188 CHR CENTRAL	0.06	0.93	14.5	46	6.45	26.31	0.44	5.16	0.2	0.12	99.53
189 189 CHR * 232269 161.3m CENTRAL SPOT 1 09-04-45E	0.14	1.17	14.62	44.28	6.40	28.11	0.7	3.59	0.2	0.16	98.73
190 190 CHR AT MARGIN SPOT 2	0.09	0.78	15.35	44.03	7.02	28.40	0.51	3.7	0.15	0.12	99.45
192 192 CHR CENTRAL SPOT 3	0.09	0.91	15.64	45.2	6.00	28.28	0.52	4.01	0.15	0.22	100.42
193 193 CHR CENTRAL SPOT 3	0.06	0.89	14.96	45.01	6.42	28.25	0.59	3.89	0.16	0.1	99.69
194 194 CHR AT MARGIN SPOT 4	0.09	0.73	15.32	44.67	6.56	28.65	0.51	3.52	0.22	0.12	99.73
195 195 CHR AT MARGIN SPOT 4	0.06	0.92	15.1	44.86	6.60	28.79	0.64	3.58	0.24	0.16	100.28
196 196 CHR CENTRAL SPOT 5	0.07	0.88	15.67	44.56	6.01	28.38	0.57	3.75	0.25	0.2	99.74
197 197 CHR AT MARGIN SPOT 6	0.09	0.83	15.38	43.99	7.28	28.58	0.52	3.62	0.31	0.14	100.01
199 199 CHR AT MARGIN SPOT 6	0.07	0.77	14.37	44.29	7.23	28.24	0.68	3.44	0.28	0.06	98.71
201 201 CHR CENTRAL SPOT 7	0.04	0.87	15.55	44.37	7.00	28.94	0.6	3.66	0.22	0.19	100.74
203 203 CHR SMALLER SPOT 8	0.08	0.79	14.45	43.82	7.13	28.10	0.55	3.47	0.2	0.13	98.01
204 204 CHR V SMALL SPOT 9	0.05	0.78	15.35	44.7	6.34	28.55	0.55	3.64	0.24	0.16	99.72
207 207 CHR * 232270 CENTRAL SPOT 2	0.08	1.89	11.19	39.47	13.10	30.84	0.65	2.07	0.14	0.15	98.26
209 209 CHR ANOTHER	0.11	1.77	0.59	35.19	30.65	31.15	0.75	0.71	0.27	0.09	98.21
210 210 CHR * 232271 182.2m CENTRAL SPOT 1 09-04-45E	0.1	1.68	10.66	40.05	13.41	30.53	0.61	1.95	0.24	0.19	98.08
211 211 CHR INT SPOT 2	0.23	1.57	1.08	37.01	28.29	29.99	0.76	0.94	0.17	0.13	97.33
217 217 CHR * 232272 SPOT 1	0	0.52	14.01	50.97	3.45	20.18	0.71	8.58	0	0.27	98.34
220 220 CHR SPOT 1	0.03	0.54	14.32	51.25	4.54	20.50	0.59	8.76	0.08	0.42	100.58
221 221 CHR SPOT 1	0.02	0.63	13.14	50.68	4.73	19.79	0.67	8.74	0	0.34	98.27
222 222 CHR AT MARGIN SPOT 2	0.01	0.62	11.98	50.4	5.73	20.14	0.78	8.26	0	0.27	97.61
223 223 CHR AT MARGIN SPOT 2	0.07	0.56	13.59	50.38	5.23	20.60	0.78	8.3	0	0.24	99.22
224 224 CHR CENTRAL SPOT 3	0	0.57	14.11	50.9	5.09	20.83	0.78	8.59	0.01	0.39	100.76
225 225 CHR CENTRAL SPOT 3	0	0.55	14.12	50.05	4.50	20.50	0.73	8.46	0.04	0.27	98.77
226 226 CHR SPOT 4	0	0.52	13.81	51.16	4.21	21.09	0.79	8.2	0	0.24	99.6
227 227 CHR CENTRAL SPOT 5	0.03	0.58	13.84	50.21	4.29	20.23	0.75	8.43	0	0.31	98.24
228 228 CHR CENTRAL SPOT 5	0	0.52	14.01	50.02	4.86	20.20	0.69	8.64	0	0.35	98.8
229 229 CHR AT MARGIN SPOT 6	0.01	0.58	13.68	50.81	3.74	20.52	0.68	8.28	0	0.38	98.31
230 230 CHR CENTRAL SPT 7	0	0.54	14.05	51.25	4.80	20.75	0.7	8.65	0.06	0.34	100.66
231 231 CHR CENTRAL SPT 7	0.02	0.54	14.02	51.34	3.76	20.64	0.7	8.47	0	0.28	99.39
232 232 CHR AT MARGIN SPOT 8	0.02	0.54	13.43	51.76	3.74	21.30	0.63	8.03	0.01	0.24	99.32
233 233 CHR SMALLER SPOT 9	0.02	0.64	13.86	51.17	3.56	20.51	0.63	8.5	0	0.32	98.86
234 234 CHR SMALLER SPOT 10	0.05	0.62	13.57	51.54	4.06	20.63	0.67	8.43	0	0.3	99.46
235 235 CHR * 232273 184.0m SPOT 1 09-19-4442	0.03	0.49	14.19	50.66	4.50	21.03	0.69	8.23	0.01	0.31	99.69
236 236 CHR AT MARGIN SPOT 2	0	0.55	13.47	51.63	4.39	21.76	0.73	7.92	0	0.26	100.27
237 237 CHR CENTRAL SPOT 3	0.02	0.48	14.4	50.45	3.93	20.99	0.66	8.22	0	0.23	98.99
238 238 CHR AT M SPOT 4	0.04	0.52	14.08	50.81	4.94	21.48	0.64	8.14	0	0.28	100.43
239 239 CHR SPOT 5	0.01	0.54	13.58	51.23	4.44	19.86	0.73	8.86	0	0.32	99.13
240 240 CHR AT MARGIN SPOT 6	0	0.42	13.04	50.84	4.83	21.00	0.64	7.99	0	0.27	98.54
241 241 CHR SMALLER SPOT 7	0.03	0.5	13.66	50.67	4.40	20.63	0.74	8.19	0	0.34	98.72
242 242 CHR SPOT 8	0	0.58	13.83	51.35	4.29	21.80	0.72	7.97	0	0.26	100.37
243 243 CHR SPOT 8	0.02	0.49	13.63	51.19	4.20	21.20	0.75	8	0.01	0.25	99.32
244 244 CHR SPOT 9	0	0.56	13.62	50.72	5.00	21.62	0.66	8.03	0	0.23	99.94
245 245 CHR SPOT 10	0.02	0.6	13.43	52.2	3.77	21.78	0.65	7.86	0.07	0.32	100.32
246 246 CHR * 232274 184.4m SPOT 1 CENTRAL, 08-19-44	0	0.57	14.06	51.51	4.31	19.35	0.51	9.59	0	0.27	99.74
247 247 CHR SPOT 2	0.01	0.55	14.05	51.08	3.76	21.76	0.64	7.84	0.01	0.3	99.62
248 248 CHR CENTRAL, SPOT 3	0.02	0.52	13.94	51.34	4.03	21.18	0.62	8.22	0.04	0.26	99.76
249 249 CHR SPOT 4	0.01	0.51	13.72	50.75	4.00	21.32	0.66	7.93	0.02	0.19	98.71
250 250 CHR CENTRAL SPOT 5	0.01	0.56	13.83	49.87	4.94	20.38	0.63	8.5	0	0.34	98.57
251 251 CHR AT M SPOT 6	0.03	0.56	13.62	51.27	4.07	21.46	0.75	7.92	0	0.2	99.47
252 252 CHR SPOT 7	0.01	0.58	13.57	49.99	5.13	20.88	0.76	8.22	0	0.2	98.83
253 253 CHR SMALLER SPOT 8	0	0.52	13.86	51.33	4.17	21.56	0.7	8.05	0	0.23	100
254 254 CHR SMALLER SPOT 9	0	0.55	13.57	50.19	4.50	21.12	0.68	7.97	0.07	0.23	98.43
255 255 CHR SMALLER SPOT 9	0	0.54	13.89	51.87	3.64	21.72	0.72	7.97	0	0.27	100.26
257 257 CHR * 232275 SPOT 1	0	0.73	14.24	50.23	4.29	20.40	0.61	8.79	0	0.35	99.21
258 258 CHR AT MARGIN SPOT 2	0.03	0.69	13.9	50.96	4.11	21.24	0.72	8.17	0	0.31	99.72
259 259 CHR ANOTHER GRAIN SPOT 3	0.06	0.72	14.15	50.77	4.46	21.04	0.64	8.47	0	0.21	100.07
260 260 CHR SMALLER SPOT 2	0	0.67	14.11	49.99	4.28	21.29	0.64	8.12	0.02	0.29	98.98
261 261 CHR ANOTHER SPOT 4	0	0.7	13.85	50.21	4.79	21.24	0.63	8.23	0.02	0.36	99.55
262 262 CHR SMALLER GRAIN 5	0.02	0.66	14.08	50.26	4.94	21.21	0.53	8.39	0	0.3	99.9
263 263 CHR SMALLER SPOT 6	0	0.72	13.91	50.11	4.20	21.29	0.67	8.09	0	0.3	98.87
264 264 CHR ANOTHER SMALLER	0	0.69	13.15	51.02	4.92	21.47	0.71	8.03	0	0.35	99.85
265 265 CHR ANOTHER	0	0.79	13.24	50.17	5.15	21.67	0.66	7.93	0	0.32	99.41
266 266 CHR ANOTHER SMALLER GRAIN	0.01	0.65	12.72	51.13	5.28	22.18	0.68	7.57	0	0.28	99.97
267 267 CHR V SMALL	0	0.69	13.23	50.77	4.27	21.99	0.71	7.57	0	0.29	99.09
268 268 CHR * 232276 195.2m L CENTRAL S-1, 08-19-444	0.01	0.54	14.33	49.64	5.07	20.11	0.66	8.86	0	0.2	98.91
269 269 CHR AT MARGIN SPOT 2	0.03	0.5	14.01	50.75	4.73	20.31	0.66	8.7	0	0.27	99.49
270 270 CHR CENTRAL SPOT 3	0	0.55	13.97	51.05	4.96	20.80	0.66	8.71	0	0.21	100.41
271 271 CHR AT MARGIN SPOT 4	0	0.57	13.7	51.02	4.67	20.57	0.72	8.6	0	0.28	99.66
272 272 CHR ANOTHER SPOT 5	0	0.57	13.82	50.66	4.94	20.48	0.59	8.69	0	0.38	99.64
273 273 CHR CENTRAL SPOT 6	0	0.61	14.01	51.09	4.16	20.44	0.64	8.74	0.01	0.33	99.61
274 274 CHR AT MARGIN SPOT 7	0	0.58	13.48	49.99	4.97	20.17	0.62	8.61	0.06	0.22	98.2
275 275 CHR SMALLER SPOT 8	0.02	0.49	13.42	51.58	4.45	20.43	0.68	8.51	0.09	0.27	99.49
276 276 CHR SPOT 9	0	0.55	13.58	50.96	4.87	20.57	0.77	8.52	0.02	0.3	99.65
277 277 CHR V SMALL SPOT 10	0	0.54	13.57	50.61	4.51	20.47	0.7	8.45	0	0.25	98.65
278 278 CHR V SMALL SPOT 10	0	0.46	12.89	50.12	5.56	19.98	0.65	8.47	0.03	0.35	97.95
279 279 CHR V SMALL SPOT 10	0	0.58	13.65	50.41	5.12	20.45	0.65	8.66	0	0.26	99.27

Big Daddy FW-08-19

	SiO2	TiO2	Al2O3	Cr2O3	Fe2O3	FeO	MnO	MgO	ZnO	NiO	TOTAL
280 280 CHR * 232277 185.8m SPOT 1 CENTRAL, 08-19-44	0	0.6	14.17	49.88	5.10	18.10	0.51	10.11	0	0.31	98.27
281 281 CHR SPOT 1 CENTRAL	0.01	0.61	14.16	50.97	5.23	18.16	0.61	10.32	0	0.31	99.85
282 282 CHR AT MARGIN SPOT 2	0	0.64	13.71	50.07	4.91	20.66	0.74	8.44	0	0.24	98.92
283 283 CHR CENTRAL SPOT 3	0	0.63	14.35	50.57	5.01	18.95	0.56	9.88	0.04	0.25	99.73
284 284 CHR AT MARGIN SPOT 4	0.01	0.67	13.68	50.89	4.90	20.52	0.64	8.7	0.02	0.37	99.91
285 285 CHR CENTRAL SPOT 5	0	0.69	13.71	50.44	4.44	20.63	0.78	8.45	0	0.27	98.97
286 286 CHR AT MARGIN SPOT 6	0	0.62	13.67	51.54	4.43	21.12	0.76	8.37	0	0.3	100.37
287 287 CHR AT MARGIN SPOT 6	0.02	0.64	13.57	51.65	4.01	20.99	0.6	8.42	0.02	0.22	99.74
288 288 CHR SMALLER SPOT 7	0	0.63	13.73	51.17	4.13	21.01	0.72	8.31	0	0.31	99.6
289 289 CHR SMALLER SPOT 8	0	0.61	13.3	50.56	4.73	20.84	0.8	8.16	0	0.31	98.84
290 290 CHR V SMALL SPOT 9	0.01	0.65	13.18	51.17	5.29	21.33	0.73	8.19	0	0.32	100.34
291 291 CHR * 232278 186.2m CENTRAL, SPOT 1, 08-19-4	0	0.46	13.49	51.5	4.63	20.26	0.72	8.69	0	0.29	99.58
292 292 CHR AT MARGIN SPOT 2	0	0.58	13.53	51.09	4.70	20.36	0.78	8.66	0.03	0.24	99.5
293 293 CHR SPOT 3	0	0.46	13.12	50.61	4.85	20.44	0.73	8.23	0.02	0.32	98.29
294 294 CHR SPOT 3	0	0.42	12.66	51.44	5.01	20.38	0.71	8.33	0.04	0.27	98.76
295 295 CHR ANOTHER CENTRAL SPOT 4	0	0.33	12.89	52.13	4.70	20.36	0.69	8.45	0.03	0.3	99.41
296 296 CHR BRIGHT MARGIN SPOT 5	0	0.25	4.13	66.05	-0.16	22.62	0.91	5.99	0	0.3	100.11
297 297 CHR ANOTHER CENTRAL, SPOT 6	0	0.48	13.07	51.79	5.05	20.37	0.74	8.66	0	0.28	99.93
298 298 CHR ANOTHER CENTRAL, SPOT 6	0	0.4	13.23	51.01	5.62	20.35	0.7	8.63	0	0.25	99.62
299 299 CHR BRIGHT MARGIN W INCL, SPOT 7	0.04	0.13	4.17	65.71	0.34	22.35	0.76	6.09	0.03	0.2	99.79
300 300 CHR CENTRAL SPOT 8	0	0.38	12.97	51.29	5.39	20.40	0.79	8.4	0	0.33	99.41
301 301 CHR AT MARGIN 9	0	0.46	12.94	51.18	4.37	20.30	0.7	8.28	0	0.35	98.14
302 302 CHR AT MARGIN 9	0	0.41	13.08	51.28	4.98	20.26	0.79	8.49	0.05	0.2	99.04
303 303 CHR SPOT 10	0	0.41	13.14	50.52	4.75	20.14	0.7	8.36	0	0.27	97.82
304 304 CHR SPOT 10	0	0.48	12.94	50.54	5.61	20.46	0.64	8.4	0	0.32	98.83
305 305 CHR SPOT 11	0.01	0.41	12.89	50.8	4.63	19.92	0.65	8.43	0.02	0.25	97.55
306 306 CHR SPOT 11	0	0.43	13.33	50.79	5.66	20.09	0.63	8.77	0.04	0.34	99.51
307 307 CHR * 232279 186.6m SPOT 1 CENTRAL, 08-20-44	0	0.58	13.78	50.67	4.43	19.12	0.66	9.25	0.06	0.38	98.49
308 308 CHR SPOT 1 CENTRAL	0	0.63	13.61	51.16	4.93	19.60	0.72	9.21	0.03	0.36	99.76
309 309 CHR AT MARGIN SPOT 2	0	0.56	12.95	52.08	4.69	20.30	0.68	8.71	0	0.36	99.86
310 310 CHR ANOTHER SPOT 3	0	0.54	13.5	51.38	4.70	19.87	0.65	8.94	0	0.43	99.54
311 311 CHR CENTRAL SPOT 4	0	0.59	13.43	51.54	3.77	19.84	0.73	8.75	0	0.42	98.69
312 312 CHR AT MARGIN SPOT 5	0	0.58	13.49	52.25	4.29	20.24	0.65	8.98	0.09	0.2	100.34
313 313 CHR SMALLER SPOT 6	0	0.57	13.22	52.09	4.44	20.08	0.81	8.85	0	0.3	99.91
314 314 CHR SPOT 7	0	0.59	12.88	51.77	5.22	20.26	0.66	8.82	0	0.32	100
316 316 CHR SMALLER SPOT 8	0	0.56	12.98	52.19	4.48	19.77	0.84	8.91	0	0.35	99.63
317 317 CHR ANOTHER SPOT 9	0	0.61	13.38	51.39	4.70	20.15	0.73	8.78	0.02	0.39	99.68
318 318 CHR V SMALL SPOT 10	0	0.62	11.82	52.98	4.36	20.35	0.78	8.43	0	0.29	99.2
319 319 CHR ** 232280 187.0m SPOT 1, CENTRAL, 08-20	0	0.61	14.33	50.87	3.62	19.35	0.66	9.32	0	0.24	98.64
320 320 CHR AT MARGIN SPOT 2	0	0.52	13.58	51.23	4.69	19.25	0.69	9.3	0	0.32	99.11
321 321 CHR SPOT 3	0	0.55	13.3	50.78	4.59	19.19	0.6	9.18	0	0.28	98.01
323 323 CHR SPOT 3	0	0.48	14.27	50.51	4.19	18.88	0.61	9.4	0.04	0.4	98.36
324 324 CHR SPOT 3	0	0.5	14.56	50.49	4.68	18.94	0.68	9.6	0	0.4	99.38
325 325 CHR CENTRAL SPOT 4	0	0.52	14.63	50.99	4.75	19.55	0.65	9.54	0	0.28	100.43
326 326 CHR AT MARGIN SPOT 5	0	0.53	14.21	50.92	4.46	19.59	0.63	9.27	0	0.3	99.46
327 327 CHR ANOTHER SPOT 6	0	0.51	14.54	50.54	4.54	18.58	0.6	9.87	0	0.32	99.05
328 328 CHR SMALLER SPOT 7	0	0.51	14.54	51.21	4.68	19.29	0.65	9.65	0	0.34	100.4
329 329 CHR SMALLER SPOT 7	0.05	0.54	14.46	50.4	4.28	18.59	0.64	9.57	0	0.39	98.49
330 330 CHR V SMALL SPOT 9	0	0.52	14.15	51.23	4.19	19.72	0.65	9.14	0.01	0.34	99.53
331 331 CHR * 232281 187.4m L GRAIN CENTRAL, 08-20-4	0	0.53	14.23	51.84	3.97	19.82	0.59	9.33	0	0.23	100.14
332 332 CHR AT MARGIN	0	0.5	14.32	51.63	4.28	19.71	0.59	9.39	0	0.28	100.27
333 333 CHR CENTRAL SPOT 1	0	0.5	14.53	51.36	3.97	18.92	0.62	9.7	0.04	0.34	99.58
334 334 CHR AT MARGIN SPOT 2	0	0.45	14.73	50.98	4.86	19.52	0.7	9.5	0	0.32	100.58
335 335 CHR AT MARGIN SPOT 2	0	0.46	14.72	50.64	4.77	19.17	0.68	9.59	0	0.34	99.9
336 336 CHR CENTRAL SPOT 3	0	0.57	14.39	51.16	4.34	19.57	0.72	9.39	0	0.27	99.98
337 337 CHR AT MARGIN SPOT 4	0	0.51	15.25	50.97	4.26	19.40	0.67	9.77	0	0.19	100.59
339 339 CHR L C ENTRAL SPOT 5	0	0.49	13.68	51.38	4.82	17.71	0.68	10.23	0	0.35	98.86
340 340 CHR L C ENTRAL SPOT 5	0	0.47	14.56	50.62	5.08	18.32	0.63	10.08	0	0.41	99.66
341 341 CHR AT MARGIN SPOT 6	0	0.53	14.26	50.64	4.52	19.08	0.68	9.49	0	0.3	99.05
342 342 CHR C SPOT 7	0	0.53	13.61	51.4	5.41	17.86	0.6	10.39	0	0.29	99.55
343 343 CHR SMALLER SPOT 8	0	0.53	14.27	51.62	3.89	19.84	0.64	9.21	0	0.27	99.88
344 344 CHR SMALLER SPOT 9	0	0.46	14.52	49.69	5.04	19.13	0.63	9.38	0	0.34	98.68
345 345 CHR SMALLER SPOT 9	0.03	0.49	14.66	51.07	4.25	19.48	0.71	9.34	0	0.28	99.89
346 346 CHR * 232282 187.8m L CENTRAL SPOT 1, 08-20	0	0.48	14.4	51.5	4.46	18.61	0.6	9.98	0	0.37	99.95
347 347 CHR AT MARGIN SPOT 2	0	0.54	14.14	51.91	4.33	19.11	0.68	9.71	0	0.32	100.31
348 348 CHR AT MARGIN SPOT 2	0	0.54	13.71	51.02	4.40	18.56	0.65	9.63	0	0.35	98.42
349 349 CHR AT MARGIN SPOT 2	0.03	0.55	14.11	51.6	3.88	18.86	0.59	9.65	0	0.27	99.15
350 350 CHR CENTRAL SPOT 3	0.03	0.49	14.02	51.59	4.69	18.97	0.69	9.61	0	0.33	99.95
351 351 CHR AT MARGIN SPOT 4	0.02	0.51	13.93	52.05	3.95	19.36	0.61	9.41	0	0.28	99.72
352 352 CHR INT SIZE, SPOT 5	0.02	0.51	13.9	51.27	4.85	19.21	0.65	9.42	0.01	0.38	99.73
354 354 CHR SMALLER SPOT 7	0	0.51	13.69	51.33	4.51	19.11	0.66	9.42	0	0.3	99.08
355 355 CHR SMALLER SPOVY 8	0.03	0.55	14.18	52.32	3.99	19.40	0.64	9.45	0.15	0.35	100.66
356 356 CHR SMALLER SPOVY 8	0.02	0.47	13.95	51.02	4.69	19.00	0.61	9.39	0.11	0.36	99.15
358 358 CHR V SMALL SPPOT 9	0.02	0.47	13.97	51.49	5.04	19.32	0.66	9.45	0.05	0.33	100.3
359 359 CHR * 232283 188.2m S 1 CENTRAL, 08-20-4456	0.03	0.54	14.65	50.66	4.75	18.93	0.73	9.69	0	0.3	99.81
360 360 CHR AT MARGIN SPOT 2	0.01	0.54	14.05	50.71	4.58	19.37	0.59	9.3	0.16	0.17	99.02
361 361 CHR CENTRAL SPOT 3	0.02	0.54	14.73	51.02	4.10	19.33	0.62	9.51	0	0.32	99.78
362 362 CHR AT MARGIN SPOT 4	0.04	0.53	14.29	51.62	4.64	19.54	0.74	9.39	0.05	0.26	100.63
363 363 CHR AT MARGIN SPOT 4	0.05	0.57	12.73	50.48	5.26	18.71	0.72	9.19	0	0.17	97.35

Big Daddy FW-08-19

	SiO2	TiO2	Al2O3	Cr2O3	Fe2O3	FeO	MnO	MgO	ZnO	NiO	TOTAL
364 364 CHR CENTRAL SPOT 5	0.02	0.52	14.57	49.99	4.74	19.33	0.54	9.31	0.07	0.35	98.96
365 365 CHR AT MARGIN SPOT 6	0.03	0.52	13.93	51.12	3.99	19.45	0.71	9.02	0	0.33	98.7
366 366 CHR SMALLER SPOT 8	0	0.61	14.53	50.79	4.74	19.54	0.69	9.52	0	0.28	100.22
367 367 CHR SMALLER SPOT 8	0.02	0.57	13.66	49.69	4.94	18.82	0.7	9.25	0	0.26	97.41
369 369 CHR SMALLER SPOT 8	0.04	0.52	14.23	50.61	3.51	19.27	0.52	9.1	0	0.27	97.72
370 370 CHR SMALLER SPOT 9	0.03	0.55	14.07	51.25	4.38	19.60	0.65	9.24	0	0.23	99.56
371 371 CHR * 232284 188.6m CENTRAL, S 1, 08-20-4457	0	0.52	14.17	52.04	4.45	18.33	0.58	10.19	0	0.46	100.29
372 372 CHR CENTRAL SPOT 1	0	0.52	13.88	51.99	4.26	18.32	0.59	10.06	0	0.37	99.56
373 373 CHR AT MARGIN SPOT 2	0.06	0.47	13.67	51.55	4.67	18.98	0.57	9.42	0	0.32	99.25
374 374 CHR CENTRAL SPOT 3	0	0.49	13.72	51.83	4.27	19.59	0.52	9.26	0.05	0.31	99.61
375 375 CHR SPOT 4 AT MARGIN	0.04	0.57	13.78	51.67	3.79	19.57	0.61	9.07	0.01	0.32	99.05
376 376 CHR CENTRAL SPOT 5	0	0.61	13.44	51.23	4.61	17.76	0.54	10.19	0	0.4	98.32
377 377 CHR CENTRAL SPOT 5	0.02	0.56	14.11	52.4	4.44	17.25	0.52	10.92	0	0.39	100.17
378 378 CHR AT MARGIN SPOT 6	0	0.57	13.67	50.44	4.86	19.28	0.57	9.22	0	0.41	98.53
379 379 CHR SMALLER SPOT 7	0	0.53	13.48	51.34	4.16	19.49	0.61	9.09	0	0.29	98.57
380 380 CHR SMALLER SPOT 8	0	0.58	13.68	51.97	4.22	20.02	0.7	9.04	0	0.31	100.1
381 381 CHR V SMALL SPOT 9	0	0.55	13.62	51.67	3.62	19.86	0.61	8.91	0.02	0.27	98.77
382 382 CHR * 232285 189.0m SPOT 1, C, 08-21-445E	0	0.6	14.02	51.87	3.96	20.14	0.68	9.04	0	0.33	100.24
383 383 CHR AT MARGIN SPOT 2	0	0.53	14.24	52.38	3.11	19.95	0.59	9.19	0	0.23	99.91
384 384 CHR CENTRAL SPOT 3	0	0.57	13.87	50.92	4.88	19.86	0.69	9.05	0.08	0.31	99.74
385 385 CHR 4 AT MARGIN	0	0.6	13.6	52.05	3.51	20.15	0.56	8.9	0.04	0.23	99.29
386 386 CHR CENTRAL SPOT 5	0	0.59	13.38	50.7	4.98	19.20	0.56	9.31	0	0.34	98.56
387 387 CHR CENTRAL SPOT 5	0	0.62	13.53	50.02	4.86	18.86	0.69	9.29	0.1	0.28	97.76
388 388 CHR CENTRAL SPOT 5	0	0.58	13.8	51.85	4.54	20.20	0.67	9.06	0.09	0.22	100.56
389 389 CHR AT MARGIN SPOT 6	0.01	0.44	13.77	51.62	3.95	19.79	0.53	8.99	0	0.28	98.98
390 390 CHR CENTRAL SPOT 7	0	0.54	13.44	52.14	4.09	19.53	0.73	9.15	0.05	0.31	99.57
391 391 CHR SMALLER SPOT 8	0	0.53	13.6	52.25	3.78	20.06	0.59	9.04	0	0.17	99.64
392 392 CHR V SMALL SPOT 9	0	0.5	13.37	52.66	3.82	20.14	0.63	8.94	0	0.22	99.9
393 393 CHR * 232286 189.4m C, SPOT 1, 08-21-445E	0.02	0.56	14.5	52.1	3.79	19.66	0.55	9.5	0	0.32	100.62
394 394 CHR C, SPOT 1	0	0.54	13.97	51.33	4.82	19.76	0.66	9.21	0.15	0.28	100.23
395 395 CHR C, SPOT 1	0	0.48	14.23	52.46	3.61	20.08	0.57	9.23	0	0.21	100.51
396 396 CHR SPOT 3	0	0.57	14.54	50.75	4.78	19.12	0.64	9.7	0	0.37	99.99
397 397 CHR SPOT 4	0	0.57	14.42	50.12	4.41	19.67	0.59	9.18	0	0.24	98.76
398 398 CHR SPOT 5	0	0.61	14.05	50.26	4.83	19.43	0.68	9.27	0	0.29	98.94
399 399 CHR SPOT 7	0	0.6	13.85	51.58	4.10	19.73	0.68	9.16	0	0.33	99.62
400 400 CHR ANOTHER SPOT 7	0	0.58	15.32	53.03	2.05	19.63	0.62	9.73	0	0.23	100.99
401 401 CHR ANOTHER SPOT 7	0	0.65	14.83	52.28	2.38	19.70	0.61	9.44	0.06	0.21	99.92
403 403 CHR V SMALL SPOT 9	0	0.65	14.72	50.94	3.13	19.48	0.66	9.31	0.01	0.29	98.87
404 404 CHR * 232287 189.8m CENT SPOT 1, 08-21-446C	0.02	0.53	13.95	50.54	4.95	18.88	0.66	9.52	0	0.3	98.85
405 405 CHR AT M SPOT 2	0	0.5	14.18	51.74	4.39	20.04	0.6	9.15	0.07	0.31	100.54
406 406 CHR ANOTHER SPOT 3	0	0.59	13.85	51.7	4.64	19.74	0.7	9.24	0.03	0.41	100.44
407 407 CHR ANOTHER SPOT 3	0.01	0.49	13.49	51.22	4.57	19.03	0.56	9.35	0.03	0.33	98.62
408 408 CHR CENTRAL SPOT 4	0	0.59	14.34	50.49	4.90	19.69	0.62	9.32	0	0.31	99.77
410 410 CHR AT M SPOT 5	0	0.5	14.26	51.66	4.07	19.87	0.71	9.2	0	0.22	100.08
411 411 CHR SMALLER SPOT 7	0	0.58	14.13	51.81	4.20	19.33	0.68	9.59	0	0.28	100.18
412 412 CHR SMALLER SPOT 8	0	0.55	13.85	52.09	4.26	20.30	0.67	8.96	0	0.35	100.61
413 413 CHR SMALLER SPOT 8	0	0.51	13.79	50.22	4.47	19.59	0.65	8.9	0	0.28	97.96
414 414 CHR SMALLER SPOT 8	0	0.52	13.43	51.43	5.06	19.75	0.73	9.11	0	0.27	99.79
415 415 CHR V SMALL SPOT 9	0.21	0.59	14.77	51.64	3.72	18.59	0.62	9.62	0.03	0.16	99.58
416 416 CHR * 232288 190.2m C SPOT 1 08-21-4461	0	0.63	13.69	50.8	5.45	19.91	0.68	9.18	0	0.29	100.08
417 417 CHR SPOT 1	0	0.48	13.6	51.27	4.12	19.97	0.71	8.76	0	0.24	98.74
418 418 CHR AT MARGIN SPOT 2	0	0.5	13.77	51.7	4.84	20.25	0.66	9.03	0	0.21	100.48
419 419 CHR CENTRAL SPOT 3	0.02	0.61	13.67	51.67	4.85	19.47	0.69	9.36	0	0.4	100.26
420 420 CHR AT MARGIN SPOT 4	0	0.65	13.52	50.79	5.22	19.75	0.74	9.11	0	0.32	99.58
421 421 CHR ANOTHER SPOT 5	0.01	0.62	13.17	51.75	4.68	20.18	0.66	8.84	0	0.32	99.76
422 422 CHR ANOTHER SPOT 6	0.01	0.68	13.35	51.15	4.63	20.29	0.56	8.83	0	0.25	99.29
423 423 CHR ANOTHER SPOT 7	0.02	0.66	13.15	51.72	4.82	20.18	0.68	8.88	0	0.28	99.91
424 424 CHR SMALLER SPOT 8	0	0.57	13.12	52.36	4.77	20.50	0.63	8.75	0.12	0.34	100.68
425 425 CHR SMALLER SPOT 8	0	0.59	12.78	52.98	3.90	20.11	0.73	8.86	0	0.23	99.79
426 426 CHR V SMALL SPOT 9	0	0.64	13.27	52	4.81	20.46	0.68	8.89	0	0.26	100.53
427 427 CHR V SMALL SPOT 9	0	0.61	12.77	50.82	4.51	19.92	0.71	8.54	0	0.29	97.72
428 428 CHR V SMALL SPOT 9	0	0.61	13.05	52.24	4.57	20.27	0.74	8.87	0	0.22	100.11
429 429 CHR * 232289 190.6m C, SPOT 1, 08-21-4462	0.02	0.48	13.17	50.3	5.97	19.35	0.62	9.13	0	0.27	98.71
431 431 CHR AT MARGIN SPOT 2	0.03	0.38	13.96	49.83	6.15	19.33	0.73	9.16	0.03	0.28	99.27
432 432 CHR CENTRAL SPOT 3	0	0.39	13.1	50.5	6.10	19.51	0.69	9.04	0	0.23	98.95
433 433 CHR AT MARGIN SPOT 4	0	0.43	13.6	50.92	5.34	19.98	0.7	8.91	0.05	0.22	99.62
434 434 CHR CENTRAL SPOT 5	0	0.39	12.1	50.87	5.97	19.30	0.67	8.76	0.04	0.34	97.85
436 436 CHR SMALLER SPOT 5	0	0.41	12.61	50.33	5.77	19.82	0.65	8.55	0	0.3	97.87
437 437 CHR SMALLER SPOT 5	0.01	0.4	13.25	51.38	5.27	20.40	0.65	8.61	0	0.27	99.71
440 440 CHR ANOTHER SPOT 6	0.01	0.46	12.66	51.76	5.87	18.99	0.62	9.42	0.07	0.35	99.62
441 441 CHR ANOTHER SPOT 7	0	0.39	13.71	51.45	5.17	20.11	0.67	8.93	0	0.31	100.22
442 442 CHR SMALLER SPOT 8	0	0.47	14.03	50.64	5.57	20.09	0.74	8.95	0	0.4	100.33
443 443 CHR V SMALL SPOT 9	0	0.47	13.51	51.11	5.03	20.59	0.66	8.56	0	0.28	99.71
446 446 CHR * 232290 C SPOT 1	0	0.53	13.77	50.83	5.18	19.58	0.6	9.26	0.03	0.31	99.57
447 447 CHR AT MARGIN SPOT 2	0	0.48	14.17	50.95	4.30	20.48	0.58	8.73	0	0.24	99.5
448 448 CHR CENTRAL SPOT 3	0	0.53	14.13	51.3	4.38	20.68	0.52	8.74	0	0.36	100.2
449 449 CHR AT MARGIN SPOT 4	0	0.51	13.58	51.61	4.72	19.92	0.64	9.06	0	0.3	99.86
450 450 CHR CENTRAL SPOT 6	0	0.55	13.9	50.94	4.72	20.27	0.69	8.79	0.08	0.29	99.76
451 451 CHR AT MARGIN SPOT 4	0.03	0.55	13.83	51.52	4.14	20.48	0.64	8.65	0.03	0.24	99.7

Big Daddy FW-08-19

	SiO2	TiO2	Al2O3	Cr2O3	Fe2O3	FeO	MnO	MgO	ZnO	NiO	TOTAL
452 452 CHR CENTRAL SPOT 5	0	0.54	14.09	50.78	4.55	20.18	0.66	8.85	0	0.34	99.53
453 453 CHR AT AMRGIN SPOT 6	0.01	0.52	13.88	50.65	4.19	20.29	0.62	8.59	0	0.28	98.61
454 454 CHR AT AMRGIN SPOT 6	0	0.56	13.89	51.43	4.23	20.70	0.7	8.54	0.04	0.35	100.02
455 455 CHR SMALLER SPOT 7	0	0.54	13.75	51.93	3.37	20.91	0.62	8.35	0	0.31	99.44
456 456 CHR SMALLER SPOT 8	0	0.59	14.05	51.62	4.12	20.75	0.64	8.67	0	0.37	100.4
457 457 CHR V SMALL SPOT 9	0.01	0.58	13.85	51.71	3.90	20.63	0.65	8.59	0.11	0.26	99.9
458 458 CHR * 232291 191.6m C SPOT 1, 08-21-4464	0	0.56	13.87	51.31	4.15	20.52	0.64	8.69	0	0.25	99.58
459 459 CHR AT MARGIN SPOT 2	0.01	0.62	13.77	51.23	3.61	21.18	0.61	8.17	0	0.26	99.1
461 461 CHR CENTRAL SPOT 3	0	0.57	13.88	49.83	4.82	20.06	0.69	8.67	0	0.33	98.36
462 462 CHR AT MARGIN SPOT 4	0.02	0.51	14.06	49.79	5.34	21.08	0.67	8.2	0	0.3	99.44
463 463 CHR CENTRAL SPOT 5	0.02	0.52	14.07	51.09	3.97	20.54	0.64	8.57	0	0.24	99.26
464 464 CHR AT MARGIN SPOT 6	0.01	0.61	13.91	50.82	4.51	21.00	0.63	8.41	0.03	0.25	99.73
465 465 CHR SPOT 7	0	0.62	13.7	50.95	4.42	21.26	0.68	8.13	0.06	0.36	99.74
466 466 CHR SMALLER SPOT 8	0	0.63	13.8	51.36	4.18	21.43	0.62	8.22	0.02	0.3	100.14
467 467 CHR V SMALL SPOT 9	0	0.56	14.01	51.48	3.96	21.16	0.68	8.3	0	0.37	100.12
468 468 CHR * 232292 192.2m SPOT 1 C 08-21-4465	0	1.02	13.82	51.06	3.66	22.39	0.59	7.91	0	0.28	100.36
469 469 CHR AT M SPOT 2	0.02	0.9	13.92	50.9	3.58	22.05	0.63	7.92	0	0.21	99.77
470 470 CHR CENTRAL SPOT 3	0	0.73	13.19	51.26	4.37	21.92	0.72	7.8	0.01	0.25	99.81
471 471 CHR AT MARGIN SPOT 4	0	0.8	13.11	51.4	3.35	21.99	0.73	7.58	0.02	0.23	98.88
472 472 CHR CENTRAL SPOT 5	0	0.88	13.41	50.29	4.51	21.57	0.65	8.04	0.03	0.26	99.19
473 473 CHR ANAOTHER SPOT 7	0	0.82	13.98	51.33	3.58	21.90	0.57	8.1	0.01	0.28	100.21
474 474 CHR SMALLER SPOT 8	0.02	0.83	13.3	50.66	4.51	21.80	0.72	7.85	0	0.23	99.47
475 475 CHR * 232293 192.6m C SPOT 1, 08-21-4466	0	0.48	14.4	52.41	3.93	19.04	0.58	9.88	0	0.32	100.65
476 476 CHR C SPOT 1	0	0.6	14.11	51.98	4.37	18.79	0.59	10.04	0	0.28	100.33
477 477 CHR AT MARGIN SPOT 2	0.02	0.54	14.12	51.48	4.52	20.82	0.61	8.64	0.01	0.36	100.66
478 478 CHR AT MARGIN SPOT 2	0	0.54	13.83	51.25	4.77	20.61	0.69	8.68	0	0.32	100.21
479 479 CHR CENTRAL SPOT 3	0.02	0.52	14.1	51.19	4.47	20.06	0.58	8.93	0.06	0.38	99.86
480 480 CHR AT MARGIN SPOT 4	0	0.55	13.83	50.76	5.02	20.87	0.69	8.52	0	0.24	99.98
481 481 CHR CENTRAL SPOT 5	0.02	0.6	13.92	51.44	4.31	20.18	0.57	8.93	0.06	0.33	99.93
484 484 CHR AT MARGIN SPOT 6	0.01	0.48	14.05	52.11	3.47	21.54	0.56	8.14	0	0.3	100.31
485 485 CHR AT MARGIN SPOT 6	0.05	0.53	13.97	50.54	4.88	20.33	0.63	8.63	0	0.3	99.37
486 486 CHR SMALLER SPOT 7	0	0.57	13.92	51.36	4.31	20.60	0.59	8.68	0	0.39	99.99
487 487 CHR SMALLER SPOT 8	0.06	0.47	13.3	51.08	5.08	20.29	0.61	8.47	0.01	0.36	99.22
488 488 CHR V SMALL SPOT 9	0.01	0.48	14.01	50.62	4.62	20.77	0.7	8.37	0	0.31	99.43
489 489 CHR * 232294 193.4m C SPOT 1 08-21-4467	0	0.55	14.26	51.4	5.00	18.49	0.56	10.2	0	0.36	100.32
491 491 CHR AT MARGIN SPOT 2	0	0.56	14.02	50.79	4.49	19.17	0.59	9.45	0	0.32	98.94
493 493 CHR CENTRAL SPOT 3	0	0.52	13.69	51.37	4.71	18.59	0.5	9.87	0	0.3	99.08
494 494 CHR AT MARGIN SPOT 4	0	0.57	13.75	52.2	3.99	20.51	0.75	8.77	0.04	0.25	100.43
495 495 CHR CENTRAL SPOT 5	0	0.51	13.29	51.19	4.91	19.19	0.58	9.3	0	0.35	98.83
497 497 CHR AT MARGIN SPOT 6	0.01	0.55	13.16	51.63	4.56	19.07	0.75	9.29	0	0.29	98.86
498 498 CHR CENTRAL SPOT 7	0	0.55	13.65	50.97	5.71	18.79	0.69	9.76	0.04	0.36	99.95
499 499 CHR SMALLER SPOT 8	0	0.59	13.76	51.01	5.22	19.97	0.61	9.13	0	0.37	100.13
500 500 CHR V SMALL SPOT 9	0	0.59	13.15	50.89	5.22	19.76	0.69	8.92	0	0.39	99.09
501 501 CHR * 232295 193.4m CENTRAL, SPT 1 08-21-446	0	0.55	14.43	51.88	3.79	20.20	0.65	9.12	0	0.28	100.52
502 502 CHR CENTRAL, SPOT 1	0.04	0.55	14.42	50.8	4.97	19.70	0.73	9.22	0	0.35	100.28
503 503 CHR AT MARGIN SPOT 2	0.04	0.58	14.27	51.25	4.35	19.29	0.55	9.5	0	0.32	99.71
505 505 CHR CENTRAL SPOT 3	0	0.61	13.68	51.13	4.93	19.30	0.6	9.5	0	0.29	99.55
506 506 CHR AT MARGIN SPOT 4	0.01	0.59	13.5	51.71	3.69	20.46	0.57	8.61	0	0.25	99.02
507 507 CHR CENTRAL SPOT 5	0.02	0.61	14.23	50.71	4.68	18.88	0.62	9.71	0	0.3	99.29
509 509 CHR AT MARGIN SPOT 6	0.01	0.57	13.99	51.77	4.00	19.70	0.67	9.23	0	0.29	99.83
510 510 CHR SMALLER SPOT 7	0	0.58	13.09	51.85	4.69	18.98	0.72	9.42	0.01	0.39	99.26
511 511 CHR SMALLER SPOT 8	0.02	0.5	14.21	51.55	4.57	19.27	0.67	9.56	0	0.26	100.15
512 512 CHR V SMALL SPOT 10	0	0.55	13.86	52.66	3.43	20.05	0.66	9.05	0	0.35	100.27
514 514 CHR V SMALL SPOT 10	0	0.58	13.32	51.45	4.50	19.26	0.65	9.36	0	0.18	98.85
515 515 CHR * 232296 193.8m C SPOT 1 08-22-4465	0.02	0.6	13.95	49.73	4.60	20.83	0.73	8.16	0	0.29	98.45
516 516 CHR C SPOT 1	0	0.55	13.87	50.32	5.06	20.44	0.61	8.67	0.07	0.26	99.35
517 517 CHR AT MARGIN SPOT 2	0	0.97	12.86	50.37	3.72	20.82	0.69	8.15	0	0.25	97.46
518 518 CHR AT MARGIN SPOT 2	0	0.57	12.37	50.13	5.36	20.32	0.63	8.2	0.01	0.28	97.33
519 519 CHR AT MARGIN SPOT 2	0	0.58	13.57	51.5	4.59	20.85	0.65	8.57	0	0.24	100.09
520 520 CHR CENTRAL SPOT 3	0	0.59	14.03	49.92	5.51	19.96	0.48	9.09	0	0.39	99.41
521 521 CHR CENTRAL SPOT 3	0	0.55	13.4	50.97	4.49	20.16	0.63	8.63	0	0.38	98.76
522 522 CHR CENTRAL SPOT 5	0	0.55	13.92	51.34	4.11	20.58	0.54	8.68	0	0.33	99.64
523 523 CHR AT MARGIN SPOT 6	0	0.58	13.73	51.42	4.11	20.41	0.56	8.79	0.01	0.22	99.42
524 524 CHR SMALLER SPOT 7	0	0.59	13.12	50.61	5.16	20.21	0.58	8.63	0.06	0.33	98.77
525 525 CHR SMALLER SPOT 8	0	0.64	13.19	50.55	4.20	20.20	0.59	8.53	0	0.24	97.72
526 526 CHR SMALLER SPOT 8	0	0.64	13.14	50.73	4.74	20.51	0.66	8.48	0	0.24	98.66
527 527 CHR V SMALL SPOT 8	0	0.55	13.41	50.26	4.54	20.22	0.57	8.49	0	0.32	97.9
529 529 CHR * 232297 194.2m CENTRAL, SPOT 1, 08-22-4	0	0.84	14.5	51.02	3.38	20.31	0.63	9.12	0	0.17	99.63
530 530 CHR AT MARGIN SPOT 2	0	0.75	13.07	50.72	5.00	20.46	0.66	8.66	0	0.23	99.05
531 531 CHR CENTRAL SPOT 3	0	0.85	13.97	50.98	4.18	20.18	0.52	9.2	0.03	0.23	99.72
532 532 CHR AT MARGIN SPOT 4	0	0.92	13.48	49.95	4.02	21.24	0.66	8.12	0	0.2	98.18
533 533 CHR AT MARGIN SPOT 4	0	0.83	13.04	51.13	4.72	20.65	0.58	8.67	0.08	0.22	99.44
534 534 CHR CENTRAL SPOT 5	0	0.73	14.91	50.73	3.09	19.85	0.59	9.24	0.07	0.22	99.12
535 535 CHR AY MARGIN SPOY 7	0	0.83	13.37	50.44	4.34	20.45	0.65	8.63	0.04	0.19	98.51
536 536 CHR SMALLER SPOT 7	0	1.57	13.55	50.97	3.00	21.09	0.66	8.86	0.06	0.22	99.68
537 537 CHR SMALLER SPOT 8	0	0.38	13.91	52.68	3.52	20.17	0.56	9	0	0.2	100.07
538 538 CHR V SMALL SPOT 9	0	0.94	12.91	50.35	5.02	20.72	0.57	8.59	0	0.24	98.84
539 539 CHR * 232298 194.6m CENTRAL SPOT 1, 08-22-44	0	0.61	14.12	50.11	5.11	19.52	0.51	9.41	0.01	0.22	99.11
540 540 CHR AT MARGIN SPOT 2	0	0.61	13.27	50.88	5.52	19.51	0.6	9.33	0	0.24	99.41

Big Daddy FW-08-19

	SiO2	TiO2	Al2O3	Cr2O3	Fe2O3	FeO	MnO	MgO	ZnO	NiO	TOTAL
541 541 CHR CENTRAL SPOT 3	0	0.55	13.98	51.12	4.86	18.81	0.6	9.83	0.01	0.25	99.53
542 542 CHR CENTRAL SPOT 3	0	0.62	14.22	51.08	4.62	19.54	0.61	9.52	0	0.24	99.99
543 543 CHR ANOTHER SPOT 5	0	0.61	13.09	50.87	5.01	19.41	0.56	9.18	0	0.29	98.52
544 544 CHR ANOTHER SPOT 5	0	0.56	13.84	51.01	4.97	19.78	0.64	9.18	0.05	0.28	99.81
545 545 CHR SMALLER SPOT 8	0	0.59	14.29	50.59	4.05	19.85	0.57	9.09	0	0.24	98.87
546 546 CHR SMALLER SPOT 7	0	0.57	14.13	51.09	5.15	19.78	0.57	9.43	0	0.29	100.5
547 547 CHR SMALLER SPOT 8	0	0.61	13.27	51.32	4.19	19.37	0.68	9.14	0	0.25	98.41
548 548 CHR V SMALL SPOT 9	0	0.62	12.98	52.14	4.43	19.95	0.61	9.04	0	0.23	99.55
549 549 CHR * 232299 195.0m CENTRAL, S 1, 08-22-447?	0	0.56	13.41	51.06	5.15	18.26	0.55	9.97	0	0.33	98.77
550 550 CHR AT MARGIN SPOT 2	0	0.55	13.73	52.17	4.36	19.26	0.69	9.52	0.03	0.34	100.22
551 551 CHR CENTRAL SPOT 3	0	0.57	13.12	50.57	5.03	18.37	0.46	9.74	0	0.25	97.6
552 552 CHR CENTRAL SPOT 3	0	0.54	13.97	50.29	5.41	18.42	0.71	9.86	0	0.32	98.97
553 553 CHR AT MARGIN SPOT 4	0	0.61	14.05	51.68	4.05	20.04	0.48	9.24	0	0.26	100.01
554 554 CHR CENTRAL SPOT 5	0	0.57	13.61	50.22	5.14	18.85	0.48	9.57	0	0.28	98.2
556 556 CHR CENTRAL SPOT 5	0	0.52	13.91	49.66	5.65	19.13	0.58	9.37	0.05	0.3	98.6
557 557 CHR SMALLER SPOT 6	0.01	0.53	14.24	50.03	4.65	19.41	0.66	9.12	0	0.36	98.54
558 558 CHR SMALLER SPOT 6	0	0.58	13.95	51.06	4.85	19.68	0.66	9.28	0	0.31	99.88
559 559 CHR CENTRAL SPOT 7	0	0.51	14.15	51.18	4.60	19.77	0.61	9.22	0	0.34	99.92
560 560 CHR SMALLER SPOT 8	0	0.57	14.06	51.2	4.59	20.15	0.75	8.99	0	0.28	100.13
561 561 CHR V SMALL SPOT 9	0	0.57	13.69	51.29	4.81	20.07	0.65	9.05	0	0.23	99.87
562 562 CHR * 232300 195.4m CENTRAL, SPOT 1, 08-22-4	0	0.45	14.48	50.53	5.01	17.81	0.57	10.35	0	0.33	99.03
564 564 CHR AT MARGIN SPOT 2	0	0.54	13.98	50.9	4.23	18.40	0.63	9.79	0	0.31	98.35
565 565 CHR AT MARGIN SPOT 2	0	0.57	13.99	50.92	4.82	18.69	0.62	9.83	0	0.29	99.25
566 566 CHR CENTRAL SPOT 3	0	0.54	14.37	51.04	5.26	16.74	0.74	11.12	0	0.29	99.57
568 568 CHR AT MARGIN SPOT 4	0.03	0.54	13.89	51.87	4.05	18.62	0.5	9.84	0	0.3	99.24
569 569 CHR CENTRAL SPOT 5	0	0.5	13.95	51.32	5.21	17.35	0.64	10.62	0	0.42	99.48
570 570 CHR AT MARGIN SPOT 6	0	0.52	13.84	50.96	5.33	18.64	0.76	9.81	0	0.29	99.61
571 571 CHR SPOT 7	0.05	0.54	14.15	51.58	4.51	17.71	0.5	10.41	0.02	0.33	99.35
572 572 CHR V SMALL SPOT 9	0	0.58	14.38	51.86	4.07	19.22	0.71	9.71	0	0.28	100.41
573 573 CHR * 232301 195.8m CENTRAL, S 1, 08-22-447?	0	0.47	14.36	51.69	5.13	16.30	0.68	11.46	0	0.3	99.87
574 574 CHR AT MARGIN SPOT 2	0	0.45	14.4	51.05	5.35	16.96	0.45	11.1	0	0.3	99.52
575 575 CHR CENTRAL SPOT 3	0	0.48	14.17	51.88	4.80	16.50	0.54	11.35	0	0.26	99.5
576 576 CHR AT MARGIN SPOT 4	0	0.57	14.13	51.92	4.59	18.25	0.51	10.41	0	0.27	100.19
577 577 CHR ANOTHER SPOT 5	0	0.49	14.12	50.79	5.04	17.40	0.53	10.6	0	0.28	98.75
579 579 CHR ANOTHER SPOT 6	0	0.54	14.55	51.42	4.87	18.31	0.59	10.4	0	0.28	100.47
580 580 CHR SMALLER SPOT 8	0	0.49	14.48	51.73	4.65	17.91	0.67	10.48	0	0.37	100.31
581 581 CHR SMALLER SPOT 8	0	0.51	14.2	51.51	4.98	17.84	0.52	10.56	0	0.33	99.95
582 582 CHR V SMALL SPOT 9	0	0.52	14.64	50.57	4.90	18.15	0.55	10.28	0.04	0.3	99.46
584 584 CHR * 232302 CENTRAL, S 1	0	0.57	14.04	51.12	4.08	17.14	0.57	10.59	0	0.33	98.03
585 585 CHR CENTRAL, S 1	0	0.58	14.02	50.56	5.05	16.93	0.58	10.84	0	0.26	98.31
586 586 CHR CENTRAL, S 1	0	0.55	14.23	51.3	4.36	16.95	0.57	10.88	0	0.32	98.72
587 587 CHR AT MARGIN SPOT 2	0	0.61	13.9	50.59	4.83	19.48	0.58	9.34	0	0.27	99.12
588 588 CHR CENTRAL SPOT 2	0	0.6	14.42	50.87	4.84	17.42	0.57	10.72	0	0.37	99.32
589 589 CHR AT MARGIN SPOT 4	0	0.54	13.81	51.12	4.68	18.47	0.63	9.82	0	0.37	98.97
590 590 CHR CENTRAL SPOT 5	0	0.53	14.3	50.82	4.59	18.70	0.66	9.79	0	0.31	99.24
591 591 CHR CENTRAL SPOT 6	0	0.52	13.93	51.09	5.29	18.62	0.62	9.94	0	0.33	99.81
592 592 CHR SMALLER SPOT 7	0	0.51	13.93	51.47	4.61	19.01	0.78	9.55	0	0.32	99.72
593 593 CHR SMALLER SPOT 8	0	0.59	13.92	51.54	4.34	19.63	0.54	9.33	0	0.39	99.84
594 594 CHR V SMALL SPOT 9	0	0.51	13.81	52.24	4.34	19.68	0.64	9.34	0	0.33	100.46
595 595 CHR * 232303 196.6m CENTRAL S 1 08-23-447?	0	0.67	14.32	50.58	5.53	17.30	0.65	10.94	0	0.24	99.68
596 596 CHR AT MARGIN SPOT 2	0	0.67	14.15	50.54	4.80	19.82	0.57	9.28	0	0.29	99.64
597 597 CHR CENTRAL SPOT 3	0	0.64	14.01	50.2	5.62	19.49	0.71	9.44	0	0.25	99.8
598 598 CHR AT MARGIN SPOT 4	0	0.56	14.18	50.35	5.21	19.76	0.59	9.24	0	0.32	99.69
599 599 CHR CENTRAL SPOT 5	0	0.66	14.12	51.03	4.96	20.10	0.7	9.19	0	0.31	100.58
600 600 CHR CWNTRAL SPOT 5	0	0.6	14.4	50.22	4.64	19.87	0.6	9.15	0	0.27	99.29
601 601 CHR SMALLER SPOT 7	0	0.55	14.27	50.17	4.89	19.61	0.59	9.25	0	0.28	99.12
602 602 CHR SMALLER SPOT 8	0	0.56	14.13	50.1	4.81	19.77	0.55	9.09	0	0.29	98.82
603 603 CHR V SMALL SPOT 9	0	0.57	14.09	49.59	5.48	20.07	0.62	8.94	0	0.23	99.04
604 604 CHR * 232304 197.0m CENTRAL S 1, 08-23-447?	0	0.55	14.74	49.57	5.42	18.90	0.68	9.72	0.04	0.31	99.39
605 605 CHR AT MARGIN SPOT 2	0	0.47	14.63	49.98	4.87	19.10	0.64	9.57	0	0.17	98.94
606 606 CHR CENTRAL SPOT 3	0	0.54	14.28	49.64	5.17	18.35	0.57	9.89	0	0.28	98.2
607 607 CHR CENTRAL SPOT 3	0	0.62	14.32	49.83	5.60	18.73	0.7	9.86	0	0.28	99.38
608 608 CHR AT MARGIN SPOT 4	0	0.61	14.56	50.33	4.79	19.37	0.6	9.56	0.03	0.27	99.64
609 609 CHR CENTRAL SPOT 5	0	0.57	14.66	48.96	5.18	19.44	0.64	9.26	0	0.24	98.43
610 610 CHR CENTRAL SPOT 5	0	0.57	14.64	49.27	5.05	19.32	0.56	9.41	0	0.25	98.57
611 611 CHR CENTRAL SPOT 5	0	0.52	14.62	50.71	4.80	19.67	0.62	9.42	0	0.29	100.17
612 612 CHR AT MARGIN SPOT 6	0	0.54	14.57	49.53	4.91	19.33	0.64	9.25	0.11	0.3	98.69
613 613 CHR CENTRAL SPOT 7	0	0.49	14.79	49.43	5.16	18.75	0.62	9.74	0	0.26	98.72
614 614 CHR SMALLER SPOT 8	0	0.5	14.89	50.76	4.82	19.70	0.69	9.48	0	0.27	100.63
615 615 CHR CXENTRAL SPOT 5	0	0.53	14.67	50.3	4.67	19.57	0.64	9.35	0	0.29	99.55
616 616 CHR AT MARGIN SPOT 6	0	0.55	14.57	49.7	4.78	19.54	0.61	9.29	0	0.19	98.75
617 617 CHR CENTRAL SPOT 7	0	0.56	14.58	50.62	5.08	19.34	0.6	9.7	0	0.27	100.24
618 618 CHR SMALLER SPOT 7	0	0.51	14.73	50.19	4.51	19.36	0.55	9.43	0.05	0.29	99.17
619 619 CHR V SMALL SPPT 8	0	0.45	14.54	50.44	5.05	19.55	0.67	9.35	0	0.28	99.83
620 620 CHR * 232305 197.4m CENTRAL S 1 08-23-447?	0	0.41	13.37	51.4	5.82	18.19	0.64	10.06	0	0.31	99.62
621 621 CHR AT MARGIN SPOT 2	0	0.41	14.14	49.29	6.68	19.18	0.69	9.48	0	0.24	99.44
622 622 CHR CENTRAL SPOT 3	0	0.39	13.35	50.53	5.85	19.98	0.59	8.85	0	0.28	99.24
623 623 CHR AT MARGIN SPOT 4	0	0.36	13.32	51.12	6.10	20.48	0.62	8.72	0.07	0.23	100.41
624 624 CHR CENTRAL SPOT 5	0	0.45	13.27	50.49	5.71	19.40	0.62	9.16	0	0.25	98.78

Big Daddy FW-08-19

	SiO2	TiO2	Al2O3	Cr2O3	Fe2O3	FeO	MnO	MgO	ZnO	NiO	TOTAL
625 625 CHR AT MARGIN SPOT 6	0	0.42	13.67	50.05	6.72	19.86	0.62	9.15	0	0.28	100.1
626 626 CHR CENTRAL SPOT 7	0	0.39	13.84	48.47	6.95	19.40	0.66	9.06	0	0.28	98.36
627 627 CHR CENTRAL SPOT 7	0	0.46	13.95	49.03	6.50	19.65	0.7	9.04	0	0.29	98.97
628 628 CHR SMALLER SPOT 8	0	0.42	13.52	48.46	6.98	19.17	0.69	9.06	0.04	0.28	97.92
629 629 CHR SMALLER SPOT 8	0	0.42	13.94	48.07	7.22	19.56	0.74	8.97	0	0.26	98.46
630 630 CHR SMALLER SPOT 8	0	0.44	14.13	49.72	6.40	20.18	0.61	9.03	0	0.25	100.12
631 631 CHR V SMALL SPOT 9	0	0.45	13.97	49.22	6.60	20.14	0.59	8.85	0.03	0.36	99.55
632 632 CHR * 232306 197.8m CENTRAL S 1 08-23-448C	0.02	0.49	14.4	50.09	5.23	19.39	0.66	9.32	0.06	0.25	99.38
634 634 CHR AT MARGIN SPOT 2	0	0.42	14.15	51.89	4.08	19.81	0.67	9.15	0	0.3	100.06
635 635 CHR CENTRAL SPOT 3	0	0.53	14.02	49.73	5.84	19.15	0.7	9.43	0	0.31	99.13
636 636 CHR AT MARGIN SPOT 4	0	0.47	13.47	51.59	4.26	19.89	0.54	8.95	0	0.26	99
637 637 CHR CENTRAL SPOT 5	0	0.52	14.49	50.41	5.10	19.91	0.71	9.19	0	0.26	100.08
638 638 CHR AT MARGINS SPOT 6	0.01	0.52	14.48	50.7	4.87	19.73	0.63	9.31	0	0.29	100.05
639 639 CHR SMALLER SPOT 7	0	0.44	14.36	49.95	5.72	19.55	0.73	9.24	0.04	0.31	99.77
640 640 CHR SPOT 8	0	0.47	14.42	50.85	4.89	19.66	0.62	9.34	0.07	0.25	100.08
641 641 CHR V SMALL SPOT 9	0.09	0.55	14.11	50.48	5.96	19.58	0.67	9.26	0.04	0.25	100.4
642 642 CHR * 232307 198.2m CENTRAL S 1 08-23-448I	0	0.58	14.29	50.19	5.34	19.62	0.58	9.4	0	0.29	99.75
643 643 CHR AT MARGIN SPOT	0.03	0.56	14.17	49.96	5.78	19.03	0.67	9.62	0	0.22	99.46
644 644 CHR CENTRAL SPOT 3	0	0.6	13.76	50.4	5.06	18.68	0.59	9.76	0	0.21	98.55
645 645 CHR AT MARGIN SPOT 4	0.03	0.61	14.5	49.83	5.55	18.94	0.55	9.81	0	0.25	99.51
646 646 CHR CENTRAL SPOT 5	0.07	0.57	14.13	50.85	5.39	18.46	0.54	9.97	0	0.34	99.78
647 647 CHR AT MARGIN SPOT 6	0	0.51	14.26	50.23	5.06	19.49	0.51	9.39	0	0.25	99.19
648 648 CHR SMALLER SPOT 7	0	0.58	13.78	51.15	4.76	19.41	0.71	9.38	0	0.23	99.53
650 650 CHR SMALLER SPOT 8	0.02	0.58	13.43	50.46	5.28	19.18	0.77	9.24	0	0.21	98.64
651 651 CHR V SMALL SPOT 9	0	0.57	14.01	50.37	5.02	19.66	0.58	9.28	0	0.18	99.17
652 652 CHR * 232308 198.6m CENTRAL, S 1 08-23-448J	0.01	0.51	13.97	50.65	5.09	16.98	0.54	10.74	0	0.28	98.26
653 653 CHR CENTRAL, S 1	0	0.55	13.71	50.27	5.06	17.39	0.47	10.41	0	0.28	97.63
654 654 CHR CENTRAL, S 1	0	0.49	14.57	51.3	4.69	16.81	0.61	11.1	0.01	0.29	99.4
655 655 CHR AT MARGIN SPOT 2	0.02	0.55	14.47	50.52	5.38	19.23	0.61	9.71	0	0.24	100.2
656 656 CHR CENTRAL SPOT 3	0	0.58	14.17	50.49	4.89	19.11	0.51	9.7	0.01	0.17	99.14
657 657 CHR CENTRAL SPOT 4	0	0.51	13.68	49.91	5.60	19.36	0.65	9.19	0	0.28	98.62
658 658 CHR CENTRAL SPOT 5	0	0.51	14.03	50.25	5.31	19.11	0.64	9.5	0	0.26	99.08
659 659 CHR CENTRAL SPOT 6	0	0.51	14.32	49.62	5.30	18.63	0.7	9.65	0	0.32	98.52
660 660 CHR CENTRAL SPOT 6	0	0.54	14.64	50.6	4.25	19.33	0.64	9.48	0	0.25	99.3
661 661 CHR CENTRAL SPOT 7	0	0.61	14.53	50.54	4.85	19.61	0.6	9.47	0	0.32	100.04
662 662 CHR SMALLER SPOT 8	0.01	0.51	13.81	50.2	4.57	19.54	0.6	9	0	0.2	97.99
663 663 CHR SMALLER SPOT 8	0	0.47	14.48	50.23	5.14	19.51	0.7	9.3	0	0.32	99.63
664 664 CHR SMALLER SPOT 8	0	0.54	14.5	50.71	4.59	19.69	0.62	9.3	0	0.34	99.83
665 665 CHR V SMALL SPOT 9	0	0.42	14.41	50.09	5.13	19.75	0.63	9.06	0	0.37	99.35
666 666 CHR AT MARGIN SPOT 9	0	0.47	14.17	50.83	4.57	19.82	0.58	9.14	0	0.22	99.34
667 667 CHR * 232309 199.0m CENTRAL, S 1 08-23-448K	0	0.49	14.75	50.61	4.79	19.59	0.58	9.48	0	0.29	100.1
670 670 CHR CENTRAL SPOT 3	0	0.52	14.9	49.69	4.66	19.00	0.65	9.55	0.01	0.34	98.85
671 671 CHR AT MARGIN SPOT 4	0.02	0.53	15.33	50.04	4.73	19.19	0.59	9.75	0.01	0.27	99.99
672 672 CHR CENTRAL SPOT 5	0	0.55	14.77	50.72	4.44	18.72	0.62	9.92	0	0.35	99.65
673 673 CHR CENTRAL SPOT 7	0	0.58	14.72	48.84	5.77	18.45	0.56	9.98	0	0.3	98.63
675 675 CHR SPOT 7	0	0.54	14.71	50.44	5.00	18.86	0.57	9.92	0	0.32	99.86
676 676 CHR SMALLER SPOT 8	0	0.54	14.88	49.42	4.88	19.34	0.55	9.44	0	0.3	98.86
677 677 CHR V SMALL SPOT 9	0	0.56	14.78	50.3	4.74	19.82	0.59	9.32	0	0.31	99.94
679 679 CHR * 232310 199.4m CENTRAL S 1 08-24-448L	0	0.6	14.35	50.6	4.98	18.07	0.59	10.3	0	0.34	99.33
680 680 CHR AT MARGIN SPOT 2	0	0.6	13.82	50.14	4.69	19.98	0.68	8.81	0	0.26	98.51
682 682 CHR CENTRAL SPOT 3	0	0.63	14.12	48.98	5.15	19.16	0.64	9.22	0.04	0.28	97.71
683 683 CHR SPOT 1 AGAIN	0	0.68	14.45	50.36	4.56	18.26	0.56	10.17	0.07	0.25	98.9
684 684 CHR SPOT 1 AGAIN	0	0.63	14.32	49.82	5.29	18.07	0.51	10.25	0	0.31	98.67
685 685 CHR SPOT 1 AGAIN	0	0.61	14.47	50.57	4.74	18.34	0.64	10.16	0	0.24	99.3
686 686 CHR AT MARGIN SPOT 2	0	0.58	14.16	50.85	5.23	19.63	0.74	9.36	0.09	0.28	100.39
687 687 CHR CENTRAL SPOT 3	0	0.63	14.18	49.81	5.10	19.75	0.52	9.24	0	0.23	98.95
688 688 CHR AT MARGIN SPOT 4	0	1.45	13.57	50.71	3.36	20.79	0.61	8.99	0	0.23	99.37
689 689 CHR CENTRAL SPOT 5	0	0.59	14.29	50.42	4.94	19.70	0.59	9.32	0	0.29	99.64
690 690 CHR AT MARGIN SPOT 6	0	0.51	13.95	51.23	4.22	19.43	0.67	9.27	0	0.24	99.09
691 691 CHR SMALLER SPOT 9	0	0.64	14.21	51.37	4.70	20.01	0.65	9.34	0	0.25	100.7
692 692 CHR SMALLER SPOT 8	0	0.59	13.87	49.81	5.54	19.40	0.62	9.29	0	0.29	98.86
693 693 CHR V SMALL SPOT 9	0	0.61	13.81	50.66	4.71	19.75	0.59	9.2	0	0.15	99.01
694 694 CHR * 232312 200.2m CENTRAL S 1 08-24-448M	0	0.48	14.46	49.86	4.87	19.00	0.61	9.46	0.01	0.34	98.6
695 695 CHR CENTRAL S 1	0	0.48	14.27	50.52	4.54	18.80	0.74	9.56	0	0.26	98.71
696 696 CHR CENTRAL S 1	0	0.49	14.48	49.95	4.64	19.03	0.54	9.51	0	0.26	98.44
697 697 CHR CENTRAL S 1	0	0.49	14.48	51.03	3.81	19.27	0.57	9.45	0.01	0.22	98.95
698 698 CHR AT MARGIN SPOT 2	0	0.44	14.44	49.89	4.81	18.95	0.68	9.43	0	0.27	98.43
699 699 CHR AT MARGIN SPOT 2	0	0.51	14.59	50.55	4.49	19.15	0.59	9.58	0	0.3	99.31
700 700 CHR CENTRAL SPOT 3	0	0.45	14.55	49.68	4.89	17.91	0.61	10.07	0.01	0.27	97.95
701 701 CHR CENTRAL SPOT 3	0	0.47	14.4	51.81	4.65	18.42	0.6	10.22	0	0.34	100.44
702 702 CHR AT MARGIN SPOT 4	0	0.5	14.46	50.29	5.10	18.62	0.69	9.87	0	0.25	99.27
703 703 CHR CENTRAL SPOT 5	0	0.5	14.49	50.38	4.32	18.90	0.66	9.56	0	0.27	98.65
704 704 CHR CENTRAL SPOT 5	0	0.5	14.43	50.15	5.05	19.22	0.56	9.5	0	0.34	99.24
705 705 CHR AT MARGIN SPOT 6	0	0.44	14.75	49.54	4.89	18.64	0.65	9.68	0	0.26	98.36
706 706 CHR AT MARGIN SPOT 6	0	0.48	14.61	50.55	4.65	19.45	0.63	9.41	0	0.29	99.61
707 707 CHR SMALLER SPOT 7	0	0.49	14.39	50.39	4.96	18.89	0.66	9.7	0	0.23	99.22
708 708 CHR SMALLER SPOT 8	0	0.46	14.31	51	4.24	19.22	0.58	9.47	0.03	0.22	99.1
709 709 CHR V SMALL SPOT 9	0	0.48	14.65	51.11	4.31	19.15	0.64	9.68	0	0.24	99.83
711 711 CHR * 232314 CENTRAL S 1	0	0.4	14.1	50.23	6.09	18.36	0.68	9.96	0	0.35	99.56

Big Daddy FW-08-19

	SiO2	TiO2	Al2O3	Cr2O3	Fe2O3	FeO	MnO	MgO	ZnO	NiO	TOTAL
712 712 CHR AT MARGIN SPOT 2	0	0.4	13.91	49.77	6.11	18.98	0.61	9.52	0	0.23	98.92
713 713 CHR CENTRAL SPOT 3	0	0.41	13.71	50.91	6.19	18.87	0.67	9.78	0	0.28	100.2
714 714 CHR AT MARGIN SPOT 4	0	0.4	13.77	49.07	6.77	19.16	0.62	9.33	0	0.25	98.69
715 715 CHR CENTRAL SPOT 5	0	0.45	13.85	50.12	6.23	18.67	0.6	9.84	0	0.25	99.39
716 716 CHR AT MARGIN SPOT 6	0	0.38	13.95	49.59	6.82	18.89	0.78	9.58	0.07	0.21	99.59
717 717 CHR CENTRAL SPOT 7	0	0.44	13.84	50.22	5.68	19.09	0.53	9.5	0	0.29	99.02
718 718 CHR SMALLER SPOT 8	0	0.38	13.56	50.37	6.36	19.30	0.63	9.38	0	0.26	99.6
719 719 CHR V SMALL SPOT 2	0	0.38	13.79	49.9	5.92	18.74	0.64	9.54	0	0.27	98.59
720 720 CHR V SMALL SPOT 2	0	0.4	13.79	50.2	6.63	19.13	0.55	9.65	0	0.27	99.96
721 721 CHR * 232318 202.6m CENTRAL S 1 08-24-4487	0.02	0.55	14.85	49.4	5.44	18.15	0.73	10.07	0.03	0.3	99
722 722 CHR AT MARGIN SPOT 2	0	0.5	14.87	50.14	4.91	18.79	0.57	9.89	0	0.3	99.48
723 723 CHR CENTRAL SPOT 3	0	0.47	15.6	50.73	3.07	18.09	0.63	10.18	0.09	0.25	98.8
724 724 CHR AT MARGIN SPOT 4	0	0.6	14.23	49.75	4.92	18.44	0.64	9.79	0.01	0.3	98.19
725 725 CHR AT MARGIN SPOT 4	0	0.53	14.13	49.36	4.99	18.10	0.6	9.8	0.04	0.28	97.33
726 726 CHR AT MARGIN SPOT 4	0	0.57	14.17	50.57	4.95	18.76	0.63	9.81	0	0.27	99.23
727 727 CHR CENTRAL SPOT 5	0	0.54	14.88	50.68	5.06	18.89	0.7	9.98	0	0.31	100.54
728 728 CHR AT MARGIN SPOT 6	0	0.59	14.78	50.27	4.68	18.76	0.7	9.89	0	0.26	99.46
729 729 CHR CENTRAL SPOT 7	0	0.64	14.81	49.98	4.79	18.30	0.7	10.14	0	0.29	99.17
730 730 CHR SMALLER SPOT 8	0.02	0.54	14.49	50.3	4.47	18.43	0.71	9.78	0	0.3	98.59
731 731 CHR SMALLER SPOT 8	0	0.6	14.4	49.7	4.28	18.68	0.59	9.61	0	0.25	97.68
732 732 CHR SMALLER SPOT 8	0	0.59	14.52	50.16	4.70	18.88	0.67	9.67	0.01	0.33	99.06
733 733 CHR V SMALL SPOT 9	0.03	0.59	14.2	50.89	4.46	18.97	0.65	9.61	0	0.24	99.19
735 735 CHR * 232319 CENTRAL S 1 08-24-338E	0.01	0.61	14.7	50.02	5.38	17.33	0.6	10.8	0	0.29	99.21
736 736 CHR AT MARGIN SPOT 2	0.02	0.6	14.54	48.79	5.95	18.63	0.69	9.75	0	0.27	98.65
737 737 CHR AT MARGIN SPOT 2	0.01	0.59	14.32	51.06	4.92	19.29	0.66	9.67	0	0.27	100.3
738 738 CHR AT MARGIN SPOT 4	0	0.64	14.24	49.95	4.91	19.12	0.63	9.43	0.12	0.34	98.89
739 739 CHR CENTRAL SPOT 5	0.06	0.6	14.26	49.65	5.57	18.33	0.56	9.88	0	0.32	98.67
740 740 CHR CENTRAL SPOT 6	0	0.56	14.44	49.88	5.42	18.66	0.57	9.92	0	0.29	99.2
741 741 CHR SMALLER SPOT 7	0	0.56	14.27	50.78	5.16	19.30	0.72	9.61	0	0.24	100.12
742 742 CHR SMALLER SPOT 8	0	0.62	13.83	50.91	4.99	20.20	0.54	9.1	0.01	0.2	99.9
743 743 CHR V SMALL SPOT 9	0.04	0.64	13.87	51.38	4.41	19.60	0.61	9.28	0	0.25	99.64
744 744 CHR * 232320 203.4m CENTRAL S-1 08-24-448E	0	0.53	16.51	51.91	1.81	19.42	0.67	9.9	0	0.2	100.77
745 745 CHR CENTRAL S 1	0	0.58	16.48	50.68	2.45	18.73	0.57	10.17	0.05	0.24	99.71
746 746 CHR AT MARGIN SPOT 2	0.01	0.54	14.09	49.46	5.81	19.62	0.72	9.07	0	0.34	99.08
747 747 CHR CENTRAL SPOT 3	0	0.67	15.36	49.97	4.27	19.24	0.55	9.86	0	0.21	99.7
748 748 CHR AT MARGIN SPOT 4	0	0.59	14.64	50.16	5.03	19.54	0.72	9.44	0	0.26	99.88
749 749 CHR CENTRAL SPOT 5	0.03	0.59	14.96	50.5	4.82	19.36	0.63	9.67	0	0.27	100.35
750 750 CHR AT MARGIN SPOT 6	0	0.64	14.29	49.89	5.48	19.70	0.63	9.35	0	0.27	99.7
751 751 CHR SMALLER SPOT 7	0	0.62	14.84	49.24	5.92	19.30	0.66	9.7	0.07	0.2	99.96
752 752 CHR SMALLER SPOT 8	0	0.57	14.59	50.2	4.89	19.56	0.69	9.37	0	0.29	99.67
754 754 CHR SMALLER SPOT 9	0	0.57	14.19	49.78	5.72	19.32	0.67	9.48	0	0.24	99.4
755 755 CHR * 232322 204.2m CENTRAL S-1 08-24-449C	0	0.57	14.71	49.82	5.31	18.67	0.61	9.98	0.02	0.24	99.4
756 756 CHR AT MARGIN SPOT 2	0.03	0.67	14.42	50.52	5.43	19.02	0.69	9.84	0	0.3	100.38
757 757 CHR CENTRAL SPOT 3	0	0.57	14.07	50.15	6.03	19.09	0.71	9.7	0	0.27	99.98
758 758 CHR CENTRAL SPOT 3	0	0.6	13.97	50.6	5.79	19.35	0.62	9.65	0	0.27	100.27
760 760 CHR AGAIN	0	0.59	13.94	49.38	6.21	18.96	0.77	9.55	0	0.27	99.05
761 761 CHR AT MARGIN SPOT 4	0	0.58	13.15	50.7	4.46	19.83	0.67	8.67	0	0.33	97.95
762 762 CHR AT MARGIN SPOT 4	0	0.59	13.4	50.58	5.83	20.05	0.63	9.04	0	0.24	99.78
763 763 CHR AT MARGIN SPOT 4	0	0.62	13.51	50.16	5.70	19.45	0.74	9.16	0.07	0.33	99.17
764 764 CHR CENTRAL SPOT 5	0	0.61	12.95	50.35	6.54	18.57	0.7	9.73	0	0.35	99.15
765 765 CHR CENTRAL SPOT 6	0	0.59	14.19	50.64	5.06	19.22	0.7	9.56	0	0.32	99.77
766 766 CHR SMALLER SPOT 7	0	0.63	14.05	50.4	5.76	19.43	0.73	9.51	0	0.34	100.27
767 767 CHR SMALLER SPOT 7	0	0.6	13.8	49.99	6.23	18.95	0.68	9.73	0	0.26	99.62
768 768 CHR SMALLER SPOTN 8	0	0.64	13.71	50.78	6.04	19.25	0.67	9.74	0	0.25	100.47
769 769 CHR SMALLER SPOTN 8	0.02	0.7	13.75	50.72	5.32	19.25	0.73	9.5	0	0.31	99.76
770 770 CHR V SMALL SPOT 9	0	0.63	14.08	50.63	4.76	19.80	0.74	9.13	0	0.32	99.61
771 771 CHR * 232324 205.0m CENTRAL S-1 08-25-4491	0	0.65	15	49.11	5.07	18.25	0.61	10.12	0	0.34	98.64
772 772 CHR CENTRAL S-1 08-25-4491	0	0.58	14.64	49.55	5.90	18.17	0.61	10.3	0	0.3	99.46
773 773 CHR AT MARGIN SPOT 2	0	0.56	14.46	49.09	4.91	18.62	0.66	9.59	0	0.24	97.64
774 774 CHR AT MARGIN SPOT 2	0	0.61	14.52	49.88	5.91	19.21	0.57	9.83	0	0.26	100.2
775 775 CHR CENTRAL SPOT 3	0	0.58	14.91	49.75	4.84	18.51	0.6	10.04	0	0.24	98.98
776 776 CHR AT MARGIN SPOT 4	0	0.53	14.66	50.3	4.42	19.15	0.74	9.46	0	0.29	99.11
777 777 CHR CENTRAL SPOT 5	0	0.63	13.54	49.79	4.72	18.73	0.62	9.34	0	0.34	97.24
778 778 CHR CENTRAL SPOT 5	0	0.63	14.34	49.91	5.30	19.24	0.6	9.61	0	0.25	99.35
779 779 CHR AT MARGIN SPOT 6	0	0.61	13.95	49.95	4.61	19.49	0.72	9	0	0.36	98.23
781 781 CHR AT MARGIN SPOT 6	0	0.6	14.65	49.94	5.02	19.08	0.72	9.63	0	0.3	99.44
782 782 CHR SMALLER SPOT 7	0	0.61	14.94	50.15	4.80	19.20	0.73	9.67	0.01	0.31	99.94
783 783 CHR SMALLER SPOT 8	0	0.57	14.68	51.04	4.46	19.49	0.73	9.56	0	0.24	100.32
784 784 CHR SMALLER SPOT 8	0	0.55	14.57	49.85	4.95	19.03	0.68	9.59	0	0.24	98.97
785 785 CHR V SMALL SPOT 9	0	0.62	15.03	50.28	4.66	18.75	0.68	10.02	0.03	0.25	99.86
786 786 CHR * 232325 205.8m CENTRAL SPOT 1, 08-25-44	0	0.61	14.54	48.89	4.61	22.27	0.83	7.41	0.07	0.15	98.92
787 787 CHR CENTRAL SPOT 1	0	0.57	14.48	50.44	4.07	22.44	0.72	7.5	0.06	0.32	100.2
788 788 CHR CENTRAL SPOT 1	0	0.58	14.59	49.18	4.71	22.03	0.65	7.7	0	0.29	99.25
789 789 CHR AT MARGIN SPOT 2	0.01	0.58	13.73	51.02	4.27	22.85	0.68	7.25	0.05	0.21	100.22
790 790 CHR AT MARGIN SPOT 2	0	0.52	13.86	49.79	5.82	22.02	0.64	7.81	0.04	0.24	100.16
791 791 CHR CENTRAL SPOT 3	0	0.57	14.53	50.11	4.32	22.03	0.65	7.83	0	0.26	99.87
792 792 CHR AT MARGIN SPOT 4	0	0.63	12.91	49.95	6.43	22.71	0.69	7.33	0	0.27	100.28
793 793 CHR AT MARGIN SPOT 4	0	0.61	12.9	49.57	5.92	22.02	0.77	7.37	0.05	0.31	98.93
794 794 CHR CENTRAL SPOT 5	0	0.6	14.7	49.66	4.89	22.37	0.7	7.74	0.07	0.18	100.42

Big Daddy FW-08-19

	SiO2	TiO2	Al2O3	Cr2O3	Fe2O3	FeO	MnO	MgO	ZnO	NiO	TOTAL
795 795 CHR CENTRAL SPOT 5	0	0.63	14.25	50.29	4.42	22.28	0.73	7.67	0	0.25	100.08
797 797 CHR AT MARGIN SPOT 6	0	0.56	12.35	50.3	5.16	21.53	0.66	7.51	0	0.23	97.78
798 798 CHR SPOT 7	0	0.59	14.09	50.06	4.89	21.79	0.65	7.83	0.12	0.35	99.88
799 799 CHR SMALLER SPOT 8	0	0.58	13.85	50.91	4.02	21.55	0.7	7.94	0.03	0.25	99.43
800 800 CHR SMALLER SPOT 9	0	0.59	13.17	50.92	4.73	22.19	0.72	7.49	0	0.28	99.62
801 801 CHR * 232752 207.0m CENTRAL SPOT 1 08-25-44E	0	0.58	14.14	50.04	4.35	20.31	0.64	8.6	0	0.34	98.56
802 802 CHR CENTRAL SPOT 1 -8-25-4493	0	0.58	14.22	50.38	4.53	20.27	0.68	8.78	0.04	0.28	99.31
803 803 CHR AT MARGIN SPOT 2	0	0.56	13.93	51.13	3.68	20.43	0.7	8.56	0	0.26	98.88
804 804 CHR CENTRAL SPOT 3	0	0.57	14.06	50.64	4.46	20.54	0.65	8.66	0	0.25	99.38
805 805 CHR AT MARGIN SPOT 4	0	0.55	13.55	51.2	4.22	20.38	0.6	8.62	0	0.29	98.99
806 806 CHR CENTRAL SPOT 5	0	0.54	14.35	50.49	4.29	20.48	0.61	8.7	0	0.28	99.31
807 807 CHR CENTRAL SPOT 6	0	0.56	14	51.47	4.24	20.07	0.62	9.02	0	0.35	99.9
808 808 CHR SMALLER SPOT 7	0	0.52	13.28	50.38	4.14	20.14	0.63	8.39	0	0.24	97.31
809 809 CHR SMALLER SPOT 7	0	0.58	13.73	51.32	4.08	20.35	0.69	8.69	0	0.28	99.31
810 810 CHR SMALLER SPOT 8	0	0.58	13.7	51.6	4.08	20.67	0.54	8.68	0.01	0.23	99.68
811 811 CHR SMALLER SPOT 9	0	0.57	13.77	51.33	3.85	20.55	0.64	8.59	0	0.22	99.13
812 812 CHR * 232754 207.6m CENTRAL S 1 08-25-4494	0	0.58	13.82	51.09	4.75	17.76	0.58	10.34	0	0.3	98.74
813 813 CHR CENTRAL S 1	0	0.5	13.93	52.17	4.35	17.57	0.57	10.63	0	0.25	99.53
814 814 CHR AT MARGIN SPOT 2	0	0.51	13.79	50.71	4.46	19.53	0.61	9.07	0	0.31	98.54
815 815 CHR CENTRAL SPOT 3	0	0.46	14.42	51.21	5.19	16.52	0.56	11.27	0	0.36	99.47
816 816 CHR CENTRAL SPOT 5	0	0.54	13.39	50.56	5.38	17.63	0.57	10.23	0	0.3	98.06
817 817 CHR CENTRAL SPOT 5	0	0.54	13.8	51.37	4.58	17.60	0.75	10.33	0	0.28	98.79
818 818 CHR CENTRAL SPOT 5	0	0.56	14.1	50.6	5.03	17.82	0.58	10.33	0	0.31	98.83
819 819 CHR AT MARGIN SPOT 6	0	0.57	13.72	50.17	4.76	19.11	0.55	9.31	0	0.3	98.01
820 820 CHR AT MARGIN SPOT 6	0	0.52	14.19	50.18	4.90	19.05	0.57	9.45	0.04	0.36	98.77
821 821 CHR CENTRAL SPOT 7	0	0.56	14.42	50.87	4.16	19.11	0.63	9.56	0	0.31	99.2
822 822 CHR SMALLER SPOT 8	0	0.47	14.21	50.85	4.44	19.73	0.67	9.06	0.02	0.33	99.34
823 823 CHR V SMALL SPOT 9	0	0.57	13.94	51.02	4.10	20.18	0.7	8.79	0.04	0.23	99.16
824 824 CHR * 232756 208.4m CENTRAL S-1 08-26-449E	0	0.59	14.67	50.08	5.17	17.79	0.54	10.51	0	0.34	99.17
825 825 CHR AT MARGIN SPOT 2	0	0.61	13.33	50.96	4.71	18.88	0.61	9.52	0	0.24	98.38
826 826 CHR AT MARGIN SPOT 2	0.06	0.57	13.5	51.31	5.84	18.97	0.74	9.66	0	0.2	100.26
827 827 CHR CENTRAL SPOT 3	0	0.6	13.96	51.35	5.02	19.17	0.63	9.75	0	0.27	100.25
828 828 CHR CENTRAL SPOT 3	0	0.57	13.8	49.34	6.11	18.73	0.71	9.62	0	0.23	98.5
829 829 CHR AT MARGIN SPOT 4	0	0.55	13.52	51.58	4.37	19.04	0.7	9.46	0.01	0.25	99.04
830 830 CHR CENTRAL SPOT 5	0	0.58	14.58	51.27	4.81	17.83	0.53	10.7	0	0.29	100.11
831 831 CHR CENTRAL SPOT 6	0	0.5	14.34	51.59	5.21	18.06	0.68	10.51	0	0.26	100.63
832 832 CHR CENTRAL SPOT 6	0	0.62	13.96	50.01	5.65	18.06	0.79	10.07	0	0.33	98.93
833 833 CHR SMALLER SPOT 7	0	0.59	14.07	51.01	4.57	19.18	0.66	9.56	0	0.26	99.44
834 834 CHR SMALLER SPOT 8	0	0.58	12.87	50.92	5.84	18.96	0.65	9.47	0.05	0.28	99.03
835 835 CHR V SMALL SPOT 9	0	0.58	13.36	50.91	5.48	18.94	0.76	9.54	0	0.28	99.31
836 836 CHR * 232757 208.8m CENTRAL S-1 08-26-449E	0	0.45	13.66	50.82	6.36	18.20	0.61	10.21	0	0.31	99.98
837 837 CHR AT MARGIN SPOT 2	0	0.41	13.5	50.22	6.48	18.47	0.71	9.77	0.03	0.28	99.23
838 838 CHR CENTRAL SPOT 3	0	0.47	14.79	49.79	5.83	18.86	0.64	9.89	0.02	0.28	99.98
839 839 CHR AT MARGIN SPOT 4	0	0.5	14.28	49.1	6.64	18.44	0.65	9.94	0	0.35	99.24
840 840 CHR CENTRAL SPOT 5	0	0.44	14.08	48.43	6.64	18.54	0.64	9.65	0	0.21	97.96
841 841 CHR CENTRAL SPOT 5	0	0.42	14.11	49.78	6.30	18.21	0.73	9.99	0	0.31	99.22
842 842 CHR AT MARGIN SPOT 6	0	0.48	14.6	48.02	6.60	18.22	0.73	9.84	0	0.33	98.16
843 843 CHR AT MARGIN SPOT 6	0	0.4	13.67	49	6.61	18.14	0.73	9.74	0	0.25	97.88
844 844 CHR AT MARGIN SPOT 6	0	0.44	14.83	49.14	6.08	18.66	0.67	9.8	0.12	0.3	99.43
845 845 CHR CENTRAL SPOT 7	0	0.36	12.38	50.48	6.76	18.06	0.76	9.66	0	0.23	98.02
846 846 CHR CENTRAL SPOT 7	0	0.46	13.26	50.1	6.32	18.75	0.58	9.52	0.04	0.37	98.76
847 847 CHR SMALLER SPOT 8	0	0.42	13.21	50.67	6.01	19.01	0.65	9.42	0	0.27	99.05
848 848 CHR V SMALL SPOT 9	0	0.38	13.89	49.4	6.09	18.99	0.74	9.23	0	0.38	98.49
849 849 CHR V SMALL SPOT 9	0	0.42	14.17	50.14	5.95	19.12	0.57	9.61	0.02	0.28	99.68
850 850 CHR * 232758 209.2m CENTRAL S-1 08-26-449F	0	0.52	13.95	50.73	5.69	16.73	0.57	11.06	0.01	0.28	98.97
851 851 CHR AT MARGIN SPOT 2	0.02	0.48	14.17	50.09	4.89	18.14	0.7	9.87	0	0.2	98.07
853 853 CHR AT MARGIN SPOT 2	0	0.55	14.38	51.59	4.76	18.71	0.68	10.06	0.05	0.29	100.59
855 855 CHR CENTRAL SPOT 3	0	0.58	14.44	51.38	4.61	18.75	0.7	10.02	0	0.27	100.29
856 856 CHR CENTRAL SPOT 3	0	0.53	14.07	50.85	5.14	18.51	0.61	9.97	0	0.33	99.5
858 858 CHR AT MARGIN SPOT 4	0	0.47	14.13	51.71	4.72	18.52	0.71	10	0	0.31	100.1
859 859 CHR CENTRAL SPOT 5	0	0.48	14.41	51.79	4.68	17.39	0.58	10.83	0	0.33	100.02
860 860 CHR CENTRAL SPOT 6	0.02	0.51	14.39	51.27	4.51	18.41	0.83	9.91	0	0.32	99.72
861 861 CHR AT MARGIN SPOT 7	0	0.58	14.04	51.27	4.52	18.66	0.73	9.81	0.1	0.24	99.49
862 862 CHR SMALLER SPOT 8	0	0.49	13.78	50.38	5.23	18.21	0.64	9.82	0.07	0.35	98.44
863 863 CHR SMALLER SPOT 8	0	0.51	14.41	51.61	4.57	18.92	0.65	9.93	0	0.25	100.39
864 864 CHR SMALLER SPOT 8	0	0.49	14.16	50.23	5.01	18.60	0.55	9.75	0.08	0.26	98.62
865 865 CHR SMALLER SPOT 8	0	0.55	14.22	50.63	4.83	18.24	0.73	9.98	0	0.36	99.06
866 866 CHR V SMALL SPOT 9	0	0.51	14.09	51.08	4.92	18.56	0.69	9.92	0	0.27	99.55
867 867 CHR V SMALL SPOT 9	0	0.59	14.44	50.91	4.53	18.28	0.81	10.09	0	0.26	99.46
868 868 CHR V LARGE GRAIN CENTRAL	0	0.55	14.06	50.84	5.22	18.82	0.59	9.86	0	0.29	99.71
869 869 CHR AT MARGIN	0	0.89	14.26	52.53	3.15	19.03	0.68	10.04	0	0.29	100.56
870 870 CHR AT MARGIN	0	0.95	13.78	51.26	3.62	18.73	0.71	9.89	0	0.21	98.79
871 871 CHR * 232759 209.6m CENTRAL S-1 08-27-449E	0	0.54	13.8	51.05	3.94	19.03	0.61	9.32	0	0.35	98.25
872 872 CHR CENTRAL S 1	0	0.56	14.64	49.74	5.38	18.93	0.6	9.76	0	0.33	99.4
873 873 CHR AT MARGIN SPOT 2	0	0.55	14.35	50.87	4.51	18.80	0.72	9.76	0	0.26	99.37
874 874 CHR CENTRAL SPOT 3	0	0.63	14.22	51.12	4.99	18.69	0.65	10.04	0.01	0.32	100.17
875 875 CHR AT MARGIN SPOT 4	0	0.54	14.14	50.71	4.65	18.97	0.74	9.55	0	0.26	99.1
876 876 CHR CENTRAL SPOT 5	0	0.66	14.03	50.24	5.09	19.29	0.64	9.47	0	0.3	99.21
877 877 CHR CENTRAL SPOT 6	0	0.6	14.54	50.04	4.89	19.01	0.71	9.63	0	0.29	99.22

Big Daddy FW-08-19

	SiO2	TiO2	Al2O3	Cr2O3	Fe2O3	FeO	MnO	MgO	ZnO	NiO	TOTAL
879 879 CHR AT MARGIN SPOT 7	0	0.6	13.65	52.02	4.26	19.33	0.63	9.5	0.05	0.27	99.88
881 881 CHR SMALLER SPOT 8	0	0.62	13.93	50.23	4.46	19.24	0.6	9.3	0	0.27	98.2
882 882 CHR SMALLER SPOT 9	0	0.55	13.78	51.26	4.60	19.25	0.68	9.41	0	0.29	99.36
883 883 CHR SMALLER SPOT 10	0	0.61	13.21	52.39	4.43	19.75	0.64	9.26	0	0.27	100.11
884 884 CHR SMALLER SPOT 10	0	0.56	13.01	52.02	4.98	19.65	0.84	9.1	0.04	0.26	99.96
885 885 CHR * 232761 210.4m CENTRAL S 1 08-27-449E	0	0.61	13.66	50.61	4.19	18.99	0.58	9.32	0	0.35	97.89
886 886 CHR CENTRAL S 1	0	0.63	15.22	50.68	3.95	19.14	0.77	9.76	0.04	0.25	100.04
887 887 CHR AT MARGIN SPOT 2	0	0.59	13.83	51.69	4.85	19.64	0.8	9.37	0	0.28	100.56
888 888 CHR AT MARGIN SPOT 2	0	0.56	13.01	50.41	5.09	19.03	0.61	9.19	0	0.27	97.66
889 889 CHR CENTRAL SPOT 3	0	0.57	14.2	51.78	4.28	18.77	0.65	9.94	0.04	0.26	100.06
890 890 CHR AT MARGIN SPOT 4	0	0.6	13.9	51.8	4.72	19.67	0.74	9.41	0	0.3	100.67
891 891 CHR AT MARGIN SPOT 4	0	0.54	13.12	52.28	3.51	20.25	0.7	8.6	0	0.23	98.88
892 892 CHR CENTRAL SPOT 5	0	0.62	14.31	50.73	4.01	19.69	0.61	9.19	0	0.3	99.06
893 893 CHR SPOT 6 AT MARGIN	0	0.54	13.55	51.2	4.38	19.65	0.75	8.99	0	0.27	98.89
894 894 CHR CENTRAL SPOT 7	0	0.62	14	50.34	4.34	19.29	0.71	9.25	0	0.24	98.35
895 895 CHR SMALLER SPOT 8	0	0.69	13.78	51.22	4.24	19.90	0.61	9.05	0.11	0.33	99.51
896 896 CHR V SMALL SPOT 9	0	0.6	14.05	50.61	4.47	19.49	0.67	9.27	0	0.23	98.94
897 897 CHR * 232763 211.2m CENTRAL S 1 08-27-450C	0	0.67	13.96	50.78	4.00	19.47	0.65	9.16	0	0.4	98.69
898 898 CHR CENTRAL S 1	0	0.66	14.24	50.93	4.06	19.40	0.71	9.38	0	0.29	99.26
899 899 CHR AT MARGIN SPOT 2	0	0.6	13.63	50.64	4.58	19.41	0.73	9.1	0	0.32	98.55
900 900 CHR CENTRAL SPOT 3	0	0.57	14.44	51.53	4.61	18.57	0.65	10.14	0.03	0.31	100.39
901 901 CHR CENTRAL SPOT 3	0	0.57	14.18	51.28	3.99	18.33	0.67	9.99	0	0.24	98.85
902 902 CHR AT MARGIN SPOT 4	0.01	0.58	14.06	50.94	3.94	19.62	0.69	9.06	0	0.3	98.8
903 903 CHR CENTRAL SPOT 5	0	0.65	13.88	50	4.80	19.43	0.67	9.14	0	0.35	98.44
904 904 CHR CENTRAL SPOT 5	0	0.64	13.97	50.09	4.70	19.54	0.7	9.09	0	0.35	98.61
905 905 CHR CENTRAL SPOT 6	0	0.56	13.28	50.84	4.96	19.93	0.59	8.86	0	0.32	98.84
906 906 CHR SMALLER SPOT 7	0	0.63	12.74	51.37	4.83	20.05	0.66	8.69	0.09	0.29	98.86
907 907 CHR SMALLER SPOT 8	0	0.67	13.51	51.28	4.12	19.83	0.75	8.88	0	0.41	99.04
908 908 CHR V SMALL SPOT 9	0	0.48	13.88	51.9	4.32	20.24	0.57	8.94	0.07	0.32	100.29
909 909 CHR * 232765 212.2m CENTRAL S1 08-27-450I	0	0.54	14.31	51.34	4.01	18.66	0.61	9.88	0	0.24	99.19
910 910 CHR AT MARGIN SPOT 2	0	0.51	14.29	50.43	4.90	18.73	0.62	9.74	0	0.32	99.05
911 911 CHR CENTRAL SPOT 3	0	0.59	14.26	52.33	3.71	19.22	0.6	9.74	0.05	0.29	100.42
912 912 CHR CENTRAL SPOT 3	0	0.52	14.38	50.47	4.45	18.50	0.57	9.83	0	0.34	98.61
913 913 CHR AT MARGIN SPOT 4	0	0.53	14.64	51.34	3.88	18.69	0.56	9.98	0	0.25	99.48
914 914 CHR CENTRAL SPOT 5	0	0.54	14.42	50.99	4.75	17.95	0.61	10.37	0	0.33	99.49
915 915 CHR CENTRAL SPOT 6	0	0.55	14.52	50.71	4.21	18.93	0.62	9.67	0	0.3	99.09
917 917 CHR SMALLER SPOT 7	0	0.56	14.42	50.22	4.92	18.38	0.71	9.95	0.02	0.28	98.96
918 918 CHR SMALLER SPOT 8	0	0.53	14.33	52.02	4.13	19.39	0.66	9.65	0	0.25	100.54
919 919 CHR SMALLER SPOT 8	0	0.45	14.32	50.91	4.26	18.90	0.62	9.54	0	0.36	98.94
920 920 CHR V SMALL SPOT 9	0	0.5	14.32	51.29	4.28	19.26	0.69	9.5	0	0.28	99.69
921 921 CHR * 232767 213.0m CENTRAL S-1 08-27-450J	0	0.42	14.45	50.68	4.21	18.58	0.64	9.72	0	0.24	98.52
922 922 CHR CENTRAL S 1	0.03	0.45	14.61	50.6	4.47	18.72	0.59	9.71	0	0.27	99
923 923 CHR AT MARGIN SPOT 2	0	0.49	14.71	51.58	3.30	19.15	0.59	9.66	0	0.15	99.3
924 924 CHR CENTRAL SPOT 3	0	0.48	14.45	51.99	4.24	18.14	0.57	10.44	0	0.21	100.09
925 925 CHR CENTRAL SPOT 3	0	0.42	14.55	50.03	4.89	17.41	0.64	10.4	0	0.27	98.12
926 926 CHR CENTRAL SPOT 3	0	0.55	14.57	50.73	4.77	17.74	0.54	10.57	0	0.26	99.26
927 927 CHR AT MARGIN SPOT 4	0	0.51	14.82	50.69	4.37	19.05	0.56	9.8	0	0.21	99.57
928 928 CHR CENTRAL 5 CENTRAL	0	0.48	14.73	51.2	4.13	18.94	0.55	9.85	0	0.26	99.72
929 929 CHR CENTRAL SPOT 6	0	0.49	15.07	51.86	3.05	19.28	0.53	9.66	0	0.36	100
930 930 CHR SMALLER SPOT 7	0	0.49	14.83	50.48	4.50	19.17	0.62	9.63	0	0.26	99.53
931 931 CHR V SMALL SPOT 9	0	0.44	14.75	51.07	3.72	19.09	0.53	9.59	0	0.29	99.11
932 932 CHR * 232769 213.8m CENTRAL S-1 08-27-450K	0	0.54	14.06	50.13	4.34	18.34	0.54	9.75	0.01	0.26	97.53
933 933 CHR CENTRAL S 1	0	0.59	14.58	50.5	5.00	18.79	0.57	10.02	0.03	0.2	99.78
934 934 CHR AT MARGIN SPOT 2	0	0.6	14.26	51.01	4.47	19.28	0.63	9.56	0	0.3	99.67
935 935 CHR CENTRAL SPOT 3	0	0.5	14.58	50.58	4.64	17.82	0.55	10.43	0.02	0.19	98.84
936 936 CHR AT MARGIN SPOT 2	0	0.54	14	51.64	4.39	19.20	0.57	9.67	0	0.22	99.79
937 937 CHR CENTRAL SPOT 5	0	0.6	14.51	50.61	4.46	18.28	0.57	10.16	0	0.28	99.02
939 939 CHR SPOT 6 AT MARGIN	0	0.54	14.48	51.46	4.36	19.25	0.65	9.7	0.02	0.25	100.28
940 940 CHR CENTRAL SPOT 7	0	0.53	14.77	50.9	4.26	18.48	0.62	10.06	0	0.31	99.5
941 941 CHR SMALLER SPOT 8	0	0.58	14.08	51.72	3.64	19.15	0.59	9.53	0.04	0.29	99.26
943 943 CHR SMALLER SPOT 9	0	0.57	14.24	51	3.89	19.21	0.6	9.44	0	0.28	98.84
944 944 CHR * 232771 214.6m CENTRAL S-1 08-27-450L	0	0.4	14.25	51.82	4.54	16.99	0.63	10.84	0	0.36	99.37
945 945 CHR AT MARGIN SPOT 2	0	0.44	13.93	50.84	5.00	18.09	0.61	10.03	0	0.31	98.75
946 946 CHR CENTRAL SPOT 3	0	0.49	14.62	50.17	5.90	17.37	0.6	10.8	0	0.33	99.69
947 947 CHR CENTRAL SPOT 5	0	0.45	13.9	50.43	4.62	17.81	0.52	10.04	0	0.3	97.6
948 948 CHR CENTRAL SPOT 5	0	0.47	14.39	50.35	5.29	17.86	0.73	10.27	0.01	0.26	99.1
949 949 CHR CENTRAL SPOT 6	0	0.46	14.31	51.23	4.54	17.63	0.55	10.48	0	0.31	99.06
950 950 CHR SMALLER SPOT 7	0	0.5	14.74	49.23	5.72	18.22	0.61	10.08	0	0.33	98.86
951 951 CHR SMALLER SPOT 8	0	0.48	14.05	50.55	4.92	18.61	0.58	9.71	0	0.38	98.79
952 952 CHR V SMALL SPOT 9	0	0.49	13.77	51.51	4.84	18.85	0.58	9.79	0	0.23	99.57
953 953 CHR * 232773 214.4m CENTRAL S-1 08-27-450M	0	0.58	15.35	49.86	3.74	18.81	0.65	9.74	0	0.29	98.65
954 954 CHR CENTRAL S-1	0	0.57	15.06	49.78	3.88	18.74	0.59	9.7	0	0.3	98.23
955 955 CHR AT MARGIN SPOT 2	0	0.61	13.89	50.54	4.48	19.00	0.56	9.52	0	0.26	98.42
956 956 CHR AT MARGIN SPOT 2	0	0.54	14.14	50.11	4.62	19.24	0.59	9.34	0	0.22	98.34
957 957 CHR CENTRAL SPOT 3	0	0.54	13.97	50.19	4.92	19.14	0.51	9.43	0.01	0.29	98.5
958 958 CHR CENTRAL SPOT 4	0	0.45	14.35	50.15	4.46	19.07	0.5	9.43	0	0.26	98.22
959 959 CHR CENTRAL SPOT 4	0	0.55	14.25	49.92	4.66	18.57	0.59	9.66	0	0.35	98.08
960 960 CHR CENTRAL SPOT 4	0	0.56	14.35	49.34	4.80	18.43	0.63	9.66	0	0.33	97.62
961 961 CHR CENTRAL SPOT 4	0	0.52	14.34	49.77	4.82	19.02	0.56	9.47	0	0.28	98.29

Big Daddy FW-08-19

	SiO2	TiO2	Al2O3	Cr2O3	Fe2O3	FeO	MnO	MgO	ZnO	NiO	TOTAL
962 962 CHR CENTRAL SPOT 4	0.02	0.53	14.18	49.85	5.31	18.70	0.64	9.56	0.12	0.32	98.69
963 963 CHR CENTRAL SPOT 5	0	0.57	13.68	49.28	5.33	18.31	0.62	9.61	0	0.3	97.17
964 964 CHR CENTRAL SPOT 5	0	0.55	14.22	50.4	4.82	19.11	0.64	9.56	0	0.21	99.03
965 965 CHR CENTRAL SPOT 6	0	0.51	14.2	50.11	4.82	18.49	0.67	9.72	0.01	0.28	98.33
966 966 CHR CENTRAL SPOT 6	0	0.5	14.16	50.26	4.78	18.62	0.67	9.64	0	0.32	98.47
967 967 CHR CENTRAL SPOT 6	0	0.43	14.21	49.61	4.99	18.51	0.54	9.58	0	0.36	97.73
968 968 CHR CENTRAL SPOT 7	0	0.46	14.07	49.7	5.40	18.77	0.62	9.57	0	0.22	98.27
969 969 CHR CENTRAL SPOT 7	0	0.46	13.65	50.83	4.42	19.27	0.48	9.24	0	0.24	98.15
970 970 CHR SMALLER SPOT 8	0	0.44	14.45	50.51	5.28	18.81	0.72	9.73	0	0.35	99.76
971 971 CHR V SMALL SPOT 9	0	0.58	14.02	51.67	3.97	19.87	0.56	9.25	0.01	0.21	99.74
972 972 CHR SPOT 1 AGAIN	0	0.55	14.99	51.18	3.66	19.04	0.56	9.86	0.01	0.21	99.69
973 973 CHR SPOT 2 AGAIN	0	0.54	14.35	51.49	4.54	19.49	0.52	9.64	0	0.27	100.39
974 974 CHR * 232775 216.2m CENTRAL S 1 08-27-450C	0	0.55	14.33	50.74	4.81	17.71	0.56	10.47	0	0.31	99
975 975 CHR AT MARGIN SPOT 2	0	0.56	14.24	50.5	4.24	18.81	0.61	9.59	0	0.31	98.44
976 976 CHR AT MARGIN SPOT 2	0	0.52	14.34	49.99	4.76	18.89	0.53	9.63	0	0.23	98.41
977 977 CHR CENTRAL SPOT 3	0	0.53	14.1	50.24	4.79	18.97	0.65	9.49	0	0.25	98.54
978 978 CHR CENTRAL SPOT 3	0	0.48	14.03	49.11	5.33	18.93	0.6	9.27	0	0.31	97.53
979 979 CHR CENTRAL SPOT 3	0	0.47	14.04	50.64	4.46	19.24	0.49	9.37	0	0.25	98.52
982 982 CHR CENTRAL SPOT 3	0	0.57	14.01	49.99	4.66	19.00	0.56	9.42	0	0.28	98.02
983 983 CHR CENTRAL SPOT 1	0	0.53	13.92	51.24	4.12	19.65	0.49	9.22	0.14	0.13	99.03
984 984 CHR AT MARGIN SPOT 2	0	0.5	13.83	49.76	5.01	19.24	0.52	9.24	0.07	0.12	97.79
986 986 CHR AT MARGIN SPOT 2	0	0.48	13.95	49.44	5.17	19.16	0.56	9.28	0.01	0.11	97.64
988 988 CHR * 232776 216.6m CENTRAL SPOT 1 08-28-451	0	0.63	14.07	50.38	4.62	19.96	0.56	9.16	0	0.09	99.01
989 989 CHR AT MARGIN SPOT 2	0	0.54	13.59	50.06	4.77	19.33	0.52	9.16	0.09	0.1	97.68
990 990 CHR AT MARGIN SPOT 2	0	0.51	16.05	53.29	0.31	18.26	0.45	10.5	0.11	0.03	99.48
991 991 CHR AT MARGIN SPOT 2	0.03	0.44	16.07	53.91	-0.29	18.64	0.44	10.19	0	0.08	99.54
992 992 CHR CENTRAL SPOT 3	0	0.59	13.97	50.18	4.97	19.49	0.6	9.28	0.14	0.1	98.82
993 993 CHR AT MARGIN SPOT 4	0	0.62	13.96	50.69	4.29	19.86	0.42	9.19	0.05	0.14	98.79
994 994 CHR CENTRAL SPOT 5	0	0.58	14.09	50.79	3.76	19.51	0.48	9.23	0.09	0.15	98.3
995 995 CHR CENTRAL SPOT 5	0	0.58	14.04	51.81	3.37	20.06	0.48	9.11	0.11	0.06	99.28
996 996 CHR AT MARGIN SPOT 6	0	0.66	13.85	51.76	3.34	19.83	0.48	9.15	0.16	0.15	99.05
997 997 CHR CENTRAL SPOT 7	0.03	0.61	13.56	51.35	3.99	19.49	0.43	9.24	0.1	0.09	98.49
998 998 CHR CENTRAL SPOT 7	0	0.61	13.65	51.94	3.90	19.70	0.51	9.29	0.12	0.14	99.47
999 999 CHR SMALLER SPOT 8	0.03	0.58	13.91	50.4	3.89	19.10	0.52	9.21	0.16	0.09	97.5
1000 *** CHR SMALLER SPOT 8	0	0.57	14.11	51.9	3.82	19.94	0.52	9.25	0.1	0.18	100.01
1001 *** CHR V SMALL SPOT 9	0	0.58	13.94	51.77	3.32	19.74	0.52	9.21	0.05	0.1	98.9
1002 *** CHR * 232778 217.4m CENTRAL SPOT 1 08-28-45C	0	0.45	14.11	50.61	5.00	19.95	0.61	9	0.2	0.14	99.57
1003 *** CHR AT MARGIN SPOT 2	0	0.48	14.45	50.1	4.28	19.64	0.59	9.13	0	0.14	98.38
1004 *** CHR AT MARGIN SPOT 2	0.03	0.48	14.57	49.2	5.24	19.01	0.55	9.45	0.01	0.19	98.2
1005 *** CHR AT MARGIN SPOT 2	0.01	0.42	14.59	48.89	4.93	19.34	0.49	9.15	0.05	0.13	97.51
1006 *** CHR AT MARGIN SPOT 2	0	0.49	14.5	49.97	4.97	19.60	0.52	9.3	0.1	0.17	99.12
1007 *** CHR CENTRAL SPOT 3	0	0.49	14.27	51.48	3.96	19.20	0.55	9.59	0	0.21	99.35
1008 *** CHR AT MARGIN SPOT 4	0	0.53	14.54	50.38	4.79	20.17	0.55	9.12	0	0.19	99.79
1009 *** CHR CENTRAL SPOT 5	0	0.44	13.98	50.19	4.44	19.03	0.44	9.4	0.03	0.11	97.61
1010 *** CHR CENTRAL SPOT 5	0	0.52	14	49.53	4.89	19.04	0.55	9.35	0	0.16	97.55
1011 *** CHR CENTRAL SPOT 5	0	0.43	14.35	50.21	4.92	19.04	0.52	9.54	0.11	0.17	98.79
1012 *** CHR AT MARGIN SPOT 6	0	0.43	14.21	50.25	4.72	20.09	0.52	8.89	0.05	0.16	98.85
1013 *** CHR CENTRAL SPOT 7	0	0.46	14.37	49.46	5.71	19.02	0.58	9.61	0.02	0.15	98.81
1014 *** CHR SMALLER SPOT 8	0	0.47	14.26	49.96	5.01	19.73	0.45	9.13	0.12	0.2	98.83
1015 *** CHR V SMALL SPOT 9	0	0.47	14.16	49.93	5.57	19.45	0.57	9.32	0.13	0.18	99.22
1016 *** CHR * 232779 217.8m CENTRAL S-1 08-28-450E	0	0.41	13.92	50.5	5.91	19.48	0.59	9.4	0.11	0.15	99.88
1017 *** CHR AT MARGIN SPOT 2	0	0.39	13.86	49.36	6.63	19.71	0.59	9.14	0.11	0.09	99.22
1018 *** CHR CENTRAL SPOT 3	0	0.41	14.09	50.07	5.69	19.90	0.5	9.12	0.07	0.18	99.46
1020 *** CHR AT MARGIN SPOT 4	0	0.43	14.07	49.73	5.51	20.12	0.45	8.98	0	0.09	98.83
1021 *** CHR CENTRAL SPOT 5	0	0.45	14.27	49.27	6.49	19.13	0.54	9.64	0.1	0.13	99.37
1022 *** CHR AT MARGIN SPOT 6	0.02	0.46	14.47	49.9	5.72	20.18	0.37	9.14	0.09	0.17	99.95
1023 *** CHR AT MARGIN SPOT 6	0.02	0.45	14.23	49.86	5.90	20.01	0.55	9.08	0.12	0.11	99.74
1024 *** CHR * 232780 218.2m CENTRAL SPOT 1, 08-28-45	0	0.46	14.11	51	4.54	18.48	0.51	9.93	0	0.23	98.81
1025 *** CHR AT MARGIN SPOT 2	0	0.52	14.18	50.91	4.90	19.14	0.49	9.72	0.12	0.13	99.62
1026 *** CHR CENTRAL SPOT 3	0	0.57	14.28	51.06	4.35	18.56	0.48	10.04	0.06	0.19	99.16
1027 *** CHR AT MARGIN SPOT 4	0	0.57	13.81	50.6	4.86	19.04	0.43	9.67	0	0.15	98.65
1028 *** CHR CENTRAL SPOT 5	0	0.53	14.47	52.14	3.97	19.46	0.49	9.79	0.13	0.06	100.64
1029 *** CHR CENTRAL SPOT 5	0	0.58	14.29	50.4	4.47	18.99	0.49	9.7	0	0.18	98.65
1030 *** CHR AT MARGIN SPOT 6	0	0.51	14.4	51.35	4.25	19.63	0.4	9.53	0.11	0.13	99.89
1031 *** CHR CENTRAL SPOT 7	0	0.55	14.38	50.84	4.68	18.92	0.58	9.81	0.1	0.18	99.58
1032 *** CHR SMALLER SPOT 8	0.04	0.57	14.35	51.08	4.33	19.08	0.47	9.68	0.08	0.16	99.41
1033 *** CHR V SMALL SPOT 9	0	0.55	14.79	49.95	4.81	19.14	0.46	9.74	0.09	0.14	99.19
1034 *** CHR * 232781 218.6m CENTRAL S 1 08-28-4513	0.05	0.61	14.18	51.54	4.45	19.16	0.48	9.67	0.09	0.26	100.04
1035 *** CHR AT MARGIN SPOT 2	0	0.6	14.06	51.39	4.46	20.04	0.43	9.26	0.14	0.19	100.12
1036 *** CHR CENTRAL SPOT 3	0	0.58	14.03	51.89	4.32	19.78	0.51	9.44	0.15	0.15	100.42
1037 *** CHR AT MARGIN SPOT 4	0	0.58	13.55	51.53	4.45	19.79	0.48	9.27	0	0.16	99.36
1038 *** CHR CENTRAL SPOT 5	0.01	0.6	13.97	51.09	4.26	19.16	0.55	9.55	0	0.21	98.97
1039 *** CHR ATR MARGIN SPOT 6	0.01	0.6	13.66	51.87	4.29	19.95	0.53	9.22	0	0.19	99.89
1040 *** CHR CENTRAL SPOT 7	0	0.57	13.67	50.55	4.79	19.39	0.45	9.34	0.03	0.19	98.5
1041 *** CHR SMALLER SPOT 8	0	0.54	13.71	51.93	4.26	20.03	0.41	9.2	0.14	0.13	99.92
1042 *** CHR V SMALL SPOT 9	0	0.53	13.66	51.26	4.92	19.76	0.49	9.31	0.03	0.15	99.62
1043 *** CHR * 232782 219.0m CENTRAL S 1 08-28-4514	0	0.55	14.4	51.95	4.15	18.43	0.55	10.28	0.05	0.21	100.15
1044 *** CHR INT SPOT 2	0	0.51	14.02	51.15	4.72	17.96	0.54	10.34	0.02	0.15	98.94
1045 *** CHR AT MARGFIN SPOT 3	0	0.54	14.05	52.14	2.98	20.34	0.35	9	0	0.13	99.23

Big Daddy FW-08-19

	SiO2	TiO2	Al2O3	Cr2O3	Fe2O3	FeO	MnO	MgO	ZnO	NiO	TOTAL
1046 *** CHR CENTRAL SPOT 4	0	0.5	14.3	51.13	4.80	20.08	0.56	9.26	0.01	0.15	100.31
1047 *** CHR AT MARGIN SPOT 5	0	0.52	14.18	51.74	3.44	20.49	0.62	8.79	0	0.15	99.58
1048 *** CHR CENTRAL SPOT 6	0	0.49	14.27	51.59	4.18	20.38	0.46	9.04	0.16	0.11	100.26
1049 *** CHR CENTRAL SPOT 7	0	0.51	14.54	50.41	4.19	19.81	0.56	9.17	0	0.16	98.93
1050 *** CHR SMALLER SPOT 8	0	0.55	14.31	51.42	4.00	19.86	0.57	9.22	0.12	0.2	99.85
1051 *** CHR V SMALL SPOT 9	0.01	0.49	14.57	51.17	4.12	20.20	0.57	9.09	0.05	0.12	99.98
1052 *** CHR * 232783 219.4m CENTRAL S 1 08-28-451E	0	0.41	14.02	50.32	5.49	20.38	0.47	8.9	0.08	0.09	99.61
1053 *** CHR AT MARGIN SPOT 2	0	0.46	14.37	50.56	4.77	20.16	0.55	8.96	0.16	0.17	99.68
1054 *** CHR CENTRAL SPOT 3	0	0.49	14.23	49.18	6.35	19.63	0.51	9.32	0.12	0.15	99.35
1055 *** CHR AT MARGIN SPOT 4	0	0.43	14.31	48.62	6.29	19.54	0.48	9.22	0.13	0.09	98.48
1056 *** CHR CENTRAL SPOT 5	0	0.46	13.62	50.73	5.64	20.11	0.57	9.05	0.02	0.11	99.75
1057 *** CHR CENTRAL SPOT 6	0.01	0.41	12.89	50.97	5.72	20.10	0.52	8.72	0.13	0.16	99.05
1058 *** CHR CENTRAL SPOT 7	0	0.46	13.81	49.6	6.46	20.59	0.46	8.73	0.2	0.12	99.78
1059 *** CHR SMALLER SPOT 8	0	0.41	13.49	49.78	5.60	20.04	0.42	8.78	0.01	0.17	98.14
1060 *** CHR SMALLER SPOT 9	0	0.37	13.37	50.75	5.65	20.55	0.49	8.59	0.13	0.15	99.48
1061 *** CHR V SMALL SPOT 10	0	0.45	13.51	51.29	5.09	20.60	0.45	8.8	0.02	0.11	99.81
1062 *** CHR * 232784 219.8m CENTRAL S-1, 08-28-451E	0	0.62	14.38	49.9	4.69	19.89	0.5	9.11	0.1	0.23	98.95
1063 *** CHR AT MARGIN SPOT 2	0	0.57	13.73	51.38	3.54	20.58	0.4	8.58	0.09	0.23	98.75
1064 *** CHR AT MARGIN SPOT 2	0	0.61	14.1	50.94	4.10	20.52	0.59	8.8	0	0.16	99.41
1065 *** CHR CENTRAL SPOT 3	0	0.63	13.75	50.79	4.31	20.36	0.57	8.74	0.05	0.22	98.99
1066 *** CHR AT MARGIN SPOT 4	0	0.58	13.69	52.06	4.34	21.12	0.43	8.63	0.17	0.17	100.75
1067 *** CHR AT MARGIN SPOT 4	0	0.59	13.83	52.29	3.43	21.20	0.54	8.54	0	0.1	100.18
1068 *** CHR CENTRAL SPOT 6	0	0.63	13.72	50.99	4.70	20.23	0.51	8.93	0.18	0.2	99.62
1069 *** CHR CENTRAL SPOT 7	0	0.64	14.28	50.98	3.84	20.65	0.47	8.81	0.03	0.19	99.51
1070 *** CHR SMALLER SPOT 8	0	0.71	13.95	51.5	3.79	20.71	0.45	8.82	0.09	0.2	99.84
1071 *** CHR V SMALL SPOT 9	0	0.62	13.66	50.88	3.49	20.23	0.45	8.7	0.02	0.15	97.85
1072 *** CHR V SMALL SPOT 9	0	0.65	13.46	50.97	4.15	19.87	0.6	8.92	0.14	0.12	98.46
1073 *** CHR * 232785 220.2m CENTRAL S-1 08-28-451F	0	0.64	13.98	50.03	4.12	19.91	0.44	8.98	0	0.15	97.84
1074 *** CHR CENTRAL SPOT 1	0	0.81	13.98	50.19	4.45	19.84	0.53	9.21	0.14	0.12	98.82
1075 *** CHR AT MARGIN SPOT 2	0	0.61	13.66	49.78	4.77	19.27	0.61	9.15	0.05	0.16	97.58
1076 *** CHR AT MARGIN SPOT 2	0	0.58	14.24	51.27	4.20	20.14	0.63	9.13	0.01	0.15	99.93
1077 *** CHR AT MARGIN SPOT 2	0	0.61	14.23	51.34	3.06	20.29	0.4	8.92	0.08	0.11	98.73
1078 *** CHR CENTRAL SPOT 3	0	0.7	14.53	50.16	4.16	20.32	0.54	8.93	0.11	0.2	99.24
1079 *** CHR SPOT 4 AT MARGIN	0	0.65	14.18	51.07	4.29	20.09	0.57	9.23	0.03	0.09	99.77
1080 *** CHR CENTRAL SPOT 5	0	0.64	14.48	50.19	4.85	20.22	0.55	9.07	0.14	0.2	99.86
1081 *** CHR CENTRAL SPOT 6	0	0.59	14.73	50.42	3.66	19.92	0.36	9.21	0.07	0.16	98.75
1082 *** CHR CENTRAL SPOT 7	0	0.64	14.44	50.15	4.02	20.46	0.47	8.75	0.15	0.18	98.86
1083 *** CHR SMALLER SPOT 8	0	0.62	13.86	51.61	3.94	20.73	0.7	8.67	0.03	0.13	99.9
1084 *** CHR SMALLER SPOT 8	0	0.68	13.9	51.92	3.90	21.08	0.53	8.59	0.12	0.29	100.62
1085 *** CHR SMALLER SPOT 8	0	0.7	13.84	52.27	3.80	20.49	0.6	8.93	0.2	0.25	100.7
1086 *** CHR V SMALL SPOT 9	0	0.67	13.62	51.21	4.03	20.69	0.44	8.67	0.08	0.17	99.17
1087 *** CHR * 232786 220.6m CENTRAL S 1 08-29-451E	0	0.6	13.56	50.29	4.05	20.37	0.52	8.47	0.12	0.13	97.7
1088 *** CHR CENTRAL SPOT 1	0	0.55	14.26	50.78	4.17	20.14	0.53	8.98	0.12	0.13	99.25
1089 *** CHR AT MARGIN SPOT 2	0	0.6	14.12	50.73	4.89	20.30	0.55	9.03	0.15	0.13	100.01
1091 *** CHR CENTRAL SPOT 3	0	0.62	14.37	50.46	4.46	19.65	0.52	9.38	0.05	0.16	99.23
1092 *** CHR AT MARGIN SPOT 4	0	0.63	14.32	50.52	5.00	20.32	0.54	9.07	0.13	0.21	100.24
1093 *** CHR AT MARGIN SPOT 4	0	0.58	14.05	51.51	4.44	20.16	0.62	9.11	0.2	0.09	100.32
1094 *** CHR AT MARGIN SPOT 4	0	0.65	13.46	50.83	4.42	20.03	0.51	8.97	0	0.14	98.57
1095 *** CHR CENTRAL SPOT 5	0	0.63	13.9	52.41	3.19	20.81	0.44	8.76	0.18	0.11	100.11
1096 *** CHR CENTRAL SPOT 6	0.01	0.6	14.4	50.91	4.34	20.45	0.6	8.86	0.05	0.31	100.1
1097 *** CHR CENTRAL SPOT 7	0	0.62	13.8	51.42	4.41	20.26	0.51	9.04	0.06	0.19	99.87
1098 *** CHR SMALLER SPOT 8	0	0.65	13.58	51.71	3.59	20.48	0.55	8.75	0.06	0.11	99.12
1099 *** CHR V SMALL SPOT 9	0	0.68	13.53	51.43	3.86	20.02	0.52	8.93	0.1	0.26	98.94
1100 *** CHR * 232787 221.0m CENTRAL SPOT 1 08-29-451F	0	0.59	14.43	51.51	4.01	20.84	0.52	8.85	0.09	0.16	100.6
1101 *** CHR SPOT 1 AGAIN	0	0.55	14.26	51.85	4.15	20.54	0.45	9.04	0.12	0.2	100.75
1102 *** CHR SPOT 1	0	0.52	13.84	50.7	4.68	20.12	0.52	8.94	0	0.18	99.03
1103 *** CHR AT MARGIN SPOT 2	0	0.59	13.8	50.98	4.86	20.90	0.65	8.61	0.07	0.11	100.08
1104 *** CHR AT MARGIN SPOT 2	0	0.53	13.62	49.57	4.99	19.37	0.61	8.92	0.1	0.26	97.47
1105 *** CHR AT MARGIN SPOT 2	0	0.56	14.2	50.1	4.79	19.88	0.55	9.05	0.11	0.19	98.95
1106 *** CHR AT MARGIN SPOT 2	0	0.7	14.04	50.93	4.42	20.95	0.5	8.67	0.13	0.19	100.09
1107 *** CHR AT MARGIN SPOT 2	0	0.52	13.94	49.21	4.98	20.33	0.54	8.51	0.12	0.11	97.76
1108 *** CHR AT MARGIN SPOT 2	0	0.56	13.95	49.86	5.47	20.49	0.58	8.69	0.17	0.16	99.38
1109 *** CHR CENTRAL SPOT 3	0	0.64	13.83	48.61	5.75	20.38	0.57	8.6	0.04	0.14	97.99
1110 *** CHR CENTRAL SPOT 3	0	0.59	13.9	49.84	5.37	20.55	0.57	8.64	0.11	0.21	99.24
1111 *** CHR AT MARGIN SPOT 4	0.01	0.63	14.22	50.37	4.76	20.76	0.58	8.68	0.08	0.17	99.78
1112 *** CHR CENTRAL SPOT 5	0	0.66	13.91	49.75	4.46	20.19	0.53	8.74	0.07	0.15	98.01
1113 *** CHR CENTRAL SPOT 5	0	0.55	13.99	49.54	4.57	20.58	0.51	8.34	0.13	0.25	98.01
1114 *** CHR CENTRAL SPOT 5	0	0.52	14.27	50.11	4.62	19.85	0.52	9	0.16	0.2	98.79
1115 *** CHR AT MARGIN SPOT 6	0.02	0.56	14.04	49.98	5.29	20.38	0.55	8.79	0.05	0.17	99.3
1116 *** CHR SMALLER SPOT 8	0	0.69	13.6	48.81	5.23	20.24	0.51	8.56	0.01	0.23	97.36
1117 *** CHR SMALLER SPOT 8	0	0.57	13.69	51.76	4.21	21.02	0.49	8.57	0.1	0.15	100.14
1118 *** CHR V SMALL SPOT 9	0	0.68	13.53	51.65	4.33	21.28	0.49	8.44	0.17	0.15	100.29
1119 *** CHR * 232788 221.4m CENTRAL S-1 08-29-452C	0	0.62	14.24	51.05	4.73	20.14	0.41	9.35	0.08	0.12	100.27
1120 *** CHR CENTRAL SPOT 1	0	0.53	13.37	49.84	5.43	19.11	0.55	9.22	0.07	0.22	97.79
1121 *** CHR CENTRAL SPOT 1	0	0.68	14.31	50.42	4.64	20.17	0.49	9.18	0.08	0.13	99.63
1122 *** CHR AT MARGIN SPOT 2	0.03	0.59	14.15	50.7	4.36	20.61	0.5	8.74	0.08	0.05	99.38
1123 *** CHR CENTRAL SPOT 3	0	0.52	14.31	50.58	4.84	20.26	0.54	9.02	0.13	0.11	99.82
1124 *** CHR CENTRAL SPOT 5	0	0.62	14.05	50.96	4.32	20.05	0.56	9.05	0.12	0.2	99.5
1125 *** CHR AT MARGIN SPOT 5	0	0.63	14.29	49.57	5.12	20.34	0.57	8.88	0.14	0.07	99.1

Big Daddy FW-08-19

	SiO2	TiO2	Al2O3	Cr2O3	Fe2O3	FeO	MnO	MgO	ZnO	NiO	TOTAL
1126 *** CHR CENTRAL SPOT 6	0	0.64	14.09	50.12	4.53	20.19	0.52	8.91	0.14	0.09	98.78
1127 *** CHR SMALLER SPOT 7	0	0.66	13.76	51.19	4.60	20.74	0.58	8.81	0	0.12	100
1128 *** CHR SMALLER SPOT 7	0	0.57	13.58	50.32	4.55	20.37	0.54	8.6	0	0.19	98.26
1129 *** CHR V SMALL SPOT 8	0	0.54	12.92	50.64	5.35	20.20	0.62	8.67	0	0.14	98.55
1130 *** CHR * 232789 221.8m CENTRAL S-1 087-29-4521	0	0.57	14.75	49.88	4.05	20.70	0.5	8.63	0.09	0.15	98.92
1131 *** CHR AT MARGIN SPOT 2	0	0.49	14.67	49.83	4.64	20.72	0.51	8.65	0.05	0.17	99.26
1132 *** CHR CENTRAL SPOT 3	0.01	0.6	13.93	50.72	4.47	20.68	0.45	8.7	0.08	0.12	99.32
1133 *** CHR AT MARGIN SPOT 4	0	0.59	14.41	50.1	4.86	20.71	0.51	8.79	0.06	0.14	99.69
1134 *** CHR CENTRAL SPOT 5	0.01	0.61	14.15	49.76	5.02	20.26	0.56	8.79	0.14	0.19	98.99
1135 *** CHR AT MARGIN SPOT 6	0.03	0.57	14.19	50.24	5.14	20.73	0.63	8.54	0.22	0.16	99.94
1136 *** CHR AT MARGIN SPOT 6	0.02	0.52	14.01	50.57	4.84	20.34	0.51	8.87	0.07	0.07	99.33
1137 *** CHR CENTRAL SPOT 7	0	0.55	13.48	48.99	6.30	19.29	0.52	9.14	0.16	0.24	98.03
1138 *** CHR CENTRAL SPOT 7	0	0.53	14.64	49.49	4.94	20.01	0.53	9.03	0.05	0.2	98.93
1139 *** CHR SMALLWER SPOT 8	0	0.49	14.62	48.96	5.28	20.17	0.51	8.83	0.04	0.25	98.62
1140 *** CHR V SMALL SPOT 9	0	0.6	13.55	49.3	5.11	19.75	0.56	8.82	0.09	0.12	97.39
1141 *** CHR V SMALL SPOT 9	0	0.54	14.13	50.16	4.87	20.76	0.48	8.62	0.13	0.11	99.31
1142 *** CHR * 232790 222.2m CENTRAL S-1 08-29-4522	0.03	0.45	14.75	50.46	4.86	20.32	0.49	9.08	0	0.1	100.05
1143 *** CHR CENTRAL SPOT 1	0.06	0.47	14.72	50.6	4.92	20.46	0.61	8.88	0.03	0.13	100.39
1144 *** CHR AT MARGIN SPOT 2	0.03	0.44	14.58	50.41	4.86	20.07	0.69	8.94	0.11	0.14	99.78
1145 *** CHR CENTRAL SPOT 3	0.04	0.48	14.11	51.61	4.78	19.22	0.52	9.72	0	0.09	100.09
1146 *** CHR CENTRAL SPOT 3	0.04	0.46	13.44	51.85	5.12	18.94	0.57	8.68	0.08	0.08	99.75
1147 *** CHR AT MARGIN SPOT 4	0.08	0.54	14.28	50.48	5.40	20.24	0.55	8.95	0.03	0.17	100.18
1148 *** CHR AT MARGIN SPOT 4	0.03	0.47	14.55	49.33	5.29	19.96	0.54	9	0	0.11	98.75
1149 *** CHR CENTRAL SPOT 5	0.02	0.66	14.84	49.62	5.47	20.32	0.47	9.22	0.12	0.13	100.33
1150 *** CHR CENTRAL SPOT 5	0	0.58	14.31	49.8	5.19	19.49	0.62	9.33	0.12	0.15	99.07
1151 *** CHR AT MARGIN SPOT 6	0.04	0.66	14.45	49.11	5.86	20.14	0.55	9.07	0	0.17	99.46
1152 *** CHR CENTRAL SPOT 7	0	0.58	14.56	48.92	5.59	19.67	0.4	9.3	0.18	0.13	98.77
1153 *** CHR SMALLER SPOT 8	0.05	0.59	14.48	49.21	5.35	20.10	0.55	8.87	0.09	0.15	98.9
1154 *** CHR V SMALL SPOT 9	0.04	0.55	14.75	48.78	4.73	19.93	0.4	8.86	0.15	0.12	97.84
1155 *** CHR V SMALL SPOT 9	0.05	0.61	15.14	49.15	4.93	20.59	0.4	8.91	0.06	0.05	99.39
1156 *** CHR * 232791 222.6m CENTRAL S 1 08-29-4523	0.03	0.63	14.31	50.16	5.08	20.32	0.5	8.89	0.15	0.27	99.83
1157 *** CHR AT MARGIN SPOT 2	0.05	0.59	13.72	49.64	5.45	20.38	0.55	8.55	0.06	0.18	98.62
1158 *** CHR CENTRAL SPOT 3	0.05	0.64	14.39	49.4	5.23	20.16	0.43	8.94	0.09	0.15	98.95
1159 *** CHR AT MARGIN SPOT 4	0.04	0.66	14.1	49.61	5.21	20.68	0.52	8.6	0.1	0.1	99.1
1160 *** CHR CENTRAL SPOT 5	0	0.66	15.13	49.5	4.15	20.90	0.49	8.74	0	0.14	99.3
1161 *** CHR AT MARGIN SPOT 6	0.1	0.59	13.92	49.99	5.46	20.43	0.42	8.69	0.09	0.06	99.2
1162 *** CHR CENTRAL SPOT 7	0	0.61	13.95	49.18	5.34	20.19	0.54	8.82	0	0.12	98.22
1163 *** CHR CENTRAL SPOT 7	0.06	0.64	14.01	49.52	5.58	20.39	0.47	8.72	0.12	0.14	99.09
1164 *** CHR SMALLER SPOT 8	0.02	0.63	13.8	50.23	4.47	20.61	0.5	8.54	0.17	0.03	98.55
1165 *** CHR V SMALL SPOT 9	0	0.63	13.83	50.05	5.24	20.96	0.59	8.49	0.06	0.15	99.48
1166 *** CHR * 232792 223.0m CENTRAL S 1 08-29-4524	0.03	0.63	14.38	49.94	4.88	21.09	0.47	8.49	0.11	0.13	99.66
1167 *** CHR AT MARGIN SPOT 2	0.02	0.62	14.51	49.31	5.07	20.41	0.53	8.73	0.18	0.17	99.05
1168 *** CHR CENTRAL SPOT 3	0.04	0.68	14.31	49.77	4.93	20.82	0.42	8.64	0.16	0.07	99.35
1169 *** CHR AT MARGIN SPOT 4	0.03	0.6	14.49	49.13	5.54	20.94	0.49	8.52	0.13	0.13	99.44
1170 *** CHR CENTRAL SPOT 5	0.05	0.58	13.67	49.62	6.06	19.99	0.53	8.85	0.15	0.19	99.08
1171 *** CHR AT MARGIN SPOT 6	0.06	0.62	14.66	49.66	5.61	20.85	0.52	8.76	0.02	0.15	100.35
1172 *** CHR AT MARGIN SPOT 6	0.07	0.54	14.4	49.06	4.93	19.74	0.51	8.77	0.18	0.15	97.86
1173 *** CHR AT MARGIN SPOT 6	0.01	0.61	14.22	49.76	5.67	21.01	0.55	8.63	0.07	0.14	100.1
1174 *** CHR AT MARGIN SPOT 6	0	0.6	13.5	48.53	5.79	19.90	0.54	8.63	0.22	0.12	97.25
1175 *** CHR AT MARGIN SPOT 6	0.06	0.59	14.32	48.51	5.47	20.43	0.61	8.33	0.24	0.15	98.16
1176 *** CHR AT MARGIN SPOT 6	0.02	0.61	14.47	49.5	5.12	20.85	0.44	8.69	0.03	0.09	99.31
1177 *** CHR SMALLER SPOT 7	0.01	0.49	14.11	49.82	5.80	20.98	0.49	8.62	0	0.1	99.84
1178 *** CHR SMALLER SPOT 7	0	0.55	13.83	48.25	5.81	20.17	0.45	8.62	0.08	0.1	97.28
1179 *** CHR SMALLER SPOT 7	0.01	0.57	14.14	48.8	6.09	20.42	0.63	8.65	0.17	0.12	98.99
1180 *** CHR SMALLER SPOT 8	0	0.59	14.05	49.62	4.49	20.74	0.42	8.42	0.1	0.18	98.16
1181 *** CHR SMALLER SPOT 8	0.03	0.63	14.12	48.94	5.00	20.69	0.47	8.37	0.15	0.11	98.01
1182 *** CHR SMALLER SPOT 8	0.02	0.57	13.99	48.31	5.38	20.63	0.44	8.36	0.06	0.02	97.24
1184 *** CHR SMALLER SPOT 8	0	0.6	14.7	48.29	5.43	20.28	0.6	8.73	0.12	0.16	98.36
1185 *** CHR * 232793 223.0m CENTRAL S 1 08-30-4525	0	0.65	14.7	48.71	5.52	20.82	0.53	8.72	0	0.14	99.24
1186 *** CHR AT MARGIN SPOT 2	0	0.54	14.49	49.23	4.96	20.45	0.61	8.59	0.18	0.15	98.71
1188 *** CHR CENTRAL SPOT 3	0	0.7	14.39	49.37	4.64	21.29	0.51	8.31	0.09	0.13	98.97
1189 *** CHR AT MARGIN SPOT 4	0	0.68	14.23	49.59	5.03	21.16	0.5	8.43	0.11	0.17	99.39
1190 *** CHR CENTRAL SPOT 5	0	0.65	13.83	50.08	4.85	21.31	0.49	8.26	0.15	0.11	99.24
1191 *** CHR CENTRAL SPOT 6	0	0.65	14.6	50.47	4.32	21.33	0.55	8.47	0.16	0.13	100.25
1192 *** CHR CENTRAL SPOT 6	0	0.54	14.21	49.14	5.01	20.61	0.56	8.37	0.21	0.19	98.34
1193 *** CHR SMALLER SPOT 7	0	0.64	14.21	49.29	5.39	20.67	0.47	8.65	0.13	0.22	99.13
1194 *** CHR SMALLER SPOT 8	0	0.58	14.46	49.58	4.82	20.66	0.7	8.57	0.06	0.14	99.09
1195 *** CHR V SMALL SPOT 9	0	0.6	14.55	49.12	4.75	21.03	0.49	8.35	0.13	0.17	98.71
1196 *** CHR * 232794 223.8m CENTRAL S-1 08-30-4526	0	0.65	13.27	50.2	4.47	20.70	0.44	8.31	0.14	0.19	97.92
1197 *** CHR CENTRAL SPOT 1	0	0.58	14.53	49.33	5.18	20.90	0.54	8.5	0.15	0.21	99.4
1198 *** CHR AT MARGIN SPOT 2	0	0.59	14.45	49.67	4.46	20.84	0.69	8.42	0.06	0.13	98.86
1199 *** CHR CENTRAL SPOT 3	0	0.62	14.24	49.66	4.84	21.35	0.43	8.29	0.04	0.21	99.19
1200 *** CHR AT MARGIN SPOT 4	0	0.64	14.33	49.11	4.60	20.90	0.56	8.29	0.17	0.14	98.28
1201 *** CHR AT MARGIN SPOT 4	0	0.65	14.29	51.11	4.04	21.57	0.55	8.33	0.08	0.18	100.39
1202 *** CHR AT MARGIN SPOT 4	0	0.63	13.8	49.36	4.46	20.92	0.48	8.11	0.19	0.17	97.68
1203 *** CHR AT MARGIN SPOT 4	0	0.69	14.22	48.75	4.61	20.88	0.49	8.3	0.13	0.1	97.71
1204 *** CHR CENTRAL SPOT 5	0	0.62	14.24	49.68	4.88	21.19	0.55	8.31	0.18	0.11	99.28
1205 *** CHR AT MARGIN SPOT 6	0.01	0.66	14.15	49.16	5.21	21.11	0.6	8.25	0.1	0.18	98.91
1206 *** CHR CENTRAL SPOT 7	0	0.63	14.04	49.4	4.40	20.88	0.57	8.28	0	0.15	97.91

Big Daddy FW-08-19

	SiO2	TiO2	Al2O3	Cr2O3	Fe2O3	FeO	MnO	MgO	ZnO	NiO	TOTAL
1207 *** CHR CENTRAL SPOT 7	0	0.61	14.26	49.01	5.07	20.65	0.57	8.47	0.14	0.15	98.42
1208 *** CHR SMALLER SPOT 8	0	0.69	13.09	49	5.36	20.82	0.5	8.17	0.1	0.06	97.25
1209 *** CHR SMALLER SPOT 8	0	0.61	14.34	49.65	4.59	21.11	0.47	8.32	0.18	0.16	98.97
1210 *** CHR SMALLER SPOT 8	0	0.65	13.87	49.44	4.96	21.05	0.52	8.32	0.06	0.09	98.46
1211 *** CHR SMALLER SPOT 8	0	0.65	14.16	49.94	4.42	21.36	0.56	8.19	0.13	0.1	99.07
1212 *** CHR V SMALL SPOT 9	0.01	0.62	14.47	48.72	4.73	20.65	0.55	8.37	0.04	0.27	97.95
1213 *** CHR V SMALL SPOT 9	0	0.62	14.57	48.22	5.07	20.85	0.41	8.41	0.12	0.1	97.86
1214 *** CHR * 232795 224.2m CENTRAL S-1 08-30-4527	0	0.69	14.8	47.41	5.48	19.33	0.49	9.21	0.2	0.13	97.19
1215 *** CHR CENTRAL SPOT 1	0	0.71	15.04	48.33	5.21	19.94	0.46	9.23	0.02	0.19	98.61
1216 *** CHR CENTRAL SPOT 1	0	0.57	15.01	49.41	4.62	19.92	0.51	9.23	0.06	0.1	98.96
1217 *** CHR AT MARGIN SPOT 2	0	0.63	14.88	50.19	4.08	20.84	0.55	8.75	0.06	0.13	99.7
1218 *** CHR CENTRAL SPOT 3	0	0.63	14.39	48.64	4.84	20.44	0.55	8.54	0.11	0.13	97.79
1219 *** CHR CENTRAL SPOT 3	0	0.55	14.44	48.68	5.43	20.58	0.6	8.49	0.1	0.22	98.54
1220 *** CHR AT MARGIN SPOT 4	0	0.68	14.42	50.1	4.65	21.29	0.54	8.48	0.15	0.08	99.92
1221 *** CHR CENTRAL SPOT 5	0.05	0.62	15.03	50.06	4.02	20.74	0.52	8.72	0	0.13	99.49
1222 *** CHR CENTRAL SPOT 6	0.06	0.59	13.49	50.23	5.27	20.17	0.52	8.67	0.14	0.12	98.73
1223 *** CHR CENTRAL SPOT 7	0.01	0.62	14.76	49.07	4.88	20.65	0.59	8.6	0.13	0.17	98.99
1224 *** CHR SMALLER SPOT 9	0	0.66	13.3	50.25	4.82	20.64	0.47	8.53	0.06	0.11	98.36
1225 *** CHR SMALLER SPOT 9	0.03	0.72	14.26	49.13	5.03	20.95	0.64	8.4	0.07	0.05	98.78
1226 *** CHR AT MARGIN SPOT 9	0.01	0.65	14.31	50.6	4.36	21.26	0.44	8.53	0.05	0.14	99.91
1227 *** CHR AT MARGIN SPOT 9	0.01	0.66	14.13	48.26	5.44	20.42	0.53	8.52	0.14	0.09	97.65
1228 *** CHR AT MARGIN SPOT 9	0	0.69	14.26	49.15	4.55	21.02	0.44	8.39	0	0.15	98.2
1229 *** CHR * 232796 224.4m CENTRAL S-1 08-30-4528	0.07	0.71	15.22	48.77	4.87	19.18	0.55	9.49	0.15	0.13	98.65
1230 *** CHR CENTRAL SPOT 1	0	0.67	14.9	47.95	5.02	19.22	0.56	9.36	0.07	0.1	97.34
1231 *** CHR CENTRAL	0.02	0.5	14.31	47.54	6.20	19.62	0.46	8.83	0.16	0.19	97.21
1232 *** CHR CENTRAL	0.03	0.51	14.14	48.86	5.63	19.76	0.46	8.94	0.09	0.13	97.99
1233 *** CHR CENTRAL	0	0.53	14.3	48.68	5.86	20.00	0.46	8.93	0.07	0.24	98.48
1234 *** CHR AT MARGIN SPOT 2	0.09	0.51	14.16	48.86	5.98	20.06	0.51	8.69	0.03	0.16	98.45
1235 *** CHR AT MARGIN SPOT 2	0.05	0.46	14.46	49.66	5.33	20.71	0.51	8.49	0.05	0.25	99.44
1236 *** CHR SPOT 2 AGAIN	0.01	0.49	14.51	49.92	5.31	20.94	0.44	8.72	0	0.12	99.93
1237 *** CHR CENTRAL SPOT 3	0.03	0.53	14.77	48.88	6.38	20.52	0.48	8.94	0.04	0.22	100.15
1238 *** CHR AT MARGIN SPOT 4	0.09	0.38	14.69	47.69	7.02	19.88	0.5	8.82	0.09	0.12	98.58
1239 *** CHR CENTRAL SPOT 5	0.04	0.5	14.45	49.1	6.16	21.18	0.5	8.34	0.15	0.19	100
1240 *** CHR CENTRAL SPOT 5	0.05	0.46	14.26	48.16	6.11	20.50	0.5	8.29	0.25	0.15	98.12
1241 *** CHR CENTRAL SPOT 5	0.01	0.46	14.25	48.09	6.69	20.97	0.52	8.37	0.04	0.12	98.85
1242 *** CHR CENTRAL SPOT 6	0	0.4	14.05	49.11	5.99	20.71	0.56	8.51	0	0.09	98.82
1243 *** CHR SMALLER SPOT 8	0.02	0.41	14.13	48.81	6.07	20.50	0.52	8.49	0.15	0.11	98.6
1244 *** CHR V SMALL SPOT 9	0.02	0.49	14.7	49.34	5.66	20.87	0.5	8.64	0.2	0.06	99.92
1245 *** CHR * 232797 224.8m CENTRAL S-1 08-30-4530	0.04	0.51	14.85	49.55	5.41	19.08	0.61	9.59	0.09	0.18	99.37
1246 *** CHR AT MARGIN SPOT 2	0.09	0.46	15.48	48.83	5.31	20.06	0.54	9.01	0	0.11	99.36
1247 *** CHR AT MARGIN SPOT 2	0.01	0.55	14.93	48.42	5.26	20.72	0.48	8.61	0.03	0.14	98.62
1248 *** CHR AT MARGIN SPOT 4	0.09	0.53	14.56	48.16	5.98	19.24	0.53	9.12	0.09	0.13	97.83
1249 *** CHR AT MARGIN SPOT 4	0.05	0.58	15.18	48.01	5.79	20.05	0.58	8.94	0.11	0.13	98.84
1250 *** CHR CENTRAL SPOT 5	0	0.42	14.25	49.52	5.31	19.61	0.62	9.02	0.11	0.19	98.52
1251 *** CHR AT MARGIN SPOT 6	0.03	0.54	14.06	49.01	5.68	20.27	0.55	8.6	0.17	0.15	98.49
1252 *** CHR AT MARGIN SPOT 6	0	0.54	14.26	49.33	4.89	20.27	0.61	8.63	0.14	0.15	98.33
1253 *** CHR SMALLER SPOT 7	0.01	0.48	14.6	49.18	4.52	20.64	0.5	8.47	0	0.14	98.09
1254 *** CHR SMALLER SPOT 7	0	0.53	14.66	49.52	3.77	20.83	0.56	8.31	0	0.19	97.99
1255 *** CHR SMALLER SPOT 7	0.01	0.58	14.56	49.94	5.10	20.93	0.51	8.69	0.12	0.12	100.05
1256 *** CHR SMALLER SPOT 8	0	0.54	14.8	49.58	5.00	20.53	0.6	8.82	0.07	0.17	99.61
1257 *** CHR V SMALL SPOT 9	0.04	0.59	14.93	48.89	5.08	20.54	0.55	8.78	0.02	0.02	98.93
1258 *** CHR * 232798 225.2m CENTRAL S-1 08-30-4531 ?	0.03	0.63	14.45	48.35	5.80	20.73	0.58	8.49	0.02	0.17	98.67
1259 *** CHR CENTRAL SPOT 1	0	0.71	14.53	47.04	5.98	20.61	0.65	8.37	0.14	0.14	97.57
1260 *** CHR CENTRAL SPOT 1	0.02	0.71	14.65	49.39	4.75	21.08	0.61	8.42	0.17	0.14	99.46
1261 *** CHR AT MARGIN SPOT 2	0.03	0.68	13.06	49.02	5.63	20.64	0.6	8.1	0.12	0.2	97.52
1262 *** CHR AT MARGIN SPOT 2	0.01	0.62	13.97	49.62	4.80	21.37	0.54	8.04	0.09	0.2	98.78
1263 *** CHR SPOT 3 CENTRAL	0	0.71	14.71	48.82	4.94	20.53	0.48	8.81	0.13	0.11	98.75
1265 *** CHR AT MARGIN SPOT 4	0	0.89	14.37	48.07	5.06	21.04	0.54	8.38	0.15	0.07	98.07
1266 *** CHR AT MARGIN SPOT 4	0	0.61	14.54	49.61	4.45	20.77	0.56	8.54	0.12	0.13	98.89
1267 *** CHR CENTRAL SPOT 5	0	0.59	14.71	49.36	4.99	21.19	0.61	8.36	0.1	0.21	99.62
1268 *** CHR AT MARGIN SPOT 6	0	0.72	14.29	49.64	5.34	21.49	0.57	8.36	0.13	0.15	100.16
1269 *** CHR CENTRAL SPOT 7	0.02	0.69	14.24	49.8	4.95	21.29	0.55	8.33	0.15	0.12	99.65
1270 *** CHR SMALLER SPOT 8	0	0.68	14.37	48.97	4.47	21.39	0.5	8.09	0.06	0.14	98.23
1272 *** CHR SMALLER SPOT 8	0	0.64	14.29	48.63	4.66	21.11	0.59	8.08	0.09	0.12	97.74
1273 *** CHR SMALLER SPOT 8	0.03	0.73	14.29	49.05	4.62	21.08	0.59	8.2	0	0.21	98.34
1274 *** CHR SMALLER SPOT 8	0	0.68	13.95	48.39	5.15	20.70	0.59	8.22	0.18	0.14	97.48
1275 *** CHR SMALLER SPOT 8	0.11	0.8	14.27	48.43	5.41	20.99	0.48	8.22	0.06	0.12	98.34
1276 *** CHR CENTRAL SPOT 1 AGAIN 08-30-4531	0	0.82	14.86	48.01	5.03	21.12	0.6	8.42	0	0.17	98.53
1277 *** CHR SPOT 1 AGAIN	0.01	0.65	14.63	48.71	5.71	21.03	0.58	8.55	0.07	0.11	99.48
1278 *** CHR AT MARGIN SPOT 2	0	0.73	14.26	48.84	5.56	21.58	0.56	8.16	0.2	0.08	99.42
1279 *** CHR CENTRAL SPOT 3	0.03	0.74	14.73	50.65	4.09	20.96	0.48	8.77	0.05	0.23	100.32
1280 *** CHR CENTRAL SPOT 3	0	0.67	14.8	49.15	4.90	20.87	0.39	8.75	0.1	0.12	99.26
1281 *** CHR AT MARGIN SPOT 4	0.02	0.68	14.88	49.97	4.47	21.08	0.5	8.56	0.19	0.24	100.14
1282 *** CHR CENTRAL SPOT 5	0	0.76	14.8	49.77	4.59	21.78	0.49	8.38	0.07	0.11	100.29
1283 *** CHR AT MARGIN SPOT 6	0.02	0.64	14.14	49.76	4.70	21.47	0.45	8.14	0.12	0.12	99.09
1284 *** CHR CENTRAL SPOT 7	0.03	0.69	14.43	49.36	5.26	21.05	0.61	8.52	0.02	0.1	99.54
1285 *** CHR SMALLER SPOT 8	0	0.69	14.37	48.71	5.33	21.20	0.61	8.25	0.08	0.2	98.91
1286 *** CHR V SMALL SPOT 9	0	0.7	14.13	49.91	5.09	21.69	0.48	8.23	0.15	0.13	100
1287 *** CHR V SMALL SPOT 9	0.01	0.69	13.98	49.3	4.44	21.33	0.49	8.05	0.07	0.11	98.03

Big Daddy FW-08-19

	SiO2	TiO2	Al2O3	Cr2O3	Fe2O3	FeO	MnO	MgO	ZnO	NiO	TOTAL
1288 *** CHR * 232799 225.6m CENTRAL S-1 08-31-4532	0	0.6	15.18	49.13	5.20	20.35	0.45	9.18	0.03	0.15	99.75
1289 *** CHR AT MARGIN SPOT 2	0	0.61	14.96	48.71	4.96	20.88	0.49	8.63	0.06	0.09	98.89
1290 *** CHR CENTRAL SPOT 3	0	0.61	15.33	48.03	5.46	20.60	0.46	8.88	0.02	0.15	98.99
1291 *** CHR AT MARGIN SPOT 4	0.06	0.79	15.59	49.03	4.37	20.90	0.46	8.83	0.07	0.1	99.76
1292 *** CHR CENTRAL SPOT 5	0	0.61	15.08	48.31	5.60	20.50	0.62	8.78	0.16	0.17	99.27
1293 *** CHR CENTRAL SPOT 6	0.03	0.7	15.26	48.45	4.80	20.74	0.54	8.69	0.07	0.09	98.89
1294 *** CHR CENTRAL SPOT 7	0.01	0.71	15.37	48.84	4.49	20.63	0.53	8.89	0.08	0.09	99.19
1295 *** CHR SMALLER SPOT 8	0.01	0.66	15.51	48.21	4.25	20.42	0.42	8.83	0.08	0.12	98.08
1296 *** CHR SMALLER SPOT 8	0	0.65	15.43	48.51	4.91	20.82	0.51	8.78	0.06	0.15	99.33
1297 *** CHR V SMALL SPOT 9	0	0.7	15.34	49.14	4.42	20.98	0.53	8.78	0.07	0.06	99.57
1298 *** CHR * 232800 226.0m CENTRAL S 1 08-30-4533	0	0.72	14.9	48.94	4.86	21.28	0.47	8.47	0.15	0.13	99.43
1299 *** CHR AT MARGIN SPOT 2	0.04	0.88	15.1	49	4.30	21.36	0.45	8.44	0.17	0.12	99.43
1300 *** CHR AT MARGIN SPOT 3	0.01	0.7	14.68	49.65	5.02	21.26	0.41	8.66	0	0.18	100.06
1301 *** CHR AT MARGIN SPOT 4	0.03	0.64	14.69	48.91	5.26	21.41	0.49	8.28	0.03	0.16	99.37
1302 *** CHR CENTRAL SPOT 5	0	0.61	14.42	48.69	5.41	20.82	0.54	8.5	0.03	0.17	98.65
1303 *** CHR AT MARGIN SPOT 6	0	0.72	14.58	49.82	4.24	21.71	0.48	8.17	0.1	0.18	99.58
1304 *** CHR SMALLER SPOT 7	0.02	0.65	14.56	49.65	4.60	21.44	0.53	8.25	0	0.2	99.44
1305 *** CHR SMALLER SPOT 8	0.02	0.76	14.59	49.34	4.50	21.76	0.48	8.1	0.06	0.17	99.33
1306 *** CHR V SMALL SPOT 9]	0.02	0.75	14.39	49.45	5.40	21.85	0.51	8.22	0.06	0.13	100.24
1307 *** CHR * 232801 226.4m CENTRAL S-1 08-31-4534	0.03	0.66	15.49	46.96	5.11	20.25	0.52	8.69	0	0.2	97.4
1308 *** CHR CENTRAL S 1	0.02	0.6	15.02	48.18	5.38	20.74	0.6	8.52	0.11	0.14	98.77
1309 *** CHR AT MARGIN SPOT 2	0	0.68	14.69	47.97	5.15	21.73	0.46	8.01	0	0.1	98.27
1310 *** CHR AT MARGIN SPOT 2	0	0.69	14.79	47.53	5.49	21.41	0.59	8.08	0	0.2	98.23
1311 *** CHR AT MARGIN SPOT 2	0.06	0.64	14.84	47.55	5.08	21.27	0.52	7.93	0	0.16	97.54
1312 *** CHR CENTRAL SPOT 3	0.03	0.8	15.04	47.77	5.46	21.25	0.5	8.37	0.15	0.13	98.95
1313 *** CHR AT MARGIN SPOT 4	0.08	0.58	14.81	48.36	5.89	21.38	0.51	8.08	0.1	0.23	99.43
1314 *** CHR CENTRAL SPOT 5	0.06	0.69	15.03	47.01	5.43	20.94	0.37	8.19	0.2	0.12	97.5
1315 *** CHR CENTRAL SPOT 5	0.06	0.69	15.09	47.29	4.96	21.49	0.48	7.87	0	0.17	97.61
1316 *** CHR CENTRAL SPOT 5	0.02	0.68	14.98	46.63	5.99	21.31	0.48	8.07	0.08	0.18	97.82
1317 *** CHR CENTRAL SPOT 5	0.04	0.75	15.18	47.2	5.78	21.41	0.46	8.21	0.07	0.2	98.72
1318 *** CHR CENTRAL SPOT 6	0.03	0.76	15.48	47.46	5.39	21.25	0.41	8.5	0.07	0.12	98.93
1319 *** CHR SMALLER SPOT 7	0	0.72	14.9	47.62	5.04	21.61	0.49	8.03	0.03	0.13	98.07
1320 *** CHR SMALLER SPOT 7	0.04	0.71	14.66	47.59	6.09	21.80	0.57	7.89	0.09	0.14	98.97
1321 *** CHR SMALLER SPOT 8	0.01	0.68	14.88	48.54	5.04	21.94	0.47	7.97	0.14	0.13	99.29
1322 *** CHR V SMALL SPOT 9	0	0.7	14.83	48.15	4.85	21.89	0.49	7.83	0.25	0.09	98.6
1323 *** CHR * 232803 227.2m CENTRAL S-1 09-01-4535	0.03	0.69	14.82	48.63	4.41	23.88	0.46	6.71	0.16	0.07	99.42
1325 *** CHR AT MARGIN SPOT 2	0.01	0.72	14.51	47.95	4.92	23.43	0.39	6.91	0.12	0.11	98.57
1326 *** CHR CENTRAL SPOT 3	0	0.66	14.49	49.39	5.61	20.09	0.45	9.3	0.06	0.09	99.58
1327 *** CHR AT MARGIN SPOT 4	0.03	0.65	14.41	48.55	4.75	23.22	0.47	6.89	0.13	0.18	98.8
1328 *** CHR CENTRAL SPOT 5	0.07	0.72	14.37	49.76	4.80	23.82	0.53	6.85	0.05	0.16	100.65
1329 *** CHR CENTRAL SPOT 5	0.03	0.76	13.59	48.51	4.86	23.43	0.33	6.66	0.13	0.17	97.99
1330 *** CHR CENTRAL SPOT 5	0.05	0.65	14.47	48.64	5.87	23.54	0.54	6.95	0.16	0.15	100.43
1331 *** CHR CENTRAL SPOT 5	0.02	0.66	14.32	48.77	4.71	23.49	0.51	6.86	0	0.12	98.99
1332 *** CHR AT MARGIN SPOT 6	0.08	0.7	14.18	48.39	5.33	23.87	0.42	6.48	0.13	0.18	99.23
1333 *** CHR SMALLER SPOT 8	0.01	0.73	14.11	48.68	4.94	24.13	0.54	6.41	0.2	0.17	99.42
1335 *** CHR V SMALL SPOT 9	0	0.64	14.12	49.74	4.41	24.17	0.49	6.5	0.24	0.14	100.01
1336 *** CHR V SMALL SPOT 9	0.04	0.68	14.26	48.81	4.62	24.29	0.44	6.32	0.11	0.14	99.25
1337 *** CHR CENTRAL SPOT 3 AGAIN	0.02	0.74	14.96	49.27	4.91	20.48	0.53	9.04	0.11	0.05	99.62
1338 *** CHR AT MARGIN SPOT 4 AGAIN	0.07	0.68	14.57	48.72	5.02	23.97	0.52	6.56	0.13	0.14	99.88
1339 *** CHR * 232805 228.0m CENTRAL S-1 09-02-4536	0	0.63	14.59	48.36	5.02	22.68	0.39	7.46	0.01	0.16	98.8
1340 *** CHR AT MARGIN SPOT 2	0	0.62	14.7	49.1	5.17	22.62	0.54	7.58	0.23	0.13	100.17
1341 *** CHR AT MARGIN SPOT 2	0	0.61	14.79	49.76	3.66	22.96	0.54	7.28	0.09	0.13	99.45
1342 *** CHR CENTRAL SPOT 3	0	0.65	14.43	48.76	4.48	23.00	0.56	7.07	0.08	0.17	98.75
1343 *** CHR AT MARGIN SPOT 4	0.02	0.56	14.93	48.84	4.56	22.50	0.56	7.44	0.16	0.1	99.21
1344 *** CHR CENTRAL SPOT 5	0	0.62	14.73	50.39	4.57	21.79	0.39	8.32	0.2	0.18	100.74
1345 *** CHR CENTRAL SPOT 5	0	0.61	14.94	50.1	3.64	22.21	0.5	7.88	0	0.19	99.71
1346 *** CHR CENTRAL SPOT 6	0.02	0.71	14.97	49.01	4.26	22.50	0.56	7.64	0	0.13	99.37
1347 *** CHR SMALLER SPOT 7	0	0.58	14.72	49.96	4.18	22.81	0.51	7.46	0.1	0.21	100.11
1348 *** CHR SMALLER SPOT 8	0	0.63	14.49	47.41	5.76	22.49	0.45	7.36	0.15	0.15	98.32
1349 *** CHR SMALLER SPOT 9	0.02	0.58	14.1	47.68	5.42	22.15	0.44	7.36	0.11	0.05	97.36
1350 *** CHR SMALLER SPOT 9	0	0.65	14.53	47.32	5.26	22.25	0.53	7.34	0.11	0.18	97.64
1351 *** CHR SMALLER SPOT 9	0	0.6	14.3	48.19	4.99	22.16	0.52	7.46	0.03	0.18	97.93
1352 *** CHR SMALLER SPOT 9	0	0.58	14.73	47.97	4.81	22.16	0.44	7.52	0.05	0.21	97.99
1353 *** CHR SMALL BRIGHT AT MARGIN	0.04	0.15	5.99	63.64	0.33	24.51	0.54	5.12	0.23	0.15	100.67
1354 *** CHR SMALL BRIGHT AT MARGIN	0.04	0.14	5.85	61.36	1.29	23.98	0.59	5	0.19	0.11	98.42
1355 *** CHR * 232806 228.4m CENTRAL S-1 09-02-4537	0	0.78	14.59	48.53	4.90	21.08	0.48	8.5	0	0.12	98.49
1356 *** CHR CENTRAL SPOT 1	0	0.71	15.19	49	4.67	21.54	0.38	8.46	0.05	0.2	99.73
1357 *** CHR AT MARGIN SPOT 2	0	0.69	15.09	47.64	5.28	22.12	0.52	7.75	0.18	0.15	98.89
1358 *** CHR CENTRAL SPOT 3	0	0.73	14.95	48.5	5.29	22.36	0.54	7.86	0.12	0.14	99.96
1359 *** CHR AT MARGIN SPOT 4	0.01	0.65	15.02	48.28	5.49	22.83	0.56	7.54	0	0.16	99.99
1360 *** CHR AT MARGIN SPOT 4	0	0.6	14.89	47.19	5.92	22.40	0.46	7.53	0.19	0.09	98.67
1361 *** CHR CENTRAL SPOT 5	0	0.67	14.95	48.08	5.59	22.22	0.42	7.93	0.01	0.2	99.51
1362 *** CHR AT MARGIN SPOT 6	0.02	0.59	14.77	48.27	5.38	22.56	0.48	7.51	0.04	0.15	99.23
1363 *** CHR CENTRAL SPOT 7	0.03	0.65	14.79	47.53	5.71	21.52	0.45	8.03	0.04	0.16	98.34
1364 *** CHR CENTRAL SPOT 7	0	0.66	14.72	46.91	6.37	21.89	0.47	7.85	0.08	0.18	98.49
1365 *** CHR SMALLER SPOT 8	0	0.66	14.59	47.96	4.87	22.45	0.59	7.36	0.07	0.1	98.16
1366 *** CHR SMALLER SPOT 8	0	0.7	14.67	47.74	5.12	22.56	0.5	7.39	0.11	0.13	98.41
1367 *** CHR V SMALL SPOT 9	0	0.69	14.5	47.75	4.93	22.60	0.45	7.23	0.16	0.17	97.98
1368 *** CHR V SMALL SPOT 9	0	0.64	14.76	48.01	4.96	22.49	0.59	7.44	0.04	0.1	98.53

Big Daddy FW-08-19

	SiO2	TiO2	Al2O3	Cr2O3	Fe2O3	FeO	MnO	MgO	ZnO	NiO	TOTAL
1369 *** CHR * 232807 228.8m CENTRAL S-1 09-02-453E	0.02	0.74	15.29	46.34	5.28	24.42	0.44	6.32	0.07	0.1	98.49
1370 *** CHR AT MARGIN SPOT 2	0.04	0.67	14.53	46.82	5.70	24.74	0.37	5.89	0.14	0.22	98.55
1371 *** CHR CENTRAL SPOT 3	0.04	0.74	14.97	46.27	5.93	24.84	0.44	6.01	0.1	0.15	98.89
1372 *** CHR AT MARGIN SPOT 4	0.06	0.72	15.27	46.61	5.78	25.06	0.42	6	0.15	0.09	99.58
1373 *** CHR AT MARGIN SPOT 4	0.04	0.77	15.05	46.71	5.35	24.90	0.48	5.98	0.11	0.15	99
1374 *** CHR CENTRAL SPOT 5	0.05	0.76	14.86	45.86	6.64	24.30	0.56	6.23	0.1	0.21	98.91
1375 *** CHR CENTRAL SPOT 6	0.03	0.72	15.21	46.16	6.21	23.27	0.48	7	0.12	0.15	98.72
1376 *** CHR SMALLER SPOT 7	0.07	0.74	15.18	46.61	6.03	25.08	0.5	5.92	0.18	0.14	99.85
1377 *** CHR V SMALL SPOT 8	0.01	0.77	14.97	46.76	5.63	24.79	0.55	6.09	0.22	0.13	99.36
1378 *** CHR V SMALL SPOT 8	0.02	0.7	14.65	46.15	6.33	24.86	0.52	6	0	0.07	98.67
1379 *** CHR * 232808 229.2m CENTRAL S-1 09-02-453E	0.04	0.75	16.3	44.88	7.07	22.26	0.53	7.89	0	0.19	99.2
1380 *** CHR AT MARGIN SPOT 2	0.02	0.84	15.95	44.91	6.67	25.26	0.51	6.11	0.17	0.07	99.84
1381 *** CHR CENTRAL SPOT 3	0.06	0.76	15.95	43.83	7.37	22.98	0.53	6.98	0.22	0.21	98.15
1382 *** CHR CENTRAL SPOT 3	0.05	0.79	15.95	44.55	7.46	23.65	0.44	7	0.14	0.14	99.42
1383 *** CHR AT MARGIN SPOT 4	0.07	0.83	15.66	44.74	6.88	24.98	0.46	6.08	0	0.16	99.17
1384 *** CHR CENTRAL SPOT 5	0.06	0.74	16.2	45.32	6.44	24.57	0.43	6.52	0.05	0.11	99.8
1385 *** CHR AT MARGIN SPOT 6	0.08	0.77	15.62	44.94	6.17	24.90	0.33	5.96	0.08	0.1	98.34
1386 *** CHR CENTRAL SPOT 7	0.05	0.79	15.92	44.79	7.11	22.29	0.52	7.74	0.02	0.14	98.66
1387 *** CHR SMALLER SPOT 8	0.05	0.78	15.78	44.12	6.81	24.61	0.51	6.06	0.14	0.16	98.34
1388 *** CHR V SMALL SPOT 9	0.09	0.77	15.53	43.97	7.34	24.97	0.54	5.7	0.17	0.16	98.51
1389 *** CHR * 232809 229.6m CENTRAL S-1 09-02-454C	0.14	0.48	14.49	44.59	8.33	26.53	0.41	4.47	0.25	0.1	98.96
1390 *** CHR CENTRAL SPOT 3	0.11	1.3	14.7	43.55	8.65	26.78	0.48	5.14	0.16	0.08	100.08
1391 *** CHR CENTRAL SPOT 3	0.05	1.28	14.73	41.6	8.39	26.13	0.58	4.99	0.19	0.11	97.21
1392 *** CHR CENTRAL SPOT 3	0.08	0.84	14.8	43.75	8.35	25.94	0.53	5.2	0.18	0.09	98.92
1393 *** CHR AT MARGIN SPOT 4	0.09	0.62	15.06	43.61	8.37	27.21	0.46	4.35	0.19	0.08	99.2
1394 *** CHR CENTRAL SPOT 5	0.09	3.26	13.5	41.14	6.91	28.98	0.49	4.24	0.37	0.15	98.44
1395 *** CHR AT MARGIN SPOT 6	0.08	0.91	15.04	44.17	8.25	27.75	0.5	4.45	0.18	0.1	100.6
1396 *** CHR AT MARGIN SPOT 6	0.1	1.16	14.78	43.19	7.95	27.58	0.45	4.39	0.12	0.05	98.97
1397 *** CHR CENTRAL SPOT 5	0.08	0.49	15	43.3	9.00	27.08	0.5	4.32	0.16	0.16	99.19
1398 *** CHR SMALLER SPOT 8	0.12	0.55	15.21	42.61	9.42	27.25	0.48	4.3	0.03	0.09	99.12
1399 *** CHR SMALLER SPOT 9	0.11	0.93	14.5	42.65	8.80	27.16	0.55	4.23	0.14	0.11	98.3
1400 *** CHR BRIGHT ZONE AT MARGIN	0.12	0.37	6.88	59.18	2.89	27.92	0.62	3.03	0.2	0.09	101.01
1401 *** CHR BRIGHT ZONE AT MARGIN	0.13	0.28	6.72	57.89	3.50	27.34	0.52	3.07	0.17	0.07	99.34

APPENDIX 6**Chromite Laser Ablation data**

²⁷ Al	82216.8	86759.55	102123.35	81248.1	103464.72	77113.66	72102.32	91494.24	86606.53	81090.34	92430.96
²⁹ Si	126.93	1261.95	86.65	95.46	151.77	207.08	90.38	463.28	357.94	234.97	262.96
⁴² Ca	<10.46	<10.56	<14.66	<10.47	<8.46	<6.16	<7.64	7.75	<6.10	7.05	<6.68
⁴⁵ Sc	7.42	7.35	7.72	7.33	10.78	6.94	6.1	9.42	6.42	8.58	8.3
⁴⁹ Ti	2336.92	2573.32	2979.5	2956.37	3923.29	2907.14	2538.01	3365.81	3139.82	3198.2	3453.35
⁵³ Cr	331110	364481.56	363027.31	343612.94	410569.94	320397.88	318539.69	344141.25	330538.03	322514.94	341398.78
⁵⁵ Mn	2680.3	3209.92	2947.99	2966.21	3004.47	2610.49	2560.46	1758.25	1782.54	1916.6	1793.12
⁵⁷ Fe	186554.67	186554.67	186554.66	201479.06	201479.05	180569.38	180569.38	20.81	20.81	20.81	161758.42
⁵⁹ Co	257.96	246.63	246.3	243.01	279.48	218.6	221.26	228.47	222.19	211.41	222.3
⁶⁰ Ni	1169.13	668.32	1276.44	986.26	1482.01	988.27	974.8	1229.19	1074.96	1086.98	1104.9
⁶⁵ Cu	1.42	0.772	2.4	0.99	1.92	2.22	1.78	2.443	1.975	1.49	2.03
⁶⁶ Zn	429.45	753.21	579.6	623.46	491.9	410.72	381.5	507.26	490.19	453.55	602.02
⁷¹ Ga	36.72	49.69	45.85	41.89	51.55	37.33	34.42	41.86	38.34	37.81	41.76
⁷³ Ge	0.359	0.654	0.54	0.381	0.476	0.431	0.408	0.501	0.453	0.443	0.438
⁷⁵ As	<0.099	<0.096	<0.099	<0.100	0.087	<0.056	<0.067	0.227	0.231	0.167	0.144
⁸⁶ Sr	0.0338	1.25	0.0182	0.0418	0.105	0.0291	0.0534	0.0424	0.11	0.0129	0.0211
⁸⁹ Y	0.0053	0.383	0.006	0.0131	0.0141	0.00393	0.00374	0.00734	0.00439	0.00831	0.00175
⁹⁵ Mo	0.06	0.068	0.076	0.087	0.099	0.08	0.086	0.067	0.0543	0.0454	0.066
¹⁰² Ru	0.0184	0.038	0.025	0.0041	0.02	0.017	0.021	0.011	0.0123	0.003	0.0098
¹⁰³ Rh	<0.00120	<0.00208	<0.00142	<0.00164	<0.00088	0.00117	<0.00129	<0.00120	<0.00120	<0.00045	<0.00051
¹¹⁵ In	0.0077	0.0062	0.0079	0.0062	0.007	0.0054	0.0057	0.0141	0.0125	0.0102	0.014
¹¹⁸ Sn	0.06	0.117	0.122	0.083	0.164	0.1	0.08	0.1573	0.1323	0.152	0.137
¹²¹ Sb	<0.0075	0.0661	<0.0162	0.014	<0.0075	0.0064	<0.0061	0.0605	0.0887	0.0593	0.0255
¹⁷⁸ Hf	0.0351	0.0244	0.0595	0.0766	0.151	0.0748	0.054	0.0726	0.0427	0.0926	0.0712
¹⁸¹ Ta	0.00199	0.0031	0.00218	0.00236	0.0099	0.00453	0.00169	0.00249	0.00181	0.00508	0.00196
¹⁸² W	<0.00241	0.0497	<0.00	0.0032	0.0094	0.0032	0.0039	0.0041	0.313	<0.00053	<0.00262
¹⁹² Os	0.018	0.0128	0.0093	0.0085	0.0123	0.0112	0.0075	0.009	0.0059	0.0071	0.005
¹⁹³ Ir	0.0061	0.0055	0.0074	0.0054	0.0036	0.0036	0.003	0.0036	0.0031	0.0042	0.0149

²⁷ Al	87277.32	82275.89	587.77	76490.69	BD 232303A	BD 232303B	BD 232303C	BD 232303D	BD 232303E	BD 232304A	BD 232304B	BD 232304C	BD 232304D	BD 232304E
²⁹ Si	223.76	<6.86	5.38	222.09	78644.05	88787.19	260.46	77750.35	85971.61	87629.93	85386.68	83574.14	90614.8	
⁴² Ca	<6.86	5.38	8.03	<4.90	203.83	<7.12	255.3	<7.67	317.14	234.01	<6.22	229.76	267.29	
⁴⁵ Sc	5.32	8.03	8.69	8.69	8.46	6.58	8.66	8.66	9.47	5.17	7.17	10.07	6.19	
⁴⁹ Ti	3084.35	3303.29	3386.43	3386.43	3430.92	3006.36	3466.38	3466.38	3248.77	3084.47	3000.88	3604.98	3046.21	
⁵² Cr	328315.47	310058.06	295066.66	295066.66	293622.34	334600.69	295080.28	295080.28	323677.78	325910.5	316710	313404.13	327402.69	
⁵⁵ Mn	1810.23	2319.51	2208.14	2208.14	2173.27	2016.1	2157.28	2157.28	2359.31	2369.41	2293.07	2365.2	2317.68	
⁵⁷ Fe	161758.42	22.28	22.28	22.28	173184.89	173184.89	173184.88	173184.88	23.78	23.78	184844.55	184844.55	184844.55	
⁵⁹ Co	220.09	218.98	210.14	210.14	204.63	224.47	206.65	206.65	229.36	231.9	222.63	222.67	228.19	
⁶⁰ Ni	1039.15	802.34	798.93	798.93	754.24	949.06	753.88	753.88	1080.39	854.72	926.51	739.71	957.87	
⁶⁵ Cu	2.04	0.408	1.94	1.94	0.302	2.92	1.038	1.038	1.008	0.7	0.823	0.576	1.83	
⁶⁶ Zn	589.34	593.58	525.73	525.73	664.29	655.79	643.21	643.21	597.91	617.17	735.6	769.33	679.02	
⁷¹ Ga	38.92	37.21	37.27	37.27	39.53	40.47	36.42	36.42	40.56	40.99	41.64	44.75	38.76	
⁷³ Ge	0.472	0.503	0.459	0.459	0.379	0.532	0.46	0.46	0.423	0.406	0.44	0.432	0.312	
⁷⁵ As	0.091	0.17	0.147	0.147	0.106	0.065	0.135	0.135	0.181	0.214	0.149	0.173	0.133	
⁸⁶ Sr	0.0124	0.653	0.0149	0.0149	0.1051	0.0177	0.0331	0.0331	0.0316	0.0249	0.0175	0.0231	0.014	
⁸⁹ Y	0.00162	0.0313	0.00172	0.00172	0.0236	0.00151	0.00174	0.00174	0.00414	0.00216	0.00223	0.0146	0.00332	
⁹⁵ Mo	0.0346	0.0798	0.0654	0.0654	0.064	0.0427	0.0524	0.0524	0.066	0.066	0.0525	0.056	0.0519	
¹⁰² Ru	0.0082	0.0078	0.0071	0.0071	0.005	0.0099	0.0053	0.0053	0.0086	<0.0028	0.0049	<0.0027	<0.0029	
¹⁰³ Rh	<0.00115	0.00289	0.00059	0.00059	<0.00125	0.00098	<0.00130	<0.00130	<0.00087	<0.00110	<0.00086	0.01	<0.00114	
¹¹⁵ In	0.01	0.0152	0.0098	0.0098	0.0109	0.0116	0.0135	0.0135	0.0132	0.00748	0.0104	0.0129	0.0084	
¹¹⁸ Sn	0.127	0.148	0.1719	0.1719	0.156	0.145	0.132	0.132	0.192	0.163	0.168	0.191	0.18	
¹²¹ Sb	0.0277	0.052	0.0796	0.0796	0.0345	0.0213	0.0168	0.0168	0.0468	0.051	0.0203	<0.0114	0.0172	
¹⁷⁸ Hf	0.0339	0.0883	0.1081	0.1081	0.105	0.0224	0.124	0.124	0.1117	0.0494	0.0839	0.173	0.0463	
¹⁸¹ Ta	0.00209	0.0075	0.0072	0.0072	0.0092	0.00187	0.0059	0.0059	0.00481	0.00229	0.0061	0.0085	0.00575	
¹⁸² W	<0.0037	<0.0029	0.0153	0.0153	0.0083	0.0049	<0.0059	<0.0059	<0.0035	<0.0041	<0.0036	0.00112	<0.00259	
¹⁹² Os	0.0092	0.0058	0.0058	0.0058	0.0079	0.0073	0.0033	0.0033	0.0035	0.0027	0.0057	0.0021	0.0032	
¹⁹³ Ir	0.0145	0.0034	0.0032	0.0032	0.0108	0.0129	0.0126	0.0126	0.0048	0.0052	0.0095	0.0038	0.0161	

²⁷ Al	109572.36	113859.48	116759.73	118015.15	117038.52	138937.86	131125.27	141358	143401.03	148150.95	80555.77
²⁹ Si	2191.64	313.76	387.31	300.98	400.52	469.33	417.47	424.73	433.6	376.65	295.38
⁴⁰ Ca	15.01	27.72	<12.40	28.78	<13.73	<9.91	<10.62	<13.39	<17.03	<12.94	13.14
⁴⁵ Sc	11.26	12.59	9.43	10.8	11.59	15.96	14.92	15.06	13.61	14.48	8.11
⁴⁹ Ti	4312.46	4466.81	3894.72	4270.62	4185.51	5389.21	5080.29	5399.17	5148.68	5406.17	3182.72
⁵³ Cr	432778.25	443242.25	419675.22	433281.31	431362.78	552542.75	523963.72	522967.88	520027.38	545285.06	311894.88
⁵⁵ Mn	3654.35	3410.24	3529.76	3407.58	3452.34	3974.57	4140.55	4056.01	4022.05	3956.89	2507.28
⁵⁷ Fe	32.5	32.5	32.5	32.5	32.5	38.14	38.14	38.14	38.14	38.14	23.35
⁵⁹ Co	318.55	310.79	309.36	304.3	300.47	376.23	367.92	357.59	355.65	369.38	220.71
⁶⁰ Ni	819.22	1468.96	1168.96	1555.63	1564.17	2012.23	1674.35	1710.77	1728.79	2074.85	1100.87
⁶⁵ Cu	0.505	0.584	0.697	1.898	1.64	2.19	1.023	2.81	1.3	2.22	0.546
⁶⁶ Zn	1076.02	930	1253.04	1066.77	720.43	872.41	977.06	1035.13	837.64	1021.39	585.86
⁷¹ Ga	59.92	55.08	50.16	53.92	50.94	67.32	64.92	67.45	64.03	66.7	40.81
⁷³ Ge	0.616	0.546	0.616	0.654	0.328	0.827	0.7	0.774	0.22	0.631	0.449
⁷⁵ As	0.175	0.268	0.133	0.175	0.098	0.265	0.274	0.223	0.39	0.257	0.156
⁸⁶ Sr	1.637	0.236	0.305	0.0393	0.218	0.0219	0.1217	0.0273	0.147	0.0238	0.374
⁸⁹ Y	0.1708	0.0161	0.0204	0.0069	0.0298	0.009	0.0149	0.0019	0.0146	0.0121	0.0266
⁹⁵ Mo	0.076	0.102	0.108	0.07	0.727	0.096	0.115	0.085	0.092	0.1	0.0705
¹⁰² Ru	0.0212	<0.0065	0.0067	0.0081	0.0214	0.0156	0.0133	0.0072	0.036	0.0082	0.0086
¹⁰³ Rh	<0.00179	<0.00132	<0.00189	0.00014	<0.0023	<0.00209	<0.00185	0.00157	<0.0016	<0.00154	0.00096
¹¹⁵ In	0.0121	0.0084	0.0054	0.0103	0.0135	0.0118	0.0213	0.0218	0.0063	0.0162	0.0095
¹¹⁸ Sn	0.24	0.226	0.176	0.15	0.135	0.275	0.302	0.276	0.168	0.208	0.1568
¹²¹ Sb	0.114	0.062	<0.0195	0.0166	0.031	0.087	0.091	0.029	0.035	0.032	0.0353
¹⁷⁸ Hf	0.169	0.127	0.095	0.123	0.141	0.178	0.168	0.235	0.157	0.2	0.1005
¹⁸¹ Ta	0.0101	0.0042	0.00387	0.0067	0.0052	0.008	0.0067	0.0085	0.0063	0.008	0.0061
¹⁸² W	0.0646	<0.0037	0.0078	0.0073	<0.0106	0.0038	<0.0063	<0.0044	0.016	0.0226	0.0089
¹⁹² Os	0.0081	0.009	0.0052	0.0086	<0.0064	0.0059	0.005	0.0125	0.023	<0.0065	0.0111
¹⁹³ Ir	0.0118	0.0153	<0.0023	0.0185	0.02	0.0083	0.007	0.0253	0.0167	0.0212	0.0142

²⁷ Al	81526.5	83975.87	87246.05	91211.85	80687.19	90825.63	90374.04	90778.32	91478.45	89612.67	90702.24
²⁸ Si	280.65	240.48	202.91	231.62	227.49	249.31	242.69	214.41	271.77	231.34	253.41
⁴² Ca	9.91	13.77	<7.79	<7.89	<7.05	<6.68	<7.09	<6.90	<6.93	<6.82	<7.93
⁴⁵ Sc	8.9	7.52	8.96	9.91	6.27	8.76	8.41	8.29	8.34	8.53	7.12
⁴⁸ Ti	3187.22	3261.32	3036.45	3366.16	2402.85	3681.46	3625.11	3586.26	3611.17	3621.89	3482.21
⁵³ Cr	314926.16	310692.66	316598.03	332494.53	286922.16	301797.44	300120.06	302098.34	305352.56	312870.88	311505.28
⁵⁵ Mn	2522.6	2558.53	2569.7	2434.19	2254.31	2265.12	2290.07	2307.2	2280.91	2361.38	2331.19
⁵⁷ Fe	23.35	23.35	23.35	23.5	23.56	23.56	23.56	23.56	23.56	23.95	23.95
⁵⁹ Co	221.07	218.18	220.57	225.23	229.41	221.07	224.96	226.22	225.7	231.9	229.98
⁶⁰ Ni	1001.31	1026.58	995.89	1091.18	682.83	717.71	692.31	691.96	720.62	820.72	833.84
⁶⁵ Cu	1.228	0.529	0.717	1.918	1.048	1.4	0.509	0.442	0.507	1.015	0.538
⁶⁶ Zn	579.25	745.7	700.59	658.47	584.64	608.26	617.5	649.32	651.54	647.89	530.01
⁷¹ Ga	39.93	44.35	38.25	41.35	37.58	40.81	40.96	41.21	42.16	41.52	38.84
⁷³ Ge	0.37	0.451	0.44	0.493	0.408	0.462	0.425	0.473	0.545	0.458	0.383
⁷⁵ As	0.176	0.125	0.132	0.12	0.124	0.095	0.129	0.142	0.137	0.096	0.082
⁸⁶ Sr	0.2203	0.554	0.034	0.0209	0.0178	0.0132	0.0143	0.0108	0.0479	0.0418	0.0119
⁸⁹ Y	0.0222	0.0227	0.0073	0.00434	<0.00151	0.00193	0.0068	0.0052	0.0177	0.00444	<0.00126
⁹⁵ Mo	0.0615	0.071	0.0482	0.0642	0.05	0.053	0.0644	0.0646	0.0543	0.0621	0.047
¹⁰² Ru	0.0134	0.0064	0.005	0.014	0.0043	<0.0022	<0.0034	0.003	<0.0022	0.1341	0.0032
¹⁰³ Rh	<0.00117	<0.00153	<0.00080	<0.00112	0.00076	<0.00069	<0.00117	<0.00158	<0.00069	<0.00123	<0.00143
¹¹⁵ In	0.00617	0.0074	0.00736	0.01	0.0152	0.0126	0.0091	0.0117	0.0101	0.0121	0.0077
¹¹⁸ Sn	0.169	0.154	0.133	0.1202	0.1052	0.1396	0.1262	0.1392	0.1276	0.1503	0.125
¹²¹ Sb	0.056	0.0285	0.0179	0.0251	0.0315	0.0375	0.0193	0.0249	0.02	0.0254	<0.0119
¹⁷⁸ Hf	0.078	0.147	0.0833	0.11	0.0315	0.1046	0.0981	0.0949	0.0894	0.0723	0.0408
¹⁸¹ Ta	0.00271	0.0069	0.00304	0.00515	0.00233	0.00645	0.00315	0.00371	0.0054	0.00213	0.0046
¹⁸² W	<0.0044	0.0235	0.0053	<0.0029	<0.0040	0.0027	0.0047	<0.0045	0.0038	0.00177	<0.0033
¹⁹² Os	0.0057	0.004	0.0052	0.0065	0.0034	0.0047	<0.0031	<0.0023	<0.0022	0.0668	<0.0033
¹⁹³ Ir	0.0118	0.0155	0.0102	0.0133	0.0106	0.0101	0.0081	0.0055	<0.00182	0.0289	0.005

	BD 232797C	BD 232797D	BD 232797E	BD 232798A	BD 232798B	BD 232798C	BD 232798D	BT 486020A	BT 486020B	BT 486020C	BT 486020D
²⁷ Al	91846.77	88970.41	95915.22	80696.83	80796.77	87540.08	89220.09	89767.31	87662.33	90932.35	90883.27
²⁹ Si	258.24	231.36	272.03	75.2	164.04	244.37	220.59	96.69	232.03	601.22	236.05
⁴² Ca	<7.75	<6.91	<6.68	<10.36	<10.04	<7.53	<7.26	<8.81	<8.47	<6.61	<7.31
⁴⁵ Sc	7.53	7.58	7.99	8.55	8.76	7.8	10.69	5.62	4.39	4.71	4.16
⁴⁹ Ti	3207.29	3480.56	3626.74	3908.96	3619.23	3542.47	3743.07	3428.55	3444.47	3570.11	3491.06
⁵³ Cr	319418	311255.66	330554.81	340186.09	324629.66	298404.97	303482.91	344168.59	301681.25	340804.22	320000.03
⁵⁵ Mn	2253.7	2282.03	2195.88	2856.59	2616.43	2281.55	2237.39	1867.96	1845.61	1933.29	1628.39
⁵⁷ Fe	23.95	23.95	186166	201712.25	201712.23	180258.41	180258.42	182979.05	182979.06	182979.05	182979.05
⁵⁹ Co	231.65	229.09	237.52	241.14	258.51	218.65	220.36	246.61	244.54	241.83	239.57
⁶⁰ Ni	882.3	879.15	921.17	831.48	745.1	735.76	785.96	952.63	726.6	718.43	890.91
⁶⁵ Cu	2.056	0.895	2.85	1.19	0.55	1.341	0.84	0.428	0.311	0.437	0.499
⁶⁶ Zn	602.43	584.13	589.95	656.19	582.28	621.13	617.43	1059.93	901.97	1256.86	1004.22
⁷¹ Ga	41.8	41.85	41.88	46.76	48.07	41.29	42.87	38.58	39.38	39.75	36.48
⁷³ Ge	0.408	0.431	0.394	0.599	0.623	0.562	0.531	0.475	0.23	0.45	0.45
⁷⁵ As	0.163	0.143	0.102	<0.096	<0.093	0.175	0.095	<0.095	<0.084	<0.068	<0.079
⁸⁶ Sr	0.0124	0.1175	0.0338	0.0173	0.0304	0.0136	0.0539	0.086	0.352	0.415	0.0497
⁸⁹ Y	<0.00194	0.0053	0.00244	0.00221	0.0074	0.00259	0.0107	0.0201	0.0461	0.0605	0.0128
⁹⁵ Mo	0.0553	0.0463	0.0587	0.1	0.073	0.068	0.087	0.066	0.086	0.126	0.065
¹⁰² Ru	0.007	<0.0035	0.0056	0.0078	<0.0028	0.0032	0.0028	0.0126	0.0124	0.0061	0.0278
¹⁰³ Rh	<0.00152	<0.00107	<0.00165	<0.00187	<0.00123	<0.00067	<0.00137	<0.00107	<0.0013	0.00105	0.00136
¹¹⁵ In	0.0117	0.0119	0.0128	0.0134	0.0104	0.0134	0.0121	0.00217	<0.0013	0.00184	0.00112
¹¹⁸ Sn	0.105	0.1245	0.1162	0.118	0.109	0.153	0.112	0.108	0.117	0.119	0.118
¹²¹ Sb	0.0327	0.0453	0.0489	<0.0079	<0.0078	0.0286	0.012	<0.0085	<0.0085	<0.0042	0.0076
¹⁷⁸ Hf	0.0392	0.0541	0.047	0.129	0.109	0.0965	0.111	0.141	0.142	0.15	0.141
¹⁸¹ Ta	<0.00151	0.00245	0.00384	0.0087	0.00482	0.0061	0.0069	0.00654	0.0118	0.0142	0.0056
¹⁸² W	0.0104	0.005	<0.0038	<0.0065	<0.0047	<0.0048	<0.0035	<0.0025	<0.00	0.00179	<0.00257
¹⁹² Os	0.0045	<0.0036	0.0055	0.0034	0.002	0.0032	<0.0024	0.0102	0.0114	0.0106	0.0187
¹⁹³ Ir	0.0094	0.0114	0.0146	0.0121	0.0077	0.0139	0.01	0.0181	0.0127	0.0193	0.0174

	BT 486020E	BT 486020F	BT 486021B	BT 486021C	BT 486021D	BT 486021E	BT 486022A	BT 486022B	BT 486022C	BT 486022D	BT 486022E
²⁷ Al	96706.36	98173.48	89369.35	95984.35	96165.1	95862.71	100248.23	95757.91	98116.18	102083.41	100356.38
²⁸ Si	272.44	221.11	325.73	221.68	244.23	236.32	205.36	126.2	258.83	251.27	263.41
⁴⁰ Ca	<8.85	<7.61	19.77	<7.06	<7.97	<7.04	<7.96	<7.69	<7.68	<6.12	<6.70
⁴⁵ Sc	6.17	5.78	4.27	4.06	4.25	4.06	5.66	6.01	5.93	5.73	5.3
⁴⁹ Ti	3668.73	3713.32	3792.29	3735.52	3754.17	3877.74	3725.54	3641	3694.83	3891.48	3826.88
⁵² Cr	338930.22	328752.03	321671.78	314949.59	325794	318616.22	355482.09	365866.47	326211.78	335156.31	328618.59
⁵⁵ Mn	1801.61	1877.95	1828.38	1787.19	1683.45	1738.74	2018.99	1934.45	2080.21	1981.63	2045.36
⁵⁷ Fe	189352.94	189352.95	194871.89	194871.86	194871.84	194871.86	200157.61	200157.61	197670.19	197670.17	197670.19
⁵⁹ Co	236.68	234.86	261.03	251.73	247.1	244.71	256.62	268.86	251.83	248.44	244.64
⁶⁰ Ni	923.33	766.11	895.07	767.14	889.86	848.01	1043.21	1073.56	1002.2	978.12	950.83
⁶⁵ Cu	0.453	0.39	0.422	0.294	0.353	0.276	0.441	0.481	0.32	0.211	0.257
⁶⁶ Zn	1211.39	1382.79	1356.64	1424.22	1351.27	1314.96	956.92	830.59	996.32	1242.2	1220.08
⁷¹ Ga	38.47	38.8	43.75	39.06	41.75	41.27	40.73	37.6	36.5	39.28	38.18
⁷³ Ge	0.383	0.434	0.313	0.482	0.433	0.399	0.476	0.366	0.405	0.468	0.411
⁷⁵ As	0.101	0.123	<0.096	0.089	0.177	0.151	<0.087	<0.083	0.137	0.114	0.111
⁸⁶ Sr	0.0208	0.0196	0.89	0.0189	0.0212	0.1161	0.0448	0.0235	0.0283	0.0386	0.0216
⁸⁹ Y	0.0103	0.0092	0.395	0.0102	0.0091	0.0396	0.0111	0.0062	0.0075	0.0108	0.0142
⁹⁵ Mo	0.0458	0.0528	0.074	0.0521	0.0431	0.0581	0.079	0.069	0.0535	0.073	0.0569
¹⁰² Ru	0.0128	0.0047	0.0092	0.0124	0.0281	0.0114	0.0204	0.0258	0.0193	0.02	0.0091
¹⁰³ Rh	<0.00094	<0.00128	<0.00195	<0.00132	0.00334	<0.00110	<0.00166	<0.00134	<0.00108	<0.00121	0.00081
¹¹⁵ In	0.00269	0.00163	0.00206	0.00255	0.00373	0.00218	0.00185	0.00265	<0.00105	0.00132	0.00203
¹¹⁸ Sn	0.142	0.145	0.173	0.169	0.199	0.167	0.105	0.121	0.138	0.182	0.159
¹²¹ Sb	0.0382	0.0285	0.0252	0.0176	0.0311	0.0395	<0.0070	<0.0060	0.0156	0.013	0.0125
¹⁷⁸ Hf	0.14	0.19	0.207	0.1008	0.102	0.133	0.097	0.084	0.148	0.125	0.15
¹⁸¹ Ta	0.0091	0.0133	0.0074	0.00654	0.00592	0.0085	0.00448	0.00476	0.0046	0.006	0.00671
¹⁸² W	<0.0093	0.0028	0.0251	0.0038	<0.0041	<0.0051	<0.00	0.00149	<0.0048	<0.0044	<0.0050
¹⁹² Os	0.0117	0.0078	0.015	0.0042	0.0144	0.011	0.0138	0.0084	0.0093	0.0083	0.0077
¹⁹³ Ir	0.0058	0.0103	0.0173	0.00258	0.0123	0.0156	0.0214	0.0153	0.0068	0.0165	0.0066

²⁷ Al	87443.86	85945.2	86710.65	75004.25	77425.59	85027.09	80759.3	81144.18	68212.22	73572.22	86544.34
²⁹ Si	106.42	276.92	235.42	104.45	112.4	227.88	234.3	353.1	98.73	118.01	319.71
⁴² Ca	21.44	<7.21	<6.78	<9.87	<6.63	<8.59	<7.96	<7.65	<8.60	<9.38	<8.11
⁴⁵ Sc	3.03	2.73	3.95	5.85	5.26	6.67	6.09	6.18	5.4	6.6	6.54
⁴⁹ Ti	4078.46	3800.85	4152.63	2072.2	1814.44	2237.2	2127.6	2126.35	2013.52	2093.65	2342
⁵³ Cr	303286.06	297916.34	293756.13	339011.22	330671.06	343629.75	329199.69	327493.13	323185.69	353887.81	349489.25
⁵⁵ Mn	2512.62	2324.59	2174.4	1229.26	1263.26	1227.71	1380.31	1359.29	1125.55	1470.13	1244.55
⁵⁷ Fe	217180.72	217802.55	217802.55	148155.52	148155.52	148155.45	148155.45	148155.45	151653.41	151653.41	151653.34
⁵⁹ Co	369.1	318.12	322.39	208.03	189.11	201.98	200.87	199.63	213.2	255.22	218.64
⁶⁰ Ni	679.7	748.32	822.07	872.77	766.73	753.22	764.95	670.79	759.04	735.63	871.5
⁶⁵ Cu	0.277	0.238	0.318	0.412	0.464	0.374	0.38	0.326	1.34	0.451	0.425
⁶⁶ Zn	1661.56	1646.2	1578.51	616.97	575.85	681.65	754.41	714.63	678.47	793.26	739.14
⁷¹ Ga	31.17	31.84	36.03	33.31	31.45	32.47	32.45	31.13	30.94	33.67	34.26
⁷³ Ge	0.714	0.443	0.409	0.599	0.284	0.416	0.524	0.444	0.485	0.464	0.513
⁷⁵ As	<0.090	0.158	0.164	<0.070	<0.048	0.086	0.128	0.147	<0.066	<0.077	0.123
⁸⁶ Sr	0.0275	0.0201	0.0129	0.057	0.0145	0.0166	0.0187	0.0762	0.0196	0.0145	0.0558
⁸⁹ Y	0.0172	0.0152	0.016	0.0046	0.00075	<0.00129	0.00162	0.00305	0.0056	0.00199	0.0095
⁹⁵ Mo	0.099	0.0553	0.0922	<0.020	<0.0129	0.0433	0.046	0.0411	0.029	0.038	0.0308
¹⁰² Ru	0.0062	0.008	0.0122	0.0091	0.0085	0.0145	0.0079	0.0141	0.0067	0.01	0.0144
¹⁰³ Rh	0.00134	<0.00147	<0.00069	<0.00159	<0.00104	<0.00117	0.00057	<0.00124	0.00131	0.00127	<0.00067
¹¹⁵ In	0.00232	0.00502	0.00205	0.0022	<0.00069	0.00122	0.0014	<0.00074	<0.00137	<0.00129	0.00288
¹¹⁸ Sn	0.216	0.196	0.228	0.081	0.0526	0.0861	0.0976	0.0764	0.059	0.0527	0.0811
¹²¹ Sb	<0.0089	0.0329	0.0331	<0.0039	0.0061	0.0155	0.023	0.0275	<0.0083	<0.0087	0.0263
¹⁷⁸ Hf	0.224	0.139	0.174	0.0274	0.0256	0.0423	0.0329	0.0241	0.0243	0.0289	0.0258
¹⁸¹ Ta	0.0121	0.0085	0.0119	0.00111	0.00202	0.00152	0.00237	0.00348	0.00104	0.00118	0.0029
¹⁸² W	0.0291	<0.0038	<0.0043	<0.00	<0.0042	0.0029	0.0005	0.0023	<0.0037	<0.0042	<0.0035
¹⁹² Os	0.0082	0.0072	0.0058	0.0094	0.0125	0.007	0.0056	0.008	0.0038	0.0063	<0.0029
¹⁹³ Ir	0.015	0.0059	0.0043	0.0115	0.0121	<0.00190	0.00215	0.00206	0.0022	<0.00106	0.0038

²⁷ Al	80395.71	74916.34	62687.44	74026.39	76779.16	79050.16	76384.85	82995.98	82679.61	79514.6	81782.38
²⁹ Si	280.13	190.08	167.2	138.25	262.76	265.45	321.1	256.44	307.67	254.91	273.75
⁴² Ca	8.14	<8.16	<9.32	<9.75	<6.67	<7.45	<6.62	<7.05	<6.95	7.42	<9.04
⁴⁵ Sc	5.84	5.52	4.06	5.85	5.6	5.86	4.87	5.55	6.1	5.97	6.11
⁴⁹ Ti	2202.81	2048.05	2084.38	2271.33	2212.25	2295.24	2310.14	2274.78	2336.13	2352.09	2347.97
⁵³ Cr	332025.75	302270.69	299745.03	342922.34	299731.75	311625.25	297482.84	323084.84	333097.31	329741.31	326007.72
⁵⁵ Mn	1472.39	1798.47	1788.27	1425.18	1805.14	1531.25	1672.1	1475.59	1392.4	1432.51	1454.61
⁵⁷ Fe	151653.36	151653.36	166344.58	166344.58	160436.97	160436.97	160436.97	20.77	20.77	20.77	161447.48
⁵⁹ Co	214.2	217.94	271.7	262.67	240.25	218.45	228.31	225.62	227.94	226.4	219.42
⁶⁰ Ni	767.22	526.02	868.79	930.38	633.63	695.13	700.79	840.02	865.19	904.08	812.24
⁶⁵ Cu	0.308	0.38	0.311	0.44	0.197	0.326	0.33	0.34	0.524	0.501	0.387
⁶⁶ Zn	786.97	708.96	861.47	684.33	825.75	767.84	760.85	810.92	784.72	756.25	766.94
⁷¹ Ga	33.03	27.54	32.49	35.38	29.09	30.85	27.73	32.23	34.1	32.98	32.19
⁷³ Ge	0.513	0.457	0.381	0.298	0.419	0.457	0.333	0.539	0.463	0.407	0.258
⁷⁵ As	0.084	0.097	<0.084	<0.084	0.113	0.123	0.171	0.265	0.236	0.221	0.204
⁸⁶ Sr	0.0676	0.0331	0.0504	0.0293	0.0241	0.0195	0.1902	0.021	0.0166	0.0176	0.0084
⁸⁹ Y	0.00408	0.00136	0.0092	0.00335	0.00142	0.0031	0.00466	0.00411	<0.00086	0.00312	<0.00121
⁹⁵ Mo	0.107	0.047	0.085	0.0374	0.0545	0.032	0.0693	0.0529	0.0441	0.0561	0.026
¹⁰² Ru	0.0138	0.0046	<0.0038	0.0039	<0.0027	<0.0029	<0.0029	0.0051	0.0045	0.0028	0.0045
¹⁰³ Rh	0.0006	<0.00113	<0.00056	<0.00103	<0.00093	<0.00084	<0.00102	0.00093	<0.00115	<0.00150	<0.00143
¹¹⁵ In	0.00172	<0.00109	<0.00114	0.00141	0.00087	0.00096	0.00265	0.0172	0.0153	0.0019	<0.00108
¹¹⁸ Sn	0.113	0.065	0.1019	0.0673	0.0708	0.0973	0.0989	0.1361	0.137	0.1103	0.109
¹²¹ Sb	0.0263	0.0355	0.0127	<0.0069	0.009	0.017	0.0491	0.1158	0.206	0.0579	0.0374
¹⁷⁸ Hf	0.029	0.0313	0.0722	0.0447	0.0578	0.0583	0.0787	0.039	0.0323	0.0374	0.028
¹⁸¹ Ta	<0.00078	0.0028	0.0066	0.00284	0.00389	0.0054	0.0075	0.00258	0.00344	0.00159	<0.00099
¹⁸² W	0.0017	0.0121	0.0445	0.0024	<0.0037	<0.0043	0.0074	<0.0043	<0.0048	0.0121	<0.0046
¹⁹² Os	0.0074	<0.0025	0.0052	<0.0018	0.003	0.0032	<0.0025	<0.0026	0.009	<0.0021	<0.0035
¹⁹³ Ir	0.0099	0.0047	0.011	0.00123	<0.0017	0.0077	0.0078	<0.00187	0.0098	<0.00148	0.014

	BT 486044E	BT 486045A	BT 486045B	BT 486045C	BT 486045D	BT 486045E	BT 486046A	BT 486046B	BT 486046C	BT 486046D	BT 486046E
²⁷ Al	81805.59	80641.36	79096.29	75245.95	80583.65	75750.88	82980.07	82113.81	78408.19	83206.02	84639.7
²⁹ Si	248.44	327.36	260.02	178.75	246.63	515.36	429.75	329.99	254.89	335.31	237
⁴² Ca	<7.00	<5.70	14.57	<4.80	<7.12	38.09	<6.05	<4.65	<4.32	<9.88	<10.84
⁴⁵ Sc	5.74	5.15	4.85	4.12	5.21	3.95	3.71	3.82	3.86	3.63	4.36
⁴⁹ Ti	2337.59	2397.53	2374.81	2348.54	2250.42	2214.83	2464.59	2496.75	2475.26	2515.14	2557.88
⁵³ Cr	321045.63	312785.69	305501.88	292944.28	309130.44	286542.56	324326.72	304139.13	311211.63	305669.78	303193.44
⁵⁵ Mn	1543.65	1592.23	1700.44	1856.7	1702.31	1940.35	2039.62	2075.83	2085.61	2210.99	2138.78
⁵⁷ Fe	161447.48	21.6	21.6	21.6	167899.17	167899.17	23.83	23.83	23.83	185233.2	185233.2
⁵⁹ Co	220.8	239.69	244.41	253.45	239.01	243.1	292.28	294.15	288.84	309.96	303.51
⁶⁰ Ni	790.18	1112	1063.07	910.01	1022.67	748.65	779.11	773.46	790.67	648.93	722.39
⁶⁵ Cu	0.338	0.642	0.32	0.291	0.414	0.303	1.078	0.518	0.321	0.182	0.387
⁶⁶ Zn	916.42	717.99	751.31	808.3	871.41	919.31	774.57	793.89	787.5	998.14	1126.71
⁷¹ Ga	31.23	34.38	32.44	30.32	32.43	30.11	32.34	32.51	31.48	30.6	33.32
⁷³ Ge	0.46	0.446	0.395	0.297	0.344	0.419	0.493	0.336	0.401	0.436	0.479
⁷⁵ As	0.104	0.198	0.207	0.184	0.147	0.345	0.263	0.22	0.203	0.14	0.153
⁸⁶ Sr	0.0108	0.0271	0.0263	0.0119	0.0099	0.1166	0.0478	0.0674	0.0545	0.0234	0.0141
⁸⁹ Y	0.00271	0.00268	0.00613	0.00333	<0.00124	0.0355	0.00466	0.00549	0.00366	0.0156	0.007
⁹⁵ Mo	0.0402	0.0501	0.0732	0.0359	0.0397	0.0408	0.0458	0.043	0.0622	0.051	0.047
¹⁰² Ru	0.0024	0.006	0.0033	0.0026	0.0049	<0.0038	0.0147	0.0025	0.0068	<0.0036	<0.0047
¹⁰³ Rh	<0.00115	<0.00080	<0.00099	<0.00103	<0.00076	<0.00069	<0.00124	<0.00080	<0.00136	<0.00069	<0.00196
¹¹⁵ In	0.00266	0.00166	0.00148	<0.00101	0.00234	<0.00067	0.00122	0.00293	<0.00090	<0.00107	0.00248
¹¹⁸ Sn	0.0959	0.1201	0.1301	0.1222	0.1002	0.1053	0.1153	0.1174	0.1013	0.12	0.125
¹²¹ Sb	0.0415	0.073	0.0834	0.0564	0.0245	0.0754	0.0565	0.0626	0.0344	0.0215	0.0397
¹⁷⁸ Hf	0.0462	0.0692	0.0688	0.064	0.0312	0.0513	0.0648	0.1192	0.099	0.104	0.0771
¹⁸¹ Ta	0.00174	0.005	0.00333	0.00445	0.00282	0.00609	0.00585	0.0119	0.00777	0.0094	0.0093
¹⁸² W	0.00058	<0.0029	<0.00191	<0.0050	<0.0027	0.389	0.0056	<0.0026	<0.0034	0.09	<0.0058
¹⁹² Os	<0.00177	0.0038	<0.0023	0.0046	0.0051	<0.0035	0.0099	<0.00219	0.0067	<0.0044	<0.0047
¹⁹³ Ir	<0.00149	0.00434	<0.00175	0.0083	0.0136	0.008	0.0132	<0.00092	0.0067	0.0068	<0.0035

²⁷ Al	97082.05	102794.17	182.66	92597.18	98915.87	100954.59	94856.84	91123.09	95073.63	93853.56	98851.68	98834.16
²⁹ Si	226.71	14.92	14.92	220.96	286.06	235.61	297.76	228.12	203.54	184.89	248.06	243.93
⁴² Ca	<6.77	3.47	3.69	<7.17	17.96	<5.93	<6.76	37.14	10.93	6.43	<7.32	<7.38
⁴⁵ Sc	4.35	4130.31	3968.55	3.69	1.89	3.48	2.85	2.23	3.42	3.57	2.39	4.54
⁴⁹ Ti	3939.74	4130.31	3968.55	3968.55	5659.92	5638.67	4732.4	4240.19	4517.51	4273.64	5093.26	4188.18
⁵³ Cr	295006.09	287802.38	278281.19	278281.19	302254.22	311777.06	292188.72	280668	291886.31	296792.22	291599.28	279774.81
⁵⁵ Mn	2468.33	2340.45	2409.97	2409.97	2480.39	2634.98	2792.51	2660.4	2774.62	2675.11	2706.84	2650.99
⁵⁷ Fe	26.67	26.67	26.67	26.67	29.23	29.23	28.77	28.77	28.77	28.77	28.77	259466.44
⁵⁹ Co	454.48	460.28	448.29	448.29	493.57	530.53	538.03	526.09	530.25	538.26	531.05	313.28
⁶⁰ Ni	691.26	645.03	644.99	644.99	666.67	869.29	847.28	757.55	801.96	745.68	859.09	516.69
⁶⁵ Cu	0.403	0.21	0.323	0.323	0.125	0.304	0.27	0.295	0.211	0.278	0.233	0.176
⁶⁶ Zn	1066.8	1360.57	1289.14	1289.14	1085.53	1528.1	1497.33	1602.1	1680.77	1554.75	1677.44	1847.59
⁷¹ Ga	39.86	36.37	37.08	37.08	32.91	46.59	37.73	37.6	36.89	33.7	38.14	22.07
⁷³ Ge	0.501	0.594	0.494	0.494	0.172	0.415	0.448	0.443	0.437	0.339	0.434	0.354
⁷⁵ As	0.25	0.158	0.151	0.151	0.14	0.145	0.25	0.102	0.117	0.157	0.121	0.188
⁸⁶ Sr	0.0324	0.263	0.0229	0.0229	0.0453	0.0223	0.0182	0.258	0.0188	0.0213	0.0264	0.0096
⁸⁹ Y	0.0114	0.0161	0.007	0.007	0.198	0.016	0.0177	0.0252	0.0177	0.01	0.0244	0.0312
⁹⁵ Mo	0.0967	0.077	0.0573	0.0573	0.073	0.0684	0.0853	0.0537	0.069	0.071	0.061	0.0579
¹⁰² Ru	<0.0043	0.0027	0.0027	0.0027	<0.0034	0.0023	0.0041	0.0048	0.0036	<0.0031	<0.0028	0.0035
¹⁰³ Rh	<0.00121	<0.00130	<0.00113	<0.00113	<0.00129	<0.00117	<0.00132	<0.00053	0.00108	<0.00139	<0.00133	<0.00151
¹¹⁵ In	0.0016	0.0303	0.00559	0.00559	<0.0015	0.00125	0.00329	0.00257	0.00134	0.00152	0.0085	0.009
¹¹⁸ Sn	0.177	0.169	0.139	0.139	0.295	0.224	0.252	0.235	0.258	0.198	0.291	0.485
¹²¹ Sb	0.1206	0.0355	0.021	0.021	0.034	0.0182	0.0729	0.0362	0.0231	0.0208	0.0275	0.0281
¹⁷⁸ Hf	0.0468	0.0588	0.0532	0.0532	0.187	0.177	0.0497	0.0373	0.0309	0.0433	0.0536	0.0148
¹⁸¹ Ta	0.0027	0.0059	0.00356	0.00356	0.0174	0.0177	0.00502	0.0069	0.0048	0.0046	0.0072	<0.00111
¹⁸² W	0.0306	0.0042	<0.0025	<0.0025	0.0162	0.0097	<0.0044	0.0052	0.0062	0.0129	<0.0066	0.0036
¹⁹² Os	0.0027	<0.0031	0.0033	0.0033	<0.0025	0.0185	0.0051	<0.0026	<0.0032	0.0034	0.0037	<0.0033
¹⁹³ Ir	0.0048	0.0082	0.0069	0.0069	0.0093	0.0213	0.0091	0.0051	0.0022	0.0039	0.0099	<0.00120

	BT 486185B	BT 486186A	BT 486186B	BT 486187A	BT 486187B	BT 486187C	BT 486187D	BT 486187E	BL 486209A	BL 486209B	BL 486209C
²⁷ Al	95520.23	98157.69	92239.37	86750.05	93619.85	92410.27	96485	95959.55	78558.48	77863.74	90509.11
²⁹ Si	244.63	491.2	582.07	312.83	292.9	233.93	344.04	234.42	513.05	98.7	248.53
⁴² Ca	11.21	13.8	25.97	14.53	16.4	<8.73	9.17	15.86	<10.73	13.18	<9.68
⁴⁵ Sc	4.65	3.68	4.98	2.98	2.858	3.58	3.98	3.5	4.21	3.71	5.51
⁴⁹ Ti	3875.06	6012.04	5235.73	3802.2	4058.89	3854.3	4083.18	4063.75	3530.72	3418.63	3348.8
⁵³ Cr	270514.88	312195.03	317190.5	297601.53	291734.84	275721.25	287230.88	285861.41	321079.75	350102.25	304869
⁵⁵ Mn	2661.31	2848.02	2837.36	2510.08	2458.48	2448.6	2441.03	2453.79	2681.46	2801.44	2669.22
⁵⁷ Fe	259466.44	278899.22	278899.22	210729.02	210729.03	210729.03	210729.03	210729.02	218035.77	218035.77	28.05
⁵⁹ Co	305.37	361.95	359.37	235.55	236.87	237.97	238.87	239.03	241.45	227	213.64
⁶⁰ Ni	542.44	522.75	437.52	198.51	202.98	192.71	195.95	193.98	160.7	223.33	110.41
⁶⁵ Cu	0.197	0.164	<0.062	0.496	0.418	0.222	0.344	0.597	1099.06	0.88	1.527
⁶⁶ Zn	1777.65	2392.79	1685.47	760.02	733.28	616.5	699.21	752.68	757.44	695.4	740.6
⁷¹ Ga	22.77	26.24	21.35	33.03	36.75	34.85	32.01	34.1	37.62	38.29	36.15
⁷³ Ge	0.404	0.524	0.23	0.333	0.393	0.311	0.349	0.445	0.462	0.533	0.542
⁷⁵ As	0.135	0.186	0.217	0.149	0.148	0.313	0.14	0.161	<0.088	<0.092	0.121
⁸⁶ Sr	0.28	0.0812	0.043	0.0554	0.0318	0.0492	0.0769	0.0279	0.0585	0.039	0.0205
⁸⁹ Y	0.0489	0.0222	0.0218	0.0112	0.0087	0.0036	0.0095	0.0071	0.0318	0.00465	<0.00161
⁹⁵ Mo	0.0684	0.08	0.119	0.064	0.072	0.08	0.068	0.0627	0.058	0.077	0.028
¹⁰² Ru	0.0156	0.0569	0.026	0.0388	0.0388	0.0301	0.0322	0.0162	0.0103	0.006	0.0034
¹⁰³ Rh	0.00157	0.006	0.0038	0.0037	0.00267	<0.0031	<0.0021	0.00308	0.019	<0.00176	<0.00164
¹¹⁵ In	0.0076	0.00437	0.0042	0.0053	0.006	0.0031	0.0057	0.00548	0.006	0.0101	0.0053
¹¹⁸ Sn	0.427	0.653	0.299	0.287	0.296	0.337	0.357	0.369	0.213	0.117	0.134
¹²¹ Sb	0.0492	0.0578	0.037	0.0524	0.0351	0.014	0.029	0.045	<0.0095	<0.0068	<0.0128
¹⁷⁸ Hf	0.0159	0.0465	0.0101	0.0132	0.021	0.0273	0.0407	0.0314	0.028	0.0111	0.0432
¹⁸¹ Ta	<0.00140	0.00357	<0.0015	0.00241	<0.00145	<0.0015	0.004	0.00235	<0.00117	0.00089	<0.00093
¹⁸² W	<0.0070	<0.0058	<0.014	<0.0039	<0.0031	<0.0068	<0.0044	0.00138	<0.0040	<0.0041	0.0096
¹⁹² Os	0.0051	0.004	0.016	0.0027	0.008	0.0056	0.0059	0.0042	<0.0029	<0.0039	0.0084
¹⁹³ Ir	0.0108	0.0159	0.0067	0.0084	0.0119	0.0078	0.0097	0.0098	0.0069	0.0082	0.005

	BL 486209D	BL 486209E	BL 486210A	BL 486210B	BL 486210C	BL 486211A	BL 486211B	BL 486211C	BL 486211D	BL 486211E	BL 486215A
²⁷ Al	84892.98	84141.84	90514.41	100237.52	94731.24	89022.79	85146.1	80388.66	100856.08	96313.37	94838.1
²⁹ Si	158.24	169.73	206.05	183.62	295.3	91.86	129.34	253.78	209.01	211.79	133.66
⁴² Ca	<5.59	<8.68	12.4	24.29	<8.16	20.5	<12.63	20.67	<11.05	22.99	27.74
⁴⁵ Sc	5.54	5.91	3.61	2.91	2.66	3.91	4.15	4.61	4.15	4.26	2.79
⁴⁹ Ti	3036.62	3122.92	4234.34	3999.45	3939.15	4105.09	4007.42	3622.48	4192.05	4419.54	4481.09
⁵³ Cr	306091.38	315806.63	307809.41	271129.72	266581.56	309641.13	352627.94	300508.97	291754.03	279365.38	285967.63
⁵⁵ Mn	2701.97	2711.07	2812.75	2710.19	2717.2	2452.71	2525.52	2523.84	2430.86	2328.09	3016.92
⁵⁷ Fe	28.05	28.05	231716.42	29.81	29.81	209874	209874.02	209873.98	27	27	239722.73
⁵⁹ Co	218.28	217.73	258.3	217.15	224.32	225.88	236.29	229.52	217.35	215.06	224.32
⁶⁰ Ni	161.76	154.58	216.83	146.22	189.22	163.18	228.04	222.71	121.05	222.9	174.55
⁶⁵ Cu	0.846	0.441	0.53	0.202	8.29	0.525	0.482	1.36	0.365	0.305	6.76
⁶⁶ Zn	679.38	799.18	1087.31	1013.44	1090.19	759.5	749.62	580.6	797.19	780.19	1034.98
⁷¹ Ga	34.94	35.32	35.97	38.56	37.34	44.81	41.84	35.28	39	40.69	36.43
⁷³ Ge	0.408	0.55	0.431	0.379	0.396	0.584	0.54	0.357	0.371	0.51	0.548
⁷⁵ As	0.046	<0.054	<0.098	<0.064	0.063	<0.092	<0.112	<0.070	<0.064	0.089	0.243
⁸⁶ Sr	0.0124	0.0128	0.0436	0.0144	0.0142	0.0239	0.0396	0.126	0.1257	0.0193	0.0259
⁸⁹ Y	0.00143	<0.00147	0.0094	0.0044	0.00122	0.0084	0.0108	0.0143	0.0177	0.0163	0.0249
⁹⁵ Mo	0.0554	0.0532	0.104	0.064	0.045	0.091	0.082	0.072	0.068	0.0476	0.04
¹⁰² Ru	0.0059	<0.0045	<0.0046	<0.0029	<0.0038	<0.0042	0.0041	0.011	<0.0022	0.00194	<0.0041
¹⁰³ Rh	0.00116	<0.00087	<0.00163	<0.00220	0.0011	0.00186	<0.00172	0.0018	<0.00227	<0.00175	<0.0027
¹¹⁵ In	0.00904	0.0067	0.0102	<0.032	0.0114	0.0084	0.0101	0.0082	0.006	0.0082	0.0068
¹¹⁸ Sn	0.1076	0.125	0.497	0.336	0.462	0.224	0.156	0.154	0.263	0.304	0.327
¹²¹ Sb	<0.0069	<0.0129	0.0058	0.0204	0.0223	<0.0082	<0.0132	<0.0056	<0.0175	0.0148	0.0258
¹⁷⁸ Hf	0.0302	0.0359	0.0336	0.0071	0.0088	0.0155	0.0109	0.0221	0.0168	0.0567	0.0181
¹⁸¹ Ta	0.0025	0.0011	0.00117	<0.00173	<0.00114	<0.00083	0.00135	0.00355	<0.00135	0.0056	0.0036
¹⁸² W	<0.0020	0.002	<0.0030	<0.0039	0.003	<0.0050	0.00071	0.00074	<0.0061	<0.0062	0.0024
¹⁸² Os	<0.0027	0.0024	<0.00146	<0.0053	<0.0035	<0.00206	<0.0029	0.0026	<0.0021	<0.0030	<0.0071
¹⁸⁹ Ir	0.0084	0.0064	<0.00173	<0.0025	<0.0025	0.00114	<0.00175	0.0117	<0.0027	<0.0034	<0.0040

	BL 486216A	BL 486216B	BL 486216C	BL 486216D	BL 486216E	BL 486217A	BL 486332A	BL 486332B	BL 486332C	BL 486333A	BL 486333B
²⁷ Al	85881.6	86325.53	86339.05	86511.45	88069.84	103331.88	86523.04	87704.55	73823.38	82990.27	84021.76
²⁸ Si	180.47	269.87	308.95	388.86	188.7	208.72	417.78	515.45	584.22	301.93	233.23
⁴² Ca	<5.68	16.07	<6.92	22.81	7.95	<13.66	<9.21	<11.84	67.78	21.78	5.21
⁴⁵ Sc	4.99	4.48	4.93	5.14	4.94	3.89	5.47	4.5	7.27	5.24	5.56
⁴⁹ Ti	3534.32	3511.71	3566.67	3582.59	3588.14	4431.63	2607.25	2350.26	2502.42	2617.4	2666.23
⁵³ Cr	307163.09	308341.66	307434.44	310985.16	308771.72	277533	345319.81	345126.03	308824.09	303320.69	306633.22
⁵⁵ Mn	2339.05	2351.51	2341.69	2359.82	2340.5	2902.65	2613.83	2574.99	2515.52	2150.22	2145.43
⁵⁷ Fe	198991.64	198991.64	198991.64	198991.64	198991.66	33.05	207308.86	207308.86	207308.86	171163.89	171163.89
⁵⁹ Co	215.13	214	213.01	215.32	215.55	257.85	282.56	286.75	251.89	226.24	230.94
⁶⁰ Ni	181.58	216.61	190.51	170.73	165.62	404.78	151.17	122.17	187.4	283.56	373.85
⁶⁵ Cu	0.513	0.616	0.591	0.328	0.416	<0.080	0.138	1.6	0.077	0.457	0.564
⁶⁶ Zn	653.17	665.39	643.09	645.14	603.06	1336.56	649.43	698.42	579.17	516	619.13
⁷¹ Ga	35.79	35.58	35.67	35.52	37.89	30.59	25.37	29.78	26	30.31	31.35
⁷³ Ge	0.544	0.497	0.598	0.588	0.447	0.539	0.43	<0.11	0.12	0.19	0.289
⁷⁵ As	0.239	0.126	0.166	0.248	0.148	0.126	<0.068	<0.083	0.25	0.167	0.077
⁸⁶ Sr	0.0189	0.0356	0.0582	0.1152	0.1228	0.0164	0.074	0.189	0.161	0.711	0.0274
⁸⁹ Y	0.00114	0.00477	0.00444	0.0337	0.0039	0.0153	0.0172	0.053	0.051	0.0158	0.0042
⁹⁵ Mo	0.0769	0.057	0.0508	0.0644	0.1	0.031	0.034	0.266	0.108	0.062	0.0603
¹⁰² Ru	<0.00184	0.0117	0.0099	0.0061	0.004	0.0064	0.0056	0.062	<0.0063	0.0066	<0.0027
¹⁰³ Rh	<0.00168	0.0036	<0.00153	0.0025	<0.0017	<0.0020	0.0025	<0.00215	<0.00217	<0.00229	0.00069
¹¹⁵ In	0.007	0.0097	0.0375	0.0086	0.0098	0.0108	<0.0022	0.0059	0.004	0.0021	0.00196
¹¹⁸ Sn	0.091	0.087	0.084	0.0715	0.0629	0.694	0.168	0.084	0.106	0.171	0.1137
¹²¹ Sb	0.0166	0.0152	0.0228	0.0169	0.0086	<0.021	0.015	0.071	0.072	0.024	<0.0117
¹⁷⁸ Hf	0.0298	0.0243	0.0229	0.0211	0.0315	0.0128	0.035	0.012	0.028	0.063	0.0376
¹⁸¹ Ta	0.0044	0.0042	0.0065	0.0056	<0.00087	0.0057	0.0038	0.0053	0.005	<0.00199	0.0017
¹⁸² W	<0.00257	0.00128	<0.00141	0.00184	<0.00091	<0.0076	<0.0088	0.032	<0.0078	<0.014	<0.0053
¹⁹² Os	<0.0030	0.0051	<0.0042	<0.0036	<0.0031	0.0103	0.014	<0.0065	<0.0047	<0.0062	<0.0041
¹⁹³ Ir	<0.00239	0.0119	0.0041	0.0113	0.0064	0.0103	0.0225	0.0091	<0.0055	0.0092	0.0057

²⁷ Al	BL 486333C	BL 486333D	BL 486333E	BL 486333F	BL 486334A	BL 486334B	BL 486334C	BL 486334D	BL 486334E
	84583.16	84938.55	84636.81	82694.1	90797.43	87469.43	89510.7	86964.8	88171.43
²⁸ Si	220.92	222.69	633.98	276.35	258.17	262.18	257.66	235.86	196.16
⁴² Ca	5.7	<5.01	<5.58	<6.37	22.57	25.45	<5.19	<5.23	<5.94
⁴⁵ Sc	6.01	5.94	5.86	5.22	6.39	6.29	6.02	5.76	5.76
⁴⁹ Ti	2720.88	2729.25	2681.6	2645.73	3017.86	2983.12	2974.22	2897.04	2909.39
⁵³ Cr	307752.06	309090.78	305550.41	307301.19	329689.16	314537.63	331141.09	319181.06	320287.59
⁵⁵ Mn	2165.71	2178.75	2159.04	2163.35	2154.32	2110.69	2086.02	2132.08	2133.08
⁵⁷ Fe	171163.89	171163.89	171163.89	171163.88	179403.38	179403.38	179403.38	179403.38	179403.38
⁵⁹ Co	231.21	230.79	227.56	229.93	252.81	244.96	257.37	246.23	248.6
⁶⁰ Ni	443.6	527.75	350.89	405	437.04	315.94	458.69	363.86	313.16
⁶⁵ Cu	0.586	0.74	0.578	0.643	0.684	0.443	1.576	0.998	0.564
⁶⁶ Zn	565.92	567.27	616.44	679.93	564.83	593.14	533.03	542.75	566.29
⁷¹ Ga	31.99	32.25	31.15	32.59	34.35	34.21	32.69	32.43	33.83
⁷³ Ge	0.338	0.417	0.321	0.271	0.387	0.466	0.442	0.427	0.421
⁷⁵ As	0.066	0.081	0.114	0.11	0.102	0.085	0.098	0.093	0.103
⁸⁶ Sr	0.0179	0.0134	0.0139	0.0086	0.0084	0.0296	0.0219	0.0167	0.0116
⁸⁹ Y	0.00109	0.00287	0.0039	<0.00200	<0.0018	0.0259	0.00603	0.0056	0.00179
⁹⁵ Mo	0.0379	0.0624	0.0528	0.062	0.092	0.054	0.0548	0.0435	0.0487
¹⁰² Ru	<0.0025	0.0055	0.0044	<0.0026	0.0035	<0.0037	0.0038	0.0063	<0.0047
¹⁰³ Rh	<0.00079	<0.00118	<0.00114	<0.00212	<0.00166	<0.00089	<0.00106	<0.00067	<0.00129
¹¹⁵ In	<0.00095	0.00253	0.00208	<0.00147	0.0014	0.00168	0.00268	0.00189	0.00298
¹¹⁸ Sn	0.124	0.1069	0.129	0.141	0.255	0.265	0.162	0.188	0.23
¹²¹ Sb	0.0147	0.0244	0.0204	<0.0116	<0.0095	0.0157	0.0181	0.0172	0.0166
¹⁷⁸ Hf	0.0398	0.0346	0.0325	0.0294	0.087	0.1024	0.0807	0.0544	0.0344
¹⁸¹ Ta	0.0055	0.00108	0.00109	<0.00161	0.0048	0.0066	0.00421	0.00433	0.00319
¹⁸² W	<0.00282	<0.0032	<0.0037	<0.0060	<0.0046	<0.0032	<0.0034	<0.0054	<0.0038
¹⁹² Os	0.0089	0.0071	0.007	<0.0029	<0.0039	0.0073	0.0028	0.0033	<0.0034
¹⁹³ Ir	0.0141	0.0167	0.0059	0.0034	0.0083	0.0142	<0.00239	0.0093	0.0053

Curriculum Vitae

Name: Jordan Laarman, PGeo.

Post-secondary Education and Degrees: Calvin College, Grand Rapids, Michigan, United States 2000-2001

The University of Western Ontario, London, Ontario, Canada 2001-2004 H.B.Sc.

Lakehead University, Thunder Bay, Ontario, Canada 2004-2007 M.Sc.

The University of Western Ontario, London, Ontario, Canada 2009-2014 Ph.D.

Honours and Awards: NSERC-IPS 2009-2011

Related Work Experience:



[KWG Resources Inc.](#)

March 2013 – June 2013 (4 months)

logged core for drill program
aided in mineral deposit targeting



[Cliffs Natural Resources](#)

July 2010 – March 2012 (1 year 9 months)

supervised drill program
logged core, described rocks

[East West Resource Corp.](#)

May 2004 – June 2010 (6 years 2 months)

geological mapping and sampling
supervised drill program
logged core, described outcrops, chip samples
produced geological and prospecting maps
produced assessment reports
aided in producing NI 43-101 reports

Nunavut Tunngavik Inc.

July 2003 – August 2003 (2 months)

geological mapping and prospecting

Teaching Assistant at the University of Western Ontario in fall 2012, fall 2010 and spring 2009

Teaching Assistant at Lakehead University 2005-2006, 2004-2005

Publications:

- 2013** **Petrogenesis and mineral chemistry of the McFaulds Lake chromite deposits** GAC-MAC Winnipeg 2013 Program with abstracts volume 36
Laarman, J.E.; Barnett, R.L.; Duke, N.A.; Weston, R.J.
- 2012** **Preliminary results on the geochemistry at the Black Label, Black Thor and Big Daddy chromite deposits in the McFaulds Lake Greenstone Belt, Ontario** Ontario Geological Survey Open File Report 6280 Summary of Field Work and Other Activities 2012
Laarman, J.E.; Barnett, R.L.; Duke, N.A.
- 2005** **Petrogenesis and PGE Mineralization of the Eva-Kitto Intrusion, Northern Ontario**
51st Annual Meeting, Nipigon, Ontario: May 24-28, 2005. Institute on Lake Superior Geology. Part 1 – Proceedings and Abstracts
Laarman, J.E.; Hollings, P.N.
- 2003** **Soapstone occurrences on Tukarak Island: A product of plume tectonics on the east margin of the Transhudson Orogen, Belcher Islands, Nunavut**
31st Yellowknife Geoscience Forum, Yellowknife, NWT, November 19-21, Program & Abstracts of Talks & Posters
Laarman, J.E.; Duke, N.A.